Proceedings of the 1st Australian Conference on Engineering Geology

ACEG 2025

23-25 July 2025



Defining the Next Challenges for Engineering Geology – Shaping our Future Together

AUSTRALIAN GEOMECHANICS SOCIETY

1st Australian Conference on Engineering Geology

Editors

Anthony Bowden
Consulting Engineering Geologist, Bowden Geotechnical

Mark Eggers
Principal Engineering Geologist, Pells Sullivan Meynink

Christopher Bennett
Senior Technical Director, GHD

Megan Packer
Principal Engineering Geologist, Pells Sullivan Meynink

© 2025 Australian Geomechanics Society Ltd, Brisbane, Australia

All rights reserved. No part of this publication or the information contained herein may be reproduced, stored in a retrieval system, or transmitted in any form or by any means, electronic, mechanical, by photocopying, recording or otherwise, without written prior permission from the publishers.

Although all care is taken to ensure integrity and the quality of this publication and the information herein, no responsibility is assumed by the publisher nor the author for any damage to the property or persons as a result of operation or use of this publication and/or the information contained herein.

ISBN 978-0-9946261-9-6

Published by: Australian Geomechanics Society Ltd
PO Box 7, The Gap, QLD 4061, Australia
operations@geomechanics.org.au
geomechanics.org.au

Conference Welcome

The AGS and IAEG are delighted to invite you to attend the inaugural Australian Conference on Engineering Geology. The conference will bring together geopractitioners from around the country who work on engineering and geohazard projects. The aim is to showcase the valuable work being carried out by engineering geologists to support Australia's economic and social development.

Acknowledgement of Country

The ACEG 2025 organising committee acknowledges that we are meeting on the traditional Country of the Turrbal people of the Brisbane and pays respect to Elders past and present. We recognise and respect their cultural heritage, beliefs and relationship with the land. We acknowledge that they are of continuing importance to the Turrbal people living today.



Gold Sponsors

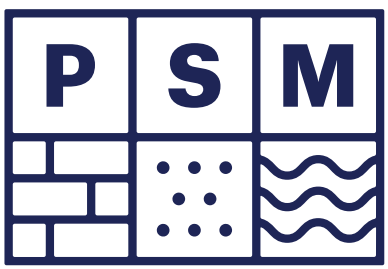
We are grateful for the generous support of our sponsors.
Their contributions make this conference possible.











Sponsors

We are grateful for the generous support of our sponsors.
Their contributions make this conference possible.

SILVER SPONSORS

ROCSCIENCE

ROCKWELL DRILLING

MACQUARIE GEOTECH

MINE GEOTECH

MGS Mapstone Geotechnical Services

GEOCHEMPET SERVICES a kiwa company

fine GEO5 ETIA TRAINING

DYWIDAG

Intrax LAND

INSITUTEK

alliance

Australian Institute of Geoscientists

SEEQUENT

TETRA TECH COFFEY

sunwater

BRONZE SPONSORS

Precision Geotechnical Services

Douglas PARTNERS

INTELLIGENT RESOURCES INC. SOFTWARE

Sigra

CONFERENCE PARTNERS

SOFITEL BRISBANE CENTRAL

1st Australian Conference on Engineering Geology Brisbane - Queensland, Australia July 2025

ORGANISING COMMITTEE

Megan Packer	Co-Chair	PSM
Christopher Bennett	Co-Chair	GHD
Mark Eggers	Technical Committee	PSM
Anthony Bowden	Technical Committee	Bowden Geotechnical
Jon Gibbs	General Manager	Australian Geotechnical Society Limited
James Robinson	Website and Support	Australian Geotechnical Society Limited

SUB-EDITORS

Alex Petty	Civil Infrastructure	PTG Consulting
Felicia Weir	Mining	PSM
Nick Roberts	Geohazards	State Growth
Tim Mote	Energy	GHD

REVIEWERS

Andrew Barclay	**Jason Hellmuth**	**Andy Law**
Joanna Sylvester	**Bari Thomas**	**Julia Bota**
Chris Hathaway	**Nick Roberts**	**Christopher Bennett**
Marc Hendrickx	**Craig O'Neill**	**Mark Eggers**
Darren Paul	**Martin Brook**	**Debra Fellows**
Megan Packer	**Felicia Weir**	**Peter Elson**
Graeme Jardine	**Ross Roberts**	**Helen Baxter-Crawford**
Tim Cartledge	**Ian Shipway**	**Tim Nash**

FIELD TRIP GUIDES

Warwick Wilmot	Maleny Bus Trip
Laurie Hutton	Brisbane Walking Tour

PUBLISHED BY

Australian Geomechanics Society Limited

Organising Committee Chairs' Welcome

Welcome to the 1st Australian Conference on Engineering Geology (ACEG)

It is with great enthusiasm that we welcome you to the inaugural Australian Conference on Engineering Geology (ACEG), taking place in Brisbane, Australia, from 23 to 25 July 2025. This landmark event is the first of its kind in the country, dedicated to enhancing the profile of engineering geology and celebrating the invaluable contributions of the professionals who contribute to our industry. Engineering geology is often overlooked by institutions, owners and companies as a key part of developing and maintaining infrastructure and mining in Australia. In the absence of a firm knowledge in how to apply geological understanding to engineering then key decisions can be missed. This application of geology was established in Australia through many of the previous practitioners like Daniel Moye, David Stapledon, and Alan Moon who helped shape how we investigate, describe, record and construct with the geological model and engineering application both in mind.

Supported by the Australian Geomechanics Society Limited (AGS) and the International Association for Engineering Geology and the Environment (IAEG), along with industry partners including the Australian Institute of Geoscientists (AIG) and the Geological Society of Australia (GSA), this conference is a testament to the collaborative efforts of organisations committed to fostering career development, expanding technical knowledge and supporting engineering geology as a specific disclipline.

With approximately 40 industry specific technical papers, two keynote speakers, three invited speakers, and a panel session, ACEG 2025 offers a diverse and engaging program that highlights both the latest advancements and the enduring challenges within engineering geology. We are fortunate to have local engineering geologist, Warwick Wilmot, host the field trip to Maleny to view the landslides of the basalt terrains. Warwick's extensive publications have significantly contributed to the understanding of the southeast Queensland (and beyond) geological landscape. For those staying more local on Friday, Laurie Hutton is kindly providing a walking tour of the city and its geology.

This conference is more than an opportunity to exchange technical insights; it is a celebration of the people who drive progress in engineering geology. We are delighted to have had the opportunity to bring together researchers, practitioners, and industry leaders to forge meaningful connections, inspire innovation, and strengthen the community that underpins this essential field.



Christopher Bennett
ACEG Co-Chair



Megan Packer
ACEG Co-Chair





Technical Committee Welcome

Dear Attendees,

On behalf of the Technical Committee we welcome you to the first ever conference in Australia dedicated to Engineering Geology. The idea for this conference was born over a beer after a long day teaching in the field on the Adelaide based Geology for Engineers course. We were reflecting on the state of our profession in Australia and felt it was time that Engineering Geology had a stronger voice in the engineering and geohazard communities. The idea for this conference is to bring Engineering Geologists together to learn, collaborate, spark ideas and build more connections. Consider this gathering as a starting point with the vision to repeat this conference every four years to help keep the conversations and connections going in the long term.

Technically we have four themes centred around engineering geology in mining, energy, civil infrastructure and geohazards with around 40 papers, two keynote and several invited speakers from Australia, China, Nepal, Canada and New Zealand. We also have a panel discussion, which is an opportunity to talk about current issues centred around education, training and professional registration.

This is a conference of the Australian Geomechanics Society, which is the Australian National Group of the International Association for Engineering Geology and the Environment. We sincerely thank the AGS for wholeheartedly embracing the idea for this conference and making a commitment to future ACEG events in the future. The IAEG is the organisation that represents our profession at the international level and we encourage all Engineering Geologists in Australia to be affiliated to the IAEG via membership of the AGS. Being involved in IAEG events and initiatives around the world is a fantastic way to take your engineering geology experience to the next level and see the strength of our profession in the global setting.

Thank you for participating in this conference, we hope you find it a memorable and fulfilling experience.



Mark Eggers
IAEG Advisory Committee



Anthony Bowden
IAEG Vice-President for Australasia

Australian Geomechanics Society National Chair Welcome

Welcome from the AGS National Chair

In a guest editorial for Australian Geomechanics in December 1999, Fred Baynes included a personal ad:

> *SEEKING SIMILAR.....*
> *Consulting engineering geologist, gosh [good sense of humour], social drinker, occasionally argumentative, enthusiast, seeks similar to develop ideas, synergy, commercial opportunities. Is it possible to connect?*

I want to welcome you to the 1st Australian Conference on Engineering Geology, what might be the ultimate 25 year response to Fred's personal ad. Little could anyone have imagined that the passage of time would bring what I now see in the conference program from Fred is a formal call to arms!

In all seriousness, Fred's editorial from 1999 is insightful, because parts of it could have been written this cool Brisbane month of July 2025. An Australian scheme for the registration of engineering geologists has not been satisfactorily resolved, and the paucity of engineering geology courses in Australia is more acute now than then. On the question of whether engineering geology is suitably appreciated by the broader geotechnical engineering community, this will always be hard to define or measure (unless anchored to the two issues of the previous sentence), but my suspicion is that some engineering geologists practicing through the last three decades may not have perceived much change. The reasons for this state of affairs are complex and to some degree may extend into market forces and educational trends that are hard to influence. But opinions vary. You can find Fred's editorial on the AGS website, as you can the September 2024 issue of Australian Geomechanics dedicated to Engineering Geology, with related editorials from several of you. There is much to discuss at ACEG1, and to occasionally argue about.

I want to thank the speakers and authors who have taken the time to engage, mostly on topics of immediate interest to Australian practice. And for wider context, just from the keynote and invited speakers, I look forward to hearing about the management of geohazards in China, Nepal and New Zealand, as well as mines in Canada and engineering geological models everywhere.

Finally, I want to thank Mark, Anthony, Megan and Christopher for their time and efforts on the organising committee, and the AGS General Manager Jon Gibbs for his efforts in supporting the planning. From preparing a proposal I read in early 2024 to making ‘it’ all happen, there is a lot of work, especially when considering that ‘it’ is an inaugural event, the stuff of precedent and future tradition.

I look forward to the conference and to speaking with many of you.





Timothy Thompson
Australian Geomechanics Society National Chair

Keynote Speakers



Xuanmei Fan
Director, State Key Laboratory of Geohazard Prevention and Geoenvironment Protection (SKLGP), Chengdu University, China

This lecture explores advancements in engineering geology, including China's extensive experience in disaster risk reduction and innovative technologies such as big data analytics, artificial intelligence, advanced remote sensing, and numerical and physical modelling. It emphasizes how these developments can address multi-hazard risks and support sustainable development in an era of rapid climate change.

BIOGRAPHY
Professor Dr. Xuanmei Fan is the Paul Marinos Distinguished World Lecturer and is the Director of the State Key Laboratory of Geohazard Prevention and Geoenvironment Protection (SKLGP) at Chengdu University of Technology, China. She obtained her PhD in Engineering Geology from the Faculty of Geo-Information Science and Earth Observations (ITC) at the University of Twente, Netherlands. Her research focuses on earthquake- and climate change-induced geological hazard chains, long-term landscape evolution, and disaster risk reduction. Her work has been extensively applied in emergency response and rescue operations following major earthquakes. Prof. Fan has served as the Principal Investigator for more than 20 national and international research projects, including a UK-China collaboration project, European initiatives, and multiple projects funded by the National Natural Science Foundation of China (NSFC). As the founding chair of the Global Partnership for Smart Informatics and Multi-hazard Reduction (SIMR), she seeks to address global challenges associated with increasing multi-hazard risks and climate change in a rapidly evolving world.



Fred Baynes
Engineering Geologists – A Call to Arms!

The implementation progress of the IAEG C25 Guidelines on Engineering Geological Models will be reviewed and lessons learnt during the roll out will be discussed. Some outstanding issues facing engineering geologists within Australia that require further effort will be suggested along with a global perspective of key issues that engineering geologists will face and their potential future contributions.

BIOGRAPHY
Fred Baynes was educated in the UK, obtaining a BSc in geology from Bristol University, an MSc in engineering geology from Imperial College and a PhD from Newcastle University relating to research on weathered rocks. After working for a site investigation contractor in the UK for a couple of years, he immigrated to Australia in 1980, where he has worked as an engineering geologist for contractors, consultants and utilities. Since 1996, Fred has been an independent consultant-engineering geologist with a continuing love of fieldwork and is now based in Central Victoria, Australia. He provides advice to major projects in the civil, mining and oil and gas sectors throughout the world. The advice provided invariably centres around "getting the geology right" and developing effective engineering geological models of all sorts to facilitate project delivery. He regularly teaches engineering geology and geology for engineers to both undergraduates and practitioners and has developed and delivered a variety of professional development courses. He has been actively involved in the IAEG since 2002 and had the honour of serving as President between 2006 and 2010.

Invited Speakers



Dr Ranjan Kumar Dahal
Uncovering geohazards impacting infrastructure in the Himalayas

This presentation will illustrate and discuss the broad range of geohazards affecting Himalayan infrastructure and society. It will discuss the part that engineering geologists are playing to address these problems and will review the impact that they and other ground engineering professionals are having on a range of projects.

BIOGRAPHY
Dr Dahal is Vice President for Asia of the IAEG and is an associate Professor of engineering geology at Tribhuvan University and a visiting professor at the Universities of Ehime and Kagawa in Japan. He has consulted extensively on projects in the Himalayas and in particular in his home nation of Nepal.



Prof D Jean Hutchinson
The impact of industry supported field courses on educational and professional outcomes

This presentation will reflect on a field school that Prof. Hutchinson taught during her career, and which covered the mining cycle and all the ways that Geological Engineers could have an impact. This course was a significant contributor to the engagement of Geological Engineers in the mining industry in Canada and on the way that mine closure planning is done.

BIOGRAPHY
Jean Hutchinson is Professor Emerita at Queens University Canada. President of Innovative Geomechanics Inc. past Vice-President for North America of the IAEG and currently a member of the IAEG Advisory Committee. During her years as Professor in Geological Engineering at Queen's University, she conducted research into slope stability (open pit and natural) and landslide hazards and risks, risk-based decision-making using monitoring techniques, applications utilizing LiDAR surveys, with applications to landslides adjacent to hydro reservoirs, and ground hazards affecting railway corridors.



Don Macfarlane
Landslides and reservoirs, the Clyde dam experience

This presentation will outline the role of engineering geology in the scoping and management of the investigations, design and construction of remedial works undertaken on 10 large landslides flanking the Clyde Dam reservoir prior to lake filling in 1992-93. It will outline the ongoing management and performance of the landslides and the role of engineering geology in that work.

BIOGRAPHY
Don Macfarlane is an applied engineering geologist with more than 45 years of experience as consultant, manager and reviewer in investigation, construction and monitoring aspects of dam and other infrastructure projects, slope stability assessments and groundwater investigations in a range of geological environments, mostly in Australia and New Zealand.

Field Trips



Warwick Wilmot
Landslide prone environments on basalt terrains in the Glasshouse Mountains

The slopes of the Maleny Plateau in the Glass House Mountains are well known to be prone to landslides. This field trip will visit several local sites to view the basaltic geology, its structure, the derived colluvial soils and the impacts of ground water outflows on ground stability.

BIOGRAPHY
Warwick Wilmot is a retired geologist who has had a wide experience in Queensland where he was employed since 1972 by the Geological Survey of Queensland in the Department of Mines. For 30 years he worked in a variety of fields, including engineering geology of dam sites, location of construction resources, mapping of urban areas, land use planning, and geological hazards.

Warwick likes to bring geology to the public, and since his retirement has written and edited numerous guidebooks in a 'Rocks and Landscape' series for the Geological Society of Australia, and has assisted national park and council staff with information signs and brochures, as well as hosting numerous public talks, community lectures and excursions.



Laurie Hutton
Walking tour of Brisbane Geology

This half-day walking tour of Brisbane City will explore the two principle geological units within which much of the Brisbane is constructed.

The Neranleigh Fernvale beds underlie much of the Brisbane CBD and therefore form the bedrock to almost all the high-rise development we see today. During the walk we will discuss how the geological history of these rocks has impacted the engineering of the city buildings.

The Brisbane tuff will be examined during the walk along the Kangaroo Point cliffs and perhaps some cliffs on the north side of the river toward New Farm. These cliffs preserve more than 20 metres of hard rock which was used extensively as a building stone for much of Brisbane's history. Its impact on the development of Brisbane will be discussed on the walk. As we will be walking beside the Brisbane River, we will also comment on the effects of the river on the city's development. We can also observe some recent sediments and discuss how we as geologists use these deposits to interpret older depositional settings.

BIOGRAPHY
Laurie Hutton is a retired Queensland geologist. He was employed for many years by the Geological Survey of Queensland as part of a team producing geological maps and has worked extensively around Queensland. Laurie retired in 2019 but maintains an active interest in geology through the Geological Society of Australia.

Contents

TECHNICAL PAPER	PAGE
Slope stability in weathered basalts *Stephen Fityus and Michael Gawn*	1
Coal Mine Engineering Geology as a Trans-Tasman learning experience in a university postgraduate course *Martin S. Brook*	4
Engineering Geology Model as a tool for the effective management of Open Pit Slopes *F.M. Weir and M.J. Fowler*	15
Understanding critical stability factors: Integrating old and new data to improve foundation stability assessments *Ben Speakman and Matthew Ferguson*	26
The specification of unprocessed rockfill for highway applications – A case study from the Coffs Harbour Bypass *A. M. Tait*	29
Rockfall hazard assessments and remediation for the major cliff precincts of Brisbane *Tharindu Abeykoon, Matthew Cochrane, Andy Law & Bruce Cheesman*	42
Management of complex geological structures using engineering geological models during tunnel construction: The Luna Park Fault Zone, Sydney *Richard Brehaut, Beatriz Estrada and Stuart Simmonds*	54
Case study on Snowy 2.0, Australia: use of LiDAR and endoscopy for assessing and modelling geological features in underground caverns *B. Potter, A. Blaise, B. Requiliani, E. Guevara and K. Stariha*	67
Application of a copula approach to quantify rainfall-induced rockfall *Farshad Bahootoroody, Davide Ettore Guccione, Klaus Thoeni and Anna Giacomini*	80
Susceptibility and mitigation of debris floods and flows in the Jenolan Karst Conservation Reserve, NSW, Australia: Bushfire and La Niña impacts *Adam Irvine and Richard Brehaut*	92
The use of empirical methods to predict landslide runout for use in rapid landslide risk asssessments following Cyclone Gabrielle, New Zealand *R. Hayes, A. Hunter and A. S. Miner*	104

Contents

TECHNICAL PAPER	PAGES
Engineering geological models in remote and difficult access terrain: A case study from Bogong High Plains Road *Davide Casagrande, Dane Pope and Katerina Irwin*	116
Slope hazard management on the Toowoomba Range Rail Corridor, Queensland *Bruce Cheesman, David Cooper, Andy Law and Matthew Cochrane*	127
Experiences communicating Landslide Risk to non-technical stakeholders *Chris Coulson and Tony Miner*	139
Risk management of coastal cliff hazards – A case study from the Surf Coast, Southwest Victoria *Kris Jelly-Butterworth*	151
Glasshouse Mountain summit routes: Balancing safety, accessibility, and tolerable risk *Sally Roberts-Kelly and Lee Moule*	165
Rockfall risk assessment at North Head, Sydney Harbour National Park, NSW *Michael Egan and Paul Roberts*	179
Landslide risk assessment in coastal settings – Recognizing the challenges and uncertainty *Andrew Hunter and Tony Miner*	188
GIS mapping of landslide susceptibility and life risk in Blue Mountains National Park *Zack Tuckey*	201
Engineering geology considerations for development on Bringelly Shale in Western Sydney *So M.M.L., Hokmabadi A.S., Zhu D., Casey T. and Terzaghi S.*	213
Neotectonic fault significance *Tim Mote*	217
Importance of detailed geomorphic interpretation in the landslide characterisation component of landslide risk assessment *Nicholas J. Roberts and Anthony S. Miner*	223
Analysis of the mechanism of landsliding, Garie Road, Royal National Park, NSW *Tim Donovan and Luke Johnstone*	234

Contents

TECHNICAL PAPER	PAGE
What is the future of Engineering Geology as a discipline in Western Australia, and Australia? *Julia Bota, Paul Baker, Patrick McManus, Andrew Shuckstes, Alex Petty, and Domenik Wolff-Boenisch*	247
The impact of industry supported field courses on the education and professional training of Geological Engineers at Queen's University, Canada *D. Jean Hutchinson*	258
The Bogong Landslide, a case study into an Australian landslide in unsaturated soils *Darren Paul, Simon Harbig, Emma O'Brien and Alana Dubowik*	269
Landslide vulnerability: Learnings from the impacts of debris flows on buildings to inform quantitative loss of life risk assessments *L. N. Agnew, R. Hayes, A. S. Miner and A. Hunter*	282
Effect of discontinuities on the survival probability of spherical blocks upon impact *Davide Ettore Guccione, Maddalena Marchelli, Oliver Buzzi and Anna Giacomini*	294
Scoping for geohazards - Environmental contrasts comparing the Engineering Geologist's role between mining, civil road tunnels, dam design and pumped hydro *Helen Baxter-Crawford*	297
Assessing the geotechnical susceptibility of caves in Pilbara iron formations to instability *Duncan Noble, James Watton, Mark Eggers and Mark Fowler*	308
Project Phoenix Pumped Hydro Energy Storage Project - Successful implementation of the Engineering Geological Model approach in support of the energy transition *Alistair Schofield*	320
Development of a geotechnical rock mass model using geochemical data and machine learning *Megan Baker, Sue Chan, Christine Lion and Daniel Strang*	336
Finite element check of GSI adjustment equation reconciling Hoek-Brown and Step-Path strengths *Norbert R P Baczynski and Alison McQuillan*	348
Engineering terrain evaluations – Opportunities and challenges of the energy transition *Tom Casey*	367
Engineering geological mapping for dam foundations - Examples from recent work *Jo Darby, Chris Hathaway, Christopher Bennett and Chris Chamberlain*	370

Contents

TECHNICAL PAPER	PAGE
Geological challenges of Brisbane's Cross River Rail project *Ralph Cammack*	391
Site investigation and geological challenges for a rail level crossing project in SEQ *Pramod Thakur and Craig Brock*	405
Reservoirs and landslides – The Clyde Dam experience *Don Macfarlane*	419
Uncovering geohazards affecting infrastructure in the Himalayas *Ranjan Kumar Dahal*	420
Engineering Geology in Australia: A profession at the fault line of policy, practice, and performance *Christian Dodge*	428
A scalable machine learning modelling tool for mapping landslide runout using a case study in Hawkes Bay, New Zealand *Alex Stokes*	450

https://doi.org/10.56295/1ACEG01

SLOPE STABILITY IN WEATHERED BASALTS

Stephen Fityus, Michael Gawn
Douglas Partners P/L, Newcastle

ABSTRACT

Tertiary basalts are widespread along the eastern Australian continental margin, extending from The Torres Strait to Melbourne in the south. In many instances, they have been extruded on, or adjacent to the Great Dividing Range, and remain prominent in the steep and elevated topography. By their nature, they weather deeply and rapidly, to form soils with undesirable engineering properties, which in the geomorphically-immature topography of the Great Dividing Range and the Great Eastern Escarpment, leads to engineering challenges for transportation infrastructure. This paper provides a description of the occurrence of these basalts around the margins of the Hunter Valley, with consideration of their control on topographic stability and geomorphic evolution. Factors such as their bedded structure, the presence of palaeosoils, and their tendency to creep are described and evaluated in the geological profiles in which they are encountered, and the engineering problems associated with them are discussed. Experiences from a recent project involving the remediation of a road, affected by basalt-hosted slope instability, are presented and discussed to provide insights into good and bad engineering practices in these geological environments.

1 EAST AUSTRALIAN BASALTS

Tertiary (Cainozoic) basalts occur sporadically along the Great Dividing Range of Eastern Australia. They have particular geological characteristics which make them problematic for civil engineering works. In particular, they are associated with slope instability of both natural and engineered slopes.

The basalt occurrences vary from localized small flows and diatremes with areas of hectares, up to areas of thousands of square kilometers. The basalts have a typical thickness of 300 m - 400 m (Knutson 1989), but smaller occurrences may have thicknesses considerably less than this. Compositions range from silica over-saturated tholeiites (less common, and often occurring as basal units) to silica over-saturated basalts (Sutherland, 1978; Knutson, 1989), which include olivine basalts, mugearites, basanites and hawaiites (more dominant in most provinces). In some sequences, units of tuff and breccia occur. Although these are generally not dominant in the sequence, they can occur locally in significant thicknesses with high clay contents including montmorillonites and halloysites (Won et al. 1983).

Basalt sequences typically comprise sequences of relatively thin flows (3 m to 10 m) which can vary in composition and structure for successive flows. Flow structures include both massive with random fracturing, or columnar, and amygdaloidal horizons within flows are relatively common. Also occurring occasionally in some sequences are palaeosol units which present as weakly-cemented, oxidized soil layers that are chemically resistant to weathering.

2 BASALT GROUND PROFILES

Basalts are renown for deep weathering to produce clay soils. This stems from their mineralogy of olivine, pyroxene and plagioclase, which are all highly susceptible to alteration and weathering in temperate environments. Less well appreciated is the presence of glass in the interstices of basalt, arising from their rapid cooling (Exon et al. 1970). Eggleton et al. (1987) reports that for Eastern Australian basalts, glass and olivine have the highest (and similar) weathering susceptibility, followed by plagioclase, then pyroxene, and then K-feldspar. The weathering process for the minerals and glass in basalt are complex, but in general, the end products are clays and oxides, amongst which halloysite and the smectites (montmorillonite, nontronite and saponite) often feature significantly (Craig and Loughnan, 1964). In addition to the rate of weathering of the minerals of basalt rocks being very fast, it has been observed that mineral alteration may even begin as the basalt cools post-eruption (Coleman, 1960).

The thickness of residual basaltic soils can vary locally, even over relatively short distances. Dahlhaus and O'Rourke (1992) suggest that this, at least in part, may be due to soil formation on different basalt flows of variable composition and texture. Residual basaltic clay soil profiles are typically many metres thick, and profiles of up to 10 m deep are not uncommon. Because of the lithological variations that can occur between adjacent flows, the texture of the residual materials in the weathered horizon can vary widely, from heavy red-brown clays of high plasticity to friable brown rotten rock which crumbles and ravels when exposed in a steep face.



Figure 1. Four weathered basalt profiles: highly plastic clay (left); crumbling friable rock (middle); tuff (right).

3 BASALT LANDSCAPES

Basalt landscapes exhibit some characteristic geomorphic features, many of which are related to landslide activity. The stacking of lava sequences on the elevated topography of the Great Divide and/or subsequent uplift has produced land slopes that are over-steep and prone to mass movement (Galloway, 1967; Young, 1983). These are typified by concave upper slopes below ridge lines and crests, and convex land surfaces adjacent to creeks (Figure 2). This is contrary to more mature landscapes in sedimentary rock landscapes in the Hunter Valley, where ridge tops are round and convex, and lower slopes are concave as they transition to valley floors. This reflects a tendency for valley walls to cut back by slides in the upper slopes on ridges, and for slide debris to accumulate in gullies faster than it can be subsequently removed.



Figure 2. Ground profile through a basalt ridge extending from the Great Dividing Range, Murrurrundi.

4 SLOPE INSTABILITY MECHANISMS.

The deep weathering profiles developed on the basalts, combined with the over-steep, immature topography in many basalt areas, leads to a variety of slope movement mechanisms that vary in scale and rate. These are summarised here.

The heavy smectite-rich clays developed over the basalts are inherently shrink-swell prone, and prone to a phenomenon known as “self-mulching” (Grant and Blackmore, 1991) whereby surface soil debris which falls into desiccation cracks when the soil is dry inhibits closure of the cracks, causing the deeper soils to be displaced toward the surface. When heavy clay soils (see Figure 1 left) occur on relatively steeper slopes, the self-mulching phenomenon can manifest as a mechanism whereby there is a downslope component of displacement in the shrink swell cycle that slowly but consistently causes the upper layers of clay soil to creep downslope. The thicknesses involved are relatively small (of the order of metres) and the process rates are slow (unmeasured, but likely to be centimetres per year), but since the phenomenon affects entire hillsides, the volumes can be collectively huge.

Where clay soils become thick and over-steep on slopes, rafts of clay soil can undergo a combination of rotational and translational sliding, leaving a scarp at the top of the slide, and creating a bulge at the toe. Such slides are almost exclusively associated with saturated ground conditions. The sliding mass may or may not break-up into a series of slices during detachment or movement. Rates of movement are likely to be of the order of metres per hour. The high cohesion in the basaltic clay soils mostly prevents the slide mass from fluidising and becoming a mudslide, but excess surface water flowing through the slide-affected area can mobilise significant soil and mud through erosion.

Despite being physically weak, palaeosol horizons present units of low chemical weathering susceptibility within deeply weathered basalt sequences, which can express (outcrop) as resistive capping levels in basalt slopes, disrupting the slope evolution process and causing the slope to become locally over-steep. Undercutting of these capping levels by more rapid erosion of deeply weathered basalt can trigger instability which penetrates the weathered rock mass. This mechanism is described in Fityus et al (2017).

Shallow instability triggered by palaeosols or local over-steepening can destabilise the ground immediately above the scarp, leading to progressive back-cutting of a slope, which may involve increasing depth with successive slices of ground. Geomorphic evidence suggests that substantial rotational rockmass slides can occur in upper slopes to leave large amphitheatre landforms which are more than half a kilometre wide and hundreds of metres high.



Figure 3. Shallow translational slide in plastic basalt soils (left); systematic upslope progression of slides (middle); amphitheatre landform below crest caused by a large deep-seated slide (right).

Roadworks which cut into weathered basalt slopes can remove slope support and induce increased loads in upslope soil masses. Creep resulting from sustained shear stresses in deeply weathered basalt soils can slowly reduce soil strengths to residual values. Where interbedded tuffs and palaeosols are present, failure can develop relatively rapidly and be difficult to arrest, once initiated.

REFERENCES

Colman, S. M. (1982) Chemical weathering of basalts and andesites: Evidence from weathering rinds: U.S. Geol. Surv. Prof. Pap. 1246, 51 pp.

Craig, D. C., & Loughnan, F. C. (1964). Chemical and mineralogical transformations accompanying the weathering of basic volcanic rocks from New South Wales. *Soil Research*, *2*(2), 218-234.

Dalhaus PG and O'Rourke MO. (1992) The Newer Volcanics. In Engineering Geology of Melbourne. Peck, Neilson, Olds and Seddon. Balkema, Rotterdam. 205 – 212.

Knutson J. (1989) East Australian volcanic geology, in Intraplate Volcanism in Eastern Australia and New Zealand. (eds. Johnson R.W, Knutson, J. and Taylor S.R.) Cambridge University Press, Sydney. pp. 89-156.

Eggleton, R. A., Foudoulis, C., & Varkevisser, D. (1987). Weathering of basalt: changes in rock chemistry and mineralogy. Clays and Clay Minerals, 35(3), 161-169.

Exon, N, Langford-Smith, T. & McDougall, I. (1970). The age and geomorphic correlations of deep-weathering profiles, silcrete, and basalt in the Roma-Amby region, Qld. Journal of the Geological Society of Australia, 17(1), 21-30.

Fityus S, Hancock G and Gibson J (2014) Landslides in Tertiary basalts at Murrurundi, Australia. Proceedings of XII International Association of Engineering Geology Congress, Torino. 1061-1064

Galloway, R. (1967). Pre-basalt, sub-basalt and post-basalt surfaces of the Hunter Valley. New South Wales, 293-314.

Grant, C. D., & Blackmore, A. V. (1991). Self mulching behavior in clay soils-Its definition and measurement. Soil Research, 29(2), 155-173.

Schon R. W. 1985. Petrology of the Liverpool range volcanics, eastern New South Wales. In: Volcanism in Eastern Australia: with case histories from New South Wales, Geol. Soc. Australia, NSW Division, Abstracts, 73–89.

Sutherland, F. L. (1978). Mesozoic-Cainozoic volcanism of Australia. Tectonophysics, 48(3-4), 413-427.

Won, G. Vickery, J and McQueen, L. (1983) Geotech investigation for a deep road cutting adjacent to the Ardglen railway tunnel Murrurundi NSW. In Collected Case Studies in Engineering Geology, Hydrogeology, and Environmental Geology. The Engineering Geology Specialist Group of the GSA, Sydney, v. 11, 423 pp.

Young, R. W. (1983). The tempo of geomorphological change: evidence from southeastern Australia. The Journal of Geology, 91(2), 221-230.

https://doi.org/10.56295/1ACEG02

COAL MINE ENGINEERING GEOLOGY AS A TRANS-TASMAN LEARNING EXPERIENCE IN A UNIVERSITY POSTGRADUATE COURSE

Martin S. Brook
School of Environment, The University of Auckland, Private Bag 92019, Auckland 1142, New Zealand

ABSTRACT

Fieldwork is at the heart of engineering geology, viewed by academics, students and industry as a ubiquitous element of geoscience tertiary education. Fieldwork is considered an extremely effective experiential (i.e. "learning-by-doing") teaching and learning method. In engineering geology, much of the learning pedagogy is focused on applied problems such as dams, tunnels, state highways and landslides, dealing with issues of "ground risk". Due to the obvious safety (and legal) implications of students visiting operating mine sites, such applied learning experiences are often confined to PowerPoint slides in classrooms, or sometimes virtual fieldtrips using a range of technologies. This can produce challenges to fostering engagement. Here, the development of a one-day graduate-level engineering geology fieldclass based at two operating open-cast mines is presented. The trip is structured to develop the students' awareness of the first priority of such workplaces, health and safety. The students then follow a mini "Cook's Tour" led by mine staff, around the open-cast mines, recording geological features, and are prompted to consider engineering hazards relating to the interaction of geology and operations. Students then log core in a mine core shed, observe and record stratigraphy and significant features such as defects and strength variability. Post-fieldtrip, the students analyse borehole geophysical logs, and undertake kinematic analysis and limit equilibrium modelling of highwall stability, incorporating this into an assessed report. Comparisons with Bowen Basin opencast and underground coal mines are encouraged, via provision of industry datasets. Opportunities, and challenges to future expansion of such fieldtrips are also discussed.

1 INTRODUCTION

This paper, which includes photographs and examples of student assessments, describes a field trip that forms the key component in the teaching of Engineering Geology to postgraduate students at The University of Auckland, New Zealand. The field trip has been developed over the past decade and the intention of this paper is to share both the experience gained during this time and also provide some photographs of some of the interesting features during the fieldtrip, along with some examples of some of the work that the students are expected to produce. The purpose of the one-day field course, part of the Earthsci 771 Advanced Engineering Geology paper, is to introduce postgraduate Engineering Geology students to the importance and purpose of site investigation in a mining context, as well as some of the typical issues in open-cut coal mines such as high wall stability, haul road stability, and associated hydrogeological issues. Students receive very little other exposure to mining operations in their studies, and visiting any work sites such as operating mines presents health and safety challenges that are beyond those typically encountered during a standard geological mapping fieldtrip, which would often be in a farmland area. Indeed, at operating worksites, appropriate PPE and inductions can present issues, while issues of accessibility, inclusivity and equity are also important considerations (e.g. Gilley et al., 2015).

Critical to the above is developing the ability of students to identify hazards and to use their geological observations and insights to make predictive judgements about short- and long-term risks to various engineering scenarios within the open-cut coal mine environment. The students visit two operating open-cut coals mines in the Waikato Coal Fields region of New Zealand's North Island (Figure 1), with both mines owned by Bathurst Resources, who are thanked for their support.

2 MINE ENGINEERING GEOLOGY TEACHING: THE BACKGROUND

2.1 NEW ZEALAND

In the late 19th and early 20th centuries, mining education was deemed very important to New Zealand's prosperity. Indeed, mining was traditionally taught at several universities in New Zealand a century ago, including the Auckland School of Mines and the Otago School of Mines (established 1878) in Dunedin. In addition, perhaps the most famous mining education institution was the Thames School of Mines, at the southwest end of Coromandel. Established in 1885, the Thames School of Mines existed until 1954. At its peak, this was the largest mining school in New Zealand, and for almost 70 years it specialised in practical scientific and industry-focused education.

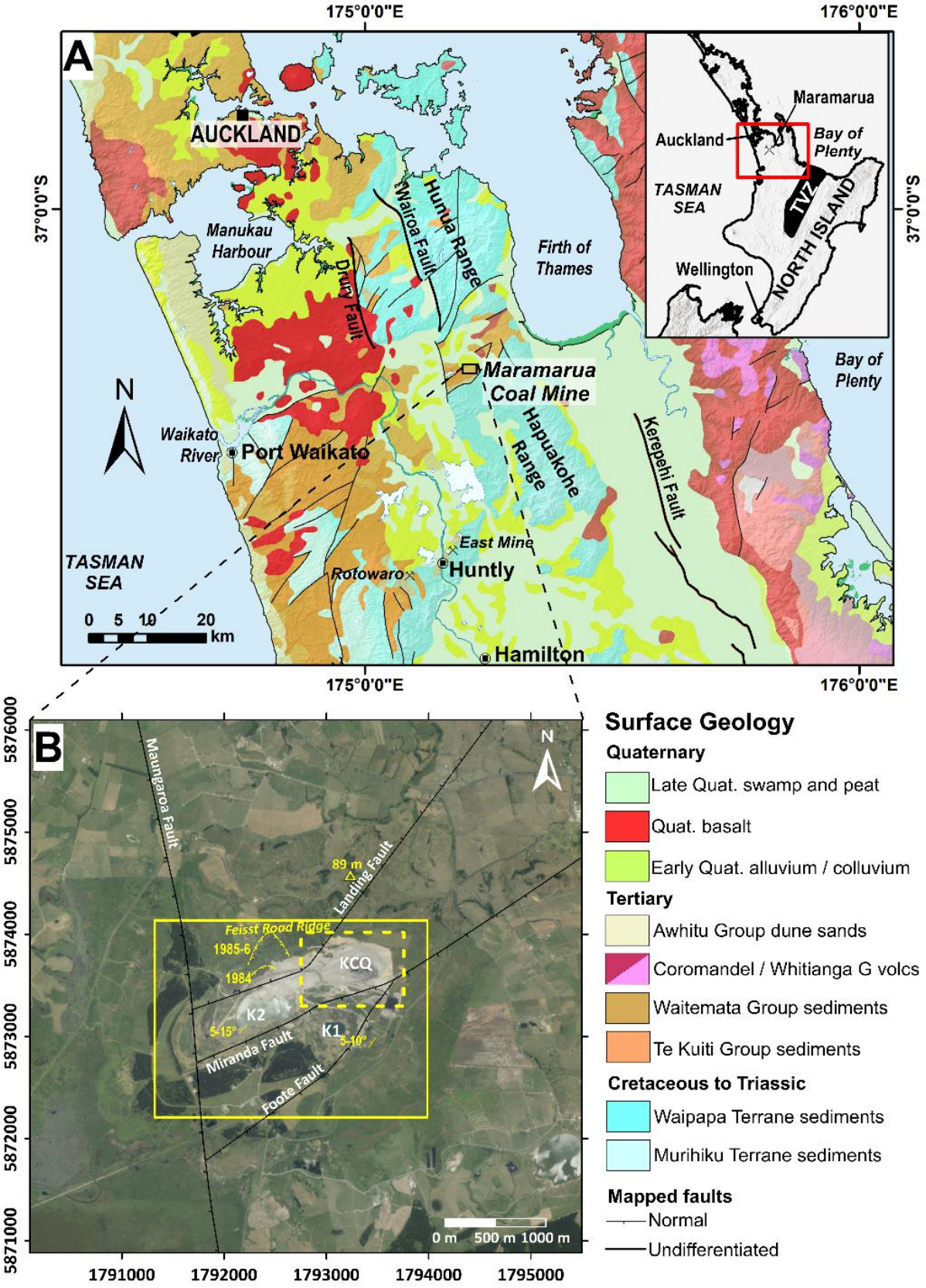


Figure 1: Location of the Waikato Coal Field and Maramarua and Rotowaro open-cut mines, with a blown-up aerial image of Maramarua as an example

Since then, however, mining education in New Zealand has suffered somewhat, and there are currently no active University mining education departments in the country, unlike Australia. Also, there are no mining-specific tertiary qualifications or papers. The lack of mining education is probably for several reasons, including general apathy in New Zealand, an anti-mining mindset (Brook 2024), long-term issues with student enrolments in STEM subjects generally (Brook, 2023a, b), and timetabling issues that plague most universities that follow the "Melbourne Model" of tertiary study. The lack of mining education is despite BSc Earth Science or Geology being taught at 6 New Zealand universities, and a considerable portion of New Zealand graduates working in mining roles overseas, as well as some at gold and coal mines, in addition to quarries, in New Zealand. In addition, civil engineering is taught at several New Zealand universities, and engineering geology master's degrees are available at the University of Auckland (and will return again soon at Canterbury University).

2.2 AUSTRALIA

Unlike New Zealand, Australia has a prevailing and long-standing tradition of mining education and has world-leading mining departments at Curtin University and the University of New South Wales, among other institutions. This includes courses and qualifications in exploration, "standard" geology, and mine geotechnical engineering etc.

3 MINE ENGINEERING GEOLOGY FIELDTRIP AT UNIVERSITY OF AUCKLAND

3.1 EARTHSCI 771 ADVANCED ENGINEERING GEOLOGY

The one-day mining fieldtrip is part of the Earthsci 771 Advanced Engineering Geology paper. This is a 15-point graduate level paper, and students take 8 x 15-point papers for a full (120 points) year of study. Nominally, a 15-point paper is equivalent to 150 hours of study (including all class contact, assessments and reading). The mine geology field trip and the associated assessments account for 50% of the assessment component for the Earthsci 771 paper. The other assessments components usually include 5 x 10% laboratory (computer modelling and soil and rock lab) assessments.

Most students taking the paper are part of the 18-month 180-point, Master of Engineering Geology programme (Brook et al., 2022, 2023). This master's programme has been taught at the University of Auckland for 7 years. Most of these students will already have studied Engineering Geology at 3rd year level during their BSc Earth Science (during Earthsci 372 Engineering Geology). Other students will take Earthsci 771 as part of their 2-year 240-point Master of Earth Science or Master of Engineering Studies. Occasionally, a student will take Earthsci 771 as part of their Earth Science BSc honors degree, or a PG Diploma in Earth Science. So, the student cohort can be somewhat mixed, but all students will have had some prior knowledge of geotechnical engineering or Earth Science to BSc 3rd year level.

3.2 THE MINE ENGINEERING GEOLOGY FIELDTRIP

The Earthsci 771 1-day mine engineering geology fieldtrip has a pre-fieldtrip component, the fieldtrip itself, and a post-fieldtrip component. All of this culminates into a single report, worth 50% of the grade for Earthsci 771.

3.2.1 Pre-fieldtrip

Pre-fieldtrip, preparation involves a desk study using geological maps, borehole data, and selected site photographs from the two open-cut mines. There is also a small selection of relevant papers published in journal articles that the students can read and review, as well as several papers in AusIMM conference proceedings. However, the number of available publications is much less than is available say, for the Bowen basin, Illawarra or Hunter valley coal fields, for example.

The purpose of the desktop reading and engagement with datasets prior to the fieldtrip is to "prime" the students prior to the site visits at the two mines. It also reinforces to the students the importance of developing a strong understanding of existing information at the start of any project, akin to the Total Geological History concept of Fookes et al. (2000), and important in developing the Engineering Geological Model, EGM (Baynes and Parry, 2024). Indeed, both these publications are provided to students in order to provide broader context, beyond the limits of the Waikato Coal Field.

Students are also briefed about what to expect at the mines, and PPE requirements are discussed. PPE can be provided to all students, although many students have existing PPE available from their workplace (many fulltime postgraduate students are employed at least part-time in the geotechnical industry and will have been in that role from the 3rd year of their BSc onwards).

Knowledge of the geology of the area underpins the fieldtrip. The coal seams (Figure 2) that are mined are within the late Eocene-early Oligocene Waikato Coal Measures (WCM), the oldest units of the Te Kuiti Group. The WCM are the basal

formation of the predominantly transgressive Te Kuiti Group, unconformably overlying an undulating erosion surface cut into deeply-weathered Mesozoic basement and grading up into shallow marine formations. The Quaternary Tauranga Group sediments (mainly pumiceous sediments) unconformably overly the Rotowaro Siltstone of the Te Kuiti Group in the area. BSc Earth Science students will have previously encountered the Te Kuiti Group in the field before at 2nd year level (e.g. Bevan et al., 2022).

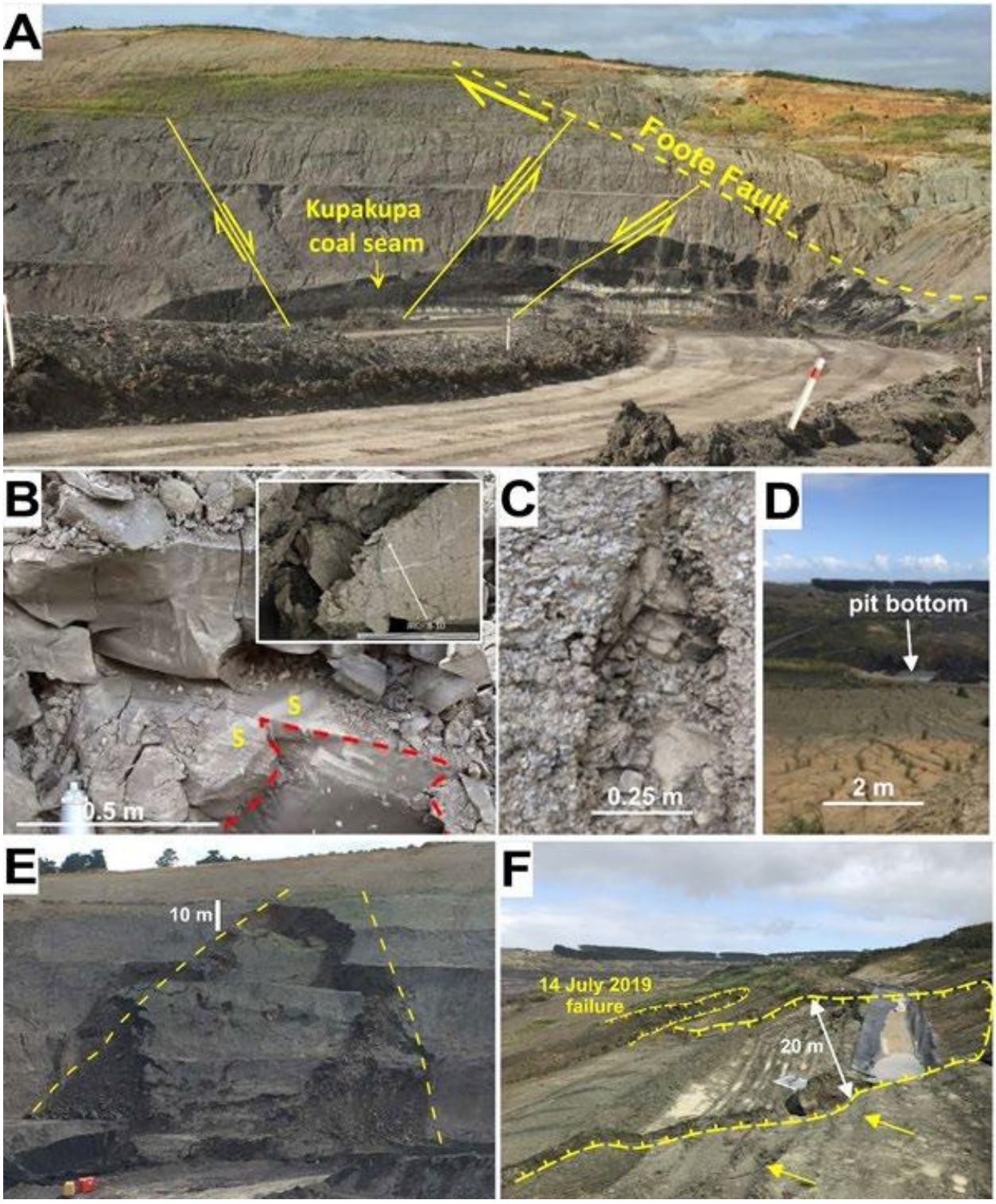


Figure 2: Engineering geology and slope issues at Maramarua mine: (A) Foote Fault and associated minor faults affecting the Kupakupa Seam; (B) smoothed shear surface (S); (C) slaking of Waikato Coal Measures; (D) weak Tauranga Group soils incised by surface runoff; (E) pit wall wedge failure; (F) rotational slump on pit wall

3.2.2 The fieldtrip day

Two mines are visited as part of the one-day fieldtrip. The first is Maramarua mine, which is 1-hour drive southeast of Auckland (Figure 1). The first part of the visit is a site induction with mining staff, and this reinforces that the absolute priority is health and safety. A technical services manager, or occasionally the site senior executive (SSE), provides an introduction in the office block, and in the boardroom, provides insights into the geology, any geotechnical issues, with TV screens showing real-time footage from the CCTV cameras operating around the mine, as a backdrop. This generates questions and discussion, and indeed the enhancement of fieldwork learning in tertiary education using visual technologies is well established (Welsh et al., 2013). The second part of the visit to Maramarua mine is a site walkover with mine staff (Figure 2). This is partly what is referred to in geoscience fieldtrip academic literature as a "Cook's Tour" (Fuller and France, 2015). These are observation-based fieldtrip components, named after the 19th century English travel agent, Thomas Cook. Some typical features they will encounter at Maramarua mine are shown in Figure 2. The floor of the pit is below sea level, so the students get to understand the importance of groundwater control.

Experiential learning activities are also important in geoscience and engineering disciplines (e.g., Fuller et al., 2010). At Maramarua mine, the students will continue their observations in the field, augmenting the desktop study, and make sketches including large-scale geomorphology, structural geology and geotechnical problems, and small-scale sedimentary features, and structural fabric. In terms of experiential activities, they make supporting measurements that can include structural orientations of bedding and joints, rock strength data from Schmidt hammer tests (Figure 2B), and assessments of the Tauranga Group soil profiles (which fail as slumps and flows) using a handheld penetrometer and a shear vane.

After Maramarua mine, the students travel by minibus to Rotowaro mine for the afternoon (Figure 3). At Rotowaro mine, following induction, the students visit the Rotowaro mine pit floor via light 4-wheel drive light vehicles (LV's). The students disembark the LV's and get to understand groundwater issues at the pit, as well as highwall stability. The legacy effects of near-surface former mine workings from the early 20th century near the surface is also evident (Figure 4). The students also consider what ground investigation approaches (invasive and non-invasive) might be appropriate to determine the existence of near-surface abandoned mines with reference to the New Zealand Ground Investigation Specification (NZGIS, 2017) and Brook (2019), and highwall monitoring technology such as InSAR (e.g. Cook et al., 2023).



Figure 3: Briefing from Bathurst resources staff regarding geotechnical issues at Rotowaro mine



Figure 4: Group of students at Rotowaro mine inspecting groundwater issues

Other activities at Rotowaro mine include engineering geological logging of core in a mine core shed. The students apply the New Zealand Geotechnical Society Guidelines (2005) to describe and characterise the properties of core in the core shed (Figure 4). For some of the civil engineering students, this may the first time they will have encountered rock core in the whole of their university studies, so it is potentially an important stepping-stone in their career development.

Application of the NZGS (2005) guidelines is important because it is utilised by contractors throughout the New Zealand civil engineering sector as well. The NZGS (2005) guidelines includes a 38-page that underpins the diagnostic 2-page fieldsheet. Thus, whether the students end up in the mining or civil sectors, this core logging aspect of the fieldtrip is important. The Australian equivalent to the NZGS (2005) would broadly be AS1726-2017.

3.2.3 Post-fieldtrip

After the field-day, the students have three weeks to compile a report, which is assessed and corresponds to 50% of the course mark for Earthsci 771. The report includes these elements: (1) desktop study information; (2) observations and data carried during the field-day; (3) highwall stability analysis; (4) rock UCS calculations; (5) rock mass characterisation.

The stability analysis that the students undertake is first of all a kinematic analysis in Dips software. Following this, the students will progress to modelling in Swedge for example, as wedge failures and bi-wedge failures are common in the Waikato Coal Measures. The more advanced students will also have read around the subject matter, and will also discuss some broader context such as non-daylighting wedge failures in their reporting. Students will also undertake modelling in Slide2 and RS2, to calculate representative Factor of Safety (FoS) and Strength Reduction factor (SRF) values. Some example values that have been produced by students are in Table 1, using a range of scenarios.



Figure 4: Logging Te Kuiti Group rock core in the core shed at Rotowaro mine using the NZGS (2005) guidelines

Table 1: Selected LEM and FEM stability modelling Factor of safety (FoS) and critical strength reduction factors (SRF) for the pit walls modelled by the students

Model scenario	RS2 Critical SRF	SLIDE2 FoS
Baseline with perched groundwater table within Te Kuiti Group	1.41	1.40
Baseline with semi-saturated groundwater conditions	1.31	1.34
Bedding-plane shears and fault gouge as individual units; semi-saturated groundwater conditions	1.14	1.17
Bedding-plane shears and fault gouge as individual units; saturated groundwater conditions	1.09	1.05

The students are also provided with geophysical logs from the mines and from these, apply the original McNally (1987) sonic to UCS curve from to estimate the UCS of the Waikato Coal Measures encountered. The final part for the students in their reports is to use the core shed descriptions and characterisation, alongside the UCS logs, to consider potential roof stability issues if the coal was extracted underground in a bord-and-pillar operation (as has previously occurred in nearby Huntly East Mine), using rock mass rating (RMR) and the coal mine roof rating (CMRR; e.g., Brook et al., 2020).

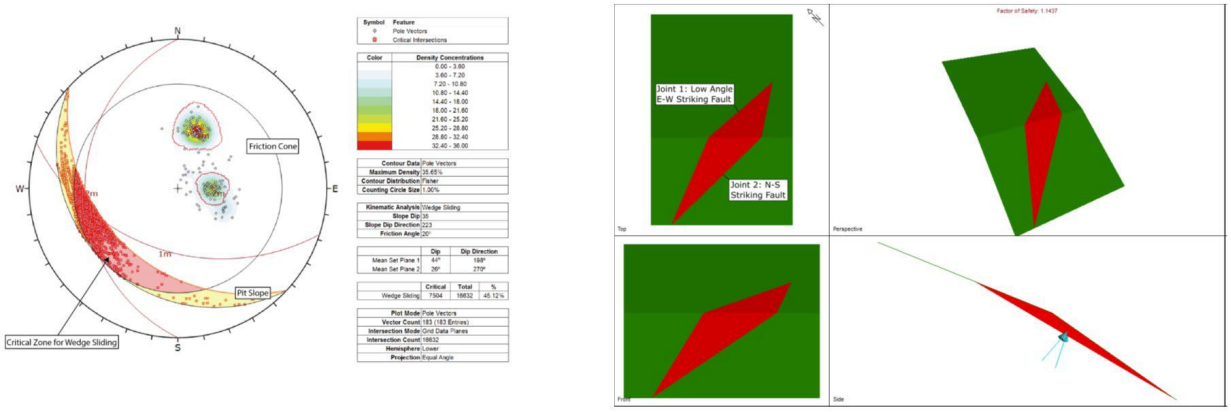


Figure 5: Post-field trip example slope stability modelling in Rocscience software: (left) kinematic analysis, right SWedge

4 THE BROADER LEARNING CONTEXT

4.1 Student reports

An important aspect of this Earthsci 771 course is that students understand the broader context of their work. The learning outcomes have varied to a minor level year-on-year, depending on exactly what access arrangements are available at the mines. Nevertheless, students always need to consider, how do the weak Eocene Waikato Coal measures compare with the much older, stronger rocks of the Australian Permian coal measures? What would this mean for highwall dimensions and overall stability differences? What are the key hydrogeological differences between extraction of the New Zealand weak rock coals and the Australian coals (e.g. Brook et al., 2016). These are important concepts, because a significant proportion of New Zealand graduates will end up working in Australian mines at some point in their career.

Thus, encouraging the students to consult the broader literature, and understand key differences between New Zealand and Australian coal measures and their respective prevailing geotechnical problems, is important. The best students will have fully contextualised their results with reference to Australian literature. Furthermore, the very best students will have also drawn parallels (and contrasts) with the management of slope stability and groundwater issues in the New Zealand civil engineering sector.

4.2 Master of Engineering Geology (MEG) at the University of Auckland

Most students who take Earthsci 771 will be enrolled in the Master of Engineering Geology (MEG). The MEG is an NZQA Level 9 programme, delivered (full-time) as either a 180-point (18 month) degree for those entering with a BSc (i.e. NZQA Level 7) or 120-point (12 month) degree for those entering with BSc Honors (or equivalent NZQA Level 8 qualification). Both the 120-point and 180-point degrees can also be taken part-time over longer durations.

The MEG programme officially is a cross-Faculty programme, led from the Faculty of Science's School of Environment, but also includes to a lesser extent at present, the Faculty of Engineering. MEG students tend to be either (1) continuing students who have undertaken a BSc Earth Science / Geology at Auckland or another domestic university, (2) international students wanting to upskill and also migrate to Australasia, and (3) returning, more mature students who have an existing degree, but wish to formalize their development with an engineering geology qualification. The motivation of the latter cohort is often to facilitate Membership, or Chartered Membership (PEngGeol) status with Engineering New Zealand. Also, graduates wishing to become a Chartered Geologist (CGeol) with the Geological Society of London, will generally need a masters-level qualification such as the MEG and a minimum 3-years of CPD.

It's important to note that there is a major emphasis on experiential learning within the MEG degree (i.e. learning-by doing; Kolb, 1984), and this has included field trips at a range of sites across Auckland and the Waikato. Note that Kolb's (1984) 4-stage cyclic experiential learning model describes two ways of grasping knowledge (1) concrete experiences and (2) abstract conceptualization. The other two modes, (3) reflective observation and (4) active experimentation, help learners transform their experience into knowledge. Each of these stages acts as a foundation for the next stage, and experiential learning exercises, such as field trips (and laboratory exercises) are a common pedagogical practice in geoscience curriculums globally (Whitmeyer et al., 2009) and in New Zealand (Fuller et al., 2010).

4.3 Competency Areas and the MEG curriculum

The key aspects of what constitute the most important aspects of engineering geology to include in university curricula have been debated for over 80 years (e.g. Terzaghi, 1961), and this continues to evolve. The core papers of the MEG curriculum do not follow all of the body of knowledge (BOK) for Professional Engineering Geologists (PEngGeol), as reported in this publication in *New Zealand Geomechanics* in 2020 (PEngGeol BOKS, 2020). Indeed, that BOK defines 98 separate core capabilities across 14 project "phases". However, the core papers of the MEG (Figure 6) do meet some of the IAEG Joint Technical Committee 3 (JTC3) proposed competency profile for engineering geology education (Turner and Rengers, 2010), that addresses both technical and professional competencies.

ASCE Category	Competency Area	Bloom's (1956) Taxonomy Level of Achievement					
		1 Knowledge	2 Comprehension	3 Application	4 Analysis	5 Synthesis	6 Evaluation
Foundational	Math	772	772	772			
	Statistics	771,772	771,772	771,772			
	Basic Science	770,771,772	770,771,772	770,771,772	770,771,772		
	Geoscience	770,771,772	770,771,772	770,771,772	770,771,772	770,771,772	770,771,772
Technical - Engineering Science	Statics						
	Mechanics of Materials						
	Fluid Mechanics	772					
	Soil Mechanics	771,772	771,772	771,772			
	Rock Mechanics	771	771	771			
Technical - Engineering Design	Numerical Modelling	771,772					
	Engineering Geology	770,771	770,771	770,771	770,771	770,771	770,771
	Hydrogeology	772	772	772	772	772	772
	Site Investigation	770,771,772	770,771,772	770,771,772	771,772	771,772	771,772
	Foundations	771	770	770			
	Underground Construction	771					
Professional	Communication	794	794	794			
	Public Policy						
	Business / Public Admin.						
	Globalisation						
	Leadership						
	Teamwork						
	Attitudes						
	Lifelong Learning						
	Professional Ethics	794	794	794			

Figure 6: Conceptual competency profile for engineering geologists based on the ASCE competency profile, as proposed by JTC3 (modified from Turner and Rengers, 2010), with Professional ASCE Competency Areas (CA's). Achieved by university = grey, and via work experience = black. MEG "core" paper numbers have been tentatively superimposed on the table (770 Engineering Geological Mapping; 771 Advanced Engineering Geology; 772 Hydrogeology). Professional CA's are covered to varying extents in the 4th "core" management-style paper. The thesis (794) covers some Professional CAs, and other CAs, depending on the topic

According to Villeneuve et al. (2015), the JTC3 was a committee of the International Society for Rock Mechanics (ISRM), the International Association of Engineering Geologists (IAEG) and the International Society for Soil Mechanics and Geotechnical Engineering (ISSMGE). The JTC3 proposed a competency profile for engineering geology education that addresses both technical and professional competencies (Figure 6), according to Bloom's Taxonomy of Learning (Bloom et al., 1956).

Note that Bloom's (1956) Taxonomy of Learning had by 2015 already been revised by Anderson and Krathwohl (2001), to reflect how learning is an active process and not a passive one. Nevertheless, Bloom's (1956) Taxonomy is a hierarchical model of cognitive skills in education, which categorizes learning objectives into six levels, from simpler to

more complex: remembering, understanding, applying, analysing, evaluating, and creating. This framework aids educators in creating comprehensive learning goals and assessments.

The ASCE Competency Areas (CAs) are shown in Figure 6 (modified from Turner and Rengers, 2010). Grey cells are what should be achieved by university studies, while black cells are what should be achieved in the workplace, according to Turner and Rengers (2010). In addition, MEG "core" paper numbers have been tentatively superimposed on the table (770 Engineering Geological Mapping; 771 Advanced Engineering Geology; 772 Hydrogeology), as well as the paper code for the 90-point thesis (794).

There are several points about these ASCE CAs in the context of the MEG degree that are worth noting. First, the attempt to map the MEG core papers to ASCE CAs is undertaken with a note of caution. This is because for some CAs, a core paper may only just be "dipping" into the respective ASCE CA, and the Bloom (1956) Taxonomy Level Achievement (1-6) may have been "achieved" only briefly as part of an assignment, rather than in a sustained manner over a full, 12-week semester. Second, knowledge and comprehension of the Rock Mechanics and Soil Mechanics CAs is implicit in two (Earthsci 771, Earthsci 772) of the core papers (Figure 6), but this actually extends beyond the ASCE-required Taxonomy Level, into "Application" (via practical exercises in this case). Third, at present, the CAs of Underground Construction and Foundations are lacking from the MEG core papers.

Fourth, a broad range of "Professional" CAs are generally lacking within three of the MEG core papers, with the exception of "Professional Ethics" and "Communication". The former is achieved approximately probably as far as Bloom's (1956) Level 3 (Application), as students need to compile undertake and quite a lengthy field form and critical review of what their thesis research will include, and who they will be interacting with (outside organisations, landowners, Māori etc). The "Communication" is achieved to a similar Bloom Taxonomy Level (3 – Application), via the compulsory research seminar all master's students must give, toward the end of their studies. The fourth MEG core paper, chosen from a list of project management-style papers, does potentially achieve some of the Professional ASCE categories, but this would vary, very much on the precise choice of paper.

5 CONCLUDING REMARKS

This article has provided an outline of the Earthsci 771 Advanced Engineering Geology one-day field trip that focused on mine engineering geology. After desktop study, the students visited two opencut coal mines in the Waikato Coal Field of New Zealand's North Island. The make observations and measurements and characterise and describe the rock masses. Post-field trip, the then undertake data modelling including highwall stability modelling using Rocscience software (Dips, Slide2, RS2 etc). The students are encouraged to envisage roof stability issues if the coal measures were to be extracted in an underground operation. Students also have to explore the broader context of mine engineering geology, with specific reference to Australian conditions, dominated by older, Permian coal measures which are significantly stronger than Eocene/Oligocene age Waikato Coal Measures. In summary, graduate engineering geologists (Paul, 2024) learn experientially in the workplace after graduation (e.g. Packer et al., 2024), and may be offered numerous on-the-job continued professional develop (CPD) training opportunities in their workplace. However, this should not preclude university academics from developing useful work-integrated learning (WIL) experiences, albeit within the prevailing staffing, budgeting, timetabling and technical constraints, typical of universities.

6 REFERENCES

Anderson, L. W. and Krathwohl, D. R. (2001). *A taxonomy for learning, teaching, and assessing: A Revision of Bloom's Taxonomy of Educational Objectives*. Longman, New York

Baynes, F. J. and Parry, S. (2024). Guidelines for the development and application of engineering geological models on projects. Version 2.0. *International Association for Engineering Geology and the Environment (IAEG) Commission 25* Publication No. 1, 81 pp.

Bevan, D., Beresford, J., Arthurs, J., Gasston, C., Brook, M. S., Prebble, W. and Brideau, M-A. (2022). Ohuka landslide, New Zealand: a low angle bedding-controlled coastal landslide at Port Waikato, North Island, New Zealand. *New Zealand Journal of Geology and Geophysics*, 65(2), 299-314.

Brook, M. S. (2019). Engineering geophysics and the 2017 New Zealand Ground Investigation Specification guidelines. *Engineering Geology*, 252, 164-167.

Brook, M. S. (2023a). Short-sighted University Geoscience Cuts in New Zealand. *Australian Institute of Geoscientists News*, 151, 19-20.

Brook, M. S. (2023b). Natural hazards, a warming climate and new resource laws – why NZ needs geoscientists more than ever. *The Conversation* 29 August. https://theconversation.com/natural-hazards-a-warming-climate-and-new-resource-laws-why-nz-needs-geoscientists-more-than-ever-212008

Brook, M. S. (2024). By not mining vital minerals, NZ is 'offshoring its own environmental footprint' – is that fair? *The Conversation* 5 June https://theconversation.com/by-not-mining-vital-minerals-nz-is-offshoring-its-own-environmental-footprint-is-that-fair-231166

Brook, M. S, Hebblewhite, B. W. and Mitra, R. (2016). Cleat aperture-size distributions: A case study from the Late Permian Rangal Coal Measures, Bowen Basin, Australia. *International Journal of Coal Geology*, 168(2), 186-192.

Brook M. S., Hebblewhite B. and Mitra, R. (2020). Coal mine roof rating (CMRR), rock mass rating (RMR) and strata control: Carborough Downs mine, Bowen Basin, Australia. *International Journal of Mining Science and Technology*, 30, 225-234.

Brook, M. S., Orense, R. P. and Richards, N. R. (2022). Geo-engineering teaching and learning during COVID-19 lockdown: The University of Auckland Experience. In: Gratchev, I. & Espinosa, H. (eds.). *Advancing engineering education beyond COVID: A guide for educators*, Taylor & Francis, New York, Ch 8, p 133-144.

Brook, M. S., Richards, N. and O'Connor. B. (2023). Development and progress of the Master of Engineering Geology degree at the University of Auckland. *New Zealand Geomechanics*, 106, 82-89.

Cook, M. E., Brook, M. S., Hamling, I. J., Cave, M., Tunnicliffe, J. F. and Holley, R. (2023). Investigating slow-moving shallow soil landslides in a vulnerable city using Sentinel-1 InSAR data. *Landslides*, 20, 427-446.

Fookes, P. G., Baynes, F. J. and Hutchinson, K. H. (2000). Total Geological History: A Model Approach to the Anticipation, Observation and Understanding of Site Conditions. *GeoEngineering 2000, Sydney, Australia*, 91 pp.

Fuller, I. C. and France, D. (2015). Securing field learning using a twentyfirst century Cook's Tour. *Journal of Geography in Higher Education*, 39(1), 158-172.

Fuller, I, C., Brook, M. and Holt, K. (2010). Linking teaching and research in undergraduate physical geography papers: The role of fieldwork. *New Zealand Geographer*, 66(3), 196-202.

Gilley, B. H., Atchison, C. L., Feig, A. D. and Stokes, A. (2015). Impact of inclusive fieldtrips. *Nature Geoscience,* 8(8), 579.

Kolb, D.A. (1984). *Experiential Learning: Experience as the Source of Learning and Development*. Prentice Hall, New Jersey.

McNally, G. H. (1987). Estimation of coal measures rock strength using sonic and neutron logs. *Geoexploration*, 24, 381-395.

NZGIS (2017). *New Zealand Ground Investigation Specification. 4 Volumes.* Available for download at. http://www.nzgs.org/library/nz-ground-investigation-specification/.

NZGS (2005). Field Description of Soil and Rock. New Zealand Geotechnical Society Inc, Wellington.

Packer, M. L, Nash, T., Bennet, C. and Doe, A. (2024). Establishing professional accreditation pathways for Australian engineering geologists in the civil design and construction industry. *Australian Geomechanics*, 59(3), 43-52.

Paul, D. (2024). The state of engineering geology in Australia. *Australian Geomechanics*, 59(3), 33-42.

PEngGeol BOKS (2020). Professional Engineering Geologist – Body of Knowledge and Skills. *New Zealand Geomechanics News*, 99, 32-37.

Terzaghi, K. (1961). Engineering geology on the job and in the classroom. *Boston Society of Civil Engineers*, 48 (2), 97-109.

Turner, A. K. and Rengers, N. (2010). *A Report Proposing the Adaptation of the ASCE Body of Knowledge Competency-based Approach to the Assessment of Education and Training Needs in Geo-Engineering*. Progress report to the: Joint Technical Committee JTC-3: Education and Training.

Villeneuve, M. C., Zimmer, V. L., Eggers, M. J., Bell, D. H., Davies, T. R. and Pettinga, J. R. (2015). Engineering geology education for the 21st century. *Proceedings of the 12th ANZ Conference on Geomechanics*, Wellington 22-25 February

Welsh, K. E., Mauchline, A. L., Park, J. R., Whalley, W. B. and France, D. (2013). Enhancing fieldwork learning with technology: practitioner's perspectives. *Journal of Geography in Higher Education*, 37(3), 399-415.

Whitmeyer, S. J. and Mogk, D. W. (2009). Geoscience field education: A recent resurgence. *Eos Transactions of the American Geophysical Union,* 90, 385–386.

https://doi.org/10.56295/1ACEG03

ENGINEERING GEOLOGY MODEL AS A TOOL FOR THE EFFECTIVE MANAGEMENT OF OPEN PIT SLOPES

F.M. Weir & M.J. Fowler
PSM

ABSTRACT

The engineering geology at every mine site has developed through complex interactions of geological processes over vast periods of time. The inherent variability between these processes and sites poses challenges in developing suitable pit slope designs due to both limited data and understanding, leading to uncertainty and associated risks.

Risk management for slope stability involves the identification, assessment, and mitigation of potential risks. A robust engineering geological model serves as an invaluable tool for effective risk management by providing insights into anticipated ground conditions. This paper provides a review of the engineering geology at three open pit mine sites from Australia and Southeast Asia. While the geological environment at each site is substantially different the underlying geological understanding enables effective slope design management and risk mitigation strategies. These strategies include the application of a geological model at a site in a highly active tectonic setting, showcasing how it facilitates identification of areas with elevated risk during operations.

The paper also presents how the engineering geology model at each site has evolved over time, particularly following slope instability events. The findings and guidelines presented herein provide valuable insights for professionals involved in slope design, enabling them to make informed decisions and enhance safety.

1 INTRODUCTION

For the design of an excavation, whether it is an open pit slope or a tunnel, an engineering model is required to represent ground conditions at a site. A critical element for the model is an appropriate understanding of the geology at the site. As highlighted by Eggers (2023), there is a trend in industry to focus on rock mass classification, with the geological component of the model often neglected, which can negatively impact the engineering design.

The management of open pit slopes in mining operations is essential for ensuring both the safety and efficiency of the excavation processes. The complexity and variability of geological conditions present significant challenges. These challenges emphasize the need for suitable engineering geological models.

An engineering geology model is a conceptual representation of the subsurface conditions at a specific site, used to support design, construction and inform risk management for a project. The primary components of the model include geology (lithology and alteration), structure, soil and rock mass, geomorphology and hydrogeology. The components of an engineering geology model are shown conceptually in Figure 1. The influence of each component on open pit slope design will vary with geological environment and site-specific ground conditions.

The complexity and variability in natural materials means that the formulation of the engineering geology model often relies on the experience of the practitioner. When developing slope designs, uncertainties and risk are always present. These uncertainties often manifest in the field of slope design, resulting in gaps and ambiguities that must be navigated. A fundamental understanding of the geological environment in terms of rock types and tectonic history can assist practitioners in predicting key failure mechanisms and likely slope performance.

At the Earth's surface, there are three primary rock types: Sedimentary, Igneous, and Metamorphic. The method of formation and inherent character for each of these rock types have significant engineering and slope design implications. For each primary group, a case study is presented that illustrates some of the challenges in slope design for that rock type.

This paper explores the application of engineering geological models as tools for the effective management of open pit slopes. It focuses on three distinct mine sites located in Australia and Southeast Asia, each with unique geological settings and challenges. Through these case studies, the paper demonstrates how a robust understanding of the local geology can inform slope design and risk management practices.

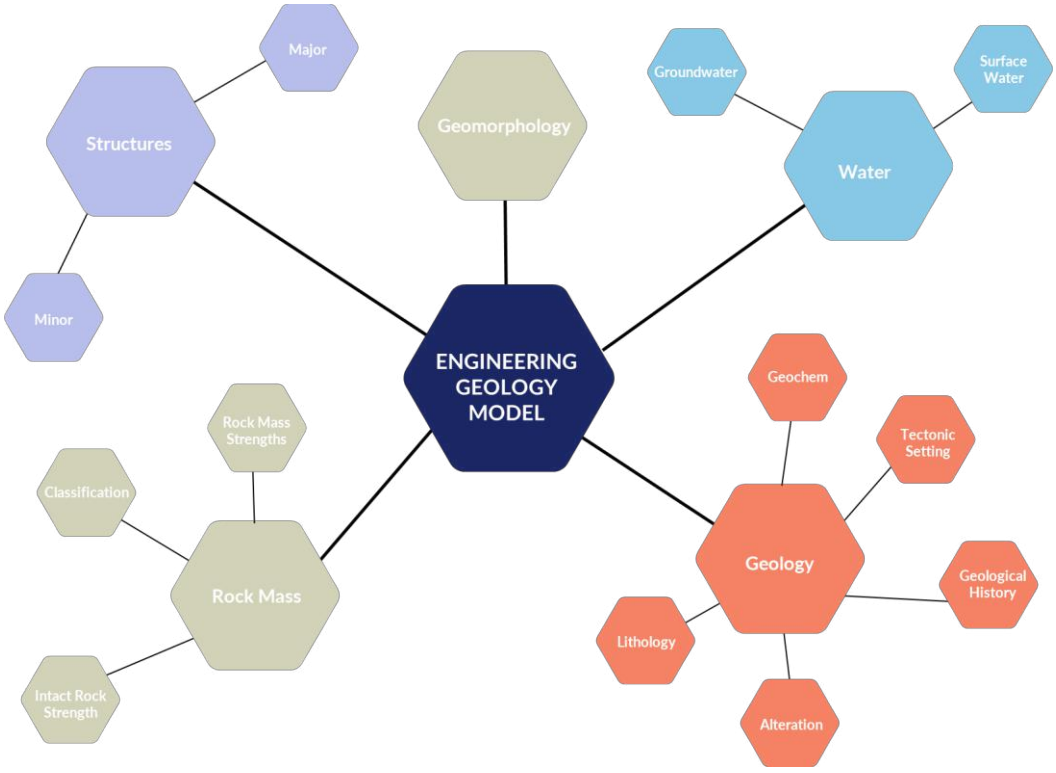


Figure 1: Conceptual understanding of the Engineering Model and its key components for open pit slope design

2 CASE STUDY SITE 1 – VOLCANIC ENVIRONMENT

2.1 Introduction

Volcanic geological environments are highly complex due to variable chemistry and rock characteristics, variable eruption styles and emplacement methods and the interaction of these with existing geomorphology. This means that volcanic igneous rocks are highly variable over short distances in depositional type, chemistry, strength and geotechnical behaviour (Weir, 2024). Adverse or irregular geological structures are also likely to be present. Examples include ring faults or dykes, faulting, autoclastic brecciation and curvi-linear jointing near intrusive plugs.

The geological complexity of these volcanic environments means that there is potentially large uncertainty in the engineering geology model. Case Study Site 1, presented here involved slope design at the base of the amphitheatre of a young strata volcano that has undergone sector collapse, multiple phases of alteration (propylitic, epithermal) and ongoing phreatomagmatic activity resulting in diatremes. This creates a geotechnically complex environment due to the co-incidence of complicated lithologies, alteration, structural, geothermal conditions, existing landslides and high seismicity. The amphitheatre forms a significant topographic feature that surrounds the active mining area and associated infrastructure with steep natural slopes, Figure 2. The existing open pit at the site is about 2.2 km long and 1.6 km wide with a depth of about 300 m (relative to sea level).

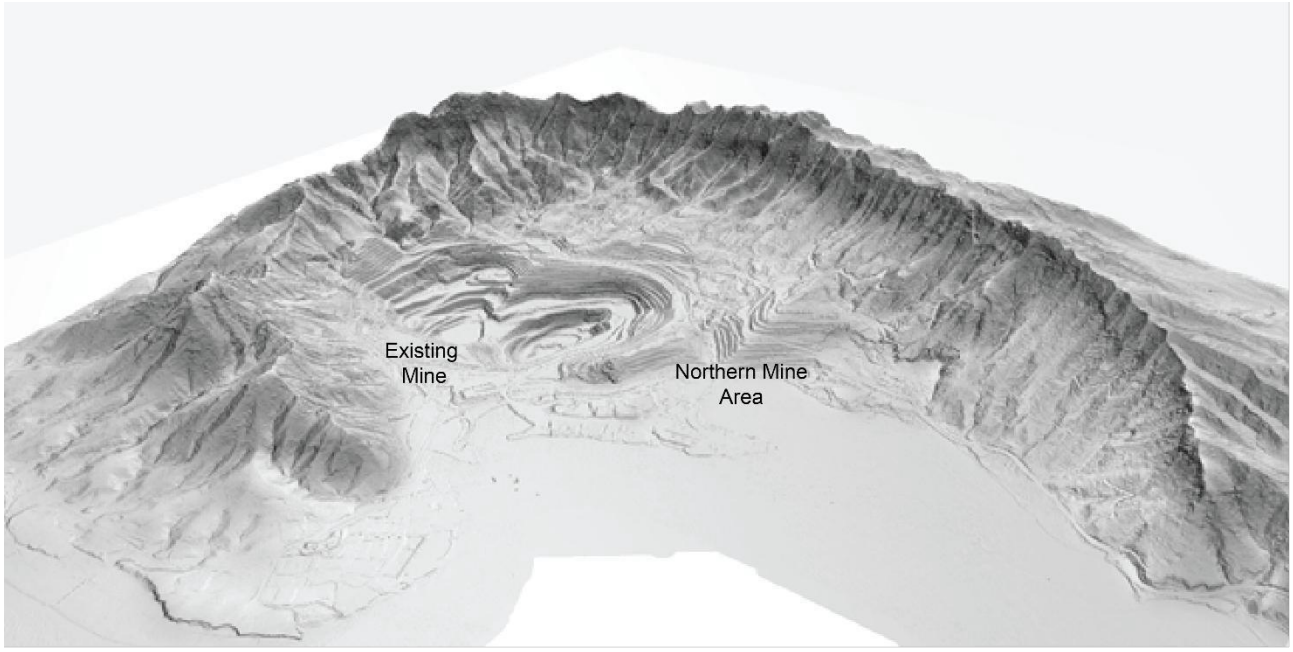


Figure 2: Oblique view towards the southwest of existing pit and volcanic amphitheatre, 2009 LIDAR surface (after Weir *et al.*, 2020)

2.2 Conceptual Model

The conceptual engineering geology model for the site was developed using modern analogues from similar volcanic environments and a combination of historical and current exposures at the mine. The modern analogues reviewed included Mt St Helens, a modern example of large-scale sector collapse of a strata volcano. The sector collapse (a large landslide), triggered by an earthquake, resulted in exposure of the magma chamber and an explosive eruption. Following this collapse, new volcanic activity commenced within the caldera. This modern example highlighted the dynamic, evolving, and overprinting nature of young volcanoes.

The sector collapse exposes the central core of the volcano to the atmosphere resulting in phreatomagmatic activity, the mixing of surface waters with magma and super-heated steam and water under pressure. The combination of reduced vertical stress due to the collapse unloading and phreatomagmatic activity is also associated with diatreme formation. Diatremes are generated by pulses of magma mixing with external water, rapid transfer of heat from magma to water, and explosion of the mixture. The diatreme contacts are typically sheared due to forceful emplacement and then compaction settlement.

Diatremes that form explosively may leave a crater. The crater can become deeper due to subsidence of the diatreme deposits. This subsidence cone or residual crater soon forms a Crater Lake, which is then often filled with epiclastic and/or fluvio-lacustrine sediments.

2.4 Diatremes at the Site

The geology at the site comprises a sequence of agglomerates, tuffs and basalts intruded by monzonite. The lithologies have typically been overprinted by various hydrothermal events, resulting in significant alteration from their primary rock types. The complicated geological history of multiple deformation episodes and pervasive alteration makes it difficult to distinguish among the twelve breccia types at the case study site and inhibits the development of a lithological model.

The soil and rock mass component of the engineering geology model for the site was developed from a framework of historical studies and recent site investigations. It represents the continuing evolution in the understanding of ground conditions. Early engineering geology models for the site were based around the existing southern mining area, where the geotechnical units were found to largely relate to the ore type/alteration model. However, as the model and mining progressed away from the volcano central core, the engineering model has evolved to incorporate the effects of late-stage phreatomagmatic activity and diatreme formation.

The first detailed characterisation of a large young diatreme at the case study site was by Blackwell (2010) in the existing mine area (L Diatreme, Figure 3). The diatreme is a polymictic, accretionary lapilli-bearing, matrix-supported breccia. It is largely unaltered, indicating a late-stage formation. Since 2010, with additional drilling data, model refinement has

focused on the L Diatreme northern extent and character. Other similar "young" diatremes were subsequently identified in core. These breccia's are characterised by:

- Fine grained, grey matrix
- Low strength rock mass
- The absence of significant alteration overprinting
- Shallow, curved structures with low defect shear strengths
- Sheared, slickensided, clay infill planes along contacts.

The Northern Diatreme is the largest of the discordant breccia bodies modelled at the case study site, Figure 3. This diatreme will form a large portion of the final pit north wall. It is characterised as a polymictic matrix supported breccia with a dark grey muddy matrix and commonly white coloured andesitic clasts. The Northern Diatreme is overlain by weakly lithified, horizontally bedded sediments, interpreted as a Crater Lake deposit. The spatial relationship between the various rock mass units is highlighted in Figure 4.

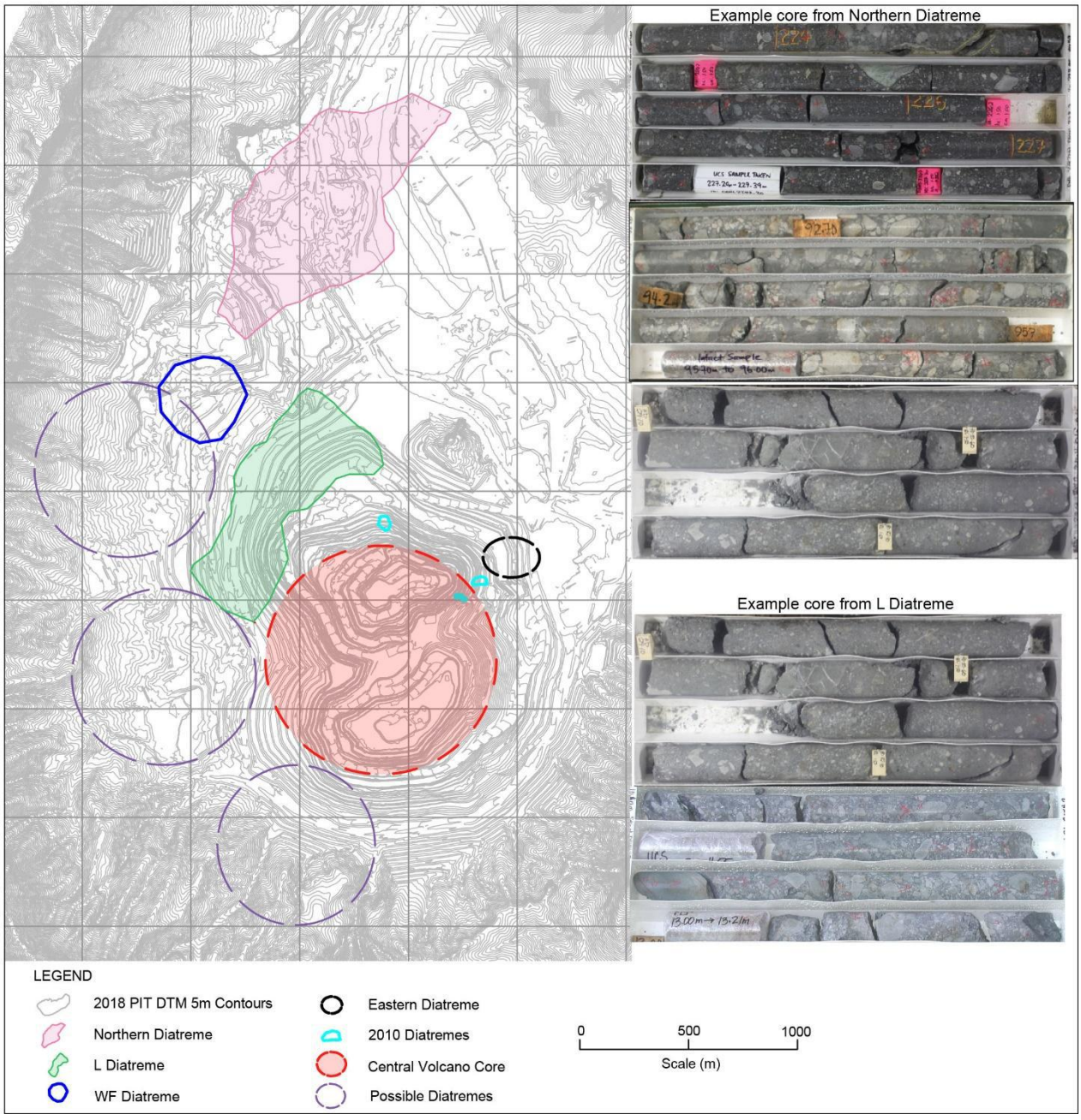


Figure 3: Identified and interpreted diatremes

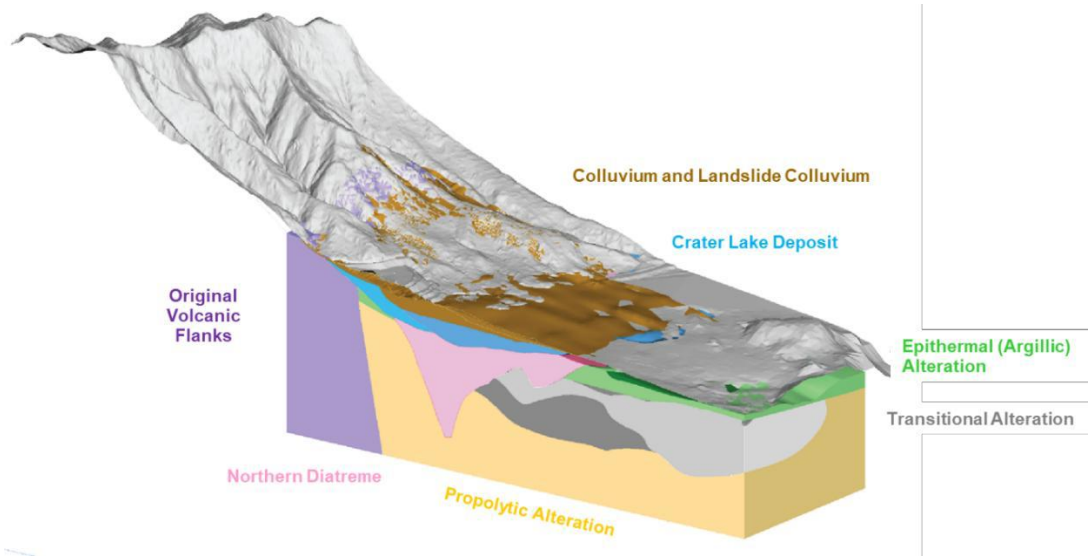


Figure 4: An oblique view of a slice through the 3D rock mass model, highlighting the relationship between the Northern Diatreme and surrounding alteration type rock mass units (after Weir *et al.*, 2020)

A number of other possible young diatremes have also been inferred from the topography and exposures, Figure 3. These typically lie along the western side of the caldera. The location of the newly identified Eastern diatreme shows the potential for other young diatremes to also be present to the east of the central core. Importantly, young diatremes do not occur in the central core. The shape of the L and Northern diatremes (with a splayed sill feature extending to the north) and the location of other young diatremes implies that the underlying basement structures have played a role in the localisation of diatreme intrusions.

2.5 Importance for Pit Slope Design

A review of site-wide historical slope performance showed that large-scale pit slope instability to date has been related to diatremes (or highly altered argillics) with pore pressures also an important influence. The failure mechanisms relating to diatremes are variable but commonly include structure.

Adverse structure conditions occurred both within and at the contact young diatremes, this is consistent with the conceptual model. Exposures of the adverse structures show a shallow to moderate dip, curved, clay-filled and variably sheared with low strength. The exact location of any such structures is difficult to predict given the shape and variability in dip. The structures within the diatremes are interpreted as commonly emplacement related.

The keys for interpretation and prediction are to use the characteristic signatures of the younger diatremes to identify them. This is to understand the structural patterns associated with diatremes and where such structures typically develop then use borehole imaging data to build and refine the structure model for that location. The identification of the young diatremes from core photos is an important tool for predicting areas of increased risk of pit slope instability at this site.

This summary has focused on the role of diatremes in slope stability at the site. Weir et al., (2020) provides a more detailed review of the evolution of the engineering geology model at this particular site.

3 CASE STUDY SITE 2 – SEDIMENTARY ENVIRONMENT

3.1 Introduction

Case Study Site 2 is a stratiform sediment-hosted Zn-Pb deposit. The site is characterized by a thick sequence of siltstone beds and occasional breccia beds that have been variably folded and faulted. The intact strength is high (ISRM), and pit design is controlled by geological structures. Being a sedimentary deposit, bedding is a dominant structure type and is considered continuous on the pit scale, with the stratigraphic units able to be traced across the entire deposit. Consequently, bedding orientation is a critical control in structural domain definition, slope design and performance of the pit slopes.

Mining to date has predominantly progressed with a footwall parallel bedding and a steep high wall, Figure 5. The joint patterns at the site show a dominant set orthogonal to bedding, which is to be expected in a sedimentary environment. Mining at the site is proposed to progress as a series of cutbacks of the highwall. Substantial work has gone into identifying

and defining the location of bedding folds where bedding in future cutbacks will dip out of the highwall. These folds are evident in the cross-section in Figure 5. The variation in joint orientations with these folds are also indicated.

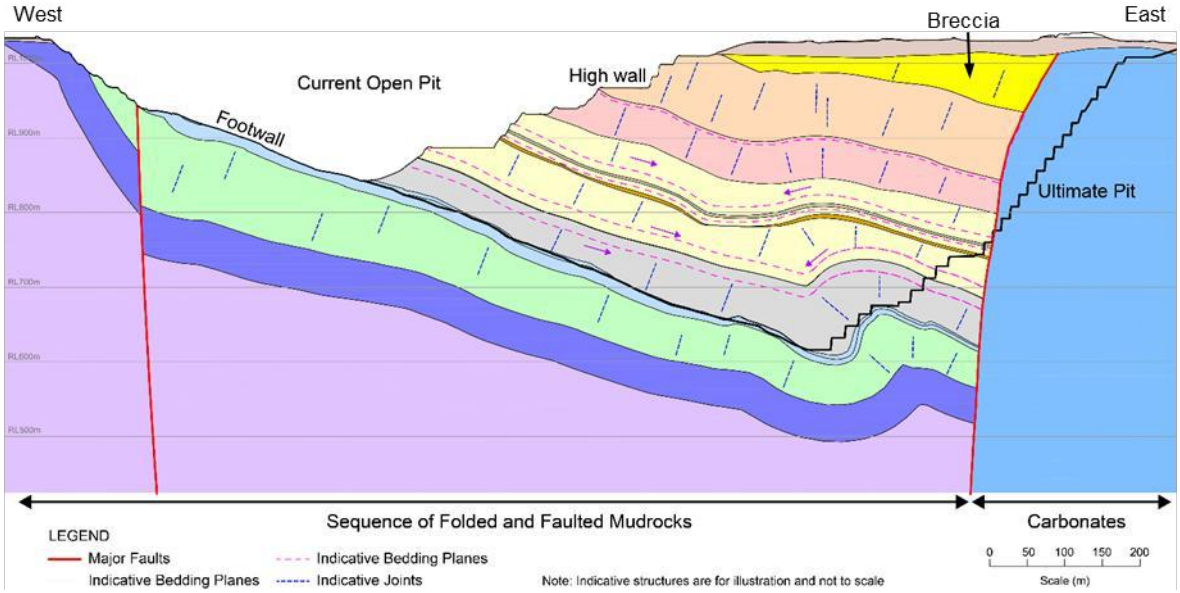


Figure 5: An East-West cross-section through a stratiform deposit showing primary stratigraphic units, bedding trends and indicative joint patterns

3.2 Instability Event

In June 2021 a multi-bench scale instability occurred in the southeast corner of the open pit. The instability developed over the course of one week, from initial detection of displacement to collapse. Geotechnical monitoring systems assisted with the identification, delineation, and safe management of the instability. The monitoring systems and management of the instability were presented by Heaven et al., 2022.

The instability occurred within a breccia unit at the top of the stratigraphic sequence, which had limited exposure in the pit wall prior to the event, Figure 5. The instability mechanism was interpreted to be step-path sliding on two closely spaced joint sets. Understanding of the ground conditions and instability mechanism was a critical element in the successful management and remediation of the slope.

3.3 Engineering Geology Model and Failure Mechanism

At the time of the instability a major study updating the engineering geology model and slope design recommendations was underway. Prior to this study data regarding the breccia unit was limited. The unit is a massive, polymictic breccia with sub-rounded clasts up to 2 to 3 m in length, Figure 6. Available data on intact strength for the breccia included field strength estimates, point load tests and unconfined compressive strength (UCS) tests. All three sources indicate for fresh rock there is a relatively high intact rock strength with values ranging between 80 and 200 MPa.

Prior to the instability the available structural data for the breccia unit consisted of limited oriented core from two boreholes. A high-resolution survey scan of the wall was completed one day prior to the instability. Photogrammetry mapping of the scan was conducted to better understand the structure orientations and conditions. The photogrammetry mapping shows two clear, joint sets that are adversely oriented for a northeast facing slope, Figure 6c. The fault plane that controlled the southern end of the instability is of a similar orientation to the dominant joint set, dipping towards the northwest (shown as red squares in Figure 6c).

Additional geotechnical drilling completed after the instability identified that the upper portion of the breccia shows an increased frequency of jointing. In addition, proximal to the fault there is a further increase in frequency of jointing and increased depth of iron staining on defects. Both at depth and away from the fault the joints are more widely spaced.

Seepage observed along structures in the pit face prior to the instability indicated a high ground water table and pore pressures acting on the slope. This was consistent with the conceptual hydrogeological model, where this area of the slope is understood to be mostly saturated with flows originating from overlying alluvial sediments associated with a nearby river. In upper units like the breccia there is groundwater recharge during the wet with subsequent slow recession during dry season.

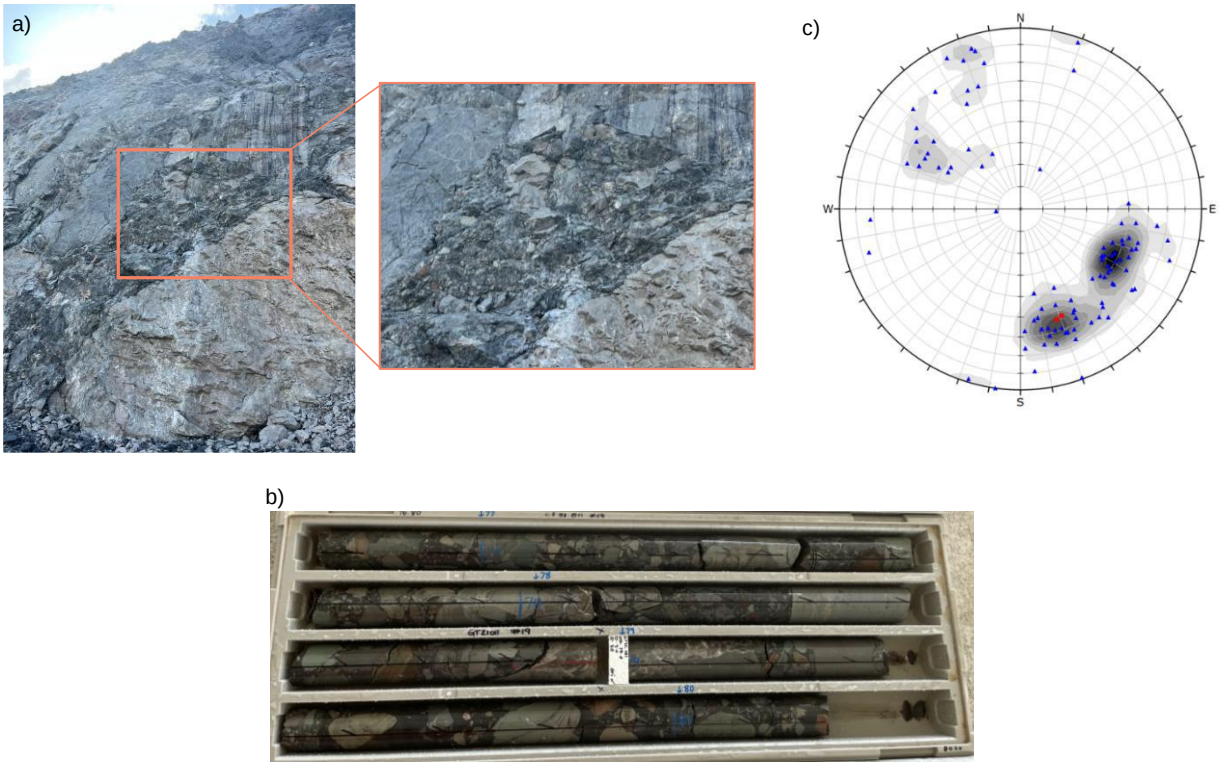


Figure 6: a) Example of the fresh polymictic breccia in recent bench face exposure, b) equivalent appearance in drill core and c) stereograph of defect orientations from remote mapping. Joints are shown in blue and faults in red. Stereograph is lower hemisphere, equal area

3.4 Failure Mechanism and Slope Management

The instability was interpreted to be structurally controlled, with the main sliding release on the southern side along a fault. The central and northern portions of the instability were likely step-path sliding along multiple closely spaced joint planes that dip out of the slope. The observations in subsequent geotechnical borehole core and bench face mapping suggest that the close spacing of the jointing was a result of proximity to a regional scale fault. The trigger for the instability was progressive mining towards the south along the slope toe which undercut some of the more persistent structures dipping out of the slope. Adverse ground water conditions also likely contributed.

A kinematic and statistical assessment of the defects was undertaken to assist reassessment of the pit slope design. This resulted in a reduction in both the bench and inter-ramp slope angles. With the adopted slope geometry there remained some risk of batter scale instability. To fully mitigate the risk of sliding due to the adversely oriented structures, the slope would have to be reoriented or flattened further. In addition, shallow batters can be difficult to execute with consideration to the limitations of drill and blast and excavation equipment. Consequently, the risk of batter scale instability was accepted and appropriately managed with the existing systems on site during mining.

The cutback was successfully completed in terms of achieving a stable inter-ramp slope. Irregular bench face geometries were experienced, largely due to the variable nature of the breccia with large, high strength clasts. Extensive seepage was again encountered during mining, which was addressed by installation of shallow horizontal drain holes.

In future cutback stages, with an increase in joint spacing away from the fault and use of the observational method the slope design was able to be steepened. This bench face steepening allowed a more practical mining approach and face development through variation to the blasting methods.

4 CASE STUDY SITE 3 – METAMORPHIC ENVIRONMENT

4.1 Introduction

Case Study Site 3 is a pegmatite lithium deposit, where the pegmatite has intruded into a regionally metamorphosed phyllite country rock, Figure 7. Pegmatite bodies enriched in spodumene are typically gently dipping, so the subvertical igneous body at this site is unusual (Phelps-Barber *et al.*, 2022; Weir *et al.*, 2023). Given the narrow, lenticular shape of the pegmatite the open pit slopes are predominantly within the surrounding country rock. A key characteristic for slope

design in these rocks is the foliated texture due to directional stresses related to regional metamorphism. The authors became involved at this site after mining had commenced and geotechnical issues were encountered in terms of both slope performance and operations. The following sections review the engineering geology model for the site and the implications for slope design and operations.

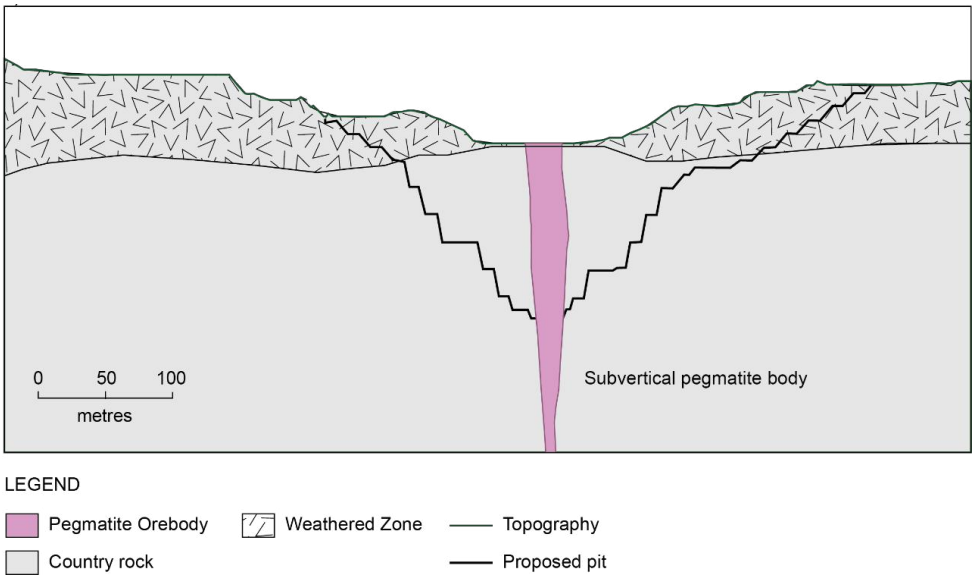


Figure 7: Cross-section through Case Study Site 3 with sub-vertical pegmatite body

4.2 Engineering Geology Model

Rock mass conditions are controlled by both the geology and surface processes at the site. The rock mass units comprise:

1. Weathered Zone - extremely weathered in-situ rock and residual soils. This zone is typically soil to low intact rock strength and is about 50 to 60 m thick. This zone is about 20 m thicker than was anticipated in pre-mining studies.
2. Fresh high strength rock - this consists of two units:
    a. Pegmatite and
    b. Metamorphosed country rock (phyllite).

The fresh rock for both the pegmatite and the phyllite has a high intact strength (>90 MPa). The presence of foliation in the phyllite country rock however results in a strong strength anisotropy. Consequently, it was important when undertaking testing that the foliation angle in relation to loading direction was carefully recorded.

The structural geology is critical to the engineering geology model and slope design for pegmatite deposits (Weir *et al.*, 2023). Two stereographs from Case Study Site 3 are presented in Figure 8. The stereographs show structures measured from oriented core of five boreholes through both pegmatite and the country rock. The pegmatite at the site is subvertical and striking north-northeast. The pegmatite stereograph shows shallowly dipping joints oriented perpendicular and parallel to the pegmatite body, which are interpreted as cooling and contact joints, respectively. Cooling related joints are oriented perpendicular and parallel to the dip of the pegmatite due to heat flow and a decrease in volume during cooling, Figure 8. Some of the jointing is of similar orientation to the meta-sedimentary country rock, Figure 8c and so may also be tectonic joints.

Within the phyllite foliation is subvertical and striking north-northeast, parallel to the pegmatite body, Figure 8c. It is likely that the magmatic fluid forming the pegmatite exploited the foliation as a plane of weakness during the intrusion event. The foliation forms closely spaced planes of weakness, particularly in the upper weathered zone, Figure 9a. Given the steep dip and character of the foliation, where the pit slopes are parallel to the foliation they are prone to flexural toppling style failures.

Standing water level observations from bores in 2021 indicate a depth to groundwater is about 0.5 to 1.6 mBGL (metres below ground level) during the wet season and between 4 to 12.5 mBGL during the dry season. The groundwater data and model are limited, particularly with regards to understanding of actual pore pressures currently acting in the slope. In addition, there are unlined mine water dams and sediment ponds directly to the south of the pit. It is considered highly likely that these structures are leaking and recharging the groundwater system, impacting slope stability.

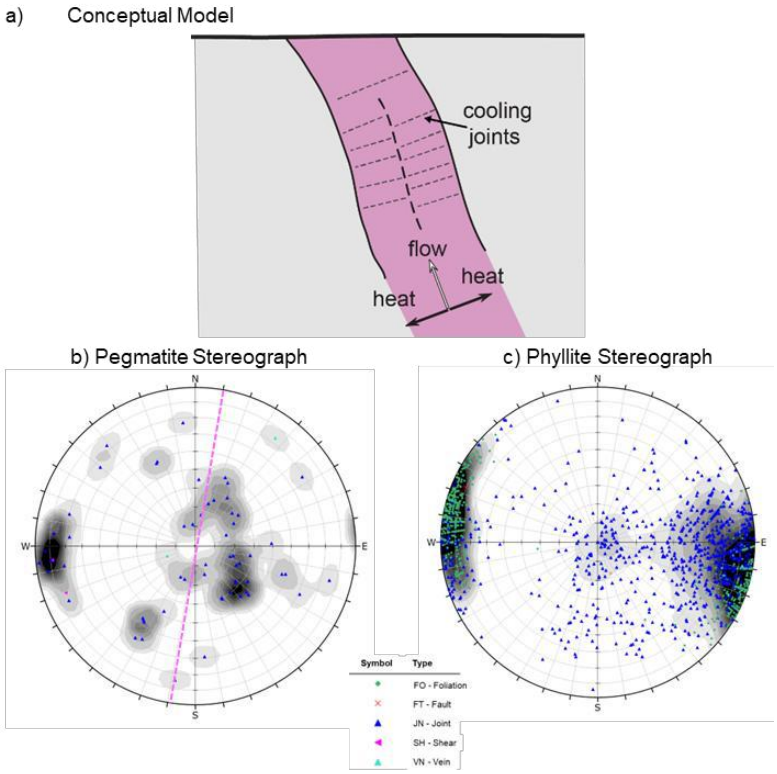


Figure 8: Pegmatite jointing patterns a) conceptual model of thermal (cooling) joints, Example structure conditions at Case Study Site 3 with stereographs from oriented core for b) Pegmatite and c) Phyllite Country Rock. Pink dashed line indicates strike of the pegmatite body. Stereographs are lower hemisphere, equal area

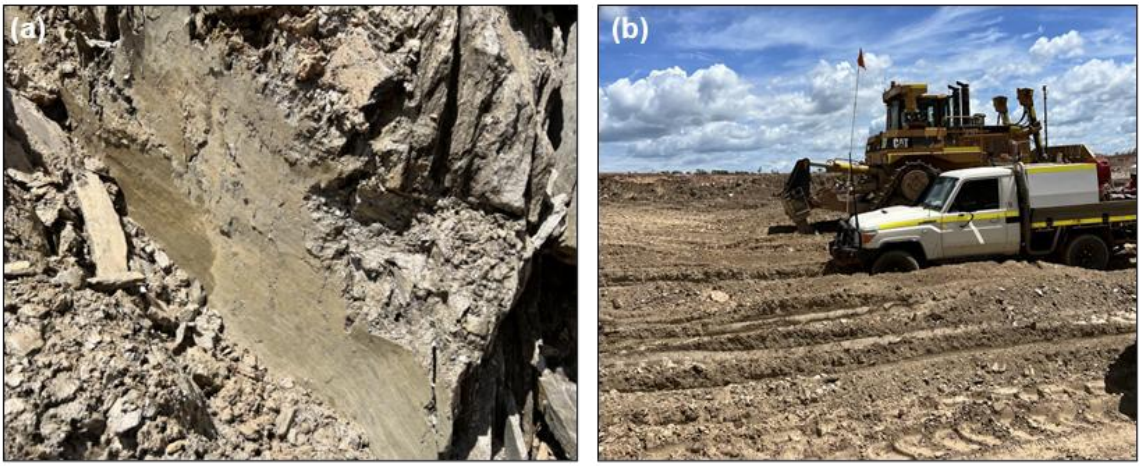


Figure 9: a) Example of a low strength foliation parting in weathered zone and (b) poor trafficability in dry conditions

4.3 Slope Design and Operational Implications

The critical failure mechanisms for consideration in slope design for each pit wall are summarised in Table 1. These were identified based on the engineering geology model and slope performance to date. To manage adverse slope performance due to toppling a small cutback and flattening of both bench face and the inter-ramp angle was undertaken for the upper weathered zone on the West wall.

Toppling failures are highly sensitive to pore pressures. To address this horizontal drain holes were also installed and lined with slotted pvc pipe to maintain the drain. The drain holes were effective at producing water and fitted with a reticulation system to capture the water and transport it to a lined sump on the end wall, rather than allowing the water to infiltrate back into the system.

Table 1: Failure Mechanisms

Pit Wall	Critical Failure Mechanism	Engineering Geology Controls
East and West Long walls	Toppling along foliation, as the pit is progressively excavated	Pervasive, closely spaced foliation in phyllite Minor faults and shears parallel to foliation Low intact strength in upper weathered zone Pore pressures
East wall	Planar sliding or wedges	Joints and shears parallel ot foliation Pore pressures
Northern and Southern End walls	One-sided wedges	Geometry and spacing of joints and foliation Pore pressures

There were other operational difficulties associated with excavation of the phyllite. The weathered phyllite is rich in micaceous minerals, which form micaceous silts and clays. These soils commonly exhibit a low in-situ density, are highly erodible and hydrophobic making dust control difficult. Durability of the slopes in the upper weathered zone is also low with slopes showing cracking and deformation with mining and exposure.

Trafficability is also a significant operational issue at the site in both dry and wet season, Figure 9b. This has resulted in significant cost associated with importing of material to the site for lining of the haul roads. A robust engineering geology model and understanding serves as a valuable tool for effective risk management by providing insights into anticipated ground conditions. These operational difficulties and associated costs could have been anticipated during early planning stages, given these are common issues associated with phyllite and other schistose rocks.

5 CONCLUSIONS

An engineering geology model is a conceptual representation of the subsurface conditions at a specific site, with the primary components of the model including geology (lithology and alteration), structure, soil and rock mass, and hydrogeology. This paper discusses the importance of engineering geology models for designing and managing open pit slopes, emphasizing risk management and the evolution of geological understanding across different mining sites. In particular, the paper emphasizes how a robust engineering geological model is an important tool for predicting likely slope failure mechanisms and aids in identifying and mitigating risks associated with slope stability in open pit mining.

The paper reviewed the engineering geology model at three open pit mine sites in Australia and Southeast Asia, highlighting how geological understanding varies yet enables effective risk mitigation strategies. Each geological environment presented posed unique challenges. In addition, the critical element of the engineering geology model (e.g. rock mass, structure or water) that influenced slope design and performance varied at each site.

The first case study focused on a volcanic site with complex geological conditions, underscoring the challenges in slope design due to high variability and potential instability from diatremes. The second case study examines a sediment-hosted deposit, where slope stability is influenced by geological structures such as bedding and faults. The third case study involved a pegmatite lithium deposit in metamorphosed rock, where foliation and groundwater conditions critically affect slope stability and operations.

Each case study illustrates how engineering geology models evolve over time, particularly after slope instability events, enhancing the understanding of ground conditions for design and management. The study highlights the need for a comprehensive geological understanding to anticipate operational difficulties and manage risks effectively in mining operations.

6 REFERENCES

Eggers, M.J. (2023). Engineering geological models in open pit slope engineering. *Proc. SSIM 2023: Third International Slope Stability in Mining Conference*, Australian Centre for Geomechanics, Perth, pp. 35-54, https://doi.org/10.36487/ACG_repo/2335_0.03.

Heaven, C., Weir, F.M., Fowler, M. and Farmer, M. (2022). Management and rehabilitation of a highwall slope instability. *Proc. Slope Stability 2022 Conference*, Tucson, Arizona USA, 17-21 October 2022.

Phelps-Barber, Z., Trench, A., and Groves, D. (2022). Recent pegmatite-hosted spodumene discoveries in Western Australia: insights for lithium exploration in Australia and globally. *Applied Earth Science*, 131 (2), 100-113.

Weir, F.M., Fowler, M.J., Sullivan, T.D., Kobler, M., and Bu, J. (2020). Evolution of a geotechnical model for slope design in an active volcanic environment. *Proc. of the 2020 International Symposium on Slope Stability in Open Pit Mining and Civil Engineering*, Australian Centre for Geomechanics, Perth, pp. 455-472.

Weir, F.M., Hemraj, D., Fowler, M.J., Watton, J.W., and Strang, D., (2023). Geotechnical slope design in hard rock lithium deposits. *Proc. SSIM 2023: Third International Slope Stability in Mining Conference*, Australian Centre for Geomechanics, Perth, pp. 449-458, https://doi.org/10.36487/ACG_repo/2335_28

https://doi.org/10.56295/1ACEG04

UNDERSTANDING CRITICAL STABILITY FACTORS: INTEGRATING OLD AND NEW DATA TO IMPROVE FOUNDATION STABILITY ASSESSMENTS

Ben Speakman[1], Matthew Ferguson[2]

[1]Engineering Geologist, Entura, Hobart, Tasmania
[2]Senior Engineering Geologist, Entura, Hobart, Tasmania

EXTENDED ABSTRACT

1 INTRODUCTION

1.1 USING TELEVIEWERS AND 3D MODELLING FOR FOUNDATION ASSESSMENTS

Televiewer and 3D geospatial modelling tools bring significant benefits to large-scale engineering and geological projects, particularly during the safety review and maintenance phases of complex infrastructure like dams and water-retaining structures. These tools augment traditional surface mapping and limited borehole data, delivering a clearer, more complete picture of the foundation rock mass. The result is more reliable design, safety, and risk management decisions.

1.2 FILLING GAPS IN BOREHOLE DATA

For historic boreholes where core samples might be missing or data is sparse, televiewers can help provide new, detailed insights. Acoustic and optical televiewers allow us to capture the orientation, size, and behaviour of foundation defects, turning what would be costly, invasive investigations into more efficient, low-risk processes. This is especially useful in well-maintained boreholes, like those used for dam drains, where televiewer data lets us understand the continuity, shape, and orientation of faults and smaller defects.

1.3 UNDERSTANDING FOUNDATION DEFECTS AND STABILITY

Understanding these factors is critical for assessing foundation behaviour, spotting potential failure modes, and evaluating foundation strength and stability. This data-driven approach not only improves structural assessments but also guides risk management and economic decisions for infrastructure upgrades. Reliable investigations using these tools can help ensure that safety and upgrade assessments are based on thorough and realistic analysis.

2 USING TELEVIEWERS IN A DAM SAFETY REVIEW

2.1 REGIONAL FAULTING

A routine safety review of a large concrete dam provided an opportunity to use televiewer surveys to improve understanding of foundation conditions.

The investigation focused on the Jurassic dolerite foundation, where faulting and discontinuities play a key role in dam stability. Three regional neotectonic features are significant to the area's broader structural setting and existing seismic risk. The closest of these is located more than 50 km from the dam, and appears to show repeated movement since at least the Cambrian, with three surface-rupturing events recorded in the late Quaternary, each displacing the ground by 2.4 to 3.1 m. No regional faults have been identified nearby aside from these neotectonic features, in part because the extensional fault system related to the Derwent Graben is not readily investigated or understood.

At the site scale, faulting trends northwest with variable orthogonal relationships, though no detailed local studies of these faults have been completed. This faulting is part of a broader regional structural trough forming the River Derwent – the Upper Derwent Graben – possibly related to the Lake Echo Scarp fault system. Studies of the Derwent Valley suggest that extensional faulting has influenced the geomorphology of the area since the Jurassic into the Cenozoic. While these regional features provide important geological context, the focus of this investigation was on the foundation faults and discontinuities most relevant to dam stability.

2.2 FOUNDATION DEFECTS FOUND DURING CONSTRUCTION

During construction, foundation defects were a major focus, with detailed surface mapping providing high-quality records of the exposed rock mass. The mapping suggests that some defects persist through the foundation at excavation scale. The most significant geological fault features identified during excavation and mapping include a metre-scale sheared zone with crushed seams, along with two smaller but similar features to the north. These faults, located beneath the left side of the dam, share moderate dips to the north. These features were extensively excavated and concrete-backfilled prior

to construction of the dam. Construction borehole logs offer some additional data, but they were not detailed enough to assess how foundation faults could influence dam stability.

2.3 USING FOUNDATION DRAINS FOR TELEVIEWER SURVEYS

The foundation drains within the dam gallery provided an opportunity to address these gaps using televiewer surveys. These drains offered a low-cost, non-destructive way to expand the dataset and improve understanding of fault continuity and persistence. To build on existing data and address uncertainties in the dolerite foundation, we conducted televiewer surveys on foundation drainage holes. These surveys covered 347 metres of foundation drains and mapped out the position and orientation of key discontinuities, like crushed seams and sheared zones. In total, we identified 868 individual discontinuities, with 121 standing out as significant, including crushed seams and sheared zones as well as weakened areas with measurable widths. We then analysed this data in stages, using orientation comparisons and detailed spatial analysis and interpretation.

3 DATA ANALYSIS AND MODEL BUILDING

3.1 COMPARING TELEVIEWER DATA WITH FOUNDATION MAPPING

To validate the televiewer data, we compared the orientations of key defects with those from prior detailed foundation mapping. This helped us identify any systematic differences between the two methods. The most detailed geological dataset for the dam site comes from foundation mapping, which provided extensive records of rock discontinuities. These features were a major focus during past investigations, with mapping, documentation, and lab testing carried out to understand their role in the stability of the concrete dam. The primary types of discontinuities at the site include joints, altered and weathered seams, sheared zones, and crushed seams. Less common or absent features include partings, sheared surfaces, and infilled seams, likely due to the nature of the dolerite and the concentrated data collection efforts around the dam footprint and nearby areas.

The dataset shows a strong prevalence of defects striking northwest, with dips ranging from 45° towards the northeast through vertical to 45° towards the southwest. Some of these defects contain decomposed zones, which required additional excavation and foundation treatment. While many defects were mapped during construction, most persist at excavation scale, are non-planar, and include joints as well as altered and moderately to highly weathered seams. This understanding comes from lab testing, site inspections, and classification systems used during design and construction. The mapping classification system assigned measured feature widths to each defect segment and categorized them as weathered, carbonate-zeolite, soft-rock defect filling, or chlorite.

Both the existing mapping datasets and the new televiewer dataset showed two main groups of non-vertical defects, with some small differences in one of the sets. We noted two other differences: high-dip angle defects appeared less often in the televiewer data and were harder to constrain, while some low-dip angle defects, visible in the televiewer surveys, were missing from the foundation mapping. These findings show why it is important to map both horizontal and inclined surfaces to accurately capture high-dip angle features, and vertical boring and mapping vertical surfaces being essential for identifying low-dip angle features.

3.2 USING 3D TOOLS FOR BETTER FOUNDATION ASSESSMENT

To go beyond basic comparisons and historic datasets, we used 3D geospatial modelling to better analyse and interpret defects (Figure 1). This allowed us to look at the continuity and persistence of these features through the foundation and to group and model related features. Using data from foundation mapping, borehole logs, and televiewer imaging, we examined details such as infills, thickness, defects around crushed seams, and the intensity of sheared zones. We also considered positions, associations, orientations, and potential shifts in defect direction. By identifying patterns across these elements, we could determine if defects extended between boreholes, which is important for understanding foundation behaviour and stability risks.

4 FINDINGS

4.1 PATTERNS IN FAULTS AND DEFECTS

Discontinuities and faults showed up throughout the foundation in clear orientation patterns, with only about 1% of these features reliably matching across borehole surveys, core logs, and surface mapping. This is likely due to the limits of the sample data and the complexity of the foundation itself. Despite the small percentage, the analysis helped us understand the persistence and larger-scale shape of many surveyed defects. The most consistent features were the thickest defects, which, after comparing various datasets, seemed likely to extend from the surface through to the foundation drains. The largest fault was linked to three persistent features showing an intermediate dip toward the northeast. Only small numbers of other faults could be confidently connected across the datasets, and in most cases, their characteristics changed between

data points. This suggests that shear strength varies depending on scale, making it difficult to estimate strength in a way that is both realistic and relevant to the load scenario.

4.2 ASSESSING FOUNDATION STRENGTH AND STABILITY

The fault models and visualisations of discontinuities we have developed are critical to understanding foundation behaviour, potential failure modes, and stability. The quantity of data reveals the real complexity of discontinuities within the rock mass, which is now better understood. This detailed picture of how these features persist, change shape, and vary over distance means we can now discount simple failure mechanisms that were once considered possible.

While the foundation mapping showed some changes in how these features appear, our findings that significant defects don't continue between boreholes give us more confidence in the foundation's high strength. Foundation mapping alone leaves unanswered questions, but these insights show a clearer picture and build confidence in the foundation.

5 IMPLICATIONS

5.1 USING DEFECT INTERPRETATIONS FOR SAFETY AND RISK DECISIONS

Getting a clear picture of the continuity, shape, and orientation of faults and smaller discontinuities is essential for understanding how the foundation will behave. This information helps us identify potential failure modes and assess the overall strength and stability of the foundation. Beyond structural assessment, this knowledge can also guide risk management and economic decisions for infrastructure upgrades. Reliable investigations that measure and interpret these factors accurately are a must. A data-driven approach ensures risk assessments are thorough with safety and upgrade decisions backed by solid analysis.

5.2 TELEVIEWER SURVEYS AS PRACTICAL AND COST-EFFECTIVE INVESTIGATION TOOLS

This case study highlights the value of televiewer surveys on existing drain holes as a low-cost, effective, and non-destructive method for subsurface data collection. The rock defect data obtained was particularly valuable for identifying flat-lying defects and improving understanding of fault continuity and potential failure modes within the foundation. Combined with other geological datasets, including surface mapping and borehole logs, this information provided a more complete basis for analysis. Developing a 3D geospatial model was key to integrating these datasets, allowing for a detailed exploration of their relationships and the identification of critical stability features.

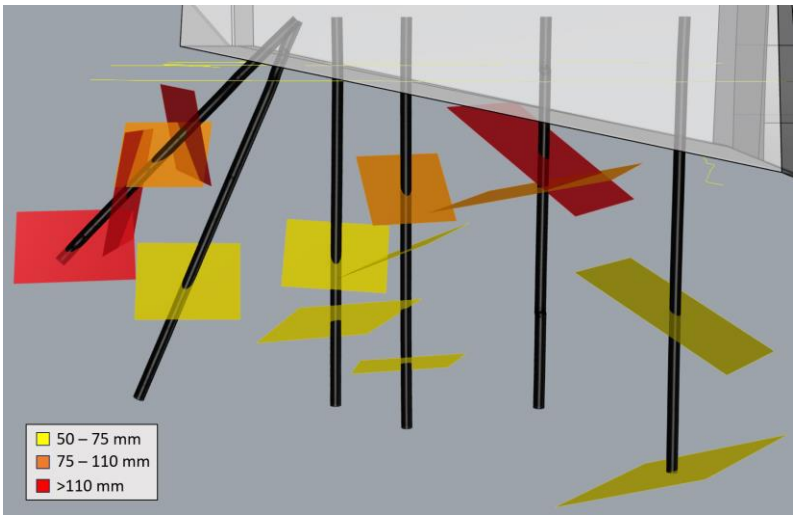


Figure 1: Extract from 3D geospatial model showing high confidence fault extents, and the lack of continuity between adjacent sample locations.

This paper is written to be accessible to a diverse audience.

https://doi.org/10.56295/1ACEG05

THE SPECIFICATION OF UNPROCESSED ROCKFILL FOR HIGHWAY APPLICATIONS - A CASE STUDY FROM THE COFFS HARBOUR BYPASS

A. M. TAIT
Engineering Geologist, Ferrovial Construction Australia

ABSTRACT

Efficient utilisation of site won materials is the key component for successful delivery of any earthworks scope. Materials and construction methods need to be fit-for-purpose, providing long term performance confidence for use in earthworks design. The Coffs Harbour Bypass project presents a unique materials management challenge with over 1M m^3 of material in cuttings requiring blasting within high strength siliceous metamorphic geology (Argillite). To meet the earthworks Specification for embankment construction this quantity would need to be crushed and processed, placing significant strain on delivery program and cost.

A project-based method specification was developed to suit the site geology and unprocessed blast condition, providing an efficient mass haul while ensuring performance requirements can be met over the design life. Laboratory testing, compaction trials and routine engineering geology assessment of the source cuts show that an unprocessed rock fill material can be produced that exhibits a well graded particle size distribution with high strength and durability properties. Analysis of these attributes show that the contract performance criteria including stiffness and post construction settlement can be met.

1 INTRODUCTION

This paper presents a case study on the use of unprocessed rockfill to construct road embankments. The paper aims to describe the material utilisation challenges faced by the hard rock geology encountered as part of the cut to fill earthworks and its implications to design, specification and construction. The case study shows the collaborative approach to use the site won rockfill and the site-specific modifications to project specification achieved resulting from research into previous rockfill use, site trials, developing testing methods, analysis and method specification development.

2 PROJECT DESCRIPTION

The Coffs Harbour Bypass is a dual carriageway highway with a total length of 14 km. The project consists of a 12 km 'greenfield' bypass of Coffs Harbour between Englands Road intersection in the south to Korora Hill in the north, and two-kilometre upgrade of the existing Pacific Motorway from Korora Hill to Sapphire Beach. The project comprises significant excavation within hard rock geology including three tunnels at Roberts Hill (158 m), Shephards Lane (321 m) and Gatleys Road (410 m).as well as cuttings up to 40m deep

The project is delivered within a Collaborative Design and Construct contract by the Coffs Harbour Bypass Team comprising:

- Transport for NSW (Principal)
- Ferrovial Gamuda Joint Venture (Contractor)
- Arcadis Sener Joint Venture (Designer)
- Aurecon (Independent Certifier)

3 EARTHWORKS SCOPE, SPECIFICATION AND DESIGN

Piccolo et al 2019, outlined the importance of a unified approach to earthworks design, construction and certification. This approach included aims to produce landform suitable for the proposed development, ensuring that construction is controlled to achieve the performance criteria, enable earthworks certification and ensuring this is achieved at the least cost. The rockfill method specification for the project was developed by engaging all delivery partners from initial concept to construction, working within the Collaborative Design and Construct contract.

3.1 SCOPE OF WORKS AND TECHNICAL CRITERIA

The geotechnical design for the highway embankment is defined in the contract Scope of Works and Technical Criteria (SWTC). This is developed by the Principal and details the performance criteria for the earthworks to provide support to the pavement in design life. These criteria include outlining the pavement design lifespan (40 years), the limits of post construction settlement (including differential settlement) to design for and stability criteria for embankment and cut design.

3.2 EARTHWORKS SPECIFICATION R44

Earthworks Specification R44 is provided by the Principal and is typically generic for all earthworks projects constructed as a TfNSW asset. The intent of earthworks specification R44 is to set out the requirements for earthworks for roadworks, in order to create a stable formation suitable for a pavement to be constructed upon using the materials from within the site. Site specific departure of the Specification can be developed to provide efficient earthworks to meet program requirements and site conditions.

R44 defines earth fill as material that derive their stability from compaction of the fine material around the coarser particles. This is specified as rock weight percentage being no less than 60% passing the 37.5mm sieve, with a maximum particle size two thirds of the layer thickness. Cohesive earth fills can be placed, compacted and tested using conventional means where the high fines content creates a soil matrix that supports the particles providing the fill with strength, stiffness and low permeability.

The Specification defines rockfill as hard sound durable rock with limited fine particles which when placed derives its stability from the mechanical interlock of the coarser particles rather than finer particles around the coarse particles.

Rockfill material shall meet the grading and strength requirements outlined in Table 1. The specification outlines the need for screening and / or processing to achieve this grading

Table 1- Earthworks Specification R44 Rock Fill Material Properties

Property	Requirement
Maximum particle dimension	300 mm
Percentage passing:	
100 mm AS sieve	0 – 20%
19.0 mm AS sieve	0 – 10%
1.18 mm AS sieve	0 – 5%
Percentage of +100 mm fraction with $I_{s(50)}$ < Annexure R44/A2.2	10% (max)
Wet/Dry Strength Variation	Max 35%

3.3 EARTHWORKS DESIGN

The earthworks are designed to meet the performance criteria set by SWTC and must be constructed in accordance with the Earthworks specification. The challenge of good earthworks design is to meet the contractual performance requirements, using the Earthworks Specification, while also providing a safe, efficient and workable solution that can be constructed to project timeframes and cost. In addition to this, the earthworks design and construction needs to be certified at completion. The role of certification lies with the Independent Certifier (IC), not affiliated with either the Principal, Designer or Contractor. To undertake the Earthworks Design, the Designer develops a Geotechnical Investigation Plan that informs an Geotechnical Interpretation Report, compiling all the geotechnical information to provide a geotechnical model and parameters to use in design.

4 PROJECT GEOLOGY

The Coffs Harbour Bypass is in the southern region of the New England Fold-Belt. The alignment sits to the southeast of the Coffs Harbour Orocline within meta-sedimentary rocks of the Coffs Harbour Sequence.

The project route is underlain by metamorphosed sedimentary rocks deposited as turbidite sequences within a regional scale accretionary wedge structural domain (Korsch 1981). The sedimentary rocks have undergone two phases metamorphism including initial low-grade metamorphism ranging from prehnite-pumpellyite to lower greenschist facies. Secondary contact metamorphism associated with granitic plutonism has occurred affecting fine sediments (Graham and Korsch 1985). The structural orogeny and metamorphic phases have created three main lithostratigraphic units than make up the Coffs Harbour sequence (Gillian, L., Brownlow, J., Cameron, R., Henley, H. 1992):

- Brooklana beds (Ccor) – thinly bedded siliceous mudstone and siltstone with rare lithofeldspathic wacke, locally chert, magnetite bearing chert and metabasalt.
- Coramba beds (Ccoc) – lithofeldspathic wacke, minor siltstone, siliceous siltstone, mudstone meta basalt, chert and jasper.
- Moombil beds – black massive, rare lithostratigraphic wacke and granule conglomerate. This unit is not present along the alignment.

The project alignment, as shown in Figure 1, is underlain by the Brooklana beds to the south and Coramba bends to the north with the boundary between the two located toward the centre of the project. Although the lithology of the metamorphic rock ranges from siliceous mudstone to greywacke sandstone, the term Argillite has been used to describe the lithology under the whole of the alignment and it is used locally to describe both Brooklana and Coramba units.

The metamorphic processes have formed a hard-durable siliceous rock. The rock fabric has been tightly folded, forming steeply dipping cleavage and defect structure that is typically very closely to moderately spaced (60 mm to 600 mm). The defect structure limits the maximum size of the excavated rock from this geology to 400 mm to 600 mm with some rare larger occurrences.

The rock strength of the slightly weathered to fresh Argillite ranges from medium to extremely high strength, with a mean value unconfined compressive strength (UCS) of 50 MPa and seismic velocity greater than 2100 m/s. The wide range of UCS is likely attributable to the test loading relative to anisotropy and cleavage of the argillite and the varying textures within the geological unit (ie meta siltstone to greywacke)

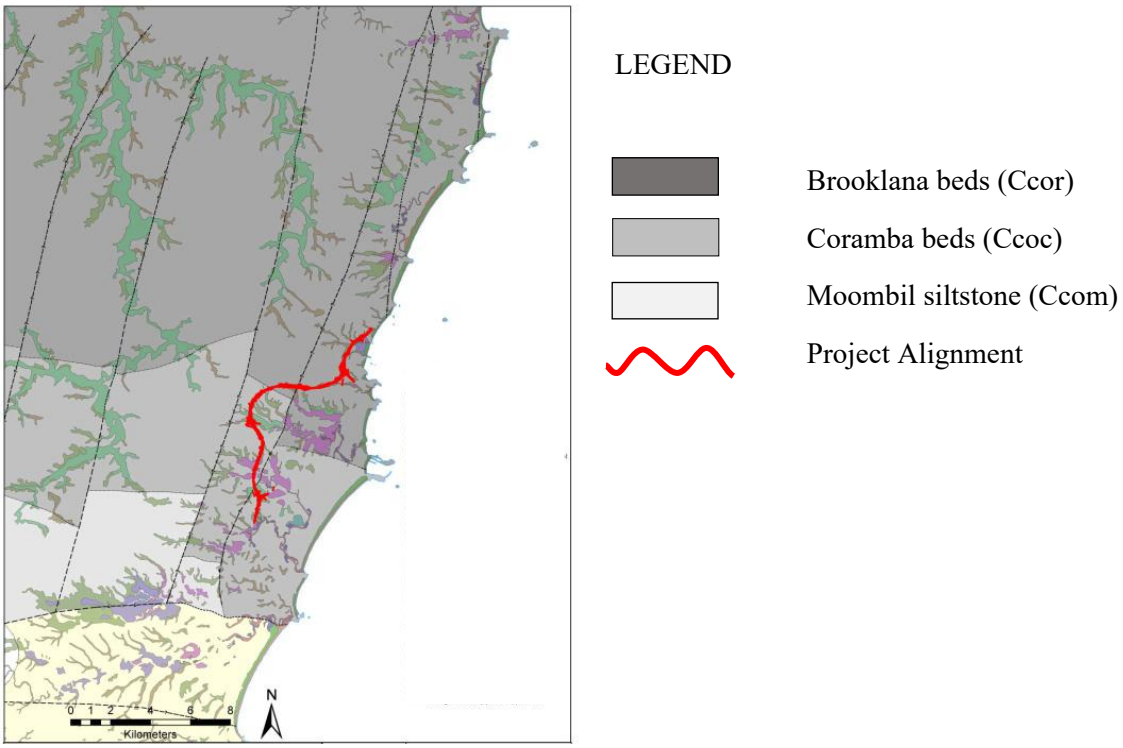


Figure 1 – Project alignment (in red) relative to regional geology (Gillian, L., Brownlow, J., Cameron, R., Henley, 1992)

5 EFFICIENT UTILISATION OF SITE MATERIALS

The design alignment through the project requires up to 3 M m^3 of cut to fill earthworks to achieve the design grade within the steeply undulating topography. This requires cuttings up to 40 m deep and fills up to 25 m high to be constructed. Geotechnical modelling of the alignment identified up to 40% of the cut mass haul occurring within marginal ripping to blasting strength material. Crushing and processing this material to the Specification rock fill or earth fill was considered cost and program prohibitive based on over 1 M m^3 required to be incorporated into embankment fill.

5.1 SUITABLITIY OF PROJECT GEOLOGY FOR ROCKFILL

During design development, local quarries within the Brooklana and Coramba formations were assessed and mapped for material as R44 rockfill. Observation and testing quarry blast piles, as presented in Photo 1, showed a durable, high strength rock. Particle Size Distribution (PSD) testing of the blast piles showed a maximum particle size in the order of 400 mm to 500 mm, up to 70% passing the 100 mm sieve and 60% retained on the 37.5mm sieve. The fine end of the grading has less than 5% passing the 1.18mm sieve with no observed 'dirty' fines (ie clay and fine sand).

The PSD positioned the unprocessed material within a non-conforming envelope between the Earth fill and Rock fill grading envelopes as shown in Figure 2. Due to the relatively small maximum particle size and the fractured nature of the rock, screening and crushing material to meet rockfill would produce significant wastage on the fine end (ie 70% of the rock would be too fine to produce rock fill). Conversely, a significant crushing and processing campaign would be required to comply to the Earth fill requirement of 60% passing the 37.5 mm sieve.



Photograph 1 - Blast pile of SW to FR argillite from Woolgoolga quarry within Coramba formation (Ccoc)

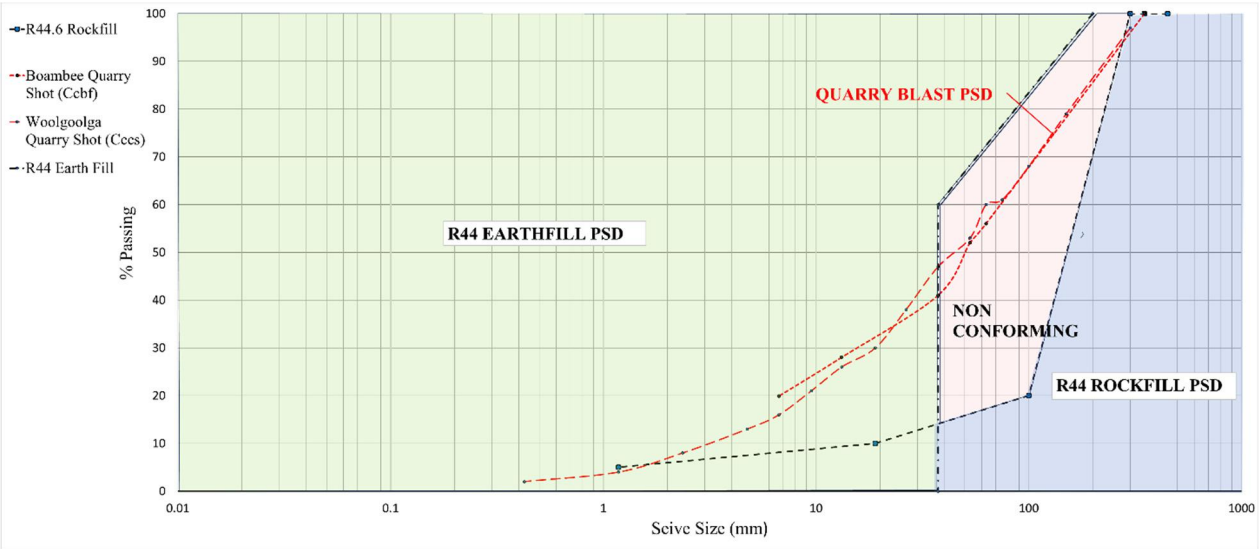


Figure 2 - Graph showing the PSD limits of R44 Earth fill and Rock fill compared to the quarry blast piles

5.2 PREVIOUS USE OF UNPROCESSED ROCKFILL

Unprocessed rock fill that has been adapted for site conditions for use in embankment construction on several sections of the Pacific Highway Upgrade. These include Alliance delivery projects at Bulahdelah, Coopernook and Kempsey. These projects included a large range of parent geology and maximum particle size.

A local example of unprocessed rockfill filling was identified as part of for Karangi Dam, located approximately 15km due west of the site (Dept of Public Works and Services 1996). The site based local quarry for the works won rock from the Coramba Formation (Ccoc). Construction reports show up to 67 000 m^3 unprocessed rock fill placed with an apparent grading less than 350 mm from observation of site photos, Photo 2 for example. Inspection of the dam site confirm this, with an observed maximum dimension of 300 mm, no apparent breakdown or significant weathering of the rock material and a good mechanical interlock of particles forming a 1.5H to 1V batter grade.

Based on the previous experience with rockfill on Pacific Highway projects and previous use of the local argillite rockfill in dam embankment construction, it was concluded that the slightly weathered to fresh argillite material could be used for embankment fill application adapting a site-specific specification for grading, strength and placement.



Photograph 2 Unprocessed rockfill dam embankment under construction at Karangi circa 1995

6 UNPROCESSED ROCKFILL TRIALS

A total of five rockfill trials were conducted on the project to develop the method specification of unprocessed rockfill for the project. The trial(s) provided research and development to support a project method specification that would meet the SWTC criteria. The initial trial (Trial #1), as shown in Photo 3, was conducted off the alignment, with subsequent trials incorporated into the project works. Two cut source locations were nominated to provide material for the trials;

- Cut 4 within the Brooklana formation (Ccor)
- Cut 16 within the Coramba formation (Ccoc)

Progressive mapping of each cut during excavation was compared to the project geotechnical model and core logs to confirm the presence of material suitable for rockfill. Where this was identified, the relevant blast bench was nominated as source material and incorporated into the trial.

The placement trials were conducted using site plant including bulldozers (Caterpillar D8) and flat drum rollers (Cat CS78B 18 tonnes) equipped with survey telemetry and intelligent compaction sensors. Each trial layer was modelled by survey and loaded into the onboard telemetry as a ‘design’ to control layer thickness.

A survey grid area of 5 m by 5 m was marked out at each trial site, with layer thickness measured after two roller passes. The survey was conducted by placing a control survey plate over the irregular surface to obtain a uniform surface for pick up for each successive survey.

Table 2 – Summary of Unprocessed Rockfill Trials

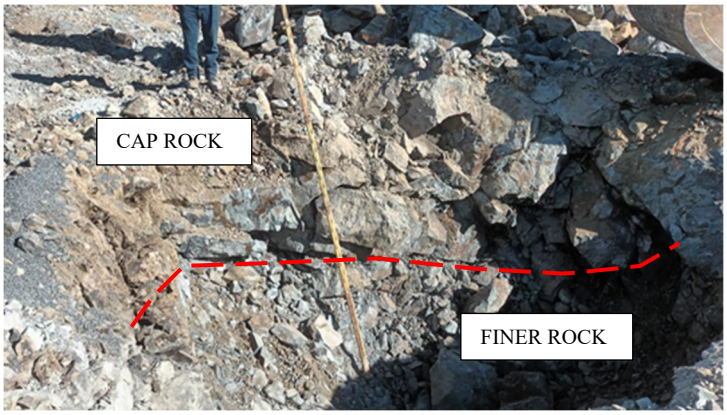
Trial Number	Geological Formation	Cut Source	Fill Area	Aims	Results	Specification Development
1	Ccoc	Cut 16	TRIAL PAD	Develop pass count vs settlement correlation Assess the effect of water conditioning Assess the particle size distribution of the blasted rockfill Assess mechanical interlock and compacted condition of the fill Assess stiffness, internal settlement and durability Layer thickness performance between 500 mm to 600 mm (Compacted)	Material shows suitable attributes for earthworks construction that are likely to meet SWTC requirements 4 to 6 passes are suitable for compaction, no significant settlement of the layer between pass 4 to 6 Reduce compacted layer thickness to 500 mm in Trial 2 Cut source management needs attention, oversize reaching the fill site and having to be dealt with during placement Particle Size Distribution testing methodology needs to be reviewed, taking entire sample back to the lab is not feasible from a technical and OHS practicality perspective Full layer moisture conditioning required	PSD does not meet Specification requirements However, trial shows material can be placed under a method specification likely to meet SWTC requirements
2	Ccoc	Cut 16	Fill 17	Reduce layer thickness to 500 mm (compacted) Site specific PSD testing methodology Cut source Management Procedure Assess the developing trend of cut source PSD Assess stiffness of the rockfill in the dry and inundated condition	PSD showing a well graded trend Results of inundation testing show settlement estimates due to stiffness contrast can be accommodated within SWTC criterial Developing QA process to manage cut source production and fill placement	Trial confirms SWTC requirements can be met Need to develop QA process
3	Ccor	Cut 4	Fill 3C	Compare rockfill performance of Trials 1 and 2 within separate geology	Material from moderately weathered to slightly weathered zone of cut Significant breakdown noted in the fill placement Variability in the cut source between medium to high strength rock, difficult to manage at the source.	**Trial failed – abandoned**. Material from moderately weathered horizon is too variable in strength and placement breakdown
4	Cccs	Cut 16	Fill 17	Refine QA process Additional inundation stiffness testing conducted	Results of ongoing PSD testing used to develop a revised specification PSD envelope Develop Quality Assurance ITP and associated documentation for cut source and fill placement	QA process developed, Method Specification drafted
5	Ccor	Cut 4	Fill 4	Repeat trial for separate geology – slightly weathered to fresh argillite Repeat trial steps from #2 and #4 to compare, can both geological sources be incorporated into one method specification?	Less variability in cut source material PSD shows good comparison to the Cccs source Placement trials show that 8 passes limit layer settlement to less than 5mm Stiffness testing in line with Cccs trials	Slightly weathered to fresh Ccor material source can be used as rockfill to meet SWTC criterial. Project Wide Method Specification Finalised incorporating both geological units.



Photograph 3 – Trial 1 site showing marked up survey grid

6.1 CUT SOURCE

The blast bench in Cut 16 for the Trial 1 source comprised a drill spacing of 2.4 m x 2.4 m drilled to an average depth of 6m. The total volume of the blast for the trial was approximately 1300 m^3. Test pits excavated within the blasted material, as shown in Photo 4 for example, revealed an upper 1 m to 1.5 m horizon of larger cap rock with maximum dimension in the order of 600 mm to 800 mm. Below this level, the particle size fined to an approximate maximum dimension of 500 mm, with an apparent distribution of particle size between 50 mm to 400 mm.



Photograph 4 – Test pit into blast material

Managing the cut source was identified as a significant aspect to the method specification. Based on the initial blasts for the trials and observation of the quality of rockfill arriving to the trial fill site, it became apparent that:

- Sorting of oversize cap rock at the source is integral to the quality of rockfill. This was reinforced on site by instructing excavator operators on the size of material to load out and oversize to put aside. It is also important that there be operator continuity at each cut source; and
- Clearly identifying the extent of the acceptable material. The engineering geologist delineates the blast bench and informs the excavator operator and leading hands on the acceptable appearance of slightly weathered to fresh material to load out.

Documentation and daily inspection of the load out face was conducted by the engineering geologist and loaded into the QA lot. This comprises a daily mapping record of the excavation face identifying suitable material and delineating material unsuitable for unprocessed rockfill material.

Photo 5 shows a typical stockpile of unprocessed rockfill ready for use.

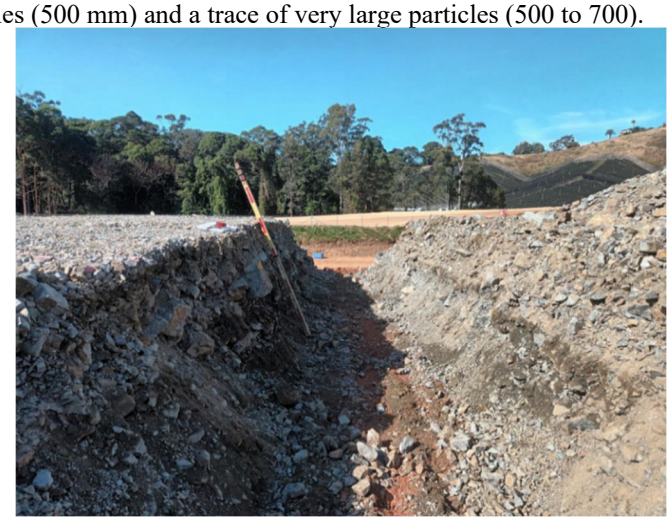


Photograph 5 - Material to be used for unprocessed rockfill trial

6.2 LAYER THICKNESS AND COMPACTION

Survey of the layer settlement between each pass showed a total of 40 mm to 60 mm of settlement after eight vibratory passes of the 18 tone flat drum roller. Up to 75% of this settlement occurred after the first 2 passes with less than 5mm of settlement occurring between Pass 6 and 8. Survey showed that the modelled loose layer thickness provided a 90% confidence on compacted layer thickness after the 8 passes of the flat drum roller. Test pits were excavated into the trial after placement to assess the condition of the rock fill. The test pits, as shown in Photo 6 for trial 1 pad, revealed:

- Good correlation with surveyed layer thickness.
- An upward fining of particle size attributed to the compactive effort and attrition of the bulldozer and roller during placement.
- Trench sides showing good definition with no slumping of the rockfill. Moisture conditioned trench side were measured at 65° to 70°.
- A homogenous mixture of rockfill with no zones of segregation, voiding or accumulation of fine material.
- Rockfill material that comprised an angular coarse gravel to cobble sized material (ie 40 mm to 200 mm) with some larger particles (500 mm) and a trace of very large particles (500 to 700).



Photograph 6 - Trial 1 test pit showing good trench side definition

6.3 PARTICLE SIZE DISTRIBUTION

Particle size distribution (PSD) testing in the large rock fill required modification to TfNSW T201 method to provide tester safety and efficiency due to the large sub sample mass required to representatively test the material.

The site-based methodology comprised:

- Sampling the face of the rock fill source with the loadout excavator equipped with a load cell. A minimum 3 tonne sub-sample is weighed and recorded by the tester and loaded into a dump truck.

- The truck dumps the sample at a purpose-built testing site comprising concrete bays with a steel base adjacent to the cut source. The load cell equipped excavator 'sieves' the sample through a custom built 100 mm slotted bucket
- The retained rock mass is measured by the excavator and material passing is representatively sub sampled to continue the PSD test in the soils laboratory.

Figure 3 presents the results of 69 PSD tests conducted as part of the trial(s), with Photo 7 showing the good mechanical interlock rock fill. Results of particle size distribution conducted from both the cut source and fill placement confirmed non-conformance to the grading requirements in R44 Specification.

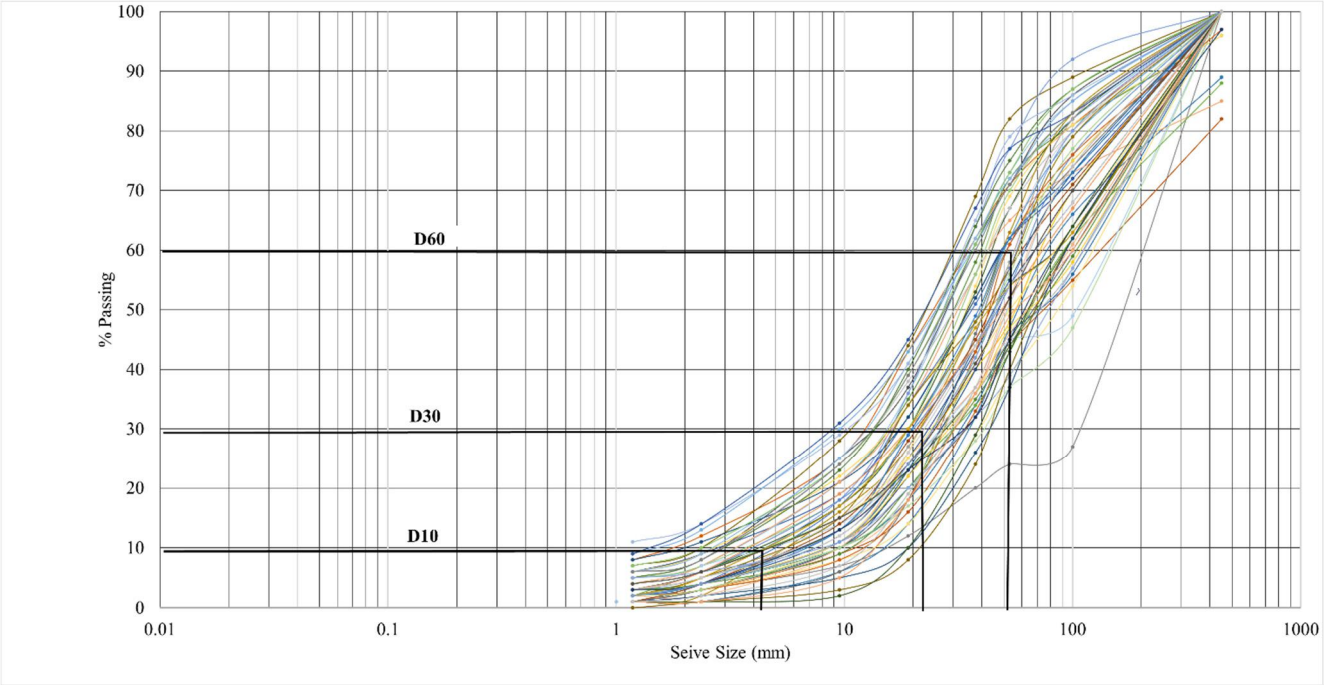


Figure 3 - Particle size distribution testing conducted during the trials



Photograph 7 – Particle size distribution and mechanical interlock exposed in Trial 1 test pit.

7 ANALYSIS

7.1 PARTICLE SIZE DISTRIBUTION COEFFICIENT

Risk associated with coarse fills is that a poorly graded PSD is developed within the compacted material. This may lead to internal erosion within the compacted mass where finer material migrates downward within the fill profile, causing voiding and potential collapse settlement. The observed condition of the compacted layers show both an interlock and point to point particle contact of the intermediate grain sizes. The packing of finer particles between this interlock of larger particles is observed in Photo 7. Uniformity coefficient (Cu) and coefficient of curvature (Cc) were used to assess the grading and potential for tight packing. Results show a well graded material with Cc between 1 and 5 and Cu greater than 4. The finer material (less than 1.18mm) is a minor component of the grading and is granular in composition. No significant cohesive fines (less than trace < 5%) were observed supporting the rock particles under compactive effort. PSD as shown in Figure 4 and strength testing was undertaken from the fill placement and compared to the corresponding source material testing for both geological sources. This comparison shows no significant breakdown post compaction for both geological sources and loss in material strength.

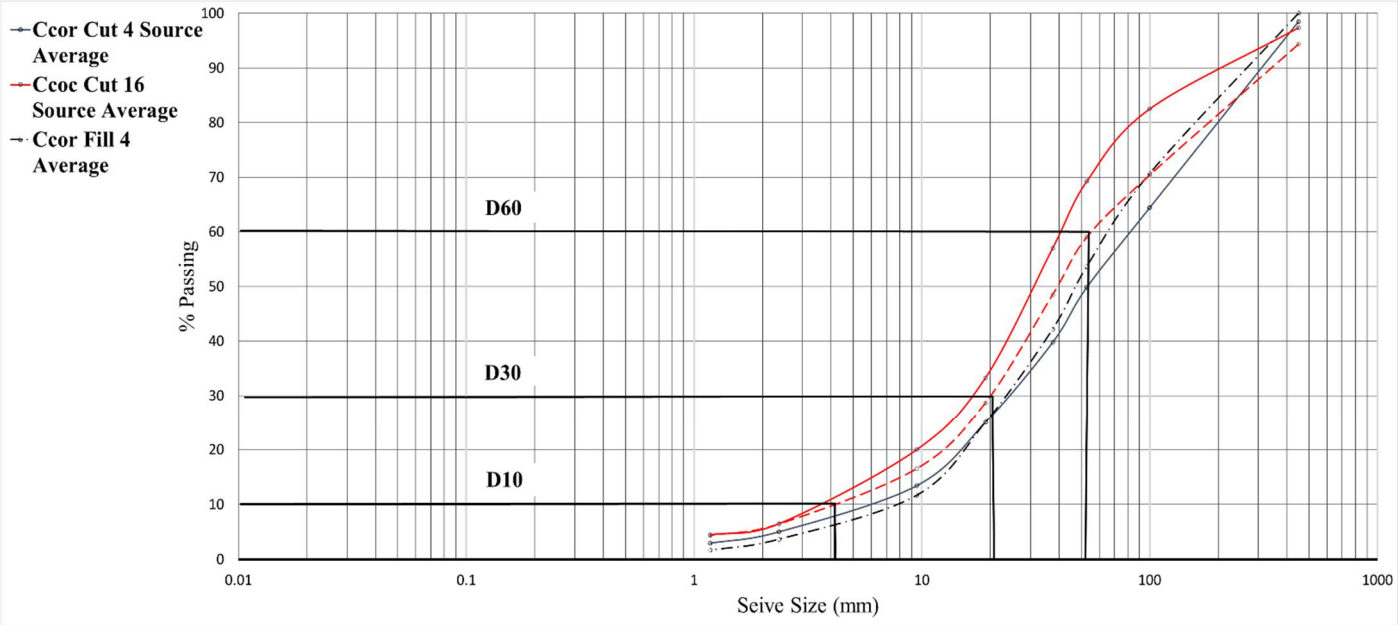


Figure 4 - Blast Source compared to Fill Placement Average Particle Size Distribution

7.2 STRENGTH AND MECHANICAL INTERLOCK

Material testing of both the Coramba and Brooklana sources show an average point load strength between 1 MPa to 6 MPa (Is50), wet dry variation that is typically below 35% and a wet strength between 200 kN to 250 kN. Both sources show very low slake durability breakdown (> 95% retained on 2nd cycle), and a high peak angle of internal friction of 43° to 48° tested on material passing the 37.5mm sieve. Strength testing shows that the parent rock is a hard durable material that is not susceptible to breakdown in both the wet and dry condition. The rock does originate from an argillaceous sedimentary source, however successive periods of deformation and burial have metamorphosed the original fabric to create a rock mass dominated by an indurated siliceous matrix and stress cleavage. .

7.3 INTERNAL SETTLEMENT

Twenty-five plate load tests were conducted on the trial fill placement. Results for Youngs modulus show a 90% confidence of E 50MPa which is in line with design assumptions for high strength rockfill.

Hunter et al 2002 provides a comprehensive review of rockfill dam deformation from over 40 concrete face rockfill dams worldwide. Results of this review show a summary of creep strain rate of compacted rockfill for medium strength to very high strength sources for embankment heights greater than 20 m. When extrapolated to an embankment height of 10 m to 15 m in line with project design, the long-term rate of settlement is estimated to be less than 0.05% of the embankment height per log cycle of time for high strength rock fill. This is shown in Figure 5. Waddell (2005) show between 0.05% to 0.16% creep strain for compacted medium strength sandstone fill.

Based on this and the high strength of the trial rockfill, a conservative creep strain rate of less than 0.1% per log cycle of the embankment thickness is considered reasonable is less than the SWTC criteria.

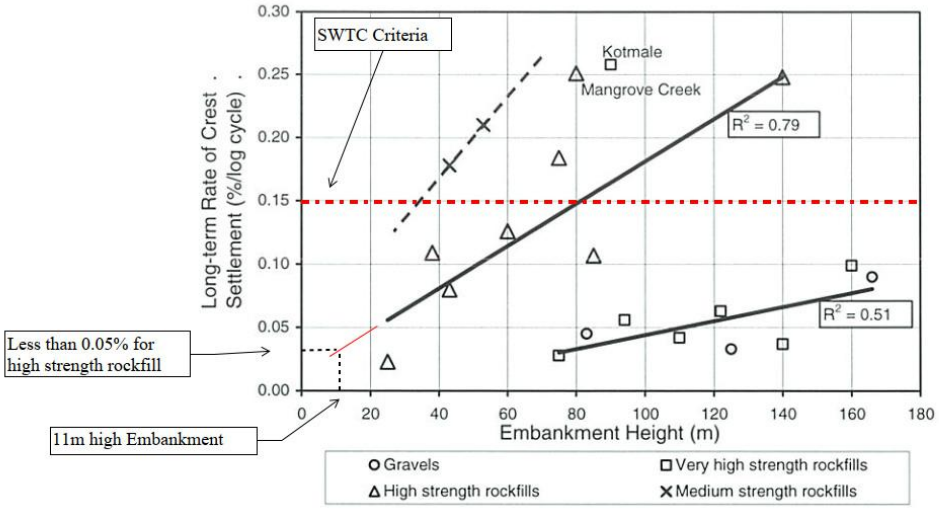


Figure 5 – Estimated long term rate of embankment settlement after Hunter and Fell 2002

7.4 HYDROCONSOLIDATION

Hydroconsolidation is a collapse compression occurring when uncompacted or partially saturated fills are inundated, causing increased, rapid settlement. In rockfill or large granular fills where the stiffness of the fill relies on the point-to-point contact between particles, the properties of the rock fragments and susceptibility to softening of the highly stressed point contacts controls the magnitude of hydroconsolidation settlement. Controlling this effect relies on controlling the strength, compaction and moisture conditioning during placement of the fill. The potential hydro consolidation effects of the rockfill after inundation were tested in Trials 2, 4 and 5. The test included conducting a plate load test in the dry condition on top of placed rockfill, then constructing a bunded area around the test site and inundating the site with water for 3 days. Measurements of settlement and an additional plate load test was conducted after the period of inundation.

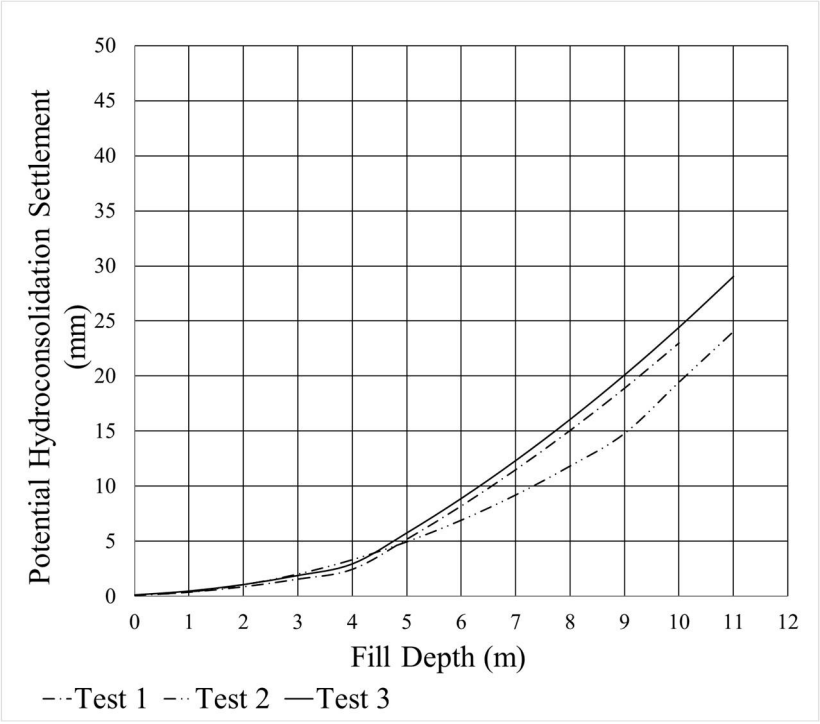


Figure 6 - Plot of Estimated Hydro Consolidation Settlement

The settlement for each 1 m layer was calculated for both the dry and inundated Youngs modulus taken from the plate load testing. The difference in settlement for each layer is plotted in Figure 5. Results of the analysis show an additional 25 mm to 30 mm of settlement may occur over a fully inundated 11m fill height (Trial Site Fill 17) due to hydroconsolidation. This would require an extreme weather event to flood the full height of the embankment and is considered unlikely. Events that flood the lower 2 m to 3 m of the embankment are more likely in flooding conditions. Based on such an event, hydroconsolidation settlement in the order 5 mm to 10 mm may occur. If the worst-case scenario of the full height of fill becoming inundated, the predicted settlement of up to 30 mm would still be acceptable from a pavement serviceability perspective noting that SWTC criteria for flexible pavements allow up to 200 mm of total residual settlement.

8 METHOD SPECIFICATION AND PROCESS CONTROL

Using the results of the trial, a method specification was developed to control the process of sourcing and placing the unprocessed rockfill. This included

- A revised PSD envelope in line with the results of testing conducted.
- Incorporating coefficient of uniformity and curvature requirements to ensure a well graded material was being placed in the fill.
- Daily cut source mapping by the engineering geologist and sorting of oversize by construction at the source.
- Regular blast and fill source strength and durability testing, including point load testing, wet / dry variation and slake durability.
- Pre modelled loose layer thickness to provide a compacted layer thickness of 500 mm.
- Minimum pass count and roller weight (18 tonne flat drum) during compaction. Each roller on the rock fill was equipped with intelligent compaction to measure pass count and coverage as well as guide on layer strength gain (CMV value).
- Test pit inspection and logging of the placed layer by the geotechnical CPS team to confirm full layer moisture conditioning and material interlock.
- Plate load testing during filling to confirm design stiffness requirements are met.

9 CONCLUSIONS

The proposed alternative of using unprocessed rock fill presented issues of conformance and certification in line with the project earthworks Specification. The identification of the issue due to geological assessment at concept stage, provided a departure to the Specification that could demonstrate adequacy to the landform requirements, be constructed in a methodical manner with the process tested, documented and certified. The modified Specification also enabled economic construction of the bulk earthworks by using the unprocessed rockfill won directly from cuts. The case study shows how a unified approach by all stakeholders can provide a best for project outcome under the Collaborative Design and Construct delivery contract.

10 AKNOWLEDGEMENTS

This paper is the result of collaborative research and development with Robert Ticknor of TfNSW and would not be possible without his contribution. Special thanks to Jim Yang (Arcadis) for peer review as well as Patrick Wong (Coffey) and Richard Kelly (SMEC) for technical guidance during the site trials. Gratitude is also expressed to the Coffs Harbour Bypass Team whose hard work and patience with the Author made this paper possible.

11 REFERENCES

Department of Public Works and Services NSW (1996). *Coffs Harbour Water Supply, Karangi Dam Raising, Geological Report on Construction.* Report No: 96-HW50

Gillian, L., Brownlow, J., Cameron, R., & Henley, H. (1992). *Dorrigo - Coffs Harbour 1:250 000 Metallogenic Map, 1st edition.* Geological Survey of New South Wales.

Graham, I. J., & Korsch, R. J. (1985). *Rb-Sr Geochronology of Course-grained Greywackes and Argillites from the Coffs Harbour Block, Eastern Australia. Chemical Geology (Isotope Geoscience Section),*58 pp. 45-54.

Hunter, G, & Fell,.R., (2002). *The Deformation Behaviour of Rockfill*. Sydney: The University of New South Wales.

Korsch, R. J. (1981). *Some tectonic implications of sandstone petrofacies in the Coffs Harbour association, New England Orogen, New South Wales*. Journal of the Geological Society of Australia, 28(3-4) pp.261-269

Piccolo, D., Mostyn, G., & Salim, A. (2019). *A unified approach to earthworks for residential, industrial and commercial developments consistent with AS3798-2007.* Australian Journal of Civil Engineering, 17(1), pp.50–62.

Transport for NSW (2021) Coffs Harbour Bypass Specification D&C R44 - Earthworks

Waddell, P., and Wong, P. (2005). *Settlement characteristics of deep engineered fills.* Australian Geomechanics Journal, 40(4), pp.57-72

https://doi.org/10.56295/1ACEG06

ROCKFALL HAZARD ASSESSMENTS AND REMEDIATION FOR THE MAJOR CLIFF PRECINCTS OF BRISBANE

Tharindu Abeykoon, Matthew Cochrane, Andy Law & Bruce Cheesman
SMEC, Level 6, 480 St Pauls Terrace, Fortitude Valley, QLD 4006, Australia

ABSTRACT

Howard Smith Wharves (HSW) and Kangaroo Point (KP) are major cliff areas within the Brisbane CBD. The cliffs are former quarries for the supply of Brisbane Tuff rock and areas for essential industries of Brisbane. The cliffs have had a history of instability, resulting in rockfalls of varying significance. Over time, the usage of these spaces has changed, necessitating a structured monitoring and maintenance strategy to manage rockfall risks. Despite previous remediation efforts, residual risks remain due to the geological characteristics, historical quarrying, and evolving site usage.

For HSW, a risk assessment was conducted in 2021 in accordance with the Landslide Risk Management Guidelines (AGS, Volume 42, No.1, 2007) to evaluate rockfall risks impacting the main entertainment areas. The risk assessment considered the potential hazards identified during site inspections and the digital survey data of slope profiles at multiple locations. The geotechnical risk assessment outlined the requirement for permanent remediation to achieve a tolerable risk.

For KP, extensive historical quarrying and high recreational usage, including rock climbing, have contributed to ongoing deterioration of the Brisbane Tuff cliffs, requiring regular inspection and maintenance to manage the rockfall risks.

The detailed design phase for the remediation required site-specific remediation solutions due to the cliff locations and site usage. Remediation works were undertaken in 2024. A variety of rockfall protection measures were designed and installed, including recessed rock dowels, spider mesh, draped mesh and secured mesh systems.

1 INTRODUCTION

Howard Smith Wharves (HSW) is a high-profile entertainment precinct constructed on the floor of a former quarry, adjacent to the Brisbane River, and located at the northern end of the Story Bridge in central Brisbane. The cliffs behind HSW have a history of instability, resulting in rockfalls of varying significance. Previous investigations and remedial measures had been implemented to mitigate some of the potential risks. However, residual rockfall risks remained as the previous remedial solutions were not intended to reduce the risks for the current site usage. A risk assessment was completed to assess the existing risks for the site in accordance with the Australian Geomechanics Society (AGS) guidelines on Landslide Risk Management (LRM) (AGS, 2007a,b,c,d,e). The assessment indicated that the geotechnical risks identified did not achieve tolerable risk ratings when assessing the risks for loss of life.

Kangaroo Point (KP) cliffs are located along the southern banks of the Brisbane River, approximately 1.5 km to the south of the Story Bridge in central Brisbane. The cliffs are a popular location for recreational activities, particularly rock climbing. Public parks are located at the crest and toe areas of the cliffs. Localised adverse rock mass properties and other factors, such as damage to the rock from quarrying, have led to a number of rockfalls occurring in the past, some of which have been significant, particularly given the current site usage.

Based on the risk assessments undertaken, SMEC was engaged to complete a detailed design for permanent remedial measures to mitigate the potential rockfall risks for areas considered to be high risk for both Brisbane City Council (Council) assets. The risk assessment methodology, processes of hazard identification, design development, optioneering, and detailed design solutions are discussed in this paper.

2 SITE DESCRIPTION AND GEOLOGICAL SETTING

2.1 SITE DESCRIPTION

The original HSW were constructed in the 1930s and 40s on the floor of a former quarry adjacent to the Brisbane River. The current development that characterises the area was largely constructed between 2017 and 2018 and comprises several public function buildings and garden areas (see Figure 1).

The geometry of the quarried cliff faces, which slope at between 65 and steeper than 90 degrees, are up to 32 m in height and 550 m in length. The geometry of the site, together with localised adverse rock mass properties and other factors such as damage to the rock from blasting during their construction, has led to a number of rockfalls occurring in the past. Some historic scaling and installation of rock bolting, buttressing, shotcreting and secured meshing had been completed. Although these remediation measures helped to reduce the likelihood and size of potential hazards, they did not remove

all hazards. Based on the site inspections, it was considered that rockfalls would continue as the geological conditions are such that the slopes would deteriorate due to both natural and human-induced processes. Hence to reduce rockfall risks, further remediation would be required.

KP cliffs are heritage-listed and were quarried for almost 150 years (quarrying works ceased at the site in 1974) to form the current near-vertical profile between 15 m to 26 m in height. The cliffs are approximately 825 m in length, and the study area extended from the Riverlife Centre south to Cox's Bluff and included the smaller cliffs known as the 'Nursery Slopes'. The Nursery Slopes are approximately 70 m in length and 6 m to 8 m in height. The popular climbing area between the cliff's café (Joey's Café) and Cox's Bluff (refer to Figure 2) has had a number of remediation stages in the last 30 years. Remediation has primarily been in the form of recessed dowels and limited coloured shotcrete support.



Figure 1: Overview of HSW cliffs



Figure 2: General view of KP cliffs

2.2 GEOLOGICAL SETTING

Figure 3 shows the cliffs to comprise two (2) distinct geological formations, the Neranleigh-Fernvale Beds (NFB) overlain unconformably to the south by the Brisbane Tuff. The KP cliffs were created by quarrying the welded tuff or ignimbrite of the Brisbane Tuff geological unit. The NFB and Brisbane Tuff are separated by an inclined geological unconformity. The unconformity is seen in the central part of the HSW site and partially visible at the southern extent of KP cliffs underlying densely vegetated residual and colluvial soil slope below Captain Cook Bridge. The unconformity is not a planar surface and rather shows the paleo-topography present at the time of the deposition of the Brisbane Tuff.

The NFB are of the Late Devonian to Early Carboniferous Period (approximately 360-320 Ma) and predominately comprise meta-sedimentary rock of argillites, phyllites and arenites with distinct and closely spaced foliation inclined moderately (30° to 45°) with dip direction around 040° (into the cliff face).

The Brisbane Tuff, the oldest of the Late Triassic Period (230-210 Ma) rocks in the area and pyroclastic rocks deposited about 226 Ma and filled an ancient river valley. The Brisbane Tuff geological unit, initially referred to as ‘porphyry’ (Gregory and McLay, 2010) is a fine to coarse-grained high to very high strength welded tuff or ignimbrite rock. It is distinctively multicoloured with phenocrysts of quartz and feldspar. Additionally, it contains pyroclasts of various origin rock types and pumice within the fine-grained tuffaceous matrix. The Brisbane Tuff generally comprises six (6) different lithologies, namely Rhyolitic tuff, ignimbrite, agglomerate, conglomerate, sandstone and shale.

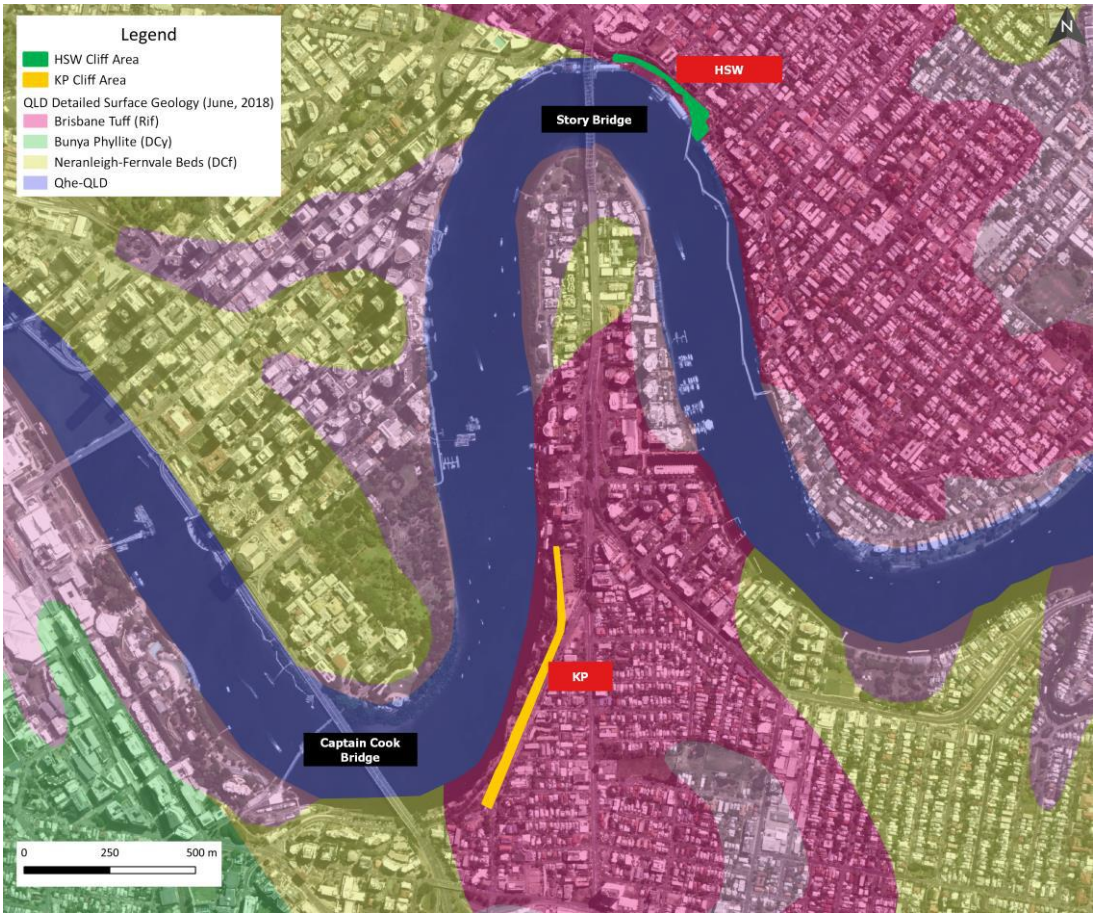


Figure 3: Extract of detailed geological release of Queensland (Department of Natural Resources, Mines and Energy, Queensland Government, 2018)

3 RISK ASSESSMENT AND DESIGN DEVELOPMENT

3.1 DESIGN PROCESS

The overall design process for slope remediation followed a structured, multi-step approach, as outlined below:

Step 1 - Review of background information and site assessment

An initial review was undertaken of available historical investigation data, supplemented by site inspections of the existing cliff faces and current land use. This process supported the identification and confirmation of primary geotechnical hazards and areas requiring further assessment. Additional survey work and geological investigations were completed in high-risk areas. At HSW, a rockfall risk assessment was conducted in accordance with AGS (2007c), while at KP, a detailed Level 2 assessment was carried out in alignment with Council's ongoing monitoring and maintenance framework (AGS, 2007a).

Step 2 - Options selection

Site-specific risk mitigation strategies were developed to address areas where rockfall risk was assessed as intolerable. For HSW, being the first to be designed, a Multi-Criteria Analysis (MCA) was undertaken to assess and rank potential mitigation options. The MCA provided a structured comparison of alternatives using weighted evaluation criteria including constructability, cost, maintenance, impact on users, and visual amenity (AGS, 2007e). Whilst no specific MCA was carried out for KP site, the process, inputs, and outcomes were largely also relevant to this site.

Step 3 - Agreed design solutions

The outcomes of the MCA at HSW, along with the preliminary recommendations for KP, were used to facilitate discussions with local authorities and other stakeholders to inform the selection of preferred design solutions for implementation.

Step 4 - Develop permanent design solutions

Finalised remedial designs were developed for implementation at identified high-risk locations. At HSW, selected options from the MCA were refined through consideration of constructability constraints and potential disruption to public use. The primary remediation measures included secured and draped rockfall mesh systems and rock reinforcement using passive dowels to stabilise both blocky rock masses and isolated hazards.

At KP, the design approach was influenced by the area's recreational use for climbing. Remediation primarily comprised recessed rock dowels to preserve the climbing surface. In non-climbing areas, additional treatments included sculpted and coloured shotcrete, and high-capacity mesh systems with profiled dowelling to conform to the rock face.

Step 5 - Residual risk evaluation

Following implementation of the final designs, a residual risk assessment was undertaken for HSW to quantify the reduction in risk to life. The assessment confirmed that the adopted permanent hazard reduction measures achieved a reduction in risk to within tolerable thresholds as defined by AGS (2007c).

3.2 HSW RISK ASSESSMENT

3.2.1 Hazard identification

Extensive site inspections and mapping programs have been carried out at HSW by Council and since 2020 by SMEC to support hazard identification and remediation prioritisation. The mapping phases included drone photogrammetry, visual inspections along the base of the cliffs, and detailed cliff face mapping at height using elevated work platforms and industrial roped access.

Hazard mapping considered the following parameters:

- Lithology;
- Discontinuity orientation;
- Degree of weathering;
- Contributing instability factors; and
- Likelihood of future deterioration.

Three primary modes of failure were evident along the cliff: planar, wedge and toppling failures. The geology and jointing orientations influenced the dominant failure types across the site. The Brisbane Tuff has dominant and persistent sets of vertical and sub-parallel joints with a variation in inclination, giving the columnar or tabular appearance. The occurrence of near horizontal basal release jointing increases the potential for toppling and planar type failures. Numerous overhangs are also present along the length of the site, which also contributes to the above failure mechanisms.

For the NFB cliff face area, the north easterly dipping foliation is the dominant feature of instability. The foliation (dipping into the cliff), in combination with sub-vertical joint sets, present toppling type failures. The closely spaced foliation surfaces are prone to weathering with clay infilling or veneers for sliding or release surfaces. These weathering properties further highlighted that deterioration of the cliff face will be an ongoing process with consequent ongoing rockfalls.

The hazard sizes generally ranged from 0.1 m to 1.0 m. Larger rock masses had predominately been supported by rock anchors, dowels and/or shotcreting in previous remediation phases. Some zones were highly fractured, forming veneers or loose flakes of rocks present on the cliff face. These zones were considered to be altered tuff, typically weaker than other zones and prone to spalling of loose fragments.

Identified triggers for rockfall at HSW include:

- Prolonged rainfall leading to percolation through discontinuities, leaching of fines, and weakening of the rock mass;
- Intense rainfall events dislodging loose material;
- Tree root growth (root jacking);
- Progressive weathering and stress relief; and
- Residual blasting damage from historical quarry operations.

3.2.2 Basis of the risk assessment

For HSW, Council had requested that the risk assessment be undertaken in accordance with AGS (2007a,b,c,d,e). This issue presents a series of LRM guidelines and further understanding of the application of the risk assessments for the recommended use by all practitioners nationwide. The assessment followed the AGS (2007c) approach and the tolerable

risk thresholds for existing (10^{-4}/annum) and new (10^{-5}/annum) developments were agreed by the client to be used as the basis of the assessment.

3.2.3 Rockfall modelling

Two-dimensional (2D) rockfall analyses were conducted across multiple representative cross-sections along cliff faces with an existing intolerable risk. To accurately account for the size and shape of individual rocks, a 'Rigid Body' analysis using the proprietary software Rocfall by Rocscience Inc. was developed. The software enables 2D statistical analysis of the energy, velocity and travel paths of the various hazards on the site. Input parameters such as ground profiles, surface conditions, and the source characteristics of rockfall hazards were derived from detailed on-site inspections, topographic survey data, and geological mapping. The software enabled the analysis of rockfall trajectories, impact energy, velocity profiles, and travel distances to support risk classification and design of mitigation measures.

Material properties used in the modelling are summarised in Table 1 and were assigned based on observed geological conditions at each cross-section. These values were selected from the conservative range recommended by Rocscience for materials with similar field descriptions and were further calibrated using evidence of recent rockfall deposits observed during site inspections.

Due to the limited availability of published restitution parameters specifically for rigid body models, the adopted normal and tangential restitution coefficients were based on values commonly used in lumped mass analyses. This approach was taken as a conservative measure, acknowledging that lumped mass restitution values tend to overestimate energy dissipation compared to rigid body dynamics. Nonetheless, this conservative bias is considered appropriate for preliminary design and risk classification purposes.

Table 1: Adopted material properties for rockfall trajectory modelling

Material Name	Material Description	Coefficient of normal Restitution	Coefficient of Tangential Restitution	Dynamic Friction Coefficient	Rolling Friction Coefficient
Rock	General cliff face	0.45	0.95	0.60	0.40
Rock	Within Unconformity - Rock fragments, debris, scattered trees	0.45	0.95	0.60	0.60
Ground [1]	Material at base of cliff	0	0	1	1

Note - 1. Properties for the Ground were selected to ignore post-impact bouncing and rolling.

3.2.4 Hazard analysis

The frequency of rockfall events is inherently variable and influenced by multiple interacting factors. Field observations and historical data indicate that most frequent events involve smaller rockfalls (<0.3 m), while larger blocks (>1.0 m) are less frequent and often previously stabilised.

3.2.5 Consequence assessment

The consequences of a rockfall event were evaluated in terms of potential loss of life, injury, or structural damage. The following factors were considered to influence the likelihood of deaths and injuries or vulnerability ($V_{(D:T)}$ / $V_{(Prop:S)}$) of persons/structures that are impacted by a rockfall:

- The volume of falling material in relation to the element/person at risk;
- Spatial location of people or structures relative to the potential impact zone;
- Type, magnitude, depth and rate of rockfall;
- Mechanism of rockfall initiation and velocity of sliding;
- Degree of protection for a person (e.g., vehicle, building, or open space exposure);
- Structural resilience or collapse potential in the event of impact.

These factors informed the assessment of the likelihood of fatality or damage and the design of targeted mitigation strategies.

3.2.6 Risk analysis

Where the AGS (2007c) method was used, the Risk of Loss of Life is defined as the risk of fatality or injury to any individual who is located within the zone impacted by the landslide; or who follows a particular pattern of life that might subject them to the consequences of the landslide.

In accordance with the AGS (2007c) LRM Guidelines for loss of life, the risk assessment was primarily based on a quantitative approach. The individual risk for loss of life can be calculated from:

$$R_{(LoL)} = P_{(H)} \times P_{(S:H)} \times P_{(T:S)} \times V_{(D:T)} \quad (1)$$

Where;

$R_{(LoL)}$ - The risk (annual probability of loss of life (death) of an individual);

$P_{(H)}$ - The annual probability of the landslide;

$P_{(S:H)}$ - The probability of spatial impact of the landslide impacting a building (location), taking into account the travel distance and travel direction of a given event;

$P_{(T:S)}$ - The temporal, spatial probability (e.g. of the building or location being occupied by the individual) given the spatial impact and allowing for the possibility of evacuation given there is a warning of the landslide occurrence; and

$V_{(D:T)}$ - The vulnerability of the individual (probability of loss of life of the individual given the impact).

The calculated risk levels were compared against the AGS defined tolerable risk criteria, guiding the design of remediation strategies to reduce risks to acceptable thresholds.

3.3 KP RISK ASSESSMENT

3.3.1 Hazard identification

A detailed Level 2 assessment of the KP cliffs was undertaken by SMEC across two phases:

1. Main cliffs, Nursery cliffs and Lower River Terrace access road slopes, and
2. Riverlife Centre cliffs.

All vertical cliff sections were accessed using either Elevated Work Platforms (EWPs) or industrial rope access techniques to ensure full visual coverage and detailed inspection. Each identified hazard was photographed, measured, and evaluated for remediation priority. The focus of the assessment was to identify unstable blocks and zones with a credible potential for detachment, posing a risk to public safety.

The following factors were identified as contributing to ongoing instability and deterioration of the KP cliff rock mass:

- Historical blasting damage, resulting in stress relief and reduced rock mass integrity;
- Weathering and strength loss along discontinuities, particularly where exacerbated by water ingress;
- Water percolation and high rainfall events, which induce transient pore pressure increases and displace rock blocks along defects;
- Root jacking from vegetation growth, causing progressive dilation of joints and formation of new fractures; and
- Recreational climbing activity, which imposes additional loading on isolated blocks and may lead to displacement of supporting material.

These mechanisms, acting individually or in combination, contribute to the overall rockfall risk profile at KP.

3.3.2 Basis of the risk assessment and hazard categorisation

The risk assessment approach adopted for KP was semi-quantitative prioritisation method to suit the nature of the site, existing data limitations, and the focus on managing risks in a recreational setting. While the AGS (2007c) framework was not specifically required, hazard prioritisation considered multiple geotechnical and contextual factors, including:

- Proximity of the hazard to high-use public zones;
- Hazard size and estimated block volume;
- Observed failure mechanism potential (e.g. planar, wedge, or toppling); and
- Anticipated trigger mechanisms such as water ingress, root jacking, and human activity.

Based on this assessment each hazard was categorised as follows:

- Category A - Remedial priority:
  - Priority 1: Scaling works to be completed before the next wet season.
  - Priority 2: Hazards requiring stabilisation to be designed and scheduled for remediation.
- Category B - Ongoing monitoring:
  - Hazards identified for visual tracking during future Level 1 and Level 2 cliff inspections, due to lower risk or uncertainty around their stability.

This prioritised approach enabled effective resource allocation and treatment scheduling in coordination with stakeholder and public safety objectives.

3.3.3 Kinematic hazard analysis

Kinematic analyses were performed to evaluate the stability of potential planar and wedge failures observed during the cliff inspections. Two-dimensional analytical tools were used, specifically:

- RocPlane by Rocscience Inc., to assess planar sliding mechanisms where failure surfaces were approximately parallel to the exposed slope face; and
- SWedge by Rocscience Inc., to analyse wedge failures formed by the intersection of two discontinuity planes and the slope surface.

Analyses were conducted under the following assumptions:

- No external loading (e.g., seismic or surcharge forces);
- Joint surfaces were considered smooth (waviness = 0°);
- Rock unit weight was assumed to be 23 kN/m³;
- Shear strength was estimated using the Barton-Bandis model; and
- No joint water pressure or ponding was considered.

3.4 OPTION EVALUATION AND DESIGN SOLUTIONS

A range of remediation options was evaluated to address the diverse rockfall hazards identified across the study areas. Preliminary mitigation measures considered included:

- Secured mesh systems;
- Draped mesh systems;
- Rockfall attenuators;
- Rockfall canopies and barriers;
- Rock bolting and anchoring;
- Shotcrete application; and
- Restrictions on building use or access in high-risk zones.

The selection and refinement of mitigation strategies were informed by site-specific hazard conditions observed during detailed inspections, as well as digital terrain models derived from topographic survey data. These inputs were used to characterise slope geometries, rockfall trajectories, and accessibility constraints.

For the HSW site, constructability was a key design consideration due to the presence of 30 m high near-vertical cliffs located directly above a high-traffic entertainment precinct. To manage this complexity, a specialist rope-access contractor was engaged during critical design stages to review construction feasibility. This collaboration informed refinements to the preferred mitigation strategies developed through the MCA process and ensured that the proposed solutions were both practical and effective for implementation in constrained urban conditions.

4 REMEDIAL SOLUTIONS

The adopted remedial solutions were developed with consideration of a range of factors, including public safety, constructability, long-term performance, cost-effectiveness, and potential reputational impacts on stakeholders. Solutions were tailored to site-specific conditions and designed to minimise disruption during construction while ensuring ongoing risk reduction.

4.1 HSW CLIFFS REMEDIATION

The detailed design for HSW cliffs incorporated the following primary remedial measures to enhance slope stability and mitigate rockfall risks.

4.1.1 Secured mesh

A high-tensile steel wire mesh secured to the cliff face with reinforcement bars (dowels) is installed with evenly spaced dowels over the entire mesh surface at a typical spacing between 1.5 m and 2.0 m. The secured mesh system effectively 'holds' the loose material into the rock face and prevents the rocks from falling.

The design of the secured mesh systems was completed in accordance with the principles documented in 'Design Software for Secured Drapery' (Brunet and Giacchetti, 2012).

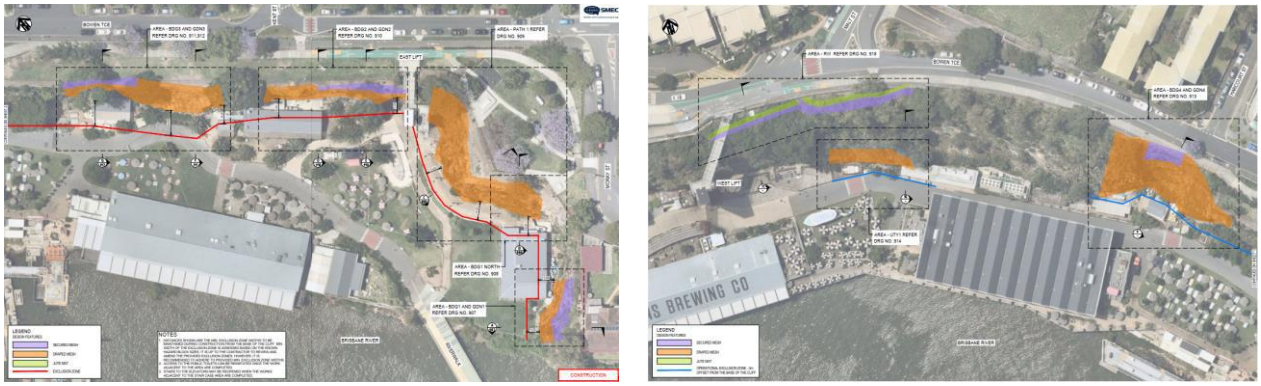
4.1.2 Draped mesh

The draped mesh system was implemented in areas with multiple hazardous blocks, anchored at the top and extending down the slope to effectively contain falling debris and direct it safely to the toe (Geobrugg ,2014). The design followed the principles outlined in the Design Guidelines for Wire Mesh/Cable Net Slope Protection (Muhunthan et al., 2005).

A single mesh type (Tecco G65/3 or similar) was adopted for both secured and draped mesh systems in matte black colour (to minimise visual impact) across the HSW cliffs. The reinforcement system includes Grade D500N self-drilling hollow duplex bars (Ischebeck Titan 40/20).

Most of the treatment areas required access from the top of the cliffs using industrial rope access methodologies (including use of Marini rigs to drill dowels) and from the base using excavators and long-reach/telescopic plant. A water mist was used at the drilling face mitigate dust generation during dowel installation.

Figures 4a and 4b illustrate the layout of remedial measures across the site, and Figure 5 presents a representative elevation and cross-sectional view of a typical treatment zone.



(a) (b)

Figure 4: HSW site layout with remedial solutions across the site

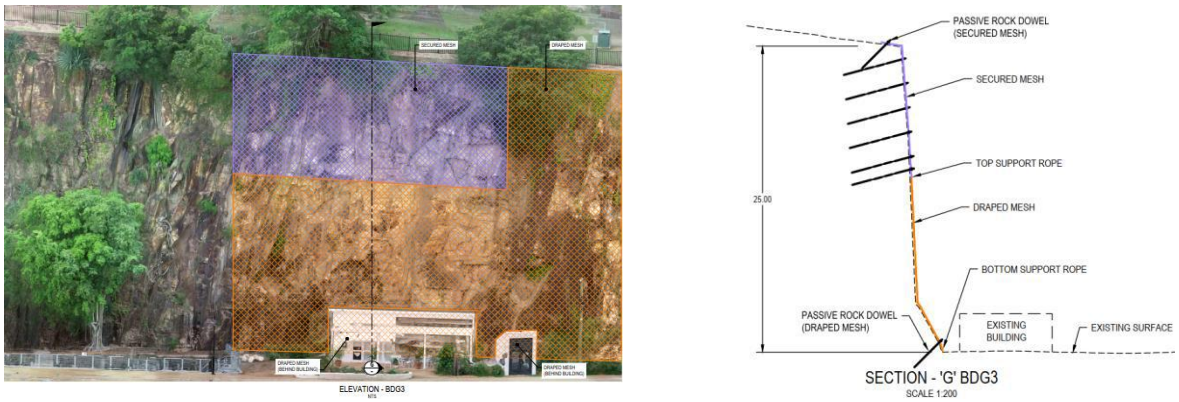


Figure 5: Representative elevation and cross-sectional view of a typical treatment zone

4.2 KP CLIFFS REMEDIATION

Remedial works at the KP cliffs addressed 24 identified hazards. The design response was informed by site usage (including recreational climbing), heritage and visual constraints, and the nature of the observed instability.

4.2.1 High-capacity wire rope mesh with dowel support

A high-strength wire rope mesh system (Spider S3-130) was selected for its capacity to conform to irregular rock surfaces while providing robust containment of unstable material. The mesh was anchored using Grade D500N self-drilling hollow duplex dowels (Ischebeck 40/16), in accordance with MRTS71 specifications.

This system was implemented in areas of highly fractured rock, particularly beneath pedestrian stairwells where foot traffic and exposure levels warranted a higher level of protection.

Figures 6a and 6b illustrate the treatment area before and after installation of the high-capacity wire rope mesh below the cliff stairs.



(a) (b)

Figure 6: High-capacity wire rope mesh remediation (a) prior to remediation, (b) post remediation

4.2.2 Recessed dowel support systems

Two dowel types were used to stabilise discrete hazards while maintaining aesthetic and recreational values:

- Glass Fibre Reinforced Plastic (GRP) Bars: Continuously threaded 1000 MPa solid GRP dowels were installed where corrosion resistance and non-interference with climbing activities were priorities.
- Stainless Steel Threaded Bars (M16): Installed with HIT-RE 500 V4 epoxy resin. Components met ASTM F568M (Class 8.8) specifications, with high-corrosion-resistant (1.4529) stainless steel washers and nuts for durability in exposed environments.

4.2.3 Sculpted and coloured shotcrete

Shotcrete was selectively applied in locations where the rock mass was highly fractured and other support measures were not feasible. The shotcrete surface was sculpted and coloured to blend with the natural rock, minimising visual impact while providing mechanical interlock with the embedded dowels. This treatment also served to consolidate surface layers and reduce progressive weathering.

To minimise the impact of remediation on climbing activities, GRP and stainless-steel bars were selected to support identified hazards. These bars met the corrosion protection requirements for permanent dowels while allowing installation with relatively smaller diameter holes. Additionally, to reduce the visual impact on the exposed rock face, the dowels were recessed into the rock and filled with mortar, colour-matched to blend with the surrounding area.

Figure 7 illustrates the final treatment of hazard locations using recessed dowels and shotcrete.



(a)



(b)

Figure 7: Remediated hazard areas at KP (a) recessed dowels (b) sculpted shotcrete

4 RESULTS AND DISCUSSION

The assessment and remediation of rockfall hazards at the HSW and KP cliffs required a structured, site-specific approach due to the complex geological conditions, historical quarrying impacts, urban interface, and evolving site usage (e.g., public access and recreational climbing).

5.1 RISK ASSESSMENT AND MITIGATION STRATEGY EFFECTIVENESS

The risk assessment framework, based on the AGS LRM Guidelines (AGS, 2007a,b,c,d,e), provided a robust methodology for evaluating and managing slope instability hazards. Dominant failure modes, including planar sliding, wedge failure, and toppling were identified through detailed inspections, digital surface modelling, and kinematic analyses using RocScience's suite of tools (RocFall, RocPlane, SWedge). This integration of field and analytical methods enabled accurate hazard delineation and prioritisation.

5.1.1 HSW rockfall modelling results

Table 2 summarises the assessed hazards and the estimated 90% rockfall impact zones prior to remediation. Hazard sizes and fall heights were derived from inspection records and digital survey data. To reflect observed variability in rock block geometry, RocFall modelling incorporated multiple block shapes, including square, rhombus, and elliptical geometries with aspect ratios between 1.5 and 2.0.

Table 2: Summary of hazards considered and Pre-remediation 90% rockfall zone

Building / Area ID	Building / Area Name	Assessed Hazard(s)		Pre-remediation 90% rockfall zone from base of the cliffs (m)
		Max. Size (m)	Fall Height (m)	
GDN1	Garden 1	0.5	Up to 20	4.0
GDN2	Garden 2	1.0	Up to 19	4.7
GDN3	Garden 3	1.0	Up to 23	8.2
GDN4	Garden 4	1.0	Up to 10	6.0
BDG1	Bougainvillea House	0.6	Up to 21	4.7
BDG2	Green House	1.0	Up to 18	5.7
BDG3	Citrus House	0.75	Up to 22	7.4
BDG4	Wisteria House	0.75	Up to 28	7.6
BDG5 (demolished)	Garden Bar	0.5	Up to 13	5.4
UTY1	Power / AC/ Composting / Storage	1.0	Up to 23	8.1
PATH1	Pedestrian path	0.5	Up to 18	4.5

5.2.1 HSW risk assessment outcomes

At HSW, the initial risk assessments indicated that loss-of-life risk exceeded the tolerable threshold (1×10^{-5}). Consequently, the Council commissioned SMEC to evaluate temporary mitigation measures, including fencing and signage, to restrict access to high-risk areas within the 90% rockfall impact zone. Following the exclusion zone installation, the residual risk was estimated between 5.4×10^{-7} and 1.0×10^{-3}, with some areas still exceeding the tolerable risk threshold.

Permanent remediation works consisted of a combination of secured mesh systems, rock dowels, and draped mesh solutions to remediate critical sections of the cliff face. These permanent hazard reduction measures have further reduced the estimated residual risk to a range of 6.2×10^{-9} to 1.6×10^{-6}, aligning with Council's tolerable risk criteria. Table 3 summarises the comparative risk levels before and after remediation.

Table 3: Summary of HSW risk assessment outcomes

Site ID	Building/ Area Name	Maximum Risk for Loss of Life Per Annum for As Existing Conditions (2,4)	Maximum Risk for Loss of Life Per Annum After Permanent Remediation
BDG1	Bougainvillea House	4.8×10^{-5}	2.9×10^{-8}
BDG2	Green House	2.4×10^{-4}	1.1×10^{-6}
BDG3	Citrus House	5.1×10^{-3}	5.1×10^{-7}
BDG4	Wisteria House	1.5×10^{-3}	1.5×10^{-7}
BDG5 (3)	Garden Bar (Demolished)	1.2×10^{-4}	1.6×10^{-6}
UTY1	Power/AC/Composting/Storage	6.2×10^{-6} (5)	6.2×10^{-9}
UTY2	Glass Processing	1.3×10^{-6}	Not Applicable
GDN1 (1)	Garden 1 (adjacent to BDG1)	6.2×10^{-4}	1.2×10^{-7}
GDN2 (1)	Garden 2 (adjacent to BDG2)	9.0×10^{-5}	5.0×10^{-7}
GDN3 (1)	Garden 3 (adjacent to BDG3)	3.9×10^{-4}	9.7×10^{-7}
GDN4 (1)	Garden 4 (adjacent to BDG4)	8.5×10^{-5}	9.7×10^{-7}
PATH1 (1)	Pedestrian Path	1.3×10^{-4}	2.8×10^{-8}

Notes
1. Existing conditions assume that the area is open for public access.
2. Excludes the temporary mitigation measures of fencing and signage to exclude end users from the more critical areas near the base of the cliffs.
3. The assessment has considered the abandonment of BDG5.
4. All assumptions associated with occupancy and frequency of entry into the assessed area are as agreed with Council.
5. Additional rockfall fence was added to reduce the potential rockfall risk on the path immediately adjacent to UTY1.

5.2.2 KP hazard assessment outcomes

At KP, a semi-quantitative hazard prioritisation approach was adopted, as AGS quantitative analysis was not required. Hazards were categorised based on location, failure potential, proximity to high-use areas, and expected triggers (e.g., root jacking, weathering, human interaction).

A total of 24 Category A (Priority 2) hazards were remediated, as summarised in Table 4. An additional 18 Category B hazards were identified for ongoing monitoring through future Level 1 and Level 2 inspections.

Table 4: Summary of KP Category A - Priority 2 remediated hazards

Recommended Remediation	Number of Hazards Identified
Wire Rope & Mesh Support (boulders adjacent to the cliff stairs)	1
Dowel Support - GRP bar	10
Dowel Support - Stainless steel bar	10
Shotcrete Support	3

5.2 CONSTRAINTS DURING IMPLEMENTATION OF REMEDIAL SOLUTIONS

5.2.1 Constructability and access constraints

The steep and near-vertical geometry of the cliffs presented significant construction access challenges. Traditional methods were unsuitable, requiring rope access techniques, EWPs and specialist drill rigs. Working within confined zones in urban environments, adjacent to pedestrian pathways, roadways, and public spaces necessitated careful scheduling around high-use periods, minimising disruption to the public and surrounding businesses.

5.2.2 Geological and environmental considerations

The Brisbane Tuff exhibited variable strength and weathering characteristics, with highly altered zones presenting weak, clay-infilled joints and fractured rock prone to localised failure. In such areas, standard mesh and dowel systems were supplemented with sculpted shotcrete to provide additional cohesion and surface control. Both HSW and KP are culturally and historically significant; consequently, all treatments had to meet aesthetic and heritage requirements, particularly where visual changes to cliff faces were a concern.

5.2.3 Stakeholder engagement and compliance

Given the high-profile nature of both sites, extensive stakeholder engagement was critical to project success. Collaboration with Council, environmental regulators, climbing communities, and the entertainment precinct management was essential to address concerns related to site usability, aesthetic impacts, and risk perception. The adoption of risk-based design methodologies and transparent communication facilitated informed decision-making and regulatory compliance.

5 CONCLUSIONS

The remediation of rockfall hazards at HSW and KP cliffs has successfully reduced risk levels to tolerable thresholds. The approach combined advanced geotechnical assessments, engineering interventions, and collaborative stakeholder engagement to address complex rock slope instability challenges. The methodologies applied in this project provide a valuable framework for managing similar geological hazards in urban environments.

6 ACKNOWLEDGEMENTS

The authors gratefully acknowledge Council for providing historical information, survey data and as-constructed drawings to facilitate this study. Further, gratitude should be extended to Brett Collins (Council) for providing technical input during the design and analysis stages of the risk assessment study including Craig Walker (Council) and Ewa Wieczorek (Council) for arranging permission for us to publish this paper.

7 REFERENCES

AGS (2007a). Guideline for landslide susceptibility, hazard and risk zoning for land use management. *Australian Geomechanics*, 42(1), 13-36.

AGS (2007b). Commentary on guideline for landslide susceptibility, hazard and risk zoning for land use management. *Australian Geomechanics*, 42(1), 37-62.

AGS (2007c). Practice note guidelines for landslide risk management*, Australian Geomechanics*, 42(1), 64-114.

AGS (2007d). Commentary on practice note guidelines for landslide risk management. *Australian Geomechanics*, 42(1), 115-158.

AGS (2007e). Australian geoguides for slope management and maintenance*, Australian Geomechanics*, 42(1), 159-182.

Brunet, G. and Giacchetti, G. (2012). Design Software for Secured Drapery. *Proc. 63rd Highway Geology Symposium*, Redding, California, USA, 91-110.

Geobrugg (2014). Rockfall drapes made of high-tensile steel wire. *The Safe and Economical Way to Guide Rockfalls*.

Gregory, H. and McLay, D (2010). *Building Brisbane's History: Structure, Sculptures, Stories and Secrets*. Warriewood, New South Wales: Woodslane Press, 180-184.

Muhunthan, B., Shu, S., Sasiharan, N., Hattamleh, O.A., Badger, T.C., Lowell, S.M. & Duffy, J.D., (2005). *Design Guidelines for Wire Mesh/Cable Net Slope Protection*. Report No. WA-RD 612.2.

Department of Natural Resources, Mines and Energy, Queensland Government (2018) *Detailed geology release - June 2018.*

https://doi.org/10.56295/1ACEG07

MANAGEMENT OF COMPLEX GEOLOGICAL STRUCTURES USING ENGINEERING GEOLOGICAL MODELS DURING TUNNEL CONSTRUCTION: THE LUNA PARK FAULT ZONE, SYDNEY

Richard Brehaut, Beatriz Estrada[1]

Stuart Simmonds[2]

[1]PSM

[2]John Holland

ABSTRACT

This paper describes the evolution of an engineering geological model developed as part of Construction Phase Services for the Sydney Metro City & Southwest Tunnel and Station Excavation project.

Barangaroo Station, located on the southern side of Sydney Harbour, comprises a 34 m deep temporary construction shaft, 35 m long crosscut adit and 230 m long crossover cavern adjacent to the north of the 28 m deep station box excavation. The site is founded within the Permian - Triassic Hawkesbury Sandstone and transected by the Northeast – Southwest trending Luna Park Fault Zone (LPFZ).

The LPFZ was anticipated to occur at the Barangaroo Cavern. During construction, the primary LPFZ plane was initially identified in probe holes before daylighting in the temporary shaft and crosscut adit. In total, the fault zone was exposed for approximately 70 m along the strike and encountered in each of the three respective underground excavations. The total zone of structural deformation was excavated over a width 50 m along the wall of the crossover cavern, equating to a true thickness of 30 m. The structure included packages of normal and strike-slip dominated displacements which combined with high angle reverse faults, Riedal shears and orthogonal transfer faults.

A three-dimensional engineering geological model was developed within a construction environment and offered rapid reproduction of encountered conditions in a format suitable for design verification during Permit to Tunnel meetings. Geotechnical borehole and field mapping records offer detailed insights into ground conditions. However, they can be difficult to visualise in two dimensions. Understanding the details of a ground model is essential in reviewing support systems that can be readily applied (and constructed) to the variable conditions encountered within a complex structural environment. The resultant model offered high-resolution imagery and interactive three-dimensional elements that could be queried and interrogated, offering increased value to numerous stakeholders.

Beyond documenting the engineering model development during construction, this paper also intends to share our observations and contribute to existing publications and the current understanding of the LPFZ within the engineering industry.

1 INTRODUCTION

The Luna Park Fault Zone (LPFZ) is considered one of the primary subvertical structural features traversing the Sydney CBD. Originally observed during the Luna Park redevelopment (Och et al., 2004), the LPFZ had only been exposed in limited locations following surficial development along the interpreted location of the fault.

The character of the LPFZ varies at each exposed location in terms of fault thickness, extent of the damage of the surrounding rock, and general rock mass condition. Accordingly, the impact of the LPFZ for urban development is also highly variable along its length.

The excavation of the Barangaroo crossover cavern exposed the LPFZ from multiple angles. This allowed for a detailed assessment of the fault zone's characteristics. This paper presents these observations and details how the engineering geological model developed in the design phase was verified during construction and communicated to designers and contractors allowing them to adapt to the encountered conditions while maintaining and optimising excavation progress.

1.1 PROJECT DESCRIPTION

The Sydney Metro City & Southwest project creates a connection from Chatswood to Bankstown via Sydney's central business district (CBD), extending the existing Sydney Metro Northwest Line by approximately 30km. The project involved the construction of:

- 15.5 kilometres of twin railway tunnels including the city's second passage under Sydney Harbour constructed using four hard rock and one slurry Tunnel Boring Machines,
- Excavation and construction of six new metro stations at Crows Nest, Victoria Cross, Barangaroo, Martin Place, Gadigal (Pitt Street) and Waterloo
- Tunnel dive structures at Chatswood and Marrickville
- Three temporary construction and service shafts at Artarmon, Blues Point and Barangaroo
- 57 cross passages providing emergency access and egress between running tunnels
- A crossover cavern located at the northern end of Barangaroo Station to permit trains to change tracks within the running alignment.

1.1.1 BARANGAROO STATION AND CROSSOVER CAVERN

Barangaroo is a waterfront precinct located on the southern side of Port Jackson (Sydney Harbour), situated to the south of Walsh Bay and extends along the shoreline past Nawi Cove towards Darling Harbour. Barangaroo occupies a reclaimed industrial site that was formerly part of Sydney's maritime infrastructure, transitioning from a docklands area into a thriving, modern commercial and recreational precinct.

The Barangaroo metro station is positioned to service the rapidly evolving western fringe of the CBD while creating the harbourside connection to the lower north shore. The following elements were included in the Tunnels and Station Excavation (TSE) contract at Barangaroo:

- Station box excavation – 215 m x 25 m, 28 m (d)
- Crossover cavern – 230 m x 22 m x 16 m (h)
- Hickson Road access shaft (temporary) – 17 m x 10 m x 30 m (d)
- Crosscut adit (temporary) – ~13 m (h) x 12 m (w) arched

Individual elements are presented in plan on Figure 1, as well as the inferred extents of the Luna Park Fault Zone, as interpreted prior to construction.

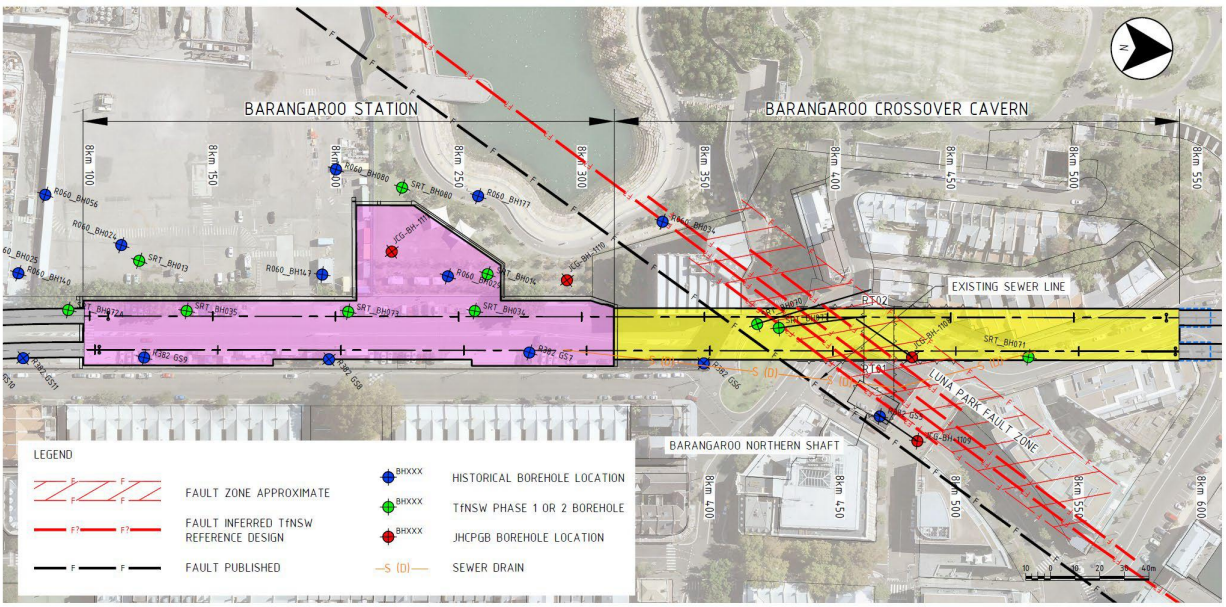


Figure 1: Barangaroo Station site plan - Station box (purple), crossover cavern (yellow). Northern access shaft and crosscut adit (dashed lines to the east of the crossover cavern) relative to the inferred extents of the Luna Park Fault Zone.

2. GEOLOGICAL SETTING

2.1 PROJECT GEOLOGY

The project is situated centrally within the Sydney Basin, which is a thick sedimentary sequence of Permian-Triassic aged rocks (290 Ma – 200 Ma). Within the project area, flat lying Lower Triassic rocks of the Hawkesbury Sandstone and Wianamatta Group dominate.

The Hawkesbury Sandstone was deposited in a fluvial paleo-environment, probably a braided river setting. Hawkesbury Sandstone is described as a medium to coarse grained, quartzose sandstone deposited in generally 1 to 3 m thick layers. These layers form primary bedding planes that range in thickness from less than 0.5 m to greater than 5 m but generally occur between 1 m to 3 m. Layers of shale breccia or clasts comprising fragments of siltstone between 50 and 4000 mm wide occur within the Hawkesbury Sandstone. They commonly occur as layers and often accumulate along primary bedding planes (Branagan et al, 1976, Pells, 2004).

Sandstone between the primary beds is described as either massive or cross bedded, the latter being referred to as 'sheet facies'.

Siltstone interbeds termed 'laminites', or 'mudstone facies', form a minor part of the unit (around 5%). Laminites typically range in thickness from 0.5 to 3 m but generally occur less than 1 m and rarely up to around 12 m. The lateral extent of these units is highly variable and can occur laterally from tens of meters to hundreds of meters (Pells, 1994). These laminate beds may be associated with increased occurring of shearing of bedding.

2.2 GEOLOGICAL STRUCTURE

The typically sub-horizontal bedded rocks of the Sydney Basin (and the cross bedded facies of the Hawkesbury Sandstone) are occasionally disrupted by regional folding and faulting. Various types of faults (normal, reverse and strike-slip) are common in the Sydney Basin (Och et al., 2009).

Concentrations or clusters of faulting and jointing are known to occur. However, the geomorphological expression of faults on the surface is limited due to extensive urban development. Therefore, the opportunity for identification of faults from surface expression is limited.

Zones of concentrated faulting and jointing have been previously identified along the Sydney Metro alignment. These zones are referred to as the LPFZ, GPO Fault Zone, the Martin Place Joint Swarm and the Woolloomooloo Fault Zone (Pells et al., 2004; Och et al, 2009). Other geological structures such as jointing and low angle thrust faulting also occur but with larger spacing and lower persistence.

2.2.1 LUNA PARK FAULT ZONE – PUBLISHED RECORDS AND DESIGN INTERPRETATION

The character and extent of the LPFZ can vary significantly at relatively short distances. Existing exposures of the fault zones in published records are described as follows:

- Miller Street rail cutting (North Sydney) - Three sub-vertical faults are documented by Longworth & McKenzie (1984) to occur within a 110 m zone. The faults strike 045 to 048° and have a fault thickness between 0.5 to 0.8 m wide comprising angular sandstone fragments within a re-cemented "rock flour". Adjacent thrust faulting was later noted by Branagan (1991).
- Luna Park (Milsons Point) - The fault zone was described as comprising two separated faults (Och et al., 2009). The eastern extent has 100 mm fault gouge with brecciated sandstone. The western extent has up to 1 m zone of observed jointing and shearing where the rock appears to be relatively intact. At the Luna Park Car Park, the character of the fault is different at the intersected walls. In the northern wall it is described as a 2 m zone of cataclastic/brecciated sandstone thinning to 1 m zone in fresher rock. In the southern wall, the LPFZ is observed as a discrete plane.
- Start City Casino Excavation (Pyrmont) - The fault zone is described (Speechley et al., 2004) as a shear zone up to 8 m wide zone comprising extremely low to very low 'sugary' sandstone with some pockets of intact medium to high strength indurated sandstone. The contact between the shear zone and the hosting sandstone is described as gradational with few defects occurring within 8 m of the edge of the observed shear zone. Steep jointing (75 - 90°) was observed adjacent to the shear zone together with brecciated shale beds dipping 10 to 15° to the west.

Based on these published observations the LPFZ was anticipated to be encountered by the Barangaroo Cavern excavation. This became a key site investigation target to constrain both site specific extents and expected geotechnical conditions. Six cored boreholes (both vertical and inclined) were drilled within the projected LPFZ lineament corridor as part of the tender and later detailed design phases. Within the proposed excavation profile fresh, high strength sandstone was intersected with localised intervals of increased fracturing. The recovered core was largely unaltered and displayed relatively discrete zones of structural disturbance, Figure 2.



Figure 2: Examples of structurally deformed, fresh Hawkesbury Sandstone from within the published LPFZ as highlighted. Borehole SRT_BH070 completed as part of the projects tender phase site investigation program.

An additional eight cored boreholes were completed by the contractor as part of its design development and risk mitigation works during early excavation of the Hickson Road temporary shaft to further assess geotechnical and hydrogeological conditions within the fault zone. Using speciality drilling equipment, low angle (15 and 30°) cored and rotary boreholes were progressively drilled within the west and southwest shafts wall. This targeted investigation allowed the sub vertical structure to be intersected more obliquely than traditional surface drilling techniques. Rising head tests were also completed to assess inflow potential within the LPFZ noting the potential hydraulic connection along strike from both Nawi Cove and Walsh Bay. The boreholes identified more intense fault gouge and deformation than previously intersected rom surface. The variable rock mass contained numerous clays seams, siltstone laminite lenses and closely spaced sub vertical joint clusters indicating a package of steep easterly/south easterly dipping shear zones were present.

3. GEOTECHNICAL VERIFICATION - CONSTRUCTION PHASE SERVICES

As part of the Construction Phase Services (CPS), the geotechnical site conditions interpreted during design were verified. The primary role as the Contractors CPS representative was to compare the encountered ground conditions during construction against the documented design assumptions and support selection criteria. If the encountered ground conditions are considered to be a departure from the design assumptions, a geological change notice was provided to the design team to formally capture the conditions and enable a timely review.

The configuration of the Hickson Road access shaft, crosscut adit and crossover cavern relative to the orientation of the LPFZ presented several geotechnical complexities. This necessitated development of a detailed three dimensional engineering geological model that could be readily updated with various data sources including boreholes, forward probe holes and geotechnical face mapping to inform both the design team and contractor throughout construction.

The following sections present selected CPS observations used to inform the LPFZ model develop during construction and aim to portray the encountered variability within the fault zone and how differently the ground conditions presented as approached from various orientations during tunnelling.

3.1.1 ACCESS SHAFT

Space constraints are commonly associated with large scale infrastructure projects in established cities. Barangaroo's Hickson Road temporary access shaft was located immediately adjacent to a live road, between two heritage bridges and active sewer connection (both considered to be sensitive structures). To accommodate these constraints, the shaft footprint at surface was smaller than its base meaning there were overhanging walls on two sides of the shaft excavation.

To manage potential instabilities, excavation was completed using relatively small lift heights, between 1.25 and 2 m. In addition to routine geotechnical face mapping, endoscope inspections were completed within the north, west and southern shaft walls. These aimed to identify adversely orientated geological structures with the potential to form unstable kinematic sliding planes as the shaft progressed through the overhanging walls at depth.

As documented by Nash et al, (2017), using endoscope inspections, it is difficult to identify defect spacing, infill, and orientation. Furthermore, assessing rock mass conditions based on recognised Sydney classification systems (Pells et al., 2008, 2019 and Bertuzzi, 2014) is nearly impossible without a full tactile assessment. This is due to the inability to measure rock strength, defect spacing and seam thickness accurately.

With close reference to adjacent cored boreholes, defect occurrences were recorded and supplemented by observations relating to gouge/clay infill, hole integrity (wash outs) and visible changes in rock mass weathering. Findings were plotted in cross section (Figure 3) and projected three dimensionally following each excavation lift to interpret the distribution of shearing withing the rock mass. A series of steep, easterly dipping shears were identified and correlated between endoscope inspection and cored boreholes drilled from within the shaft confirming a viable failure mechanism. In response, cable anchors were proactively installed from upper levels to address the identified mechanism which subsequently daylighted within the lower southwest wall.

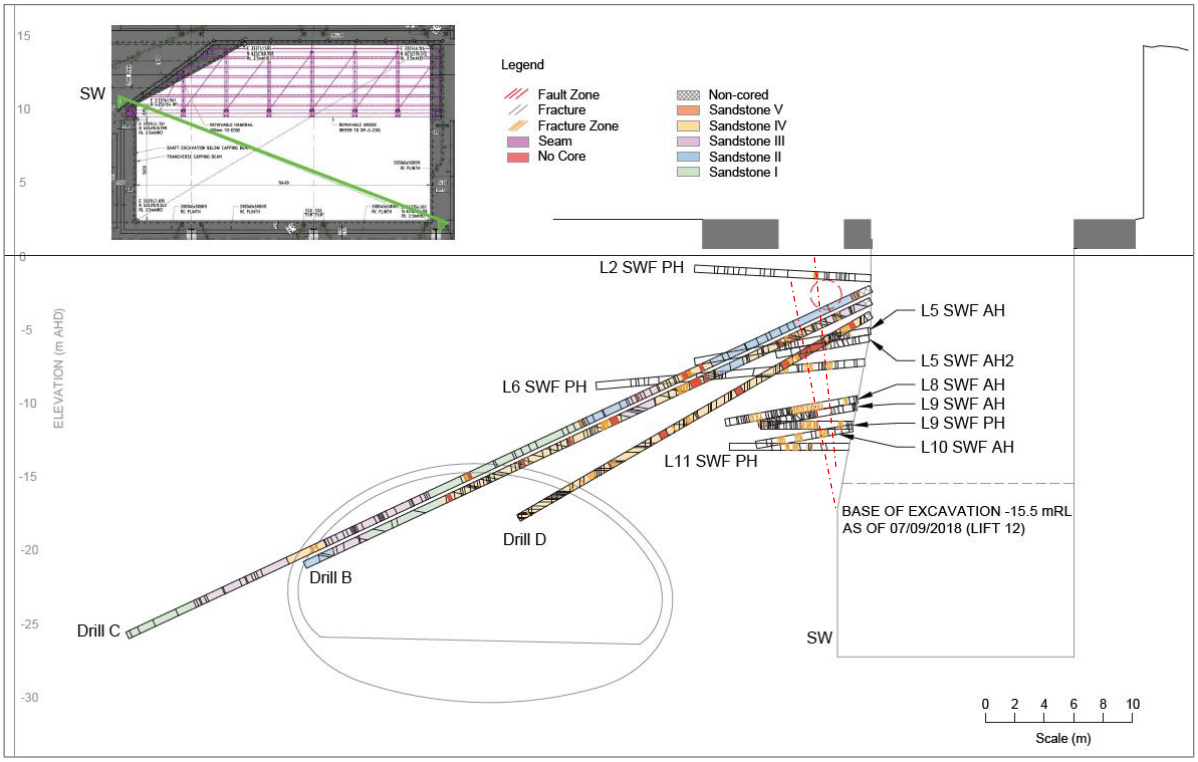


Figure 3: Cross section illustrating cored borehole and probe hole endoscope coverage within the southeast wall of the Hickson Road temporary access shaft. Adversely oriented kinematically sliding planes inferred to intersect at the base overhanging wall.

Localised instabilities were managed within subsequent excavation lifts beneath the crown level of the crosscut adit portal between -15 and -20 mRL where overbreak was observed up to 800 mm along daylighting shears, Figure 4 and Figure 5.



Figure 4: Subvertical shear daylighting in shaft wall at the crown level of the crosscut portal. Highly altered sandy clay breccia and gouge breaking away from the planar, slickensided subvertical shear at rear. Material was readily disaggregated by hand.



Figure 5: Subsequent excavation lift (approx. -20 mRL) where steeply dipping shears daylighted approximately 2.5 m vertically beneath initial plane. Note undulating defect surface and undercutting of wall along discrete sub horizontal joints

Forward probe holes were drilled and inspected with endoscopes from the base of the access shaft showing multiple zones of shearing and fault gouge material. This information was incorporated into the construction three-dimensional model to assess the forward extent and character of faulted ground prior to tunnelling. Pre-excavation support, including spiling bars, were installed. However, the bearing of the crosscut adit (260°) obliquely undercut the fault zone, which exhibited variable rock quality.

3.1.2 CROSSCUT ADIT AND CAVERN EXCAVATIONS

Geotechnical face mapping was undertaken by an experienced team of engineering geologists and geotechnical engineers using 4G enabled tablets. This hybrid digital mapping approach allowed highly detailed observations to be efficiently captured while summarising the following geotechnical attributes:

- Rock mass descriptions
    - Lithology
    - Weathering
    - Field estimated strength
    - Colour

    - Defect spacing
    - Rock class (as per Pells et al 2008, 2019)
- Defect characteristics
    - Defect type
    - Orientation
    - Shape and Roughness
    - Infill, thickness and spacing
- Design validation and nomination of additional support requirements.

An example of a CPS mapping records completed during verification of ground conditions within the crosscut adit is illustrated in Figure 6.

During excavation (late 2018), the use of photogrammetry or 3D colourised laser scanning surveys was not well established in heavy civil tunnel construction projects throughout Australia. While the technology was available, practical workflows that did not impede construction were still maturing.

At the time of construction, creation of full digital twins was not standard practice. Instead, face mapping records were georeferenced within the three-dimensional CPS engineering geological model for every advance within the LPFZ. Detailed mapping observations, combined with borehole and probe hole data, helped verify and refine the design geotechnical model, Figure 7.

Following completion of the crosscut adit's top heading, a full cross section of the LPFZ had been exposed. Both stages of excavation and primary support provided unique perspective as the fault zone was approached from different orientations. The CPS interpretation of geotechnical conditions was presented during daily Permit to Tunnel (PTT) meetings and provided a basis to confidently predict the expected conditions within the mainline cavern excavation, orientated to traverse obliquely along strike of the structure. The information informed both design team and the Contractor to forecast ground support requirements and production rates respectively.

Barraclough et al, (2021) describes the application of the CPS engineering geological model in development of additional ground support types, including a hybrid detail, to cater to the encountered conditions. Due to the oblique orientation of the fault relative to the crossover cavern, the hybrid support type enabled the Contractor to maintain a heavy configuration in areas of faulted ground while permitting lighter ground support on side of the cavern with more favourable conditions. This collaborative team approach negated program delays, allowing assembly and launch of a slurry TBM required for the harbour crossing to the Blues Point Shaft on the north shore.

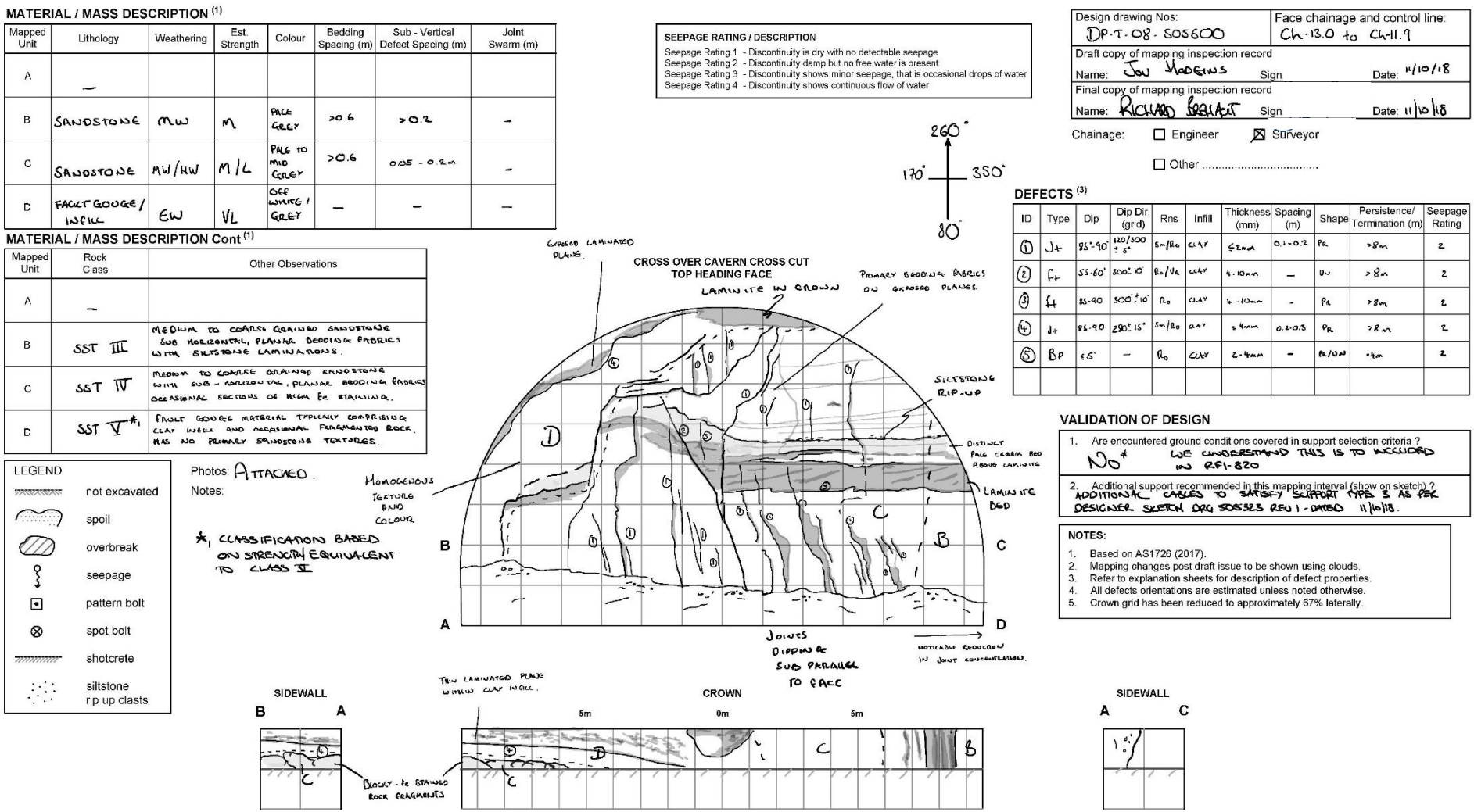


Figure 6: Example of detailed geotechnical face mapping records completed for individual tunnelling advances capturing the variable character of the LPFZ during construction.

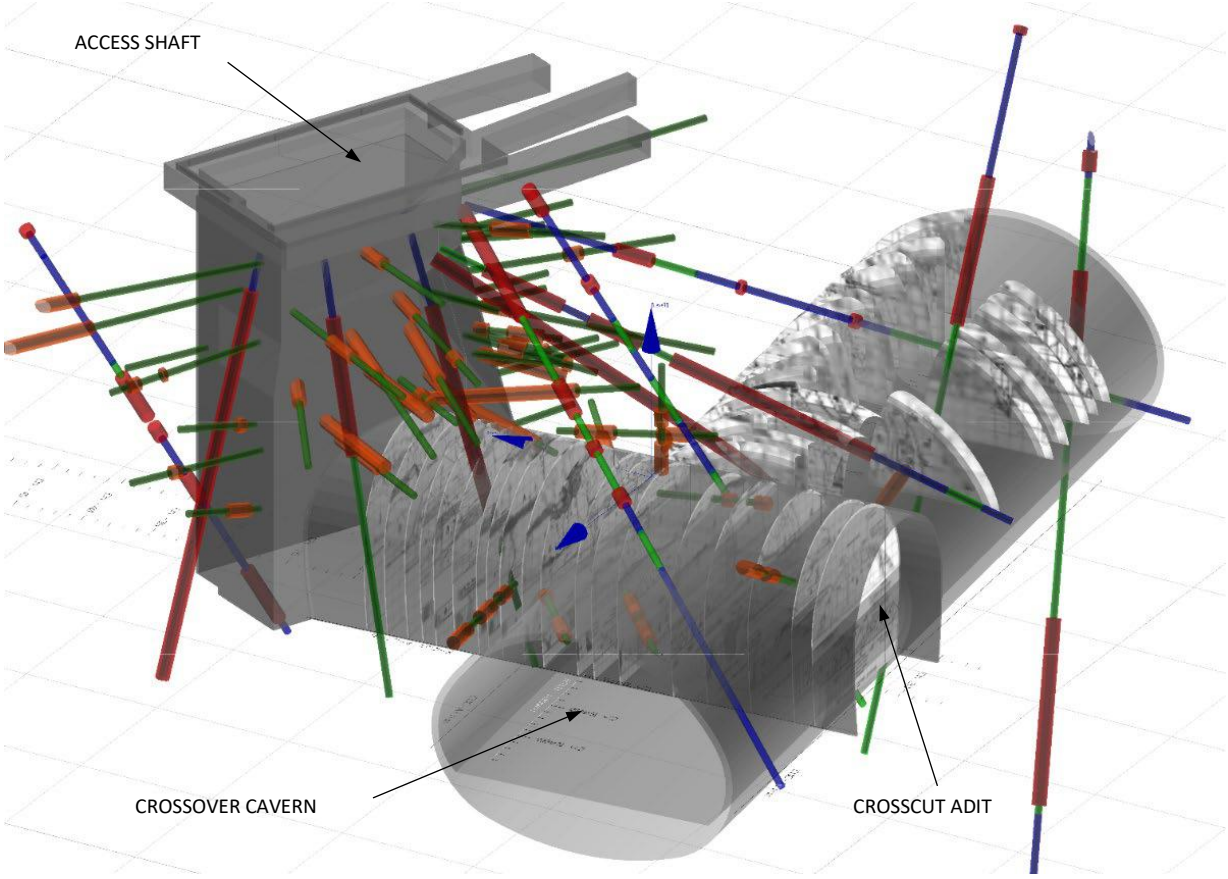


Figure 7: Oblique view showing data density of CPS face mapping, borehole and probe hole inspection records within the LPFZ portion of the Barangaroo crossover cavern looking south east. Boreholes (inclined) are displaying relative to the Pells classification - Blue Class I/II, Green Class III, Red Class IV/V. Probe holes (sub horizontal) presented using project specific classification for faulting - Green – Not fault affected, Orange – Fault affected.

4. SUMMARY OF ENCOUNTERED CONDITIONS WITHIN THE LPFZ

The sub vertical LPFZ, striking northeast (020 to 040°), was encountered for a length of approximately 50 m along the Barangaroo crossover cavern and temporary access excavations. The total exposure equated to a true thickness of approximately 30 m. The delineated extents of the LPFZ as included in the project geotechnical interpretive report and published literature were shown to be well aligned. The fundamental refinement in our understanding of the ground conditions was to characterise the nature and variability of ground conditions. Having the opportunity to excavate the fault zone from numerous orientations and over extended distances permitted a level of interpretation not achievable through the review of boreholes and limited surface exposures.

As encountered at Barangaroo, the LPFZ comprises a series of distinct structural deformation intervals. Individual aspects of the broader fault zone are summarised below with selected face mapping intervals included for reference in Figure 8 and Figure 9. The fault extents are also presented in plan as projected within the three-dimensional CPS engineering geological model in Figure 10.

- **Fault Core** - Three primary shear planes were observed within the central fault core of the LPFZ, orientated 75-85°/125-135° and 65-70°/090-100° (Dip/DipDirection) respectively and diverging with depth. These structures were infilled by up to 300 mm (true thickness) highly altered, soft mottled white and grey, highly plastic, sandy CLAY breccia. A magnesium coating was observed on the bounding slickensided shear surfaces, Figure 4 to Figure 6.

- **Fault Disturbed** – The rock mass located immediately west of the "fault core", is described as typically low strength highly fractured sandstone with persistent defects spacing less than 200 mm. Fault breccia's are observed to anastomose along strike resulting in changes to local scale shape and infill, Figure 8.
- **Fault Margins** - Two fault "margin" zones were encountered further west of the "fault disturbed" zone, summarised as corridors comprising discrete structures with minimal clay infill and associated sympathetic jointing with a true thickness of approximately four to five metres, Figure 9.

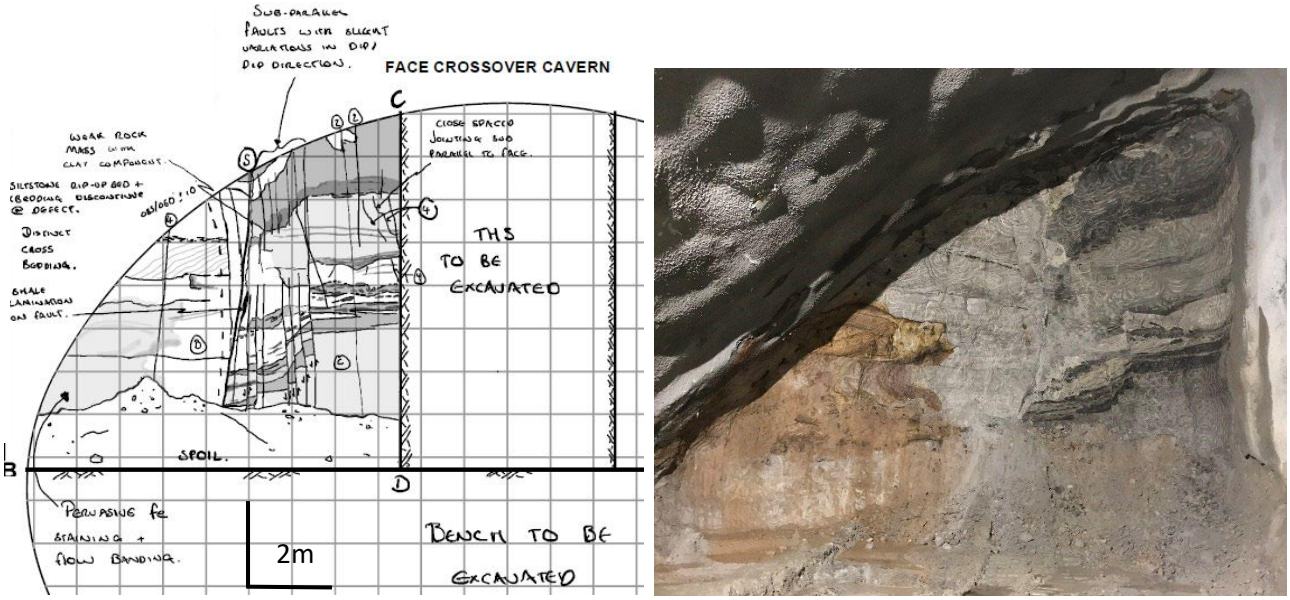


Figure 8: CPS face mapping excerpt of the Fault Core/Fault Disturbed Zones from the south left side, southbound heading. Laminite beds provided marker horizons to assess displacement between individual fault planes. Localised zones of moderately weathered sandstone were also observed on multiple occasions owing to preferential water flow along the fault.

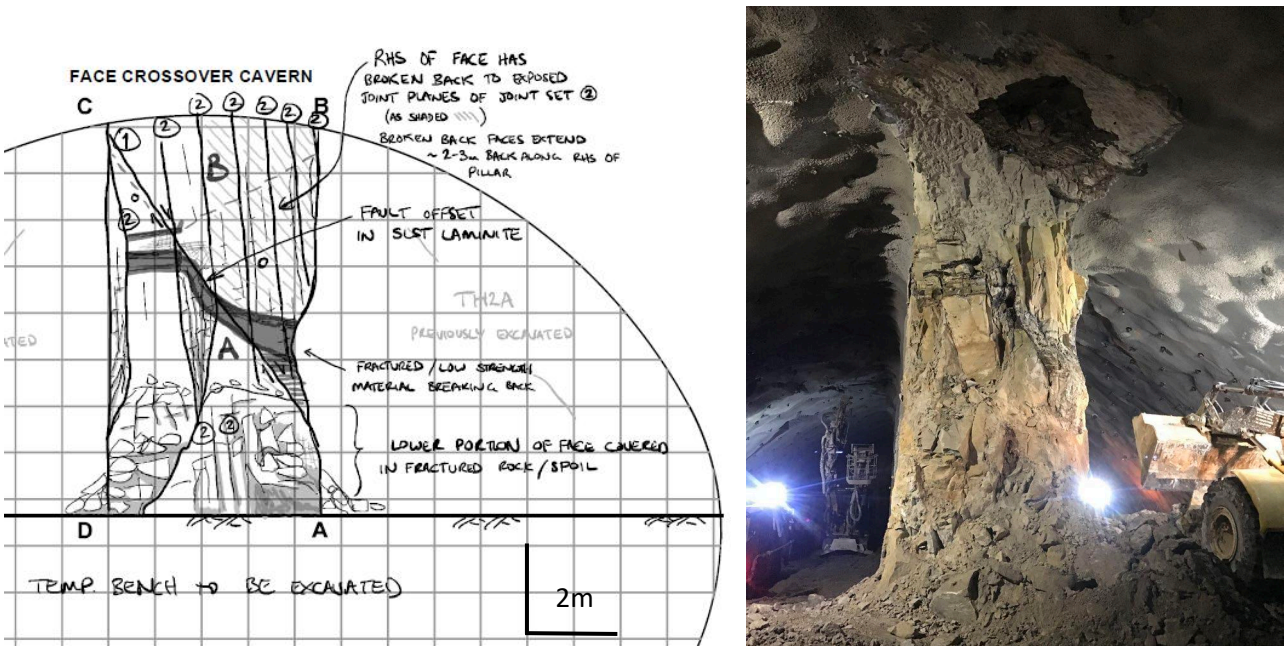


Figure 9: CPS face mapping excerpt of the Fault Margin Zone from the central cavern pillar (CH8476.6m) being excavated as part of a three stage, top heading advance. Image looking toward 350°.

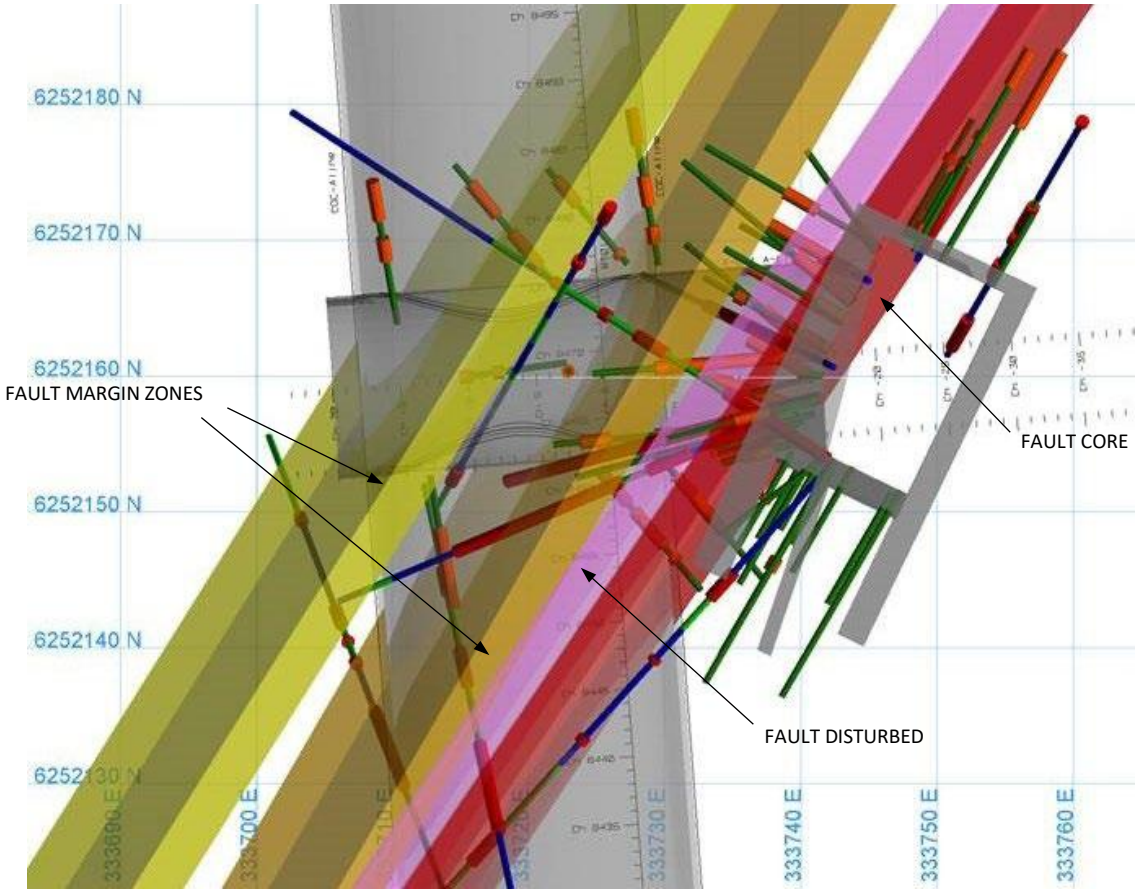


Figure 10: Plan view summary of the CPS model illustrating exposed extents of the LPFZ with the Barangaroo crossover cavern. Interpreted zones delineated as follows: Fault core – red, Fault disturbed – magenta, Fault margin zone – orange and yellow.

Normal and strike-slip movements were interpreted along individual fault planes with the LPFZ. At a local scale within the excavation, other high angle reverse faults, Riedal shears and orthogonal transfer faults were observed to have taken up strain within the deformation zone. Absolute displacements were unable to be measured, particularly with respect to strike slip movements. The presence of laminate lenses provided clear marker horizons for assessing local scale vertical displacements within construction faces.

To the east of the immediate LPFZ boundary were a series joint clusters and discrete faults (100 to 300 mm offset and minimal infill) orientated subparallel to the main fault plan. Also associated with the eastern fault boundary was a localised zone of moderately weathered rock. These features may act a marker boundary should the structure be encountered in future developments.

The potential for groundwater connection to the adjacent harbour was identified as a risk during detailed design. However, the underground excavation experienced no notable groundwater inflow on either side of the fault during construction. The small inflows that did occur were consistent with rates estimated during rising head testing at the Hickson Road shaft and were equal to less than 1.0 L/s.

5. CONCLUSIONS

As part of the Sydney Metro City & Southwest Project the Barangaroo crossover cavern underground excavation provided a unique opportunity to observe and characterise the LPFZ. The integration of geotechnical data from boreholes, probe holes, and detailed geotechnical face mapping enabled the development of a comprehensive three-dimensional model that supported design verification and construction decision-making.

The LPFZ was observed to comprise distinct structural deformation zones, including a fault core with significant clay-rich shear planes, a fault-disturbed zone with high fracture intensity, and fault margin zones with discrete faulting and

joint clusters. The ability to assess the LPFZ from multiple excavation orientations greatly improved the broad understanding of fault variability and ground response to tunnelling. As echoed by Och et al (2012), it is hoped that these learnings can be applied to future projects that may encounter the structure, particularly in the interpretation of site investigation data and development of ground support designs.

The observations from this study contribute to the broader geological understanding of the LPFZ and highlight the importance of ongoing refinement of engineering geological modelling during construction.

6. ACKNOWLEDGEMENTS

The authors wish to acknowledge the commitment and dedication of our colleagues who contributed to the construction phase services delivery for the project. The quality of observation and resulting mapping detail has created an excellent record of the encountered conditions and are a credit to the individuals that created them.

Further appreciation is extended to the construction and management team from John Holland CPB Ghella Joint Venture for their collegial approach and valued contributions as we progressed through some of Sydney more structurally complex tunnelling conditions. A perspective of the completed northern half of the cavern excavation is included in Figure 11.



Figure 11: View of the final excavation profile of the Barangaroo crossover cavern.

7. REFERENCES

Barraclough, P., Brierley, R., Amon, A. and Simmonds, S. (2021) Sydney Metro City & Southwest TSE – design and construction of the Barangaroo Cross Over Cavern through the Luna Park Fault Zone. *Proceedings of the Australasian Tunnelling Conference,* 235 - 254

Branagan, D., Herbert, C. and Langford-Smith, T. (1976) An outline of the geology and geomorphology of the Sydney Basin, Science Press, Department of Geology and Geophysics, University of Sydney

Branagan, D.F. (1991). Geology of the Pyrmont-Ultimo Area, Sydney. *Twenty Fifth Newcastle Symposium on Advances in the Study of the Sydney Basin.*

Bertuzzi, R. (2014), Sydney sandstone and shale parameters for tunnel design, Australian Geomechanics Journal, 49(2), 95-104.

Nash, T.R., Shen, B., and Bertuzzi, R. (2017). Geotechnical validation for Sydney Tunnels. *Proc., 16th Australasian Tunnelling Conference, Australasian Tunnelling Society, Engineers Australia.*

Och, D.J. Offler, R., Zwingmann, H., Braybrooke, J., & Graham I.T. (2009). Timing of brittle faulting and thermal events, Sydney region: association with the early stages of extension of East Gondwana. *Australian Journal of Earth Sciences, 56,* 873-887.

Och, D.J. Davies, S. Gilchrist, D. Kotze, G. Bowden, A and McNally, G (2012), Ground investigation in the Sydney CBD - A more sustainable model for the future. *Australian Geomechanics, 255-260.*

Pells, P.J.N. (1994). Engineering geology of the Triassic rocks of the Sydney area. www.pellsconsulting.com

Pells, P.J.N., Mostyn, G.R., and Walker, B.F. (1998). Foundations on sandstone and shale in the Sydney region, *Australian Geomechanics, 33(2),* 17-29.

Pells, P.J.N., Och, D.J., & Braybrooke, J.C. (2004). Map and selected details of near vertical structural features in the Sydney CBD. *Distributed at the Australian Geomechanics Society Sydney Chapter Mini-Symposium.*

Pells, P.J.N., Mostyn, G., Bertuzzi, R., & Wong, P.K. (2019). Classification of sandstones and shales in the Sydney region: A forty-year review. *Australian Geomechanics,* v.54: No. 2.

Speechley, L., Walker, B., & Scholey, G. (2004). Some examples of variability within Hawkesbury Sandstone. *Australian Geomechanics, 39(3),* 23 - 30.

https://doi.org/10.56295/1ACEG08

CASE STUDY ON SNOWY 2.0, AUSTRALIA: USE OF LIDAR AND ENDOSCOPY FOR ASSESSING AND MODELLING GEOLOGICAL FEATURES IN UNDERGROUND CAVERNS

B. Potter *SHL*
A. Blaise *Tractebel*
B. Requiliani *Webuild*
E. Guevara *Webuild*
K. Stariha *SMEC*

ABSTRACT

Snowy 2.0 is a major pumped hydropower project currently under construction in Australia that will complement the existing Snowy Mountains hydroelectric system, adding an additional 2200 MW to the national energy grid. The Power Station Complex (PSC) for the project comprises 3 caverns, a shaft, and some 10 km of Drill and Blast excavated tunnels, at a depth of over 750m. The Machine and Transformer halls within the PSC are excavated using an observational approach to excavation, requiring a thorough understanding of encountered conditions and excavation behaviour.

Traditional mapping techniques in tunnels face challenges due to limited accessibility and visibility. This case study describes the use of survey controlled Light Detection and Ranging (LiDAR) scans of the excavated face to augment traditional mapping, used together with downhole endoscopy and optical televiewer (OTV) to identify and project major defects in 3D modelling softwares. Integrating these technologies has allowed for comprehensive defect detection, persistence and waviness assessments on the cavern scale, and accurate orientation measurements which can be combined with defect conditions assessed in traditional mapping. This is key in the observational approach to excavation, providing a highly accurate geological model which allows a verification of design assumptions, comparison of geological features to monitoring, highlighting areas where bolt shear may be of concern, and ensuring a comprehensive and accurate owners model for the operations phase of the scheme.

1 INTRODUCTION

The Snowy 2.0 project is a major pumped-storage expansion of the iconic Snowy Mountains Hydroelectric Scheme, which forms a vital part of Australia's energy transition towards a low-emissions future. The existing Snowy Hydro Scheme is a major hydroelectricity and irrigation system located in the Snowy Mountains, New South Wales, Australia. Built between 1949 and 1974 it is considered one of the civil engineering wonders of the world, with a 4.1 GW capacity. The existing scheme comprises 16 dams, 8 hydropower stations, and 145 km of tunnels.

Snowy 2.0 is an augmentation of the existing scheme, and is currently under construction. It will add 2,200 MW of energy generation capacity, with storage of 350,000 MW hours. At full capacity Snowy 2.0 will be able to generate for almost one week without pumping.

The Snowy 2.0 project is led by Snowy Hydro Limited as the owner, with SMEC providing technical engineering support to the owner for the geotechnical and tunnelling scopes in particular. The principal contractor for the civil works is Future Generation Joint Venture, a consortium comprising Webuild, Clough, and Lane, responsible for the civil construction works. The design joint venture is composed of Lombardi, Tractebel, and Coffey, with cavern design specifically falling under Tractebel's scope within the joint venture.

Similar to the existing scheme, Snowy 2.0 involves extensive underground works, both in terms of scale and intricacy, and is situated within a complex and highly variable alpine geological and hydrogeological setting. The underground works comprise ~33 km of TBM driven tunnels, ~10 km of drill and blast tunnels, three deep shafts, and a large power station complex located ~750 m underground. Of particular note within the power station complex are the Machine Hall (MHA) and Transformer Hall (THA), which are amongst the largest, widest and deepest caverns in the world. The MHA and THA are approximately 310,000 m³ and 160,000 m³ volume, 33 and 20m span and 61.5 and 46m height respectively.

Although comprehensive site investigations were undertaken prior to works commencing, the depth and extent of underground works and access constraints for surface investigations prevented a full characterisation of ground conditions prior to excavation. As such, an observational approach to excavation has been adopted across the project, with a continuous assessment of excavation performance and verification of design assumptions ongoing.

This has been particularly key for the MHA and THA where, due to the height of the structures, it is imperative to understand as early as possible whether the conditions are within design assumptions, whether the excavation is behaving as expected, and whether appropriate support and construction staging have been applied. Once excavation proceeds beyond a certain depth, any re-works in the crown will become remarkably challenging. The MHA and THA have a design life of 150 years.

Due to the depth of the excavation, shearing along geological discontinuities is considered to be a risk, potentially compromising installed support. The location and nature of any geological structures is therefore of key interest and has been the subject of many varied investigations. These have ranged from cored holes both from the surface (over 1km long) and from within adjacent excavations and the caverns themselves, to construction records such as geological mapping and endoscope imagery undertaken within drainage and monitoring holes. To supplement traditional mapping techniques, the project has invested in the use of survey controlled Light Detection and Ranging (LiDAR), to scan the excavated face and allow for a spatially and colour accurate record of the exposed rock. The compilation and processing of these scans has allowed for the accurate tracing of geological discontinuities within the excavations to date.



Figure 1: Layout and location of the original Snowy Hydroelectric scheme, with the Snowy 2.0 project currently under construction in orange

Integrating these technologies has allowed for the generation of highly accurate 3D geological models maintained by the designer, contractor, and owner, in Rhino 6, Leapfrog Works 2024.1 and Maptek's Vulcan 2024.4 (alongside sister software PointStudio and GeologyCore, herein 'Vulcan Package') respectively. These are used to confirm design assumptions and inform Hold Points within the cavern construction, allow for optimisations in construction staging, and form a permanent record of encountered conditions. Not only is our understanding of the location of defects improved, but also the understanding of defect properties, in particular persistence and waviness, which are otherwise difficult to obtain from localised sources such as cored holes and traditional face maps. Excavation is able to proceed safely, ensuring that all major defects are monitored and that support integrity is maintained.

This paper will explore the innovative approaches and technologies integrated into the cavern excavations, highlighting how they contribute to the successful implementation of an observational approach to tunnelling.

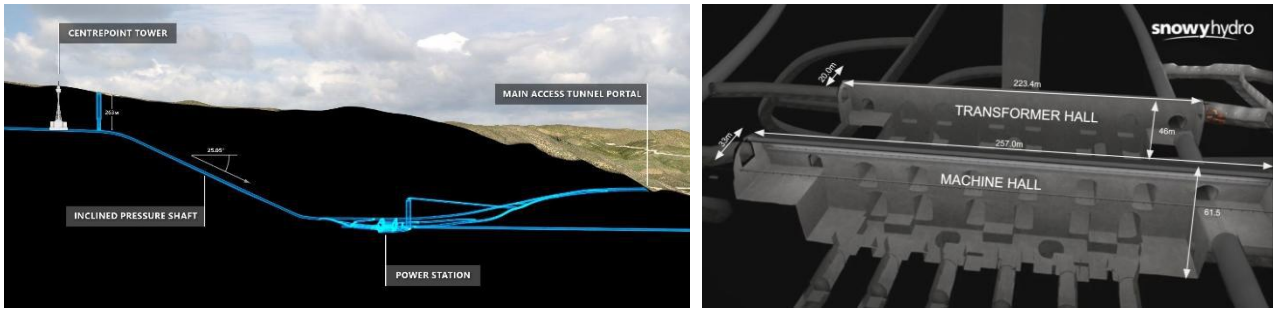


Figure 2: a) Schematic showing the main underground works area on Snowy 2.0 (excluding the Headrace and Tailrace tunnels); and b) Schematic of the Machine and Transformer halls within the Power Station Complex.

2 METHODOLOGY

2.1 DATA SOURCES

The geological model for the MHA and THA is fed with several data sources, as follows:

1. Site investigations, comprising cored holes and in-situ testing - both from the surface and underground
2. Downhole imagery in percussion-drilled probe holes - both exploratory holes directly ahead of the excavation, and holes in the cavern crown for drainage and shear displacement monitoring. Imagery is collected using Optical Televiewer (OTV) and/or Endoscope camera inspection, and drilling parameters are also recorded.
3. Geotechnical mapping is undertaken at each advance, as per ASTM D4879-08.
4. LiDAR scanning of the exposed rock face is undertaken at each advance.

2.1.1 Site Investigations

The Machine and Transformer Halls have been targeted with several phases of geotechnical investigations throughout the design phase of Snowy 2.0. A total of 7 cored boreholes were progressed from the surface into the Power Station Complex area, up to 1057 m in length. Given the cavern's depth of up to 750 meters below ground, and access constraints on the surface, geotechnical drilling from the surface is time-consuming and costly. To enhance geological understanding and confirm design assumptions, additional cored boreholes have been drilled from adjacent excavations as they progressed close to MHA and THA, and from within the caverns themselves. These have included multiple oriented cores into the pillars between the caverns, and a 250-meter-long horizontal core along the axis of the THA crown. Oriented core, and Optical Televiewer (OTV) and/or Acoustic Televiewer (ATV) imagery in these holes allowed for an understanding of defect frequency, orientation and condition prior to cavern excavations commencing.

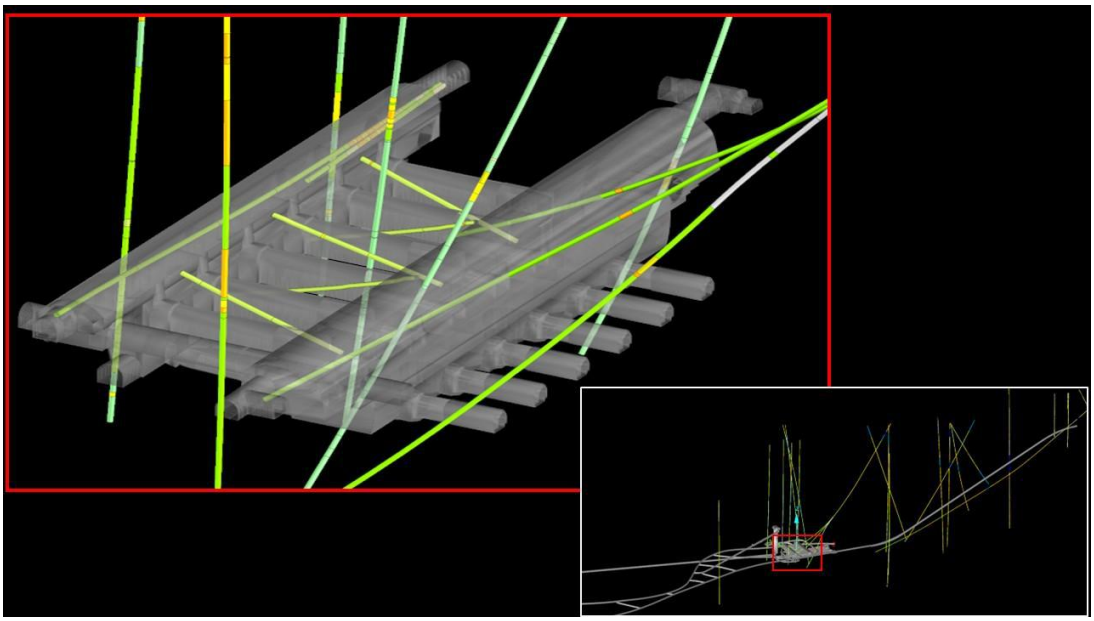


Figure 3: Cored holes undertaken from the surface (refer to inset) and underground at power station cavern (main figure), looking north-north-west. Colours indicate lithology, adjacent tunnels removed for clarity.

2.1.2 Downhole Imagery

Endoscope camera and Optical Televiewer (OTV) are performed in probe holes ahead of the excavation face, and also at the perimeter of the excavation (drainage holes, multi-strand anchors for corbels, and shear displacement monitoring holes) to gain advanced understanding and characterisation of joint set orientations in the rock mass around the excavation periphery. Downhole imagery allows (1) to detect major joints or shear planes which might have not yet been encountered ahead of the cavern excavation, i.e., joints striking out only later in the excavation at the lower part of the cavern, and (2) to follow the evolution of a critical discontinuity at different stages.

To capture endoscope footage, the project utilises a DGRT Wireline Digital Camera 360 View Model 003169, or a SeeSnake CS6X. These capture a forward-facing video of the hole as the tool is inserted or extracted. Contractor's geologists analyse endoscope videos, and note the depth and description of major defects. Endoscope is typically used in place of OTV, where the latter cannot be attained due to physical constraints.

To capture OTV, the project utilises a QL40 OBI-2G Optical Borehole Imager which implements a high-resolution CMOS digital sensor combined with a fisheye lens. This produces a clear 360º continuous-unwrapped digital picture of the borehole walls. OTV images are processed and interpreted using the software WELLCAD (v5.6). Features are classified by type and aperture (such as bedding, parting, closed joint, open joint, seam, etc), and the Rock Quality Designation is calculated. Data can be exported with orientation and categories of the picked features in .csv format.

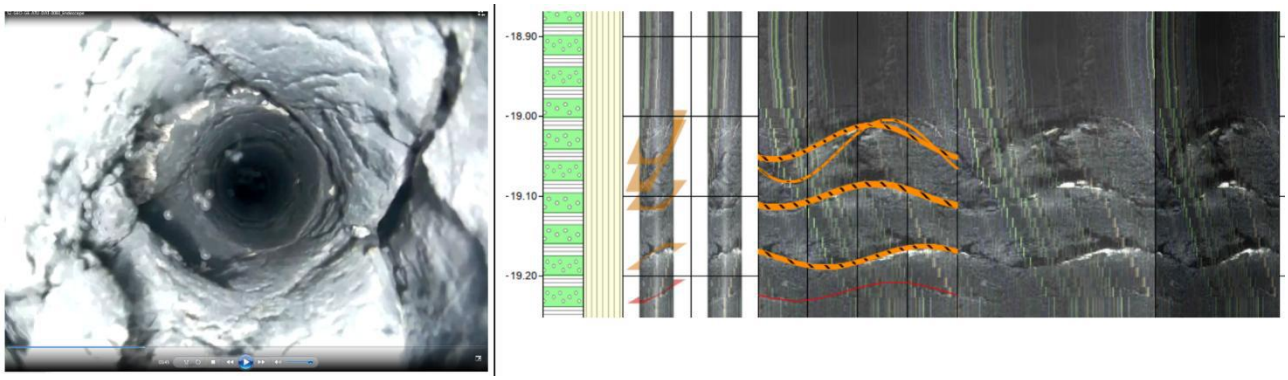


Figure 4: Discontinuity detected in an endoscope (left) vs data available from interpreted OTV (right)

2.1.3 Face Mapping

Geotechnical mapping is undertaken at each advance, as per standard ASTM D4879-08. The face is mapped by the contractor's geologists, who document detailed descriptions of the discontinuities and defect sets encountered. They also assign a suite of geotechnical parameters which are used as the basis for geomechanical classifications such as the Geological Strength Index (Hoek, Carter, Diederich 2013), Q-system (Barton et al. 1974) and Rock Mass Rating (Beniawski 1989) as well as assigning project-specific Ground Types and Ground Behaviours. These all inform the support class required for the tunnel advance as well confirming the ground conditions remain within the design limitations. A new digital acquisition system is currently being implemented for geotechnical mapping through TUGIS software. This software will streamline the import process of mapping data and pictures into a database which will simplify the modelling of geological features both in TUGIS and other modelling softwares.

2.1.4 LiDAR

During the course of survey and geotechnical inspections of freshly excavated faces, LiDAR scans are collected by the contractor's survey team using a Leica RTC360 at millimetric accuracy as a part of the project's employer's requirements. These LiDAR scans allow for survey and colour accurate 'point clouds' of the excavated advance. The point cloud effectively captures the surfaces of discontinuities and lineaments, as the face is scanned from a single origin, capturing shadows cast by protruding surfaces. Thus, by importing these scans, discontinuities can be identified and traced without having to georeference and extensively interpret mapping records. This allows for continuous tracking of defects across multiple advances and headings. Note that this paper focuses exclusively on LiDAR scans on rock surfaces, although the project also utilises LiDAR scans of shotcrete surfaces for as-built records and long-term monitoring.

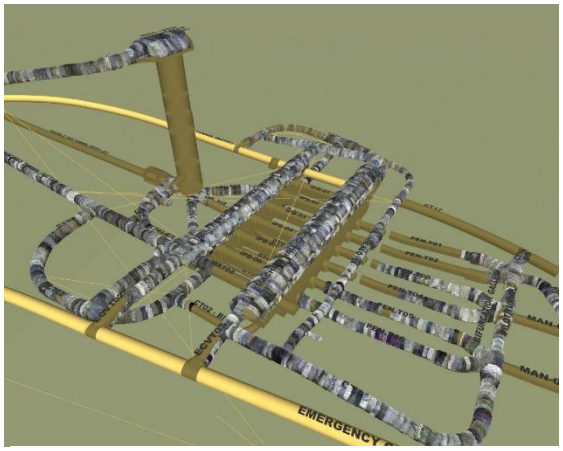


Figure 5: Revizto model of LiDAR scans captured through the excavation of D&B tunnels in the PSC area.

2.2 INTEGRATION AND MODELLING

Collected geological data is integrated into 3D geological models maintained by the designer, contractor, and employer as follows:

- The Designer maintains a geological model in Rhino 6, which is used to feed a digital twin in 3DEC, (Tonioni et al 2024), (Hernandes et al 2025), supporting the observational approach to excavation and informing Witness and Hold Points throughout the cavern excavations. Encountered geological conditions are modelled to assess predicted excavation behaviour and resulting support adequacy.

- The Contractor maintains a geological model in Leapfrog Works, which is a factual summary of major structures encountered in excavation. This provides insight into whether any features may be expected within the remainder of works, and whether this will have an impact upon construction. This will also form the basis of an as-built record.
- The Employer maintains a geological model in the Vulcan package for verification and risk mitigation. This provides an additional layer of rigour, helping to enhance geological insights and ensure that the Owner's model for operations will contain a comprehensive understanding of encountered conditions and any features requiring monitoring. This approach mitigates operational risks by ensuring potential geological challenges are identified and managed proactively.

The outcomes of the probe holes and explorative investigations are corroborated by the advancements in geotechnical mapping. The table in Figure 6 summarises the diagram flow to process the Geomodel used by the Contractor - starting from the input process, followed by the tools and techniques used to generate finally the model output. The different data sources, and how they are integrated into each model, is tabulated below in Table 1.

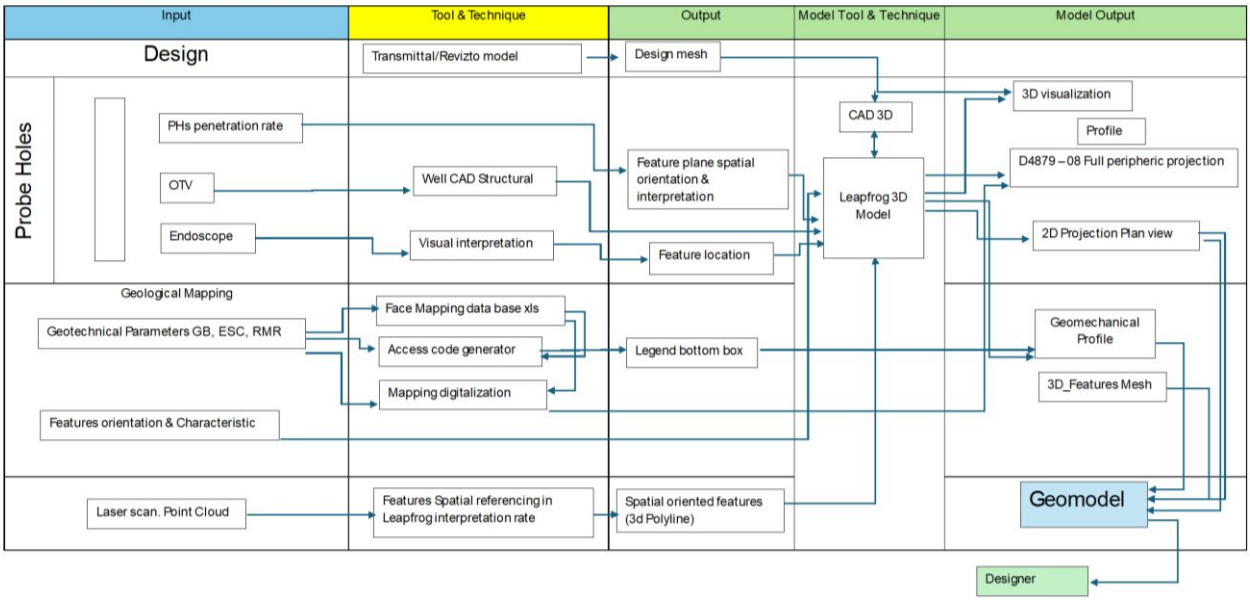
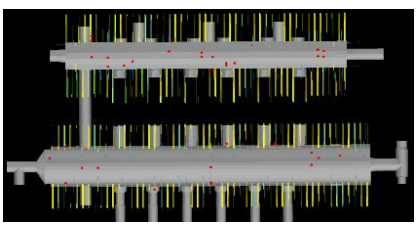
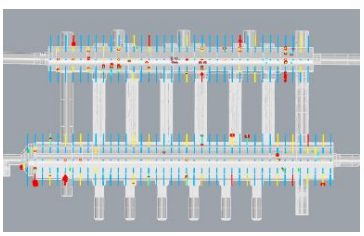
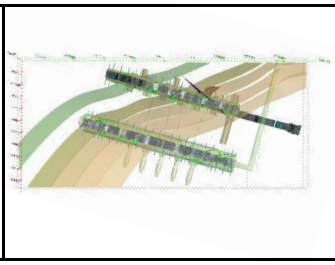
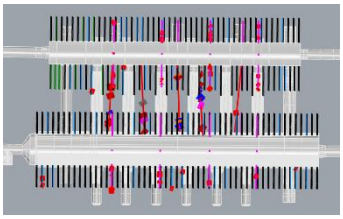
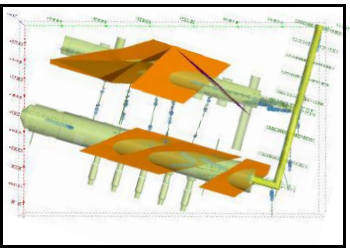
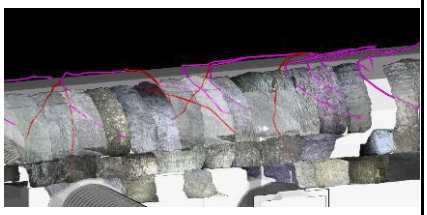
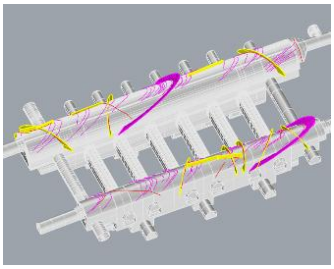
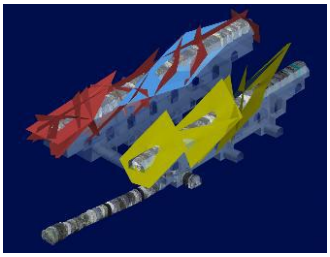
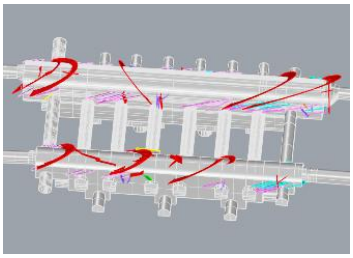
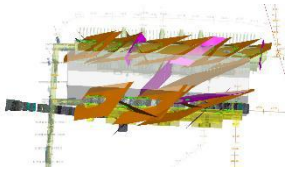


Figure 6: Conceptual map for the development of Geomodels - in use on Snowy 2.0 by the Contractor

Table 1: Methodology for modelling various data sources in each software package

Data Source	Vulcan Package	Rhino 6	Leapfrog Works
Endo-scope	Depths of defects encountered in each hole are recorded by geologists, imported as point data, and plotted as a point along the drill hole.		
			
OTV	OTV data is exported from the WellCAD .tfd file and saved as a .csv, which can then be imported and displayed as structurally orientated planes.		

	The OTV image itself can also be imported, but relies either on a license extension not available on the project, or a georeferenced image.		
LiDAR	Imported as las or laz files. Discontinuities are traced by creating lines between selected points. A simple projection to a plane can then be made using these points, or using the 'Fault Manager' to account for waviness.	Import of LiDAR is limited, this model relies on export of lines and surfaces of defects picked in the Vulcan Package with cross-checking of traditional mapping.	Processing and interpretation of true colour LiDAR is challenging, therefore this model imports defects as traces or projections
			
Traditional Mapping	Each map has a coordinate assigned, to which the data from mapping (defect type, orientation, properties, etc) is aligned.		Mapped features are traced into a geomechanical profile in AutoCAD 3D, and then integrated into Leapfrog.
	This data is then imported into the Vulcan database, with features typically displayed as structurally oriented discs.		

2.3 DESIGN VERIFICATION

The observational method is currently implemented for the excavation of the PSC. This is supported by the Rhino 6 geomodel and associated 3DEC digital twin (Tonioni et al 2024, Hernandes et al 2025), which are used to inform design control points (Witness Points and Hold Points) defined along the excavation of the PSC. The main objectives of the observational method for design verification are:

- To confirm (or update) the geological conditions and model,
- To confirm the validity of the design (for the actual geological conditions and model),
- To provide design adjustments if the actual conditions differ from the expected design scenarios.

The digital twin model is based on 2 levels of analyses:

- The first level of analyses is the investigation of main discontinuities that can be potential critical areas for the PSC in terms of compliancy of the rock support with the acceptance criteria. The geomodel is continuously updated with the data collected, developed in Sections 2.1 and 2.2 above. Identified potential critical discontinuities are plotted in Rhino 6 geomodel.
- The second level of analyses is developed with 3DEC to carry out "back analyses" identifying the rockbolts exceeding the design criteria based on updated parameters. Georeferenced discontinuities from Rhino 6 geomodel are one of the updated parameters that are inputs of the 3DEC model.

3 RESULTS

3.1 DATA INTEGRATION AND COMPILED MODEL

The integration of LiDAR scans, face mapping, cored holes, downhole endoscopy, and OTV imaging enabled precise identification and tracking of geological features throughout and between the adjacent MHA and THA. This allowed for a detailed understanding of feature orientation and location, which is particularly critical in areas such as intersections with IPB galleries and access tunnels. See below Figure 7 to Figure 9 displaying the final locations of defects tracked in each software, up to the current state of excavation.

Tracing features across multiple datasets also allowed the spatial extent of individual features to be interpreted. Accurate tracing of major features encountered in the sidewalls of the excavations (from LiDAR and mapping), combined with investigative data between and above the caverns (imagery in perimeter holes and cored holes), allowed for a significantly improved understanding of persistence as compared to traditional face maps alone, which are by their nature limited to the field of view. Projecting features between caverns allowed for alignment with information from cored pillar holes and imagery in perimeter holes, showing where features are expected to intersect the pillars. Shears aligned with bedding exhibited significant persistence, typically extending beyond the cavern span, whereas non-bedding-aligned features displayed variable continuity. Additionally, LiDAR scan traces verified that shears exhibited waviness across all orientations, at scales which were much clearer from adjacent LiDAR scans than from individual maps. This allowed for the verification of design assumptions on dilation angle.

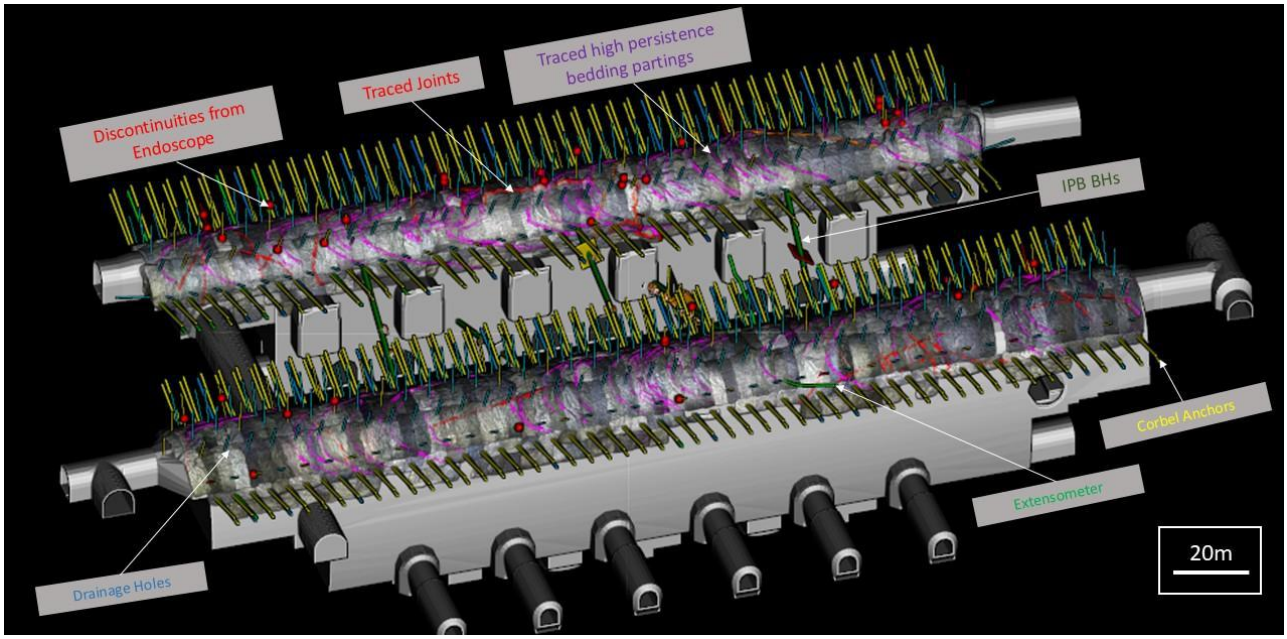


Figure 7: Vulcan package complete geomodel up to current state of excavation, looking north-west

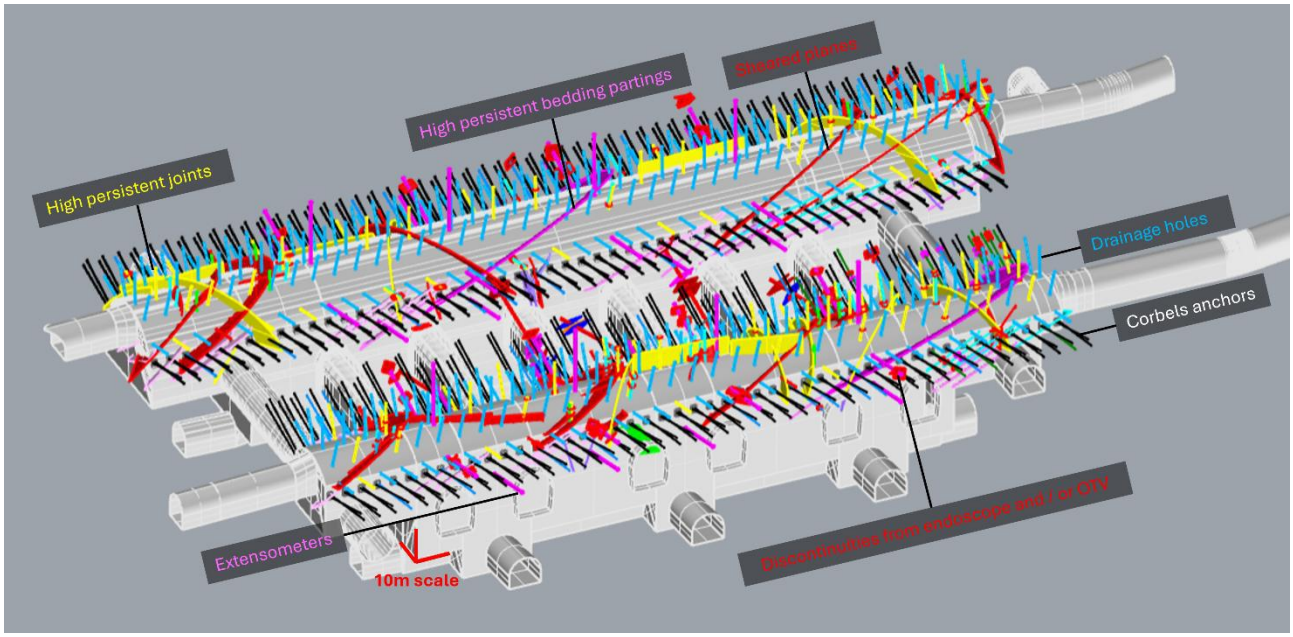


Figure 8: Rhino 6 complete geomodel up to current state of excavation, looking north-west

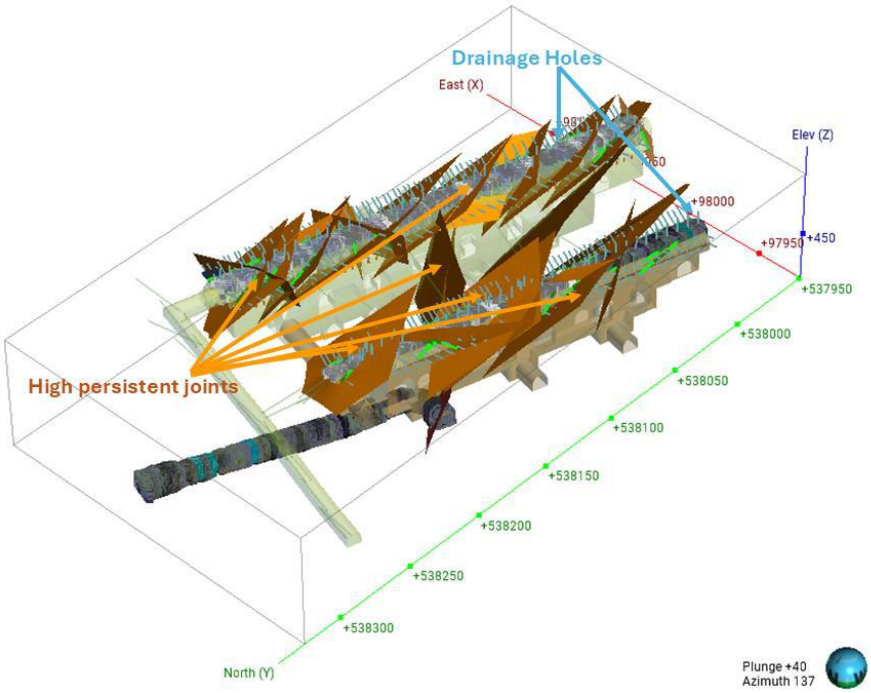


Figure 9: Leapfrog geomodel up to current state of excavation, looking north-west

3.2 CASE STUDY: OVERBREAK IN THA/IPB INTERSECTION

The case study below shows the importance of tracking the location and orientation of features proximal to sensitive locations, in this case, the intersection of the THA and an Isolated Phase Busbar (IPB) gallery. During the geological mapping of each excavation, geological overbreak (GOB) may be identified by the site geologist, occurring when intersecting defects result in the excavation profile exceeding that of design. One such event was identified in the sidewall of the THA, at the future location of the crown of a tunnel immediately adjoining the cavern, as demonstrated in Figure 10 below.

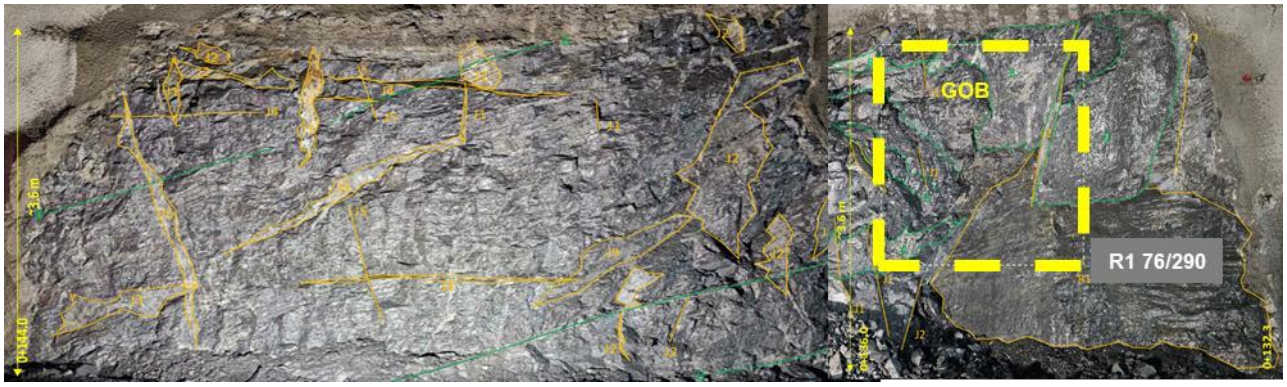


Figure 10: Mapping TH upstream Ch. 132.3 to 144.0

By importing the LiDAR scans of this advance and those neighbouring, the same discontinuity was able to be identified across multiple advances and even benches. This meant it could then be traced directly using the LiDAR scan as demonstrated in Figure 11 below. The orientation of this defect was consistent between both traditional mapping and LiDAR; dip 70 to 80°, dip direction 280 to 290°.

In the construction phase boreholes so far undertaken, this defect has not been detected, thus suggesting that it has a relatively low persistence. However, as construction continues benching down, it allows for additional support to be installed if required, boreholes to be conducted to refine the interpretation of the persistence of the feature, and the targeting defects for shear displacement monitoring should there be a concern it poses a geotechnical risk, such as shearing of installed support.

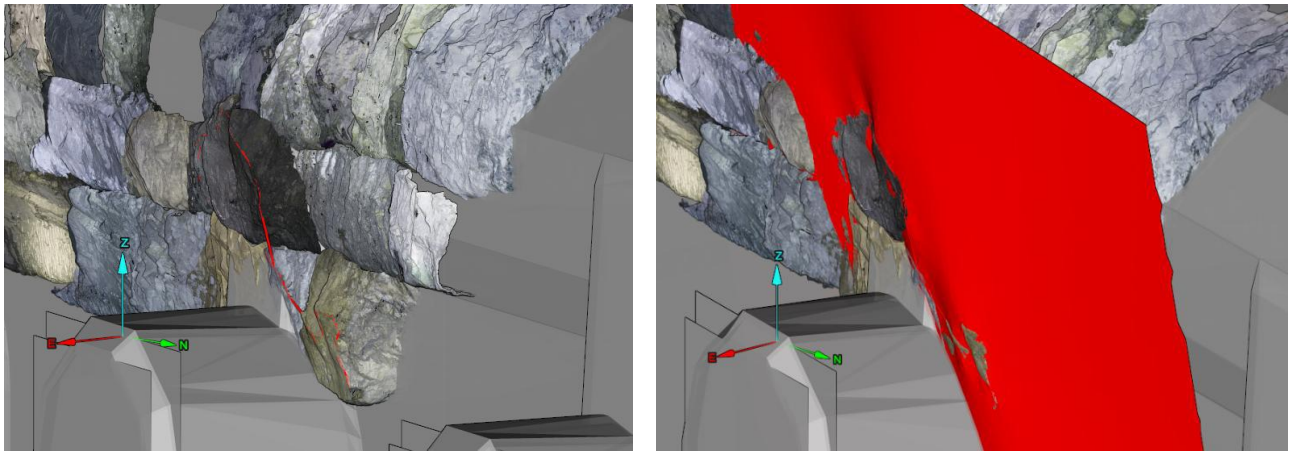


Figure 11: a) Combinations of multiple advances' LiDAR scans, with defect described above traced (red line), looking south-west; b) Projection of trace in 11a, looking south-west

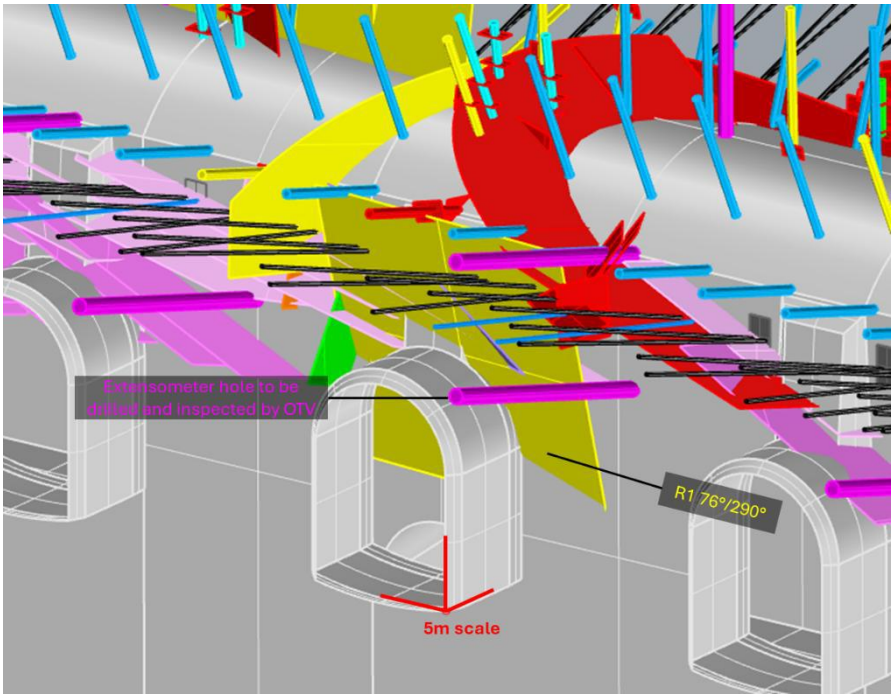


Figure 12: Rhino 6 model, Zoom on TH upstream Ch. 132 to 136, showing all data available in the surrounding of IPB 3. 'R1' represents the joint identified in Figure 11.

4 DISCUSSION

The adoption of 3D geological models has proved to be a success on Snowy 2.0, with each model presenting benefits specific to the targeted use and adopted software package. In general, the adoption of 3D modelling softwares has been found to have the following advantages over traditional mapping compilation methods, as follows:

- Allow the rapid visualisation of the main geological features from multiple data sources, with a higher precision resulting from spatially accurate sources such as LiDAR and OTV. Improved understanding of the nature of features, including persistence, waviness etc.
- Comparison of engineering designs within the model - allows for verification of design assumptions, and highlights areas where amendments to design or construction activities, sequencing and monitoring are required.
- Allows features to be projected to future advances to ensure the geologists target the features of interest for more rigorous assessment as they become visible.
- It is fast and simple to add new data and amend interpretations.
- Export of interpretations to 3D BIM models, such as Revizto, for a project wide audience

Table 2: Benefits and limitations specific to each software package used on Snowy 2.0

	Vulcan Package	**Rhino 6**	**Leapfrog Works**
Benefit	- Rapid visualisation of as-built geology by ease of import of LiDAR scans. - Ability to create defect surfaces that demonstrate the exhibited waviness of the defect, rather than just planar discs or projections.	- Easy extract of the Rhino 6 geomodel for 3DEC model input - Less costly	- Cross sections can be easily cut from anywhere in the 3D model on demand and are automatically regenerated when the model is updated. - The interpolant function can easily provide extended interpretations of features, such as bedding. - User-friendly, easy to learn and common to industry.
Limitation	- Cost (more expensive than competitors)	- LiDAR scans limitation due to the big-size data set that is time-	- Leapfrog Works has some limitations for geotechnical modelling, including processing

	- Software is targeted towards mining use cases, rather than tunnelling or civil. - The modelling process can be very complex and rigorous compared to other software, though it is improving noticeably in development of the newer 'Vulcan GeologyCore'.	consuming for import into Rhino 6 model - Planar features modelled in Rhino 6, simplified visualisation that does not show waviness. One single orientation is defining the planar visualisation. - Specific geological modelling tools are not available, requires manual coding	time and the need to adjust model extents. - The importation of LiDAR Data inside the model is not a direct process. It requires an elaboration. In addition, importing big-size datasets is time-consuming. - LiDAR data import requires a high-performance computer.

Table 3: Benefits and limitations of each data source

Data Source	Benefit	Limitation
Endoscope	- Real-time image of the entire holes. - Observation of groundwater inflow - Shear displacement in the hole can be captured - Provides detail of rock colour, weathering condition (when image is clear) - Inexpensive	- Downhole depth in records can be inexact - Captures only a forward-facing view of the hole, meaning defect size and aperture (etc.) can appear distorted or exaggerated. - The camera orientation is not recorded, likewise identified defects cannot be oriented (like they can be in OTV). - Difficult to correlate the features observed with other endoscopes if not interpolated with OTV. - Visual point data, unable to interpret large scale waviness, roughness, persistence or provide a quantified measure of rock quality.
OTV	- Features type can be categorised - Feature orientation can be accurately captured - Feature aperture can be accurately captured. - Attains accurate downhole survey of the hole, capturing any deviation	- Cannot be performed when the hole dips > +15º from horizontal (Project specific safety condition). - Visual point data, unable to interpret large scale waviness, roughness or persistence. - Captures only the sidewalls of the hole - Specialised software is required to view and interpret the data file
Lidar Data	- Create the most accurate as built geological record possible with high density, spatially accurate point clouds. - Defects can be accurately traced and modelled without the need of georeferencing maps etc. providing an accurate representation of orientation, persistence, and waviness.	- Data-heavy point cloud files can be difficult to store, import and utilise without specialised software and advanced hardware. - Variable underground lighting conditions result in variations in the quality of colour in the scan. - Ensuring appropriate data quality can be challenging. Projects should specify the requirements of LiDAR scans to be not only accurate, but of consistent point densities and lighting. Although it can be difficult to achieve good lighting in a tunnel under construction, poor and inconsistent tunnel lighting results in the colour of scans ranging from black to white, resulting in a "zebra" effect, discernible in figures above.
Geotechnical (traditional) mapping	- Detailed geotechnical analysis of each feature, including roughness and infilling. - Overview of waviness that cannot be detected by an OTV related to the difference in scale - Stress (i.e. audible, spalling) and water (i.e. damp, dripping) conditions can be observed and documented	- Human error/typos. - Less accuracy of defect orientations as the geologist cannot physically measure the surface (personnel must remain ~2 to 4 meters behind the face due to unsupported ground restrictions) - Subjective assessments based on experience of geologist

In addition to the points above, geomodels developed by both the Contractor and Designer have allowed the targeting the placement of shear displacement monitoring holes according to identified discontinuities observed in-situ. The objective of this monitoring is to check for any shear displacement along features which may impact the integrity of installed support. The contractor undertook the monitoring at the completion of excavation of each bench, using endoscope camera inspections to check the feature conditions and the absence of movement. Beyond the first three benches, ongoing shear displacement monitoring has been refined based on the shear potential observed in previous records and geo models.

The designer has successfully utilised the Rhino 6 geological model to inform the 3DEC model for several Hold and Witness points in the cavern excavations to date. Figure 13 shows the geological model from Rhino 6 developed for Hold Point 2, and the 3DEC twin numerical model refined taking the Rhino 6 geomodel as input. The reassessment of the design at this control point resulted in the prediction of a lower number of rock bolts exceeding the design criteria at the end of the excavation than what was foreseen during the original design. This has allowed for the adjustment of excavation sequencing and the installation of the rock support, and has also given room to updating the re-bolting strategy.

The Owners geological model has in particular been successful in identifying highly persistent features from LiDAR scanning across multiple advances, including several features which were not clear from traditional mapping methods. This has been used to not only feed the Contractors and Designers models of major structures, but to ensure that the owner's model for Operations and Maintenance will contain an accurate representation of encountered conditions. This will assist in understanding any unexpected excavation behaviours across the 150-year design life of the structure, and allow for targeted and efficient treatment as required.

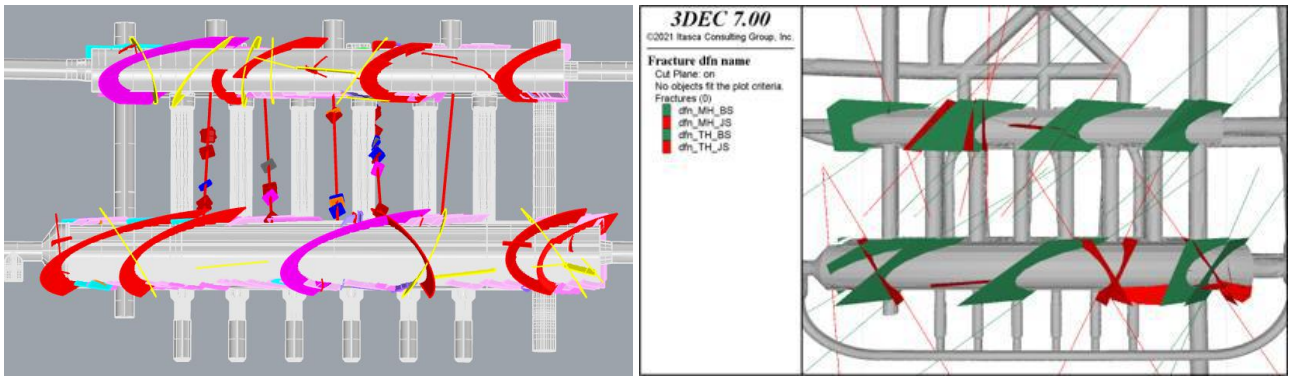


Figure 13: Comparison of models developed for Hold Point 2; a) Rhino 6 Geomodel; and b) 3DEC numerical model

5 CONCLUSION

The Snowy 2.0 project presents significant geotechnical challenges due to the complexity and scale of its underground excavation works, including some uncertainty in ground conditions even within key structures such as the Machine and Transformer Halls. To address these challenges, an observational approach to excavation has been adopted, leveraging the use of multiple models and numerous sources of data to continuously refine geological models and compare expected conditions and excavation behaviour to design assumptions.

This study has demonstrated how integrating multiple data sources - such as LiDAR scanning, traditional mapping, downhole endoscopy, and Optical Televiewer (OTV) imaging together with early-stage site investigations - enhances geological modelling. Accurate tracing of major features using LiDAR and mapping, combined with investigative data from perimeter and cored holes, significantly improved the understanding of feature location and persistence beyond the limitations of traditional face maps, including above and between the caverns. LiDAR scan traces verified feature waviness. The case study of the THA/IPB intersection showed how LiDAR scans can be used to trace a feature beyond the extent which would be noted in traditional mapping, and how this has allowed the feature to be tracked and investigated at a key location where it may impact excavation and support.

By integrating multiple data sources within multiple 3D geomodels, the project has strengthened design verification and improved geotechnical risk management both for during the construction and operation phases of the power station. This integrated approach not only supports safe and efficient excavation, but also provides a valuable and robust framework for future underground projects.

REFERENCES

ASTM D4879-08, July 2008. Standard Guide for Geotechnical Mapping of Large Underground Openings in Rock.

Barton, N., Lien, R. and Lunde, J., 1974. Engineering classification of rock masses for the design of tunnel support. Rock Mechanics and Rock Engineering, 6(4), pp.189-236.

Bieniawski, Z.T., 1989. Engineering rock mass classifications. New York: Wiley.

Geological Strength Index (Hoek, Carter, Diederich 2013), Q-system (Barton et al. 1974) and Rock Mass Rating (Bieniawski 1989).

Hernandes, J., Blaise, A., Tonioni, P.L., Lambrughi, A., Chapman, B. and Ching, I., 2025. Digital Twin Model as aid of the Observational Method for the Snowy 2.0 caverns excavation. World Tunnel Congress (WTC 2025), Stockholm, Sweden.

Hoek, E., Carter, T.G. and Diederichs, M.S., 2013, June. Quantification of the geological strength index chart. In ARMA US rock mechanics/geomechanics symposium (pp. ARMA-2013). ARMA.

Shen, B., Nash, T.R., Bertuzzi, R. and Clarke, S.J., 2015. Use of monitoring data during construction to refine cavern design. FMGM 2015, Sydney, Australia.

Thirukumaran, S., Oliveira, D. and Asche, H., 2021. Successful Design of Large Span Caverns in the Challenging Ground Conditions.

Tonioni, P.L., Toussaint, A., Lignier, P., Thermann, K., Lambrughi, A. and Ching, I., 2024. Snowy 2.0 – Implementation of a “twin numerical model” as computational tool of the “observational method” during the excavation of a large cavern under high in situ stress. World Tunnel Congress (WTC 2024), Shenzhen, China.

https://doi.org/10.56295/1ACEG09

APPLICATION OF A COPULA APPROACH TO QUANTIFY RAINFALL-INDUCED ROCKFALL

Farshad Bahootoroody[1], Davide Ettore Guccione[1], Klaus Thoeni[1], Anna Giacomini[1]
[1]*Centre for Geotechnical Science and Engineering, The University of Newcastle, Callaghan, NSW 2308, Australia.*

ABSTRACT

Rockfall hazards threaten coastal infrastructure, particularly under high rainfall conditions that accelerate slope degradation. This paper presents a copula-based statistical analysis of the relationship between rainfall and rockfall volume at Susan Gilmore Beach, Newcastle, NSW, Australia. Over a two-year monitoring period, drone-based photogrammetry surveys captured volumetric changes across 28 time intervals. To emphasise larger, more hazardous events, the 75th percentile of daily rainfall was paired with the 75th percentile of observed rockfall volumes. Correlation measures (Pearson's r and Kendall's τ) indicated moderate to strong dependencies, prompting assessment of three Archimedean copulas (Gumbel, Clayton, and Frank). Goodness-of-fit tests identified the Gumbel copula as the best model for capturing upper-tail dependence, linking high rainfall to substantial rockfall volumes. Joint and conditional probabilities derived from the copula framework revealed that extreme precipitation markedly elevates the likelihood of significant rockfalls, surpassing insights from conventional linear correlation. The findings underscore the value of nonlinear, tail-focused statistical approaches in hazard characterisation. The conditional probability provides explicit likelihoods of specific rockfall volumes for given rainfall amounts, offering the potential to define risk thresholds and inform targeted mitigation strategies. By integrating high-resolution 3D monitoring with an advanced copula-based model, this study provides a robust methodological template for analysing rainfall-triggered instability in coastal cliff environments.

Keywords: rockfall hazard assessment, probabilistic analysis, copula modelling, conditional probability

1 INTRODUCTION

Rockfall hazards pose risks to infrastructure and public safety, as sudden collapses can endanger lives and disrupt transport corridors and facilities. This risk is particularly relevant in Australia, where extensive coastal cliffs vary in lithology and height. Intense rainfall is a well-established trigger for rockfalls (Delonca et al., 2014). Climate change exacerbates the urgency of this issue, as extreme rainfall events are projected to increase in frequency and intensity, potentially amplifying cliff retreat and instability (Contino et al., 2017; Ansari et al., 2015; Melillo et al., 2020; Vessia et al., 2020). Therefore, precisely understanding the rainfall–rockfall relationship is crucial for hazard mitigation planning and climate resilience in these vulnerable coastal zones.

Recent studies have increasingly focused on enhancing rockfall prediction models and climate impact assessments (Matsuoka, 2019; Nissen et al., 2021; Leyva et al., 2022; Birien and Gauthier, 2023; Malsam and Walton, 2024; Mirhadi and Macciotta, 2023). The lack of comprehensive and high-resolution historical rockfall datasets and insufficient records of weather conditions at the time of failure have made it difficult to establish clear relationships between weathering processes and rockfall occurrence. This challenge is further compounded by the inaccessibility of hazardous slopes, inconsistencies in monitoring techniques, geological variability, and limitations in data precision and temporal coverage. These constraints are particularly problematic for short-term analyses that require detailed, high-frequency observations.

Despite advances in remote sensing and monitoring techniques, establishing robust correlations between rainfall and rockfall occurrence remains challenging. Studies relied primarily on cross-correlation or simple linear models (Delonca et al., 2014; Leyva et al., 2022; Bajni et al., 2021), often with limited temporal resolution and qualitative volume estimates. More recent investigations (Birien and Gauthier, 2023; Malsam and Walton, 2024) have employed high-resolution, lidar-derived data and terrestrial laser scanning (TLS) to track thousands of discrete rockfall events over shorter intervals. Although these efforts have shed light on the role of rainfall, temperature, and weathering, the underlying relationships can exhibit strong nonlinearity and tail-dependent behaviour that conventional correlation measures (e.g., Pearson's coefficient) fail to capture. In most studies, correlation analyses, often using the Pearson correlation coefficient, assess linear relationships between normally distributed variables (Schober et al., 2018; Hazra and Gogtay, 2016). However, this method fails to capture nonlinear dependencies, common in climatology, where data distributions are skewed (Schoelzel and Friederichs, 2008). Schirmacher and Schirmacher (2008) and Hashemi et al. (2015) highlighted its limitations, showing that different dependence structures can yield identical coefficients, leading to misleading conclusions.

To address these limitations, copula-based modelling offers a flexible framework for describing complex, nonlinear dependence structures in geotechnical data (Nelsen, 2007; Ningrum et al., 2017). Unlike linear correlation, copulas provide a means of isolating and quantifying how extreme rainfall events coincide with large-volume rockfalls—a phenomenon referred to as "tail dependence." This approach has found success in various risk assessment contexts, including landslide hazard evaluation (Motamedi and Liang, 2014; Li et al., 2018) and slope stability analyses (Wu, 2015; Wang and Li, 2018). Nonetheless, applications of copula theory to short-term, high-resolution rockfall datasets remain relatively scarce, underscoring the need for further exploration.

Against this backdrop, the current study aims to quantify the rainfall–rockfall volume relationship at Susan Gilmore Beach (SGB) in Newcastle, NSW, Australia, using a copula-based statistical approach recently proposed by the authors (Bahootoroody et al., 2025). Rainfall, among other factors such as freeze–thaw cycles, thermal fluctuations, wave action resulting in undercutting, root jacking from vegetation growth and geological conditions, has been identified as one potential rockfall trigger. In the current study, rainfall has been chosen as the primary trigger to illustrate the application of copula theory. While the proposed approach can accommodate the inclusion of other triggers in future research, it currently serves as a foundational step. This initial focus allows for a thorough evaluation of the method's applicability and effectiveness before expanding its scope to include additional triggers. Over a two-year period (2022–2024), high-resolution drone photogrammetry surveys were performed to capture volumetric changes resulting from rockfalls across 28 time intervals. The research objectives are threefold: (1) to characterise the magnitude and frequency of rockfalls using refined 3D data acquisition; (2) to assess the suitability of various copula families (Gumbel, Clayton, and Frank) in modelling rainfall-driven rockfall dependence; and (3) to leverage joint and conditional probabilities to improve hazard assessment. By integrating advanced geospatial monitoring with rigorous statistical modelling, this study demonstrates how nonlinear dependence insights can inform more targeted and effective risk management strategies for coastal cliff instability.

2 METHODOLOGY

This study employs a novel copula-based approach to model the dependency between rockfall volume and rainfall (Bahootoroody et al., 2025). The methodology of the copula-based approach is briefly reported here. Full details of each step can be found in Bahootoroody et al. (2025). Copula modelling is a powerful statistical approach for capturing dependencies between variables by constructing joint distributions from their marginal distributions. Unlike traditional multivariate models, copulas provide flexibility in defining dependence structures (Genest and Favre, 2007).

According to Sklar's theorem (1959), for any two random variables, U and V, with a joint cumulative distribution function (CDF) denoted as $H(u, v)$, there exists a copula function C that links their marginal distributions:

$$H(u,v) = C(F_U(u), F_V(v)) \quad (1)$$

where F_U and F_V represent the marginal CDFs of U and V, respectively. This relationship generalises to higher dimensions, allowing the construction of a multivariate dependence structure while preserving the individual behaviour of each variable (Embrechts et al., 2001). Figure 1 illustrates the structured methodology used to estimate the conditional probability of rockfall volume based on rainfall, employing a copula-based approach. The process is divided into two main stages: Data Processing and copula Fitting.

The first stage begins with data collection (Step 1), where rainfall and rockfall volume datasets are gathered. Next, the dataset is split into training and validation subsets (Step 2) to ensure a robust model evaluation. Subsequently, an Empirical Cumulative Distribution Function (ECDF) is constructed (Step 3) to analyse the distribution characteristics of the variables. These distributions are then transformed into a standard uniform distribution (Step 4), enabling compatibility with copula modelling. Finally, correlation measures such as Pearson's correlation and Kendall's tau are computed (Step 5) to quantify the relationship between the variables.

The second stage, copula Fitting, starts with selecting the most suitable copula function (Step 6) to model the variables' dependence structure. The goodness-of-fit of the chosen copula is assessed (Step 7) to ensure an appropriate model fit. Once validated, the copula joint probability distribution is constructed (Step 8), allowing for a comprehensive probabilistic representation of the relationship between rainfall and rockfall volume. In the final step, the conditional probability of rockfall volume given rainfall is estimated (Step 9), providing critical insights into hazard assessment. The entire process is implemented through a Python script explicitly developed for this research, ensuring computational efficiency and reproducibility.

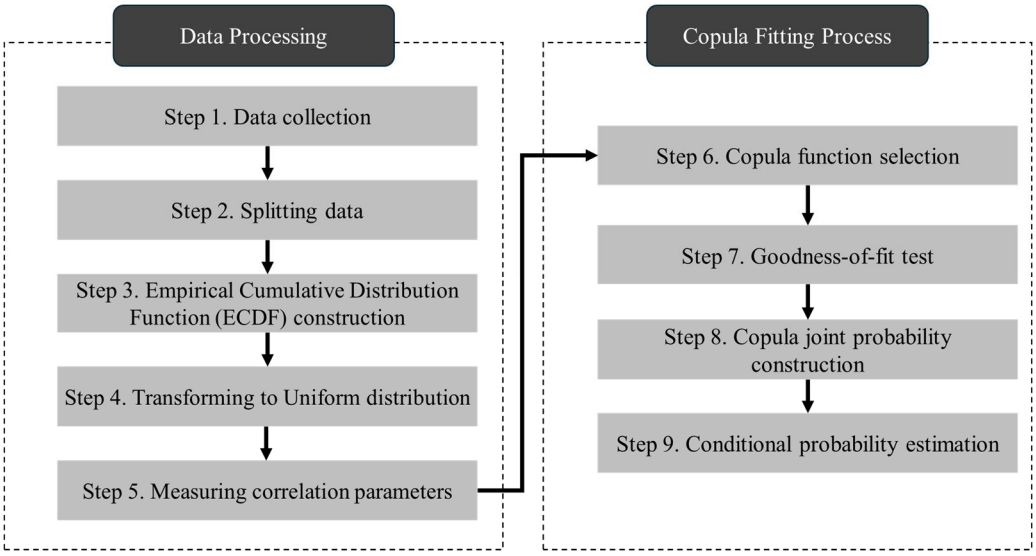


Figure 1. The schematic overview of the copula-based framework details data processing and copula fitting for conditional probability estimation.

2.1 DATA PROCESSING

The data processing stage prepares the dataset for copula modelling by transforming raw data into a format suitable for dependency analysis. This involves data collection, dataset splitting, distribution transformation, and correlation assessment.

The process begins with data collection (Step 1), where the variables of interest are obtained. Further details on data sources and characteristics are provided in Section 4.1. After collection, the dataset is split into training and testing subsets (Step 2) using an 80:20 ratio, where 80% of the data is used for copula modelling, while the remaining 20% is allocated for estimating conditional probability. A stratified random sampling approach is applied to ensure that both subsets maintain representative characteristics (Tippett, 1931).

To facilitate copula-based dependency modelling, the Empirical Cumulative Distribution Function (ECDF) is constructed (Step 3) for each variable. The ECDF is a non-parametric method that estimates the cumulative probability distribution based on observed data (Bernards et al., 2020; Parzen, 1962). Since copula modelling requires uniform marginals, the empirical cumulative distribution function (ECDF) is applied to transform the raw data variables into a uniform distribution:

$$\hat{F}_{(u)} = \frac{1}{n}\sum_{i=1}^{n} I(U_i \leq u) \tag{2}$$

where I is an indicator function that equals 1 if $U_i \leq u$ and 0 otherwise. The transformation is applied to obtain uniform variables u and v in the unit interval [0,1] (Step 4), which is essential for copula modelling, as it allows dependency structures to be analysed independently of their marginal distributions (Papaefthymiou and Kurowicka, 2009; Bedford and Cooke, 2001).

Following this, correlation parameters are computed (Step 5) to quantify the relationship between variables. Pearson's correlation coefficient is employed to measure linear dependence (Embrechts et al., 2001), while Kendall's tau (Kendall, 1938) is used to assess monotonic associations, offering a nonparametric alternative suitable for capturing nonlinear dependencies (Nelsen, 2007).

This stage establishes a structured foundation for copula fitting and conditional probability estimation by transforming the dataset into a uniform scale and quantifying dependencies.

2.2 COPULA FITTING PROCESS

The copula fitting stage establishes the dependency between variables by selecting an appropriate copula function, validating its effectiveness, constructing the joint probability distribution, and deriving conditional probabilities. The process begins with choosing a copula function (Step 6), which defines how the relationship between the variables is modelled. Copulas are classified into different families, with two primary categories commonly used in statistical modelling: elliptic and Archimedean copulas. Archimedean copulas were selected for this study due to their established application in modelling rainfall patterns (Wang et al., 2017; Ma et al., 2013; Zhang and Singh, 2019; Villarini et al., 2008). This family includes the Clayton, Frank, and Gumbel, which provide different ways to capture dependency patterns, including strong lower or upper tail dependencies. The dependence copula parameter θ is estimated based on

Kendall's tau (τ). Table 1 summarises the mathematical relationship between θ and τ in three Archimedean copulas (Sepúlveda-García and Alvarez, 2022).

Table 1. Copula density function c in a bivariate case, for some popular Archimedean copulas used in geotechnics, and simplified relationships between Kendall's tau (τ) and the copula parameter (θ) (modified after Sepúlveda-García and Alvarez (2022).

Copula	$C(u, v; \theta)$	Relationship $\tau - \theta$
Frank	$-\frac{1}{\theta}\ln\left[1+\frac{\left(e^{-u\theta}-1\right)\left(e^{-v\theta}-1\right)}{e^{-\theta}-1}\right]$	$\tau = 1-\frac{4}{\theta}+4\frac{D_1(\theta)}{\theta}$
Gumbel	$\exp\left[-\left((-\ln u)^{\theta}+(-\ln v)^{\theta}\right)^{1/\theta}\right]$	$\tau = 1-\frac{1}{\theta}$
Clayton	$\left[u^{-\theta}+v^{-\theta}-1\right]^{-\frac{1}{\theta}}$	$\tau = \frac{\theta}{2+\theta}$

The selection of an appropriate copula is based on the characteristics of the dataset and the type of relationship observed. Following the selection, a goodness-of-fit evaluation (Step 7) determines how well the chosen copula represents the data. This is achieved using the Akaike Information Criterion (AIC) (Akaike, 1974) and Bayesian Information Criterion (BIC)(Schwarz, 1978), which assesses the trade-off between model complexity and fit quality. These metrics are defined as follows:

$$AIC = 2k - 2l \tag{3}$$

$$BIC = k\ln N - 2\ln l \tag{4}$$

where l is the likelihood function, k is the number of model parameters, and N is the sample size. The copula function yielding the lowest AIC and BIC values is considered the best fit for the dataset. Once the copula function is validated, the joint probability distribution is formulated (Step 8). This step constructs both the copula probability density function (PDF) and the cumulative distribution function (CDF), which collectively define the dependence between variables. These distributions offer insight into the probability of joint occurrences, revealing key patterns such as clustering and tail dependencies. To enhance interpretability, graphical representations such as contour plots and 3D surface plots can be generated to visualise how probability distributions change across different values of the variables.

Finally, the conditional probability of one variable given another is estimated (Step 9). This probability quantifies the likelihood of rockfall occurring for a given level of rainfall and is derived using the copula model. Mathematically, the conditional probability of V given a specific U threshold is computed using:

$$P(V \leq v | U = u) = \frac{\partial C(u, v)}{\partial u} \tag{5}$$

This step quantifies the likelihood of exceeding certain rockfall volumes under given rainfall conditions, providing a probabilistic framework for hazard assessment.

3 APPLICATION

The coastal cliffs of Susan Gilmore Beach in Newcastle, NSW, Australia, were selected as the study site to assess the dependency between rockfall volume and rainfall using the copula approach. The cliffs at Susan Gilmore Beach belong to the Newcastle Coal Measures of the Sydney Basin and consist of Late Permian-aged sedimentary rocks. The lithology includes sandstone, siltstone, shale, conglomerate, and coal seams, with key stratigraphic units such as the Dudley Coal Seam, Bogey Hole Formation, Yard Coal Seam, Bar Beach Formation, and Tighes Hill Formation (Watman et al., 2023). The rock mass exhibits a blocky structure due to near-vertical joint sets and horizontal bedding planes, contributing to its instability. Weathering and erosion of weaker fine-grained layers, such as shale and siltstone, lead to the undercutting of more resistant sandstone and conglomerate, increasing the likelihood of rockfalls (see

Figure 2).

Watman et al. (2023) conducted a study on the Susan Gilmore cliff, in which the structural controls on rockfall susceptibility were characterised through geostructural mapping using Sirovision (Datamine, 2022). Structural mapping revealed a total of 1,576 discontinuities across the cliff. Three principal sets of near-vertical joints and a distinct set of nearly horizontal bedding planes were identified throughout the entire cliff (Figure 3a).

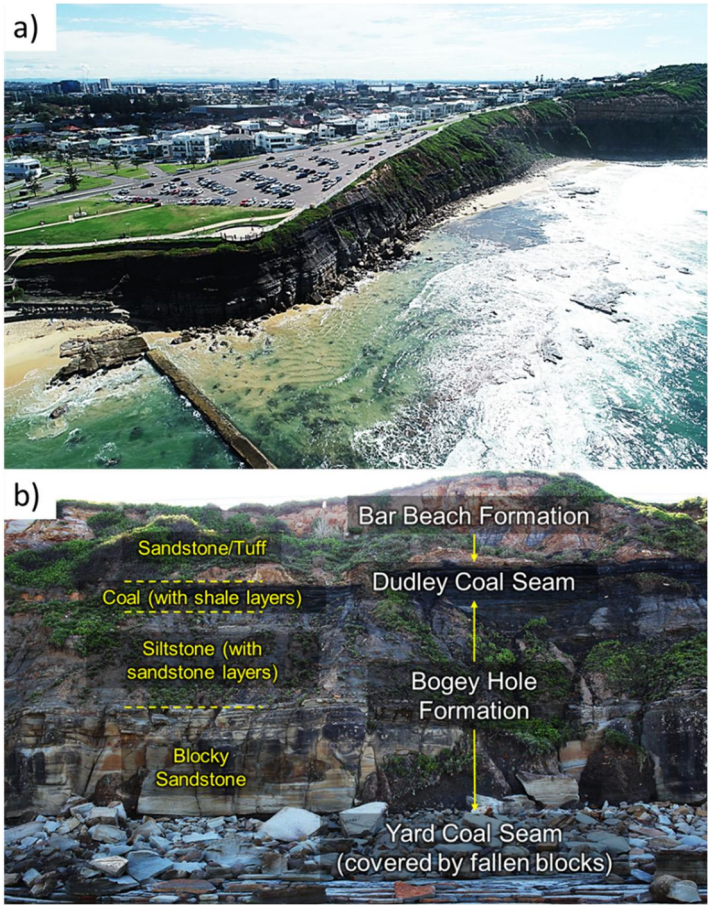


Figure 2. a) Panoramic view and b) stratigraphic units outcropping along Susan Gilmore cliff photo, modified after Watman et al. (2023).

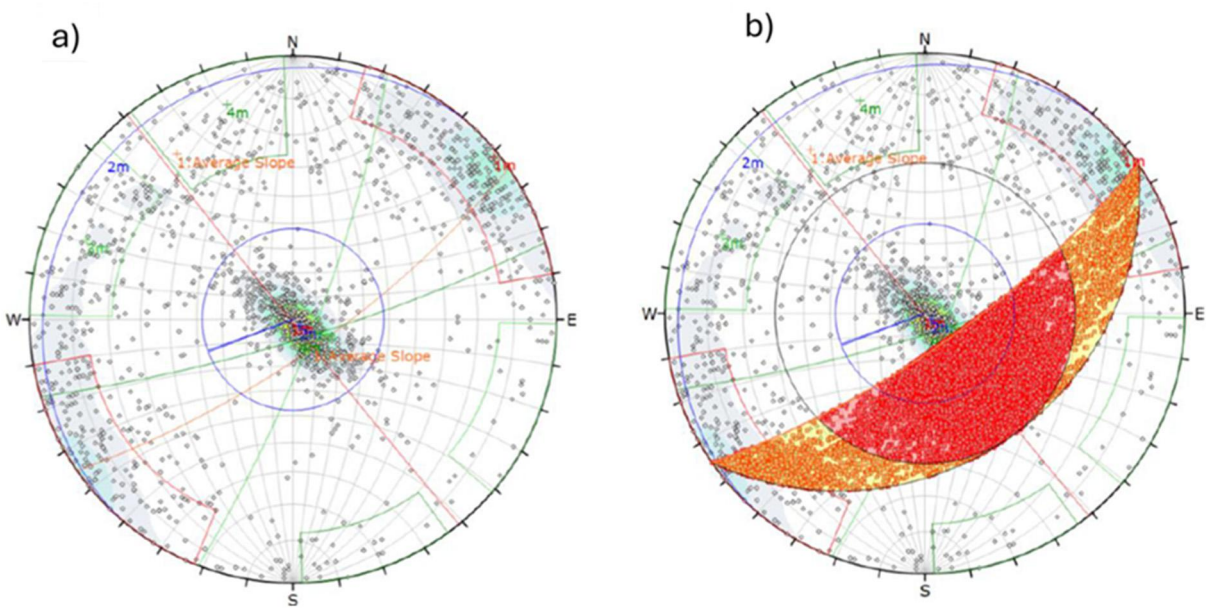


Figure 3. a) Overall stereonet and b) results from kinematic analysis for wedge sliding along the entire cliff, modified after Watman et al. (2023).

Figure 3a and Table 2 indicate three prominent near-vertical joint sets (89/231, 81/163 and 80/111), along with the set of near-horizontal bedding planes (4/311). The evaluation of the overall stereonet (Figure 3a) reveals that the possible rockfall failure mode of the cliff is direct toppling, wedge sliding and planar sliding. Kinematic analysis was performed

for the overall stereonet. The Dips output for wedge sliding is shown in Figure 3b. Besides wedge sliding, analyses were conducted for direct toppling, planar sliding, and flexural toppling. The findings from these analyses are summarised in Table 3. This table indicates that wedge sliding is the most likely failure mode for the given cliff, accounting for 13.9% of potential failures, followed by direct toppling at 6.8%, and planar sliding at 5.8%.

Table 2. Summary of orientations of structures at Susan Gilmore Beach cliff, modified after Watman et al. (2023).

set	Dip [°]	Dip Direction [°]
Red (joints)	89	231
Pale green (joints)	80	111
Dark green (joints)	81	163
Blue (bedding)	4	311
Slope	75	145

Table 3. Summary of kinematic analysis results, modified after Watman et al. (2023).

Failure Mode	Critical Intersections/ Poles	Total Intersections/ Poles	Critical Proportion [%]
Wedge Sliding	172,204	1241005	13.9
Direct Toppling	84,027	1241005	6.8
Planar Sliding	92	1576	5.8
Flexural Toppling	29	1576	1.8

3.1 DATA COLLECTION

To develop the dataset for analysis, rockfall events and rainfall measurements were recorded over a monitoring period from November 17, 2022, to November 27, 2024, during which the cliffs were surveyed 28 times at irregular intervals. Table A1 in APPENDIX A provides the monitoring intervals. Rockfall detection and volume estimation were conducted using drone-based photogrammetry. Geospatial data acquisition involved using a DJI Phantom 4 RTK drone for high-resolution aerial imaging. These datasets were processed into 3D mesh models to facilitate change detection analysis. Rockfall source areas and volumetric changes were identified using CloudCompare (Girardeau-Montaut, 2020) plug-in called "VoxFall" recently developed by the authors (Farmakis et al., 2025). Figure 4 demonstrates the cumulative frequency and magnitude (block volume) relationship of the data obtained from the 2-year observation. Note that the frequency has been normalised by the year. The figure also shows that a power-law distribution fits the observed data quite well. Furthermore, the Rainfall data was obtained from the Bureau of Meteorology (BoM), Newcastle Nobbys Signal Station AWS.

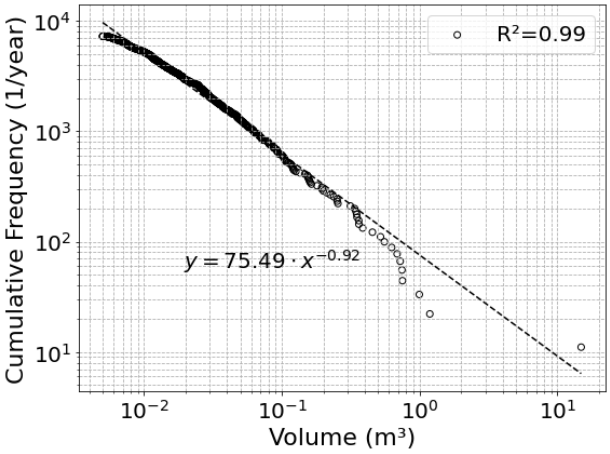


Figure 4. Relationships between the annual cumulative frequency and magnitude in a log-log plot.

3.2 DATA PREPROCESSING

As the exact timing of rockfall events was unknown within each monitoring period, a statistical approach was used to represent rockfall volume and rainfall. The 75th percentile of rockfall volume was selected to characterise the upper range

of observed events, ensuring that significant occurrences were captured. This value was then correlated with the 75th percentile of daily rainfall recorded in the same period, providing a representative dataset for analysis. The 75th percentile was selected to emphasise larger rockfall events and higher rainfall intensities, as these more hazardous occurrences are critical for risk mitigation and infrastructure planning, ensuring that preventive measures are designed for significant, rather than minor, fluctuations (Liu et al., 2022). Figure 5 and Figure 6 illustrate these distributions using box plots of rockfall volume and rainfall across all monitoring periods. Figure 7 presents the 75th percentile rockfall volume (m^3) and 75th percentile rainfall (mm) across monitoring periods, illustrating potential correlations between rainfall intensity and rockfall occurrences, with rockfall data represented as log-scaled bars and rainfall trends as dotted lines.

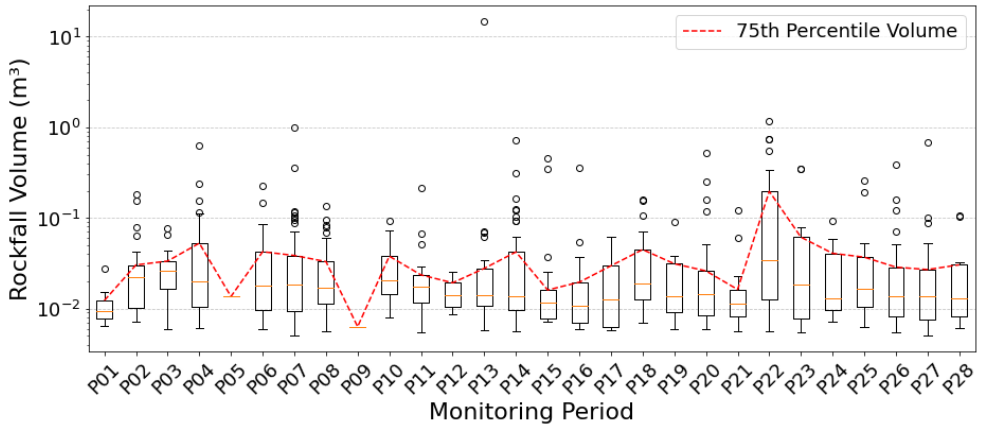


Figure 5. Boxplot of rockfall volumes across monitoring periods, with the 75th percentile volume shown as a red dashed line, highlighting variations in rockfall magnitude over time.

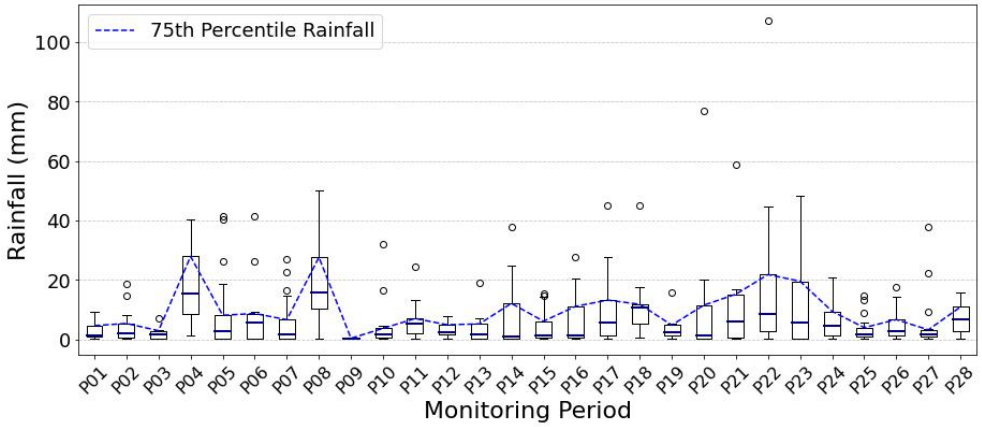


Figure 6. Boxplot of rainfall across monitoring periods, with the 75th percentile rainfall shown as a blue dashed line.

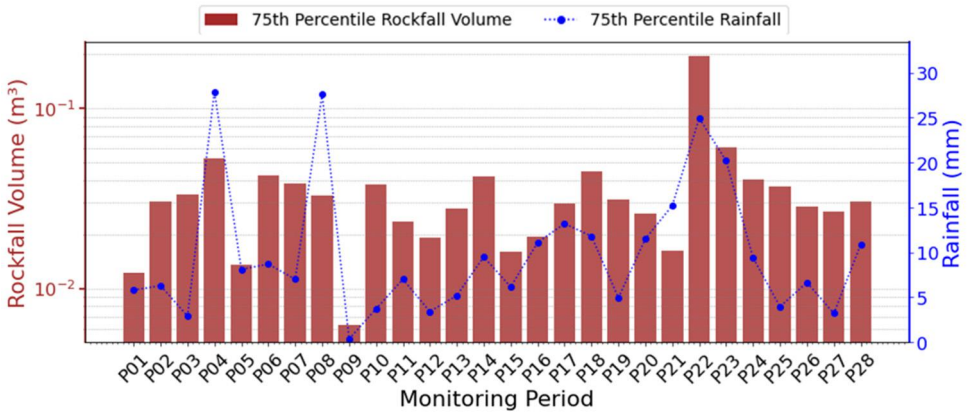


Figure 7. Comparison of 75th percentile rockfall volume and 75th percentile rainfall over monitoring periods.

After preprocessing, the dataset (28 period-wise observations of paired rockfall and rainfall values) was divided into a training subset and a testing subset in an approximately 80:20 ratio. A stratified random sampling approach (Tippett, 1931) was employed to ensure that the split was representative of the overall data distribution. In practice, this meant that

22 observations (about 80%) were randomly selected for copula model analysis, and the remaining 6 observations (about 20%) were reserved for checking the conditional probability.

4 RESULT AND DISCUSSION

4.1 EXPLORATORY DATA ANALYSIS

An exploratory data analysis was conducted to understand the underlying patterns and relationships in the training dataset, focusing on the trends, correlations and distribution between variables. The scatter plot illustrates the relationship between the rockfall volume and rainfall, with a fitted trend line indicating a positive correlation (see Figure 8). The logarithmic y-axis highlights variations in rockfall magnitude across different rainfall values. The correlation between these variables has been computed and is presented in Table 4, using Pearson's correlation and Kendall's tau. Pearson's correlation, which measures linear dependence, indicates a relatively strong relationship, while Kendall's tau, which assesses monotonic associations, suggests a moderate nonlinear trend.

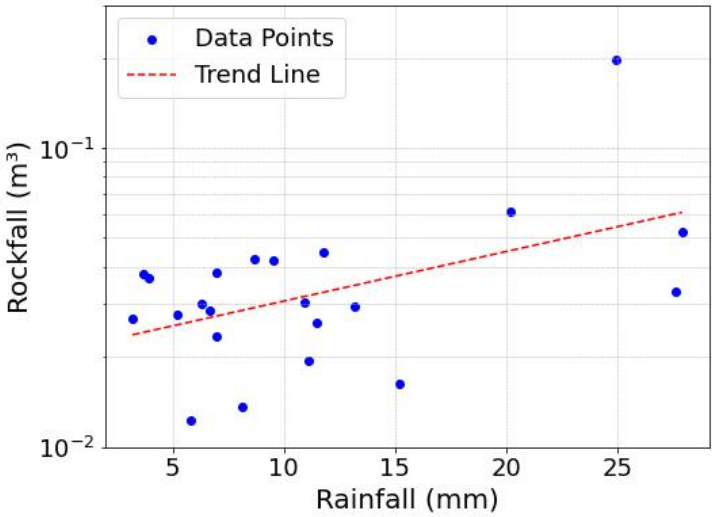


Figure 8. The scatter plot of 75th percentile rockfall volume vs. rainfall shows a moderate positive correlation with a fitted trend line.

Table 4. Pearson correlation and Kendall's tau coefficient between rockfall volume and rainfall

Pair	Pearson correlation	Kendall's tau
Rockfall-Rainfall	0.54	0.30

4.2 COPULA FITTING PROCESS

Copula fitting process starts with constructing the histograms of rockfall and rainfall to represent the frequency distribution of rockfall volume and rainfall, while ECDFs were fitted to illustrate the cumulative probability of each variable (see Figure 9). This visualisation highlights the skewness and distribution characteristics of the data, offering insights into the presence of extreme values and their potential influence on subsequent statistical modelling. Since copula modelling requires uniform marginal distributions, each variable's data was transformed using its ECDF. Figure 10 this step's result was a pseudo-observations in which rockfall and rainfall marginals were approximately uniform on the interval [0,1]. By using ECDFs, no specific parametric distribution needed to be assumed for rockfall or rainfall; the empirical distributions preserved the data characteristics and made them suitable for copula fitting.

Table 5 presents AIC and BIC Goodness-of-fit results and the copula parameter (θ) for the three Archimedean copulas (Gumbel, Clayton and Frank). The Gumbel copula exhibits the lowest AIC and BIC, indicating that it provides the best fit among the tested models. The Gumbel copula is an asymmetrical Archimedean copula known for its ability to model upper tail dependence, consistent with the expectation that extreme rainfall might strongly coincide with extreme rockfall volumes.

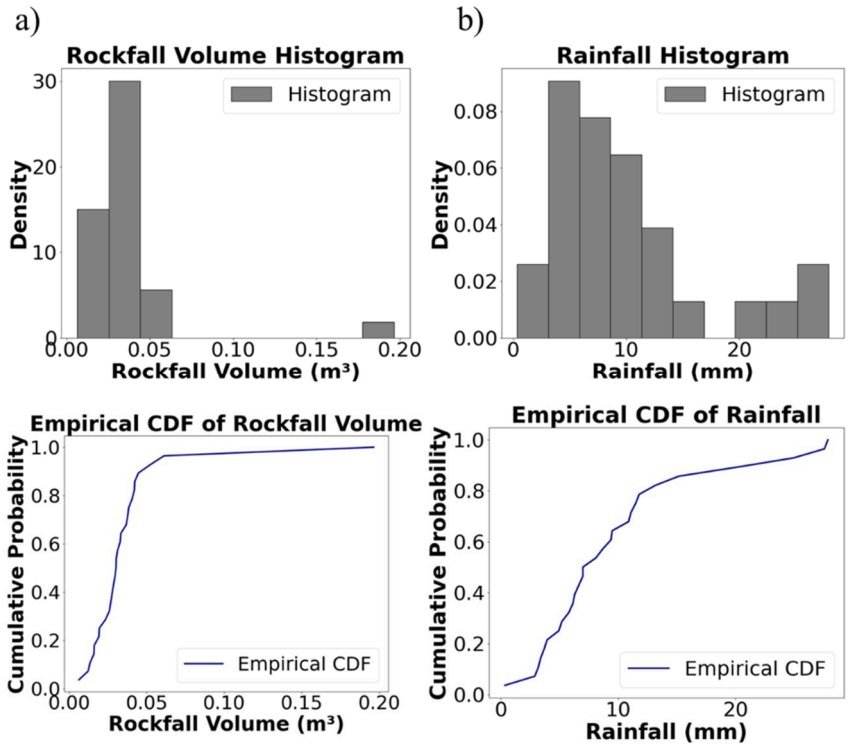


Figure 9. Histograms and ECDF of a) rockfall volume and b) rainfall, illustrating their statistical distribution and cumulative probability.

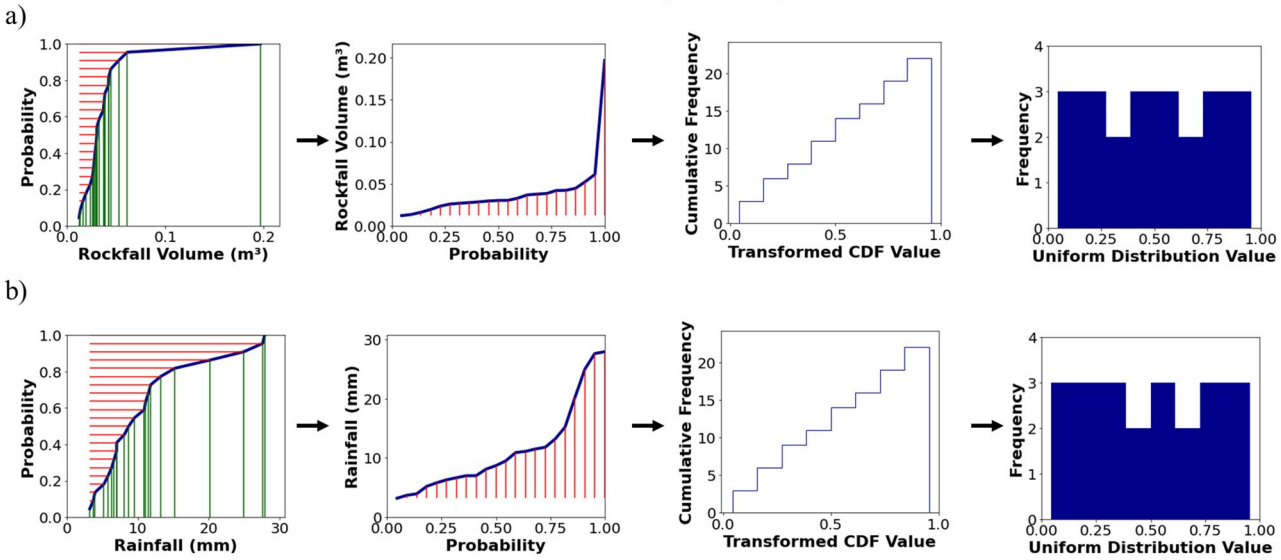


Figure 10. Transformation and uniformisation of a) rockfall volume and b) rainfall, demonstrating the mapping from the original empirical distributions to a uniform distribution through the cumulative distribution function (CDF).

Table 5. AIC and BIC values of the copula function

Copula	**AIC**	**BIC**	***θ***
Gumbel	-2.56	-4.63	1.05
Clayton	-0.88	-1.99	0.10
Frank	0.92	-1.96	50.02

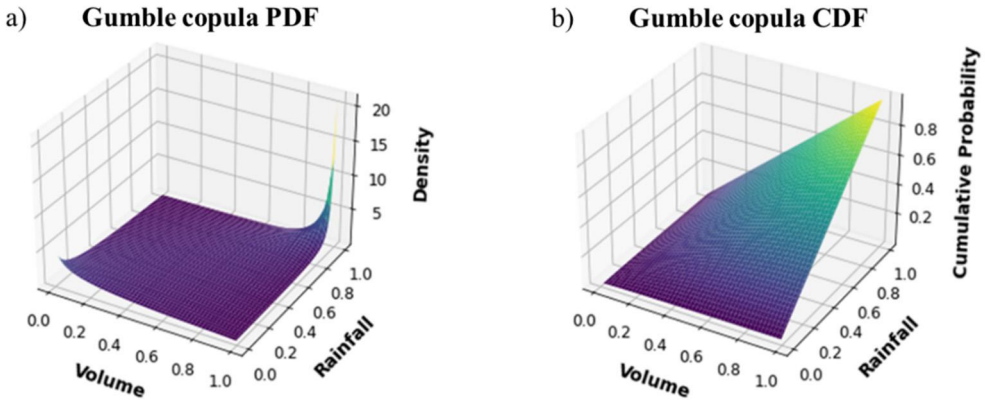


Figure 11. Gumbel copula-based Joint a) PDF and b) CDF of Rockfall Volume and Rainfall.

Following the selection of the Gumbel copula family, the process of fitting the copula to the transformed uniform data commences. Figure 11 shows the three-dimensional Gumbel copula-based joint PDF and CDF of the rockfall volume and rainfall. The concentration of density near 0 and 1 in the Gumbel copula-based joint PDF highlights a strong dependence on extreme rockfall volume and rainfall values. The high density in these regions suggests that low rainfall is typically associated with minimal rockfall activity, whereas high rainfall tends to correspond to significant rockfall events. The dependence between rockfall volume and rainfall is assessed by examining the conditional probability of volume for a given rainfall amount, as estimated from the Gumbel copula joint CDF. Figure 12 graphically demonstrates the changing conditional probability for various rockfall volumes. Each curve in the figure represents the likelihood of rockfall occurrence across various volumes corresponding to a given rainfall level. The rainfall values in Figure 12 are derived from the testing dataset and were not included in the copula-based analysis.

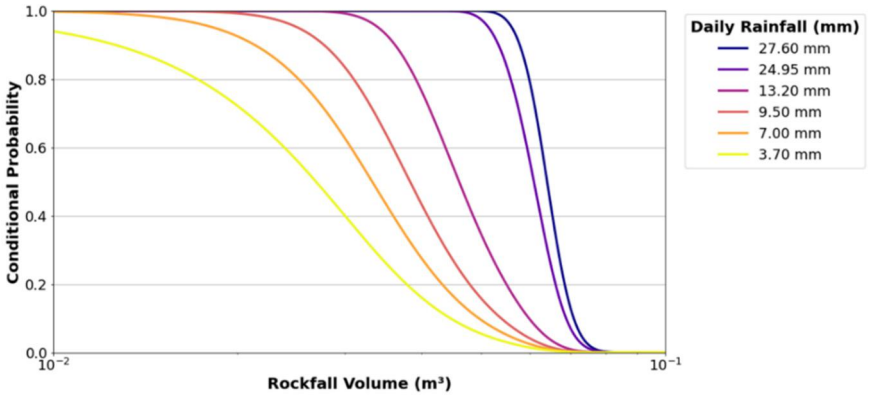


Figure 12. Conditional probabilities of the rockfall volume are given by specific amounts of rainfall.

5 CONCLUSION

This study employed a copula-based approach to investigate the relationship between rainfall and rockfall volume along the coastal cliffs of Susan Gilmore Beach, Newcastle, NSW, Australia. By utilising drone-based photogrammetry and 3D point cloud analysis, rockfall occurrences were systematically tracked over a two-year period (2022–2024), providing a detailed dataset for assessing rainfall-induced rockfall activity. Through this probabilistic modelling, the analysis captured nonlinear dependencies that traditional correlation techniques often fail to recognise, allowing for a more comprehensive understanding of how rainfall influences rockfall detachment.

The findings indicate that copula modelling is a powerful tool for estimating rockfall probability under varying rainfall conditions, as it provides greater flexibility in capturing complex relationships beyond linear assumptions. The integration of conditional probability functions enhances the ability to predict rockfall likelihood with reduced uncertainty, particularly in high-rainfall scenarios where traditional models struggle to account for variability in detachment patterns. Additionally, the conditional probability function P(V|U) derived from our copula model quantifies the likelihood of specific rockfall volumes for given rainfall amounts, enabling the definition of risk thresholds and informing targeted mitigation strategies. Furthermore, high-resolution 3D change detection methods have enabled a more accurate representation of rockfall source areas and volume changes, reinforcing the effectiveness of combining geospatial monitoring with statistical modelling in hazard assessment.

This research underscores the need for advanced analytical methods in understanding rainfall-driven rockfall processes, particularly in unstable coastal environments. The outcomes emphasise the importance of integrating meteorological data with real-time monitoring to improve hazard assessment strategies and inform risk management decisions. Expanding the

dataset with real-time monitoring systems and applying machine learning techniques could further refine predictive capabilities, contributing to more effective hazard mitigation in vulnerable coastal regions.

ACKNOWLEDGEMENTS

This work was supported by the Australian Research Council (DP210101122).

APPENDIX A

Table A1. Monitoring periods with start and end dates, and duration in days.

Monitoring Period	Start Date	End Date	Day Number	Monitoring Period	Start Date	End Date	Day Number
P01	17/11/2022	16/12/2022	29	P15	30/11/2023	9/01/2024	40
P02	16/12/2022	23/01/2023	38	P16	9/01/2024	5/02/2024	27
P03	23/01/2023	21/02/2023	29	P17	9/01/2024	22/02/2024	44
P04	21/02/2023	3/03/2023	10	P18	5/02/2024	22/02/2024	17
P05	16/12/2022	31/03/2023	105	P19	22/02/2024	28/03/2024	35
P06	3/03/2023	31/03/2023	28	P20	28/03/2024	8/04/2024	11
P07	31/03/2023	16/05/2023	46	P21	8/04/2024	24/04/2024	16
P08	16/05/2023	31/05/2023	15	P22	24/04/2024	27/05/2024	33
P09	31/05/2023	21/06/2023	21	P23	27/05/2024	26/06/2024	30
P10	21/06/2023	27/07/2023	36	P24	26/06/2024	25/07/2024	29
P11	27/07/2023	29/08/2023	33	P25	25/07/2024	29/08/2024	35
P12	29/08/2023	28/09/2023	30	P26	29/08/2024	1/10/2024	33
P13	28/09/2023	31/10/2023	33	P27	1/10/2024	31/10/2024	30
P14	31/10/2023	30/11/2023	30	P28	31/10/2024	27/11/2024	27

REFERENCES

Akaike, H. (1974). A new look at the statistical model identification. *IEEE transactions on automatic control,* 19**,** 716-723.

Ansari, M., Ahmed, M., Rajesh Singh, T. & Ghalayani, I.(2015). Rainfall, a major cause for rockfall hazard along the roadways, highways and railways on hilly terrains in India. *Engineering Geology for Society and Territory-Volume 1: Climate Change and Engineering Geology*, 2015. Springer, 457-460.

Bahootoroody, F., Giacomini, A., Guccione, D., Thoeni, K., Watman, A. & Griffiths, D. V. (2025). Predictive modelling of rainfall-induced rockfall: a copula-based approach - under review. *Georisk: Assessment and Management of Risk for Engineered Systems and Geohazards (Under Review)*.

Bajni, G., Camera, C. a. S. & Apuani, T. (2021). Deciphering meteorological influencing factors for Alpine rockfalls: a case study in Aosta Valley. *Landslides,* 18**,** 3279-3298.

Bedford, T. & Cooke, R. M. (2001). Probability density decomposition for conditionally dependent random variables modeled by vines. *Annals of Mathematics and Artificial Intelligence,* 32**,** 245-268.

Bernards, R., Van Westering, W., Morren, J. & Slootweg, H. (2020). Analysis of energy transition impact on the low-voltage network using stochastic load and generation models. *Energies,* 13**,** 6097.

Birien, T. & Gauthier, F. (2023). Assessing the relationship between weather conditions and rockfall using terrestrial laser scanning to improve risk management. *Natural Hazards and Earth System Sciences,* 23**,** 343-360.

Contino, A., Bova, P., Esposito, G., Giuffré, I. & Monteleone, S. (2017). Historical analysis of rainfall-triggered rockfalls: the case study of the disaster of the ancient hydrothermal Sclafani Spa (Madonie Mts, northern-central Sicily, Italy) in 1851. *Natural Hazards and Earth System Sciences,* 17**,** 2229-2243.

Datamine (2022). Sirovision Software 6.2.2. Australia.

Delonca, A., Gunzburger, Y. & Verdel, T. (2014). Statistical correlation between meteorological and rockfall databases. *Natural Hazards and Earth System Sciences,* 14**,** 1953-1964.

Embrechts, P., Lindskog, F. & Mcneil, A. (2001). Modelling dependence with copulas. *Rapport technique, Département de mathématiques, Institut Fédéral de Technologie de Zurich, Zurich,* 14**,** 1-50.

Farmakis, I., Guccione, D. E., Thoeni, K. & Giacomini, A. (2025). VoxFall: Non-parametric volumetric change detection for rockfalls. *Engineering Geology,* 352**,** 108045.

Genest, C. & Favre, A.-C. (2007). Everything you always wanted to know about copula modeling but were afraid to ask. *Journal of hydrologic engineering,* 12**,** 347-368.

Girardeau-Montaut, D. (2020). CloudCompare (2.11.3) . [Software].
Hashemi, S. J., Ahmed, S. & Khan, F. I. (2015). Correlation and Dependency in Multivariate Process Risk Assessment. *IFAC-PapersOnLine,* 48**,** 1339-1344.
Hazra, A. & Gogtay, N. (2016). Biostatistics series module 6: correlation and linear regression. *Indian journal of dermatology,* 61**,** 593-601.
Kendall, M. G. (1938). A new measure of rank correlation. *Biometrika,* 30**,** 81-93.
Leyva, S., Cruz-Pérez, N., Rodríguez-Martín, J., Miklin, L. & Santamarta, J. C. (2022). Rockfall and Rainfall Correlation in the Anaga Nature Reserve in Tenerife (Canary Islands, Spain). *Rock Mechanics and Rock Engineering,* 55**,** 2173-2181.
Li, H., Xu, Q., He, Y. & Deng, J. (2018). Prediction of landslide displacement with an ensemble-based extreme learning machine and copula models. *Landslides,* 15**,** 2047-2059.
Liu, T., Mcguire, L. A., Oakley, N. & Cannon, F. (2022). Temporal changes in rainfall intensity–duration thresholds for post-wildfire flash floods in southern California. *Natural Hazards and Earth System Sciences,* 22**,** 361-376.
Ma, M.-W., Ren, L.-L., Song, S.-B., Song, J.-L. & Jiang, S.-H. (2013). Goodness-of-fit tests for multi-dimensional copulas: Expanding application to historical drought data. *Water Science and Engineering,* 6**,** 18-30.
Malsam, A. & Walton, G. (2024). Seasonality of rockfall triggers and conditioning factors interpreted from a lidar-derived rockfall database. *Engineering Geology,* 333**,** 107500.
Matsuoka, N. (2019). A multi-method monitoring of timing, magnitude and origin of rockfall activity in the Japanese Alps. *Geomorphology,* 336**,** 65-76.
Melillo, M., Gariano, S. L., Peruccacci, S., Sarro, R., Mateos, R. M. & Brunetti, M. T. (2020). Rainfall and rockfalls in the Canary Islands: assessing a seasonal link. *Natural Hazards and Earth System Sciences Discussions,* 2020**,** 1-26.
Mirhadi, N. & Macciotta, R. (2023). Quantitative correlation between rock fall and weather seasonality to predict changes in rock fall hazard with climate change. *Landslides,* 20**,** 2227-2241.
Motamedi, M. & Liang, R. Y. (2014). Probabilistic landslide hazard assessment using Copula modeling technique. *Landslides,* 11**,** 565-573.
Nelsen, R. B. (2007). An introduction to copulas, *Springer science & business media*.
Ningrum, O. W., Tarno, T. & Di Asih, I. M. (2017). Perhitungan Value at Risk Pada Portofolio Saham Menggunakan Copula (Studi Kasus: Saham-Saham Perusahaan Di Indonesia Periode 13 Oktober 2011-12 Oktober 2016). *Jurnal Gaussian,* 6**,** 231-240.
Nissen, K. M., Rupp, S., Kreuzer, T., Guse, B., Damm, B. & Ulbrich, U. (2021). Quantification of Meteorological Conditions for Rockfall Triggers in Central Europe.
Papaefthymiou, G. & Kurowicka, D. (2009). Using Copulas for Modeling Stochastic Dependence in Power System Uncertainty Analysis. *IEEE Transactions on Power Systems,* 24**,** 40-49.
Parzen, E. (1962). On estimation of a probability density function and mode. *The annals of mathematical statistics,* 33**,** 1065-1076.
Schirmacher, D. & Schirmacher, E. (2008). Multivariate dependence modeling using pair-copulas. Technical report.
Schober, P., Boer, C. & Schwarte, L. A. (2018). Correlation Coefficients: Appropriate Use and Interpretation. *Anesthesia & Analgesia,* 126**,** 1763-1768.
Schoelzel, C. & Friederichs, P. (2008). Multivariate non-normally distributed random variables in climate research–introduction to the copula approach. *Nonlinear Processes in Geophysics,* 15**,** 761-772.
Schwarz, G. (1978). Estimating the dimension of a model. *The annals of statistics***,** 461-464.
Sepúlveda-García, J. J. & Alvarez, D. A. (2022). On the use of copulas in geotechnical engineering: a tutorial and state-of-the-art-review. *Archives of Computational Methods in Engineering,* 29**,** 4683-4733.
Sklar, A. (1959). Fonctions de répartition à n dimensions et leurs marges. *Publications de l'Institut de Statistique de l'Université de Paris,* 8.
Tippett, L. H. C. (1931). The Methods of Statistics*,* London, UK, *Williams & Norgate*.
Vessia, G., Di Curzio, D., Chiaudani, A. & Rusi, S. (2020). Regional rainfall threshold maps drawn through multivariate geostatistical techniques for shallow landslide hazard zonation. *Science of the Total Environment,* 705**,** 135815.
Villarini, G., Serinaldi, F. & Krajewski, W. F. (2008). Modeling radar-rainfall estimation uncertainties using parametric and non-parametric approaches. *Advances in Water Resources,* 31**,** 1674-1686.
Wang, F. & Li, H. (2018). The role of copulas in random fields: characterization and application. *Structural Safety,* 75**,** 75-88.
Wang, Y., Li, C., Liu, J., Yu, F., Qiu, Q., Tian, J. & Zhang, M. (2017). Multivariate Analysis of Joint Probability of Different Rainfall Frequencies Based on Copulas. *Water,* 9**,** 198.
Watman, A., Guccione, D. E. & Bahootoroody, F. T., K. Giacomini, A. (2023). Rockfall instability analysis of coastal cliffs: A case study along Susan Gilmore Beach (Newcastle, NSW). *14th Australia and New Zealand Conference on Geomechanics (ANZ2023).* Cairns.
Wu, X. Z. (2015). Modelling dependence structures of soil shear strength data with bivariate copulas and applications to geotechnical reliability analysis. *Soils and Foundations,* 55**,** 1243-1258.
Zhang, L. & Singh, V. P. (2019). Copulas and their applications in water resources engineering*,* Cambridge, *Cambridge University Press*.

https://doi.org/10.56295/1ACEG10

SUSCEPTIBILITY AND MITIGATION OF DEBRIS FLOODS AND FLOWS IN THE JENOLAN KARST CONSERVATION RESERVE, NSW, AUSTRALIA: BUSHFIRE AND LA NIÑA IMPACTS

Adam Irvine & Richard Brehaut
Pells Sullivan Meynink

ABSTRACT

This study assesses debris flood and flow susceptibility within the Jenolan Karst Conservation Reserve (JKCR), New South Wales, Australia, following the 2019 to 2020 summer bushfires and the prolonged 2020 to 2023 La Niña weather pattern. The bushfires significantly altered catchment hydrology by reducing vegetation cover and increasing sediment availability, while the subsequent extreme rainfall events triggered an increase in erosion and debris movement.

A detailed geological, geotechnical, and geomorphological assessment was conducted, incorporating the Melton Ratio to evaluate catchment susceptibility to debris floods and flows. The findings informed engineering solutions, including the design of debris barriers aimed at mitigating sediment transport and protecting downstream infrastructure. The study provides insights into the long-term impact of bushfires and extreme weather events on debris mobilisation, emphasising the importance of proactive mitigation strategies.

1 INTRODUCTION

Debris floods and flows are natural hazards with significant potential to impact infrastructure. These events are particularly common in steep and mountainous terrain where heavy rainfall, geological conditions, and land disturbances contribute to increased sediment mobilisation. Unlike conventional fluvial floods, debris floods and flows transport large volumes of sediment and organic material, which can cause extensive damage to infrastructure.

Following the 2019 to 2020 summer bushfires, the Jenolan Karst Conservation Reserve (JKCR) experienced a notable increase in debris flood and flow activity. The impacts of bushfire altered catchment hydrology by reducing vegetation cover, increasing soil water repellency, and exposing loose sediments to erosion. The bush fires were then followed by a three year La Niña climatic pattern between 2020 and 2023 which delivered record breaking rainfall and widespread flooding across eastern New South Wales, Australia. The bushfires, combined with the subsequent La Niña period, contributed to intensified debris movement and subsequent deposition across the reserve.

Surveyors Creek forms one of three main tributaries to the Jenolan River. The JKCR catchments are prone to debris floods and flows with records of debris flood and flow activity dating back to 1919, including instances where debris floods and flows have caused damage to property and resulted in sedimentation of the Blue Lake being of detrimental effect to the reserves amenity. Between 2020 and 2024, four intense rainfall events have triggered debris flood and flow events, which historically, is a large increase in frequency and occurrence.

This study presents an assessment of debris floods and flows, covering key aspects such as site and geological characteristics, definitions of debris floods and flows, and the impact of bushfires on their generation. It includes a desktop study reviewing site precedents, hydrology, and terrain, alongside site observations. The assessment employs both quantitative and numerical methodologies to evaluate debris flood and flow susceptibility, with findings integrated into the development of engineering design.

2 SITE DESCRIPTION AND GEOLOGY

The JKCR is a geologically significant area located in the Central Tablelands of New South Wales, Australia. It lies approximately 175 km west of Sydney and 30 km east of Oberon. The reserve is renowned for its extensive network of limestone caves that have been shaped by hydrological and geological processes. The caves are situated within a deeply incised, uplifted plateau that is characterised by steep gorges, rugged terrain, and karst formations.

Surveyors Creek is one of three main tributaries of the Jenolan River. Situated to the west of Jenolan Caves, it flows north before doglegging eastward beneath Carpark 1 and Caves House through a series of open and closed culverts before traversing beneath the Grand Arch before entering the Blue Lake, Figure 1. This system is prone to debris floods and flows originating within Surveyors Creek. A notable feature of the lower catchment is Surveyors Creek Dam, located above Carpark 1. This concrete structure provides limited flood and debris retention capacity, estimated at between approximately 1,500 and 2,500 m^3. The catchment is characterised by a steeply incised valley, plunging up to 400 meters

from adjacent ridge lines and many slopes exceeding 50°, contributing to high erosion rates and frequent debris floods and flows. Slope steepness increases toward the northern part of the catchment toward Surveyors Creek Dam.

The catchment features quartz sandstone and cherty siltstone of the Silurian Campbells Group after Branagan et al (2014), and overlying colluvial deposits. The quartz sandstone unit is composed of light to dark grey, blocky, fine to medium grained sandstones with minor slates and the cherty siltstone unit is composed of thinly bedded radiolarian-rich black siltstones, interbedded with slates and minor quartz sandstone (Branagan et al, 2014). A key feature of the site is the presence of a persistent layer of surficial loose granular colluvium which overlies the bedrock and provides a primary sediment source for debris floods and flows.

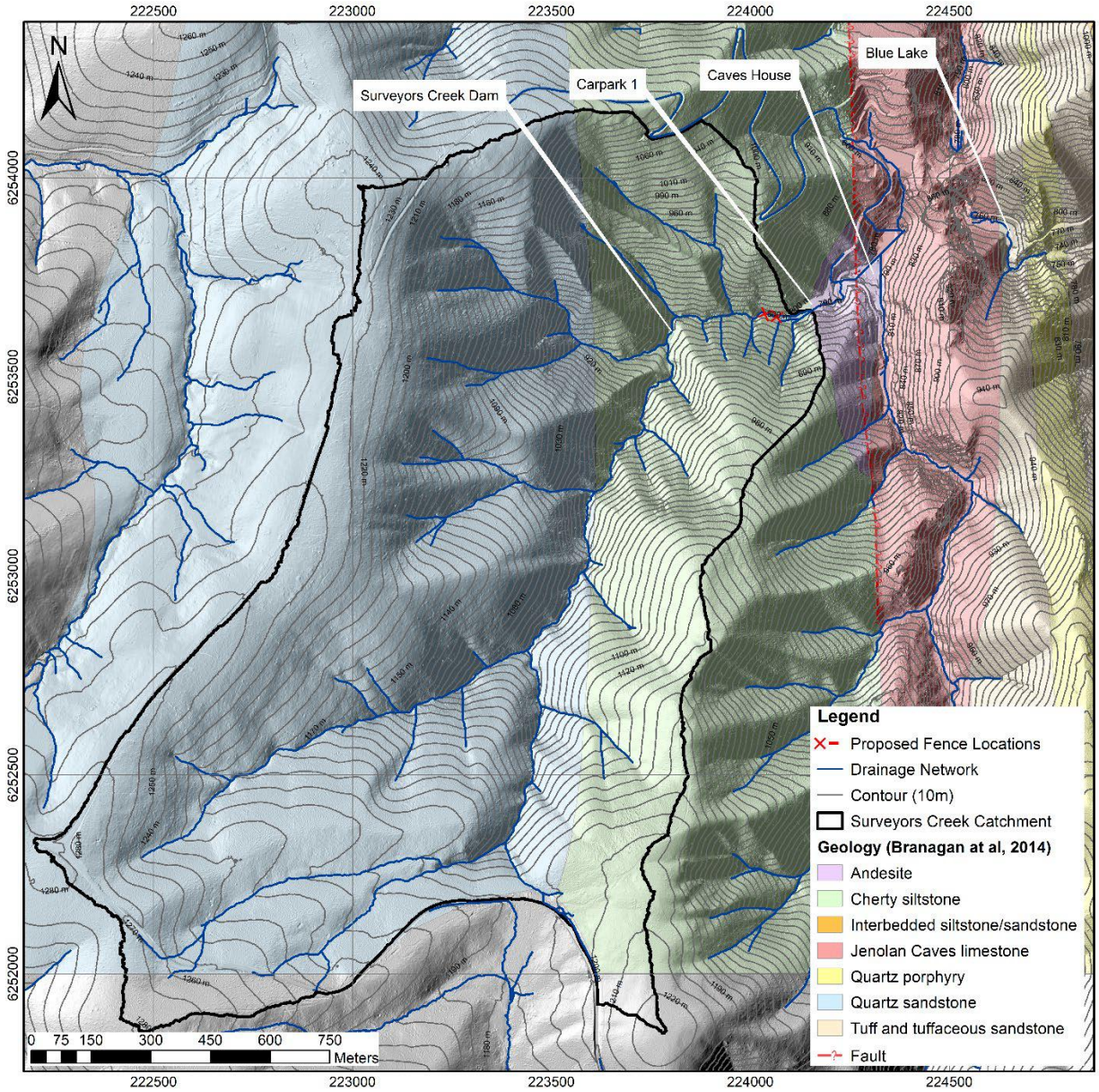


Figure 1: Surveyors Creek catchment and geology after Branagan et al (2014)

3 DEFINING DEBRIS FLOODS AND FLOWS

Debris flows occur when masses of poorly sorted sediment, agitated and saturated with water, surge downslope in response to gravity. The United States Geological Survey (USGS) define debris flows as having a sediment concentration above 60%. The velocities of debris flows vary according to slope angle but can range from walking pace up to 50km/hr in steep terrain. A debris flow can have more destructive potential than a debris flood.

Debris floods are defined by Hutchinson (1988) as hyper-concentrated flows of water laden with gravel, sand, and silt. They are defined by the USGS as a water flow involving 'normal' sediment concentrations, generally between 5% and

10% sediment volumes, though may extend up to 60% (hyper-concentrated flow). A debris flood is not a landslide but is a mass transport phenomenon with destructiveness similar to that of water, but less than that of debris flows. Objects impacted by debris floods are typically surrounded or buried by flood debris but are often undamaged (Hungr et al., 2001).

Both debris flows and debris floods are triggered and controlled by water and have the potential to travel a considerable distance from their source. The extent and effect of debris flows and floods are variable in terms of trigger mechanism, volume, and velocity, and depend on site factors including the geology, geomorphology, hydrology, and climate.

4 THE BUSH FIRE EFFECT

Intense rainfall is the primary trigger for debris floods and flows. However, the bushfires have significantly altered catchment hydrology increasing debris flood and flow susceptibility. Bushfires reduce vegetation cover, expose loose sediments and soil to direct rainfall which in turn increases runoff and erosion, and makes reestablishment of vegetation difficult. Overtime, as tree roots decay, the soil loses reinforcement, which provides an ongoing sediment source. Table 1 summarizes the post-fire effects on debris generation, adapted from DeGraff et al. (2015) and Parise & Cannon (2012). The 2019 to 2020 summer bushfires have significantly contributed to the increased debris movement at JKCR.

Table 1: Effect of bushfires on generation of debris floods and flows

Timeframe Relative to the Fire	Cause of Failure
During	-
Immediately After (0 to1.5 years)	Surface runoff process
	Changes to hydrologic response of drainage basin
Long Term (1.5 to 10 years)	Landslide failures through mobilisation of sediment due to tree root decay
	Changes to hydrologic response of drainage basin

5 DEBRIS FLOOD AND FLOW ASSESSMENT

5.1 SITE PRECEDENT

Factual accounts from previous events, geomorphological evidence and the terrain evaluation presented in the following Sections have informed this assessment. As discussed, several debris floods and flow events have occurred in the past five years with historical photographs documenting debris floods and flows occurrences as far back as 1919.

Figure 2 shows the February 2020 debris event that affected Caves House, the Grand Arch, and nearby buildings, as reported by the Canberra Times. It is understood sand, gravel, cobbles, and boulders were transported by debris floods from all three Jenolan River tributaries, including Surveyors Creek.



Figure 2: Flooding at Jenolan Caves in February 2020 looking towards the western side of the Grand Arch

5.2 HYDROLOGY

JKCR experiences a temperate climate with seasonal temperature variations, occasional snowfall, and bushfire-prone dry periods. Rainfall is relatively evenly distributed annually. Figures 3 and 4 present monthly mean precipitations and maximum daily rainfall intensities from available data sources.

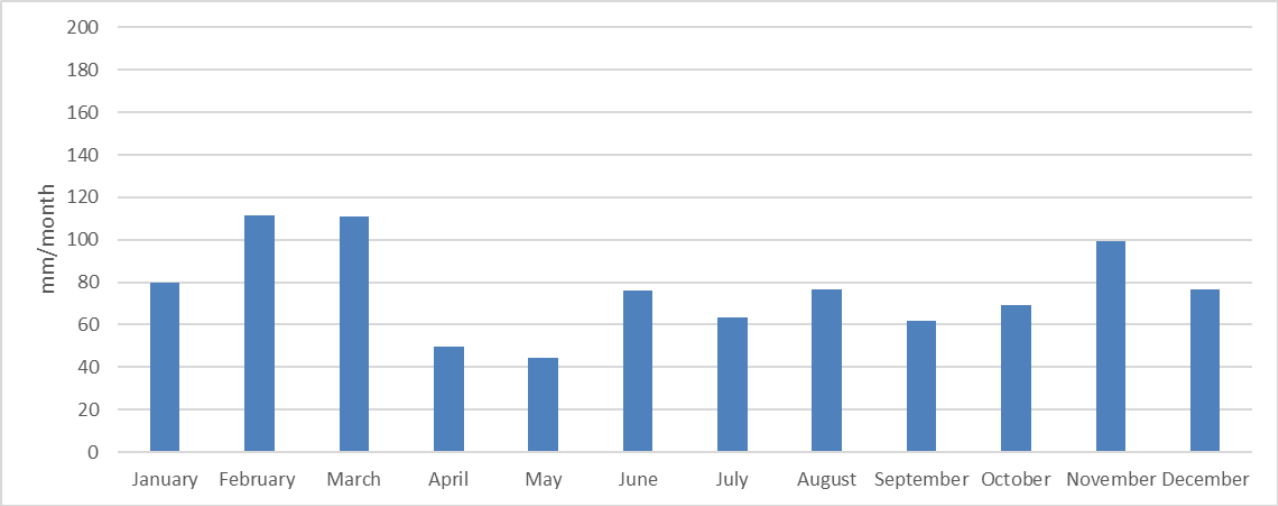


Figure 3: 2000 to 2023 monthly mean precipitation

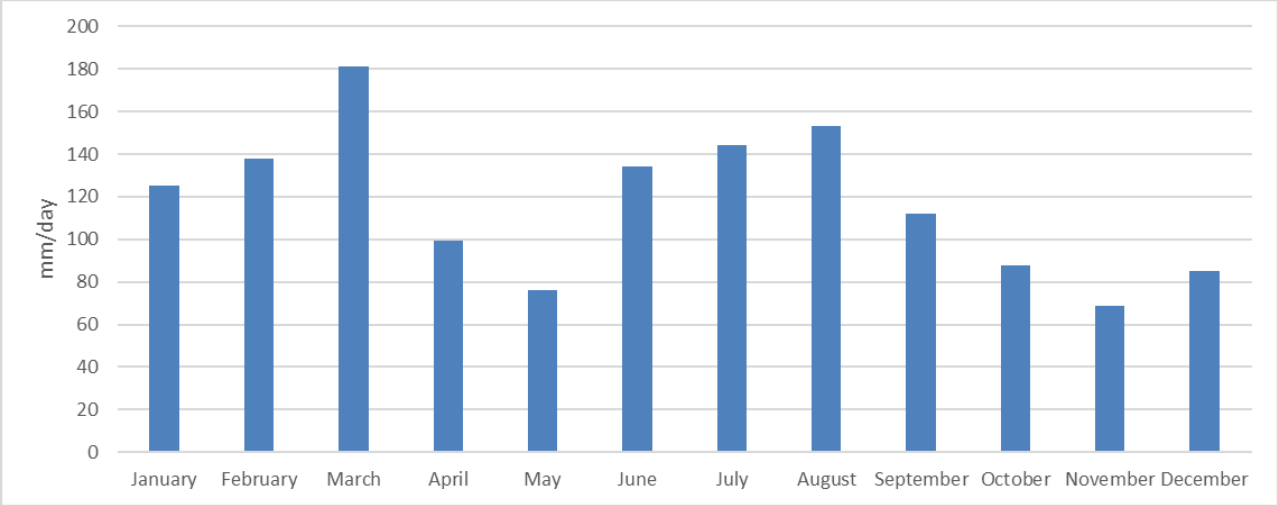


Figure 4: 1905 to 2023 short term rainfall intensity (maximum single day rainfall per month)

As part of our work at the JKCR, Intensity – Frequency – Duration (IFD) curves have been formulated, Figure 5. The major, recent storm events that have triggered debris floods / flows are presented in red on the IFD curves and include:

- February 2020 (an approximate 1:100 year event)
- March 2021 (an approximate 1:75 year event over 24 hours, or a 1:20 year event beyond 24 hours)
- July 2022 (an approximate 1:5 to 1:10 year event)
- April 2024 (an approximate 1:5 to 1:10 year event).

Figure 5 also plots the largest storm events recorded between July 2022 and April 2024 in green, that did not result in observable debris floods or flows. Analysis of Figure 5 suggests debris events are triggered when rainfall exceeds approximately 85 mm over 24 hours, or 110 mm over 48 hours, representing between a 1 in 2 and 1 in 5 year event.

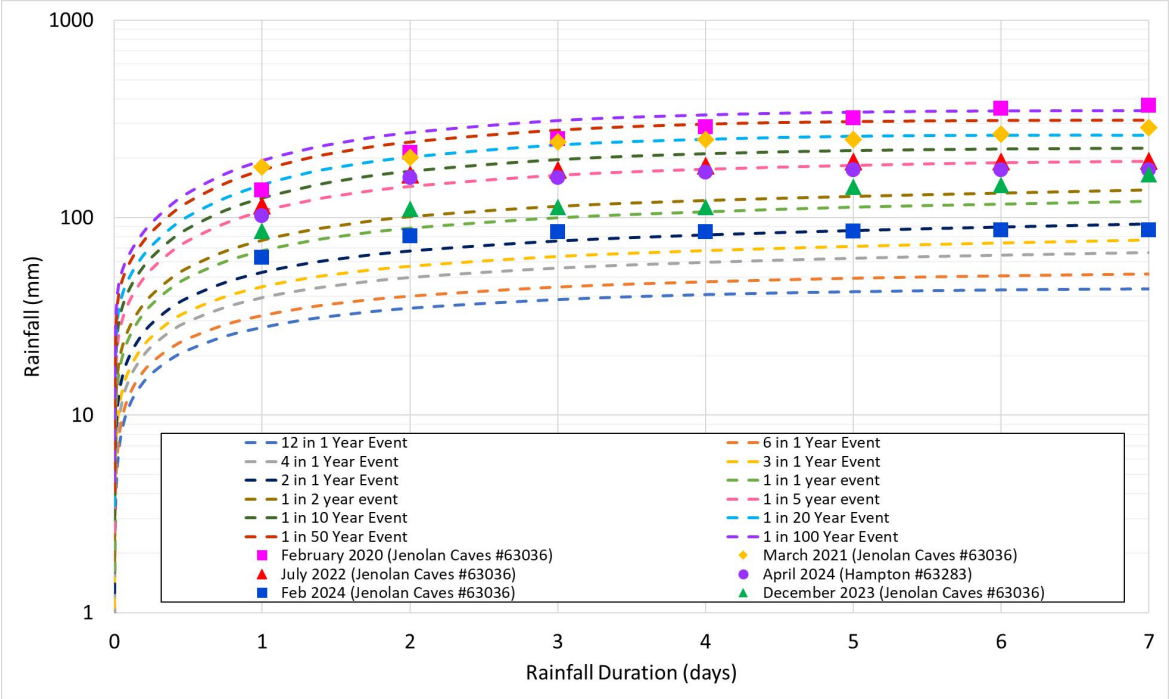


Figure 5: IFD curves for the JKCR. Recent storm events that resulted in debris floods or flows are presented in red and recent storm events that did not result in debris floods or flows are presented in green

5.3 TERRAIN ASSESSMENT AND SITE WALKOVER

A terrain assessment was undertaken prior to a site walkover and geomorphology mapping campaign. The terrain assessment is presented with the qualitative susceptibility assessment in Section 5.4.2. The assessment is based on geomorphological signatures observed in the DEM topography which was subsequently verified and updated in the field via the use of a mobile GIS application.

A focus of the terrain assessment was identification of sediment in storage that may be susceptible to mobilisation leading to generation of debris floods or flows. The following terrain units were identified across the site:

- Bedrock
- Scree
- Colluvium overlying bedrock
- Colluvial Apron
- Alluvium
- Anthropogenic.

Bedrock is observed along some ridges and within stream beds. Typically, scree slopes and boulder fields have formed below outcropping rock providing a source of sediment in storage.

A typical feature of the JKCR topography is the presence of a thin surficial layer of colluvium overlying bedrock, Figure 6. The surficial layer is typically loose, angular, sandy fine to coarse gravel with silt, trace cobbles and is estimated to be less than one metre thick in most cases. It is interpreted to be the primary source of sediment in storage. Development of the thin, granular colluvium is attributed to several factors including:

- Steep slopes and high erosion rates promoting rapid runoff, minimal topsoil development and slow vegetation establishment
- Extreme climate contributing to mechanical breakdown of bedrock
- High insitu stress resulting from deep valley incision (unloading of overlying rock reducing vertical stress, leading to basin uplift, rock mass dilation, fracturing and accelerated erosion).

Colluvial aprons are formed along the flanks of Surveyors Creek which is actively eroding and over steepening portions of the lower valley slopes, Figure 7. Material accumulation is interpreted to be a product of gravity driven, slope wash processes (such as landsliding) that deposit near the source and provides a source of sediment in storage. Due to the relatively steep gradient of Surveyors Creek and the resulting erosive force, the stream bed has incised down into bedrock resulting in only isolated deposits of alluvium.



Figure 6: Examples of loose colluvium present on the hill slopes

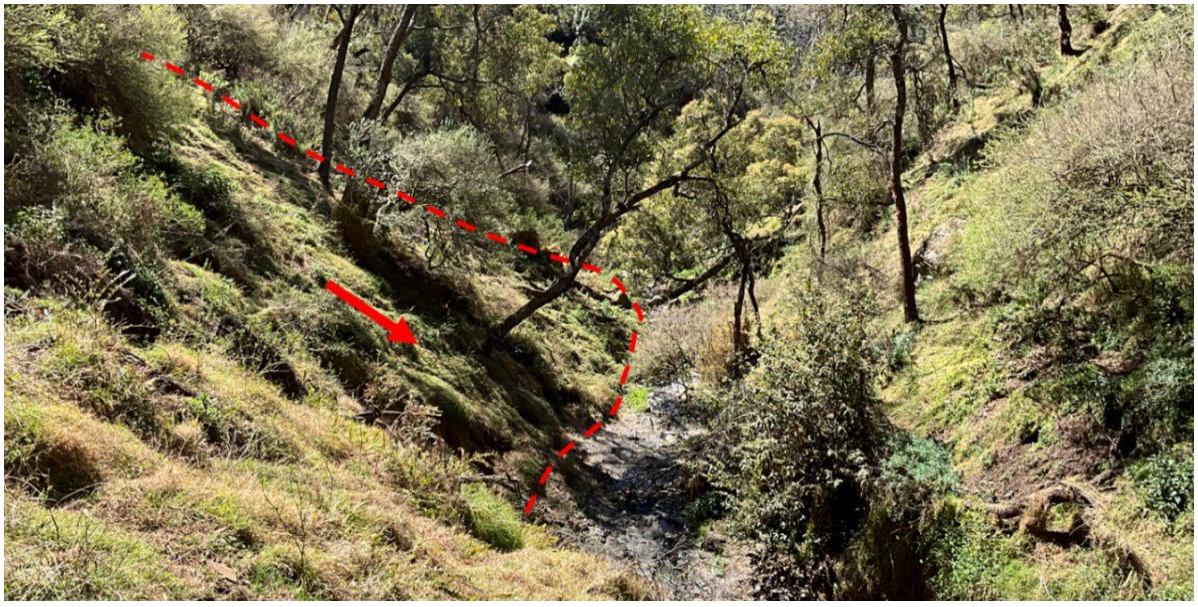


Figure 7: Colluvial apron formed through landsliding along the flank of Surveyors Creek

5.4 DEBRIS FLOOD AND FLOW SUSEPTIBILITY

5.4.1 Preamble

Assessment of debris flood and flow susceptibility was undertaken utilising a GIS based approach. The assessment has adopted both a qualitative evaluation and a numerical approach to assess debris flood and flow susceptibility.

5.4.2 Qualitative Assessment

A qualitative assessment of debris flood and flow potential has been undertaken considering the physical and geomorphological attributes of each catchment that feed into Surveyors Creek. This has included consideration of the following metrics, many of which were observed during the site walkover:

- Catchment area
- Slope gradient
- Steam / gully axis gradient
- Evidence of landsliding
- Evidence of debris in storage.

Table 2 summarises the qualitative assessment for individual metrics throughout the wider catchment. 'Debris Potential' (DP) has been assigned to each catchment to communicate the qualitive potential for generation of debris floods or flows based on some common susceptibility metrics widely referenced in the literature, Figure 8. Each catchment has been allocated a DP based on a qualitative appraisal as follows:

- Major debris potential
- Moderate debris potential
- Minor debris potential.

Table 2: Qualitative assessment of debris flood and flow potential

Catchment ID	Catchment Area (m^2)	Mean Slope Gradient (°)	Mean Stream / Gully Axis Gradient (°)	Evidence of Landsliding	Evidence of Debris in Storage	Debris Flood / Flow Potential
1	310,345	10	7	Minor	Not visited	Minor
2	603,727	17	11	Minor	Not visited	Minor
3	300,151	18	11	Minor	Not visited	Minor
4	228,102	22	21	Minor	Yes [1]	Moderate
5	199,788	27	20	Yes	Yes	Moderate
6	366,102	27	25	Yes	Yes	Major
7	176,617	33	23	Yes	Yes	Major
8	128,923	35	26	Yes	Yes	Major
9	147,097	31	27	Minor	Yes [1]	Moderate
10	86,114	34	26	No	Yes [1]	Moderate

[1] Loose surficial colluvium layer across the catchment

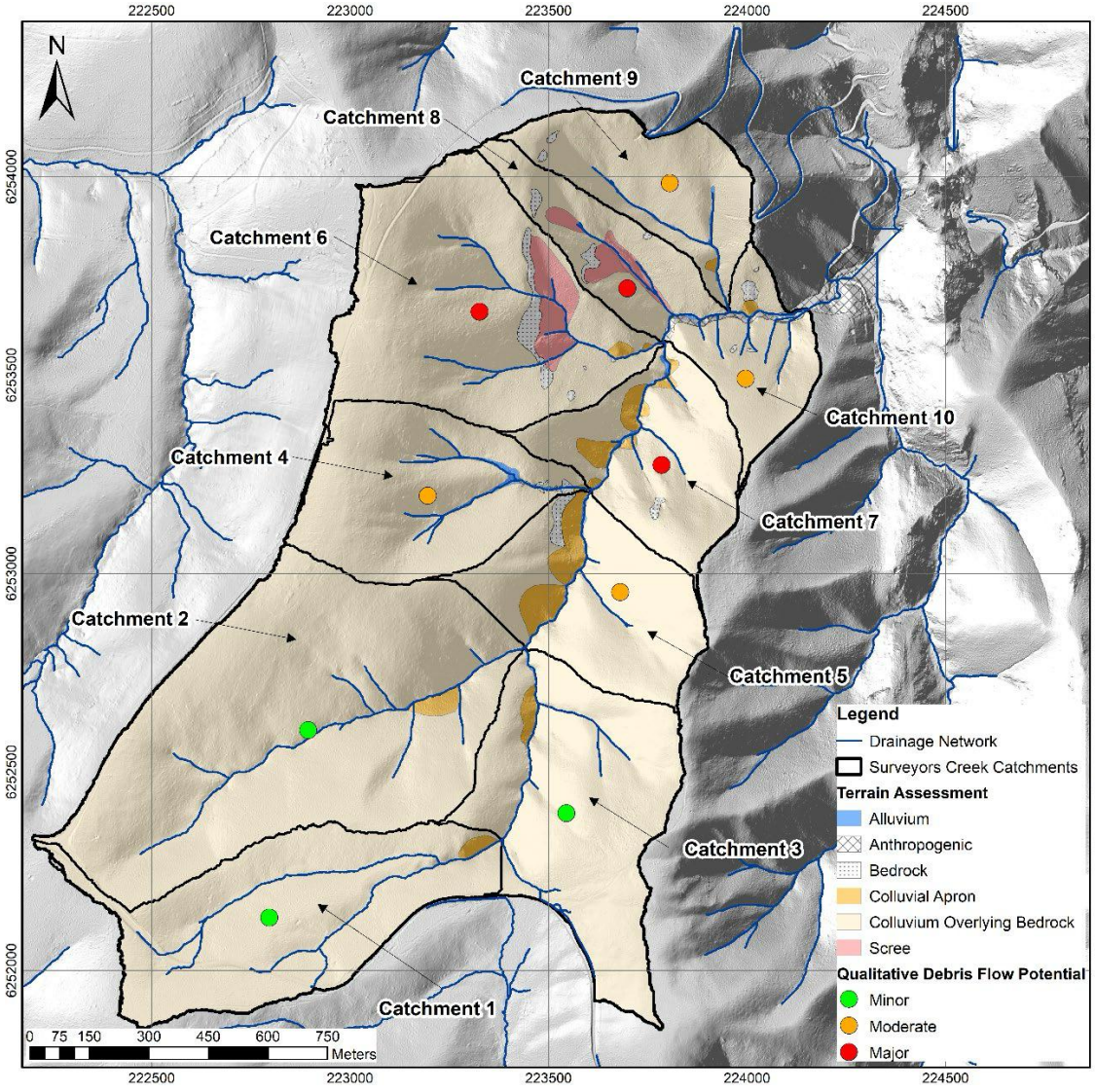


Figure 8: Terrain analysis and quantitative debris flood and flow susceptibility assessment

On this basis, debris flood/flow susceptibility broadly increases toward the north of the catchment where increased debris is observed in storage coupled with a significant increase in slope gradient.

5.4.3 Numerical Assessment

Morphometric catchment parameters of Surveyors Creek tributaries have been used to assess the susceptibility to debris floods and flows using the Melton Ratio (MR) after Melton (1957). The ratio is defined as:

$$R = H / \sqrt{A} \quad (1)$$

Where:

- R is the Melton Ratio
- H is the relief of the catchment, defined as the difference between the highest and lowest elevation
- A is the area of the catchment.

The MR for those Surveyors Creek catchments assessed are presented on Figure 9. Walsh and Davies (2010) define the following MR for defining susceptibility after Jackson et al (1987) and Wilford et al (2004):

- MR ≤ 0.30 – conventional fluvial processes are dominant (i.e., normal flooding)
- MR ≥ 0.30 & ≤ 0.6 – catchments that are prone to debris floods
- MR ≥ 0.6 – catchments that are prone to debris flows.

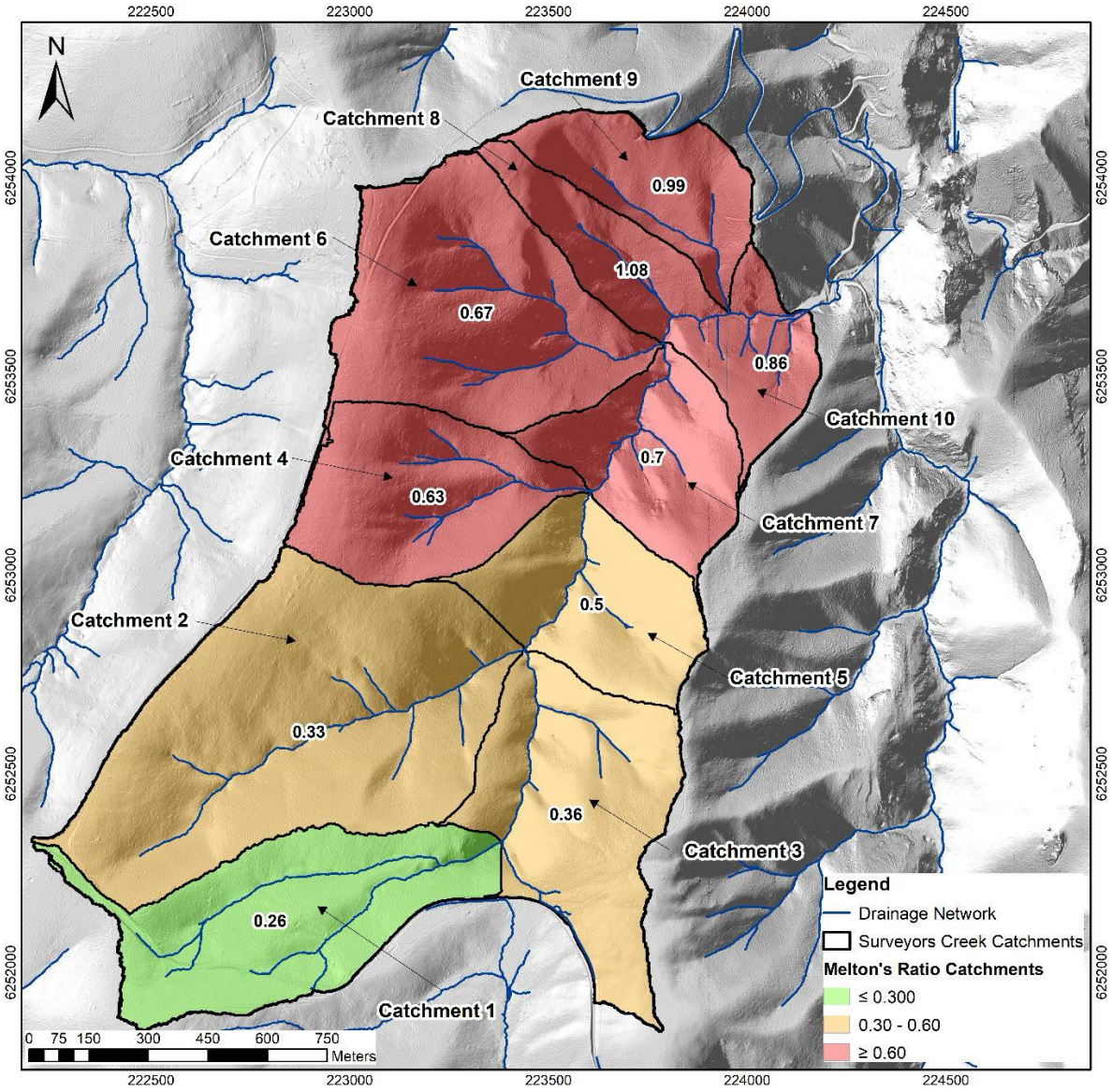


Figure 9: Melton Ratio numerical debris flood and flow susceptibility assessment

6 ENGINEERING DESIGN DEVELOPMENT

6.1 BASIS OF DESIGN

Based on site precedent, the debris susceptibility assessment and acknowledging that the JKCR will be prone to debris floods and flows until vegetation is re-established, it was recommended that a debris retention system be installed to complement the Surveyors Creek dam by providing additional debris catch capacity.

Recognising that debris generation is a natural and ongoing process, design of additional debris retention aims to reduce debris migration by retaining material within Surveyors Creek. This management strategy allows debris removal to occur 'offline' (away from public amenities) minimising operational disruptions and preserving the reserves amenity.

Design of a debris retention system requires estimation of typical debris volumes and the required retention capacity; this can be estimated by:

- Direct assessment – calculation of debris volumes from previous events
- Empirical assessment based on catchment area (NZGS, 2023)
- Hydraulic assessment – calculation for a range of annual recurrence intervals by multiplying clearwater flood volumes by a debris bulking factor (NZGS, 2023).

In this study debris volumes have been calculated utilising the direct and empirical assessment methodologies.

6.2 DEBRIS VOLUME AND THE REQUIRED RETENTION CAPACITY

6.2.1 Direct Assessment

The direct assessment estimates debris volumes based on past events and site-specific data. Following the April 2024 storm (approx. a 1:5 year event, see Figure 5), approximately 500 m³ (up to 35 % of Surveyors Creek Dams retention capacity) of debris was retained behind Surveyors Creek dam.

Although no historical records exist to quantify other single event debris volumes originating from Surveyors Creek, previous Blue Lake infilling events (Feb 2020, March 2021, April 2024) provided further basis for estimating debris volumes.

The Blue Lake has an estimated debris retention capacity of 15,000 to 20,000 m³ and is fed by three catchments:

- McKeowns Valley catchment (approximate catchment area = 21.5 km2)
- Camp Creek catchment (approximate catchment area = 2.65 km2)
- Surveyors Creek catchment (approximate catchment area = 2.57 km2).

Assuming each catchment has a similar sediment generating potential and contributes a volume of debris to the Blue Lake proportional to the catchment area, the approximate contribution of debris to the Blue Lake from each catchment is estimated as:

- McKeowns Valley – 80 %
- Camp Creek Catchment – 10 %
- Surveyors Creek Catchment – 10 %.

Based on this proportional contribution, Surveyors Creek may have deposited as much as 2,000 m³ of debris into the Blue Lake in the February 2020 or March 2021 event. It is therefore estimated Surveyors Creek requires a minimum retention capacity of 2,000 m³ for comparable events. This required catch capacity calculated is broadly equivalent to the capacity of Surveyors Creek Dam provided sediment buildup behind the dam is minimised.

6.2.2 Empirical Assessment

Figure 10 presents a summary of some empirical relationships between catchment area and debris volumes for granular debris flows (NZGS, 2023).

The total catchment area of Surveyors Creek (~2.6 km2) is presented on Figure 10 in green indicating:

- A 50th percentile volume estimate after Marchi et al (2019) of 4500 m3
- Typical volumes between approximately 12,500 and 55,000 m3 for most other authors
- A 98th percentile volume estimate after Marchi et al (2019) of 125,000 m3.

The empirical volume estimates above consider the entire Surveyors Creek catchment rather than just those catchments assessed to be prone to debris flows. When considering catchments prone to debris flows (i.e., MR ≥ 0.6, see Section 5.4.3), the total catchment area is ~1.2 km2 as shown on Figure 10 in red, indicating:

- A 50th percentile volume estimate after Marchi et al (2019) of 2,500 m3
- Typical volumes between approximately 6,000 and 32,000 m3 for most other authors
- A 98th percentile volume estimate after Marchi et al (2019) of 62,000 m.

Based on the empirical assessment, and considering only those catchments assessed to prone to debris flows (i.e., MR ≥ 0.6), Surveyors Creek Dam capacity is exceeded above the 50th percentile volume estimate after Marchi et al (2019).

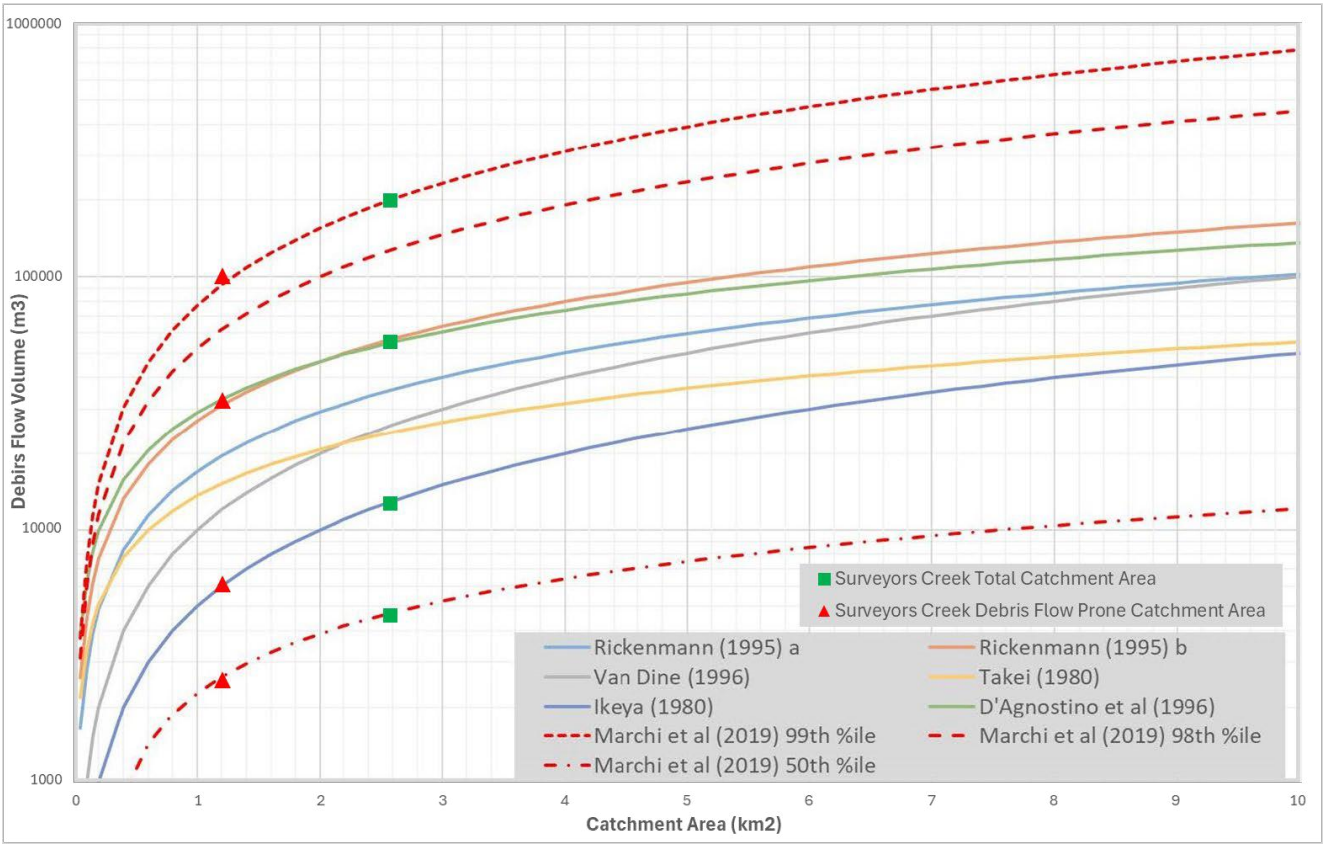


Figure 10: Relationship between debris volume and catchment area (after NZGS, 2023)

6.3 MITIGATION OPTIONS

There are several different options to provide additional debris catch capacity including:

- Debris retention basins
- Check dams
- Flexible barriers (debris fences)
- Natural barriers (placed boulders, logs etc.).

Given site constraints, ease of construction, and the ability to catch debris while allowing water to pass, flexible barrier(s) were recommended to provide additional catch capacity as required.

6.4 DEBRIS FENCE DESIGN

The primary design considerations included in the proposed debris mitigation system are discussed in the following sections.

6.4.1 Location

Due to site constraints, two potential locations for debris fences between the Surveyors Creek Dam and Carpark 1 (see Figure 1) were assessed which aim to provide a balance of the following:

- Location relative to active tributaries and debris sources
- Cross sectional area and subsequent retention capacity
- Accessibility for both construction and ongoing maintenance (including debris removal).

6.4.2 Retention Capacity

Both debris fence locations were calculated to have a retention capacity between 350 and 450 m3, or between 700 m3 and 900 m3 if debris fences are installed at both locations.

Including Surveyors Creek Dam this brings the debris retention capacity of Surveyors Creek to between 1,850 m3 and 2950 m3 if one debris fence is installed, and between 2,200 m3 to 3,400 m3 if both debris fences are installed.

Our assessment indicated there are no other practical alternatives to provide additional catch capacity without significant expenditure and therefore the retention system cannot achieve typical empirical capacities reported in the literature. Installation of the debris fences would increase the debris retention capacity by up to 30% if both fences are installed providing additional protection in the system if Surveyors Creek Dam reaches capacity. Options to increase the dams retention capacity were not considered due to heritage and cost relative to the proposed fences. Based on the direct assessment of debris volume, the system achieves the required capacity for similar events that have occurred over the past five years, providing some redundancy in design, particularly if Surveyors Creek or the debris fences are not at 100% capacity prior to an event.

6.4.3 Specification and Design Parameters

Due to the creek dimensions at the nominated locations, the Geobrugg VX System was recommended which incorporates a primary ring net mesh, support ropes and anchors. It was further recommended that rock armour be placed to support the flanks (anchors) from scour and erosion under both normal flow and flood (debris) events.

Debris floods are expected to be the dominant mechanism with higher frequency that debris flows. The following debris type and density have been adopted for design which assume sediment concentrations consistent with an upper bound debris flood density:

- Debris type:
  - Debris composed of sandy fine to coarse gravel, cobbles, boulders, and driftwood
- Debris density between:
  - 50% debris (2,200 kg/m3) and 40% water = 1,600 kg/m3 and
  - 30% debris (2,200 kg/m3) and 60% water = 1,200 kg/m3.
- Debris velocity:
  - Less than 5 m/s, consistent with typical debris flood velocities.

The intention of the debris fence system is to intercept and retain debris prior to it reaching the Blue Lake. From field observation we anticipate sandy fine to coarse gravel is the dominant material type to be retained, and for this purpose a finer secondary mesh to capture finer debris was recommended to be installed as part of the fence design.

It should be understood that the system is a filter barrier that allows flow to pass through whilst retaining larger sediment. The system is not designed to retain fine materials which are anticipated to filter through the debris fence under normal flow conditions. However, it is expected that some retention of finer particles will occur during events where debris fills up behind the fence and reduces flow velocity, however if sediment levels are not maintained behind the debris fence it is expected that finer sediments will erode and filter downstream over time.

Additional parameters required for debris fence design include anchor bond strength and specific hydraulic parameters (debris impact velocity and peak discharge) which are not reproduced in this paper.

6.4.4 Maintenance

Effective performance and longevity of debris fences require ongoing maintenance and inspection. This includes replacing damaged components and management of debris levels, particularly following rainfall events that have approached the documented thresholds known to increase debris flood and flow susceptibility. Within Surveyors Creek this also includes maintenance of debris levels within the dam to maintain the systems retention capacity.

The proposed debris fences have been located such that debris levels can be maintained from the upstream side via the use of excavators, however there may be a need from time to time to maintain debris levels from the downstream side which requires disassembling and reassembling of the debris fence(s).

7 CONCLUSION

This study has assessed the susceptibility of debris floods and flows in the Jenolan Karst Conservation Reserve following the 2019 to 2020 summer bushfires and the prolonged La Niña climatic pattern that extended from 2020 to 2023. By integrating geological, hydrological, and geomorphological analyses, along with the application of the Melton Ratio, we have identified key factors contributing to debris mobilisation and transport within Surveyors Creek.

The findings highlight that bushfire-induced vegetation loss, coupled with intense rainfall, significantly increases the likelihood of debris flood and flow events. Catchments in the north of the study area exhibit the highest susceptibility, with debris in storage observed on steep slopes.

To enhance site resilience, flexible debris fences have been proposed to supplement the retention capacity of Surveyors Creek Dam. These structures provide a pragmatic, cost-effective approach to intercept debris and minimise downstream impacts on the Blue Lake and adjacent infrastructure. While the mitigation measures proposed in this study provide immediate risk reduction, ongoing monitoring, maintenance, and adaptive management are essential to ensure long-term effectiveness.

References

Branagan, D.F., Pickett, J.W., & Percival, I.G. (2014). Geology and geomorphology of Jenolan Caves and the surrounding region. *Proceedings of the Linnean Society of New South Wales, 136*, 99–130.

DeGraff, J.V., Cannon, S.H., & Gartner, J.E. (2015). The timing of susceptibility to post-fire debris flows in the western United States. *Environmental & Engineering Geoscience*, *21(4),* 277–292.

Hungr, O., Evans, S., Bovis, M., & Hutchinson, J. (2001). A review of the classification of landslides of the flow type. *Environmental & Engineering Geoscience, 7*(3), 221–238.

Hutchinson, J.N. (1988). General report: Morphological and geotechnical parameters of landslides in relation to geology and hydrogeology. In Bonnard, C. (Ed.), *Proceedings, Fifth International Symposium on Landslides*, Vol. 1 (pp. 3–36). A.A. Balkema, Rotterdam.

Jackson, L.E. Jr., Kostaschuk, R.A., & MacDonald, G.M. (1987). Identification of debris flow hazard on alluvial fans in the Canadian Rocky Mountains. *Reviews in Engineering Geology, 7*, 115–124.

Marchi, L., Brunetti, M.T., Cavalli, M., & Crema, S. (2019). Debris-flow volumes in northeastern Italy: Relationship with drainage area and size probability. *Earth Surface Processes and Landforms, 44*, 933–943.

Melton, M.A. (1957). *An analysis of the relations among relief, slope, and drainage basin characteristics*. *Bulletin of the Geological Society of America, 68*(8), 1,149–1,174.

NZGS (2023). *Slope Stability Geotechnical Guidance Series*. Unit 1 – General Guidance. New Zealand Geotechnical Society, December 2023.

Parise, M., & Cannon, S.H. (2012). Wildfire impacts on the processes that generate debris flows in burned watersheds. *Natural Hazards, 61*, 217–227.

Welsh, A., & Davies, T. (2011). Identification of alluvial fans susceptible to debris-flow hazards. *Landslides, 8(2)*, 183–194.

Wilford, D.J., Sakal, M.E., Innes, J.L., Sidle, R.C., & Bergerud, W.A. (2004). Recognition of debris flow, debris-flood, and flood hazard through watershed morphometrics. *Landslides, 1*, 61–66.

https://doi.org/10.56295/1ACEG11

THE USE OF EMPIRICAL METHODS TO PREDICT LANDSLIDE RUNOUT FOR USE IN RAPID LANDSLIDE RISK ASSSESSMENTS FOLLOWING CYCLONE GABRIELLE, NEW ZEALAND

R. Hayes, A. Hunter and A. S. Miner
GHD

ABSTRACT

In February 2023, a severe weather event triggered widespread landslides across the coastal towns of Muriwai, Karekare and Piha, New Zealand, causing extensive damage and resulting in fatalities. In response, there was an urgent need to conduct area-wide landslide risk assessments on individual properties with respect to future debris flow hazards. This paper focuses on the development of rapid methods to predict landslide runout, using established empirical methods. With an inventory of 160 mapped landslides empirical-statistical relationships were established between runout distance, landslide volume, and downslope angle. Variation in data correlations ultimately necessitated the adoption of separate empirical models for Muriwai and Piha/Karekare.

These simple empirical-statistical models were combined with flow accumulation modelling to predict both landslide distance and direction. The method ultimately proved highly effective for the rapid delivery of risk assessments but highlighted the importance of using observational data, incorporating site-specific factors that influence landslide runout behaviour and applying a degree of judgement.

1 INTRODUCTION

Cyclone Gabrielle was an extreme weather event that occurred in February 2023, causing widespread flooding and >140,000 landslides (Geonet, 2023) across regions in the north and east of New Zealand's North Island. At $14.5 billion, the event became the costliest weather-related disaster in the country's history (phcc.org.nz). Dozens of landslides occurred in the coastal settlements of Muriwai, Piha and Karekare, located in the Waitakere Ranges region on the West Coast of Auckland, resulting in widespread damage to built infrastructure and the loss of two lives.

Prior to Cyclone Gabrielle the Auckland region was already under a state of emergency following a series of extreme weather events in January 2023 including the "Auckland Anniversary" storm when 160 mm of rainfall fell in just 6 hours, estimated to be a 1 in 250-year event (NIWA, 2023). Critically therefore it is implied that the slopes that failed in Muriwai, Piha and Karekare were already subject to a reduction in strength due to oversaturation.

As part of the emergency response following the event Auckland Council completed a preliminary assessment of risk to life using the rapid building assessment placarding system (building.govt.nz) in which buildings were either given unrestricted access (white placard), restricted access (yellow placards) or prohibited access (red placards). Following the initial emergency response an area-wide quantitative risk assessment was carried out on individual placarded properties to assess risk to life with respect to future landslide hazards, using the Australian Geomechanics Society Landslide Risk Management Guidelines, commonly referred to as AGS (2007).

A crucial element of the quantitative risk assessment process is understanding both the direction and reach of a future landslide hazard. Given the urgency for an outcome for homeowners and the requirement for speed and consistency in the assessments to facilitate the Auckland Council policy developed for a "buy out scheme" (Roberts, 2024), a rapid method for predicting landslide runout was required. This paper discusses the use of published empirical methods to develop predictive landslide runout models using observed landslide behaviour from the previous event which subsequently informed the quantitative risk assessments.

2 LANDSLIDE RISK ASSESSMENT PROCESS

Use of AGS (2007) quantitative risk assessment to estimate risks to loss of life for the person-most-at-risk was mandated by Auckland Council to be applied to each individual property. The Individual Risk-to-Life is defined as the risk of fatality or injury to any identifiable (nominated) individual who lives within the zone impacted by the landslide; or who follows a particular pattern of life that might subject them to the consequences of the landslide. In this instance this was a person occupying a building at risk of being impacted by a landslide. The risk of 'loss-of-life' to an individual is calculated from:

$$R_{(LoL)} = P_{(H)} x\ P_{(S:H)} x P_{(T:S)} x V_{(D:T)} \quad (1)$$

Where,

$R_{(LoL)}$ is the risk (annual probability of loss of life (death) of an individual).

$P_{(H)}$ is the annual probability of the landslide.

$P_{(S:H)}$ is the probability of spatial impact of the landslide impacting a building (location) taking into account the travel distance and travel direction given the event.

$P_{(T:S)}$ is the temporal spatial probability (e.g. of the building or location being occupied by the individual) given the spatial impact and allowing for the possibility of evacuation given there is warning of the landslide occurrence.

$V_{(D:T)}$ is the vulnerability of the individual (probability of loss of life of the individual given the impact).

The main objective of the risk evaluation is to compare the assessed risk to risk levels that are considered acceptable or tolerable to the community to enable informed policy decisions. These risk levels ultimately formed the basis of categorising each property for the "buy out" scheme and revising the original placards given during the rapid building assessment process. The risk acceptance criteria adopted by Auckland Council was a tolerable risk value of 10^{-4}/annum. It is important to distinguish between "acceptable risks" and "tolerable risks". AGS (2007) states that tolerable risks are within a range that society can live with so as to secure certain benefits. It is a range of risk regarded as non-negligible and needing to be kept under review and reduced further if practicable. Acceptable risks are usually considered to be one order of magnitude lower than tolerable risks.

It is essential to recognise that there is an inherent level of uncertainty within the quantitative risk assessment process. Typically landslide risk assessments are based on a variety of different information that ranges from well-established knowledge to judgements, educated guesses and tentative assumptions. The effect of uncertainty is not usually implicitly stated. One of the main factors that influences the dependability of a landslide risk assessment is the nature and quality of evidence used to generate probability. In this study, the use of observed landslide behaviour from the previous event has been calibrated with published empirical methods for predicting landslide runout when estimating the probability of spatial impact ($P_{(S"H)}$).

3 STUDY AREA

The study areas are situated on the west coast of Auckland (Figure 1). Piha and Karekare are located within the Waitakere Ranges and Muriwai is approximately 8 km north of the ranges. The geomorphological and geological settling at Piha and Karekare are in contrast to those in Muriwai.

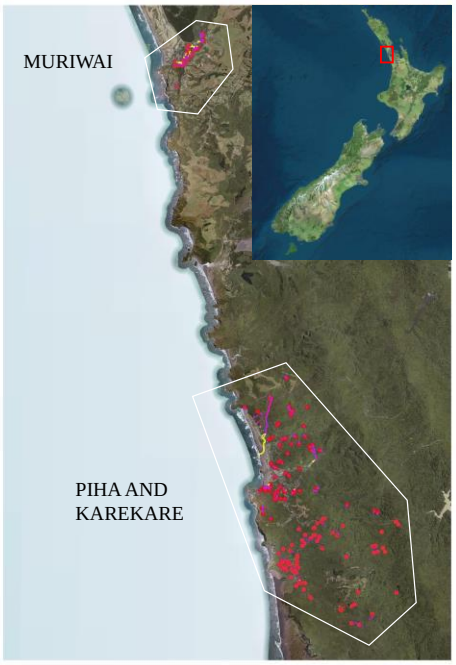


Figure 1: Landslides mapped in the coastal settlements of Muriwai, Piha and Karekare on the West Coast of Auckland

3.1 GEOMORPHOLOGICAL SETTING

Muriwai is characterised by an approximate 1.5 km-long escarpment that divides the township (Figure 2). The majority of the settlement is situated on the low-lying slopes beneath the escarpment and associated coastal terrace to the west (near sea level). There is a vertical elevation difference of approximately 80 m between the lower terrace and the higher plateau above the escarpment to the south and east. The centre of the escarpment is delineated by a north-west trending ridgeline, where slopes on the escarpment north of the ridgeline are typically 30° and have an 80 m vertical elevation and the slopes to the south are less well defined and variably have less than 50 m vertical elevation. The edge of the plateau is characterised by distinct crescent shaped scarps associated with past landslide events.

Piha and Karekare are situated on the western sloping margin of the Waitakere Ranges, which in contrast to the Muriwai area are characterised by a relatively steep, dissected topography with sharp ridgelines (Figure 2). The slopes are typically forested with dense native vegetation. Piha, approximately 3.5 km north of Karekare is bisected by the Piha Stream which divides the southern and central portions of the settlement. Although the majority of the settlement occupies much of the coastal backshore and elevated sand dunes, many properties also occupy the gently sloping, low lying stream flood plains in the central portion of the settlement as well as relatively steep hillsides in the southern portion up to 280 m RL. The settlement of Karekare occupies less of the low lying coastal area and is linearly distributed along two main roads (Karekare Road and Lone Kauri Road) which traverse both the low lying flood plain of Karekare Stream within the main valley feature and steep hillsides up to 320 m RL. Geomorphic features interpreted as relic landslide scarps are also common in the landscape.

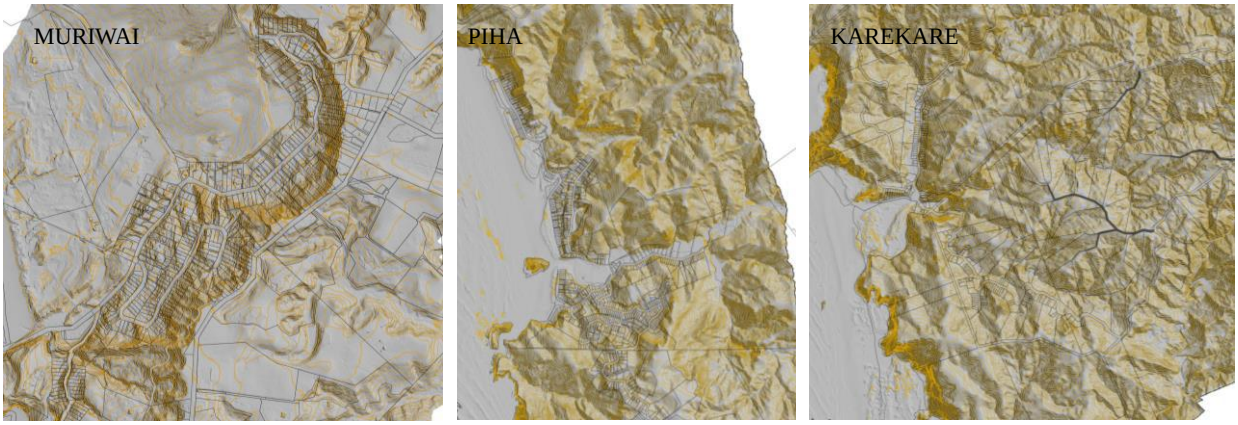


Figure 2: Muriwai and Piha/Karekare areas exhibit significantly different geomorphological characteristics

3.2 GEOLOGICAL SETTING

The geomorphological features described above are generally a consequence of the underlying geology. Muriwai is underlain by the Awhitu Sand Formation, part of the Kaihu Group coastal deposits (Pliocene age <2 Mya), which unconformably overly Miocene age volcanic and volcaniclastic deposits, and form the escarpment slopes. The Awhitu Sand Formation is characterised by dense to very dense sand in the top 30 m generally comprising fine to coarse clayey sand. Below 30 m the formation becomes a moderately weathered, massive to thickly bedded sandstone with very low to low strength. The beds are subhorizontal, discontinuous and cross bedded, consistent with costal dune formation, notably containing occasional discontinuous laminated to thick layers (generally <0.1 to 1 m) and lenses of silt, clay and peat.

The Awhtiu Sands have relatively high concentrations of iron which has oxidised near the modern day surface developing a binding cement giving the sands rock mass properties. The upper profile has been less affected by iron cementation and/or prone to dissolution due to exposure to weathering. The occurrences of fine grained or highly cemented layers tend to act barriers to groundwater, resulting in localised saturation of unconsolidated layers.

The hillsides in Karekare and Piha are underlain by the Piha Formation and Lone Kauri Formation, part of the Waitakere Group Volcanics. The Waitakere Ranges, which formed approximately 25 Mya are the remnants of a large volcanic system, the centre of which was approximately 200 km offshore. The Piha Formation and Lone Kauri Formation are submarine volcanic breccia conglomerate and terrestrial extrusive (subaerial basaltic andesite flows and pyroclastics) and shallow intrusive rocks, respectively. The rock mass is similarly massive with widely spaced joints. Critically the soil weathering profile developed within each formation is shallow (<1 m) typically comprising silts and clays with gravel to boulder sized rock fragments. Colluvial deposits are common on lower slopes and within incised gullies.

4 LANDSLIDE HAZARDS AND INVENTORY

Following the event Auckland Council captured high resolution LiDAR data and aerial photography of the study areas. An attempt was made to undertake a DEM change analysis using pre event LiDAR data (LINZ, 2018) to identify landslides through obvious areas of ground surface change between the pre and post event DEM's, however this provided mixed results, potentially a result of contrasting resolution and survey techniques. Ultimately it was manual work with aerial photography in combination with the new LiDAR data which proved the most effective way to systematically map over 200 landslides, recording characteristics such as the zone of depletion and zone of accumulation. Subsequent targeted ground truthing was pivotal to confirm the presence of landslides and their runout extents as well as develop observational engineering geological models for each site under assessment.

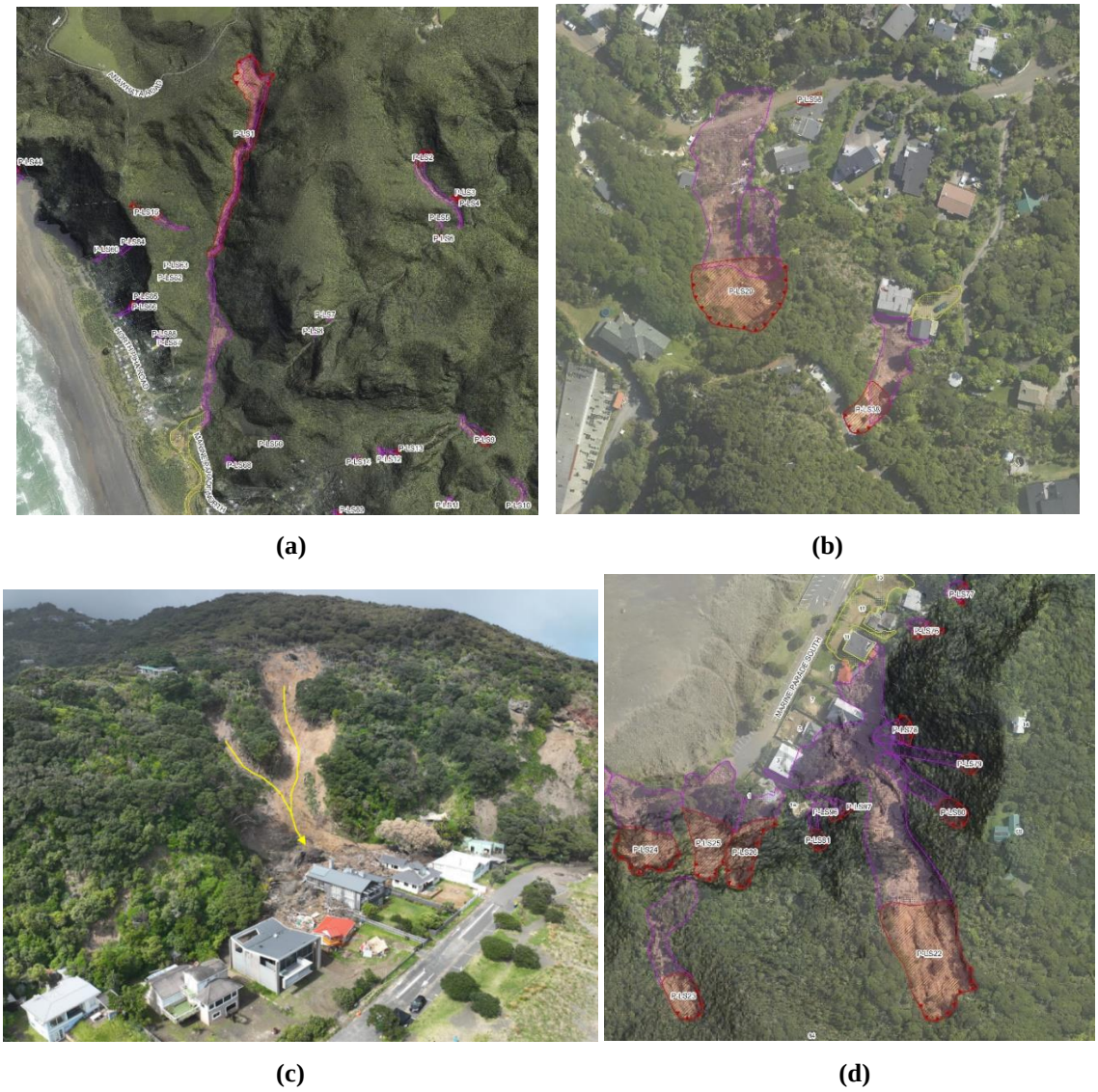
Landslides that occurred on natural slopes throughout Muriwai, Piha and Karekare initiated as small to large slides (either translational or rotational) at their source area which subsequently became fluidised under surface and subsurface water flows to transition into debris flows, defined as extremely rapid debris flows according to the Hungr et al. (2014) classification system. A debris flow is referred to exclusively by Hungr et al. (2014) as a channelised landslide, whereas a landslide consisting of flowing debris on an open slope is referred to as a debris avalanche. In this study, the term debris flow is adopted universally. A common factor across the entire study areas was the relatively shallow depth of the initial slides, which was generally <1m occasionally up to 2m.

In Muriwai landslides initiated from a common source area, the crest of the main escarpment (Figure 3). The main scarps were measured up to 70 m in width, and they typically had a runout which extended well beyond the base of the escapement on the flatter coastal terrace below. Smaller landslides occurred on topographic spurs within the escarpment and were less likely to have a runout extending to the escarpment base. The topography of the escarpment is not deeply incised, rather characterised by shallow and relatively open gullies, drainage features and spurs which resulted in minimal debris flow confinement. Key preparatory factors likely to have contributed to the failures include cementation of the sands susceptible to dissolution and lenses and layers of fine grained composition acting as aquicludes (multiple occurrences and anecdotal evidence of groundwater emanating from the zone of depletion).



Figure 3: Examples of landslides which occurred on the main escarpment in Muriwai

Generally, much smaller in volume than Muriwai, the landslides in Piha and Karekare were widely distributed, rarely clustered. With no distinct correlation with regards to source location, they typically initiated on slopes >25°. The critical preparatory factors considered is the permeability contrast between the shallow soil profile (typically residual soils and colluvium) and the underlying rock mass and the relatively steep dip of the rock surface on which the soils lie. As a reflection of the topography, the degree of confinement varied significantly with runout distances up to 1 km mapped where landslides entered incised gully features (Figure 4).



(a) **(b)**

(c) **(d)**

Figure 4: (a) Example of confined landslide in Piha with a runout extent over 1km. (b) Examples of landslides terminating on build infrastructure in Piha. (c) Example of landslide amalgamation at Marine Parade South in Piha. (d) Mapped landslides at the same location. Illustrating difficulty when differentiating separate debris flow runouts

In addition to the morphology of the topography, landslide runout direction and distance was often influenced by other factors including the type and density of vegetation, the presence of the built environment in the runout path (Figure 4), the accumulation (entrainment of additional soil in the runout path or amalgamation with other debris flows) (Figure 4) or depletion (deposition of debris along the runout path or splitting of a single debris flows in different directions) of debris volume.

5 REVIEW OF EMIPIRCAL RUNOUT METHODS

The AGS (2007) guidelines highlight the importance of the ability to predict landslide runout distance and velocity to reliably determine the extent it will affect property and persons downslope. This involves understanding the slope characteristics, mechanism of failure and characteristics of the downhill path. The guidelines indicate the importance of established empirical methods such as Hunter and Fell (2002) and Corominas (1996) to estimate runout distance. Where empirical methods are used for travel distance predictions, much judgement is required and it is important to calibrate the methods with observed landslide behaviour in the study area to reduce uncertainty and improve accuracy in the prediction model.

Empirical runout models for natural landslides that rely on statistical geometric correlations have long been established as a useful tool for predicting the runout distance to inform landslide risk assessments. The earliest empirical runout

relationship was developed by Heim (1932) who proposed that the distance a landslide travels is proportional to its fall height defining the "Fahrböschung" angle (F-angle) as the tangent of the ratio of fall height (H) to horizontal runout distance (L) between the crest of the source zone and the toe of the deposit (Figure 5).

A number of authors have since expanded upon Heim's work, adopting an inverse correlation between landslide volume and Fahrböschung angle (Scheidegger 1973; Li 1983; Corominas 1996; Finlay et al 1999; Hunter and Fell 2002). These authors have also incorporated other variable factors such as path morphology, landslide classification, and obstructions in attempt to improve the Fahrböschung-volume correlation for more site specific adaptation. Hungr et al (2005) provides a concise overview of some these established methods, highlighting a lack of agreement among researchers with respect to volume for both large landslides (Hsü 1975) and small landslides (Hunter & Fell 2003) as a predictor for landslide mobility.

Corominas (1996) studied the effect of deflection, confinement and vegetation as obstacles for different landslide classifications. Dividing events into more homogeneous groupings produced distinct trends (although required the subdivision of an already small data set).

Finlay et al.'s (1999) data was a mixture of good and modest quality information which is reflected in the large scatter of the predicted travel distances, hypothesising that at low volumes, other factors like slope angle, path confinement, geology, groundwater, and failure mechanism have more of an effect on runout than at larger volumes, as small landslides do not develop the large energy/momentum that overshadows these factors.

Hunter & Fell (2002) revised previous work using more selective good quality data. Interestingly, they found significant improvement in their predictive models for travel distance angle (F-angle) by including the downslope angle below the source area (Figure 5). This applied to "rapid" slides on steep natural slopes. The downslope angle is defined as the average angle of the portion of the downslope from the landslide source area to the point where the slope begins to flatten out (Hunter & Fell, 2002).

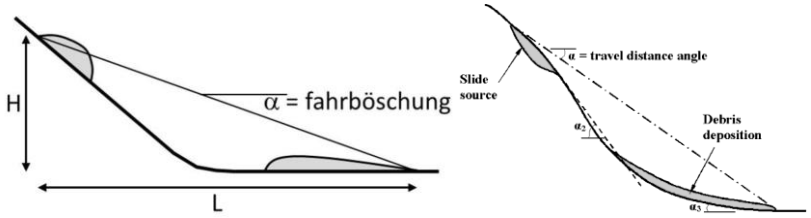


Figure 5: (Left) Fahrböschung angle definition, where H is the elevation difference between the source zone crest and toe of the runout and L is the plan distance between the source zone crest and toe of runout (after Heim, 1932). (Right) Definition of downslope angle below source area α_2 for slides on steep natural slopes (after Hunter & Fell, 2002)

More recent work by Brideau et al. (2021) using the correlation between landslide volume and Fahrböschung angle compiled a large dataset from previous published work (i.e. Scheidegger 1973; Li 1983; Corominas 1996) in combination with unpublished New Zealand landslides triggered by earthquakes and rainstorm events. They separated a series of plots for different landslide types, glacier versus unglaciated environments, travel path morphology and triggers (earthquake or rain). Clear variability in the data was evident, attributed to a range of site-specific and analysis specific conditions.

Other established methods include the correlation based on Galileo scaling laws, between landslide volume and the area covered by the deposit, which has been documented for rock avalanches and lahars (e.g. Li 1983, Iverson et al 1998). Whitall (2020) found good correlation with a length versus height relationship favourable for small open pit failures with small volumes at bench scale and showed that mobility of pit slope failures appear relatively insensitive to volume up to approximately 10,000 m^3.

6 EMPIRICAL RUNOUT ASSESSMENT USING CASE STUDY DATA

An inventory comprising 160 mapped landslides (32 in Muriwai and 128 in Piha and Karekare) formed the dataset used to develop empirical-statistical relationships between the H/L ratio and both landslide volume and downslope angle (Figure 6 and 7). Given the contrasting geomorphological and geological conditions at Muriwai compared to Piha and Karekare, the data was separated for the analysis. The data within each study area was divided into subsets for multiple linear regression analyses based on the influence of path morphology (degree of confinement) on the runout distance. At Muriwai three subsets were used; unconfined (slopes with little to no confinement), partially confined (landslide may enter a topographic drainage feature which has some influence on direction of travel) and confined (landslide typically entered a distinct gully / drainage feature, becoming channelised). At Piha and Karekare a simpler approach was adopted in an attempt to reduce ambiguity in the risk assessment process, two subsets were defined (unconfined and confined).

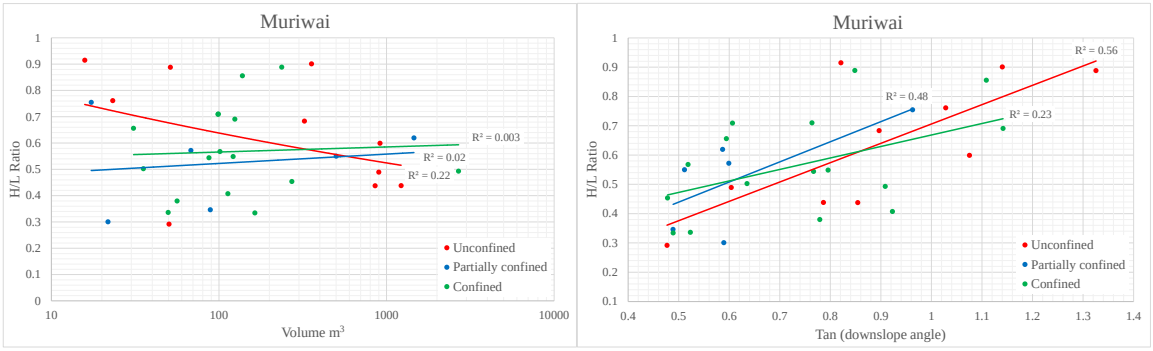


Figure 6: Empirical relationships for Muriwai landslides with different travel path morphologies for (left) H/L ratio and volume and (right) H/L ratio and downslope angle

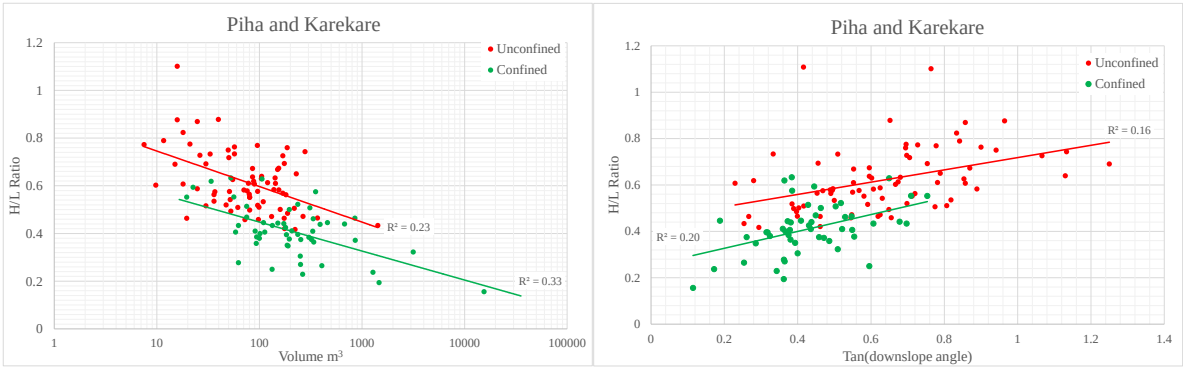


Figure 7: Empirical relationships for Piha and Karekare landslides with different travel path morphologies for (left) H/L ratio and volume and (right) H/L ratio and downslope angle

Interestingly the relationship between landslide volume and runout distance for the Muriwai data shows a broad scatter of data with a poor correlation between the H/L ratio and landslide volume. Adopting volume as the main variable, the most common empirical relationship in the published literature to predict landslide runout, did not appear useful in the case of Muriwai. The Hunter and Fell (2002) predictive method for "rapid" landslides on steep natural slopes in dilative soils correlates H/L with the downslope angle and degree of confinement. Using this method, the Muriwai landslide data shows a stronger correlation. The 'partially confined' travel path in particular was found to be very similar to the respective Hunter and Fell (2002) regression line (Figure 8). A comparison exercise of this method with the measured F-angles for several of the February 2023 landslides typically found agreement within a few degrees.

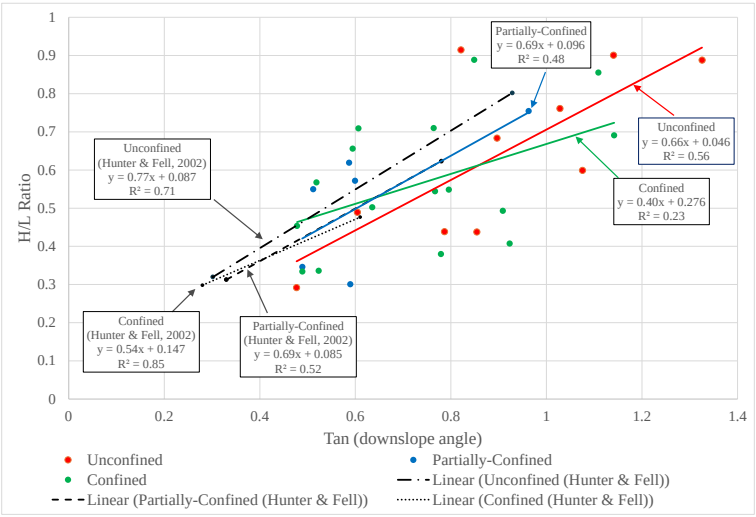


Figure 8: H/L ratio versus downslope angle relationship for Muriwai data together with Hunter & Fell (2002) relationships for rapid landslides on steep natural slopes in dilative soils.

The Piha and Karekare data show a clearer trend of reducing H/L with increased volume. It also demonstrates the dominant influence the degree of confinement had on the landslide runout behaviour for the February 2023 landslides.

The coefficient of determination R^2, for the best fit regression lines is 0.23 and 0.33 for unconfined and confined flows, respectively which can be considered 'weak to moderate' correlations. As a comparison, the data is also presented on a H/L ratio versus the tangent of the downslope angle and regression lines established. While there appears to be a correlation, there is a broader degree of scatter in the data relative to the relationship with volume.

7 RAPID LANDSLIDE RISK ASSESSMENTS

As part of the immediate emergency response there was a requirement for Auckland Council to make rapid decisions with regards to which homes were at risk from further landslide hazards and therefore required evacuation. The use of the Fahrböschung (F) angle was adopted by measuring runout distances of seven landslides, mapping the minimum and maximum F-angles from the crest of the escarpment across the remainder of the affected downslope areas (Roberts, 2024) (Figure 9). The results ranged from 22° to 25°. Each home was subsequently assigned a placard. The assessment is a good example of the effectiveness of the F-angle approach as an initial screening tool, but was not intended for use in longer term decision making or planning (i.e. adoption in the quantitative landslide risk assessment process).

Ultimately, in the case of Muriwai, the landslide risk assessment process was guided by a computer simulated three-dimensional debris flow assessment (RAMMS software) which estimated the landslide runout behaviour of future landslide hazards initiating from the escarpment crest (Figure 9).The modelling process took nearly six months and therefore the use of empirical-statistical relationships established between H/L ratio and downslope angle for predicting landslide runout was adopted as an interim method where rapid decision-making was required. Empirical methods were also used to further verify the RAMMS modelling outputs and the observed landslide runouts.

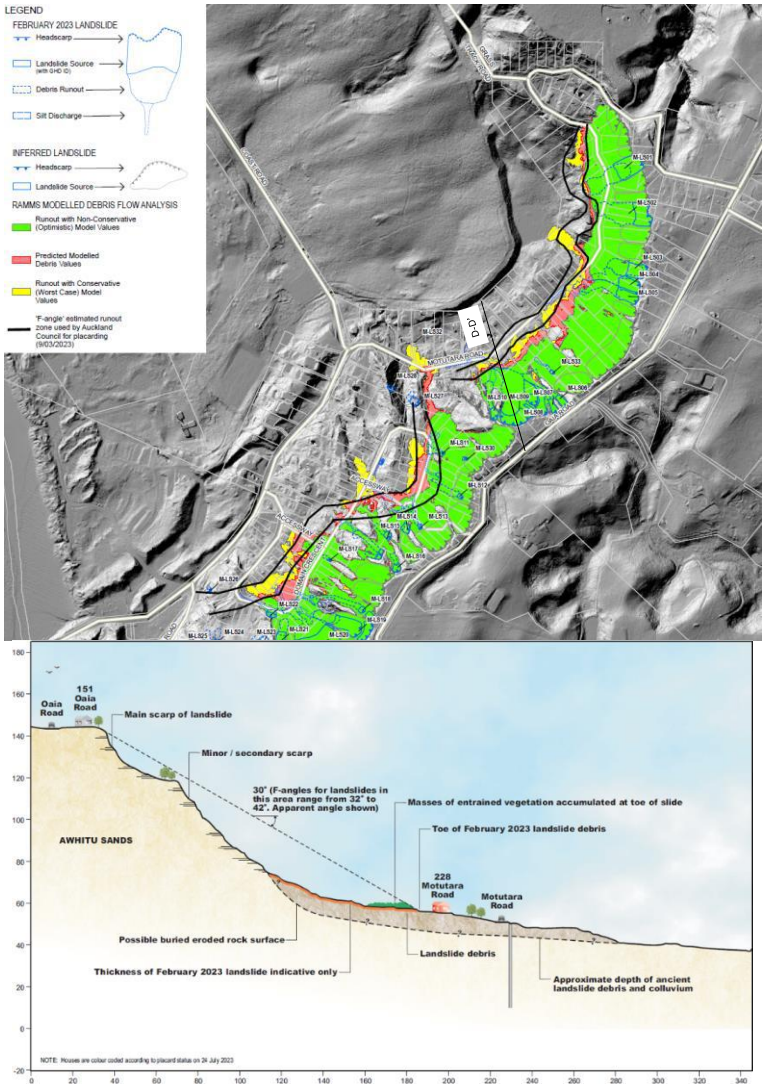


Figure 9: (Top) Results of RAMMS modelling showing simulated debris flow extents in Muriwai and best and worst case F-angles (black lines). (Bottom) Illustrative cross section (D-D') showing F-angle measurement.

The use of numerical analyses were considered inappropriate for Piha and Karekare due to both time constraints and the dispersed nature of the sites requiring assessment. Therefore, the development of empirical-statistical relationships formed an integral element of the risk assessment process. The probability of spatial impact $P_{(S:H)}$ was partitioned into two separate conditional probabilities,

$$P_{(S:H)} = P_{(S':H'2)(H)} x\, P_{(S':H'2)} \quad (2)$$

Where,

$P_{(S':H'1)}$ is the probability that if the landslide occurs it travels in the direction of the site under assessment

$P_{(S':H'2)}$ is the probability that is the landslide occurs it will travel to at least the site under assessment and will impact the property.

Given the understanding that the direction of debris flow runout is typically determined by the nature of the slope morphology below the source area, a rapid method for predicting flow direction was required. Flow accumulation analysis was completed using the 2023 DEM. This is a GIS tool typically used for hydrological modelling and deriving accumulated flow from a DEM. Assuming a landslide source area (typically slopes >25° above the site under assessment), the tool provided a rapid solution to determine the potential direction a landslide would travel (Figure 10). If the slopes are generally unconfined a landslide is assumed to travel perpendicular to the contours i.e. straight down the slope towards the site under assessment, a high probability of 0.8 to 1.0 was adopted. If debris is likely to become channelised (confined) by entering a topographic feature, and the site is within the down slope path of the channel, a probability of 0.8 to 1.0 was adopted. Where the channel is likely to direct the landslide away from the site, a low probability of 0.05 was adopted. The flow accumulation analysis was also used to help determine whether the potential landslide hazard would be defined as unconfined or confined for the purposes of assessing travel distance.

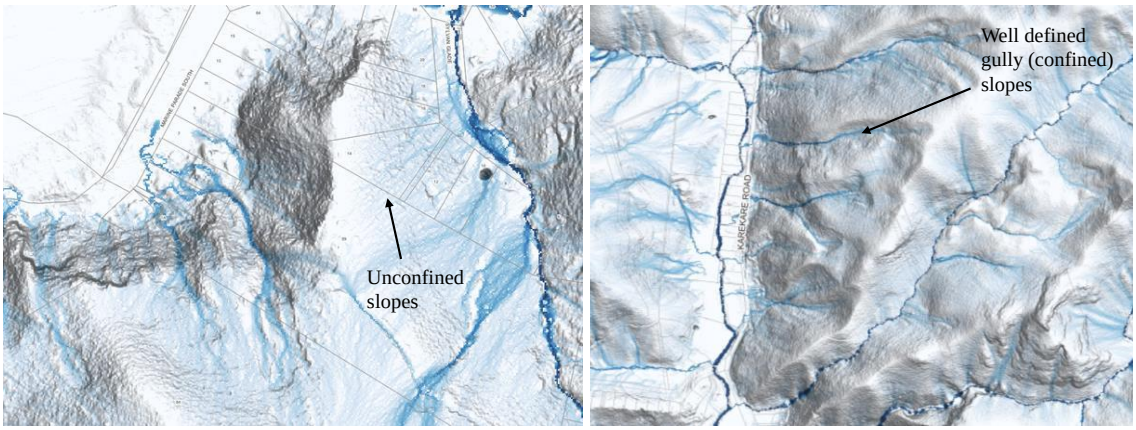


Figure 10: Examples of flow accumulation analysis used as a rapid tool to predict the likely behaviour of debris flows occurring above the sites. (Left) Unconfined slopes. (Right) Landslides likely to become channelised in gully features (confined)

To estimate the volume of a future landslide hazard which could be consistently applied to each site under assessment, a 'most likely significant landslide' definition was adopted. This was determined by analysing the range of February 2023 landslide volumes in combination with the respective level of damage inflicted. It was found that once the volume reached approximately 100 m³, most debris flows resulted in partial or complete collapse of a building. To predict the landslide travel distance, the corresponding F-angle for either unconfined or confined flow was determined using the best fit linear regression line on the H/L ratio versus volume plot. The F-angle was transposed onto a cross section from the assumed landslide source through the predicted travel path and site under assessment and landslide runout extent determined by its intersection with the topography. A probability of 1.0 was adopted where the F-angle projected beyond the building, 0.5 where it projected to the rear of the building and 0.0001 where it fell short of the building. Noting that observational behaviour took precedence where relevant i.e. if a previous landslide within close proximity to the site travelled further than predicted runout, a greater travel distance was assumed.

A particular site within Piha worthy of discussion is North Piha Road. A number of properties requiring a landslide risk assessment located along the backshore of Piha beach lie at the base of an escarpment on which six landslides occurred during the February 2023 event. Both empirical and numerical approaches were adopted to compare the predicted runout of future landslide hazards occurring above 35 properties. A series of section lines were produced along the escarpment and the F-angle projection lines applied (Figure 11). A numerical analysis utilising DHI's proprietary software MIKE Zero 2023, typically used to model surface water flow, and similar to RAMMS, simulated debris flows incorporating

material parameters based on the behaviour of landslides in the previous event. A reasonably good correlation was found between the predicted landslide runout extent for both the empirical and 3D modelling approaches (Figure 11). Judgement was weighted towards evidenced based behaviour of previous landslides where significant discrepancy was observed.

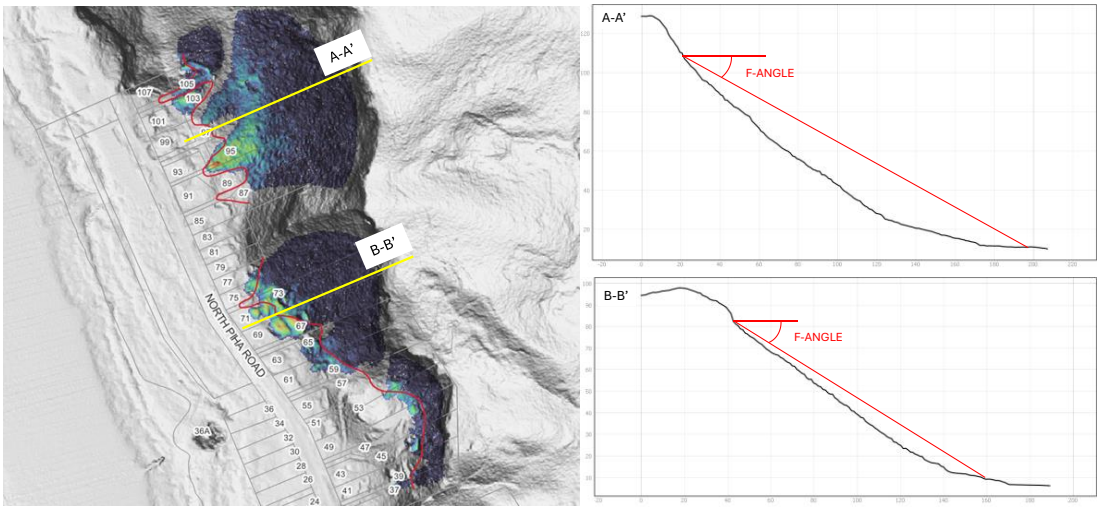


Figure 11: (Left) Modelled debris flow runout extents using MIKE Zero 2023 and estimate extent based on F-angle modelling (red line). (Right) Examples of F-angle transposed onto cross section through two sites

The approach of selecting a single value from the best fit regression lines on the H/L ratio versus volume plot proved effective for this assessment. The AGS (2007) guidelines, and others (i.e. McDougall, 2017) suggest a probabilistic approach could be used to limit uncertainty by defining the probability of exceedance of a specific landslide volume. Alternatively, the level of uncertainty in the dataset could be accounted for by using confidence intervals. Figure 12 shows the lower bound 50% confidence interval for unconfined and confined flows, i.e. where in 50% of cases, the true average H/L ratio will fall within this range. As a result, a more conservative approach, given the scatter of data could be to adopt the H/L ratio corresponding to this lower bound line.

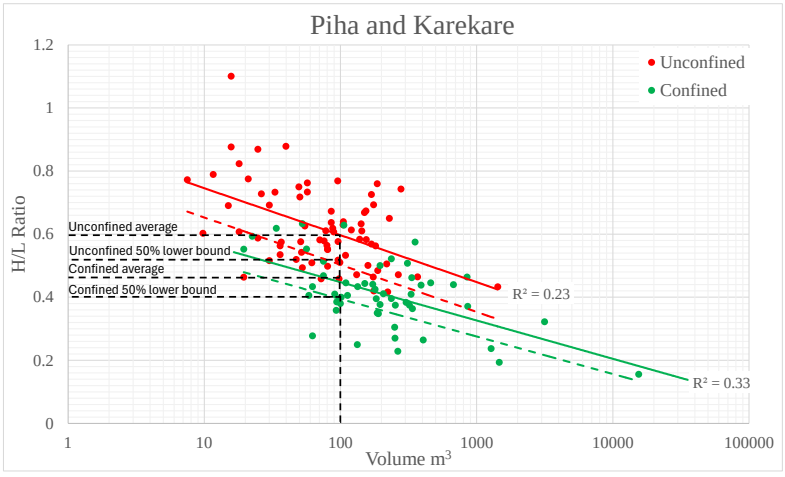


Figure 12: Empirical relationship between volume and H/L for Piha and Karekare data showing lower bound 50% confidence intervals

8 DISCUSSION

The adoption of well-established empirical-statistical methods for predicting landslide runout proved to be a highly effective approach in supporting the rapid delivery of area-wide landslide risk assessments in Muriwai, Karekare, and Piha. This success was largely driven by the early development of an extensive landslide inventory, similarities in landslide classification within each study area and the recognition of the role that downhill morphology played in controlling both landslide direction and reach.

To enhance the accuracy of spatial impact probability for the Piha and Karekare study areas, the probability was partitioned to account for both travel direction and distance. Combing the empirical-statistical models with simple flow

accumulation modelling proved particularly valuable. The assessment methods developed were relatively systematic and straightforward to apply, which was crucial given the variable site-by-site topographic conditions, the number of practitioners utilising them and the paucity of time under which assessments had to be made. Developing a standardized approach early on in the process including the probability values to be applied to given conditions ensured consistency in risk assessment outcomes across different locations. Additionally, the importance of applying judgment when allocating probabilities based on observed behavior from the event was evident. While empirical models were very informative, judgement of the results was necessary to account for site-specific nuances and uncertainty.

Variability in observational landslide runout data introduced significant scatter to the empirical-statistical models, particularly between the two study areas. The general scatter reflects uncertainty in the adopted F-angles when predicting landslide runout distance. A more conservative approach to capturing this uncertainty in future assessments could be to plot the probability of exceedance or confidence intervals and select predicted values accordingly. Several site-specific factors have been postulated for the contrasting H/L and volume correlations between the Muriwai and Piha and Karekare data:

- The effect that source material properties may have on debris flow behaviour. Muriwai are soils dominantly sandy whereas the Piha and Karekare material were fine grained soils.
- In many instances at Muriwai it was difficult to differentiate between debris flows due to the amalgamation. Therefore, the measured runout extents do not reflect their true behaviour.

The variability in the general dataset could be attributed to a number of influencing factors which might include:

- The impact of the built environment, such as driveways, buildings and roads, which often resulted in extended or reduced travel distances.
- The accumulation or depletion of debris along the runout path (including amalgamation or splitting of flows), which altered the overall volume of material.
- The type and density of vegetation within the runout path.
- Successive landslides originating from the same or adjacent source areas in the days or weeks after the initial event, leading to combined flows, resulting in extended runouts. This reflects the importance of early reconnaissance following the event.
- A relatively narrow range of volumes in the dataset, leading to weaker correlation strength within the predictive models.

Numerical methods proved useful in both Muriwai and North Piha and the results of these assessments appeared to show reasonably good correlation with the empirical-statistical predictive models. Several authors have provided comprehensive comparisons between empirical-statistical methods and numerical methods that rely on process based modelling (McDougall 2017, Brideau et al 2021, Komu et al 2022) but a summary of some key lessons from this study include:

- Empirical-statistical methods are a simple but powerful tool for both initial screening and adoption in the quantitative assessment where a sufficient dataset is established using past landslide events, but it is important to reflect uncertainty in the predictions.
- The appropriate published correlation needs to be adopted, and the recognition and incorporation of site specific variable factors is critical to produce an effective prediction model.
- Empirical-statistical runout models should be complimented with other additional yet simple tools where possible, particularly where there is ambiguity with respect to landslide direction or the degree of confinement.
- Evidenced based observational behaviour is essential, and should often take precedent when applying judgement to the selection probability values
- Numerical runout methods can provide detailed runout models providing useful outputs such as debris thickness and velocity. They rely on calibration with accurate observations of previous site specific landslides.
- RAMMS modelling worked well for Muriwai but took several months. However, RAMMS modelling could not be calibrated with the recorded landslide data in North Piha and therefore the selection of software applicable to the site and data is important.

9 REFERENCES

Australian Geomechanics Society (AGS), (2007). *Landslide Risk Management*. Journal and News of the Australian Geomechanics Society. 42(1).

Brideau, M.-A., de Vilder, S., Massey, C., Mitchell, A., McDougall, S. and Aaron, J. (2021). Empirical relationships to estimate the probability of runout exceedance for various landslide types, *Landslides*.

Corominas, J. (1996). The angle of reach as a mobility index for small and large landslides, *Canadian Geotechnical Journal*, 33, 260–271.

Finlay, P.J., Mostyn, G.R. and Fell, R. (1999). Landslides: Prediction of travel distance and guidelines for vulnerability of persons, *Proceedings of the 8th Australia New Zealand Conference on Geomechanics*, ed. Vitharana and Colman, Hobart, Australian Geomechanics Society, 105–113.

Geonet (2023). Over 140k landslides mapped following Cyclone Gabrielle, Geonet News, 29 September. Available at: https://www.geonet.org.nz/news/4OeHpYPDO4f19HicJA0Lj7.

Heim, A. (1932). Landslides and human lives (Bergstruz and Menchen leben), Translated by N. Skermer, BiTech Publishers, Vancouver, B.C, 195.

Hsü, K.J. (1975). Catastrophic debris streams (sturzstroms) generated by rockfalls, *Geological Society of America Bulletin*, 86, 129–140.

Hungr, O., Corominas, J. and Eberhardt, E. (2005). Estimating landslide motion mechanisms, travel distance and velocity, Hungr, O., Fell, R., Couture, R. and Eberhardt, E. (eds), *Landslide Risk Management, Balkema, Rotterdam*, 99–128.

Hungr, O., Leroueil, S. and Picarelli, L. (2014). The Varnes classification of landslide types, an update, *Landslides*, (11), 167–194.

Hunter, G. and Fell, R. (2002). Estimation of travel distance for landslides in soil slopes, *Australian Geomechanics*, 37(2) 65-82.

Hunter, G. and Fell, R. (2003). Travel distance angle for rapid landslides in constructed and natural soil slopes, *Canadian Geotechnical Journal*, 40(6), 1123–1141.

Iverson, R.M., Schilling, S.P. and Vallance, J.W. (1998). Objective delineation of lahar-inundation hazard zones, *Geological Society of America Bulletin*, (110), 972–984.

Komu, M.P., Nefeslioglu, H.A. and Gokceoglu, C. (2023). A review of the prediction methods for landslide runout, Proceedings, 87, 3.

Land Information New Zealand (LINZ) (2018). Auckland North LiDAR index tiles (2016-2018), LINZ Data Service. Available at: https://data.linz.govt.nz/layer/105090-auckland-north-lidar-index-tiles-2016-2018/ .

Lee, E.M. (2015). Landslide risk assessment: The challenge of communicating uncertainty to decision-makers, *Quarterly Journal of Engineering Geology and Hydrogeology*.

Li, T. (1983). A mathematical model for predicting the extent of a major rockfall, *Zeitschrift für Geomorphologie*, 24, 473–482.

Ministry of Business, Innovation and Employment (MBIE) (n.d.), Rapid building assessment placarding system, Building Performance. Available at: https://www.building.govt.nz/managing-buildings/managing-buildings-in-an-emergency/rapid-building-assessment-placarding-system.

NIWA (2023). 'Auckland suffers wettest month in history', NIWA News, 2 February. Available at: https://niwa.co.nz/news/auckland-sufferswettest-month-in-history.

Primary Health Care & Community (PHCC) (2024). The long shadow of Cyclone Gabrielle: A brief review 12 months on, PHCC Briefing, [online] Available at: https://www.phcc.org.nz/briefing/long-shadow-cyclone-gabrielle-brief-review-12-months.

Roberts, R. (2024). A case study on managed retreat from landslide risk – lessons learnt in Auckland, New Zealand *Geotechnical Society NZ Geomechanics News*, June. ISSN 0111-6851.

Scheidegger, A.E. (1973). On the prediction of the reach and velocity of catastrophic landslides, *Rock Mechanics*, 5, 231–236.

Whittall, J., Mitchell, A. and McDougall, S. (2020). Runout of open pit slope failures: an update, in Dight, P.M. (ed.), *Slope Stability 2020: Proceedings of the 2020 International Symposium on Slope Stability in Open Pit Mining and Civil Engineering, Australian Centre for Geomechanics, Perth*, 1149–1162.

https://doi.org/10.56295/1ACEG12

ENGINEERING GEOLOGICAL MODELS IN REMOTE AND DIFFICULT ACCESS TERRAIN: A CASE STUDY FROM BOGONG HIGH PLAINS ROAD

Davide Casagrande[1], Dane Pope[2], Katerina Irwin[3]

[1]*Senior Engineering Geologist, PSM, Geelong*

[2]*Principal, PSM, Geelong*

[3]*Lead Engineer – Geotechnical Design, DTP, Melbourne*

ABSTRACT

A significant landslide closed access to Falls Creek via Bogong High Plains Rd in October 2022. An investigation into the potential to open a temporary four-wheel-drive access to Falls Creek via steep terrain adjacent to Lake Guy was completed. The site had difficult access, remote location and limited time for investigation.

For a small project area there was significant variation in slope performance and geology, including colluvium and residual soils overlying exposed granodiorite and metamorphic bedrock. The study considered the rich history of engineering geological studies associated with past hydropower projects to establish broad structural controls on the topography before developing the local engineering geological model. Traditional desktop, geomorphological and field mapping techniques were adopted to characterise the slopes and assign appropriate domains. The domains then directly informed the assessment of landslide hazards and remedial design advice. Landslide hazards were assessed using the Department of Transport and Planning "Roadside Geotechnical Hazard Risk Management" guideline. Domains were validated with a series of test nails/bolts as mobilisation of slope stabilising contractors was imminent.

The case study highlights that meaningful, cost-effective engineering models can be developed without traditional intrusive site investigation methods and that engineering geological models should underpin landslide assessment and remediation.

1 INTRODUCTION

The Bogong High Plains area presents substantial challenges for engineering geological modelling due to its remote location, steep terrain, and landslide-prone slopes. In October 2022, a significant landslide obstructed access to Falls Creek, necessitating a temporary emergency access route to be designed for controlled, four-wheel-drive passage across challenging terrain near Lake Guy, Figure 1. The Department of Transport and Planning (DTP) proposed a 550 m long access track, with slope angles ranging from 30° to 68° and slope heights up to 5.5 m to provide temporary connectivity while minimising impact on the surrounding environment.

Historical studies highlight the complexities in this region, where weathering and structural variability affect slope stability (Beavis, 1949; Kenny, 1937).

Given the challenging terrain and limited access in the Bogong High Plains area, the investigation primarily focused on ground-truthing the LiDAR survey and soil nail/rock dowel boreholes and acceptance tests. The ground-truthing of the LiDAR was focused on geological units, structural features, and slope performance.

This approach is consistent with the guidelines of the International Association for Engineering Geology and the Environment (IAEG) Guidelines (Baynes and Parry, 2022), which recognise that in remote, complex terrain, limited data can be reconciled with observational insights through conceptual domain-based engineering geological models.

This study summarises the geological model that considered slope performance and provides targeted remediation strategies for high-risk areas.

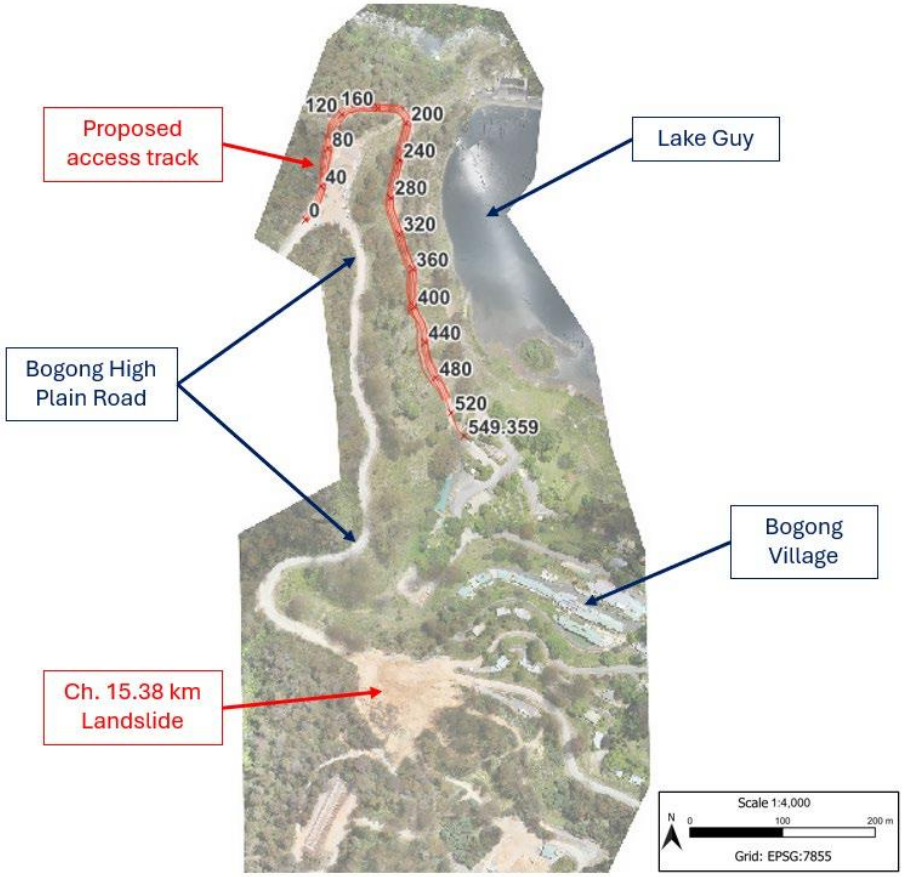


Figure 1: Proposed access track highlighted in red

2 GEOLOGICAL SETTING

The Geological Map of Feathertop (Geological Survey of Victoria (GSV) Report 125, 2005a) indicates the Site lies within the contact between Lower Silurian aged migmatite (Som) and Cobungra Granite (G549), Figure 2, both from the Omeo Metamorphic Complex (OMC). The "Som" was formed during regional metamorphism, and it is a gneissic rock with thin layers in dark minerals gneiss and schist and it includes small bodies of fine to medium-grained granite. The "G549" is a grey biotite-muscovite granite, coarse to medium grained with K-feldspar phenocrysts. It contains bodies of migmatite, gneiss and quartz and could be foliated.

To the south, the Site is near the boundary of Lower Devonian East Kiewa Granodiorite, a grey, medium grained biotite granodiorite with some muscovite.

Morand et al. (2005) outlines physiographic setting of Bogong region as follows:

- Much of the Bogong region is mountainous. There are three distinct landforms: plateaus (High Plains), dissected uplands and intermontane valleys.
- The plateaus are interpreted as the remnants of a moderately undulating landscape that preceded the current, more rugged eastern highlands. The plateaus generally lie above 1700 m elevation. The plateaus landform is developed on a variety of different rock types and incorporates the dissected remnant of Cainozoic basalt flows.
- The dissected uplands are the predominant landform and consists of a rugged valley and ridge topography with many hundred metres of relief. Very little geological control, either from rock type or rock structure, is evident in the morphology of this landform. Several straight streams are developed along presumed joints and a few faults, such as the Tawonga Fault. Only minor streams are controlled by the strike of bedding and foliation.
- Amidst the valley and ridge topography of the dissected uplands there are several broader flooded valleys. Most of these intermontane valleys are the result of north-flowing rivers changing from their mountain river track into their downstream valley track.

A more detailed description of the geological unit specific to the Site is presented in Table 1 and Figure 2.

Table 1: Summary of geological units documented on the Feathertop Geological Map (GSV, 2005a)

Geological Unit	Description
Cobungra Granite (G549, Figure 2)	• Is a medium grained equigranular muscovite–biotite leucogranite. Biotite grains are much smaller than muscovite. • This rock formed as accumulations of melt produced during development of the OMC (William and Wilson, 1999). • In the highest-grade of the complex, melt segregations from the Som were mobilised into intrusive granitic bodies. • Heterogeneous rock unit with an irregular shape, occupying much of the central part of the OMC between Mount Beauty and the Omeo area. • In Bogong the boundary of the pluton is gradational with the surrounding migmatite, but it locally intrudes gneiss and schist. • Area mapped as G549, Figure 2, may contain outcrop of Som. • Even in unfoliated samples, deformation is pronounced. • Biotite is usually more abundant than muscovite.
OMC migmatite (Som, Figure 2)	• Gneissic rock with two components: light coloured granite or pegmatite and darker gneiss rich in biotite. • Most migmatite is layered, with layers of the two components. Leucosomes (melt layers) regularly interlayered with biotite-rich gneiss. A strong gneissosity is parallel to this layering, which can be overprinted by gently plunging, west-verging crenulation folds. This rock is derived from the Pinnak Sandstone, which has been metamorphosed. • Heterogeneous rock that may contain patches of laminated quartz gneiss and various granite such as C549, Figure 2. • Relic bedding may be seen near the boundary with metasedimentary gneiss. • This rock has been folded by upright crenulations folds.

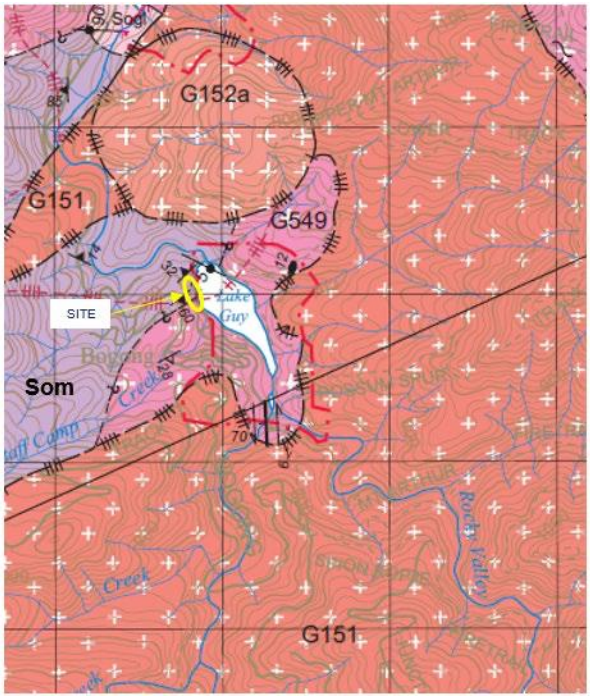


Figure 2: Extract from Geological Map of Feathertop (GSV, 2005b)

3 INVESTIGATION METHODS

Observations were conducted on accessible exposed slopes, road cuttings, and the temporary access track, Figure 3. To further understand the geological conditions and assist with developing engineering control measures, subsurface investigations were carried out, involving the following activities:

- Auger and air percussion drilling was completed at five locations along the access track to a maximum depth of 7 m.
- Nineteen slope cuts were excavated and cleaned along the batter of the temporary access track and Bogong High Plains Road using a 6-tonne excavator.

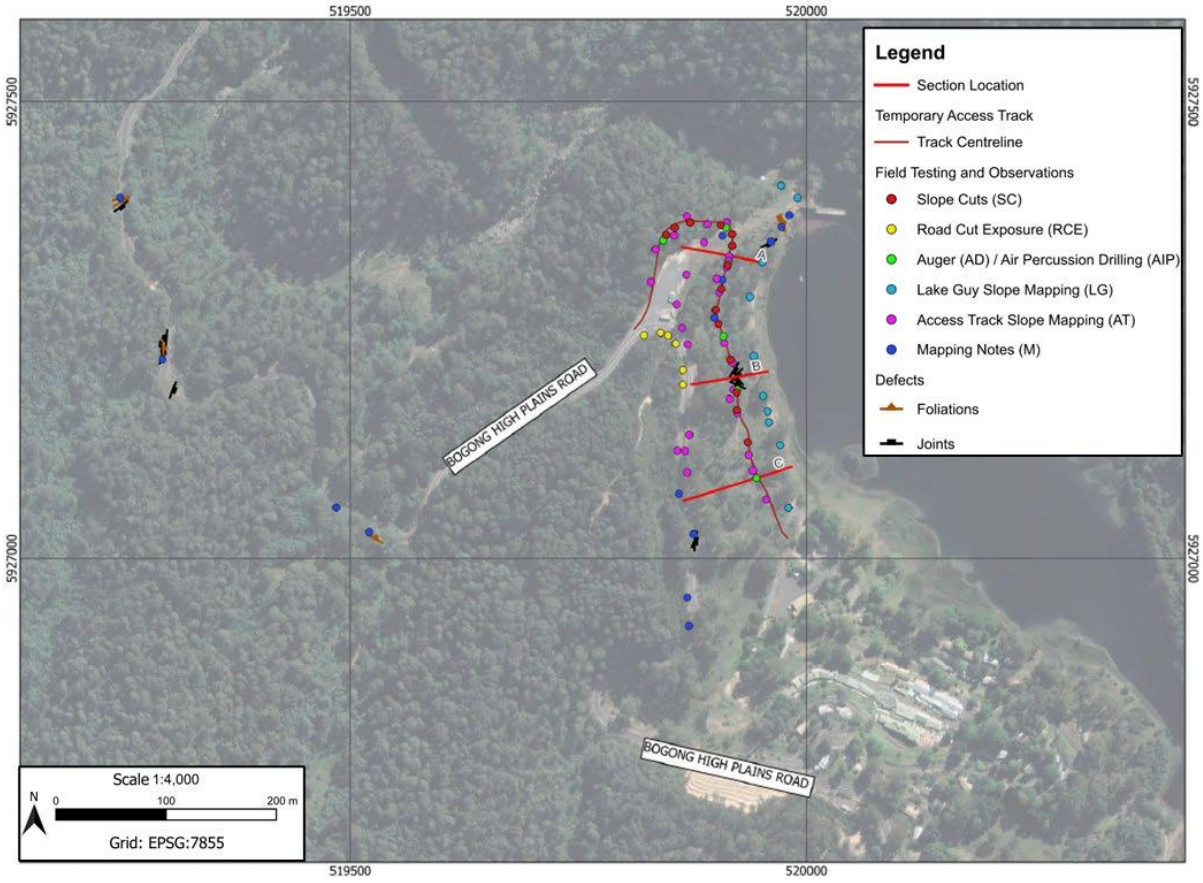


Figure 3: Field testing, observations and section locations

4 ENGINEERING GEOLOGICAL MODEL

A preliminary conceptual model was developed prior to fieldwork based on desktop assessment of the Feathertop geological map (GSV, 2005b), historical records from the Kiewa Hydroelectric Scheme (Beavis, 1948; Kenny, 1937), and analysis of high-resolution LiDAR imagery. The site was interpreted to lie within a contact zone between migmatitic gneiss and granodiorite, with topographic and geomorphic features suggesting strong structural control on slope development.

It was anticipated that the slopes would be mantled by variably thick colluvium and residual soils, underlain by either highly weathered bedrock or fresh rock exposures depending on slope aspect and elevation. Structural features such as foliation in the metamorphic units and exfoliation joints in the granodiorite were expected to influence slope stability, particularly where they daylighted on steep slopes. Gully features, slope concavities, and historical landslide scars introduced further uncertainty into the interpretation.

Uncertainties in the preliminary model included:

- The lateral extent and thickness of superficial deposits.
- The depth to competent bedrock across the alignment.
- The condition and orientation of structural defects in fresh and weathered rock.

- The degree to which geomorphology had reworked or obscured in situ geological structures.

The conceptual model was refined using field observations obtained during the investigation program described in Section 3. Slope cuts, temporary track exposures, and mapped features were assessed to characterise lithology, structural fabric, and soil–rock transitions, which informed the delineation of engineering geological units.

4.1 GEOLOGICAL UNITS

The geological units identified during the fieldwork are summarised in Table 2. The depth below surface of the geotechnical units is difficult to differentiate, and three representative cross-sections are presented in Figure 4.

Table 2: Detailed summary of geological units

Unit	Description
Colluvium (COL1 & COL2)	• Derived from ancient debris flow and more recent Bogong High Plains Road construction • Highly variable but often defined by: – COL1: Matrix supported. Matrix is SAND trace silt to SAND with silt and gravel: fine to coarse grained, light brown, orange, gravel is sub-angular up to 10 mm. Boulders up to 800 mm of highly to slightly weathered (HW to SW) granodiorite, medium to very high strength, dry to moist, loose to medium dense. – COL2: Matrix supported. Matrix is SAND trace silt: fine to coarse grained, dark brown, orange. HW gravels and cobbles, moist, medium dense to dense. • Boulders and cobbles are commonly present from Ch. 0 m to Ch. 400 m along the temporary access track slopes with the following properties: – Highly to moderately weathered – High to very high strength. • Thickness of colluvium is variable across the Site and controlled by slope angle. Colluvium thickness is inferred from Slope Cuts, and it varies from 0.5 m to 2.5 m.
Residual (RES)	• Derived from rocks of BEDROCK1 and BEDROCK2 • Mostly dominated by: – SAND with silt and gravel: fine to coarse grained, brown to orange, gravel is sub-angular up to 10 mm, moist, medium dense, typically weakly cemented • Thickness of RES is variable across the Site and controlled by subsurface weathering.
Bedrock (BEDROCK1)	• Observed on the Temporary Access Track between Ch. 210 m and Ch. 290 m, and between Ch. 350 m and Ch 370 m. • Observed along Bogong High Plains Road between CH. 13.58 km and CH. 14.28 km. • Observed along Lake Guy Access track and near the Lake guy Dam outlet. • Mostly defined by: – BEDROCK1: Heterogenous metamorphic rock, MIGMATITE, fine to coarse grained, dark grey colour, crenulation folds and lamination, boulders subcrop and outcrop with dimension varying from 1.5 m to > 10m, very high strength, moderately weathered to fresh – BEDROCK2: Heterogenous igneous rock, GRANITE/GRANODIORITE, medium grained equigranular muscovite-biotite, dark grey to pale grey colour, evidence of contact metamorphism, boulders subcrop and outcrop with dimension varying from 1.5 m to > 10m, very high strength, moderately weathered to fresh. • Dark mineral, biotite, and hornblende (50 – 60 %) and white mineral, feldspar, muscovite, and quartz (40 – 50 %). • Bedrock is typically observed as sub cropping boulders with dimensions varying from 1.5 m to > 10 m.

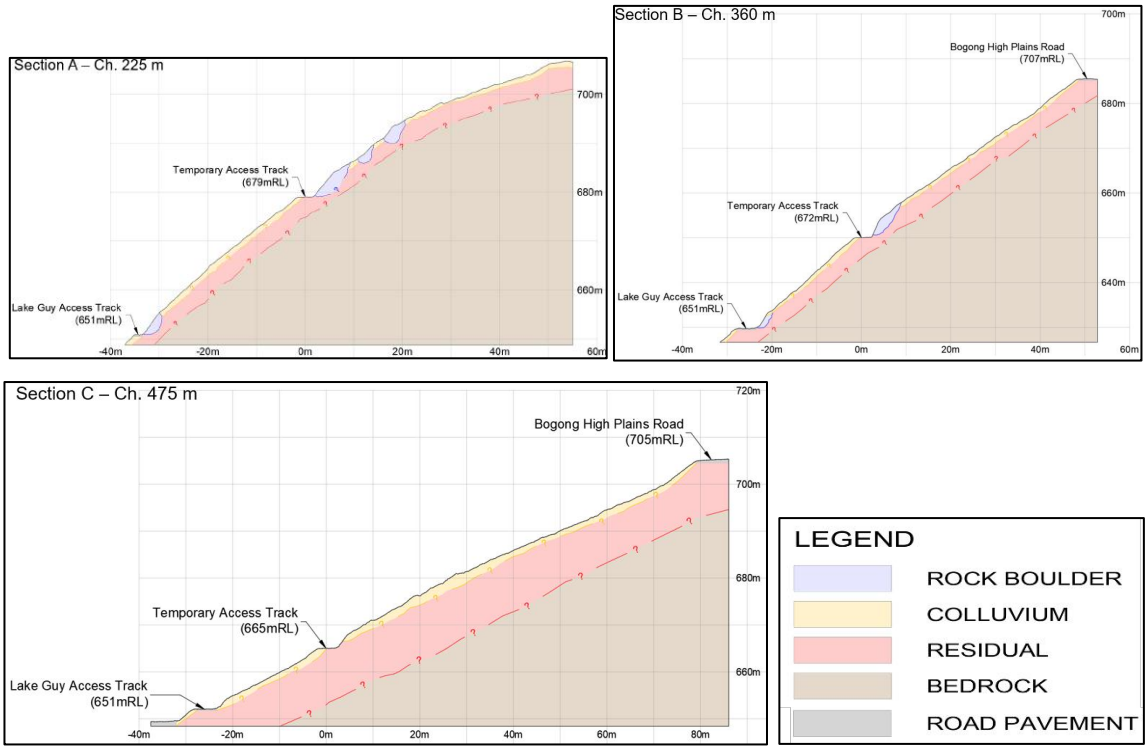


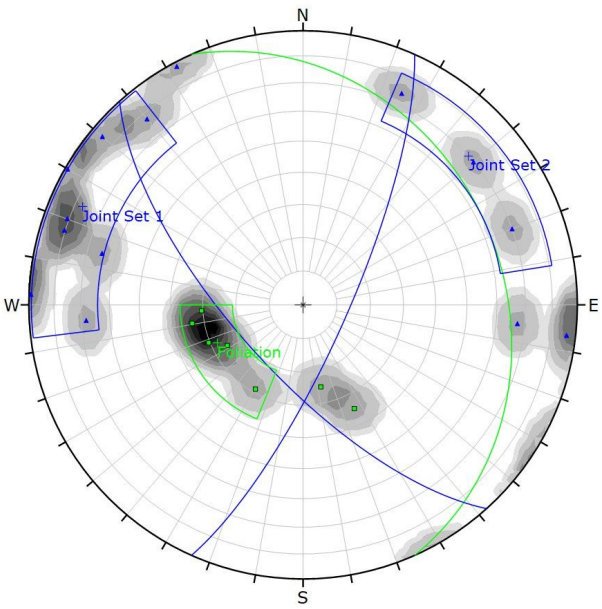
Figure 4: Representative cross-sections

4.2 GEOLOGICAL STRUCTURE

One aim of the investigation is to understand whether stress relief joints in the BEDROCK2 and foliation in BEDROCK1 control slope stability. The development of a site wide engineering geological model allows for a comprehensive assessment of potential mechanisms to be undertaken.

4.2.1 Field mapping

Bedrock exposures of BEDROCK1 and BEDROCK2 units along Bogong High Plains Road present as a moderately to extremely weathered foliated and massive rock mass respectively. Geotechnical face mapping from available exposures is presented on a stereonet in Figure 5.



Symbol	TYPE	Quantity
	FO	7
	JN	14

Color	Density Concentrations
	0.00 - 1.50
	1.50 - 3.00
	3.00 - 4.50
	4.50 - 6.00
	6.00 - 7.50
	7.50 - 9.00
	9.00 - 10.50
	10.50 - 12.00
	12.00 - 13.50
	13.50 - 15.00

Contour Data	Pole Vectors
Maximum Density	14.86%
Contour Distribution	Fisher
Counting Circle Size	1.0%

	Color	Dip	Dip Direction	Label
Mean Set Planes				
1m		28	66	Foliation
2m		77	114	Joint Set 1
3m		70	228	Joint Set 2

Plot Mode	Pole Vectors
Vector Count	21 (21 Entries)
Hemisphere	Lower
Projection	Equal Area

Figure 5: Stereographic projection of BEDROCK1 and BEDROCK2 defects.

4.2.2 Cleavage and Foliation

Some outcrops have a mineral lineation that is parallel to regional folds, with the mineral lineation, Figure 6, usually dipping a low to moderate angle to the southeast.



Figure 6: Sample taken from road cut in BEDROCK1 on Bogong High Plains Road, showing an example of mineral lineation and crenulation folds following the black minerals

The observed foliation had a dip of 25° to 35° towards 030° to 090°. PSM notes that there is uncertainty about the validity of defect measurements due the potential for disturbance and rotation from landslide activity. Nonetheless, it was anticipated that foliation could have unfavourable orientations at the Site where BEDROCK1 was exposed in cuttings and slope aspect was towards the east/northeast (e.g. CH. 100 m to 200 m, Figure 1). Between these Chainages, cuttings were dominated by colluvium and residual soils without relict foliation observed.

4.2.3 Joints

The joints are mostly relict joints in BEDROCK2 or overturned joints in BEDROCK1, Figure 7. The joints in BEDROCK1 may have formed from lineation or foliation overturned by folds documented in the area. Two joint sets were mapped within the temporary access track:

- Joint Set 1: sub-vertical set dipping from 75° to 85° towards the east
- Joint Set 2: sub-vertical set dipping from 60° to 75° towards the west – southwest

Note that stress relief joints were not observed however, evidence of planar slide was documented in areas of BEDROCK2. Basal landslide angles ranged from 25° to 40°.



Figure 7: View of a jointed BEDROCK1 on Bogong High Plains Road Ch. 13.88 km.

4.2.4 Faults

Faults were not observed on site. However, with regards to published information on faults in the project area:

- The Nelse Shear Zone strikes northwest through the broader project area.
- During construction of Lake Guy Dam (originally called Junction Dam) and the Number 2 Tail Race Tunnel minor faults and shears were mapped, Figures 8 (State Electricity Commission (SEC), 1950) and 7 (Beavis, 1949).
- Approximately 300 m from the No. 2 Power Station in the Number 2 Tail Race Tunnel, Figure 9, the tunnel alignment intersected a basic porphyrite dyke, which was intruded along a fault line. The dyke itself was sheared, indicating both pre- and post-dyke shearing, Figure 9 (Beavis, 1948, 1949)

Given that the proposed access track was predominantly in surficial soils and with some bedrock exposures, it was considered unlikely that the faults would directly control stability.

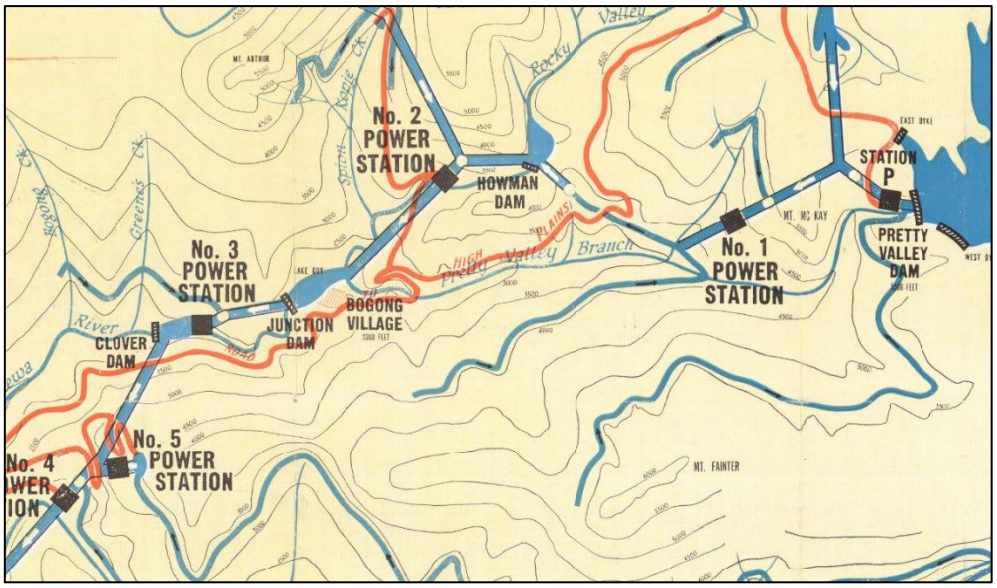


Figure 8: Plan of Kiewa hydroelectric project (SEC, 1950)

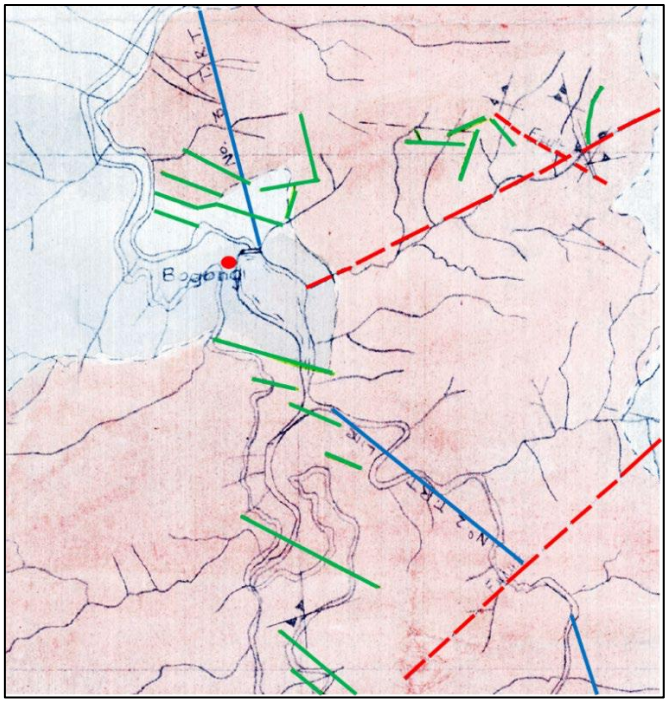


Figure 9: Extract from the geological plan of the Kiewa Scheme (Beavis, 1948). Faults are marked with dashed red lines, dykes with a green line, Tail Race Tunnels with a blue line, and the Site location with a red circle.

4.2.5 Groundwater conditions

While no groundwater was encountered directly in the cut slopes or test pits, signs of wet soils were observed in select areas, and seepage was observed in two minor gullies.

The Visualising Victoria's Groundwater (VVG, 2023) database confirms that regional groundwater depth generally exceeds 20 metres and reduces to less than 5 m (essentially at the surface) in proximity to Lake Guy.

5 SLOPE PERFORMANCE, HAZARDS AND REMEDIATION

5.1 LANDFORM DOMAINS AND SLOPE OBSERVATIONS

Based on soil type, rock mass characterisation and terrain evaluation, the Site was divided into five domains (D1-D5), each exhibiting distinct slope characteristics, Figure 10 and Table 3.

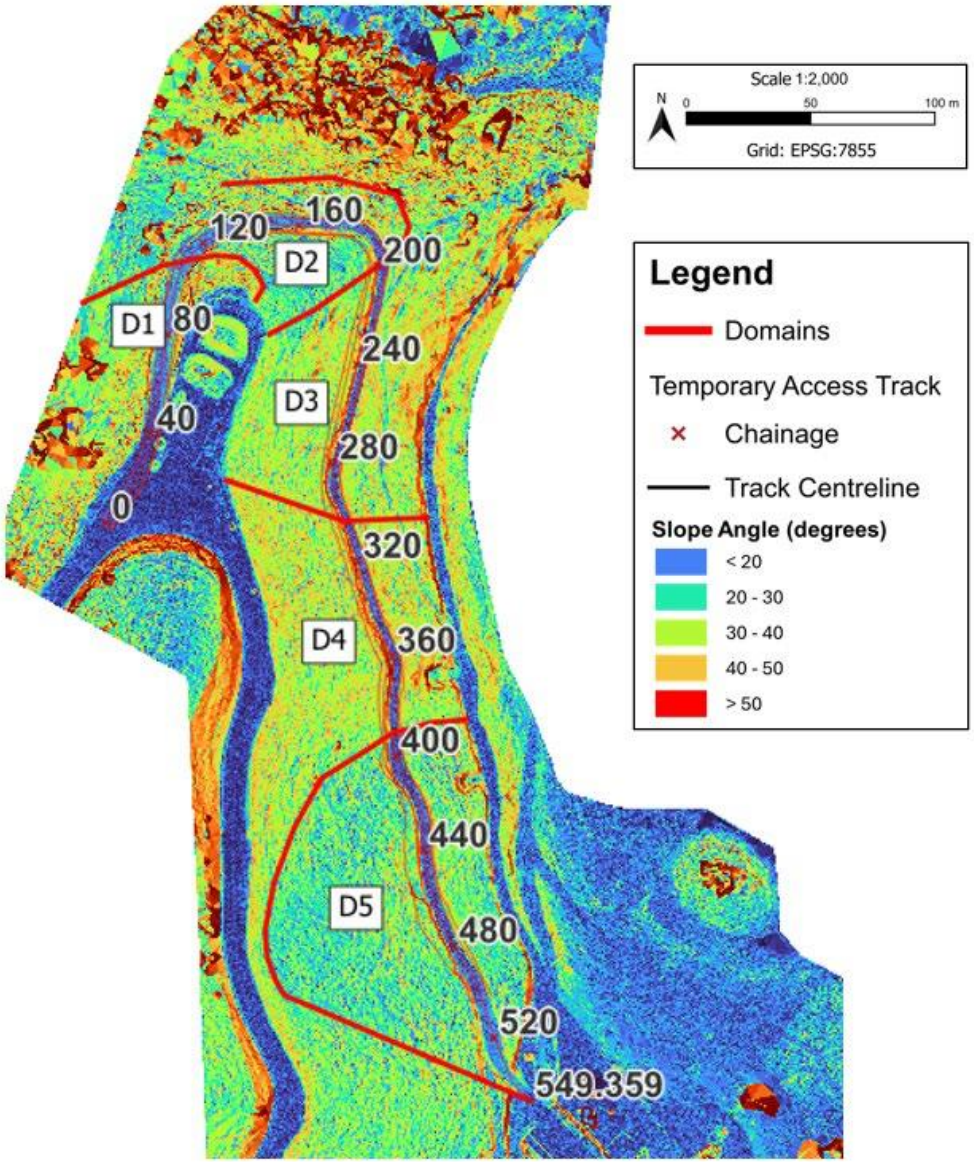


Figure 10: Slope map with two inferred planar slides marked by black ovals

Table 3: Site Domains

Domain	Chainage	Rock mass and soil characterisation	Slope observation	Slope performance
D1	Ch. 0 m to 110 m	COL1 and RES	Downslope 40° Upslope 25° - 35°	No sign of instability observed
D2	Ch. 110 m to 200 m	COL1 and RES Scattered boulders	Downslope 40° Upslope 25° - 35°	Minor slip in COL1 recorded. The upslope angle controls stability of the area
D3	Ch. 200 m to 305 m	COL1, RES and BEDROCK1	Downslope 45° Upslope 40° - 45°	Minor slips observed in COL1, and RES caused by recent construction.
D4	Ch. 305 m to 390 m	COL1, COL2, RES and BEDROCK2	Downslope 40° Upslope ~ 45° From Ch. 385 m ~ 35°	One inferred planar slide observed in COL2, RES and BEDROCK2, and one minor slip in COL1, COL2 and RES along Lake Guy Access track
D5	Ch. 390 m to 550 m	COL2 and RES Scattered boulders of BEDROCK2	Downslope 25° - 35° Upslope 30°	One inferred planar failure in COL2 and BEDROCK2 observed along Lake Guy Access track

5.2 HAZARD ASSESSMENT AND CONCEPTUAL REMEDIAL OPTIONS

The risk assessment framework was based on the Department of Transport and Planning (DTP) "*Roadside Geotechnical Hazard Risk Management"* guideline (2018). This guideline states that DTP *"undertakes risk management of roadside geotechnical hazards in accordance with the Australian Geomechanics Society (AGS) Practice Note Guidelines for Landslide Risk Management 2007"*. It is important to note that the DTP guideline was developed *"specifically for the risk assessment of roadside geotechnical hazards"* and that the guideline has specific definitions regarding risk tolerance criteria that do not directly translate to AGS (2007) suggested criteria. The differences in the guidelines are not the subject of this paper.

While the AGS Landslide Risk Management Framework (AGS, 2007) provides a robust methodology for formal risk assessment, the project adopted the DTP guidelines. Nevertheless, the first principles technical process required for delineation of landform domains and identification of slope hazards is relatively consistent between the two guidelines. This is particularly the case when recognising hazard types, slope performance indicators, and consequence pathways.

Hazards and consequences of failure for each landform domain were developed, Table 4. Similarly, conceptual remediation options were developed per domain, Table 4.

Table 4: Hazard assessment and conceptual remedial options

Domain	Chainage	Hazard	Consequence	Conceptual Remediation
D1	Ch. 0 m to 110 m	• Metastable cut slopes • Debris flows.	• Temporary closure of road • High maintenance.	• Appropriate permanent batter angle.
D2	Ch. 110 m to 200 m	• Metastable cut slope • Small changes in stress could result in slumping soil. • Debris flows and rock fall: 300 to 600 mm boulders in sand matrix.	• As per D1 and, • Over excavation • Need for strengthening. • Impact vehicles at low speed.	• Soil nailing • Appropriate permanent batter angle.
D3	Ch. 200 m to 305 m	• Very high strength boulders with undefined dimension – mobilised by earthworks • Rockfall • Slips between boulders.	• As per D2 and • Over and under excavation.	• Soil nailing • Rock meshing. • Loose boulders removal.

D4	Ch. 305 m to 390 m	• Very steep upslope but dense soil and less boulders, more cobbles • Wet area with gullies • Debris flows.	• As per D2.	• Combination of surface and sub-surface drainage • Appropriate permanent batter angle • Soil nailing.
D5	Ch. 390 m to 550 m	• No or scattered boulders, loose soil. But slope flatten • Metastable cut slopes • Debris flows.	• As per D2.	• Appropriate permanent batter angle.

6 SUMMARY

The landform domains provided a systematic approach to identifying hazards and develop appropriate conceptual remediation. The observed variability in geological conditions across the Site highlighted the importance of site-specific stabilisation measures tailored to each domain.

The study demonstrates that simple, proven field methods should always be considered when developing a site-wide engineering geological model. This is particularly the case in difficult access and remote terrain. Fortuitously, the difficult access to the Site was well supported by readily available historical records associated with the Kiewa Valley Hydro Scheme (Kenny, 1937; Beavis, 1948, 1949; GSV, 2005a). This reinforces the importance of the historical catalogue provided by the Geological Survey of Victoria that can be accessed under Creative Commons Licence.

7 ACKNOWLEDGEMENTS

The author wishes to thank the Victorian DTP for permission to publish this paper. The views expressed in this paper are those of the author and do not necessarily reflect the views of the Victorian DTP.

8 REFERENCES

Australian Geomechanics Society (AGS) (2007). *Practice Note Guidelines for Landslide Risk Management 2007*. Australian Geomechanics, Vol. 42, No. 1, pp. 1–75.

Baynes, F.J. & Parry, S. (2022). *Guidelines for the development and application of engineering geological models on projects*. International Association for Engineering Geology and the Environment (IAEG), Commission 25 (C25).

Beavis, F.C. (1948). No. 2 Power Station line Geological Report. *Geological Survey of Victoria,* Victoria.

Beavis, F.C. (1949). Geological report on No. Junction Line, Kiewa Hydroelectric Scheme. *Geological Survey of Victoria,* Victoria.

Department of Transport and Planning (DTP) (2018). *Roadside Geotechnical Hazard Risk Management Guideline*. Melbourne: Victorian Government.

Geological Survey of Victoria (GSV) (2005a). *Report 125: Structural trends in the Bogong region*. Department of Primary Industries, Victoria.

Geological Survey of Victoria (GSV) (2005b). *Geological Map of Feathertop*. Department of Primary Industries, Victoria

Kenny, J.P.L. (1937). Bogong High Plains, Proposed Reservoir. *Geological Survey of Victoria,* Victoria.

Morand, V., Cayley, R.A., Moore, D.H. and Willman, C.E. (2005). Physiographic setting of Bogong region. *Geological Survey of Victoria,* Victoria.

PSM. (2024). *PSM4933-306L: Bogong High Plains Road, Geotechnical and Slope Performance Investigation*. PSM Engineering Consultants.

State Electricity Commission of Victoria and Shell Company of Australia. (1950). *Kiewa on the map [cartographic material]: Guide to Kiewa Hydro-Electric project*. *State Electricity Commission of Victoria (SEC)*. Available at: https://nla.gov.au/nla.obj-2807716806

Visualising Victoria's Groundwater (VVG). (2023). *Groundwater Database*. Available at: www.vvg.org.au (Accessed: February 2023).

Williams, M. & Wilson, G. (1999). Heterogeneous rock units and their implications in the Omeo Metamorphic Complex. *Journal of Australian Geology*, 47(2), 125-134.

https://doi.org/10.56295/1ACEG13

SLOPE HAZARD MANAGEMENT ON THE TOOWOOMBA RANGE RAIL CORRIDOR, QUEENSLAND.

Bruce Cheesman, David Cooper, Andy Law & Matthew Cochrane
SMEC, Level 6, 480 St Pauls Terrace, Fortitude Valley, QLD 4006, Australia

ABSTRACT

The Toowoomba Range Rail Corridor (TRRC) forms part of the West Moreton Line and runs from Harlaxton to Murphy's Creek. This section of track is approximately 26 km in length and was built circa. 1860's, through the steep terrain and complex geology of the Toowoomba Range. This section of the rail corridor has been subject to historic and ongoing slope instability which has impacted on the operational use of the railway. Over the past five years a programme of routine and emergency site assessments have been conducted to ensure safe operation of the railway. The assessments have been supplemented by UAV-obtained LiDAR and photogrammetry data to create Digital Terrain Models (DTMs). These DTMs have significantly aided in the assessing, planning and managing of slope maintenance activities.

Additionally, automated instrumentation has been installed in high-risk instability zones using GNSS satellite-based movement monitors, track tiltmeters and inclinometers.

The above methodologies have facilitated the development of a comprehensive register of instability events, zones of concern, associated risks and required maintenance works. This register also includes recommendations for further work at all assessed slope sites. This has proven extremely beneficial in assisting the Asset Owner with prioritising and targeting critical locations during the limited Scheduled Corridor Access System closures (SCAS closures) available.

An outline of the remediation works undertaken for one of the larger landslides at Chainage (CH.) 141 km, which reactivated and mobilised following the intense rainfall events in February/March 2022, is also presented.

1 INTRODUCTION

The diverse geological, geomorphological, hydrogeological, vegetation and climatic setting of the TRRC (also known as the Main Range Railway) have posed ongoing challenges for the safe operation of this critical transport link, which is essential for the export of goods from Queensland's interior.

Historically, instability events have impacted cut and fill slopes, structures (retaining walls, culverts, tunnel portals etc) and naturally occurring slopes above and below the rail corridor. To manage the effects of ongoing slope instability, the Asset Owner, has adopted a systematic programme of visual assessments, monitoring and maintenance of the rail corridor, including:

- Emergency and routine visual assessments by qualified engineering geologists.
- The use of UAV for capture of LiDAR and photogrammetric data and its storage in cloud-based software platform that manages and visualises spatial data.
- The installation of track and slope monitoring instrumentation providing cloud-based storage and real time web-based access to the data.
- Regular slope maintenance works including scaling and vegetation removal directed by qualified engineering geologists during SCAS closures.
- Construction of more significant remediation solutions when required.

One of the key challenges with this process has been determining which slopes should be prioritised for remedial works. Because slope instability events along the TRRC are often triggered by periods of elevated rainfall intensity and or changes in vegetation such as root jacking, slope conditions are prone to significant deterioration over relatively short timeframes. The dynamic nature of the processes driving these changes requires a flexible approach to determining where to direct resources to best manage slope risk along the corridor as conditions change over time.

2 PROJECT SETTING

The TRRC is heritage listed and is located directly north-east of the township of Toowoomba, Queensland (Figure 1). The project setting in terms of location, geology/geomorphology and a summary of the history of the site are provided below for context.



Figure 1: Site Location (Qld Gov, 2025)

2.1 SITE DESCRIPTION

The TRRC climbs some 365 m from Murphy's Creek CH. 131.400 km (245 m AHD) at the base of the Great Dividing Range to the summit at Harlaxton CH. 157.790 km (610 m AHD). This is the section of rail corridor described in this paper and has a length of approximately 26.4 km.

The rail line follows the contours of spurs and ridges, with the railway typically set in along ascending hillsides and banks that sit to the north of the track. Responding to the terrain, numerous built features including tunnels, cuttings, culverts, bridges, embankments and stabilising works occur along the extent of the railway.

2.2 GEOLOGY AND GEOMORPHOLOGY

Published geological information (GSQ, 2018) shows the TRRC (Figure 2) to be underlain by:

- Miocene Epoch (22-25 Ma) olivine basalt of the Main Range Volcanic Group at the western end toward Toowoomba.
- Mid-Jurassic Epoch (163-174 Ma) sandstone and siltstones of the Koukandowie Formation from approximately Murphy's Creek Road intersection to approximately Holmes Yard.
- Early Jurassic Epoch (174-200 Ma) Gatton Sandstone from Holmes Yard toward Murphy's Creek.

Both the Gatton Sandstone and Koukandowie are part of the Marburg subgroup and form the sedimentary basement rocks which underly the Main Range Volcanics on the Toowoomba Range.

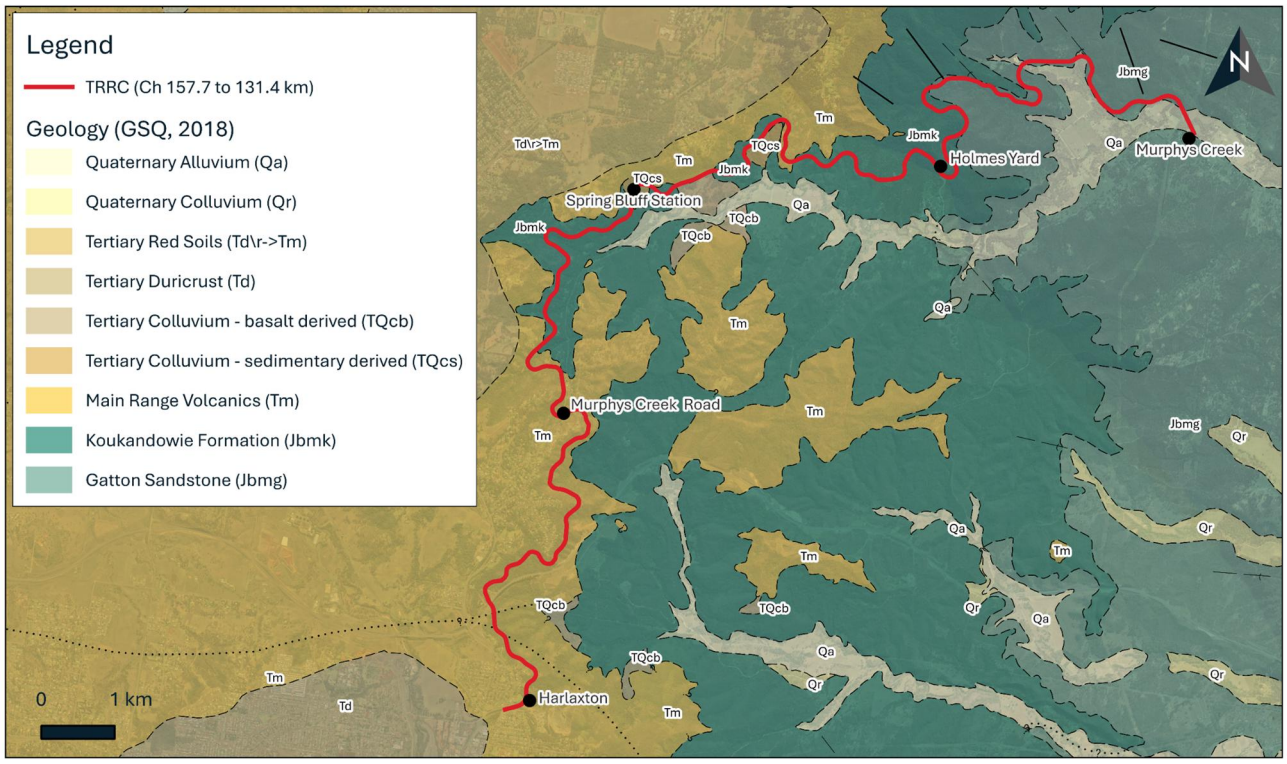


Figure 2: Geological Map (GSQ, 2018)

2.2.1 Main Range Volcanics

The Main Range Volcanics comprise a series of basaltic flows, most just a few metres thick, with discontinuous beds of tuff and agglomerate in some areas. These volcanics occur between Murphy's Creek Road and Harlaxton, with occasional outcrops south of Spring Bluff Station, predominantly along spur ridge lines. Typically, the terrain in this geological unit is steep, with exposed rock outcrops and boulders visible on cleared slopes. Common failure modes include rockfalls, boulder roll, debris slides, and occasional large landslides. Some basaltic flows have an altered upper horizon that has preferentially weathered. In some locations, this has led to undercutting of more competent basalt blocks, increasing their potential for instability. This appears to be a primary failure mechanism in basaltic cuttings, as shown in Figure 3.



Figure 3: Rail cutting showing competent basaltic blocks progressively undercut

Volcanic tuff is observed near the rail intersection with Murphy's Creek Road (previously Ballard railway station) where they are seen in layers of 10-15 m in thickness (see Figure 4).



Figure 4: Typical rail cutting in Tuff

2.2.2 Marburg Subgroup

The Koukandowie Formation and Gatton Sandstone form two of the major components of the Marburg subgroup (see Figure 5). This group is typically described as "Fine to coarse-grained, thin- to very thick- bedded, crossbedded, quartzose to lithofeldspathic sandstone, interbedded with polymictic pebble and minor cobble conglomerate, siltstone and claystone; minor coal and basalt, fossil wood ferruginous oolite" (GSQ, 2018). These units are typically found east of Murphy's Creek Road. The Gatton Sandstone typically comprises much thicker beds of sandstone. Areas of instability and/or existing failures are often observed where flat-lying relatively competent sandstone has been undercut by less resistant shales and siltstones. This appears to be a primary mechanism for failure within these cuttings.



Figure 5: Typical rail cuttings in the Koukandowie Formation (left) and Gatton Sandstone (right)

2.3 SITE HISTORY AND SLOPE INSTABILTY

The TRRC was the earliest railway crossing of the Great Dividing Range in Queensland (and in Australia) between Murphy's Creek and Harlaxton. It was built by railway builders Peto, Brassey and Betts between 1865-1867 for the colonial government of Queensland. Along the route, engineering features responded to challenging and variable terrain, as demonstrated in the provision of nine tunnels, numerous culverts, cuttings and embankments, and extensive use of curved track. The line originally included the construction of 47 bridges (mostly timber), but these have been gradually replaced by culverts and embankments.

The regional setting of the TRRC is one of known slope instability, as detailed by W.F Willmott (1984). Historically, slope instability events along the corridor are often triggered by periods of elevated rainfall intensity. This has led the Asset Owner to develop a network of weather stations and rainfall intensity-based triggers which allow pre-defined actions such as closing the rail line and undertaking Emergency Inspections of the corridor prior to re-opening the corridor to rail traffic.

In recent years, major climatic events such as those in January 2011 and 2013 (Ex-Tropical Cyclone Oswald) resulted in significant damage and remediation (e.g. CH. 141.1 km, CH. 153.3 km and CH. 155.6 km) and most recently in January 2022 when much of the line was impacted by superficial slope failures. One notable exception was the reactivation of a previous landslide, which resulted in the loss of an unused access road (see Section 6.2).

3 SLOPE RISK ASSESSMENTS

3.1 HAZARD IDENTIFICATION

In 2019/2020, SMEC was engaged by the Asset Owner to undertake a series of slope risk assessments for the cuttings and embankments along the TRRC. The initial scope was to identify slope hazards with the potential to impact the rail line. Over time the assessments have expanded to consider hazards within the natural terrain above and below the cut and embankment slopes, as well as hazards which could also affect the rail corridor access roads.

A total of one hundred and seven (107) slope sites were assessed. Initial site assessments were carried out on foot, with observations predominantly made from track level, limited access to slope crests was available. Dense vegetation often restricted visual assessments of embankment slopes. For each slope site, an Asset Condition Report was compiled, documenting slope extents, geological conditions, identified hazards including an assessment of likelihood and consequence of each hazard impacting the track. The reports also included recommendations for hazard management and/or mitigation strategies, with indicative time frames in which to conduct the mitigation works.

3.2 RISK ASSESSMENT FRAMEWORK

The risk assessment was qualitative in nature and was undertaken in line with the Asset Owners' risk framework (QR, 2018). The assessment evaluates hazards based on the likelihood of occurrence and potential consequences to the rail track and rail traffic.

3.2.1 Likelihood

The assessment of likelihood considers both the potential for a hazard to mobilise (probability of detachment) and its ability to impact the track (probability of travel). This was based on engineering judgement with consideration given to field based evidence of past events, documented incidents, slope geometry and clear space between the slope and the track. A summary likelihood ratings and descriptors from the asset owners risk framework are presented in Table 1

Table 1: Likelihood Descriptors

Likelihood Term	Likelihood Description
Certain	>100 times/year, Always occurs,
Highly Likely	11 to 100 times/year, regularly occurs
Likely	2 to 10 times/year, periodically occurs
Possible	Once a year, occasionally occurs
Unlikely	Once every 10 years, infrequently occurs
Improbable	Once every 100 years, almost never occurs
Rare	Once every 1000 years, has never occurred

3.2.2 Consequence

In general, to align the risk assessment framework consistently through the assessments the consequence categories were assigned based on service disruption, financial impact and safety concerns. The consequence terms adopted are summarised in Table 2.

Table 2: Consequence Descriptors

Consequence Term	Consequence Description
Catastrophic	>28 days service disruption, multiple fatality
Critical	14 to 28 days service disruption, multiple fatality
Very High	7 to 14 days service disruption, single total permanent disability injury or fatality
High	3 to 7 days service disruption, 1 – 10 major injuries (reportable to WH&S QLD)
Moderate	1 to 3 days service disruption, 1 – 10 serious injuries (lost time injury)
Low	< 1 day service disruption, 1 – 10 minor injuries
Very Low	No disruption, no injury

3.2.3 Risk Assessment

The qualitative risk assessment was conducted for each identified hazard assigning a Risk Rating (e.g., High, Medium, Low) to each. The worst-case scenario determining the overall slope risk rating for each site. Table 3 provides a summary of the derived risk ratings for the initial site assessments in 2020.

Table 3: Summary of risk assessment outcomes for TRRC in 2020

Overall Risk	Cuttings	Embankments	Total
Very Low	0	0	0
Low	5	0	5
Medium	82	7	89
High	8	5	13
Extreme	0	0	0
Total	**95**	**12**	**107**

4 SLOPE PRIORITISATION CHALLENGES

For each site, a Priority Ranking score was assigned based on the Asset Owner's risk framework, with scores derived from likelihood and consequence values within the risk matrix. The ranking aimed to identify which slopes should be prioritised for remedial works.

From the initial risk and priority assessments, the 10 most critical sites were selected for targeted maintenance during future SCAS closures. However, several challenges arose with this prioritisation approach:

- Many hazards fell under the same consequence and likelihood parameters, resulting in identical risk ratings and priority scores for multiple slopes.
- In some cases, hazards of a lower risk rating received higher priority scores to those of a higher risk rating owing to the structure of the risk matrix. For example:
  A Medium-Risk hazard with a 'Possible' Likelihood (4) x 'High' Consequence (4) = Priority Score 16, while a High-Risk hazard with a 'Certain' Likelihood (7) x 'Low' Consequence (2) = Priority Score 14.

This rigid approach to a priority framework did not account for temporal changes in environmental triggers for instability, such as wet weather, seasonal vegetation growth, or periods of drying out.

To supplement the slope prioritisation, a schedule of routine site visits was established to visually monitor key hazards for signs of deterioration. These visits were complemented by ad-hoc emergency callouts as and when requested, either following slope instability events, or episodes of wet weather exceeding 50 mm rainfall/24 hrs.

5 ADDITIONAL MONITORING & DATA CAPTURE

Since 2020, additional site data has been routinely collected, allowing for further refinement of the initial risk assessments. The additional data has been obtained by:

- Carrying out detailed slope assessments at individual sites, via roped access during SCAS closures.
- Observing the processes and rates of slope deterioration at individual sites over time.
- Undertaking remedial works at select locations.

In addition to routine and emergency site visits, further site data has been acquired through the installation of slope monitoring devices and the acquisition of a 3D reality capture of the rail corridor using LiDAR and photogrammetry. These enhancements have contributed to establishing a more robust slope risk management along the rail corridor.

5.1 INSTRUMENTATION

Several types of instrumentation have been utilised along the TRRC for differing purposes at differing times including topographic survey of structures/markers, tiltmeters, standpipe piezometers, and inclinometers for specific sites to support analysis and development of remedial solutions.

One of the most utilised instrumentation types currently is a system patented by Kurloo which is based upon Global Navigation Satellite System (GNSS) and the Internet of Things (IoT) and their cloud computing technology. The basis of the system is that the accuracy of a point in x/y/z determined by GNSS increases with the length of time observation. At one end of the scale a 1 second reading might give 5-10 m uncertainty in location whereas a continuous operation reference station (CORS) may achieve 1-5 mm accuracy. The Kurloo devices are installed at the top of a metal post which can be driven or concreted into the ground, are solar powered and can deliver 0-3 mm accuracy in x/y/z according to the manufacturers. Arrays of these instruments have been installed at several critical sites across the project (see Figure 6). A typical output from the web-based portal which allows customisation for the project and alert triggers to be set is presented in Figure 7.



Figure 6: Kurloo instrumentation embankment monitoring

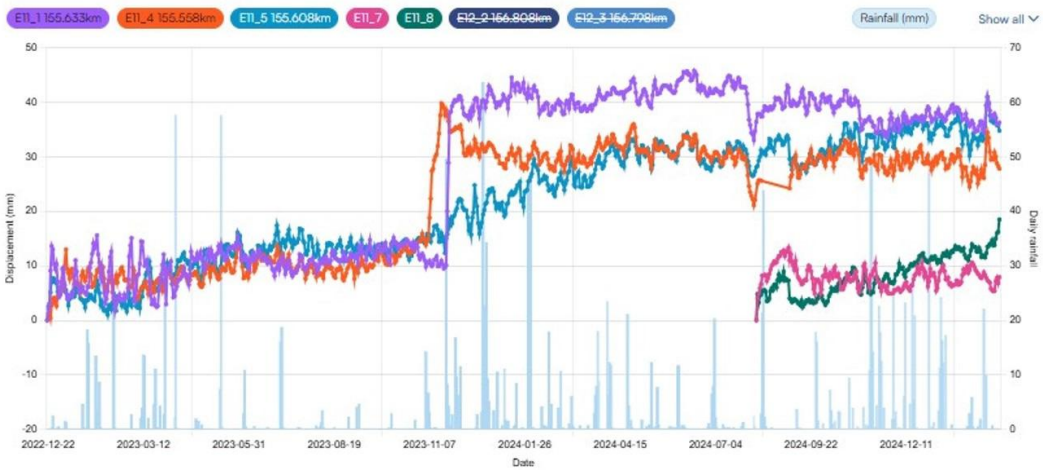


Figure 7: Typical web-based output

5.2 AERIAL PHOTOGRAMMETRY AND 3D VISUALISATION

To support asset management, the Asset Owner engaged SKAND in 2022 to conduct a topographic survey and host a 3D reality capture of the rail corridor. LiDAR and photogrammetry data were obtained via UAV with the outputs accessible through an online portal hosted by SKAND. The photogrammetry data provides a valuable tool for visualising slopes and identifying key features, including:

- Potentially unstable rock blocks and their dimensions.
- Locations of past remediation zones that may be subject to Cultural & Heritage protections (e.g., old stone pitched walls).
- Critical rail infrastructure such as pressure sensors and greaser devices.

This enables the slope management team to review the assessed hazards, understand site constraints, and identify any assets in the area which may require extra protection measures to be put into place before maintenance works can commence.

While photogrammetry offers detailed surface visualisations, dense vegetation can obscure key slope features. To address this issue, hillshaded DTMs were generated from the LiDAR data. This allows for a clearer visualisation of the ground surface to be achieved in densely vegetated areas. Integrating the hillshades with photogrammetry in the 3D model has proven invaluable for planning slope assessments and maintenance during limited SCAS closures by:

- Assisting the review of initial hazard assessments.
- Identifying key targets for roped access inspections.
- Helping to detect potential instabilities beyond cut slopes within the natural terrain that may require additional inspections.
- Ensuring critical infrastructure (e.g., sensors, greasers) is identified protected before scaling activities, to prevent damage from machinery or falling blocks as they are scaled from the slopes.

Figure 8 illustrates how the combined photogrammetry and hillshade visualisations can be used to highlight visible instabilities in the rock slope and to identify additional zones of concern that may exist within the natural terrain beyond the cut slope crest.

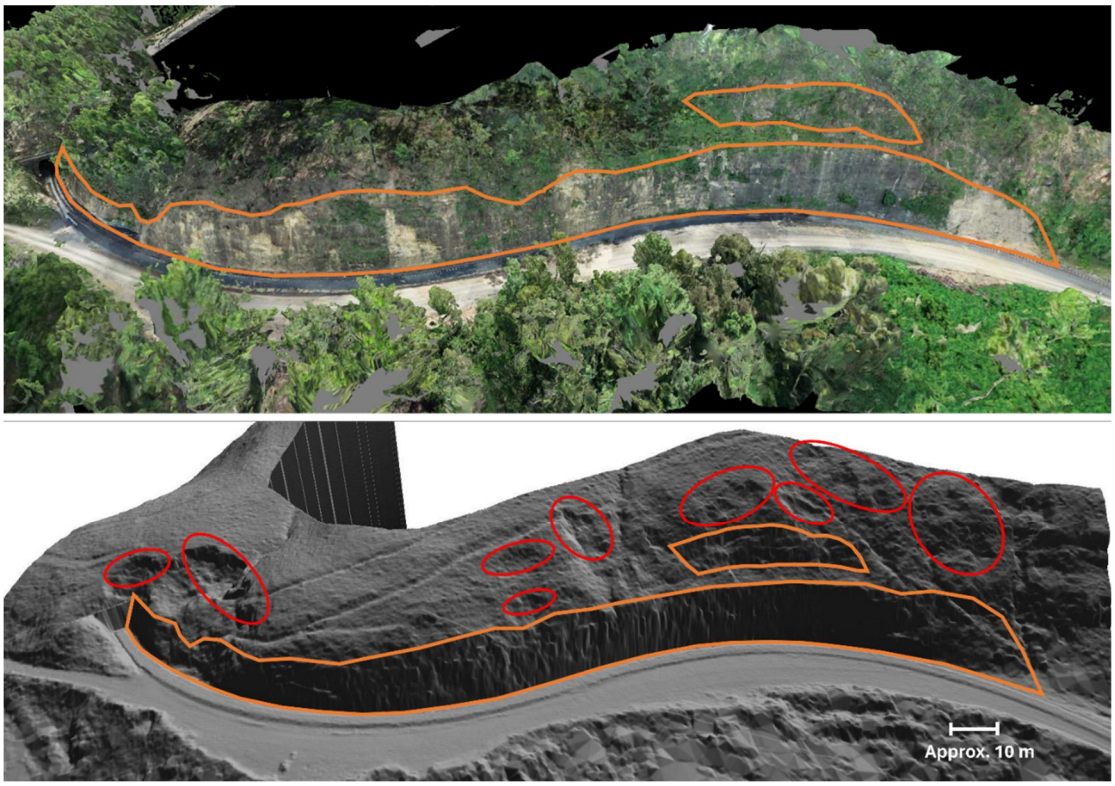


Figure 8: (Top) photogrammetry with rock slope details and extents indicated (orange). (Bottom) 3D hillshade showing additional zones to be assessed located within the vegetated natural terrain above the cutting (red).

Utilising this approach to review site locations when planning future slope maintenance activities has significantly improved efficiency in scaling and inspection campaigns during the limited SCAS closures. Additionally, the 3D visualisations serve as an effective communication tool, helping convey hazard scale and mitigation needs to the Asset Owner.

6 SLOPE MAINTAINANCE REGISTER

Over time, site observations have been compiled to form a recent slope history at each site. These histories document the initial risk assessment observations, recommendations for slope works, recent instability events, and remedial works that may have occurred over time at each site.

The compilation of this data led to the creation of a 'Maintenance Register,' a live document which can be used to track changes in site conditions. It is updated following routine or emergency assessments, scaling works, or as new recommendations and indicative timeframes for remedial works are established. By tracking slopes that have experienced recent deterioration, ongoing instability, or are overdue for inspections, the asset management team can respond dynamically to changing site conditions. This approach is more aligned with the Asset Owner's needs, allowing for flexible and targeted management of slope risks.

6.1 INTEGRATED SYSTEM FOR RISK MANAGEMENT

In 2023, the Asset Owner's risk framework was revised (QR, 2023), triggering an update to the initial risk assessment. This update incorporated the new risk framework, and results of ongoing maintenance works and assessments conducted since the start of the project. Information detailed in the Maintenance Register enabled this task to be streamlined.

As part of the updated assessment, the Maintenance Register was integrated directly into the revised risk assessment document, the intent being to ensure the register is maintained allowing a more data-driven approach to managing slope risks to be adopted moving forward.

6.2 OUTCOMES

At the start of this project, slope assessments and scaling works were typically carried out on a case-by-case basis in response to emergency callouts following rockfalls or landslide events. Over time, routine visits and slope works have been implemented to improve risk management of the corridor slopes.

A key factor driving the regular slope works has been the availability of a clear record of activity at each slope site. Documenting this information in the 'Maintenance Register' provides the asset management team with the data needed to justify and implement a more proactive slope maintenance schedule. This integrated approach has led to a significant reduction in emergency callouts over the past four years.

Between January 2020 to December 2021 a total of 18 emergency callouts occurred associated with instability events. For the period January 2022 to December 2024, a total of 11 emergency callouts were requested associated with instability events, representing a 38% reduction in unplanned track closures.

Following the risk framework update, the revised 2024 risk assessment is summarised in Table 4.

Table 4: Summary of Revised Risk Assessment Outcomes for TRRC IN 2024

Overall Risk	Cuttings	Embankments	Total
Low	31	0	31
Medium	64	9	73
High	2	4	6
Extreme	0	0	0
Total	97	13	110*

Note: *Three sites were added in 2024 as these sites were not accessible for initial 2020 assessments.

7 REMEDIATION MEASURES

As part of the slope risk assessment process, recommendations for remedial measures have been made to better manage slope risks along the corridor. In the short term, prescriptive measures such as routine scaling and roped access assessments are commonly adopted. For more long-term solutions, permanent designs have been developed to the concept stage, with detailed design and construction completed for one site to date.

7.1 PRESCRIPTIVE MAINTENANCE

Prescriptive maintenance measures adopted along the TRRC have included roped access inspections, scaling activities, and vegetation management. These efforts typically aim to reduce the likelihood of future rockfalls and mitigate slope deterioration due to root jacking (Figure 9 & Figure 10). While these measures are lower cost compared to permanent solutions, they require repeat visits to address ongoing slope deterioration.



Figure 9: (Left) Rockfalls induced by root jacking, trimming and poisoning of critical vegetation is often utilised. (Right) Roped access assessment and the use of air bags to remove large localised blocks from the slope face.



Figure 10: (Left) Extensive scaling via roped access and the use of hand tools. (Right) Mechanical scaling of larger zones of problematic rock mass via long reach excavator.

7.2 PERMANENT REMEDIATION (CH. 141 KM EMBANKMENT STABILISATION)

The embankment below the rail line is positioned on a historical landslide area, which was reported to have occurred following a rainfall triggering event in 2012. The landslide was reactivated following extreme rainfall event in February 2022 where approximately 450 mm was recorded over a four-day period. A landslide scarp of approximately 80 m long developed with up to 6 m of downwards displacement. The landslide continued slow displacement predominately associated with each rainfall event. A detailed design was undertaken to support the upper access track and mitigate the slope instability.

Remediation works were undertaken between July 2023 and October 2023 comprising:

- Soil nails and shotcrete to upper access track: to aid long-term stability of the slope by mitigating potential erosion issues, assisting drainage control and decreasing the risk of global slope instability.
- Site-wide drainage: to mitigate potential scour/erosion from the site and to mitigate water infiltration into the slope. The drainage system aimed to slow the flow velocity at the pipe exits of existing culverts (using a pit), down the chute (by added bevels/steps), and along the slope (using a rock mattress/gabion) and to collecting the water and convey it away from the slope.
- Regrading the slope: to flatten the slope steepness, which results in a reduction of shear stress acting on the soil, hence creating more stable slope conditions.
- Vegetation: was added to the slope surface. The roots of the vegetation hold the soil in place and reduce the effects of erosion.

Figure 11 shows the condition of the landslide prior to and following the remediation works.



Figure 11: (Top) Reactivation of an existing failure at CH. 141.1 km resulted in the mid-slope access road experiencing 6 m downwards displacement. (Bottom) Post construction condition of the slope following remedial works undertaken in 2023.

8 CONCLUSIONS AND ACKNOWLEDGEMENTS

Information regarding the frequency of instability events, particularly in sparsely populated areas, is often poorly documented (Shipway & Cooper, 2019). This has considerable impact on the risk assessment process when determining the likelihood of a hazard occurring. Clearly documenting any instability events, recommendations for remedial works with suggested timeframes for completion, and any maintenance works undertaken at each slope site, provides an

important knowledge framework for successfully assessing and managing risks to the rail operation both now and in the future.

The Maintenance Register implemented on this project has proven invaluable to the asset management team to efficiently identify and prioritise critical slopes for remedial works during limited SCAS closures, ensuring a proactive and organised approach to slope maintenance is achieved.

The authors gratefully acknowledge the Asset Owner for providing historical information and data to facilitate this study. Further, acknowledgement is extended to Kurloo and SKAND for their specialist equipment and technology.

9 REFERENCES

Geological Survey of Queensland (2018). Detailed 1:100,000 Surface Geology of Queensland, *digital dataset, Queensland Department of Natural Resources and Mines, Brisbane*. Available from: https://www.business.qld.gov.au/industries/mining-energy-water/resources/geoscience-information/maps-datasets/digital-data/geological-mapping).

Queensland Government (2025). Satellite image of South East Queensland. *Queensland Globe*. Available from: https://qldglobe.information.qld.gov.au/.

Queensland Rail (2018). Specification QR MD-13-561 Risk Assessment Criteria *(Version 5.0)*.

Queensland Rail (2023). Specification QR MD-13-561 Risk Assessment Criteria *(Version 6.7)*.

Shipway, I.C.F and Cooper, D. (2019). Judgements of landslide frequency and their effects on risk assessment in the coastal dune systems of South East Queensland. *Proc. 13th ANZ Conference on Geomechanics.* International Society for Soil Mechanics and Geotechnical Engineering.

Willmott, W.F., (1984). Slope stability and its constraints on closer settlement in the foothills of the Toowoomba Range, Gatton Shire. *Geological Survey of Queensland.* Record 1984/44.

https://doi.org/10.56295/1ACEG14

EXPERIENCES COMMUNICATING LANDSLIDE RISK TO NON-TECHNICAL STAKEHOLDERS

Chris Coulson
AECOM

Tony Miner
GHD

ABSTRACT

The language used by practitioners to communicate the concepts and results of a landslide risk assessments can be misunderstood by the end-user of such information. The authors draw on their experiences of how risk assessment outcomes, using language outlined in references such as the Australian Geomechanics Society Practice Note Guidelines for Landslide Risk Management (AGS 2007c), can be perceived differently by clients.

We explore the definitions and language used by practitioners and clients, and how they can perceive the meaning of the same words differently. Whilst technical practitioners deal in likelihoods, consequences, probability and uncertainty, non-technical end users may understand and perceive risk assessment outcomes to be more precise or definitive than the geoprofessional may intend.

Our aim is to identify issues and misconceptions in the risk assessment process and suggest some clarity to enable better communication of uncertainty and the true meaning of what is a challenging and at times unknowable predictive process. The authors hope the findings and views in this paper can be used to supplement the requirements of AGS (2007c) so that our clients can make informed decisions, and stakeholders have a better appreciation of landslide risks.

1 INTRODUCTION

Clients require landslide risk assessments to make management decisions regarding assets on or near slopes, and often to communicate such decisions to stakeholders. To do this, geotechnical engineers and engineering geologists (geoprofessionals) report landslide risk assessments (LRA) in a very structured manner – we help define the problem, analyse hazards, likelihoods, and consequences to estimate a risk, provide guidance regarding tolerability, and suggest management options. The AGS (2007c) Practice Note guidelines require LRA reports to document the data gathered, the logic applied, and conclusion reached in a defensible manner. Indeed, the guidelines go on to say that full documentation of these results provides evidence of completion, provides transparency in the light of uncertainty, enables the assessment to be re-examined or extended at a later date, and enables the assessment to be defended against critical review. As professionals working in an industry where litigation and insurance claims are unfortunately all too common, there is merit in us striving to meet these requirements.

In achieving our aim to create logical, transparent, and defendable professional reports, we use language and conventions that have narrow or specific technical definitions and meaning. There should be little room for alternate technical interpretations of our work, and a well-written report should be clearly understood by our peers. But commonly our clients and key stakeholders are not fluent in the language of landslide risk. The number of people impacted by landslides in Australia is relatively low when compared to notable other natural hazards such as bushfire and flood. Limited societal and client exposure to, and experience with, landslides has likely meant the community perceptions of risk associated with landslides is not as mature as with bushfire and flood hazards. Many clients may only have a very basic concept of what a landslide is. So, whilst we strive to produce well-written and technically accurate landslide risk reports, perhaps we're letting down the most important stakeholder in the task we're undertaking. Clients need to decide if the assessed risk is tolerable, what to do about it, and how to communicate their decision to stakeholders. The authors have experienced that landslide risk reports often don't provide the information to allow clients to achieve this.

This paper explores different aspects of communication from geoprofessionals to clients and stakeholders, including observations by the authors, and suggests approaches that could result in improved outcomes.

2 RISK TERMINOLOGY

2.1 PROBABILITY

Probability can be defined as a measure of the uncertainty about whether a particular event (e.g. a landslide or a particular level of landslide-related damage) will occur in the future. Probability is quantitatively expressed as a number between 0 and 1, with 0 indicating an impossible outcome and 1 indicating that a particular outcome is certain (Lee and Jones, 2023).

The outcome of a quantitative landslide risk assessment, conducted in accordance with the AGS (2007c) guidelines, will be an annual probability of loss of life of an individual. Whilst this is often paraphrased as a "risk to life" due to a landslide hazard, it remains a prediction of a possible (or the sum of many possible) outcomes. However, following the framework for landslide risk management described in the AGS (2007c) guidelines will not result in a certain or absolute outcome – it will not tell us when the next landslide will occur, how large it will be, or the consequences to property and life. Instead, the annual probability provides a best estimate of an outcome based on the judgement of the geoprofessional, with due consideration of the available evidence. There is uncertainty in the process of assessing the probability of loss of life, often a significant amount of uncertainty. Whilst we, as geoprofessionals, may have an appreciation of this uncertainty, how do clients and stakeholders interpret and use the probabilistic outcomes of a landslide risk assessment?

2.2 HOW LIKELY IS IT?

Landslide risk, in the context of Australian industry practice, is typically the result of the probability of an event occurring and the consequence should that event occur. Qualitative terms for likelihood such as likely, possible, unlikely, high, moderate, low, are commonly used within society to imply how frequent a given event might occur. Acknowledging societal use and acceptance of such terms in everyday language, efforts are made to align these with specific quantified landslide recurrence intervals in guidelines such as AGS (2007c). While geoprofessionals might like to assume our clients read every word in our reports and are familiar with the quantified meaning of qualitative terms, clients will often focus on the Executive Summary and recommendations when making decisions. Terms describing landslide frequency might be included in these sections without the context of implied recurrence intervals.

In 2020 the online research group YouGov published the results of a survey looking at how Britons perceive probability (Smith, 2020) and it showed that perceptions of probability vary amongst individuals in the same society. More than 1,500 respondents were asked to rank a list of 'probability' descriptors between 0 and 10, where 0 is 'Completely certain not to happen' and 10 is 'Completely certain to happen'. Four of the descriptors in the YouGov survey are the same or similar to qualitative measures of likelihood terms in AGS (2007c), and the survey results for these descriptors are presented in Figure 1.

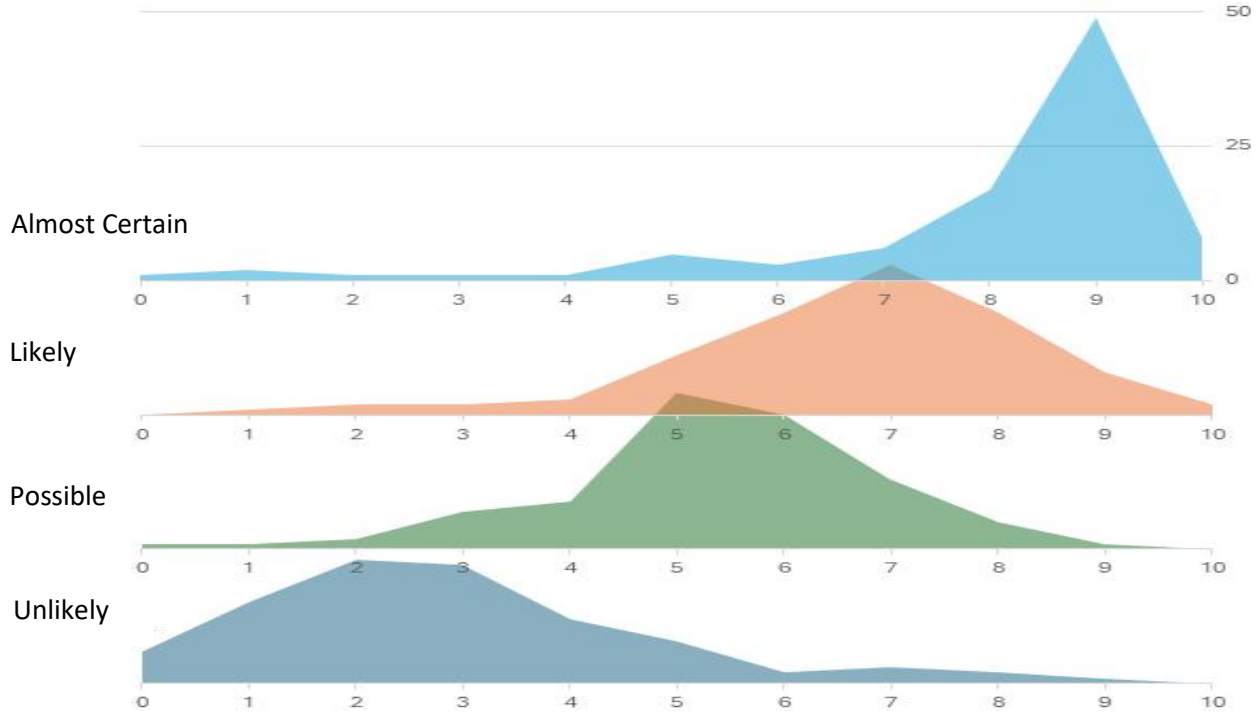


Figure 1: YouGov survey results showing proportion (%) of responses for qualitative likelihood terms

The most common interpretation for Almost Certain was 9 out of 10, but interestingly only 49% of respondents selected this. The consensus across the remaining three descriptors was less definite, with 7 out of 10 for Likely (only 28% of respondents associated 7 with Likely) 5 out of 10 for Possibly (29% of respondents associated 5 with Possible), and 2 out of 10 for Unlikely (23% of respondents associated 2 with Unlikely).

Of further interest is the range of responses that respondents perceived such terms to mean. For example, looking at survey responses selected by more than about 10% of respondents, Likely could mean anything between 5 and 9 out of 10.

The wide spread of responses indicates differences in the way people perceive probabilities. The YouGov research concluded that perceptions of probability are varied and complex and finding a way to communicate such concepts in a way that everyone understands or accepts is difficult (Smith, 2020). Such a variation in responses has been observed by the authors of this paper in workshops and meetings discussing landslide risk.

2.3 RISK ASSESSMENT LANGUAGE

To be able to communicate the outcomes of a landslide risk assessment in a way that someone unfamiliar with the intricacies of AGS (2007c), the geoprofessional requires some knowledge of how such technical terms are being interpreted by the stakeholder and how aware the stakeholder might be of the risks being described.

The authors have experienced similar differences in how clients and stakeholders perceive the meaning of risk terminology and understanding quantitative risk. Table 1 lists some of the interpretations or implied meanings that have been encountered by the authors when communicating with clients and stakeholders.

3 SOCIETAL RISK AWARENESS AND PERCEPTION OF LANDSLIDES AND OTHER NATURAL HAZARDS

Different groups in a society have varying perceptions of risk in relation to natural hazards such as flooding, bushfires, and landslides. Clients engaging geoprofessionals for landslide risk assessments will also have various understandings and perceptions of landslide hazards.

The New Zealand Natural Hazards Commission (Toka Tū Ake EQC, 2023) observes that risk perception may ultimately be more important in affecting behaviour and choices than actual risk. They found that people may dismiss information that encourages action that is inconvenient to them. When communicating risk, it is important to ensure people do not underestimate risk, or think a risk is worse than it really is. But Toka Tū Ake EQC point out that simply providing more information does not necessarily lead to better communication.

Raaijmakers et al (2008) identified that conventional methods of risk analysis (with risk as a product of likelihood and consequences, which AGS (2007c) is founded upon) don't allow for a pluralistic approach that includes the various risk perceptions of stakeholders or lay people within a given social system. Work on flood risk in Spain considered societal risk perceptions in addition to conventional likelihood-consequence approach, and identified three broad categories of risk awareness:

1. Expert awareness or perception of risk assessment, with the least uncertainties about probabilities and consequences of the hazard.
2. Underestimation of probability of occurrence of the hazard or consequences of the hazard.
3. Ignorant of their risk exposure.

Clients and stakeholders can fall within any of the categories listed above.

Looking at these categories through a landslide risk lens, the first category would include the geoprofessional undertaking landslide risk assessments and well-informed stakeholders. An example of the second category might be a visitor to a beach that has unstable cliff warning signs, and who doesn't understand or misinterprets the information being presented. Using the same example, someone in the third category might be an international visitor who is unfamiliar with the hazard and unable to read the language of or interpret the importance of the messages on the sign. Experience provides a basis for these scenarios. A reduced effectiveness of signage that warns beach users of cliff hazards has been observed, rendering such management actions as sometimes being ineffective (Aucote et al 2012). Cui et al (2023) made similar observations, identifying that the level of risk awareness possessed by tourists and visitor is influenced by their familiarity with similar natural hazards. As such, 'warning' signage does little to address visitor ignorance of an unfamiliar hazard.

Alcántara-Ayala et al (2016) observed that when people have more experience with disasters, that experience shapes their perceptions to a greater extent. Conversely, when there is a lack of experience or it is considered as being remote, it is more likely judgements will be based on information obtained through the media, their own intuition, and immediate social networks.

Table 1: Examples of alternate interpretations to specific landslide-related language

Term	Landslide-related definition	Alternate, or non-technical, interpretation
Hazard	A condition with the potential for causing an undesirable consequence. The description of landslide hazard should include the location, volume (or area), classification and velocity of the potential landslides and any resultant detached material, and the probability of their occurrence within a given period of time[1].	A source of danger or harm, such as a snake, or a pothole in the road. Or sometimes, a natural hazard like flood, storms, tsunami earthquake. Not often considered with a sense of probability of likelihood of occurrence.
Risk	A measure of the probability and severity of an adverse effect to health, property or the environment. Risk is often estimated by the product of probability x consequences. However, a more general interpretation of risk involves a comparison of the probability and consequences in a non-product form[1].	A hazard (without consideration of the consequence of occurrence). Or sometimes Likelihood (i.e. "what is the risk of a landslide occurring this year?"). Events that have probabilities of occurrence that are predictable and outcomes that can be estimated with some confidence[2].
Uncertainty	Result of imperfect knowledge concerning the present or future state of a system, event, situation or population under consideration. The level of uncertainty governs the confidence in predictions, inferences or conclusions[3]	Events where probabilities of occurrence are difficult to predict, and outcomes are challenging to quantify[2].
Tolerable risk	A risk within a range that society can live with so as to secure certain net benefits. It is a range of risk regarded as non-negligible and needing to be kept under review and reduced further if possible.[1]	If someone gets hurt but doesn't die.
Acceptable risk	A risk for which, for the purposes of life or work, we are prepared to accept as it is with no regard to its management. Society does not generally consider expenditure in further reducing such risks justifiable.[1]	Acceptable is when no one dies.
Possible	The event could occur under adverse conditions over the design life[1].	Although it might seem possible, if it hasn't happened in living memory, then it won't happen. "I would be very surprised if I saw that occur…"
10^{-4}	0.0001	What does that mean?
Rainfall ARI	The average or expected value of the periods between exceedances of a given rainfall total accumulated over a given duration. It is implicit in this definition that the periods between exceedances are generally random[4].likelihood thru rainfall proxies are ARI and AEP…	A 1 in 100-year event only happens once every hundred years
Person most at risk	Individual risk will usually be the governing consideration for most residential developments, and the person most at risk generally has the greatest spatial temporal probability[1].	Isn't everyone at risk? Surely, we need to consider everyone exposed to the landslide?

[1.] AGS (2007c); [2.] Infrastructure Australia Assessment Framework (IA, 2021); [3.] Adapted from New Zealand Dam Safety Guidelines (NZSOLD, 2024), [4] Australian Water Information Dictionary online (BOM, 2025)

Information from the media regarding natural hazards can also affect the perception of the severity of an event. Although the media information may not accurately reflect the severity or frequency of natural hazards, it can change the way these events are perceived in a community (Alcántara-Ayala et al, 2016). Raaijmakers et al (2008) observe that risk awareness increases when

1. a society is confronted with a hazard; and
2. information and education about the hazard is widely available, and this information has implications for appropriate actions.

Awareness may lead to higher levels of worry, and as a consequence, higher preparedness. A better prepared society will then worry less about the risk it is prepared for, but over time reduced worry may lead to a decline in awareness of the risk. This is because individuals forget risks to which they or their communities have not been exposed to for a long period. Notwithstanding, worry is a valuable indicator in determining public preferences in the trade-off between risk and benefit. This means a high level of worry concerning a risk will lead to a greater societal basis for risk reducing measures (Raaijmakers et al, 2008).

Media-worthy landslides tend to be less common than other natural hazards in Australia, and as such the community is generally less aware of the impacts that landslide hazards can have. An intense rainfall event in Western Victoria triggered over 200 landslides in the Gariwerd (Grampians) National Park during January 2011. Surveys and interviews of residents, local businesses, and emergency response personnel captured the impacts on the community during the emergency and the recovery (Ollerenshaw et al, 2014). Feedback from the community, emergency services, and recovery services, all expressed that the nature and scale of the events – both of the flooding and of the landslides – were wholly unexpected and unprecedented and therefore difficult to prepare for and respond to. Although unexpected for the residents and emergency response organisations, there are good historic records of two similar landslide events in 1916 and 1934. The individuals responding to the surveys were not familiar with the history of the area, and it seems the broader community had forgotten risks to which they had not been exposed to for almost 80 years.

So how should a geoprofessional assist a client develop a considered appreciation of landslide risk, such that they can make informed decisions?

4 RISK AWARENESS AND UNCERTAINTY WHEN COMMUNICATING TO CLIENTS

The experience of the authors has been that when preparing landslide risk assessment reports for clients,

1. the executive summary and recommendations are often used to make decisions, and
2. elements of landslide risk reports are reproduced in stakeholder or community communications, often selectively and/or without an appreciation of the uncertainty associated with the outcome.

The reporting standards for a landslide risk assessment, as required by AGS (2007c), includes 15 elements that should be included (or an explanation provided as to why one of these elements is missing). Clearly the outcomes, assumptions, and limitations of these elements, and how each might contribute to the degree of uncertainty inherent in the findings and recommendations of a landslide risk assessment, cannot be succinctly summarised into an executive summary.

The following sections explore ways to assist clients to make binary decisions based on probabilistic (uncertain) outcomes, and how these decisions could be communicated to stakeholders.

4.1 EXPLAINING RISK AND UNCERTAINTY TO DECISION MAKERS

The inherent uncertainty in a risk assessment might be understood by a practitioner or informed client but is often not appreciated by less informed clients or stakeholders. Clients and decision-makers might seek binary answers (yes/no, safe/unsafe) from landslide risk assessments, and are looking for clear recommendations and advice on how to implement remedial measures. They might interpret terms like Risk and Uncertainty in terms of a business or project management, (Saunders, 2016), which as shown in Table 1 can be subtly, albeit sufficiently different to generate a misalignment of expectations regarding the degree of confidence a landslide risk assessment might be reporting.

Various definitions of risk and uncertainty exist in other industries, and as an example The Infrastructure Australia Assessment Framework (IA, 2021) defines risk and uncertainty in the following ways (terms underlined by authors, not IA).

- Risk is defined as events that have probabilities of occurrence that are predictable and outcomes that can be estimated with some confidence.
- Uncertainty is defined as events where probabilities of occurrence are difficult to predict, and outcomes are challenging to quantify.

AGS (2007c) openly acknowledges that the assessment of landslide frequencies is particularly difficult at frequencies in the order of 10^{-4} (1 in 10,000) or less, because methods involving the review of historic data are not applicable. As landslide frequency is a fundamental LRA input, the potential for confusion and misjudgement in decision making can be inherent on the understanding of what a client considers to be “risk”.

The United Kingdom governmental Guidelines on the Use of Scientific and Engineering Advice in Policy Making (DBIS, 2010) explores how scientific and engineering advice should be sought and applied to enhance the ability of government policy makers to make better informed decisions. The guidelines, prepared by the Government Chief Scientific Adviser, provide an insight into how governments consider and incorporate scientific and engineering advice in decision making. Amongst other advice, the guidelines acknowledge:

1. Evidence in public policy making contains varying levels of uncertainty that must be assessed, communicated and managed,
2. Experts should not be pressed to come to firm conclusions that cannot be justified by the evidence available,

3. As a result, levels of uncertainty should be explicitly identified and communicated directly in plain language to decision makers.

The authors consider these points very important, regardless of whether the client is a government authority, or a private entity. So how can the uncertainty inherent within landslide risk assessments be communicated and understood by a client in a way that still allows informed decisions to be made?

Lee (2015) notes that landslide risk assessments contain degrees of randomness (aleatory uncertainty, natural variability) and imperfect knowledge (epistemic uncertainty). Aleatory uncertainty is described as being a property of the system (that is, a property of nature) independent of the observer's knowledge of it or evidence for it. It cannot be reduced by further study, as it expresses the inherent variability of a phenomenon. Epistemic uncertainty is described as the level of understanding of a problem. In many situations, difficulties in estimating future landslide activity are due to a lack of knowledge about ground conditions, failure mechanisms and the circumstances that could lead to failure, rather than randomness. Knowledge uncertainties are due to things we could, in principle, know but do not in practice.

Methods for describing uncertainty associated with landslide risk assessments is the subject of a recent paper by Paul and Miner (2025), which introduces a range of methodologies to communicate an improved understanding of uncertainty. As different stakeholders will have different capabilities and/or knowledge regarding landslide risk assessments, three levels (or tiers) of communication style have been developed to assist communicating the uncertainty associated with landslide risk.

- Tier1 is where uncertainty is communicated through a qualitative descriptor based on an index rating, related to the state of knowledge of site conditions (*e.g., Risk of loss of life for the individual most at risk is* 1.7×10^{-4} *with MODERATE confidence. Risk estimation is based on observation and a degree of belief*).
- Tier 2 is where quantitative risk (probability) is communicated as a range centred on a best estimate with an upper and lower bound, whereby the broader the range means the greater the uncertainty *(e.g., Risk of loss of life for the individual most at risk ranges between* 2.6×10^{-5} *and* 1.1×10^{-3} *with best estimate of* 1.7×10^{-4}).
- Tier 3 is where quantitative risk (probability) is communicated as confidence limits derived from a log-normal distribution centred on a best estimate and relative to a nominated evaluation criterion. *(e.g., Based on an initial risk estimate of* 1.7×10^{-4}*, there is a 74% chance the risk is unacceptable relative to a nominated evaluation criterion*).

The policy maker is generally responsible for increasing risk awareness, so how can geoprofessionals assist in providing sound advice to promote improved awareness across society? In the aftermath of the worldwide COVID-19 pandemic, Intemann (2021) considered the role of scientific communication in facilitating (or undermining) public trust in science and science-based policy recommendations. Whilst no set rules were identified that will always result in responsible or effective communication that facilitates trust for everyone, the following recommendations were made.

1. Have a clear sense of who your audience is and what they care about in relation to decision-making.
2. Strive to present information that is not only accurate but relevant to the kinds of decisions those audiences want to make.
3. Develop targeted, audience-specific messaging in cases where there are populations who have different circumstances, needs, and interests.
4. Explain – as clearly and concisely as possible – why the evidence for the findings being presented is epistemically reliable or competent.
5. Try to present evidence, findings, or recommendations in ways that acknowledge or speak to a diversity of values or serve a diversity of public interests.
6. Remind audiences how science works (or set expectations for what might change).
7. Articulate benefits and risks in a balanced manner.

Aspects of a LRA report, if clearly presented, can help the policy maker communicate decisions to stakeholders. A well-developed landslide inventory, for example, might assist the client gain an appreciation of landslide risks that stakeholders may not be aware of or that society has forgotten about.

4.2 SUPPORTING CLIENTS COMMUNICATING LANDSLIDE RISK CONCEPTS WITH STAKEHOLDERS

Technical risk information can be challenging to communicate in a way that will resonate and be meaningful for communities. Language barriers and subjective perceptions of risk can exacerbate this challenge. When the client of a LRA is a policy maker, reports prepared in accordance with AGS (2007c) provide a logical, transparent, and defendable basis for the client to implement policy. What these reports don't necessarily do is help the policy maker with raising awareness of landslide risk within the community. Fischhoff et al (2011) note that risk communication is required in situations when people need good information to make sound choices, and it differs from public affairs (or public

relations) communication by its commitment to accuracy and its avoidance of spin. They go on to recommend communications must be evidence-based and consistent with the science, avoiding things known not to work or ignoring known problems. Communications should also be reviewed and evaluated, because even the best science cannot guarantee results.

The USGS Landslide Handbook (Highland et al, 2008) provides landslide-specific risk communication guidance, identifying that for communication of hazard information to be useful, the nontechnical user must be able to

1. Perceive likelihood, location, and severity of the hazard so that the end-users become aware of the danger,
2. Convey the risk to others, and
3. By using the information, be able to directly to deduce a threat and know where and how to evacuate.

Research into development of flood and other natural hazard risk communications can also provide guidance that may be of relevance when considering landslide hazards. In a study looking at developing flood risk communication strategies in Europe, Bradford et al (2012) observed that scientists and the public at large perceive risk in very different ways. Exploring the role of public perception in developing flood risk communication strategies, the study made recommendations that may have parallels when improving landslide risk awareness, depending on the type(s) of landslide and hazards at risk. The recommendations highlighted:

1. The need for clear tailored information regarding preparedness, mitigation and evacuation,
2. Benefits in capturing personal accounts from victims and use this in future communications, and
3. That communications should not evoke fear amongst vulnerable communities.

Whilst the first recommendation is similar to the likelihood-consequence-risk framework of the USGS Landslide Handbook, the second and third recommendations aim to improve the risk awareness of stakeholders, drawing similar conclusions to the work of Raaijmakers et al (2008).

The Natural Hazard Risk Communications Toolbox (Aukland Council, 2014) is a useful reference that provides simple explanations of a range of natural hazard risk terminologies and provides suggestions for how to communicate these concepts. The toolbox was developed to increase understanding of basic hazard and risk concepts, by providing consistent content for communication materials used within council and externally to stakeholders, politicians and the community. The toolbox contains written and visual materials to describe frequently used local natural hazard risk management concepts, including case studies from the Auckland area (where possible). It provides one set of definitions, with the aim to create a consistent and integrated approach to communicating natural hazard risk management.

In the immediate response to the worldwide COVID-19 pandemic, Goldstein (2020) found that tailoring effective scientific communications requires perspective-taking, insight, humility, and knowledge of the target audiences. USGS Landslide Handbook, AGS (2007c), and to a lesser degree the Aukland Natural Hazard Risk Communication Toolbox perhaps don't address this level of engagement with landslide-affected communities as acutely as the perspective-taking insight described by Goldstein.

There has been a steady increase in community engagement across broader natural hazard and climate change risks during the past decade or so (LTAR, 2023). A Delphi survey of specialists across a range of areas including planning, strategic policy, emergency preparedness, community development, and climate risk research identified the following nine issues that experience has shown to exacerbate the challenges of community engagement in a natural hazard and climate change risk.

1. The high-stakes nature of the conversations, often evoking emotions such as anger, denial, fear, and distrust.
2. Uncertainties, which can lead to a lack of commitment to address the issue.
3. The highly technical content, and the challenges in explaining technical aspect of the risk.
4. The spatial and temporal variability of hazard risk, which are neither static nor predictable.
5. Different individual risk capacities and appetites between (and within) communities.
6. Lack of clarity about who owns and pays for the risk hinders the engagement process.
7. Identifying and coordinating people with necessary expertise and skills to collaborate as a team.
8. Engagement underutilisation by decision makers, who avoid seeking community feedback in risk situations.
9. Capability and capacity challenges to ensure engagements are supported by good risk engagement expertise and leadership skills.

The specialists surveyed by LTAR (2023) provided the following advice for practitioners engaging in community conversations with stakeholders, which align closely with the themes of perspective-taking, insight, humility, and knowledge of the target audiences explored by Goldstein (2020).

- Being open, honest, and genuine about listening to feedback
- Work with other practitioners and learn from them

- Talk to someone who has done it before, particularly if you're new to working in a given community
- Localise your processes, and demonstrate how science applies to local impacts.
- Know how to deal with grief when engaging with people affected by hazards.
- Tools tested with communities are the best, provided they are suited to the situation and community context.
- Use a set of principles but tailor to your process to the local context and setting.

5 LANDSLIDE RISK MANAGEMENT IN PRACTICE

5.1 CASE STUDY 1: AGS LRM GEOGUIDES

To help a stakeholder assess the acceptability of landslide risk, the Geoguides (AGS 2007e), an accompaniment to the main AGS LRM technical guidelines (AGS, 2007a,b,c,d), are written in less technical, plain English. To help improve people's intuitions about the magnitude of risks rather than provide insight regarding risk acceptability, Geoguide LR7 includes quantitative risk estimates for a variety of more common hazards, expressed as the annual probability of death.

Risk perception research suggests, however, that these sorts of comparisons may not be very satisfactory even for this purpose (Slovac, 1987). Perceptions and attitudes towards risk are determined by a variety of quantitative and qualitative characteristics, not only by the sort of unidimensional statistics used in tables such as the one presented in Geoguide LR7 and reproduced in Table 2, below. Instead, difficulties in understanding probabilistic processes, biased media coverage, misleading personal experiences, and the anxieties generated by life's gambles contribute to the denial of uncertainty, misjudging risks (sometimes overestimated and sometimes underestimated), and judgments of fact to be held with unwarranted confidence. Strong personal views ("*I wouldn't want to be in a plane crash, so I'll drive because I'm a safe driver*") are often resistant to change because they influence the way that subsequent information is interpreted, even when new facts, such as those in Table 2, are presented.

Table 2: Examples of alternate interpretations to specific landslide-related language

Risk (deaths per participant per year)	**Activity/Event Leading to Death** (NSW data unless noted)
1:1,000 (1 death per 1,000 participants per year)	Deep sea fishing (UK)
1:1,000 to 1:10,000	Motor cycling, horse riding, ultra-light flying (Canada)
1:23,000	Motor vehicle use
1:30,000	Fall
1:70,000	Drowning
1:180,000	Fire/burn
1:660,000	Choking on food
1:1,000,000	Scheduled airlines (Canada)
1:2,300,000	Train travel
1:32,000,000	Lightning strike

5.2 CASE STUDY 2: SIGNAGE STUDY AT BARWON HEADS, VICTORIA AUSTRALIA

Early in 2006 a study was conducted to find out the general public's beliefs concerning the dangers of falling rocks from cliff faces at Barwon heads, Victoria, Australia. The study was conducted to develop improved ways to discourage people from entering dangerous rockfall areas.

Results from the study (Aucote et al, 2010; Aucote et al, 2012) suggest that the warning signs used at the site were not sufficiently detailed to provide all participants with enough information to make informed decisions about safe behaviours. Interestingly, 40% of respondents thought signs were erected merely to stop the responsible authority getting sued.

Figure 2 presents a detailed interpretation of the perceived messaging of the Australian standard sign depicting an unstable cliff rock fall hazard. The land manager had a perceived duty-of-care to display this signage in order to inform the public about potential hazards after it had been recommended as part of an earlier landslide risk assessment.



Table 1. Five interpretations of the warning signs and the percentage of participants who endorsed them.

Interpretation of signage	%
Do not go too close to the cliff face	39.5
Do not climb the cliff face	23.6
Do not stand under/next to cliff face	13.2
Do not climb and Do not stand under/next to cliff face	18.4
General warning to be careful – could not state what "careful" entailed	5.3

Figure 2: Interpretation of the perceived messaging of the unstable cliffs sign (from Aurecote et al, 2012)

As a result of further ongoing risk assessments and a recent detailed signage audit, the following improvements have now been incorporated into the revised signage:

- Internationally recognised hazard pictograph (exclamation mark) and large font warning.
- Photos of the site showing area people will be exposed to the hazards
- Written description of what the hazard is (together with rockfall pictograph)
- Clear description that safe access along beach not possible at certain times (high tide)
- QR code for latest tidal information

Examples of the revised signage are shown in Figure 3.



Figure 3: New signage to inform the public of unstable cliff hazards

6 CONCLUDING REMARKS

The authors have shared some of their experiences and outlined challenges in communicating concepts of probability, risk and uncertainty to clients who may have varying degrees of understanding, knowledge, and perception of landslide hazards. A key outcome for us is to highlight the need to better communicate what we as geoprofessionals are undertaking within the restrictions of our professional duties and requirements, while at the same time providing our clients with outcomes they can use to make informed decisions. Often these two focuses don't align. How societal risk perceptions and associated community messaging of other natural hazards is framed and broadcast offers insight to how landslide risk communication might be improved.

To start bridging this communication gap, we believe that the geoprofessional should consider the following suggestions when working through a landslide risk assessment for a client.

At the start of the project:

- Spend more time at proposal or Request for Quote stage explaining what can be achieved and what limitations and inherent uncertainty exists.
- Listen to what the client is asking for. Often this is different to how the scope in a Request for Quote written (because of misalignments in risk assessment language, or unrealistic expectations regarding what a LRA report will provide). Make sure the scope is clarified prior to commencing the project.
- Clarify with the client that LRA does not lead to a binary outcome. Aleatory uncertainty and epistemic uncertainty cannot always be reduced to negligible levels.
- Inform the client of what a LRA report typically contains (what will be provided) so they have an understanding of what the outcomes might mean for them and their decision-making processes.
- Adequately communicate to the client that LRA reports are not necessarily a statement of how stable a slope is, but rather an estimate of possible future landslides, which in most cases has been based on limited information (when compared to engineering reports from other disciplines).

When reporting LRA findings for the client

- Spend more time at proposal or Request for Quote stage explaining what can be achieved and what limitations and inherent uncertainty exists.
- Appreciate how the client understands concepts such as uncertainty and probability.
- Understand how the client or Stakeholder intends to use the findings of a LRA report, and present the report in a way that the client can use.
- Draw attention to the consequences of landslide events. Consider using terms such as 'dangerous' landslide events. When communicating to a non-technical audience, consider using terms such as 'dangerous' in lieu of 'risk' as this communicates a harmful outcome that 'risk' might not.
- Include a glossary to help address misalignment in understanding of risk terms.
- Include, where possible, some form of quantification when using qualitative terms (possible, likely, etc) in Executive Summaries. This needs to be balanced with a clear statement regarding the uncertainty underlying the findings and recommendations of a LRA.

When discussing LRA outcomes with the client

- Ensure the client has the tools to be able to communicate the findings of a LRA report to upper management, decision makers, and/or policy makers. A well-written Executive Summary that includes a statement regarding the uncertainty underlying the findings, together with supporting evidence (such as a landslide inventory) should help with this communication.

The Authors agree there is still much work to do unpacking societal perceptions of landslide risk and how we, as geoprofessionals, can best contribute to this broader discussion. However, we believe highlighting the communication gap is an appropriate starting point for further advancement in effective risk assessment and management for all stakeholders.

7 ACKNOWLEDGEMENTS

The Authors would like to thank the following colleagues for their support with this paper: Paul Gangell and Timothy Miller-Backhous, Barwon Coast Committee of Management

8 REFERENCES

Aukland Council (2014). Natural Hazard Risk Communication Toolbox. https://www.civildefence.govt.nz/resources/natural-hazard-risk-communication-toolbox, accessed 20 May 2025.

Australian Geomechanics Society (AGS) (2007a). Guideline for landslide susceptibility, hazard and risk zoning for land use management. *Australian Geomechanics*, 42(1), 13-36.

Australian Geomechanics Society (AGS) (2007b). Commentary on guideline for landslide susceptibility, hazard and risk zoning for land use management. *Australian Geomechanics*, 42(1), 37-62.

Australian Geomechanics Society (AGS) (2007c). Practice note guidelines for landslide risk management. *Australian Geomechanics*, 42(1), 64-114.

Australian Geomechanics Society (AGS) (2007d). Commentary on the practice note guidelines for landslide risk management. *Australian Geomechanics*, 42(1), 115-158.

Australian Geomechanics Society (AGS) (2007e). The Australian GeoGuides for Slope Management and Maintenance. *Australian Geomechanics*, 42(1), 159-182

Aucote, H., Miner, A., and Dahlhaus, P. (2010). Rockfalls: predicting high-risk behaviour from beliefs. *Disaster Prevention and Management*, 19(1), 20-31

Aucote, H., Miner, A., & Dahlhaus, P. (2012). Interpretation and misinterpretation of warning signage: perceptions of rockfalls in a naturalistic setting. *Psychology, Health & Medicine*, 17(5), 522-529

Bradford, R., O'Sullivan, J., van der Craats, I., Krywkow, J., Rotko, P., Aaltonen, J., Bonaiuto, M., De Dominicis, S., Waylen, K., and Schelfaut, K. (2012). Risk perception – issues for flood management in Europe. *Natural Hazards and Earth Systems Science*, 12, 2299–2309

Bureau of Meteorology (BOM) (2025). Australian Water Information Dictionary. http://www.bom.gov.au/water/awid/index.shtml accessed 21 February 2025

Cui, A., Fountain, J., and Espiner, S. (2023). Communicating natural hazard risks to Chinese visitors: a case study from New Zealand. *Front. Sustain. Tour*. 2:1192124. doi: 10.3389/frsut.2023.1192124

Department for Business, Innovation, and Skills (DBIS 2010). *The Government Chief Scientific Adviser's Guidelines on the Use of Scientific and Engineering Advice in Policy Making*. UK Government Office for Science, Crown Copyright URN 10/669

Fischhoff, B., Brewer, N., and Downs, J. (eds.) (2011). *Communicating Risks and Benefits: An Evidence-Based User's Guide*. Food and Drug Administration (FDA), US Department of Health and Human Services, August 2011.

Goldstein, C., Murray, E., Schnoes, A., and Wang, M. (2020). Science Communication in the Age of Misinformation. *Annals of Behavioural Medicine* 54:985–990

Guzzetti, F., Mondini, A., Cardinali, M., Fiorucci, F., Santangelo, M., and Chang, K. (2012). Landslide inventory maps: New tools for an old problem. *Earth-Science Reviews* 112 (2012) 42–66

Highland, L.M., and Bobrowsky, P. (2008). *The landslide handbook—A guide to understanding landslides*: Reston, Virginia, U.S. Geological Survey Circular 1325

Infrastructure Australia (IA) (2021). *Guide to risk and uncertainty analysis – Technical guide of the Assessment Framework*. Commonwealth of Australia

Interman, K. (2021). Science communication and public trust in science. *Interdisciplinary Science Reviews*, 48(2), 350-365

Lee, M. (2015) Landslide risk assessment: the challenge of communicating uncertainty to decision-makers. *Quarterly Journal of Engineering Geology and Hydrogeology* 49(1), 21-35

Lee, M. and Jones, D. (2023). *Landslide Risk Assessment, Third Edition*. ICE Publishing

Let's Talk About Risk (LTAR) (2023). *Natural hazard and climate change risk community engagement: A framework to aid engagement design*. Let's Talk About Risk, https://www.resorgs.org.nz/our-projects/risk-and-resilience-decision-making/lets-talk-about-risk/.

NZSOLD (2024). *New Zealand Dam Safety Guidelines*. New Zealand Society on Large Dams

Ollerenshaw, A., Dahlhaus, P., McDonald, K., Courvisanos, J., Graymore, M., Thompson, H., Sheil, H., Miner, A., and Corbett, J. (2014). *Understanding the 2011 Grampians Natural Disaster, addressing the risk and resilience Final Report*. Centre for eCommerce and Communications, Federation University Australia

Paul, D. and Miner A. (2025 in press). Practical communication of uncertainty in quantitative landslide risk assessment. *Australian Geomechanics Society Journal*, Volume 60 No.1

Raaijmakers, R., Krywkow, J. and van der Veen, A. (2008). Flood risk perceptions and spatial multi-criteria analysis: an exploratory research for hazard mitigation. *Natural Hazards* 46:307–322

Saunders (2016). *Differentiating between Risk and Uncertainty in the Project Management Literature*. http://fionasaunders.co.uk/wp-content/uploads/2016/07/Differentiating-between-Risk-and-Uncertainty-in-the-Project-Management-Literature.pdf accessed 18 February 2025

Smith, M. (2020). *How likely is likely*? YouGov. https://yougov.co.uk/politics/articles/32255-how-likely-likely accessed 29 January 2025

Toka Tū Ake EQC (2023). *Natural Hazard Risk Tolerance Literature Review*. Natural Hazards Commission, Aotearoa New Zealand Government, July 2023

https://doi.org/10.56295/1ACEG15

RISK MANAGEMENT OF COASTAL CLIFF HAZARDS – A CASE STUDY FROM THE SURF COAST, SOUTHWEST VICTORIA

Kris Jelly-Butterworth
Senior Engineering Geologist, GHD

ABSTRACT

Coastal cliffs pose a significant and unpredictable landslide hazard to users of coastal areas. The surf coast region of Southwest Victoria encompasses more than 50 km of coastline from Torquay to Lorne. The region is a world-class surfing destination and attracts hundreds of thousands of visitors each year, from all over the world. The coastline is variable, with low-lying sand dunes juxtaposed with large sea cliffs. From Torquay to Aireys Inlet, cliffs comprise variably cemented Paleogene aged sediments of very low- to low strength sandstone, calcarenite and limestone with soil horizons, transitioning to the Cretaceous rocks of the Otway Basin around Lorne. This combination of unstable cliffs and the popularity of the area for coastal users presents a challenge to manage the geotechnical risk whilst preserving public amenity. This case study looks at how GHD aided the Great Ocean Road and Parks Authority (GORCAPA) in understanding the hazard and risk posed by coastal cliffs and how GORCAPA moved away from traditional reactive management methods to a more proactive approach. Part of this involved identifying “hotspot" areas where resources could be better targeted to monitor and mitigate risks. A key aspect was development of a Trigger Action Response Plan (TARP) and integration with the wider Coastal and Marine Management Plan (CMMP). The TARP allows GORCAPA staff to understand the actions that need to be undertaken following certain events and, tied to the CMMP, aids in a more proactive response to developing cliff risks. The reality of risk management for this area, with multiple hazards meant that only the consequences of the hazard could effectively be reduced. Restricting access to large expanses of popular beaches in the region is not feasible, therefore other strategies were deployed, including education programs in local schools, improved hazard signage and improved communication of hazards with the public via social media streams. The implemented approach has mitigated the likelihood and severity of potential casualties. An effective risk management program is essential to keeping users of the coastline safe and informed about hazards posed by cliffs.

1 INTRODUCTION

Southwest Victoria boasts a varied and rugged coastline with towering sea cliffs, sea stacks, offshore platforms, reefs and caves to low lying sandy beaches and dunes. The Surf Coast area, comprising more than 50 km of coastline extending from Torquay to Lorne, has an abundance of these geomorphic features. The varied nature of the coastline and the underlying geology are the reason for the world-class surfing environment in this region. The combination of natural beauty and coastal activity/amenity brings millions of visitors each year – with 5.5 million visitors to the Great Ocean Road Region in the 12 months to September 2024 (Tourism and Events Victoria 2024).

The coastal environment presents a number of potential geotechnical hazards, the most common being landslide hazards associated with coastal cliffs including rockfall and slide/flow-type mechanisms. With large numbers of visitors to the area every year, hundreds of thousands of people may be exposed to these hazards, possibly without understanding the risk posed by coastal cliffs. In 2021/2022, a 30-m-high cliff face collapsed near Bells Beach, part of the Surf Coast. A group of six people were sitting under the cliff face at the time, with three people struck by falling debris, leading to one person being killed with the other two sustaining injuries as a result (ABC News 2021). This highlights the risk to the public posed by coastal cliff hazards in the region.

According to the Guidebook to Public Land Management in Victoria (CJC & GCLS 2023), under the *Crown Land (Reserves) Act 1978, (Vic),* it is the responsibility of local land managers/authorities, such as local councils and other state authorities appointed by the Department of Energy, Environment and Climate Action (DEECA), to manage the land and to protect the coastline. This includes understanding the risk posed by coastal geotechnical hazards, managing risk and effectively communicate this risk to the public.

This case study focuses on the risk management strategy implemented for an area of coastline between Torquay and Aireys Inlet (shown in Figure 1A, 1B below), managed by the Great Ocean Road Coast and Parks Authority (GORCAPA), a Victorian State Government entity (known as the Great Ocean Road Coast Committee, or GORCC, prior to December 2020). GHD were first engaged by GORCC/GORCAPA to undertake a baseline geotechnical risk assessment between Torquay and Aireys Inlet in 2012, with a review and update of the risk assessment undertaken in late 2019 and early 2020.

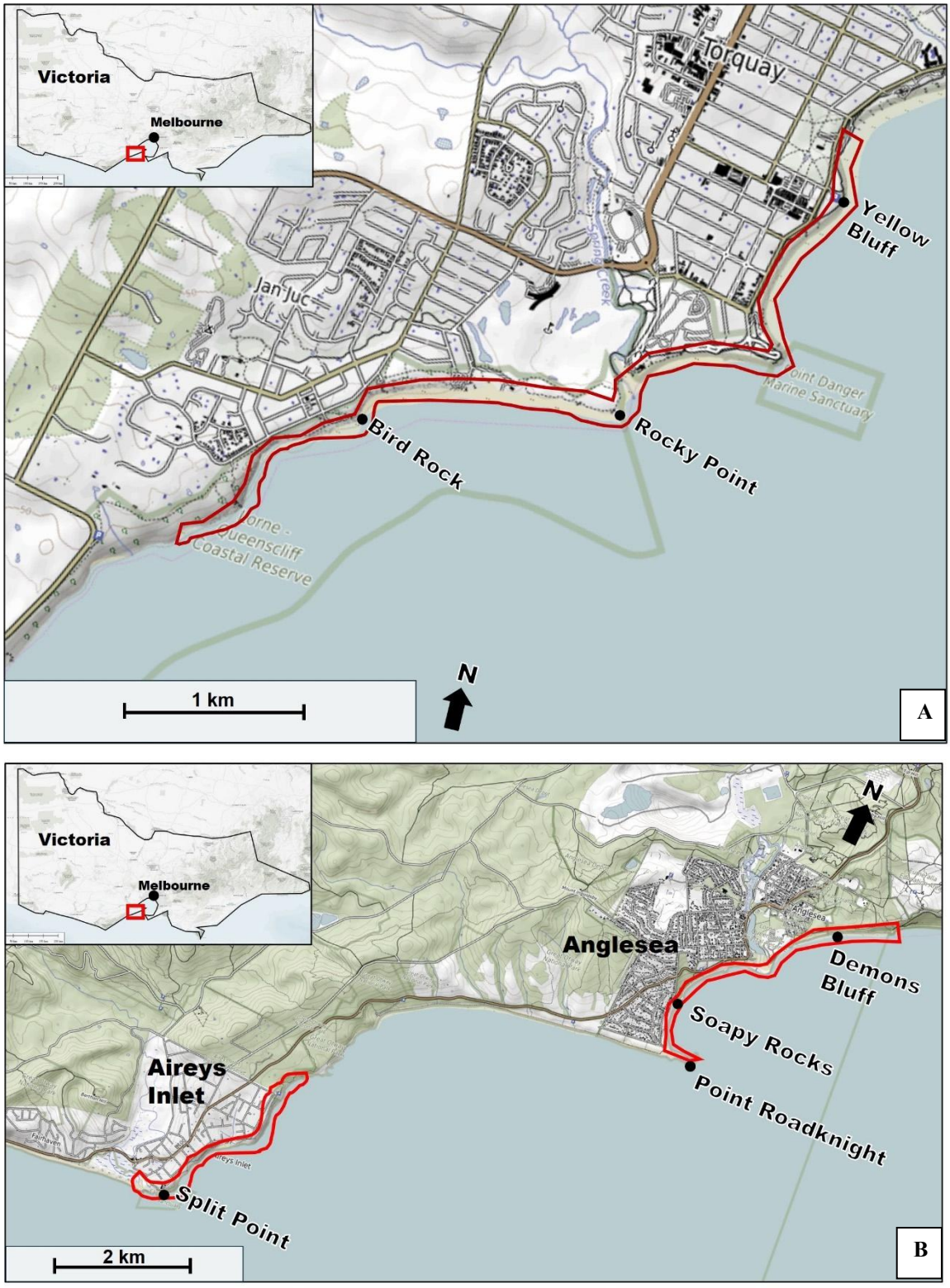


Figure 1: Area location maps. A: Torquay and Jan Juc areas. B: Anglesea and Aireys Inlet areas. Red outlines indicate the coastline that was assessed in GHD 2012 and GHD 2020. Map overlays from OpenTopoMap

As a part of the risk assessment and review process, GORCAPA were keen to identify areas of particularly high-risk cliff areas ("hotspots"), develop erosion trigger points and setbacks for clifftop amenities, undertake an audit of cliff risk signage and a review of the current cliff monitoring methodology and recommendations for improvement. The report and its findings would provide a basis for input to GORCAPA's Coastal and Marine Management Plan (CMMP). In 2023, the Victorian Government through the Department of Energy, Environment and Climate Action (DEECA) released its

long-term coastal framework and guidelines for coastal risk management and guidelines – Victoria's Resilient Coast. Coastal risk management activities undertaken by land managers is now also expected to align with this framework.

2 GEOLOGICAL SETTING

This case study uses the geological stratigraphy initially used in the GHD 2012 study, to allow for continuity. This is based on the 1:63,360 geological map produced in 1968 and the work of Abele (1979). The author is aware that the geological stratigraphy was updated in 2014 as part of the Victorian Seamless Geology project and geological mapping is now available in 1:50,000 scale.

The geology of the coastline from Torquay to Aireys Inlet is dominated by two major Paleogene to Neogene aged formations/groups of rocks – the Oligocene to Eocene aged Demons Bluff Formation (Te) and the Miocene to Oligocene aged Torquay Group (To). The Paleogene and Neogene rocks are folded into a series of gently dipping anticline and synclines with a gentle south-east plunge. Recent deposits comprising alluvium (Q1, Q2) swamp/lake deposits (R2) and recent sand dunes (R3) overly or abut the older rock units.

2.1 TORQUAY AND JAN JUC

The coastal cliffs in the Torquay and Jan Juc areas comprise the Torquay Group (To), as shown in Figure 2. The Torquay Group comprises two main formations – the Jan Juc and Puebla formations, with three defined limestone members within each formation (Point Addis and Waurn Ponds limestone Members in the Jan Juc Formation and the Zeally Limestone Member within the Puebla Formation). These formations are described in detail by Abele (1979) in several measured coastal cliff sections. The Point Addis Limestone Member is not encountered in this part of the project area and is described in the Anglesea and Aireys Inlet sections below.

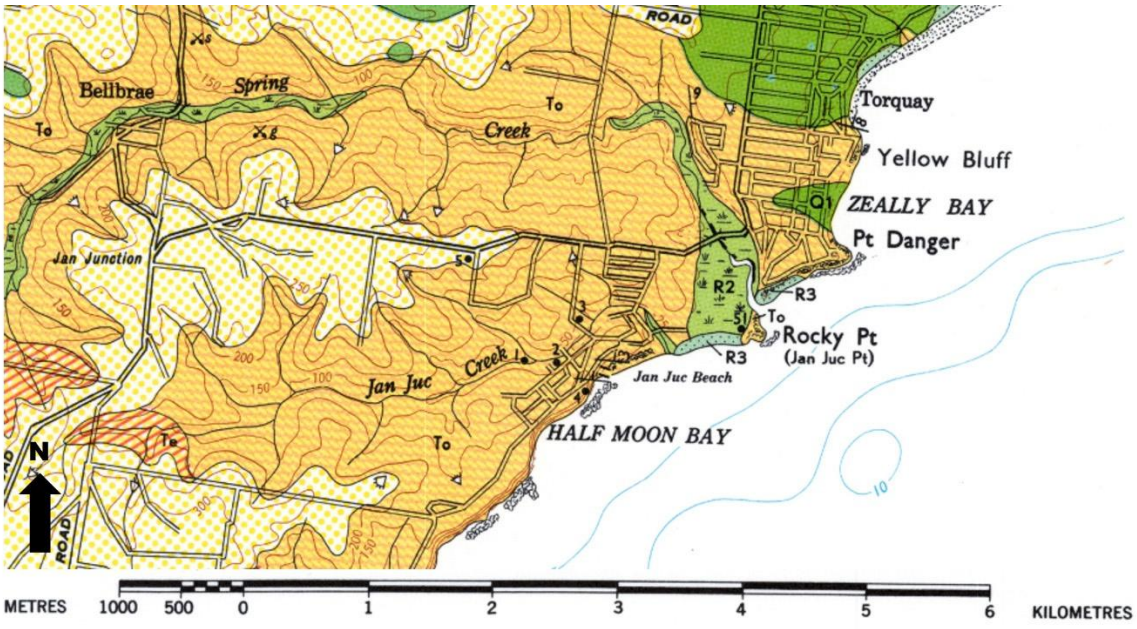


Figure 2: Surface Geology of coastline of interest - Torquay to Jan Juc (Extract from 1:63,360 Anglesea map sheet, Geological Survey of Victoria, 1968). Q1 = alluvium, R2 = swamp/lake deposits, R3 = sand dunes, To = Torquay Formation

The Jan Juc Formation generally comprises silty glauconitic marl and clayey sandy calcarenite, noted to be highly friable. The calcarenite layers are more strongly cemented, more ferruginous and more resistant than the marl beds (Abele 1979), leading to an irregular weathering pattern on cliff faces, as shown in Figure 3A. The Jan Juc Formation is exposed in the lower part of the cliffs from Bird Rock to Fisherman's Steps beach.

The Puebla formation overlies the Jan Juc Formation and is the main component of the cliffs from Bird Rock to Yellow Bluff. The rocks of the Puebla formation comprise grey, yellow-grey-brown to grey, orange clayey silt and silty clay, commonly calcareous, with thin cemented limestone and calcarenite interbeds. Calcareous concretions are present either in layers or scattered throughout the unit. The upper beds are commonly strongly weathered and ferruginous (Abele 1979). Typical outcrops of the Puebla Formation are shown at Yellow Bluff, Figure 3B, 3C. The Zeally Limestone Member is an intermediate layer within the Puebla Formation and outcrops in coastal cliffs from Jan Juc beach, Rocky Point, to Point

Danger and just south of Yellow Bluff. The unit comprises grey, orange to pale orange sandy bryozoal calcarenite. The calcarenite has a rubbly texture due to the differentially cemented nature of the rock. This texture is well illustrated in a cliff section at Rocky Point, Jan Juc (Figure 3D).

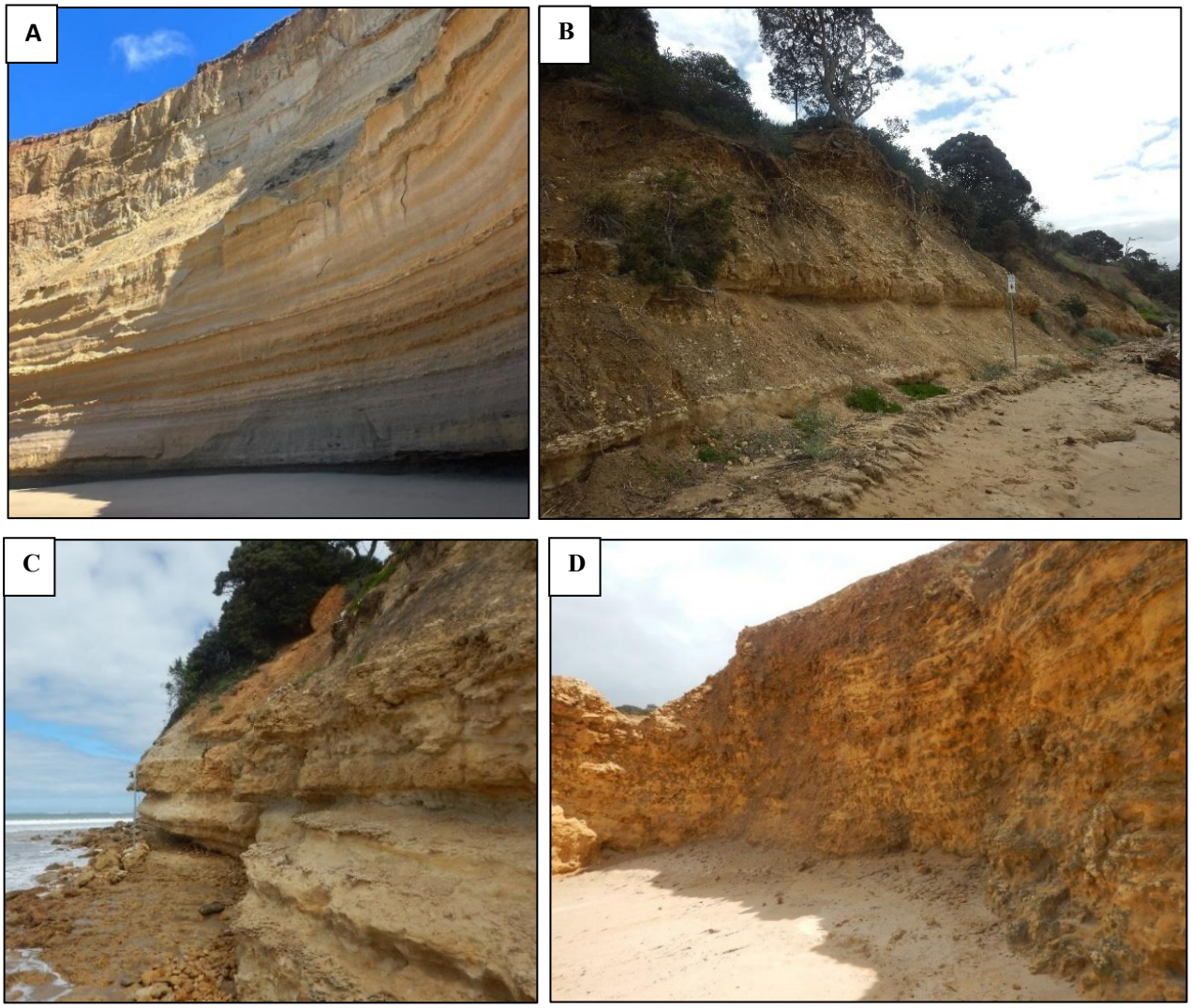


Figure 3: Typical outcrops of the Jan Juc Formation (A – Near Bird Rock GHD 2023), Puebla Formation (B and C, near Yellow Bluff GHD 2020) and Zeally Limestone Member (D, Rocky Point, Jan Juc GHD 2020).

2.2 ANGLESEA AND AIREYS INLET

The coastal cliffs in the Anglesea area comprise the Demons Bluff Formation (Te). In Aireys Inlet, the Demons Bluff Formation units are overlain by Torquay Group (To) rocks, comprising the Point Addis Limestone Member of the Jan Juc Formation. The relationship of the surface geology is shown in Figure 4.

The Demons Bluff Formation is made up of two members: the Anglesea Siltstone Member (which includes the previously differentiated Addiscot Greywacke Member) and the Angahook Member. The Anglesea Member makes up the vast majority of the Demons Bluff Formation and consists of a poorly stratified homogenous brown-black to brown-grey carbonaceous, pyritic clayey silt to fine sand and silty clay. Where intensely weathered, it presents as grey-red to pale-brown (Abele 1979). A conspicuous feature in the coastal cliffs at Demons Bluff is the abrupt change in colour of the Anglesea Member sediments from dark grey to pale brown, as is shown in Figure 5. This colour change is thought to represent a diagenetic change rather than an obvious erosional or lithological change (Abele 1979).

In contrast to the Anglesea Member, the Angahook Member is more heterogeneous/lithologically varied. The Angahook Member comprises basalt, tuffaceous sediments, tuff breccias, quartz sand and gravel, sandy clay and clay. These materials are well exposed in the Aireys Inlet area (as shown in Figure 6A, 6B), as well as near Point Roadknight and Soapy Rocks west of Anglesea. Basalt is observed at the base of the cliffs at Aireys Inlet near Split Point. Further east/north-east, the unit grades into tuffaceous sediments, poorly to well cemented, in part well laminated/bedded that

grade to more massive pyroclastic units with large boulders of basalt and other rocks. At Soapy Rocks in Anglesea, the Angahook Member is well described with laminated clay, tuffaceous mudflow, tuff breccia, tuff, tuffaceous sand and clayey silt. A 10-m-thick reddish brown and yellow ferruginous sandy clay overlies this tuffaceous succession (Abele 1979).

The Point Addis Limestone Member overlies the Angahook Member at Aireys Inlet. The Point Addis Member generally consists of grey-orange to very pale orange sandy bryozoal calcarenite, locally interbedded with silty or sandy marl. The calcarenite is poorly cemented and poorly stratified (Abele 1979)

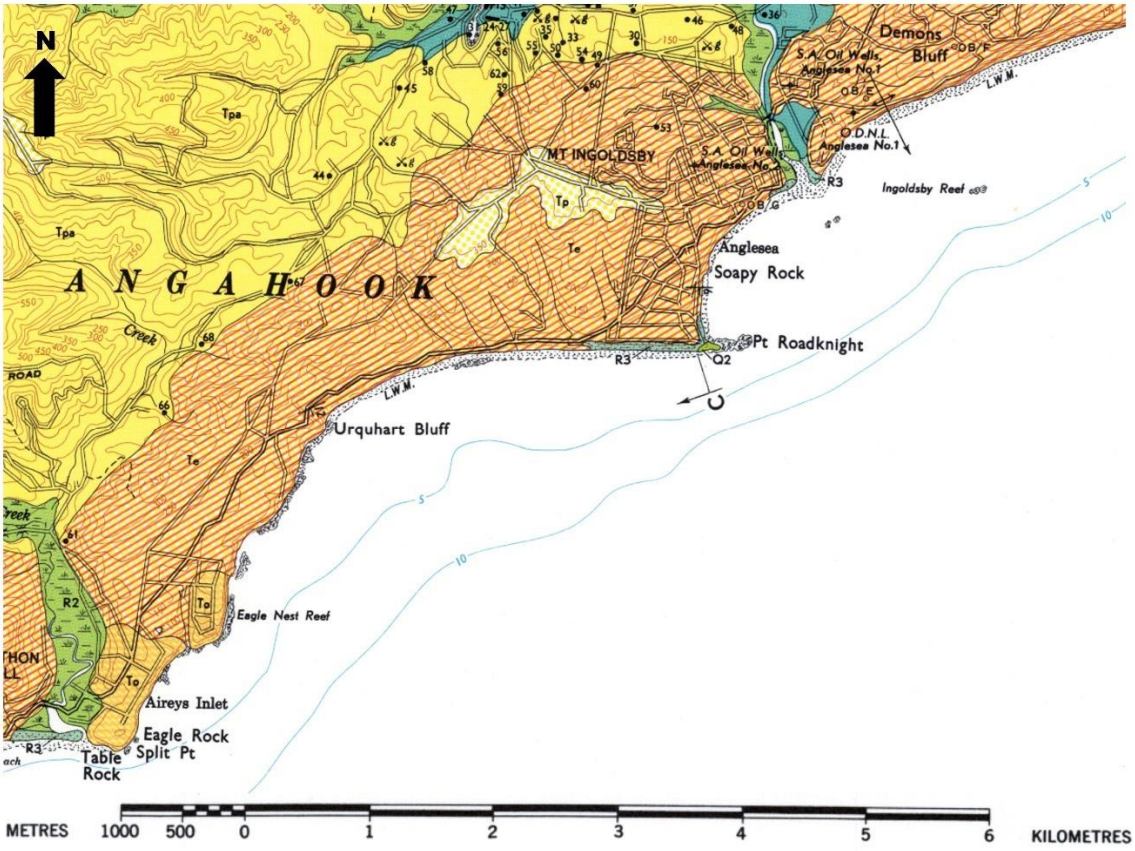


Figure 4: Surface geology of the coastline of interest – Anglesea to Aireys Inlet (Extract from 1:63,360 Anglesea map sheet, Geological Survey of Victoria, 1968).Q1, Q2 = alluvium, R2 = swamp/lake deposits, R3 = sand dunes, Te = Demons Bluff Formation, To = Torquay Formation.



Figure 5: Drone capture showing typical outcrop of the Anglesea Member, in the Demons Bluff cliffs, Anglesea (Provided by GORCAPA)

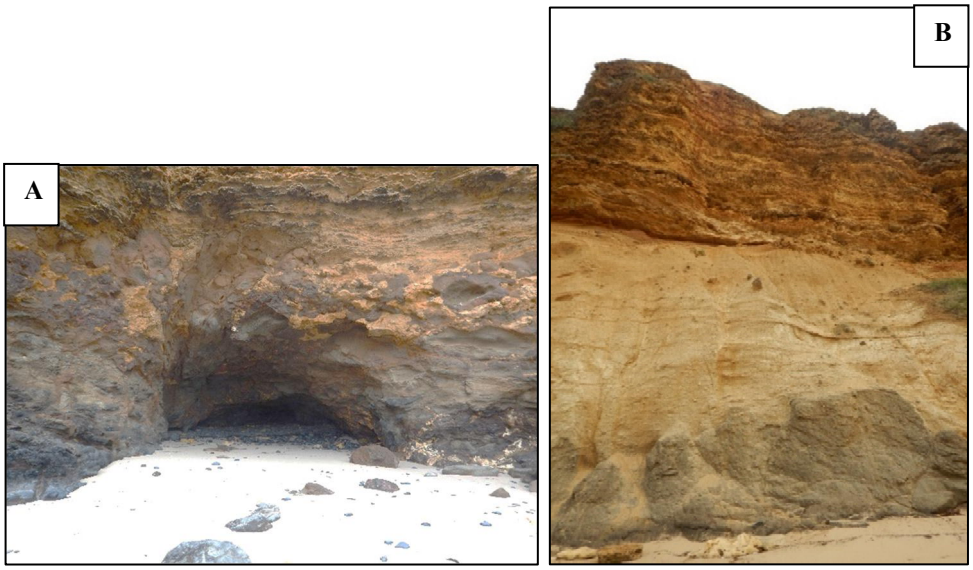


Figure 6: Typical exposures of the Angahook Member at Aireys Inlet, showing lithological diversity from basalt/basaltic sediments (A) to tuffaceous sediments and pyroclastic sediments (B). Photo B shows the contact of the Point Addis Limestone Member and the Angahook Member (GHD 2020)

2.2 GENERAL REMARKS

The geological make-up of the coastline of interest is lithologically varied, although one key property is shared between all the rocks which comprise most of the cliffs: they are all poorly or variably cemented. This poor induration means that the rocks are very-low-to low strength and soil strength in part. The cliffs that have formed are mostly near vertical, and this is reflective of dynamic and active coastal processes of recession under current sea levels. Therefore, the cliffs are more susceptible to erosion and stability issues compared with higher strength rocks.

3 HAZARD AND RISK ASSESSMENT

GHD were first engaged by GORCC/GORCAPA to undertake a baseline geotechnical risk assessment between Torquay and Aireys Inlet in 2012, with a review and update of the risk assessment undertaken in early 2020. The risk assessment methodology employed is briefly described in the following sections.

2.1 2012 AND 2020 ASSESSMENT

The initial baseline risk assessment by GHD (2012) included the following elements.

- Definition of hazard types observed during site visit (Based on AGS (2007a) terminology, see Table 1)
- Hazard zoning for each of the identified danger types, based on the estimated frequency of each danger type occurring (Table 2), for the coastline of interest (areas split and numbered 1 to 17). Frequency of each danger type was estimated utilising aerial photography, photo comparisons of the same geographic areas against previous report photos, anecdotal evidence of previous failures and general literature for similar failure types.
- Qualitative/semi-quantitative risk assessment was undertaken for cliff top property (paths, lookouts, car parks and other infrastructure) following the guidance in AGS (2007c)
- Quantitative risk assessment for risk to life was undertaken for cliff top users and beach users.

The risk to life for the individual most at risk was calculated using the method from AGS (2007c).

$$\boldsymbol{R}_{(\mathrm{lol})} = \boldsymbol{P}_{(\mathrm{h})} x\, \boldsymbol{P}_{(\mathrm{s:h})} x\, \boldsymbol{P}_{(\mathrm{t:s})} x\, \boldsymbol{V}_{(\mathrm{d:t})} \quad (1)$$

where:

- $\mathbf{R}_{(\mathrm{lol})}$ is the risk (annual probability of loss of life (death) of an individual).
- $\mathbf{P}_{(\mathrm{h})}$ is the annual probability of the hazardous event occurring.
- $\mathbf{P}_{(\mathrm{s:h})}$ is the probability of spatial impact on the beach area.
- $\mathbf{P}_{(\mathrm{t:s})}$ is the spatial temporal probability, i.e. the probability of the individual occupying the beach area at time of the event.
- $\mathbf{V}_{(\mathrm{d:t})}$ is the vulnerability of the individual (probability of loss of life of the individual given the impact).

The initial estimates of risk to life showed annual probability of death for the person most at risk to be significant. This was assessed to be due to the uncertainty involved with estimating user numbers and the frequency of events accurately. Due to the number of assumptions required, the decision was made to reduce the calculated risk by an order of magnitude for each area.

The GHD (2020) risk assessment update included

- Review of the 2012 risk assessment methodology
- Updated risk assessment, utilising updated user numbers provided by GORCAPA
- Identification of "hotspot" areas for targeted increased surveillance and assessment
- Hazard signage audit
- Review of GORCAPA coastal management plan
- Initial development of a Trigger Action Response Plan (TARP) to aid GORCAPA in coastal risk management.

The revised risk assessment also noted risk levels to be significant, similar to that assessed in 2012. Again, this was thought to be due to the uncertainty in assumptions and estimations made for user numbers and hazard frequency, such as a blanket 4% increase year on year in visitor numbers with few/no physical counts being undertaken and general lack of information related to landslide frequency. Due to this, the assumptions behind the calculations were essentially the same as those in 2012 and produced conservative risk level estimates. A general recommendation was made that GORCAPA look to improve the recording of landslide events (i.e. build a landslide inventory) and look to improve data on user numbers for cliff top and beach amenities.

Table 1: Slope Stability Danger Classification (GHD 2012)

Classification	Danger Type	Description	Example From Site
A	Small rotational and translational slides	Less than 1000 m^3 displaced material. Initial failure is likely to be rapid. Example: Failure of infilled sinkhole, Aireys Inlet	
B	Large rotational and translational slides	Larger, generally deeper, slides than those in 'A' above, involving greater than 1000 m^3 displaced material. Example: Soapy Rocks Landslide, Anglesea	
C	Minor falls/topples	Failure of less than 1 m^3 of material from cliff face. Failure likely to be extremely rapid. Example: Rock fall, Yellow Bluff, Torquay	

D	Major falls/topples	As in 'C' above, with greater than 1 m^3 of failed material. Example: Cliff failure, Demons Bluff, Anglesea	
E	Rill and gully erosion	These are often ephemeral features and are formed by erosion of the land surface by flowing water. Example – Rills/Gullies adjacent to Anglesea SLSC	

Table 2: Descriptors for hazard zoning, adapted from AGS (2007a) (GHD 2012)

Hazard descriptor	Falls, topples and small slides on natural cliffs (Danger classes A, C, D)	Large slides on natural slopes (Danger class B)
	Number/annum/km of cliff	Annual probability of active sliding
Very High	>10	10^{-1}
High	1 to 10	10^{-2}
Moderate	0.1 to 1	10^{-3} to 10^{-4}
Low	0.01 to 0.1	10^{-5}
Very Low	<0.01	$<10^{-6}$

2.1.1 Hotspots

As part of the 2020 Cliff Risk Assessment Review (GHD 2020), GORCAPA were keen to identify particularly high-risk areas to focus monitoring resources on. Termed "hotspots", these were defined as areas of the coast where risk ratings (for risk to life and risk to property) were classified as Very High, High or Moderate. These areas were recommended to be prioritised for increased surveillance to improve understanding of the frequency of hazards and the number of users in order to improve assumptions made. The following areas were identified as hotspots

- Zone 1 – Yellow Bluff
- Zone 3 – Rocky Point
- Zone 6 – Bird Rock
- Zone 7 – Jan Juc: Sparrows to Boobs/Steps
- Zone 8 and 9 – Anglesea East (Demons Bluff/Demons Bluff to Anglesea River Estuary)
- Zone 10 – ASLSC to Soapy Rocks
- Zone 11 – Anglesea West
- Zone 12 and 13 – Soapy Rocks and Point Roadknight
- Zone 14 and 15 – Aireys Inlet – Sunnymead Beach to Sandy Gully Beach

2.1.2 Signage Audit

A signage audit was undertaken along the coastline of interest. This was completed by taking a GPS-located point at every hazard/warning sign encountered during the site walkover of the coastline areas of interest. Signs were then classified based on type, with nine different varieties of signage identified. The signs were then assessed based on their compliance with relevant Australian standards – AS1319:1994 (Safety signs for the occupational environment) and AS2416.1:2010 (Water safety signs and beach safety flags). Essentially, hazard signs fall into one of two classes: Warning or Danger sign types, with each having specific criteria as per the standards. Warning signs typically should have a black pictogram which has a simple depiction of the hazard, on a yellow background in a diamond shaped black bordered box. Danger signs should include the words "Danger" and include red, black and white colouring to highlight the importance of the information.

The signage audit found five different styles of warning sign (three types shown in Figure 7A, 7B, 7C) depicting the same hazard – unstable cliffs. Some had accompanying text in English, others had only the pictogram with no words. Spatial distribution was generally quite random, with some areas having more signs than others for no obvious reason. With so many varieties of the same sign, communication of the hazard could become confused/unclear.



Figure 7: Cliff hazard signage examples from the signage audit. A, B and C – sign examples as observed by GHD in 2020 in the GORCAPA managed areas, three different varieties of sign all communicating the same hazard. D, E – Signs from Parks Victoria managed areas, communicating the hazard posed using words, pictograms, colour and photographs of the actual hazard to clearly communicate the hazard and risks, including contact details/places to obtain further information as required.

Example signage from other land management agencies, such as Parks Victoria, were used to compare against those found in the GORCAPA managed land area and showed what could be achieved. For example, at popular sites along the Great Ocean Road, Parks Victoria had combined Warning signage compliant with the Australian standards with a photograph of similar hazard/failure, in order to visually communicate the risk. Signs observed are shown in Figure 7.

2.2 TARP DEVELOPMENT

Following completion of the risk assessment update, signage audit and review of GORCAPA monitoring plan, GHD recommended development of a TARP. TARPs are used extensively within mining settings in relation to pit stability, intrinsically linked to detailed monitoring of slope stability, to document clear actions and responsibilities associated with geotechnical failures of differing scales. Parallels can be made with mining pit slopes and coastal cliffs in terms of geotechnical failures of varying scale. The underlying idea behind the proposal of a TARP for the coastal environment

was to avoid implementing a complex system of various trigger points and setbacks for each individual cliff area/hazard, essentially making it more practical for GORCAPA coastal reserve staff to implement. The initial TARP proposed by GHD included

- Triggers related to the cliff slope conditions, for beach users, cliff top assets >5m to the edge of the cliff and cliff top assets <5 m to the edge of the cliff.
- Triggers rated from low to very high, with green, yellow, amber and red alert levels, based on the potential failure size/potential for failure to impact on public paths and lookouts
- For each trigger/alert level, a corresponding response level was nominated, containing the person responsible and the actions required to be undertaken.

For example, an orange alert level (high) trigger is noted for clifftop assets >5 m from the cliff edge constituting tension cracks or failure observed between 5 and 10 m from public areas of the asset (i.e. paths or lookouts). Responsibility lies with the GORCAPA Coastal Reserve Manger (CRM) – with actions to be taken including notifying coastal staff of the alert level, preparing to close the asset, notifying stakeholders of the situation. GORCAPA operations staff then would be told to continue to monitor the situation and provide feedback to the CRM in case of worsening condition.

GORCAPA later built on the draft TARP and updated and amended it to fit their operations, as well as tie in with an updated CMMP. Figure 8 shows the triggers defined by GORCAPA (2020). It is noted that all measurements in terms of distances and volumes are estimated from a safe distance and not measured by GORCAPA staff to maintain safety.

Risk Level	Beach Users			Cliff Top User
	Potential or actual failure of cliff face (Erosion, soil/rock falls, ground displacement).	Loss of cliff crest	Tension cracks within Xm from cliff crest.	Tension cracks or failures within Xm from a public area, walking track or lookout.
Low	Volume < 1m³	<2m	<2m	>10m
Medium	1m³ < Volume <25m³	2-5m	2-5m	10-7m
Significant	25 m³< Volume < 100 m³	5-10m	5-10m	7-5m
High	Volume > 100m³	>10m	>10m	<5m

Figure 8: Excerpt from GORCAPA Understanding Geotechnical Risk Manual (2020) showing the Triggers defined for each risk level/alert level.

Responses per risk level trigger, from GORCAPA (2020), include

- **Low**: On-going routine monitoring as per the CMMP
- **Medium**: CRM to assess situation, monitor, communicate with staff on the location, nature and expected conditions associated with the failure. External communication: inform public via Website and Social Media outlets). For Beach user risk: audit of local signage to ensure signs are legible and free from damage. GORCAPA Staff: avoid hazard area, report any change in conditions to CRM.
- **Significant**: CRM: same actions as Medium, but with addition of contacting a geotechnical consultant if cliff top users are at risk from the hazard/failure and preparing to close the asset/restrict access to a safe location if practicable and notify other stakeholders. For Beach users: consider temporary signage and fencing to prevent access to failure zone if practicable. GORCAPA Staff: avoid hazard area, report any change in conditions to CRM.
- **High**: CRM: same actions as Significant, but for cliff top risk close the asset and restrict access, notify stakeholders. Investigate and formulate recovery plan (formal risk assessment may be required). GORCAPA Staff: avoid hazard area, report any change in conditions to CRM.

4 COASTAL AND MARINE MANAGEMENT PLAN

This section briefly explores the implementation of the recommendations of the 2020 risk assessment in terms of GORCAPA's CMMP.

4.1 UPDATED SIGNAGE

Following the recommendations of the signage audit completed in 2020, GORCAPA committed to upgrading and improving hazard signage. Cliff hazard signs were replaced/upgraded with standardised symbology and wording along the coastline (Figure 9). In addition, GORCAPA also implemented different signage to communicate the hazards at beach and coastal path entrances, taking cues from the Parks Victoria examples in incorporating photographs of the hazard, as well as additional information available in other languages access via the website/QR codes on the sign (Figure 9).



Figure 9: Updated signage examples found at Jan Juc and Anglesea. A: Unstable cliff warning sign, showing a clear pictogram of the hazard and advice on what to do to avoid the hazard. B: Photographic sign depicting typical failures, as well as showing the correct usage of paths. A QR code also links viewers to the GORCAPA website for further information which is also in other languages.

4.2 MONITORING

Monitoring of cliff condition lies at the heart of the CMMP. The purpose of the monitoring is to

1. Assemble an inventory to assist with understanding landslide frequency for future risk assessment.
2. Reassess previously noted hazard conditions.
3. Identify imminent failures and initiate actions (in line with the TARP).

There are two scales of monitoring: regional and local. Regional monitoring covers a large area, with methods that are easily and cheaply undertaken across the area. The local scale is targeted at hotspot areas (as identified by the regional scale methods), covers a smaller area in finer detail, and may be more time consuming and expensive.

Methods employed to undertake monitoring, scale and frequency are summarised in Table 3. The monitoring plan will also allow for better quality landslide frequency data to be collected to inform future risk assessment updates.

Table 3: Monitoring methods summary (GORCAPA CMMP 2021)

Monitoring Method	Scale	Description	Capture Frequency
Aerial Imagery Analysis	Regional and Local	Assessment of shoreline and clifftop position over time using GIS software and aerial imagery captured at different points in time	Yearly
Photogrammetry[1]	Local	Elevation data obtained from drone photography	Cliff – Yearly
Geotechnical Assessments	Regional and Local	Visual geotechnical risk assessments undertaken by a consultant	Regional – 10 years Local – as required
Day to day observations by GORCAPA staff	Regional	Detailed information captured by GORCAPA staff undertaking day-to-day duties	Daily

Monitoring Method	Scale	Description	Capture Frequency
Information provided by the public	Regional	Detailed information received from the public through GORCAPA's communication channels	Daily
Cliff Assessments by GORCAPA Staff	Local	Involves the completion of a cliff risk assessment pro forma, photo capture and evaluation against GORCAPA's Trigger Action Response Plan (TARP)	After high rainfall events/storms Every 3 months

[1.]Photogrammetry is currently undertaken by the Victorian Coastal Monitoring Program (VCMP) run by Deakin University on behalf of DEECA at certain sites along the coast and processed through the software platform Propeller. For sites outside of the VCMP, GORCAPA has adopted drone photogrammetry using its own pilots and the software Drone Deploy.

4.3 EDUCATION AND COMMUNICATION

In addition to the CMMP, GORCAPA have been undertaking different methods of communicating the dangers posed by the coastal cliff hazards to local users and visitors to the coastline. Communication of hazards/failures or imminent cliff failures are communicated via GORCAPA's social media streams (e.g. Facebook, Instagram), in addition to the local signage. Communication via local print media is also used to keep the local population apprised of developments with hazards or temporary closures of paths/lookouts/beaches. During the peak season, GORCAPA also implement geofenced marketing strategies, which involves targeted adverts appearing on phone apps/websites when people enter the GORCAPA managed coastal zone. The adverts highlight the coastal hazards and how to stay safe around cliffs. This demonstrates an innovative way to reach visitors who may be new to the area and have no prior knowledge of the coastal hazards. GORCAPA has also previously been involved in education programs in local schools (Environmental Education Program), helping to educate local children on coastal hazards and how to be safe around cliffs, however, this program is no longer in operation. GORCAPA has also been training coastal staff in how to identify geotechnical hazards, linked to the TARP. These workshops were run in conjunction with GHD to help GORCAPA staff be more confident in identifying potential failures and implementing the TARP.

5 DISCUSSION

This case study highlights the difficulty in managing geotechnical hazards posed by coastal cliffs in weak rocks. The geology of the cliffs in this study area makes them highly susceptible to landslide hazards but has also led to the development of reefs and submerged rock platforms that contribute to the appeal of the area for coastal amenity.

The risk assessment methodology adopted for the risk assessment was undertaken in general accordance with AGS(2007a, b, c, d, e). Previous risk assessment (prior to 2012) along the coastline of interest had included the superseded AGS (2000) method, as well as bespoke assessment methods from other geotechnical consultants. In 2020, the New South Wales National Parks and Wildlife Service (NPWS) commissioned Golder Associates to develop clear guidance for geotechnical practitioners, setting out preferred methods for calculating individual and societal risk associated with trails and lookouts within state parks, to allow comparisons with NPWS selected risk criteria for individual and societal risk (Golder Associates 2020). This methodology is based on the AGS (2007a, b, c, d, e) and ANCOLD (2003) guidelines, but presented in a user-friendly format, particularly in terms of walking paths and lookouts. This method was used for risk assessment at a cliff top path at Jan Juc beach by GHD in late 2022 (GHD 2023), and the results gave a similar risk profile to the 2020 assessment, but with better definition of societal risk. This method might be useful applied to the coastline of interest in future risk assessment updates.

However, any method for risk assessment is only as good as the input data. Good quality data such as monitoring data on landslide frequency, size/volume, runout distance, and user numbers for cliff top amenities and beaches is crucial to further refine risk assessments, reduce conservatism in assumptions and focus risk management activities.

The formalised monitoring plan within the GORCAPA CMMP is important for future risk assessment work and should lead to an improved landslide inventory to improve estimates of frequency. Some issues have been identified, particularly with drone photogrammetry data. The VCMP is generally based on the Propeller online platform, and the raw data from the surveys is processed by Deakin University and Melbourne University on behalf of DEECA and uploaded to the platform. Simple volume differencing is possible within Propeller, as well as comparing surveys over a date range to assess changes. However, there are concerns that the software cannot differentiate between vegetation and topography, leading to poor measurements/false topography. GORCAPA and other similar land managers don't have the internal capability/budget to undertake this sort of data processing/validation/correction. This is leading to valuable drone data

being under-utilised in landslide risk management. Further support from specialists will be required to aid land managers in processing this data and understanding changes occurring to cliffs and help understand if triggers are being met as per the TARP.

A key challenge identified during the risk assessment process was how to mitigate the identified risks to an acceptable level of risk. In the coastal environment, methods usually employed to reduce the likelihood (frequency) of events (such as engineering of slopes, rock bolting, rock-fall mesh, rock-fall barriers) are likely to be less effective due to the interaction with seawater and storms/wave action. These engineering solutions tend to be expensive to implement, and generally beyond the budget of most land managers. Therefore, the only other options available to mitigate the risk are those related to reducing the consequence of the hazards – reducing the chance of people/property being within the zone of influence of the failure.

The TARP, tied to the CMMP, creates a much more proactive response to cliff risk. Monitoring streams feed in to identifying potential issues early, sometimes before a failure occurs, meaning the TARP can be activated based on the risk posed and responses can be implemented. Education on how to identify geotechnical risk, for the operational staff undertaking their daily duties on the coast, is crucial in the success of the TARP process.

Effective communication of the hazard/risk posed by cliffs in the coastal environment is key. Signage alone is unlikely to be effective in communicating the hazard to all users of the coastline. Therefore, utilising different media streams (such as social media, websites and print media), with content available in different languages, to reach as wide an audience as possible is an important strategy. This aids land managers to meet their obligations in terms of managing coastal cliff hazard and risk as far as is reasonably practicable.

The implemented approach to risk management in the GORCAPA managed area of the coastline has mitigated the likelihood and severity of potential casualties related to cliff hazards.

ACKNOWLEDGEMENTS

The author would like to acknowledge GHD and GORCAPA for permission to discuss the case study herein, especially Caleb Hurrell – Coastal Operations Manager, GORCAPA. With thanks also to Tony Miner (Technical Director, GHD) for discussions on layout and content.

REFERENCES

ABC News (2021). Man killed from falling debris as 30-metre-high cliff collapses at Bells Beach. Available at: https://www.abc.net.au/news/2021-12-31/police-and-emergency-services-at-an-incident-at-bells-beach/100733532 (Accessed: 16 February 2025)

Abele, C. and Hancock, S.J (1968). *Anglesea Geological Map,* No. 833 Zone 7, 1:63360. Melbourne: Geological Survey of Victoria (reprinted 1980 by Geological Survey of Victoria)

Abele, C. (1979). *Geology of the Anglesea area, Central Coastal Victoria*. *Geological Survey of Victoria Memoir 31*. Melbourne: Geological Survey of Victoria. 72 pp.

ANCOLD (2003). *Guidelines on Risk Assessment*. Melbourne: Australian National Committee on Large Dams, Inc.

Australian Geomechanics Society (AGS) (2000). Landslide risk management concepts and guidelines. *Australian Geomechanics Journal*, 35(1), 49-92

Australian Geomechanics Society (AGS) (2007a). 'Guideline for Landslide Susceptibility, Hazard and Risk Zoning for Land Use Planning'. *Australian Geomechanics Journal*, 42(1), 13-36.

Australian Geomechanics Society (AGS) (2007b). 'Commentary on Guideline for Landslide Susceptibility, Hazard and Risk Zoning for Land Use Planning'. *Australian Geomechanics Journal*, 42(1), 37-62.

Australian Geomechanics Society (AGS) (2007c). 'Practice Note Guidelines for Landslide Risk Management'. *Australian Geomechanics Journal*, 42(1), 64-114.

Australian Geomechanics Society (AGS) (2007d). 'Commentary on Practice Note Guidelines for Landslide Risk Management'. *Australian Geomechanics Journal*, 42(1), 115-158.

Australian Geomechanics Society (AGS) (2007e). 'Australian GeoGuides for Slope Management and Maintenance'. *Australian Geomechanics Journal*, 42(1), 159-182.

Climate Justice Clinic (CJC) and Gippsland Community Legal Service (GCLS) (2023). *Guidebook to Public Land Management in Victoria*. Melbourne: Monash University, 66 pp.

Crown Land (Reserves) Act 1978 (Vic). Available at: https://www.legislation.vic.gov.au/in-force/acts/crown-land-reserves-act-1978/133 (Accessed: 16 February 2025)

GHD (2012). *Report on coastal stability study and risk assessment – coastal reserves between Torquay and Aireys Inlet*. Melbourne: GHD Pty Ltd, 146 pp.

GHD (2020). *Torquay to Aireys Inlet Coastal Cliff Stability Review*. Melbourne: GHD Pty Ltd, 109 pp.

GHD (2023). *Rockfall and Landslip Assessment at Jan Juc*. Melbourne: GHD Pty Ltd, 28 pp.
Golder Associates (2020). *NSW National Parks and Wildlife Service – Guidelines for Quantitative Risk to Life Calculations for Landslides*. Melbourne: Golder Associates Pty Ltd, 113 pp.
Great Ocean Road Coast and Park Authority (GORCAPA) (2020). *Understanding Geotechnical Risk Manual*. Torquay: Great Ocean Road Coasts and Parks Authority
Great Ocean Road Coast and Parks Authority (GORCAPA) (2021). *Coastal Monitoring Program (CMMP) Final Draft*. Torquay: Great Ocean Road Coast and Parks Authority, 50 pp.
Standards Australia (1994). *AS1319:1994. Safety signs for the occupational environment.* Sydney: Standards Australia.
Standards Australia (2010). *AS2416.1.2010. Water safety signs and beach safety flags.* Sydney: Standards Australia.
Tourism and Events Victoria (2024). Regional research. Available at: https://tourism.vic.gov.au/research-and-insights/regional-researchegional research (Accessed: 16 February 2025)

https://doi.org/10.56295/1ACEG16

GLASSHOUSE MOUNTAIN SUMMIT ROUTES: BALANCING SAFETY, ACCESSIBILITY, AND TOLERABLE RISK

Sally Roberts-Kelly and Lee Moule
EDG Consulting PTY LTD

ABSTRACT

The Glasshouse Mountains National Park located in Southeast Queensland, Australia is formed around a group of 11 volcanic peaks. The variety of walking tracks within the remarkable natural environment and panoramic views attainable at the peaks mean the national park is increasing in popularity with locals and tourists alike. Two of these peaks, Mount Tibrogargan and Mount Beerwah, include summit routes that have exposed, steep rock sections that are explicitly recommended only for fit, experienced hikers and rock scramblers by Queensland Parks and Wildlife Service (QPWS).

These two noted summit routes present unique challenges for managing slope risk due to their exceptionally steep topography and natural hazards. This paper explores the application of quantitative geotechnical risk assessment processes to reduce risk for track users while maintaining accessibility to these popular natural sites.

The tolerable risk levels for more challenging trails like these are typically aligned with other perceived high-risk recreational activities, such as climbing, scuba-diving and skiing. Assessing what is considered tolerable risk helps strike a balance between public safety and accessibility. This process is a risk-based compromise between maintaining access to the natural landscape, minimising invasive infrastructure, and reducing exposure to hazards.

Ultimately, to allow continued public access, there is a need for regular risk assessments and review of risk management to uphold safety standards while allowing the public to engage with these fulfilling national park experiences.

1 INTRODUCTION

The Glasshouse Mountains National Park encompasses eleven volcanic peaks and is located in Southeast Queensland, Australia. This area is renowned for its beautiful and unique scenery, with the park attracting thousands of visitors annually, including hikers, picnickers, and climbers. Among its many trails, the summit scrambling routes of Mount Tibrogargan and Mount Beerwah are popular with those looking for a challenge, due to their difficult terrain and breathtaking views from the peak. These routes are explicitly recommended for fit, experienced hikers and rock scramblers due to their steep and often rough profile.

As the number of park visitors grows, balancing risk reduction and safe access to the park's summit routes for all users is an increasing challenge. Striking the balance between safety and accessibility is an increasingly complex task for Queensland Parks and Wildlife Service (QPWS), particularly given the abundance of natural hazards and the unique track topography of each route. Effective geotechnical risk management is needed to allow continued public access on these scrambling trails while minimising the likelihood of accidents and injuries for park users.

The objective of this paper is to explore how quantitative geotechnical risk assessment can be used to effectively manage these two summit scrambling routes within the Glasshouse Mountains National Park. As the risk to users cannot be entirely eliminated, QPWS is tasked with the responsibility to reduce exposure and enhance hiker awareness, balancing public safety with the recreational value of the summit routes.

This paper focuses on the geotechnical aspects of risk management, relating to slope stability and rockfall hazards. It does not address access in relation to First Nations cultural and heritage perspectives. Other risk considerations such as an individual's competency are discussed, however this paper is not informed by these aspects.

2 BACKGROUND AND SITE DESCRIPTION

2.1 GEOLOGICAL AND GEOGRAPHICAL OVERVIEW

Mount Beerwah and Mount Tibrogargan are two prominent peaks within the Glass House Mountains, which are a collection of volcanic plugs formed from magma intrusions during the late Oligocene, approximately 27 to 26 million years ago (Willmott, 2007). Mount Tibrogargan is located about 3 km southwest and Mount Beerwah about 6.5 km west of the Glass House Mountains Township. These and other peaks are shown in Figure 1.

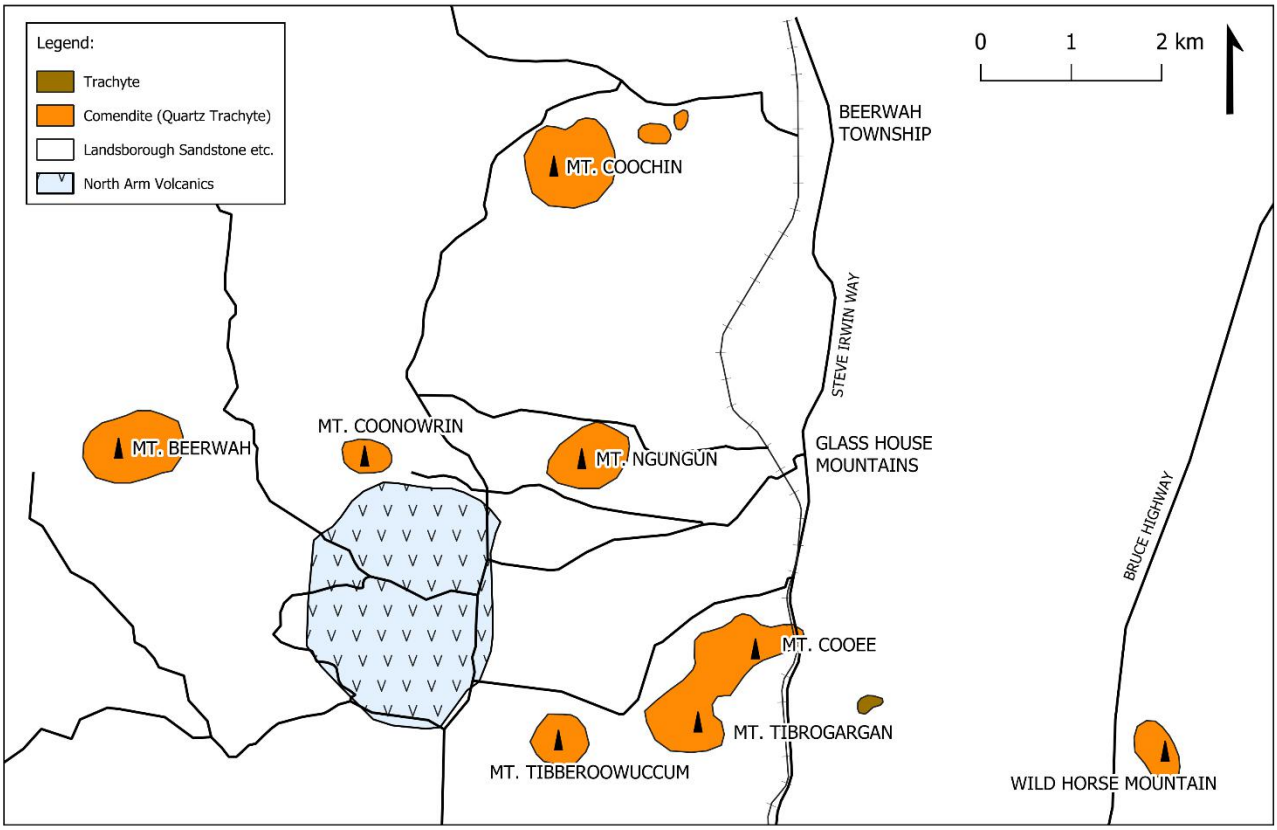


Figure 1: Glasshouse Mountains Geology (Willmott, 2007)

The Glass House Mountain formations are remnants of a volcanic complex which formed when Australian continental crust passed over 'hot spots' in the earth's mantle. They formed as magma intruded into older sedimentary rock layers, solidifying into plugs of alkali rhyolite, trachyte, and related volcanic rocks. Mount Beerwah is composed mainly of alkali trachyte, while Mount Tibrogargan consists of a bluish alkali rhyolite (comendite) (Willmott, 2007). As these volcanic bodies cooled, contraction within the rock led to the formation of vertical columnar joints, visible today in features like the "Organ Pipes" on Mount Beerwah and blocky structure of Mount Tibrogargan (as shown in Figure 2).



Figure 2: Left: Mount Beerwah 'Organ Pipes' Columnar Jointing, Right: Mount Tibrogargan blocky structure

Over millions of years, the basalt flows, and then subsequently the surrounding softer sedimentary rocks, primarily Landsborough Sandstone, eroded away, exposing the harder volcanic plugs. The peaks now stand as isolated remnants of the once majority volcanic landscape due to their greater resistance to weathering. Groundwater has also played a role in shaping the landscape by seeping along defects, weakening the rock, and creating shallow caves on the mountain faces.

2.2 GLASS HOUSE MOUNTAIN TRAILS INFORMATION

The Mount Tibrogargan summit access route follows the mountain's western ridgeline, while Mount Beerwah, the highest peak in the Glass House Mountains National Park, has its summit access route on the northern face. Despite their difficulty, these routes attract hikers of all skill levels. Regular foot traffic has caused significant anthropogenic erosion, making the summit routes visible in aerial photography, as shown in Figure 3.

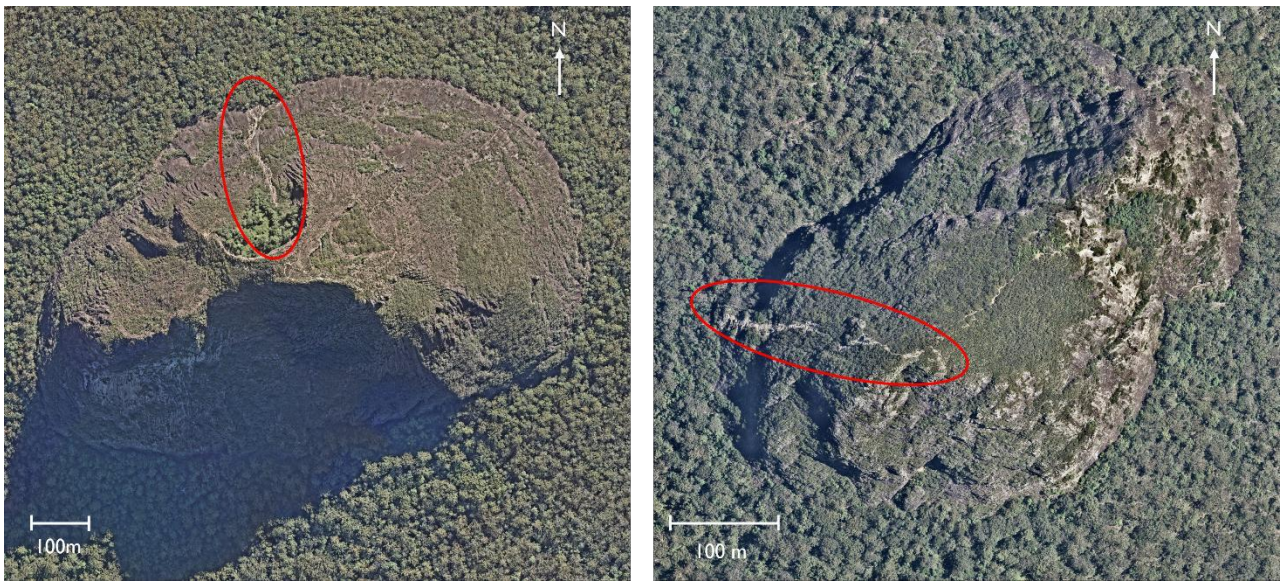


Figure 3: Plan view of Mount Beerwah (L) and Mount Tibrogargan (R) showing the summit access routes clearly eroding the slope faces (© Nearmap, 24 December 2024).

The Queensland Parks and Wildlife Service (QPWS) provides detailed information on various walking trails within the Glass House Mountains National Park, assigning each a specific grade to indicate its level of difficulty (Queensland Parks and Wildlife Service, 2025). However, the summit routes for Mount Beerwah and Mount Tibrogargan are absent from this grading system due to their unique challenges and higher assessed risk.

Among the graded routes, examples include:

- Mount Beerburrum Summit Walk
  This track is classified as Grade 3, meaning it presents a moderate challenge. It includes a steep 750 m concrete section that can be slippery, requiring reasonable fitness and appropriate footwear. The full return distance is 3.5 km, with an estimated completion time of 1 hour and 30 minutes.
- Yul-yan-man Track
  Rated as Grade 5, this track is designed for experienced hikers with rock scrambling skills. It offers a challenging adventure with access points from both the Beerburrum and Tibrogargan trailheads.

In contrast, QPWS provides information about the summit routes for Mount Beerwah and Mount Tibrogargan at the bottom of the Glass House Mountain Journeys webpage, following all other graded trails, and precedes the section on the webpage with a safety video. The absence of a grading system serves as a subtle warning, reinforcing the challenges and risks involved. QPWS strongly advises that only those with sufficient experience and preparation attempt these climbs. To support this, a comprehensive cautionary information sheet is available on the website, including detailed descriptions and profile maps (see **Figure 4**).

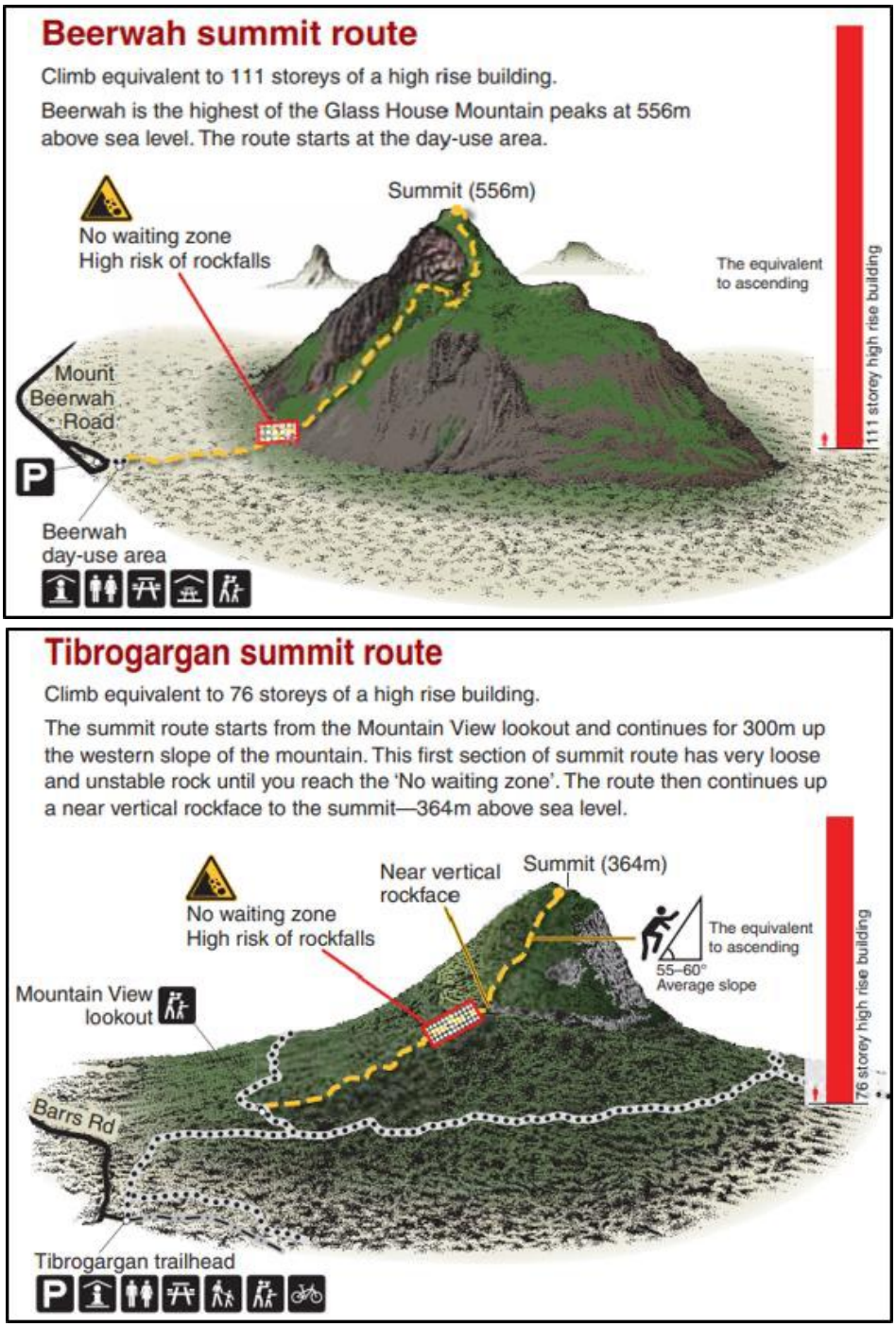


Figure 4: Glass House Mountains summit route profile maps; Top: Mount Beerwah, Bottom: Mount Tibrogargan (© State of Queensland. Queensland Parks and Wildlife Service. MA787 August 2022).

2.3 VISITOR DEMOGRAPHICS AND USAGE TRENDS

Usage data provided by QPWS shows approximately 36,000 and 25,000 counts at the Mount Tibrogargan and Mount Beerwah summit routes in 2023, respectively. Data was collected using a variety of installed automated loggers, including motion and heat sensors. It is assumed that an individual hiker triggers the usage monitoring apparatus twice, on ascent and descent, so actual usage figures are half of the above. Usage patterns indicate that most hikers make the ascent during the day at weekends and public holidays. When the 2023 Mount Tibrogargan usage data is compared to data collected in 2016, an increase in usage of approximately 38% is evident. It may be assumed that Mount Beerwah has seen a similar increase. The increasing usage highlights the need for effective risk management strategies.

3 RISK MANAGEMENT FRAMEWORK

3.1 PRINCIPLES OF GEOTECHNICAL RISK ASSESSMENT

Assessing geotechnical risk is critical for understanding and managing hazards in all areas where geotechnical hazards are present. The process follows a structured approach to evaluating potential ground-related risks, ensuring informed decision-making and mitigation strategies (AGS, 2007). The key principles include:

1. Hazard Identification – Recognising potential geotechnical hazards such as rockfalls, landslides, and erosion through geological surveys, historical data, and site investigations.
2. Risk Analysis – Assessing both the likelihood of hazard occurrence and its potential consequences, using qualitative (e.g. risk matrices) or quantitative (e.g. probabilistic models) methods.
3. Risk Evaluation – Comparing assessed risks against regulatory guidelines and acceptable thresholds to determine the need for intervention.
4. Mitigation and Control Measures – Implementing engineering solutions (e.g. slope stabilisation, drainage), monitoring systems (e.g. inclinometers), and administrative controls (e.g. hazard zoning, access restrictions).
5. Uncertainty Management – Accounting for variability in ground conditions, geological processes, and modelling assumptions through conservative design and sensitivity analysis.
6. Continuous Review and Adaptation – Risk assessments should be updated as new data becomes available, environmental conditions change, or unexpected events occur, ensuring ongoing refinement of risk mitigation strategies.

By following these principles, geotechnical risk assessment provides a systematic framework for managing ground hazards, reducing potential impacts on infrastructure and public safety.

3.2 RELEVANT GUIDELINES AND INDUSTRY BEST PRACTICE

For public recreational activity, ideally risk should be eliminated. This is quite often not possible, or eliminating the risk devalues the benefit of the activity. Instead, to allow continued amenity to the public, the risk must be managed in a way that balances the risk and benefit. ISO 4980:2023 provides a framework for regulatory decision-making based on legal, organisational, and societal considerations. The methodology of this standard is outlined in Section 6.1.2.

As stated in the AGS Guidelines (AGS, 2007) defining tolerable risk criteria is the responsibility of the regulator because the implications affect the community at large. For National Parks in Queensland, the regulator is Queensland Government's Department of Environment, Tourism, Science and Innovation (DETSI). QPWS operates within DETSI.

ISO 4980:2023 differentiates between tolerable risk and acceptable risk specific to a recreational activity as follows:

- Tolerable risk: A risk that is deemed manageable under the given circumstances but still requires monitoring and mitigation where possible. It acknowledges that some level of hazard is inherent in recreational activities.
- Acceptable risk: A risk level that does not require further action because it aligns with the expected and reasonable exposure associated with the activity.

According to the standard, risk criteria for a recreational activity should be established based on:

1. External Context – Regulatory requirements, legal frameworks, cultural attitudes, and societal expectations.
2. Internal Context – Organisational policies, facility objectives, and the purpose of the activity.
3. Nature of the Activity – The inherent risks versus the intended benefits (e.g., rock climbing involves unavoidable fall risks but provides significant physical and mental reward to the climber).
4. User Demographics – The abilities, experience, and decision-making capacity of participants (e.g., children's play areas may have lower tolerable risk thresholds than adult adventure activities).
5. Risk Reduction Measures – The effectiveness of interventions such as equipment, training, supervision, and emergency response systems.

An assessment team to define appropriate criteria should comprise at least three members with expertise in the relevant activity. This should include designers, site managers, and activity leaders, with a team leader that has significant experience in risk assessment and facilitation.

3.2.1 Industry Landslide Risk Tolerances

As an example of quantified tolerance levels, there are many differing tolerances for landslide risk used around the world with different regulators citing differing technical guidance for their nominated tolerance. Table 1 shows a multitude of regulators, their nominated risk tolerance for loss of life and cited reference. The variance across multiple industries

highlights the uncertainty inherent in the practice of quantifying risk. For example, three different entities across New South Wales have tolerable limits that differ by more than three orders of magnitude.

Table 1: Individual Loss of Life Risk Criteria for various Regulatory Bodies (Leroi et al., 2005).

Regulatory Body	Industry	Description	Risk/Annum	Reference
Health and Safety Executive, United Kingdom (HSE)	Land use planning around industries	Broadly acceptable risk.	10^{-6}/annum, public and workers	HSE (2001)
		Tolerable limit	10^{-4}/annum, public	
			10^{-3}/annum, workers	
Department of Urban Affairs and Planning, NSW, Australia	Land use planning for hazardous industries	"Acceptable" (tolerable) limits	5×10^{-7}/annum, hospitals, schools, childcare facilities, old age housing	
			10^{-6}/annum, residential, hotels, motels	
			5×10^{-6}/annum, commercial developments	
			10^{-5}/annum, sporting complexes	
Australian National Committee on Large Dams	Dams	Tolerable limit	10^{-4}/annum, existing dam, public most at risk	ANCOLD (2003)
			10^{-5}/annum, new dam or major augmentation, public most at risk	
Australian Geomechanics Society (AGS) guidelines for landslide risk management	Landslides (from engineered and natural slopes)	Suggested tolerable limit	10^{-4}/annum, public most at risk, existing slope	AGS (2000)
			10^{-5}/annum, public most at risk, new slope	
Hong Kong Special Administrative Region Government	Landslides from natural slopes	Tolerable limit	10^{-4}/annum, public most at risk, existing slope	Ho et al. (2000), ERM (1998), Reeves et al. (1999)
			10^{-5}/annum, public most at risk, new slope	
Iceland Ministry for the Environment Hazard Zoning	Avalanches and landslides	"Acceptable" (tolerable) limit	3×10^{-5}/annum, residential, schools, day care centres, hospitals, community centres	Iceland Ministry for the Environment (2000), Arnalds et al. (2002)
			10^{-4}/annum, commercial buildings	
			5×10^{-5}/annum, recreational homes	
Roads and Traffic Authority, NSW, Australia	Highway landslide risk	Implied tolerable risk	10^{-3}/annum	Stewart et al. (2002), RTA (2001)

4 SITE HAZARD IDENTIFICATION AND RISK ASSESSMENT

4.1 IDENTIFIED HAZARDS

Across the two summit routes there are four significant hazards that were commonly identified, these are all associated with the fall of rock blocks, described in points 1-4 below and shown in Figure 5. Mount Beerwah also has a unique mass flow hazard, described in point 5 below.

1. Large scale rockslide, triggered by erosion and/or heavy rainfall.
    - Defined as multiple rocks with many greater than 0.6 m (average dimension) in size moving as a group, which are likely to disaggregate as they travel and affect the entire width of the track.
    - Will trigger movement of other loose blocks as they travel downhill. The masses are mainly located adjacent to the existing track either as in situ or slightly disturbed rock masses.
2. Release of individual large blocks from the outcropping rock masses defining the upper slopes, triggered mainly by erosion and heavy rainfall, some maybe levered off the slope by the action of roots.
    - Defined as a single rock greater than 0.6 m in size initiating as a singular object but likely to disaggregate into smaller pieces if it travels downslope.
    - The blocks may be funnelled down the summit access route and may trigger other blocks to move as they travel downhill.
3. Release of individual medium blocks, triggered by erosion/rainfall or in some cases, hikers.
    - Single boulder between 0.2 m and 0.6 m in size initiating as a singular object but likely to disaggregate into smaller pieces as it travels and affect a smaller proportion of the track width.
    - Medium blocks are less likely than larger blocks to trigger additional rockfall as they move downhill.
4. Release of individual small blocks, triggered mainly by hikers, with minor releases due to rainfall.
    - Single rock fragment less than 0.2 m in size but typically greater than 60 mm in size initiating as a singular object.
    - The individual small blocks break up with travel but are unlikely to disaggregate to less than 60 mm in size. They will affect a localised section of the track and are unlikely to trigger other hazard detachments.
5. Large scale mass flow of soil and rock, triggered by a bush fire followed by heavy rainfall.
    - This is defined as a semi-liquidised flow of debris from the soil bowl immediately below the columnar cliffs of Mount Beewah that will move with high velocity and would affect the entire width of the access route.



Figure 5: Examples of hazard types 1 to 4, as shown by photo number.

Whilst this paper explores only the geotechnical risk associated with the Mount Beerwah and Mount Tibrogargan summit hikes, to define a suitable broader risk tolerance for a recreational activity such as hiking, the regulator must consider all possible hazards. These might include:

- Falls from height – Steep terrain and exposed rock faces increase the likelihood of falls.
- Slips and trips – Uneven, loose surfaces, wet conditions, and eroded tracks create hazards.
- Heat exhaustion and dehydration – High temperatures and limited shade can affect hikers.
- Wildlife encounters – Venomous snakes and insects present potential risks.
- Navigation errors – Poor signage or misjudging terrain can lead to getting lost.

4.2 ADOPTED METHODOLOGY FOR ASSESSING RISK

Historically, risk assessments for the summit routes have been conducted using a 'person most at risk' (PMaR) approach, following the AGS 2007 guidelines. This method identifies the individual or group most vulnerable to potential hazards and evaluates the likelihood and consequences of harm specific to them. Societal risk was calculated and found to be little different, due to the frequency of the PMaR visits relative to an average person. Other methods that may be applicable to the summit routes are introduced below, and further discussion is given in Section 6.1.

4.3 RISK ASSESSMENT FACTORS AND OUTCOMES

Quantitative risk assessments for both mountains have provided estimates for the annual risk of loss of life (R(LoL)) for the 'person most at risk'. The PMaR for each summit route is defined as a competent and capable hiker who climbs the mountain almost every day outside of peak hours but occasionally climbs during peak hours due to personal schedule.

They are exposed to the instability hazards for 2 hours during the ascent/descent during daylight hours. The calculated values for these hikers exceed the commonly accepted tolerable risk threshold for the general public (10^{-4}/year) and approach the limit of tolerability for workers (10^{-3}/year). Specifically:

- Mount Tibrogargan: The revised R(LoL) for the PMaR is 9.3×10^{-4}, suggesting a level of risk comparable to high-risk recreational activities such as hang-gliding or scuba diving (refer Section 4.4).
- Mount Beerwah: The R(LoL) for the PMaR is 7.6×10^{-4}, indicating a slightly lower but still significant risk level.

Given these findings, QPWS continues to implement a risk management strategy that adheres to the 'As Low As Reasonably Practicable' (ALARP) principle. Ongoing mitigation measures include track monitoring, controlled scaling, seasonal and event-specific closures, and targeted signage to inform hikers of the inherent risks. While risk cannot be entirely eliminated, these interventions aim to reduce exposure and enhance hiker awareness, balancing public safety with the recreational value of the summit routes. While there are wider assumptions underlying the risk assessments in accordance with AGS 2007 guidelines, these are not discussed here, as they do not directly relate to the paper's focus on balancing risk and accessibility.

4.4 RISK ASSESSMENT METRICS AND TOLERABLE RISK THRESHOLDS

We agree that the adoption of a tolerable risk criterion is appropriate for the Mount Beerwah and Tibrogargan summit access routes. This is based on hikers acknowledging that there is inherent risk in the activity, but they are still willing to tolerate this risk in order to secure the benefits of the experience when undertaking the activity. Health and Safety Executive, United Kingdom (HSE) agree that 10^{-4} per year is the boundary between unacceptable and tolerable for members of the public for a risk that is "in the wider interests of society" (HSE, 2001). HSE also suggests that 10^{-3} lives per year is the upper limit of the tolerable region for workers in industry.

To compare the calculated total risk for the person most at risk of 9.33 x 10^{-4} per year for Mount Tibrogargan and 7.6 x 10^{-4} per year for Mount Beerwah, other recreational activities with similarly assessed risk levels are provided in Table 2.

Table 2: Activities corresponding to a 1 x 10^{-3} risk of fatalities/year (Lee and Jones, 2023)

Activity	Number of times activity is required per year for 10^{-3} risk of fatalities
Hang-gliding	116 flights
Surgical anaesthesia	185 operations
Scuba diving	200 dives
Rock climbing	320 climbs
Mount Tibrogargan Summit Access Route	200 ascents & descents – five during peak traffic(1)
Mount Beerwah Summit Access Route	200 ascents & descents – five during peak traffic(1)

Notes: (1) Peak traffic times are associated with heightened anthropogenic block dislodgement triggers.

In our opinion, tolerable risk criteria are difficult to quantify for the person most at risk as individual tolerances vary when considering the recreational nature of the activity involved in walking the route. Adoption of residential risk levels may therefore be overly conservative, and adoption of industry worker's risk levels appears the opposite. Therefore, a value between 1 x 10^{-4} per year and 1 x 10^{-3} per year for tolerable risk appears appropriate for the two summit routes.

5 RISK MITIGATION AND MONITORING

5.1 CURRENT MITIGATION STRATEGIES

The levels of risk for the summit routes as previously calculated are considered marginally tolerable. Consequently, QPWS takes all practical measures to reduce risk and/or further refine the assessment of risk in accordance with the principle of ALARP. These strategies of ALARP include signage, warnings, removal of routes from walking track maps, seasonal and event-specific closures, additional public information online, and public education. The mitigation strategies are not factored into the risk assessment as the associated behavioural outcomes have not been quantified.

5.1.1 Signage

Signage has been installed at key points along the summit access routes, including the trailhead, the base of the no-stopping zone, and the upper sections of the route. These signs warn hikers of the dangers posed even by smaller dislodged rock fragments, which can become life-threatening projectiles. They also encourage responsible behaviour by advising hikers to watch their footing, stay on the designated path to minimise erosion, and avoid disturbing loose rocks. The signage outlines the risks and challenges of the climb and provides guidance on proper preparation for the ascent (as shown in Figure 6 and Figure 7).



Figure 6: Glass House Mountains summit route information signs, (© Queensland Parks and Wildlife Service).

5.1.2 Public Information

As discussed in Section 2.2, QPWS have implemented a segregated public information management strategy for the summit routes. Information on the summit routes has generally been removed from the standard hiking maps and plans for the Glass House Mountains National Park. Information for these routes is available in a separate section of the QPWS Glass House Mountains webpage, which has been structured so that users must view the warnings and critical skills information before reaching the maps associated with these routes near the base of the webpage. The webpage includes an information video at the top with rangers and local first responders outlining the risks and previous incidents on the summit routes. The summit route information signage, as shown in **Error! Reference source not found.**, has been designed to summarise the hazards and consequences, while providing details on how to reduce personal risk with planning, using appropriate equipment and supplies.

5.2 TRACK MONITORING AND CLOSURES

A monitoring program for the summit routes helps assess the accumulation of small and medium-sized rock fragments and, where possible, track the movement of larger blocks. While the entire route is reviewed, particular focus is given to areas where debris tends to accumulate. QPWS staff conduct routine inspections, photographing higher-risk areas as needed to track the changes to conditions over time. Additionally, regular track users and local climbing clubs play an active role in reporting any significant changes.

When any new hazards are identified or changes observed by the QPWS team, a professional geotechnical site assessment is recommended. Based on the scale and nature of the geotechnical hazard, the QPWS management team can temporarily close the track until the hazard is assessed and mitigated if required.

Following cyclones, bushfires, or severe wet weather events/storms impacting the mountains, it is recommended that the track is closed. Following these events the routes may require scaling and/or geotechnical assessment and is opportune under the same track closure. Based on previous experience QPWS request a geotechnical assessment if they are concerned about reopening the track. Closure following rain events of 50 mm or more would:

- Allow the track to be assessed to ensure that large scale hazards have not been mobilised.
- Reduce the likelihood of climbers mobilising loose rock because of slippery conditions.
- Potentially have other benefits in injury reduction from slips and falls.



Figure 7: Glass House Mountains summit route information sign, (© Queensland Parks and Wildlife Service).

6 DISCUSSION

6.1 DIFFERING RISK PERCEPTION AND CULTURE

Perceptions of acceptable and tolerable risk in outdoor activities vary widely across society. The design of infrastructure within national parks can influence how visitors perceive personal responsibility for their safety. A study of three U.S. national parks by Rickard (2014) found that as government agencies construct more paths, signs, and shelters, visitors increasingly transfer the perceived responsibility for their safety to park management. Similarly, research by Gstaettner et al. (2022) in Western Australian national parks found that first-time visitors were the least likely to perceive parks as dangerous, whereas those with repeat visits or previous traumatic experiences in similar environments had heightened risk awareness.

Changing societal expectations, particularly among younger generations, have contributed to a culture where documenting risk-taking through social media is seen as integral to the experience (Palmer, 2004). Activities once considered extreme—such as outdoor bouldering, snowboarding, and standing on precarious ledges—are now embedded in mainstream culture, media, and advertising. This normalisation has shifted these once-thrilling pursuits into common weekend activities, reinforcing the perception that anyone can participate, often without the necessary experience, knowledge, or appreciation of the risks involved (Palmer, 2004).

Unlike many other extreme sports, summitting the Glass House Mountains lacks a tangible "barrier to entry" that might deter inexperienced or unprepared individuals. Comparable activities such as scuba diving or rock climbing typically require specialised equipment, creating an inherent restriction. In contrast, the accessibility of these summit routes allows anyone to attempt them, potentially fostering a false perception of lower risk compared to activities of similar risk levels.

Glass House Mountains National Park offers a variety of trail environments and difficulty levels, but visitor decisions are not always based on trail complexity. Anecdotal observations from QPWS staff and regular park visitors suggest that the summit routes are often attempted by less experienced hikers, drawn more by the challenge and the opportunity for social media content without an understanding of the trail's difficulty. In contrast, other equally complex trails that offer fewer social media-worthy moments tend to attract visitors who are more focused on the challenge itself and have a better grasp of the risks involved.

6.1.1 Differing Person Most at Risk

In previous risk assessments of the Mount Beerwah and Mount Tibrogargan summit routes, the Person Most at Risk (PMaR) has been defined by EDG as an individual who summits the respective mountain 200 times per year, with five of those trips occurring during peak traffic periods. This definition assumes that the greatest exposure to hazards comes from sheer frequency of visits. However, past assessments have not accounted for the relative inexperience or unpreparedness of some hikers and the associated risks.

It could be argued that someone trekking the summit routes as frequently as the assessed PMaR is likely to be a competent, fit, and well-equipped individual with an explicit understanding of the safest routes. While they may be more exposed to hazards such as rockfalls, they are also theoretically far less likely to suffer injuries from slips, trips, or falls compared to an inexperienced, unfit tourist during any single outing. Future risk assessments may benefit from considering these additional risk factors to ensure a more comprehensive approach to public safety.

6.1.2 ISO 4980:2023 Framework

As a future alternative, ISO 4980:2023 provides a comprehensive risk assessment framework that may be applicable to the summit routes of Mount Beerwah and Mount Tibrogargan. The methodology evaluates risk based on two key factors: the severity of potential harm and the likelihood of occurrence. Severe injuries require stricter controls, while risk-benefit trade-offs determine whether an activity's value justifies the level of risk due to exposure to the hazards. The process follows the typical risk assessment process of identifying hazards, estimating risk levels, comparing them to predefined criteria, and implementing mitigation strategies where necessary. If risks exceed acceptable thresholds, adjustments must be made. This standard differs to previously undertaken risk assessments as it considers all potential hazards associated with the activity, offering a broader scope of evaluation.

6.1.3 Societal Risk

An alternative risk assessment was undertaken with recent usage data to quantify the societal risk based on the total number of people potentially exposed to the hazards. This approach applied a theoretical average individual's exposure and calculated the cumulative probability of loss of life using F-N criteria in accordance with the New South Wales Parks and Wildlife Service Guideline Document (Golder, 2023). The resulting probabilities were slightly lower than that

estimated using the PMaR method outlined earlier (5.86×10^{-4} and 7.81×10^{-4} for Mount Beerwah and Tibrogargan, respectively) though both remained within the same order of magnitude.

Previous risk assessments have largely focused on risks to individuals. However, societal risk may also need to be considered if an event impacting a large group simultaneously is plausible. At Mount Beerwah and Mount Tibrogargan, this could be relevant in the event of a large debris slide or flow, similar to Hazard 5 identified in Section 4.1, occurring during peak traffic hours when multiple climbers are on the mountain. For societal risk assessments, industry best practices are outlined in ANCOLD (2022).

6.2 BALANCING RISK AND ACCESSIBILITY

Under Queensland and Australian law, QPWS has a duty of care to national park visitors. The visitor safety policy (DETSI, 2001) states that while QPWS must manage and inform visitors of known risks as far as reasonably practicable, it cannot eliminate all risks in natural areas. Visitors are expected to remain vigilant, conduct their own research, and take personal responsibility for their safety.

Balancing legal and ethical responsibilities with societal expectations is key to effective risk management. While national parks inherently involve risks, and while people enjoy the thrill and challenges of nature, effective risk management allows visitors to adapt and respond safely in ever-changing and sometimes unfamiliar conditions. Gstaettner et al. (2022) found that while risk management and control are valued aspects of national park experiences, excessive management can diminish people's awareness of danger and their sense of responsibility in preparing for risks (in line with the observations of Rickard noted in Section 6.1).

In the case of summit routes, adopting a tolerable risk criterion is considered appropriate, as users generally accept a higher level of risk compared to everyday activities—recognising that climbing to the summit carries inherent danger, but that the experience and challenge justify the exposure. However, this level of risk is only considered tolerable when supported by appropriate management strategies, which may include temporary closures during periods of elevated risk.

In line with growing demand for more challenging tracks, QPWS developed the Yul-yan-man Trail in 2019— a Grade 5 track designed to offer a rock scrambling experience while maintaining a lower geotechnical risk profile than the summit routes.

Despite alternative trails, some thrill-seeking visitors will always wish to attempt the higher risk summit routes. To align visitor risk perception with similar extreme sports, QPWS could consider installing an entry barrier, such as a fence with a gated access point. This would not restrict access but encourage hikers to engage with warning signage and create a tactile obstacle similar to equipment requirements in other higher risk activities.

7 CONCLUSIONS

Risk perception varies widely among stakeholders of the Glass House Mountains National Park, shaping both QPWS decisions and visitor behaviour. While some hikers seek to minimise or eliminate risk, others embrace it as an inherent part of the outdoor experience. Societal shifts have led to an increasing number of inexperienced hikers attempting high-risk summit routes without fully understanding the dangers involved. This underscores the need for a nuanced risk management approach that acknowledges these trends while striving to reduce geotechnical risks to levels as low as reasonably practicable.

Balancing risk and accessibility remains a key challenge. While QPWS has a duty of care to manage and communicate risks, it cannot eliminate them without compromising the natural experience visitors seek. The development of trails like Yul-yan-man demonstrates an effort to provide challenging yet lower-risk alternatives. By maintaining this balance, QPWS can preserve accessibility while fostering informed decision-making and personal responsibility among visitors.

8 ACKNOWLEDGEMENTS

We would like to thank Nat Smith from QPWS for his guidance and provision of recent data, as well as Tim Thompson and Katie Rose of EDG Consulting for their support.

9 REFERENCES

AGS (Australian Geomechanics Society) (2000) 'Landslide risk management concepts and guidelines', *Australian Geomechanics*, 37(1).

AGS (Australian Geomechanics Society) (2007) 'Practice note guidelines for landslide risk management 2007', *Australian Geomechanics*, 42(1), pp. 63–114.

ANCOLD (Australian National Committee on Large Dams Inc.) (2022) *Guidelines on Risk Assessment*. Melbourne: ANCOLD. ISBN 0731 027 620.

Department of Environment, Tourism, Science and Innovation, DETSI (2001) *Operational policy- Visitor safety policy QPWS/2021/5869*, accessed 24 February 2025, https://parks.desi.qld.gov.au/

Golder Associates Pty Ltd (2023) 'Guidelines to Quantitative Risk to Life Calculations for Landslides' *New South Wales National Parks and Wildlife Service.*

Gstaettner, A.M., Rodger, K. and Lee, D., 2022. Managing the safety of nature? Park visitor perceptions on risk and risk management. *Journal of Ecotourism*, *21*(3), pp.246-265.

Ho, K.K.S., Leroi, E. and Roberds, B. (2000) 'Quantitative risk assessment: Applications, myths and future directions', in *GeoEng 2000 Invited Papers*. Lancaster, PA: Technomic, pp. 209–312.

HSE (Health and Safety Executive, United Kingdom) (2001) *Reducing Risks, Protecting People*. London: Her Majesty's Stationery Office.

Iceland Ministry for the Environment (2000) 'Regulation on hazard zoning due to snow- and landslides, classification and utilization of hazard zones, and preparation of provisional hazard zoning', *6 July 2000*.

Leroi, E., Bonnard, Ch., Fell, R. and McInnes, R. (2005) 'Risk assessment and management', in Hungr, O., Fell, R., Couture, R. and Eberhardt, E. (eds) *Proceedings of the International Conference on Landslide Risk Management*, Vancouver, Canada, 31 May–3 June. Leiden: A.A. Balkema, pp. 159–198.

Palmer, C (2004), Death, danger and the selling of risk in adventure sports. U*nderstanding lifestyle sports: consumption, identity and difference*. Routledge, Taylor & Francis, pp. 55-69.

Queensland Parks and Wildlife Service (QPWS) 2025, *Glass House Mountains—Things to do*, Queensland Government, accessed 12 February 2025, https://parks.desi.qld.gov.au/

Rickard, L. (2014). Mountain and handrails: Risk, meaning, and responsibility in three national parks. *Environmental Communication*, 8(3), 286–304.

Stewart, I.E., Baynes, F.J. and Lee, I.K. (2002) 'The RTA guide to slope risk analysis version 3.1', *Australian Geomechanics*, 37(2), pp. 115–148.

Willmott, W. (2007) *Rocks and Landscapes of the Sunshine Coast*, 2nd edn. Brisbane: Geological Society of Australia, Queensland Division.

https://doi.org/10.56295/1ACEG17

ROCKFALL RISK ASSESSMENT AT NORTH HEAD, SYDNEY HARBOUR NATIONAL PARK, NSW

Michael Egan[1] and Paul Roberts[2]
JK Geotechnics, Sydney, NSW, Australia[1]
JK Geotechnics, Sunshine Coast, QLD, Australia[2]

ABSTRACT

A large rockfall in excess of 9,000 m^3 occurred on 10 August 2016 near Sydney's iconic North Head lookouts, within the Sydney Harbour National Park, NSW. JK Geotechnics (JKG) was engaged by NSW National Parks and Wildlife Service (NPWS) to carry out a detailed geotechnical assessment of the existing sandstone cliff faces and cliff top areas. The assessment included a walkover inspection of the cliff top, an aerial drone survey of the cliff faces and targeted inspections of selected portions of the cliff faces using abseiling techniques. Following the inspections and a subsequent risk assessment, NPWS partially restricted access at one of three cliff top lookouts, with the remaining two lookouts permanently closed.

Following a hazard reduction burn within the national park on 17 October 2020, several open and persistent joints became exposed across the ground surface immediately behind the cliff faces. JKG reinspected the cliff top areas for additional signs of instability, reviewed historical information and provided updated geotechnical advice for two proposed lookouts located near the cliff edges (namely, Burragula and Yiningma). The results of the inspection confirmed that the observed open joint traces generally corresponded to structural features identified during the previous JKG geotechnical assessment completed in 2016 following the rock fall. An updated risk assessment informed the minimum set back distances of the proposed lookouts from the cliff edges. JKG also carried out numerous inspections during the demolition and construction phases and the lookouts were safely and successfully constructed circa June 2023.

1 INTRODUCTION

The Fairfax walking track at North Head offers stunning vantage points for picturesque views of Sydney Harbour, the Tasman Sea, and the Sydney city skyline, as well as providing opportunities for seasonal whale watching and viewing the start of the world famous Sydney to Hobart yacht race. In 2016, three cliff top lookouts along the walking track were temporarily closed due to safety concerns following the collapse of an approximately 85 m wide section of the coastal cliff line within the national park. A comprehensive rockfall risk assessment was subsequently undertaken resulting in restricted access at one lookout and closure of the remaining two. In 2020, a hazard reduction burn exposed several open joints across the cliff top areas, and an updated risk assessment was carried out at the request of NPWS to better inform the set back distances from the cliff edges of two proposed lookouts that were eventually constructed in 2023. This paper summarises the site history, geological setting, the fieldwork and risk assessment methodology, and the landslide risk mitigation measures that were implemented both in the design and construction phases.

2 ASSESSMENT METHODOLOGY

Two separate geotechnical assessments of the cliff faces and cliff top areas were carried out in 2016 and 2020; the former assessment comprised the following works:

- An initial aerial drone survey of the cliffs within the site area to gain an initial appreciation of the topographic, surface drainage and geological conditions of the site area and select areas of the cliff faces for subsequent abseil rope inspections;
- Using industrial rope access abseiling techniques, detailed inspection of five locations along the cliff face; including the three original lookout locations (Lookouts One, Two and Three) and an unofficial fisherman's cliff face access; and
- From the crest of the cliff faces, where access was possible, a detailed walkover inspection at the lookouts, with particular attention to mapping the pattern of jointing across the cliff top areas.

In 2020, following the aforementioned hazard reduction burn, a follow-up geotechnical assessment was requested by NPWS as several open and persistent joints became apparent across the cliff top areas. JKG surmised that the joints were either open and covered with vegetation or at least partially infilled with sand at the cliff top surface and the sand infill collapsed into the joint during or immediately after the reduction burn. The additional assessment included a specific

focus on the open joints and their potential impact on the previous risk calculations and advice. The levels of risk to both life and property were assessed in the JKG 2016 report using the Australian Geomechanics Society (AGS) 'Practice Note Guidelines for Landslide Risk Management' (AGS 2007c). In 2020, to inform the societal risk assessment associated with groups of visitors to the cliff top area, JKG adopted the NPWS 'Guidelines for Quantitative Risk to Life' (NPWS 2020). A summary of the risk assessment procedure and analysis results is presented in Section 4.

3 SITE FEATURES

3.1 LOCALITY AND HISTORY

The coastal cliff lines at North Head are positioned on the northern and eastern sides of Sydney Harbour National Park. The Sydney Harbour National Park comprises North Head, South Head, and several adjacent landforms lining Sydney Harbour, with the national park first gazetted in 1975 (NPWS, 2004). Prior to this time, primarily before and during World War II, North Head contained defence facilities such as gun emplacements, bunkers and tunnels. Some of the previous infrastructure can still be seen today. The historical Quarantine Station and a water resource recovery facility are also located on the western side and at the north-eastern end of North Head, respectively.

3.1 SITE DESCRIPTION

From the North Head Scenic Drive carpark, Fairfax Walking Track extends to the south toward Lookout One (now named Burragula, meaning 'sunset'), then eastward to Lookout Two (now closed) situated over the south-eastern corner of the cliff face, and then north to Lookout Three (now named Yiningma, meaning 'cliff edge'). From Lookout Three, the walking track returns to the carpark to the north-west. Figure 1 shows the site area.

In the vicinity of the walking track and lookouts, the sandstone cliff faces are a maximum height of between approximately 50 m and 70 m above the wave cut platform. The cliff faces typically comprise sub-vertical sandstone bedrock faces with occasional shale bands (typically about 1 m thick) of the Hawkesbury Sandstone, overlying Narrabeen Group interbedded sandstone, siltstone and shale exposed over the basal section of the cliff faces. Over various portions of the cliff faces, 'step' and undercut features are evident.



Figure 1. Aerial photo showing the site area at the southern end of North Head (image sourced from Nearmap, January 2025)

The cliff faces and their outline (in plan) are controlled by orthogonal sub-vertical joint planes typically orientated (bearing) approximately north-south (bearings ranging between approximately 007° and 030°) and east-west (bearings ranging between approximately 080° and 130°). The sandstone is generally sub-horizontally bedded and locally bedded (or cross bedded) at a maximum of approximately 17°.

The basal portion of the cliff face, where not covered by older (and more recent) rock fall debris, is characterised by the aforementioned Narrabeen Group (estimated to be approximately 25 m thick) which has typically been eroded to form a major undercut feature present over a majority of the length of the cliff faces.

3.1.1 Previous cliff face collapse

The previous rock fall impacted an approximately 85 m long section of the cliff face located about 300 m to the west of Lookout One. At this location, the cliff face was a maximum height of about 20 m and the majority of the rock fall debris comprised large sandstone blocks (defined by the orthogonal joint sets described above) and extended seaward at least 20 m; see Figure 2.

From a review of the JKG site observations and previous photographs prior to the collapse, the likely cause of the rock fall was considered to be ongoing erosion of the undercut section at the base of the cliff. This process had ultimately resulted in the undermining of the jointed rock mass, leading to an overturning moment of sufficient magnitude to induce toppling failure of the upper jointed rocks. Ephemeral hydrostatic pressures associated with temporary collection of water in open joints was also considered to be an additional potential trigger mechanism. The identified release surfaces of the rock fall are outlined below and indicated on Figure 2:

- Over the eastern section of the cliff, an approximately 030° trending sub-vertical joint (Joint 1);
- Over the western end, an approximately140° trending sub-vertical joint (Joint 2); and
- Over the central section, a localised sub-vertical joint (Joint 3) trending approximately 100°, extending east from Joint 1 and intersecting Joint 2.

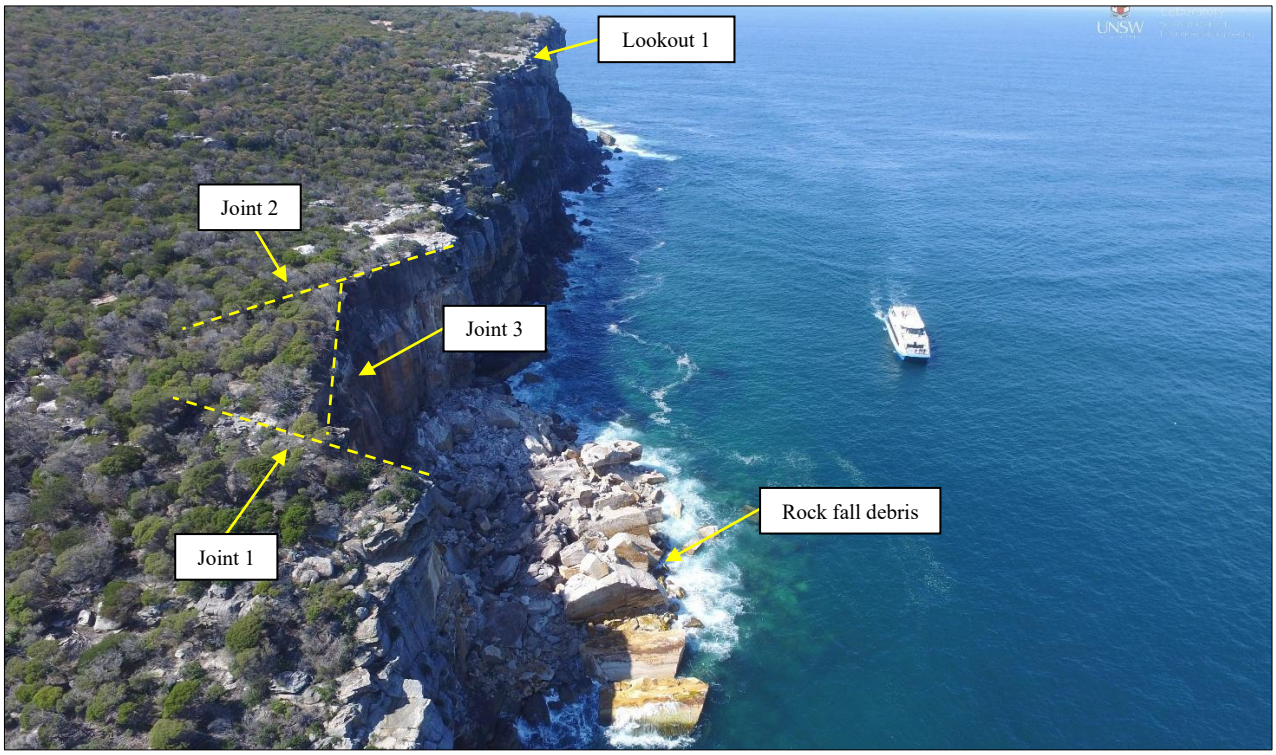


Figure 2: Oblique view of the cliff face and Lookout One following the rock fall (image supplied by NPWS, 2016)

3.1.2 Lookout One

The original Lookout One was located at a minimum set back distance of approximately 0.3 m from the edge of the cliff. An open, sub-vertical joint (Joint 4) trending at approximately 130° was intermittently exposed in the sandstone bedrock between approximately 20 m and 29 m landward (i.e. to the north) of the cliff edge. Figure 3 presents a cross-sectional sketch of the cliff face at Lookout One.

Several overhangs (maximum horizontal 'depth' of approximately 3 m) were present within the upper sections of the cliff. Below these overhangs, a second more extensive overhang feature extended over a horizontal distance (east-west) of about 40 m. The overhang was present below the full length (east-west) of the lookout, extended down the cliff face a

maximum vertical height of about 26 m, and had a maximum horizontal 'depth' of about 9 m. The base of the overhang was covered with soil and sandstone debris (gravel and cobble sized) which was typically overgrown.

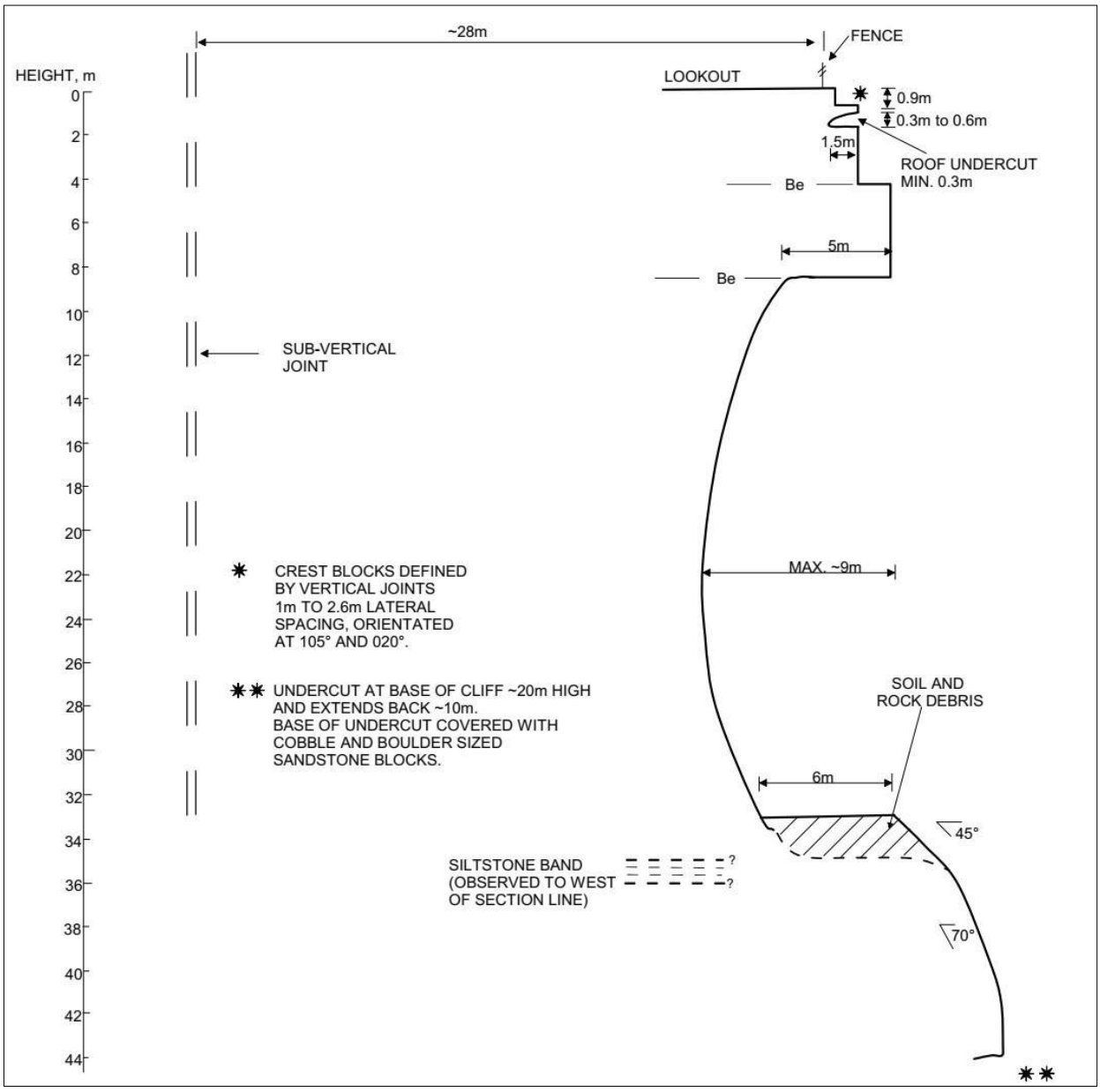


Figure 3: Cross-sectional sketch of the cliff face and cliff top area at Lookout One (looking east)

3.1.3 Lookout Two

The original Lookout Two was located at a set-back distance of approximately 1.8 m from the edge of the cliff. The crest of the cliff was characterised by an overhang feature that was approximately 6 m below the lookout surface. A second overhang feature (about 8 m high with a maximum horizontal 'depth' of about 2.4 m) was present about 1 m below the upper overhang. Below the second overhang, the cliff face had a stepped profile which extended down to about 37.5 m below the lookout surface where cobble and boulder sized sandstone blocks had collected on a flat sandstone ledge (3 m maximum width). A sub-vertical cliff face then extended down a further 7.5 m to the roof of the persistent undercut feature. The undercut was a maximum of about 25 m high, with a maximum horizontal 'depth' of about 5 m, and extended down to the wave cut platform below.

An open, sub-vertical planar joint (Joint 5) orientated at approximately 020° was located approximately 1 m to the east of the former lookout area and extended northward parallel with the cliff line. The open joint defined the western margin of a large column of sandstone at least 20 m high.

3.1.4 Lookout Three

The original Lookout Three was located at a set back distance of between approximately 1 m and 3.2 m from the edge of the cliff, and approximately 17 m seaward (i.e. to the north-east) of the walking track. Figure 4 presents an oblique view of the lookout during the 2016 assessment.

From the Fairfax walking track, access to the lookout was along a sand/gravel surfaced walking path and a number of voids and depressions were observed which impacted both the access path and adjacent cliff top area to the south-east. The voids and depressions appeared to be associated with soil loss through a persistent open joint (Joint 7) orientated at approximately 120° within the underlying bedrock. Joint 7 steeply dipped down to the north-east at between approximately 70° and 90° and had a sub-parallel alignment to Joint 8 observed in the cliff face below the north-western side of Lookout Three. Joint 7 and Join 8 were set back approximately 8 m and 13 m from the cliff edge, respectively. The north-western side of the cliff face adjacent to the former lookout also exposed a sub-vertical planar joint (Joint 9) orientated at approximately 012° (i.e. trending back into the cliff face).

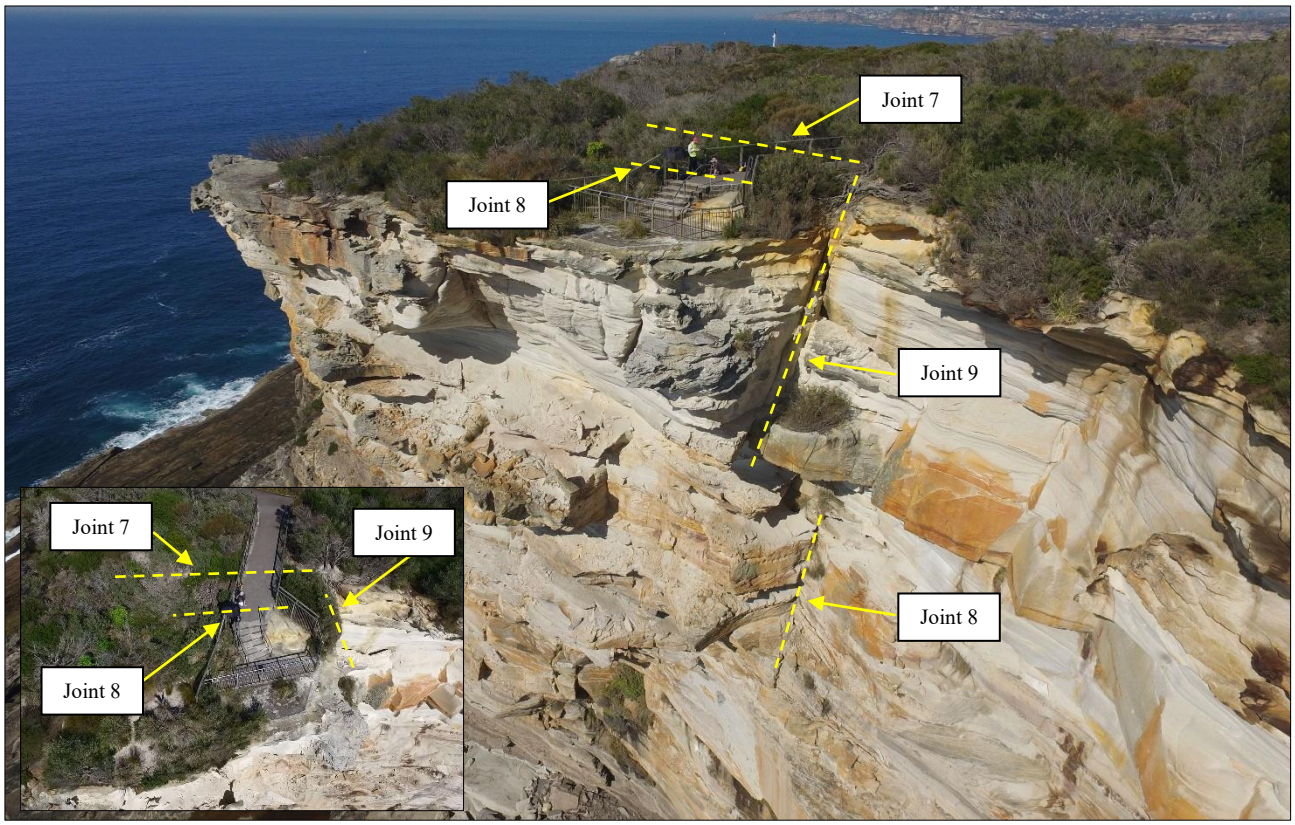


Figure 4: Oblique views of Lookout Three (images courtesy of NPWS, 2016)

The upper approximately 6 m of the cliff immediately below the lookout was characterised by a number of overhang features ranging between about 2 m and 4 m height and 'depths' of between about 0.4 m and 6 m. Several additional overhangs (maximum horizontal 'depth' of approximately 4.5 m) were observed down the cliff face. The persistent undercut feature had a maximum height of about 25 m, with a maximum horizontal 'depth' of about 5 m, and extended down to the wave cut platform below.

4 RISK ASSESSMENT

4.1 GEOLOGY AND FACTORS AFFETCING CLIFF FACE STABILITY

The foreshore cliff faces at North Head comprise Hawkesbury Sandstone and Narrabeen Group bedrock of Triassic age (around 245 to 210 million years ago). It is evident that the topography of the cliff faces at North Head have been influenced by the orthogonal joint sets identified during the inspections. The principal orthogonal joint sets were generally orientated approximately north-south (ranging between about 007° and 020°) and east-west (ranging between about 080° and 130°). The open nature of numerous joint planes in the cliff lines is the result of horizontal stress relief. In the case

of North Head the stress relief is, in large part, due to the formation of the valley feature which in the recent geological past was flooded as sea levels rose in response to post glacial ice melt to form what we now know as Sydney Harbour.

Factors affecting cliff face stability generally include undercutting, toppling, and basal shear/sliding (Kotze et al., 2024). However, based on geotechnical observations during the various JKG inspections, the most pertinent failure mechanism at North Head involves undercutting of the more erodible basal rock mass (i.e. the Narrabeen Formation) leading to toppling of the overlying competent (but jointed) rock mass (i.e. Hawkesbury Sandstone).

4.2 RISK ANALYSIS

4.2.1 General

The rockfall risk assessment at North Head followed the methodologies outlined in AGS 2007c and NPWS 2020. Site inspections of the cliff faces and cliff top areas, as well as review of aerial drone surveys, identified critical zones of instability, in particular immediately below the original lookouts.

A toppling failure analysis was completed for the observed open and sub-vertical joints located landward of the cliff edges at each lookout. Toppling of the rock mass is controlled by such factors as the weight of the overhanging portion (i.e. forming the overturning forces), possible water pressure in the open joint and horizontal release plane (i.e. bedding parting), and the distance of the open joint from the cliff face (i.e. forming the restoring forces). Figure 5 provides a diagram of the various features to be considered for a toppling failure analysis.

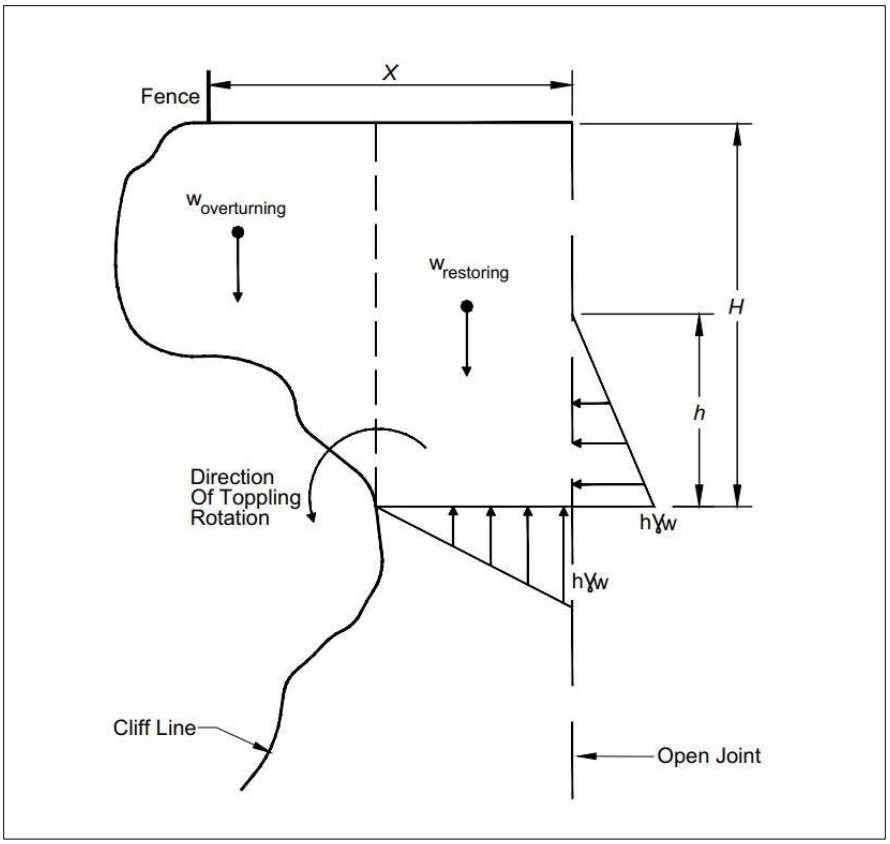


Figure 5: Example of toppling failure

The analysis was completed assuming the identified joint (based on the site observations) was 'dry' (Case 1), and also the situation where the head of water within the sub-vertical joint was half the height above the point of toppling, i.e. 2h = H (Case 2). For Case 2, hydrostatic pressure was assumed to be acting on a sub-horizontal bedding parting at the base of the overhanging section. In addition, an assessment of a theoretical joint set back approximately 4 m from the cliff edge (a typical lateral spacing for joints in the Hawkesbury Sandstone) was also completed. Water collecting over the full height of the joint was not considered realistic considering the open and interconnected nature of the jointed rock mass which was assessed to naturally drain.

For the identified joints, the results of the topping failure analysis indicated a Factor of Safety (FOS) greater than 1.5 at each lookout was achievable for both Cases 1 and 2. However, for a theoretical joint in close proximity to the cliff edge, the FOS was less than 1 for both cases.

For the identified overhangs over the upper sections of the cliff, the situation where no joint was present was also assessed. In this instance, a tensile strength of 2 MPa (i.e. low strength) was assumed for the intact bedrock, and the sandstone was therefore considered to have sufficient strength to resist brittle (i.e. tensile) failure (based on the methodology outlined in Young et al., 2009).

The results of the topping analysis coupled with the assessment of brittle failure, indicated that the approximate annual probability of instability, both over the upper reaches (i.e. overhangs) and mid-sections (i.e. persistent undercut feature) of the cliff faces, was considered to range between 1 x 10^{-2} (i.e. Likely) and 1 x 10^{-4} (i.e. Unlikely), as defined in AGS 2007c.

4.2.2 2016 risk analysis using AGS 2007c

The Australian Geomechanics Society (AGS 2007c) framework for landslide risk assessment applies a qualitative approach to evaluate the risk to property, and a semi-quantitative method to assess the risk to life. The probability of failure was estimated based on field observations (obtained during the 2016 assessment) and the geotechnical assessment presented in Section 4.2.1 above. Based on the likelihood of instability, the assessed risk to property (under former existing conditions) for each of the three lookouts ranged between Low and Moderate, which was considered to be 'Acceptable' and 'Tolerable' in accordance with AGS 2007c, respectively.

For the risk to life, typical temporal, vulnerability and evacuation factors were adopted based on previous experience in similar cliff top environments. A spatial probability of 1 was adopted; that is, the affected person or persons were assumed to be present immediately above the specific hazard if instability occurred. This approach may be regarded as slightly conservative at Lookout One due to its large area and the non-persistent nature of several geotechnical features within the upper reaches of the cliff face, although it was considered a reasonable assumption for the remaining smaller lookouts (i.e. Lookout Two and Three) which had more restricted entry and exit areas.

Based on information supplied by NPWS, two cases were considered for the risk to life, they were: 1) an individual visiting the lookout, and 2) a tour group of say 30 people visiting the lookout as part of a guided tour. In accordance with AGS 2007c, under former existing conditions, the risk to life for the individual most at risk was assessed to be 'Acceptable', and the risk to life for the entire tour group of 30 people was assessed to be within the 'Tolerable' to 'Acceptable' range.

The above assessment was provided to NPWS along with specific landslide risk mitigation measures to reduce the 'Tolerable' risk levels at each of the three lookouts. This advice essentially restricted access to Lookout One, and prevented any further use of Lookout Two and Lookout Three, which were subsequently permanently closed by NPWS.

4.2.3 2020 risk analysis using NPWS 2020

In 2020, approximately four years after the initial geotechnical assessment was completed and following a hazard reduction burn which exposed several open and persistent joint traces across the cliff top areas, the risk to life for groups of visitors from the previous AGS 2007c risk assessment was reviewed and updated based on the recently published guidelines outlined in NPWS 2020. The guidelines were prepared by Golder on behalf of NPWS and adopted the criteria for the individual most at risk from AGS 2007c, and the criteria for societal risk from ANCOLD 2003, with the intention of *"seeking to develop clear guidance that can be provided to geotechnical practitioners setting out preferred methods for calculating individual and societal risk so as to allow comparison with these criteria"*.

Between the initial assessment in 2016 and subsequent assessment in 2020, access remained restricted at Lookout One, with the other two smaller lookouts (i.e. Lookout Two and Three) permanently closed, and so only Lookout One was considered at that stage. Using the NPWS 2020 guidelines, the previously assessed 'Acceptable' risk level for the individual most at risk (using AGS 2007c) was confirmed.

The societal risk, which is defined as *"the risk of multiple fatalities or injuries in society as a whole: one where society would have to carry the burden of a landslide causing a number of deaths",* was also considered for a group of individuals or tour group at Lookout One. NPWS indicated that the number of visitors at Lookout One was between approximately 9100/month during summer (when the National Park is open for 14 hours/day) and 9400/month during winter (when the National Park is open for 12 hours/day). Additional information provided by NPWS indicated that the maximum expected size of a tour group was approximately 20 people, and an average of 4 tour groups visited the area annually. Under former existing conditions at Lookout One, the societal risk for a group of individuals or tour group, ranged between 'Tolerable - ALARP' (i.e. As Low As Reasonably Practical) and 'Unacceptable'.

Following provision of the above risk assessment to NPWS, several options for the 'treatment of risk' for Lookout One included: 1) accepting the risk and carrying out on-going monitoring, 2) avoiding the risk by permanently closing the lookout, 3) reducing the consequence of risk by a combination of limiting visitor numbers, posting warning signs, further restricting access etc., or 4) reducing the consequence of risk by designing a new lookout such that the probability of the lookout being impacted by cliff face instability would be greatly reduced. Option 4 was selected by NPWS and a subsequent societal risk assessment at Lookout One and Lookout Three indicated an 'Acceptable' level of risk could be achieved for new lookout structures at these cliff top locations (now known as Burragula, and Yiningma, respectively) even with a predicted 50% increase in visitor numbers following construction. This societal risk assessment could only be achieved if appropriate landslide risk mitigation measures were adopted. Lookout Two remained permanently close.

A risk assessment for the construction phase was undertaken for Lookout One (Burragula), where workers carrying out demolition of the original lookout structures and construction would be working seaward of set back distances recommended by JKG. From advice provided by the project structural engineer (SDA Structures), construction loading on the surface of the cliff face overhang (shown in Figure 3) ranged between approximately 7.5 kPa and 12 kPa, which accounted for workers, reinforcement and formwork, and 'wet' concrete. The surcharge loads represented only a 0.2% increase in the required tensile strength to maintain the overhang in its current form. As such, based on the additional temporal information (i.e. construction period) provided by Glascott (the builder) and assumed spatial, vulnerability and evacuation factors, the assessed societal risk during the construction period was considered 'Acceptable' provided that additional risk mitigation measures, as outlined in Section 4.3 below, were implemented.

The design and construction methodologies of the proposed lookouts was therefore heavily influenced by the geotechnical assessments undertaken by JKG, specifically the 2020 assessment of societal risk.

4.3 LANDSLIDE RISK MANAGEMENT MEASURES

In order to reduce societal risk levels, the proposed lookout locations were required to satisfy the below criteria defined by JKG:

- Prevent structural loads being imparted onto the potentially unstable sections of the cliff face which could increase the likelihood of instability; and
- Prevent the new lookouts from being damaged should cliff face collapse occur.

Based on the sectional profiles of the cliff faces in the vicinity of the proposed lookouts, the following JKG advice was provided to NPWS prior to the design stage of the new lookouts:

- To reduce the likelihood of cliff face instability impacting the lookout, either from collapse of the upper portion of the overhangs or the entire lower overhang, the footings supporting the new lookout must be located a minimum set back distance of 8 m and 4 m of the existing fence lines at Lookout One and Lookout Three, respectively;
- Any portions of the lookout seaward of these set back distances must be designed as cantilevered and supported by foundations located landward of these set back distances; and
- The proposed areas of the new lookout foundations would need to be cleared of vegetation and inspected by a geotechnical engineer to check for the presence of any traces of open sub-vertical joint planes and to confirm the above mentioned set back distances.

During construction of Lookout One (Burragula), a maximum of five workers were permitted on the seaward side of the set back distances provided above, and each worker was required to be attached to harnesses and safety ropes with anchor points landward of any area of cliff face instability. Additional landslide risk mitigation measures during demolition of the existing lookouts were also implemented, including using hand held demolition equipment or tracked plant (i.e. excavators) well landward of any zones of instability, and using a spotter at all times.

5 CONSTRUCTION OF LOOKOUTS

Demolition and construction at Lookout One (Burragula) and Lookout Three (Yiningma) commenced in early 2022 and regular geotechnical inspections were carried out by JKG in relation to the aforementioned landslide risk mitigation measures and other design related issues, such as: 1) confirming appropriate demolition plant and safety equipment was being used, 2) defining the nominated set back distances of all load bearing structures, 3) inspecting the bedrock surface in localised trenches for the signs of any sub-vertical joint traces, and 4) assessing the exposed whether the rock mass was suitable for the design allowable bearing pressure.

During the inspections, several of the persistent joints identified during the earlier assessments were locally exposed in footing excavations and were subsequentially 'bridged over' with sacrificial formwork and additional reinforcement, or a Bondek slab, in accordance with advice from SDA Structures. It was noteworthy that a strong breeze could be felt in

one localised section of an open joint (Joint 4) exposed at Lookout One, with the air most likely being blown through the open joint exposed within the cliff face approximately 20 m to the south-east.

Figure 6a and Figure 6b presented below show Lookout One (Burragula) prior to and following construction, respectively.



Figure 6a Lookout One pre construction (looking east, image courtesy of NPWS, 2016)

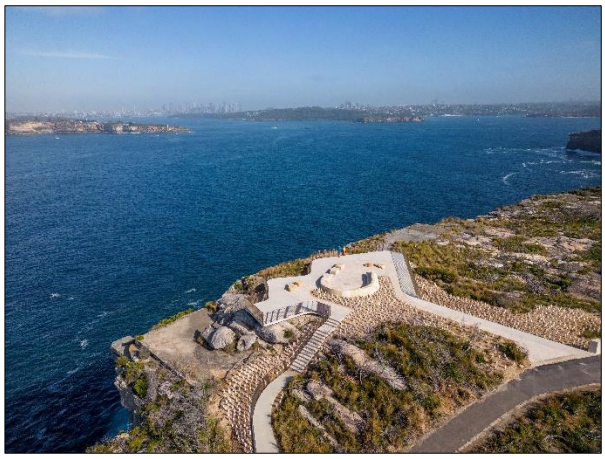


Figure 6b: Lookout One following construction (looking south-west, image courtesy of NPWS, 2023)

6 CONCLUSIONS

Design of the new lookouts at North Head was governed by the geotechnical constraints at the site, and in particular their geological structure and associated risks. Refining the risk levels between two geotechnical assessments completed nearly four years apart, in particular a refined approach to societal risk, resulted in updated design and construction related advice intimately informed by a risk management approach. This specific geotechnical advice was actioned by NPWS, the project consultants and builder, resulting in a safety conscious design and construction of two partially suspended lookouts which cantilever seaward in close proximity to the existing cliff lines, providing expansive views of Sydney Harbour and the Tasman Sea.

7 ACKNOWLEDGEMENTS

The authors acknowledge NPWS for their permission to publish this paper, and in particular Katherine Ashley of NPWS for her assistance prior to and during construction of the lookouts. The successful project outcome was in large part due to the willingness of NPWS to engage with various stakeholders, including community and consultants, to deliver a user friendly and safety focused project that is expected to be enjoyed by locals and visitors for many years to come.

The efforts of the architectural design team from Chrofi and Bangawarra should also be acknowledged. The central focus of their design was around ‘Connecting with Country’ and the history of the area. The architectural collaboration for the lookouts received high praise, being awarded the NSW AIA Architecture Medallion, the NSW AIA Rober Woodward Award for Small Project Architecture, and the AIA National Nicholas Murcutt Award for Small Project Architecture.

8 REFERENCES

Australian Geomechanics Society (AGS) (2007c). Practice Note Guidelines for Landslide Risk Management, *Australian Geomechanics*, 42 (1), 63-114

Golder Associates Pty Ltd (2020). NSW National Parks & Wildlife Service Guidelines for Quantitative Risk to Life

Kotze, G., Hunter, A. & Field, D. (2024). A 30 Year Review of Rockfall Frequency and Coastal Cliff Regression on the Northern Beaches of Sydney, Australia, *Australian Geomechanics*, 59 (3), 57-71

NSW National Parks and Wildlife Service (2004). Sydney Region, Fire Management Plan Sydney Harbour and Botany Bay (La Perouse Precinct) National Parks

Young, R. W. and Wray, R. A. L. (2000). The Geomorphology of Sandstone in the Sydney Region, in McNally, G. H. and Franklin, B. J., eds. *Sandstone City*, Springwood, NSW: Conference Publications 55-73

Young, R. W., Wray, R. A. L. and Young A. R. M. (2009). *Sandstone Landforms*, Cambridge: Cambridge University Press

https://doi.org/10.56295/1ACEG18

LANDSLIDE RISK ASSESSMENT IN COASTAL SETTINGS – RECOGNIZING THE CHALLENGES AND UNCERTAINTY

Andrew Hunter and Tony Miner
GHD

ABSTRACT

Coastal hazards present a common threat to many Australians given the extensive utilisation of our vast coastal margins. These hazards can take the form of cliff collapse, rockfalls, landslides, karstic features and coastline regression and involve the interface between these terrestrial processes and coastal agents of change including wave action, tidal surge and storm events.

This paper looks at the challenges faced by practitioners and managing authorities when managing public safety on the coast through the undertaking of landslide risk assessments. We look at the adaptation of standard risk assessment approaches to the coastal environment and discuss the use of geomorphic analysis to assist in the determination of key inputs into the risk assessment process. In particular, we review the role of process rates and coastal regression to inform likelihood determination through geomorphic analysis of past coastal erosional environments and the role of sea level and climate variations. Whilst the concepts and approaches discussed in this paper could be applied to many coastal settings and scenarios, this paper considers risk assessment as applied to landslide hazards in coastal conditions with focus on below cliff / beach level users and does not deal with cliff top infrastructure.

The nature of landslide hazards, techniques for assessing likelihood, consequence and the estimation of landslide risk is discussed in the context of coastal settings. We also highlight the challenges faced in delineating the patterns of use by the public, the varying potential for impact within different hazard zones and the complications associated with risk mitigation.

1 INTRODUCTION AND BACKGROUND

The coastline of mainland Australia is vast, extending for about 34,000 km with about 50 % of the Australian population residing within 7 km of the coast. Rocky coasts account for about 40% of the coastline forming dramatic coastal cliffs and headlands (Kennedy et, al. 2012). With over 10,000 beaches on mainland Australia, the Australian population has traditionally had a strong affinity for the beach and the beach is often considered central to the Australian culture. While most Australians are somewhat familiar with beach safety hazards such as rips, waves, currents and marine life, our experience suggests there is a general sense of unfamiliarity with coastal landslide hazards.

Rocky coasts commonly comprise small beaches that are semi-enclosed between steep headlands. The beaches, often known as headland-bay beaches or pocket beaches are typically bow shaped with headlands at each end. These beaches are particularly common along the coasts of New South Wales and the southern Victorian Coast. The nature of the headlands and associated cliffs vary dramatically depending mainly on geological controls. At some beaches, coastal cliffs extend around the backshore parts of the shoreline, such that the beach face extends directly to the toe of the cliffs. Cliffs and rock overhangs offer shade and shelter to beachgoers and are often an attractive place for individuals and groups of people to congregate.

Horizontal shore platforms (also called rock platforms) at the foot of coastal cliffs, are also a common feature along the coasts of New South Wales and southern Victoria. In fact, the term ‘shore platform’ was coined by the famous American geologist, James Dwight Dana while visiting New Zealand and New South Wales during 1839 and 1840 as the geologist to the United States Exploring Expedition (Dana, 1849). During the early 1900’s, mostly in the period prior to WWII, many coastal rockpools were constructed in NSW on these shore platforms and many of these pools have heritage listings. The rockpools remain very popular, enticing large numbers of visitors to headland areas and have become iconic landmarks, particularly in Sydney. In addition to pool users, visitors are also enticed to shore platforms and associated coastal cliff areas by formalised walkways, informal walking routes between adjacent beaches and rock or spear fishing sites (Figure 1).

Owing to the aggressive coastal weathering and wave action, rockfalls are a common occurrence at many coastal cliffs. Based on data compiled mainly using the National Library of Australia’s Trove database, coastal landslides have resulted in at least 24 fatalities in Australia since 1926 (Appendix A, Table A1). However, we acknowledge this is probably an underestimate given entries in Trove post 1954 are still somewhat limited because of copyright restrictions, according to

landslide fatality statistics compiled by Roberts and Miner (2023). This accounts for about 44% of all known natural landslide deaths in Australia (excluding construction and mining related landslides). Despite this, there is often a public disregard or lack of awareness of these dangers. This paper aims to frame the challenges and difficulties associated with landslide risk assessment in dynamic coastal environments which are often quite different from other settings more commonly investigated by geotechnical practitioners. We also explore the challenges often faced in mitigating and communicating these risks to the public.



Figure 1: Typical scene showing a rockpool constructed on a shore platform adjacent to coastal cliff.

2 THE USE AND APPLICATION OF RISK ASSESSMENT IN COASTAL ENVIRONMENTS

Risk can generally be defined as "a measure of the probability and severity of an adverse effect to health property or the environment" (AGS, 2007e). Coastal landslide risk can then be further defined as the likelihood that a particular coastal landslide hazard will occur and may involve possible consequences to elements at risk located within that coastal setting.

Risk assessment has been applied across many facets of modern life and can be defined as *"the process of making a decision recommendation on whether existing risks are tolerable and present risk control measures are adequate, and if not, whether alternative risk control measures are justified or will be implemented. Risk assessment incorporates the risk analysis, risk estimation and risk evaluation phases"* (adapted from Fell et al. 2005). Landslide risk assessment in Australia has generally adopted the "state of the art" guidelines published by the Australian Geomechanics Society (AGS) published initially in 2000 and updated in 2007.

In coastal environments, landslide risk assessment is the process by which coastal landslide hazards are identified, their likelihood estimated, the consequences of such hazards determined through assessment of their direction and travel distance and their ability to adversely impact and interact with valued elements at risk such as beach users which may include sunbathers, beachcombers, users of rockpools and other associated beach infrastructure such as changing rooms, toilet blocks or coastal paths.

3 CHALLENGES FOR DETERMINING RISK COMPONENTS

In its simplest form, risk assessment is conducted through the estimation of likelihood and consequence. The most fundamental estimation of the annual probability of loss of life $R_{(LOL)}$ for a nominated element at risk from a specific hazard type involves the product of an annual probability of occurrence of a particular hazard $P_{(H)}$ and a series of conditional probabilities associated with spatial factors. These are; direction and reach of the hazard $P_{(S:H)}$, temporal exposure of the element at risk $P_{(T:S)}$ and the vulnerability of the element at risk $V_{(D:T)}$ (AGS 2007a). In addition, an element at risk may be exposed to one or multiple hazards, or there may be multiple elements at risk (i.e. an exposed population) which encounter one or multiple hazards.

Limitations in our knowledge of each of these risk components introduces uncertainty and inaccuracy to the final estimate of risk. Further uncertainty may be introduced through error in measurement and observation, variable judgement and bias of the assessor. Uncertainty can also arise from the unpredictability of natural systems (Paul and Miner, 2025).

The following sections describe challenges and difficulties associated with the fundamentals of hazard identification and the components involved in the estimation of risk, with specific emphasis on the application of risk assessment to coastal settings.

4 HAZARD VARIABILITY

AGS (2007) broadly defines a landslide as: *"the movement of a mass of rock, debris, or earth (soil) down a slope (AGS, 2007)"*. Landslides are generally described through a combination of material and movement type. According to Hungr et al. (2014) material types include: rock, clay, mud, silt, sand, gravel, boulders, debris peat and ice. Types of movement include: falls, topples, slides, spreads, avalanches, flows and slope deformation such as solifluction. Other terms such as collapse or creep are also sometimes used colloquially. Hence, landslides comprise numerous combinations of material and movement types, and familiar examples of landslide descriptions include rockfalls, clay slides and debris flows.

Similarly for coastal settings, a wide range of potential hazards are possible and hazard identification and description is critical to undertaking any coastal landslide risk assessment. Coastal hazard settings can comprise soft and hard cliffs as well as coastal bluffs, sand dunes and moderate to steep slopes, with potential hazard types presented in Table 1.

Table 1- Compilation of various types of coastal landslide hazards (adapted from Hungr 2014)

Type of Movement	Rock	Soil
Falls	Rockfall	Clay / silt fall Boulder fall
Topple	Rock block topple Rock flexural topple	Sand/gravel/silt topple
Slide	Rock rotational slide Rock planar Slide Rock wedge slide	Clay /silt slide Gravel / sand/debris slide
Flow	Rock avalanche	Sand / silt/ debris dry flow Sand /silt/ debris flow-slide Debris flow Mud flow

The diversity of hazard types means an assessor must make detailed and thorough observations to establish a conceptual geological model which then yields the potential mechanisms of failure and the range of possible hazards. In some cases, geological or terrain features may be concealed (such as hidden discontinuities and defects) thus making assessment of mechanism(s) and coastal landslide hazard types difficult.

5 DIFFICULTIES IN FREQUENCY DETERMINATION

5.1 OBSERVATIONS AND INVENTORIES

The assessment of landslide frequency in coastal settings can be especially challenging due to the dynamic nature of the environment. Rockfall debris is often rapidly washed away by wave action, removing all evidence of the event, sometimes within hours depending on tides and swell (Figure 3). While debris from very large failures may remain for longer, over time the material is reworked, broken up and transported across shore platforms and the beach by wave action. Given enough time and weathering, the recent rockfall debris becomes indistinguishable from other talus and boulders along the shoreline, limiting geotechnical practitioners' ability to draw upon knowledge of past events.



Figure 2: A very large coastal cliff collapse / rockslide of approximately 40,000 m^3 occurred at Jarosite Headland in Victoria. Only 100 m to the southwest of the site of a fatal rockfall of only 2 m^3 occurred killing 1 person and injuring 2 others just a month earlier.

Rockfall inventories can provide an important insight into event frequency, however such records are rarely collected by managing authorities. Kotze et al. (2024) presented the results of a 32-year study of rockfall frequency on Sydney's Northern Beaches aimed at mitigating adverse effects of rockfalls from coastal cliffs in the local government area. Due to the length of that study, both large-scale and small-scale events were captured in the inventory, allowing assessments of coastal cliff regression to be made. Muller et al. (2006) presented the results of ongoing studies into rockfalls at a coastal headland known as The Bluff, at Barwon Heads, Victoria. A rockfall inventory was assembled from review of terrestrial photos taken from permanent vantage points over a period of 12 years with such data providing critical insight into the relationship of hazard volume and frequency. More recently studies by Anna Giacomini at the University of Newcastle are helping to highlight inventory and monitoring to assist with hazard identification, likelihood and travel distance analysis (Watman et al., 2023). However, such studies are the exception and generally little is known about rockfall history at the majority of sites.



Figure 3: Large rockfall from coastal cliff with destroyed warning sign on right. Debris was completely washed away within a few days.

5.2 REMOTE SENSING

In this increasingly digital age, remote sensing methods are often spruiked to solve all manner of problems. Unfortunately, in coastal settings remote sensing methods to assess long term rockfall frequency and cliff regression may be of limited use. Small magnitude rockfalls, which usually occur more frequently, are often of more interest to practitioners undertaking risk assessments and these methods typically don't address these knowledge gaps. For example, in most Australian states publicly available lidar data extends back for perhaps up to 15 years and the resolution is variable. Lidar is also only suitable for identifying large magnitude, episodic cliff failures whereby 'metres' of cliff line has failed between successive surveys. Due to vertical occlusions and resolution issues, smaller scale rockfall frequency cannot be assessed. Traditional aerial photography, while available over longer time periods, is also limited by resolution issues, lighting and camera azimuths.

Repeat drone mounted lidar or photogrammetric surveys of coastal cliffs aimed at comparing changes over long periods of time would be of great benefit to future risk studies however this information is typically not available to practitioners given the relatively recent emergence of the technology.

5.3 GEOMORPHOLOGY AND PROCESS RATES

When sufficient data is available, knowledge of local geology and geomorphic processes can be used to develop process rate models to help predict the size and volume of future landslide events (e.g. Moon et al. 2005). Knowledge of the geometry of the slope can then be used to estimate rates of slope retreat. Flentje (2012) compiled a summary of published escarpment retreat rates for parts of NSW. We have updated this to include a broader area of south-east Australia and to highlight the methodology used to determine these retreat rates (Table 2).

Table 2: Escarpment retreat rates – Southeastern Australia (modified from Flentje, 2012)

Retreat Rate (m/1000 years)	Geological Unit(s) / material	Location	Source	Methodology	Interval (years)
0.6	Narrabeen Group, Illawarra Coal Measures & Hawkesbury Sandstone	Illawarra Escarpment	Flentje, 2012	Plate tectonic reconstruction	70 Ma.
1	Regional cross section	Southeastern coastline	Thom et al, 2010	Plate tectonic reconstruction	30 Ma.
0.3	Hawkesbury Sandstone	Illawarra Escarpment	Flentje, 2012	Landslide inventory	<100
0.3 to 3	Narrabeen Group	Lawrence Hargrave Drive (Coalcliff to Clifton)	Moon et al., 2005	Landslide inventory and geomorphic assessment	<100
1 to 40	Narrabeen Group	Newcastle coastal cliffs	Delaney, 2005	Shore platform retreat	6,500
0.5	Granite and granodiorite - Bega Batholith	Bega Valley, NSW	Heimsath et al., 2000	Plate tectonic reconstruction	100 Ma.
0.5	Hawkesbury Sandstone and Narrabeen Group	Bulli Pass, Illawarra Escarpment, NSW	Hunter et al., 2022	Landslide inventory	120
2.9	Narrabeen Group	Northern Beaches Peninsula coastal cliffs, Sydney	Kotze et al., 2024	Landslide inventory	32
0.9	Cabramurra Basalt	Toolong Range, Snowy Mountains, NSW	Caine et al., 1968	Radiocarbon dating	35,000
9	Arkose	Point Sturt, Otway Coast, VIC	Gill et al., 1983	Shore platform retreat	6,000
18	Siltstone	Northeast of Point Sturt, Otway Coast, VIC	Gill et al., 1983	Shore platform retreat	6,000

It is important to recognise that the rates in Table 1 have been determined using a variety of different methods, each with different levels of uncertainty and accuracy. The published escarpment retreat rates are in many instances very long-term averages, and in some studies have been estimated over periods ranging from less than 100 years to 100 million years. Climatic conditions and sea levels have fluctuated substantially over these time periods. It should be self-evident that the prevailing climate at any particular time is a key factor influencing landside processes and therefore great caution should be given to the appropriateness of adopting long-term average rates as a means to estimate event likelihood over a near-term period that may only span years or decades.

Coastal risk assessments need to consider the highly episodic nature of landsliding at coastal cliffs which in many cases may be more strongly dependent on local conditions than broader escarpment scale rates of retreat. For example, following a large-scale cliff collapse (i.e. full height failure) whereby a cliff may retreat by several metres in a single event, the cliff may remain in a 'static equilibrium' state for long periods of time (i.e. potentially hundreds or thousands of years) until such time that processes such as erosion and wave action trigger a further collapse. It is also important to recognise that small volume, high frequency events such as small rockfalls can often pose higher risks to individuals than large failures. It is therefore useful to consider how these events contribute to the overall process rates. Furthermore, events at either end of process rate curves (i.e. very small magnitude and very large magnitude events) are often the events we know the least about.

Shore platform development has sometimes been used to infer rates of coastal cliff retreat by using knowledge of sea levels during the Holocene epoch. The most common shore platforms in eastern Australia were classified by Sunamura (1992) as 'Type B' platforms, which comprise a near-horizontal, intertidal rock surface extending from the cliff to the low tide level with a marked drop at their seaward edge (Figure 4). The formation of shore platforms has been debated for decades, particularly with respect to the amount of erosion caused by wave action versus the lowering of platforms by subaerial processes (Trenhaile, 2002). However, it is widely agreed that recession of coastal cliffs is essential for Type B platform development (Sunamura,1992).

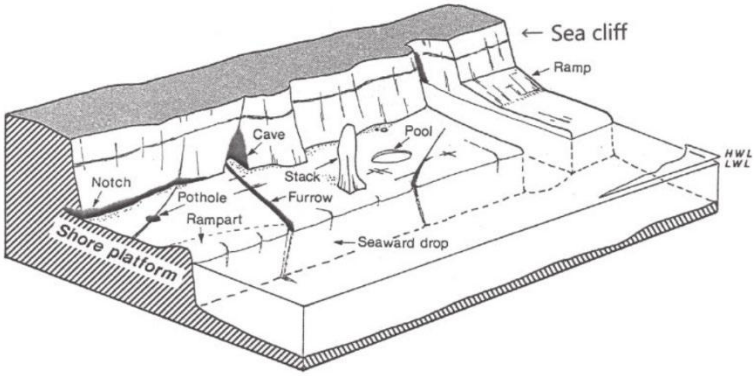


Figure 4: Type B horizontal shore platform morphology (Sunamura, 1992).

Woodroffe (2003) notes there is considerable debate as to whether the seaward edge of shore platforms retreats under current sea levels, with the low-tide scarp often inferred to mark the position of the old shoreline before erosion of the platform. If it is assumed that the seaward edge of the low tide scarp is essentially 'static', it is possible to estimate the average rate of cliff regression since sea levels rose to their present positions around the Australian coastline at the end of the last glacial marine transgression in the mid Holocene Epoch. According to Thom et al. (1985) this was about 6,500 ± 250 years ago. While this method appears to offer an elegant solution to estimating cliff regression rates, it also introduces a number of uncertainties. For example, it is widely recognized that wave energy is partly expended on the low-tide scarp and is further dissipated as waves travel across the platform, meaning that under present sea level climatic conditions, waves are ineffective erosional mechanisms (Trenhaile, 2011). Furthermore, modelling by Trenhaile (2000) showed the rate of platform width extension decreased with time and a state of equilibrium has often been reached.

It reasons that average rates of cliff regression over the last 6,500 are very unlikely to be representative of current conditions given that the initial rates of erosion following the stabilisation of sea levels about 6,500 years ago would have been very rapid and have progressively slowed. This is demonstrated in the process rate model (developed for the cliff pictured in Figure 1 using a long-term inventory study) in Figure 5. To further complicate this issue, it is also well documented that some shore platforms may have been inherited from earlier periods of the Holocene when sea levels were at a similar or higher level to todays (Trenhaile, 2011). This inconsistency has been recognised in two recent coastal studies in NSW. Kotze et al. (2024) found that cliff regression rates estimated using shore platform geomorphology were about 1.5 to 6 times greater than cliff regression rates estimated using a long term rockfall inventory. Furthermore, Kennedy et al. (2012) dated the exposure age of shore platform rocks in the Illawarra region using cosmogenic dating methods and found that the cliff retreat rates were orders of magnitude faster than those proposed by Flentje (2012).

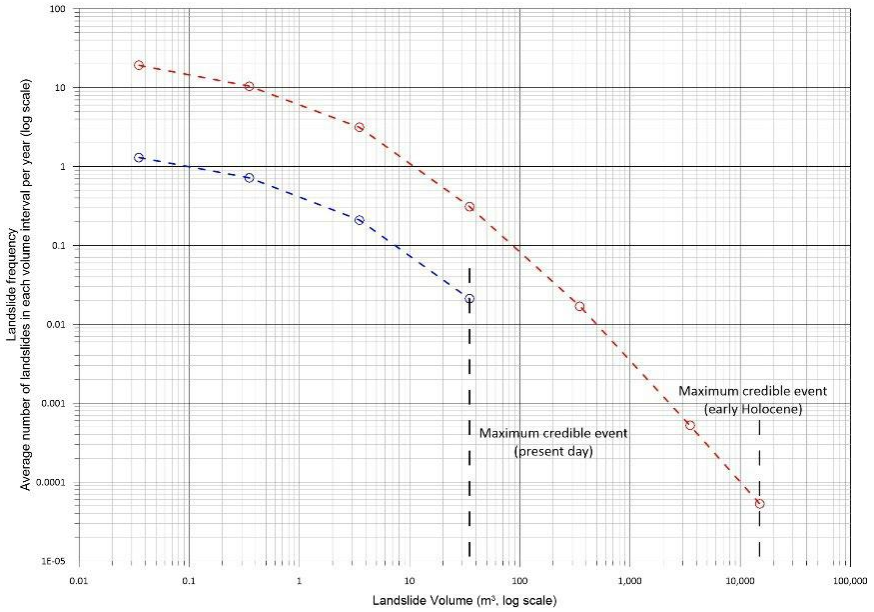


Figure 5: Process rate model showing landslide volume curve (blue) for cliff pictured in Figure 1. Red curve represents postulated process rate estimated using average rate of shore platform retreat.

In our opinion cliff regression rates estimated using shore platform relationships are in most cases not representative of present conditions or the time period of relevance to the risk assessment, which is typically less than say 100 years. Therefore, inventories (if available), together with observations and 'degree of belief' approaches should be used to inform process rates and associated likelihood values as the event likelihoods are more representative of conditions under current climatic and coastal conditions. However, it is suggested that rates still be compared with published process rates as a 'sensibility check' based on all available evidence and information.

6 CHALLENGES ASSESSING CONSEQUENCE

In beach and coastal settings, temporal probability, spatial probability and vulnerability are inextricably linked. Identifying the person most at risk as defined by AGS (2007c) can be challenging due to seasonal usage patterns and without long term familiarity of a site it is often not obvious who has the highest exposure to hazards. Some of the common scenarios that need to be considered in risk assessments include:

Seasonal usage patterns: Some beach settings have very high numbers of users over warmer months and visitation typically reduces over cooler months. For example, over warmer months, individuals and groups often have the most exposure however the exposure of other individuals such as pool users, walkers and anglers may be constant throughout the year. Managing authorities typically don't have definitive usage numbers available, so it is often necessary to estimate beach usage, introducing more uncertainty.

Human behaviours: Unlike built environments, individuals have practically unrestricted access to any area of the coastline and while behaviours are unpredictable, they are usually influenced by tides, swell, weather and other beach conditions. Longer term (i.e. many repeat visits) observations helps to inform these judgements. Cliffs and rock overhangs provide shade and are inducements for individuals to sit and congregate below, often for long periods of time. All beach settings will have a combination of mobile (i.e. walkers) and static (i.e. sunbathers) usage scenarios that need to be considered separately. One approach to simplify temporal and spatial patterns of usage is to estimate risks for defined zones as presented in Figure 6.

Beach Conditions: Tides, swell, weather and other beach conditions affect how individuals use the beach. During periods of large swells, rockpools may not be used at all. High tides and swells often result in individuals occupying higher parts of the beach such as directly below cliffs, which increases vulnerability. Large swells also remove sand from parts of beaches and expose shore platforms. This can often mean spatial probability needs to be given close attention because rocks will travel further and fragment on impact (Figure 7). However, the removal of sand from shore platforms changes usage patterns. For example, some groups from the exposed population are instead more likely to visit other parts of the beach that has sand.

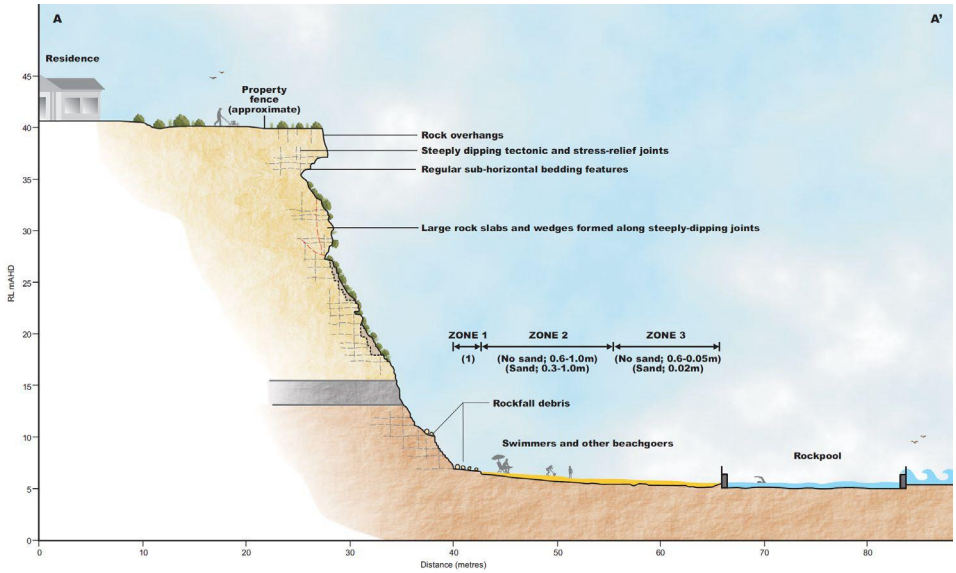


Figure 6: Typical risk scenario showing hazards, elements at risk and ranges in rockfall reach probability (in brackets).

Beach conditions and human behaviours are essentially 'known unknowns' and it is not possible to estimate these scenarios with certainty. This inevitably leads to assumptions being made for a range of scenarios. It is suggested that all reasonably foreseeable scenarios should be included in the risk assessment to assess the person most at risk.

The issue of seasonal usage patterns also introduces challenges to risk assessment because averaging exposure over a year may not realistically reflect risks during summer periods, while adopting a 'worst case' scenario means risks throughout much of the year are over estimated.

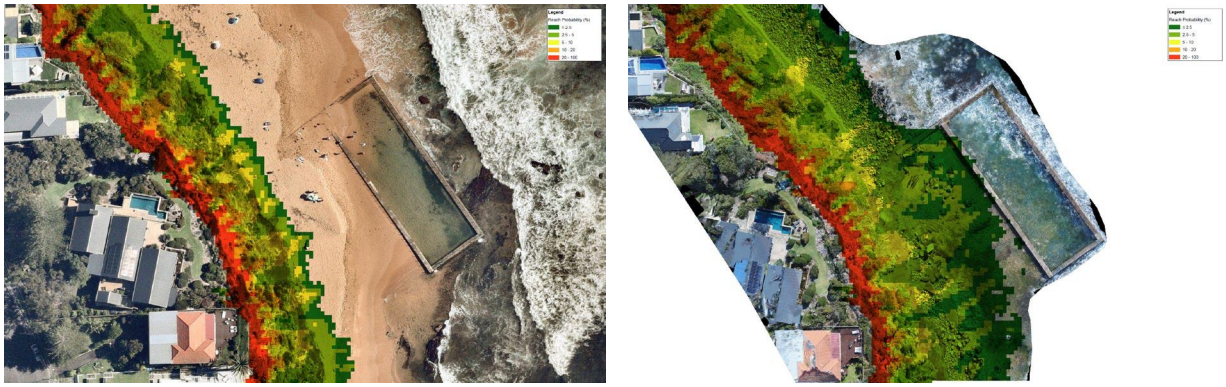


Figure 7: Example of 3D rockfall modelling for coastal cliff in NSW showing the dampening effect of sand on reach probability: Left with sand on beach, Right with exposed shore platform of hard rock.

7 CHALLENGES WITH RISK MITIGATION AND TREATMENT

In the context of coastal cliffs, Bird (1994) notes that when accidents occur, there is invariably a demand that something be done to make them 'safer'. Furthermore, geotechnical practitioners often feel a sense of obligation to propose mitigation works given risk management is a core tenant of the AGS (2007c) risk management guidelines. However, in most circumstances the 'sanctity' of the natural setting and visual amenity preclude the application of hard engineering solutions. Furthermore, owing to the vast extent of publicly accessible coastal cliffs and the scale and number of hazards, these hard engineering works are usually cost prohibitive to managing authorities.

Consequently, to balance mitigation costs and risk, the establishment of hazard warning signage is often an attractive option for managing authorities due to the low cost, ease and speed of installation and almost complete lack of other alternatives. There is often a perception that signage provides effective protection against personal injury claims with respect to legislation such as the Civil Liability Act 2022 (NSW). Legal precedence court rulings involving general warning signage for any forms of hazards can be subjective, for example whether the messaging, number of and location of the signage is appropriate. However, the importance of warning signage has been noted during inquests into a number

of coastal rockfall fatality cases. The Beaumaris case involved the death of a 3-year-old boy who was killed by a rockfall while sitting at the toe of cliffs at Beaumaris, Port Phillip Bay. Bird (1994) reported that the Deputy Coroner of Victoria found that the local council had contributed to the accident by failing to erect warning notices.

On September 27, 1996, four adults and five children were killed by a rockfall at Huzzas Beach, Western Australia in what later became known as the 'Gracetown tragedy'. The people were sheltering from a heavy rainstorm under a large rock overhang, which collapsed suddenly without warning. The coronial inquiry found the deaths were accidental. The Coroner added riders that authorities responsible for cliff areas should monitor the potential hazards of rockfall and should work together so that potential risks be effectively managed, while also noting that a minimum response to danger areas would be to erect warning signs (Gordon, 1999).

The ultimate responsibility for increasing public awareness falls to the managing authority of an asset and this cannot be contracted to other parties. However, the placement of signage in coastal settings is often problematic. Signs placed near the toe of cliffs are often damaged by landslides and, in order to read the signs, individuals can unknowingly be within the hazard runout zone because there is a perception that only the area behind the sign is hazardous. Furthermore, erecting signs further away from the cliffs, such as on rock platforms or beaches is usually not feasible due to damage from waves. Placement of signs at access points to the beach may be more appropriate in some instances, although this requires a level of understanding of human behaviour which is by nature unpredictable.

Despite signage at many coastal cliff locations our observations suggest that there is a sense of public unfamiliarity with coastal hazards and perhaps also a disregard for signage (Figure 8). Insights into the psychology of the public's beliefs about rockfalls and associated high risk behaviour, and public interpretation of coastal rockfall hazard warning signage is offered by Aucote et al. (2010, 2012). The study found that many people doubt the validity of warning signs. Approximately two thirds of participants in the study thought that warning signs were erected even when there was only a small chance of injury, about one third thought that warning signs were erected even if rocks were not falling on a regular basis, and about 40 % thought that the main reason authorities put up warning signs was to avoid being sued. Aucote et al. (2012) also found that interpretation of warning signage was also variable with less than 40% of participants correctly interpreting the messaging to keep a clear distance from the cliffs (Figure 9).



Figure 8: Examples of apparent disregard or unawareness of rockfall hazards, despite signage.

Interpretation of signage	%
Do not go too close to the cliff face	39.5
Do not climb the cliff face	23.6
Do not stand under/next to cliff face	13.2
Do not climb and Do not stand under/next to cliff face	18.4
General warning to be careful – could not state what "careful" entailed	5.3

Figure 9: Five interpretations of warning signs and the percentage of participants who endorsed them (Aucote et al. 2012).

The study by Aucote et al. (2012) assessed that comprehension of signage was hampered by a lack of prior knowledge of the particular risk, a failure to think carefully about the situation and misleading pictorials on signs. To attempt to overcome these

issues, recently installed signage at some coastal sites the authors are involved with have been designed to include; actual photographs of the site and rockfalls, annotated hazard zones, QR codes and additional instructional information (Figure 10).

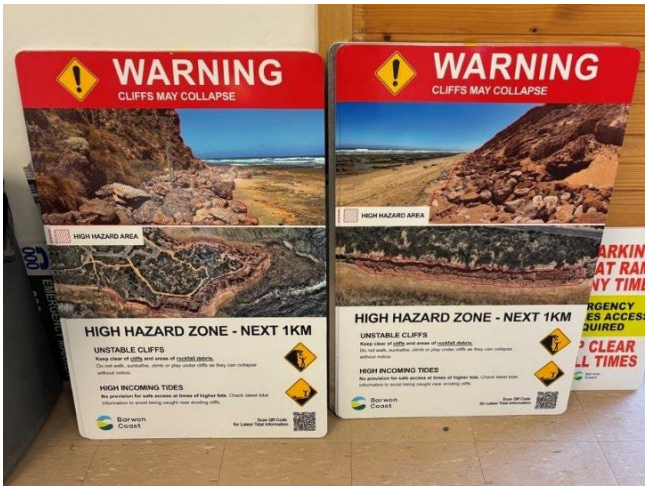


Figure 10: Examples of recent rockfall warning signage.

8 DISCUSSION

Risk assessment is a valuable tool in assessing natural hazards including coastal landslide hazards. It provides a structured framework and process for assessment that can be largely replicated by different consultants and provides standard outcomes in the form of an annual probability of loss of life or damage. However, the quantitative nature of risk assessments should not be taken to imply greater precision and accuracy than can be feasibly achieved and this is particularly apparent in coastal settings. Limitations in knowledge and uncertainty exist for all input components of the risk process and these are rarely adequately relayed in the final assessment, thus somewhat clouding the probabilistic nature and inherent uncertainty of the advice.

The review of risk estimates against certain criteria may result in a determination of "tolerable risk". Such a determination is usually made prior to an event but the question remains; does "tolerable" remain "tolerable" in the immediate aftermath of a hazardous event? Experience suggests that managing authorities and the general public, perceive risks to be unacceptable after coastal cliff deaths, regardless of the level of estimated risk.

Whilst most Australians living near the coast are familiar with beach safety hazards such as drowning or fauna interactions, our review of coastal landslide fatalities suggests an unfamiliarity with coastal landslide hazards, despite these hazards being responsible for a large proportion of the total landslide deaths in Australia. Perhaps this is because Australians aren't very familiar with landslide hazards generally, or perhaps individuals are more likely to be exposed to landslide hazards in coastal settings as opposed to other settings such as residential buildings, driving or other recreational activities.

This review of the challenges and difficulties with undertaking coastal risk assessments has found there is probably similar levels, if not more uncertainty associated with inputs to coastal hazard estimates compared with other landslide assessments. This is partly due to the difficulties in accurately identifying the location of hazards which may have hidden defects or uncertain failure mechanisms, the lack of coastal rockfall inventories, difficulties interpreting rates of cliff retreat and unpredictable human behavioural patterns. Consequently, we have imperfect knowledge of the nature of the hazard, the likelihood of occurrence and knowledge of travel distances meaning ultimate estimates of risk levels for coastal landslide hazards contain significant inherent uncertainty.

This paper has highlighted several challenges associated with the determination of key probability inputs for coastal risk assessments. Assessment of these inputs should be based on all available evidence and information and shouldn't rely on one stream of evidence. It should also be recognised that judgement and 'degree of belief' approaches are often vital in coastal settings given the paucity of information. It is therefore incumbent on practitioners undertaking coastal landslide risk assessments to better communicate such challenges and associated uncertainties to clients to allow more informed and appropriate decision making.

9 ACKNOWLEDGMENTS

The authors wish to thank David Field for assisting with figure preparation and his review comments. Isabella Jaukovic is also thanked for her comments on the paper.

10 REFERENCES

AGS (2007a) Guideline for Landslide Susceptibility, Hazard and Risk Zoning for Land Use Management. *Australian Geomechanics*, 42(1), 13-36.

AGS (2007c). Practice Note Guidelines for Landslide Risk Management. *Australian Geomechanics*, 42(1), 63-114.

AGS (2007e). Australian GeoGuides for Slope Management and Maintenance. Australian Geomechanics Society.

Australian Geomechanics, Vol 42, No1,

Aucote, H.M., Miner, A., & Dahlhaus, P. (2010). Rockfalls. Predicting high-risk behaviours from beliefs. *Disaster Prevention and Management*, 19, 20–31.

Aucote, H.M., Miner, A., & Dahlhaus, P. (2012): Interpretation and misinterpretation of warning signage: Perceptions of rockfalls in a naturalistic setting, *Psychology, Health & Medicine*, DOI:10.1080/13548506.2011.644247

Caine, N., and Jennings, J. N. (1968). Some blockstreams of the Toolong Range Kosciusko State Park, New South Wales. *Journal and Proceedings, Royal Society of New South Wales* 101, 93–103.

Bird, C., F. (1994). Cliff Hazards and Coastal Management. *Journal of Coastal Research*, 299–309.

Dana, J.D., (1849). *United States Exploring Expedition* (v.10 (1849) [Geology Text]). G. Putnam. Retrieved from https://doi.org/10.5962/bhl.title.68069

Delaney, M.G., (2005). Coastal cliff line stability and regression in the Newcastle Region, *Australian Geomechanics*, 40 (1), 31 – 38.

Fell, R., Ho, K.K.S., Lacasse, S. and Leroi, E. (2005). A framework for landslide risk assessment and management. In *Landslide Risk Management*, Editors O Hungr, R Fell, R Couture and E Eberhardt, Taylor and Francis, London, 3-26.

Flentje, P., (2012). Evolution of the Illawarra Escarpment Terrain. *Australian Geomechanics*, 47(1), 1- 16.

Gill., E., D. and Lang., J., G., (1983). Micro-erosion meter measurements of rock wear on the Otway Coast of Southeast Australia. *Marine Geology*, 52 (1983) 141-156.

Gordon, F. (1999). The Rockfall of Huzzas Cliff, Gracetown, Western Australia. In *Proceedings 8th Australia New Zealand Conference on Geomechanics: Consolidating Knowledge*. Australian Geomechanics Society.

Heimsath, A. M., Chappell, J., Dietrich, W. E., Nishiizumi, K., & Finkel, R. C. (2000). Soil production on a retreating escarpment in southeastern Australia. *Geology*, 28(9), 787-790. https://doi.org/10.1130/0091-7613(2000)28<787:SPOARE>2.0.CO;2

Hungr, O., Leroueil, S. & Picarelli, L. (2014) The Varnes classification of landslide types, an update. *Landslides* 11, 167–194. https://doi.org/10.1007/s10346-013-0436-y

Hunter A., J., Flentje, F and Moon A. T. (2022). Bulli Pass Landslide Risk Management Part 1 – Hazard Assessment. *Australian Geomechanics*, 57(3), 97-113.

Kennedy, DM, Brighton., B, Sherker., S and Woodroffe., D. (2012) 'Towards a Typology of Rocky Coasts in the Context of Risk Assessment'. *Proceedings of the 21st NSW Coastal Conference,* Australian Coastal Society Ltd.

Kotze., G., Hunter., A., J. and Field., D. (2024). 'A 30 Year review of Rockfall Frequency and Coastal Cliff Regression on the Northern Beaches of Sydney, Australia'. *Australian Geomechanics*, 59(3), 57-71.

Moon A.T., Wilson R.A. and Flentje P.N. (2005). Developing and using landslide size frequency models. In: Hungr O, Fell R, Couture R and Eberhardt, E (eds) *Landslide Risk Management*, CRC Press, 681-690.

Muller., B. J., Dahlhaus., P. G. and Miner., A. S. (2006) Coastal rockfall hazard identification, Barwon Heads, Victoria. Australian Geomechanics, 41 (3), 85-92.

Paul., D. and Miner., A.S. (2025) Practical communication of uncertainty in quantitative landslide risk assessment, *Australian Geomechanics*, 60(1).

Roberts., N., J. and Miner., A., S. (2023). Collating southeast Australia's slope-failure casualties. *Proceedings of the 14th Australia and New Zealand Conference on Geomechanics, Cairns 2023 (ANZ2023).*

Sunamura, T., (1992), *Geomorphology of Rocky Coasts*. Wiley, Chichester

Thom, B.G. and Roy, P.S., (1985), Relative Sea Levels and Coastal Sedimentation in Southeast Australia in the Holocene. *Journal Sedimentary Petrology* Vol. 55, 257-64.

Thom, B. G., Keene, J. B., Cowell, P. J. and Daley, M., (2010). East Australian marine abrasion surface. *Geological Society special publication* 346(1), 57-69.

Trenhaile, A.S., (2000) Modelling the development of wave-cut shore platforms. *Marine Geology*, 166 (1) 163-178

Trenhaile, A. S., (2002). Rock coasts, with particular emphasis on shore platforms. *Geomorphology*, 48: 7-22.

Trenhaile, A. S., (2010). The effect of Holocene changes in relative sea level on the morphology of rocky coasts. *Geomorphology*, 114, 30– 41.

Trenhaile, A. S (2011), 'Predicting the response of hard and soft rock coasts to changes in sea level and wave height', *Climatic Change*, vol. 109, 599-615.

Watman., A, Ettore Guccione., D, Bahootoroody., F, Thoeni., K and Giacomini., A. Rockfall instability analysis of coastal cliffs: A case study along Susan Gilmore Beach (Newcastle, NSW). *Proceedings of the 14th Australia and New Zealand Conference on Geomechanics, Cairns 2023 (ANZ2023).*

Woodroffe., C. D, (2003). *Coasts : form, process, and evolution*, Cambridge University Press, New York.

Young, A. (1972). *Slopes*, Edinburgh: Oliver and Boyd

Appendix A: Table A1 – Summary of reported Australian coastal landslide fatalities

Date	Location	State	Description	Number Killed	Number Injured
February, 1926	Kurnell	NSW	A couple were taking tea under an overhanging rock when several loosened pieces of rock fell on top of the male, killing him. One man aged 35 died	1	0
April, 1927	One Mile (Port Stephens)	NSW	A landslide hurtled down onto a party of campers at One Mile Beach, killing one and injuring another. It is thought that the landslide was caused by recent torrential rain accumulating in a crevice about three parts of the way up the hill. One male, aged 23, died, three persons injured (SMH 18/4/1927). One male aged 42: injuries to knee and back. Two other males treated for bruises and abrasions.	1	3
August, 1929	Merewether Beach, Newcastle	NSW	A fall of earth on the cliff face at Merewether injured three people who had been collecting coal from an outcrop. Three males injured (SMH 9/9/1929). Male, aged 65; broken ribs, broken right arm, abrasions and shock; One boy (aged 7), broken arm, head injuries and shock; One boy (aged 6), abrasions to the forehead and shock.	0	3
29 January 1933	Bulgo Beach/ Otford	NSW	Roy Burns (15) was killed by a landslip at Bulgo Beach.	1	0
2 September 1936	Amity Point, North Stradbroke Island	QLD	20-foot-high sea cliff collapsed at Amity Point, burying two children under several tonnes of sand. One child died. They had been tunnelling into a sand cliff formed some months before by marine erosion. The girl, aged 7, was rescued uninjured, but prolonged efforts to resuscitate her brother, aged 13, were unsuccessful (SMH 3/9/1936).	1	0
1 November 1948	Cape Schanck	VIC	Two brothers were killed when trapped by an avalanche of rocks while fishing under a 200 ft cliff at Simpson's Bay near Cape Schanck. The men were Colin Bibby (33) married of Glen Iris and Kenneth Bibby (34) married of Flemington. Three other men miraculously escaped injury. They rushed desperately for cover as they were showered by small rocks	2	0
September 1950	Back Beach, Sorrento, Mornigton Peninsula	VIC	A sea cliff at Sorrento collapsed on top of a man and a girl, burying but not killing them. Two people injured, and a rescue attempt was mounted (SMH 18/9/1950). One man and a 13-year-old girl were buried.	0	2
13 April 1952	Demons Bluff Cliffs, Anglesea	VIC	Young man and woman caught in landslide while sitting at base of steep cliffs	0	2
August 1952	Lobster Beach, Broken Bay	NSW	The movement of a group of boys up a steep hill is believed to have started a landslide at Lobster Beach. One boy was killed by a falling rock. The landslide occurred on a 'mountain'- categorised as a hill. The landslide was believed to be induced by the movement of the boys over the boulders. One male aged 17 died when he was crushed by a boulder (SMH 3/8/1952).	1	0
April 1958	Port Willunga, Adelaide	SA	Rocks and rubble fell from a cliff onto a party who were about to eat lunch in a cave by the beach at Port Willunga. Two men were killed, and one woman was injured. Two males (37, ?) killed, (SMH 6/4/1958) one woman critically injured with multiple fractures.	2	1
1960's	Lawrence Hargrave Drive, Stanwell Park	NSW	Reported (not confirmed), in a Motor Vehicle Accident due to landslide on Lawrence Hargrave Drive in 1960's	1	0

Date	Location	State	Description	Number Killed	Number Injured
1 January 1990	Beaumaris Cliffs, Beaumaris	VIC	3-year-old boy killed by rockfall near cliffs	1	0
January 1996	Sorrento Back, Beach, Sorrento	VIC	A 7-year-old boy sheltering under a sandstone and limestone cliff was killed when a rock half the size of a car fell on him. Cliffs are unstable and crumble, so accidents occur regularly.	1	0
27 September 1996	Huzzas Beach, Gracetown	WA	A 14m high cliff on the south side of Cowaramup Bay collapsed, killing 5 children and 4 adults and injuring 2 children and 1 adult. There was a surfing event on the beach at the time and people took shelter at the base of the cliff during a heavy rainstorm.	9	3
16 January 1997	Fishery Beach, Bremer Bay	WA	A group of people were abseiling at a Scripture Union youth camp. One person, not on the camp, was belaying when a large rock fell from above and, dislodging other rocks, hit this person. The cause of the rock fall was unknown and, as the only preceding rainfall that month was 1mm in the 24 hours to 9am on 15 January, rainfall was not the trigger. The person died about seven and a half hours later while being flown from the local hospital to Perth.	1	0
18 February 1998	Totem Pole, Tasmania	TAS	British tourist and climber Paul Pritchard travelled to Tasmania to climb an infamous sea stack named the Totem Pole on Tasmania's east coast in 1998. As Mr Pritchard was at the base preparing to climb, a rock fell on his head. He suffered a severe head injury and became a hemiplegic as a result of the accident.	0	1
4 November 2001	Jan Juc Beach	VIC	An 18-year-old man was walking with friends along the beach at the time of a large rock fall from an 50 m. He was buried up to his shoulders in the landslide. His two companions managed to jump clear. It took three hours to rescue him because of dangerous conditions caused by continuing rock falls. He was flown to hospital with crush injuries to both legs.	0	1
21 February 2004	Bangalley Headland, Avalon	NSW	Two Austrian tourists stood on a blocky sandstone ledge at the top of a coastal cliff. The block that they had been standing on, collapsed. One man fell forward over the cliff and was found dead beneath the boulder, sand and debris. The other fell backward on to the headland and suffered a few scratches and psychological trauma. The ground under the rock was unstable due to wind erosion.	1	1
6 September 2014	Sam Fiszman Park, Bondi Beach	NSW	A man climbing a cliff face fell 5m, hit his head on a rock ledge, then fell another 2m, when the rock that he was holding on to, while trying to take a photo of his friends at the top of the cliff, gave way. His friends phoned emergency services, and he was rescued by helicopter, assessed by paramedics, and airlifted to hospital. He had head injuries and a suspected broken collar bone.	0	1
22 November 2015	Depot Beach	NSW	A young man was standing on the edge of a limestone cliff, looking for a good place to surf, when it "crumbled beneath his feet". He lost his footing and fell more than 20m. Several people, including two nurses, rendered first aid until paramedics arrived in the Snowy Hydro Southcare helicopter. He was flown to the Canberra Hospital, suffering from two broken arms, a broken jaw, chipped teeth, punctured lung and fractured T8 vertebra. He was operated on over the next two days and was expected to make a full recovery.	0	1
3 December 2021	Jarosite Cliffs, Bells Beach	VIC	A 28-year-old man died after a 30-metre cliff face collapsed at Bells Beach.	1	0

https://doi.org/10.56295/1ACEG19

GIS MAPPING OF LANDSLIDE SUSCEPTIBILITY AND LIFE RISK IN BLUE MOUNTAINS NATIONAL PARK

Zack Tuckey
Jacobs Group (Australia) Pty Ltd

ABSTRACT

Blue Mountains National Park is part of a world heritage-listed conservation area managed by New South Wales National Parks and Wildlife Service, spanning over one million hectares of protected wilderness on the western outskirts of Sydney. The park encompasses an uplifted tableland of Triassic sandstone, underlain by shale, claystone, and coal measures. The escarpment is incised by rivers and streams, forming deep valleys surrounded by cliffs. Some of the most popular walking tracks receive hundreds of thousands of annual visitors and follow steep routes that connect the top of the escarpment to the valleys below via switchbacks, stairways and ladders that pass under high cliffs and overhangs. Typically, a new rockfall or debris slide is reported in the park about once per month, and over the last decade, landslides have infrequently caused serious injuries and fatalities; more frequently, they have caused major damage to walking tracks and fire trails.

Previous landslide risk assessments in the park have usually been focused on life risk for bushwalkers, with assessments undertaken on a site-specific basis in response to past instability or incipient slope failure. Under the National Parks *Landslides and Rockfalls Procedures*, the results of quantified risk assessments are used to estimate societal risk and develop appropriate risk mitigation strategies. Despite many years of reactive and site-specific landslide risk assessment, the park contains hundreds of kilometres of trails and walking tracks, and many locations have never been subject to any form of landslide risk assessment. This paper presents methods and findings of a proactive GIS investigation of landslide susceptibility and risk across 3400 km^2 of Jamison and Grose Valley, encompassing the most visited regions of the park. A landslide susceptibility map was produced from analysis of digital elevation models, expected rainfall intensity, bedrock geology, and hillslope erosion datasets. The concept of a "synthetic landslide return period" is introduced to link GIS-based landslide susceptibility scores to potential life risk for track and road users. The resulting susceptibility and risk maps can be interrogated to rank the relative landslide risk exposure of linear infrastructure, and identify locations that may require additional administrative risk management, site investigation, or engineered slope risk mitigation works.

1 INTRODUCTION

Blue Mountains National Park is one of the most visited bushwalking destinations in Australia, located on the western margin of the Sydney Basin. The park is managed by the New South Wales National Parks and Wildlife Service (NPWS) and contains hundreds of kilometres of walking tracks and fire trails; the most popular tracks receive hundreds of thousands of annual visitors and traverse under high sandstone cliffs and across steep terrain subject to frequent rockfall and landslides. In 2019 NPWS first published landslide risk management procedures based on the quantitative risk assessment (QRA) framework of the Australian Geomechanics Society (2007). When landslide hazards pose an unacceptable societal risk to life, NPWS seeks to mitigate the risk in accordance with the *ALARP* principle, which tests whether risks have been reduced *as low as reasonably practicable*, such that the level of risk reduction is proportionate to the cost and environmental impact of the works, as well as the safety risks faced by workers undertaking remediation activities. Until recently, landslide hazards in the park have usually been managed using a reactive approach, with site-specific investigations undertaken in response to new or incipient slope instability.

Decades of local NPWS staff experience have produced a good understanding of the slope failure mechanisms and frequency of instability for some of the most landslide-prone locations in the park. Despite this extensive institutional experience, many locations have never been subject to formal landslide risk assessment. Following an internal review of landslide risk, NPWS commissioned a proactive GIS study to investigate spatial trends in landslide susceptibility and risk across a 3400 km^2 region spanning most of Jamison Valley and Grose Valley. The primary goal of the study was to develop a GIS methodology that could be used to rank the relative landslide risk exposure for all walking tracks and fire trails using a standardised approach, allowing for direct comparison and ranking of assets by relative landslide risk exposure. The outputs of the study included a GIS "heat map" of landslide susceptibility, with walking tracks and fire trails divided into 10 m long sections and colour-coded according to a series of derived measures for landslide susceptibility and life risk.

This paper describes the GIS mapping methodology, tailored to the geological setting of the Blue Mountains, and introduces the concept of a "synthetic landslide return period" that links landslide susceptibility to annualised life risk. The resulting GIS "heat map" and colour-coded track alignments provide a useful tool to visualize the spatial variation in

landslide risk across multi-kilometre tracks and trails that traverse across variable terrain, and the entire GIS database is hosted on a web viewing platform to allow NPWS to interrogate the dataset and generate customised map sheets. The "synthetic return period" approach provides a semi-quantitative assessment of relative life risk that, over time, can be benchmarked against empirical landslide magnitude-frequency records collected by NPWS, increasing confidence in the critical QRA parameter P_H which represents the estimated annual probability of landslide initiation.

2 LANDSLIDES IN BLUE MOUNTAINS NATIONAL PARK

2.1 GEOLOGICAL AND PHYSIOGRAPHIC SETTING

The Blue Mountains are an uplifted sandstone tableland that has been deeply incised by rivers and creeks, with cliff up to 200 m high surrounding the Jamison and Grose Valleys. The communities of Katoomba and Blackheath are built on top of the uplifted sandstone plateau, with park visitors typically accessing Jamison Valley and Grose Valley by descending steep switchbacks, fabricated metal and carved bedrock stairways that connect the top of the escarpment to the valley trails below. The topography of the park is dominated by prominent escarpment cliffs. Figure 1 shows an isometric view of the publicly available 2 m resolution digital elevation model (DEM) near Katoomba, coloured by slope angle. A continuous 18 km stretch of walking tracks traverses across the steep upper talus slopes and along the base of the cliffs between Narrow Neck in the west and Wentworth Falls in the east. The slope gradient decreases with distance away from the upper cliffs, before descending into the nested v-shaped valleys of Govetts Leap Creek in the Grose Valley and Kedumba River in the Jamison Valley, which have eroded beneath the Illawarra Coal Measures and into Shoalhaven Group, which forms the basal unit of the Sydney Basin.

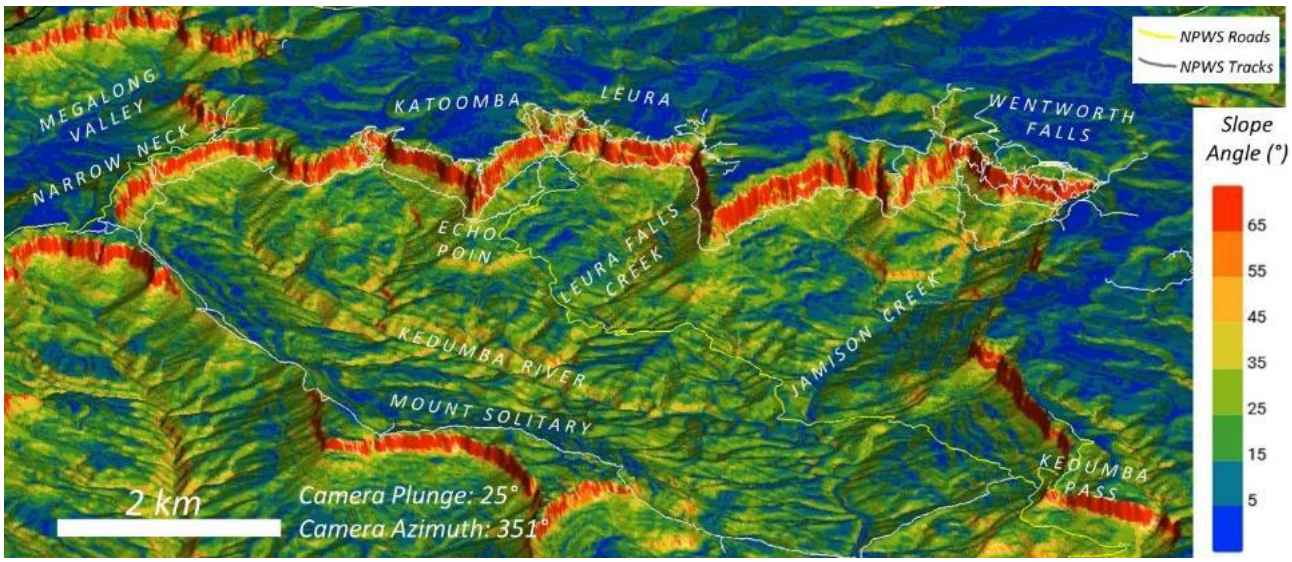


Figure 1: Isometric view of regional elevation model centred on Jamison Valley, coloured by slope angle

The network of valley trails includes many routes that traverse along the base of the sandstone cliffs within the "rockfall shadow" of the escarpment. Figure 2 shows an interpreted cross section and annotated photogrammetry image highlighting the key geological units and walking tracks that traverse across the cliffs near Wentworth Falls. Zones of geologically frequent rockfall are inferred from the presence of overhangs and pale, fresh sandstone.

The upper cliffs are comprised of the massive, quartzose Banks Wall Sandstone of the Narrabeen Group, which is locally up to 120 m thick. The Banks Wall Sandstone is underlain by the Mount York Claystone, a marker unit of weak, red-brown claystone that that forms a continuous bench in the middle of the cliffs that can be traced for kilometres across the escarpment. The lower cliffs are formed by the Burra-Moko Head Sandstone, an early Triassic quartzose to quartz-lithic sandstone that is up to 110 m thick, underlain by interbedded claystone, shale, and quartz-lithic sandstone of the Caley Formation, which forms the basal unit of the Narrabeen Group and the Permian-Triassic boundary. The late Permian Illawarra Coal Measures outcrop at the base of the cliffs, comprising coal seams, torbanite (oil shale), siltstone, and minor sandstone layers. Through the late 1800s and into the early 1900s numerous underground mining operations extracted torbanite and coal from these formations using the room and pillar technique, producing extensive networks of mine workings more than 200 m below the crest of the escarpment. Underground coal mining operations have been associated with major cliff collapses at various locations throughout the Blue Mountains including at the Newnes oil shale mine between 1911 and 1915 (Pells et al., 1987), the Dogface Rock landslide of 1931 above the Katoomba Colliery (Tuckey, 2023) and more recent failures at Nattai North Colliery in the 1960s and 1970s (Cunningham, 1988).

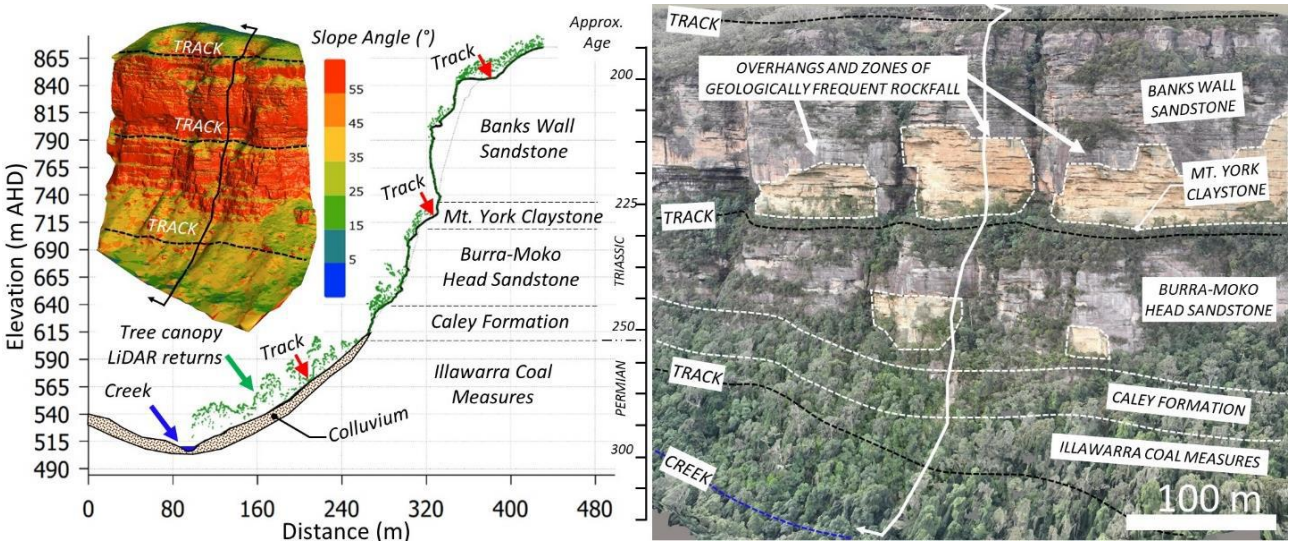


Figure 2: Interpreted LiDAR cross section and photogrammetry imagery of the cliffs near Wentworth Falls

The next section presents examples of typical landslide mechanisms observed throughout the park.

2.2 ESCARPMENT RETREAT AND LANDSLIDE MECHANISMS

Following uplift of the Blue Mountains during the late Triassic, the geomorphic processes shaping the landscape have been dominated by erosion by stream incision and gravity-driven slope failures. Rockfalls are ubiquitous along the escarpment cliffs, being products of the long-term processes of valley incision and escarpment retreat that have produced the modern landscape. Figure 2 shows the conceptual sequence of v-shaped valley incision into Jamison Valley, occurring due to the variations in rock mass strength between the stronger Narrabeen group sandstones at the top of the escarpment and the weaker underlying Illawarra Coal Measures, Shoalhaven Group, and Devonian basement rocks.

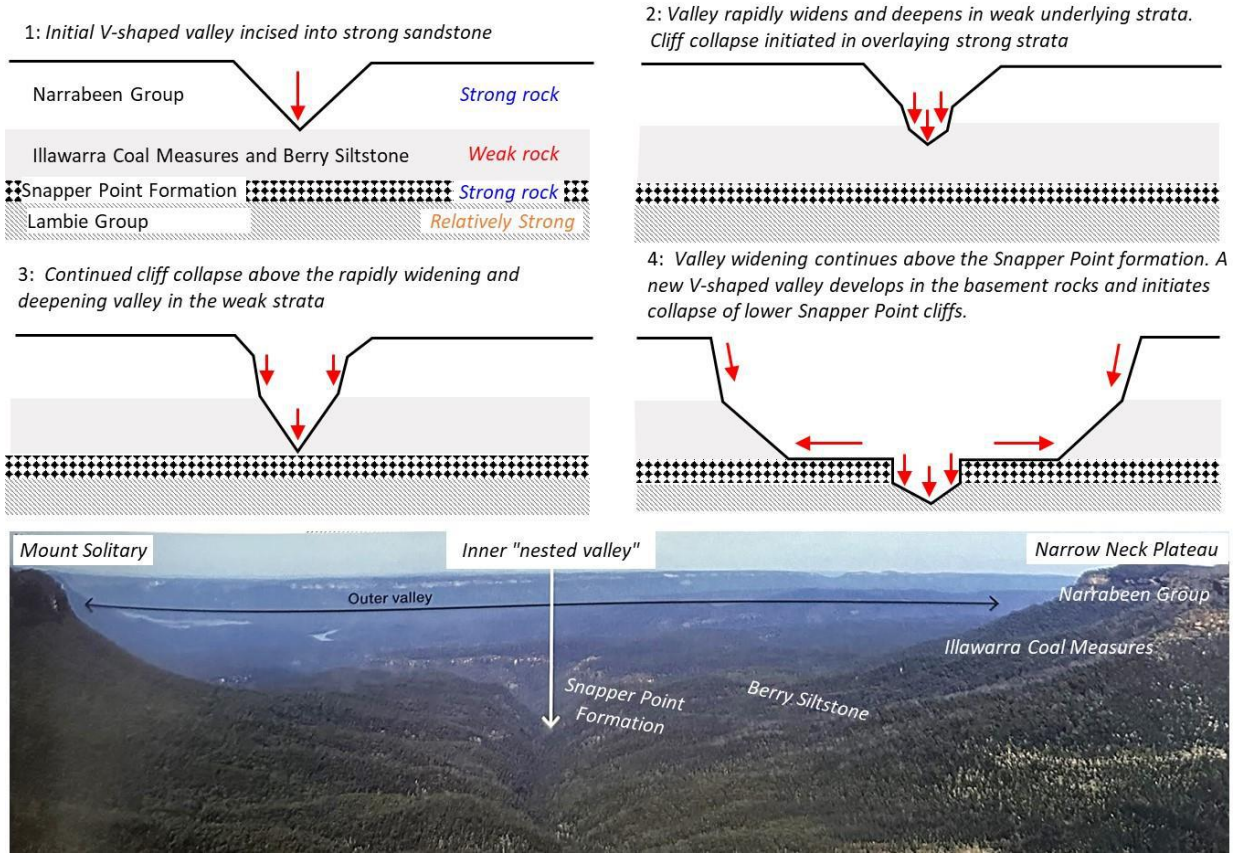


Figure 3: Formation of nested river valleys in the Jamison Valley (modified after Hatherly and Brown, 2022)

NPWS records and area staff experience suggest that the most common landslide types in the Blue Mountains include (1) **rockfalls and topples** initiating from the sandstone cliffs, varying in scale from discrete failure of centimetre-scale blocks, up to rock mass-scale cliff collapse events; (2) **debris slides** initiating on steeper sections of the colluvial talus slopes and valley rim (typically involving basal shearing along the interface between soil and bedrock driven by intense or prolonged rainfall); and (3) channelised **debris flows** that initiate along the upper slopes of the valley rims, with runout along creeks or ephemeral drainage lines, usually triggered by short intense rainfall events.

Rockfalls in the Narrabeen Group sandstone rocks often involve failure of overhanging or undermined blocks of sandstone. Two regionally ubiquitous vertical joint sets interact with subhorizontal bedding to produce cubic to tabular-shaped blocks that are kinematically free to detach from the cliffs. Failure is promoted by the preferential erosion of weak shale and claystone layers that degrade with cyclical changes in moisture content. Where tracks pass directly under natural or excavated overhangs, blocks may freefall just a few metres directly onto the track; other rockfalls have involved long runout of blocks onto tracks that traverse the valley slopes below the base of the cliffs. Rockfall initiation may be promoted by tree root jacking, elevated pore pressures from intense rainfall events, or may occur with no obvious external trigger, as the culmination of slow, long-term crack subcritical growth driven by gravitational stresses.



Figure 4: Conceptual sketch of time dependent rockfall initiation and examples of recorded rockfall impacts

Debris slides commonly occur on the talus slopes immediately upslope from walking tracks, or localised "hanging swamps" that have developed around the rim and middle benches of the escarpment cliffs. Collapse may be triggered by short, intense rainfall or prolonged wet periods that cause the soil to become saturated, reducing its effective shear strength. Failures often comprise a mixture of granular residual and colluvial soils, boulders, and vegetation (Figure 5). Slopes may show evidence of slow, long-term creep, with potential for sudden, rapid acceleration if pore pressures become sufficiently elevated to induce undrained failure.



Figure 5: Conceptual sketch and example of a debris slide in colluvium and residual soil

When debris slides initiate near creeks or ephemeral drainage lines along the crest of the escarpment, they can transition to channelised debris flows that entrain additional material along the runout path, producing a highly mobile, fluidised mixture of bouldery debris along with trees and surficial vegetation. Where drainage lines run over the crest of vertical cliff faces, the fluidised mass free-falls and may reach velocities exceeding 100 km/h. Recent debris flows in the Jamison Valley have produced runout distances of hundreds of metres; several were triggered by short, intense rainfall events during the La Niña weather conditions in the summers of 2020, 2021, and 2022 (Figure 6).

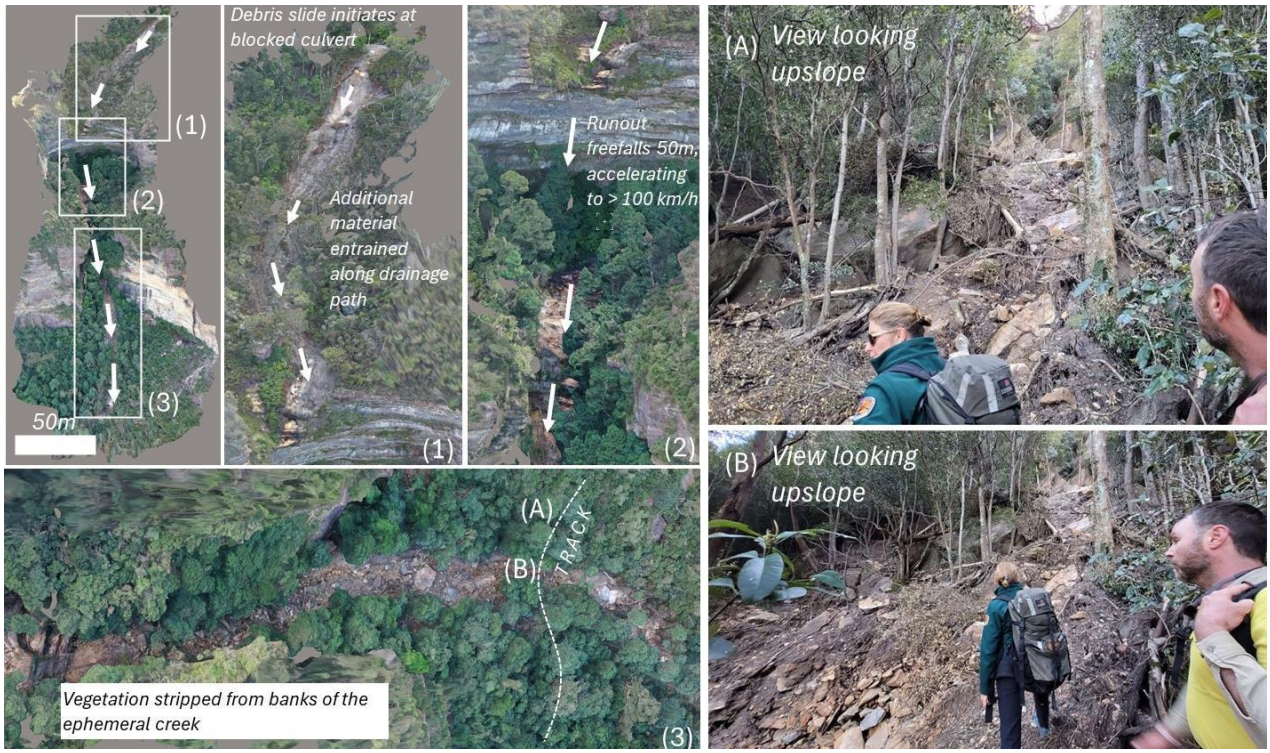


Figure 6: Example of a channelised debris flow in Jamison Valley (occurred in 2022)

A review of historical landslides undertaken for this study shows that the magnitude-frequency relationship appears to conform to a log-normal or negative exponential distribution, in agreement with published empirical trends observed in diverse geological environments around the world (e.g. Hungr et al., 1999). Most events comprise small, localised slumps or rockfalls with edge dimensions in the order of 1 m or less. However, there is also evidence for very large, deep-seated landslides with volumes in the millions of cubic metres. Figure 7 shows two examples including a recent multi-lobe debris slide on the southern flanks of Mount Solitary that occurred in early 2022, promoted by intense La Niña rainfall, and an ancient landslide at Carne Creek dated to 13,000 years, with estimated volume of 30 Mm^3 (Tomkins et al., 2007).

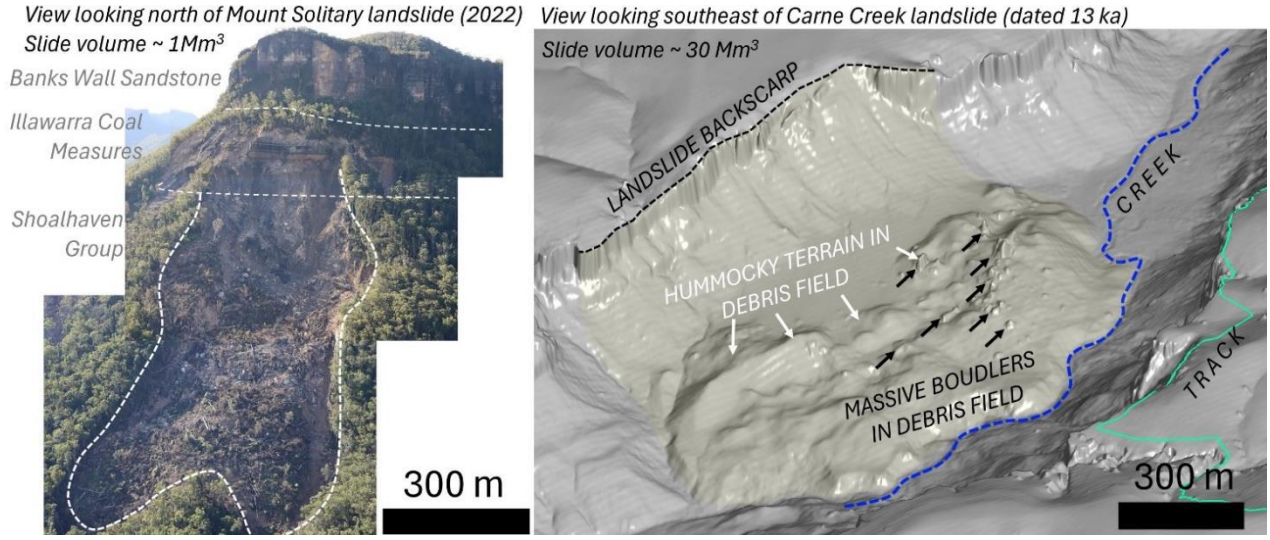


Figure 7: Examples of very large recent and ancient rock and debris slides with volumes exceeding 1 Mm^3

The Mount Solitary landslide was a low-consequence event because no walking tracks or other assets are near the runout path. However, other recent landslides have damaged walking tracks and critical fire trails, including a debris slide complex with volume in the tens of thousands of cubic metres that destroyed a section of Rodriguez Pass in Grose Valley in 2022. Previous QRA results for Rodriguez Pass, including consideration of risk to workers in re-establishing the trail through a landslide area, led NPWS to abandon the existing trail and develop an alternative access route into the valley.

The following sections introduce the concepts, methods, and results of the GIS landslide susceptibility and life risk mapping exercise. The landslide susceptibility rubric is specifically tailored to the landslide mechanisms described above, and the approach for estimating life risk uses empirical trends in landslide magnitude-frequency to link the landslide susceptibility score to an estimated "synthetic return period" for landslide initiation.

3 GIS LANDSLIDE SUSCEPTIBILITY MAPPING

3.1 LANDSLIDE SUSCEPTIBILITY CONCEPTS

Researchers and geoscience practitioners have published landslide susceptibility maps across a wide range of geological environments, resolutions, and scales. Caleca et al. (2025) presented a continental scale landslide susceptibility and risk mapping investigation spanning the European mountain ranges at 100 m resolution. Domínguez-Cuesta and Bobrowsky, (2013) produced a 1 km resolution Canada-wide landslide susceptibility map. Flentje et al. (2011) developed a 25 m^2 resolution qualitative landslide susceptibility map of the Sydney Basin. Smaller-scale examples include landslide susceptibility and hazard zoning maps produced for ski resorts in Kosciuszko National Park and the Victorian alpine region, and slope hazard zoning maps of the former Pittwater council (now part of Northern Beaches council) in Sydney; the production of these smaller-scale maps was initiated following the coronial enquiry into the Thredbo Landslide of 30 July 1997 (Leventhall and Kotze, 2008).

In broad terms, susceptibility describes the relative likelihood of landsliding. Common inputs into GIS-based landslide susceptibility maps include measurements of key terrain parameters such as slope angle, usually derived from a digital elevation model (DEM). Other spatial data may include bedrock and surficial geology units, gridded rainfall intensity data for a specific return period, vegetation cover and bushfire intensity mapping data, and proximity to watercourses (Corominas et al, 2014). Landslide inventory data may also be included, if the spatial extents of known or potential landslide features have been delineated through traditional geomorphology terrain analysis, or by using emerging techniques such as time-series change detection or machine-learning (Cochrane et al., 2024). Each of the input GIS datasets are assigned a weighted, numeric point score that contributes to the overall landslide susceptibility value. There is no universally accepted methodology for calculating landslide susceptibility, and the relative importance of each input dataset depends on site-specific engineering geology factors that control the expected landslide types. For this study, the landslide susceptibility "heat map" rubric was developed to consider the combined potential for the most common landslide failure mechanisms and impact scenarios:

- **Scenario 1:** A debris slide initiates at or near walking track level, with the source zone transporting downhill and potentially causing loss of the track or other asset. This scenario is particularly relevant for walking tracks that traverse across steep sections of the colluvial talus slopes.
- **Scenario 2:** A rockfall or debris slide initiates above the track and runs out onto the slopes below. This is the most common scenario for rockfall impacts to tracks that pass under the high escarpment cliffs. The likelihood of spatial impact is related to the "rockfall shadow" of the escarpment.

Figure 8 shows conceptual cross sections for both scenarios, along with corresponding examples of previous landslides where failure has either occurred near track level or involved runout of rockfalls initiating far above the track.

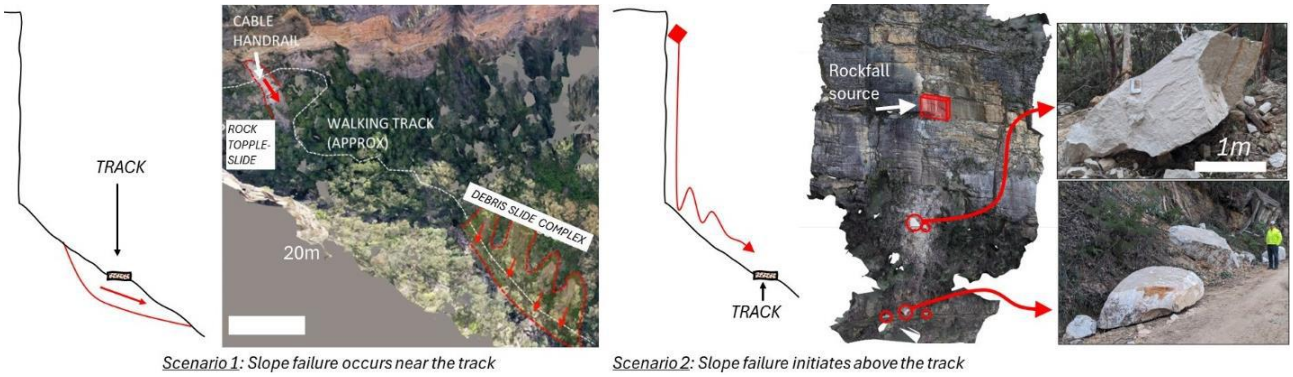


Figure 8: Landslide susceptibility combining the potential for localised instability and impact from above

3.2 GIS MAPPING METHODOLOGY

The landslide susceptibility scoring framework included five spatial input layers; these were selected based on data availability and expected correlation with the two landslide or rockfall impact scenarios described in the previous section. Data from each input layer were assigned a point score varying from 0 (nil susceptibility) to 100 (highest susceptibility). Weighting parameters were iteratively modified until the resultant "heat map" reflected the empirical evidence that most landslides and rockfalls occur in the immediate "rockfall shadow" of the escarpment cliffs and around the steepest sections of the valley side slopes, and incised creek channels. Table 1 summarises key details of each input data source.

Table 1: Summary of input GIS data and ranking for landslide susceptibility

Input Layer	Data Source *(Rationale)*	Data Range	Weighting
Horizon Angle	Publicly available LiDAR, 2 m resolution *Spatial likelihood of rockfall impact*	0 to 90°	35
Mean annual erosion using the Revised Universal Soil Loss Equation (RUSLE)	Modelled Hillslope Erosion over New South Wales, 100m resolution. Yang et al. (2017) *Shallow soil landslides triggered by rainfall*	0 to 25 t/ha/year	25
Slope Angle	Publicly available LiDAR, 2 m resolution *Soil or rock slide potential; runout distance*	0 to 90°	20
Rainfall IFD 7-day rainfall 50% AEP	Bureau of Meteorology, 2.5 km resolution *Orographic effects; higher rainfall areas are more susceptible to landsliding*	125 to 215 mm	15
Geology	NSW *Seamless Geology* (Colquhoun et al., 2022). *Weaker/more erodible units expected to correlate with increased frequency of landsliding*	Qualitative Point Ranking	5
		Total Susceptibility Points	**100**

The "rockfall shadow" of the escarpment is a key factor influencing the potential for impact under Scenario 2 (rockfall initiation above the site). Proximity to the cliffs is quantified using the "horizon angle" measured from every pixel in the map to the highest point on the surrounding terrain. The horizon angle is analogous to the energy line, which is used to estimate rockfall kinetic energy with the cone method, where rockfall velocity v is calculated from the vertical distance Δh between any point on the terrain and the projected energy line (Castelli et al., 2021). Figure 9 illustrates the concept, showing how a track directly under the cliffs would have an apparent horizon angle approaching 90° and effectively 100% probability of spatial impact. Horizon angle and probability of spatial impact decrease with distance away from the cliffs.

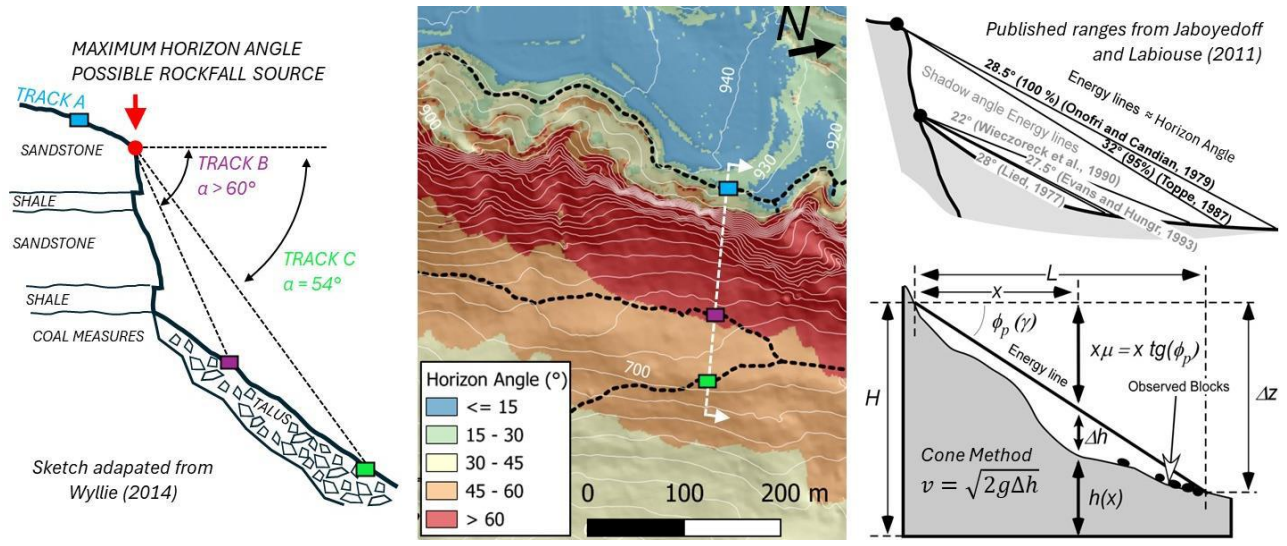


Figure 9: Illustration of the rockfall shadow concept, quantified by measuring maximum horizon angle

Empirical measurements of rockfall reach angle or Fahrböschung, measured from the source zone to the furthest runout block, can be used to develop a range of credible energy line values for a specific site (Field and Hunter, 2024). It is

important to note that the horizon angle is distinct from the "shadow angle", which is instead measured from the apex of the talus slope (i.e. the base of the cliffs) to the furthest runout block (Evans and Hungr, 1993).

In summary, the susceptibility input weightings reflect the expectation that topography dominates the potential for landsliding. Geological map units are assigned the lowest relative weighting, accounting for only 5% of the total landslide susceptibility score. Qualitative point scores were assigned to each geological unit, with the highest susceptibility scores assigned to alluvial and colluvial soils. The relatively weaker coal measures rock units were assigned higher susceptibility scores than the overlying massive sandstones of the Narrabeen Group. Despite the limited influence assigned to the geological unit layer, the role of geology is implicitly accounted for in the DEM-derived terrain measurements, because present-day landforms are a product of long-term escarpment retreat processes which in turn are controlled by geology.

3.3 GIS MAPPING RESULTS

Figure 10 shows plan views of the five input layers and resultant project-wide "heat map" of landslide susceptibility. Each pixel in the landslide susceptibility map has a score varying from a minimum of 0 (negligible probability of landslide impact) to a maximum of 100 (worst-case, highest likelihood of landslide impact). The data were interrogated to develop qualitative landslide susceptibility classes varying from *low* to *very high* as a visualisation aid.

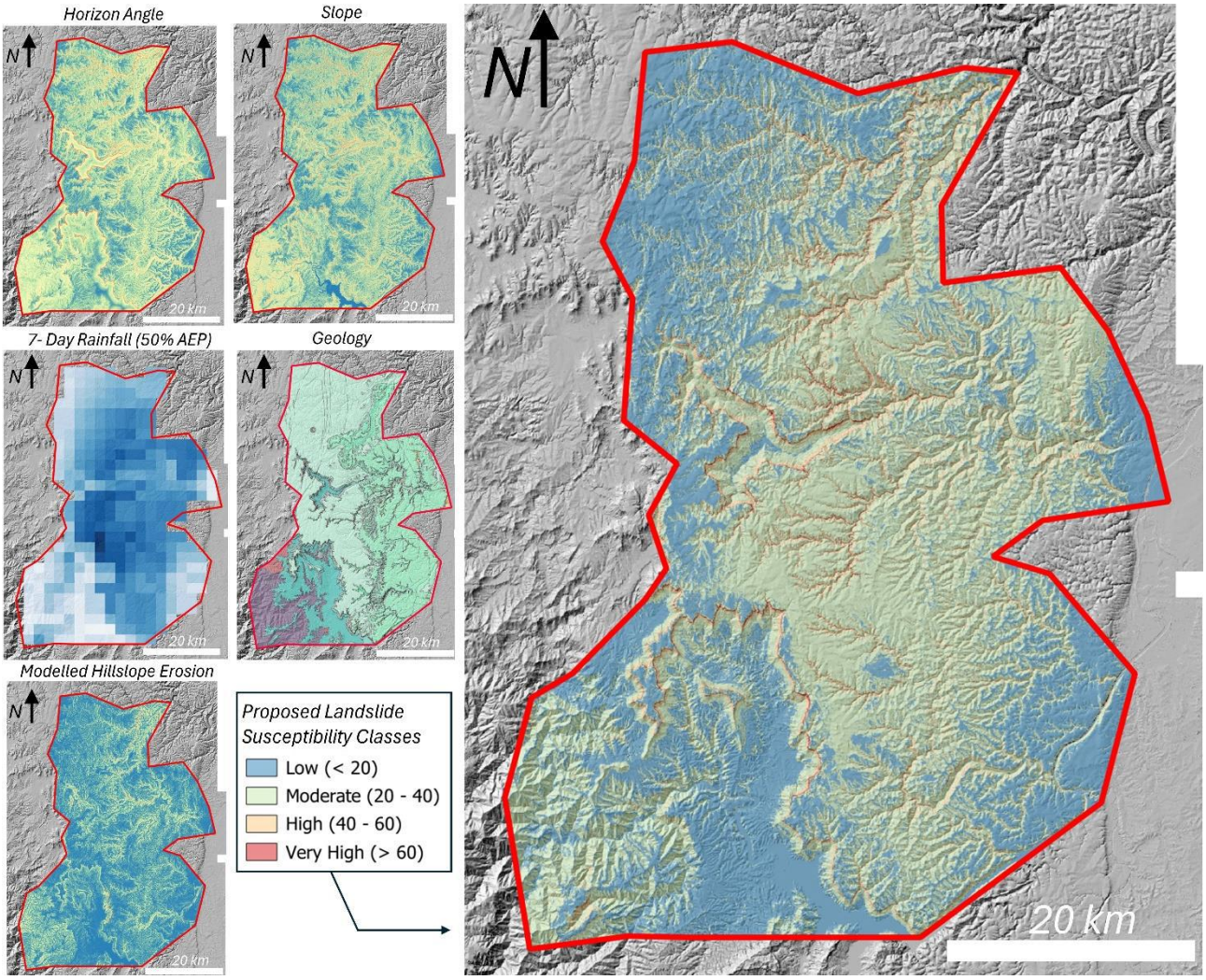


Figure 10: Plan view of input layers and resultant project wide "heat map" of landslide susceptibility

Linear assets including walking tracks and roads were split into 10 m long segments, with each segment assigned a single numeric landslide susceptibility score by sampling the maximum value from the underling heat map, within a 20 m wide buffer zone. An algorithm was developed to evaluate the terrain on either side of a track or road, and preferentially sample susceptibility values on the upslope side, to avoid very high landslide susceptibility scores for clifftop walking tracks that traverse near the upper crest of the escarpment. Figure 11 presents the resulting histograms and cumulative frequency curves of landslide susceptibility for the complete project-wide map (left), along with the corresponding results for

walking tracks (right). The statistics show that landslide susceptibility roughly conforms with a lognormal or negative exponential distribution, which is typical of many natural phenomena including landslide magnitude-frequency relationships (Hungr et al., 1999). Under the proposed susceptibility classification framework, approximately 90% of the map area is assigned a *low* to *moderate* landslide susceptibility score. In contrast, 70% of walking track length falls into the *low* to *moderate* susceptibility classes; 22% of the total walking track length is subject to *high* landslide susceptibility and 8% of walking track length is subject to *very high* landslide susceptibility.

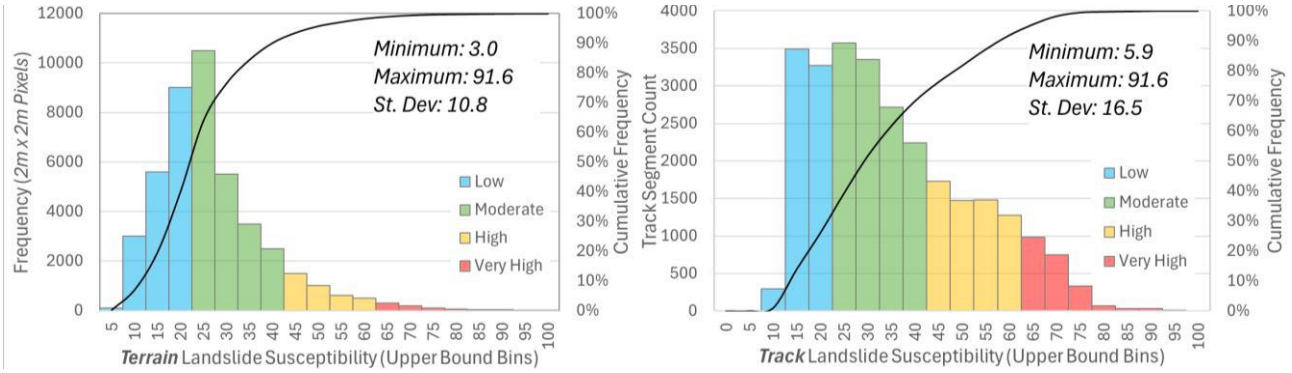


Figure 11: Histogram and cumulative frequency curves for landslide susceptibility of terrain and tracks

The data show that walking tracks are subject to higher landslide susceptibility than the overall terrain, reflecting the reality that these tracks have been constructed through steep terrain along the escarpment cliffs and upper reaches of the valley side slopes. The tracks with the highest landslide susceptibility include:

- **Cliffside tracks** that traverse along the base and intermediate benches of the escarpment cliffs. The most common slope failures affecting these tracks are expected to involve rockfalls initiating from the cliffs or overhangs, falling directly onto the walking track (no long-distance runout is required).
- **Gully and slot canyon tracks** that pass through steep creek lines connecting the upper escarpment with the valleys below. The most common slope failures affecting these tracks are expected to involve debris flows and potentially rockfalls initiating from the rim of narrow slot canyons.
- **Valley tracks** that traverse along the base of the escarpment cliffs, across the steep upper talus slopes, such as Federal Pass and Wentworth Pass. The most common slope failures affecting these tracks are expected to involve debris slides initiating in over-steepened sections of the talus slope or cut slopes above the track, and debris flows following major rainfall events, impacting the tracks at creek and drainage line crossings.

3.4 LINKING LANDSLIDE SUSCEPTIBILITY TO LIFE RISK

Estimation of risk to life requires an annualised landslide return period (representing the QRA parameter P_H) and a temporal exposure parameter representing the probability that people will be present on the track or road when a landslide occurs (analogous to the QRA parameter $P_{T:S}$). Whereas susceptibility scores vary from 0 to 100, landslide return periods for a given site may vary from several per year, up to many thousands of years. To account for this variation, an exponential relationship was used to derive an artificial "synthetic return period" (SRP) from the susceptibility score, reflecting a similar trend to the negative exponential form of landslide magnitude-frequency data (e.g. Hunter et al., 2022). Figure 12 shows two proposed exponential relationships to estimate SRP from the underlying susceptibility score.

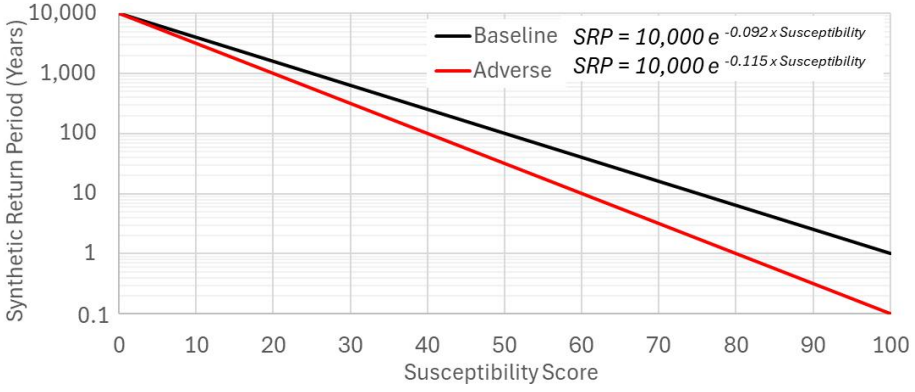


Figure 12: Proposed relationships between landslide susceptibility score and synthetic return period

Both SRP relationships assume a return period of 10,000 years for a susceptibility score of zero. The "baseline" relationship adopts an upper bound return period of 1 landslide per year for a score of 100. The "adverse" relationship adopts an upper bound return period of 0.1 years for a score of 100, corresponding to roughly one slope failure per month. It is important to note that the SRP estimates are not rigorously calibrated to historical landslide records, and they are not intrinsically linked to any specific failure mechanism or landslide size; rather, they have been selected to represent relative "base case" and "adverse" estimates of potential landslide frequency, for regional scale comparison of relative risk. In recent years, a new rockfall or landslide has been reported somewhere in the park about once per month. Many more landslides may occur in remote areas away from tracks and roads; furthermore, some fraction of rockfalls will either overshoot a track or road, or may come to rest on the slopes above the track, and thus go undetected.

Temporal exposure for park visitors was calculated for every track segment using annual visitation data provided by NPWS. Walkers were assumed to be travelling at 3 km/h through a notional "impact zone" that could vary in size from 1 m for a small rockfall, up to larger slope failures which could impact a complete 10 m long track segment. After calculating the synthetic QRA parameters for each track segment, the relative life risk can be interrogated in terms of a "synthetic fatality return period" with roads and tracks colour-coded to highlight the highest risk locations, accounting for both (1) landslide susceptibility; and (2) track visitation and the corresponding temporal exposure. Figure 13 shows an extracted map near Katoomba, with terrain coloured by landslide susceptibility, and tracks coloured by "synthetic life risk" categories under baseline conditions, for a landslide impacting a full 10 m track segment.

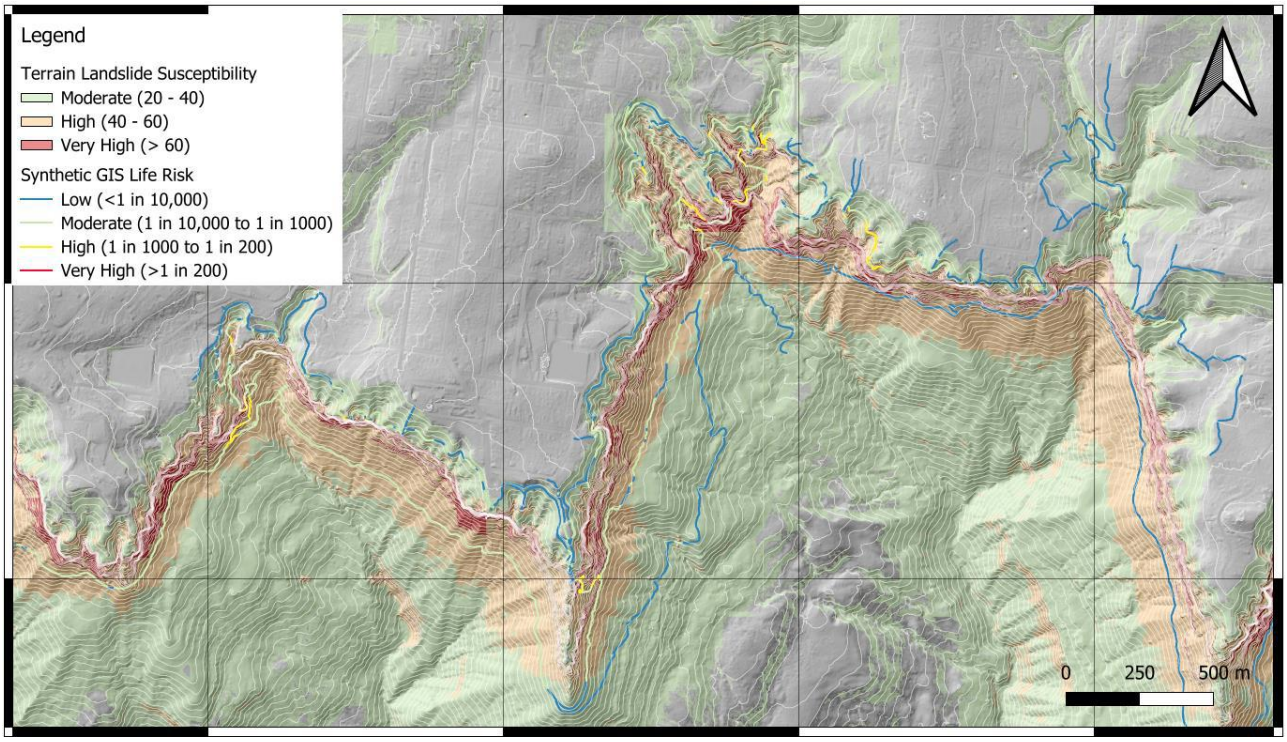


Figure 13: Tracks coloured by synthetic life risk, overlain on landslide susceptibility raster

Based on the proposed GIS risk classes, and considering a landslide that impacts a full 10 m long track segment, the walking track dataset is classified as 97.6% *low* to *moderate* life risk by track length. Only 2.3% of walking track length is classified as *high* life risk, and less than 0.1% falls into the *very high* life risk category.

4 DISCUSSION

Qualitative inspection of the regional scale mapping results confirmed that the *high* and *very high* risk areas broadly correspond with locations of known landslide impacts and high visitation; however, it must be emphasized that all estimates of life risk from this GIS analysis should be only used only to rank the relative risk of track and road assets and prioritise locations for site-specific investigation. The mapping results are intended to rapidly highlight the walking tracks and road sections subject to the highest life risk; they are not a conclusive determination of whether an asset is subject to *tolerable* or *unacceptable* societal risk in terms of the AGS (2007) risk assessment framework. In the near-term, the results will be used to highlight locations of *high* or *very high* risk where no previous geotechnical investigations have been undertaken and prioritise these areas for site-specific inspection and quantitative risk assessment.

There are several important limitations to the methodology. Although the landslide susceptibility score considers the potential for both debris slide and rockfall impact, initiation triggers may differ depending on the failure mechanism. Whereas brittle rockfalls may initiate with little warning, as the culmination of slow, gravity-driven subcritical crack growth, debris slides are known to correlate with intense rainfall or prolonged wet weather, when walkers are less likely to be present. Consequently, post-processing workflows to estimate life risk must adopt different weighting parameters for the temporal exposure parameter $\boldsymbol{P_{T:S}}$ to reflect the reduced likelihood that walkers will be present during wet weather.

Furthermore, this investigation defined landslide susceptibility as the potential for rockfall impact or localised instability of steep slopes: channelised debris flows are under-represented in the project wide susceptibility map. Preliminary investigations have demonstrated that hydrologic simulation techniques can be integrated into the GIS mapping methodology to highlight track sections subject to debris flow risk. Figure 14 shows an example from the Jamison Valley, where the accumulated flow depth for an input storm event is calculated using the publicly available 2 m resolution DEM. Track sections coloured by the simulated flood depth give a proxy indication of debris flow potential, showing a good match with two observed debris flows, and highlighting areas that may be impacted in the future.

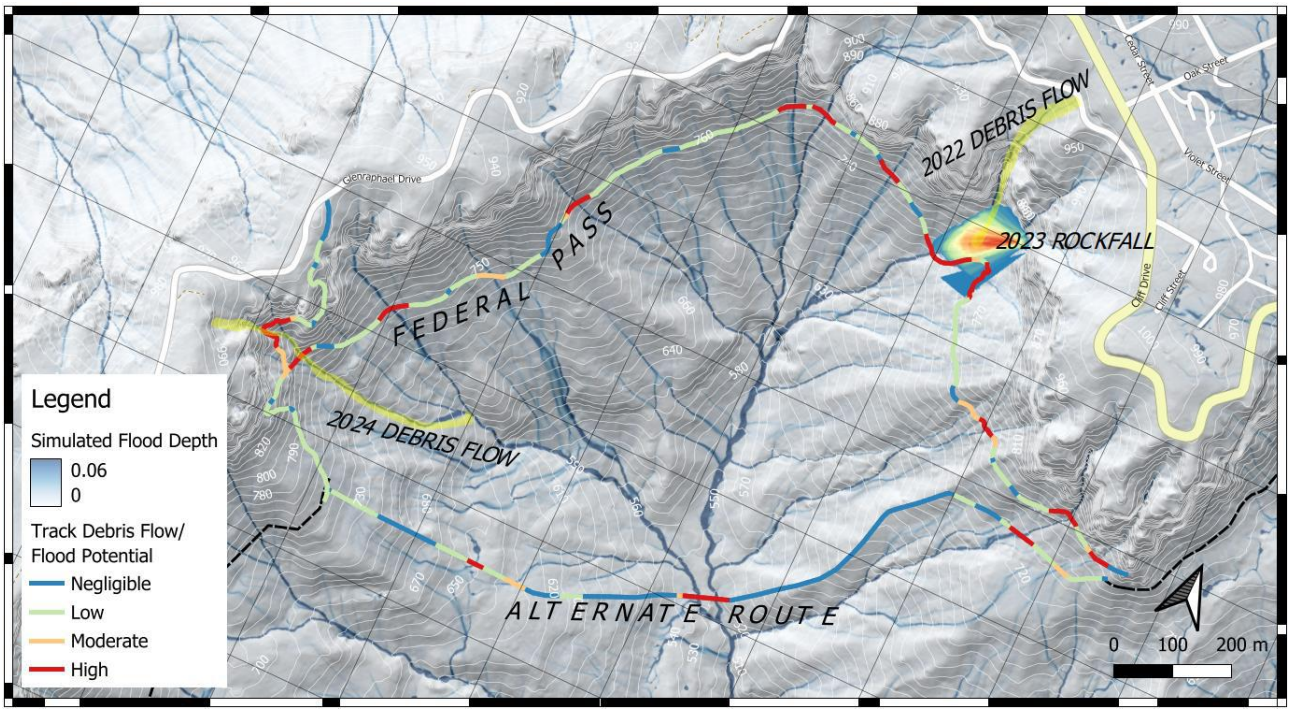


Figure 14: Example of a hydrologic simulation for overland flow to highlight creeks and drainage lines

Future developments could further improve confidence in the landslide susceptibility mapping by incorporating change detection techniques, with comparison of successive aerial LiDAR surveys. Over time, the landslide susceptibility scoring rubric can be refined to better reflect areas of real, observed instability.

5 CONCLUSIONS

This investigation produced a GIS database covering approximately 3400 km^2 of Blue Mountains National Park centred around the communities of Katoomba and Blackheath. The database includes topography and cadastral data, as well as a selection of five geospatial layers that were used to estimate susceptibility to impact from rockfalls and debris slides. The GIS database is hosted on a web viewing portal that allows NPWS to view the maps, interrogate the data, and generate localised plans as needed for areas of planned track work, or as part of the incident response to reported landslides.

A "synthetic return period" approach can be used to link landslide susceptibility to life risk based on the negative exponential form of empirical landslide magnitude-frequency data. The resulting heat maps of landslide susceptibility and life risk reflect the empirical observation that landslide susceptibility is highest near the steep escarpment cliffs, and on the steepest sections of the valley side slopes and incised creek channels.

6 REFERENCES

Australian Geomechanics Society (AGS) (2007). Practice note guidelines for landslide risk management. *Australian Geomechanics Journal*, 42(1), 63-114.

Caleca, F., Lombardo, L., Steger, S., Tanyas, H., Raspini, F., Dahal, A., Nefros, C., Mărgărint, M.C., Drouin, V., Jemec-Auflič, M. and Novellino, A. (2025). Pan-European landslide risk assessment: From theory to practice. *Reviews of Geophysics*, 63(1).

Castelli, M., Torsello, G. and Vallero, G. (2021). Preliminary modeling of rockfall runout: Definition of the input parameters for the QGIS plugin QPROTO. *Geosciences*, 11(2), 88-114.

Cochrane, M., Cheesman, B., Pyke, A., and Kelly, R. (2024). Creation of city-scale landslide susceptibility maps using machine learning. In: *Proceedings of the Australian Geomechanics Society Symposium (Sydney Chapter)*, November 2024.

Colquhoun G.P., Hughes K.S., Deyssing L., Ballard J.C., Folkes C.B, Phillips G., Troedson A.L. & Fitzherbert J.A. (2022). New South Wales Seamless Geology dataset, version 2.2 [Digital Dataset]. Geological Survey of New South Wales, Department of Regional NSW, Maitland.

Corominas, J., van Westen, C., Frattini, P., Cascini, L., Malet, J.P., Fotopoulou, S., Catani, F., Van Den Eeckhaut, M., Mavrouli, O., Agliardi, F. and Pitilakis, K. (2014). Recommendations for the quantitative analysis of landslide risk. *Bulletin of engineering geology and the environment*, 73, 209-263.

Cunningham, D.M. (1988). A rockfall avalanche in a sandstone landscape, Nattai North, NSW. *Australian Geographer*, 19(2), 221-229.

Domínguez-Cuesta, M.J. and Bobrowsky, P.T. (2013). Proposed landslide susceptibility map of Canada based on GIS. *Landslide Science and Practice: Volume 3: Spatial Analysis and Modelling*, 375-382.

Evans, S.G. and Hungr, O. (1993). The assessment of rockfall hazard at the base of talus slopes. *Canadian Geotechnical Journal*, 30(4), 620-636.

Field, D. and Hunter, A. (2024). Methods for assessing remote rockfall hazards above transport corridors. *Australian Geomechanics Journal*, 59(3), 75-97.

Flentje, P., Stirling, D. and Chowdhury, R. (2011). Landslide inventory, susceptibility, frequency and hazard zoning in the Wollongong and wider Sydney Basin Area. *Australian Geomechanics Journal*, 46(2), 41-49.

Hatherly, P. and Brown, I. (2022). *The Blue Mountains: Exploring Landscapes Shaped by the Underlying Rocks, Uplift and Erosion*. Windy Cliff Press.

Hungr, O., Evans, S.G. and Hazzard, J. (1999). Magnitude and frequency of rock falls and rock slides along the main transportation corridors of southwestern British Columbia. *Canadian Geotechnical Journal*, 36(2), 224-238.

Hunter, A., Flentje, P., and Moon, A. (2022). Bulli Pass Landslide Risk Management Part 1 – Hazard Assessment. *Australian Geomechanics Journal*, 57(3), 97-113.

Jaboyedoff, M. and Labiouse, V. (2011). Preliminary estimation of rockfall runout zones. *Natural Hazards and Earth System Sciences*, 11(3), 819-828.

Leventhal, A.R. and Kotze, G.P. (2008). Landslide susceptibility and hazard mapping in Australia for land-use planning—with reference to challenges in metropolitan suburbia. *Engineering Geology*, 102(3-4), 238-250.

NSW National Parks and Wildlife Service (2019). *Landslides and Rockfalls Procedures*. NSW Department of Planning, Industry and Environment, Sydney NSW.

Pells, P.J.N., Braybrooke, J.C., Mong, J. and Kotze, G.P. (1987). Cliff line collapse associated with mining activities soil slope instability and stabilization. In: Soil *Slope Instability and Stabilisation*; Walker & Fell (Eds.), Balkema, Rotterdam, 359-385.

Tomkins, K.M., Humphreys, G.S., Macris, J., and Hesse, P. (2007). Landslides in the Sydney basin: is there a seismic link. In: Clark, D. (Ed.) *Potential geologic sources of seismic hazard in the Sydney Basin*. *Proceedings volume of a one day workshop*, Geoscience Australia Record 2009/11 (GeoCat # 65991), 100-108.

Tuckey, Z. (2023). The role of progressive brittle fracture in the 1931 landslide at Dogface Rock, Katoomba. *Australian Geomechanics Journal*, 58(3), 77-93.

Wyllie, D.C. (2014). *Rock fall engineering*. CRC Press.

Wyllie, D.C. and Mah, C. (2005). *Rock slope engineering*. CRC Press.

Yang, X., Gray, J., Chapman, C., Zhu, Q., Tulau M., McInnes-Clarke, S. (2017). Digital mapping of soil erodibility for water erosion in New South Wales, Australia. *Soil Research*. 56(2), 158-170.

https://doi.org/10.56295/1ACEG20

ENGINEERING GEOLOGY CONSIDERATIONS FOR DEVELOPMENT ON BRINGELLY SHALE IN WESTERN SYDNEY

So M.M.L., Hokmabadi A.S., Zhu D. Casey T.
Arup Pty Ltd

Terzaghi S.

Aosullivan and Associates (AUS)

1 1INTRODUCTION

Western Sydney is expected to undergo a substantial transformation over the coming decades, with planning for extensive residential developments and significant infrastructure projects. This rapid urban expansion requires a thorough understanding of the engineering geological behaviour of significant geological formations, in particular the Bringelly Shale. This formation is known for its high potential for shrink-swell behaviour and susceptibility to rapid degradation when exposed to wetting and drying cycles, and further exacerbated by human activities, such as excavation and earthworks, which disrupt its equilibrium state.

This paper shares project experiences to inform construction practices in the Bringelly Shale and highlights the importance of incorporating engineering geological practices. A case study demonstrates the value of developing an engineering geological model to evaluate the combined impact of removing protective sandstone caps on hills containing Bringelly Shale and the influence of subvertical joints, excavation and rainfall infiltration, in the rapid degradation of subsurface materials and impact on slope stability. Similar lithological conditions can be expected throughout Western Sydney.

Additionally, this paper outlines key considerations (e.g., identifying backfilled farm dams, understanding saturation zones, and soil creep) which should be assessed in early phase planning and design when working in Bringelly Shale, to manage and mitigate significant risks to foundation design, deep excavations, and linear infrastructure. Early identification of these risks is essential for informing planning decisions and guiding necessary investigations to support effective and safe design practices.

2 GEOLOGICAL SETTING OF BRINGELLY SHALE AND ITS ENGINEERING SIGNIFICANCE

The Bringelly Shale of Wianamatta Group is a major sedimentary formation outcrop in western Sydney, primarily confined to the Fairfield Basin, extending from the northwest near Penrith, Liverpool, Camden, Campbelltown, and part of Hawkesbury and Parramatta region (Figure 1). This unit predominantly comprises a sequence of alternating shale, claystone, siltstone, followed by decreasing order of volumetric abundance by sandstone, coal, and highly carbonaceous claystone and tuff (Herbert 1983). The Wianamatta Group was deposited during the Triassic Period and is believed to be the result of a major marine regression. The depositional environment of laminated silt of the Bringelly Shale in lagoons, marshes, levees and backswamps whereas the sandstone unit was formed in both barrier-bar and alluvial channel environments. Therefore, sandstone units are commonly juxtaposed with the shale and claystone-siltstone, but the sandstone within the Bringelly Shale generally occur sporadically and in layers of limited lateral extent (Herbert 1983). As sea levels dropped due to regional uplift associated with the breakup of Gondwana and onset of compressional forces in eastern Australia during Early to Mid-Cretaceous, the previously formed rock exposed and the surrounding weaker and more erodible siltstone and claystone beds eroded, leaving the more resistant sandstone unit. These sandstone remnants often form topography highs such as ridges or crest of hills. As such, the characteristic topography of the Bringelly Shale is generally undulating and numerous outliers of ridge tops.

The Bringelly Shale is characterised by a high proportion of a mixed layer illite-smectite, resulting in a high shrink-swell potential and susceptibility to rapid degradation when exposed to wetting and drying cycles.

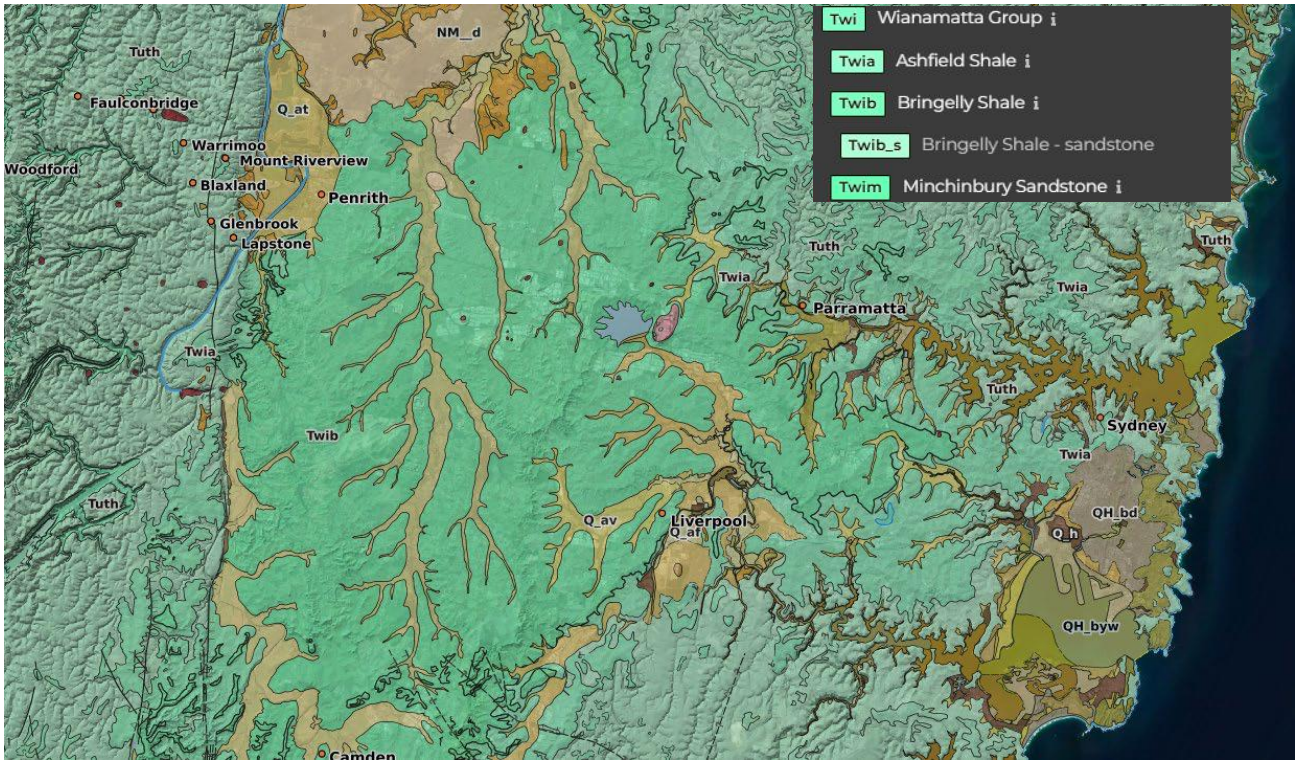


Figure 1: Geological map of Sydney and outer Sydney region (extracted from MinView https://minview.geoscience.nsw.gov.au)

3 CASE STUDY OF SLOPE STABILITY ISSUE OVERVIEW

The site of the case study, located on a hilltop underlain by the Bringelly Shale Formation in western Sydney, was developed during 2021 to 2022, which was one of the wettest years in Sydney on record. During construction work, the top 4-5m of the hill was removed to form a level platform, with retaining walls constructed at the perimeter below the platform. In addition, excavation for trenches and shafts further exposed the deep levels of the ground. To monitor the performance of the retaining wall and slope movement outside the wall, inclinometers were installed around the perimeter of the platform. These inclinometers recorded gradual and steady movement at the west and northwestern portion of the site, with displacement ranging between 10mm and 30mm within about 10 months. Major movement occurs at approximately 10-12m below the final formation level. The retaining wall did not provide adequate resistance to the excessive movements; therefore, stabilisation measures were required.

A review of the ground conditions, based on pre- and post- ground investigation information, revealed that the original ground prior to excavation comprised a thin layer of residual soils overlying predominantly weathered sandstone to a depth of 5-6m and underlain by siltstone and mudstone. After excavation, the sandstone cap was mostly removed and the interbedded siltstone, claystone and shale were exposed. The rock was generally extremely weathered to moderately weathered with very low to medium strength, extending to approximately 12m below the final formation level. The beddings were sub-horizontal with inclined to subvertical joint sets dipping from ~40° to 80°, and the presence of clay seams ranging from 0mm to 30mm. Extensive highly fractured rock zones, which were also described as shear zone in some boreholes, were identified at the northwestern portion of the site. Below this zone, moderately to slightly decomposed siltstone and sandstone overlaying fresh rock was encountered. Healed fractured rock was also observed underlying the sandstone cap, possibly associated with tectonic movement, local faulting, crush under self-weight or stress relief when overlying beds were eroded. The fractures were subsequently healed or cemented with clayey materials, silica or calcite. It is postulated that these materials were derived from surrounding materials and deposited either as water flow or through moisture ingress due to suction.

Based on the vibrating wire piezometers (VWPs) and standpipe readings, the global groundwater level was recorded at about 20m below the final ground surface level, with multiple perched water tables vary spatially at various depth, about 10 to 12m below ground and 15m below ground

4 CASE STUDY FINDINGS AND IMPLICATION

The removal of the sandstone cap exposed the interbedded siltstone and claystone, which were no longer protected from surface water infiltration. The heavy rainfall events experienced on site along with the fractured nature of the bedrock facilitated the propagation of water, resulting in moisture change in deeper rock layers. Subsequent trenching activities led to increased water infiltration into the rock layers, causing the interbedded siltstone and claystone to undergo shrink-swell cycles due to wet-dry conditions after heavy rainfall events. The presence of clay seams within this zone may induce transient perched water tables and may have exhibited shrink swell in response to the rainfall events, which could have further reduced slope stability and caused excessive movement. Also, high perched water tables were expected in the rock layers during and shortly after the rainfall events. These water tables induce additional hydrostatic water pressure behind the retaining wall and reduce effective stress within the fractured zones and decreasing factor of safety against sliding.

It is noted that areas other than the northwestern portion of the site appear to have less movement as the rate of movement reduced significantly after a few rainfall events in 2022, while the northern part of the site continued to move even in the absence of working loads on the platform. It is possible that the ground may have reached full saturation after several rainfall events following the removal of the sandstone cap and gradually reached an equilibrium state where any change in moisture content would not trigger noticeable shrink swell type behaviours. However, the northwest of the site, where continued movement was observed, may be related to extensive fractured zones and prevalent sub-vertical joints falling water infiltration. The slope instability may have been triggered by shrink swell behaviour between rock blocks or simply by jacking the blocks apart due to increased water pressure, or a combination of the two.

This case study highlights the importance of understanding geological setting and recognising the geological units have reached their equilibrium under current tectonic regime. The sandstone unit within the Bringelly Shale, typically found at the top of the topography, serves as a protective layer for the underlying siltstone and shale. The removal of this protective layer disrupts the natural equilibrium, increasing the risk of instability. Developing a comprehensive engineering geological model to assess ground conditions, lithological properties, existing geological defects and the impact of human activities for mitigating potential geotechnical risks and should be incorporated into engineering projects.

5 OTHER CONSIDERATIONS IN THE BRINGELLY SHALE

In addition to slope stability due to site formation at the crest of the hill, various engineering works such as building structures, deep excavation and installation of lineament infrastructure (e.g. pipelines) are expected to be widespread as part of the urban expansion. The following section discusses other considerations that should be incorporated into an engineering geological model for projects involving the Bringelly Shale.

5.1 IDENTIFYING FARM DAMS

Western Sydney primarily consists of agricultural lands where farm dams are commonly built and often backfilled without proper treatment. The fill material is likely site-won and derived from the Bringelly Shale, making it prone to shrink-swell behaviour. The presence of shrink-swell-prone fill materials has significant implications for foundation design. Variations in fill thickness and moisture content can result in excessive movement or differential settlement or foundation upheaval in shallow foundations. For piled foundations, swelling of backfill materials beneath the base slab can induce uplift pressures, especially when groundwater levels fluctuate, increasing tensile forces in piles.

Identifying farm dams early in the design phase is important for managing these risks. This includes a comprehensive desktop such as reviewing historical aerial imagery to locate potential former farm dams which have been decommissioned or any existing farm dams, which can guide targeted ground investigation to determine the depth, extent and properties of backfilled materials. Laboratory testing, such as free swell and degree of saturation assessments, can be conducted to evaluate swell behaviour. These findings can inform appropriate mitigation strategies such as removal and replacement with non-reactive engineered fill, lime treatment followed by compaction, or designing foundation to accommodate anticipated ground movements.

5.2 IDENTIFYING SIGNS OF SOIL CREEP

Soil creep, induced by the long-term shrink swell behaviour of expandable clays in the weathered bedrock of the Bringelly Shale, is a slow and steady downward movement. This is not unique to the Bringelly Shale derived soil, but their high shrink-swell potential may expedite the process during moisture change cycles. The shrinkage-induced cracks allow precipitation to reach deeper ground levels, reducing confinement and increasing the likelihood of downslope soil movement when swelling. This occurs when shear stress is sufficient to produce permanent deformation but not exceed

the shear strength to trigger shear failures. Also, wet-dry cycles contribute to the formation of blocky clay layers through repeated expansion. This process also facilitates incremental lateral movements and the development of shear bands and slickensides within the weathered profile. Although soil creep is not an immediate safety hazard, it presents long-term impacts on buried infrastructure, particularly linear structures like pipelines. Over time, this graduate movement can exert stress on pipelines, potentially leading to deformation, joint displacement, or even service disruptions. Soil creep of the Bringelly Shale can occur on slopes as gentle as 10°.

Assessing the soil creep risk requires a desktop study, including a review of historical aerial imagery to identify visible signs of creep such as terracettes, tilted trees, or irregular surface undulations. Additionally, Digital Elevation Models (DEMs) can be used to generate slope maps, which helps identify areas where creeping behaviour is more likely to occur. These can guide targeted ground investigations to confirm subsurface conditions and evaluate potential mitigation measures including monitoring, strengthening of pipelines, or strategic routing where feasible.

5.3 SWELLING POTENTIAL IN ROCK IN EXCAVATIONS

Deep excavations in the Bringelly Shale must account for the potential swelling pressure of the rock. In its natural state, the rock at depth is typically under the groundwater table and saturated. However, dewatering is often required during deep excavation under the groundwater table. This can cause the rock to transition from a saturated state to an unsaturated state, inducing matric suction within the shale. Over time, as groundwater recharges into the excavation, the shale will reabsorb moisture, leading to swelling. This swelling pressure exerts additional lateral forces on walls that need to be considered in design.

The degree of saturation should be evaluated to assess swelling potential. To select appropriate rock samples for laboratory testing, core box photos can be reviewed to evaluate oxidation levels, which can indicate past moisture fluctuations. Rock in unoxidized zones may have remained saturated for an extended period, while heavily oxidized rock may have already undergone moisture-driven changes. This means the swelling potential can differ between these zones, free swell and swelling pressure tests should be conducted on both non-oxidized and oxidized zones samples to obtain an understanding of the swelling behaviours.

6 SUMMARY

The Bringelly Shale's high shrink-swell potential and susceptibility to rapid degradation poses challenges for construction if not managed properly. Human activities, such as excavation, exacerbate these issues. By incorporating engineering geological practices, such as desktop studies and development engineering geological models can help identify risks during the planning and design phrases. The case study highlights the importance of the sandstone cap in protecting the underlying siltstone and shale from water infiltration, preventing further degradation. Similar lithological conditions, where sandstone caps overlay weathered shale are anticipated at hilltops within the Bringelly Shale Formation. Therefore, any future development involving hilltop excavation should conduct detailed geological assessments before construction. Other considerations include identifying farm dams, assessing soil creep, and evaluating the degree of saturation to assess the swelling potential. A good understanding of these factors is essential for mitigating geotechnical risks in the region.

7 REFERENCES

Herbert, C. (1983). Geology of the Sydney 1:100,000 Sheet 9130. New South Wales Geological Survey, Sydney.

https://doi.org/10.56295/1ACEG21

NEOTECTONIC FAULT SIGNIFICANCE

Tim Mote
GHD Pty Ltd

ABSTRACT

This paper presents a sensitivity analysis on the significance of neotectonic faults at various slip and distance scenarios to seismic hazard ground motion estimates. The analysis implements neotectonic faults into an exemplar probabilistic seismic hazard analysis (PSHA) with no prior known neotectonic faults by iterating 15 hypothetical neotectonic distance-slip scenarios combining, five site-to-fault distances (5, 10, 20, 50, and 80 km) with three slip rate scenarios (~ 1 m/Myr, 10 m/Myr, and 100 m/Myr). The results show the relative increase in calculated ground motion through the addition of the distance-slip fault scenario as a percentage to the baseline hazard (no faults) to demonstrate the significance of neotectonic faults to seismic hazard in an Australian critical infrastructure design context. The sensitivity analysis provides insights to inform decision making in support of more detailed paleoseismological studies following initial desk study/screening level assessments of neotectonic faults near a site.

1 INTRODUCTION

Australia is often perceived as a seismically stable region due to its intraplate setting within the Australian tectonic plate, far from active plate boundaries. However damaging earthquakes do occur and almost all earthquakes, especially larger ones, occur on existing faults.

Accounting for ground motions from earthquake recurrence intervals on known active faults is a fundamental step in probabilistic seismic hazard analysis (PSHA). In tectonically active regions, a fault is typically considered active if it has moved within the Holocene epoch (approximately the last 11,700 years) or within the Late Pleistocene epoch (approximately 35,000 years ago). Australia has a relatively low number of Holocene active faults compared to tectonically active regions.

In an Australian seismotectonic context “Neotectonic” faults are faults that have demonstrable or probable movement during the current crustal stress field orientation which started in the Pliocene and late Miocene (i.e., the past 5-10 million years) and may have the potential for displacement in the future (Clark et al. 2011; Sandiford et al. 2004). Neotectonic faults are important sources in Australian seismic hazard assessments because they represent recent tectonic activity in the region. They reflect the present-day tectonic stress regime and are interpreted as more likely to rupture again, making them a locus of future earthquake recurrence. As such, neotectonic faults that could significantly contribute to the design basis ground motions for critical infrastructure should be identified and be accounted for.

Over the past two decades, research into understanding neotectonic faulting and incorporation into Australia’s current state of seismic hazard assessment has progressed. The Geoscience Australia National Seismic Hazard Assessment (NSHA18 Allen et al, 2018, NSHA23 Allen at all 2023) incorporated neotectonic faults. The ANCOLD (2019) Guidelines for Design of Dams and Appurtenant Structures for Earthquake requires … *neotectonic faults that could significantly contribute to the ground motion for the dam should be identified and be accounted for in the seismic hazard assessment.*

Numerous recent studies have shown the significance of neotectonic faults to critical infrastructure in Australia through paleoseismic field investigations (e.g., Clark et al., 2021, Ninnis and Clark, 2019, and Mote et al., 2021, and Griffin et al., 2024). While the incorporation of neotectonic features is acknowledged in the current state of practice, the level of effort required to adequately characterise neotectonic faults to understand their significance to ground motions has not yet been mainstreamed. In regions with low rates of tectonic activity and landscape development (e.g. Australia), fault activity characterization is difficult (McMoran and Hull, 2013). Assessing the location and activity of neotectonic faults can be technically challenging, time intensive, and affect design and construction schedules.

This paper will present a sensitivity analysis of the impact to design basis ground motions from adding hypothetical single neotectonic fault scenarios to an exemplar PSHA with no prior neotectonic faults. The analysis will iterate through 15 hypothetical neotectonic distance-slip scenarios combining: five site-to-fault distances (5, 10, 20, 50, and 80 km) with three slip rate scenarios (~ 1 m/Myr), 10m/Myr, and 100m/Myr) to estimate the relative increase in calculated ground motions as a percentage over the baseline hazard (no faults) at three select annual exceedance probabilities (AEP).

2 NEOTECTONIC ASSESSMENT BACKGROUND

An Australia-wide assessment of active faulting based on neotectonics data was initiated by Clark et al. (2011) and expanded into the Geoscience Australia Neotectonic Feature Database (NFD) (Clark and McPherson, 2012). The data were derived from the analysis of Digital Elevation Models (DEMs), aerial photos, satellite imagery, geological maps, and paleoseismic

studies. At the time of this paper the catalogue contains 406 neotectonic features, (neotectonics.ga.gov.au). Verifying these features as neotectonic faults (or not) is an ongoing process. The catalogue is not a complete representation across Australia, as such site-specific seismic hazard assessments need to identify and account for neotectonic faults, accordingly.

Several recent studies highlight and provide insight into the significance of neotectonic faults. Sommerville et al. (2017) summarised conditions under which identified neotectonic faults contribute significantly to seismic hazard in Australia and states that ground motion levels decrease rapidly with increasing closest distance from a fault. They found identified faults rarely dominate the probabilistic hazard if they are 20 km or more from the site. Ninis and Clark (2019) presented a paleoseismic study which identified 2 or 3 M7.0 earthquakes on the Avonmore Scarp in last ~80,000 years, highlighting their significance to hazard estimation. Clark et al. (2021) presented a paleoseismic study for the Meadow Valley Fault and found that potentially damaging ground motions might be generated out to distances of 50-70km from the fault, but noted uncertainty in the likelihood that the fault might generate significant ground motions within a time frame relevant to infrastructure stability. Griffin et al. (2024) presented a paleoseismic study showing three earthquakes on Jindabyne Thrusts since ~40,000 years ago that are significant to critical infrastructure in the Snowy Mountains. Quigley et al. (2024) showed there are 216 NFD fault traces within 100 km of 428 ANCOLD dams and suggested that detailed analyses of fault-based hazard may be particularly relevant for dams within 20 to 30 km of faults with sufficient length (e.g., ≥ 20-30 km) to produce M ≥ 6.7 to > 7.0 earthquakes and sufficiently high slip rates (e.g., ≥ 0.1 mm/yr) to potentially contribute to seismic hazard at time-scales commonly of interest for critical infrastructure (e.g., ≤ 1:5,000 to 1:10,000 AEP). Ninis et al. (2018) provided a methodology to incorporate bedrock faults that are aligned favourably with the current stress regime with slip rates of 1 to 2 m/Myr. In their study 11 total faults, over distances from 10 to 60 km were added to a PSHA to show a 10 to 20% increase in peak ground acceleration (PGA) across a range of AEPs.

A recurring theme in all of these studies is the value of the more rigours paleoseismic studies, be it field or desk-based, to reduce uncertainty and add confidence into the assessment of neotectonic faults that could have significant impact to design basis ground motions estimates.

3 SENSITIVITY ANLYSIS

3.1 METHODOLOGY

The sensitivity analysis methodology involved developing an exemplar PSHA for a location in Northern NSW/Southern Queensland, where no neotectonic faults in the current Geoscience Australia NFD are identified (Figure 1). It is important to note that in this area, the NFD is not complete and there are many mapped regional bedrock faults that are favourably aligned with the current stress regime to allow reactivation.

The exemplar fault parameters (e.g. maximum magnitude) were based on typical neotectonic faults located in eastern Australia with three mean slip rate scenarios (~ 1 m/Myr, ~10m/Myr, and ~100m/Myr). The slip rates scenarios were selected to represent orders of magnitude of ground deformation. For reference, a 1 m/Myr slip rate is arguably the lower limit of recognisable fault displacement expression given erosion rates, and a 100 m/Myr slip rate is comparable to active slip rates in high seismicity areas (e.g. a Pleistocene rupture). In line with the typical PSHA methodology, the slip rate scenarios were implemented with weighted distributions across upper, preferred, and low estimates, to capture epistemic uncertainty.

The PSHA model followed the ANCOLD (2019) guidelines and incorporated inputs from NSHA23 (Allen et al., 2023). A full detailed description of the PSHA implementation is beyond this paper. The key model components are summarised below:

- Site V_{s30} of 760 m/s.
- NSHA23 earthquake catalogue.
- Three seismotectonic models; two distributed seismicity/areal-source models (GHD site-specific and AUS6) and one smoothed seismicity models (RF23). Both AUS6 and RF23 implementations were extracted from NSHA23.
- Ground motions prediction equations applied for non-cratonic Australia.
- Faults were added to baseline model with no consideration of double counting between fault and areal sources.
- The hypothetical fault characterisation including length, dip, seismogenic depth was used to calculate a maximum magnitude distribution is summarised in Table 1.
- b-values distribution was adopted from the local site-specific areal source zone
- Neotectonic faults were modelled with an exponential magnitude recurrence model (i.e., Guttenberg - Richter) with a minimum magnitude of M5.0. While many Australian PSHAs apply weighted exponential and characteristic magnitude recurrence models to capture uncertainty, implementing only the exponential model in this study is considered conservative.

The model was run to develop baseline ground motions (e.g. no neotectonic fault contributions). The model was then re-run, iteratively, with a single neotectonic fault added to the model for 15 hypothetical distance-slip scenarios: five site-to-fault distances (5, 10, 20, 50, and 80 km) with the three slip rate scenarios (Low, Moderate, High).

Results were computed for three AEP (1:475, 1:2000, and 1:10,000) representing typical design basis AEP for critical infrastructure over three ground motion parameters (PGA with spectral periods of 0.2 s and 1.0 s). For reference the baseline PGA at a 1:10,000 AEP for the exemplar site is ~0.1g.

Table 1: Neotectonic Fault Characterisation

Length (km)	Fault Type	Dip Angle (weight)	Depth (weight)	Mmax Mw (weight)
170	Reverse	60 (0.2)	10 (0.2)	7.2(0.2)
		65 (0.6)	15 (0.6)	7.3(0.6)
		70 (0.2)	25 (0.2)	7.4(0.2)

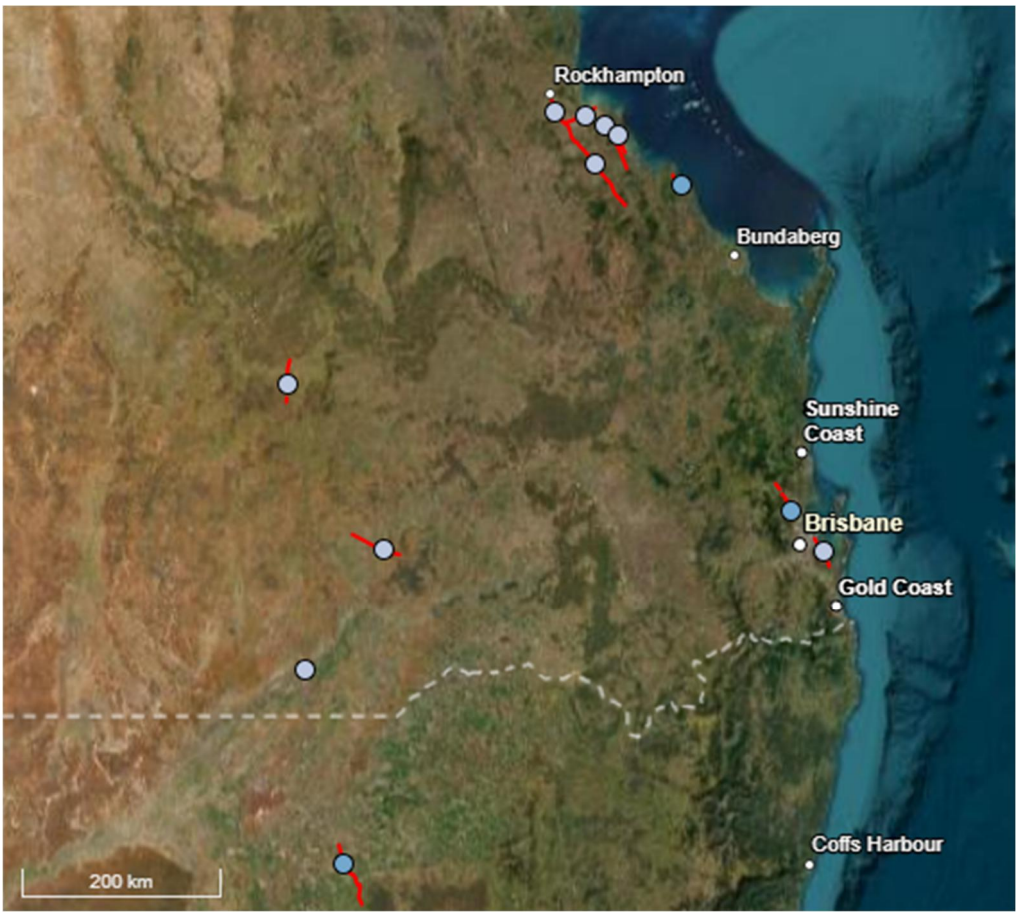


Figure 1: Extract from Geoscience Australia NFD for Northern NSW/Southern Queensland highlighting the sparsity of neotectonic faults (red) identified in the region (www.neotectonics.ga.gov.au)

3.2 SENSITIVITY RESULTS

The sensitivity results are presented in Figure 2 for three ground motion parameters (PGA, 0.2 s, and 1.0 s) and three AEPs (1:475, 1:2,000, and 1:10,000).

Each line represents the relative increase in calculated ground motions through the addition of the distance-slip fault scenario as a percentage to the baseline hazard (no faults). The percentage increase is shown in log scale on the y-axis and distance from site-to-fault on the x-scale. The three slip scenarios are delineated by line style (Low Slip = solid, Moderate Slip = dotted, High Slip = dashed). The three AEP scenarios are separated by colour (1:475 AEP = orange, 1:2,000 AEP = blue, 1:10,000 = red).

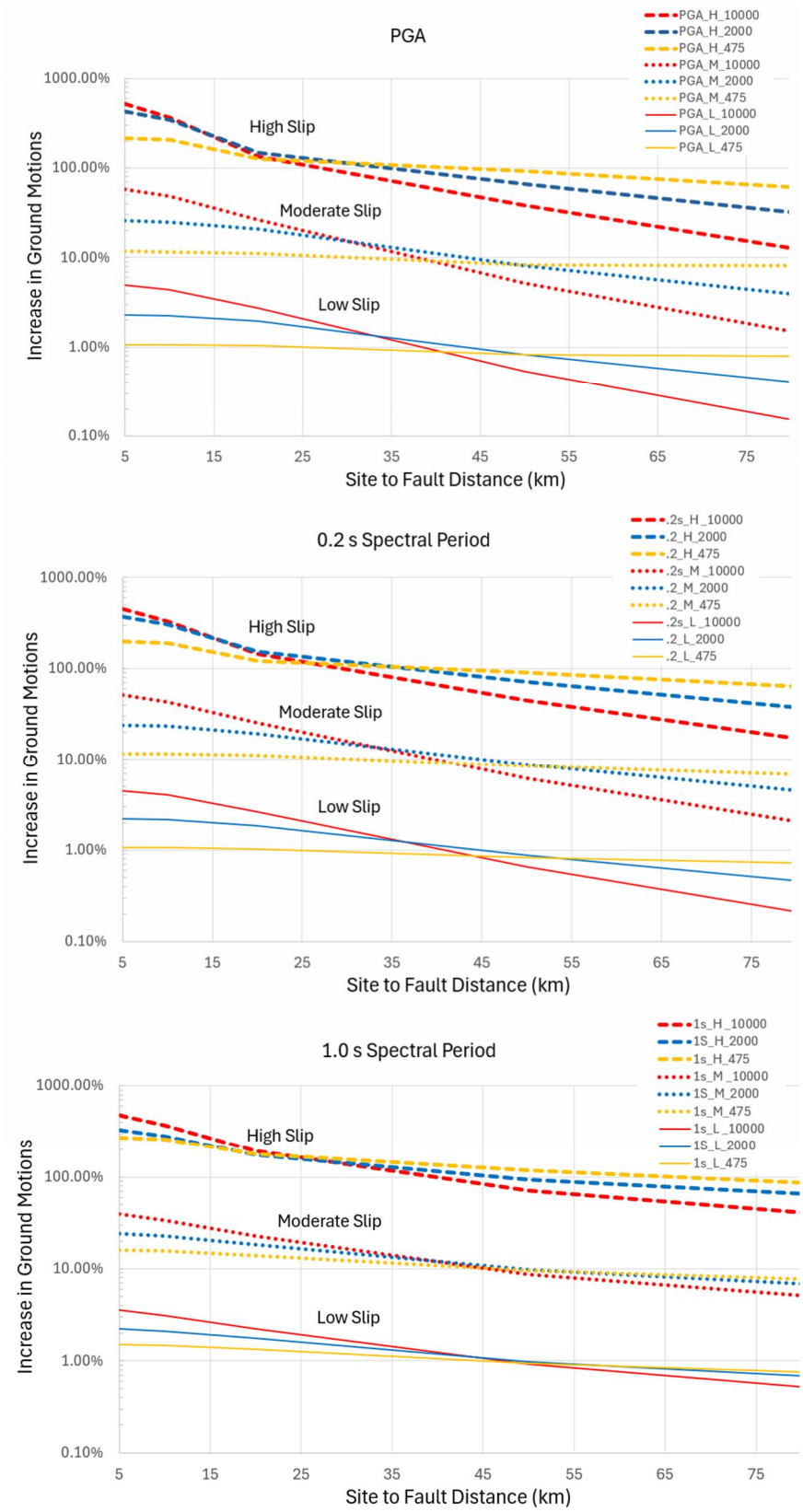


Figure 2: Relative percentage increase in ground motions from fault distance-slip scenarios. PGA (top), 0.2 s (middle), 1.0 s (bottom). The three slip scenarios are delineated by line style (Low Slip = solid, Moderate Slip = dotted, High Slip = dashed). The three AEP scenarios are separated by colour (1:475 AEP = orange, 1:2,000 AEP = blue, 1:10,000 = red).

4 DISCUSSION

The sensitivity results show a similar pattern across all ground motions parameters and AEPs. As expected, adding neotectonic fault scenarios with increasing slip, from Low to High Slip, corresponds to larger increases in relative ground motions to the baseline, respectively.

The Low Slip scenarios have little increase to ground motions across all scenarios. They only increase the baseline hazard by a few percent when the site-to-fault distance is less than ~10km at 1:2,000 and 1:10,000 AEPs.

The High Slip scenarios increase the baseline hazard ground motions by over 100% for all ground motions parameters and AEPs for distances less than ~25 km. As expected, the High Slip scenarios are over 2 x the baseline hazard. The 1.0 s results show this increase out to ~45 km, reflecting the influence in ground motion from large earthquakes at distance.

The Moderate Slip scenarios report an increase typically between 10% and 100% out to distances of 45km.

Across all slip scenarios, at 1:475 AEP the relative change in ground motions with increasing distance is expressed with a relatively flat line (comparable change across all distances) compared to a steeper slope at 1:10,000 AEP where the relative increase drops off faster with distance. This steeper slope for 1:10,000 AEP reflects the greater contribution from the baseline (e.g. background) seismicity at these lower probabilities (e.g., long return periods).

Consideration of these exemplary results can start to provide insight into what slip rate scenarios on potential neotectonic faults at known distances will contribute significantly to ground motion estimation at a site. While state of practice guidance directs accounting for neotectonic faults that could significantly contribute to the ground motion, there is no explicit commentary on what significant contribution means. For example, taking a 10% increase as an arbitrary threshold for engineering significance, these exemplar results can be interpreted to provide insight on contribution of faults and support decision making and justification for more detailed characterisation of neotectonic faulting through paleoseismological investigations.

- A High Slip scenario contributes significantly (e.g. >10%) to the ground motions at all distances and AEPs. While the contribution drops with distance for PGA, at 1.0 s the increase in ground motions is still significant. This highlights the importance of identifying and confidently quantifying slip rates for these neotectonic faults.
- A Moderate Slip scenario contributes significantly (e.g. >10% - 100%) to ground motions at site-to-fault distances less than 45 km. The contribution is more significant in the lower probabilities. This highlights the importance of identifying and confidently accounting for neotectonic faults within 45km.
- A Low Slip scenario fault increases the ground motions less than the 10% arbitrary threshold. This suggests that these low slip neotectonic faults are not significant to the ground motion estimates (assuming a 10% threshold of significance).

These insights can be used to inform decision making to support more detailed paleoseismological studies following initial desk study/screening level assessments of potential neotectonic faults near a site. As often is the case, the significance of a potential neotectonic fault needs to be communicated, and often quantified, to decision makers to justify the investment in increased effort.

Notably, as a single exemplary PSHA, the analysis presented here has inherent site-specificity with its geographical location as well as the implementation of the PSHA model (e.g. site Vs30, local areal sources, fault characterization, ground motion models, etc.). It is not intended as a generalization for all of Australia.

5 SUMMARY

Although the incorporation of neotectonic faults is now standard in the current state of Australian seismic hazard assessment practice, the level of effort required to adequately characterise neotectonic faults to understand their significance in contributing to ground motions has not yet been mainstreamed.

A sensitivity analysis was carried out by iteratively adding 15 hypothetical neotectonic distance-slip scenarios, five site-to-fault distances (5, 10, 20, 50, and 80 km) with three slip rate scenarios, to an exemplar PSHA with no previous mapped neotectonic faults.

The results show a relationship between distance-slip scenarios on neotectonic faults and an increase in estimated ground motions. For this exemplar, it reiterates the significance of neotectonic faults with slip rates more than ~100 m/Myr, shows that slip rates of ~10m/Myr can significantly increase ground motions at distances less than ~50km, and neotectonic faults with slip rates of 1m/Myr have little contribution. This sensitivity analysis has inherent site-specificity in its geographical location as well as details in the implementation of the PSHA model. More work is needed to expand the analysis to adequately capture a range of seismotectonic settings in Australia and support broader understanding of neotectonic fault significance to

critical infrastructure ground motions. Nevertheless, these insights can start to help inform decision making in support of more detailed paleoseismological studies following initial desk study/screening level assessments of potential neotectonic faults near a site.

The findings of this study and other paleoseismic studies on neotectonic faults can be used to develop guidance on the requirements of paleoseismic assessments for critical infrastructure in Australia.

6 AKNOWLDEGEMENTS

The author wishes to thank Dr Brendan Duffy and Dr Narges Khajavi for their valuable discussions on neotectonic faulting and assessment practice in Australia. Comments from an anonymous reviewer were very much appreciated.

7 REFERENCES

Allen, T., Griffin, J.D., Clark, D., Cummins, P., Ghasemi, H. & Ebrahimi, R. (2023). The 2023 National Seismic Hazard Assessment for Australia: Model Overview. *Record 2023/53. Geoscience Australia, Canberra.*

Allen, T.I., Griffin, J., Leonard, M., Clark, D. & Ghasemi, H. (2018). The 2018 National Seismic Hazard Assessment: Model Overview. *Record 2018/27. Geoscience Australia, Canberra.*

ANCOLD (2019). Guidelines for Design of Dams and Appurtenant Structures for Earthquake. *Australian National Committee on Large Dams.*

Clark, D., McPherson, A. & Collins, C. (2011). Australia's seismogenic neotectonic record. *Geoscience Australia Record, 11, pp.1–95.*

Clark, D. & McPherson, A. (2012). Neotectonic Features Database. Geoscience Australia. [online] Updated December 20, 2019. *Available at: https://pid.geoscience.gov.au/dataset/ga/74056 [Accessed 26 Jun. 2025].*

Clark, D., Stephenson, J. & Allen, T. (2021). Ground shaking potential relating to eastern Australian active faults, an example of the Bendigo Region with relevance to water reservoirs and tailings dams. *Proceedings of the 2021 ANCOLD Conference.*

Griffin, J., Clark, D., Kemp, J., Stirling, M., King, T., Kulesza, O., La Greca, J., Sharma, A., Quigley, M., Ninis, D., Pietsch, T., Eaton, B. & Wilcken, K. (2024). Large Earthquake Recurrence in the Snowy Monaro Region: New Findings to Inform Dam Safety. *Proceedings of the 2024 ANCOLD Conference.*

McMorran, T. & Hull, A. (2013). Fault rupture hazard assessments for dam foundations: examples from contrasting tectonic environments. *Proceedings of the 2013 ANCOLD Conference.*

Mote, T.I., Vitharana, N., Johnstone, L. & Illangakoon, K. (2021). Active Fault Assessment for a Proposed Pumped Hydro Energy Storage Project in South Australia. *Proceedings of the 2021 ANCOLD Conference.*

Ninis, D., Borleis, E. & Peck, W. (2018). Evaluating potentially active tectonic faults for probabilistic seismic hazard assessments in Australia. *Proceedings of the 2018 ANCOLD Conference.*

Ninis, D. & Clark, D. (2019). Fault Investigation Practice in Australia and New Zealand: Why Australian Dam Owners and Operators Should Care About Collecting Active Fault Data. *Proceedings of the 2019 ANCOLD Conference.*

Quigley, M., Werner, T., Tang, Y., Clark, D., Griffin, J. & Yang, H. (2024). Exposure of Australian Dams to Earthquakes on Proximal Faults. *Proceedings of the 2024 ANCOLD Conference.*

Sandiford, M., Wallace, M. & Coblentz, D. (2004). Origin of the in situ stress field in south-eastern Australia. *Basin Research, 16(3),* pp.325–338.

Somerville, P., Skarlatoudis, A. & MacFarlane, D. (2017). Conditions under which identified faults contribute significantly to seismic hazard in Australia. *Proceedings of the 2017 ANCOLD Conference, Hobart, Australia.*

https://doi.org/10.56295/1ACEG22

IMPORTANCE OF DETAILED GEOMORPHIC INTERPRETATION IN THE LANDSLIDE CHARACTERISATION COMPONENT OF LANDSLIDE RISK ASSESSMENT

Nicholas J. Roberts[1,2], Anthony S. Miner[3]

[1]Mineral Resources Tasmania, Rosny Park, Tasmania, Australia;
[2]University of Tasmania, Sandy Bay, Tasmania, Australia; [3]GHD, Geelong, Victoria, Australia

ABSTRACT

Inventories are foundational to landslide hazard characterisation, and thus risk assessment, but commonly suffer from inadequate landslide detection and interpretation. Bare-earth LiDAR models offer excellent opportunities to identify and understand diverse slope failures from their landscape signatures. However, LiDAR's utility is rarely fully leveraged because of unfamiliarity with its datasets and underappreciation of the geomorphic subtleties they record. We illustrate challenges – and some solutions – to interpreting and documenting landslide features with wide-ranging geomorphic distinctiveness using LiDAR through the worked example of a hilly 2.8-km^2 site in Tasmania. Its size and undulating slopes are representative of typical residential subdivisions and development-pressured land fringing many Australian cities. Previous high-level, reconnaissance mapping did not identify any landslides at this site. However, iterative, site-focused landform mapping using publicly available LiDAR data and complementary open-access datasets reveal diverse slope movements. They range from fresh-looking, indisputable landslides to very subdued features suggesting much older movements, all of which should be further considered during site visits. Improved landslide hazard characterisation in this example highlights key factors influencing landslide inventorying: LiDAR's utility in conveying diverse geomorphic indicators; complementarity of geospatial techniques for interrogating elevation data; contributions from supplemental information sources; inverse proportionality between land extent and mapping detail; value of mappers' previous experience; and benefits of discussion-based landscape interpretation. Expanding site inventories into adjacent terrain and to consider evidence of additional geohazards enhances both identification and likelihood-consequence estimation of hazard scenarios. Robust landslide inventories such as this improve the entire risk assessment process and enable better risk management.

1 INTRODUCTION

Geomorphic interpretation is critical to landslide inventories, which in turn are the foundation to all other aspects of landslide mapping, spanning from susceptibility mapping, through probabilistic hazard mapping, to risk mapping. Inventories also play a key role in local-scale landslide risk assessment by helping identify conceivable hazard scenarios as well as guiding the location and form of detailed site investigations. Robust inventories necessitate not only capturing of conspicuous landslide evidence but also identifying and interpreting muted and subtle features that indicate, or even only hint at, the occurrence and behaviour of much older slope movements. Bare-earth LiDAR models (Dong & Chen, 2017) have become critical tools in developing landslide inventories (e.g. Mazengarb & Stevenson, 2010; Miner et al., 2010) including detailed characterisation of specific landslides (e.g. Cook et al., 2022; Choi et al., 2024) and, where it is available, should be heavily used in those activities. Beyond providing exceptional detail on the location, extent, type, and behaviour of landslides, geomorphic subtleties conveyed by bare-earth LiDAR models can provide insights into landslide failure depth, relative age, and contributing factors (cf. Griffiths & Whitworth, 2012). However, the power of such data is commonly underutilised. This shortfall, which hinders hazard characterisation and ultimately landslide risk management, reflects the relatively limited attention to landslide geomorphology (cf. Crozier, 2010) and all-too-common unfamiliarity with LiDAR's range of capabilities. This is not surprising given that geomorphology – a key field in leveraging the utility of LiDAR – is limited in engineering training in Australia, even in many geoscience programs.

We illustrate the challenges faced in interpreting and documenting landslide features with varying degrees of geomorphic distinctiveness through a worked example. The landslide inventory presented herein is for a 2.8-km^2 site in Tasmania covered by publicly available State LiDAR datasets. It demonstrates LiDAR's capabilities in conveying even very subtle geomorphology as well as the importance of those landforms in driving landslide investigations that support appropriate landslide risk management. Our specific objectives are threefold: 1) highlight information that can be gleaned from bare-earth LiDAR elevation models; 2) provide pointers on maximising usefulness of LiDAR datasets, including integrating complementary information sources; and 3) demonstrate an appropriate level of detail for site-scale landslide inventory. Careful geomorphic mapping, as demonstrated here, greatly improves landslide characterisation and the consequent insights that can inform landslide risk assessment and management.

2 BACKGROUND

2.1 RISK ASSESSMENT PROCESS

Risk assessment and risk management enable some aspects of society to successfully coexist with hazardous processes. In Australia, the approach for slope failures follows the nationally recognised Australian Geomechanics Society (AGS) Guidelines for Landslide Risk Management (AGS, 2007a,b,c,d,e). A revision of the guidelines – for Australia and New Zealand – will be released in 2026.

Risk assessment can be summarised in five fundamental questions: 1. what might happen? (i.e. hazard characterisation); 2. how likely is it? (i.e. frequency analysis); 3. what would be the impact? (i.e. consequence analysis); 4. how important is it? (i.e. risk estimation and evaluation); and 5. what can be done? (i.e. risk management). This paper demonstrates the criticality of geomorphic interpretation to the first question and provides insights into how such interpretations can help address the second question. It aligns with initial components of Baynes and Perry's (2022) workflow for engineering geological models as well as the 'landslide characterisation' component of hazard analysis in AGS (2007a) (Figure 1).

2.2 GEOMORPHIC INTERPRETATION IN LANDSLIDE MAPPING

Geomorphic interpretation is key to identifying and describing past landslides and provides a basis for constraining where future landslides may occur (Griffiths and Whitworth, 2012). Information derived at this stage of investigation supports all aspects of landslide mapping as well as site-specific landslide risk assessment (cf. Figure 1a). Unfortunately, landslide geomorphology has historically received much less attention than other Earth-surface processes (Crozier, 2010).

LiDAR offers one of the best opportunities for landslide characterisation (Miner et al., 2010; Griffiths and Whitworth, 2012), regardless of project scale and scope. Beyond providing greater landform detail than most other remotely sensed datasets, bare-earth elevation models derived from LiDAR data reveal geomorphic indicators that are otherwise too subtle to recognise or entirely obscured by vegetation. Other datasets need to be considered in conjunction with LiDAR, including geologic mapping, historical aerial photographs, archival information, and local knowledge. Additionally, other modern remote sensing technics can provide important, complementary insights into landslides (e.g. Roberts et al., 2019; Cook et al., 2022; Choi et al., 2024). However, LiDAR datasets should be central to landslide mapping when available.

2.3 DATASETS AVAILABILITY

In Australia, Tasmania has some of the best coverage of open-access data for landslide characterisation. Much of it is available through online map viewers and associated GIS web services. All parts of the state are covered by multiple eras of aerial photography since 1930, with most now searchable and freely downloadable. LiDAR datasets are publicly accessible for ~75% of the state and are expanded annually; hillshades and contour lines are available from LIST Map (https://maps.thelist.tas.gov.au) whereas point clouds and gridded digital elevation models (DEMs) are available from ELVIS (https://elevation.fsdf.org.au). Geologic mapping varies across several scales down to 1: 25 000 although surficial units are commonly underrepresented in favour of underlying bedrock. Open-access drilling records comprise drill holes, auger holes, and test pits, with archived drill core available for viewing. Tasmania has an extensive landslide mapping program, although its ~10,000 identified and possible landslides largely reflect moderate-scale reconnaissance mapping.

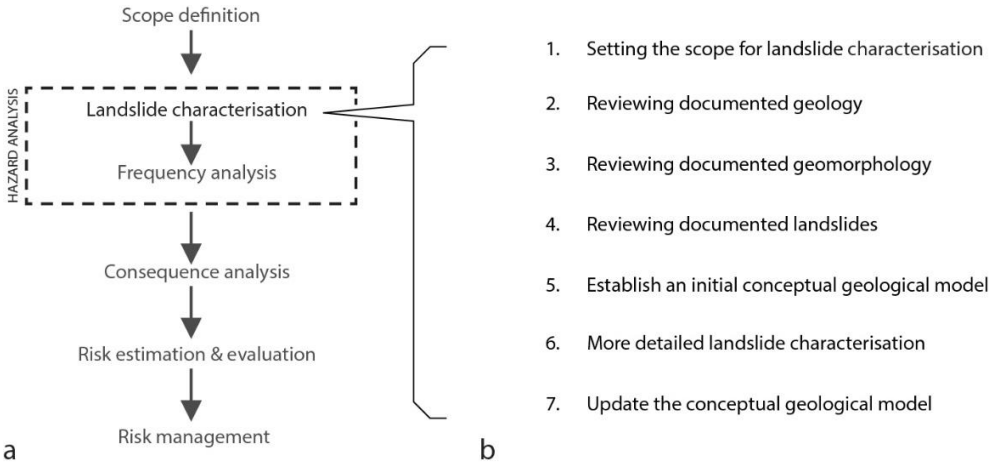


Figure 1: Context of hazards characterisation as a) a component of the landslide risk assessment process (simplified from AGS 2007a) and b) comprising the seven key steps formalised herein.

Dataset availability is highly variable elsewhere in Australia. LiDAR coverage is sporadic and only sometimes freely accessible (cf. ELVIS). Landslide mapping is particularly limited in most areas and, where it exists, is typically difficult to access. Geoscience Australia's listing of landslides and landslide-triggering events (GA 2012; Leiba 2013) provides some helpful details but is highly irregular in spatial-temporal coverage with spatial referencing limited to estimated point coordinates.

3 LANDSLIDE CHARACTERISATION PROCESS

Landslide characterisation forms the foundation of risk assessment (Figure 1a). We formalise landslide characterisation into seven steps (Figure 1b), elaborated below. This paper focuses specifically on LiDAR dataset usage in the recognition and understanding of landslide features to support three tasks: identifying processes and consequent hazards; interpreting the behaviour and timing of past movements; and estimating the character and likelihood of future movements.

3.1 SETTING THE SCOPE FOR LANDSLIDE CHARACTERISATION

Spatial extent and intended land use together dictate the scope and resolution of landslide characterisation. Necessary site background includes determining clearance and land-use history, aided by insights from historic imagery and topographic maps. Geographic bounds determine the nature and diversity of ground conditions that will be encountered, including slope geometries, materials, and processes. The types and density of land use determine exposure to hazards. They additionally may aggravate existing hazards and produce new hazards. Critically, hazard characterisation, and thus inventory area, should extend beyond just the spatial extent of the project area; insights from adjacent, analogous landscapes provide key opportunities for identifying and understanding existing and potential hazards.

3.2 REVIEWING DOCUMENTED GEOLOGY

Existing geologic information is a fundamental starting point for understanding hazards because of its insights into material properties and their spatial and stratigraphic variability. Both mapping and subsurface information should be considered, although their availability will depend on the scale, purpose, and quality of past work. Beyond geologic maps and drilling, any available soil maps and geophysical surveys should be considered. Rock and soil units determine geomechanical and hydrological properties. Additionally, they provide a starting point for geomorphic interpretation by indicating emplacement processes.

3.3 REVIEWING DOCUMENTED GEOMORPHOLOGY

Geomorphology provides complementary information to geology. Tell-tale landforms left by geologically recent processes remain coupled to their geologic records, enhancing understanding of those processes operating in and responsible for the landscape. In many cases, those processes also represent hazards. Regrettably, geomorphology is not commonly mapped in Australia. However, topographic and geologic mapping provide some insights into, respectively, landscape form and material properties. In the rare instances where geomorphology is mapped, it is typically either very localised or limited in detail. This partially reflects Australia's commonly mature landscapes and relatively slow process rates (cf. Taylor, 1994), which complicate geomorphic interpretation because constituent landforms are generally subdued.

3.4 REVIEWING DOCUMENTED LANDSLIDES

Existing landslide inventories and mapping provide a starting point for identifying and understanding past mass movement types, magnitudes, drivers, and frequencies. These resources are key sources of previous assessors' interpretations of the landscape. They typically include information from a variety of sources, some of which may be challenging to obtain (e.g. local knowledge) or altogether unavailable (e.g. confidential reports). Critically, if mapping is out of date, existing inventories may not represent current conditions or, possibly, even the most recent state of understanding. This is most likely to be the case as most mapping is only periodically refreshed. Furthermore, the information provided can range from limited to excessive (Mazengarb et al., 2010).

Unfortunately, landslide inventories and maps will not already exist in most cases, leaving the responsibility of identifying and interpreting landslides wholly to the current investigator. Even where landslide maps exist, they are commonly difficult to access because they are held by local authorities or commercial consultants; such mapping may be privileged information and thus not publicly available. A key exception is Tasmania's statewide, publicly available landslide inventory (Mazengarb and Stevenson, 2010). As the coverage, recency, and detail of the inventory is highly variable, it should be viewed as a reconnaissance-level depiction of mass movements.

Ancillary sources (e.g. aerial and orbital imagery, archival newspapers) should be considered. They provide complementary information including soil moisture, vegetation type, land use, and above-ground features removed from bare-earth LiDAR models. Additionally, information from different eras can constrain the timing of past landscape change.

3.5 ESTABLISHING AN INITIAL CONCEPTUAL GEOLOGICAL MODEL

Initial conceptual geological models formulate what landscape conditions and processes exist as well as how they influence hillslope evolution (cf. Baynes and Perry, 2022). They are the first call for understanding context and implications of landslide mechanisms. Formation of the conceptual model is directly influenced by the quality, extent, and scale of previous datasets and their interpretation. All existing information should be considered, including landslide mapping, geologic mapping, geomorphic mapping, and subsurface investigations (detailed logs, driller's logs, and even information from groundwater wells). The mapping scale and detail of previous inventories thus directly impacts model development. To a degree, previous assessors' conceptual model will be reflected in their landslide inventories, as these are heavily influenced by their interpretations.

3.6 UNDERTAKING MORE DETAILED LANDSLIDE CHARACTERISATION

This is the start of the new contributions of the current assessor. It may also be the only landslide mapping for the area. Even if not, previous work will likely have been at a smaller scale (i.e. less detailed), using poorer data (e.g. high-altitude aerial photography). Any features already captured are likely the most obvious ones. Mapping should consider multiple representations of the landscape at hand. However, those representations will depend heavily on available datasets.

New LiDAR-based mapping will be limited to superficial features. Geomorphology provides great insight into surface conditions and processes, but also reflects conditions below surface (e.g. estimates of failure depth based on landslide type and extent). However, subsurface conditions cannot be adequately understood from geomorphology alone.

3.7 UPDATING THE CONCEPTUAL GEOLOGICAL MODEL

The initial conceptual model is updated by considering previous work and adding new landslide interpretations. In some cases, particularly where little new information is available, that model may only slightly change. Alternatively, the model will change drastically where the new assessors' interpretations differ from those previous and, especially, where new insights are available. This is particularly relevant where previous work did not have the benefit of geomorphic insights provided by bare-earth LiDAR elevation data.

4 CASE STUDY

The following case study uses a real landscape in a hypothetical scenario to demonstrate the above seven-step landslide characterisation process. It emphasises the importance of geomorphic interpretation for site-specific landslide mapping (section 3.6) and ensuing conceptual geological model revision (section 3.7). All datasets presented are publicly available through online sources (detailed in section 2.3). The specific locality is unimportant and, thus, not indicated.

4.1 SCOPE

The project area is a rural agricultural site with mixed vegetation cover (Figure 2a) bordering the suburban fringe of an urban area. The fictitious scenario proposes subdivision of a parcel for moderate-density, detached or semi-detached, residential housing. We have extended the study area to be considered in mapping and conceptual model development beyond the dimension of the project area to ensure adequate context for thorough hazard characterisation.

4.2 GEOLOGIC MAPPING

Site geology, as depicted in Tasmania's 1:25 000 geologic map series (Figure 2b), spans just a few material types (cf. Corbett et al., 2014): Jurassic (ca. 170 Ma) Tasmanian Dolerite, which is locally deeply weathered; Cenozoic alluvium spanning gravelly Quaternary (< ca. 2.6 Ma) and predominantly fine-grained Palaeogene-Neogene (ca. 66-2.6 Ma) sediments; and Cenozoic ferricrete formed within colluvial cover and the older alluvial sediments.

No subsurface information is available within the study area, although nearby boreholes provide general context. Core logs through pre-Quaternary alluvium ~1 km away record weathered, very weak sedimentary rock to at least 10 m depth. Logs through dolerite ~3-4 km away indicate <1 m of residual soil over slightly weathered dolerite near ridgelines in contrast to ~1-1.5 m residual soil overlying at least 10-15 m of very deeply weathered dolerite lower on slopes.

4.3 GEOMORPHIC MAPPING

No geomorphic mapping has yet been published for this area. However, topographic and geologic information (Figure 2b) provide some helpful insights. General slope profiles, the substantial age of most geologic units, and the formation of ferricrete all suggest development of a thick colluvial apron. Mapped alluvium of wide-ranging ages indicates long-lasting fluvial influences as well as minimal modification of pre-Quaternary sediments. *In situ* weathering necessary to produce the ferricrete further reflects mature, relatively stable landscapes.

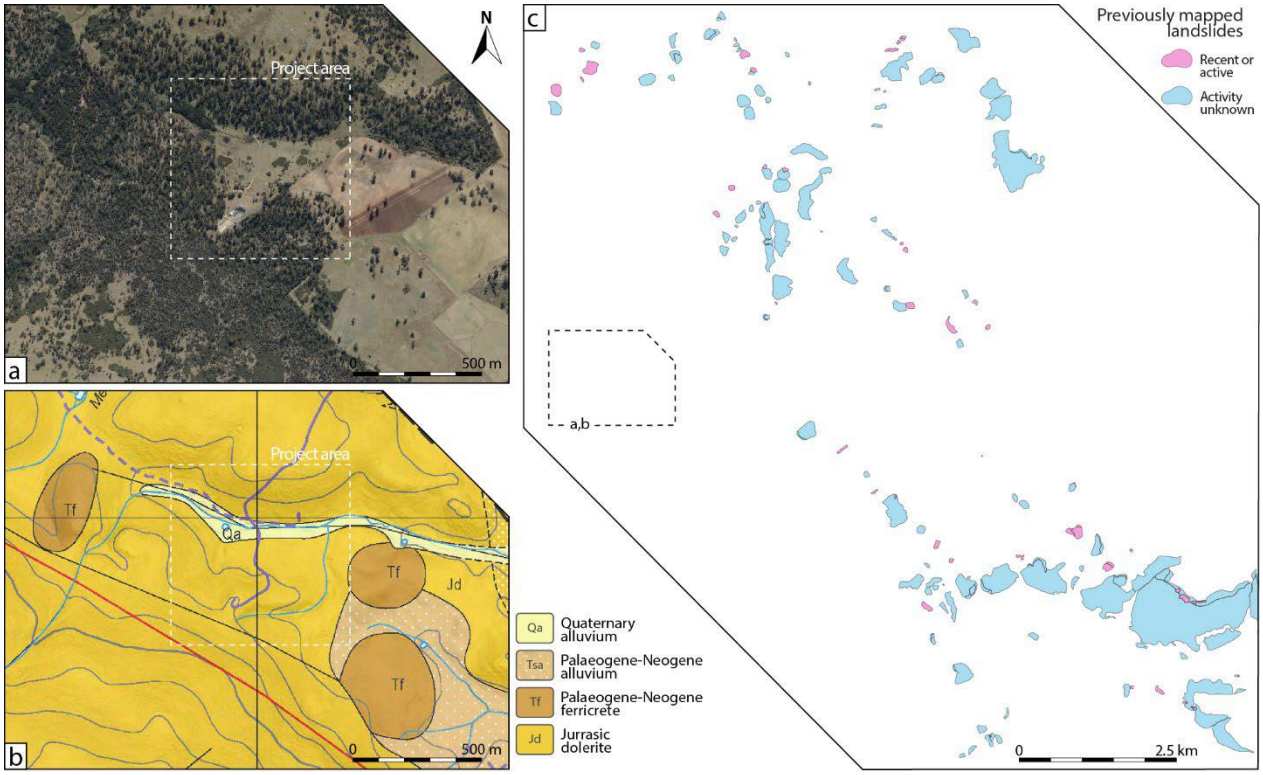


Figure 2: Available background information for the study area: a) recent aerial photograph; b) 1: 25 000 geologic mapping; and c) regional landslide mapping. All datasets are viewable in LIST Map.

4.4 LANDSLIDE MAPPING

Despite the study area's reasonably landslide-prone terrain and coverage by various information sources, no slope failures have been previously documented. No landslides are indicated in MRT's statewide landslide database (Figure 2c) or the most detailed published geologic mapping (Figure 2b). No landslide impacts are indicated in MRT's landslide damage dataset or could be found through searches of archival newspapers in the National Library of Australia's Trove repository.

4.5 INITIAL CONCEPTUAL GEOLOGICAL MODEL

Topographic and geologic information enable formation of a basic conceptual geological model focusing on the main, southwest slopes (Figure 3). Fresh dolerite occurs near surface in uppermost slopes with depths of deeply weathered dolerite and thinner overlying residual doleritic soils increasing down slope; soil-strength materials derived from dolerite exceed 15 m near slope toes, and residual soils are expected to become finer. Valley bottoms are covered by older (probably pre-Quaternary) alluvium with incised, narrow corridors of younger (Quaternary) alluvium along channels.

Insufficient landslide information hinders the demonstration of past failure mechanisms as well as the anticipation of future failure types, locations, and magnitudes. However, based on the simple conceptual model, debris slides are most likely to

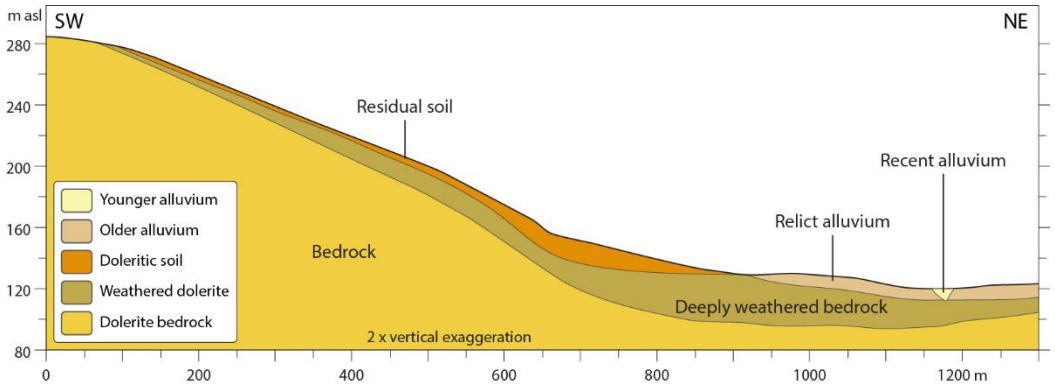


Figure 3: Initial conceptual geological model.

occur in coarse-grained mid-slopes and earth slides in fine-grained lower slopes. Small rotational or compound landslides (i.e. riverbank slumps) are likely to be concentrated along modern river channels, particularly near sharp cutbanks.

4.6 LANDSLIDE INVENTORY PRODUCTION

The authors mapped together while discussing interpretations, enabling efficient identification, description, and basic evaluation of features. The most obvious features were mapped first. Each subsequent mapping pass identified progressively more subtle features aided by insights from more obvious analogues already detected and by the interpreters' growing familiarity with the landscape. The landslide inventory was thus iteratively expanded with each pass identifying additional landslide features, albeit of progressively lower confidence. Notably, mapping leveraged complimentary ways of viewing the LiDAR models and their derivative representations (Figure 4) as well as ancillary datasets (e.g. Figure 2a,b).

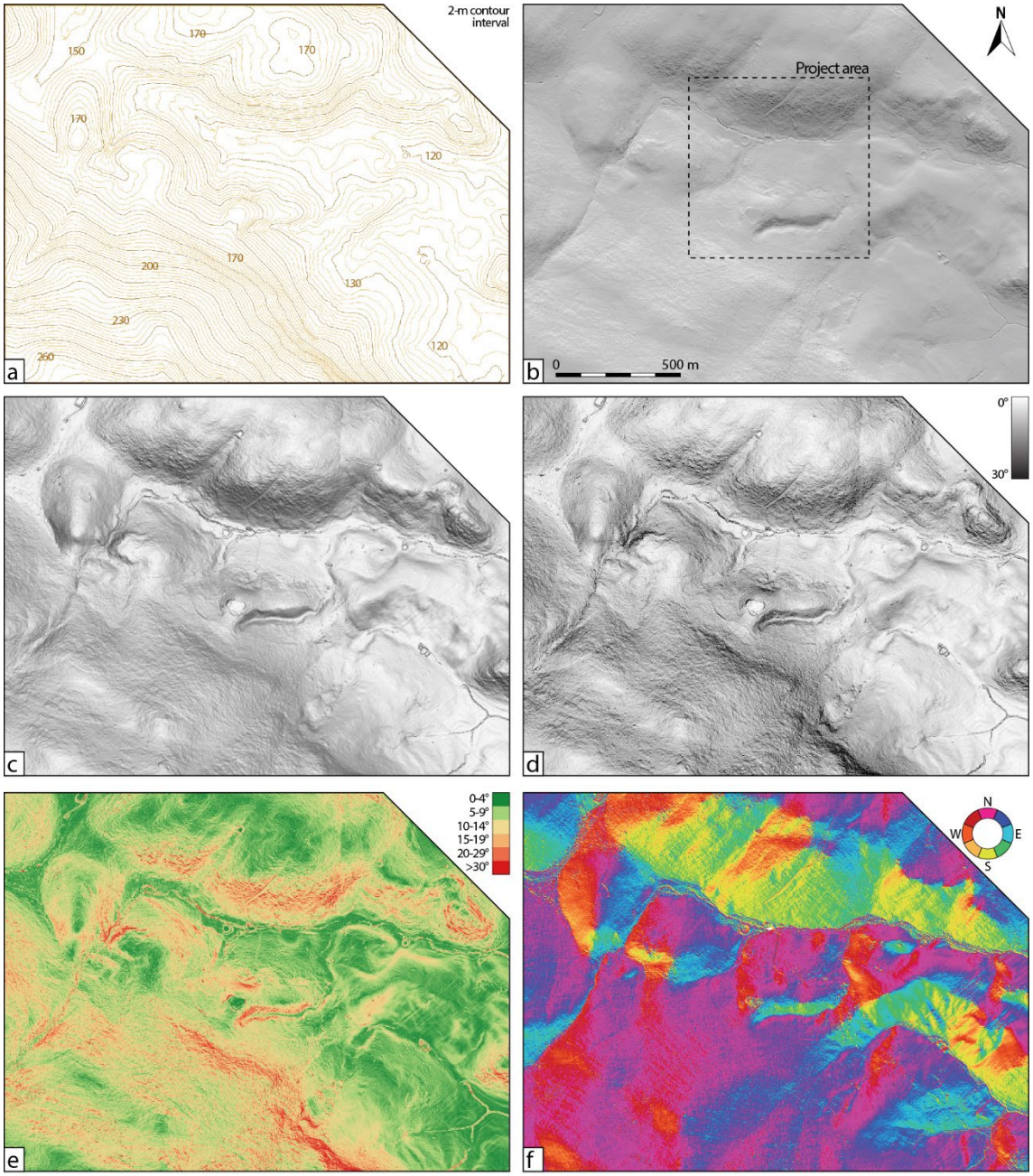


Figure 4: Diverse topographic representations of the same bare-earth LiDAR dataset: a) QGIS-generated contour lines; b) QGIS-generated hillshade; c) LIST Map hillshade; d) GlobalMapper slopeshade: e) QGIS-generated slope map; and f) QGIS-generated aspect map. Each is influenced by user-selected preferences, with some similar products appearing different ('b' vs 'c') and some different products appearing similar ('c' vs 'd').

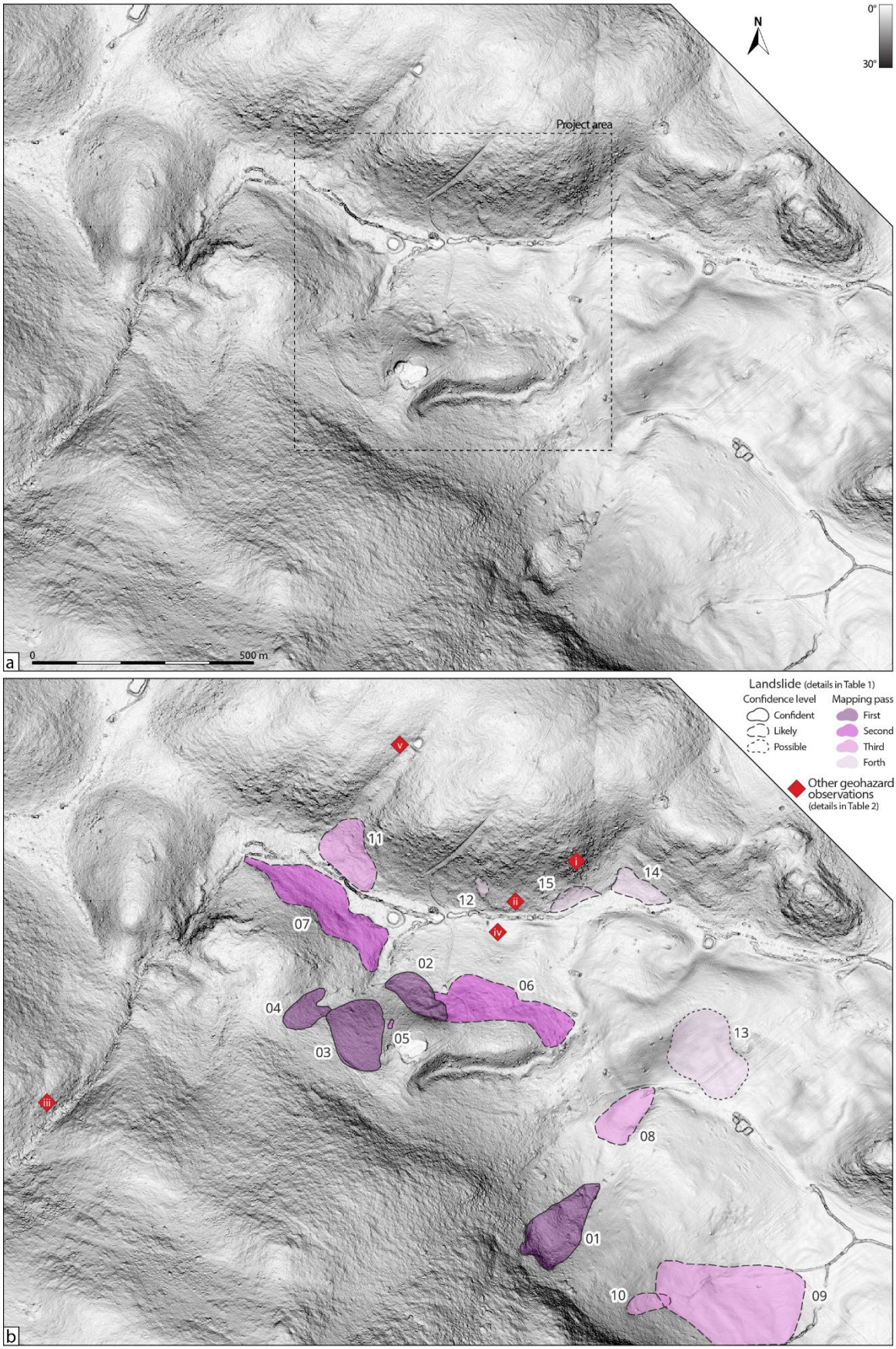


Figure 5: Iterative mapping with slope shader (Figure 4d) as base map. Identified features comprise landslides (polygons: details in Table 1) and other observations related to geohazards (diamonds: details in Table 2).

Table 1: Basic details of mapped landslides.

Feature	Pass	Type	Confidence	Rating*	Comment
01	1	Earth slide	Confident	1	Most obvious feature; pronounced headscarp, toe, & internal lobes
02	1	Debris slide	Confident	2	Conspicuous lobes becoming more muted toward western margin
03	1	Debris slide	Confident	3	Subtle, suggesting either greater age, shallower depth, or both
04	1	Debris slide	Confident	3	Subtle, suggesting either greater age, shallower depth, or both
05	2	Earth slide	Confident	2	Sharp boundaries, but very small; visible easily at very large scale
06	2	Debris slide	Likely	3	Similar to adjacent feature 02 but more degraded appearance
07	2	Debris slide	Likely	3	Similar to adjacent feature 02 but more degraded appearance
08	3	Earth slide	Likely	4	Muted but confidence increased by analogous feature upslope
09	3	Earth slide	Likely	2	Muted boundaries but distinct internal structure; confidence increased by likely analogous features (08 & particularly 01)
10	3	Earth slide	Likely	3	Very subtle, degraded morphology; limits visible in 3D perspective
11	3	Debris slide	Likely	4	Toe displaces stream but other limits unclear; mechanism uncertain
12	4	Debris slide	Possible	5	Lobate feature probably in soil with coarse rockfall; possibly evidence of how this colluvial apron evolves
13	4	Earth slide	Possible	5	Very muted downslope-trending ridges ending in lobes
14	4	Debris slide	Likely	4	Noted when examining LIST Map hillshade
15	4	Debris slide	Likely	4	Noted when examining LIST Map hillshade

* Qualitative rating of feature clarity:
1 - Landslide of identifiable type with sharp geomorphic features
2 - Landslide of identifiable type with subtle/degraded geomorphic features
3 - Landslide of identifiable type with subtle/degraded geomorphic features, limits difficult to determine
4 - Likely landslide, type and/or limits uncertain
5 - Speculative at best

We identified 15 landslide features within and adjacent to the project area through five iterative passes (Figure 5; Table 1). The slope-shaded DEM (Figures 4d, 5) was the main source of interpretation. However, differing visualisations benefited feature identification and characterisation by providing additional insights into landforms and the processes they reflect. For instance, some subtle landslide features (nos. 14 and 15) were not readily apparent in the slope-shaded DEM but were clearly evident in the LIST Map hillshade (Figure 4c vs 4d). Topographic profiles and 3D perspective views assisted in recognising and interpreting many features. Landslide features were primarily identified from LiDAR datasets, although ancillary datasets provided useful insights and context.

The main identified landslide mechanisms are earth slides and debris slides. Subtle features indicate that rock fall and debris flow could occur locally. Mapping identified several various geomorphic features of interest related to additional geohazard scenarios at the site (Figure 5b; Table 2): hints of dolerite outcrops producing rock fall (i) that may form colluvial aprons along some slope toes (ii); a likely bedrock channel that could carry debris flows (iii); tunnel gullying (iv); and a farm dam that could produce a channelised outburst flow (v). Attribution at minimum should include the fields in Table 1. Free-form comments or notes provide a critical summary that helps map users understand the rationale behind the identification of a given feature.

Table 2: Basic details of other geohazard observations.

Feature	Pass	Type	Confidence	Comment
i	3	Rockfall	Likely	Scabby texture indicates heavily jointed bedrock at or near surface
ii	4	Colluvial apron	Possible	Lobate aprons suggest debris accumulation from suspected rockfall sources
iii	4	Bedrock channel	Likely	Shallow bedrock forms a channel that could carry saturate debris
iv	2	Tunnel gullying	Confident	Deep, narrow, locally covered channel suggesting subsurface erosion
V	3	Farm dam flood source	Possible	Earthen dam impounding a small reservoir, if it failed, could release a small but extremely rapid flood down the channel below

4.7 REFINED CONCEPTUAL GEOLOGICAL MODEL

Geomorphology recognised using bare-earth LiDAR data helped to confirm and refine the initial conceptual geological model, including expansion to the area's northern slopes (Figure 6). Notably, the detailed hillslope characteristics determined using DEM representations, profiles, and 3D perspectives provide key additional insights into material properties and formative processes. Steepness, morphology, and texture were particularly useful. Rough patterns on steeper slopes in the study area's north indicate the main departure from the initial conceptual model: dolerite bedrock is near and locally at surfaces in middle to upper slopes whereas debris, possibly from rock fall, mantles slope toes.

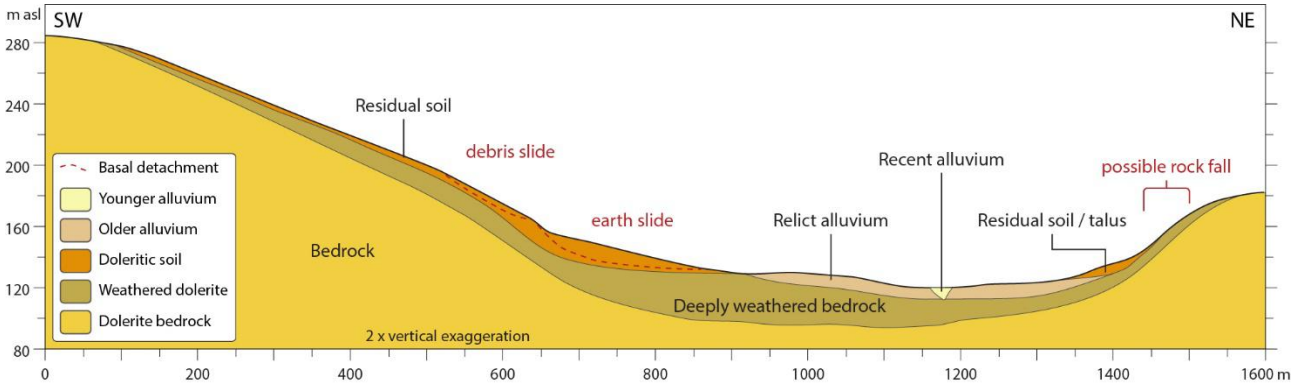


Figure 6: Revised and expanded conceptual geological model.

The initial conceptual model reasonably explains moderate-to-gentle slopes elsewhere in the study area. Surface textures along slope toes support the previous expectation of substantial, downslope-fining colluvial deposits on most slopes. Spatial distributions of landside mechanisms, as interpreted from geomorphic expression, further support the previously expected extents and relative depths of weathered and sedimentary units. Thus, the revised conceptual geological model is similar to the initial one but adds recognition that locations of the most common landslide types are determined by the thickness and fineness of dolerite-derived slope deposits.

5 DISCUSSION

A structured approach to landslide mapping helps achieve better consistency and overall quality. The worked example herein helps demonstrate various factors and considerations in landslide mapping, particularly when using bare-earth LiDAR DEMs. Their careful interpretation will help improve landslide inventories of any scale.

5.1 CASE STUDY FINDINGS

The above case study illustrates subtleties and capabilities of bare-earth LiDAR DEMs for landside mapping. It also demonstrates the vast improvement in site-specific landslide characterisation that LiDAR datasets enable when thoroughly investigated. No landslides were identified at the site during previous geologic or regional landslide mapping. By contrast, careful LiDAR DEM interpretation identified numerous relevant features: five landslides; ten suspected landslides; and additional geohazard scenarios including tunnel gullying and channelised outburst from a small farm dam reservoir. Each of these features and processes could negatively impact current and future site uses. Each must be carefully considered throughout the risk assessment process to determine whether proposed future development is appropriate and if landslide risk management is necessary to achieve tolerable risk levels.

Subtleties in bear-earth LiDAR datasets indicate significant potential geohazards at the site and many more past landslides than most practitioners or land managers would likely have expected. Landslide potential elsewhere in Australia is probably similarly underappreciated. The case study site is representative of landscape conditions and development pressures in the periphery of urban areas across Australia's Eastern Uplands (cf. Pain et al., 2011). It is thus relevant to development-pressured regions not only in Tasmania but in landslide-affected parts of mainland Australia.

5.2 INSIGHTS INTO LIDAR-BASED LANDSLIDE MAPPING

There is no single way to best utilise LiDAR datasets. The general process and specific activities herein provide some guidance on its effective use for landslide mapping. Project area, resourcing, and purpose together determine mapping scale, thresholds for what is or is not considered, the degree to which features are split or amalgamated, and the level of detail in attribution.

5.2.1 Specifics of the mapping process

Some best practices within the mapping process, as demonstrated in the case study, are strongly recommended. Mapping should extend beyond the designated project area. How far, however, depends on consistency of physiography, geology, and geomorphology. The aim is to consider representative conditions that will help inform processes and possible hazards at the project site. Nearby areas may have better information or more informative features, thus providing clearer demonstration of processes and hazards at play. Conversely, looking too far away may add too much complexity or variation in preparatory conditions, landslide mechanisms, and failure triggers.

Best practice uses multiple, complimentary information sources. Beyond being the best available datasets, these should provide differing information types (e.g. ground cover, elevation, and reported observations) and, where possible,

represent different eras to help inform rates of landscape changes (e.g. multitemporal aerial photography and satellite imagery). In the case of LiDAR, using multiple representations of bare-earth elevations is especially important to provide different perceptions and perspectives that support robust interpretations (cf. Figure 4). Where LiDAR datasets are unavailable or of poor quality, new LiDAR collections may be critical to project success.

Making multiple passes allows mapping to systematically progress from the most obvious to the least distinct features. This helps to calibrate the assessor in recognising the range of morphology types and their gradual degradation in a given landscape. Beyond leveraging obvious features to assist in interpreting more muted analogues, this approach helps inform the relative antiquity and activity of previously mapped landslides.

Many details can be interpreted remotely from LiDAR datasets. However, the range and confidence of information remain limited without field confirmation and detailed investigation. Given the numerous attributes that could be included in a landslide inventory (cf. Mazengarb et al., 2010), careful consideration is necessary to avoid superfluous data while ensuring that sufficient information is provided, not only for present needs but for anticipated future inventory uses. Inventories should also convey the level of interpretation confidence, which commonly reflects the degree of geomorphic clarity.

5.2.2 Scale and detail

Mapping scale and detail will depend on four factors: extent of area, complexity of area, purpose of work, and resources available. Notably, workload increases geometrically, not arithmetically, with project scale. For instance, by necessity of its areal extent, Tasmania's extensive statewide landslide inventory – considered to be one of the best in Australia – does not capture all obvious or potential landslide features and commonly groups contiguous landslides into landslide areas or landslide complexes. Additionally, the detail of Tasmania's statewide mapping differs from location to location based on mapping date, available base datasets, risk profile, relevance to past projects, and who specifically did the work. Mapping at larger scale for more targeted projects – such as specific subdivisions, lots, or infrastructure corridors – should greatly expand upon available regional-scale mapping.

5.3 IMPORTANCE OF EXPANDING BEYOND EXISTING MAPPING

Absence of previously mapped landslides is no guarantee that landslide evidence is lacking in the landscape. This is particularly the case where LiDAR now provides new opportunities for detailed geomorphic mapping that was far more challenging and potentially impossible with earlier datasets and information, such as aerial photograph interpretation and on-site inspections. Simply stating "no mapped landslides" is insufficient for landslide characterisation; site assessors must evaluate the study site at an appropriate scale and explain what they have done.

Any existing mapping should be considered a starting point for site-specific inventories. Site investigators must consider not only what is already known about a site, but what might have been missed in previous mapping due to scale, data availability, or purpose. The small area of site-scale investigations enables far more detailed interpretation and mapping. Do not assume that previously mapped landslides are the only features present or accurate representations of current slopes. Any mapping captures a landscape at a point in time. New landslides will eventually occur, and existing ones can change in extent, mechanism, or obviousness. Additionally, other natural and anthropogenic processes will modify slopes.

6 CONCLUSIONS

We developed a seven-step landslide characterisation process that leverages the geomorphic utility of LiDAR datasets. Detailed geomorphology conveyed in bare-earth LiDAR models is largely independent of vegetation cover and provides critical insights on the location, extent, and mechanisms of past landslides. It also provides evidence that helps approximate landslide age. A worked case study demonstrates the proposed steps. Additionally, it highlights the importance of thorough geomorphic interpretation in landslide mapping, with impacts on the entire landslide risk management process.

LiDAR is one of the most effective tools available for producing robust, appropriately detailed landslide inventories. It is especially powerful for understanding Australia's relatively old landscapes and generally slow processes, where subtle geomorphology complicates the identification and interpretation of landslide features. Our landslide characterisation process and case study illustrate several additional key points. Landslide mapping requires multiple passes to maximise LiDAR's benefits. More detail must be considered at site-scale than small-scale mapping exercises, with the former highly likely to identify additional features. Expanding landslide inventories spatially beyond the study site and to include related geohazards enhances the identification and subsequent likelihood-consequence estimation of hazard scenarios. Landscape interpretation involving discussion amongst assessors, combined with their previous mapping experience enhances comprehensive recognition and understanding of landslide features. Robust landslide inventories directly improve subsequent risk assessment steps and enable better risk management.

Critically, data sources and past interpretations are not infallible. They represent a point in time within ever-changing landscapes. Features in addition to previous mapping very likely exist, having either gone unrecognised or occurred since.

We make the following key recommendations:

- When available, LiDAR data should feature extensively in desktop mapping and guide on-site investigation.
- Complementary geospatial techniques and visualisations should be employed when interrogating elevation data.
- LiDAR data need to be used in combination with supplemental information sources such as other modern technologies, historical imagery, archival records, and local knowledge.
- Mapping requires field verification, acknowledging that subtle features may be most apparent in LiDAR datasets.
- Because of the dynamic nature of landscapes, landslide mapping should be periodically updated.

Having completed a robust landslide characterisation, the rest of the risk assessment process can then more effectively proceed beginning with frequency analysis, which can itself be guided by LiDAR-based geomorphic interpretation.

7 ACKNOWLEDGEMENTS

NJR publishes with permission of the Director of Mines, Tasmania. An anonymous reviewer provided helpful comments.

8 REFERENCES

AGS (Australian Geomechanics Society). (2007a). Guideline for landslide susceptibility, hazard and risk zoning for land use management. *Australian Geomechanics*, 42(1), 13-36.

AGS (Australian Geomechanics Society). (2007b). Commentary on guideline for landslide susceptibility, hazard and risk zoning for land use management. *Australian Geomechanics*, 42(1), 37-62.

AGS (Australian Geomechanics Society). (2007c). Practice note guidelines for landslide risk management. *Australian Geomechanics*, 42(1), 64-114.

AGS (Australian Geomechanics Society). (2007d). Commentary on the practice note guidelines for landslide risk management. *Australian Geomechanics*, 42(1), 115-158.

AGS (Australian Geomechanics Society). (2007e). The Australian GeoGuides for Slope Management and Maintenance. *Australian Geomechanics*, 42(1), 159-182.

Baynes, F.J. & Parry, S. (2022). *Guidelines for the development and application of engineering geological models on projects*, IAEG Commission 25 Publication No. 1, 129 pp.

Choi, S.-K., Ramirez, R.A., Lim, H.H. & Kwon, T.-H. (2024). Multi-source remote sensing-based landslide investigation: the case of the August 7, 2020, Gokseong landslide in South Korea. *Scientific Reports*, 14: 12048.

Cook, M.E., Brook, M.S., Hamling, I.J., Cave, M., Tunnicliffe, J.F., Holley, R. & Alama, D.J. (2022). Engineering geomorphological and InSAR investigation of an urban landslide, Gisborne, New Zealand. *Landslides*, 19, 2423-2437.

Corbett, K.D., Quilty, P.G., & Calver, C.R. (2014). *Geological evolution of Tasmania*, Geological Society of Australia Special Publication 24. Tasmania Division, Geological Society of Australia, 639 pp.

Crozier, M.J. (2010). Landslide geomorphology: An argument for recognition, with examples from New Zealand. *Geomorphology*, 120(1-2), 3-15.

Dong, P. & Chen, Q. (2017). *LiDAR remote sensing and applications*, CRC Press, Boca Raton, Florida, 220 pp.

GA (2012). Landslide Search. Geoscience Australia (updated June 2018), viewed 1 December 2024, <https://id.geoscience.gov.au/dataset/ga/74273>.

Griffiths, J.S. & Whitworth, M. (2012). Engineering geomorphology of landslides, in J.J. Clauge & D. Stead (eds), *Landslides Types, Mechanisms and Modeling*, Cambridge University Press, pp. 172-186

Leiba, M. (2013). Impact of landslides in Australia to December 2011. *Australian Journal of Emergency Management*, 28(1), 30-36.

Mazengarb, C. & Stevenson, M. (2010). *Tasmanian Landslide Map Series: User Guide and Technical Methodology*, Tasmanian Geological Survey Record 2010/01, Mineral Resources Tasmania, Department of State Growth, 44 pp.

Mazengarb, C., Flentje, P., Miner, A.S. & Oscuchowski, M. (2010). Designing a landslide database: lessons learnt from Australian examples', *11th Congress of the International Association of Engineering Geology and the Environment*, Auckland, 6 pp.

Miner, A.S, Flentje, P., Mazengarb, C. & Windle D.J. (2010). Landslide Recognition using LiDAR derived Digital Elevation Models-Lessons learnt from selected Australian examples', *11th Congress of the International Association of Engineering Geology and the Environment*, Auckland, 9 pp.

Pain, C.L., Gregory, L., Wilson, P., & McKenzie, N. (2011). *The Physiographic Regions of Australian – Explanatory Notes*, Australian Collaborative Land Evaluation Program and National Committee on Soil and Terrain, Canberra, 30 pp.

Roberts, N.J., Rabus, B.T., Clague, J.J., Hermanns, R.L., Guzmán, M.-A. & Minaya, E. (2019). Changes in ground deformation prior to and following a large urban landslide in La Paz, Bolivia, revealed by advanced InSAR. *Natural Hazards and Earth System Science*, 19, 679-696.

Taylor, G. (1994). Landscapes of Australia: their nature and evolution, in R.S. Hill (ed), *History of the Australian vegetation: Cretaceous to Recent*, University of Adelaide Press, pp. 60-79.

https://doi.org/10.56295/1ACEG23

ANALYSIS OF THE MECHANISM OF LANDSLIDING, GARIE ROAD, ROYAL NATIONAL PARK, NSW

Tim Donovan[1] and Luke Johnstone[2]

[1]Associate Engineering Geologist, Aurecon [2]Engineering Geologist, AtkinsRéalis

ABSTRACT

Once landslide movement is identified, it is important to employ the necessary investigation techniques to characterise the landslide type and analyse the mechanism of mass movement. Defining the geometry of the landslide slip surface and presenting this with confidence within the engineering geological model is fundamental to the development of the appropriate remedial design solution.

A large landslide developed along Garie Road, Royal National Park in March 2022 following a series of intense rain events. Tension cracking along the centreline of the road progressed quickly to large scale deformation as a slow-moving landslide developed retrogressing to the south and west. This paper presents a case study of the engineering geological and geotechnical assessment of the Garie Road landslide using various investigation techniques including drone terrain evaluation, landslide mapping, detailed core logging and instrumentation review. The data collected to analyse the landslide mechanism is presented and validated through a literature search and comparison of a similar Illawarra escarpment landslide. The comparative study was fundamental in identifying similar basal sliding in close proximity to the interface between the Bald Hill Claystone and the Bulgo Sandstone.

1 INTRODUCTION

1.1 SITE LOCATION

Garie Road is situated approximately 30 km south of Sydney CBD within the Royal National Park. The landslide location is located along a north-south trending section of Garie Road that is approximately 400 m to the west of Garie Beach. The landslide location is presented in Figure 1.

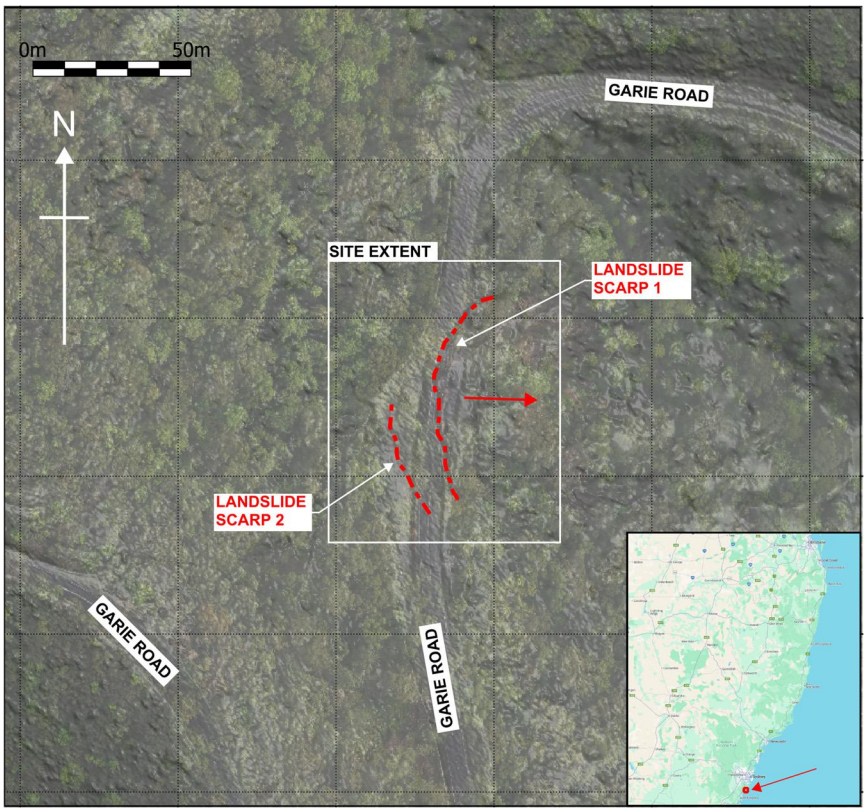


Figure 1: Location and scarp extents of the Garie Road landslide

1.2 SITE GEOLOGY AND GEOMORPHOLOGY

Reference to the Seamless NSW Geological Maps (Colquhoun, et al., 2021) indicates that the site geology comprises (from an upslope to downslope direction) the Hawkesbury Sandstone, Newport Formation, Bald Hill Claystone and Bulgo Sandstone (Figure 2). The landslide site is directly underlain by the Bald Hill Claystone and the top of the underlying Bulgo Sandstone is between ~12 m to 17 m below road level.

An Unmanned Aerial Vehicle (UAV) drone survey was flown over the failed extent of the road and surrounding upslope and downslope areas. An output from the UAV survey was a LiDAR Digital Terrain Model (DTM) that is utilised as the topographic surface in Figures 2, 3, 6, 8 and 10.

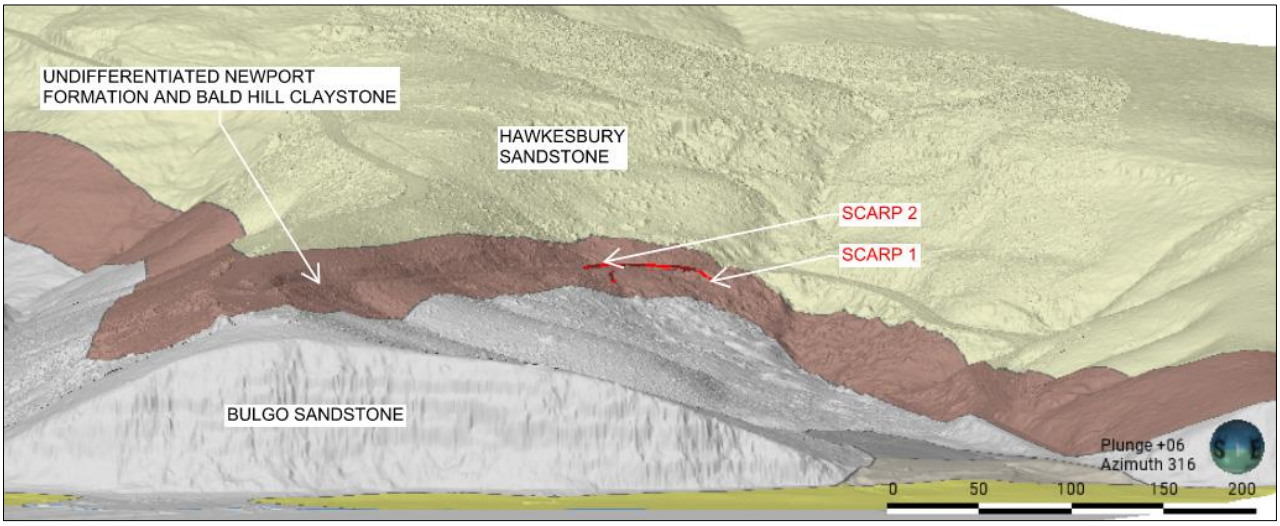


Figure 2: View of the Seamless NSW Geological Maps (Colquhoun, et al., 2021) overlain on the DTM (MES, 2022) of the Garie Road landslide and coastal cliffs. Note: no differentiation is provided on the Seamless NSW Geological Maps between the Newport Formation and the Bald Hill Claystone however the Bald Hill Claystone was mapped as an individual unit on site.

Descriptions of the geological units are presented Table 1.

Table 1: The geological units present in the vicinity of the Garie Road landslide site (Colquhoun, et al., 2021) and (Pells, 1994).

Sub-group	Formation	Map Unit	Period	Description
Hawkesbury Sandstone		Tuth	Middle Triassic	Medium to coarse grained quartz sandstone with minor shale and laminate lenses.
Gosford Sub-group	Newport Formation	Tng_b	Early Triassic	Interbedded shale and sandstone sequence. The unit has a gradational boundary to the underlying Bald Hill Claystone and is interbedded with the overlying Hawkesbury Sandstone.
Clifton Sub-group	Bald Hill Claystone			Chocolate brown to red-brown kaolinitic claystone with silty and sandy grey and mottled grey-brown zones, with minor laminated and thinly bedded siltstones and sandstones ranging up to 3 m thick. The Bald Hill Claystone is primarily kaolinite (50% to greater than 75%) with quartz and feldspar as the remainder. Hematite is the primary secondary mineral and source of the red-brown colour.
	Bulgo Sandstone	Tncu		Fine to medium grained grey-brown to green quartz-lithic sandstone with lenticular brown shale/claystone and siltstone interbeds, sporadic minor polymictic pebble conglomerates.

Garie Road traverses an undulating hillside that slopes at approximately 20-30° to the east. The road corridor is typically 10 m wide and was constructed using cut and fill techniques. The embankment on the downslope side of the road is ≤5 m in height with a gradient of 20° to 40°. At the landslide location, the road corridor widens to approximately 30 m, where the toe of the natural slope to the west is set back from the western edge of Garie Road. It is understood that this widened area is where the previous alignment of Garie Road existed prior to being straightened in the 1960's with the introduction of fill to span the valley.

Site topographical and drainage features are illustrated in Figure 3, which presents an oblique view of the Garie Road landslide site illustrating the topography and incised drainage channels and immediate surrounding area.

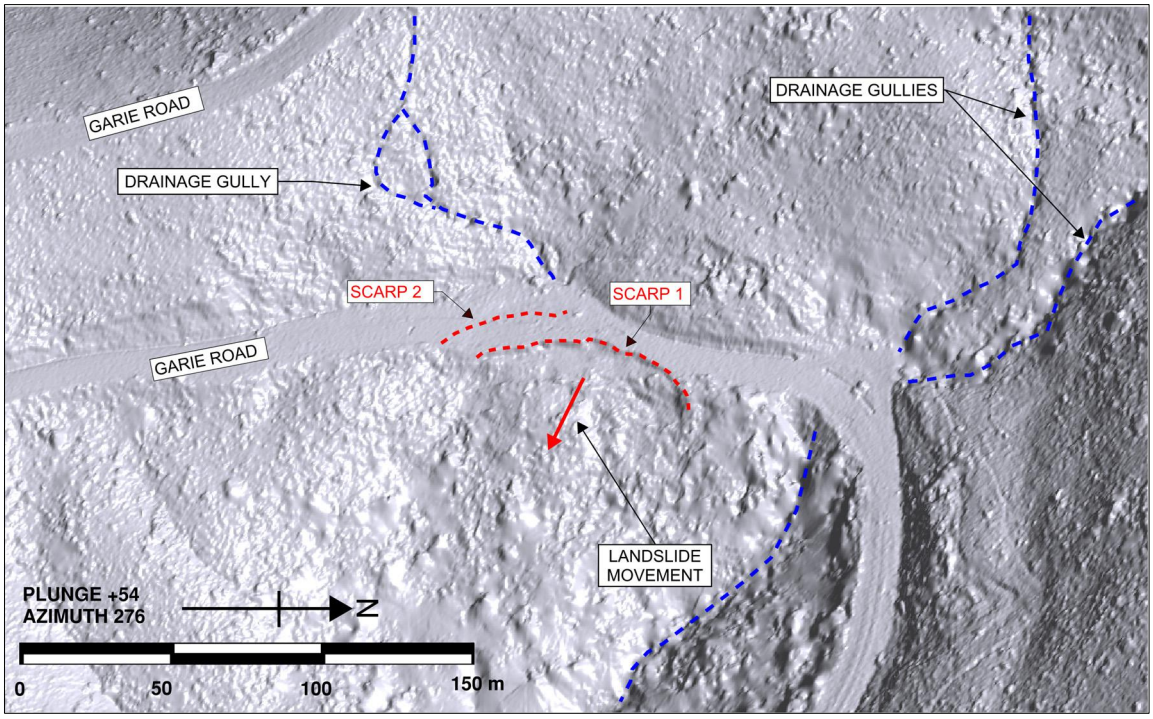


Figure 3: View of the DTM (viewing west) of the Garie Road Landslide site and surrounding area. Source of DTM is MES (2022).

1.3 DEVELOPMENT OF THE LANDSLIDE

The east coast of New South Wales (NSW) experienced severe rainfall in early to mid-2022 associated with the La Nina weather cycle resulting in widespread flooding and significant landslide damage to road and rail infrastructure across the state networks (Flentje, et al., 2022).

In early March 2022, a large landslide developed on Garie Road with the movement direction downslope and to the east. With additional heavy rain events, the landslide grew, retrogressing across the road to the west and some distance to the south between March 2022 and October 2022 (Figure 4). The landslide eventually encompassed the entire road, rendering it impassable by any vehicle.

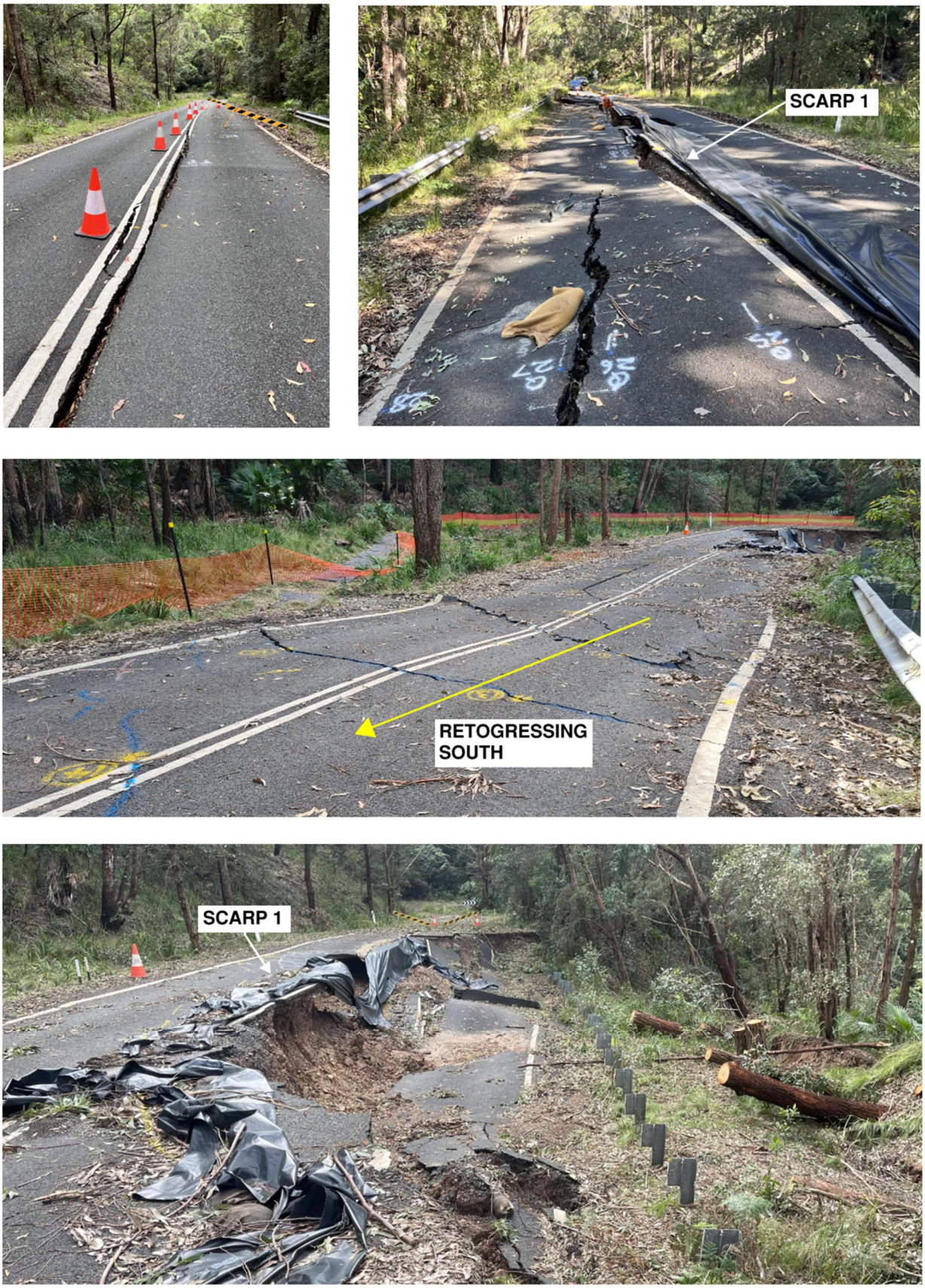


Figure 4: Photos showing the development of the Garie Road landslide. Top left - vertical and horizontal displacement along road centreline (30 March 2022). Top right - significant progression of the deformation (4 April 2022). Middle - landslide retrogressed south (early July 2022). Bottom - Scarp 1 condition (July 2022).

Within 24 hours of the initial ground instability, a series of surface survey monitoring points at various locations were installed above and below the observable scarps to record the ground movement. The movement and rainfall observations are summarised below and in Figure 5:

- **Early March 2022:** 268 mm of rainfall was recorded within two consecutive days. Site observations recorded longitudinal cracking along the centre line of the road and crescent shaped cracking at the northern and southern end of the developing zone of instability.
- **Early April 2022:** 352 mm of rainfall was recorded in five days. This resulted in progression of the instability and a significant landslide backscarp was now evident with ~1 m of vertical displacement.
- **April to July 2022**: Scarp 1 increased to 2.7 m vertical displacement.
- **Early July 2022:** 755 mm of rainfall was recorded within seven days. This resulted in additional vertical displacements of up to 160 mm in the areas surrounding Scarp 1 and the landslide retrogressed to the south. Movement at Scarp 1 slowed and stabilised at ~3 m of vertical displacement.
- **Early to mid-October 2022**: 287 mm of rainfall was recorded in 13 days, resulting in additional instability and a retrogression of Scarp 1. A secondary Scarp 2 (Figure 1) opened to the west of Scarp 1 with vertical displacement ranging from 300 mm to 400 mm with creep of surrounding areas. Survey data recorded 3.3 m of maximum vertical displacement at Scarp 1 in October 2022.
- **November 2022 to April 2023:** The landslide movement stabilised and the surface survey monitoring was terminated in April 2023 due to early construction activities on site.

The above summary is presented graphically in Figure 5 which illustrates the rainfall data near Garie Road (sourced from the nearest Bureau of Meteorology station, Darkes Forest, Kintyre) and the resulting vertical slope movement recorded by the survey monitoring points.

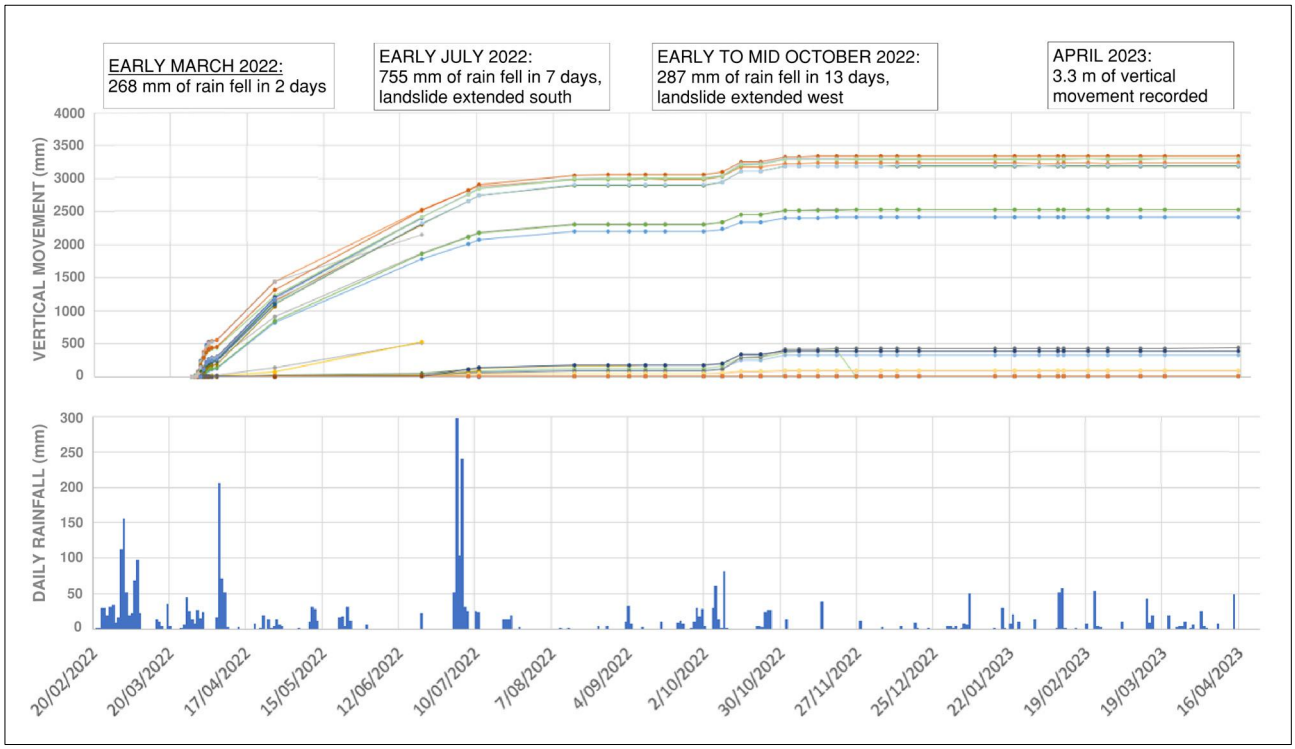


Figure 5: Landslide vertical movement plotted from key survey monitoring points (coloured lines) installed below Scarp 1 and rainfall plot from March 2022 to April 2023. The rainfall data is taken from the BOM database for the Darkes Forest, Kintyre rain gauge.

2 ASSESSMENT METHODOLOGY

Various intrusive and non-intrusive investigation techniques were employed at the Garie Road landslide site to provide the required data to create an Engineering Geological Model (EGM) and characterise the landslide and its mechanism of mass movement:

- **UAV drone survey**:
  Flown over the failed extent of the road and surrounding upslope and downslope areas. The outputs from the UAV survey were high resolution photogrammetry and a LiDAR generated DTM.

- **Engineering geological and geomorphological mapping:**
  Mapping of the zone of instability and surrounding areas including the upslope and downslope (limited access) to the landslide. The mapping assessed the extent and key features of the landslide, key geomorphological features and soil and rock exposures/outcrops.

- **Intrusive geotechnical investigation**:
  A phased geotechnical investigation was undertaken comprising:
  - Twelve cored boreholes.
  - Five (5) seismic refraction lines totalling 450 m in total length, one (1) along the road, one (1) along the toe of the road/landslide and three (3) perpendicular lines in a down slope direction, intersecting boreholes where possible for calibration purposes.

- **Instrumentation installation and monitoring:**
  Geotechnical monitoring instruments were installed in selected boreholes:
  - Four (4) manual inclinometers (refer Figure 8).
  - One (1) Vibrating Wire Piezometer (VWP).
  - Three (3) standpipe piezometers.
  - Four (4) boreholes allocated for downhole imaging with Optical Televiewer (OTV) and Acoustic Televiewer (ATV) methods.

- **Literature Review:**
  A literature review was undertaken on any known documented slope instability within the Bald Hill Claystone, particularly within the Illawarra Escarpment which the Garie Road landslide site forms the escarpments northern limit.

- **Engineering Geological Model:**
  The factual data from the intrusive and non-intrusive investigations was presented in an EGM (produced in Leapfrog software by Seequent). The EGM presents the distribution of the assigned engineering geological units within 3D space and assisted in the characterisation and interpretation of the landslide and its mechanism of mass movement.

3 INVESTIGATION RESULTS

3.1 UAV DRONE SURVEY

The UAV survey produced high quality orthomosaic photos of the landslide and its features, particularly the downslope inaccessible area to the landslide. A key observation from the orthomosaic photos was the identification of the extent of felled trees on the downslope that had been uprooted due to the landslide movement. The lower limit of the felled trees was taken to be the toe of the landslide daylighting from the slope face. This point was georeferenced and inputted into the EGM.

The DTM was a valuable output from the UAV survey and was interrogated to assess additional scarps that could not be observed during the mapping due to steep inaccessible slopes or dense vegetation. In addition, the DTM provided information relating to the geomorphology and drainage characteristics of the site (Figure 3).

3.2 ENGINEERING GEOLOGICAL MAPPING

The engineering geological and geomorphological mapping is presented in Figure 6 and a typical mapped outcrop of the Bald Hill Claystone is presented in Figure 7.

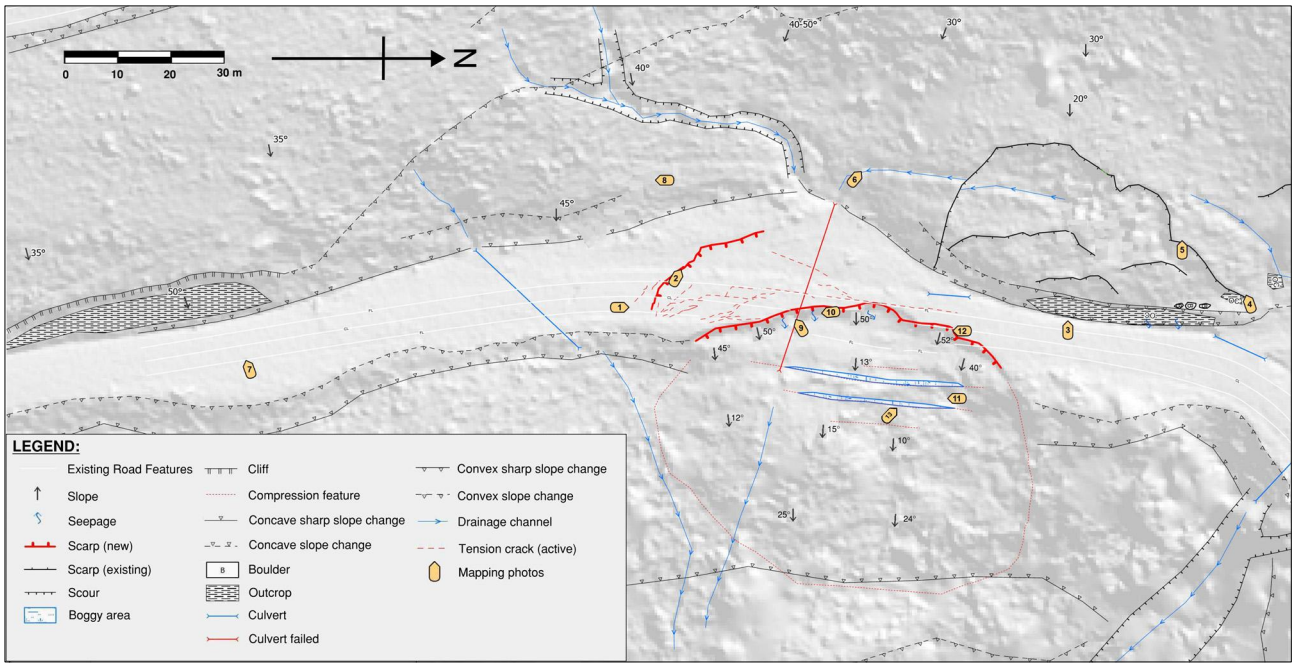


Figure 6: Engineering geological map of the landslide and surrounding area. Source of DTM is MES (2022).

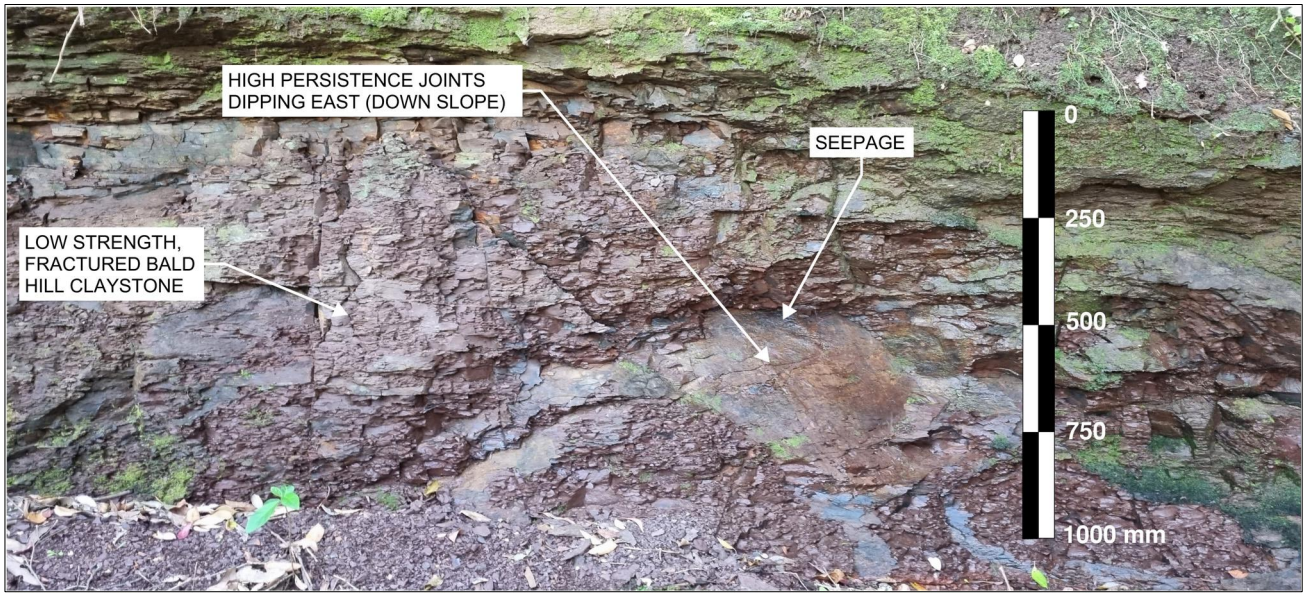


Figure 7: Typical Bald Hill Claystone rock cutting present on the upslope of Garie Road immediately to the north of the landslide

The following is a summary of the key features mapped:

- The landslide was relatively large; the dimensions were assessed to be approximately 80 m in width and 60 m in length from landslide backscarp to toe. The landslide toe extended significantly beyond the road reserve into the National Park to the east.

- The landslide backscarps in the road and road reserve were inclined relatively steep, dipping ~65° to the east.
- A historic scarp was mapped on the immediate downslope to the main landslide with approximately ~2 m of vertical displacement. This historic scarp was less obvious due to compression features resulting from the recent instability.
- Some historic scarps were also mapped on the upslope above the road cutting that is present at the northern end of the site, but with no recent displacement or instability observable.
- The Bald Hill Claystone outcrops are typically highly fractured with their surface being comprised of angular interlocking gravel and cobble sized claystone fragments, separated by clay infilled defects.
- A key outcrop observation was a number of higher persistence smooth joints with groundwater seepage, dipping approximately 60° east (general slope failure direction).

3.3 BOREHOLES AND GEOPHYSICS

A site plan indicating the locations of the exploratory holes, inclinometer locations and seismic refraction lines is presented in Figure 8.

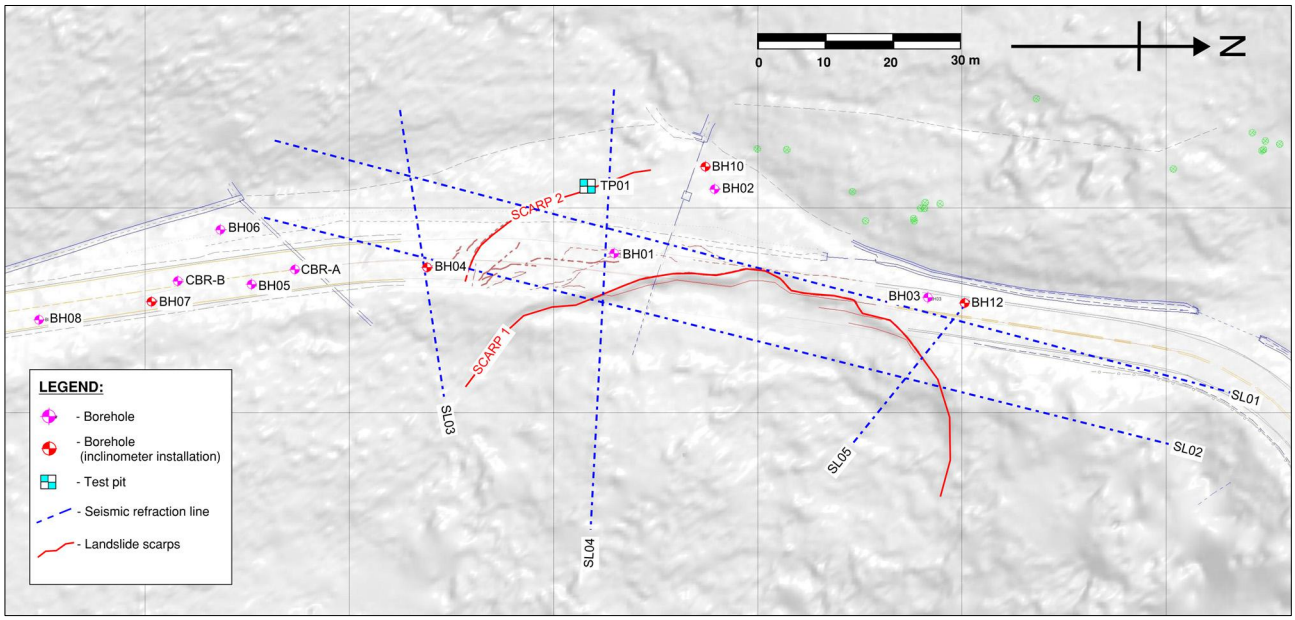


Figure 8: Geotechnical investigation site plan at the Garie Road landslide site. Source of DTM (MES, 2022).

The following presents a summary of the key conclusions from the borehole and geophysical investigation:

- The ground profile generally comprised variable depths of fill, typically underlain by colluvium. These surficial soils were underlain by varying weathering grades of the Bald Hill Claystone, underlain by the more competent Bulgo Sandstone.
- The colluvium comprised highly variable cohesive soils with a significant silt, sand and gravel component, generally stiff to very stiff.
- The residual soil and extremely weathered rock of the Bald Hill Claystone generally comprised very stiff clays with gravel of extremely weathered to highly weathered claystone, siltstone and sandstone. This unit was sometimes difficult to distinguish from the overlying colluvium.
- The highly weathered or better Bald Hill Claystone was typically claystone with siltstone and minor (<10%) sandstone beds (typically highly fractured with weathered joints). This unit ranged from very low to medium strength with an assessed Geological Strength Index (GSI) ~ 40.
- A pale weathered zone of reduced strength (named ‘weak zone’ from here in) was encountered in boreholes BH06, BH08, BH10 and BH12 within the Bald Hill Claystone in close proximity (within ~1 to 2 m) to the underlying interface of the Bulgo Sandstone (Figure 9). This weak zone was logged varying from 350 mm to 800 mm thick where the material had been recovered.

- The Bulgo Sandstone was fine to medium grained, competent sandstone (in contrast to the nature of the overlying Bald Hill Claystone) typically high to very strength with an assessed GSI ~70. The sandstone has a clay/silt matrix between the sand grains hence a relatively low permeability. In some of the logged core, the interface of the Bald Hill Claystone and the underlying Bulgo Sandstone was transitional with an interbedded zone (Pells, 1994).

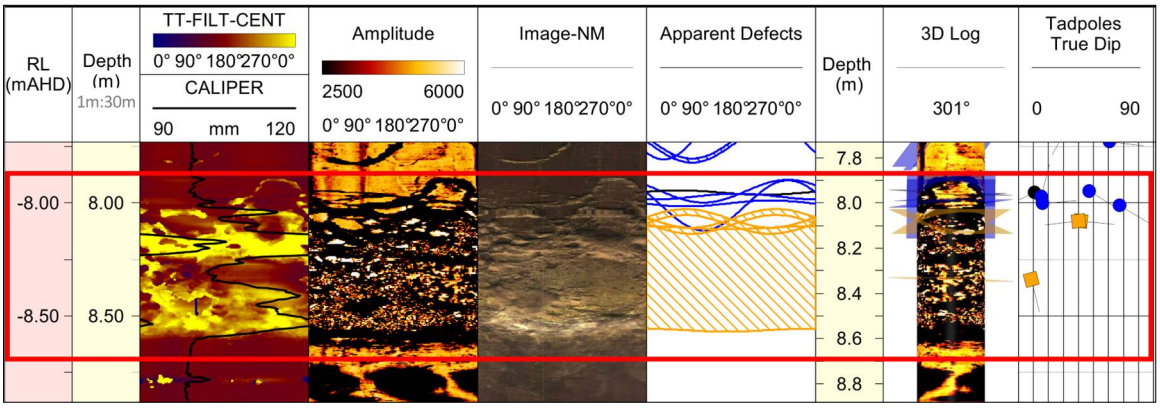


Figure 9: Weak zone clearly identified in the downhole OTV and ATV logs between 8.05 m to 8.5 m depth in BH12

3.4 INSTRUMENTATION REVIEW

The installed inclinometers and standpipe piezometers were monitored manually at fortnightly intervals post installation and then increased to weekly after intense rain events. Initially, only minor movements (<2 mm) within the zone of error were recorded from the relatively dry period from April 2023 to April 2024.

Due to initial construction activities on site only two inclinometers BH10 and BH12 remained operational. In early May 2024, 344 mm of rain fell over twelve days and inclinometer monitoring of BH10 and BH12 was undertaken on a weekly basis. In BH10 which was located towards the western edge of the landslide where no instability had been previously recorded, 55 mm of displacement was recorded on 12 June 2024 at ~9 m depth (Figure 10). The recorded movement within the BH10 inclinometer was within a zone of core loss ~1 m above the upper logged 'weak zone' observed in BH10 (Figure 12).

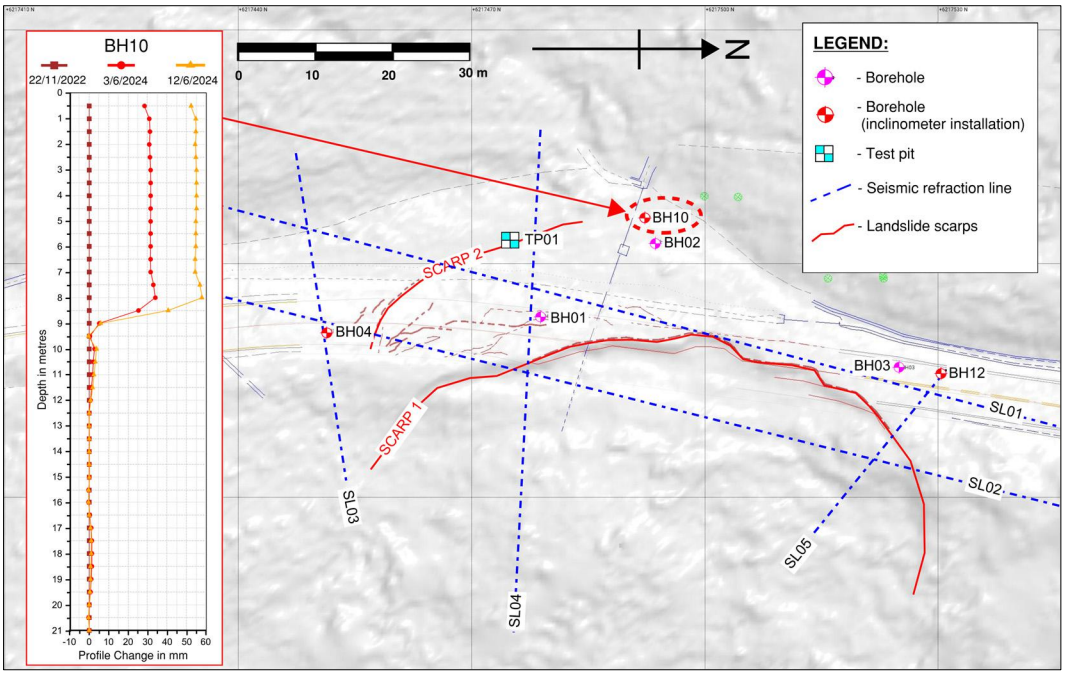


Figure 10: Ground movement at ~9 m depth recorded in BH10 inclinometer in June 2024.

4 INSIGHTS FROM ANALOGUE LANDSLIDE IN THE BALD HILL CLAYSTONE

A literature review has identified a similar case study of landsliding in the Bald Hill Claystone, at a site located on the Illawarra Escarpment, NSW. Stone (2012) and Flentje & Leventhal (2012) reported a case study at Site 43 on the South Coast Railway where a landslide developed on a side-fill embankment within a gully feature in response to the 1989 El Nino rain event (Figure 11). The total movement recorded was ~700 mm up to mid-July 1989 at the onset of dry weather (Stone, 2012).

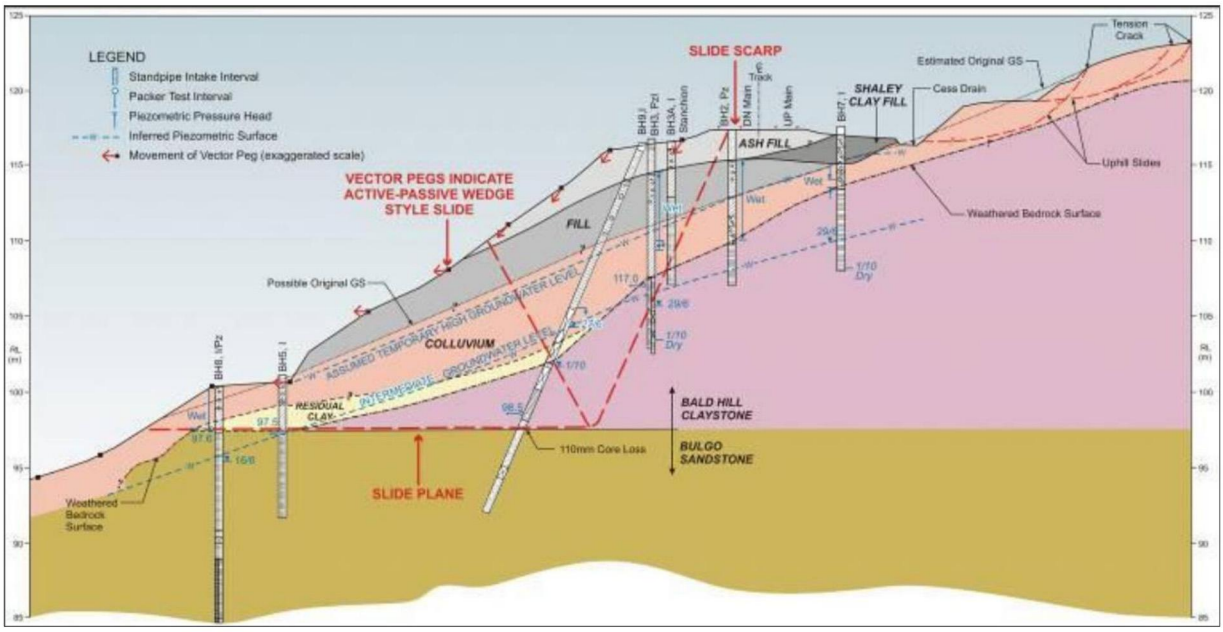


Figure 11: Site 43 – South Coast Railway Cross Section (Flentje & Leventhal, 2012)

The Site 43, South Coast Railway landslide had the following characteristics:

- The ground profile comprised the following units in depth order: fill, colluvium, Bald Hill Claystone and the Bulgo Sandstone as the basal unit.
- Sliding was identified at the interface of the Bald Hill Claystone and the underlying Bulgo Sandstone.
- Superficial instabilities were mapped on the upslope to the main landslide.
- The main backscarp to the landslide was relatively steep, in the order of 65° dip.
- Progressive movement was experienced until the onset of dry weather.

Stone (2012) described the Site 43 landslide as a rotational/flat planar feature (active-passive wedge model) extending 19 m deep below the track and along the Bald Hill Claystone/Bulgo Sandstone interface. The geometry of this failure was stated to be very well defined by the inclinometers and vector peg measurements.

At Site 43, Stone (2012) describes white clay gouge material encountered within a remedial construction excavation that was identified to be the landslide slide plane at the Bald Hill Claystone / Bulgo Sandstone interface (Figure 12). The Garie Road geotechnical investigation encountered a similar weak zone (soil strength material ranging to zones of XW/HW rock) within the Bald Hill Claystone in BH06, BH08 and BH10 and BH12; ~350 mm to 800 mm thick and 1 to 2 m above the interface of the Bulgo Sandstone. Figure 12 displays the remarkably close similarities between the slide plane gouge verified in an excavation at Site 43 of the South Coast Railway (Stone, 2012), to the Garie Road identified ‘weak zone’. The authors of this paper believe this is the same zone of weak material that is prone to landsliding in both case studies.

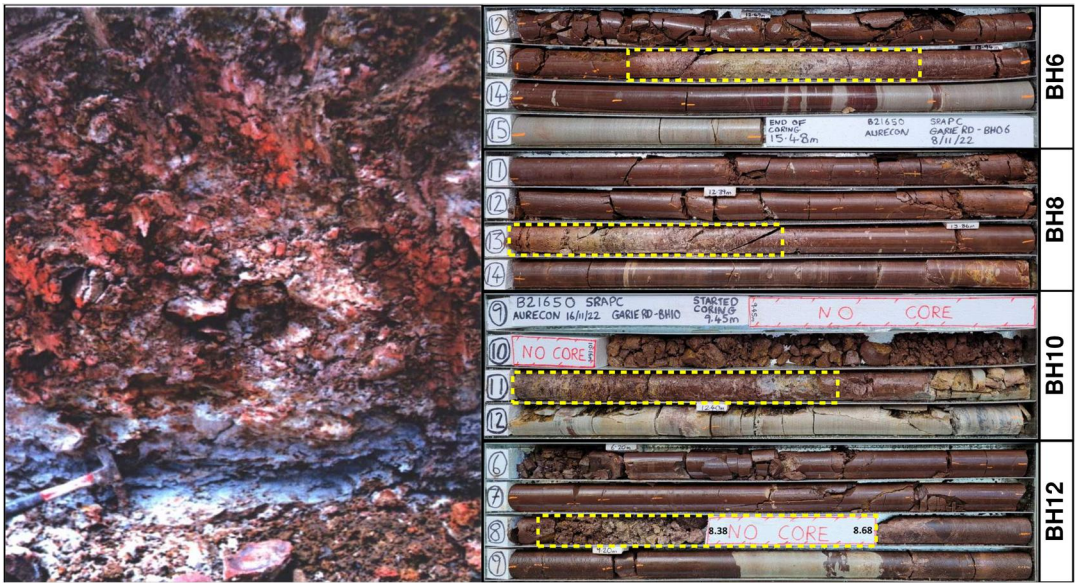


Figure 12: Left image - pale white clay 'gouge' associated with a zone of sliding in the Bald Hill Claystone at Site 43 (Stone, 2012). Right images - BH06, BH08 BH10 and BH12 core displaying a similar pale white weathered clay zone (yellow dashed boxes) within the Bald Hill Claystone, 1 to 2 m above the interface with the underlying Bulgo Sandstone.

5 ENGINEERING GEOLOGICAL MODEL

The data collected during the investigation was assessed and used to develop the EGM. Engineering geological units were assessed at an appropriate scale largely based on rock weathering grades or type of deposit (e.g. colluvium and fill). The 'weak zone' was assigned an individual project engineering geological unit given its importance within the ground model and landslide mechanism.

A 3D cross section of the EGM is presented in Figure 13.

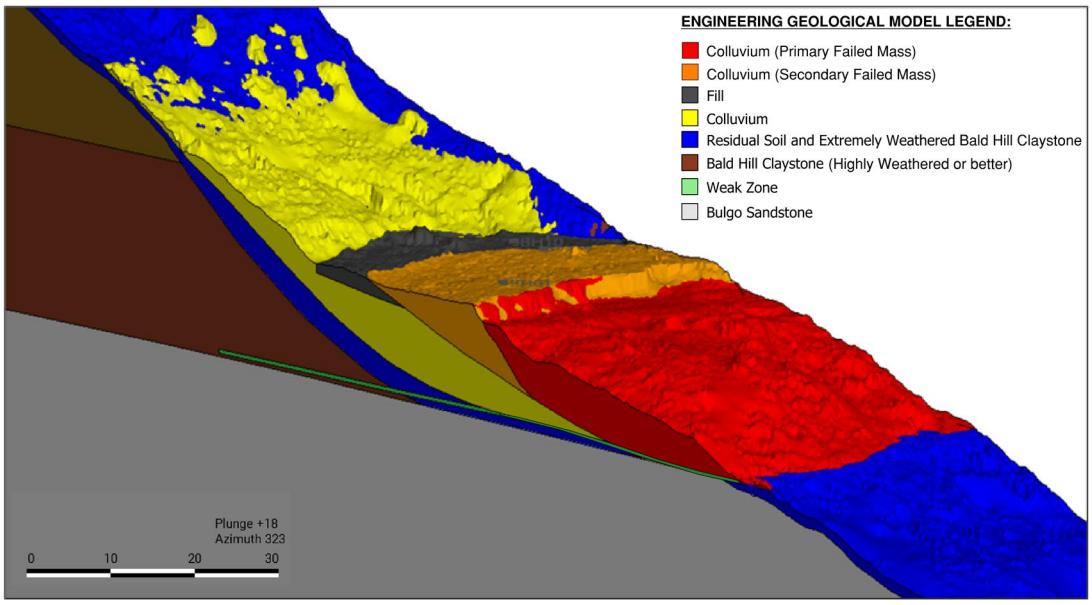


Figure 13: Cross section through the Leapfrog developed EGM. Source of DTM (MES, 2022).

In the EGM, the landslide was interpreted to have a backscarp in the order of ~65° dip and an assessed planar basal sliding plane ~13 m below ground level at the Scarp 1 location. The geometry of the landslide was defined based on the engineering geological mapping, intrusive investigation results and comparison with the published literature (Flentje & Leventhal, 2012; Stone, 2012).

6 DISCUSSION

The characteristics and mechanism of mass movement of the Garie Road landslide have been assessed by a number of instructive and non-intrusive investigation techniques, a literature review and the development of an EGM. The following is a summary of the landslide characteristics and the components of the mechanism of mass movement:

- The landslide is a pore pressure driven; slow moving 'stick-slip' landslide as demonstrated by the rainfall vs ground monitoring data (Figure 5). Ground movements accelerated subsequent to intense rain events with retrogression of the landslide and slowed or ceased during periods of dry weather.
- The mechanism of mass movement is a large slide with both a rotational and translational component. The backscarp to the landslide is assessed to be semi-rotational measured dipping at ~65° to the east at the ground surface. The basal slide plane is the translational component of the landslide mechanism sliding on the weak zone within the Bald Hill Claystone close to the interface of the underlying Bulgo Sandstone. The assessed dip of the basal slide plane is just ~5° to the east, approximately parallel to the sub-horizontal top of the Bulgo Sandstone.
- The Garie Road landslide has a number of close similarities to the Site 43 South Coast Railway landslide site, namely the same zone of sliding within the white clay gouge 'weak zone' is common to both landslides (Figure 12). In addition, both landslides have similar backscarp and basal slide plane geometry, the presence of superficial instabilities on the upslope and progressive movement was experienced until the onset of dry weather (Flentje & Leventhal, 2012; Stone, 2012).
- The ground movement recorded in the BH10 inclinometer at ~9 m depth in June 2024 is assessed to be a retrogression of a new backscarp trending up at a similar geometry to the existing Scarp 1 and 2 from the 'weak zone' basal slide plane. This inclinometer movement further validated the landslide movement is within the identified 'weak zone'.
- The steep joints with high persistence dipping approximately 60° to the east (general slope failure direction) mapped within the Bald Hill Claystone road cuttings are assessed to provide a preferential weak surface for the formation of backscarps during high intensity rainfall events.
- In addition, the steep dip high persistence joints are assessed to provide a preferential pathway for surface water infiltration into the lower Bald Hill Claystone. During intense rain events groundwater is concentrated at the interface of the relatively low permeability Bulgo Sandstone where degradation of this zone occurs forming the 'weak zone' that is prone to landsliding.
- The mechanism of landsliding presented is an example of the Illawarra Escarpment retreat (Flentje, 2012).

The components of the mechanism of landsliding comprising a semi-rotational backscarp and a sub-horizontal basal slip plane formed at the location of the 'weak zone' is presented in Figure 14.

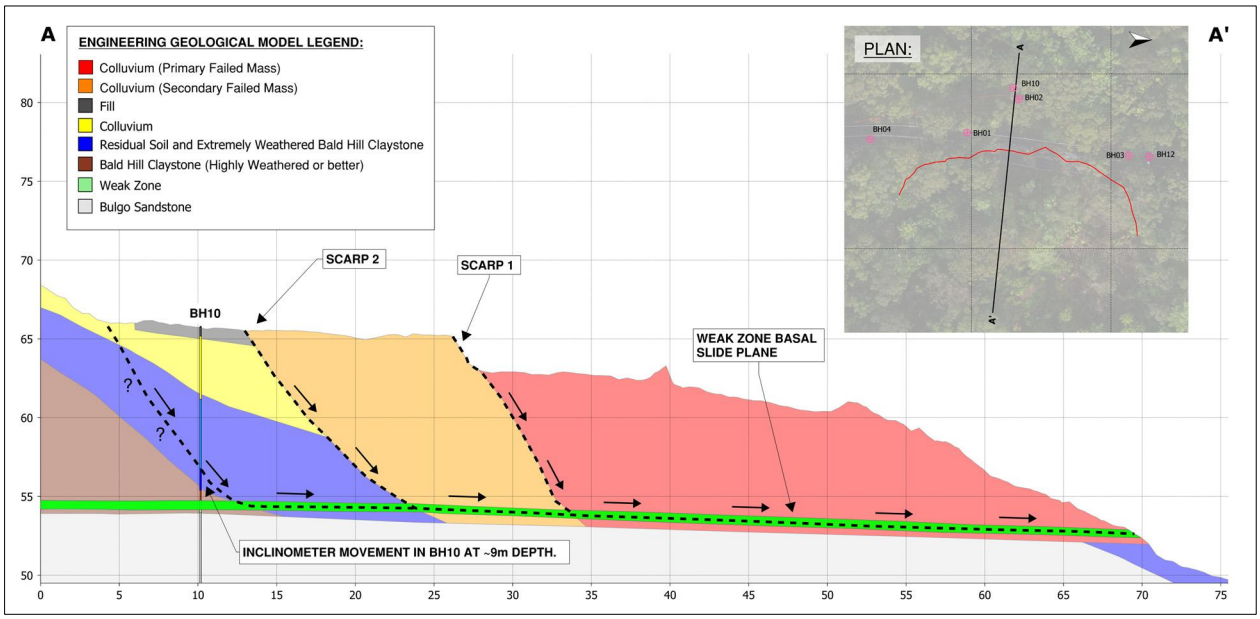


Figure 14: Cross section A-A' through the EGM displaying the assessed mechanism of landsliding at Garie Road.

7 CONCLUSIONS

The Garie Road landslide was triggered by 268 mm of rain that fell in two consecutive days in early March 2022. The landslide was slow moving, retrogressing to the south and west over the subsequent months in response to further intense rain events. The landslide demonstrated 'stick-slip' style movement in response to periodic elevated pore water pressures.

This paper presents a case study of the assessment of the landslide through the various investigation techniques including drone terrain evaluation, landslide mapping, detailed core logging and instrumentation trends. The data collected was inputted into an EGM which allowed an interpretation of the components of the mechanism of mass movement, comprising a steep semi-rotational backscarp and a translational basal slide plane ~60 m in length dipping at just ~5° to the east. The location of the basal slide plane was interpreted to be at the location of the identified 'weak zone' within the Bald Hill Claystone in close proximity to the underlying Bulgo Sandstone.

The assessed landslide mechanism has been validated through comparison of the similar Illawarra escarpment landslide at Site 43 on the South Coast Railway (Flentje & Leventhal, 2012). At this landslide site, a trench excavation revealed white slide plane clay gouge identified to be the failure surface at the Bald Hill Claystone / Bulgo Sandstone interface. This case study builds on the previous knowledge of known landsliding at the interface of the Bald Hill Claystone / Bulgo Sandstone; allowing better understanding and mitigation of similar landslides on Australia's civil infrastructure network.

8 REFERENCES

Colquhoun, G. P., Hughes , K. S., Deyssing, L. & Ballard, 2021. *New South Wales Seamless Geology dataset, version 2.1 [Digital Dataset],* s.l.: Geological Survey of New South Wales, Department of Regional NSW.

Flentje, P., 2012. Evolution of the Illawarra Escarpment Terrain. *Australian Geomechanics,* 47(1), pp. 1-16.

Flentje, P. et al., 2022. A Photographic Essay on Landslides across Southeastern New South Wales Triggered by the Rainfall Events of 2022. *Australian Geomechanics,* 57(3), pp. 115-134.

Flentje, P. & Leventhal, A., 2012. Illustrative sections depicting landslide susceptibility of the Illawarra Escarpment. *Australian Geomechanics 47,* pp. 17-33.

Pells, 1994. *Engineering Geology of the Triassic Rocks of the Sydney Area,* Sydney: Pells Sullivan Meynink Pty Ltd.

Stone, P. C., 2012. Landslide impacts on the South Coast Railway during the 1988-90 El Nino event. *Australian Geomechanics Vol 47,* pp. 79-110.

https://doi.org/10.56295/1ACEG24

WHAT IS THE FUTURE OF ENGINEERING GEOLOGY AS A DISCIPLINE IN WESTERN AUSTRALIA, AND AUSTRALIA?

Julia Bota[1], Paul Baker[2], Patrick McManus[3], Andrew Shuckstes[4], Alex Petty[5] and Domenik Wolff-Boenisch[6]
[1]HATS Consulting Pty. Ltd., [2]GHD Pty. Ltd., [3]Ground Recruitment Pty Ltd., [4]Newman College Perth, [5]PTG Consulting Pty Ltd and [6]Curtin University Perth

ABSTRACT

Engineering geology plays a key role in infrastructure development, risk mitigation, and engineering solutions. However, the discipline faces significant challenges in Western Australia (WA) and across Australia, particularly in workforce sustainability and academic pathways. Unlike New Zealand, where engineering geologists make up a substantial portion of the geotechnical workforce, Australia lacks dedicated tertiary education programs for engineering geology.

This paper examines the current state of engineering geology in WA and Australia and explores factors influencing its future, including the limited availability of specialised university programs, market forces favouring the mining sector, and the declining interest in and teaching of geosciences at secondary and tertiary education levels. Data from LinkedIn and Ground Recruitment Pty Ltd highlights the disparity in proportions of engineering geologists and geotechnical engineers in Australian practice compared to New Zealand. Further, a LinkedIn poll of Australian geotechnical professionals confirms that while geology is widely recognised as fundamental to geotechnical engineering, the number of dedicated engineering geologists remains low in Australia.

We discuss the implications of this workforce gap, questioning whether geotechnical engineers can adequately fulfill engineering geology roles and whether industry trends undervalue the contribution of engineering geologists. Additionally, we assess ongoing initiatives, including university-led field courses and industry collaborations aimed at fostering interest in engineering geology among students.

The paper highlights the apparent benefits of increased industry engagement, education reform, and professional development opportunities to secure the future of engineering geology in Australia. Without targeted efforts, the discipline risks further decline, potentially impacting the quality and safety of geotechnical engineering practices in the region.

1 INTRODUCTION

The engineering geologist plays a key role in the planning and design of commercial, industrial, and public developments, by conveying the impact geology and geomorphology has on engineering projects. The engineering geologists' understanding of the interaction between the earth and the proposed structure assists in the development of a safe and cost-effective design.

Sourcing of engineering geologists to work in consultancy and engineering practice in WA is currently difficult. There are no industry ready engineering geologists born and educated in WA. Graduate engineering geologists are generally degree qualified geologists who are then upskilled and trained on the job or are degree qualified engineering geologists who migrate temporarily or permanently to WA from overseas.

A large proportion of the experienced engineering geologists practicing in WA were born and educated in other countries e.g. New Zealand, United Kingdom and South Africa. For example, the University of Auckland offers a Master of Engineering Geology allowing for further training of geology graduates in the engineering geology discipline. In Australia, the University of NSW offers a Master of Engineering Science (Geotechnical Engineering & Engineering Geology). There are currently no masters courses dedicated purely to Engineering Geology in Australia. During nationwide economic booms, consultants and engineering companies have been able to import skilled engineering geologists from overseas with relative ease (via skilled migrant visas). However, outside of a booming economy, relocating engineering geologists from overseas is not a simple task if skilled migrant visas require the satisfaction of a more rigorous assessment criteria to obtain a visa.

Sourcing of engineering geologists to sustain our discipline in WA is now proving to be a serious challenge. This paper will detail what is currently happening in WA to deliberately encourage geologists into the engineering geology discipline.

It is noted that there are pathways for engineers to undertake postgraduate training in geology and practice engineering geology (Paul, 2024), however this paper focusses on geologists, reflecting the authors own journeys into the discipline.

Parts of the discussion and interpretation presented in this paper represent the opinions of the authors, informed by our experiences and observations. The paper will explore how we may maintain the discipline in the future and if there is anything practitioners can do to support this. The paper will present data and statistics that may provide a better understanding of the problem and therefore assist in achieving the objective.

2 IS THERE A PROBLEM?

There are currently no WA based Tertiary academic avenues, e.g. Master of Science courses, available for specialist engineering geology study. It is generally thought that this is because Tertiary education is primarily focussed on the State's large mining sector and therefore exploration and mining geology. To illustrate, this paper provides data from Curtin University that demonstrates the career destinations of graduates completing Curtin's Applied Geology undergraduate degree course. This may also be reflective of global trends where there has been a general shift away from geoscientific research.

The problem with encouraging young geologists may be linked to starting salaries for graduate engineering geologists, which are much lower than starting salaries for geologists working directly in the mining sector. But if that is the case, why haven't market forces closed this gap?

Is it possible that some projects are still being progressed without the involvement of an engineering geologist at all? Or is the engineering geology part of these projects being completed by individuals that lack the necessary background to do the tasks properly? Not every organisation who executes engineering projects employ an engineering geologist, so how are geological hazards identified and appropriately assessed?

Are we doing enough to:

- promote our discipline to young people considering a career in science;
- demonstrate our value to the industries we serve;
- market ourselves to other disciplines within our industry?

This paper uses data provided by Ground Recruitment Pty Ltd. for geotechnical professionals (made up of engineering geologists and geotechnical engineers) in consultancy and engineering across Australia and New Zealand. The data highlights the vast differences in the proportions of geotechnical engineers compared to engineering geologists in the workforce in WA, across Australia and New Zealand and opens a discussion as to why this is the case. The LinkedIn data on the geological workforce in Australia and New Zealand supplied by Ground Recruitment Pty Ltd reveals some interesting trends:

- In Australia, only 9% of all geologists work as engineering geologists, whereas in New Zealand, this figure is significantly higher at 67%.
- A significant portion of geologists in Australia, just over half, are in WA, although only 3% of geologists in WA identify as engineering geologists on LinkedIn.
- The data shows that engineering geologists make up 41% of geotechnical professionals in New Zealand, compared to an average of 12% across Australia.
- In Australia, Tasmania stands out with the highest ratio of engineering geologists working as geotechnical professionals in Australia at 23%, while Victoria has the lowest mix at 8%.

These findings indicate a notable disparity in the distribution and specialisation of geological professionals choosing to be engineering geologists between Australia and New Zealand, as well as within different regions of Australia. The differences highlighted by this data are significant. The authors of this paper are all based, and work, in Perth, WA. It is therefore difficult to accurately address the questions around this topic. However, there is clearly something fundamentally different about New Zealand and Australia.

The LinkedIn data provided by Ground Recruitment Pty Ltd demonstrates the vast differences between the geotechnical workforce in New Zealand compared to Australia. The authors of this paper believe this is driven by the severity and frequency of geological hazards present in New Zealand (e.g. seismicity, active volcanoes, landslide hazards etc.) compared to Australia. The relative size of the mining and civil industries in these countries may be a factor resulting in more investment in mining in Australia compared to more investment in geohazard mitigation in New Zealand. And in support of the New Zealand geotechnical workforce, a Masters in Engineering Geology is available in New Zealand. Some questions that could be asked include:

- Are the different proportions between Australia and New Zealand more workplace or salary driven?
- Is the role of the engineering geologist typically the same in New Zealand as it is in WA? In New Zealand, are engineering geologists performing what would traditionally be considered geotechnical engineering tasks in the Australian workplace?
- Are the differing proportions simply because of the array of geological hazards present in New Zealand that must be well understood and addressed by the engineering solution / design, i.e. the engineering community is more aware of the benefits of engineering geology and therefore employ a greater proportion into their geotechnical teams?
- Is the requirement for a chartered engineer to sign off on designs influencing any shift in focus away from the importance of engineering geology in design in some Australian states? It is noted that New Zealand has a body of registered Professional engineering geologists (PEngGeol) which is assessed and governed by Engineering New Zealand (the equivalent to Engineers Australia). Accreditation pathways are available to Australian professional engineering geologists; however, some are not discipline specific or recognised by state legislation (Packer, M. et al., 2024),

This paper also presents School Curriculum and Standards Authority (SCSA) data that shows the decline in teaching of earth science in WA high schools over the last ten years. It also discusses the support provided to earth science education by Australian Earth Science Education (AusEarthEd) across WA.

There is a decline in enrolments in earth sciences based higher education at a global scale, which indicates that this issue spans much further than just engineering geology (Vafeas, N., 2023 and Rogers, S. L., et al., 2024).

3 UNDERVALUED OR NOT NEEDED?

There is considerable overlap in the skills, expertise and perspectives both engineering geologists and geotechnical engineers bring to ground engineering projects. Their roles complement each other.

The engineering geologist is typically on-site during site investigations, coordinating ground intrusive works and in situ testing, logging to AS1726-2017 and sampling, and all the while thinking about a geological model for the site, possible geohazards, environmental impact and possible sustainability wins. You could argue a geotechnical engineer could do all this site work, and in addition, return to the office to focus on the engineering design of foundations, retaining walls and other built-environment structures.

So, maybe engineering geologists aren't needed at all?

Engineering tasks are increasingly commoditised and perhaps this philosophy can be extended to include geotechnics. For some projects, such as straightforward developments at locations where the geotechnical risks are low due to relatively homogenous or well understood ground conditions, an engineering geologist is not likely to provide much added value compared to a geotechnical engineer. Afterall, the engineering properties of a soil are derived from particle size and how those particles interact; particle mineralogy plays only a minor role. For rock, is it necessary to understand the lithology provided rock mass characteristics and strength are logged accurately?

An appreciation of geomorphology and geology becomes more valuable the larger and more complex the project is. With increasing project size (footprint area or linear length, for example) and complexity comes an increased likelihood of variability in ground conditions and exposure to geohazards, and opportunities for sustainability wins. This is where engineering geology comes to the fore.

A recent acknowledgment of the importance of understanding the engineering geology of a site comes from the Global Industry Standard on Tailings Management (ICMM, 2020) which emphasises the importance of robust site characterisation including detailed geological and hydrogeological assessments. This acknowledgement is partly in response to high profile failures of tailings storage facility embankments including, Los Frailes, Spain, 1998, and Mount Polley, Canada 2014. In the case of Los Frailes, the embankment was constructed on a layer of marl (clay containing calcium carbonate), which deteriorated over time. The deterioration was primarily due to acid (in the tailings) dissolving calcium carbonate reducing the strength (strain weakening behaviour) of the clay which contributed to a foundation failure and subsequent collapse of part of the embankment (Eptisa, Servicios de Ingeniera S.A., 1998). One of the conclusions of the independent expert engineering and review panel for the Mount Polley failure (Independent Expert Engineering Investigation and Review Panel, 2015) was "the design did not take into account the complexity of the sub-glacial and pre-glacial geological environment associated with the Perimeter Embankment foundation…site characterisation failed to identify a continuous glaciolacustrine layer…and failed to recognise it was susceptible to undrained failure when subject to the stresses associated with the embankment".

As the world shifts to a low-carbon emissions future, there is an increasing investment in renewable energy projects across Australia. In the Pilbara region of WA, tier-one resources companies such as BHP, Rio Tinto and Fortescue are investing

heavily in decarbonising their operations. Solar and wind farms have large footprints, and in addition, these power generating assets need to be connected to an integrated power grid meaning hundreds of kilometres of transmission line infrastructure, substations and battery storage facilities are needed. As Baynes, Fookes and Kennedy, 2005 point out, the "total engineering geology" approach requires involvement of engineering geologists in investigation, risk management, design and construction supervision that relate to ground engineering. Engineering geologists are best placed to identify and assess geohazards that could impact construction; in the Pilbara these include rockfalls, karst (and non-karst near-surface cavities), collapsible soils, reactive soils, and asbestiform minerals.

While the above examples highlight the importance of engineering geology in mitigating geohazards, having engineering geologists involved in projects is not just about reducing risk and mitigating geohazards. Through their unique perspectives of the interfaces between the natural and built environments, engineering geologists can play an important role in sustainable development and in delivering the United Nations (UN) Sustainability Development Goals (SDGs) (Lagesse et al, 2022).

According to Lagesse et al, 2022, engineering geologists can contribute to all 17 of the UN SDGs with the strongest overall contributions to SDG 7 (Affordable and clean energy), SDG9 (Industry, innovation and infrastructure), SDG 12 (Responsible consumption and production) and SDG11 (Sustainable cities and communities). The most significant contribution to these SDGs comes through engineering geologists' involvement in infrastructure development through:

- site characterisation (including engineering geological model development), assessing geohazards and informing the planning, efficient design and construction of infrastructure;
- reducing costs and time overruns during construction due to unforeseen ground conditions;
- assessing the re-use of excavation spoil and developing material treatment and remediation strategies to minimise transportation of, and importation of materials, and minimising construction waste.

It is difficult to quantify the potential cost savings of sustainability wins and the dollar value of risks mitigated by employing an engineering geologist with the necessary years of experience in site characterisation, geotechnics and construction support. Paradoxically, society finds it much easier to assign a dollar value to the economic impact of the damage caused by a high-profile catastrophic failure(s). Perhaps the engineering geology community needs to do more to self-promote its contributions to engineering projects, not just in terms of reducing the risk of catastrophic failures and geohazards, but also the benefits of engineering geologists working with engineers throughout the project lifecycle not just in the geotechnical site investigation / characterisation phase but being involved through to the engineering and construction phases of projects.

Projects with a significant geotechnical component, are typically those projects where the engineering requires interpretation and judgement, and the best outcomes for such projects generally do not come from thinking of engineering as a commodity. This is particularly true for a field such as geotechnical engineering where experience and judgement is required to assess and manage risk; and that judgement is called upon from scoping and safely executing the geotechnical site investigation(s), through to interpreting the factual data, applying that data appropriately to creating geotechnical models, undertaking engineering design, preparing technical specifications for construction, and supporting construction by observing and responding to as-encountered ground conditions and facilitating modifications to design as needed.

So, what do Australian based geotechnical practitioners think about the importance of geology in geotechnical engineering practice?

As part of this paper, a LinkedIn poll was completed. The poll comprised a single question with a choice of four answers. The question was: "As a Geotechnical Professional in Australia – what role does geology play in geotechnical engineering practice". The answer choices were deliberately picked to provide a range of responses to the question without specific 'for' or 'against' answers. The four possible answers were:

1. Fundamental for all sites
2. Depends on the complexity
3. Importance is overstated
4. Geotech testing is sufficient

The poll was run for a period of two weeks with a focus on gaining input from both geotechnical engineers and engineering geologists. In total there were 315 respondents. Figure 1 provides the summary responses for all respondents. It indicates that 73% (231) of respondents feel that geology is fundamental for all sites and 25% (79) voted depends on the complexity.

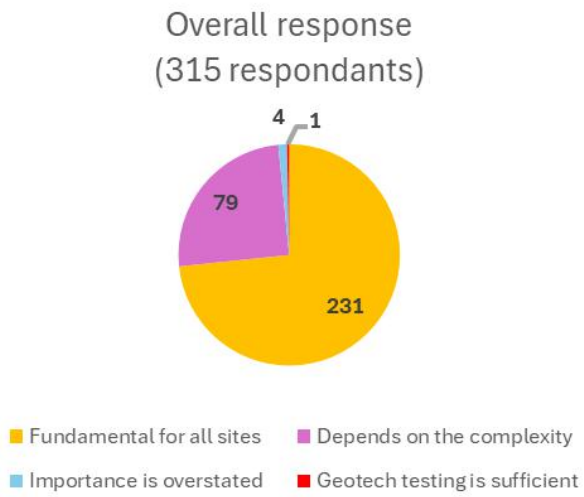


Figure 1: Overall Response Summary

Figure 1 clearly shows that geology is important to all those who responded, with only five respondents not picking either answer 1 or 2.

Of the 315 respondents, the primary job title discipline has been derived. This has been completed by using their current LinkedIn profile job title. Where their title includes the word 'geotechnical' or 'engineer' they have been designated an 'engineer' and where the word 'geologist' is included they have been designated a 'geologist'. Where their current position is less clear, they have been designated 'other'. These include titles such as Technical Director, Practice Director, Branch Lead, Director etc. Using these designations, Figure 2 depicts the breakdown of respondents. It is noted that the respondents included a variety of experience levels from graduates to experienced directors and senior principals. However, a specific breakdown of the experience levels has not been included in this paper given the limited nature of using LinkedIn polls.

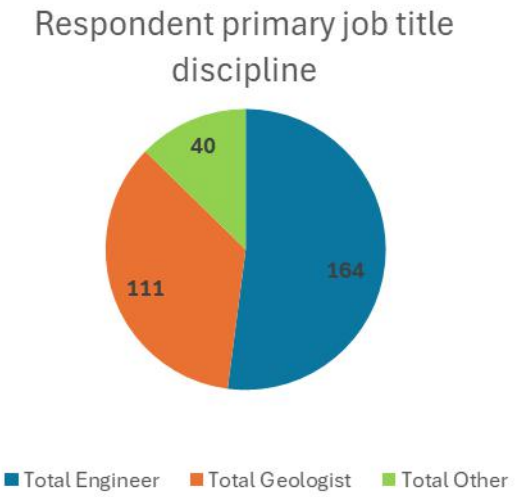


Figure 2: Summary of Respondent Primary Job Titles

The breakdown of respondents provides a good dataset from both the engineering and geology disciplines. This indicates that both geotechnical engineers and engineering geologists value the importance of geology in geotechnical practice. This is further demonstrated in Figures 3 and 4 which provide the breakdown of responses for answers 1 and 2 by job title designation.

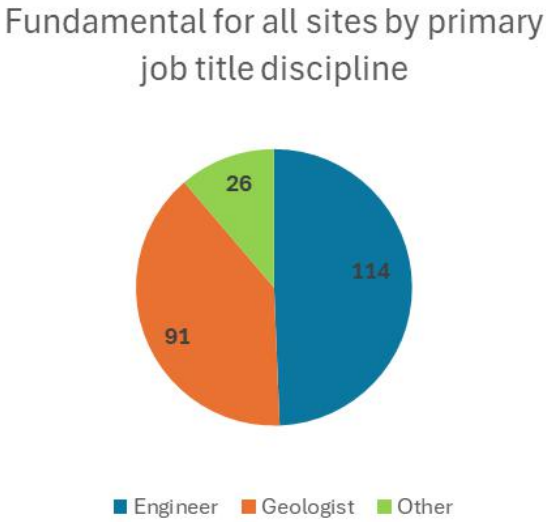


Figure 3: Summary of Respondent Primary Job Titles for Answer 1 (Fundamental for all sites)

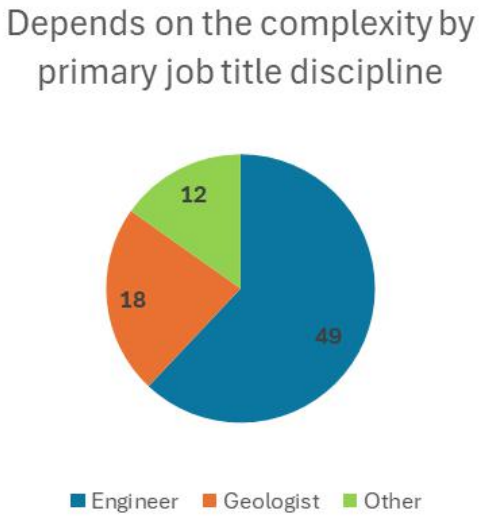


Figure 4: Summary of Respondent Primary Job Titles for Answer 2 (Depends on complexity)

Based on Figures 3 and 4, 82% of the geologist designation respondents indicate that geology is fundamental for all sites (answer 1), compared to 70% for the designated engineers. Further to this, 16% of the geologist designation respondents indicate that it depends on the complexity (answer 2), whilst 30% of the engineers indicate this answer. Note, that answers 3 and 4 only received 5 responses of a total of 315 (~1.5%) and these have not been further analysed.

Perhaps unsurprisingly, the geologists have a higher percentage of respondents indicating that geology is fundamental for all sites, compared to engineers. However, the number and percentages of engineers also indicating the importance of geology is perhaps unexpected, given the premise of this paper.

Clearly (at least based on a small poll of industry peers) the wider community of geotechnical professionals across a range of experience levels value the importance of geology in geotechnical practice. Therefore, common sense would suggest that engineering geologists are important for every project. This appears to be in contrast to the data presented in Section 2 which indicates that engineering geologists make up only 8% (Victoria) to 23% (Tasmania) of the Australian geotechnical professional workforce. Why do we appear to have such a small contingent of engineering geologists in Australia given the value of geology that has been indicated? Are engineering geologists undervalued or not needed? Perhaps the poll question of whether *geology* is important can assist in answering this question. Do geotechnical engineers realise the importance of geology, butnot appreciate the inherent importance of engineering geologists to understanding the geology? Do geotechnical engineers feel comfortable undertaking the role of an engineering geologist? Should this be an acceptable practice? Could geotechnical engineers be upskilled and trained in engineering geology? This paper presents the facts and

data to support the necessity of incorporating geology in geotechnical practice, while also exploring who is best placed to provide that input – engineering geologists or suitably trained geotechnical engineers.

4 PERSPECTIVES FROM SECONDARY EDUCATION

If we assume that there is a continued need for geology as applied to ground engineering, we must ensure a supply of new skilled specialist talent. A good place to begin our effort is with the development of an interest in earth science and engineering in our younger population. We cannot hope to attract new geoscientists to the engineering industry if there is a lack of awareness of the need, or a recognized value placed on the pursuit. All Australian states and territories offer Earth and Environmental Science (EES) as a senior secondary ATAR (Australian Tertiary Admission Rank) subject (except for Victoria, which offers environmental science) (ACARA, 2024). Western Australia offers a 4-unit, two-year EES ATAR that addresses most sub-disciplines in geology and environmental science, including a brief introduction to geological hazards and seismic design. These courses are excellent places to encourage young people to join our craft.

Data available online from the School Curriculum Standards Authority (SCSA, 2024) shows that only 10 out of about 400 secondary schools in WA offered EES in 2023. Only 115 students sat the EES ATAR Western Australian Certificate of education (WACE) examination in the WA in 2024, down from 167 in 2020. Andrew Shuckstes has been teaching EES to secondary students in Perth WA since 2016. During this time, he has made several observations including:

- Students attending high school are largely unaware or misinformed about engineering as a technical discipline and are totally unaware of geology as an applied skill for engineering.
- Senior secondary science educators in WA lack experience, subject knowledge and skills necessary for EES education. These teachers are sparsely resourced for practical and other educational opportunities for interested students.
- Experienced professionals rarely transition to teaching from engineering or geology. There are likely several reasons for this observation including the perceived challenges of working with young people and the significant reduction in remuneration resulting from the transition.
- For those of us teaching EES, there are several government and privately supported organizations that support pre-Tertiary EES education across Australia. These organizations include AusEarthEd (Australian Earth Science Education), TESEP (Teacher Earth Science Education Program), GA (Geoscience Australia), GSA (Geoscience Australia). These organizations aim to provide teacher professional development, publications and resources up to Year 12 ATAR EES.
- EES WACE scores are scaled down by WA SCSA, resulting from a calculated relative simplicity compared to other ATAR sciences like Physics and Chemistry. This makes EES less attractive to those candidates wanting to maximize their ATAR score because they know they will lose some of their marks in EES for their ATAR score.
- EES is often chosen by students who want to experience practical and tactile science without the challenge of Physics and Chemistry. Students who choose EES are often less academic with less developed mathematics and language skills than those pursuing other science ATAR subjects.
- EES WACE results in WA are low (average score was not above 60% since 2016, and below 50% in 2024) and have been getting lower for the last 10 years. This data is available to the public and discourages many students from considering the subject.
- EES is not a prerequisite or a recommended secondary subject for any university course in WA. This makes it less attractive to strategic subject choice for senior secondary school.

The WA economy is a resource export economy, dominated by metals, fuels and foods. Geology at our universities has traditionally focussed on metals and hydrocarbons (Kalgoorlie has the Curtin School of Mines), along with the academic geology we are all familiar with like palaeontology and mineralogy. Secondary students are largely unaware that there are alternative pathways for geologists such as civil engineering and environmental science. If we take the observations above at face value and apply them to our analysis of enrolments at university, it gives clear reasoning as to why we have limited interest in engineering geology as a career choice.

The lack of interest in EES, and thus geology as a secondary school subject is dependent on several factors:

- A lack of exposure and emphasis for EES during primary and junior secondary schooling.
- The perceived difficulty of technical subjects like geology, physics and chemistry.
- The strategic aspect of ATAR scores for students who wish to achieve higher ATAR scores irrespective of the subject by choosing "easier" subjects.
- Opportunities that are endorsed by the school community that offer a perceived easier and more certain ATAR that allows entry to university through alternative pathways.

If we want to encourage Australian students to consider geology or more specifically engineering geology, we must begin at the primary and secondary stages of education. We must, as a professional community, offer assistance and encouragement to institutions that deliver education to young people about the appeal of geotechnical pursuits. Government and industry supported organization like AusEarthEd, TESEP, GA and GSA or even Engineers Australia are a good place to start. A slightly different approach is to convince schools to encourage geology as a subject in secondary and tertiary education through advertising or voluntary school visits. Another possibility is for engineering consultancies to hire interested geologists, and to use workplace education to train junior geologists to apply their craft to engineering. There are many engineering geologists who were developed in this way resulting in many years of valuable geological input to engineering. In short, it is up to us to initiate the change and either grow talent from young children or grow talent from older interested professional people.

5 MOVING INTO GEOLOGY CAREERS AFTER GRADUATION

Besides looking at the secondary education angle, it is important to understand where geology students end up after finalising their tertiary degree. To this end, we reviewed publicly available and internally gathered data from Curtin University (Bentley Campus). It is one of the few Australian campuses still offering a specialised Bachelor of Applied Geology program (mind, not a BSc with a major in geology) and two associated double degrees (Geology and Finance and Geology and Environmental Science). Curtin also offers a BSc majoring in Earth Science and is about to launch an additional major in Environmental Sciences. In recent years, several Australian campuses have reduced or restructured their geology programs due to financial or institutional changes. Some standalone geology departments have been closed or consolidated into broader earth science or environmental science schools at institutions such as Australian National University (ANU), University of Melbourne, University of Sydney, University of Newcastle and Macquarie University.

Finding out where geology graduates end up is elusive as there is no official repository for this kind of information. At Curtin, the data that are available go back to voluntary reporting from graduates who inform the course coordinator of their starting position. Records of destinations have been kept systematically since 2019 and allow a glimpse into the predominant first employment industries.

As per the pie chart given in Figure 5, 75% of Curtin graduates start out in the 'minerals' sector. This is a broad definition and includes all aspects of the mineral resources sector. The 2nd largest batch goes on to do an Honours degree. This is not strictly a starting position, so once graduated, this cohort enters any of the other categories, inflating their numbers. Assuming a similar distribution, it means that the minerals sector takes up close to 90% of all the geologists from Curtin. This is not surprising given the economic importance of mining in WA.

Of the remaining numbers, twice as many geologists end up in the environmental sector (i.e. consultancy) compared to the energy sector (mostly oil and gas exploration). This impression that the environmental sector attracts more graduates than the oil and gas sector (O&G) is skewed because a certain (unknown) number of respondents are double degree graduates (geology and environmental science) and thus from the onset focussed to work in the environmental field. It should also be noted that some of those marked down in the Minerals and Environment category find positions as hydrogeologists or engineering geologists and not all noted under Minerals are in exploration or mining geology but work for resource companies in different roles (anecdotal evidence via email communication with graduates after entering the workforce).

Finally, numbers may be further skewed because one group/category may report back to the course coordinator preferentially compared to the other sectors (e.g. reticence to report entering the O&G sector given the situation around climate change or keenness to share first working experiences in a mining environment).

It is thus hard to pin down how many graduates move into engineering geology. Yet, inasmuch as this crude statistic can give a wider picture of the situation in WA, it indicates that, conservatively, less than 10% of Curtin graduates start in environmental consultancy, the category to which engineering geology consultancy belongs. Personal communication with interested 3rd year students who are asking for contacts and possibilities to do internships in this field (while taking the unit 'Hydrogeology and Engineering Geology') is consistent with this low percentage but suggestive of a mark closer to ≤5%. Whatever the true numbers, it is hard not to infer that the Minerals sector is siphoning off the bulk of graduate geologists (including double degrees with economy) that are vital for other areas, among them consultancy in engineering

geology, hydrogeology, and/or environmental contaminant remediation. And while genuine interest in exploration and resources geology may play its legitimate role in this imbalance, other factors may well contribute to this monopoly on human resources, not least the disproportionate entry salaries (and their propagation).

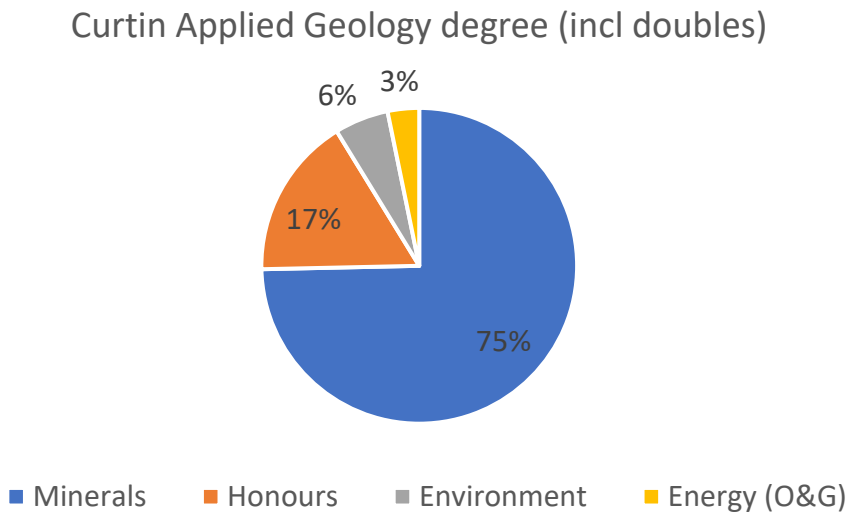


Figure 5: Different industry sectors taking up BSc Geology single and double degree graduates (n=217) from the School of Earth and Planetary Sciences at Curtin from 2019-2024. (Note, these are not all graduates but only those who voluntarily report back where they found their first employment)

6 CONCLUSIONS

The data presented in the paper indicates that engineering geologists form a relatively small proportion of the geotechnical workforce in Australia when compared with other countries including New Zealand. The paper recognises that market forces have driven the contrast between Australia (which has a large resource sector particularly in WA) compared to New Zealand (which is home to numerous geological hazards). But the paper highlights that there is very limited earth science education in Australian schools, and limited tertiary education available for engineering geologists in Australia. Interest in geosciences as a career is declining globally. We could continue to source engineering geologists from overseas, but we may be missing the opportunity to incorporate locally trained geologists with a good knowledge of Australia's vast and sometimes unique geological domains. There is therefore justification for attempting to increase the number of Australian trained engineering geologists.

We know that geology is important in geotechnical practice. This is demonstrated by several high-profile catastrophic engineering failures attributed, at least in part, to poorly understood ground conditions. The LinkedIn poll data indicates that geotechnical practitioners in Australia value the importance of geology, and the vast majority (73%) believe it is fundamental for all sites. It is therefore clear that geological knowledge, and engineering geology, is an important engineering discipline. If this is the case, who is currently performing the geological work in geotechnical practice? Based on the proportion of geologists in the Australian geotechnical workforce indicated by the Ground Recruitment Pty Ltd data, geotechnical engineers may be performing a geological role on their projects. Can engineers identify where they have more complex or hazardous geological conditions without having the geological training and experience that a geologist would contribute? There is a fundamental difference between engineering and science. Is this well understood?

Given the resource driven market conditions in Australia, and particularly in WA, it seems unlikely that Master of Engineering Geology program will be offered by WA universities in the near future, A program of this kind is currently under development at UNSW. This raises the question, will geologists from other states consider relocating or enrolling remotely to pursue further qualifications in engineering geology? Perhaps we need to upskill geotechnical engineers in geology? Could that be a solution? Offering a university micro credential for interested geologists, or more courses on engineering geological themes for geotechnical engineers to complete may also be beneficial. Could the expanding set of courses organised and operated by the AGS plug this gap going forwards?

7 DO WE ALREADY HAVE THE ANSWER?

The AGS has been running geotechnical and geological mapping courses in Perth for many years. These courses are actively supported by local practising engineering geologists willing to share their knowledge and expertise. These initiatives are crucial for providing the specialist engineering geology skills and knowledge to individuals working in the discipline in WA. The skills and knowledge offered on these courses are necessary for any WA engineering geologist to learn. These mapping courses would be vital to those who are isolated from other practitioners because they are the only engineering geologist in their company or WA office location, and also for engineering geologists who qualified elsewhere and may not be familiar with WA geology. It is clearly important that these courses continue.

Over the last few years, a few additional things have been happening in WA that may be assisting in encouraging geologists into the engineering geology discipline.

Final year students undertaking the Bachelor of Applied Geology at Curtin University, Perth study a Hydrogeology and Engineering Geology unit (Unit 3003). Domenik Wolff-Boenisch is the Unit Coordinator for this unit and maintains. strong industry links and resources. Paul Baker, GHD Pty Ltd has been collaborating with Dom as an Adjunct Associate Lecturer to contribute to this unit for the past six years. During those six years, Paul and Dom have overhauled the course content to align it with the latest standards and guidelines and adjusted the content so it is relevant to current industry needs. For example, an introduction to tailings storage facilities has been added. Paul prepares and delivers some lectures, but the main contribution is being present for the weekly workshops where students work through practicals on desktop studies and geological models, soil and rock mechanics as well as introducing hazards such as rockfalls, sinkholes and landslides to the undergraduates. He also introduces site investigation techniques and the importance of understanding groundwater and aquifer systems. During the practical sessions, it is apparent that approximately 20% of the students have an aptitude for engineering geology and for many it comes as a revelation that being an engineering geologist is a viable career path. However, the discrepancy between starting salaries in the resources industry (exploration and mining) and engineering/consulting gives graduates a very difficult choice between the two irrespective of how much the applied aspects of engineering geology may appeal to them.

In 2021, Paul Baker published his LinkedIn article ‘It’s hard to find home-grown engineering geologists in Perth’. The article asked if there were any engineering geology topics that potential employers of engineering geologists would like to see included in a university course. In response to this article, Julia Bota (HATS Consulting) and Alex Petty (PTG Consulting Pty Ltd) contacted Paul to discuss supporting the Applied Geology Unit GEOL3003. Dom had been considering introducing a field course as part of the unit, and Julia and Alex were able to contribute to the planning and preparation of the field course. A half day engineering geology field course was subsequently held in 2023 and 2024 as part of Unit GEOL3003. It was hoped that by showcasing the role of the engineering geologist to the students and providing them with more industry connections that some may show an interest in pursuing a career in engineering geology.

It may be too early to state that this course has had a significant impact on encouraging students to follow engineering geology as a career. It should be noted that the two graduates who attended the Curtin University field course that have entered the profession in Perth have joined GHD Pty Ltd. (with Paul Baker) and PTG Consulting Pty Ltd (with Alex Petty), two of the three engineering geologists who lectured at the field trip. More time is needed to demonstrate the effectiveness of this kind of engagement. However, with support from individual volunteer practitioners, a short introductory field course is something that could be extended to other universities who provide Geology degrees across WA and Australia.

Whilst all the initiatives presented above are certainly helping to raise the profile of engineering geology at a higher education level, it is important to note that, once students reach university, they have already chosen their overall subject. There are currently no specific programmes or initiatives for engaging high school students with engineering geology as a discipline. This issue is discussed further in the Australian Geoscience Council’s Australian Tertiary Geoscience Education Profile 2022 report, which states that the lack of exposure and awareness of geosciences in Australian secondary schools remained one of the significant contributary factors with the low number of students entering geosciences higher education programs in Australia.

If we are to encourage Australian students to consider geology or more specifically engineering geology or geological engineering, we must begin at the primary and secondary stages of education. We must, as a professional community, offer assistance and encouragement to institutions that deliver education to young people about the appeal of geotechnical pursuits. Government and industry supported organization like AusEarthEd , CORE, TESEP, GA and GSA or even Engineers Australia are a good place to start. This could be supplemented by members of our community visiting schools and talking about careers in engineering geology.

It is positive to see that a couple of graduates have already been placed in roles who have recently completed the Curtin University Applied Geology Bachelor GEOL3003 Unit (Hydrogeology and Engineering Geology). Perhaps a few more individuals getting involved with mentoring potential engineering geologists and supporting universities in maintaining strong industry links will assist in maintaining, or even increasing, representation of engineering geologists within the geotechnical community in Australia.

REFERENCES

Australian Curriculum, Assessment and Reporting Authority (ACARA) (2024) Earth and Environmental Science, Version 8.4, (https://v8.australiancurriculum.edu.au/senior-secondary-curriculum/science/earth-and-environmental-science/), February 2024.

Baynes F.J., Fookes P.G, and Kennedy J.F. (2005). The total engineering geology approach applied to railways in the Pilbara, Western Australia. *Bulletin of Engineering Geology and the Environment,* 64(1):67-94.

Eptisa, Servicios de Ingeniera S.A. (1998) Investigation of the Failure of the Aznalcollar Tailings Dam cited on Tailings Info (https://tailings.info/casestudies/los frailes.htm on 23 December 2024.

Independent Expert Engineering Investigation and Review Panel (2015). Report on Mount Polley Tailings Storage Facility Breach. January 30, 2015.

International Council on Mining and Metals (ICMM) (2020): Global Industry Standard on Tailings Management, August 2020.

Lagesse, R.H. et al, 2022. The role of engineering geology in delivering the United Nations Sustainable Development Goals. *Quarterly Journal of Engineering Geology and Hydrogeology.* Volume 55, Issue 3, 2022.

Packer, M., Nash, T., Bennett, C., and Doe, A. (2024) Editorial. Establishing professional accreditation pathways for Australian engineering geologists in the civil design and construction industry. *Australian Geomechanics*. Volume 59, No. 3, 2024.

Paul, D. (2024). The state of engineering geology education in Australia. *Australian Geomechanics.* Volume 59, No. 3, 2024.

Rogers, S. L., Giles, S., Dowey, N., Greene, S. E., Bhatia, R., Van Landeghem, K. and King, C. (2024) "You just look at rocks, and have beards" Perceptions of Geology from the United Kingdom: A qualitative analysis from an online survey. *Earth Science Systems and Society, The Geological Society of London.* Volume 4, Article 10078, February 2024.

School Curriculum and Standards Authority (SCSA) (2024) Student achievement data (https://senior-secondary.scsa.wa.edu.au/data), 4 February 2024.

Vafeas, N. (2023). The fall of geoscience – an unintended consequence of well-intended climate advocacy, LinkedIn Article (https://www.linkedin.com/pulse/fall-geoscience-nicholas-vafeas-uwuce/), 6 November 2023.

https://doi.org/10.56295/1ACEG25

THE IMPACT OF INDUSTRY SUPPORTED FIELD COURSES ON THE EDUCATION AND PROFESSIONAL TRAINING OF GEOLOGICAL ENGINEERS AT QUEEN'S UNIVERSITY, CANADA

D. Jean Hutchinson, Ph.D., P.Eng. (ON & BC), FEIC, FCAE
Professor Emerita, Queen's University and Vice President, Innovative Geomechanics Inc.

ABSTRACT

The capstone Geological Engineering course taught at Queen's University for two decades has given students the opportunity to explore the mining cycle by visiting mine, mill, smelter and tailings sites over a seven day field school. Learning about the challenges and potential solutions during the site visits from the passionate and creative site guides was very effective and inspiring. Many students reported that learning about these sites and projects inspired them for the first time to think about a career in mining. Many of the students who took these courses are working in the geological engineering aspects of the mining industry now, perhaps inspired by this course.

1 INTRODUCTION

The industry supported Geological Engineering field course discussed in this paper has been attended by many hundreds of final year and graduate students over the past two decades at Queen's University. In addition to classroom time, the course included five working days on mineral exploration sites, mine and mill sites, processing and mine waste facilities.

The field course has been supported by industry for more than 20 years, with companies providing detailed and extensive guided site visits for the students and instructors. Visits to mines, mills and tailings sites has given the students a concentrated and technically excellent introduction to these concepts, the past successes and failures at the sites, and the evolving approaches to understanding and managing challenges at the sites. Student engagement has been enhanced by pre-trip exercises focussed on assessing the mining cycle, the circular economy and the specific sites to be visited, and evening discussions and reports during the field trip. A final assignment, including a report and presentation summarizing a problem encountered at one of the sites and potential engineering solutions, provided the class members with an opportunity to focus on a topic of interest, and to hear from and ask questions of their classmates on a range of topics.

The students benefitted tremendously from learning about the issues and solutions from the people working on them and the opportunity to make personal observations about the sites. The industry "tour guides" were very generous of their time and knowledge, providing background materials and documents about the issues being discussed and areas being visited, and giving the students a "real" picture of the challenges and opportunities at their workplaces. One of the most valuable outcomes was the opportunity for students to ask questions of the site contacts to understand the technical issues, as well as the societal perception and regulatory environment being considered at each facility. Industry members appreciated the opportunity to inform students about their work, encourage them to find work at mine sites and other facilities, and to introduce them to the smaller communities they live and work in.

The consideration of the mining cycle as a central theme to the course provided students with a better understanding of the environmental and societal effects of mining and the importance of a multi-disciplinary approach to the solutions. Discussions of the professional aspects of work in this sector, including policy and regulations, changes to technical and professional practice guidance and regulations resulting from past failures, and risk-based decision making both during mining and for post operational landscapes, provided students with a more comprehensive perspective, and some skills usable after graduation.

Many students taking the course had never visited or worked in mining prior to the trip. Almost all students, over the years, were motivated by the experience, enjoying the challenges and comprehensive, and multi-disciplinary approaches to the problems. A significant number of the students trained in this way are now contributing to this sector, and effecting change in both practice and the perception of mining.

The support of industry in this course was an essential contribution to the outcomes. It was often not easy to justify the time taken by site personnel with very busy jobs, to prepare and guide the tours. In spite of this, the students were provided exceptional tours every year. In addition, the significant and legitimate safety concerns with having casual visitors on these sites was addressed by extensive pre-trip safety instruction and discussions, site specific visitor inductions, and smaller tour groups at each site to permit sufficient personnel to observe and manage safety.

2 GEOLOGICAL ENGINEERING PROGRAM DESIGN

The Geological Engineering program at Queen's is designed to meet the requirements of the Canadian Engineering Accreditation Board, and to provide students the knowledge and skills required to work in geotechnical, geoenvironmental, mineral exploration and geophysics specializations. The program is structured to include foundational building blocks in both geology and engineering, as well as mandatory and elective courses in the key areas of specialization. Field and / or laboratory teaching is a fundamental component of all of the courses offered. The conceptual design of the program is illustrated in Figure 1, including a general overview and a more detailed listing of the core topics to be covered in each area. This material was developed by Dr. Mark Diederichs during a significant program revision and redesign in 2011.

3 GEOLOGICAL ENGINEERING COURSE DESIGN

The professional accreditation of engineering programs in Canada requires that student competence be assessed against a number of graduate attributes for which learning outcomes are measured. The Geological Engineering degree program is built year by year, through:

- foundational courses in general engineering in first year;
- geo "materials" courses in second year, including mineralogy, sedimentary geology and stratigraphy courses, a field mapping school, as well as mechanics and strength of materials;
- geo "mechanics" courses in third year, including soil mechanics, rock mechanics and hydrogeology, mineral exploration, structural geology, geophysics and geochemistry; and
- geo "engineering" design courses in fourth year, including mandatory courses in engineering design and numerous electives to permit some specialization by the students.

All of the Geological Science and Geological Engineering courses at Queen's include "hands on samples" and/or computer labs and many have field trips to sites of interest in the local area. The emphasis on field based teaching has been maintained by the department, through financial support from alumni, and field trip fees paid by the students, in spite of financial pressures to reduce or remove these courses. As an example of the importance the department places on field based teaching, all faculty position postings indicate that interest in field based teaching is an asset.

At Queen's University, all engineering students undertake the Engineering Design and Practice Sequence (EDPS) set of courses, to develop "competence in design process methods and tools, problem analysis, creativity, economics and entrepreneurship, engineering communications, professionalism, and ethics" (Frank et al, 2011). The early year courses within the sequence are common across all of the engineering disciplines, to lay the foundational knowledge from a multi-disciplinary perspective. During the second half of the degree, each engineering program offers design courses relevant to the subject(s) they cover. In the case of Geological Engineering, this includes the integration of geological knowledge into geotechnical, geoenvironmental, mineral exploration and geophysics projects and designs. In addition to a full year, multi-disciplinary team design project, the Geological Engineering students took the capstone field course discussed in this paper. The field course was intended to expose students to then-current challenges and opportunities within the mining cycle, by visiting numerous sites over a seven day trip, with associated academic exercises assigned and completed before, during and after the trip.

The capstone field course for Geological Engineering students at Queen's University focussed on the mining cycle, and the ways that program graduates can become involved in mining related work, including mineral exploration, geological model development and ore evaluation modelling, extraction, processing, waste reuse or disposal including progressive decommissioning, closure planning and implementation, and throughout the process, the support for informed decision making through engagement with stakeholders.

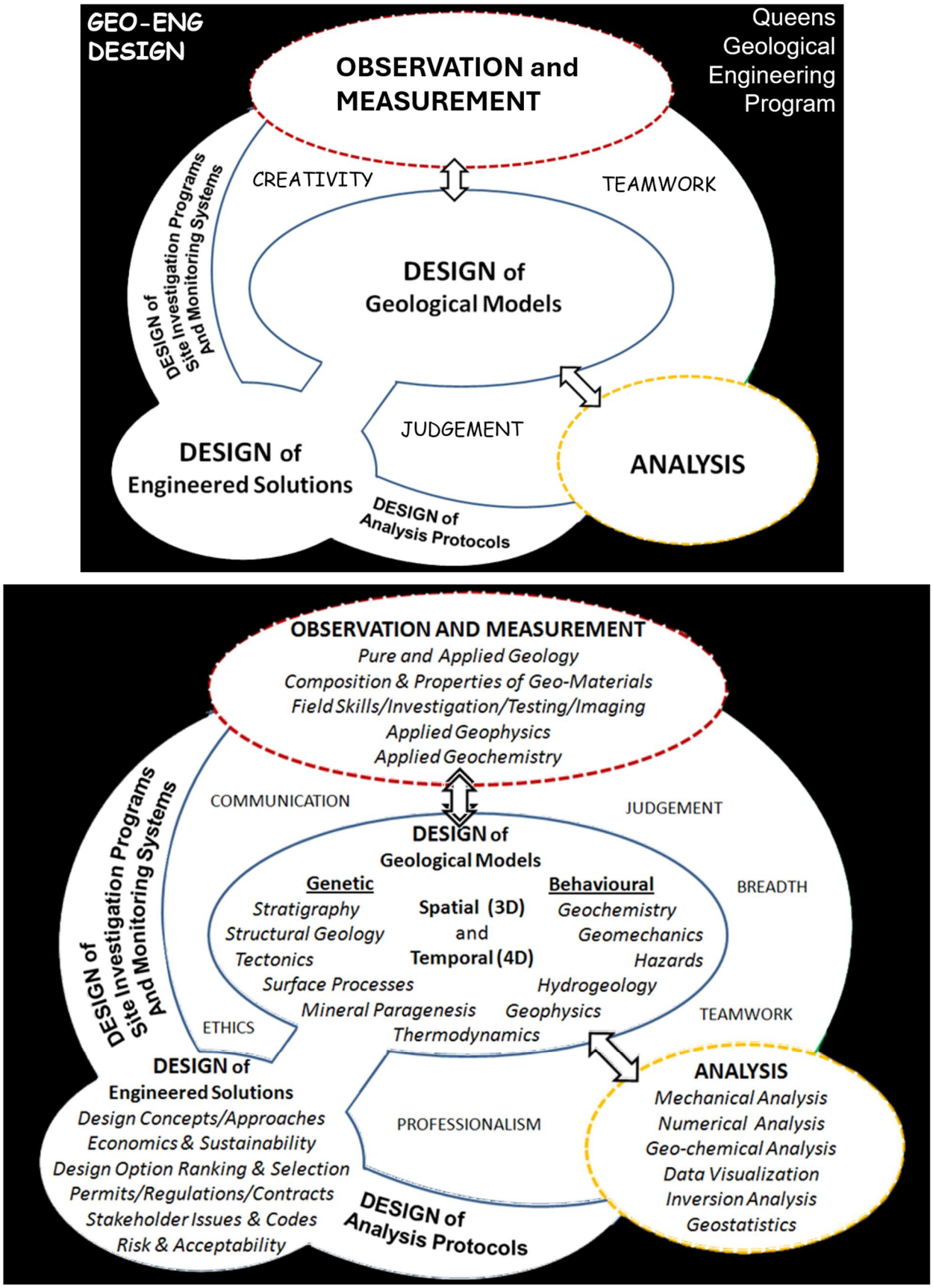


Figure 1: Geological Engineering program design at Queen's University, in general (upper image) and including specific topics included in various courses (lower image). Images courtesy of Mark Diederichs, 2011.

4 CAPSTONE FIELD COURSE STRUCTURE

The work included within the field course comprised attendance at a number of lectures, completion of pre-, during- and post-trip assignments, and attendance during all days of the field trip (except in the case of illness). Because this course was offered in the final year of the Geological Engineering program, the students were already well prepared with pre-requisite information, as they had already taken many geology, science and engineering courses, including structural geology, mineralogy and mineral exploration, as well as numerous courses covering the mechanics and design of rocks and soil, the mechanical influence and chemistry of water and waste, were familiar with mineral exploration including using geochemistry and geophysics, and had considered stakeholder perspectives and communication with the public about Geological Engineering projects. Lectures included discussions of all of the stages of the mining cycle, including the circular economy whereby waste is diverted for other uses; and how evolving technologies, public knowledge and perceptions, as well as regulations and technical guidelines must be considered to support evidence based decision making and to retain (if possible) the social license to complete resource projects.

The assignments for the course are described in more detail during the course, but a one page summary sheet was also provided, to give the students an easily accessible reminder of the work to be completed and the deadlines. A sample is given in Appendix A.

A typical route for the trip is shown in Figure 2, travelling from Queen's University in Kingston to the mining hubs and communities of Sudbury and Timmins, Ontario.

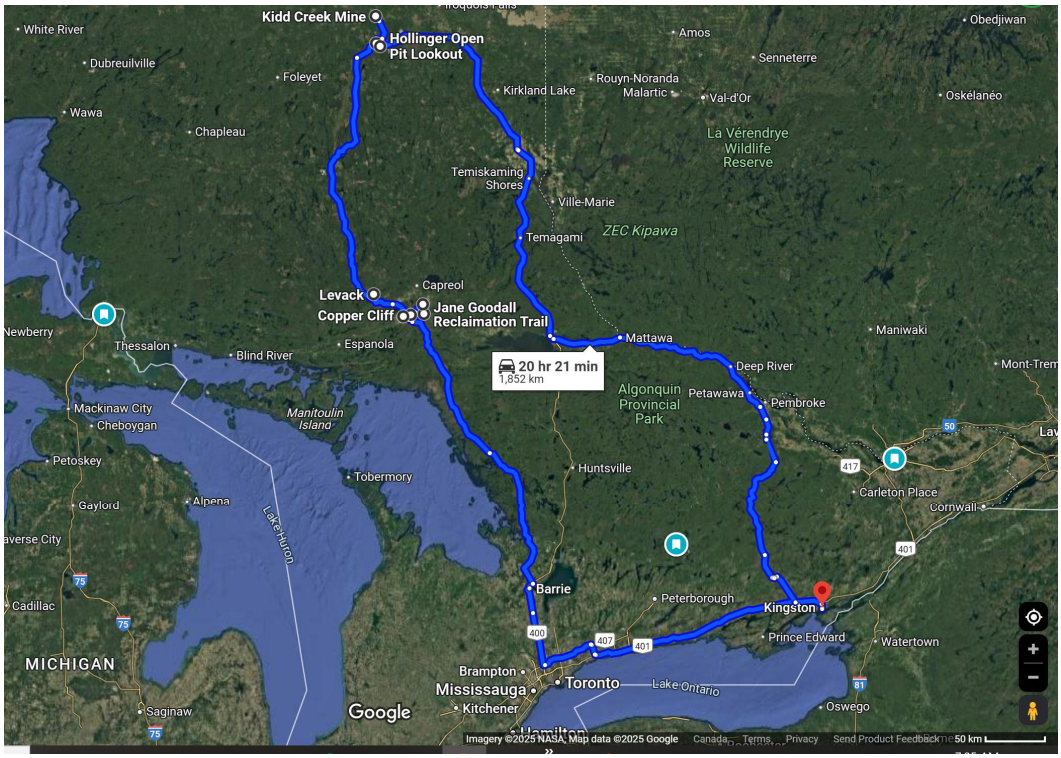


Figure 2: Typical field course route between Kingston, Ontario and the mining hubs and communities of Sudbury and Timmins, Ontario.

Technical lectures offered prior to and during the trip included physical and environmental considerations in the assessment, design, operation, progressive rehabilitation and closure of open pit and underground mines, including crown pillars, tailings impoundments, waste rock piles and general mine infrastructure. Speciality lectures were offered by faculty members regarding mine waste management, acid rock drainage testing and mitigation, milling and smelting processes, and mineral exploration for orebodies similar to those visited on the trip. Guest lecturers discussed indigenous stakeholder consultation and indigenous ways of knowing about the land, post mining landform design and other topics of interest.

4.1 PRE-TRIP ACTIVITIES

At the start of the course, each student selected a site and a design topic from a list of sites provided. The topic selections were reviewed and approved as they were submitted by the students, and direction was given by the instructors to ensure that a breadth of topics was being considered by the class members. Some background materials were provided, particularly those which are not easily found, grouped as: Geological information and Mineral exploration, Geotechnical issues, Geoenvironmental issues, Regulations and Closure planning, Mining and Milling, Tailings dams, Stakeholder communications and public policy, Impacts of legacy mining, History of Sudbury and History of Timmins.

The students were tasked with researching and writing a brief summary report to develop an understanding of the technical challenges at the site as well as in the broader industry, and to generate a list of two or three questions to be asked during the site visit. They were also directed to include consideration of the geological setting / geological model where applicable. These documents were compiled and made available to all students at the start of the field trip travel day, to give them more broadly based knowledge, before visiting the first site.

The students benefitted tremendously from learning about the issues and solutions from the people working on them and the opportunity to make personal observations about the sites. The industry "tour guides" were very generous of their time and knowledge, providing background materials and documents about the issues being discussed and areas being visited, and giving the students a "real" picture of the challenges and opportunities presented by their workplaces during the site visits. One of the most valuable outcomes was the opportunity for students to ask questions of the site contacts to understand the technical issues, as well as the societal perception and regulatory environment being considered at each facility. Industry members appreciated the opportunity to inform students about their work, encourage them to find work at mine sites and other facilities, and to introduce them to the smaller communities they live and work in.

It was also important for the students to consider the societal perspectives related to the resource extraction industry. For a second pre-trip assignment, they were assigned a persona, and a "for" or "against" perspective for a resource project that was under consideration or protest at the time they took the course. The points of view represented included:

- In favour: Geotechnical Consultant, Geoenvironmental Consultant, Mayor of the local community, Mining Company Board member, Lawyer representing First Nations communities to negotiate Impact Benefit Agreement,
- In opposition: Geoenvironmental Consultant, Mayor of downstream community, Mining Watch Canada representative, Lawyer specializing in land use rights and First Nations claims representing First Nations communities in opposition,
- Neutral, fact checking for regulations and facts about the specific cases: Ministry of Northern Development and Mines, Ministry of the Environment at both Federal and Provincial levels.

This required the students to complete some less conventional research, using newspapers, popular magazines and web pages, in addition to any other published materials in order to understand the project, the technical and societal challenges and to consider the many different viewpoints that are expressed in these discussions. Each person was given the opportunity to make a statement from their persona's perspective and to ask questions of their "opponent". The objective was to have the students consider multiple perspectives, the nuances of deciding whether challenging resource projects will be permitted and the impact of historical mining operations and practices on current day understanding and perspectives, both good and bad. At the end of the exercise, the students were asked to critique the information that they provided, and were asked which side of the discussion they were personally aligned with, and whether they thought the project should be permitted to advance or not.

4.2 DURING-TRIP ACTIVITIES

The students had several assignments during the trip. All had to write a legible field note book for every day of the site visits, recording factual information and observations, as well as personal observations and questions. While the latter information is not normally included in a professional field note book, it was helpful for the students with their development of critical thinking and considering the course themes and questions. The field notebook was turned in at the end of the trip, reviewed and marked. This process provided the students with some feedback on their work, and ensured that the students were engaged with and listening to the site contacts at all times. The site personnel made favourable remarks on this exercise regularly, and were often interested in the drawings students were doing to work out complex ideas or record visual observations.

At the end of each day, on the trip back to accommodation, ¼ of the students were tasked with writing out two or three questions that might be addressed during the discussions held each evening. These questions ranged from clarification of concepts discussed during the site visit, to more open ended discussions about the role of scientists and engineers and the development of new approaches and methods, to more philosophical discussions about the impact of mining on economic

development and opportunities versus environmental impacts / loss of pristine sites, to name just a few topics. The instructors reviewed the submissions and selected several for the discussions.

After the last discussion of the evening, which were often quite animated and had to be terminated to permit sufficient sleep before the next day, the students each wrote a half page summary of the most important lesson they learned that day and any residual questions remaining.

On the bus home, after the last day, the students wrote a short reflection of their experiences on the trip. They were asked to comment on the impact of the course on their understanding of the resource cycle, the major lessons learned from discussions with the site contacts and for any suggested changes for future years. They also had the opportunity to provide anonymous course reviews at the end of term, where they could comment on the course both positively and negatively, in terms of the teaching team, the effectiveness of the assignments to support their learning and any recommendations for what should be kept and what they would recommend changing for future years of the course. Comments drawn from these reflections are included later in the paper in the discussion of the impact of the course on students.

4.3 POST-TRIP ACTIVITIES

The final deliverable for the course was a Geological Engineering design report and professional presentation. The students worked in pairs on this, generally combining diverse interests and perspectives on the topic they selected. They were tasked with considering an ongoing challenge at the sites visited, based on a thorough understanding of the geological setting and the technical issues, and developing conceptual designs for possible solutions, and a monitoring and decision making framework to guide final selection and optimization. This work took place for several weeks after the trip. At the end of the academic term, the full class attended all of the presentations and were encouraged to ask questions of their classmates. This deliverable was the most scrutinized during engineering accreditation reviews to assess the students' abilities to work through a credible engineering design process.

5 FIELD COURSE PLANNING CONSIDERATIONS

The design of the course changed over time, mostly in response to changing opportunities to visit sites, and considering lessons we learned from running the course and soliciting input from students about the course content and structure.

Each instance of the course was designed to expose students to exploration, extraction (open pit and underground), processing (milling and smelting) and waste management (tailings, waste rock, effluent, and mining impacted water). As noted before, several discussions explored the opportunity to reuse waste materials and to consider long-term solutions and conditions, providing an opportunity for students to develop a more holistic and critical perspective of the sites visited.

In addition to the pedagogical design of the course, other challenges and solutions include:

Challenge 1: Ensuring students are prepared.

When the course was initiated, several sites rejected visit requests, due to the poor reputation and behaviour of university groups coming to site unprepared, uninterested, sleep deprived and hung over. To combat these problems the course was designed to introduce the students to the sites and concepts before the visit, through lectures and assignment work, and to engage them in exercises every day during the trip. A contract was developed with the students, and signed by them, in which they agreed that they would not drink or take drugs during the trip, and that they would bring and wear all required PPE. The field trip safety plan was developed and discussed with the students during class time to ensure all aspects were included and the hazards and mitigations were well understood. For many of the students, this course provided their first opportunity to visit an industrial site, and for almost all of the students, an opportunity to visit an underground operation, so this preparatory work and the focus on health and safety was essential.

Challenge 2: Ensuring students are engaged with the site contacts.

The level of high quality and focussed student engagement was a constant source of pride for the instructional team. Most sites welcomed us back year after year, indicating that the trip was a highlight for the site contacts. All of the pre- and during- trip work was designed to give the students information and knowledge, make them curious about the issues and solutions, and require them to be attentive at all times during the contacts with the site contacts.

Challenge 3- Justifying industrially based field courses in an academic environment.

While many people at this conference understand the value of field based learning and engaging with the most pressing problems in our resource industries, this type of course and the instructional component offered by the field contacts are not typical of most university courses. Indeed, most administrators initially thought of these as field trips, not courses, with a focus on passive observation. This type of trip requires much higher than usual per-capita spending, compared to on campus courses, and particularly when compared to large enrollment seminar courses without any lab or tutorial

content. Higher instructor to student ratios are required for field based teaching, to ensure the students are safe in unfamiliar industrial settings. There are significant travel and accommodation expenses.

At Queen's, a field trip fund has been created and generously supported by alumni and companies, all of whom recognize the value and importance of field based training opportunities. This has the advantage of providing funding but also demonstrating the significance of these types of courses to our alumni, who also support other initiatives across the university. An annual report was prepared for alumni and donors to provide an update on the course each year, including quotes from some of the students' reflections, used with their permission.

Challenge 4 – Ensuring the H&S of all students.

As noted above, the students were involved in all aspects of planning the field trip safety form, considering potential hazards, impacts and actions. However, this could not prepare them for a trip to an industrial site or underground. As a result, the class participated in a "trial run" to a tourist mine, built out of an old near surface mine with both shaft and adit access. They could gauge their own level of comfort with the environment, and we used the displays to present the geological setting, the different support systems used at the site, and various excavation methods. Having developed a level of comfort first, the students were then better prepared to engage in the technical learnings during the site visit and to better understand their personal responsibility for safety. This also meant that they paid strict attention during the site specific safety briefings provided by the H&S personnel at each site. After twenty years and site visits by hundreds of inexperienced students, there were limited number of incidents, although there were two lost time incidents involving students rolling their ankles on rough drift floors under water.

6 INDUSTRY SUPPORT

This course would not have been possible without the tremendous support by industry and site personnel. At almost every site, there were multiple person-days expended to prepare for the visit by providing advance information, planning for the visit including on site transportation, and the inclusion of several technical personnel at each site to cover all of the aspects to be discussed, and post-trip follow up with the student teams with any remaining questions. At the end of each trip, we asked the students to calculate the number of hours expended by the guides and to estimate the cost of salaries to have the guides working on our behalf and not on their regular jobs – a very eye opening exercise.

A number of the site contacts would pro-actively contact us each year before agreeing to other requests for site visits, because they valued the interaction with our students so highly. There are no formal metrics of the value of this course to industry, but a number of graduates moved to the mining communities we visited or similar small communities to take up employment, and more work in resource related industries as a direct result of this experience.

7 IMPACT ON STUDENTS

There are no formal metrics to measure the impact of this course on students, either during their program and when they started working. However, as noted above, the students wrote a "reflection" assignment about the trip.

Hundreds of students have taken the course in the final year of their program at Queen's University, and the vast majority reflected that the course had increased their understanding and positively improved their perspectives on both the benefits and solutions to the impact of mining and the role of Geological Engineers within the mining cycle. Many wrote that they were inspired by the passion of the site contacts and the opportunities and challenges presented by the mining and processing industries to consider work in this field which they had not considered before the trip. A selection of comments is included below to demonstrate both the value of a field course and the interactions with the site personnel.

> "During our tours we met workers who had recently graduated from university, and others who have spent their whole careers in the mining industry and have reached high ranks within their companies. It was interesting to see the knowledge and responsibility that the engineers-in-training or geologists-in-training had gained at their job. Everyone was extremely welcoming, helpful and answered all of our numerous questions."
>
> "For any of us who were not too sure about heading into the mining industry, this trip has cleared up any misunderstandings and shown us how safe they are as well as what our future jobs may be. This trip has been a great learning experience and I enjoyed every part of it."
>
> "The field trip was an incredible experience. It provided me with the opportunity to visit multiple underground mines and see the dynamic workings. It is an excellent opportunity to take the concepts learned in the classroom and see how they are applied in multi-million dollar operations. It is a truly amazing feeling to be 7500 feet below surface and see copper stringer mineralization in person in the drift walls. It is very encouraging to see how far the industry has come and progress that has been made

for every component of the mining cycle. It also makes me wonder where the mining industry could be headed given that technology continues to advance each and every year support and extraction techniques continue to be refined. One of the most special moments of the trip for me was visiting the tailings ponds at Strathcona (see Figure 3). I questioned myself if I was looking at a tailings pond or a lake in Muskoka. I thought it was so remarkable that they were able to use the physical geography of the land to their advantage and produce an amazing treatment system. I thought it was incredible that they were able to grow different varieties of crops on the tailings slime with no trace metal elements. I thought this was so promising for the future of mining and a step closer to how the mining industry could be perceived in a different light."

David Bonneau

"Given the uncertainty involved with mine design, and geological uncertainty, it was especially interesting to see the ingenuity employed by management. Part of being a geological engineer is being able to identify, evaluate and ultimately create a plan of action for unique problems. After visiting this mine, the methodologies employed to identify and mitigate potential hazards was especially interesting, and forced me to think unconventionally.



Figure 3: Final polishing pond contained within tailings facility at Strathcona Mill, Levack, Ontario.

The course described in this paper was the inspiration for the field based course included in the professional Masters of Earth and Energy Resources and Leadership program also offered at Queen's University[1]. The students in this program are from numerous countries, and the program is designed to be of benefit to professionals with a wide variety of background knowledge and areas of practice, for both mining and energy resources. The field trip route for this course is in western Canada, and generally includes visits to a copper producing open pit mine, mill and tailings dam, a smelter, a proposed coal mine at a brownfields site, a gas processing plant, and a hydroelectric dam and powerhouse. The reflections offered by these students provides an opportunity to measure the impact of this type of course at a later stage in their careers, and for people with a variety of very different educational backgrounds. While not directly relevant to the practice of Geological Engineering, the comments selected below are intended to highlight the outcomes and value of this field course from the professional students' perspectives.

"As an economist and policy professional by background, the field school gave me an opportunity to visit physical sites of operation (including mine sites, reclamation sites, hydro facilities, and oil and gas production sites). Speaking with the operators of these facilities provided me with the technical insights into the challenges that various operations face in driving production operations and implementing physical changes that respond to regulatory requirements. The field school provided me with a platform to understand the extractive sectors in a way that was not possible from an office setting, nor from within

[1] https://www.queensu.ca/earthenergyleadership/

the government in a policy-making capacity. This broadened perspective enabled me to immediately apply better practices in the development and amendment of government policies and regulations, with a stronger lens to developing policy that can practically and efficiently be implemented by operators."

Mark Zanewick

"What stood out most was the openness and generosity of the industry professionals we engaged with on-site. They not only exchanged technical insights but also unvarnished perspectives on leadership, operational culture, and responsible resource development. The opportunity to engage directly with professionals who operate in world-class operations was both exceptional and significant, and their insights have had a lasting effect on me.

The experience profoundly reshaped the way I approach my own projects. It broadened my perspective and reignited my motivation to return to my home country, Peru, with a more strategic and purpose driven mindset. Today, I lead a family-run mining group dedicated to the generation, development, and production of mining projects, with a strong emphasis on community engagement. The field school played a pivotal role in refining my strategic thinking and strengthening my ability to navigate the complex intersection between project development and stakeholder management. "

Manuel Rodrigez

8 CONCLUDING STATEMENT

The unique and special opportunity to educate students in the field is a key element of a comprehensive geological education. Although this concept is well understood by most engineering geologists / geological engineers, these types of courses are increasingly under threat and disappearing from University curricula, due primarily to budget pressures and retirement of faculty members capable of and interested in teaching field courses. As a result, a significant opportunity to expose students to field work is being missed, preventing them from understanding the value and importance of in situ learning and the excitement of working in the field, and delaying the development of their ability to think about observations within a larger picture of the geological model and anticipated material behaviour.

One of the student reflections provides an excellent summary of student perceptions of the important and impact of this course:

"When we talk about the value of the learning environment in Geology, a learning environment where students and their professors alike enjoy small classes and excellent hands-on learning opportunities, it is easy to get hung up on the differences between geology and bigger faculties. Something I believe is very important to consider when comparing geology to these other programs, however, is the nature of the work geology and geological engineering graduates find themselves doing. Many students, myself among them, chose geology as a discipline partly because it allowed for outdoor employment. The outdoor office is a very different environment than any classroom can emulate, and the way one works outdoors is often quite different from their indoor work habits. The development of real world skills for fieldwork at the university level is a godsend for employers, as mine have told me repeatedly, and in my (albeit inexperienced) opinion is a crucial part of an education in geological sciences or engineering. By making fieldwork a mandatory part of our program, the school is enriching everyone's education. For people similar to myself, who find themselves more comfortable in the field than the classroom, it is an opportunity to learn a great deal. I can honestly say that I learned more in one week in Sudbury and Timmins than I have learned in the majority of term-long courses I've taken, and more importantly, the things I learned to identify and/or understand are the exact same things I will likely be dealing with in my career, as opposed to classroom or laboratory models. Those people who find fieldwork to be a more daunting learning environment than the classroom may not learn as much about geotechnical issues during a field trip such as the one I just enjoyed, but they will come away from the trip with different lessons about overcoming any personal discomfort and enhancing productivity in the same fieldwork situations they will no doubt find themselves in again once entering the workforce."

Cam MacKay-Stotesbury

Organizations like AGS (https://australiangeomechanics.org/courses/) and AIG (https://www.aig.org.au/professional-development/events/) are needed to fill this gap, and to support further professional growth and development. These efforts are to be commended, encouraged and supported.

9 ACKNOWLEDGEMENTS

The field schools discussed in this paper were the result of many people's work, collaboration and enthusiasm. Grateful acknowledgements are due to:

Co-instructors: Rob Harrap and Dr. Heather Jamieson and the many graduate students who worked as Teaching Assistants on this course.

Company representatives – GEOE 410: Glencore – Strathcona Stephanie Marshall, Samantha McGarry and Joe Fyfe; Glencore – Kidd Creek Mine Dave Counter; Vale – Samantha Espley and Quentin Smith; Hollinger Mine – Josh Metcalfe and John Henning.

Queen's Alumni supporting the Field Education fund - in particular Mike Rose and Sue Riddell Rose who provided the initial substantial investment in the fund and also provided funds earmarked for the early versions of this course.

Queen's Students – for exceptional engagement, critical thinking and fun times, including gamely watching "The Core", "Volcano" and other assorted geology disaster movies with me on our long drives.

10 REFERENCES

Frank, B.M., Strong, D.S., and Sellens, R. 2011. The Professional Spine: Creation of a Four-year Engineering Design and Practice Sequence. Proceedings of the Canadian Engineering Education Association (CEEA), June. DOI: 10.24908/pceea.v0i0.3586

Appendix A:

Assignment summary sheet for GEOE 410 field school. The timing of the activities is indicated by the highlighted text – Pre-trip as yellow, During-trip as teal, and Post-trip as green.

GEOE 410 Assignments: Fall, 2022

Assignment 1: Select a topic of interest from the list provided. Conduct research on that topic, in general terms and also specifically related to one of our sites, if you can find them. Write a summary of the topic, including at least three technical references – from the collection posted on Teams and/or your own search. Generate two or three technical questions related to this topic that you hope to ask when on the trip.

- Summary report due: Sun Oct 2 at 23:59.
- Max length = 2 pages, point form text. List questions and references on an additional page, as well as any key figures.
- Individual, 20%.

Assignment 2: Keep a professional, complete, organized and legible field notebook. This includes recording the time and date of your visit, the weather conditions and the name and title of the people you meet on each site. Take care to distinctly identify each area visited, using the local names. Be sure to attribute important factual statements to the appropriate speaker. You may later use some of these statements as (personal communication, name, 2022) in your report.

- Due Friday October 14th, at the time that you board the bus for home.
- Individual, 20%.

Assignment 3: When you depart the bus at the end of your assigned day, propose one or two issues, in writing, for group discussion that evening. This should be relevant to observations you have made while on site. Participate in the discussion period every evening, remaining respectful and factual at all times.

- Due at the end of bus ride on your assigned day.
- Contributions to the evening discussion are expected throughout the trip.
- Individual, 15%.

Assignment 4: Provide a technical summary of each day, at the end of the discussion period, including the most interesting engineering fact that you learned. If additional questions arise, that have not been answered during the discussions, please add these to your summary. Please submit on individual pieces of paper.

- Due at the end of the evening discussions on T, W and Th on the trip.
- Maximum length = 1 page / day.
- Individual, 10% total, 3.33% / day.

Assignment 5: Write a reflection on your experiences of the trip. What did you learn? How did the field setting support this learning? Some of this content may be used in promotional material related to field education funding or in letters of thanks to field fund donors. Please advise if you would like to remain anonymous, if we do use any quotes from your reflection.

- Reflection due: Friday October 14th, at the dinner stop.
- Individual, 5%.

Assignment 6: In a team of two, propose a design solution to one of the issues encountered during the trip. Conduct additional research, as required, to support your analysis. Once your topic has been approved, prepare a 15-minute presentation, outlining statements of the engineering issue and the design scope, including observations and findings from the trip, and justify the selected solution. Your work should result in a fact based, technically feasible and justified solution, including high level economic analysis for the option selected.
The powerpoint file should include figures and tables, photos from the field trip if appropriate and available, and multiple technical sources. All of these items must be fully referenced in the slides and included in a reference list. Where possible links to the references should be embedded in the ppt file. Each slide should include full speaker's notes to summarize the information conveyed – this can be in point form, but must be fully referenced.

- Thurs October 20th by 23:59 – topic title and one paragraph each for problem statement & project scope, submitted by one member of your pair.
- Sunday Nov 6 by 23:59 – ppt files submitted electronically.
- Tuesday Nov 8 – presentations in class period.
- Deliverables include:
  - Ppt file with full referencing and speaker's notes.
  - Your team of two making a presentation of your design solution.
- Pairs, 30%.

https://doi.org/10.56295/1ACEG26

THE BOGONG LANDSLIDE, A CASE STUDY INTO AN AUSTRALIAN LANDSLIDE IN UNSATURATED SOILS

Darren Paul, Simon Harbig, Emma O'Brien, Alana Dubowik
WSP, Melbourne, Victoria

ABSTRACT

Over the course of two weeks between 28 September and 12 October 2022 a landslide estimated to have mobilised a volume of 30,000 m^3 of soil occurred on north-facing slopes near Bogong Village in Victoria. Debris arising from the landslide blocked Bogong High Plains Road – the main road to one of Australia's largest ski resorts, Falls Creek, and forced the evacuation of Bogong Village downslope of the landslide. The road needed to be re-opened before May 2023 to allow access to the resort for the 2023 ski season, it being the only road to the resort. Understanding the processes that caused the landslide became critical to informing the design and safe execution of interim works to re-open Bogong High Plains Road. Various lines of evidence including video of the landslide occurring, geomorphological evidence, investigations and analysis informed the development of an engineering geological model for the landslide. The model indicated anomalously deep extremely weathered micaceous granodiorite with a high void ratio at the sheared contact between two plutons. Perhaps owing to their northerly aspect and high evapotranspiration, the soils comprising these slopes preserve high soil suctions. A loss of soil suction arising from wetting fronts that developed over the course of three successive La Niña years was assessed to have triggered the landslide. On the basis of this model, interim works were designed to safely remove a sufficient volume of soils to re-open a single lane of the road. Following the interim works, permanent landslide mitigation was provided, the basis of which was to promote the preservation of soil suctions whilst preserving the natural landscape adjacent to Alpine National Park as far as practical. Understanding the response of the unsaturated soils to prolonged rainfall was critical to informing the design of interim and permanent landslide mitigations. This paper describes the development of the engineering geological model for the Bogong landslide and how the model then informed interim and permanent works to reopen the road and to prevent further landslides.

1 INTRODUCTION AND BACKGROUND

The Bogong landslide occurred upslope of Bogong High Plains Road and Bogong Village as indicated in Figure 1.



Figure 1: Aerial photograph of the Bogong landslide taken 11 November 2022

The cut road batter at the site of the landslide had exhibited signs of instability in the past, including in 2017 at which time the road batter was cut back and benched, with an overall slope angle of about 60° and height of about 15 m (Figure 2). The Bogong landslide of October 2022 was preceded by three years of above average rainfall induced by La Niña climate conditions. Approximately two weeks before the landslide, tension cracks were observed on a track about 90 m back from the roadway (Figure 3). Ongoing movement was observed before the landslide, which ultimately displaced approximately 30,000 m^3 of soil. Spoil and vegetation were deposited across both lanes of the road, completely blocking access between the major towns of Mount Beauty and Falls Creek and threatening Bogong Village downslope of the landslide (Figure 1). Falls Creek is an alpine resort reliant on income from tourism, particularly in winter, making the financial consequences of not opening the road before the 2023 ski season significant and demanding a rapid response.



Figure 2: Left: Road Batter in May 2017 at completion of excavation. Right: Road Batter on 8 October 2022 following landslide initiation



Figure 3: Left: Cracking observed on Spring Saddle Track, 28 September 2022. Right: Cracking observed in face of batter, 5 October 2022

The immediate response involved making the site safe and constructing a bypass road around the landslide. However, the bypass road was steep, unsealed and suitable only for four-wheel drive access. Bogong Village at the base of the landslide was evacuated and, subsequent to that, the works began to clear debris from the top of the landslide working down and clearing material that could safely be removed from the toe of the landslide using remote controlled equipment.

However, a robust interim solution was needed to provide access during the upcoming 2023 ski season and then an ongoing permanent solution required beyond that. Development of that solution required a thorough understanding of what caused the landslide and if the landslide mechanisms could act in the future and threaten access to Falls Creek. The compressed timeframe over which that understanding could be gained added to the challenge of understanding the geology, making the site safe and getting the road open.

2 EVIDENCE COLLECTED

The following evidence was collected to assist with the development of an engineering geological model of the Bogong landslide and to inform the basis of both the interim and permanent designs:

- Photographs and videos of the site, before, during and after the landslide event.
- Site observations collected by geotechnical engineers on site after the landslide event and during the initial clearance works.
- Geotechnical boreholes, including groundwater information.
- Publicly available geological and rainfall information.
- Surface survey information including both photogrammetry and LiDAR collected regularly using UAV techniques.
- Monitoring data, i.e. tilt sensors, collected continuously during clearance works.

Video and photographs taken in October 2022 on the day material reached the road indicate that material detached from the natural 40° slope upslope of benches 1 and 2. The debris travelled as a non-saturated soil (poured over like sand rather than flowed as a liquid) over the lower two benches. Based on the video and photos, slope materials did not detach from the lower two benches. However, materials may have been stripped from the benches as debris flowed over them. Seepage was not observed from the face, nor did it appear to be associated with the material detachment. Over the subsequent week further material detached from above Bench 2, causing debris to bury the lower benches and the buildup of a colluvial fan at the toe of the slope as indicated in Figure 2.

Comparison between LiDAR survey acquired before and after the landslide indicated a zone of soil depletion upslope of Bench 2 where material has detached and a zone of soil accumulation, where material has been deposited downslope of Bench 2. This is illustrated in the cross section in Figure 4. The location and geometry of the slip surface could be estimated through the survey comparison. Note that some material mobilised by the landlide was retained in the source area due to incomplete transportation to the zone of accumulation.

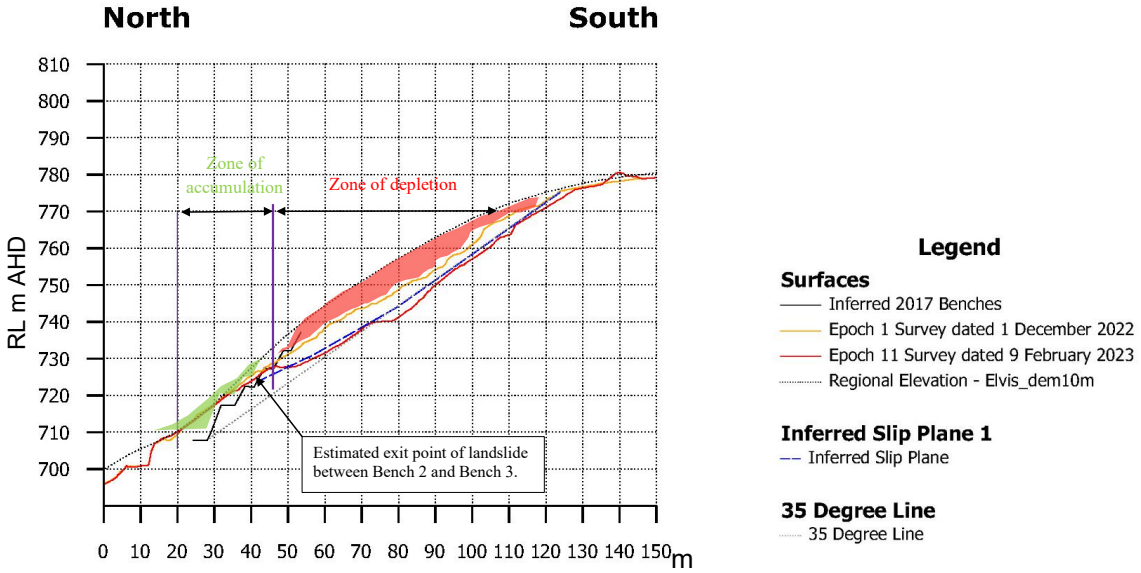


Figure 4: Indication of zones of accumulation and depletion associated with the October 2022 landslide

In early January 2023, debris clearance works sought to cut the slope bank to the landslide plane by removing the loose debris. Observations of the cleared surface indicate that the landslide plane was relatively shallow, with an angle of about 35° from the horizontal as indicated in Figure 5 and as confirmed by LiDAR and photogrammetry survey.



Figure 5: Crest of landslide, 12 January 2023 taken from Spring Saddle Track. Excavation has cut back to in situ material.

On 18 January 2023, in response to heavy rainfall (24 mm recorded at Falls Creek over the hours preceding the event), a crack opened within a batter slope about 10 m below the crest of the cutting made by the clearance works. Subsequent photogrammetry survey indicates the extent of the cracking and that it occurred on a slope of about 36° to 37° and regressed back to an angle of about 35°. Rills and gullies formed due to softening and erosion of the soils (Figure 8). Observations consistently indicated that where landsliding had occurred, it had occurred on sloping ground steeper than 35°, as measured from the horizontal and regressed back to 35°. This angle is consistent with the angle of repose for the debris at the base of the slope and suggested a friction angle within the soils of about 35° (Figure 6). The geomorphic evidence was consistent with triaxial evidence subsequently obtained.



Figure 6: Loose debris at toe of slope, 13 February 2023

Geotechnical investigations included drilling boreholes up to 40 m depth immediately upslope of the landslide headscarp and on its flanks. These boreholes did not encounter groundwater, indicating a deep groundwater table well below the landslide and suggesting that raising of the permanent groundwater table was unlikely to be a factor in the observed instability. Boreholes encountered unusually deep residual and extremely weathered micaceous granitic soils that appear to be associated with a sheared contact between two granite intrusions, consistent with geological map indications. The soils were typically partially saturated, although based on site observations, the moisture content of near surface materials respond rapidly to wetting and drying. Observations of earthworks indicated that steep batters can be cut when the material is in a partially saturated state. However, upon wetting or drying these steep batters collapse and regress. Measurements of loose, dry material in stockpiles indicated a consistent angle of repose for the material of 35°, an angle confirmed by LiDAR and photogrammetry survey.

3 POSTULATED LANDSLIDE MECHANISM

The apparent lack of free water or soil saturation associated with the landslide was a key indication that it was not triggered by the development of positive pore pressures within the slope, for example a rising groundwater table, which was confirmed through borehole groundwater measurements. Furthermore, the deep, fine-grained soils, lack of persistent structure (joints or other defects), the preceding above average rainfall and northerly aspect to the slope were assessed to be consistent with a landslide mechanism involving a loss of soil strength due to a loss of suction stresses. An engineering geological model was developed for the landslide based on a loss of suction stresses in the slope caused by increased moisture content.

In an unsaturated soil, suction stresses are induced by negative pore water pressures and strength is gained in the soil through apparent cohesion. Once the soil becomes saturated or the suction stresses are dissipated through a loss of soil structure, this gained strength or apparent cohesion is lost. Residual granitic soils exposed in slopes with a northerly or northwesterly aspect in Victoria have been recognized as prone to landslide upon saturation, Nyman (2013); Nyman et al., (2019). The relative difference between precipitation and evaporation on slopes with northerly or northwesterly aspect is greatest, which gives slopes of this aspect the potential to develop high soil suctions and suction stresses. Few landslides are observed in residual granites in Victoria during 'typical' climate conditions (neutral conditions between La Niña and El Niño events). However, based on the experience of the author's of this paper, soil wetting induced by prolonged or extreme rainfall in La Niña phases sees an increase in landslide and debris flow activity, particularly within granitic soils, which is what is inferred to have occurred at Bogong.

Similar landslide mechanisms in granitic soils been studied in locations such as Hong Kong, for example, Henscher and Lee, (2010). Figure 7 illustrates the concept of rainfall induced landslides caused by a loss of soil suction. As in this example, the 2022 Bogong landslide occurred in soils well above the water table that were not significantly influenced by positive pore water pressure. Note that no significant seepage or evidence of positive pore pressure development was observed to be associated with the Bogong landslide.

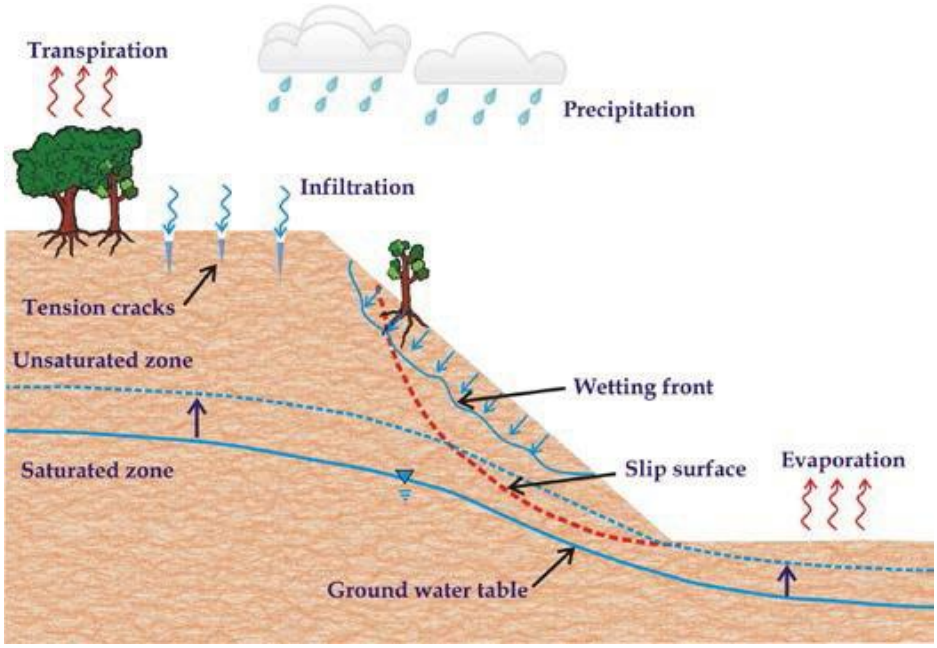


Figure 7: Concept for rainfall induced landslide in unsaturated soils, after Rahardjo et. al. (2011)

Strain in the form of tension cracks was first noticed upslope of the landslide, before there was any evidence of rupture in the face of the cutting at the toe of the landslide. It is postulated that the wetting front advanced into the slope commencing at the crest near what would become the headscarp of the landslide with the less saturated soils downslope. The tension cracks and some of the more permeable rocky strata within the slope may have been a conduit for water infiltration with the slope, effectively pushing displacement from upslope due to loss of strength in that area.

Whilst the loss of soil suction model for the landslide was consistent with observation, measuring the soil-water characteristics to help inform its geotechnical behaviour under unsaturated conditions takes a long time, with testing to derive a soil-moisture characteristic curve potentially taking months. Whilst this testing was ultimately done and used to help verify the model (see section 5), it occurred well after it was necessary to develop an interim design and get the road open. The project proceeded on the basis that the landslide mechanisms involved a loss of soil suction.

Observations and testing were undertaken to gather information on the basic geomechanical properties of the soils as follows:

- Classification testing, which indicated the material ranged span clayey sand, silty sand and sand. The proportion of fines ranged between 35% and 50% and were predominantly a low-plasticity silt. The materials are sufficiently fine grained to support high suction stresses, but permeable enough to be vulnerable to surface-water infiltration and loss of suction.
- The in situ bulk density ranged between 2.0 t/m^3 and 2.1 t/m^3, reducing to about 1.5 t/m^3 when disturbed and loose. These relatively low densities are consistent with the mica content and structured nature of the soils.
- Triaxial testing indicated an internal angle of friction consistently between 33° and 35°, consistent with the geomorphic evidence.
- Pinhole dispersion tests indicated the soils to be ‘erosion resistant’ whereas the Emerson class tests found the compacted material to be Class 5, moderately dispersive. This is consistent with the observations of gully erosion after heavy rains (Figure 8) and loss of trafficability, noting that rapid drying (within 24 hours) and return to trafficable conditions was observed.



Figure 8: Gully erosion after heavy rain, 18 January 2023

The interim design was advanced based on the assessment of soil properties set out above assuming a landslide mechanism involving a loss of soil suction.

4 BASIS OF REMEDIAL DESIGNS

Linked to the assessed landslide mechanism, the objectives of both the interim and permanent designs were to:

- Safely remove soil from and open the road, initially one lane for the interim remediation and two lanes for the permanent remediation.
- Reduce the risk to road users and residents of Bogong Village to a level tolerable by the road regulator.

- Preserve soil suctions insofar as is possible whilst also reducing reliance on suction stresses for stability.
- Given the location on the edge of Alpine National Park, preserve the natural landscape and ongoing maintenance requirements in the permanent solution by avoiding hard engineering measures wherever possible.

Estimation of the angle to which the slope should be cut back in both the interim and permanent case was undertaken using an infinite slope analysis adapted for unsaturated soil conditions after Lu and Godt (2009). This method was adopted because the sliding plane of the October 2022 landslide was roughly planar and persistent over a large area and because through approximation, this method allows consideration of suction stresses induced by unsaturated conditions without knowledge of the full soil-water characteristic curve (SWCC), noting this was not available within the short time frame over which remedial designs needed to be developed.

Lu and Godt (2008) provide a series of equations and examples for various soil types, including silty and sandy soil types similar to those underlying the site and which are prone to a loss of suction in response to wetting. These are based on the modification of a 'classic' infinite slope stability equation to consider the effects of apparent cohesion developed through soil suction stresses. This generalized infinite slope equation is noted for use in the assessment of stability within silty or sandy unsaturated soils above the water table where slope failure (factor of safety reduces below 1.0) is likely to occur in a weakened zone a few metres below the ground surface and furthermore, that failure occurs as the soil nears saturation and suction stresses approach 0.

Equation 1 is for stability analysis of unsaturated slopes as provided by Lu and Godt (2008):

$$F = \frac{\tan \emptyset\prime}{\tan \beta} + \frac{2c\prime}{\gamma H_{ss} \sin 2\beta} - \frac{\sigma^s}{\gamma H_{ss}} (\tan \beta + \cot \beta) \tan \emptyset' \quad (1)$$

Where:

- F is the factor of safety
- $\emptyset'$ is the effective friction angle in degrees (°)
- c' is the effective cohesion
- β is the slope angle in degrees (°) as measured from the horizontal
- H_{ss} is the depth to the sliding plane from the ground surface
- σ^s is the suction stress which is related to the volumetric water content
- γ is the soil unit weight

The first term in the equation relates to the internal friction or friction angle of the soils, the second to the cohesion and the third to the apparent cohesion or strength attributed to suction stresses. It was conservatively assumed there is no cohesion on the basis of the low plasticity and silty/sandy composition of the soils and based on observation that the soils are completely dry such that $\sigma^s = 0$, then a factor of safety, F of 1 is achieved when the slope angle approaches the friction angle. This is analogous to the angle of repose adopted by the landslide debris that accumulated at the toe of the slope and provides evidence in support of a friction angle of about 35° within the disturbed, loose residual soils.

LiDAR and photogrammetry survey indicated that the landslide had a depth to the sliding plane (H_{ss}) of up to about 7 m. Based on the Equation 1, and assuming no cohesion, a friction angle of 35°, a slope angle of 40° (indicated by survey and shown in Figure 4) and depth of 7 m to the failure plane, a factor of safety greater than 1 is maintained with as little as 0.25 kPa of soil suction. If the slope angle is reduced to 35°, the factor of safety with -1 kPa of suction stress is 2.0. Based on assessment using Equation 1, the effect of suction stresses on stability within these materials is significant and it is likely that prior to the landslide, the stability of the slope was dependent upon the preservation of suction stresses. Lu and Godt (2008) indicate a suction stress of -1 kPa can be achieved in unsaturated silty and fine sand materials with volumetric moisture contents as low as 10% and that with wetting, suction stress does not significantly reduce until the degree of saturation is above about 90%. Given the emergency nature of the works and in the absence of testing to assess the soil-moisture characteristics at the early stage of the project, these typical estimates were adopted to help confirm the postulated landslide mechanism. As set out in Section 5, field and laboratory testing was subsequently undertaken to test this hypothesis. The interim remedial design involved:

- Removing debris and cutting the slope back such that batter slopes were no steeper than 35°, estimated to be the maximum angle at which stability could be preserved (Factor of Safety greater than 1) if suction stresses were lost.
- Providing erosion control matting over the slope whilst in a temporary condition to reduce erosion and runoff.
- Opening of one lane of the road once the slope had been sufficiently cut back to uncover the lane in conjunction with monitoring and the implementation of a trigger/action/response plan (TARP).

The permanent design then involved:

- Providing 10 m wide benches to prevent debris reaching the road in the event there were to be instability on a batter slope. The overall slope angle was 27° and based on Equation 1 is estimated to have a factor of safety of about 1.4 under conditions where suction stresses are lost. The batter slopes themselves had a factor of safety approaching 1 under conditions where suction stresses were lost, necessitating the need to provide the benches to prevent landslides arising on the batters from reaching the road.
- Preserving the natural soil structure as far as practical. No fill was placed as part of the landslide remediation.
- Revegetating the slope using a mix of native vegetation to help preserve soil suctions.
- Proving bench drains to direct surface water off the landslide as efficiently as possible.
- Providing access tracks to help reduce surface water infiltration and to allow future slope maintenance such as clearing drains, removing debris and maintaining vegetative cover.

Images of the completed permanent works are shown in Figure 9 and Figure 10 and the designed permanent slope profile in Figure 11.



Figure 9: Far field view of remediated slope (bench 10 m wide)



Figure 10: View along completed bench (bench 10 m wide)

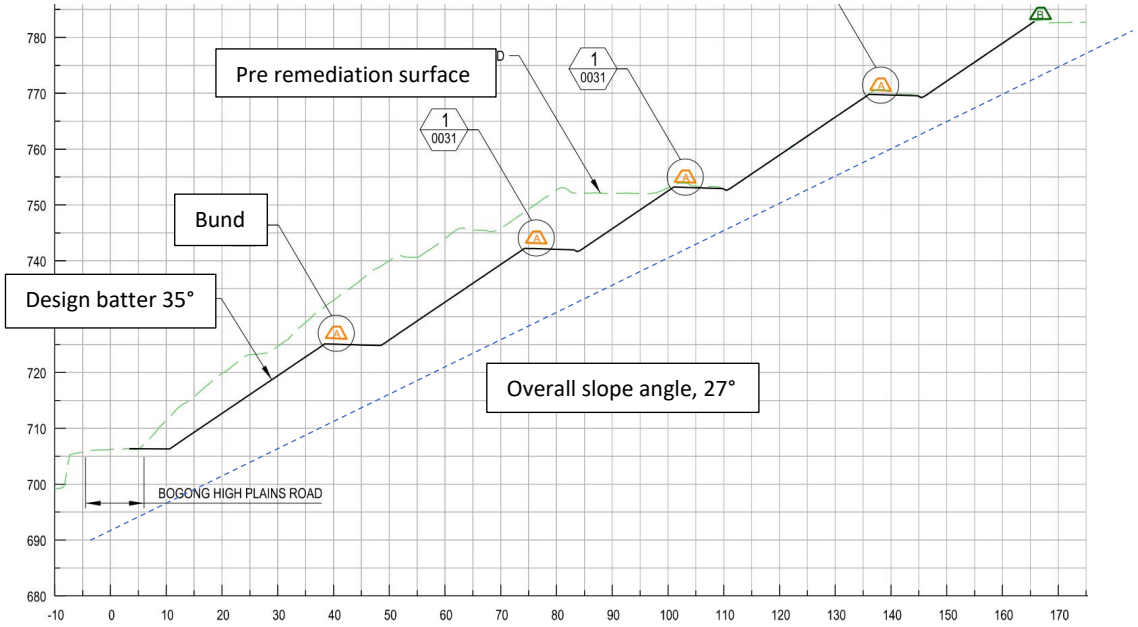


Figure 11: Typical cross section through remediated landslide (scale in m)

A risk assessment was undertaken to assess the risk to road users noting that achieving a risk level that could be tolerated by the road regulator was a requirement of the design. The key input to the risk assessment was the probability of a landslide, related in this case to the degree of saturation within the soils. Guidance was taken from literature to estimate the probability of failure for the slope within which the global factor of safety is expected to reduce to 1.4 every 50 years or so in response to wetting. Kavvadas et. al. (2009) presents a relationship between factor of safety and probability of failure for cohesive soils as indicated in Figure 12. On this diagram, V_{cu} is the coefficient of variation of c_u, (the undrained shear strength) and is a function of the certainty in that parameter calculated as the standard deviation divided by the mean for that parameter. The higher the coefficient of variation, the less certainty in the parameter and the higher the probability of failure. There was limited strength data on which to base an estimate of the coefficient of variation for the soils of the Bogong landslide. However, the observations that were undertaken, which included triaxial tests plus observations of the landslide, suggest a coefficient of variation of between 0.05 and 0.3 based on the measured friction angle and cohesion respectively. Whilst a highly uncertain estimate due to limited data, this is a low coefficient of variation, which is consistent with observations. Assuming a coefficient of variation of 0.25, a Factor of Safety of 1.4 correlates to a probability of failure of about 0.05.

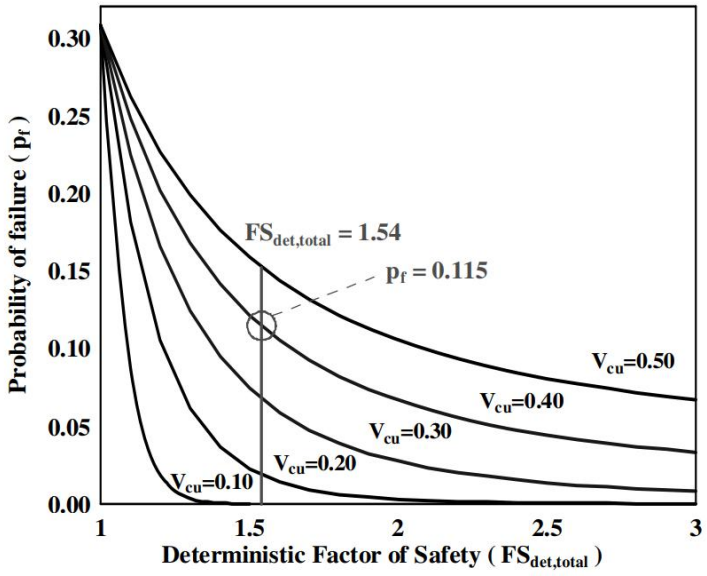


Figure 12: Extract from Kavvadas et.al. (2009) showing relationship between factor and safety and probability of failure for cohesive soil

This estimate is consistent with Read and Stacey (2009), who provide Table 1 indicating a general relationship between factor of safety and probability of failure and suggesting via interpolation a probability of failure of 5% (0.05) for a factor of safety of 1.4.

Table 1: General Relationship Between FOS and PoF, extract from Read and Stacey (2009)

Consequence of failure impacting on public safety, infrastructure, environment, land or property	Acceptable (mean) FOS	Acceptable minimum PoF
Not Serious	1.3	10%
Moderately Serious	1.6	1%
Very Serious	2.0	0.5%

Based on these indications, albeit it relatively uncertain, a probability of failure of 0.05 was assumed for global instability of the four-bench design. Assuming the probability of the slope becoming saturated is about 1 in 50 (0.02) and the probability of failure under that condition is 0.05, the probability of global failure was estimated as the product of 0.02 × 0.05 = 0.001 or 1 in 1,000. This corresponds to an 'Unlikely' probability and 'Medium' risk assuming the consequences of another similar landslide would be 'Major' when assessed using the risk matrix as shown in Figure 13 after the road regulator. This assessed risk level was sufficient to satisfy the road regulator and the road was permanently reopened back to two lanes on that basis.

Table 1: Risk estimation matrix for road geotechnical hazards.

Likelihood	Consequences				
	1 or C1 CATASTROPHIC	2 or C2 MAJOR	3 or C3 MEDIUM	4 or C4 MINOR	5 or C5 INSIGNIFICANT
A or L1 ALMOST CERTAIN	VH	VH	H	H	M
B or L2 LIKELY	VH	H	H	M	L-M
C or L3 POSSIBLE	H	M-H	M	L-M	VL-L
D or L4 UNLIKELY	M-H	M	L-M	L	VL
E or L5 RARE	M	L-M	L	VL	VL
F or L6 NOT CREDIBLE	VL	VL	VL	VL	VL

Estimated based on bulk earthworks

Target

Figure 13: Extract from VicRoads Technical Note TN-96 (Vicroads, 2022)

5 VERIFICATION OF LANSDLIDE MECHANISM

To further investigate the postulated landslide mechanism, in-situ soil moisture and soil suction sensors were installed and laboratory testing undertaken to establish a SWCC. Four soil moisture sensors and two soil suction sensors were installed between 0.5 m and 1 m depth in clayey sand material (residual granitic soil to extremely weathered granite). Sensors were installed in three auger holes (two sensors per auger hole) in remediated benches 1, 3 and 4. Auger holes were excavated using a hand auger with the moisture sensors embedded in the hole sidewalls (in-situ soil) and suction sensors placed in compacted backfill at the base of the hole. Holes were backfilled by hand with spoil at approximately 100 mm increments and tamped by hand. Laboratory testing was undertaken on a single undisturbed tube sample taken from bench 3 in similar clayey sand material (residual granitic soil).

A SWC-150 pressure plate device was used to measure volumetric water contents for matrix suction values on the drying and wetting curve of less than 1000 kPa. A WP4C water potential meter was used to measure water contents for matrix suction values on the drying curve above 1000 kPa. Figure 14 shows the SWCC developed. Testing covered suction stages ranging from 9 kPa to 316 kPa on the wetting curve and between 77 kPa and 147 MPa on the drying curve. These corresponded to a variation in volumetric water content of between 18.9% and 46.9% on the wetting curve and 3.9% and 26% on the drying curve.

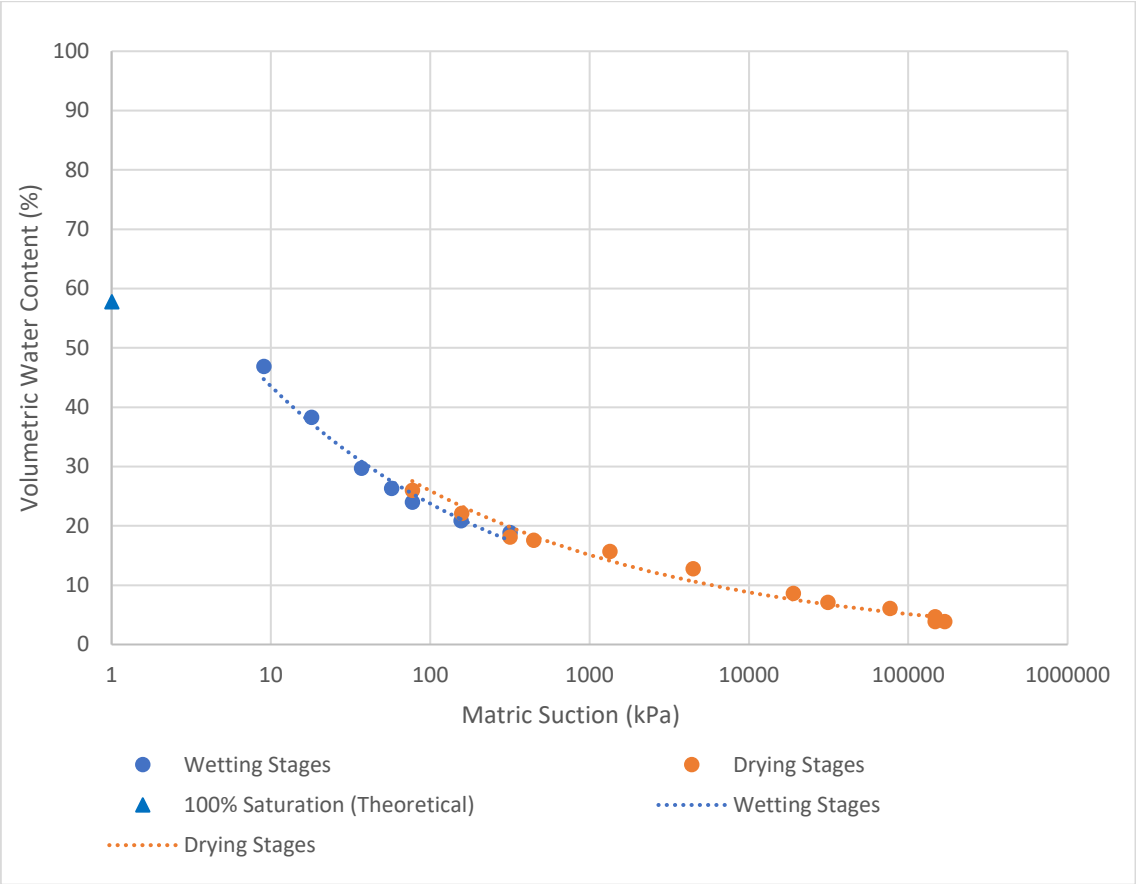


Figure 14: Soil water characteristic curve

The relationship measured between volumetric soil moisture and rainfall over a six-month period is presented in Figure 15. More than six-months of in-situ soil moisture data indicated a strong relationship between rain events and soil moisture, generally a sharp increase in soil moisture in all four sensors in response to a rain event followed by a gradual decrease in soil moisture. Smaller, but more frequent, rainfall events during September appear to correspond to a higher average soil moisture.

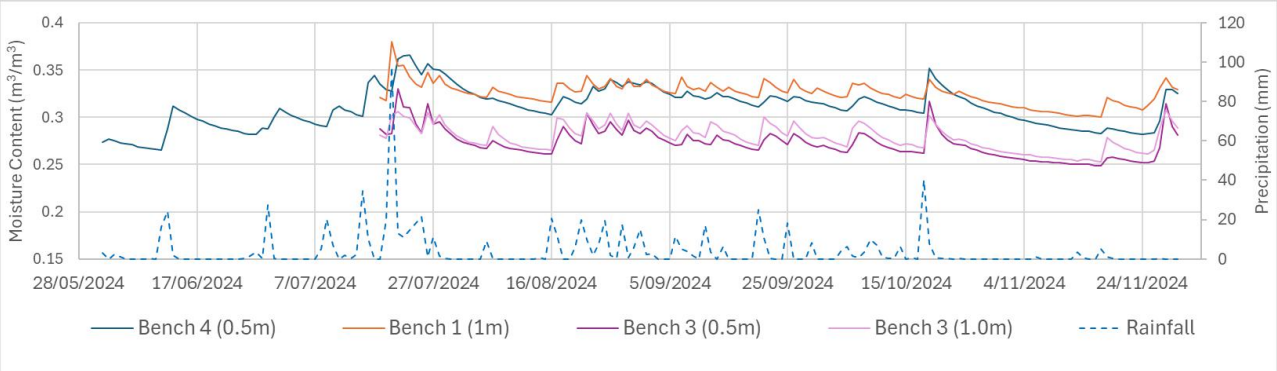


Figure 15: Measured relationship between rainfall and soil suction

The SWCC developed in Figure 14 was used to convert the in-situ volumetric soil moisture measurements into a matric soil suction. Site-measured soil moisture was between 25% and 40%, which fell between laboratory measured moisture conditions, i.e. not outside the range of available data points used to generate the SWCC. Rainfall together with the measured soil suction and corresponding soil suction developed from the measured soil moisture and SWCC is plotted in Figure 16.

The measured soil suction generally followed a similar, but inverse, pattern as the soil moisture with sharp decreases in soil suction measured following rain events followed by a gradual increase in periods of no rainfall. During winter and spring months (July to October) several instances of zero suction occurred, likely due to frequent rainfall events during this period. Compared to the measured soil suctions, the soil suctions estimated by SWCC were significantly higher, showed more variation and did not show instances of zero suction.

These differences could be due to the SWCC better estimating soil matric suction for in-situ soil compared to the disturbed soil at the base of the borehole in which the sensor was installed. Another potential cause for differences could be the differences in soil composition tested in the laboratory compared to the soil the sensors were installed in.

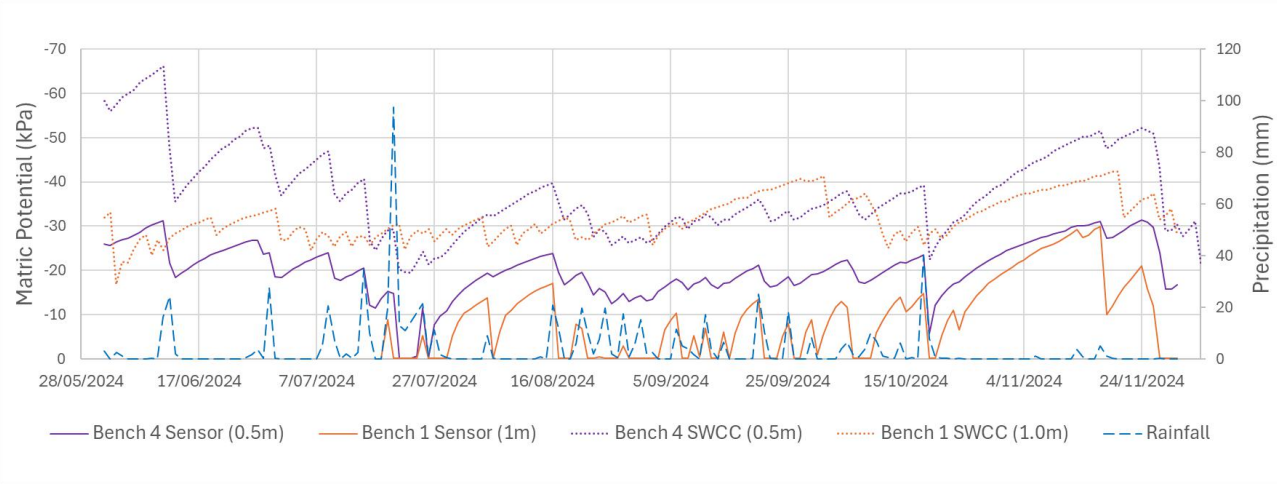


Figure 16: Relationship between rainfall, and estimated matric suction and estimated matrix suction from SWCC

The soil moisture and suction data presented in Figure 15 and Figure 16 indicate two important behaviours of the residual granitic soil consistent with the postulated landslide mechanism:

- The soil suctions are sensitive to rainfall and show seasonal change with frequent rainfall events causing a loss of suction.
- Disturbed soil appears to hold significantly less suction as implied by the differences in SWCC estimated suction and measured suctions from the sensors installed in backfilled material.

Measured soil suctions ranged between 0 kPa and -31 kPa, whereas estimated soil suctions ranged between -16 kPa and -66 kPa. This significant change in effective cohesion support the model that that the Bogong landslide could have occurred due to a general increase in soil moisture during a period of increased rainfall leading to a reduced overall matric soil suction in the slope. Furthermore, if disturbance of the in-situ soil occurred due to failure of the soil matrix, it is likely a significant amount of suction (and therefore effective cohesion) would have been lost near the zone of failure.

6 CONCLUSIONS

Understanding the landslide mechanism was crucial to the selection and design of remedial works for the Bogong landslide. Given the emergency nature of the event, that understanding had to be developed using the best evidence available at the time. Deep residual granites combined with a northerly slope aspect and the apparent lack of free water in the landslide were suggestive of a landslide mechanism involving a loss of soil suction stresses induced over a period with prolonged, above average rainfall.

Remedial solutions were developed in line with this postulated mechanism and involved cutting the slope back to an angle such that reliance on suction stresses for stability was reduced along with works to preserve suction stresses, including drainage and revegetation.

Based on the studies undertaken into the Bogong landslide, landslide mechanisms in southern Australia involving a loss of soil suction is an area for further study. It is postulated that slopes in southern Australia with a northerly aspect are more susceptible to this type of landslide mechanism because they have the greatest differential between precipitation and evapotranspiration. Deeply weathered soil profiles, such as those typical of granitic rocks, can maintain oversteep angles, including in human-made slopes such as road cuttings due to their partial saturation. Approaches to landslide mitigation measures that focus on the preservation of soil suctions in lieu of hard engineering measures should be pursued.

7 REFERENCES

Kavvadas, M., Karlaftis, M., Fortsakis, P., Stylianidi, E. (2009) Probabilistic analysis in slope stability, *Proceedings of the 17th International Conference on Soil Mechanics and Geotechnical Engineering,* pp1650 – 1653.

Lu, N., Godt, J. (2008), Infinite slope stability under steady unsaturated seepage conditions, water resources research, Vol 44 (11) W11404.

Henscher, S.R., Lee, S.G. (2010) Landslide mechanisms in Hong Kong, in *Weathering as pre-disposing factor to slope movements, Geological Society of London, Special Publication 23*. pp 77 – 103.

Nyman. P. (2013) Post-fire debris flows in southeast Australia: initiation, magnitude and landscape controls, PhD thesis, University of Melbourne.

Nyman, P, Rutherford, I.D., Lane, P.N.J., Sheridan, J.,(2019) Debris flows in southeast Australia linked to drought, wildfire and the El Nino-southern oscillation, *Journal of the Geological Society of America*, 47 (5).

Rahardjo, H., Satayanaga, A., Leong, E.C. (2011) Unsaturated soil mechanics for slope stabilisation, *Unsaturated soils: theory and practice, Jotisankasa, Sawangsuriya, Soralump and Mairaing (ed.),* Kasetsart University, Thailand. Pp.103-117

Read, J., Stacey, P., (2009) Guidelines for Open Pit Slope Design, *CSIRO Publishing*

VicRoads. (2022) Technical Note TN096, Version 3, available from https://content.vic.gov.au/sites/default/files/2024-05/Technical-Note-TN-096-Risk-Management-of-Road-Geotechnical-Hazards.pdf.

https://doi.org/10.56295/1ACEG27

LANDSLIDE VULNERABILITY: LEARNINGS FROM THE IMPACTS OF DEBRIS FLOWS ON BUILDINGS TO INFORM QUANTITATIVE LOSS OF LIFE RISK ASSESSMENTS

L. N. Agnew, R. Hayes, A. S. Miner, A. Hunter
GHD

ABSTRACT

A significant weather event in February 2023 triggered numerous landslides in the townships of Muriwai, Piha and Karekare in the Waitākere area on Auckland's West Coast. The event caused widespread damage to residential buildings and resulted in two deaths. Most landslides materialised as debris flows. Due to their high velocity and ability to travel long distances, debris flows pose a significant risk to life. Vulnerability can be described as the conditional probability of death (given a landslide impact), or as a conceptual measure of overall human susceptibility, sensitivity or proneness to landslide hazards (human vulnerability). The former is often related to the collapse of occupied buildings and thus is indirectly, a function of structural vulnerability.

This case study found the extent and nature of damage to residential buildings, and therefore vulnerability of the occupants, varied considerably. Typically, extent of damage depended on debris flow volume, and the recency of construction of the building. Building collapse due to inundation was common, however other 'atypical' instances of damage included buildings being 'rafted' downslope and the occupants escaping unharmed, trees entrained in the top of the debris penetrating the upslope side of buildings, buildings being undermined and remaining intact, and significant volumes of debris resting against the upslope wall but resulting in minimal, if any, damage. This variability indicates there can be significant uncertainty in the outcome of a landslide risk assessment, which can be difficult to quantify.

AGS (2007c) includes a table of example vulnerability values for a limited number of inundation and building damage scenarios, adapted from Finlay et al. (1999). In some instances, there are wide ranges in the data and a practitioner must use judgement to select an appropriate value. Should the building collapse, which occurred with many of the buildings impacted by landslides in Muriwai, Karekare and Piha, AGS (2007c) recommends a value of 1 (death is almost certain) be adopted. A revised and expanded set of vulnerability values adopted for the study site is presented in this paper.

Human behaviour is a key factor of human vulnerability (Pollock & Wartman, 2020) and had a large influence on the resulting number of deaths as many residences that suffered significant damage were either unoccupied or evacuated. Had this not been the case, the survivability in many properties would likely have been low. Records of human behaviour are often poorly persevered during an event (Pollock & Wartman, 2020), and it is difficult to predict the influence of human behaviour in a risk assessment. As such, human behaviour is generally ignored during the risk assessment process in favour of the worst-case scenario approach.

1 INTRODUCTION

1.1 WAITĀKERE LANDSLIDE EVENTS

Two significant weather events in January and February 2023 were the result of ex-tropical cyclone Hale and Gabrielle, respectively. As a consequence of these weather events, Auckland experienced its wettest period since records began, accumulating over 45% of its average, annual rainfall in approximately one month (Fowler, 2023). Following cyclone Gabrielle an already saturated Auckland experienced catastrophic flooding and slope instability. One of Auckland's worst affected regions was the Waitākere Ranges.

The Waitākere Ranges are a chain of hills located along Auckland's West Coast, approximately 25 km long (north to south) and approximately 25 km to the west of central Auckland. The ranges are comprised of various volcanic sequences which originate from the flanks of the Waitākere Volcano, the centre of which is located approximately 200 km offshore and is approximately 15 – 25 million years old. These sequences were uplifted approximately 3 – 5 mya and generally contain volcanoclastic conglomerates, ash and igneous intrusions (Hayward, 1979). The Waitākere Ranges are home to smaller, generally coastal, settlements in discrete locations along the length of the ranges.

As a function of the early 2023 rainfall events, resultant land instability observed in the Waitākere Ranges was generally expressed as debris flows and avalanches (which included rocks, trees, and other vegetation), and to a lesser extent rockfalls. Many of the debris avalanches became saturated debris flows as they travelled downslope. These flows resulted

in significant damage to buildings and infrastructure. Tragically, two fatalities occurred as a result of debris flow impacts on private dwellings in Muriwai. A similar storm event in Muriwai in 1965 also claimed two lives. Fortunately, early warning weather systems had predicted the February 2023 storm, which meant that many inhabitants of affected areas had evacuated their houses prior to the ensuing instability, following directions from local and regional authorities. Figure 1 presents an example of typical damage observed in the aftermath of the event.



Figure 1: Complete destruction of a dwelling in Muriwai resulting from debris flow impact.

1.2 POST-LANDSLIDE RISK ASSESSMENT PROCESS

Immediately following the landslide event, rapid building assessment of residential buildings was undertaken by Auckland Council. This system utilised a "traffic light" approach allowing Auckland Council building inspectors to classify buildings as white (unrestricted access), yellow (temporary or partially restricted access), and red (no access permitted). These rapid building assessments were intended as a preliminary assessment of risk to occupants, as a function of the buildings damage and/or its perceived risk of further damage at the time.

Following the rapid building assessments, Auckland Council commissioned GHD to undertake loss of life landslide risk assessments on more than 100 properties over a 7-month period. Properties of the worst affected Waitākere settlements of Muriwai, Piha, and Karekare were assessed as part of this work. The risk assessments were to be conducted as quantitative, loss of life assessments in accordance with the Australian Geomechanics Society, Guidelines for Landslide Risk Assessment and Management, 2007 (AGS, 2007).

1.3 VULNERABILITY TO LANDSLIDES

The term "vulnerability" as used in this paper and in the referenced literature has different contextual definitions. This paper explores vulnerability in the dual context of the following:

- Vulnerability as a "specific conditional probability" within the context of a calculation of the probability of loss of life assuming impact from a landslide, as defined by AGS (2007c), and
- Human Vulnerability to landslides when used as a measure of overall susceptibility, sensitivity or proneness to landslide hazards. In this context, human vulnerability includes overall considerations of spatial and temporal factors, the degree of injury or impact and interplay of human behaviour on the potential outcome for the possible occurrence of a hazard.

This paper intends to document observations from Waitākere following the Cyclone Gabrielle weather event and how these observations may inform both the conditional probability related to vulnerability of the occupants of effected houses and the overall concepts of human vulnerability.

2 AGS 2007 GUIDELINES FOR LANDSLIDE RISK ASSESSMENT AND THE ROLE OF VULNERABILITY AS A CONDITIONAL PROBABILITY TERM

2.1 SUMMARY OF THE GUIDELINES

The AGS 2007 Guidelines for Risk Assessment and Management are a landslide risk management (LRM) framework to assess (i.e. evaluate hazard and consequence against a tolerance criteria) and manage (i.e. mitigation, land use planning, etc.) the risk posed by landslides to properties and persons.

Risk assessments can be performed qualitatively or quantitively. Qualitative assessments are an assessment of likelihood and consequence using prescribed outcome descriptors and values that correspond to specified probability descriptors. Generally, this method is useful for assessments that require repeatability, however, they can be restrictive as the assessor is limited to the outcomes or possibilities as prescribed by the descriptors. It is generally accepted that qualitative risk assessments are not sufficient for the assessment of loss of life risk, due to the difficulties of incorporating conditional probabilities (such as spatial and temporal probability) into a likelihood and consequence matrix. As such, AGS requires that 'loss of life' risk assessments are to be estimated quantitatively.

Quantitative assessments are numerical assessments where each element of the assessment is assigned a probability between 0 (not occurring) and 1 (definitively occurring). Quantitative assessments are useful as they can be adapted for scenarios that are not specified by generic qualitative descriptors and allow for direct comparison with tolerable 'loss of life' risk criteria. However, it must be recognised that quantitative risk assessments have an inherent level of uncertainty which is not usually implicitly stated. The equation for quantitatively calculating the risk of loss of life is defined by AGS (2007) as follows.

$$\mathbf{R}_{(LoL)} = \mathbf{P}_{(H)} \times \mathbf{P}_{(S:H)} \times \mathbf{P}_{(T:S)} \times \mathbf{V}_{(D:T)}$$

Where,

$\mathbf{R}_{(LoL)}$ is the risk (annual probability of loss of life (death) of an individual).

$\mathbf{P}_{(H)}$ is the annual probability of the landslide.

$\mathbf{P}_{(S:H)}$ is the probability of spatial impact of the landslide impacting a building (location) taking into account the travel distance and travel direction given the event.

$\mathbf{P}_{(T:S)}$ is the temporal spatial probability (e.g. of the building or location being occupied by the individual) given the spatial impact and allowing for the possibility of evacuation given there is warning of the landslide occurrence.

$\mathbf{V}_{(D:T)}$ is the vulnerability of the individual (probability of loss of life of the individual given the impact).

Although it is the responsibility of the managing authority to determine what is ultimately deemed a 'tolerable risk', the AGS guidelines present suggested tolerable loss of life risks for the person most at risk (Table 1). Acceptable risks are usually considered to be one order of magnitude lower than tolerable risks.

Table 1: AGS suggested tolerable loss of life individual risk.

Situation	Suggested Tolerable Loss of Life Risk for the Person Most at Risk
Existing slope (1) / Existing Development (2)	10^{-4} / annum
New Constructed Slope (3) / New Development (4) / Existing Landslide (5)	10^{-5} / annum

2.2 VULNERABILITY TO THE INDIVIDUAL

Establishing the vulnerability to an individual can be highly subjective. This is because vulnerability is generally assessed empirically using published information or, if an event is large enough, proxies from the same event.

Vulnerability is described in the AGS guidelines as: "The degree of loss to a given element or set of elements within the area affected by the landslide hazard. It is expressed on a scale of 0 (no loss) to 1 (total loss). For property, the loss will be the value of the damage relative to the value of the property; for persons, it will be the probability that a particular life (the element at risk) will be lost, given the person(s) is affected by the landslide.". For a person, this is essentially asking: if the landslide occurs, travels in the direction of the person most at risk, reaches their location, and they are present at the time of impact, what is the probability that they will die? Collecting data with respect to the vulnerability of an individual in the aftermath of a catastrophic event is challenging, as such, vulnerability is generally expressed as a function of

structural vulnerability as this data is more readily available and measurable following an event. The influence structural vulnerability has on the vulnerability of an individual is reflected in the table of vulnerability values for various inundation and building damage scenarios as adapted by Finlay et al. (1999) presented in AGS (2007).

Table 2: Vulnerability values from Finlay et al. (1999).

Case	Range in data	Recommended value	Comments
Person in open space			
If struck by a rockfall.	0.1 – 0.7	0.5	May be injured but unlikely to cause death.
If buried by debris.	0.8 – 1.0	1.0	Death by asphyxia almost certain.
If not buried.	0.1 – 0.5	0.1	High chance of survival.
Persons in a vehicle			
If the vehicle is buried/crushed.	0.9 – 1.0	1.0	Death is almost certain.
If the vehicle is damaged only.	0 – 0.3	0.3	High chance of survival.
Person in a building			
If the building collapses.	0.9 – 1.0	1.0	Death is almost certain.
If the building is inundated with debris and the person is buried.	0.8 – 1.0	1.0	Death is highly likely.
If the debris strikes the building only.	0 – 0.1	0.05	Very high chance of survival.

3 PUBLISHED INFORMATION ON OVERALL HUMAN VULNERABILITY

3.1 DEFINING HUMAN VULNERABILITY

Human vulnerability is often discussed as the conceptual susceptibility of people to landslides and is generally considered to be a function of both structural vulnerability and human behaviour. The factors influencing human vulnerability can affect the spatial ($\mathbf{P}_{(S:H)}$) and temporal ($\mathbf{P}_{(T:S)}$) probabilities, as well as the vulnerability ($\mathbf{V}_{(D:T)}$). Discussion on structural vulnerability and human behaviour from relevant literature is presented in the following sections.

3.2 STRUCTURAL VULNERABILITY

3.2.1 Factors influencing structural vulnerability

Structural vulnerability (sometimes termed physical vulnerability) at its simplest, is a function of the construction material, type of landslide, velocity of the landslide, and impact pressure of the landslide. However, other factors such as, height of the building, size of the building, number of floors, age of the building, location of openings, and type of foundation can also impact the structural vulnerability (Papathoma-Köhle et al., 2017). Kang & Kim (2015) derives relationships for structural vulnerability from inundation depth, flow velocity and impact pressure, for both non-concrete and reinforced concrete framed buildings, presented in Figure 2.

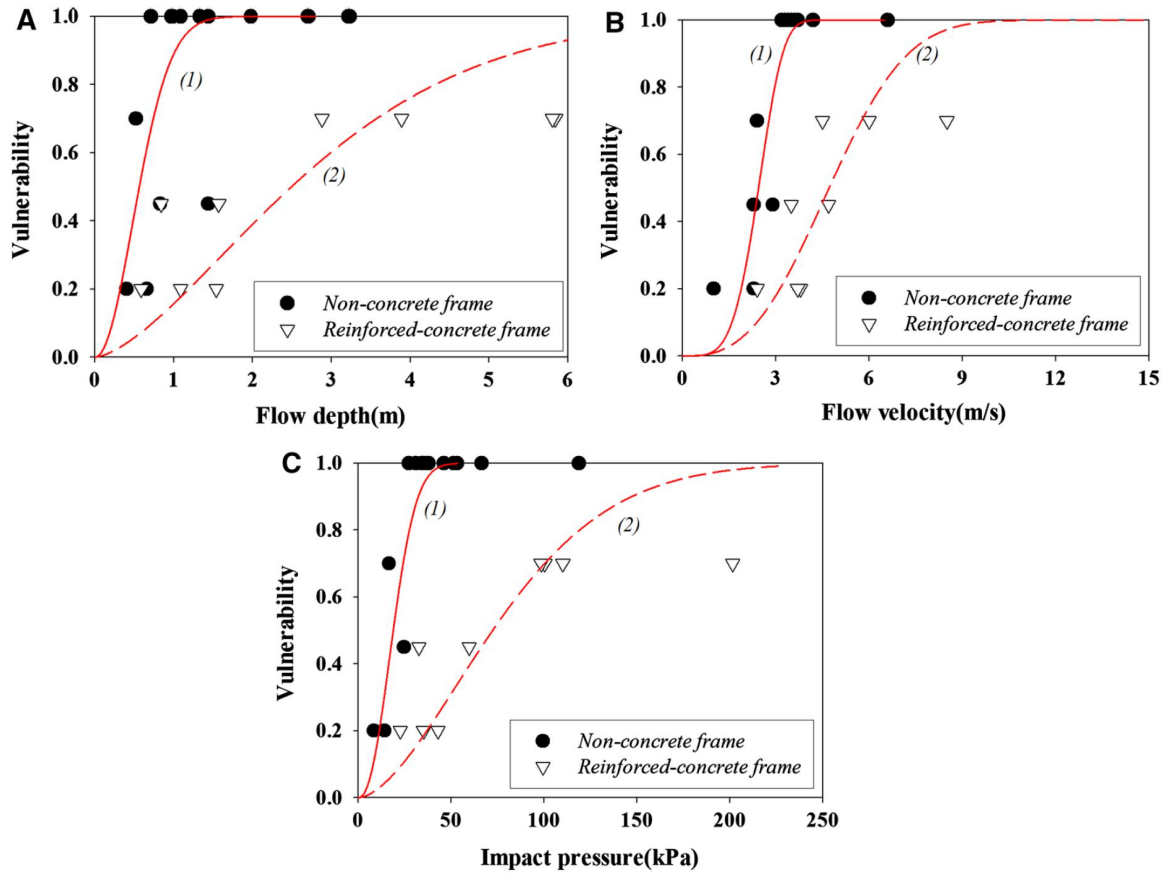


Figure 2: Graphs of vulnerability against flow depth (A), flow velocity (B), and impact pressure (C) from Kang & Kim (2015).

3.2.2 Damage of different building types

As indicated by Kang et al. (2015), timber framed buildings (non-concrete framed buildings) generally have less resistance to landslide damage resulting from debris flows or rockfalls than masonry or concrete structures. A study of debris flows in Korea by Kang and Kim (2015) indicates that for timber framed buildings, complete building collapse can be the result of debris heights between 0.97 - 3.89 m. Massey et al. (2018) determined that for timber framed buildings collapse occurred at flow depths of about 1.4 - 1.6 m. Pollock & Wartman (2020) determined that for most structures (including concrete framed buildings), inundation greater than 2.5 m resulted in complete building collapse regardless of building material type. Based on this, one could infer that inhabitants of concrete framed buildings are likely to have lower vulnerability than those living in timber or other less rigid material-type structures. However, as Pollock & Wartman (2020) points out, the structural resilience of rigid materials may be both a blessing and a curse. Although debris may exert less damage on rigid structures at low and moderate inundation depths, if the debris intrudes into the building through structurally weak areas such as windows and doors, debris may fill the building rather than exiting, thus trapping and burying the occupants. Pollock & Wartman also concluded that at inundation depths capable of collapsing buildings regardless of construction material, falling masonry or concrete slabs may be more deadly than the landslide itself.

Massey et al. (2018) collated structural damage assessments resulting from debris flows including data sets from Italy, Austria, South Korea, Hong Kong, Spain, Switzerland, and New Zealand. The resulting damage ratio to debris height graph is presented in Figure 3. Although a generally increasing trend with debris height was noted for the damage ratio, there was still much variability in the data with an instance of a 3.0 m debris height resulting in a damage ratio of 0.15, and an instance of a 1.15 m debris height resulting in a 1.0 damage ratio. This speaks to the variability of outcome when assessing a structures vulnerability, and the need to consider other factors for example, debris flow velocity and foundation type.

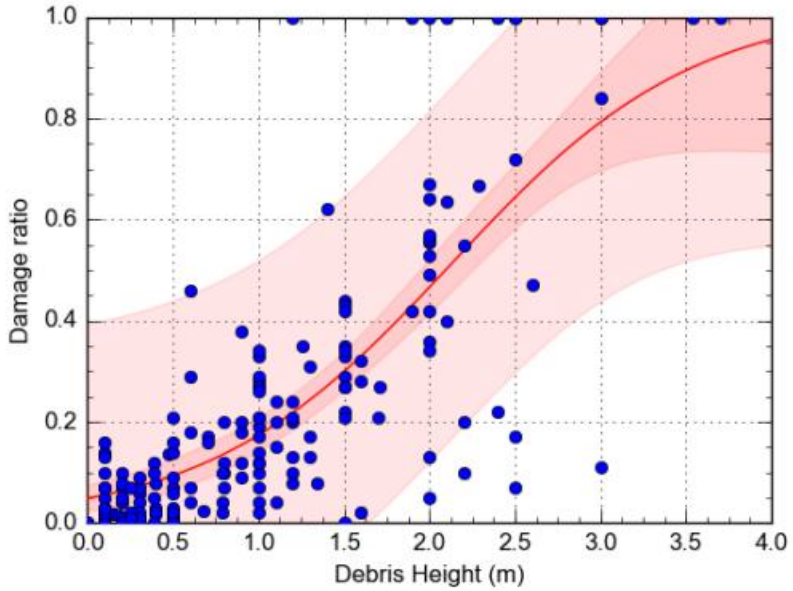


Figure 3: Damage ratio vs debris height from Massey et al. (2018).

3.3 HUMAN VULNERABILITY

3.3.1 Influence of human behaviour

While still considered to be related, the interplay between structural vulnerability and human vulnerability is generally not considered to be a direct relationship (Pollock & Wartman, 2020). This is likely due to inherent differences in coping potential between individuals and the ability of humans to act to dynamically to change their vulnerability (Crozier & Glade, 2005). The effect that dynamically reacting to a situation had on human vulnerability was investigated by Pollock & Wartman (2020). Conclusions drawn from this study indicated that awareness of an approaching threat, even if its location and nature were unknown, sharply decreased the odds of death, with those who were not aware eight times more likely to be killed. Of those who were able to identify a threat, actions taken included moving away from the perceived direction of the threat, escaping vertically to a higher floor or the top of furniture, or sheltering in a prepared refuge area in their home. Those who took no protective action were five times more likely to be killed. The survival rate of individuals on the second or third floors, including attics and roofs, was 95%, with those on the ground floor 12 times more likely to be killed.

Pollock & Wartman (2020) also documents the socioeconomic component to human vulnerability. They concluded that economically developing nations have significantly greater human vulnerability than developed nations at almost all inundation depths. In their study individuals in developing nations had six times the likelihood of death of those in developed nations.

3.3.2 Building inundation and occupant causes of death

Pollock & Wartman (2020) indicates that there is a mild correlation between human vulnerability and inundation depth. Additionally, they go on to state that the greatest increase in probability of death is observed between 0 and 2 m, although no fatalities are recorded below inundation depths of 0.8 m, likely due to the intrusion of debris into buildings through structural weak points such as windows, commonly set at heights of ~1 m, after which debris may overwhelm and bury occupants (Massey et al., 2018; Totschnig et al., 2011). Despite this, the maximum building inundation depth survived by an individual in the study was 9.6 m, the victim survived with severe injuries. Given this, Pollock & Wartman concluded that at intermediate inundation depths, human behaviour is the most significant factor in landslide mortality. The main causes of death from landslide impacts are traumatic injury and asphyxiation generally as a result of burial or physical impacts from the landslide or building (Pollock & Wartman, 2020; Massey et al., 2018).

4 OBSERVATIONS OF BUILDING DAMAGE IN THE WAITĀKERE LANDSLIDE EVENTS

4.1 INUNDATION FROM DEBRIS FLOWS

The settlements of Muriwai, Piha, and Karekare were initially established prior to 1940 with residential development becoming more widespread through the mid to late 1900s. New Zealand's building code came into effect in 1992 after the passing of the Building Act in 1991 which was repealed and replaced in 2004. Many dwellings constructed before the introduction of the Building Act and Code still exist today. The majority of dwellings constructed before the year 2000 are timber framed with light weight cladding, whereas in recent years concrete has become an increasingly favoured building material. This difference in age of the dwelling and material type produces a stark contrast in the ability of a dwelling to withstand the effects of inundation.

Observations of many dwellings effected by landslides indicated that generally, debris flow heights of between 0.5 – 1.0 m resulted in the collapse of buildings. However, some atypical instances of inundation were also observed. These included recently constructed (concrete framed) buildings that were able to withstand larger volumes of inundation (>5 m), including large volumes of debris resting against the upslope side of dwellings resulting in minimal damage (Figure 4). In these cases, while the dwellings remained mostly intact, debris often entered the dwellings through weak points such as windows and doors. Figure 5A presents an example of this where the same dwelling is encased in debris (visible through window in background of photo) and the debris has penetrated an upslope widow, depositing material in the living room.

Other examples of inundation not resulting in complete building collapse included dwellings where landslide debris (greater than 0.5 m in height) had entered a portion of the dwelling or had displaced a dwelling from its original location. The example presented in Figure 5B is a scenario where debris greater than 1.0 m in height, has entered the dwelling and the dwelling has not collapsed. This image highlights the variability in an individual's spatial probability ($\mathbf{P}_{(S:H)}$). If the occupant of the dwelling is in the kitchen (background of the photograph engulfed in debris) during the landslide event their spatial probability would almost certainly be 1.0, as they would be expected to be engulfed in the debris, likely resulting in a vulnerability ($\mathbf{V}_{(D:T)}$) of 1 also. However, if the occupant of the dwelling is in the living room (foreground of the photograph) at the time of the landslide event, their spatial probability might instead be somewhere between 0 – 0.5, given that they might only be slightly impacted by debris or not at all, likely resulting in a much lower or non-existent vulnerability. Additionally, the same is true in Figure 5A, considering a person sitting on the couch by the window adjacent to the debris would have a different vulnerability than a person sitting on a couch on the other side of the room.

Other atypical instances of inundation included dwellings being "rafted" downslope by multiple to tens of meters, and the dwellings remaining relatively intact (Figure 6A). Residents of Karekare confirmed that there was at least 1 instance of people occupying their house during the events, which was then picked up and "rafted" downslope by approximately 20 m. Once the dwelling came to rest it was mostly intact and the occupants were able to escape the dwelling physically unharmed. Figure 6B illustrates an example of a dwelling which has been rafted downslope by more than 10 m, and in doing so completely destroyed the lower-level, while the upper-level remains almost completely intact. In this example, the vulnerability of a person occupying the lower-level would likely be between 0.8 – 1.0, whereas a person who is occupying the upper-level is likely to have a significantly lower vulnerability of about 0.05 given the upper-level remained largely intact.

4.2 THE EFFECTS OF VEGETATION

Many of the slopes which failed during the events comprised a significant amount of vegetation. Vegetation type varied from small, dense shrubs to large, well established pine trees. While vegetation can have a stabilising effect on slopes, it was observed that this stabilising force was overcome by the force of the debris flow, resulting in vegetation becoming entrained within the debris, ultimately increasing the overall debris flow volume. The different effects vegetation had on dwellings within the project site included:

- Trees, shrubs and other vegetation becoming entrained within the landslide debris, subsequently increasing the volume of the debris impacting dwellings,
- Tall trees (in this case mainly pines) being carried downslope and penetrating the upslope side and roofs of dwellings (Figure 7).

4.3 THE IMPACTS OF ROCKFALL

Although rockfall hazards can pose a significant risk to dwelling occupants, there were limited instances of rockfall impacting dwellings during or following the landslide event. Given the geology of the area (volcanoclastic conglomerates, ash, and intrusions) headscarps formed by the landslides often exposed profiles of residual soil (which commonly included

core stones) and weathered rock. Additionally, colluvium hung up on the slopes following the event usually contained large core stones. As a result of ongoing weathering and degradation of these exposed profiles and colluvium, the release of rocks from the failure areas resulted in rockfalls impacting close to dwellings. There were no observed instances of rockfalls causing death, injury or significant building damage.

4.4 UNDERMINING SCENARIOS

The regression of landslides below building platforms and building foundations was also observed. Damage from the undermining of a building varied and was ultimately dependant on how close to the building the landslide regressed, and the foundation system and material type of the building. Generally, flexible structures (such as light weight timber framed buildings) were able to withstand a significant agree of undermining, on the order of 3+ m (Figure 8), whereas rigid concrete framed structures were more susceptible to damage from undermining. However, quantifying the amount of undermining required to cause collapse proved difficult as no examples of complete building collapse resulting from undermining was observed. Given this, it was assessed that survivability is likely to be relatively high in an undermining scenario where the building does not completely collapse.

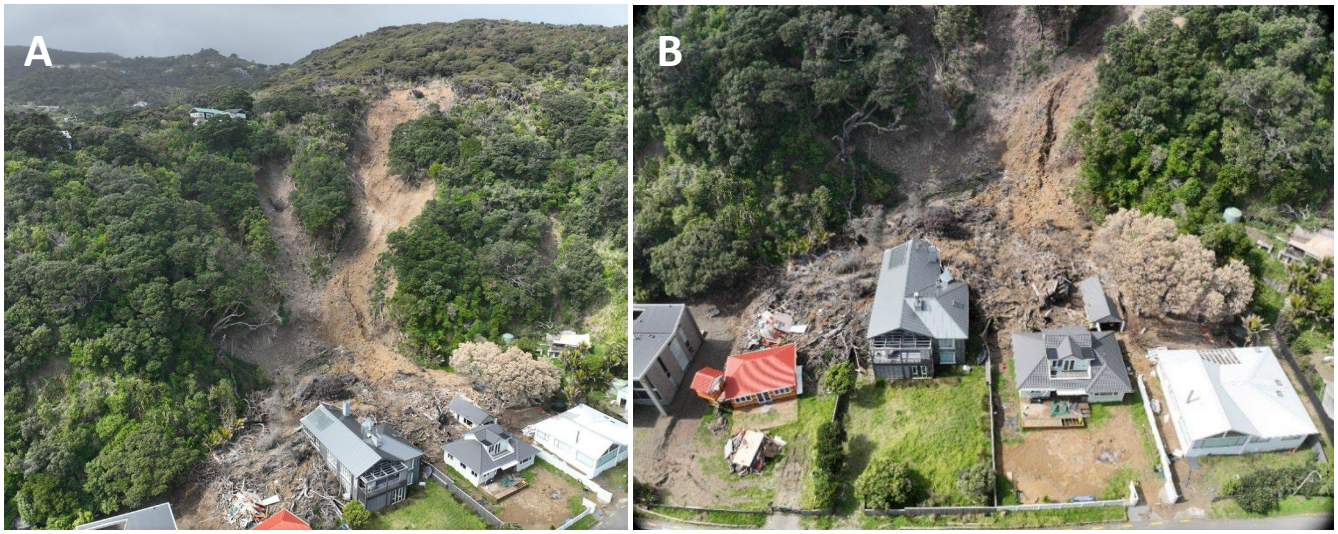


Figure 4: (A) Aerial photograph of a landslide and debris flow that has impacted several houses. Debris height is approximately 5-6 m behind the middle house. (B) Aerial photograph of dwellings affected by a large debris flow, showing older (pre-1970s construction) red, left house moved completely off foundations and grey middle house (post 2000s construction) remains in place.



Figure 5: (A) Landslide debris entering into the living room of dwelling by penetrating windows and wall. Dwelling is encased in debris as evidenced by debris visible through window in background. (B) Photograph of the inside of a dwelling which landslide debris has entered. In the background of the image, covered in debris, is the kitchen, the foreground contains the living room.



Figure 6: (A) Dwellings which have been rafted downslope from their original locations remaining relatively intact. (B) Photograph of a dwelling which has been rafted and toppled over by a landslide, with lower-level of the dwelling completely destroyed, while the upper-level remains mostly intact.



Figure 7: Photographs of a dwelling which has been impaled by a tall pine tree. Both photos are of the same dwelling taken at ground level and from the headscarp, respectively.



Figure 8: Photograph of a landslide undermining a timber framed dwelling. Leading edge of the dwelling is undermined by approximately 3 m.

5 DISCUSSION

5.1 OBSERVATIONS FROM WAITAKERE

5.1.1 Vulnerability as a conditional probability

The guidance presented in AGS (2007) for assessing the conditional probability term, vulnerability is limited and the adapted table from Finaly et al. (1999) presents vulnerability values for a limited range of scenarios. AGS (2007) also only provides guidance for vulnerability resulting from inundation, which is generally associated with debris flows. Other landslide mechanisms, such as rockfall or undermining from landslide regression, are either generic or not explicitly catered for. As such, adapted table(s) of vulnerability values incorporating available data, expert judgement and site-specific information are required to adequately cater for the observed instances of damage.

Given the large volume of properties requiring rapid risk assessments, a standardised approach to assessing the loss of life risk was created out of necessity. This involved standardising the assessment of vulnerability. As discussed above, the adapted table of vulnerability values presented in AGS (2007c), adapted by Finaly et al. (1999), did not adequately cater to the building damage scenarios observed in the field. Therefore, further adaptations of the table included combining it with information from the TfNSW Guide to Slope Risk Analysis (RMS, 2014) as well as observations of damage to buildings and structures resulting from the landslides in Muriwai, Piha, and Karekare. The table is presented as Table 3.

Published vulnerability data for rockfall events in New Zealand was poorly known at the time. Given this, and the fact that there were no observed instances of rockfall causing death, injury or damage to buildings, vulnerability values related to rockfall have not been included.

Table 3: Expanded set of vulnerability values for inundation and undermining scenarios.

Case	Range	Typical value used for Waitakere Assessments	Comments
Person in a building that collapses under impact from debris flow	0.8 -1.0	0.9	Death is almost certain. Evacuation unlikely to occur
If building is inundated with debris and the person is buried	0.8 -1.0	0.8	Very high potential for death Evacuation unlikely to occur
If building is inundated with debris but no collapse occurs and the person is not buried	0.01 -0.1	0.1	High chance of survival Evacuation unlikely to occur
If the debris strikes the building only	0.001-0.05	0.01	Very high chance of survival
If failure occurs below the building and results in significant collapse	0.5-0.8	0.6	Moderate to high potential for death. No forewarning signs with evacuation unlikely to occur.
If failure occurs below the building and results in partial collapse	0.01 -0.1	0.05	High chance of survival. Signs of building distress should provide occupants with opportunity to take evasive action.
If failure occurs below the building and results in damage. No collapse occurs.	0.001-0.05	0.005	Very high chance of survival. Evacuation almost certain.

5.1.2 Human vulnerability

More recently published human vulnerability data is limited and biased towards human vulnerability as a function of structural vulnerability, given that human behaviour in an event is difficult to predict and measure. From the published literature it is clear that structural vulnerability varies considerably for each building and each scenario as each study presented in Section 3 concluded different debris heights resulted in complete building collapse. This misalignment is likely due to the variability in different material types, foundation types, building openings, building age, landslide

volume, landslide speed and energy, etc. This uncertainty inherently requires an applied level of judgement and caution when applying these results to a given vulnerability assessment.

Pollock & Wartman (2020) indicates that human behaviour (including the ability to dynamically react to a situation, awareness of an approaching threat, emergency preparedness, level of education on potential hazards, etc.) is a key factor in human vulnerability and notes that this information is usually poorly preserved in the aftermath of an event. This was true of Waitākere. While evacuations were undertaken by local and regional authorities some residents chose to stay. Of those who stayed, it is not known which houses were occupied at the time of the event, or the preparedness of residents or their level of education and understanding around the potential hazards. Had it not been for these evacuations, however, it is almost certain that many more people would have lost their lives. Consequently, as there were minimal casualties for an event of this scale, estimating the vulnerability (both human vulnerability and the conditional probability) for the many atypical cases becomes difficult as there are few examples to compare to, which results in the application of judgement and inherent uncertainty.

Observations of building damage from Waitākere generally agree with Kang & Kim (2015) that as debris heights approach 1 m, the possibility that a dwelling will collapse is very high. However, many atypical examples of inundation that contradict this observation were observed, including instances of about 5 m of debris flow height resulting in minimal building damage, buildings "rafting" downslope with debris, and bottom floors of buildings being destroyed but upper floors remaining intact. Additionally, human vulnerability can vary spatially when considering internal building inundation scenarios. Furthermore, quantifying the impact that entrained vegetation has on landslide debris volume and structural vulnerability (and therefore vulnerability) is difficult, given the inherent variability in cover, type and outcome.

5.2 UNCERTAINTY IN EVALUATING VULNERABILITY

A key conclusion from the review of published literature and observations from the Waitākere landslide events is that there is a significant amount of uncertainty in predicting the outcome as it relates to human vulnerability to a given landslide. This is primarily due to the range of available outcomes for any single event, outcomes which rely heavily on many contributing factors, and/or factors that are difficult to quantify. For example, it is difficult to predict if a building experiencing "total" inundation will be picked up and "rafted" downslope, or if the building is completely destroyed, and if this impact on the building will result in a person's death. The same is true for most hazards presented by landslides (e.g. internal building inundation, undermining of buildings, impacting rockfalls, etc.). There is a degree of 'randomness' generated by catastrophic events, which results in uncertainties that are difficult to quantify. This randomness and uncertainty often requires practitioners to adopt a precautionary approach, often resulting in the assessment of a worst-case scenario, which assumes the person is in the wrong place at the wrong time. This essentially eliminates human behaviour which, as highlighted by Pollock & Wartman (2020), is a key factor in human vulnerability.

The main method for evaluating both human vulnerability and adopting a specific conditional probability value for vulnerability is having proxies on which to draw upon, however, this is made difficult by limited published information. Estimating human vulnerability for larger scale events is in many respects easier because the damage scenarios can be more certain, given can be more site-specific data to draw from. However, for smaller scale events evaluating vulnerability can be difficult due to variability in building construction and limited proxies. Furthermore, given that human vulnerability is often a function of structural vulnerability, and geotechnical practitioners are not structural engineers, probability estimates rely on a significant amount of professional judgement and experience. Thus, for smaller scale landslide events, uncertainty in the vulnerability value is likely to be much greater and consistency between practitioners is likely to be variable.

Uncertainties related to the element at risk also impact the assessment of vulnerability. Generally, the element at risk is considered to be the occupant with the highest exposure to the hazard (i.e. the person with the highest temporal probability). The two people who tragically lost their lives during the event were inside a dwelling in Muriwai after it was inundated by a debris flow. The dwelling subsequently collapsed killing both inside. However, these two people were not regular occupants of that dwelling, rather they were volunteer firefighters who had intervened to remove the occupants from this dwelling, after an initial debris flow impacted the dwelling but didn't completely destroy it. In other words, they were people with a low temporal probability.

6 CONCLUSION

- The term vulnerability needs to be understood in terms of the context that it is being used. As discussed, it can relate to a specific conditional probability used in the calculation of loss of life or as an overall human susceptibility to landslide hazards.
- Conditional probability values of vulnerability presented in AGS (2007) have limited scenarios and broad ranges in the data.

- Additional recommendations based on observations from the Waitakere landslide event have been included to provide a broader range of possibilities associated with similar events.
- The concept of overall human vulnerability must take into account consideration of human behaviour aspects impacting spatial and temporal probabilities.
- The performance of various types of buildings against various types of inundation scenarios is well documented in published literature. However, there is much variability in the published results likely due to nuances in building design. As such, proxies using published information should be selected carefully.
- Structural vulnerability as a result of undermining of buildings and rockfall is not well documented in published literature.
- For many landslide hazards, human behaviour is the leading factor in determining human vulnerability. Evacuations in Waitākere likely saved many lives. However, behavioural information is often poorly preserved in the aftermath of a catastrophic event. Additionally, human behaviour can include intangibles that are difficult to measure, such as an individual's level of education, preparedness, and awareness of an approaching hazard.
- Estimating both overall and specific aspects of vulnerability is an uncertain process given the many different contributing factors and given the lack of available behavioural information, which inform all the possible outcomes. This uncertainty in outcome generally forces practitioners to adopt a conservative, worst-case scenario approach, assuming a person is in the wrong place at the wrong time, which removes the behavioural aspect entirely.

7 REFERENCES

Australian Geomechanics Society (AGS), (2007). *Landslide Risk Management*. Journal and News of the Australian Geomechanics Society. 42(1).

Crozier, M.J. and Glade, T., (2005). *Landslide hazard and risk: issues, concepts and approach*. Landslide hazard and risk, Landslide Hazard and Risk. 1, 1–40).

Finlay, P.J, Mostyn, G.R, Fell, R. (1999). *Landslides: Prediction of Travel Distance and Guidelines for Vulnerability of Persons. Proc* 8th. Australia New Zealand Conference on Geomechanics, Hobart. Australian Geomechanics Society, ISBN 1 86445 0029, 1, 105-113.

Fowler, A.M., (2023). *Auckland deluge 2023: A historical perspective.* Journal of Hydrology (New Zealand), 62(1), 35-52.

Hayward, B.W. (1979). *Eruptive history of the early to mid miocene Waitākere volcanic arc, and palaeogeography of the Waitemata Basin, Northern New Zealand*. Journal of the Royal Society of New Zealand. 9(3), 297–320.

Kang, H.S. and Kim, Y.T., (2015). *The physical vulnerability of different types of building structure to debris flow events*. Natural Hazards, 80, 1475-1493.

Kang, H.S., Pradhan, A.M.S. and Kim, Y.T., (2015). *Physical Vulnerability Characteristics of Buildings by Numerical Simulation of Debris Flow*. In The 2015 World Congress on Advances in Structural Engineering and Mechanics (ASEM15), Incheon, Korea. 41.

Massey C.I., Thomas K.-L., King A.B., Singeisen C., Horspool N.A. and Taig T., (2018). *SLIDE (Wellington): vulnerability of dwellings to landslides* (Project No. 16/SP740). Lower Hutt (NZ): GNS Science. 76 (GNS Science report; 2018/27). doi:10.21420/10.21420/G2DD2Q.

Road and Maritime Services (RMS) (2014). *RMS Guide to Slope Risk Analysis.* Version 4. Transport for New South Wales Document ILC-AM-TP1-601-G01. New South Wales Government.140

Papathoma-Köhle, M., Gems, B., Sturm, M. and Fuchs, S., (2017). *Matrices, curves and indicators: A review of approaches to assess physical vulnerability to debris flows.* Earth-Science Reviews, 171, 272-288.

Pollock, W. and Wartman, J., (2020). *Human vulnerability to landslides*. GeoHealth, 4(10), p.e2020GH000287.

Totschnig, R., Sedlacek, W., & Fuchs, S. (2011). *A Quantitative Vulnerability Function for Fluvial Sediment Transport*. Natural Hazards, 58(2), 681–703.

https://doi.org/10.56295/1ACEG28

EFFECT OF DISCONTINUITIES ON THE SURVIVAL PROBABILITY OF SPHERICAL BLOCKS UPON IMPACT

Davide Ettore Guccione[1], Maddalena Marchelli[2], Oliver Buzzi[1], Anna Giacomini[1]
[1]*Centre for Geotechnical Science and Engineering, The University of Newcastle, Callaghan, NSW 2308, Australia*

[2]*Department of Environment, Land and Infrastructure Engineering (DIATI)- Politecnico di Torino, C.so Duca degli Abruzzi 24, I–10129 Torino, Italy*

ABSTRACT

The fragmentation of rocks upon impact is a complex and not well-understood phenomenon. To model this fragmentation accurately, the first question to address is whether a falling block will fragment upon impact. This can be determined if the survival probability of the rock, i.e. the probability that the rock block does not fragment, is known. However, predicting this probability is challenging, as no existing model or method can accurately forecast the survival probability of natural rocks. Recently, the authors have developed a model that can predict the survival probability of brittle rocks under collinear impact, building on a preliminary breakthrough for brittle spheres. However, natural blocks may contain discontinuities, which can increase the probability of fragmentation occurring not only due to breakage but also due to the disaggregation of the rocks along these discontinuities. The present work introduces an experimental campaign in which fully persistent and filled discontinuities were inserted into mortar spheres. The angle of the discontinuities with respect to the impact surface, as well as the impact velocity, was varied to obtain an experimental survival probability for blocks with discontinuities. The results were compared with the survival probability of intact blocks, showing how the discontinuities significantly reduce the range of energy required to break the spherical block.

1 INTRODUCTION

Rockfalls are particularly dangerous among landslide hazards, posing risks to people, structures, and infrastructure Understanding and predicting these events is crucial for effective risk management. Forecasting block trajectories and their kinematic parameters is essential for implementing mitigation measures (Volkwein et al., 2011). Rockfall events often involve fragmentation, where rock blocks break into pieces or disaggregate along fractures (Corominas et al., 2017). Despite its prevalence, the fragmentation process in rockfalls is not fully understood. Studies have shown that factors like block shape, impact angle, discontinuities, impact velocity, and soil characteristics influence fragmentation patterns (Giacomini et al., 2008; Wang and Tonon, 2011). While existing models provide insights, a universal fragmentation model and comprehensive predictive trajectory model are still lacking. Current models require site-specific parameters and handle post-impact kinematics stochastically, highlighting gaps in knowledge and the need for further research (Marchelli and De Biagi, 2019; Matas et al., 2020; Lanfranconi et al., 2024).

Guccione et al. (2021a) proposed a model that can predict the fragmentation survival probability (SP) of brittle homogeneous spheres upon impact from the input parameters of both block and slope material resulting from statistical analysis of Brazilian test and unconfined compressive tests. However, this prediction model is not valid if the sphere contains defects or, more specifically, preexisting discontinuities. In this paper, an extensive campaign of drop tests on artificial rocks of simple shape (spheres) with discontinuities is presented to investigate the experimental survival probability of these specimens and compare it with the prediction model of homogeneous spheres.

2 EXPERIMENTAL METHODS

For this study, two types of sphere specimens with discontinuities were made: containing 1 discontinuity (1Dsc) (Figure 1a) or 3 discontinuities (3Dsc) (Figure 1b). The spheres were cast in 3Dsc-printed moulds (Figure 1c) and glued together to create discontinuities. A total of 182 and 202, 1Dsc and 3Dsc specimens were created, respectively. Both the matrix (sphere) and discontinuity were made using mortar of different mass proportions. The mortar for the matrix is made of silica sand, Portland cement, hydrated lime, and water (3:1:0.25:1 by mass), and included a cement accelerant (2% by weight of cement weight) for faster curing. Material characterization tests (Brazilian tests (BT), unconfined compressive tests (UCS), and toughness tests) following ISRM standards were conducted for each batch. To simulate rock discontinuities, a weaker mortar type (3.5:0.8:1:1.2 by mass) was used. All specimens were cured for 2 weeks in a humid environment and 4 weeks in an oven at 40°C before testing. The mass of the specimen is about 1kg. Results of material characterization of both materials are reported in Table 1.

The two series of drop tests (1Dsc and 3Dsc) were performed using a specifically designed setup to study the fragmentation of blocks upon impact, developed by Guccione et al. (2021b). The setup allows the release of the blocks (in freefall) from height up to 5.1 m (equivalent impact velocity of 10 m/s). The impacted material is an instrumented concrete slab to simulate an impact against hard rock. More details about the setup as well as the characteristics of the slab can be found in Guccione et al. (2021b). Four impact velocities were used: 4, 5, 6, and 7 m/s for 1Dsc and 1.5, 3, 4 and 5 m/s for 3Dsc. Different orientations (θ) of the discontinuities with respect to the impacted surface (slab) were considered (Figure 1c). The "impact position" θ were grouped into 9 categories (one every 10°): 0-10°, 11-20°, 21-30°, 31-40°, 41-50°, 51-60°, 61-70°, 71-80°, and 81-90°. To ensure a good representation of all possible θ, at least 5 drop tests were conducted for each category, with a total number of tests for each impact velocity equal to 50. The exception was for 4 m/s of 1Dsc where, due to a manufacturing issue, only 25 samples were used. Note that the spheres were dropped without rotation. The SP is obtained from the following equation:

$$SP = \left(1 - \frac{N_f}{N}\right) \cdot 100 \quad \textbf{(1)}$$

where N is the total number of drop tests and N_f represents the number of tests that result in fragmentation (or desegregation). The SP can be described in terms of either impact velocity or impact kinetic energy. The impact velocity (or impact kinetic energy) at which there is a 37% probability of survival is referred to as the critical impact velocity (v_{crit}) (or critical kinetic energy). According to experimental evidence provided by the authors, the survival probability of brittle spheres in drop tests can be approximated as a linear function (Guccione et al. 2021a).

Table 1: Material characterization of the matrix and discontinuity material.

Parameter	Unit	Matrix	Discontinuity
Unconfinement Compression Strength (from UCS) σ_y	MPa	16.69	8.51
Secant Young Modulus (from UCS) Y_b^s	MPa	2021*	1316
Tangent Young Modulus (from UCS) Y_b^t	MPa	3385	2082
Poisson ratio (from UCS) ν_b **	-	0.20*	0.20
Diameter of specimen used for BT d	m	0.053*	0.053
Height of specimen used for BT h	m	0.029*	0.029
Tensile Strength (from BT)	MPa	2.11	1.05
Critical Force (from BT) F_{BT}^{cr}	N	5398*	2801
Weibull shape F factor (from BT) m_{BT-F}	-	7.29*	5.19
Critical Work (from BT) W_{BT}^{cr}	J	1.372*	0.707
Weibull shape W factor (from BT) m_{BT-W}	-	3.75*	4.02
Mode I fracture toughness (from toughness tests) K_{Ic}	MPa ·m$^{1/2}$	0.350	0.181

* Impact for prediction model of SP for homogeneous sphere (Guccione et al. 2021a).
** assumed.

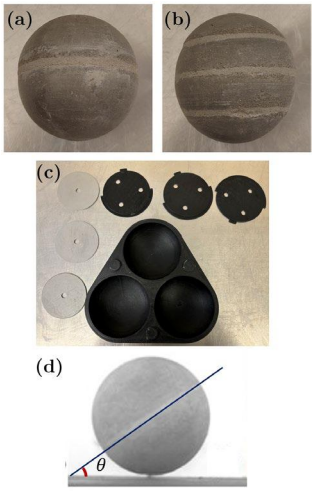


Figure 1: (a) Sphere with 1Dsc; (b) Sphere with 3Dsc. (c) Moulds used to cast the spheres. (d) Angle between discontinuity in impacting surface

3 RESULTS

Figure 2 reports the experimental SP (expressed in terms of impact velocity) for both 1Dsc and 3Dsc. Each point represents at least 50 tests, with the exception of impact velocity 4 m/s where only 25 drop tests were performed. The Linear interpolation of the experimental data for both series of drop tests is also shown in the figure. The experimental SPs are compared in the same figure with the predicted SP of homogeneous spheres of the same diameter (100 mm). Note that the input parameters of the block material for the predicted SP are reported in Table 1. For conciseness, the input parameters of the slope (concrete slab here) are not reported here but it can be found in Guccione et al. (2021a).

By comparing the three SPs, it is clear how the presence of preexisting defects (1Dsc) and the number of these defects (1Dsc vs 3Dsc) on the block influence the probability of fragmentation occurring. Clearly, less kinetic energy is required to observe fragmentation of blocks with discontinuities (compared to a block of the same dimension but without defects). The v_{crit} are 6.0 m/s and 3.7 m/s for 1Dsc and 3Dsc, respectively. These are about 20% and 50% less than that of the homogeneous blocks (7.3 m/s). The fragmentation (both for breakage of the intact material or disaggregation along the discontinuities) of blocks with 3D can start being observed at an impact velocity > 0.2 m/s (SP = 100%), particularly for θ > 45°. This is more than 95% less than the value for 1Dsc (2.0 m/s) or homogeneous blocks (5.6 m/s). Finally, it is interesting to note that the two experimental SPs look parallel. This is probably due to similar characteristics (in strength)

of the discontinuities. The shift of the SP is given by the fact that 3Dsc has more defects compared to 1Dsc, therefore it is more likely to break compared to the blocks containing a single defect.

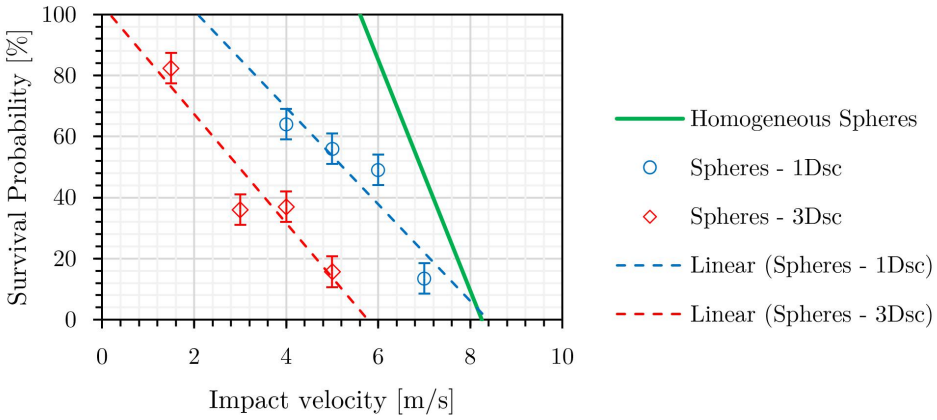


Figure 2: Comparison of experimental SP of spheres with 1Dsc and 3Dsc with predicted SP for homogeneous spheres (Guccione et al. 2021a). Symbols represent experimental data, while dashed line represent linear interpolation of the experimental results. Uncertainty in the point estimates (± 5%) is shown as error bars.

4 CONCLUSION

This paper presents the results of an experimental study focusing on the determination of the SP in drop tests of spheres with discontinuities. The results have shown how the fragmentation of blocks containing preexisting defects can occur at a much lower impact velocity compared to homogeneous blocks of the same size. Although this paper brings new insights into the significance of block defects for the SP, more research is needed. The challenge now is to be able to predict the occurrence of fragmentation considering the effect of discontinuities in an accurate yet practical manner. This is key for a more realistic rockfall assessment.

ACKNOWLEDGEMENTS

This work was supported by Australian Research Council (DP210101122 and IE230100410), Rocscience Inc and Marie Curie Postdoctoral Fellowship 2022 (Call Horizon-MSCA-2022-PF-01, grant GA101103401 - RIDETHERISK project). The help received from Dr Michele Spadari, Elena Cozacenco and Wesley Murphey with preparing the samples and conducting the experiments is also gratefully acknowledged.

REFERENCES

Corominas, J., Mavrouli, O. and Ruiz-Carulla, R. (2017). Rockfall occurrence and fragmentation. In *Advancing Culture of Living with Landslides: Volume 1 ISDR-ICL Sendai Partnerships 2015-2025*, Springer International Publishing, 75-97.

Giacomini, A., Buzzi, O., Renard, B. and Giani, G.P. (2009). Experimental studies on fragmentation of rock falls on impact with rock surfaces. *International Journal of Rock Mechanics and Mining Sciences*, 46(4), 708-715.

Guccione, D.E., Buzzi, O., Thoeni, K., Fityus, S. and Giacomini, A. (2021a). Predicting the fragmentation survival probability of brittle spheres upon impact from statistical distribution of material properties. *International Journal of Rock Mechanics and Mining Sciences*, 142, 104768.

Guccione, D.E., Thoeni, K., Fityus, S., Nader, F., Giacomini, A. and Buzzi, O. (2021b). An experimental setup to study the fragmentation of rocks upon impact. *Rock Mechanics and Rock Engineering*, 54(8), 4201-4223.

Lanfranconi, C., Frattini, P., Agliardi, F., Stock, G.M., Collins, B.D. and Crosta, G. (2024). Field evidence and indicators of rockfall fragmentation and implications for mobility. *Engineering Geology*, 341, 107704.

Marchelli, M. and De Biagi, V. (2019). Optimization methods for the evaluation of the parameters of a rockfall fractal fragmentation model. *Landslides*, 16(7), 1385-1396.

Matas, G., Lantada, N., Corominas, J., Gili, J., Ruiz-Carulla, R. and Prades, A. (2020). Simulation of full-scale rockfall tests with a fragmentation model. *Geosciences*, 10(5), 168.

Volkwein, A., Schellenberg, K., Labiouse, V., Agliardi, F., Berger, F., Bourrier, F., Dorren, L.K., Gerber, W. and Jaboyedoff, M. (2011). Rockfall characterisation and structural protection–a review. *Natural Hazards and Earth System Sciences*, 11(9), 2617-2651.

Wang, Y. and Tonon, F. (2011). Discrete element modeling of rock fragmentation upon impact in rock fall analysis. *Rock Mechanics and Rock Engineering*, 44, 23-35.

https://doi.org/10.56295/1ACEG29

SCOPING FOR GEOHAZARDS - ENVIRONMENTAL CONTRASTS COMPARING THE ENGINEERING GEOLOGIST'S ROLE BETWEEN MINING, CIVIL ROAD TUNNELS, DAM DESIGN AND PUMPED HYDRO

Helen Baxter-Crawford
SMEC

ABSTRACT

The Engineering Geologist plays a pivotal role, using their geological background to nominate possible geohazards, specifically associated with a project's lithological conditions. An artifice of being a "specialist on everything", the Engineering Geologist is often expected to use their varied project experience to advise on how the nominated hazards are identified in the field, develop health and safety management plans and generate solutions that will allow for project development to continue, through mitigation or elimination for construction and design stages.

This paper explores a series of case studies, comparing the understanding of site specific geohazards associated with 1) iron ore open pit mining in the Pilbara, 2) civil road tunnel construction projects in Sydney, 3) dam foundation design at Mount Bold Dam, and 4) the geohazards already identified and under consideration for the proposed pumped hydro energy storage project, Borumba. It delves into the geohazards associated with each project and discusses what factors influence safety considerations, and which impact design, construction and/or waste management. Specific geohazards discussed are airborne hazards (fibrous and silica minerals); effects of dewatering, including dispersive or dissolvable materials; geomorphology; waste rock and water; and man-induced geohazards. It discusses the Engineering Geologists role in proofing the risk and actions required to enable project development to work around or with the hazard, via engineering control and mitigation.

It explores the factor of project scale, the influence that has on geohazard considerations and in particular the quantum of investigation required.

1 INTRODUCTION

Engineering geology is a dynamic and wide-ranging field. By default or by circumstance, the engineering geologist (EG) needs to be equally as widely versed in all sub-sectors of the discipline, firstly due to the overall shortage of EG's globally and secondly as a means of adjusting to variations in markets. For a fulfilling and lasting career, the EG professional needs flexibility and adaptability to enable a jump from commodity to commodity or sector to sector. As a result, the EG field demonstrates highly skilled individuals with significant cross-pollination of experience, environments, technologies and methodologies in modelling and design.

Identifying geohazards is one area where the EG can greatly support a project to optimise design and safety. Geohazards come in two forms:

1. Natural geohazards are the effects of the ground on a project, independent of the planned ground modifications, like existing landslides and swelling soils, and
2. Activated geohazards which are the effects the ground has on the project, directly influenced by the action of project development, like release of hazardous particulates from excavations, development of ground instabilities due to changes in groundwater regime, and effects of stress on excavations.

The EG is an asset to the design engineer. Engineers are more able to become niche specialists - geotechnical, dams, open-pit mining, and underground mining for example. The primary (geo)hazards that an engineer may focus on for design and construction considerations would be:

- Overall stability relating to natural geohazards
- Local ground instability related to activated geohazards (including stress related), arising during construction,
- Dust and spoil management as a consequence of changes to the form of rocks by the process of excavation.

Within a singular commodity or sector, the amount of rigour required to assess the impact on each may be limited – the data is well understood and can be logically addressed. The lithological and mineralogical properties of rock and soil are direct and indirect inputs into each hazard type and the EG would advise if the properties are typical or outside the norm and direct the degree of further investigation/assessment required.

The EG cements their position in a project when things change or there is a shift to something new, for example:

- Expansion of an open pit below the ground water table,
- Expansion of a city's metro rail network,
- New remote technology may uncover or support previously dismissed geohazards, and
- Intrusive site investigations may suggest the state geological survey mapping requires updating.,

Such case studies are discussed in this paper.

The inclusion of the pure study of mineralogy for any geohazard assessment cannot be understated. A background understanding of the minerals that may be present in any particular rock or soil type will focus the EG for what activated geohazards may form with project development and help shape the site investigation, inputs required for risk assessments and resultant risk profile of the site.

Further, the project scale may, but not always dictate the likelihood of geohazards being present and this must be considered in both the risk assessment and the site investigations. For example:

- A singular mine may be extracting one commodity but depending on the geological environment and mechanism in which mineralisation has occurred, the ore may be contained within one or more lithologies or alteration zones and the background mineralogy and inherent quantum of hazardous minerals may be different – this could be critical for products like gold and copper.
- A tunnel may be over 20 km long and contained within a single stratigraphy or be 2 km long and cover multiple lithological/stratigraphical units.
- A dam may have a 200 m span and have abutments in two totally different rock types or be 700 m long and founded within a singular unit.
- The footprint of a pumped hydro project is much more likely to contain infrastructure in completely different stratigraphic units and depending on the infrastructure being developed in each, the natural and activated geohazards that present may be totally unique for each.

2 ENVIRONMENT 1 – OPEN PIT MINING IN THE PILBARA

The author worked for over a decade at various mining operations in the Pilbara iron ore region of Western Australia. During this time, the author developed a rich understanding on the local geological units, namely the ore bearing units of the Dales Gorge and Marra Mamba Banded Iron Formations and the overlying Tertiary Detrital sequences, Figure 1.

The focus of projects the author was involved with was geotechnical – expanding and/or optimising existing mines in the folded and faulted bedrock environment and designing new green fields operations.

The banded iron formations (BIF) of the Dales Gorge and Marra Mamba Formations consist of inter bedded cherts, shales and iron bearing laminated sequences. The shales form discrete, distinct and continuous marker horizons with a clear, repeatable gamma downhole geophysical signature. The units are stratigraphically continuous (other than where folded or faulted) for thousands of kilometres. Where folding has resulted in dip slopes, the continuity, waviness and friction angle of the beds are critical inputs for slope design. Undercutting of the beds, may result in planar slide at bench and inter-ramp scale.

With respect to the geohazard focus of engineers outlined above, the following commentary is made with regards to iron ore mining in the Pilbara:

1. Overall stability relating to original landforms and geomorphology – within the bedrock units, the overall stability is typically governed by the dip slopes; ancient landslide surfaces are rare, limited to localised block falls.
2. Local ground instabilities that result during pit excavation are usually related to the kinematic relationship between the dip of the beds, slope angle and bed friction angle. Some allowance for small scale planar slide or wedge formation is expected with the unstable material captured on catch berms.
3. Dust is a common issue within most mining operations and dust suppression mechanisms are used during normal day to day activities by means of water carts and exclusion zones. The minerals present in the "dust" generated by mining activities are not considered high-risk, so the requirement to wear dust masks is typically a case-by-case site requirement or related to daily assessment of wind conditions.
4. Spoil rock – The beauty of the Pilbara's iron ore deposits is the majority of excavated material is ore. Spoil rock is typically limited to areas of required excavation to fit the pit design in units like the West Angela Shale, Whaleback Shale and the Mt McRae Shale. The Mt McRae shale is a known reactive shale and therefore considered a hazardous material – the unit contains nodules of pyrite, benign due to oxidation when weathered, but when unweathered, pose an acid drainage problem as well as a potential for spontaneous combustion,

especially when stored inappropriately in waste dumps, (Waters & O'Kane, 2003). The unit underlies the Dales Gorge Iron Formation and as such typically forms the footwall of Dales Gorge deposits. The issues with pyritic shale management are so well understood, that standard operating procedures are in place at most sites that intersect this unit.

5. Spoil water: During the early 2000s very few of the Pilbara iron ore sites had developed below water table, so water spoil management wasn't a significant consideration, at least from a geotechnical perspective.

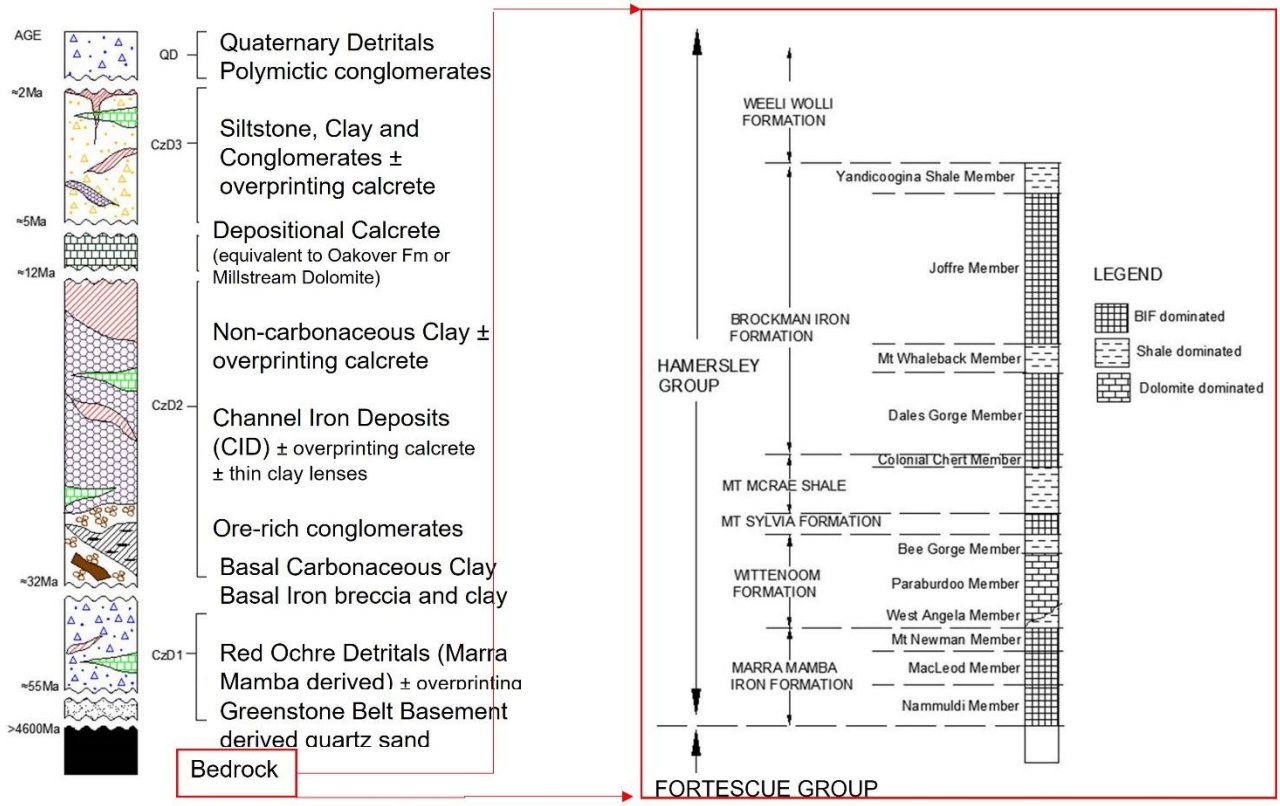


Figure 1: Stratigraphic Column for the Pilbara Iron Ore sequences and overlying Tertiary Detritals, after Baxter 2016 in (Eggers, Griffiths, Parry , & Culshaw, 2016).

A key additional geohazard, directly related to mineralogy of the Banded Iron Formations (BIF) that forms the bedrock is the potential presence of naturally occurring asbestos (NOA). For the mineralised zone of the deposits, any NOA is typically altered (to tiger iron) and regarded as non-hazardous, and so is not a considered factor in dust mitigation and safety. Only in unweathered and unaltered BIF would NOA be expected. As such, many of the mining operations develop their ore body delineation through the use of low expense reverse circulation drilling, with assay geochemical testing and gamma geophysical survey under the strict control of a risk management plan that dictates the holes are terminated 3m below (or one drill run) the base of mineralisation so as to avoid exposure of NOA during the exploration process.

At one particular site where the author led a geotechnical site investigation of drilling and mapping to optimise and expand existing operations, the initial pit configurations, already under development had been designed based on a rudimentary ore body model with correlations of major beds made purely by interpreting between 50 x 50m spaced holes with geophysics.

The orebody was located in the Marra Mamba Iron Formation, specifically the Newman Member, with the unmineralized optimised pit slope to be developed in the lower-most portion of Newman and the underlying McLeod Member. The ore was centred within a synclinal fold hinge. The inter-ramp slope of the pit followed the approximate dip slope, but benching had been poorly achieved. Use of blasting and digging without presplits had effectively resulted in a 120 m high slope with bench face angles parallel to bedding (essentially parallel to the planned inter-ramp angle) and limited to zero catch berm capacity.

As part of the optimization site investigation, diamond drilling was introduced with the intent to penetrate 50 m behind the pit slope and allow development of a design with suitable bench face angles and catch berm capacity, and ultimately expansion of the mine. Use of the diamond rig brought new risk management documentation requirements to the project - the operations staff had been averse to geotechnical core drilling due firstly to the potential for NOA intersection, but

secondly as they were unfamiliar with diamond drilling. Despite diamond drilling being commonplace in the early 2000s it had never been observed at this site so substantial, safe work method statements had to be developed to ensure that diamond drilling was actioned as safely as possible. The proposed drilling of unweathered and unmineralized BIF meant the risk of encountering NOA increased and so further risk management systems had to be implemented, including development of a substantial risk management plan in order to gain permits for the drilling to take place. Put simply, the risk management plan detailed the use of wet drilling to minimise NOA fibres becoming airborne and inspection of all rock core for fibres. Were any found, a sampling and testing protocol was implemented to allow for laboratory testing to confirm the intersections. Had any intersections been found, these zones would have been demarcated in the geological model for the mine.

The geotechnical program completed at the site resulted in two key outcomes for geohazard assessment:

1. No asbestos was encountered, but risk management plans were developed and the work paved the way for further geotechnical investigations at other deposits within this operation.
2. The synclinal shape of the fold that formed the pit became much better understood. The diamond drilling and mapping indicated that the ore body did not uniformly parallel the bedding and further, bedding was not uniform in dip – with the new deeper penetrating data, the model was updated, resulting in a shift of the fold hinge by some 200 m, compared to the ore-body drilled model, Figure 2. The laboratory testing and mapped data allowed for an improved understanding on design friction angles and resulted in a suitable and constructable bench-berm configuration.

For this project, the value-add of the engineering geologist being engaged to identify and develop work systems that would allow geological assessment beyond the ore zone to be completed were:

1. The development of safety protocols and risk management plans that were informed and useful,
2. A revised model that allowed for safer but also more economical pit development.

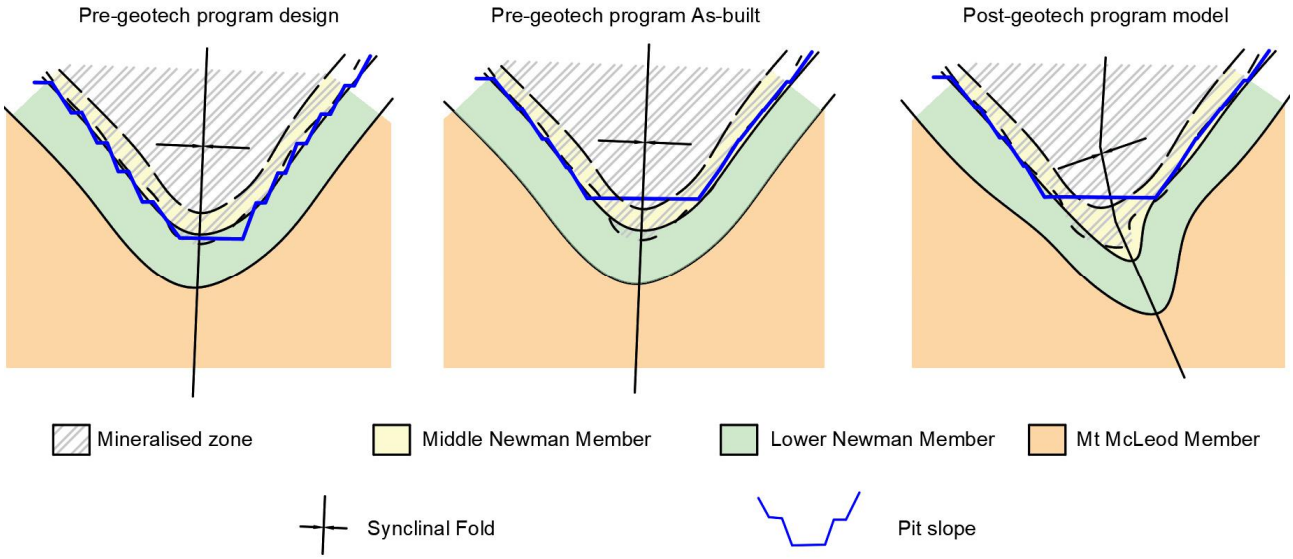


Figure 2: Schematic of the modifications to the model resulting from the geotechnical drilling. Not to scale

By 2007, several operations had begun exploring the feasibility of extending below the water table to extract ore. The author had significant involvement in the early stages of below water table expansion site investigations and design for the Marandoo deposit, with ore contained in the Marra Mamba Iron Formation, and expansion below Tertiary Detrital soil and rock sequences.

Beyond the aforementioned geohazards, the introduction of pit excavation below the water table introduced a new geohazard system, whereby the change in groundwater regime had the potential to destabilise the carbonate balance which could lead to a potential for sinkhole formation from the dissolution of calcium carbonate in the form of calcrete.

Additionally, as the footwall of the pit expansion was contained within the Marra Mamba Iron Formation, a similar risk-based approach to the potential for NOA intersection in the BIF units was implemented.

Calcrete, formed from precipitation of calcium carbonate at the top of an ancient groundwater table, was observed about 30 m below the ground surface throughout the detrital sequences, though with very limited penetration into the ore body.

Critically, the thickest and most well-developed calcrete concentrations (with assay records indicating CaCO3 in abundance of 20%) occurred behind the proposed pit slope adjacent to the main ore transport rail line. The act of dewatering the pit posed a risk that it could destabilise the delicate balance where the CaCO3 remained as rock and could cause dissolution (Baxter, 2012). This could be the catalyst for unravelling of the overlying clastic low strength rock (with zones of soil strength material) and promote the formation of sinkholes.

The diamond-RC twins and geochemical relationships were used to characterise the calcrete mass condition (Baxter, Eggers, Muhairini, & Smith, 2015), Figure 3, and extrapolate the signature patterns between boreholes to develop a model of calcrete development intensity and thereby define potential areas of higher risk for sinkhole development where preventative remediation treatment could actioned if required.

The geotechnical program completed at the site resulted in two key outcomes for geohazard assessment:

1. No asbestos was encountered, but risk management plans were developed and used.
2. The calcrete study and model allowed for identification of high-risk areas to be monitored and further assessed in event remediation was required prior to dewatering.

For this project, the value-add of the engineering geologist being engaged to identify and develop work systems that would allow the appropriate geological assessments to be undertaken were:

1. Refinement of safety protocols and risk management plans that were informed and useful,
2. Accurate modelling of high-risk areas, to inform ground monitoring systems to be used during the mine development.



Figure 3: Variation in calcrete overprinting texture (After Baxter, 2012)

3 ENVIRONMENT 2 – TUNNELLING IN SYDNEY

The author has worked numerous tunnel projects across Australia and the Asia-Pacific over the last 20 years. The Sydney Basin experience has involved road header, drill and blast and Tunnel Boring Machine (TBM) tunnels ranging from 1 km to 14 kms length, crossing a maximum of three stratigraphic units with a typical drill ratio of one borehole per 100 to 200 m, and higher ratio at caverns/station boxes or where tunnels overlapped. This drill ratio reflects the relative simplicity of Sydney's stratigraphy. By contrast, the 7 km Brisbane Airport Link crossed three stratigraphic units with a drillhole to tunnel length spacing of 30 to a maximum of 200 m.

With respect to the geohazard focus of engineers, the following commentary is made about tunnelling in Sydney:

1. The geomorphology of Sydney is such that existing landslides within the natural surfaces are very localised and while the tunnel alignment should be reviewed, and portal areas mapped, landslides would rarely be a key focus for the investigations.
2. Tunnelling in Australia is controlled through the use and implementation of controlled, well-practised international methods for construction so the risk of instability related activated geohazards should be engineered for in the design. Small scale wedge fallout is usually addressed through the use of spot bolts or a change to the support class from the predicted. Recent occurrences of ground movements through to surface have human factors as the primary contributors. Stress issues are very localised and generally situation specific. The Sydney trains, roads and metro networks are relatively shallow (maximum around 80 m depth) and the strength of the Sydney stress regime is low. Exceptions are where other stress factors occur like valley bulge as indicated from the Northside Storage Tunnel.
3. Consideration as to the impacts of silica dust released from excavation processes has on tunnellers has been a focus of recent years, however, at the authors first tunnelling project in 2003, the supply and use of disposable P2 dust masks was optional, with most choosing not to wear and not being appropriately educated to understand why they should. By 2008, they were expected to be carried and used on an as needs basis. Self-rescuers were considered a more important piece of safety equipment, with detailed training sessions on use and reporting mechanisms in place to report those not carrying one underground. By 2016, P2 was the minimum requirement with most sites moving to fit-tested personal options. Legislation is following suit, with guidelines for the minimum number of times annually any staff member is allowed to be exposed, before mandatory health surveillance testing is required. Silica exposure is a very real activated hazard from excavations in the quartzose Hawksbury Sandstone.
4. Spoil rock from Sydney's Hawkesbury Sandstone is like gold - its readily able to be sold off as a reuse product as engineered fill. The Ashfield Shale is not as valuable and often is repurposed within a site. Neither are considered hazardous.
5. Waste-water management and groundwater seepage control is a project within a project for road and transit tunnels. While the maximum groundwater inflows at a single location (for example flowing from a bed or joint) in Hawkesbury Sandstone that the author has observed is in the order of 10L per minute (more than what is delivered by a standard shower head), Figure 4a. When this occurs, the total lugeon value for a 1 km segment of tunnel may be higher than designed, particularly if the zone is structurally affected (fault zones) or forms a gravitational low. The deepest point of the M8 tunnel at Arncliffe is an example where both increased structure and flow direction coalesce to form a zone of significant groundwater inflow and ongoing management.

Other geohazards the engineering geologist may need to identify within the Sydney tunnelling environment are:

- Shrink-swell potential for Ashfield Shale. This characteristic of the unit is well known and actively monitored for during construction as a risk mitigation measure, but this natural geohazard could become more of an issue as tunnelling pushes to the west of Parramatta with continued urban development.
- Beyond simple management of waste-water, continued maintenance of the sumps and drainage systems is needed in the Hawkesbury Sandstone to keep the drainage clear of bacterial iron precipitate sludge, Figure 4b. This activated geohazard “sludge” doesn't always appear to develop, but where observed, begins to form within weeks to months of excavation. It effectively forms a geohazard as if the drainage systems are not adequately maintained, groundwater seepage becomes an ongoing issue for tunnel users.
- Over the last 20 years there have been several cases of significant ground instability occasioning serious damage and in one situation, death in Sydney. A direct result of these incidents has been a change to the immediacy of ground support requirements with the inclusion of shotcrete application almost immediately upon excavation. This limits the amount of time geologists have to collect the factual mapping data to groundtruth the design and provide updates to the assumptions made for the subsequent tunnelling section. Use of shotcrete as a support medium has been adopted in civil tunnel conventional (roadheader and drill and blast) rock tunnels throughout Australia. The key activated geohazard risk is that the observational method adopted as part of the construction methodology is substantially time-constrained and unable to be verified. Features that could be telling of changes

to stress and groundwater conditions are not readily observable and key geological structures may not be identified.

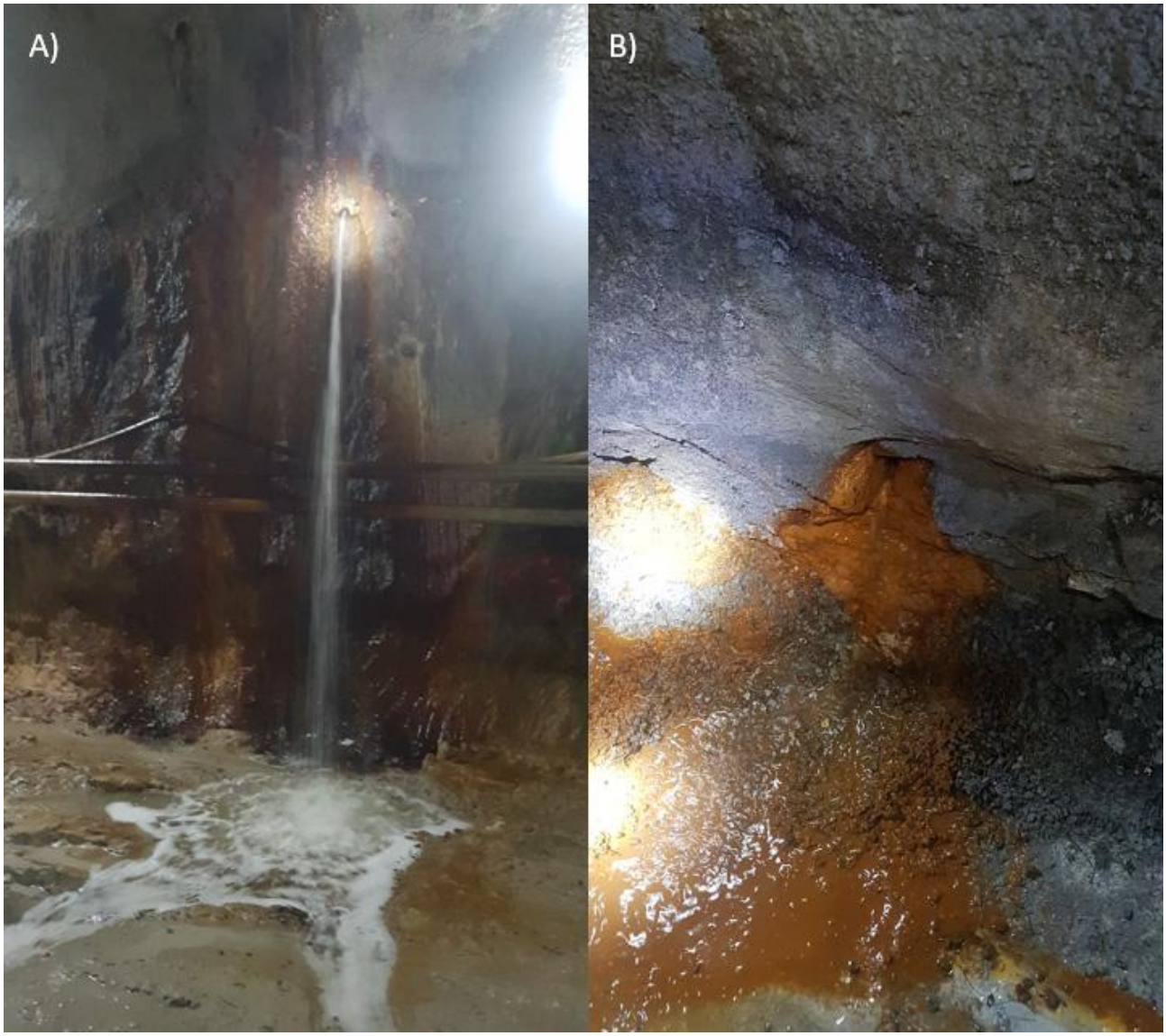


Figure 4: a) flow of water from structure in M8 tunnel with iron precipitation beginning to develop. b) bacterial sludge beginning to develop in association with flowing water in M8 tunnel.

The value-add of the engineering geologist being engaged to identify geohazards and develop work systems that would allow the appropriate geological assessments to be undertaken in Sydney tunnels are:

1. Refinement of safety protocols and risk management plans that were informed and useful,
2. Identification of high risk areas (for shrink-swell response, for excessive groundwater inflows) and provision of advice for drainage and treatment requirements.

4 ENVIRONMENT 3 – DAMS

The author is relatively new to the dams' sector, working on various projects over the last four years, though observes similar geohazard issues arise as observed within mines or tunnels, but with a higher potential consequence should the geohazard result in failure.

Many dams within the Australian portfolio are presently undergoing either 20-year risk reviews and full dam risk assessments, some as the first phase into upgrades; others to simply ensure they are compliant with current ANCOLD regulations.

One such dam looking for potential upgrade is Mount Bold Dam in the Adelaide Hills, straddling the Onkaparinga River. The main dam is founded on a phyllitic rock mass belonging to the Woolshed Flat Shale.

With respect to the geohazard focus of engineers outlined above, the following commentary is made about the dam:

1. Excavation of the existing dam was completed to slightly weathered rock. Historic photos demonstrate vertical to near vertical temporary faces prior to dam concrete pouring and back filling.
2. Stress is related to regional scale earthquake loading with the dam and reservoir within the neotectonic zone associated with the Willunga Fault.
3. Local ground instabilities during construction of any upgrade are considered possible with the right abutment forming a dip slope and sub-vertical joint release planes present. Such small (<10 m3) scale slide and wedge derived instabilities have been observed along access roads to date so are known to be possible. This is expected to be controllable by means of bench scale slope design and use of catch berms, or if the available space is not conducive to a benched approached, then through the use of short-term face support, like bolting. Long term, any new excavation would likely be covered with dam concrete or fill and thereby be stabilised. The rock mass strength of the less weathered and unweathered foundation rocks would suggest piping is unlikely. Larger scale ground movements are discussed following.
4. Dust is expected to only be an issue during construction of any dam upgrade and would likely be mitigated using conventional methods like water trucks. The mineralogy is being tested to assess the risk of airborne silica, though this is unlikely to be an issue with the anticipated excavation methods.
5. Spoil rock and water would need to be controlled during any excavation for the upgrade, to avoid contamination downstream. Substantial fill already exists on the lower downstream slopes that may need removal for the upgrade. These aspects are yet to be properly considered at this time with no design in place.

Previous workers at the site have suggested zones of inferred colluvium present on the right abutment downstream slope may be of landslide origin. The area of concern has been repeatedly identified as a risk, mapped (and drilled), discounted and raised again over many years of study.

Several phases of LiDAR (Light detection and ranging) have been imaged over the last 20 years, with the most recent incorporating cleaning of the digital data to remove vegetation from the imagery and at the highest resolution available to date. This latest data set expresses the character of the upper slope of the right abutment far better than any mapping of the highly vegetated slope would allow, Figure 5. Further work is ongoing in this space but the improvements in LiDAR technology in recent years are such that the author encourages all sites with inconclusive landslide understanding to recapture their local data.

The value-add of the engineering geologist being engaged to identify geohazards and develop work systems that would allow the appropriate geological assessments to be undertaken for this dam are:

1. Review of the dam foundation rock mineralogy to assess the risk to personnel from excavation practises, should the dam upgrade proceed. The last excavations for the dam were completed nearly 100 years ago, and as such, so such systems were in place,
2. Identification of high-risk areas for ground movement using the latest technological tools and supported by traditional ground-truthing techniques.

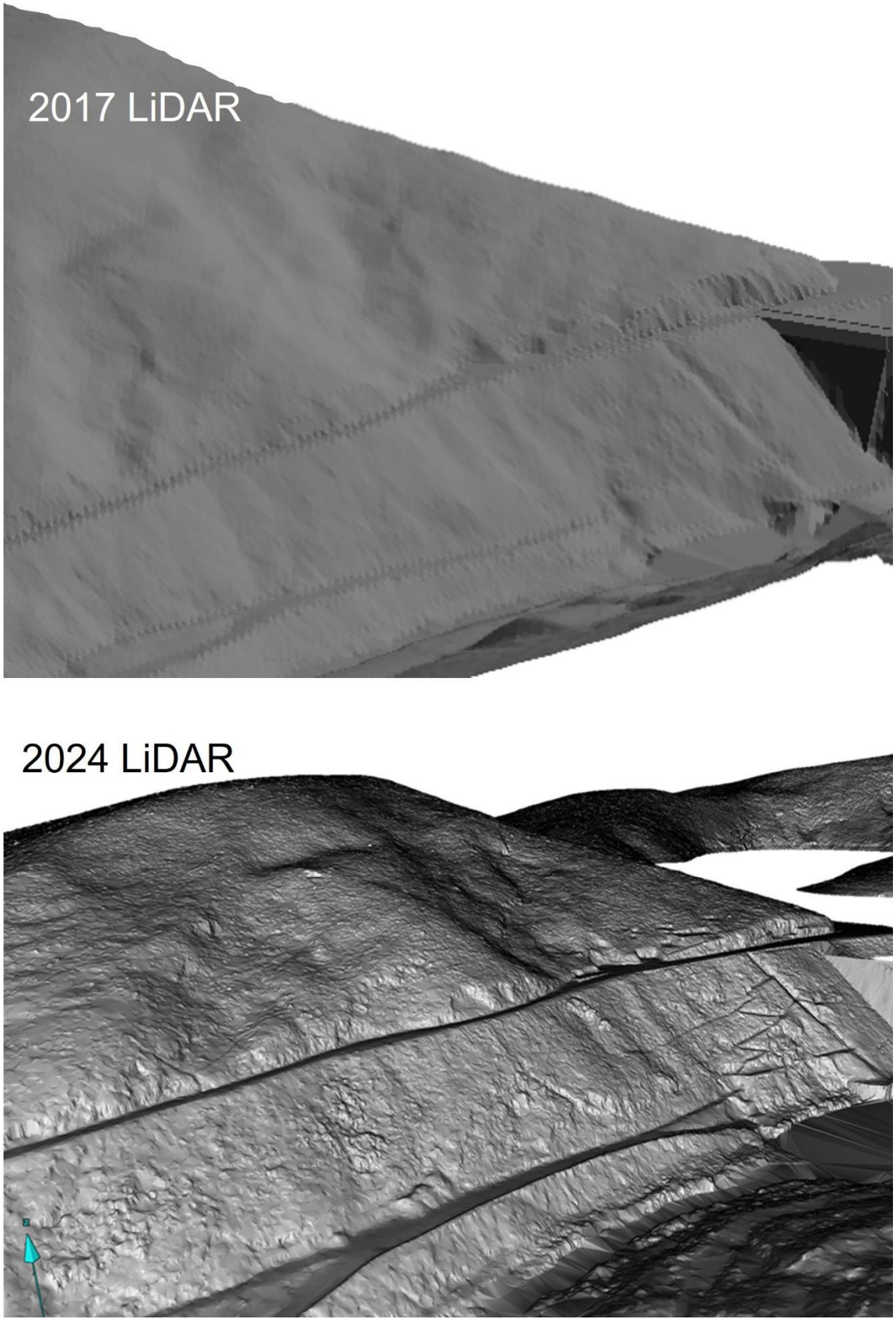


Figure 5: Comparison in LiDAR quality between 2017 and 2024

5 ENVIRONMENT 4 – PUMPED HYDRO

The scale of pumped hydro projects is such that multiple stratigraphic sequences can be contained within one project footprint. The author has been working as Qwners Engineer for the Borumba Pumped Hydro Energy Storage (PHES) project, assisting in recognising potential geohazards for the early investigation stages and assisting in developing risk management plans to allow work to progress. The geohazard predictions are proactive, used to pre-emptively action safe work processes and advocacy for the sustainability goals of the project. The site covers tunnels and caverns within a meta-sediment laminated rock mass, with portal in a granitic intrusion; upper reservoir dams in the same meta-sediment unit and in a granodiorite intrusion; and a lower reservoir dam within a sequence of metavolcanics, not seen in the upper reservoir; as well as other excavations for camp and road developments crossing a variety of rock and soil units. The Mt Mia Serpentinite is inferred as present on the Queensland geological survey map within the site bounds, though the key infrastructure sites do not intersect. This unit and its inferred fibrous minerals habit has been considered and incorporated within a risk management plan for geotechnical drilling with key safeguards active until sufficient data has been captured to identify any high risk or known occurrence areas. Despite the very low expectation of fibrous mineral intersection, until all areas are proofed as clear, every drilling/mapping intersection on the project is being marked on a GIS-portal based map indicating:

- Not observed
- Fibrous minerals observed (not tested)
- Fibrous minerals observed (tested negative)
- Fibrous minerals observed (tested positive).

The area is very remote, green fields with some areas of dense vegetation, and others (the granitic zones) used for cattle grazing. The Queensland geological survey mapping is showing low reliability with differences observed during initial field work. The inferred boundaries of granitic intrusions don't match observations and the main unit targeted for cavern development is lithologically different to the inferred stratigraphy of the survey map, with site workers considering it to belong to a different sequence. As such, the early drilling has been very important in delineating which lithologies (and minerals) are expected and both the natural and activated geohazard considerations required, both at site investigation stages, for sustainability and disposal considerations in design with reuse of excavated material within the project bounds being a key sustainability goal, and for construction health and safety.

To further remotely define the unit boundaries, a closely spaced airborne geophysics survey has been completed using helicopter which has proven highly favourable in identifying unit boundaries and particularly the Mt Mia Serpentinite.

With respect to the geohazard focus of engineers outlined above, the following commentary is made about the project:

1. Excavation of the dam foundations are expected to be developed by digging methods. Tunnelling for the caverns is proposed to be drill and blast - the rock mass is tending high to very high strength based on early drilling data, so this is a suitable, economical method.
2. Stress increases would predictably be expected at the depth of the cavern, proposed some 500 m below ground surface. Testing is underway to identify the dominant stress direction and develop a cavern orientation best suited for conditions to de-risk the excavation.
3. Data is being collected to capture the blockiness characteristics of the rock masses being tunnelled such that local ground instabilities are considered and captured in the design. To further de-risk the construction stage, a permit to tunnel (PTT) system is planned to inform and permit construction of the exploratory tunnel in defined segments, with a detailed forward probing plan to collect data and inform design. The PTT process allows the designer to review forward probing data and confirm the early support predictions are suitable or require modification, with the PTT discussions advising which areas are approved for excavation and the support systems and monitoring requirements that are required. With respect to ground instabilities on the surface, any areas of slope excavation, including portals are being mapped to capture the understanding of existing historic landslides, with data collected input into models for stability analyses. Access roads are subject to inspection protocols to assess for indicators of changes in slope behaviours following rainfall with these protocols updated as and when changes to the road usage (including vehicle quantity) occurs.
4. Mapping is progressing to assess the geomorphological character of the site and generate a landslide risk map.
5. Tunnelling to access the cavern locations is expected in the moderate silica meta-sediments and high silica granitic rock masses. Excavation in these units would follow standard dust suppression and mandatory dust mask health requirements used elsewhere in the country. Health and safety regulations are being followed with respect to health monitoring of employees.
6. The mineralogy of tunnel spoil is being assessed for reuse purposes, stockpiling and to inform health and safety understanding. Pyrite has been observed in the granitic rock mass from the proposed tunnel and is presently being assessed to understand the form and quantity of the mineral such that its effects can be appropriately

controlled/mitigated. Geochemistry of groundwater is also being assessed as there are strict controls on the mineralogical make-up of reservoir water and contamination.

As new lithologies are being encountered, the mineralogy is being assessed for fibrous mineral potential, influence on stability, and other characteristics via petrographic assessment and various suites of geochemical laboratory testing. Reuse and/or permanent storage of excavated materials on site is a key sustainability goal for the project.

The value-add of the engineering geologist being engaged to identify geohazards and develop work systems that would allow the appropriate geological assessments to be undertaken at Borumba are:

1. Pro-active identification of potential hazardous minerals across the entire project,
2. Pro-active mapping and remote survey controls to inform natural geomorphological geohazards allowing variations to design to be considered at early project stages,
3. Pro-active development of risk management plans that are informed and useful, and constantly updated,
4. Identification of high-risk areas across each facility area of the project, to be further informed by ground-truthing.

6 DISCUSSION ON ENGINEERING GEOLOGIST'S ROLE

The Engineering Geologist plays a pivotal role on any project, using their geological background to nominate possible geohazards, specifically associated with a projects lithological conditions. The EG needs to develop sufficient familiarity with the stratigraphy, lithology and mineralogy of a site to be able to advise on the potential issues that may be encountered and be able to communicate how to identify and manage risk and provide solutions to assist the engineers with their design through to construction.

The case studies presented in this paper demonstrate that while the infrastructure environment changes, and the stratigraphic and lithological environments changes, the author is repeatedly faced with similar geohazards, particularly those related to airborne dust and lung health. All require proofing, but the stratigraphic and lithological understanding (and associated mineralogical understanding) were the basis for suggesting the geohazard presence and nominating controls and investigation methods to define the risk to the project. Only stress and surface ground instabilities were dictated by topographic variations more than being distinctly related to geology/mineralogy.

The safe work practises and mitigation measures to contain airborne dust particles during construction is a common theme for all work environments. The engineering geologist has been at the forefront of firstly identifying the high-risk minerals, then assisting health and safety teams in developing risk management plans that allow work to continue while managing the health and safety of employees.

Overall, the Engineering Geologists role never changes when it comes to geohazard (natural and activated) identification. Just the environment does.

7 ACKNOWLEDGEMENTS

The Author would like to thank Queensland Hydro and SA Water for permission to publish this paper.

8 REFERENCES

Baxter, H. (2012). Pilara Cenozoic Detrital Sequences and Associated Geohazards. *AGS Symposium.* Perth.

Baxter, H., Eggers, M., Muhairini, A., & Smith, J. (2015). The effect of carbonate alteration on Detrital mass strength and implications for geotechnical slope design. *Iron Ore Conference 2015*, (pp. 429 - 435). Perth.

Eggers, M. J., Griffiths, J. S., Parry , S., & Culshaw, M. G. (2016). *Developments in Engineering Geology.* London: The Geological Society of London.

Waters, P., & O'Kane, M. (2003). Mining and Storage of Reactive Shale at BHPBilliton's Mt Whaleback Mine. *6th International Conference on Acid Rock Drainage*, (pp. 155-161). Cairns.

https://doi.org/10.56295/1ACEG30

ASSESSING THE GEOTECHNICAL SUSCEPTIBILITY OF CAVES IN PILBARA IRON FORMATIONS TO INSTABILITY

Duncan Noble, James Watton, Mark Eggers and Mark Fowler
PSM

ABSTRACT

Natural caves are common features of the iron formation strike ridges in the topography of the Pilbara Region of Western Australia, which are also host to many of Australia's major iron ore deposits. These caves are increasingly being recognised for their ecological and heritage value. Consequently, there is an emphasis on preserving the structural integrity and minimising potential impacts caused by nearby mining activities, while also reducing risk to personnel undertaking research or monitoring activities within the caves.

The morphology and engineering geology of the Pilbara iron formation caves are central to understanding potential failure mechanisms and triggers to rockfall in the caves. A methodology has been developed for assessing geotechnical susceptibility of the caves to instability, which is used to inform risk and impact assessments for nearby mine developments. The approach uses detailed engineering geological observations to identify susceptible features and potential hazards to personnel working in and around the caves as part of ecological and heritage monitoring.

1 INTRODUCTION

The Pilbara Region is home to some of the world's largest iron ore mines. Deposits currently in production include open pit mining operations with strike lengths of tens of kilometres. These deposits are often situated along prominent ridges of banded iron formation (BIF) and chert, which also commonly host caves and overhangs. These caves are home to several native bat species and often have cultural heritage value as a result of millennia of indigenous occupation of the region.

Over recent years high-profile cases of damage or destruction of cultural heritage sites by mining activities, as well as a growing focus on environmental protection in general, have resulted in increased attention on the responsibility of iron ore miners to preserve the environmental and/or heritage value of these sites. This is usually achieved through:

- Identification of important sites
- Careful documentation of geotechnical conditions
- Development of vibration limits and/or exclusion zones to reduce the likelihood of unacceptable damage due to mining activities, and
- Ongoing monitoring of the impacts of these activities on the sites.

The purpose of this paper is to summarise the occurrence, morphology and engineering geological condition of typical features that are susceptible to instability in naturally occurring iron formation caves in the Pilbara. The engineering geological assessment of a cave site is usually undertaken to achieve one or more of the following three objectives:

1. To document the pre-mining condition of the site to aid in identifying any future impacts that may result from mining activities or natural degradation
2. To assess the susceptibility of the site and specific geotechnical features to mining induced impacts (termed 'susceptible features')
3. To identify rockfall hazards that may impact safe access to the site for archaeological or environmental surveys and monitoring activities.

The threshold for what is considered 'damage' may vary depending on the purpose of the study; for example, minor rockfall may be acceptable in a bat roosting site, but unacceptable for cultural heritage preservation. Regardless of the main purpose, the basis of each of these three objectives is to undertake detailed engineering geological observations of the rock mass and structural character of the cave and features that may impact stability of the site.

This paper presents an overview of the assessment process and the typical geotechnical features observed in a cave environment. Guidance is provided on the qualitative assessment of both the susceptibility of these features and the whole site to instability or mining impacts (termed 'qualitative susceptibility assessment').

A desktop study should be undertaken prior to the site visit to understand the regional geological setting, any mapped or inferred major structures, local topography, and proximity of the site to existing or planned developments. Although the

desktop study is essential to the overall geotechnical assessment of caves, the focus of this paper is on the field observations and how they are used to assess susceptibility.

2 GEOLOGY AND GEOMORPHOLOGY

The regional bedrock geology of the Pilbara broadly comprises granites overlain by Archean to early Proterozoic banded iron formation (BIF), shale, dolomite, volcaniclastics and mudstones. Bedded iron ore deposits are predominantly hosted within the Brockman Iron Formation, Marra Mamba Iron Formation, and to a lesser extent, the Cleaverville Iron Formation.

The Pilbara has undergone numerous deformation events resulting in regional scale folding and thrust faulting, producing prominent strike ridges of the more resistant BIF and chert lithologies, while the more erodible shales and dolomites form intervening valleys, commonly partially infilled with Tertiary-Quaternary aged clastic transported materials and lacustrine deposits.

Prominent escarpments are a common feature along the BIF strike ridges, both at the contacts with the adjacent erodible units, and where surface water drainage has cut deep gullies through the bedrock. These escarpments can be very steep to overhanging and may be tens of metres high. The base of these escarpments is typically covered by an apron of colluvium. An example of a typical cave-hosting BIF escarpment is shown in Figure 1.

Bedding is a common feature of the outcropping bedrock and often forms partings at spacings of 50 mm or less to several metres. Shale bands interbedded with the BIF and chert units often form weaker, more erodible layers, which can result in overhangs and ledges in the escarpment and within the caves.

The upper few tens of meters of the bedrock are often altered by near-surface processes, which can result in overprinting of bedding textures and the development of a massive, vughy rock mass.



Figure 1 - A typical Pilbara iron formation escarpment hosting numerous caves

3 CAVE FORMATION AND MORPHOLOGY

The mechanisms of iron formation cave development are not fully understood (Brandi et al. 2019), however they are typically inferred to have formed in two ways:

1. Through near-surface alteration processes, which result in a net volume loss in the rock mass and the development of voids. Near-surface BIF rock mass, exposed to meteoric water, is commonly hydrated. This

process includes alteration and recrystallisation of the iron oxide minerals from hematite to geothite, often overprinting the bedding fabric of the rock (Tardy et al. 1990), resulting in a massive rock mass with relatively little structure. The hydration process also includes a volume reduction through the concentration of iron oxides and dissolution of siliceous minerals, resulting in a vughy rock mass. It is this volume change that creates the initial voids leading to cave development.

2. Through mechanical breakdown, usually as a result of pervasive structure such as bedding or closely spaced joint sets. In the Pilbara, this is commonly closely spaced bedding partings, which form the roof or wall of the cave. Conjugate joint sets orthogonal to bedding may facilitate block formation with successive block release over a long period of time resulting in the development of a void.

Each of these cases can have different features susceptible to instability, associated rockfall mechanisms, and hazards. Examples of these two typical cave morphologies are presented in Figure 2. Features common to both cave types are shown schematically in Figure 3, including some of the susceptible features discussed later in this paper.

Caves assessed by the authors of this paper, comprising more than 150 sites, have ranged from shallow overhangs in escarpments less than a few cubic metres in volume, to multi-chambered caves extending tens of metres into the rock mass and encompassing several hundred cubic metres of internal space. The full extent of some of these caves is unknown as some areas are too narrow or are deemed unsafe or unnecessary to access.

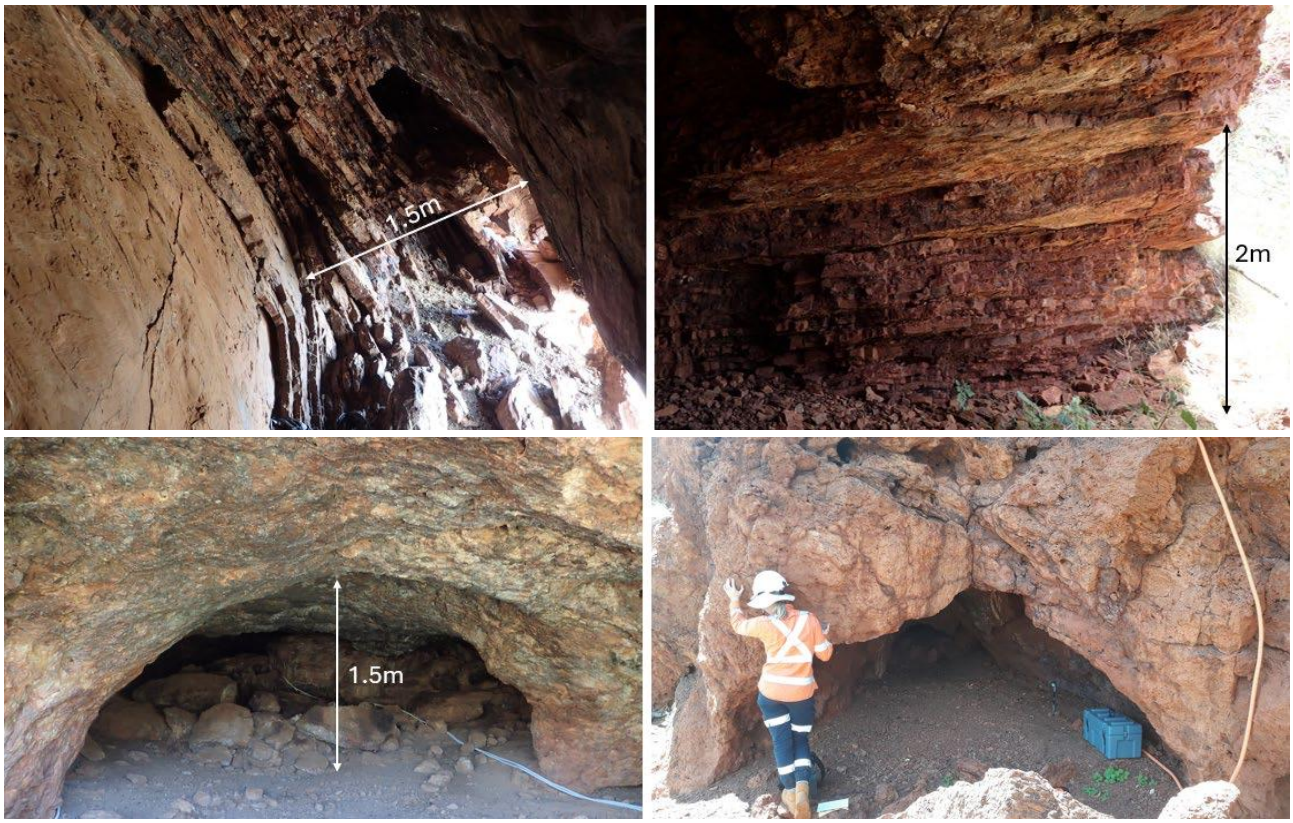


Figure 2 - Top: Examples of caves formed on steeply (left) and shallowly (right) dipping bedding. Bottom: Examples of caves formed in hydrated BIF rock mass.

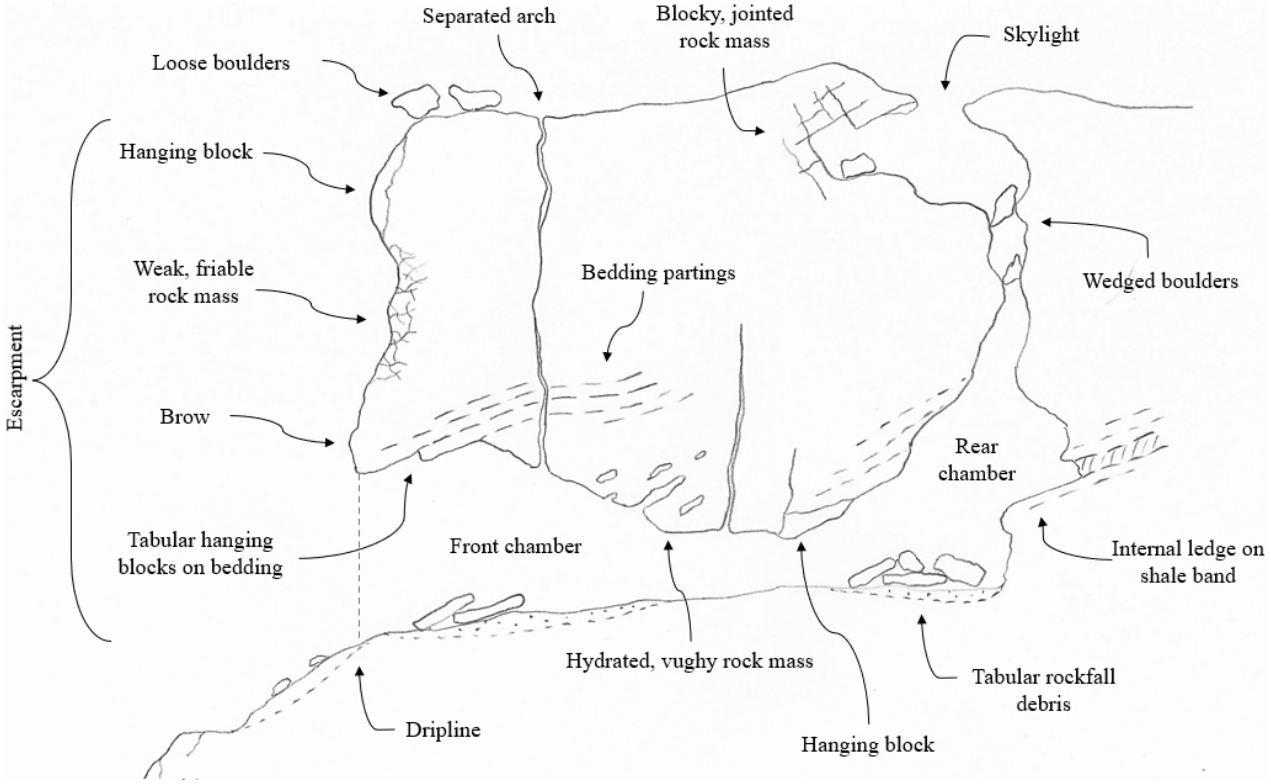


Figure 3 - Schematic cross-section of a cave showing key morphological and engineering geological features

4 ENGINEERING GEOLOGICAL OBSERVATIONS

Detailed engineering geological observations form the basis of the qualitative susceptibility assessment. The study area should be defined prior to beginning the assessment, as the cave itself may not always be the area most susceptible to instability. Often the escarpment immediately outside (or some distance from) the cave entrance is assessed to be more susceptible to rockfall than the interior of the cave. In the case of ecological preservation (e.g. bat populations), rockfall from the escarpment may not be a concern; however, for a heritage site or a hazard assessment, this may be as important as the cave itself.

The focus of the observations should be on:

1. Rock mass condition, including rock type, estimated strength, structure and defect descriptions
2. Morphology of the cave and/or escarpment, including interpretation of formation mechanisms
3. Large to intermediate (regional to outcrop scale) structures, including bedding partings, joints, veins and faults and shears
4. Evidence of past rockfall events and interpretations of mechanisms and potential triggers
5. Observations of specific hazards, such as hanging blocks or perched boulders, or areas of loose or unstable blocky rock mass.

Australian Standard AS1726:2017 provides a detailed methodology for item 1, describing the rock material, including lithological and structural features. These observations are integral to forming a geotechnical model of the site and interpreting failure mechanisms and susceptibility. However, given the significant existing body of literature on this topic, these aspects of the assessment are not described in detail here. The focus of this discussion is on Items 2 to 4. Observations of susceptible features (Item 5) is described in Section 5.

4.1 MORPHOLOGY

Morphology of the site (Item 2) should be described using common terms such as those presented in Figure 3 and should include measurements or estimates of cave dimensions. Aspects particularly important to the susceptibility assessment include the cave span, shape and height, the brow and roof thickness, and observations of any areas that are not directly accessible but may still be a source of rockfall, such as high ledges and overhangs, or wide cracks in the walls and roof.

Morphology can also be used to help in the interpretation of rockfall mechanisms that have contributed to the formation of the cave, which are likely to be the same mechanisms responsible for many of the susceptible features at the site. For

example, the distinctive tabular morphology of the roof profile in the examples in Figure 2 (top), indicating formation and/or growth by repeated tabular rockfall from bedding partings.

4.2 STRUCTURE

Observations of structures (Item 3) are focused on features that are significant to the formation of the cave or to its stability, such as bedding partings, persistent joints, veins or shears. These structures should be described in detail, as set out in AS1726:2017. They should also be mapped and photographed for future reference. Where the cave is an important habitat for fauna, dilation or movement of large structures, especially those that connect the interior of the cave to the ground surface, may lead to changes in climatic conditions within the cave. Ecologically, this may be considered unacceptable damage in some cases.

Major structures, such as faults, may also act as pathways for structurally guided vibration waves where they intersect the blasting location in the nearby mine and pass close to the cave site. This can potentially result in local amplification of blasting vibrations proximal to the fault (e.g. Li et al. 1997). While it is important to note any major structures in the field, many of these larger features may be better assessed through a thorough desktop study prior to the field assessment. While essential to the assessment, the desktop study is not discussed further in this paper.

4.3 PAST ROCKFALL

Evidence of past rockfall events (Item 4) may include rockfall debris on the floor of the cave or the slope below the escarpment or brow. Other evidence includes rockfall source scars, the appearance of which can give some indication of the timing of the rockfall event with surfaces that appear fresher/less weathered than the surrounding rock mass usually indicating relatively recent rockfall.

Evidence of trigger events leading to rockfall is typically more difficult to interpret. In some cases where the timing of the rockfall event can be estimated to within a period of weeks or months it may be possible to infer a trigger event such as a nearby blast, drilling activity, earthquake, or significant weather event. Comparison of photographs from previous site visits, or debris found on ‘scat sheets’ used in some environmental surveys can be very helpful in estimating the timing of a rockfall event. In other cases, it may be possible to infer a trigger from observations within the cave, such as evidence of recent water flow, or roots growing from the source defect. Figure 4 shows examples of recent rockfall events inside caves, including rockfall onto a scat sheet and relatively ‘fresh’, clean surfaces indicating recently broken rock debris.

Morphology of past rockfall scars and rockfall debris can also provide evidence for possible mechanisms. The example in Figure 5 shows a large pile of rockfall debris interpreted to have fallen during a roof-collapse event, evidenced by the tabular shape of the blocks, the surfaces of which match the sources scars along bedding. In addition, the roof morphology includes a significant step between the area of large rockfall debris and an area relatively free of large blocks, indicating that roof collapse has not yet occurred in this part of the cave.

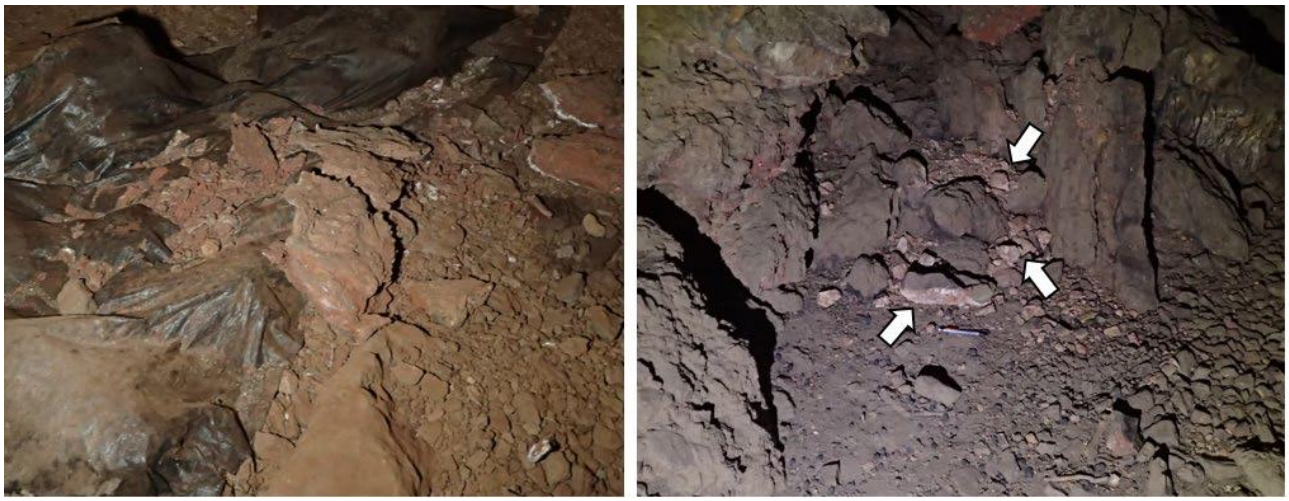


Figure 4 - Examples of inferred recent (approximately within the past year) rockfall debris on a plastic scat sheet (left) and on top of older debris (right).

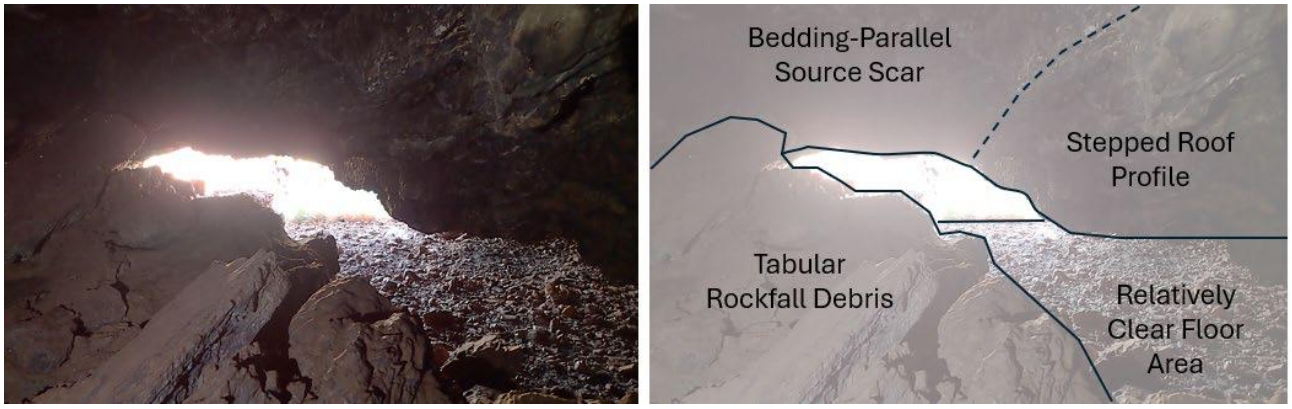


Figure 5 - Left: a photo of the interior of a cave showing significant rockfall debris on one side, coincident with a rockfall source area defined by bedding planes. Right: an interpretation of the same photo; rockfall debris is inferred to be the result of a partial roof collapse event along bedding partings on the left side of the photo.

5 SUSCEPTIBLE FEATURES

Any susceptible features observed within the site should be described, photographed and included on a detailed schematic plan of the site to allow them to be identified quickly during future site visits. Common susceptible features observed in Pilbara iron formation caves are described in this Section.

5.1 HANGING BLOCKS

Hanging blocks in the rock mass are bounded by defects in the walls, roof or in the escarpment. Hanging blocks are typically found on intersecting joint sets, along bedding partings, or bounded by randomly oriented defects. Important observations to record include:

- Location in the site
- Size and shape of the block (e.g. tabular, rhomboidal, etc.)
- Defect types and surface conditions, including openness indicating dilation, infill, roughness, shape and persistence
- The perceived degree of interlocking of the block with the surrounding rock mass. This is closely related to the assessment of defect conditions but also takes into account the interaction of bounding defects and their orientations
- Interpreted impact zone, including possible runout area.

Some examples of hanging blocks are presented in Figure 6.

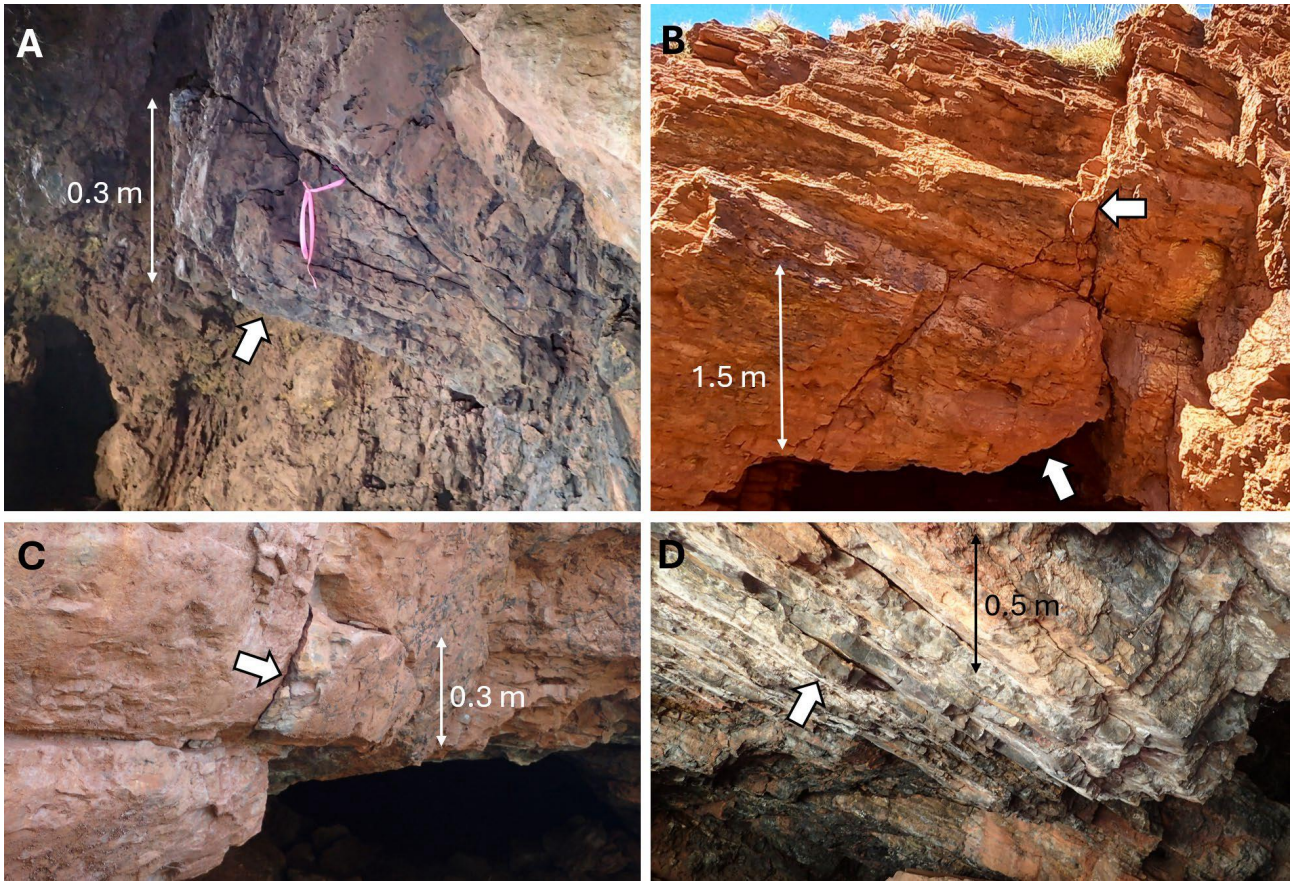


Figure 6 - Examples of hanging blocks bounded by open defects. A) A block hanging on an open joint within a cave. B and C) Hanging blocks in the cave brow. D) Tabular hanging blocks on bedding in the roof of a cave.

5.2 LOW STRENGTH ROCK OR VERY BLOCKY ROCK MASS

Areas of lower rock strength or highly fractured, dilated rock mass can be susceptible to fretting and rockfall. These features often occur in isolated areas of a site and may be associated with increased rockfall debris. Defects may be randomly oriented fractures, or repeated structures such as intersecting joint sets, closely spaced bedding partings or fault damaged rock mass, Figure 7. Lower strength, friable rock mass is more common within shale lithologies.

These features can be highly susceptible to triggers such as ground vibrations or disturbance from direct contact with people or objects.

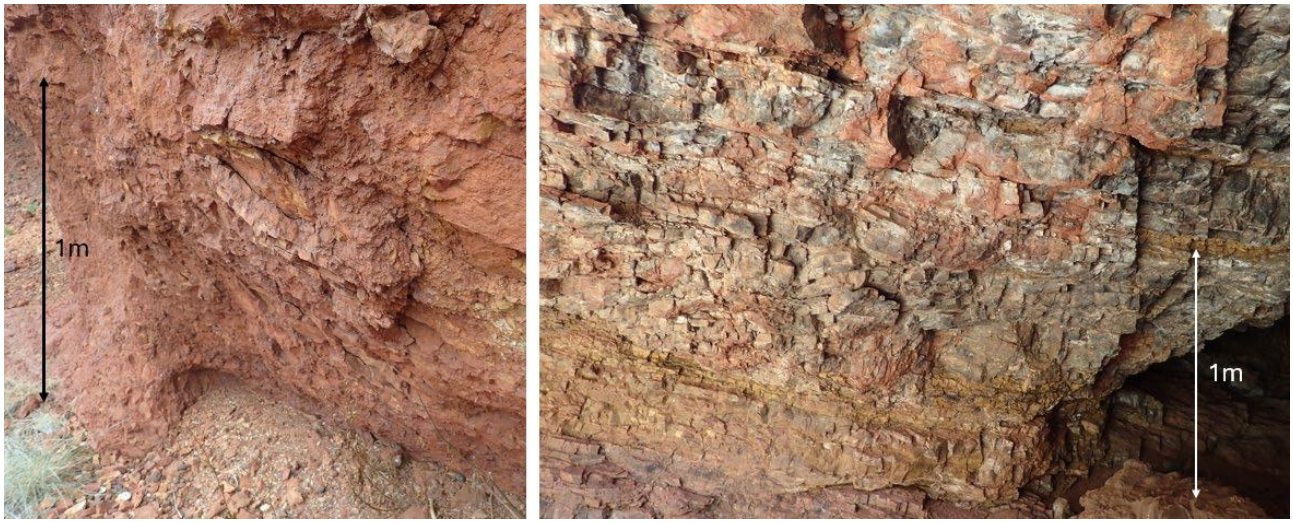


Figure 7 - Examples of blocky, friable rock mass outside (left) and inside (right) caves.

5.3 LOOSE OR PERCHED BOULDERS

Loose or perched boulders are often found on the escarpment or brow (Figure 3) but can also be found on internal or external ledges, or wedged within cracks in the roof or walls, Figure 8. Observations should include size and location of the rocks, and angle and condition of the supporting surface. The interpreted impact zone, including possible runout area should also be noted.

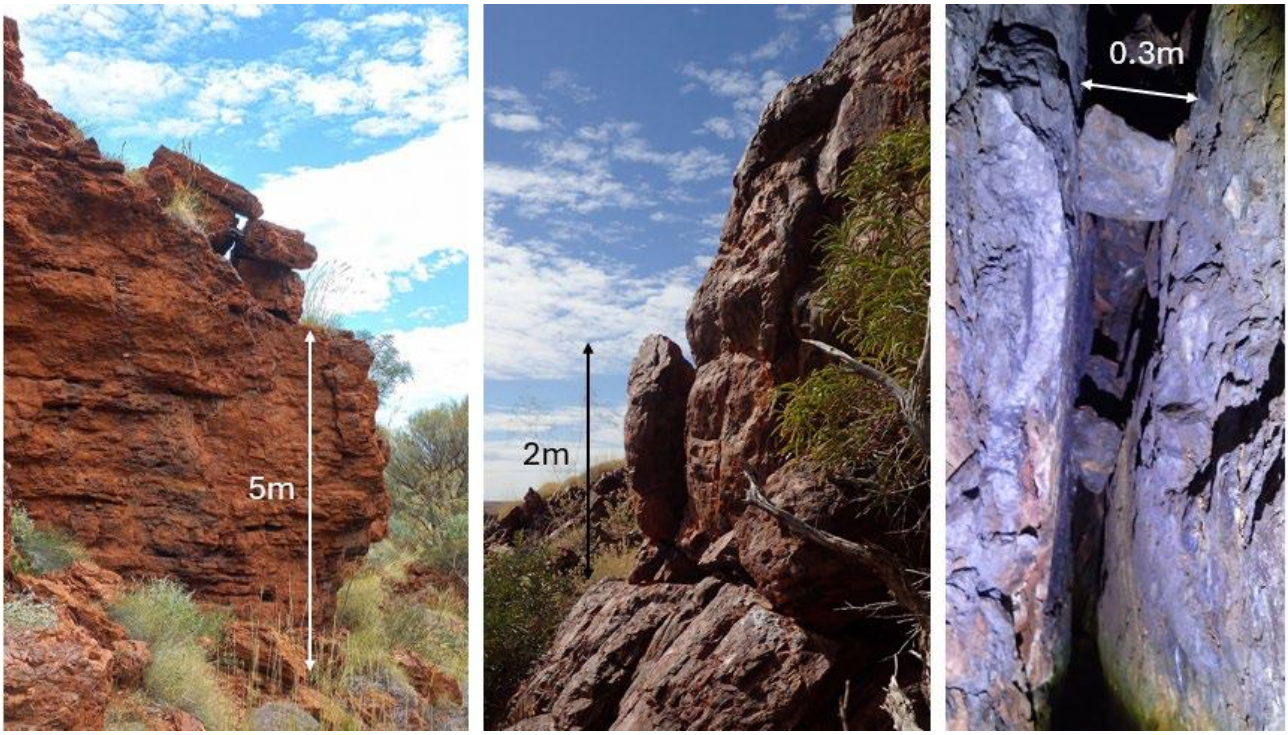


Figure 8 - Examples of loose or perched rocks on escarpments and within a vertical crack in the roof of a cave.

5.4 PILLARS

Pillars can form between entrances to a cave, or within smaller entrances termed ‘windows’. They are narrow columns of rock remaining after the surrounding rock mass has collapsed or eroded away. Examples shown in Figure 9 include a large pillar formed along bedding partings between two entrances, and a pillar between windows eroded in a relatively weak rock mass.

Along with location and size of the pillar, the estimated strength of the intact rock and presence of any defects through the pillar are important observations to make when assessing susceptibility. The pillar may also be supporting blocks or sections of the cave roof, which may be an additional hazard if the pillar were to collapse.

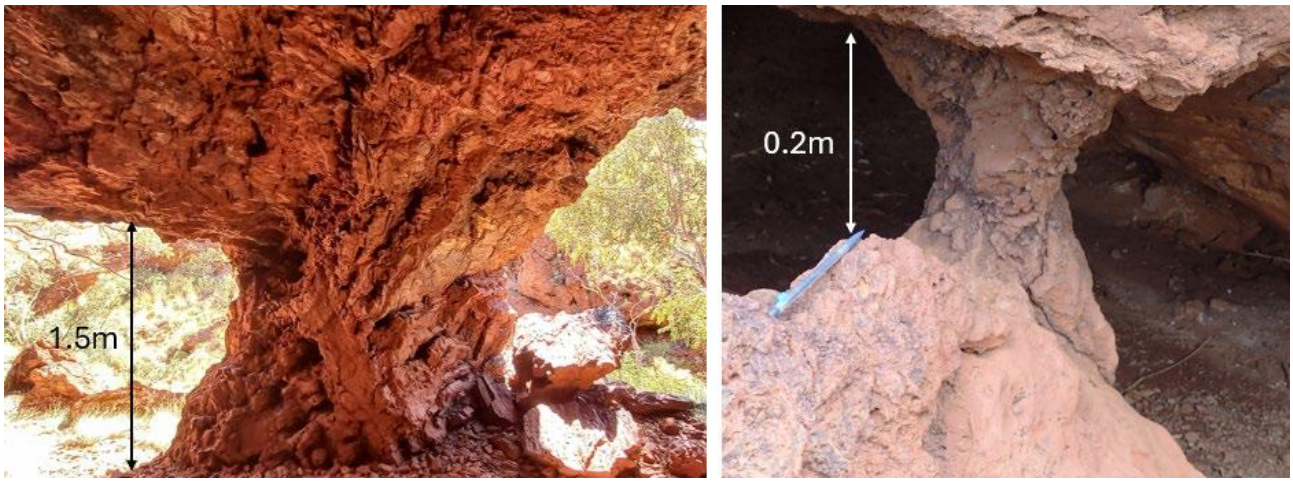


Figure 9 -Examples of structurally controlled (left) and rock mass controlled (right) pillar development

5.5 SEPARATED ARCHES OR COLUMNS

These features are large sections of the roof arch or overhang that are separated from the escarpment or outcrop by a persistent defect or multiple, intersecting defects. Separated arches (Figure 3) can tilt away from the rock formation over time, presenting a significant rockfall hazard. The examples shown in Figure 10 also include loose rocks wedged in the bounding defect.



Figure 10 – Examples of separated arches. The left and centre photos are the same separating defect, viewed from the inside (left) and the outside above the cave entrance (centre). In the centre photo the cave entrance is below and to the left. The right photo is another separating defect, viewed from the side of the cave with the entrance around the outcrop to the right.

5.6 COLLAPSE HAZARDS

Wall, escarpment or roof collapse hazards are usually interpreted through observations of:

- Loosened, blocky, dilated rock mass such as a rock mass cut by many open, intersecting defects, resulting in relatively little contact between blocks. Although in-situ, the rock mass may have the appearance of a pile of loosely stacked rocks, Figure 11
- Roof or escarpment sub-parallel, persistent defects, usually bedding partings or a pervasive joint set, Figure 12



Figure 11 - A cave entrance viewed from outside and inside, showing dilated, blocky, loosened rock mass. Daylight was visible through the defects from the inside.



Figure 12 - Examples of potential collapse hazards including escarpment-parallel joints (left), and roof-parallel open joints (top right) and bedding partings (bottom right)

6 SUSCEPTIBILITY ASSESSMENT

In cave geotechnical studies, susceptibility is defined as the potential or propensity for cave ground and ecological instability. There is no inference on the likelihood, frequency or probability of cave instability. The assessed susceptibility level of observed geotechnical features is an input into a risk assessment for personnel or equipment in the caves, or as an input to the assessment of suitable blast exclusion zones and/or vibration limits to reduce the chance of unintended damage to the sites. As such, it is important that susceptible features are not only identified and described but assessed in terms of their propensity to instability triggers such as vibrations from blasting or earthworks, or weather events such as heavy rainfall or high winds.

Observations contributing to the assessment of susceptibility are often qualitative in nature, as monitoring of specific susceptible features is not common in Pilbara caves. Observations that may inform susceptibility can include:

- The **degree of interlocking** of a hanging block with the surrounding rock mass, for example, a hanging block that has some visible rock bridging with the surrounding defect (i.e. defects do not entirely bound the block), or where bounding defects are rough or irregular, requiring significant dilation of the defect or breaking through asperities before the block can fail.
- Any **support provided by the rock mass**. For example, a tabular block hanging from an open, planar bedding plane in the roof may be considered highly susceptible, while a joint bounded block in the wall, on a shallowly dipping lower defect may be considered to have lower susceptibility. The same applies to the surface on which a perched or loose boulder is resting.
- The **strength of the rock mass**. Low intact rock strength in a friable rock mass is likely to be more susceptible than high strength rock in a blocky rock mass. Likewise, low strength or erodible defect infill may result in higher susceptibility of hanging blocks in a blocky rock mass.
- For **roof collapse hazards**, the width of the roof span and the roof profile are important features with wide, flat roof profiles typically being more susceptible to collapse than short spans and arched roofs.
- **Dilation of defects** bounding separated arches, as well as the height of the arch, dip of the bounding defect and estimate of where the centre of gravity lays relative to the footprint of the structure.
- **Evidence of water seepage**. Water seepage through defects bounding susceptible features can result in increased pore pressures (reduced effective normal stress) and washout of defect infill as well as slaking of low strength materials.

- The presence of **past rockfall debris** at the site, particularly if the source or mechanism is interpreted to be the same as the susceptible feature being assessed.

The above criteria can be used to compile a qualitative susceptibility chart based on the engineering geological characteristics and susceptible features important to the caves being assessed, as controlled by the geological and geomorphological setting of the project. An example for a particular mining area in the Pilbara is presented in Figure 13.

Susceptibility	Low	Medium	High
Block or boulder rockfall hazards	None observed or, if observed: • Potential impact (including inferred runout zone) not considered adverse	Specific hazards observed but not considered highly susceptible, e.g.: • Appears to have some degree of rock/soil mass interlocking (blocks) or toe embedment (boulders) • Not entirely bounded by visible defects • Blocks supported from below • Rock fall debris does not appear recent (weathered surfaces, dust/dirt covered etc.) • Inferred runout zone considered marginal	Specific hazards observed and considered highly susceptible e.g.: • Blocks hanging from the roof or walls with little observable interlocking • Significantly dilated bounding defects • Perched boulders with little or no toe embedment • Evidence of recent rockfall from susceptible feature • Inferred runout zone considered highly adverse
Rock mass/structure	• 'Massive' rock mass, or • Widely spaced defects that do not form blocks at the cave scale • No large, open defects persisting through cave walls or roof • No structural defects controlling cave/escarpment geometry (e.g. bedding, joints, fault or shears) • Dry conditions	• Structurally significant open defects, e.g. those that persist from the cave interior to the ground surface, or that bound large blocks of rock • Intersecting defect sets forming blocks • Structural defects control the cave/escarpment geometry • Water seepage from defects or rock mass	• Persistent, sub-horizontal defects in the cave roof • Three or more intersecting defect sets – very blocky rock mass • Persistent escarpment-parallel defects • Highly fractured and dilated rock mass • Cloudy/turbid flowing water, or increased flow/seepage rates
Cave or slope morphology	• Near-round, arched cave roof • Shallow to moderate escarpment slopes • Narrow cave spans	• Wide cave spans in massive rock mass • Low/flattened arched cave roof • Moderate to steep escarpment slopes • Pillars or columns	• Wide cave spans in jointed/bedded rock mass • Flat roof profiles • Separation of arches or columns/slabs from the escarpment • Narrow pillars and/or those with weak or loosened rock mass

Figure 13 – Example of a qualitative susceptibility chart

Ranking of qualitative susceptibility can be used to assess appropriate mitigation and controls depending on the objective of the geotechnical assessment, for example whether it be for heritage or ecological preservation, or risk to individuals entering the cave for monitoring. For risk to individuals, residual susceptibility can be assessed, which considers common controls to reduce the exposure of people and equipment to the observed susceptible features, such as monitoring and avoidance. In some circumstances, the residual ranking may indicate the risk is not sufficiently reduced, in which case entry should be prohibited and specialist advice sought.

In previous studies, the authors have occasionally been asked to provide an estimate of Rock Mass Rating (RMR_{89}) through field assessment of the Geological Strength Index (GSI) using nomographs such as that presented in Marinos and Hoek (2000). These estimates have then been used in blasting evaluations by the mine or blasting specialists in an attempt to predict the level of damage that may result from the expected vibrations at the site. While this approach may be useful for the rock mass and cave structure as a whole, it does not capture the specific susceptible features identified in the field assessments such as individual hanging blocks, which may be more susceptible than would be inferred from the overall RMR_{89} or GSI for the site. In cases where any degree of damage to the site is considered unacceptable, (for example, an important cultural heritage site) the authors do not consider this approach alone to be adequate to reduce the risk of adverse outcomes.

A cave geomechanical index (CGI) was proposed by Brandi et al. (2020) for assessing natural cave span stability in iron formation rocks in Brazil. The index utilises estimates of the RMR_{89}, hydraulic radius, ceiling shape, and ceiling thickness of each cavern to assess an indicated susceptibility of the span to structural instability from blast induced vibrations. Although Brandi et al. (2020) concluded that the index correlates well with observed cave collapse events in Brazil, the results have not correlated well with the qualitative assessments undertaken by the authors for Pilbara caves. Of note is that the CGI is strongly influenced by the hydraulic radius, while the roof span is not explicitly considered. Many of the caves qualitatively assessed as high susceptibility are characterised by persistent sub-horizontal defects in the roof, or large controlling defects. These factors do not appear to be adequately accounted for in the CGI assessment. For example, persistent sub-horizontal defects only result in a reduction of the RMR_{89} by five points, resulting in no change to the CGI in some cases.

At sites of high importance, it may be useful to install monitoring equipment on specific features to quantitatively assess susceptibility and monitor for changes to stability, this may include:

- Tilt meters to measure the movement of hanging blocks, perched boulders or separated arches
- Vibrating wire crack meters or extensometers to measure dilation of defects
- Cameras to record instances of rockfall.

These should be used in conjunction with on-site vibration monitoring to assess the susceptibility of the instrumented features to recorded levels of ground vibrations. Where a maximum ground vibration limit is implemented as a control to mitigate the risk of damage to a site, the adopted ground velocity limits should be assessed based on the perceived susceptibility of the site and the level of damage that is considered tolerable. Where the set ground vibration limits at a site are exceeded, a follow-up engineering geological site assessment should be undertaken to document any visible or measurable damage to previously documented susceptible features, or development of any new susceptible features. Cave entry should be limited to geotechnical specialists until an updated susceptibility assessment has been undertaken.

7 CONCLUSIONS

Natural caves in Pilbara iron formation rocks are increasingly being studied by prospective and active mine operators to assess the risks to cultural heritage sites and/or to preserve the unique fauna of the cave environments. The aim of these studies is to preserve structural integrity and minimise the impacts of mining activities on the cave sites, while also reducing risk to personnel undertaking research or monitoring activities within the caves.

Assessing the geotechnical susceptibility of the caves to instability should focus on detailed engineering geological observations to identify susceptible features and assess their level of susceptibility to ground vibrations or weather impacts. These detailed engineering geological assessments are integral to anticipating potential impacts of nearby mine developments and natural degradation processes on the sites.

Brandi, I., Sebastião, C. S., Ferreira, M. L., Lima, H. M. de ., & Gama, M. F. P.. (2019). Physical stability of iron ore caves: geomechanical studies of a shallow underground cave in SE Brazil. *REM - International Engineering Journal*, 72(2), 217–225.

Brandi, I., Barbosa, M., Barata, A., De Paula, R., Correa, T., Lima, H. and Osborne, R. (2020). Cave Geomechanical Index (CGI). Classification and Contribution to the Conservation of Natural Caves in the Iron Mines, *Geoconservation Research*, 3(2), pp. 134-161.

Li, Y., Ellsworth, W., Thurber, C., Malin, P. and Aki, K. (1997). Fault-Zone Guided Waves from Explosions in the San Andreas Fault at Parkfield and Cienega Valley, California. Bulletin of the Seismological Society of America, Vol 87, No. 1, pp. 210-221.

Marinos, P. and Hoek, E. (2000) GSI: A Geological Friendly Tool for Rock Mass Strength Estimation. *Proceedings of the GeoEng 2000 at the International Conference on Geotechnical and Geological Engineering,* Melbourne, 19-24 November 2000, 1422-1446.

Standards Australia. (2017). AS 1726:2017, Geotechnical site investigations

Tardy, Y., & Trolard, F., & Roquin, C., & Novikoff, A., (1990). Distribution of hydrated and dehydrated minerals in lateritic profiles and landscapes. *Chemical Geology.* 84.

https://doi.org/10.56295/1ACEG31

Project Phoenix Pumped Hydro Energy Storage Project - successful implementation of the Engineering Geological Model approach in support of the energy transition

Alistair Schofield

GHD

1 ABSTRACT

ACEN Phoenix Pty Ltd (ACEN Phoenix) engaged GHD to complete prefeasibility and feasibility investigations on Phoenix Pumped Hydro, a proposed pumped hydropower project in regional NSW. The aim of these works was to develop a thorough understanding of site-related geological and geotechnical hazards early in the project, to guide design and enable more accurate cost estimation, whilst reducing, where possible, the need for intrusive on-site investigations. The Engineering Geological Model (EGM) approach can be used to effectively identify and assess geological relationships and geotechnical properties and provides an important framework to enable thorough understanding of geomechanical behaviour and potential hazards (Schofield and Roberts, 2024). On this project, the conceptual geological model was refined in near real-time as the detailed geological mapping identified and delineated an unmapped complexly folded and faulted dolerite sill intruded prior to regional deformation. The investigations were rescoped to provide confidence in the interpretation and hence allowing design optimisation to exploit more favourable geotechnical conditions.

This project demonstrates the benefits of the use of fundamental geological skills as part of the Engineering Geological Model approach in large civil engineering projects to optimise design and deliver both time and cost savings through appropriate and scientific targeting of intrusive investigations.

2 INTRODUCTION

The planned Phoenix Pumped Hydro scheme will be constructed on a greenfield site in Central-West NSW on the eastern side of Lake Burrendong between the population centres of Wellington and Mudgee. It will have an installed capacity of approximately 810 MW for a nominal duration of 12 hours.

The concept design of the scheme allows for construction of new upper and lower reservoirs with an interconnecting waterway and other ancillary infrastructure. There is an approximately 330 m head difference between the reservoirs which means approximately 12 GL of water storage is required in each reservoir to provide the 810 MW of generation.

The concept design conveyance arrangement comprises an excavated vertical shaft and tunnel from the upper reservoir to the surface powerhouse excavated to below the minimum operating level of the lower storage. The installed capacity of 810 MW adopts three standard reversible fixed-speed Francis pump-turbine units of 270 MW capacity. The connection to the network consists of a 330 kV transmission line to a new connection on the existing 330 kV Wellington to Mt Piper line.

Uniquely, GHD identified the site and undertook initial assessments and studies regarding feasibility and site suitability using internal funding mechanisms with ACEN Phoenix ultimately taking on development of the project. GHD was then engaged to complete prefeasibility and feasibility investigations and design. The aim of these works was to develop a thorough understanding of site-related geological and geotechnical hazards early in the project, to guide design and enable more accurate cost estimates. The Engineering Geological Model approach was utilised, as it enables effective identification and assessment of geological relationships and geotechnical properties and provides an important framework to enable thorough understanding of geomechanical behaviour and potential hazards (Schofield and Roberts, 2024) and a scientific approach to the scoping, completion and use of data from intrusive geotechnical investigations.

This paper discusses the engineering geological model development process and findings that were used to guide the geotechnical investigation and demonstrates how following a logical and staged approach with identification of hazards and gaps is an effective approach to understanding ground risk for major projects.

3 ENGINEERING GEOLOGICAL MODEL GUIDELINES

In order to maximise information gathered, the geotechnical and engineering geology assessments of the site were conducted in stages to allow for an iterative development of the geological model, as per the Engineering Geological Model (EGM) Guidelines (Baynes et al 2022). The Engineering Geological Model (EGM) approach facilitates effective identification and assessment of geological relationships and geotechnical properties to ensure a thorough understanding of geomechanical behaviour and potential hazards.

The guidelines provide a valuable framework for development and use of geological models in engineering geology. All available information was utilized to develop a conceptual geological model which will be continually revised as new data becomes available through the rest of the design process, construction and into operation.

4 DESKTOP STUDY

This part of the process studied the regional geological, geomorphological and geophysical characteristics of the site. The published geological mapping and associated mapping reports and memoirs were reviewed to both identify the geology of the site and to understand the processes that contributed to the geological conditions present.

The desktop review identified that the site is dominated by a thick sequence of folded low-grade metasedimentary and possibly volcanic rocks. These materials were deposited in a deep marine environment known as the Hill End Trough which is thought to be part of a large back arc basin system formed during the Lachlan Orogen in the Late Silurian to Early Devonian (approx. 390 to 425 million years ago (Ma)).

Figure 1 shows the 1:100,000 scale Geological Survey of NSW map (Morgan et al, 1999) of the project area which is dominated by the Cunningham Formation with a small area of Merrions Formation towards the north. Approximate locations of the upper and lower reservoir are also presented.

A summary of the geological mapping codes with Formation/Unit names and lithological descriptions is presented in Table 1.

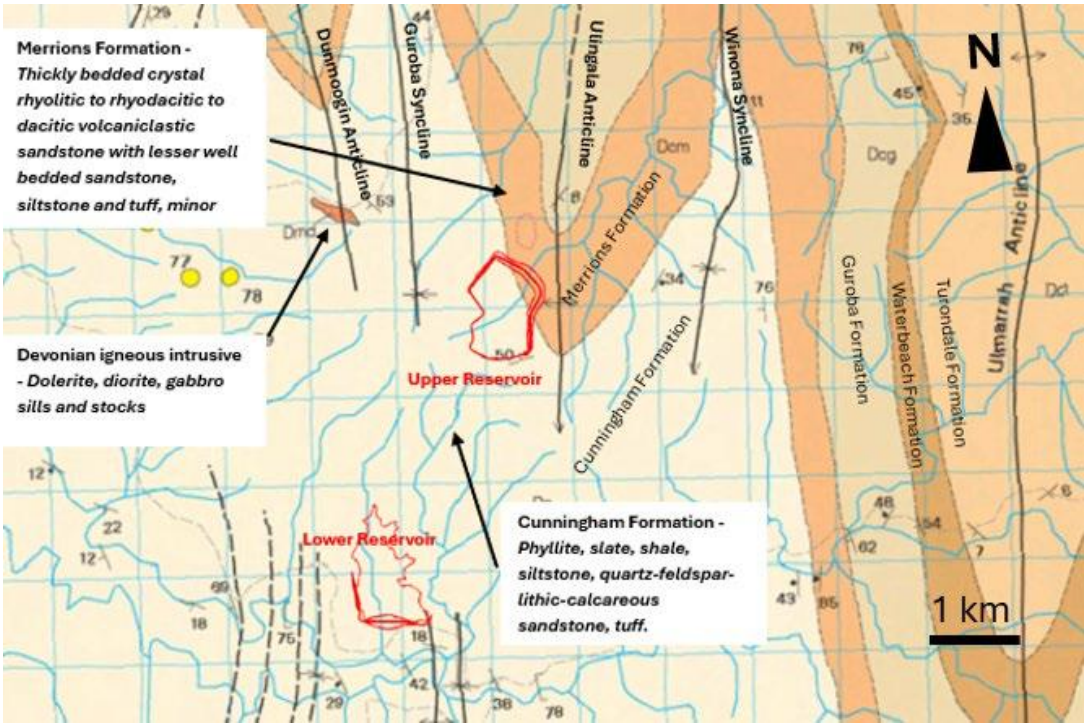


Figure 1: Site geology with project elements shown (after Morgan et al, 1999)

Table 1: Regional bedrock geological units (units in bold are within project boundaries)

Geological map code (youngest to oldest)	Unit Name	Description
Dmd	Not named	Dolerite, diorite, gabbro sills and stocks
Dn	Cunningham Formation	Phyllite, slate, shale, siltstone, quartz-feldspar-lithic-calcareous sandstone, tuff.
Dcm	Merrions Formation	Thickly bedded crystal rhyolitic to rhyodacitic to dacitic volcaniclastic sandstone with lesser well bedded sandstone, siltstone and tuff, minor lava and ignimbrite.
Dcg	Guroba Formation	Thinly to thickly bedded, muddy crystal lithic, rhyolitic to rhyodacitic volcaniclastic sandstone interbedded with lesser tuff, siltstone, phyllitic shale and paraconglomerate.
Dcw	Waterbeach Formation	Well bedded to laminated slate, siltstone and phyllitic shale with lesser lithic, feldspathic sandstone
Dct	Turondale Formation	Thickly bedded, crystal lithic, rhyolitic to rhyodacitic volcaniclastic sandstone interbedded with lesser thinly bedded, pelagic and volcaniclastic sandstone, siltstone and phyllitic shale; minor rhyolitic tuff and conglomerate.

The Cunningham Formation is thought to have been deposited via a combination of marine sedimentation punctuated by submarine debris flows and turbidity currents comprising clay, silt and volcaniclastic sand. Some limestone debris or blocks, resulting from failures along the edge of a carbonate shelf, may also be found in the Cunningham formation (Meakin and Morgan et al, 1999). This mode of deposition may lead to the presence of laterally variable rock types.

The Merrions Formation represents a deposit of volcanically derived material comprising sediments (probably volcaniclastic sandstones) and porphyritic igneous rocks thought to have been lava erupted and emplaced submarine. The clasts present in the sediments match the mineral assemblages present in the lava flows indicating they have been derived from erupted lava (Cas, 1976).

High quality, 1m resolution lidar data was available for the site. Using this data colluvium and alluvium was identified which is not shown on the published geological maps. The lidar data also revealed bedding or foliation structure of the metasedimentary rock across the landscape and an interpretation of the regional scale structural geology was completed. This interpretation indicated the presence of at least four major folds and smaller scale parasitic folding on these main fold limbs, and several short fault strands across the project area. Based on this structural interpretation it was identified that the bedding dip and lithology would be variable across the project area, and that the folded structures may have also lead to the presence of bedding parallel shears and ramp flat thrust, wedge and hinge faulting associated with stresses induced during the folding process.

As surface instability in the form of landslides is a key hazard to surface penstocks (with the exact configuration yet to be decided at the time), a geomorphological assessment was undertaken along the waterway route to identify possible landslides. Although areas of instability, in the form of translational earthflows and rockslides, were identified, these were away from the waterway route. An anomalous feature, of uncertain origin, was also identified in the topography. This feature coincided with a regional geophysical anomaly noted in the airborne radiometric survey data as shown in Figure 2. This radiometric anomaly was similar to one that coincided with a diorite outcrop on the published geological map. The Merrions Formation is also clearly visible in the radiometric data. The radiometric mapping overlaid on the geological mapping with key components of the project and geological features labelled is presented in Figure 3. The areas of landsliding and this geomorphological and geophysical anomaly were added to the itinerary for the geological reconnaissance mapping stage.

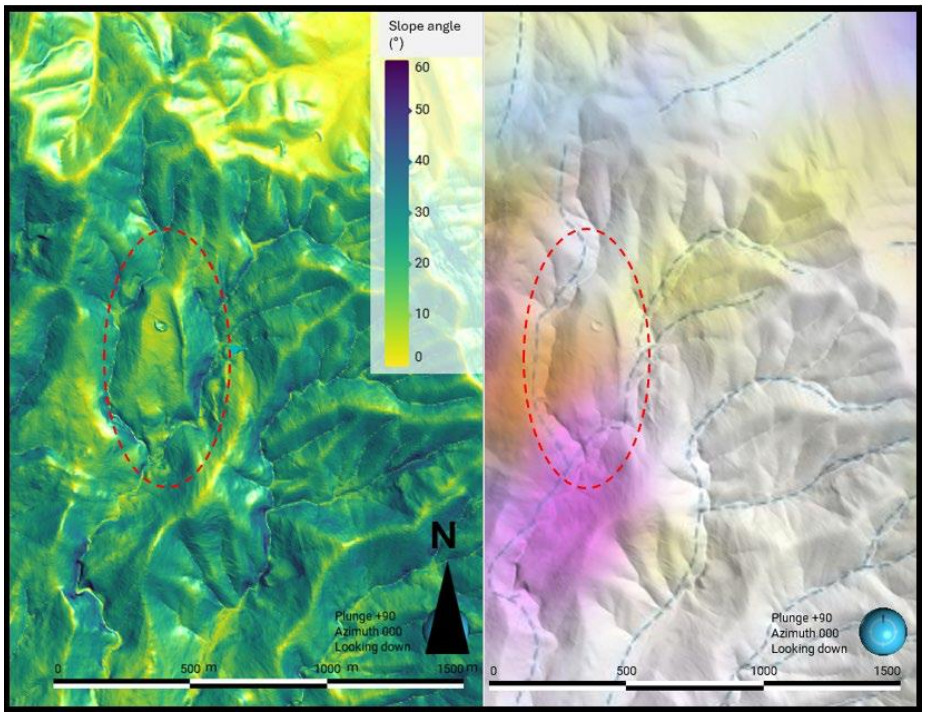


Figure 2: Geomorphological (left) and radiometric anomaly (right)

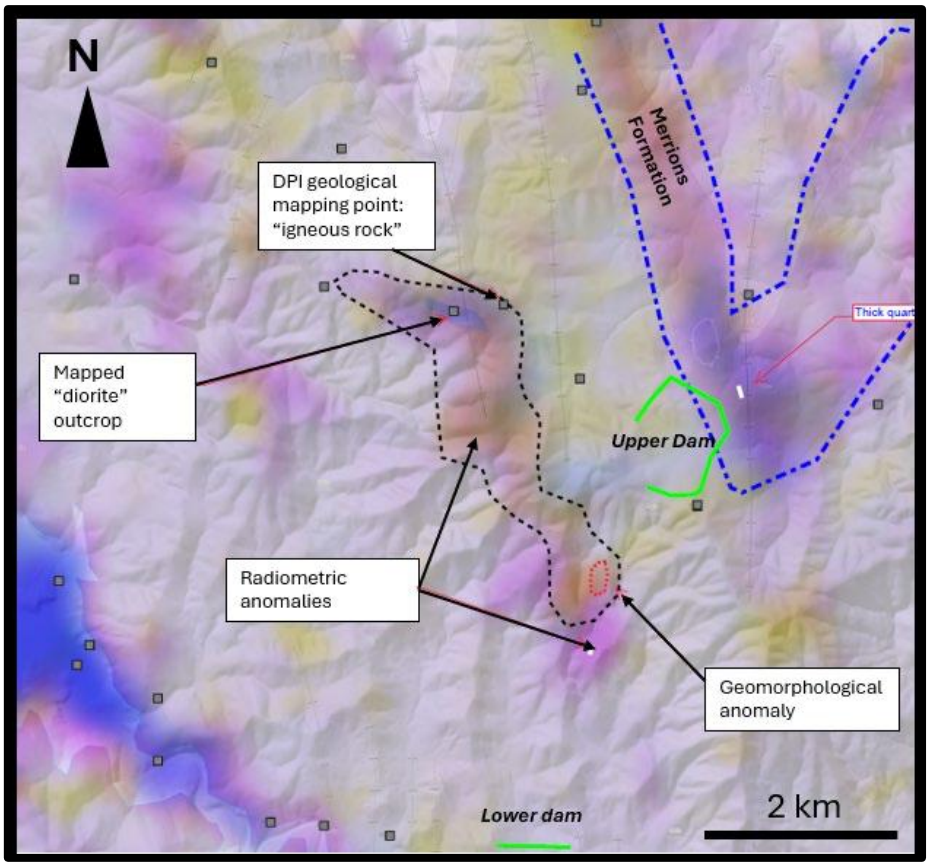


Figure 3: Igneous rock and radiometric anomalies possible indicating broader extent of igneous rock outcrop (DPI = NSW Department of Primary Industries) (after Minview, 2022)

5 GEOLOGICAL RECONNAISSANCE MAPPING

To inform the development of the conceptual geological model, which would be used to develop a scope of works for intrusive geotechnical investigations, geological reconnaissance mapping was completed. The primary aim of this mapping was to identify lithological and geotechnical characteristics and variability in areas of the upper and lower reservoir and along the waterway alignment. Anomalies as discussed in the previous section were also included in the itinerary and assessed. Collection of dip and dip direction structural data of significant features such as foliation, major joints and crushed seams was completed opportunistically.

The mapping identified a number of rock types across the broader project area including:

- A very high strength, slightly weathered volcaniclastic sandstone located in the north eastern part of the project area and which is believed to be part of the Merrions Formation
- A moderately weathered, medium strength fine grained meta-argillite (metasedimentary rock) with dominant foliation
- Fresh, extremely high strength vein quartz up to 1.8 m width

The mapping suggested that the foliation in the metasedimentary rock is broadly aligned in a north south direction. The collected measurement data is presented graphically as a stereo plot in Figure 4. The concentration of poles representing the subvertical north-south striking cleavage and the variable bedding dip (from 20º to the south east to 80-90º to the west and east) and a southerly plunging fold have been marked in the figure. This geological structure is consistent with the Geological Survey of NSW mapping data and the structural mapping completed using the lidar data.

Bedding was difficult to ascertain in many outcrops and is therefore underrepresented in the dataset. The difference between cleavage foliation and bedding in an outcrop on the right abutment of the lower dam is illustrated in a photograph taken during the inspection presented in Figure 4.

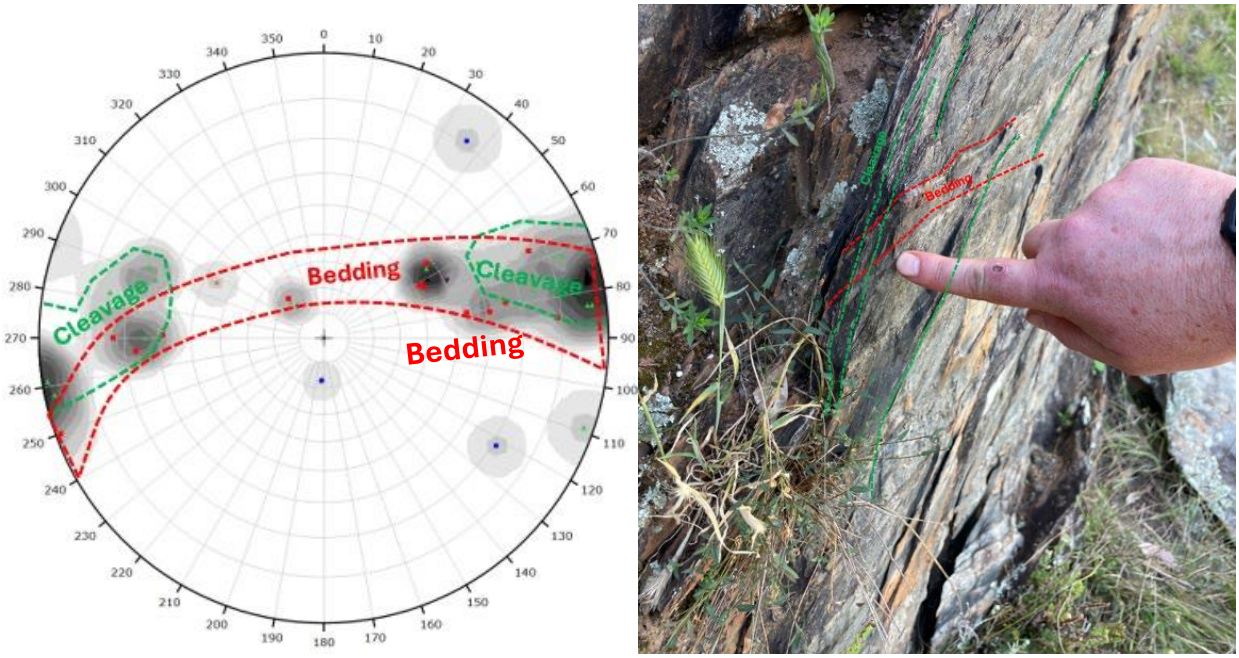


Figure 4: Stereo plot showing results of mapping across the project area (orientated towards true North) (left) and image of site rock showing relationship between cleavage and bedding (right)

Upon field examination of the anomalous area of geomorphology identified during the desktop stage, a reddish orange clay soil and differing vegetation was observed. A weathered rock outcrop was identified in a farm dam excavated in the centre of the feature. The rock identified was an extremely weathered to highly weathered mafic medium grained igneous rock that had developed characteristic “onion skin” concentric weathering. Quartz veins were observed within the exposure with an approximate north to south strike. Subsequent petrographic testing completed on hand specimens identified the rock to be a greenschist grade metamorphosed dolerite and gabbro. The highly weathered gabbro rock was

low to medium strength. These features are shown in Figure 5. Hand held radiometric equipment could have been utilised to help identify the location of the anomaly but was not considered necessary at this early stage of the project.



Figure 5: Reddish orange clay associated with weathering of igneous rock (left) and gabbro and concentric weathering and quartz vein (right)

6 TERRESTRIAL GEOPHYSICAL SURVEYS

Seismic refraction tomography surveys and subsequent Frequency Time Analysis (FTAN) of surface waves (Rayleigh and Love) was completed by the GHD geophysics team to provide both a P-wave and S-wave velocity profile (Natale et al, 2004). The geophysical surveys were completed predominantly at the location of dams in the upper and lower storage but also at the proposed powerhouse location. They allowed for identification of features possibly associated with differentially weathered bedding and/or geological structures such as bedding parallel faults. The orientation of the possible structure was checked against the regional geological and reconnaissance mapping and found to generally agree. An example of the geophysical survey results is presented in Figure 6.

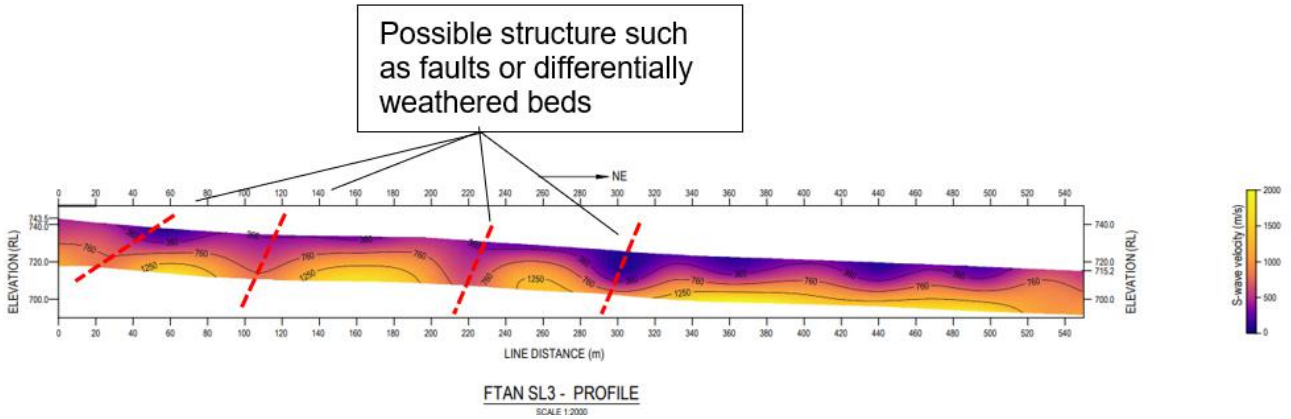


Figure 6: Geophysical survey results presented as FTAN

7 CONCEPTUAL GEOLOGICAL MODEL

Following the desktop study and geological reconnaissance mapping, an initial conceptual geological model was developed to identify potential hazards and opportunities related to the site's geology. This conceptual understanding

helped identify various engineering geological opportunities, uncertainties, and hazards, providing a framework for planning intrusive investigations.

7.1 ROCK (UNITS AND STRUCTURE)

The site is dominated by the folded metasedimentary rocks comprising a mixture of metasiltstone, phyllite and fine to medium grained sandstones. The folding of these rocks has imparted a strong axial planar cleavage in the rocks (particularly the argillaceous rocks) that strikes along the fold axes which is in a generally north to south direction. Two main anticlines and two main synclines plunging towards the south have been identified in the project footprint. A number of complex smaller folds and possible thrust faults have also been interpreted to be present from the interpretation of available lidar data.

The presence of bedding shears and other faulting associated with the folding was considered highly likely. Other faulting including thrust faulting associated with regional tectonic stresses were also considered to be present.

Orthogonal jointing patterns were noted in some of the metasedimentary rock units. The main defect sets are considered to comprise a relatively consistent cleavage set, with additional joint sets that are associated with the folding.

A previously unmapped area of fine to medium grained mafic igneous rock was encountered between the upper and lower reservoirs during the walkover.

Petrographic thin section analysis, completed on hand specimens collected during the walkover, identified these rock types as meta-dolerite and meta-gabbro. Petrographic analysis also identified the presence of actinolite which is a mineral common in altered basic volcanics across eastern Australia. However, this actinolite was noted to be in an acicular and prismatic habit but not in a fibrous or asbestiform habit.

Thick quartz veins were expected across the site aligned with the regional structure.

7.2 SOILS

Soil development across the site was minimal resulting in a generally thin layer (up to approximately 1 to 2 m thickness) of colluvium present on the slopes. This depth of soil is expected to increase towards the base of the valleys where it is reworked into alluvial deposits, but it is anticipated that the depth of soil will generally not exceed 5 m across the site. However, localised, deeper but relatively narrow zones of soil associated with deep weathering of beds or faults were also anticipated. The geophysical surveys indicated that discrete zones of possibly soil strength material could occur to depths of up to 20m below surface.

7.3 HYDROGEOLOGY

It was uncertain how the hydrogeological model and permeability of the rock mass may be impacted by shears and faults; it may be relatively high along these features; or these features may be of low permeability causing localised changes of groundwater conditions over short distances. As permeability of structural features represents a hazard to the project this will be investigated in future stages of geotechnical investigation.

7.4 SUMMARY

In summary, the initial conceptual geological model identified that the rock mass is relatively complex with numerous folds, faults, different lithological units and bedding parallel and bedding cross-cutting igneous intrusions and faults. There is a potential for high permeability along faults and shears. A 3D block model sketch was developed to illustrate the geological relationships and hazards. This sketch (presented as Figure 7) does not show all intrusions and faults or true dips of features and is for illustrative purposes only. Also omitted are lower angle thrust faults and overturned folds.

The ground conditions were identified as being potentially complex at the site, but risks associated with this complexity were deemed to be able to be managed by appropriate scoping of geotechnical and geological investigations and laboratory testing. Materials suitable for construction were identified to be available at the site.

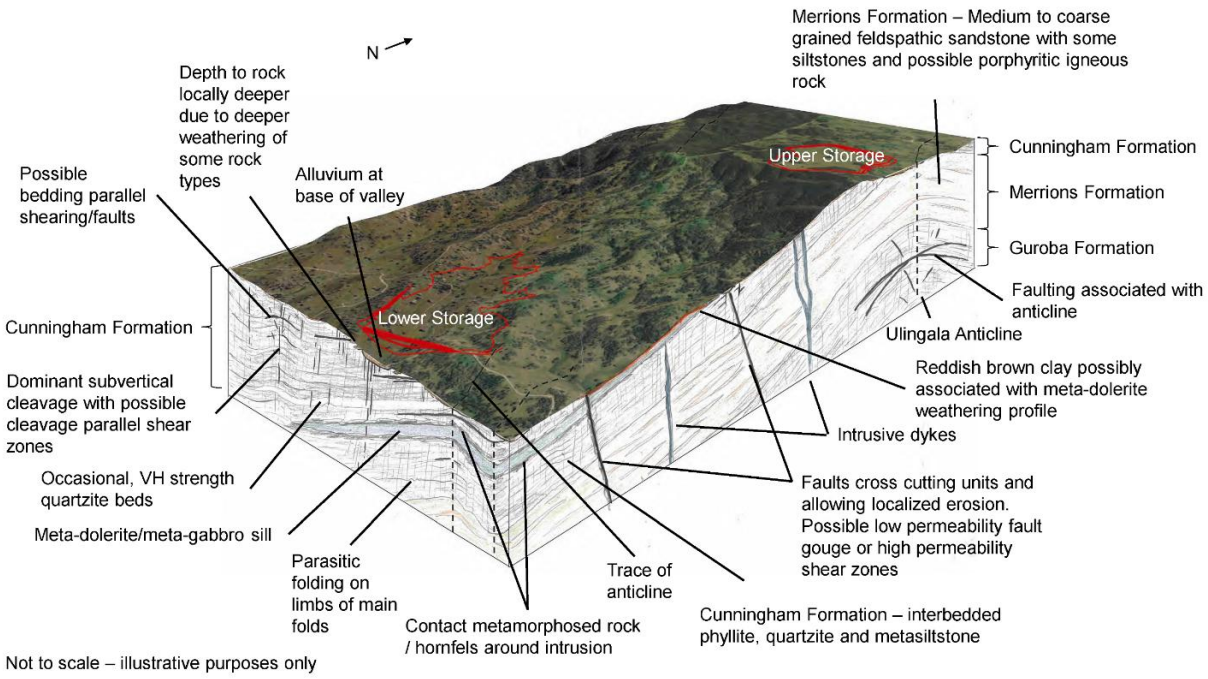


Figure 7: Illustration of conceptual geological model

8 GAP ASSESSMENT AND GEOTECHNICAL RISK REGISTER

Following the desktop study and site walkover and reconnaissance geological mapping, the developed conceptual geological model enabled identification of several hazards and opportunities for the project: It was identified that the geological and geotechnical conditions related to the metasedimentary rock would dominate the majority of the upper and lower dams as well as the bulk of the waterways if an underground option was chosen and that the igneous intrusion would potentially play an important role in design development for the project, depending upon the characteristics of this intrusion below surface. The geological conditions and resultant issues and opportunities are outlined in the table below.

Table 2 Geological Hazards and Opportunities

Geological Condition	Issues	Opportunity	Elements of project potentially impacted
Rock structure	Interbedded and folded and faulted sedimentary sequence leading to variable geotechnical properties such as rock mass strength and permeability (dam foundations) and differing support requirements in tunnels	Relatively predictable north-south striking folds and presence of possible “marker beds” means that major groups of rock units can be understood across the project area and allowed for in design and construction.	All
Phyllite/meta-siltstone rock with dominant cleavage	Excavated rock may be unsuitable for use as rockfill due to tabular nature of blocks. Tunnels and shafts will possibly require more support than in rocks with less structure. Potential instability controlled by rock structure in excavations.	The rock may be easier to excavate due to presence of cleavage. Tunnelling and shaft excavation in the weaker phyllite rock will require less excavation effort than harder rocks in area. Some dams (such as Kangaroo Creek) have effectively used	All

Geological Condition	Issues	Opportunity	Elements of project potentially impacted
	Phyllite rock likely to be unsuitable for use as concrete aggregate due to shape and clay content. Possible durability issues and breakdown of rock once exposed as rockfill.	tabular rock as rockfill – lessons can be learned from such dams	
Vein quartz	Rock will require additional effort to excavate and will be highly abrasive to equipment. Silica dust generation may be high.	Vein quartz expected to have good geotechnical properties	Tunnel and shafts
Igneous meta-gabbro/meta-dolerite rock intrusion along waterway route	This rock may be more abrasive to tunnelling and could be more deeply weathered than the phyllite resulting in more complex anchoring of any surface penstocks. Petrographic analysis indicates presence of the mineral actinolite which elsewhere may take the form of asbestiform minerals with potential health impacts on construction workers. Excavation in the igneous rock may be slower due to more widely spaced joints and higher strength	This area may prove useful for development of quarries for rockfill, concrete aggregate and potentially sand. Better geomechanical conditions may be encountered in the igneous intrusion than in the surrounding metasedimentary rock leading to reduced ground support requirements. Petrographic testing currently indicates that the actinolite is not fibrous and presents a reduced risk to health (in line with other rock dust related illnesses). Additional appropriate testing will be completed to confirm this.	Waterway Rock Quarry Powerhouse
Contact between igneous intrusion and country rock (surrounding metasedimentary rock).	Thermally metamorphosed metasedimentary rock may be of very high strength and abrasive. Alteration may have also reduced strength of igneous rock/metasedimentary rock in vicinity of the contact. Possible brecciation along contact may increase permeability along contact.	Contact may be “tight” and have lower permeability than the shears and crushed seams expected in the metasedimentary rocks. Lower contact could be used as a stratigraphical marker to help constrain the geological interpretation.	Waterway Rock Quarry Powerhouse
Thin residual soil and alluvial/colluvial cover at lower and upper storage and escarpment slopes	Minimal soil available for earthfill Possible instability should seepage from upper storage occur.	Potential for shallow anchoring of surface penstock into competent rock Reduced excavation support required in upper section of shafts Ability to excavate steeper cut slope batters (foliation and bedding dependent due to potential reduced slope stability parallel and subparallel to bedding and foliation). Possibly shallow depth of preparation for rockfill or concrete faced rockfill dam foundations.	Waterway Upper dam Powerhouses

Geological Condition	Issues	Opportunity	Elements of project potentially impacted
"Dip-slope" failures in vicinity of waterway route	Movement of slope could jeopardise waterway. Excavation into slope for access tracks could cause significant failure or requirement for stabilisation.	These areas are relatively easy to identify and can be avoided	Waterway
Pyrite and other sulphide minerals present in the less weathered metasedimentary rocks	Upon excavation, the sulphide minerals may oxidise causing a number of issues including volume expansion and degradation of cut slopes and tunnel walls and possible rockfill. Oxidation would result in release of sulphuric acid and sulfates with potential environmental affects and degradation of concrete structures/shotcrete. Spoil may need to be treated onsite or disposed of offsite.	Testing can be completed to assess this issue. Acid sulfate issues are known and managed at rock fill dams such as Corin Dam in the ACT.	Tunnels, shafts, powerhouses Rock quarries
Groundwater	Groundwater conditions are largely unknown and folded and faulted geological strata could allow for discrete zones of high permeability below dams or into underground excavations.	Minimal surface seepages were observed indicating possible deep groundwater. Faults and strata may also be relatively impermeable.	Upper and lower storage, tunnels and shafts, powerhouse.

9 GEOTECHNICAL INVESTIGATION SCOPING

Following on from the development of the conceptual geological model and identification of hazards and gaps in knowledge, GHD commenced scoping of a targeted phase of preliminary geotechnical investigations.

The investigation scope included:

- Detailed geological mapping across the storage areas and along the penstock routes and of the igneous geology identified in the previous stage to build on the preliminary mapping completed previously. This would provide more information on geological structure, slope instability and lithological variations across the project area. Potential quarry locations were also included in the mapping scope, particularly with respect to the presence of possible igneous rock.
- Excavation of test pits/trenches across the upper and lower storage areas, waterway and possible quarry and borrow areas to depths of between 3 and 4 m or refusal on rock. In possible borrow areas and dam foundations, test pits would be extended for up to 15m in length to allow mapping of the subsurface profile.
- Cored boreholes of varying depth at key locations at the upper storage dams, inlet, waterway, powerhouse and lower storage dam location. These boreholes were oriented as much as possible to maximise intersection of varying geology by inclining the opposite direction to the anticipated foliation/bedding dip direction
- In-situ testing including permeability testing and televiewer surveys were scoped to be completed in all boreholes to allow for an understanding of the depth of "destressing", permeability and rock structure.
- Vibrating wire piezometer installation in six boreholes and dataloggers deployed to monitor seasonal variation of piezometric levels.
- Reverse circulation (RC) boreholes for installation of groundwater monitoring wells at select locations downstream of each embankment and between the two storages. The monitoring wells are to be used for long term water level monitoring and water sampling and were installed within vertical boreholes and constructed such that the invert of the screened interval is located approximated 10 m below first water strike.

Each monitoring well was equipped with water level sensors and dataloggers and sampled quarterly to characterise groundwater quality to provide information for the engineering design of the project and to enable development of

baseline hydrogeological conditions at the site and inform on potential impacts to the underlying aquifer and associated ecosystems.

Whilst downhole measurement of P-wave and S-wave velocity and flowmeter assessments of groundwater flow were not utilised at this stage of investigations they will be beneficial in future stages of investigation.

In the early stages of this project in-situ stress was assessed using a combination of desktop review of regional conditions combined with innovative laboratory testing techniques which will be the subject of a future paper. In-situ stress testing will be completed in future stages of geotechnical investigations now that a good understanding of the geological structure has been developed to assist in targeting of test locations and types.

The information gathered during the geological and geotechnical investigations, would be used to confirm the conceptual geological model or allow for revision.

10 INTRUSIVE INVESTIGATIONS AND RESULTS

The aim of the geological and geotechnical investigations was to characterise the general geological conditions and answer key gaps and provide information to assess the identified project risks and enhance understanding of the impact of these conditions on the various components of the project.

The intrusive investigations completed at the site included excavation of 45 no. test pits, some of which were extended to show a wider exposure of the geological materials, and a total of 15 no. geotechnical boreholes drilled to depths varying from 20 m to 340.6 m below surface. The shallower boreholes were drilled for the dams forming the upper and lower reservoir whilst the deeper holes were for collection of information for the underground waterways which had become the favoured design approach by the commencement of the investigations.

The intrusive investigations identified that the predominant lithology was a fine grained metapelite/metasedimentary rock with occasional beds of fine to medium grained quartzose sandstone that varied in thickness from laminations to medium beds. XRD testing of the sandstones identified that they are quartzose with some carbonate cement and pyrite mineralisation. The sandstone also appeared to be less subjected to metamorphism than the metapelite. Where possible, laboratory testing was targeted at either beds of metapelite or the sandstone to provide information on the range of possible geotechnical properties that could be encountered.

Two boreholes targeted the igneous rock with the results indicating that this was a folded intrusive sill. A zone of silicified hornfels was encountered at the contact between the dolerite sill and the country rock.

Photographs of core from the metasedimentary unit and the dolerite are presented in Figure 8 and Figure 9.



Figure 8: Typical interbedded metasiltstone and sandstone (left) and dolerite (right)

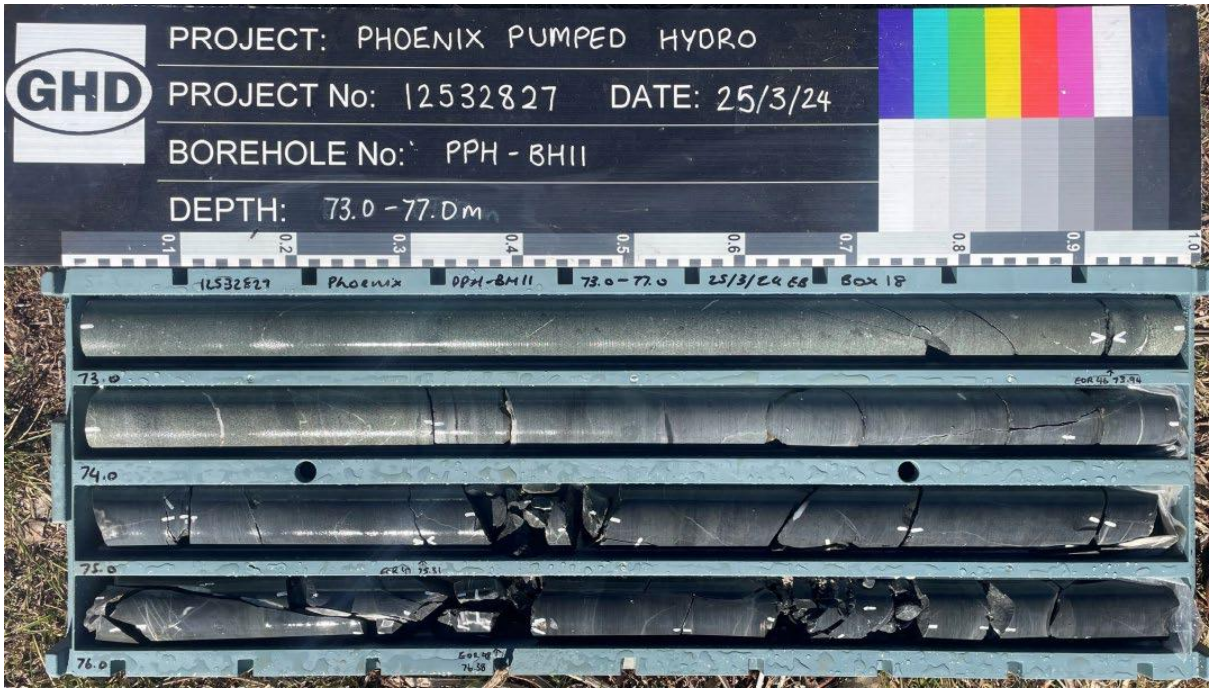


Figure 9: Core through base of sill at 73.95m

In-situ packer permeability testing was completed in each borehole with contiguous testing completed where possible. Generally low Lugeon values were encountered but there were some high takes associated with discrete seams within the rock mass at shallow depths.

A suite of laboratory testing was also completed to understand the variability of key geotechnical parameters and geochemical characteristics. This testing included:

- Unconfined compressive strength (UCS) testing
- Point load testing (PLT)
- Brazilian tensile strength testing
- Density testing
- Cerchar abrasivity testing
- Net acid production and net acid generation testing for assessment of acid sulfate rock
- Petrographic and quantitative x-ray diffraction of rock samples for a combined purpose of assessment of acid sulfate, asbestiform mineral habit screening and also calculation of Equivalent Quartz Content for use in assessment of Rock Abrasivity Index
- Direct shear testing of natural defects

It was identified prior to strength testing that premature failure of samples along foliation may result in a lower-than-expected estimation of strength in the metasedimentary rocks. A wide scatter in testing results was also observed in the results from testing of the dolerite with this possibly related to microscopic fracturing of the dolerite imparted during folding but which cannot be observed at hand specimen scale. Additionally, when compared with the estimated strength using an approximate relationship of Brazilian tensile strength testing to UCS as per Ribeiro et al (2015) (*UCS=Brazilian tensile strength x 10)* a significantly lower strength was encountered with the UCS and PLT testing in the interbedded sedimentary rocks. This was attributed to failure upon foliation in the metasedimentary rock. The lower strengths did also not match with the field descriptions of strength (generally high to very high).

PLT results are presented in Figure 10 showing the large scatter of testing results in the dolerite, and overall lower strength results in the metasedimentary rock. In general, the metasiltsone was medium to high strength and the dolerite was very high to extremely high strength.

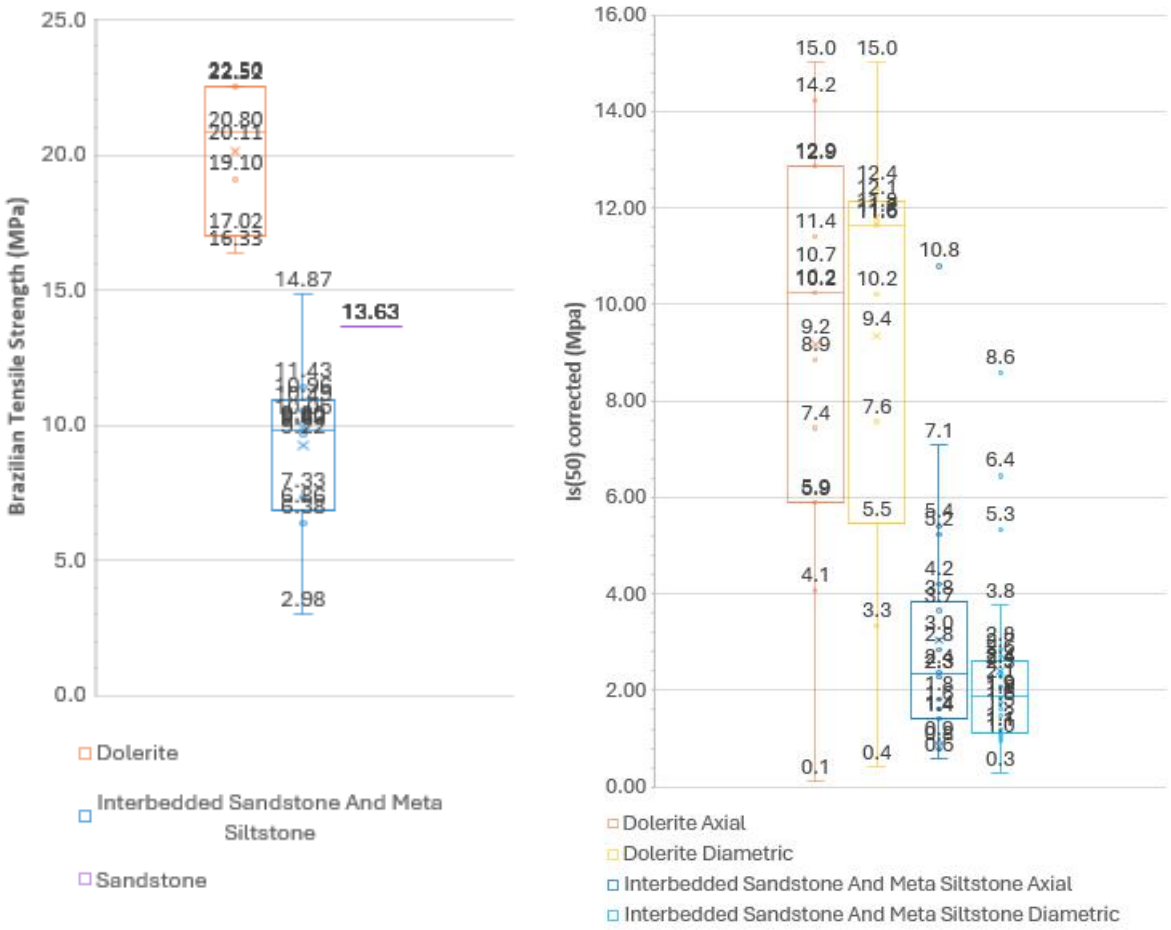


Figure 10: Brazilian tensile strength (left) and point load testing results (right)

Cerchar abrasivity testing was found to have a large scatter of results which likely relates to the relatively constrained test length (10 mm) which may not travel over the most abrasive mineral crystals or grains in the rock. The rock abrasivity index as outlined by Plinninger, 2010 appeared to provide much more consistent results related to the varying rock types present across the site with both the metasiltstone and dolerite being about the same abrasivity with the hornfels having the greatest abrasivity.

With all sedimentary rock derived from a deep ocean environment there is a potential for the presence of pyrite and other sulfides which can oxidise upon exposure to the atmosphere. This can have both environmental and engineering implications, with the potential for acidic water and sulfate damage to steel and concrete. As pyrite was frequently logged in the borehole core either as defect coatings, as nodules or disseminated through the rock substance, it was determined that testing was required to assess the hazard. A number of geochemical tests were completed with the results indicating that in most cases the rock has sufficient carbonate or other buffering minerals to neutralise the acid produced. Additional testing is required to confirm this at future stages of design.

Due to the presence of actinolite, an amphibole mineral resulting from alteration of pyroxenes, and the potential for these minerals to be asbestiform in habit, a preliminary screening exercise was completed using petrographic analysis methods. In addition, engineering geologists completing the mapping and logging were briefed on the potential presence of asbestiform minerals and its identification prior to the geotechnical investigations commencing. A naturally occurring asbestos management plan was also prepared to manage the health and safety risks if asbestiform minerals were encountered. To date no asbestiform actinolite has been encountered with the dominant crystal habit being acicular or prismatic.

The drilling investigations also confirmed the hydrogeological model with a fractured bedrock aquifer with sheared zone controls on increased permeability. The aquifer is in some locations semi-confined due to weathering and alluvium and colluvium cover.

11 DETAILED GEOLOGICAL MAPPING

Detailed geological mapping was completed at scale of 1:1000 over the project area primarily to gain information on the lithological variation across the site but also to collect structural geological data. The mapping was completed during the initial stages of the drilling investigations with the aim of allowing findings to influence the remaining scope of the intrusive investigations.

The mapping was able to determine the complex boundary of a mafic sill which has intruded into the metasedimentary rocks by a combination of a dominant brownish red soil colouration and hornfelsed zone that was found to be more resistant to weathering and erosion in the landscape. Once the structure of the sill was better understood, a review of high-resolution aerial photography revealed that the contrasting-coloured soils also gave an indication of the location of the sill, albeit affected in some locations by colluvial processes.

The detailed geological mapping was successful in confirming the geological structure away from the intrusive boreholes that had been drilled immediately prior to the mapping and provided almost immediate information to update the conceptual geological model and revise the drilling investigation scope to provide confirmation of the structure and geotechnical implications.

12 OPTIMISATION OF DESIGN DURING INVESTIGATIONS

A preliminary structural interpretation was completed immediately after completion of detailed geological mapping and this, along with the collected borehole data, supplemented the conceptual geological model which was assessed and then visualised in 3D space in Seequent's Leapfrog Works. The detailed surface geological mapping allowed for confirmation of the outcrop location and structural orientation and the boreholes provided information on the subsurface shape of the sill. Using this information, the sill was modelled in 3D and it was realised that the powerhouse silos could be repositioned and rotated to make better use of the dolerite and its more advantageous geotechnical characteristics (higher strength and wider joint spacing). Prior to the cessation of the drilling program, an additional borehole was designed and drilled to allow confirmation of the sill structure and the revised powerhouse location was confirmed. Figure 11 shows a geological section with the relocated powerhouse to be largely within the dolerite sill.

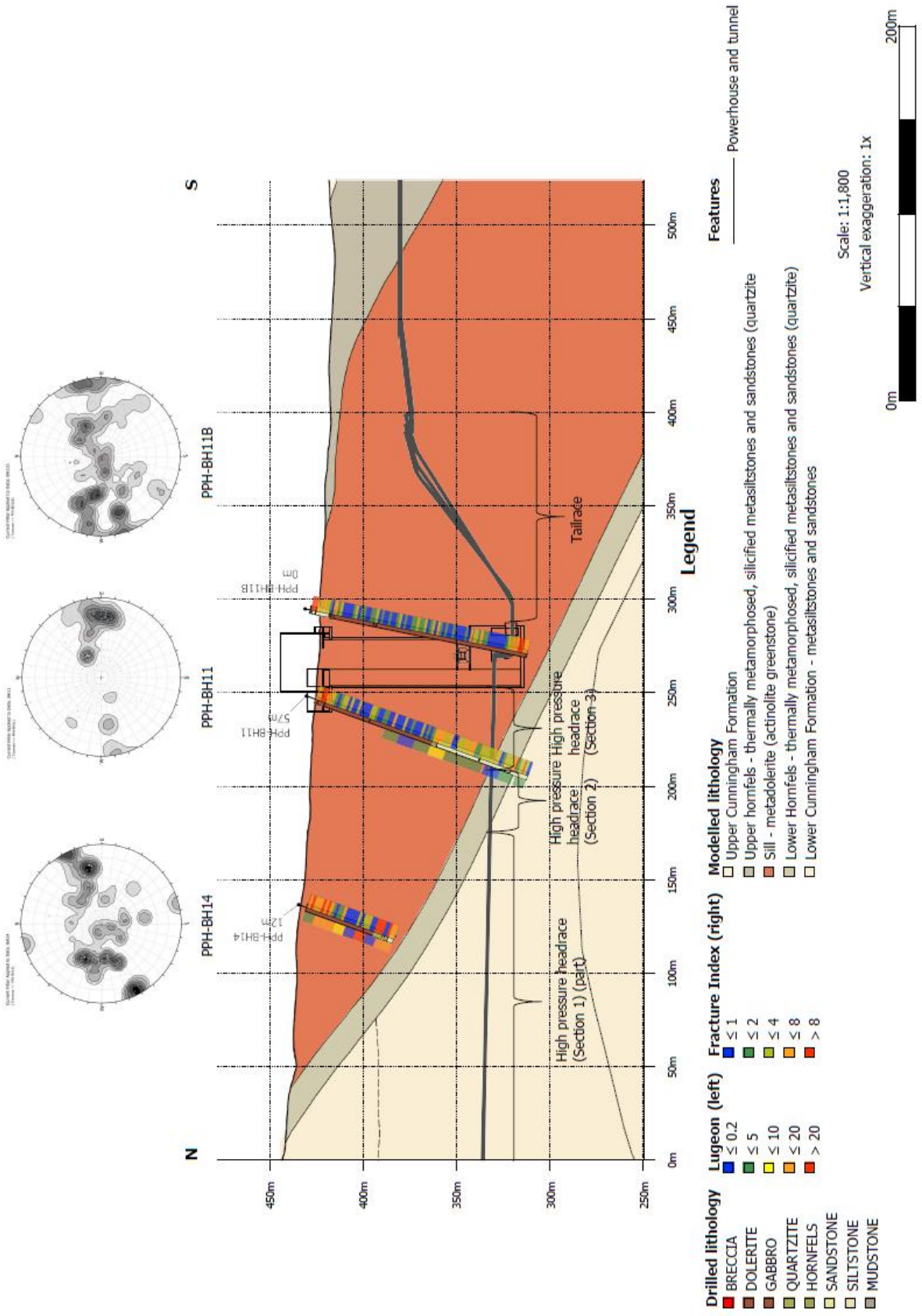


Figure 11: Geological section through powerhouse after relocation of structure

13 CONCLUSIONS

The use of “traditional” geological skills such as detailed surface geological mapping, understanding and application of structural geology concepts alongside the use of surface and aerial geophysical data, intrusive investigations, in-situ testing and laboratory testing in conjunction with 3D geological model visualisation allowed for the efficient and rigorous understanding of the engineering geology of the site.

The staged geotechnical investigation approach and iterative development of a conceptual geological model as part of the engineering geological model knowledge framework not only allowed for the effective delivery of a feasibility design for a complex pumped hydropower project but also allowed for agile and rapid optimisation of the project during design to better make use of more favourable geotechnical conditions. The engineering geological model development framework provides a methodical and technically rigorous approach to the understanding and management of ground hazards.

The rapid optimisation in the midst of the geotechnical investigations was only possible due to the effective transfer of data and verbally communicated information from site to the office and this information being used in the interpretation immediately. This approach was only viable as GHD was completing both the design and the investigations. This approach is recommended for all projects with compressed timeframes and the requirement for the use of ground investigation data in the design process in near real time of collection.

14 ACKNOWLEDGEMENTS

The author is grateful to ACEN Phoenix for permission to write this paper and their recognition of the importance of engineering geology in renewable energy projects. Thanks also to Dr Brendan Duffy and Ryan Hayes who completed the detailed geological mapping which proved the immense value of surface geological mapping and the rest of the GHD team who completed and managed the geotechnical investigations.

15 REFERENCES

Baynes, F.J. and Parry, S. (2022) Guidelines for the development and application of engineering geological models on projects. International Association for Engineering Geology and the Environment (IAEG) Commission 25 Occasional Publication No. 1, 130 pp.

Cas, R. (1976) The Merrions Tuff – Its Genesis, Bulletin of the Australian Society of Exploration Geophysics, 7(1), pp. 14-25.

Meakin, N.S. and Morgan, E.J. (1999) Dubbo 1:250 000 Geological Sheet SI/55-4, 2nd Edition: Explanatory Notes. Geological Survey of New South Wales, Sydney.

Morgan, E.J., Scott, M.M. and Cameron, R.G. (2000) Euchareena 1:100 000 Geological Sheet 8732, 1st edition. Geological Survey of New South Wales, Sydney & Geoscience Australia, Canberra.

Natale, M., Nunziata, C. and Panza, G. (2004) FTAN method for the detailed definition of Vs in urban areas, in Proceedings of the 13th World Conference on Earthquake Engineering.

New South Wales Department of Primary Industries (NSW DPI) (2025) MinView, New South Wales Government, Sydney. Viewed April 2025 [https://minview.geoscience.nsw.gov.au/#/?lon=148.5&lat=-32.50000&z=7&l=].

Plinninger, R. (2010) Abrasivity assessment using the "Rock Abrasivity Index (RAI)” - Following eight years of application, in Geologically active: proceedings of the 11th IAEG Congress, Auckland, New Zealand, 5-10 September 2010.

Ribeiro, P., Oliveira, M. and Nelson, P. (2015) Correlation Between Uniaxial Compressive Strength and Brazilian Tensile Strength Using Different Rock Types, 10.20906/CPS/GJ-13-0005.

Schofield, A. and Roberts, N. (2024) Applying the engineering geological model approach to Quaternary glacial geology in western Tasmania, Australian Geomechanics Journal.

https://doi.org/10.56295/1ACEG32

DEVELOPMENT OF A GEOTECHNICAL ROCK MASS MODEL USING GEOCHEMICAL DATA AND MACHINE LEARNING

Megan Baker, Sue Chan, Christine Lion and Daniel Strang
PSM

ABSTRACT

In mining, the development of a realistic and well-informed engineering geological model can be challenging. Mining projects typically present with sparse geotechnical data and variable ground conditions, resulting in challenges with the interpretation of geotechnical unit boundaries, and the development of a three-dimensional model. This paper presents a case study where geochemical data collected for orebody knowledge definition was used to develop a rock mass model to inform pit slope design. During model development, borehole domaining assisted by machine learning was trialed to improve model reliability and enhance efficiency. This paper has demonstrated that an automated approach to rock mass classification using geochemical data is an effective and useful method which can be incorporated into the geotechnical model development process.

The methodology adopted for rock mass classification and model development is summarised below:

- Rock mass classification of geotechnical boreholes based on logging data and core photographs.
- Selection of 'twin' reverse circulation (RC) boreholes (adjacent to geotechnical boreholes).
- Comparison of downhole geochemical data against the logged rock mass unit intervals.
- Identification of geochemical signatures associated with each rock mass unit.
- Trial of machine learning methods to identify and classify rock mass units using geochemical data.
- Apply the results of the machine learning to a wider dataset with the objective of producing a 3D rock mass model.

1 INTRODUCTION

The concept of using 'indirect' data sources (i.e. geochemical and geophysical data) to interpret the boundaries of geotechnical detrital units in the Pilbara was introduced by Baxter (2016). The methodology described uses secondary data sources (collected during geological investigations) to supplement geotechnical site investigation data and in turn increase the confidence of the geotechnical model. This methodology has also been used by Noble, Hemraj and Eggers (2021), where geochemical signatures for Cenozoic cover sediments were identified and applied to a series of 2D cross sections which were then used to interpret the geotechnical model.

This paper aims to expand on the work completed by Baxter (2016) and Noble et al (2021), by using machine learning methods to assign rock mass unit boundaries based on geochemical signatures. The current methodology for assigning rock mass units using geochemical data has only been applied in a 2-dimensional sense, with boreholes being characterized along key geotechnical sections. Although the development of geotechnical sections in areas of elevated geotechnical risk is crucial for analysis and slope design, the current method for assigning domains is time consuming, relies heavily on interpretation and assumes that the areas of highest geotechnical risk are known. Machine learning methods however, are expected to provide a quick approach to assigning rock mass domains and will likely require minimal manual interpretation of the data, providing the human geologist/engineer more time for detailed interpretation. Machine learning methods will also allow for the processing of large datasets which can be used to develop a 3-dimensional model. This paper presents the results of a machine learning trial where machine learning methods have been used to interpret geotechnical rock mass unit boundaries using geochemical data.

2 BACKGROUND

The dataset available for the machine learning trial is from an iron ore deposit in the Pilbara Region of Western Australia. The projects mineralisation is hosted in the Marra Mamba Iron Formation (of the Hamersley Group) which is buried beneath Cenozoic aged detrital sediments. These Cenozoic detrital sediments are geotechnically challenging due the high variability in the rock mass conditions and the uncertainty surrounding the spatial distribution of units.

The project itself is proposed to be a large open pit operation with the construction of relatively shallow (~120 m deep) satellite pits which will be spread over a large area (approx. 200 km^2). The project is currently in the early stages of design and has limited geotechnical data with only eight (8) geotechnical boreholes drilled across the proposed development

area. Therefore, defining the spatial distribution of the geotechnical units is key to the geotechnical model and the overall slope design.

3 GEOLOGICAL OVERVIEW

The project is located in the Hamersley Province in the Pilbara region of Western Australia. Archean to lower-Proterozoic bedrock sequences in the area comprise the Marra Mamba Iron Formation, the lower most unit of the Hamersley Group. Dominant lithologies of the Hamersley Group include banded iron formation (BIF) interbedded with shale, dolomite, and acid volcanics which are intruded by dolerite sills and dykes.

Iron enrichment for the deposit is concentrated within the Detrital sequence and the BIF of the Marra Mamba Iron Formation. The Marra Mamba Iron Formation outcrops in the north along the Chichester range and is buried under Cenozoic aged sediments towards the south. These Cenozoic sediments contain Detrital Iron Deposits (DID) which are hematite-goethite rich colluvial/alluvial deposits derived from the erosion of banded iron ores hosted in the Marra Mamba Iron Formation. A geology map of the Pilbara Region showing the Hamersley group rocks and known occurrences of channel iron deposits is shown in Figure 1.

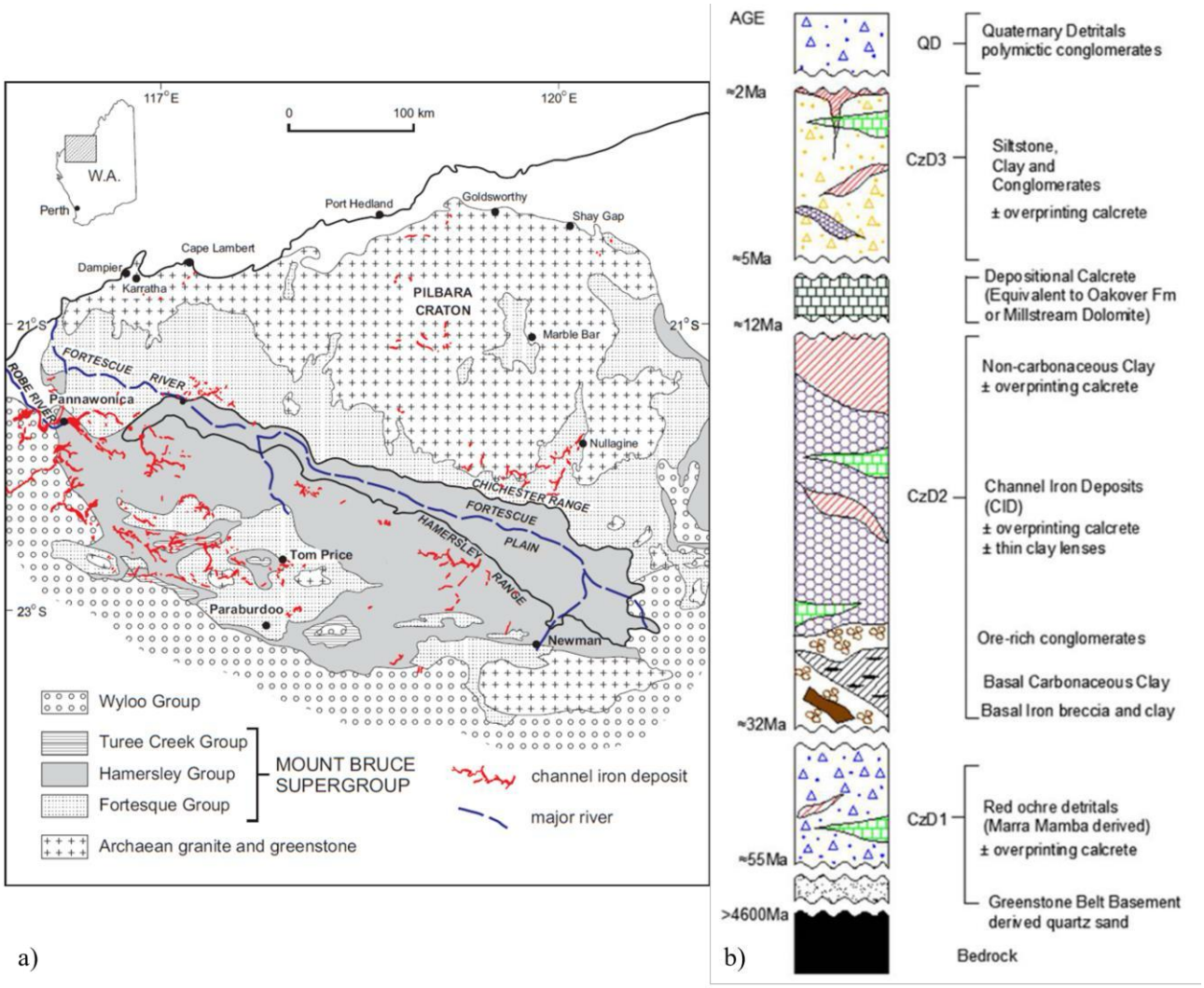


Figure 1: (a) Geology and Channel Iron Deposits of the Pilbara Region (Stone, 2005); (b) Suggested Stratigraphic column for Pilbara Cenozoic Detrital sequences (Baxter, 2016).

3.1 GEOLOGICAL HISTORY OF CENOZOIC DETRITALS IN THE PILBARA

The DID settings are typically hosted in Marra Mamba to Brockman Iron Formation Strike Valley (MBSV) environments. Figure 1 shows a suggested stratigraphic column for the Cenozoic detrital sequences produced by Baxter (2016). The DID sequences have been grouped based on their geological nature and depositional character. These three main detrital groups are described below.

- CzD1 (Cenozoic Detritals 1), oldest
  - Red ochre detritals, including a hematite conglomerate, basal conglomerates and a cemented vitreous hardcap
- CzD2 (Cenozoic Detritals 2)
  - Iron rich pisolites, lacustrine clays, overprinting calcretes and iron rich conglomerates with varying degrees of cementation
- CzD3 (Cenozoic Detritals 3), youngest.
  - Alluvial sediments such as siltstones and conglomerates.

4 AVAILABLE DATA

Limited geotechnical data was available for the project. The data available included:

- Eight (8) geotechnically logged diamond boreholes with core photographs
- Seventy-Eight (78) historic diamond boreholes with geological logging and core photographs. Three (3) of which were used in this assessment.
- Eleven (11) neighbouring Reverse Circulation boreholes (RC) with the following data:
  - Geological logging
  - Geochemical assay results including weight percentages of the elements Fe, SiO_2, Al_2O_3, P, Mn, LOI, S, TiO_2, CaO, MgO, K_2O and Zr
  - Geophysical data including density, gamma, resistivity and susceptibility for 8 of the 11 RC holes
- An additional ~9,500 RC boreholes were available across the project with geological logging and geochemical assay data. Geophysical data was also available for most of these boreholes (~8,970 holes).
- A geological model with the following surfaces:
  - Base of CzD3
  - Base of CzD2
  - Base of Detritals
  - Base of Archean units, i.e. Mount Newman, MacLeod and Nammuldi Members.

The diamond boreholes available were primarily drilled for geometallurgical purposes and were often not cored through the detrital sequence. Therefore, only three of the historic diamond boreholes were used in this assessment as rock mass classification could not be completed without core photographs.

Machine learning requires a complete dataset to train the model and make reliable predictions. An incomplete dataset may disrupt the learning process and generate inaccurate results. As geophysical data was not available for all of the neighbouring twin RC holes, the geophysical data has been excluded from the machine learning model.

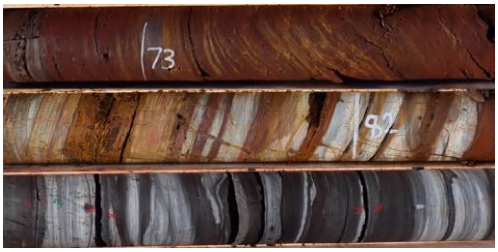
5 GEOTECHNICAL ROCKMASS UNITS

Rock mass units were assigned based on the interpreted stratigraphy of the geotechnically logged boreholes. The lithology, strength, geotechnical conditions and variability of each unit were considered when grouping rock mass types with similar geotechnical characteristics. Several geotechnical rock mass units occur within the detrital sequence. The typical characteristics and strengths of each rock mass unit are described in Table 1. The field estimated strengths are based on AS 1726:2017 Geotechnical site investigations (Standards Australia, 2017) and the CANMET 'Pit Slope Manual' (Herget, 1977). Typical photos of each rock mass unit are shown in Table 1.

Table 1: Observed Geotechnical Rock Mass Units

Geotechnical Rock Mass Unit	Field Estimated Strength	Example Photograph
Quaternary Detritals A polymictic conglomerate of BIF, hematite and shale clasts in a moderately consolidated silty matrix. Clasts are typically sub-angular and range from fine gravel to cobble.	Very stiff soil to low rock strength (S4 to R2)	

Geotechnical Rock Mass Unit	Field Estimated Strength	Example Photograph
Calcrete Typically observed as orange-brown and white overprinting of the shallow detritals and clayey units. Vigorous reaction with HCL. The presence of calcrete is indicative of saline groundwater.	Low to medium rock strength (R2 to R3) ~10% Extremely low rock strength (R0)	
Gravelly Siltstone Fine to coarse gravels of sub-rounded to sub-angular BIF and hematite in a silt matrix. Commonly moderately consolidated and matrix dominated. Pisolitic zones occur towards the base of the unit.	Very stiff soil to very low rock strength (S4 to R1)	
Pisolite Fine to medium pisoid nodules in a silt matrix. Pisoids are rounded to sub-rounded and are strongly magnetic. Moderately consolidated to unconsolidated in parts.	Very stiff soil to very low rock strength (S5 to R1), cemented in parts (~20% R2 to R4)	
Lacustrine Clay A clay-rich unit comprising ~60% clay and ~40% gravelly clay and breccia. Typically, massive with occasional relict bedding. Mottled texture in areas due to iron staining and manganese alteration.	Very stiff soil to extremely low rock strength (S4 to R0)	
Hematite Conglomerate Fine to medium gravels of sub-rounded to sub-angular hematite clasts in a silt matrix. Predominantly clast supported with a silt matrix. Moderately consolidated and indurated in parts.	Bimodal strength, typically low to high rock strength (R2 to R4), with ~10% very stiff to hard soil (S4 to S5)	
Cemented Detritals Iron rich gravelly, cemented and hydrated detritals. Overprinting of the clastic texture occurs in parts as the rock has a 'welded' appearance. When hydrated it is difficult to distinguish from in-situ Canga/Hardcap units. Vughy in parts.	Low to high rock strength (R2 to R4), ~5% very high rock strength (R5)	
Clayey Breccia Colluvium Highly variable in appearance from a gravel dominated breccia to cobbles and boulders of Canga interspersed with laterally discontinuous clays. Clast sizes and proportions are highly variable.	Bimodal strength, typically very stiff soil to very low rock strength (S4 to R1), ~15% low to high rock strength (R2 to R4)	

Geotechnical Rock Mass Unit	Field Estimated Strength	Example Photograph
Cangarised BIF Highly to extremely weathered BIF, non-magnetic and steely in parts. Vughs often elongated parallel to bedding and occasionally infilled with clay. Bedding typically indistinct and overprinted.	Very low to high rock strength (R1 to R4) with pockets of (~10%) very stiff to hard soil (S4 to S5)	
Archean Bedrock Interbedded Shale and Banded Iron Formation (BIF). Occurs as hydrated, highly to moderately weathered, mineralised and Fresh. Hematite and goethite rich zones occur when mineralised. Fresh BIF is present at depth.	**Mineralised BIF**: Friable to medium rock strength (S5-R3) **Weathered BIF:** Medium to high rock strength (R3 to R4) **Fresh BIF:** medium to very high rock strength (R2 to R5)	

6 TWIN ASSESSMENT

To distinguish geochemical signatures for each geotechnical unit, a comparison of diamond core and RC twin boreholes was undertaken. The twin holes are pairs of cored and RC holes located as close as possible to each other (up to 20 m) and are usually positioned on the same drill pad. All diamond holes with logged geotechnical rock mass units were reviewed for the twin assessment. Assay data from each twin hole was compared with the rock mass unit boundaries of the corresponding geotechnical borehole to identify marker signatures in the unit boundaries. A typical comparison log showing the logged geotechnical units of the diamond borehole and the geochemical data of the RC hole is shown in Figure 2. The example presented shows obvious geochemical variations downhole which can be correlated back to the boundaries of the different detrital units.

Geotechnical Borehole Rock Mass Units	Depth (m)	RC Borehole Geochemical Assay Data											
		Fe (%)	SiO2 (%)	Al2O3 (%)	P (%)	Mn (%)	LOI (%)	S (%)	TiO2 (%)	CaO (%)	MgO (%)	K2O (%)	Zr (%)
Quaternary Detritals	0 - 10	17.16	58.1	10.55	0.025	0.04	4.88	0.019	0.593	0.11	0.3	0.487	0.018
Gravelly Siltstone	10 - 12	17.98	48.95	16.11	0.022	0.03	6.49	0.019	1.201	0.1	0.36	0.568	0.031
	12 - 14	18.91	47.39	16.36	0.023	0.03	6.62	0.016	1.238	0.1	0.31	0.46	0.033
	14 - 16	18.08	47.75	16.86	0.022	0.02	7.05	0.016	1.215	0.12	0.29	0.412	0.03
	16 - 18	27.03	41.76	11.95	0.021	0.02	5.57	0.023	1.046	0.07	0.22	0.278	0.027
	18 - 20	37.65	27.78	10	0.025	0.03	6.7	0.03	0.785	0.05	0.16	0.14	0.02
Cemented Detritals	20 - 22	54.68	6.37	4.72	0.027	0.005	9.83	0.037	0.198	0.03	0.09	0.018	0.005
	22 - 24	56.74	5.14	4.36	0.023	0.01	9.1	0.028	0.113	0.02	0.08	0.016	0.005
	24 - 26	42.25	14.48	13.02	0.025	0.04	10.57	0.025	0.54	0.05	0.16	0.024	0.015
Lacustrine Clay	26 - 28	12.38	37.36	30.69	0.013	0.01	12.5	0.009	0.79	0.11	0.31	0.029	0.019
	28 - 30	6.44	41.1	34.09	0.009	0.02	12.8	0.006	1.957	0.1	0.31	0.037	0.035
	30 - 32	3.28	42.43	36.05	0.007	0.06	13.16	0.002	2.594	0.07	0.27	0.023	0.041
	32 - 34	3.36	42.12	36.29	0.008	0.04	13.18	0.002	2.68	0.04	0.24	0.025	0.04
	34 - 36	3.75	38.89	37.43	0.01	0.02	14.57	0.006	2.758	0.04	0.23	0.024	0.049
	36 - 38	2.8	41.5	36.09	0.019	0.1	13.36	0.008	3.843	0.06	0.23	0.022	0.056
	38 - 40	1.23	45.23	35.63	0.036	0.005	11.21	0.001	1.956	0.08	0.84	2.702	0.027
	40 - 42	25.01	27.11	21.24	0.079	0.36	11.29	0.005	1.077	0.08	0.64	1.603	0.026
Banded Iron Formation	42 - 44	37.62	17.92	13.77	0.072	0.83	11.73	0.013	0.729	0.06	0.28	0.048	0.017
	44 - 46	59.46	3.42	1.84	0.063	0.19	8.75	0.006	0.098	0.01	0.09	0.022	0.002
	46 - 48	59.31	4.47	3.37	0.047	0.14	6.55	0.006	0.259	0.01	0.08	0.012	0.007
	48 - 50	59.75	3.86	2.21	0.065	0.21	7.4	0.008	0.118	0.01	0.07	0.017	0.003
	50 - 52	60.3	3.71	1.91	0.072	0.2	7.25	0.008	0.096	0.01	0.08	0.016	0.003
	52 - 54	46.04	27.15	1	0.063	0.2	5.03	0.005	0.042	0.01	0.09	0.022	0.003
	54 - 56	45.13	28.67	0.95	0.064	0.24	5.01	0.006	0.043	0.01	0.1	0.024	0.003
	56 - 58	40.37	33.06	2.09	0.069	0.36	5.77	0.009	0.118	0.02	0.13	0.033	0.005
	58 - 60	55.67	9.27	2.23	0.123	0.36	7.51	0.008	0.088	0.02	0.12	0.02	0.001
	60 - 62	55.09	5.4	3.63	0.141	0.84	9.81	0.007	0.159	0.02	0.1	0.126	0.003
	62 - 64	58.98	3.7	1.59	0.155	0.33	9.2	0.006	0.066	0.02	0.07	0.057	0.002
	64 - 66	50.62	17.85	0.87	0.143	0.16	7.84	0.005	0.059	0.02	0.07	0.02	0.003

Figure 2: Example comparison log showing inferred rock mass units in the geotechnical borehole (left) and the assay data of the nearby RC twin (right)

7 GEOCHEMICAL SIGNATURES

Geochemical signatures were derived for each rock mass unit during the twin assessment. A series of histograms were produced for each unit to compare element percentages. Using the histograms, grade cut off values were determined based on the spread of the data. Rock mass units which indicate strong geochemical signatures include, lacustrine clay and calcrete. Iron rich units such as hematite conglomerate, pisolite and cemented detritals have very similar geochemical signatures and are difficult to differentiate. Due to the nature of the clayey breccia colluvium, a mixed breccia and clay, there are large variations in the geochemistry. These variations make the unit difficult to distinguish.

The geochemical signatures identified for the project are presented in Table 2.

Table 2 – Geochemical signatures identified for the project

Unit	Typical Assay Value (%) (1)										
	Fe	SiO2	Al2O3	LOI	Mn	CaO	MgO	TiO2	K2O	S	P
Quaternary Detritals	<30	>40	8-18	3-12	<1	<6	<3	0.3-1.3	0.4-1.9	<0.3	0.02 - 0.04
Gravelly Siltstone	10-50	10-60	8-22	4-12	<1	<1	<1	0.7-1.5	<1.5	<0.2	0.01-0.08
Pisolite	25-50	<35	10-25	3-13	<1	<1	<1.5	1-1.7	<0.3	<0.1	<0.04
Calcrete	<15	30-40	7-12	>10	<1	>10	>4	<0.5	<1	<0.5	<0.03
Cemented Detritals	35-60	<25	4-15	5-13	<1	<1	<1	<1.2	<0.2	<0.1	<0.15
Hematite Conglomerate	30-50	<40	<15	<12	<3	<1	<1	<0.6	<0.2	<0.1	<0.07
Lacustrine Clay	<35	10-50	16-40	10-15	<1	<1	<1	<3	<0.2	<0.1	<0.1
Clayey Breccia Colluvium	10-50 (varies)	5-75	5-25	<12	<1	<1	<1	<1.2	<0.2	<0.1	<0.06
Canga	>35	<30	2-10	5-15	<2	<3	<2.5	<0.8	<0.5	<0.2	0.01-0.03
Bedrock	varies	varies	<5	<15	<2	<1	<1	<0.5	<0.2	<0.4	<0.15

(1) The highlighted cells indicate elements which have diagnostic signatures for specific units

8 MACHINE LEARNING

In order to use the geochemical signatures identified and apply the signatures to a large dataset, a fast and reasonably accurate algorithm is required to domain boreholes based on the geochemistry. Machine learning is a form of artificial intelligence that can be used to analyse large datasets. It identifies and learns patterns from data to make decisions with minimal human intervention. Machine learning has fast processing capabilities and once the model is trained, it requires minimal input to generate results. Because of these factors, machine learning has been trialled to domain the boreholes with geochemical data.

During the machine learning trial, many different algorithms were tested and used to develop the classification model. In this paper we present the final results obtained with the best performing models.

8.1 DATA STATISTICS

The primary case study for this paper has a relatively small dataset with only 11 geotechnically logged diamond boreholes with RC twins. The twin RC boreholes have geochemical assay data in 2 m intervals and occasionally 10 m intervals. Some assay intervals used for training contained multiple inferred geotechnical units. In this instance, the dominant detrital unit (i.e., the unit covering over half of the assayed interval) was adopted for the entire interval. The available assay data for the project comprises weight percentages of the following elements, Fe, SiO_2, Al_2O_3, P, Mn, LOI, S, TiO_2, CaO, MgO, K_2O and Zr. Machine learning relies on data consistency. Therefore, elements without a complete dataset (e.g. Zr) were not used to build and train the model.

Table 3 summarises the available samples of geochemical data for each geotechnical unit. The Marra Mamba Iron Formation and gravelly siltstone units represent 58% of the total population of data. Some detrital units such as hematite conglomerate, calcrete and silcrete comprise less than 2% of the whole dataset. These units with low sample numbers tend to have specific geochemical or geotechnical characteristics and have therefore been kept independent to avoid noise in the data.

Table 3 – Number of Samples for Each Geotechnical Rock Mass Unit

Unit	Number of Samples	Percentage (%)
Quaternary Detritals	19	6
Gravelly Siltstone	82	24
Pisolite	33	10
Calcrete	2	<1
Cemented Detritals	31	9
Hematite Conglomerate	6	2
Lacustrine Clay	9	3
Clayey Breccia Colluvium	13	4
Canga	21	6
Silcrete	2	<1
Bedrock	123	36
Total	**341**	**100**

8.2 MACHINE LEARNING MODEL

Due to the small size of the available dataset, a 10-fold cross validation method was used to build and evaluate the model. For each iteration 90% of the data was randomly selected to train the model, and the remaining 10% was used to test the model. The representation of each rock mass unit in the dataset was imbalanced, with some units, such as the Marra Mamba Iron Formation, representing 36% of the dataset and the lacustrine clay only representing 3%. Due to the data imbalance, the model will not perform well at identifying lacustrine clay unless it has strong distinguishable geochemical characteristic. A two-step method for model development was adopted to overcome this issue:

1 Build a model to identify two units: Marra Mamba Formation versus 'the rest'
2 Build a model that classifies the remaining detrital units.

8.3 MODEL PERFORMANCE

After testing different methods, which we will not detail here, the Random Forest Classifier (RF) algorithm for both steps was adopted, as it provided an overall accuracy of 82% in assigning rock mass units. In machine learning and data analysis, the common metrics for evaluating a models performance include sensitivity/recall, specificity, precision and F-score. F-score is a measure of a model's accuracy and is the harmonic mean of precision and recall. A high F-score indicates high precision and recall while a low F-score suggests poor model performance. When working with imbalanced datasets, the F-score is an important metric to consider as it can indicate whether the model is overpredicting or underpredicting certain classes. Table 4 presents the sensitivity, specificity, precision and F-score results for all units classified by the RF model algorithm.

In terms of the model performance, we observe that:

- Marra Mamba Formation, gravelly siltstone, lacustrine clay, Quaternary detritals, cemented detritals and pisolite all have an F-score greater than 70%
- The F-score could not be calculated for hematite conglomerate as none of the samples were predicted correctly in the cross-validation
- Comprising more than a half of the total population, both Marra Mamba Formation and gravelly siltstone can be predicted with high accuracy by the machine
- Lacustrine clay has the third-highest F-score with a precision of 100% and a sensitivity of 67%. This indicates that no other lithology samples are classified as lacustrine clay mistakenly, however, some lacustrine clay samples are incorrectly predicted as other units

- Both Quaternary detritals and cemented detritals have a sensitivity higher than the precision as false positive results are greater than false negative results for these lithologies. This means samples tend to be predicted into these lithologies mistakenly
- Pisolite, calcrete, clayey breccia colluvium, and lacustrine clay are classified with higher precision than sensitivity. The false negative results for these lithologies are greater than the false positive results, indicating that their samples tend to be predicted as other lithologies.

Table 4: Specificity, sensitivity, precision and F-score results for all units

Unit	Sensitivity (average %)	Specificity (average %)	Precision (average %)	F-score (average %)
Quaternary Detritals	89	98	71	79
Gravelly Siltstone	87	92	78	82
Pisolite	64	98	81	71
Calcrete	50	100	100	67
Cemented Detritals	84	95	65	73
Hematite Conglomerate	0 (1)	99	0	Undefined (2)
Clayey Breccia Colluvium	38	99	56	45
Lacustrine Clay	67	100	100	80
Canga	57	97	52	55
Bedrock	86	95	91	88

(1) The highlighted cells indicate results with <50% sensitivity, specificity, precision or F-score
(2) Metrics are undefined when the calculations result in a division by 0 and there are no positive predictions.

8.4 RESULTS

The data imbalance and the size of the dataset are the limiting factors for this case study. The rock mass unit with the highest weighting was classified first to reduce the data imbalance when classifying the remaining units. The model developed can classify Quaternary detritals, gravelly siltstone, pisolite, cemented detritals, lacustrine clay and the Marra Mamba Iron Formation (bedrock) with >70% confidence. Overall, the RF method has proven successful in classifying rock mass unit boundaries using the case study data. However, additional samples are required to train the model and improve the accuracy when identifying the calcrete, hematite conglomerate, clayey breccia colluvium, and canga.

9 MACHINE LEARNING TRIAL OF A SECONDARY CASE STUDY

The original focus of this work was to trial machine learning methods using data from one project only (the project discussed in previous sections). As this project has limited geotechnical information, data from another project (case study 2) has also been trialled to compare models built from small and medium-sized datasets.

The secondary case study (case study 2) is another iron ore deposit in the Pilbara Region of Western Australia. The project has a similar geological setting with Cenozoic detrital sequences overlying Banded Iron Formation. The geotechnical rock mass units are also very similar except for a few additional units including calcareous lacustrine clay and calcrete (>20% CaO).

9.1 DATA STATISTICS – CASE STUDY 2

The second case study has a dataset of 249 RC boreholes with previously interpreted detrital units and accompanying assay data. The available assay data comprised Fe, SiO_2, Al_2O_3, P, Mn, LOI, S, TiO_2, CaO, MgO and K_2O measurements. Boreholes along two geotechnical sections were selected to test the model. The testing dataset comprises 1,839 samples across 11 units. Table 5 summarises the available samples of geochemical data for each geotechnical unit.

Table 5 – Number of Samples for Each Geotechnical Rock Mass Unit (Case Study 2)

Unit	Training		Testing		Total	
	No. of Samples	Percentage (%)	No. of Samples	Percentage (%)	No. of Samples	Percentage (%)
Quaternary Detritals	1447	23	384	21	1831	22
Gravelly Siltstone	742	12	262	14	1004	12
Calcareous Lacustrine Clay	4	0.063	7	0.38	11	0.13
Calcrete <20%	151	2.4	24	1.3	175	2.1
Calcrete >20%	154	2.4	14	0.76	168	2.0
Cemented Detritals	208	3.3	507	28	715	8.7
Silcrete	12	0.19	0	0	12	0.15
Hematite Conglomerate	300	4.7	55	3.0	355	4.3
Clayey Breccia Colluvium	467	7.3	26	1.4	493	6.0
Lacustrine Clay	72	1.1	19	1.0	91	1.1
Canga	506	7.9	4	0.22	510	6.2
Bedrock	2330	36	537	29	2867	34.8
Total	**6393**	**100**	**1839**	**100**	**8232**	**100**

9.2 MACHINE LEARNING MODEL

The Quaternary detritals and bedrock units represent 22% and 35% of the dataset respectively. As these units constitute a large proportion of the total dataset, they outweigh the other classes. To balance the weighting, we developed a two-step method using the RF classifier with the following steps:

1. Build a model to identify three units: Quaternary detritals, bedrock and 'the rest'
2. Build a model that classifies the remaining detrital units.

For this case study, we defined geological 'rules' to attempt to provide stratigraphic control when defining rock mass domains. The geological rules applied include defining the boundaries of lithologies in a bottom-up and top-down manner. The geological rules include:

- Setting the boundary bottom-up for bedrock and canga, i.e. canga can only occur immediately above bedrock
- Setting the boundary top-down for Quaternary detritals and gravelly siltstone, i.e. gravelly siltstone occurs directly beneath Quaternary detritals
- The top and bottom predicted calcrete intervals in a borehole defined the calcrete boundaries.

9.3 MODEL PERFORMANCE

In conjunction with the geological rules, the RF classifier algorithm provided the best results with an overall model accuracy of 83%. Table 6 presents the sensitivity, specificity, precision and F-score results for all units. We observe the following regarding model performance:

- Calcrete >20%, calcrete <20%, Quaternary detritals, bedrock, cemented detritals and gravelly siltstone all have an F-score greater than 70%:
    - The units constituting around 70% of the whole dataset, Quaternary detritals, bedrock and gravelly siltstone, can be predicted with high accuracy by the model
    - With the distinct geochemical signature for calcrete, the model can identify calcrete with high accuracy
- The F-score could not be calculated for calcareous lacustrine clay and canga because none of the samples were predicted correctly. Calcareous lacustrine clay has insignificant training and testing data (i.e. less than 10 samples); canga also has a small testing dataset (i.e. 4 samples)
- For units with F-scores lower than 70%, the units were typically classified incorrectly and mistaken for units with similar geochemistry:
    - Lacustrine clay had an F-score of 59%, a precision of 100% and a sensitivity of 42%. Therefore, no other units' samples were mistakenly identified as lacustrine clay, however, some lacustrine clay

samples were mispredicted. lacustrine clay was mistaken as either clayey colluvium or gravelly siltstone.

- Hematite Conglomerate was incorrectly classified as clayey colluvium and cemented detritals. Those units are basal detrital units with similar lithologies (i.e. clay and breccia).

Table 6: Specificity, sensitivity, precision and F-score results for all units (Case Study 2)

Unit	Sensitivity (average %)	Specificity (average %)	Precision (average %)	F-score (average %)
Quaternary Detritals	86	97	89	88
Gravelly Siltstone	82	95	75	79
Calcareous Lacustrine Clay	0	100	Undefined (2)	Undefined
Calcrete <20%	100	100	96	98
Calcrete >20%	100	100	100	100
Cemented Detritals	86	94	85	85
Hematite Conglomerate	33	98	37	35
Clayey Breccia Colluvium	42	99	41	42
Lacustrine Clay	42	100	100	59
Canga	0	100	0	Undefined
Bedrock	87	95	87	87

(1) The highlighted cells indicate results with <50% sensitivity, specificity, precision or F-score
(2) Metrics are undefined when the calculations result in a division by 0 and there are no positive predictions.

9.4 RESULTS

To summarise, the model developed using the data from the secondary case study and using geological rules had very similar results to the primary case study. The model can classify the units Quaternary detritals, gravelly siltstone, calcrete >20%, calcrete <20%, cemented detritals and bedrock with >70% confidence. However, the model performs poorly (<50% F-score) when identifying the calcareous lacustrine clay, lacustrine clay, clayey breccia colluvium, hematite conglomerate and canga units.

Figure 3 compares the downhole model prediction and the human-interpreted lithology boundaries for a geotechnical cross-section developed for the project. A good correlation exists between the model-predicted units and the human-interpreted lithology boundaries.

10 MACHINE LEARNING TRIAL OF A BALANCED DATASET

In machine learning, the model's accuracy depends on the data's quality and availability. The training and testing datasets selected in the secondary case study were selected by grouping boreholes along geotechnical sections. Using this method of grouping, the training and testing datasets have different weights for each detrital unit. For instance, cemented detritals comprised 3.3% of the training dataset and 28% of the testing dataset. Machine learning relies on a balanced dataset to ensure sufficient training and testing of the data.

In this section, a balanced dataset has been used for training and testing of the secondary case study data. Table 7 shows the number of training and testing samples for each identified unit in the balanced dataset. Samples were randomly picked for testing and training, and the data was not kept in stratigraphic order. Therefore, geological rules were not applied.

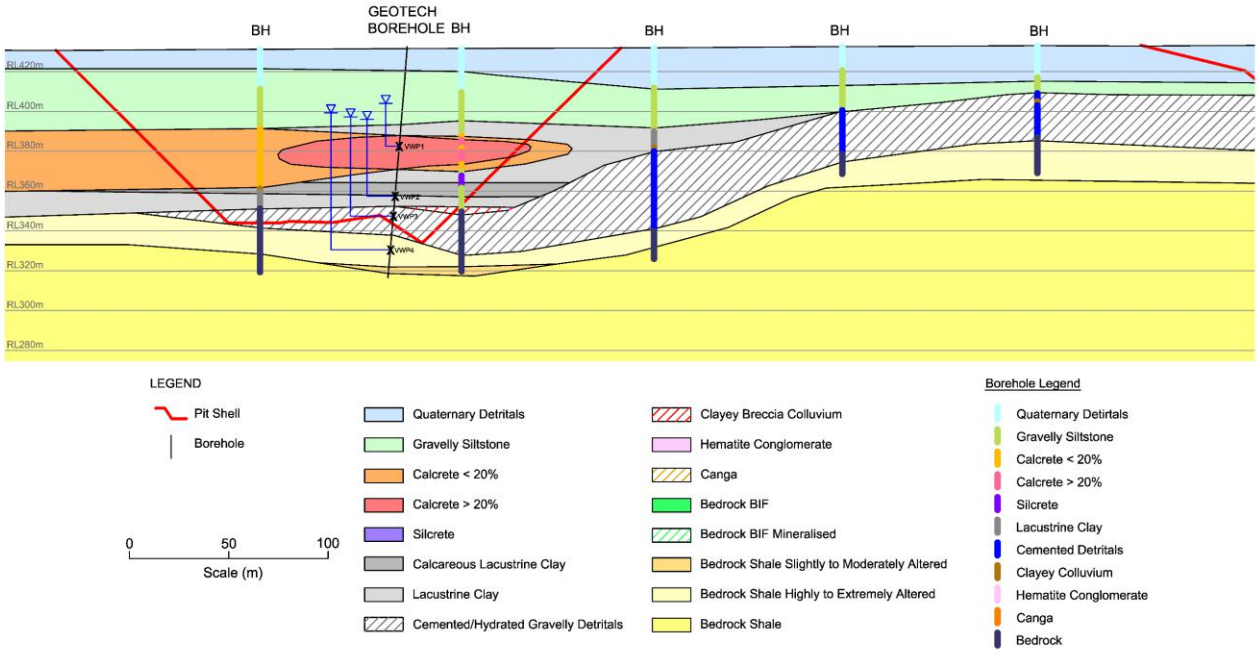


Figure 3: Comparison of Model predicted borehole intervals and the manually interpreted unit boundaries

Table 7 – Number of Samples for a Balance Dataset (Case Study 2)

Unit	Training		Testing	
	No. of Samples	Percentage (%)	No. of Samples	Percentage (%)
Quaternary Detritals	1464	25	367	22
Gravelly Siltstone	803	14	201	12
Calcareous Lacustrine Clay	8	0.14	3	0.18
Calcrete <20%	140	2.4	35	2.1
Calcrete >20%	133	2.3	35	2.1
Cemented Detritals	571	9.8	144	8.7
Silcrete	9	0.15	3	0.18
Hematite Conglomerate	285	4.9	70	4.2
Clayey Breccia Colluvium	394	6.7	99	6.0
Lacustrine Clay	72	1.2	19	1.1
Canga	408	7.0	102	6.2
Bedrock	1568	27	575	35
Total	**5855**	**100**	**1653**	**100**

10.1 MODEL PERFORMANCE

The RF classifier algorithm with the balanced dataset returned the best results with 92% overall model accuracy. Table 8 presents the sensitivity, specificity, precision and F-score results for all the units. Except for lithologies with a very limited sample size, namely calcareous lacustrine clay and silcrete, all other lithologies have an F-score greater than 70%. If the proportion of each lithology is similar between the training and testing dataset, the accuracy in identifying the units increases significantly. Therefore, the use of a balanced dataset provides the best results for training the model.

Table 8: Specificity, sensitivity, precision and F-score results for the balanced dataset (Case Study 2)

Unit	Sensitivity (average %)	Specificity (average %)	Precision (average %)	F-score (average %)
Quaternary Detritals	96	98	95	95
Gravelly Siltstone	87	98	87	87
Calcareous Lacustrine Clay	33	100	100	50
Calcrete <20%	97	100	92	94
Calcrete >20%	100	100	100	100
Cemented Detritals	90	99	87	88
Silcrete	0	100	Undefined (2)	Undefined
Hematite Conglomerate	83	100	89	86
Clayey Breccia Colluvium	81	99	86	83
Lacustrine Clay	68	100	72	70
Canga	92	100	94	93
Bedrock	95	97	94	95

(1) The highlighted cells indicate results with <50% sensitivity, specificity, precision or F-score
(2) Metrics are undefined when the calculations result in a division by 0 and there are no positive predictions. units

11 CONCLUSION

The inclusion of machine learning into the model development process has proved successful in this trial. The random forest (RF) classifier algorithm demonstrated high accuracy when domaining the boreholes and is a useful method which can be used for future projects. Borehole domaining of the primary dataset was achieved with 82% overall model accuracy using the RF method. When training and testing the model built from the secondary dataset, 92% model accuracy was achieved with the inclusion of a balanced dataset.

The use of a balanced dataset when training and testing the model has proven to significantly increase the model accuracy. Rock mass units with small sample sizes such as calcareous lacustrine clay and silcrete do not have sufficient data to train the model and classify the units correctly. To improve the accuracy when predicting these units, additional twin geotechnical boreholes and RC boreholes are required to increase the data available to train the model. The success of the model largely depends on the size of the dataset and how balanced the dataset is. Therefore, collecting adequate/sufficient data to train the model is key for model accuracy and confidence.

This paper has demonstrated that an automated approach to identification of detrital units using geochemical data is an effective method for classifying boreholes. The approach to borehole domaining using machine learning can be successfully applied to a large borehole dataset and in turn can be used to develop a 3D model. This methodology will significantly reduce the time required for manual interpretation and allow the geologist/engineer greater time for detailed interpretation.

12 REFERENCES

Baxter, H. (2016). Geophysics, geochemistry and engineering geology: how disciplines combine to improve mine slope design in the Pilbara detrital valleys of Western Australia. Geological Society, London, Engineering Geology Special Publications, 27(1), pp.81-92.

Herget, G. (1977). Pit Slope Manual Chapter 2 – Structural Geology. CANMET (Canada Centre for Mineral and Energy Technology, formerly Mines Branch, Energy, Mines and Resources Canada), CANMET REPORT 77-41; Appendix A (pp 88).

Noble, D.P., Hemraj, D.J. and Eggers, M.J. (2021). Improving reliability of the geotechnical model for Cenozoic cover sequence sediments in the Pilbara, Western Australia (pp. 373-386). Australian Centre for Geomechanics.

Standards Australia. (2017). Geotechnical Site Investigations. AS 1726:2017.

Stone, M.S. (2005). Depositional history and mineralisation of Tertiary channel iron deposits at Yandi, Eastern Pilbara, Australia. University of Western Australia.

https://doi.org/10.56295/1ACEG33

FINITE ELEMENT CHECK OF GSI ADJUSTMENT EQUATION RECONCILING HOEK-BROWN AND STEP-PATH STRENGTHS

Norbert R P Baczynski[1]; Alison McQuillan[2]
Prime Geotechnics Pty Ltd, Australia[1]; Rocscience, Australia[2]

ABSTRACT

Rock mass strength is impacted by the coalignment of geological defects and intact rock (IR) bridges. The greater the alignment of geological defects and smaller the rock bridges, the weaker the rock mass strength. Current versions of the 1980s Hoek-Brown Method (HBM) for rock mass strength considers rock mass blockiness and defect condition via a Geological Strength Index (GSI) chart. This chart was refined several times, but these revisions still do not directly consider coaligned defects and bridges. Step-Path Method (SPM) evolved in mid-1970s to assess strength implications of coaligned defects and IR bridges. Early SPM models were simple; but progressively evolved to consider more complex situations. In late 1980s, computer software was written to assess rock mass shear strength by Monte-Carlo statistical simulation of defect and IR bridge along failure paths through slopes. Since mid-2000s, EXCEL spreadsheets have aided this type of assessment. SPM often computes a lower rock mass strength than HBM. Based on 230+ case studies an equation was proposed in 2019 to adjust the GSI index in HBM based on relative occurrences of coaligned defects and IR bridges along failure paths. The general equation is $GSI_{Design} = \{GSI_{General\ Rock\ Mass} - [0.4 \times (\%\ coaligned\ defects)] + [1.2 \times (\%\ IR\ bridges)]\}$. With the above adjusted GSI, HBM computes near-same rock mass strength as SPM. Appropriateness of above GSI adjustment equation with respect coaligned defects is checked by two-dimensional (2D) jointed finite element (FE) modelling. Results are presented and discussed. The method is presented for alternative strength inputs into jointed rock masses to account for the presence of co-aligned defects dipping into the excavated slope.

Key words: Hoek-Brown, Step-Path, rock mass strength, GSI adjustment, finite element analyses

1 INTRODUCTION

Hoek-Brown (HBM) (Hoek and Brown, 1980) and Step-Path (SPM) (Jennings, 1970; Baczynski, 2000) methods assess rock mass (RM) shear strength. HBM considers rock mass blockiness and joint condition via a Geological Strength Index (GSI) chart. SPM considers the occurrence of coaligned defects and intact rock (IR) and/or rock mass (RM) bridges between these coaligned defects along potential failure path in slopes. Where coaligned defects are absent, HBM and SPM compute the same RM strength. As occurrence (%) of co-aligned defects increases, SPM strength progressively decreases until with 100% coaligned defect occurrence RM strength is same as coaligned defect strength. Thus, SPM strength is in between HBM strength and defect strength; yielding lower factors of safety (FOS) in limiting equilibrium analyses (LEA) of rock slope stability. Bar and Baczynski (2019) finite element modelled one slope case and inferred that SPM was a geotechnically logical approach. To reconcile differences between HBM and SPM rock mass strength estimates, Baczynski (2019) developed an GSI adjustment equation based on 230 case studies.

$$GSI_{Design} = \{GSI_{General\ Rock\ Mass} - [0.4 \times (\%\ coaligned\ defects)] + [1.2 \times (\%\ IR\ bridges)]\} \quad (1)$$

The 0.4 and 1.2 coefficients in this equation are generally applicable (correlation coefficients of 0.72 to 0.86); but they do somewhat vary (0.35-0.53 and 1.0-1.5) with rock type and mi (<11, 11-19 and >19) groupings respectively; with some groupings achieving better correlation coefficients of 0.98.

In this paper, the coaligned defects component of the GSI adjustment equation is checked by two-dimensional (2D) jointed finite element (FE) modelling. RS2 software (Rocscience, 2024) is used. Objectives, methodology, FE slope models, analysis results, conclusions and recommendations are presented and discussed. Baczynski (2019) suggested GSI adjustments due to intact rock bridges between coaligned defects was not investigated.

2 HOEK-BROWN METHOD

Hoek-Brown Method (HBM) for estimating rock mass strength was developed by Hoek and Brown (1980) and is now widely used. Inputs are unconfined compressive strength (UCS), shape of the triaxial strength curve (mi), rock mass blockiness and geological defect condition – estimated via the Geological Strength Index (GSI) chart (Hoek and Brown, 1997) and blasting disturbance (D). GSI is based on Bieniawski (1986, 1989) rock mass rating (RMR) index; but can also be estimated via Barton et al (1974) and other classifications, including Deere (1963) Rock Quality Designation (RQD). GSI chart was revised several times to make HBM better suited to specific ground situations; especially defect orientation in the rock mass. With respect to Step-Path Method (SPM), Truzman (2007) GSI chart is useful, if the term "intensity" is equated to "relative occurrence of geological defects that are coaligned with the failure path direction" (Baczynski, 2018). Figures 1 (a) and 1(b) show examples of two GSI charts.

3 STEP-PATH METHOD

Jennings (1970) detailed a basic Step-Path Method (SPM) for bedding planes failures in rock slopes. Since then, SPM has considered progressively more complex geotechnical conditions (Baczynski, 2000; Baczynski 2019). Although SPM is not widely used; it provides an approach to statistically quantify the extent to which geological defects coaligned with failure path direction and the IR / RM "bridges" between these defects contribute to RM shear strength. HBM strength is still assigned to those rock mass regions where coaligned defects do not statistically occur.

Figure 2 shows conceptual step-path methodology.

In Figure 2A, slope failure path complexity ranges from one set of coaligned defects to a composite situation. In the latter, the failure path traverses along a major backscarp fault, a central zone across the defect pattern and has HBM rock mass strength and then steps along short coaligned defects near slope toe. Figure 2B shows the three conceptual step-path "cell" types – coaligned defects, intact rock and rock mass.; with cells being shear-box tested individually and together. Figure 2C shows a multiple "cells" test; with anticipated shear strength dependent on relative occurrence of cell types. Figure 2D plots the expected shear strength relationship between the three cell types and SPM.

Strength relationship is intact rock > HBM rock mass > SPM rock mass > geological defect.

4 HBM-SPM 2019 RECONCILIATION

Baczynski (2019) reconciled HBM and SPM rock mass strength estimates by GSI adjustments; based on 230 case studies. Adjustments were computed via Microsoft EXCEL spreadsheet (Lambert and Frye, 2022) and ROCLAB-1.0 software (Rocscience, 2007).

Figure 3 (A to C) shows reconciliation plots for all rock types combined, sandstone and siltstone, respectively. As per 2019 paper, the method and adjustment equations are valid for GSI<75 and only yield sensible results when geological defects shear strength is less than HBM rock mass strength.

GSI adjustment Equation 1 for all rock types combined was presented in Section 1. Equations 2 and 3 are for sandstone (SS) and siltstone (SL) rock types, respectively.

$$GSI_{Design} = \{GSI_{SS\ Rock\ Mass} - [0.55 \times (\%\ SS\ coaligned\ defects)] + [1.0 \times (\%\ SS\ IR\ bridges)]\} \quad (2)$$

$$GSI_{Design} = \{GSI_{SL\ Rock\ Mass} - [0.41 \times (\%\ SL\ coaligned\ defects)] + [1.6 \times (\%\ SL\ IR\ bridges)]\} \quad (3)$$

Statistical correlation coefficients for the linear trends shown in Figure 3 range from 0.87 to 0.98.

5 FINITE ELEMENT MODELLING SOFTWARE

Modelling was done via RS2 two-dimensional (2D) jointed finite element (FE) software (Rocscience, 2020, 2024).

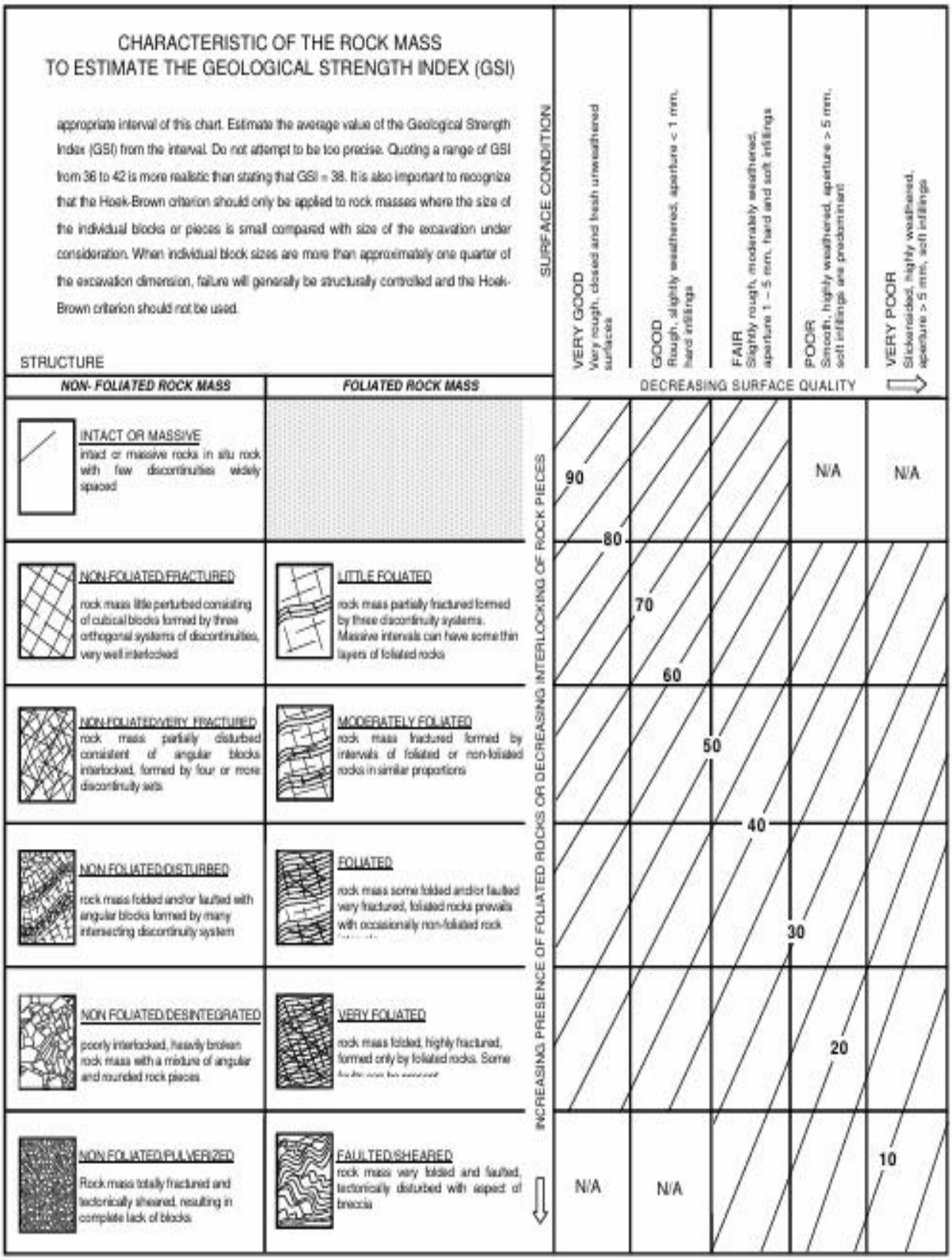
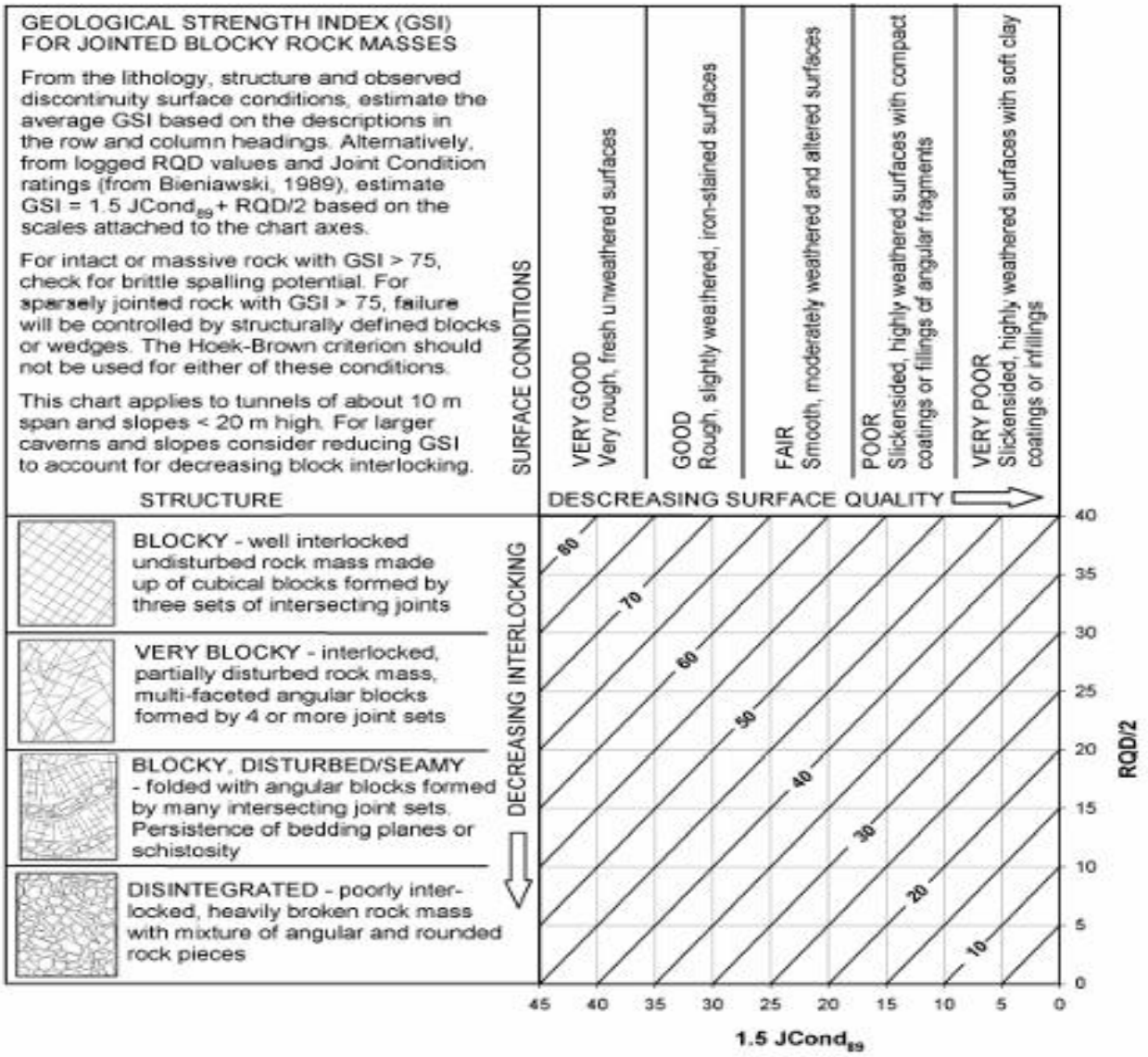


Figure 1(a): Truzman (2007) GSI chart



Condition of discontinuities	Very rough surfaces Not continuous No separation Unweathered wall rock	Slightly rough surfaces Separation < 1 mm Slightly weathered walls	Slightly rough surfaces Separation < 1 mm Highly weathered walls	Slickensided surfaces or Gouge < 5 mm thick or Separation 1 – 5 mm Continuous	Soft gouge > 5 mm thick or Separation > 5 mm Continuous
Rating	30	25	20	10	0

Guidelines for classification of discontinuity conditions

Discontinuity length (persistence) Rating	< 1 m 6	1 to 3 m 4	3 to10 m 2	10 to 20 m 1	More than 20 m 0
Separation (aperture) Rating	None 6	< 0.1 mm 5	0.1 – 1.0 mm 4	1 – 5 mm 1	More than 5 mm 0
Roughness Rating	Very rough 6	Rough 5	Slightly rough 3	Smooth 1	Slickensided 0
Infilling (gouge) Rating	None 6	Hard infilling < 5 mm 4	Hard filling > 5 mm 2	Soft infilling < 5 mm 2	Soft infilling > 5 mm 0
Weathering Rating	Unweathered 6	Slightly weathered 5	Moderate weathering 3	Highly weathered 1	Decomposed 0

Figure 1(b): Hoek et al (2013) GSI chart

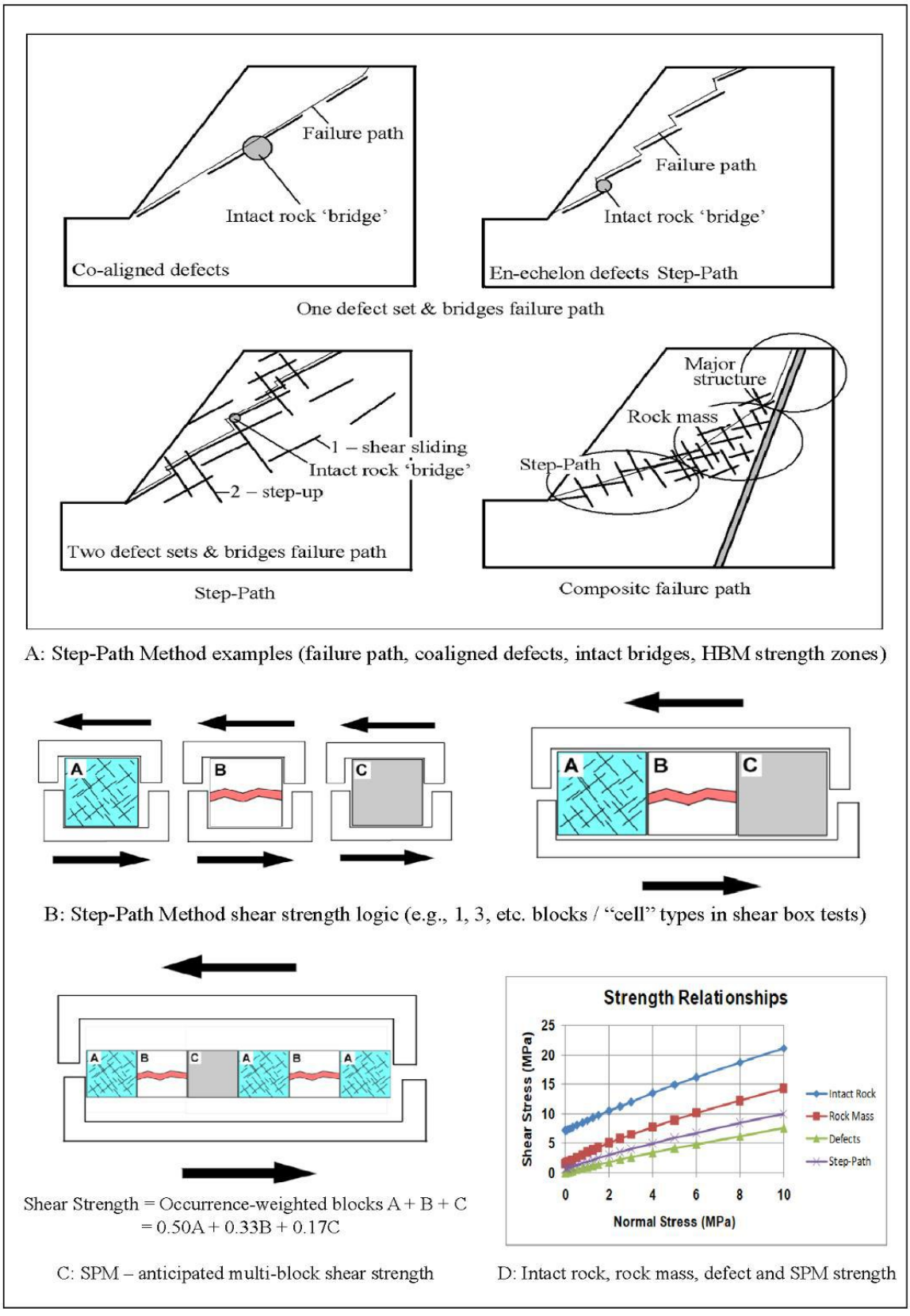


Figure 2: Step-Path model (Baczynski, 2019, 2022)

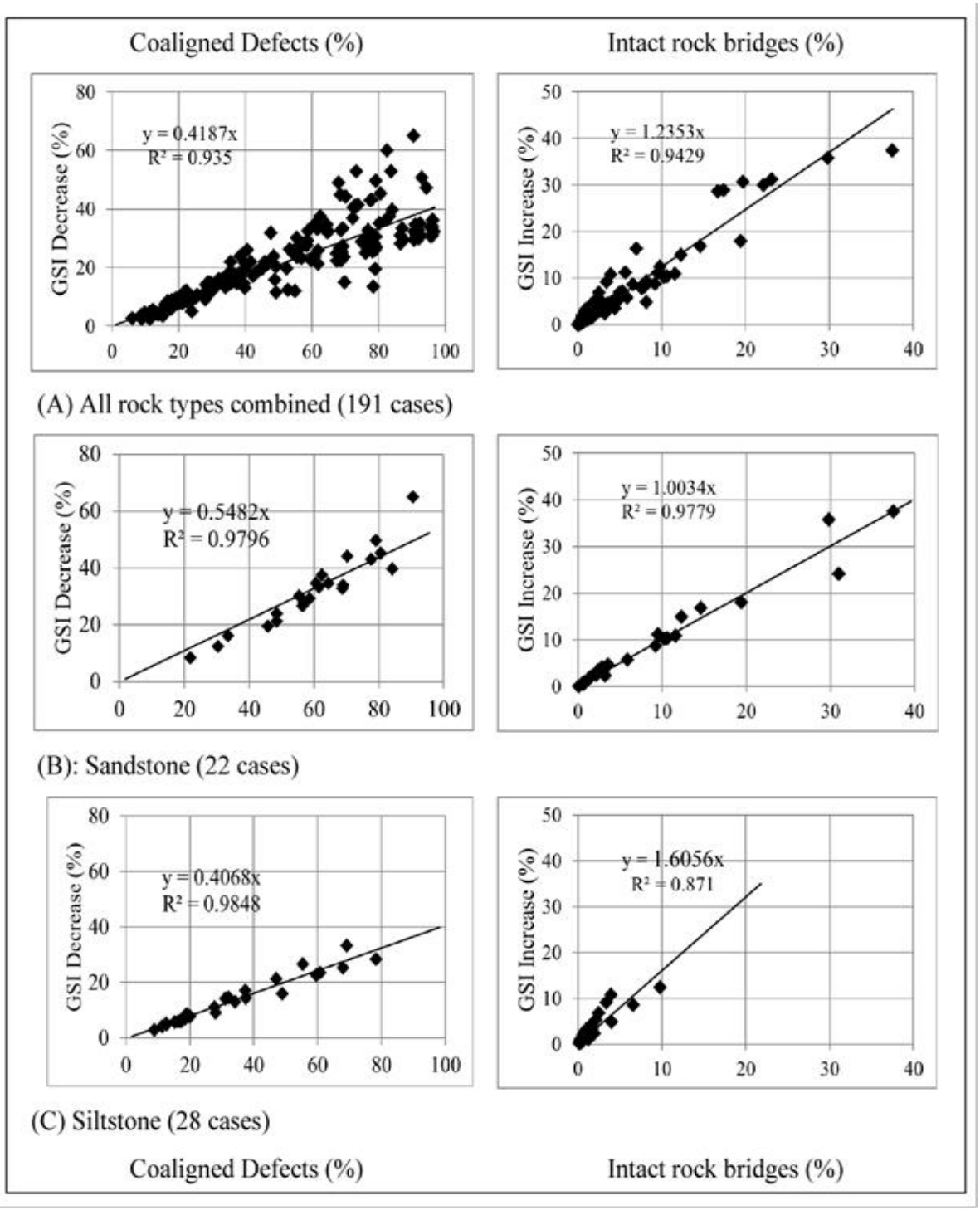


Figure 3: GSI adjustments (at 2 MPa normal stress) for relative occurrence of coaligned defects and intact rock bridges along failure paths through rock mass slopes (Baczynski, 2019)

6 MODEL SLOPE GEOMETRY

Various slope geometry models were considered, trialled and refined. Results in this paper are for 280m and 710m high slopes with overall face angles of 44°; as shown in Figures 4. Slope face in some models was vertically surcharged. This

was an attempt to simulate slope-scale direct shear tests and to reduce SRF from the often achieved >2 to ≤ 1.1. If applied, surcharge is flagged in this paper.

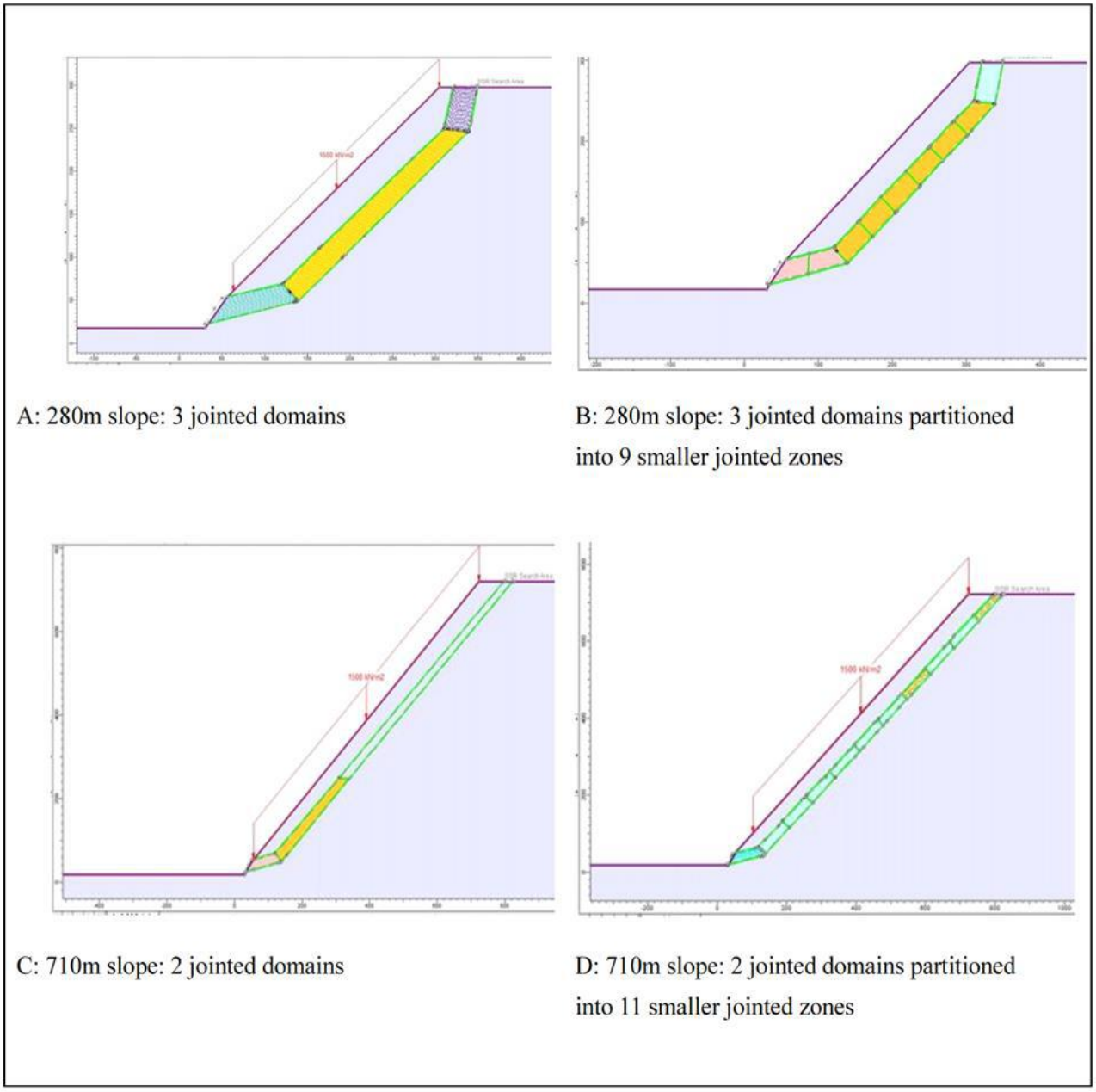


Figure 4: RS2 finite element slope models: jointed domains surrounded by unjointed rock mass

A 25m thick jointed area was located 30m behind the 280m high slope face. This area exited at slope toe and 30m behind slope crest. Ground on either side was unjointed. There were three joint-dip domains; each had one joint set. In the Upper, Central and Lower Domains joints dipped at 78°, 44° and 13° into the pit void, respectively.

Geometry of 710m high slope was similar to 280m high slope; but Central Domain was much longer. In most analyses, Upper Domain was deleted and Central Domain extended to ground surface.

With jointed domains, models broadly simulated slab-sliding conditions; with change in failure path trend at slab toe and in some models at slope crest. Nevertheless, this path is still similar to slip-circle failure with large radius and shallow depth traverse behind slope face.

In most analyses, three jointed "domains" were further partitioned into several shorter, each same length, jointed "zones". Such partitioning is akin to SPM concept of an assemblage of adjacent "cells" / blocks in Figure 2. As per Figure 4, there were 11 such jointed zones in 710m high slopes and 9 in 280m high slopes.

7 COALIGNED DEFECTS

Probability of occurrence, defect and bridge lengths and spacing between coaligned defect lines are discussed.

7.1 OCCURRENCE

Relative occurrence of coaligned defects in a rock mass may range between 0 and 100%.

"Joint-Ratio" setting in Joint Properties of RS2 software designates defect occurrence in each Jointed Zone. For comparison of RS2 results, a 0.8 "joint ratio" was usually used. Thus, if defects occurred in every jointed zone along slope failure path; defect occurrence was 80%. If a defect occurrence of 90% needed to be modelled, then the "Joint-Ratio" could be reset to 0.9.

In simplest models, all defects in specific jointed zones could be just deleted to reduce defect occurrence along failure paths. For example, with 0.8 joint ratio, each of the 9 jointed zones in the 280m high slope contained 80/9 = 8.9% of the coaligned defects. If defects were deleted in 3 of 9 zones, then 80 – 8.9 x 3 = 53.3% coaligned defects existed along the failure path. This approach was used to FE model the conceptual mean sandstone 2019 case study.

Coaligned defect occurrence in 2019 case studies was derived by slope face mapping. This value was rarely a convenient multiple of 8.9% occurrence in each of 9 jointed zones. Such situations were accommodated by dividing field occurrence by 8.9 to determine how many of the 9 jointed zones needed to contain defects in them and adjusting length of one zone to achieve the desired outcome. For example, a 56% mapped occurrence equates to 56/8.9 = 6.3 jointed zones. In this situation, length of one zone was increase by 0.3 (reducing the adjacent zone to 0.7 of its original length). Coaligned joints were assigned to 5 zones, plus the zone with 0.3 increased length. This resulted with joints in 6.3 zones and HBM rock mass strength (without joints) in the other 2.7 zones.

7.2 LENGTH

Figure 5 shows the mean defect length statistical model for 33 of the 230 Baczynski (2019) case studies that were RS2 modelled. Median and mode lengths are ~3m; this length was adopted

EXCEL-ROCLAB simplified SPM only considers cumulative lengths of each component (i.e., coaligned defects, intact rock bridges, rock mass bridges, HBM rock mass areas without coaligned defects) to compute shear strength.

In the original Step-Path STEPSIM Monte-Carlo simulation software (McMahon, 1979) and revised STEPSIM4 (Little et al, 1996-2000; Baczynski, 2000) coaligned defect length was a key input. Statistical models were based on field mapping and laboratory test data for defect type (fault, joint) and its occurrence, length, shear strength, cutoff probability by other defect sets, intact rock and rock mass "bridge" length for not cut-off defects and shear strength of these bridges. STEPSIM4 simulated 5,000 to 15,000 step-paths to develop failure path shear strength model.

7.3 ROCK MASS BRIDGES AND COALIGNED DEFECTS LINE SPACING

Length of rock mass (RM) bridges between coaligned defects is related to defect length and joint ratio. For example, with joint ratio of 0.8 and constant 3m defect length, RM bridge length is 0.77m. If defect length is increased to 5m, 10m, or 20m; respective RM bridge lengths increase to 1.3, 2.55 and 5.2m. Spacing between multiple lines of coaligned defects was purposely made same as RM bridge length. This approach ensured that slope failure path was not unintentionally restricted to traversing along a specific line(s) of coaligned defects (i.e., if bridges between the lines were longer), but was able to freely develop across multiple lines.

It perhaps worth noting that rock mass RQD with modelled bridge lengths and joint-line spacing is 100%. Hence, modelled defects in present finite element analyses do not impact "blockiness" rating along vertical axis of GSI Index charts. In this instance, often-cited perception that GSI rating should be somehow increased in HBM model to compensate for defects that are seemingly being considered twice lacks substance.

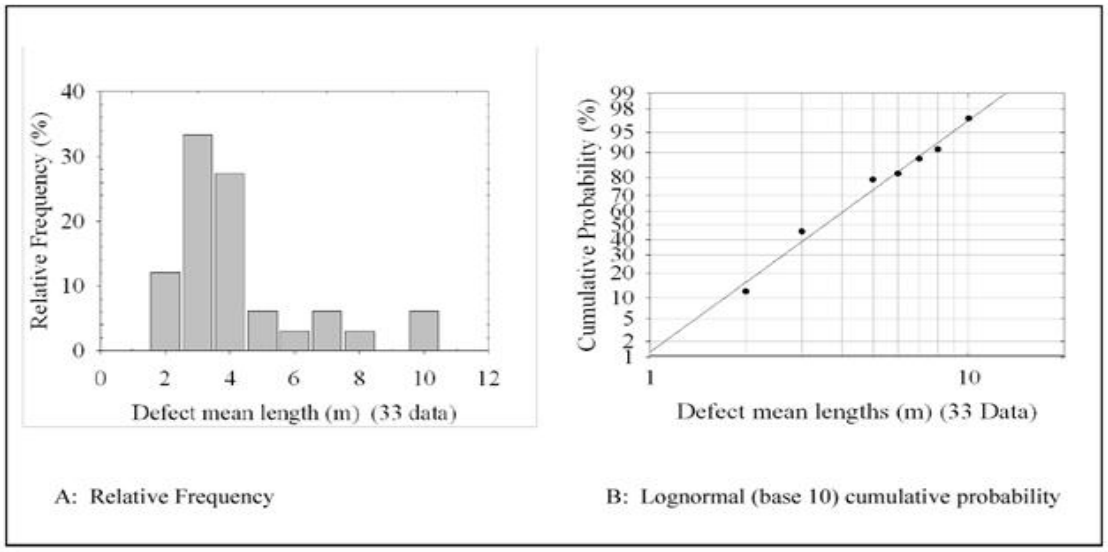


Figure 5: Mean sandstone and siltstone defect mean lengths in 2019 SPM case studies RS2 analysed

8 ROCK MASS AND DEFECT GEOTECHNICAL PARAMETERS

Table 1 details the range of rock mass and geological defect parameters that were considered in RS2 two-dimensional (2D) jointed finite element (FE) models. The Bandis-Barton model for joint shear strength was adopted (Barton, 1976, 2018; Barton and Bandis, 1990, 2017)

Table 1: RS2: Rock Mass and Defect Geotechnical Parameters

A: Hoek-Brown Rock Mass Strength						
Model	**Rock UCS (MPa)**	**GSI**	**mi**	**D**	**Young's Modulus (E) (GPa)**	**Poisson Ratio**
Conceptual Sandstone	30	60	17	0	250 x UCS 7.5	0.18
Sandstone 22 Cases	15-49	42-78	17	0	250 x UCS 3.8 – 12.3	0.18
Siltstone 11 of 28 Cases	25-100	35-65	7-15	0	250 x UCS 6.3 – 25.0	0.18
B: Geological Defects: Bandis-Barton shear strength						
Model	**JCS (MPa)**	**Roughness (JRC)**	**Base Friction $Ø_b$**	**Length (m)**	**Joint Stiffness (GPa/m)**	
					Normal	**Shear**
Conceptual Sandstone	30	6	30	3-20	4GPa: 1 case, otherwise 0.1	4GPa: 1 case, otherwise 0.01
Sandstone 22 Cases	15-49	5-11	30-32	3	0.1	0.01
Siltstone 11 of 28 Cases	25-100	4-8	29	3	0.1	0.01

9 STRESS REGIME AND STRENGTH REDUCTION FACTOR

Vertical stress is hydrostatic based on intact rock density of 24 kN/m3. Whilst the Poisson's Ratio is stated as 0.18; horizontal stress in finite element analysis was same as vertical stress.

RS2 finite element analyses specifically computed the SRF for jointed material domains only.

10 GSI ADJUSTMENT CALCULATIONS

This is a four steps process. Firstly, compute the strength reduction factor (SRF) for the model with joints. Then, repeat analysis for the model without joints. Aim is to determine the GSI reduction needed for the unjointed model to yield same SRF as the jointed model. The steps are:

Step-1: Do RS2 analysis for the candidate slope with the required HBM rock shear strength (say, UCS=30; GSI=60; mi=17; D=0) and required occurrence (say, 56%) of coaligned defects in jointed zones. Outcome depends on both HBM and joint shear strengths. Say, this yields SRF=1.53

Step-2: Redo RS2 analysis without coaligned defects in jointed zones. Outcome only depends on HBM shear strength (i.e., same inputs as indicated in Step-1). Say, this yields SRF=1.78

Step-3A: Redo Step-2 RS2 analysis but with GSI=60 reduced to GSI=50. Say, this yields SRF=1.68. This is higher than SRF=1.53 in Step-1

Step-3B: Redo Step-2 RS2 analysis but with GSI=60 reduced to GSI=40. Say, this yields SRF=1.58. This is still higher than SRF=1.53 in Step-1

Step-3C: Redo Step-2 RS2 analysis but with GSI=60 reduced to GSI=30. Say, this yields SRF=1.48. This is now lower than RS2 Step-1 result of 1.53.

Step-4: By further RS2 analyses within GSI=31 to GSI=39 range establish GSI value in the unjointed model that yields SRF=1.53; same as the SRF in Step-1. Alternatively, interpolate existing RS2 analysis result to reach same conclusion. In this example, SRF outcome for the jointed model in Step-1 is achieved when GSI=35 (and, UCS=30, mi=17, D=0) in the same model but without any coaligned joints in the jointed zones.

Step-5: Calculate the GSI adjustment; i.e., 60-35 = 25

11 FINITE ELEMENT RESULTS

Figures 6 to 10 summarize RS2 jointed finite element results.

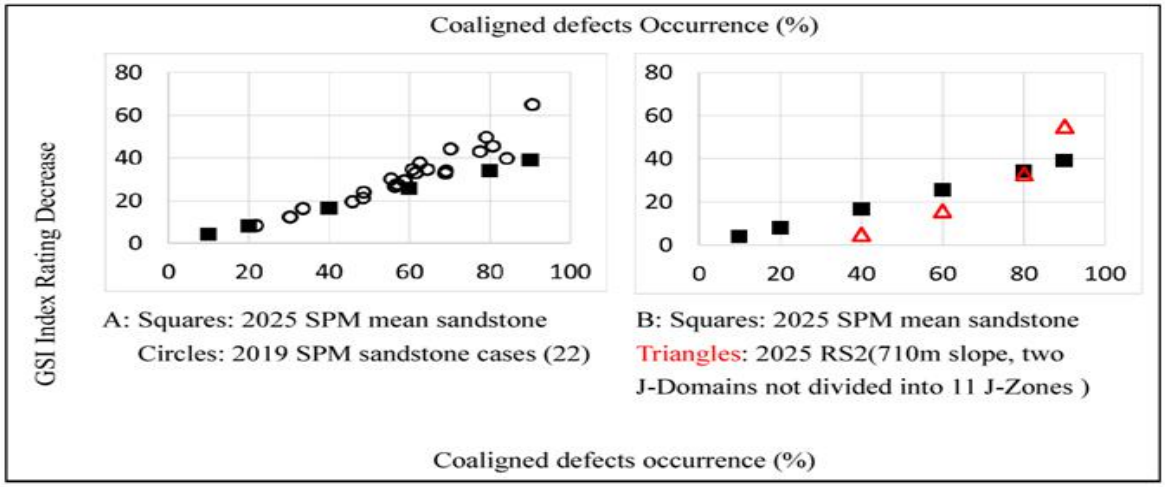


Figure 6: RS2 finite element results for 2025 SPM mean sandstone case study

11.1 STEP-PATH METHOD LOGIC CHECK

Initial FE analyses checked validity of SPM logic. A mean conceptual sandstone model (see inputs in Table 1) was tested over 10-90% coaligned defect occurrence range. Black circles in Figure 6A are actual Baczynski (2019) results for 22 sandstone case studies (as derived by EXCEL-ROCLAB calculations); black filled squares are 2025 likewise-derived results for mean sandstone test model.

As per Figures 4A and 4C, 280m and 710m high slope models each initially had three jointed domains. Joints in Upper, Central and Lower Domains dipped at 78^o, 44^o and 13^o towards pit void, respectively. In subsequent 710m slope models, Upper Domains was abolished and Central Domain extended to ground surface. The red triangles in Figure 6B are RS2-derived GSI adjustments for 30-90% coaligned defect occurrence in the two jointed domains of 710m slope model. Whilst a match exists between SPM-predicted and RS2-achieved GSI adjustments at 80% coaligned defect occurrence, RS2 analyses indicate lower GSI-adjustments for lower coaligned defect occurrences; trending to 0% GSI adjustment below 30% coaligned defect occurrence. RS2 re-analyses of the same models with much reduced Mohr-Coulomb joint shear strength inputs failed to significantly alter the overall outcome.

On reflection, initial FE analyses were not honouring the Step-Path concept in Figure 2. Defects of particular defect set tend to occur in clusters / zones (Baczynski, 1980 a, b).

Extent of clusters in directions parallel and normal to a defect set's mean plane may be defined in terms of conditional probabilities (i.e., the greater the intensity of the defect set in a "cell", the greater the likelihood that immediately adjacent cells will also have high intensity and vice-versa). It is worth noting that if defects were randomly distributed, line-sampled defect spacing would not be lognormal. The SPM rock mass model conceptually comprises an array of adjacent relatively small size "cells" which may have 1 or more through-going coaligned defects in each cell. Defect occurrence is simply estimated by partitioning line traverse slope face mapping data into 5m or 10m segments (or akin 5m x5m or 10m x 10m mapping windows) and determining how many line-segments / mapping windows contain specific defect sets in them.

Figures 4B and 4D show that the SPM "cells" concept was achieved in RS2 models by partitioning the 2 jointed domains in 710m high and 3 jointed domains in 280m high slopes into 11 and 9 smaller jointed "zones", respectively. Partitioned jointed "zones" were used in all subsequent RS2 analyses.

11.2 SINGLE-LINE VERSUS MULTI-LINE COALIGNED DEFECTS

Figure 7 shows GSI adjustment outcome for models with single-line and multi-lines of coaligned defects. Multiline RS2 model yields similar results to SPM. Single-line results are 60-70% less.

11.3 COALIGNED DEFECT LENGTH IMPACT

Figure 8 shows RS2 analysis GSI adjustments for multiline models with 3m long coaligned defects and 0.77m rock mass bridges and line spacing and with 10m long defects and 2.55m bridges / line-spacing. GSI adjustments for shorter defects and bridges are similar to somewhat higher than SPM predicted; those for longer defects are generally less, especially for defect occurrences > 60%.

11.4 RS2 ANALYSIS OF 2019 SPM CASE STUDIES

Twenty-two (22) sandstone and 11 siltstone of Baczynski (2019) case studies were RS2 modelled. Results are shown in Figures 9 and 10.

In spite of the data scatter in Figures 9A and 9B, there is good agreement between 2019 SPM-predicted and 2025 RS2-achieved GSI adjustments for sandstone and siltstone case studies. The two linear trend lines coincide in Figure 9B.

Figures 9C to 9E plot the respective results for sandstone case studies without and with the cases being partitioned with respect GSI (i.e., GSI>73 and GSI<74). Half of sandstone cases were for GSI>73. This GSI is near upper limit of Baczynski (2019) GSI adjustment equation's application. After partitioning, RS2 analyses of GSI<74 group (Figure 11D) achieved a reasonable match with 2019 SPM-predicted results. In GSI>73group, SPM predicted higher GSI adjustments than RS2 modelling.

11.5 JOINT STIFFNESS IMPACT ON RS2 RESULTS

Joint normal and shear stiffness testing data was not available for any of the 230 Baczynski (2019) case studies. Such data is rarely collected during routine geotechnical investigations and was not an input to HBM and SPM analyses. A large volume of literature exists on joint stiffness but values vary considerably between authors. Papers include Bandis et al (1983), Moorzad and Aminpoor (2008), Kulatilake et al (2016), Han et al (2023), Niktabar et al (2023) and Wang et al (2024). As per Table 1, 0.1 GPa/m and 0.01 GPa/m were adopted for normal and shear defect stiffness. Only one suite of RS2 analysis was done with joint stiffness increased up to 4 GPa/m. With stiffer defects, the RS2 computed SRF increased by 5-10%.

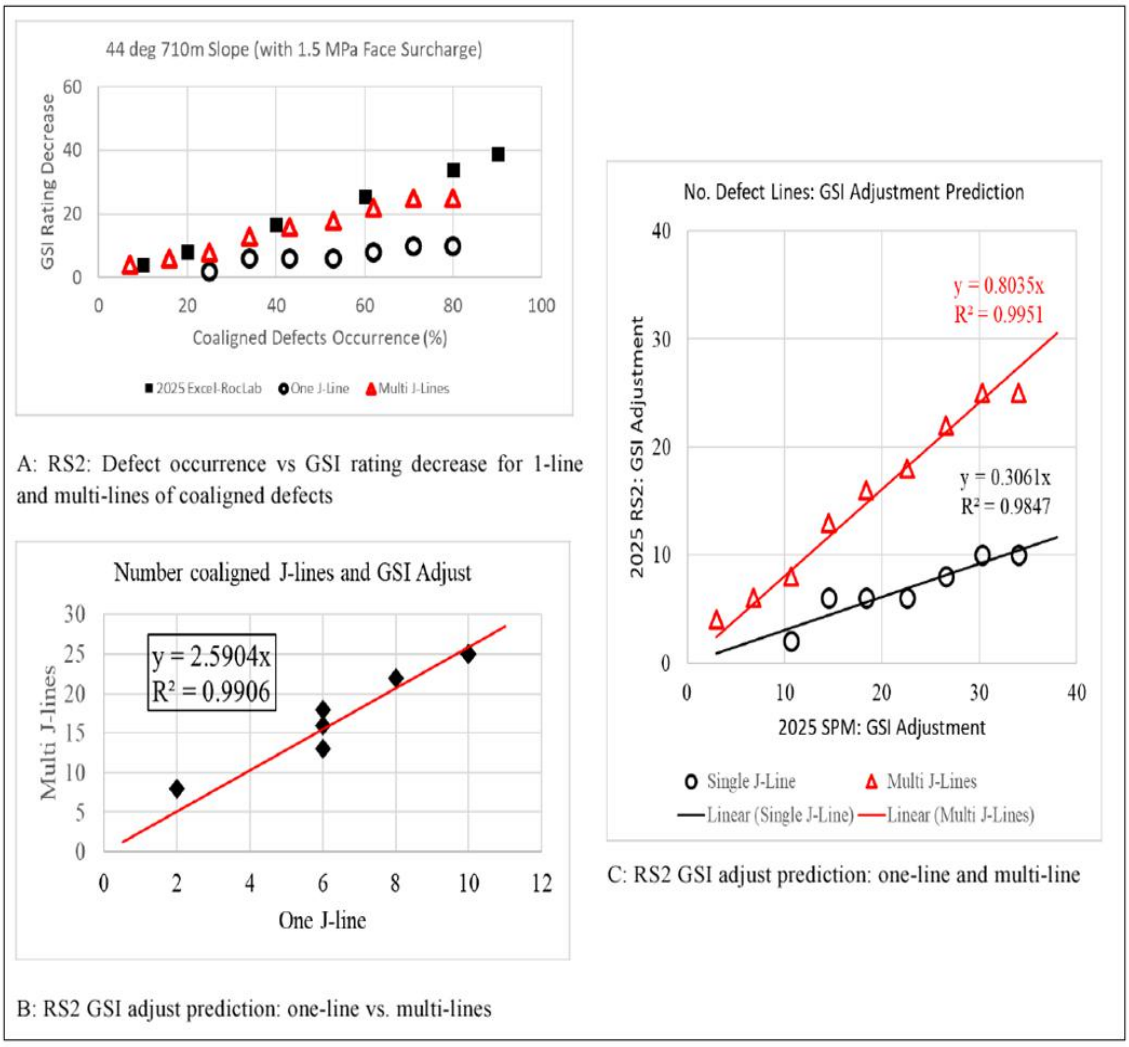


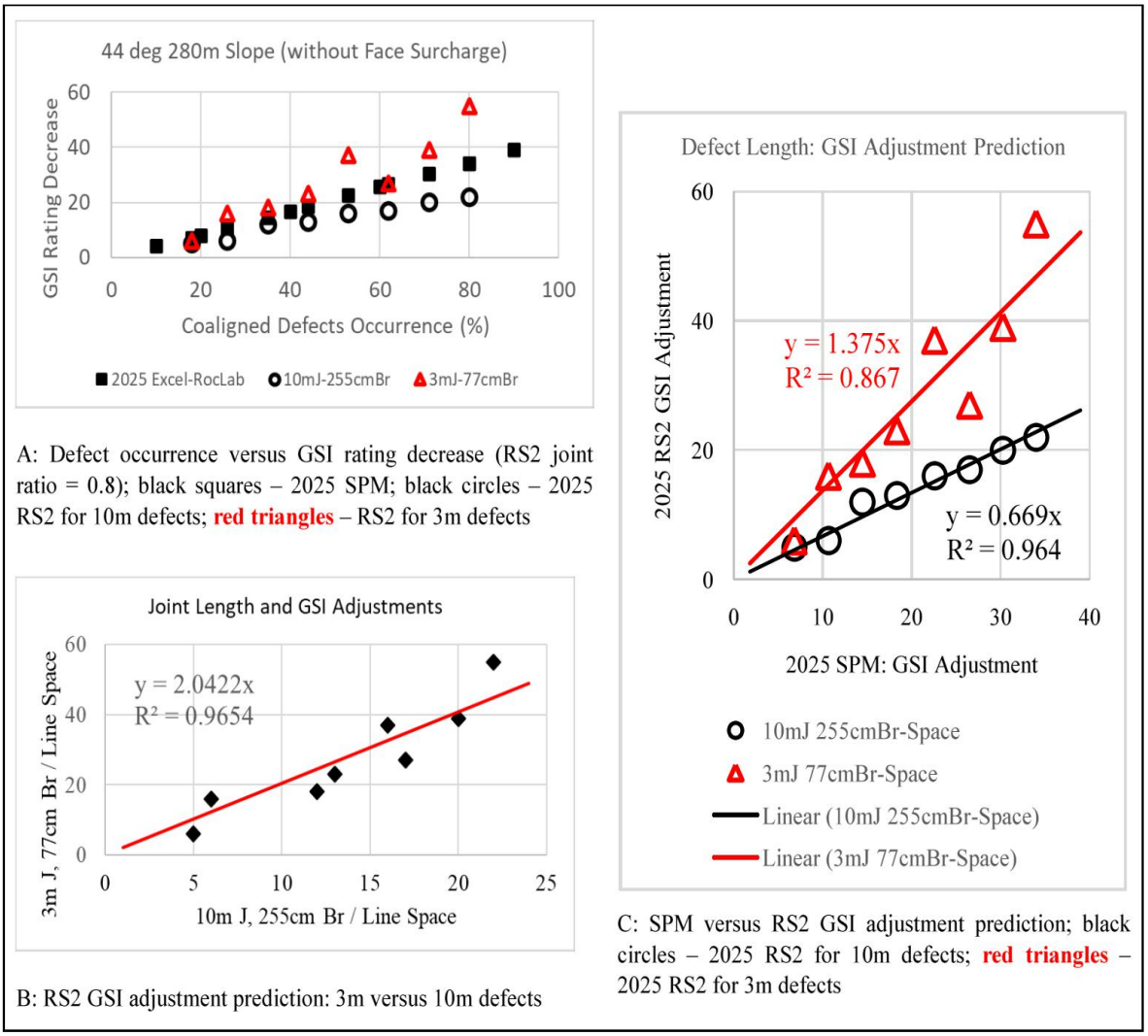
Figure 7: 2025 SPM mean sandstone: RS2 derived GSI adjustments for one and multi-lines of co-aligned defects

11.6 2019 SPM VERSUS 2025 RS2 GSI-ADJUSTMENT PREDICTION

Figures 10A to 10F indicate that RS2 finite element analyses have confirmed SPM logic for predicting GSI-Adjustments in HBM rock masses for GSI <74 situations. Correlation coefficients for sandstone and siltstone trendlines in Figures 10B, 10E and 10F are 0.92, 0.91 and 0.98; respectively.

In view of various factors (e.g., number of lines of coaligned defects, defect length and defect stiffness, and also likely the number of smaller joint zones partitioning larger jointed domains) that had been shown to impact RS2 modelling outcomes, there has been a fairly strong confirmation of Baczynski (2019) SPM logic and GSI adjustment equations

reconciling SPM and HBM rock mass strength estimates. This GSI adjustment model applies to those defects that are significantly coaligned with the failure path through the rock slope; with sliding into the excavation direction.



A: Defect occurrence versus GSI rating decrease (RS2 joint ratio = 0.8); black squares – 2025 SPM; black circles – 2025 RS2 for 10m defects; **red triangles** – RS2 for 3m defects

B: RS2 GSI adjustment prediction: 3m versus 10m defects

C: SPM versus RS2 GSI adjustment prediction; black circles – 2025 RS2 for 10m defects; **red triangles** – 2025 RS2 for 3m defects

Figure 8: 2025 SPM mean sandstone: RS2 derived GSI adjustments for multi-lines of 3m and 10m long defects

11.7 NON-LINEARITY OF GSI MODEL

Figure 11 best explains the reason for the upper GSI limit stated in Baczynski (2019) GSI-adjustment equation. In Figure 11A, spacing between shear strength curves increases with increasing GSI. In the 1-3 MPa normal stress range that likely exists in many shallow-seated rock slope failures, spacing between the plotted curves is fairly similar up to GSI~70; but widens significantly for higher GSI values.

This normal stress impact above 3 MPa is again highlighted in Figure 11B. Figure 11C and 11D closer examine this matter. The GSI vs shear strength trend is linear for GSI<70; then there is non-linear transition between GSI=70-90; and perhaps a linear trend at GSI>90. Baczynski (2019) had suggested that perhaps the GSI trend could be considered in terms of two linear relationships, somewhat as shown in Figure 11D; with the transition point at about GSI=75. But this consideration was not further pursued. It suffices to note that the present RS2 finite element analyses infer that 2019 published GSI adjustment equations may overestimate GSI adjustments for coaligned defect occurrence in rock masses with GSI>72, and that the cut-off limit for SPM GSI adjustments should perhaps be somewhat reduced from the published GSI=75 to perhaps GSI=72 or 73.

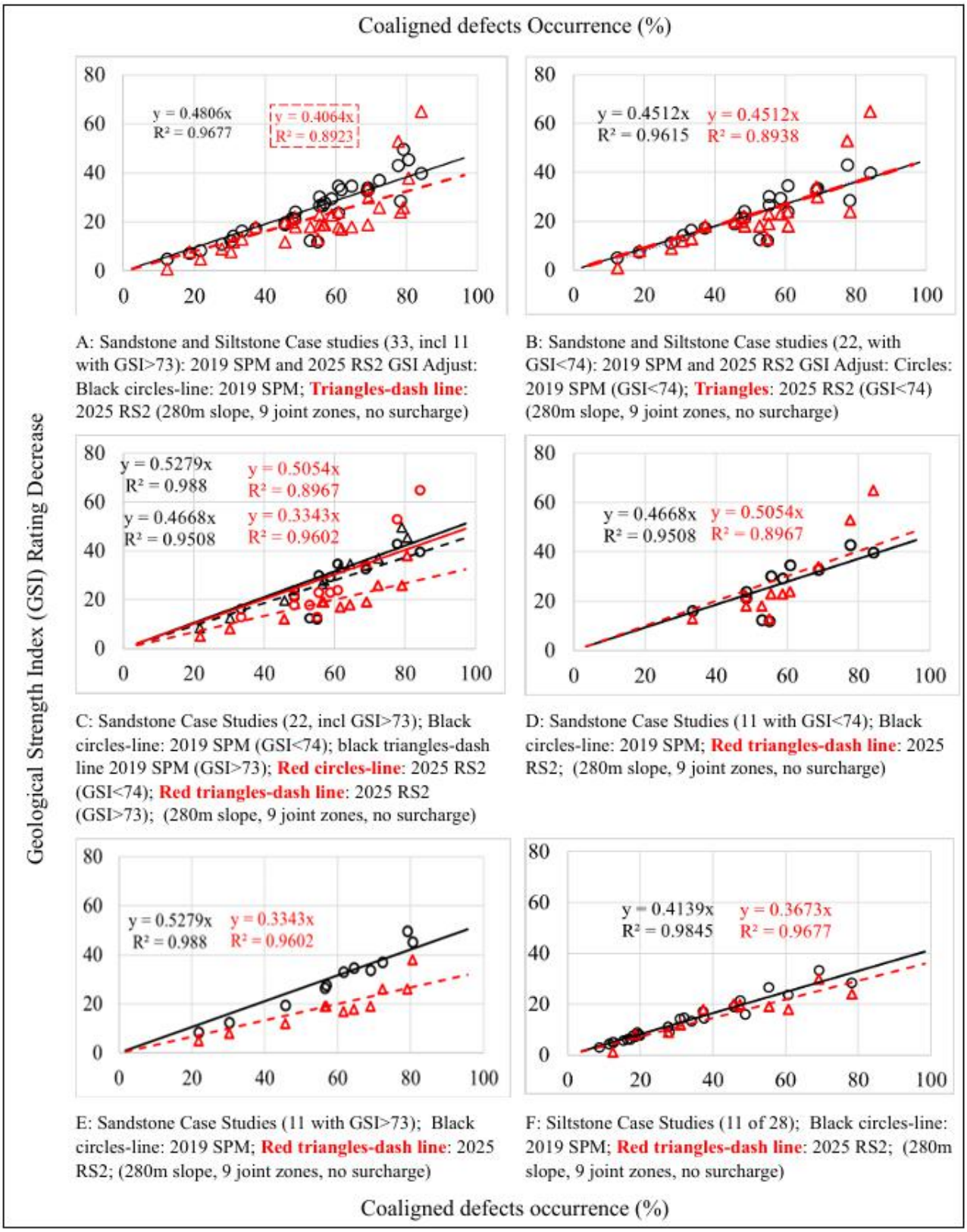


Figure 9: RS2 finite element results for 2019 SPM sandstone and siltstone case studies

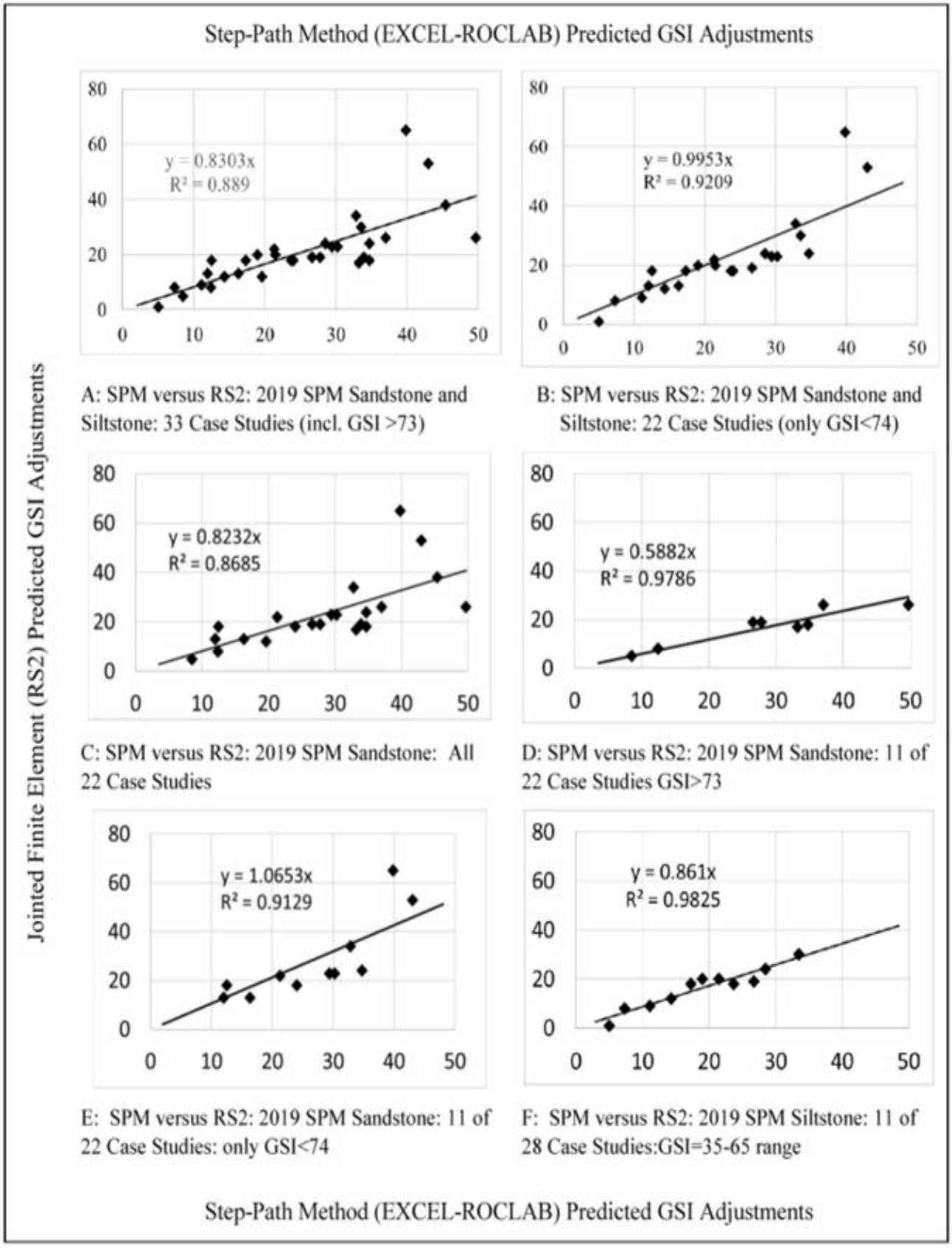


Figure 10: Step-Path Method versus RS2 finite element predicted GSI Adjustments

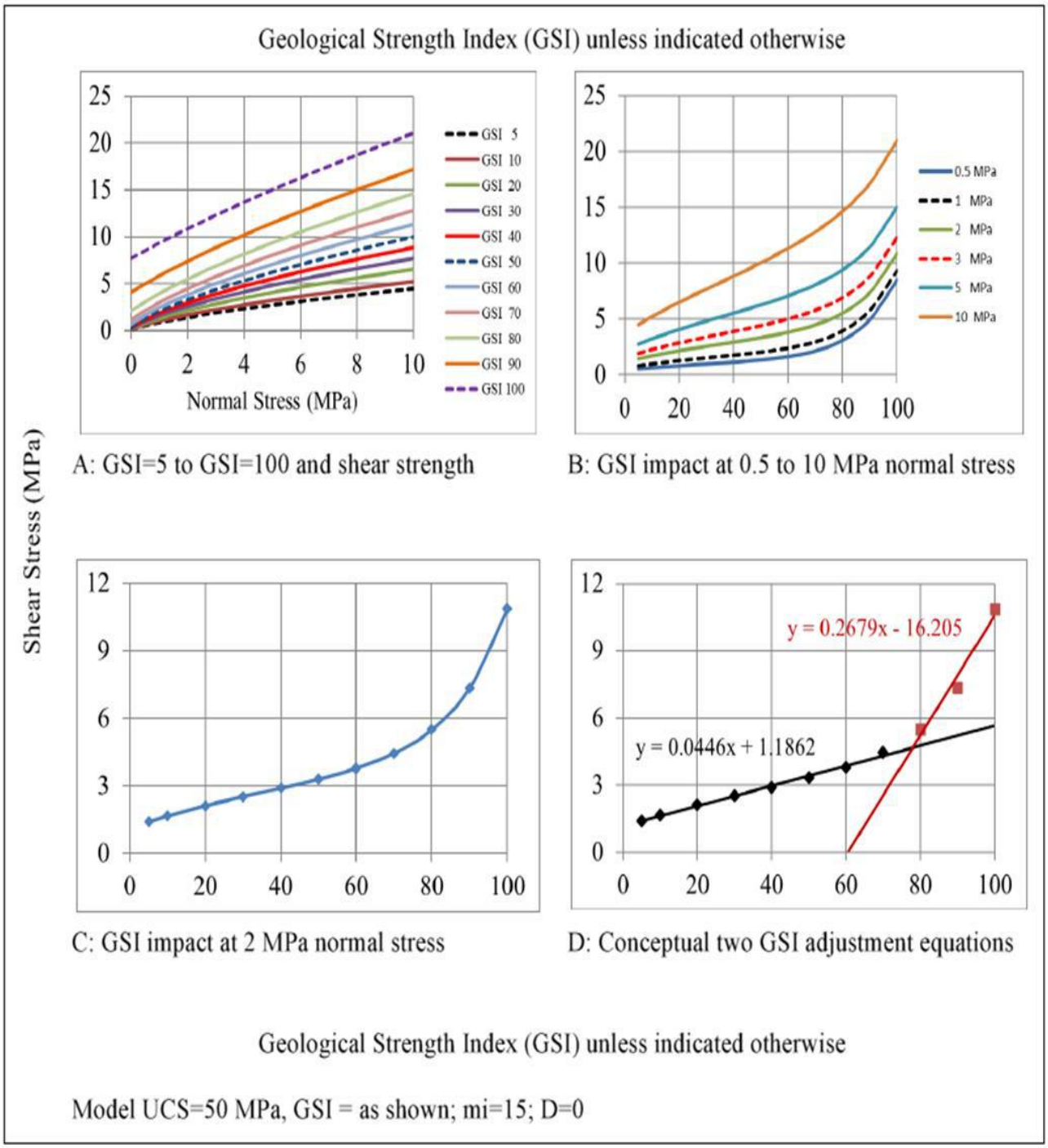


Figure 11: Shear stress outcome due to non-linearity of GSI Index model (Baczynski, 2019)

12 DISCUSSION

The GSI adjustment equation comprises two parts. Firstly, there is a negative GSI adjustment for the relative occurrence of geological defects that are coaligned with slope failure paths. Secondly, there is a positive GSI adjustment for the relative occurrence of intact rock bridges between the coaligned defects. Finite element modelling presented in this paper checked the coaligned defects component. All modelled bridges were rock mass strength. Validation of intact rock bridges is still required.

Completed RS2 analyses assessed two model types. The first was a near-mean conceptual sandstone model; second comprised all of the 22 sandstone and 11 of 33 siltstone case studies in Baczynski (2019).

Conceptual models aimed to broadly check the validity of negative GSI adjustments logic and to understand how various factors impacted outcomes. Factors included single and multiple lines of coaligned defects along failure paths, defect occurrence in clusters (zones), length, rock mass bridge lengths (and line spacing) between them, shear strength and normal / shear stiffness. Irrespective of their potential numerical modelling importance, defect stiffness and rock mass dilation are not inputs to GSI index in the HBM. Hence, these should not be deemed additional constraints to be considered in reconciling SPM and HBM strengths via GSI adjustments.

Slope face of some models was 1.5 MPa vertically surcharged to achieved 2-3 MPa normal stress on dipping defect surfaces and thus provide results in same stress range as considered in Baczynski (2019). Results are summarized in Sections 11.1 to 11.5.

Figures 9 and 10 and Sections 11.6 summarize the results of 2019 case study FE modelling. Initial intention was to just FE model all of the 22 sandstone cases to check validity of 2019 GSI adjustment equation. Eventually, 11 siltstone cases were also modelled. The selected siltstone subset aimed to have FE results over the full range of coaligned defect occurrences (10% to 80%) and to consider siltstone from several locations.

13 FUTURE NUMERICAL MODELLING

To date, 33 of the 230 case studies in Baczynski (2019) had been FE modelled. Ideally, the rest or at least a greater number of these cases should likewise be modelled.

In real rock masses, not all defects are perfectly coaligned with failure paths. As coalignment decreases, the negative GSI adjustment will likewise decrease. It is anticipated that this GSI decrease will likely resemble the Snowden adjustment that already exists in the RS2 software (Rocscience, 2020). There's an opportunity to check this situation with the already created RS2 models.

The positive GSI adjustment impact of intact rock bridges between coaligned defects has not been FE checked. This work is required to fully validate the 2019 published GSI adjustment equation. Presently considered rock mass bridges were 0.77 to 5.2m long. Intact rock bridges are typically very much shorter (often 0.01 to 0.3m) and rarely exceed 1m. A new suite of FE models will be required to assess intact rock bridges.

14 CONCLUSIONS

Coauthors conclude that two-dimensional, jointed RS2 finite element analyses had overall verified the Step-Path Method logic and approach of negative GSI adjustments in Hoek-Brown Method for coaligned defect occurrence along failure paths in rock slopes. Coaligned defects are those that near-parallel the failure path trend and dip into the pit excavation. The positive GSI adjustment impact of intact rock bridges between coaligned defects remains to be FE checked.

Baczynski (2019) GSI-adjustment equation adjustments are valid for rock masses with GSI $\leq$ 73; this upper-bound GSI is marginally less than originally suggested, where co-aligned defects dip into the excavation.

Before using these GSI-adjustment equation(s), the analyst should check that the process is not confounded by joint shear strength exceeding Hoek-Brown rock mass strength.

Defect shear strength curve should not cross over the Hoek-Brown rock mass shear strength curve within the normal stress interval (say 1-3 MPa) of slope stability analysis interest. Geotechnical inputs to HBM and Bandis-Barton shear strength analysis equations are not identical. Hence, strength curve cross-overs may occur for low mi and low UCS in HBM equation and for moderate to high JRC and JCS values in Bandis-Barton equation. In reality, geological defects are rarely stronger than rock masses, apart from situations where the rock is extremely weathered to decomposed and defects are very rough and strongly cemented (e.g., quartz, iron oxide).

15 ACKNOWLEDGMENTS

This jointed finite element analysis would not have been possible without Rocscience RS2 software being provided for an extended trial period. Time, assistance and patience of Jiwoo Ahn of Rocscience Australia are much appreciated.

16 REFERENCES

Baczynski, N.R.P. (1980a). Zonal Concept for Spatial Distribution of Fractures in Rock. *Proc. 3rd Aust. NZ Conf. Geomech.*, Wellington, New Zealand, 12-16 May 1980, Vol.2, pp. 2-29 to 2-33.

Baczynski, N.R.P. (1980b). Rock Mass Characterization and Its Application to Assessment of Unsupported Underground Openings. *PhD Thesis*, Department of Mining & Metallurgy, University of Melbourne, Vic., Australia, dated 25 Nov. 1980, 233p., 66 Figures, 15 Tables, Appendix 1 (5p.)

Baczynski, N.R.P. (2000). STEPSIM4 Step-Path Method for slope risks. *GEOENG 2000, Pro Int Conf Geotech & Engng. Geol*, Melbourne, Australia, 2, 86

Baczynski, N.R.P. (2018). Step Path adjusted Hoek Brown GSI Chart. *Proc. 10th Asian Rock Mech. Symp., ARMS10, The ISRM Int. Symp. 2018*, 29 Oct – 3 Nov, Singapore, 12p

Baczynski, N.R.P (2019). GSI adjustments for directional Hoek-brown strength calibrated by Step-Path case studies. *Aust Geomech J.*, 54(3), p51-78.

Baczynski, N.R.P (2022). Step-Path Method for rock slopes. *University of Queensland, Course UQ CIVL 4280, 2022 Advanced Rock Mechanics*, Guest Lecture, 15 Aug 2022, PPTX PowerPoint, 136 slides.

Bandis, S.C., Lumsden, A.C. & Barton, N.R. (1983). Fundamentals of rock joint deformation. *Int. J. Rock Mech. Min. Sci. Geotech. Abstracts,* 20(6), pp 249-268.

Bar, N. & Baczynski, N.R.P. (2019). Slope failure risks by engineering geological logic and the Simplified Step-Path Method. *13th Aust NZ Conf Geomechanics*, Perth, Australia, 5p.

Barton, N., Lien, R., & Lunde, J. (1974). Engineering classification of rock masses for the design of tunnel support. *Rock Mech.*, 6(4), pp 189-236

Barton, N.R. (1976). The shear strength of rock and rock joints. *Int. J. Rock Mech. Min. Sci. Geotech. Abstracts*, 13(9) pp 255-279

Barton, N.R. & Bandis, S.C. (1990). Review of predictive capabilities of JRC-JCS model in engineering practice. In *Rock Joints, Proc. Int. Symp on rock joints*, (ed. N. Barton and O. Stephansson), pp 603-610, Rotterdam, Balkema.

Barton, N.R. & S.C. Bandis, 2017. Characterization and modelling of the shear strength, stiffness and hydraulic behaviour of rock joints for engineering purposes. *Rock Mechanics and Engineering*, Ed. Xia-Ting Feng, Vol. 1, Ch. 1, pp. 3-40. Taylor & Francis.

Barton, N. (2018). Barton-Bandis Criterion. In Bobrowsky, P., Marker, B. (eds) *Encyclopedia of Engineering Geology*. Geology. Encyclopedia of Earth Sciences Series. Springer, Cham.

Bieniawski, Z.T. (1976). Rock mass classification of rock masses and its application in tunnelling. *Proc. Third Int. Cong. Rock Mech. ISRM*, Denver, 11A, 27-32.

Bieniawski, Z.T. (1989). *Engineering rock mechanics classification*. New York, Wiley.

Deere, D.U. (1963). Technical Description of Rock Cores for Engineering Purposes. *Rock Mech. Engng. Geol.*, Vol 1, pp.16-22.

Han, G, Chen, Z., Xiang, J., Gao, Y., Zhou, Y., Tang, Q. & Chen, W. (2023). Numerical simulation study on shear properties of rock joints under CNS boundary conditions. *Geotech. Geol. Engng.,* Vol 42, pp.1351-1371

Hoek, E. & Brown, E.T. (1980). Empirical strength criterion for rock masses, *ASCE J Geotech Div*, 106 (9), pp 1013-1035

Hoek, E. & Brown E.T. (1997). Practical estimates of rock mass strength. *Int J Rock Mech Min Sci*, 34(8), pp 1165-1186

Hoek, E, Carter T.G. & Diederichs, M.S. (2013). Quantification of the Geological Strength Index Chart. *Proc 47th US*

Rock Mechanics / Geomechanics Symp, 23-26 June 2013, San Francisco CA, USA.

Jennings, J.E (1970). A mathematical theory for the calculation of the stability of slopes in open cast mines. *Proc. Symp. Planning Open Pit Mines*, PWJ van Rensberg (ed), Johannesburg, Balkema (Cape Town, 1971), pp 87-102

Kulatilake, P.H.S.W., Shreedharan, S., Sherizadeh, T., Shu, B., Xing, Y. & He, P. (2016). Laboratory estimation of rock joint stiffness and frictional parameters. *Geotech. Geol. Engng.,* Vol 35, 13p.

Lambert, J. & Frye, C. (2022) Microsoft Excel (Office 2021 and Microsoft 365) Step-by-Step", Microsoft Corporation & Pearson Education, Inc., 67p

Little, T.N. Cortes, J.P. & Baczynski, N.R. (1997-2000). Risk-based slope design optimisation study for the Ok Tedi copper-gold mine. Vol 1 to 8 & Executive Summary, Ok Tedi Mining Limited, Mine, Technical Services Dept., Geotech. Engng. Section, internal report

McMahon, B.K. (1979). Report to Bougainville Copper Limited on slope design studies, Pan Hill, McMahon, Burgess & Yates, Sydney, internal report.

Niktabar, S.M.M.; Rao, K.S., Shrivastova, A.K., & Scucka, J. (2023). Effect of varying stiffness of rock joints under 0cyclic shear loads, *Materials,* Vol 16, No. 4272, 20p.

Noorzad, A. &, Aminpoor, M. (2008). Effect of joint stiffness values on stresses of jointed rock. *ISRM Int Symp 2008, Fifth Asian Rock Mech. Symp. (ARMS5),* 24-26 Nov 2008, Tehran, Iran, pp. 437-443

Rocscience (2007). Roclab 1.0, Users Guide, 19p.

Rocscience (2020). RS2: Slope Stability Verification Manual. Parts 1 to 4, 441p

Rocscience (2024). RS2: Joint Analyses Verification Manual. 108p

Truzman, M. (2007). Statistical summary of rock mass characterization for tunnels of the Caracas-Tuy Medio Railway Project", *Proc XXIII Pan-American Conf Soil Mech Geotech Engng*, Margarita Is, Venezuela, 2, pp 877-882

Wang, B., Jiang, Y., Zhang, Q., & Chen, H. (2024). Shear behaviour of intermittent joints subjected to shear cycles under constant normal stiffness conditions: effects of loading parameters. *J. Rock Mech. Geotech. Engng,* Vol 16 (2024), 43p.

https://doi.org/10.56295/1ACEG34

ENGINEERING TERRAIN EVALUATIONS – OPPORTUNITIES AND CHALLENGES OF THE ENERGY TRANSITION

Tom Casey
Arup

ABSTRACT

As traditional energy (oil/gas) companies and other investors look to develop integrated export-scale green hydrogen hubs and onshore renewable power generation, the vast open spaces of Australia, are being explored to unlock the abundant and reliable renewable energy resources (wind/solar), supporting our energy transition.

The Clean Energy Council of Australia reported [1] tens of billions dollars of large-scale renewable energy projects are under construction across Australia, with almost 40% of Australia's energy generation from renewable sources in 2023.

Renewables in Australia, both onshore and offshore, are shown to be reliable, affordable and sustainable. Australia is one of the windiest and sunniest countries on the planet and a large proportion of regional communities are reported to be supportive of developments with the right engagement, reaping the benefits of jobs, consistent income and local investment that comes with large scale projects. Combined with the prospect of pumped hydro power storage (PHES) and battery energy storage systems (BESS), discussions on requirements for "base load" and "firming" (by coal or gas fired power stations) are likely near obsolete.

The energy transition is a complex topic, and the physical constraints of our environment will have a significant impact.

Challenges of physical environment and simplifying complexity

Many energy transition projects will be set across extensive, remote or minimally developed landscapes of varied terrain and geology; crossing innumerable natural features and obstacles, encountering a spectrum of complexity at surface and in the subsurface. Understanding of the range and significance of engineering constraints and cost drivers is key to early decision making on project feasibility, in pre-FEED/FEED assessments and in subsequent execution and operational phases.

Engineering Terrain Evaluations (ETE); methodical and multi-phased assessments, are performed with the goal to simplify and characterise the complexities of these vast sites into a spatial framework, defined by broad landscape areas (terrain units) with a consistent range of geological and terrain conditions. Each terrain unit can be considered as a single unit from a planning or costing perspective, defining significant engineering constraints and cost drivers.

In simple terms, the principal purpose of an ETE is to identify sources of geohazard risk and evaluate the implications for project feasibility, site selection/suitability and high-level inputs to layout optimisation. This approach represents best practice approach when considering assessment of large-scale sites; and helps inform both SME and non-technical parties within owner/developer organisations.

The challenge for studies on such projects is rarely to do with managing large volumes of information and data, as many are remote locations with sparse site observations, limited to no detailed records (bores), topographic surveys and mapping. Rather, it is the need to determine the range of anticipated characteristic conditions, by extracting key geological/geomorphological information from limited sources and reliance upon expert judgement/experience of engineering geologist/geomorphologists. Knowledge and experience in this context is invaluable.

Recent experience

Recent project experience in Western Australia (Pilbara), South Australia (Eyre Peninsula) and Queensland, considered power generation sites of several thousand square kilometres and/or linear infrastructure corridors extending of many hundreds of kilometres. All projects adopted a broadly consistent approach to the terrain evaluation, which resulted in clear, concise and actionable advice, informing technical and commercially driven aspects of projects and client teams.

Initial screening established those geohazards that may be significant for power generation plant (wind turbine and solar arrays) and associated infrastructure/facilities, including roads, cables and pipelines within power generation envelopes. Simple hazard-risk models were then developed to identify how these geotechnical hazards ('geohazards') can lead to specific adverse consequences.

Preliminary terrain classification (mapping) was generally guided by two main factors; (i) topography; defining surface geomorphology and terrain ruggedness; and (ii) geology, defining the shallow sub-surface conditions. These two factors

[1] https://cleanenergycouncil.org.au/advocacy/industry-snapshot

can be considered in terms of relative complexity ratings, where topography was referred to as “Site Complexity”, and the sub-surface ground conditions, referred to as “Geotechnical Complexity”.

Site complexity reflects the constraints on layout of power generation plant and routing of access roads, buried cables and pipelines. In low relief/near level terrain, standard geometric grid layouts can be adopted, whereas in terrain of increasingly rugged, high relief and steep terrain, the impacts can be felt in the wind regime at site or could result in shading of PV.

Geotechnical complexity accounts for ground-related hazards and impacts upon foundation and subgrade conditions and can impose significant construction costs (cost drivers) requiring mitigation.

A simple five-class qualitative assessment (Low, Medium-Low, Medium, High, Very High) was made for the level of site and geotechnical complexity in each terrain unit defined, and points plotted on a matrix for ease of comparison.

The value in this approach is how it enabled differences in complexity between terrain units to be qualitatively rated or ranked, and understood in terms of broad impacts to both construction and maintenance cost (including investigation, design and mitigation costs) and the residual risks to which the project would be exposed. The difference is measured in terms of whether standard engineering considerations/solutions apply, versus requirements for special measures and more design and construction considerations or indeed zones to exclude/avoid.

This simple approach to defining the complexity of a site was most usefully applied to the large power generation envelopes and other development sites where layout was a critical design issue. This approach establishes a consistent framework for assessment of large sites/broad corridor complexity, it does not wholly address requirements appropriate to long linear infrastructure corridors (transmission), and specifically routing constraints for buried pipelines.

Subsequent studies targeted increased characterisation of threats to the project posed by indirect and/or temporal hazards, including extreme wind (tropical cyclone), fluvial flood, bush fire, seismicity, tsunami and coastal erosion. Studies further informed layout and routing constraints, mitigation measures for specific hazards, and identified requirements for detailed analysis/modelling or where design codes may be lacking. Material sourcing studies aimed to inform planning for construction material supply potential from local borrow sites and regional commercial supply .

Each stage of an ETE aims to minimise and characterise uncertainty; and to achieve this requires the right people, skills and expertise. These skills are core to experienced engineering geologists and geomorphologists. When deployed on projects in a timely manner, anticipated geohazards can be identified, managed appropriately and effectively communicated to decision makers, technical specialists and stakeholders, to achieve positive outcomes.

Opportunities with the modern digital age

The need for experienced people will never diminish, and the wealth of geospatial data currently available can present challenges in simplifying the complexities of site conditions into a meaningful framework for identification and management of risks. With the right experience, combined with state-of-the-art data analysis and application of AI/ML techniques, opportunities exist to provide repeatable outputs with greater insights. Much of the data used in recent projects was a rich mix of publicly accessible geospatial mapping (including geology) and digital elevation models (initially 1 sec SRTM data, and subsequently detailed LiDAR). Data which is widely used in common geospatial analysis.

Application of generative AI (e.g. Large Language Models) in geospatial analysis, is going to be a valuable tool in augmenting the desktop study process, but is unlikely to replace the human expertise factor, not yet anyway. As with any complex modelling or assessment process, the saying “rubbish in, rubbish out” remains true, in the absence of sufficient, quality data and inadequate understanding of the problem or conditions being considered.

Recent reports suggest that more than 90% of students are using AI to complete work; and whilst this approach may build perceived proficiency in using these digital tools, it is unlikely to build knowledge and deep learnings on the particular topic. The AI landscape is rapidly developing, reliability and accuracy will most likely improve, but there will remain elements of uncertainty that cannot adequately be predicted; and that will need application of expert judgement, based on years of experience, knowledge gathering, learning in the field and at the desk.

The importance of technical guidance, knowledge sharing and experience of global geohazard risk expertise is invaluable and it is clear that knowledge sharing and technical mentoring by senior industry expertise will be critical for development of future generations of engineering geologists (EG).

Challenges of the professional landscape in Australia

Skills and labour shortages are impacting the energy transition, and so it is imperative that industry advocates for the necessary skills and people. AI is useful, but it will not replace our jobs, yet.

Geologist remains on the Australian skills shortage list and yet geoscience and engineering geology undergraduate/post-graduate course are declining (globally) and so the supply of graduate/postgraduate geoscientists/EG's will follow.

Industry recognition and avenues for professional registration of geologists in the engineering sector in Australia are inadequate and likely contribute to the attrition of skilled geoscience expertise and resources.

The absence of an impactful route to professional registration/accreditation of geologists and recognition within the engineering sector critically undermines and devalues the skills and expertise of engineering geologists in industry. Particularly for those EG professionals in the early stages of their careers and who have not spent time overseas, notably in the UK or US.

The peak bodies, professional organisations and routes to professional registration in the UK and US, are a good examples of the type systems and professional pathways that promote application and collaboration of the diverse range of geoscience, engineering geology and geotechnical engineering skills, with relative parity of recognition. These pathways can always be better, but they are a good starting point.

In Australia, this critical gap and weakness in professional registration of EG's has influence beyond the sector/industry. Specifically, poor perception of geology within engineering sector as a long term career option, particularly for the generation currently in the tertiary education (if they even know of it as an option).

Persistent historical perceptions of geology and careers in geology across the Australian education system, appear somewhat skewed towards those of mining/mineral extraction and hydrocarbon industries; those typically of adverse environmental impact and significant contributors to climate change and global warming. Some of these industries continue to play a vital part in society of today; however, it is clear that things must change, and the younger generations are becoming more vocal on the urgency for change.

Unfortunately, awareness of alternative careers and the valuable role of geologists in supporting society, protecting it from the impacts of natural hazards is poor [2] (Australian Geoscience Council, Project Geoscience survey).

We have seen the impact of this poor perception and awareness playing out in recent times, with closure of distinguished, long standing geoscience and engineering geology undergraduate/post-graduate courses in Australia, New Zealand and the UK. The reasons are multifaceted, both commercially driven and reducing enrolment, but the result is the same, severe impact to the supply of trained geoscientists available to industry in support of the ever-increasing geohazard challenges.

For a continent which faces increasing severity and incidence of climate and weather-related geohazards; the society and built environment are encroaching into ever more remote and challenging terrain (both onshore and offshore); the pressures of increasing population and urbanisation, and developments pushing into poorer and potentially more adverse terrains; the need for more experienced engineering geologists is ever more critical to manage risks that come from this friction of natural hazards, human made risks and potential disasters.

Where to from here?

The diverse range of skills required to tackle geological and climate related threats to society and communities worldwide, should be an easy theme to promote to younger generations. Early STEM engagement in schools is critical to developing awareness and enthusiasm required to prime interest for tertiary studies/training and into professional practice. Some are making efforts in this space, but more is required.

The growth of digital skills, AI technology and application to such engineering studies for energy transition projects described, present a unique platform to influence perceptions and engage interest of younger, more digitally savvy generations in the range of rewarding careers in engineering geology and broader geosciences.

Whether future generations of geoscientists come into the engineering by chance or by choice, the industry in Australia must improve the environment into which they come, and provide meaningful pathways for professional recognition.

As we are all keenly aware from our professional practice of the geosciences, the past is the key to the future and we must learn and act for the benefit of all, or face the consequences.

Acknowledgements

Discussion presented draws heavily on recent experience in Western Australia/South Australia/Queensland (confidential), learnings and knowledge sharing by global geohazard risk expert and 24th Glossop Lecture and Medal recipient, Dr Mark Lee (Ebor Geoscience Ltd, UK), to whom I am immensely grateful for his generosity and guidance. Opinions and observations are those of the author and do not necessarily represent affiliated organisation(s) or named expertise.

[2] https://www.agc.org.au/wp-content/uploads/2025/02/Fiftyfive5-AGC-Project-Geoscience-SUMMARY-19122024.pdf

https://doi.org/10.56295/1ACEG35

ENGINEERING GEOLOGICAL MAPPING FOR DAM FOUNDATIONS - EXAMPLES FROM RECENT WORK

Jo Darby[1], Chris Hathaway[1], Christopher Bennett[1], Chris Chamberlain[2]
[1] GHD, [2] Engineering Mapping Australia

ABSTRACT

This paper explores the importance of engineering geological mapping of dam foundations to enable the assessment of engineering geology characteristics that influence geotechnical parameters, analysis and design of dam foundation design.

The paper provides examples from recent project work where foundation data is recorded by the engineering geologist using technology such as drone - mounted Light Detection and Ranging (Lidar). This approach improves the spatial accuracy of mapped geological features and aids the engineering geologist in producing geological foundation records for as built records.

The paper also describes the process for identification and description of geological features exposed at the foundation surface and includes a methodology for description of geological features using Australian Standard AS1726 - Geotechnical Site Investigations to assist with the assessment of the origin of each defect and describe the associated engineering properties.

Correct assessment of engineering properties is critical for developing a foundation geotechnical model and assessing the foundation kinematics. Recent project work has demonstrated that detailed engineering geological mapping is essential in developing a comprehensive engineering geological model and geotechnical model as required by ANCOLD (2020) and IAEG/C25 (2022) guidelines.

1 INTRODUCTION

It is best practice that foundations of large infrastructure dams and those with significant risk profiles are carefully documented from an engineering geology and geotechnical viewpoint to provide a record of conditions which become permanently hidden once construction is complete. This paper focuses on the engineering geological mapping of rock foundations and explores:

- The purpose and historical approach of engineering geological mapping for dam foundations.
- The importance of understanding the geological model, engineering geological model and geotechnical model, and origin of defects in engineering assessment and design.
- The use of technology to aid data collection during engineering geological mapping of foundations.
- The application of engineering geological mapping to design and construction.
- The benefits to asset owners of having detailed engineering geological mapping.

Project work from three recent example projects, ‘Project A’, ‘Project B’ and ‘Project C’ are presented herein and are used to demonstrate the importance of detailed engineering geological mapping for dam construction and post-construction dam needs. ‘Project A’ focuses on engineering geological mapping undertaken for a dam risk assessment, ‘Project B’ focuses on engineering geological mapping undertaken for design and ‘Project C’ focuses on construction phase engineering geological mapping.

2 ENGINEERING GEOLOGICAL MAPPING OF DAM FOUNDATIONS

Throughout the history of dam construction varying levels of engineering geological mapping of foundations have been undertaken - often dependant on available time, budget, resources, technology and perceived needs. The engineering geologist must balance these variables and apply them (as required) to processes such as high-level geological reconnaissance mapping, detailed engineering geological mapping during construction and post-construction engineering geological mapping to fill data gaps identified in the engineering geological model or geotechnical model.

2.1 PURPOSE OF ENGINEERING GEOLOGICAL MAPPING AT DAM SITES

The practice of engineering geological mapping at dam sites extends from initial green field assessment through to the construction and post-construction phases. Initial geological reconnaissance mapping of a proposed dam site provides input to site selection and preliminary design and may feed into later construction stage activities and post construction monitoring. Construction phase engineering geological mapping is typically performed to provide a record of encountered ground conditions for design verification and to guide foundation preparation. Construction phase and additional post

construction engineering geological mapping may be used for future input to risk assessment, forensic engineering and the design of further investigations at the site.

For dam foundation mapping in Australia, guidance is provided by the Australian National Committee on Large Dams' (ANCOLD) Guidelines for Geotechnical Investigations of Dams their Foundations and Appurtenant Structures (ANCOLD, 2020). More explicitly, the ANCOLD guidelines for Concrete Gravity Dams (ANCOLD, 2013) identify adequate engineering geological mapping of a dam foundation as a specific input to determining if 'well defined' strengths and their associated factors of safety can be adopted. Further guidance on engineering geological mapping for engineering purposes and its place in the Engineering Geological Model is provided in the International Association of Engineering Geologists' (IAEG) C25 Guidelines for the Development of Engineering Geological Models on Projects (IAEG, 2023). Several other publications are available that provide more general guidance on the mapping and information gathering process to assist in planning and logistics (e.g., Basic Geological Mapping by Lisle et al., 2011).

The basic engineering geological mapping process is similar for all dam types, however, must be tailored for the specific site and project conditions. Site specific requirements for mapping may be guided by the site geology, access constraints or the availability of resources (personnel and technology).

Engineering geological mapping for dam foundations needs to adequately record ground conditions for purposes specific to dam design and safety that include assessment of:

- The presence of low strength material that may control foundation strength or be susceptible to erosion.
- The presence of leakage pathways.
- The presence of kinematically unfavourable failure mechanisms.
- The adequacy of the rock mass to resist deformation.
- The shear strength of the foundation.
- The appropriate level of the foundation.

2.1.1 Historical Approach

The role of engineering geology in dam construction is well documented since in the early 20th century and mapping of ground conditions is a long - recommended practice. Herbert Lapworth in his lectures describes "geological mapping" and provides examples of the economic benefits to dam construction of adequate geological investigation (Lapworth, 1908) and further describes the importance of investigation trench mapping in dam foundations as part of site evaluation/selection (Lapworth, 1912).

The importance of engineering geology in dam design and construction was further demonstrated throughout the early 20th century following several dam failures that were attributed to geological conditions in the foundation. The failure of the Saint Francis Dam and the loss of more than 430 lives, in part resulting from 'defective foundations' (Wiley, 1928), became somewhat of a catalyst in the United States for the enlightenment of engineers as to the importance of understanding the geological conditions at a dam site (Burwell and Moneymaker, 1950).

The basic approach to engineering geological mapping for foundations is relatively unchanged from 100 years ago, with fieldwork focussing on the survey of rock exposures and defects, the measurement of feature orientation (strike / dip, dip / dip direction), properties (e.g., thickness and spacing), and sketching of these features to show their distribution and to allow interpretation of 'unseen outcrops' (Lapworth, 1908). Similarly, the basic tools of mapping remain the same, with early dam foundation engineering geological mapping utilising tools that are still used by geologists today including a pocket-book, compass, clinometer, tape and hammer (Lapworth, 1908).

Through the 20th century, advancements in digital technology were reflected in changes to mapping processes and the introduction of cameras, hand-held GPS, computers and GIS allowed for improvements in data capture and processing. McAffrey et al. (2005) identified that the cost and physical bulk of digital field equipment in the early 2000s was prohibitive to their widespread use, however, accurately predicted that in future these would become "more streamlined physically, durable, with long-life batteries and wireless connectivity". In recent years, engineering geological mapping of dam foundations has moved in step with significant advancements in technology and now regularly includes the use of drones, photogrammetry, digital logging tools and 3D models. However, technology should provide a supporting role as nothing supersedes the importance of physical observations made by an engineering geologist in the field.

2.2 GEOLOGICAL, ENGINEERING GEOLOGICAL AND GEOTECHNICAL MODELS

ANCOLD (2020) describe the progressive development of geological, engineering geological and geotechnical models:

1. Geological Model: a conceptual model based on the tectonic setting and regional geology of the project site.

2. Engineering Geological Model: builds upon the Geological Model, highlights the geological aspects of the project site and present them in a way engineers understand, incorporates field investigations.
3. Geotechnical Model: builds upon the Engineering Geological Model, characterises the geotechnical properties of critical to the project site and is used by civil and geotechnical engineers to assist analysis (stability, groundwater flow, erosion potential etc), incorporates laboratory testing and instrumentation results.

Establishing a geological model will help with understanding the geological setting of dam foundations and dam sites. A good geological model will then be used to inform future ground investigations (geotechnical drilling and engineering geological mapping) and be developed into an engineering geological model and subsequently a geotechnical model. These models will develop and evolve over the life of the asset and assist in inform future design. Geotechnical investigations (engineering geological mapping and geotechnical drilling) will confirm the assumptions made to develop the models or assist in developing and changing the models further. Geotechnical investigations feed into model development and vice versa; the geological, engineering geological and geotechnical models feed into the development of geotechnical investigations.

Engineering geologists need to have a good grasp of the civil engineering design intent when undertaking engineering geological mapping so they can better assess and anticipate key ground conditions within the foundation or surrounding rock exposures. From a project perspective, this will require involvement in the design development process with the engineering design team to ensure that the full exposure to the civil engineering design aspect is provided. Without the understanding, engineering geologists run the risk of incorrectly identifying the defect type described in Section 2.3 while undertaking geotechnical investigations and critical engineering geological risks associated with the intended design.

Our example 'Project B' first developed a conceptual geological model using available literature and existing geotechnical investigation information. The model showed the different geological units present at the dam site and large regional type faults. The geological model was then developed into an engineering geological model, followed by a geotechnical model as our understanding of the geological conditions grew as further geotechnical investigations (geotechnical boreholes and engineering geological mapping) were undertaken at the dam site. The geotechnical model shows the distribution of the geotechnical units within the dam foundation as well as investigation data such as engineering geological mapping and laboratory test results. The models have been built using three-dimensional (3D) modelling software to help visual the geological information in three-dimensional space. The geotechnical model was instrumental in informing the geological and geotechnical conditions during dam upgrade design work and assisting in the analysis need to support design.

2.3 IMPORTANCE OF UNDERSTANDING THE ORIGIN OF THE DEFECT

Understanding the origin of geological defects is a key element to assessing the geotechnical parameters needed to undertake design and analysis for dam foundations. Recording the geotechnical properties of each defect in detail during engineering geological mapping assists in understanding the foundation rock mechanics and geotechnical parameter development.

Australian Standard AS1726 - Geotechnical Site Investigations (AS1726) defines a defect as a (natural) "discontinuity, fracture, break or void in the material or materials across which there is little or no tensile strength". The process in which a defect is formed relates to the geological setting (depositional history) and structural development (phases of deformation) of the project area. Understanding the geological setting and structural development of a project area will guide an engineering geologists initial understanding of what types of defects may be present locally within a dam foundation. A detailed description of the geological and geotechnical properties enables the connection between the two scales (regional and local). The connection between how a defect is formed and its geological and geotechnical properties is described in Figure 1 (Fell et al., 2015). Correlation of geological defects with their intrinsic geotechnical properties is noted in historical engineering geological mapping of dam and hydropower projects such as at Tumut 2 Underground Power Station and Kangaroo Creek Dam by David Stapledon (1961 and 1967).

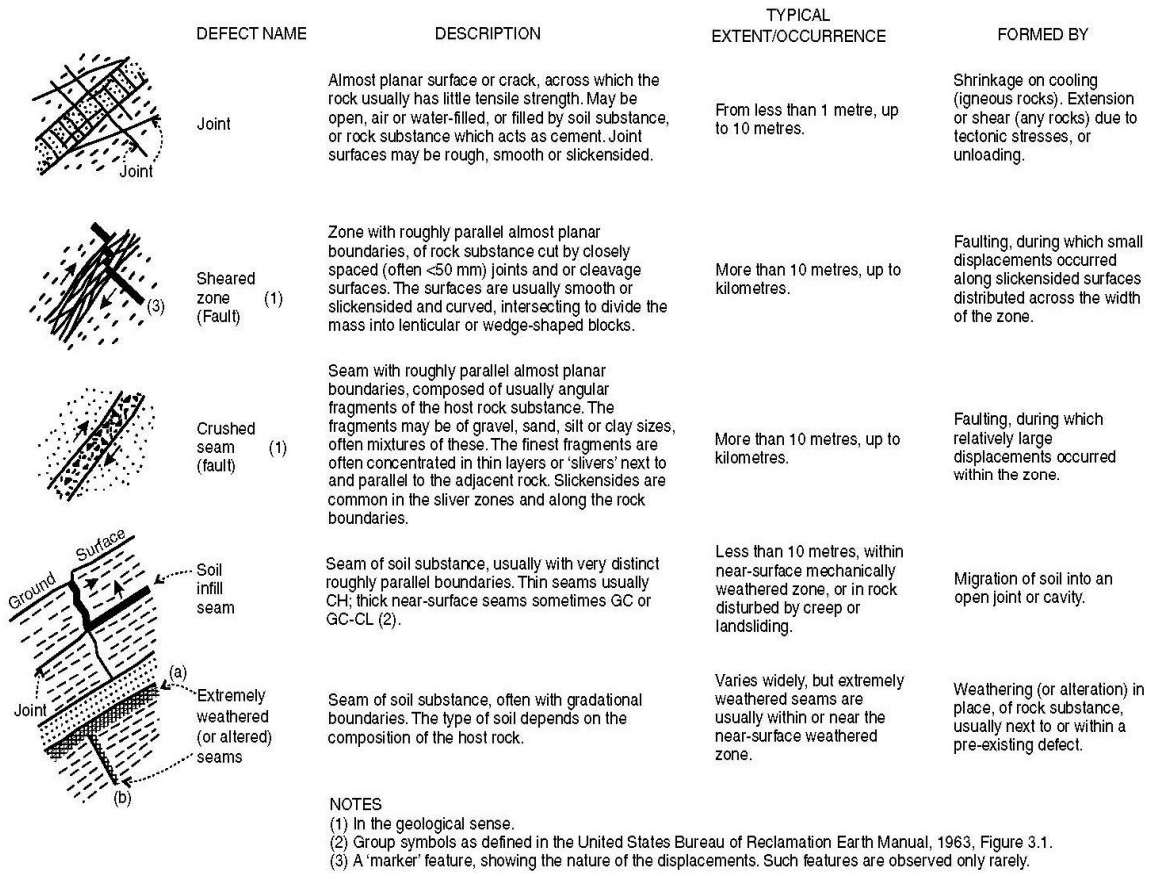


Figure 2.1 Common defects in rock masses.

Figure 1: Figure 2.1 from Fell et al., (2015) describing common defect / features and origins

Whether the engineering shear strength of a rock defect should be assumed to be at peak shear strength or residual shear strength, is inferred by its origin. Rock defects formed through faulting (movement) such as crushed seams, sheared surfaces, sheared seams and sheared zones are assumed to have already overcome peak shear strength to generate movement and are therefore assumed to be at residual shear strength. Rock defects that do not display any form of movement such as partings and joint are assumed to be at peak shear strength as the peak shear strength has not been overcome to generate displacement along the defect. AS1726 provides a framework for defect descriptions and is reproduced in Table 1 with interpretation of the appropriated shear strength applicable to each defect type (peak or residual).

Table 1: Summary of defect types, descriptions origin and engineering shear strength. Descriptions modified based on Table 22, Clause 6.2.5.2, AS 1726-2017, Geotechnical Site Investigations.

Type	Description	Engineering shear strength
Parting[1]	Tensile crack / fabric related. A surface or crack across which the rock has *little or no tensile strength*. Parallel or sub-parallel to layering (e.g. bedding) or a planar anisotropy in the rock material (e.g. cleavage). May be open or closed. Includes bedding, cross bed, foliation, cleavage partings. Formed without movement of the rock mass and is a part of the rock fabric.	Peak shear strength – rock on rock contact.
Joint	See Figure 1 above. Tensile crack. Formed without significant movement of the rock mass.	Peak shear strength – rock on rock contact.
Extremely Weathered Seam	See Figure 1 above. Weathered in-situ material. Shear strength depends on the extent of weathering across the seam and consideration should be made on the scale and thickness of the defect.	Peak shear strength – soil/rock strength.
Infilled Seam	See Figure 1 above. Opening infilled with transported material. Scale and thickness are important, and soil characteristics should be described, especially plasticity.	Residual shear strength – soil strength.
Sheared Surface[2]	Fault related surface. A near planar, curved or undulating surface which is, polished or slickensided and which *shows evidence of shear displacement*. Formed by movement.	Residual shear strength – rock on rock contact.
Crushed Seam	Fault related seam. Seam of *soil material* with roughly parallel almost planar boundaries, composed of *disoriented, usually angular fragments of the host rock* material which may be more weathered than the host rock. The seam has *soil properties*.	Residual shear strength – soil and rock fragment interaction.
Sheared Seam	Fault related seam. Seam of *soil material* with roughly parallel almost planar boundaries, composed of soil materials with roughly parallel near planar, curved or undulating boundaries cut by closely spaced joints, *sheared surfaces* or other defects. Some of the defects are usually curved and intersect to divide the mass into lenticular or wedge-shaped blocks.	Residual shear strength – soil strength integration.
Sheared Zone	Fault related zone. *Zone of rock material* with roughly parallel near planar, curved or undulating boundaries cut by closely spaced joints, *sheared surfaces*, crushed seams, sheared seams or other defects. Some of the defects are usually curved and intersect to divide the mass into lenticular or wedge-shaped blocks.	Residual shear strength – combination of rock on rock contact and soil / rock interaction.

3 ENGINEERING GEOLOGICAL MAPPING TECHNIQUES

The fundamentals of engineering geological mapping have not changed significantly over time however, the techniques used to acquire and document data has significantly improved, largely as a result of improvements in technology and because of standardisation. Recent projects have utilised drone survey and imagery to complete engineering geological mapping in an efficient and effective manner. They have also used mobile photograph applications to take and document photographs of defects as well as recording defect characteristics using scanline mapping techniques.

3.1 USE OF TECHNOLOGY TO AID IN DATA COLLECTION

Engineering geological mapping of dam foundations was originally performed using traditional survey techniques with basic instruments such as grid paper and measuring tapes and utilised photographs where available (e.g. photographs taken from above in crane boxes during construction). As technology has advanced and become more readily accessible, engineering geological mapping techniques now include tools such as digital cameras and compasses (including mobile phones), drones, hand - held GPS and LiDAR, that have significantly improved the quality and speed in which geological data can be captured and documented.

3.1.1 Unmanned Aerial Vehicles (UAV or Drones)

Technology such as UAV or drones can assist the engineering geologist during mapping to improve accuracy and efficiency. Images captured by drones of cleaned foundations can be used to generate base maps that enable the engineering geologist to spatially capture geological features with a high degree of accuracy, in terms of feature shape, length, width and position. Engineering geological mapping can be carried out by hand on sheets overlaying the base map utilising drone imagery. This method allows for efficient data collection and line work compared to other methods such as grid paper using a chainage and offset approach.

Drone images can help engineering geologists identify the large scale geological features that might not be clear when standing on the ground. The image captured provides a bird's eye view of a dam foundation or rock outcrop and geological features with a long persistence will be easier to spot and trace. This helps to reduce bias in data collection and allows for defect persistence to be recorded more accurately.

In some cases, drone imagery might be captured during or after mapping has been completed. The engineering geologist is then able to transpose their work onto the latest imagery, adjusting and amending line work as required.

Drone images of cleaned foundations also provide a good photographic record of construction to supplement the engineering geological mapping sheets produced by the engineering geologist.

In our example 'Project A', drone images were captured part way through engineering geological mapping (during the foundation cleaning process), allowing the engineering geologists to mark out and record coordinates for mapping control points. These control points were used to geospatially rectify the images captured by drone. The engineering geologists on site were then able to quickly record geological boundaries and defects / features allow for more time to be spent describing geological and geotechnical properties and addressing the design purpose the engineering geological maps needed to address. Drone images streamlined the mapping workflow and allowed for efficient data collection over a short time frame. An example of the aerial imagery capture by drone is presented in Figure 2 and the corresponding engineering geological mapping is presented in Figure 3.

In our third example 'Project C', high resolution drone images were captured daily throughout the foundation preparation process by project surveyors, with timing scheduled around the morning and lunchtime construction breaks to maintain project consistency with other teams. The geospatial accuracy of these images was very high (centimetre - scale image resolution) and the resulting base images also contained valuable foundation level information and key foundation control point information that defined the extents of discrete construction lots. An example image is presented in Figure 4.

The resulting engineering geological mapping was able to document geological features to a high resolution while also accurately recording foundation levels. The foundation images, engineering geological mapping and levels were then stored and manipulated digitally as the construction work progressed, allowing an as-constructed foundation model to be produced using 3D geological modelling software. The high level of documented foundation detail will be invaluable in the event that foundation conditions should need to be interrogated in future (e.g. during future safety review or future risk assessment).

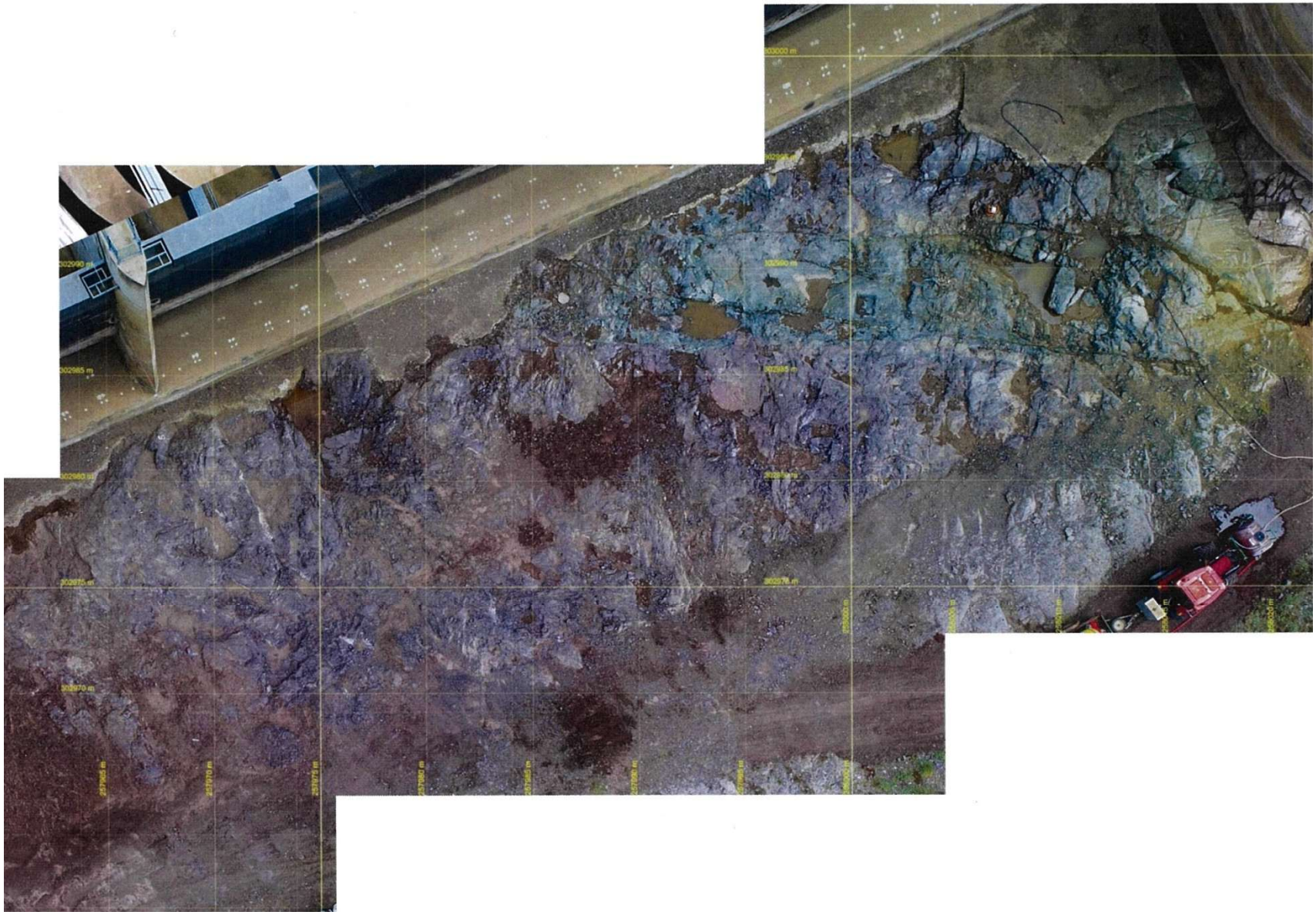


Figure 2: 'Project A' base map created from stitched drone images. The drone imagery has captured the rock foundation near the end of the cleaning process. Different lithologies can be identified by the different colours of the rock and defects can be identified as lineaments

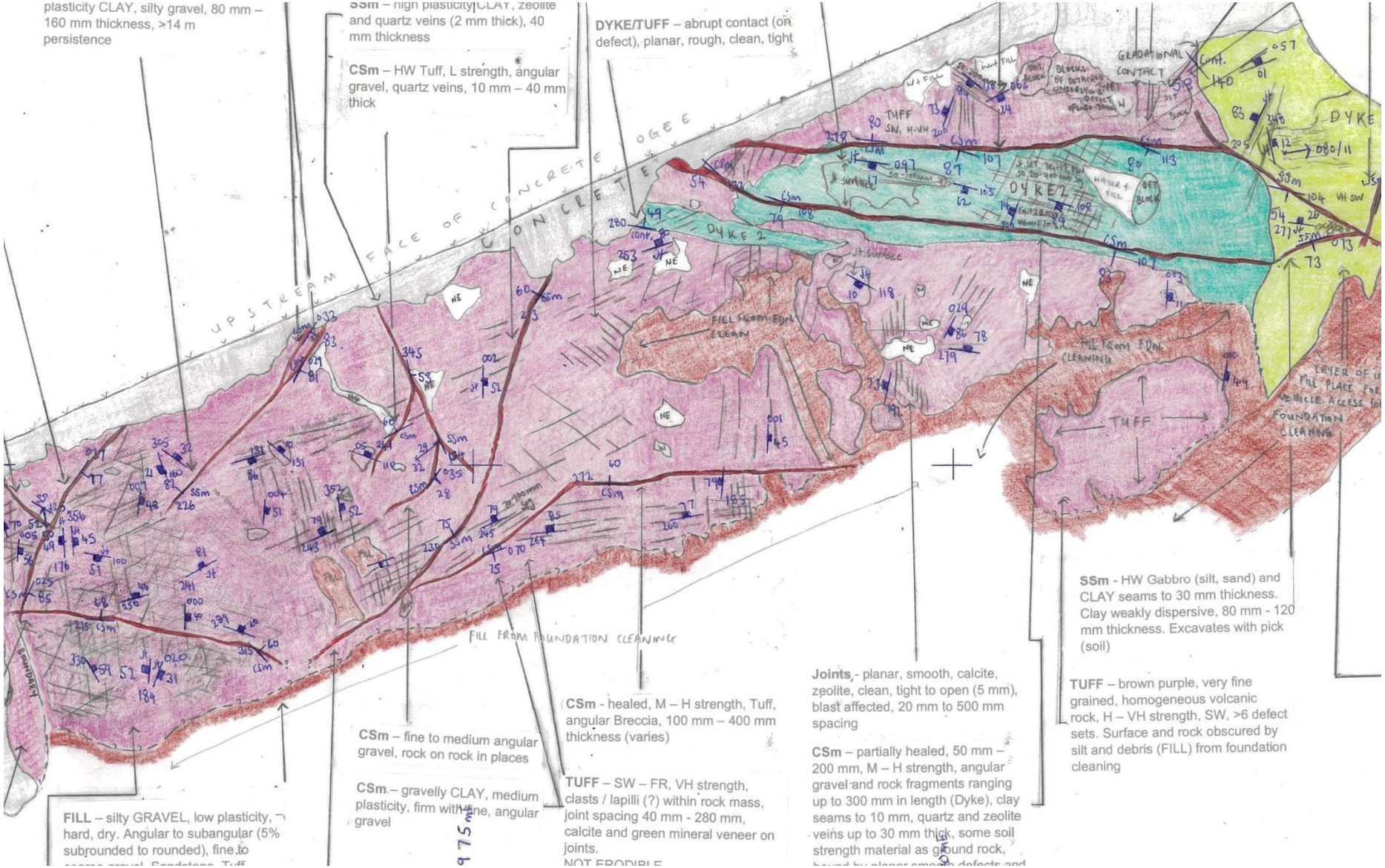


Figure 3: Project A' engineering geological map created using the base map shown in Figure 2, where key defects and lithologies have been documented and described

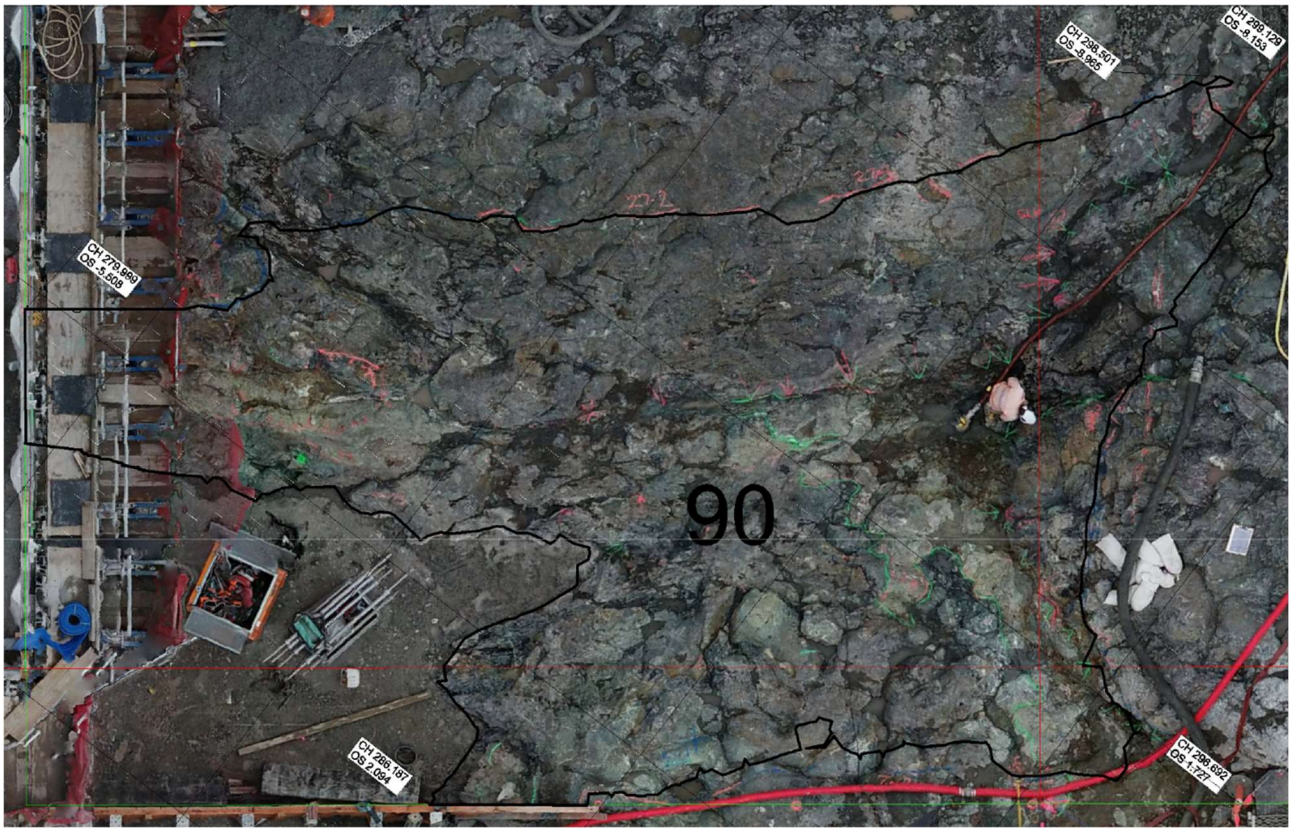


Figure 4: "Project C" example of a base mapping sheet for a specific foundation area showing foundation extents and construction limits. In the example, foundation lot 90 is delineated by the black outline and engineering geologists used this aerial image to complete engineering geological mapping for this foundation lot

3.1.2 Photographs

A consistent documentation process undertaken as part of engineering geological mapping includes providing a photographic record of mapped geological features such as lithologies, geological faults and rock defects. These photographs supplement the engineering geological mapping sheets and are valuable tools for communicating to others the geological conditions of the site. Nowadays, the cameras inbuilt into cell phones are of better or equal quality to that of basic digital cameras making this a readily available tool for engineering geological mapping.

In our examples 'Project B' and 'Project C', hundreds of photographs were taken during engineering geological mapping. Photographs captured each mapped defect and geological features, as well as general photographs of each mapping lot or cleaned rock outcrop. The volume of photographs highlights the need to have an effective and efficient data management system to track and store all the photographs. Photographs were marked on mapping sheets with an identification (ID) and a direction arrow to denote the field of view the photograph has captured. Photographs were taken using a camera application that watermarked photographs with geospatial information such as, the GPS position the photograph was taken from, what direction the photograph is looking in and the feature number and photograph ID. These photographs will be reviewed in the future alongside the mapping sheets throughout the life of the dam.

3.2 DEFECT DATA

The importance of recording detailed data during engineering geological mapping was highlighted during the construction boom of large infrastructure during the 1960s to 1980s, where the emphasis was on meticulous collection of observational data and accurate descriptions of materials and processes (Legget, 1979 and Griffiths, 2014). Observations taken in the field by engineering geologists are crucial to later phases of design and understanding foundation conditions. Figure 5 from Griffith (2004) highlights the information that engineering geology maps should contain and the importance of understanding the purpose of this information and why it is being documented.

Table 8. *Data to be recorded on an Engineering Geology map (Griffiths 2004)*

Geological data

- Map units (chrono- and/or lithostratigraphy)
- Geological boundaries (with accuracy indicated)
- Description of soils and rocks (using standard engineering codes of practice)
- Description of exposures (cross-referenced to field notebooks)
- Description of state of weathering and alteration (note depth and degree of weathering)
- Description of discontinuities (as much detail as possible on the nature, frequency, inclination and orientation of all joints, bedding, cleavage, etc.)
- Structural geological data (folding, faulting, etc.)
- Tectonic activity (notably neotectonics, including rates of uplift)

Engineering Geology data

- Engineering soil and rock units (based on their engineering geological properties)
- Subsurface conditions (provision of subsurface information if possible; e.g. rockhead isopachytes)
- Geotechnical data of the engineering soil and rock units
- Location of previous site investigations (i.e. the sites of boreholes, trial pits, and geophysical surveys)
- Location of mines and quarries, including whether active or abandoned, dates of working, materials extracted and whether or not mine plans are available
- Contaminated ground (waste tips, landfill sites, old industrial sites)
- Man-made features, such as earthworks (with measurements of design slope angles, drainage provision, etc.), bridges and culverts (including data on waterway areas), tunnels and dams

Hydrological and hydrogeological data

- Availability of information (reference to existing maps, well logs, abstraction data)
- General hydrogeological conditions (notes on: groundwater flow lines; piezometric conditions; water quality; artesian conditions; potability)
- Hydrogeological properties of rocks and soils (aquifers aquicludes, and aquitards; permeabilities; perched water tables)
- Springs and seepages (flows to be quantified wherever possible)
- Streams, rivers, lakes and estuaries (with data on flows, stage heights and tidal limits)
- Man-made features (canals, leats, drainage ditches, reservoirs)

Geomorphological data

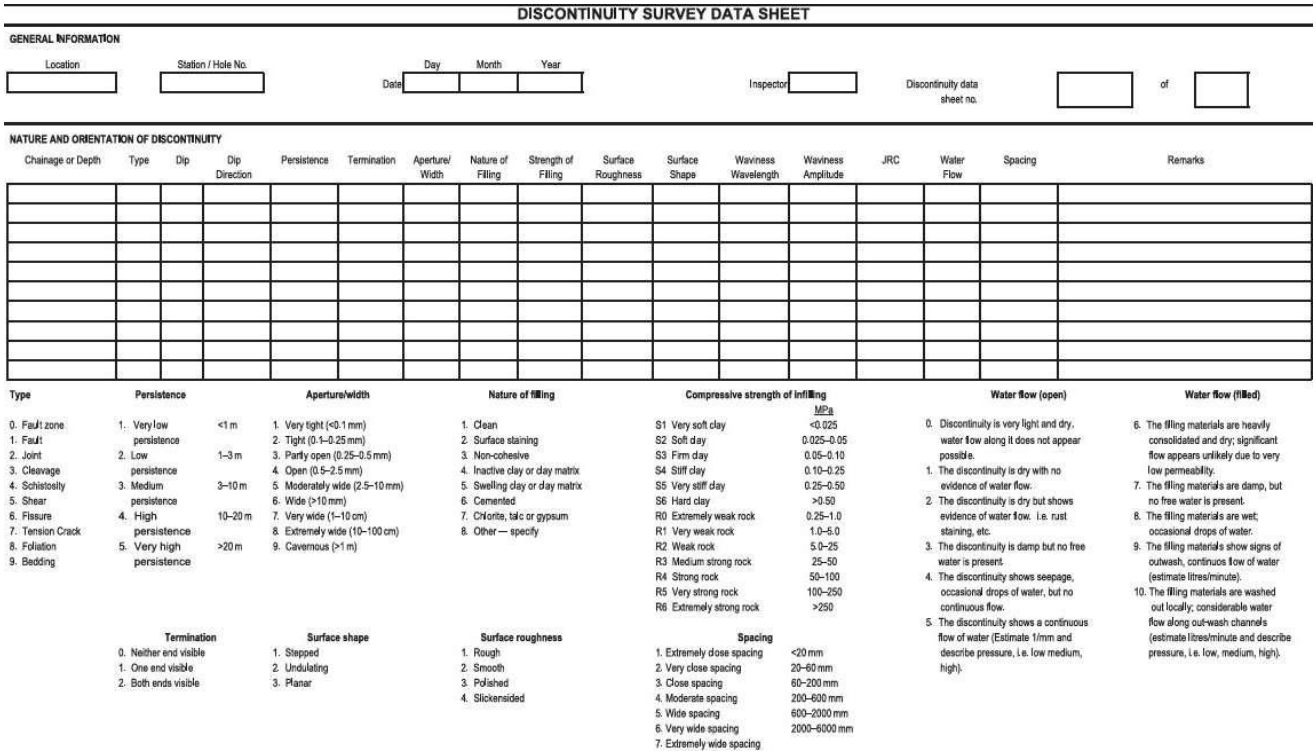
- General geomorphological features (ground morphology; landforms; processes; Quaternary deposits)
- Ground movement features (e.g. landslides; subsidence; solifluction lobes; cambering)

Geohazards

- Mass movement (extent and nature of landslides; type and frequency of landsliding; possible estimates of runout hazard; snow avalanche tracks)
- Swelling and shrinking, or collapsible, soils (soil properties)
- Areas of natural and man-made subsidence (karst, areas of mining, over-extraction of groundwater)
- Sand and dust hazard, mainly but not solely in areas of limited vegetation cover
- Flooding (areas at risk; flood magnitude and frequency; coastal or river flooding)
- Coastal erosion (cliff form; rate of coastal retreat; coastal processes; types of coastal protection)
- Seismicity (seismic hazard assessment)
- Vulcanicity (volcanic hazard assessment)

Figure 5: Extract from Griffiths (2004) Table 8 - Data to be recorded on an engineering geology map

In our example 'Project B' defect data was captured using a scanline template developed from Wyllie and Mah (2004) presented in Figure 6. The standardised template was implemented to assist the engineering geologists in recording the relevant geotechnical data in a methodical and consistent manner. AS1716 was used as a framework for the defect descriptions recorded on the scanline sheets.



DISCONTINUITY SURVEY DATA SHEET

GENERAL INFORMATION

Location | Station / Hole No. | Date: Day Month Year | Inspector | Discontinuity data sheet no. | of

NATURE AND ORIENTATION OF DISCONTINUITY

Chainage or Depth	Type	Dip	Dip Direction	Persistence	Termination	Aperture/ Width	Nature of Filling	Strength of Filling	Surface Roughness	Surface Shape	Waviness Wavelength	Waviness Amplitude	JRC	Water Flow	Spacing	Remarks

Type
0. Fault zone
1. Fault
2. Joint
3. Cleavage
4. Schistosity
5. Shear
6. Fissure
7. Tension Crack
8. Foliation
9. Bedding

Persistence
1. Very low persistence <1 m
2. Low persistence 1–3 m
3. Medium persistence 3–10 m
4. High persistence 10–20 m
5. Very high persistence >20 m

Aperture/width
1. Very tight (<0.1 mm)
2. Tight (0.1–0.25 mm)
3. Partly open (0.25–0.5 mm)
4. Open (0.5–2.5 mm)
5. Moderately wide (2.5–10 mm)
6. Wide (>10 mm)
7. Very wide (1–10 cm)
8. Extremely wide (10–100 cm)
9. Cavernous (>1 m)

Nature of filling
1. Clean
2. Surface staining
3. Non-cohesive
4. Inactive clay or clay matrix
5. Swelling clay or clay matrix
6. Cemented
7. Chlorite, talc or gypsum
8. Other — specify

Compressive strength of infilling

	MPa
S1 Very soft clay	<0.025
S2 Soft clay	0.025–0.05
S3 Firm clay	0.05–0.10
S4 Stiff clay	0.10–0.25
S5 Very stiff clay	0.25–0.50
S6 Hard clay	>0.50
R0 Extremely weak rock	0.25–1.0
R1 Very weak rock	1.0–5.0
R2 Weak rock	5.0–25
R3 Medium strong rock	25–50
R4 Strong rock	50–100
R5 Very strong rock	100–250
R6 Extremely strong rock	>250

Water flow (open)
0. Discontinuity is very light and dry, water flow along it does not appear possible.
1. The discontinuity is dry with no evidence of water flow.
2. The discontinuity is dry but shows evidence of water flow. i.e. rust staining, etc.
3. The discontinuity is damp but no free water is present.
4. The discontinuity shows seepage, occasional drops of water, but no continuous flow.
5. The discontinuity shows a continuous flow of water (Estimate 1/mm and describe pressure, i.e. low medium, high).

Water flow (filled)
6. The filling materials are heavily consolidated and dry; significant flow appears unlikely due to very low permeability.
7. The filling materials are damp, but no free water is present.
8. The filling materials are wet; occasional drops of water.
9. The filling materials show signs of outwash, continuos flow of water (estimate litres/minute).
10. The filling materials are washed out locally; considerable water flow along out-wash channels (estimate litres/minute and describe pressure, i.e. low, medium, high).

Termination
0. Neither end visible
1. One end visible
2. Both ends visible

Surface shape
1. Stepped
2. Undulating
3. Planar

Surface roughness
1. Rough
2. Smooth
3. Polished
4. Slickensided

Spacing

1. Extremely close spacing	<20 mm
2. Very close spacing	20–60 mm
3. Close spacing	60–200 mm
4. Moderate spacing	200–600 mm
5. Wide spacing	600–2000 mm
6. Very wide spacing	2000–6000 mm
7. Extremely wide spacing	

Figure 6: Extract from Wyllie and Mah (2004) Appendix II, discontinuity survey data sheet denoting the geological parameters needing to be described during engineering geological mapping

3.3 SUITABLY TRAINED ENGINEERING GEOLOGISTS

ANCOLD (2020) describe that a suitably trained engineering geologists are needed to carry out geotechnical investigations of dam foundations, including undertaking of engineering geological foundation mapping during the construction stage. Suitable training typically starts at university postgraduate level as part of a specific engineering geology degree (MSc or PhD) which usually includes development of a core competence in both soil and rock mechanics through specific course work. Training then extends into employment and by registration with the governing technical body in the country of employment.

Griffiths (2014) discusses that an engineering geologist should have sound knowledge of geology and geomorphology and understand the way soil and rocks behave under conditions of changing stress as well as the requirements of engineering. A suitably trained engineering geologist will be able to understand and visualise the geological, engineering geological and geotechnical models (depending on the stage of the project) and how their observations of the geological conditions sit against these models. Other professionals without appropriate core training in engineering geology are unlikely to be able to possess these skills to understand how the geological conditions will influence the engineering design.

4 APPLICATION OF ENGINEERING GEOLOGICAL MAPPING INFORMATION

Detailed information from engineering geological mapping of dam foundations undertaken during construction is required to validate the engineering geological model and / or geotechnical model as well as verify assumptions made during design. Having detailed defect data from engineering geological mapping is invaluable to the asset owner who will need to undertake different assessments and design during a dam's life.

Engineering geological mapping is required to verify and inform design as it is 'real data' comprised of observations, not assumptions of the geological conditions and characteristics of the foundation or surrounding areas. Understanding the data the engineering geological maps contain will allow for different assessments such as stability assessments, erodibility assessments and risk assessments to be undertaken with an increased certainty of the geological conditions. Engineering geological mapping should also be incorporated into the engineering geological model and / or geotechnical model to assist with design and identifying gaps of data and understanding.

4.1 UNDERSTANDING DATA FROM ENGINEERING GEOLOGICAL MAPPING

Engineering geological mapping should provide a multitude of geology and geotechnical data of the dam foundation or surrounding rock exposures that needs to be processed in such a way that it can be used to input into design or analysis. The collected data needs to be able to answer the purpose which it was intended for – the design / analysis needs and objectives.

Engineering geological mapping data provides an opportunity to characterise geological features / defects in a way that geotechnical drilling does not allow for. Geotechnical drilling provides a small physical sample (millimetre / centimetre scale) with the expectation to inform the geological and geotechnical conditions of a large area (boreholes are often hundreds of metres apart), whereas engineering geology mapping is undertaken on rock exposures (large areas) and provides larger scale (metres) geological / geotechnical information. This enables the engineering geologist to see more of the foundation conditions on the basis that more rock is exposed. Geological features can be traced into the foundation and matched with defects when engineering geological mapping is paired with geotechnical drilling data.

Understanding of the geological and geotechnical characteristics of geological features allows for design to be undertaken with more certainty. ANCOLD (2013) has specified that engineering geological mapping is one of the requirements to achieving 'well defined' parameters. For many existing dams, engineering geological mapping undertaken during construction does not contain enough detail to satisfy the 'well defined' criteria and additional engineering geology mapping of nearby rock exposures maybe a necessary step to try achieving 'well defined' parameters.

Data from engineering geological mapping can be brought back into the engineering geology model and / or geotechnical model to undertake the processes shown in Figure 7.

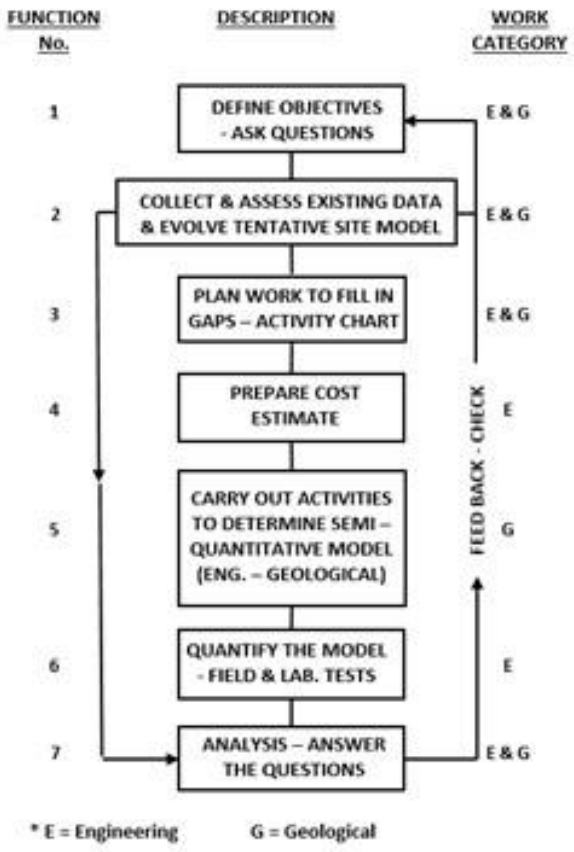


Figure 7: Extract from Stapledon (1982) showing the proposed approach to how investigations and design / analysis integrate with one another

In our examples 'Project B' and 'Project C' engineering geological mapping has been incorporated into the engineering geological models and geotechnical models. This data has been used to assist in understanding and communicating the

geological conditions within the foundation and to identify further data gaps where future geotechnical investigations may be required.

4.2 DEVELOPMENT OF KINEMATIC SECTIONS

Kinematic sections are required to allow assessment of foundation stability for different potential failure modes including those identified in ANCOLD (2013 and 2020). The guidelines illustrate eight basic modes of kinematic failing to be assessed. Sliding within the foundation, along kinematically viable failure surfaces and overturning at the base of the kinematically viable failure surface are highlighted as the most important potential failure modes for concrete gravity dams (Figure 8). Engineering geological mapping data should be sufficient in detail to allow for the development of sections that reflect foundation conditions at different sections of a dam and hence the development of kinematic sections based on that data.

Detailed engineering geological mapping (1:100 and 1:50 scale) will assist in identifying potential failure paths within the foundation. Different failure paths and potential failure modes may exist for different areas a dam, and it is important that the geological mapping is able to document geological defects / features and their geotechnical properties that will contribute to these potential failure pathways and failure modes.

To develop suitable kinematic sections, defect characteristics / sets should be defined using data collected during engineering geological mapping (construction or subsequent investigations). Each set will have an influence on foundation stability. Defect sets of a low angle (dipping upstream or downstream) will create potential sliding surfaces, whereas steeply dipping defects sets with a similar strike to a dam's axis can act as back release surfaces. For each defect set, an average orientation, defect type, persistence, spacing, wavelength, shape and roughness can be determined from engineering geological mapping data. Defect sets can then be presented on kinematic sections representing real defect data.

Engineering geological mapping provides large (metre scale) and small (millimetre) scale defect data. True defect roughness, shape, waviness and persistence cannot accurately be determined by geotechnical drilling data. Defect data gathered by drilling only shows the small scale geotechnical properties which are not always incorporated into stability analysis. The large scale geotechnical properties will likely govern stability, however this is dependent on their nature.

Kinematic sections developed for our example "Project B" have combined engineering geological mapping data from different phases of investigations. Engineering geological mapping completed at the time of construction does not adequately describe the geotechnical properties of each mapped geological feature and therefore only orientation data and defect type have been included in the development of project sets (Figure 9). Subsequent engineering geological mapping has documented the geotechnical properties of over 1000 defects (predominantly crushed seams and sheared seams / zones as they have been assessed to govern dam stability), allowing for development of defect sets, their geotechnical properties and detailed kinematic sections (Figure 10).

Kinematic sections have been developed for each dam foundation area (left abutment, primary spillway and right abutment) to cater for differences in dam load conditions and also for different geological foundation conditions. Using mapping data collected in each area to address the different potential failure modes, the changing orientation of the dam axis and geological conditions across the site. The foundation conditions do not allow for defect data to be easily matched between boreholes; therefore, geological mapping has been pivotable in enabling stability analysis to be undertaken. An example kinematic section is presented in Figure 11. Geological materials sampled during mapping has allowed for the refinement of preliminary geotechnical parameters.

Mode	Condition	Comments
1. Shear along concrete-rock contact 	Shear along weak discontinuity at or near concrete–rock contact.	Possible if weak foundation or poor excavation and/or foundation treatment. Infrequent mode. Check for condition, particularly in old dams.
2. Development of non-compression zone leading to shear 	Development of non-compression zone (a computed crack) leading to shear along the concrete–rock contact.	Can occur even in good foundations.
3. Shear along planar discontinuity 	Shear along planar or near planar discontinuity in rock foundation.	Frequent mode.
4. Shear along stepped discontinuities 	Shear along stepped discontinuities or along surfaces stepping down between parallel discontinuities in rock foundations.	If step(s) not large then failure surface may be approximated by an inclined plane. Large steps may require higher level of analysis.
5. Shear through jointed rock mass 	Shear through highly jointed rock mass (both natural or blast induced) or through weak rock mass.	Infrequent mode. May be used in moderately jointed rock masses (with an adjustment to the assigned Hoek-Brown rock mass strength). Failure surfaces usually approximated as being planar.

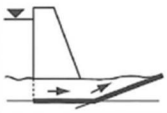
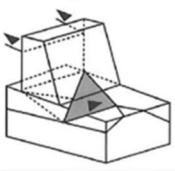
Mode	Condition	Comments
6. Shear along combined discontinuities 	Shear along a combination of two or more discontinuities.	Occasional: usually assume planar mode (3) during initial assessment. Limit equilibrium analysis can be used for more detailed analysis.
7. Toppling 	Loads at toe of dam causing toppling of bedded rock formation.	Infrequent but should be evaluated in bedded or highly jointed (parallel) rocks. If dam heel lifts block may continue movement by shearing through toe (mode 2).
8. Wedge 	Wedge formed beneath block by combination of major faults, shears and/or joint sets.	Infrequent but should be evaluated where major features such as faults/shears cross foundation and combine with jointing. Rigid body, 3-dimensional analysis.

Figure 8: Extracts from ANCOLD (2013) (Figure 7.1 and 7.2) illustrating kinematically feasible failure modes

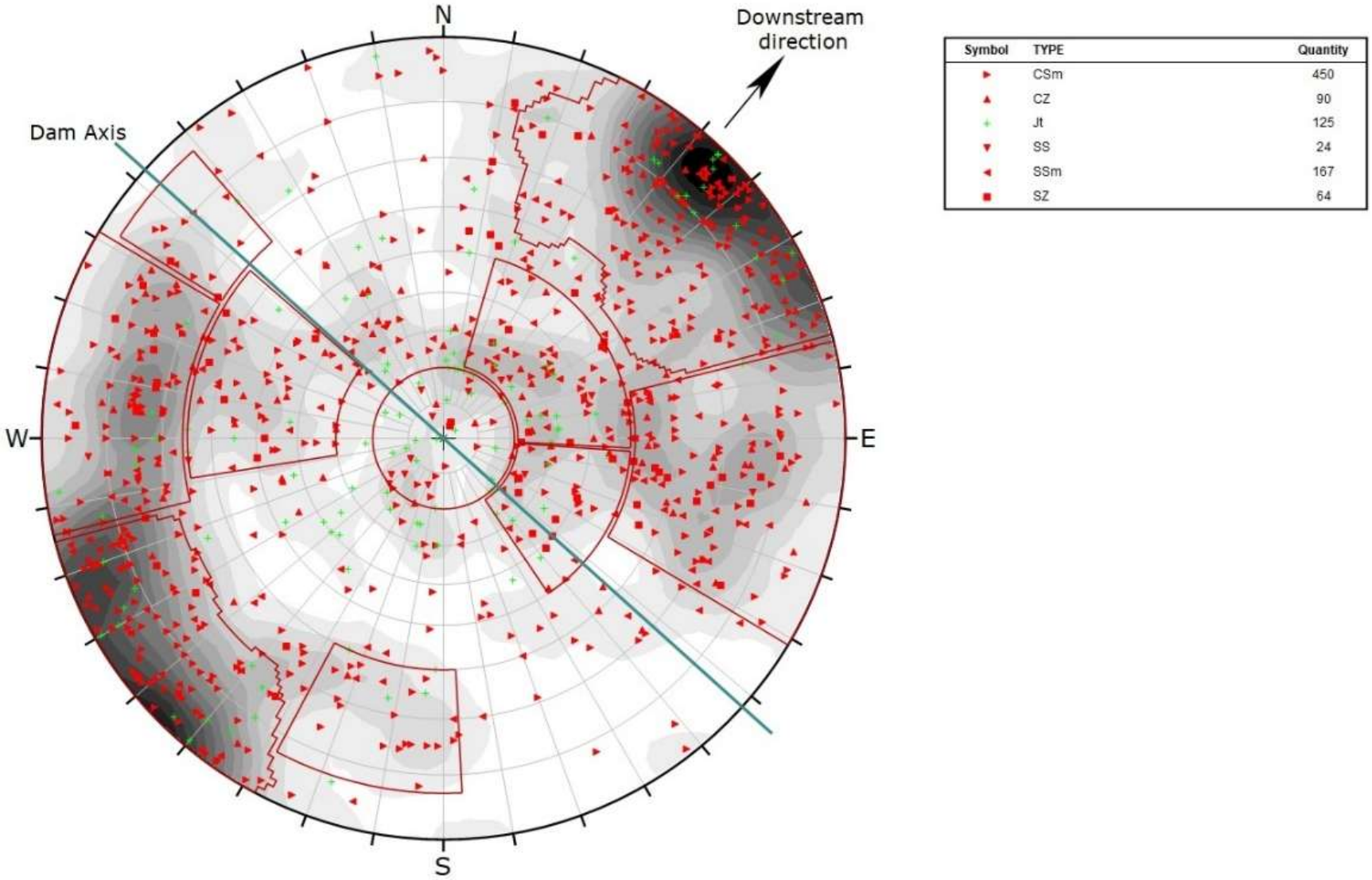


Figure 9: Stereographic projection of engineering geological mapping data from 'Project B', identifying set windows of defect data documented during engineering geological mapping

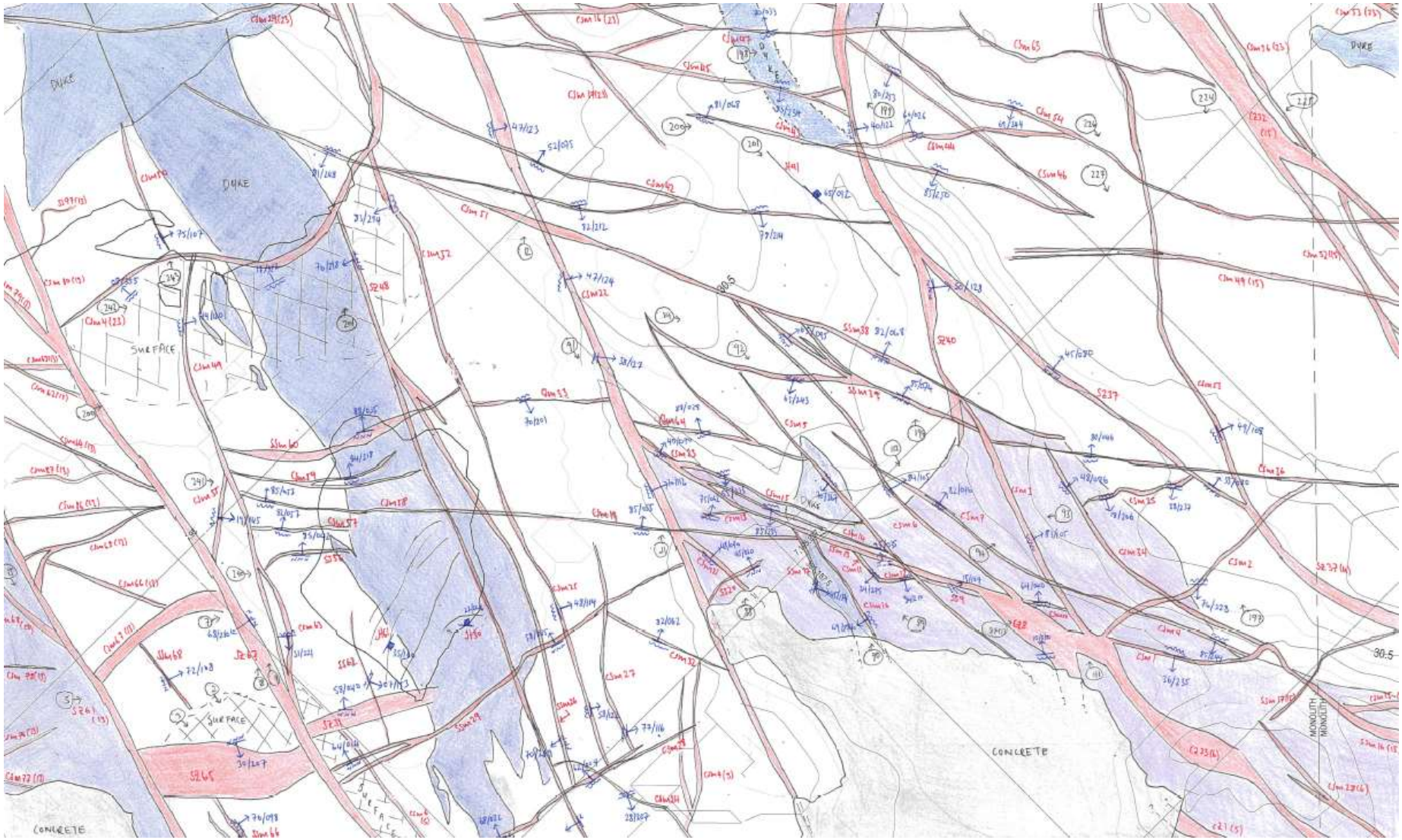


Figure 10: Engineering geological mapping sheet from example 'Project B', mapping has been undertaken at 1:50 scale showing key defects and lithology outlines. Key defects are identified as defects likely to govern dam stability and are important to assess dam stability

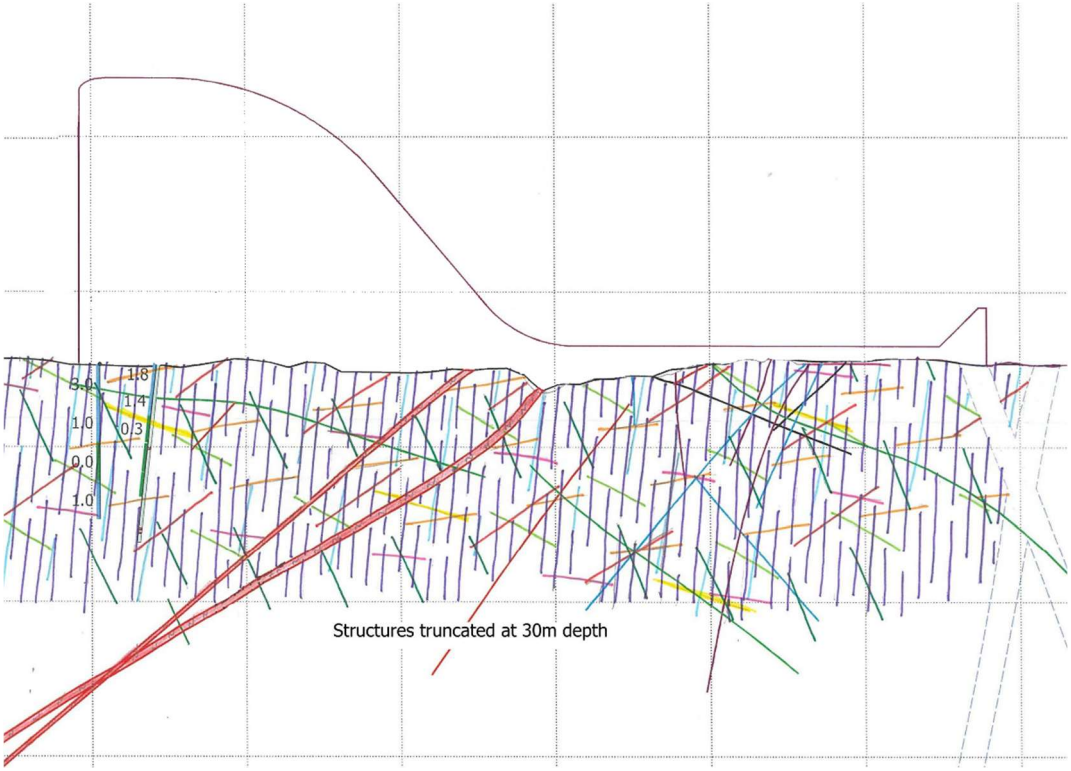


Figure 11: Typical kinematic section for dam stability assessment from 'Project B'. Project defect sets are shown in different colours, the persistence and spacing of each set as been determined from engineering geological mapping

4.3 FOUNDATION EXCAVATION AND MAPPING DURING CONSTRUCTION

The role of an engineering geologist on site during construction is to assess that a suitable foundation material has been achieved during excavation, adverse kinematic blocks are removed, adverse geological features are treated, and the final foundation surface has been engineering geologically mapped before construction materials are placed. The engineering geologist is often under a tight timeframe / budget to complete all these tasks to allow construction to progress as planned. It is important to budget enough time to allow the engineering geologist complete detailed engineering geological mapping as once the foundation is covered by concrete or construction materials it is not seen again, and the mapping data will be relied upon throughout the life of the asset. The design and construction team should be aware of the importance of engineering geological mapping and the role it plays as part of the overall excavation, preparation and material placement process during construction.

As is the nature of dam construction sequencing, the foundation is often revealed gradually and sporadically, and progress is typically at the whim of the construction process. Adequate personnel and processes should be in place to account for this uncertainty, and a full time site presence is therefore typically required on larger projects to ensure that a record of the foundation can be made with minimal impact to construction activities.

The engineering geological mapping should document the key geological features that may influence and govern dam stability. Due to time constraints, it is not possible to map every defect, so it is important the engineering geologist understands the engineering geological model and / or geotechnical model to help identify the key geological features.

In the event that encountered ground conditions are not as anticipated, a feedback process should be in place that includes independent assessors, designers and constructors to ensure agreement is reached as to a particular course of action (e.g., additional excavation, stabilisation or re-design). A Foundation Inspection Committee has been found to be a favourable way of managing this process and helps avoid a potentially adversarial relationship between engineering geologist, designer and constructor due to competing project drivers. The project lead engineering geologist is a key member of the Foundation Inspection Committee.

Construction phase engineering geological mapping of dam foundations typically seeks to provide a record of the rock mass for the purpose of guiding foundation preparation, verification of design and as a future record of the ground conditions encountered. The process of verification may reveal conditions that are adverse and were not anticipated that may require additional design consideration and / or construction activities (and ultimately cost); it is therefore vital that

the mapping process forms part of the construction quality assurance (QA) process (e.g., as part of the Specification and Inspection and Test Protocols). Engineering geological mapping should form a hold point in the construction QA process and the requirements of mapping should be clearly stated in the construction specification.

In our example ‘Project C’, it was important engineering geological mapping documented the crushed seams, sheared seams and sheared zones located at the boundaries of different geological lithologies as they were assessed to government dam stability. Engineering geologists on site were responsible in ensuring that foundation met the specified design criteria, that no adverse material had been left within the foundation and kinematically adverse features had been either be appropriately treated or removed. Engineering geological mapping formed a hold point within the construction sequence, before the Foundation Inspection Committee would meet to agree that all the additional hold points had been completed to a satisfactory standard, such as the foundation and mechanical clean down. Once all the hold points have been signed off and the Foundation Inspection Committee was satisfied with the foundation preparation, concrete placement was able to commence. Engineering geological mapping was incorporated into the engineering geological model in almost real-time and used to inform the engineering geologists on site of potential adverse kinematic blocks in future foundation lots. An example mapping sheet is presented in Figure 12, this mapping sheet was produced utilising the base mapped present in Figure 4 in Section 3.1.1.

Throughout the life of a dam, there is a requirement to undertake risk assessments and dam safety reviews to ensure that the asset is still safe and performing as intended. Engineering geological mapping will be assessed and relied upon to inform stability and erosion assessments. As outlined in Section 3.2, engineering geological mapping data should record the geological engineering properties of the rock mass and geological features / defects as this will directly inform the assessments.

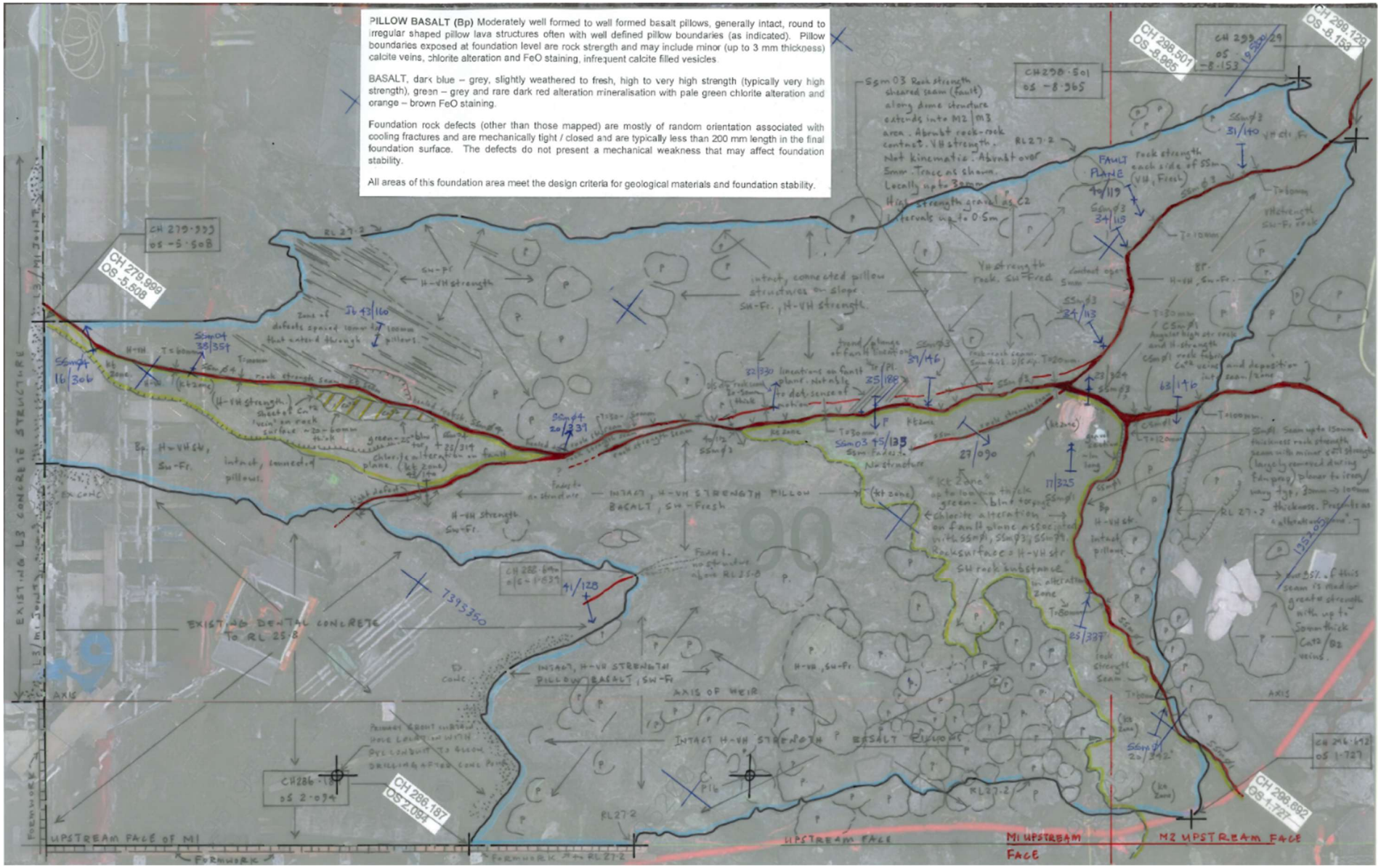


Figure 12 "Project C" example of final mapping sheet for the foundation area shown in Figure 4. Note the manual production method for the mapping sheet overlay.

4.4 KEY BENEFITS TO THE DAM OWNER

Throughout the life of a dam, the dam must comply with dam regulatory bodies and meet current day regulations. A dam will be expected to have regular risk assessments and dam safety reviews carried out and may even need upgrades to meet newer regulations. Detailed engineering geological mapping will be advantageous to owners in terms of time and budget. If engineering geological mapping undertaken during construction and subsequent investigations are completed to a high standard and have captured sufficient geological defects / features and geotechnical parameters, it will be adequate to assist in the required safety reviews and risk assessments and subsequent tasks / assessments. For existing dams where engineering geological mapping completed during construction has not been able to capture the required detail (due to time, budget and technology constraints), owners will need to undertake further investigations to answer gaps in the existing data. This not only adds financial costs to owners, but it also adds to the time taken to complete the safety review or risk assessment.

Where dams are required to undergo upgrades to meet present day regulations, detail engineering geological mapping will again be advantageous to the owner. As outlined in Section 4.1, engineering geological mapping allows for more certainty in design and gives owners the opportunity to achieve 'well defined' parameters. To gather geological data is a costly and timely exercise if no detailed engineering geological mapping is available.

In our example 'Project A', data gaps were identified during a risk assessment of the dam and no engineering geological mapping was available for the dam. Unfortunately for the owner, this meant engineering geological mapping needed to be undertaken at additional cost and time to fill in the identified data gaps. The completed engineering geological mapping will be used to complete future assessments and analysis.

5 SUMMARY

Engineering geological mapping will always be a key piece of data required to understand the geological conditions present at a dam site and specifically within the foundation. The methodology for engineering geological mapping has developed with advancements in technology and this has allowed for data to be collected faster and with greater spatial accuracy. Understanding the geological setting prior to commencing mapping is critical to ensuring that data recorded during engineering geological mapping (such as the origin of the defect) is in accordance with the geological, engineering geological and geotechnical models and defect properties critical to the success of the design are appropriately evaluated.

It is important that a suitably trained engineering geologist undertakes engineering geological mapping and other geotechnical investigations for dams to ensure that observations are recorded correctly, and the appropriate engineering geological information is documented. Data from engineering geological mapping should be appropriate for further design (e.g. construction and dam upgrades) and analysis (e.g. stability assessments, erodibility assessments, risk assessments, dam safety reviews) and its potential future uses should be considered during the planning of the engineering geological mapping. If engineering geological mapping is lacking in data or has not sufficiently addressed the design purpose, performing further engineering geological mapping and geotechnical drilling post-construction maybe a complex and costly undertaking.

6 REFERENCES

Australian National Committee on Large Dams (ANCOLD) (2013). Guidelines on Design Criteria for Concrete Gravity Dams.

Australian National Committee on Large Dams (ANCOLD) (2020), Guidelines for Geotechnical Investigations of Dams, their Foundations and Appurtenant Structures.

Australian Standard, AS 1726:2017. Geotechnical Site Investigations. Standards Australia, 2017

Burwell, E. B., Moneymaker (1950), Geology in Dam Construction, *The Geological Society of America, Engineering Geology (Berkey) Volume*

Fell, R., MacGregor, P., Stapledon, D., Bell, G. and Foster, M., 2015. Geotechnical Engineering of Dams: Second Edition (2nd ed.). *CRC Press*, Boca Raton

Griffiths, J.S. (2004). Engineering Geology: Geological Maps. *In: Selley, R.D., Cocks, R & Plimer, I. (eds) The Encyclopedia of Geology, Vol. 1.* Elsevier, Oxford, 463-473.

Griffiths, J.S. (2014). The 14th Glossop Lecture: Feet on the ground: engineering geology past, present and future. *Quarterly Journal of Engineering Geology and Hydrogeology, Vol. 47*, 116-143

International Association for Engineering Geology and the Environment (IAEG) (2022), Guideline for the development and application of engineering geological models on projects, *IAEG commission 25 publication No. 1*

Lapworth, H. (1908), The Principles of Engineering Geology, Two Lectures to the Students of the Institution in Session 1907-1908

Lapworth, H. (1912), The Geology of Dam Trenches, A Scientific Analysis of the Engineering Problems Involved, *Scientific American Supplement No. 1895*

Leggit, R.F (1979). The 13th Terzaghi Lecture: Geology and geotechnical engineering. *Journal of the Geotechnical Division, ASCE, 105*, 342-391.

McCaffrey, K. J. W., Jones, R. R., Holdsworth, R. E., Wilson, R. W., Clegg, P., Imber, J., Holliman, N., Trinks, I. (2005), Unlocking the Spatial Dimension: Digital Technologies and the Future of Geoscience Fieldwork, *Journal of the Geological Society, Vol. 162, Issue 6*, 927-938

Stapledon, D.H. (1967). Geological Investigations at the Site for Kangaroo Creek Dam, South Australia. *Trans. Institution Engineers Australia, Vol. CE9, No.* 1, 31–43.

Stapledon, D.H. (1961). Thesis: Geological Studies for the Planning and Construction of Tumut 2 Underground Power Station. *University of Adelaide Economic Geology Department.*

Stapledon, D.H. (1982). Subsurface Engineering – in Search of a Rational Approach. *Australian Geomechanics News, 4*, 26-33.

Wiley, A. J., Louderback, G. D., Ransome, F. L., Bonner, F. E., Cory, H. T., Fowler, F. H. (1928), Report of the Commission Appointed By Governor C. C. Young to Investigate the Causes Leading to the Failure of the St. Francis Dam. Near Saugus, California.

Wyllie, D.C., & Mah, C. (2004). Rock Slope Engineering: Fourth Edition (4th ed.). *CRC Press*.

https://doi.org/10.56295/1ACEG36

GEOLOGICAL CHALLENGES OF BRISBANE'S CROSS RIVER RAIL PROJECT

Ralph Cammack
PSM

ABSTRACT

The Cross River Rail project includes a new rail line in Brisbane, comprising surface rail and station upgrades, twin running tunnels and four new underground stations at Boggo Road, Woolloongabba, Albert Street, and Roma Street. This project has provided valuable insights into the geological conditions of the Brisbane CBD through large-scale investigation and construction activities. This paper presents case studies of particularly challenging ground conditions encountered during the project, emphasizing the need to consider geotechnical variability and uncertainty in the design phase, as well as the verification of these conditions during construction. The findings presented may serve as a reference for future ground engineering projects in Brisbane.

1 INTRODUCTION

Cross River Rail (CRR) is a new 10.2 km rail line in Brisbane, Australia. It extends from Dutton Park south of the CBD to Bowen Hills in the north comprising 5.9 km of twin running tunnels and four new underground stations at Boggo Road, Woolloongabba, Albert Street and Roma Street, Figure 1. The Pulse consortium which included the joint venture of CPB Contractors, BAM International Australia, Ghella and UGL (CBGU JV) was awarded the contract to design, construct and maintain the Tunnels, Stations and Development (TSD) works.

The project traversed several geological units, with some adverse and challenging ground conditions encountered. Case studies are presented for selected examples including a major fault zone intersecting Roma Street Station, a low-angle persistent fault at Albert Street Station and a highly variable geological unconformity encountered at the invert of the Boggo Road Station. These case studies demonstrate the importance of considering geotechnical variability and uncertainty in the design phase, along with the verification and flexibility to respond to adverse ground conditions during construction.

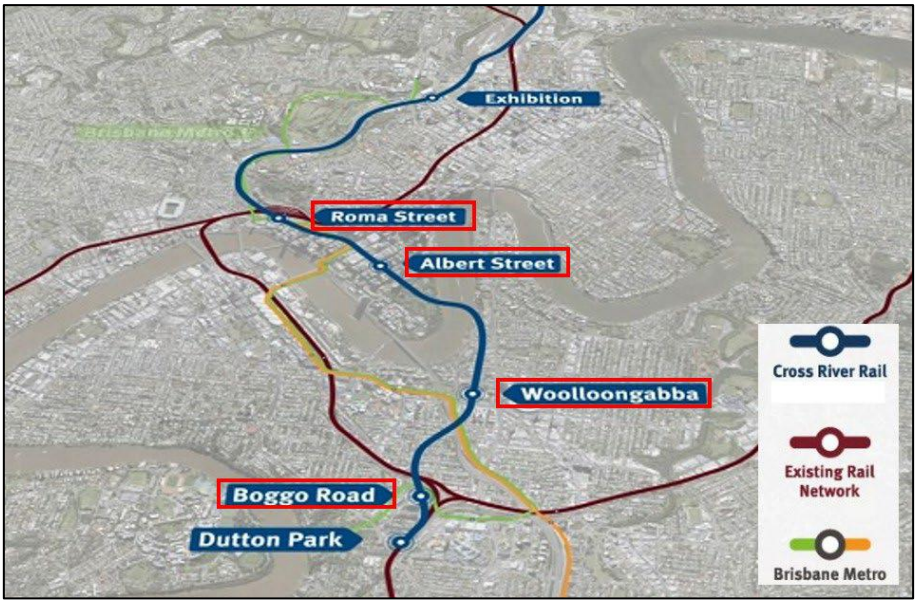


Figure 1: CRR alignment showing the location of the underground stations (www.crossriverrail.qld.gov.au).

2 GEOLOGICAL OVERVIEW

The main geological units encountered at CRR are presented in plan as Figure 2 and described in a stratigraphic column in Table 1. The Neranleigh-Fernvale Beds (NFG) basement rocks are prevalent in the central and northern parts of the project, including the Brisbane CBD. The overlying Brisbane Tuff and Aspley Formation rocks are prevalent in the central and southern parts. Weathering has degraded the rock near the surface to variable depths. Geological unconformities occur between the geological units, which can comprise zones of poor quality sheared or soil strength materials, contrasted with more competent rock above and below. There are multiple significant faults in the Brisbane

CBD, Figure 2. The Normanby Fault Zone (NFZ) strikes northwest to north-northwest through the project area and comprises a wide zone of fault splays, fault gouge and brecciated rock, separated by more competent rock 'fault blocks'. A detailed description of the rock mass units and structural geology conditions encountered at the CRR project and referred to in this paper is provided in Cammack et. al. (2022). Geotechnical design parameters are also presented in that paper.

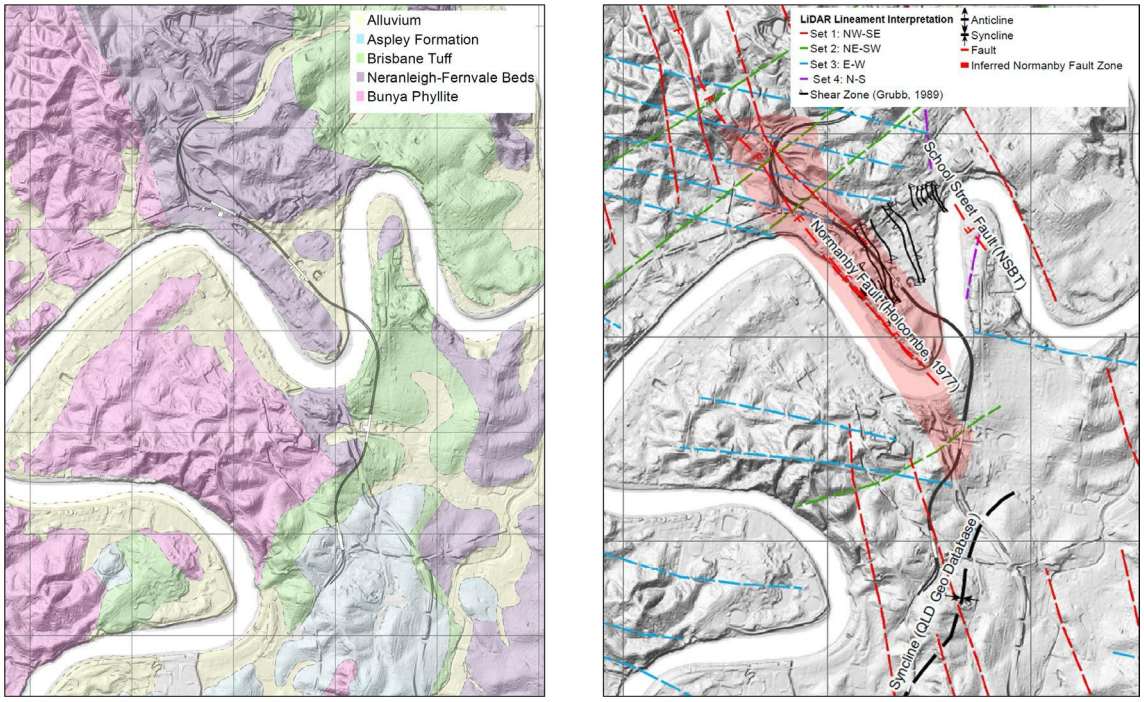


Figure 2: Geological plan and structural geology lineaments showing the CRR alignment.

Table 1: CRR geological units – stratigraphic column and general description

Unit	Period	Age	Rock Type	Description
Aspley Formation (Aspley)	Triassic	200 to 230 Ma	Sedimentary	Conglomerate, sandstone, shale, minor coal. Bedded with orthogonal sub-vertical joint sets and occasional shears and faults. Classified for CRR as either Conglomerate Dominant (CD) or Siltstone Dominant (SD).
Brisbane Tuff (Tuff)			Volcanic/ sedimentary	Rhyolitic tuff, ignimbrite, agglomerate, conglomerate, sandstone, shale. Jointed with sub-vertical orthogonal to conjugate sets and sub-horizontal set and occasional shears and faults, often steeply dipping.
Neranleigh-Fernvale Beds (NFG)	Devonian - Carboniferous	300 to 400 Ma	Metamorphic	Phyllite, arenite, meta-greywacke, quartzite derived from a siliceous parentage (chert, jasper), basic metavolcanics, metamorphosed to greenschist facies. Strongly foliated in places (generally dipping to the NE), with frequent foliation partings and foliation parallel shearing. Joint set antithetic to foliation, along with subvertical joints. Significant shears and faults in places.

3 CASE STUDY 1 – FAULT ZONE AT ROMA STREET STATION

3.1 GEOTECHNICAL MODEL

Roma Street Station is located within the NFG geological unit on the northern edge of the Brisbane CBD. Several of the initial investigation boreholes encountered a major fault zone, which was inferred to be associated with the regional NFZ. Additional boreholes were proposed at the design phase to increase confidence in the ground model at critical locations,

including the adit and cavern intersections. However, the boreholes were not able to be completed due to surface constraints including the operating railway station, Inner Northern Busway and other buildings. The location and extent of the fault zone was therefore inferred based on the available information, and was interpreted to intersect the cavern, adits and main shaft Figures 3 and 4. The rock mass was classified into NFG1 to NFG5 (fresh to weathered) units, and fault zone materials including Fault Disturbed Zone (FDZ) and Fault Crush Zone (FCZ). The fault zone materials were assessed to be of significantly lower strength and stiffness compared to the surrounding high strength NFG rocks and were considered to have potential implications for the cavern and shaft stability, ground loading and founding conditions.

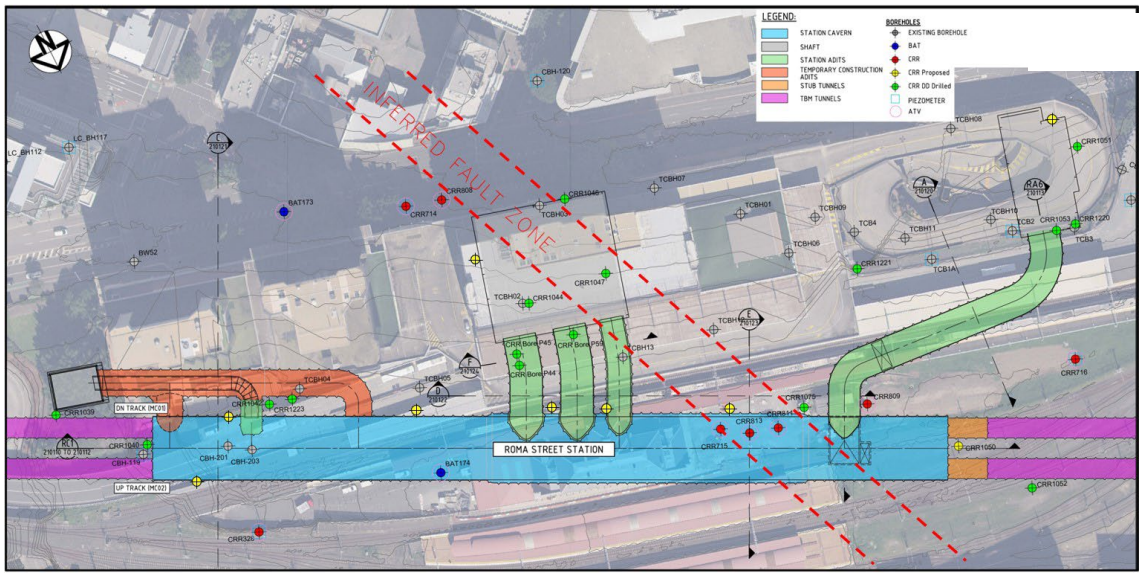


Figure 3: Roma Street Station borehole plan, showing inferred fault zone.

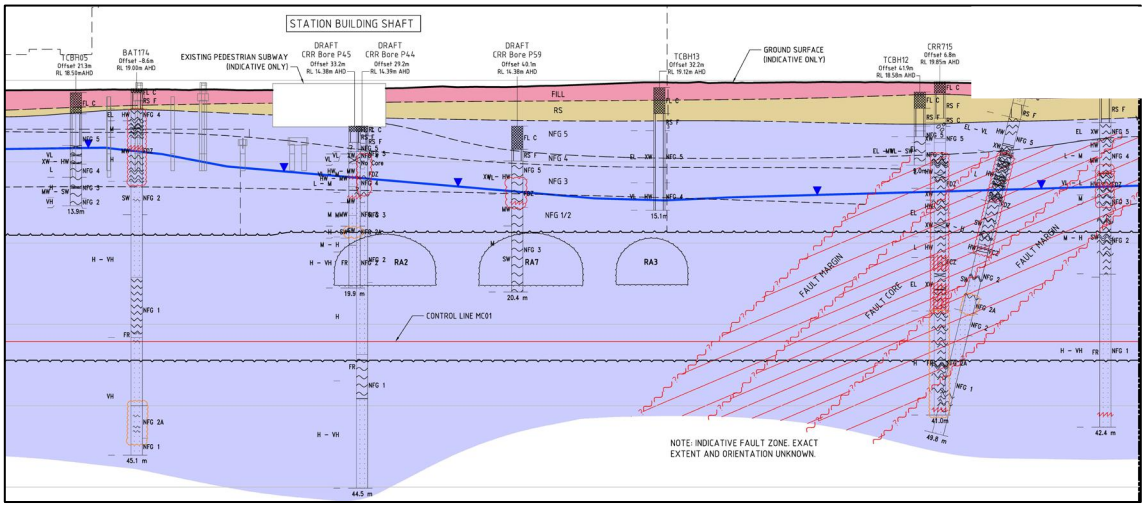


Figure 4: Roma Street Station geotechnical section – showing inferred fault zone intersecting the cavern.

3.2 DESIGN CONSIDERATIONS

Several ground support and ground reinforcement types were included in the Roma Street Station cavern design 'toolbox' to cater for the range of expected ground conditions within the fault zone, as described in detail by Shen et. al. (2022) and Cammack et al. (2023). These included:

- A passive shotcrete lining primary cavern crown support type, combined with a three-heading excavation sequence to minimise span width and allow verification of ground conditions in the lead heading, Figure 5.
- A heavily bar reinforced passive shotcrete primary lining support and temporary collar structure if a fault zone was encountered at the intersection of the cavern and adits.

- A widened elephant's foot foundation for the shotcrete arch primary lining, with micropiles and wall support under the footing in the fault zone, Figure 5.
- Removal and concrete replacement of fault zone materials in the cavern invert, Figure 6.
- A permanent concrete lining with thickness and reinforcement which catered for ground loading from the fault zone.

These were assigned during construction via the Permit to Tunnel (PTT) and Hold Point processes based on the encountered conditions. The anticipated ground deformation was also assessed during design, and a series of monitoring trigger levels were defined to alert the designer if the ground was not behaving as expected during construction. Design solutions were also adopted for the main shaft to address these adverse ground conditions however these are not presented in this paper.

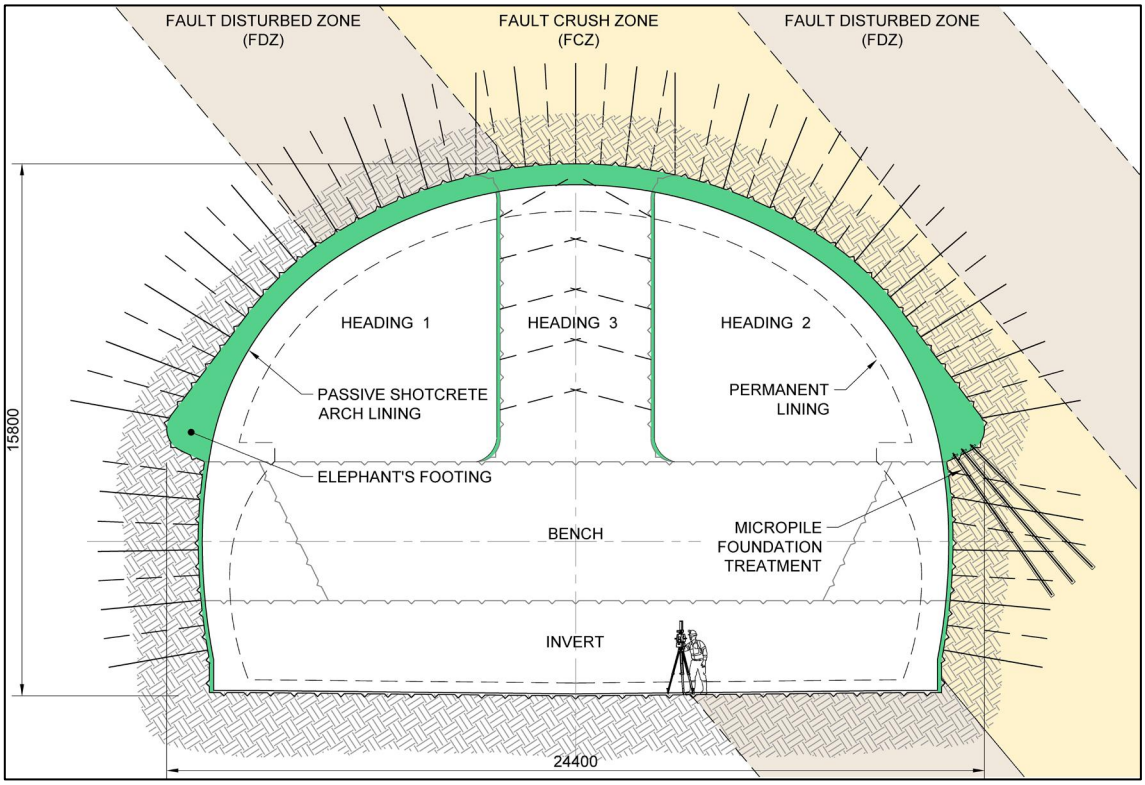


Figure 5: Roma Street Station cavern – showing passive shotcrete arch lining and micropiles at the elephant's footing foundation (Shen et. al. 2022).

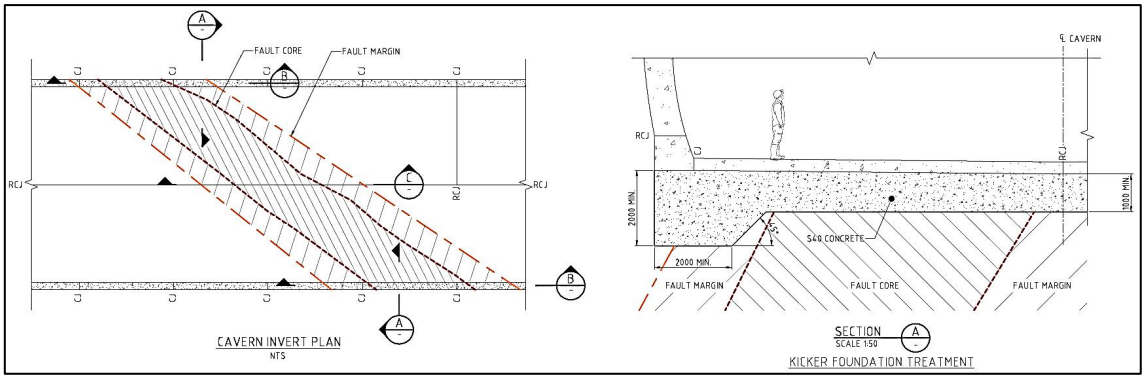


Figure 6: Roma Street Station cavern invert foundation treatment.

3.3 CONSTRUCTION OUTCOMES

Verification of the fault zone was undertaken during construction via geotechnical mapping, endoscopes, piling inspections, plate load testing and monitoring. Mapping of the cavern and adits detailed a 5m to 10m wide fault core comprising variable FCZ (typically 1m to 4m wide) and FDZ (typically 2m to 5m wide), steeply dipping to the northeast. The FCZ materials comprised fault brecciated rock with seams of fault gouge material, ranging from matrix to clast supported and soil to very low rock strength. The FDZ materials comprised highly disturbed and brecciated rock with frequent crush and shear zones, generally clast supported and ranging from very low to medium rock strength. The core was surrounded by a fault margin zone comprising NFG and FDZ materials, around 5m to 10m in thickness either side. A zone of increased rock mass disturbance was observed adjacent to the fault margin in places, characterised by increased jointing, minor warping and folding of foliation and increased weathering of geological structures. Figure 7 presents the fault zone as mapped in the crown of the cavern and adits. The encountered fault zone extent and characteristics were generally consistent with the design assumptions, and the design solutions were implemented without delay or modification. Figure 8 presents a photograph of the fault zone in the cavern heading. Figure 9 presents the removal of the fault zone in the cavern invert. The fault did not occur at the cavern intersection with the adits and therefore the bar reinforced concrete collar was not required.

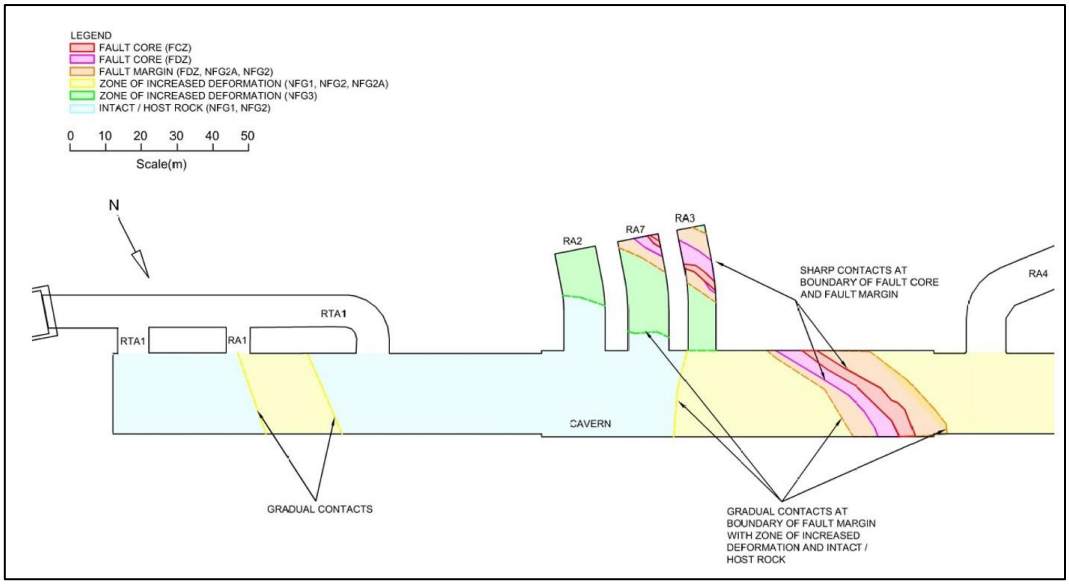


Figure 7: Roma Street Station rock mass units encountered in the cavern and adit crown during construction (Cammack et. al. 2023).



Figure 8: Fault zone encountered in the Roma Street Station cavern heading during construction.



Figure 9: Excavation of fault materials for the Roma Street Station cavern invert floor treatment.

4 CASE STUDY 2 – LOW-ANGLE FAULT AT ALBERT STREET STATION

4.1 GEOTECHNICAL MODEL

Albert Street Station is located within the NFG geological unit in the Brisbane CBD. Initial investigation boreholes indicated a persistent gently dipping fault intersecting the proposed station cavern and shafts. This feature was interpreted to be a low-angle listric thrust fault splay associated with the NFZ. Additional boreholes were drilled during the detailed design phase as buildings were demolished for the project, providing a reasonable level of confidence in the fault characteristics and location for the geotechnical model, Figures 10 and 11. The fault was observed to occur along a lithofacies contact between overlying fine grained phyllite and underlying coarser grained meta-sediments in the NFG, dipping to the east at around 15°. It comprised up to 0.5m thick FCZ brecciated rock and fault gouge material, often bounded by FDZ or fractured NFG rock, Figure 12. The fault was assessed to be of low shear strength and stiffness and was considered to have potential implications for shaft and cavern stability, ground loading, founding conditions, and as a potential source of displacement which could impact adjacent high-rise buildings and other infrastructure.

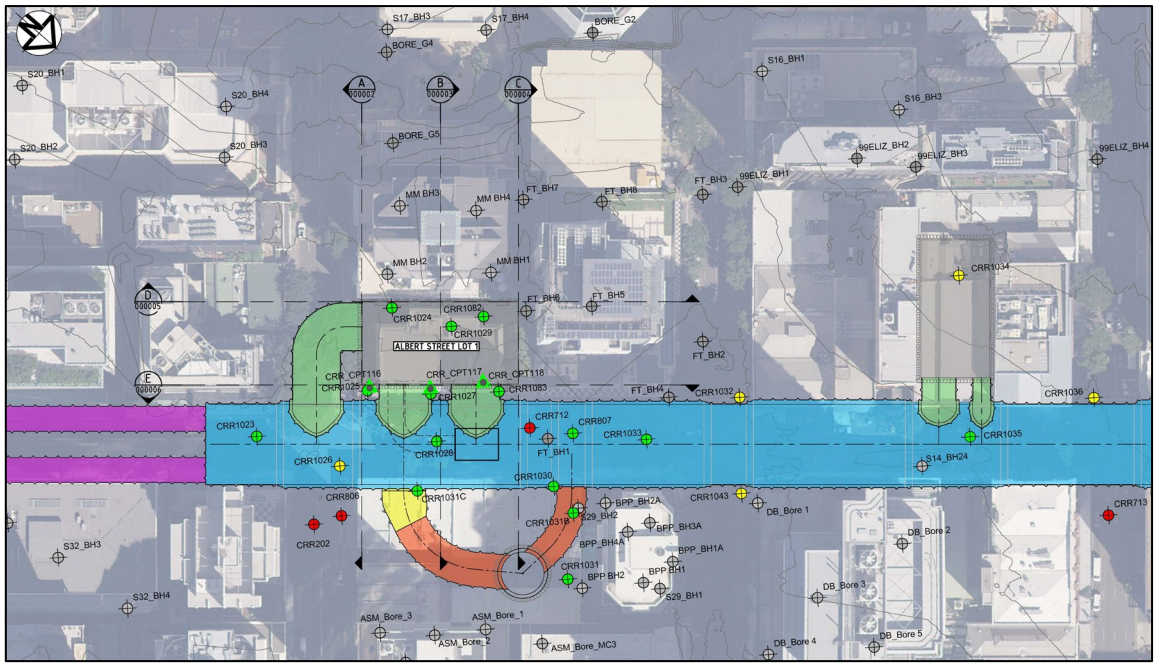


Figure 10: Albert Street Station borehole plan (refer to Figure 2 for legend).

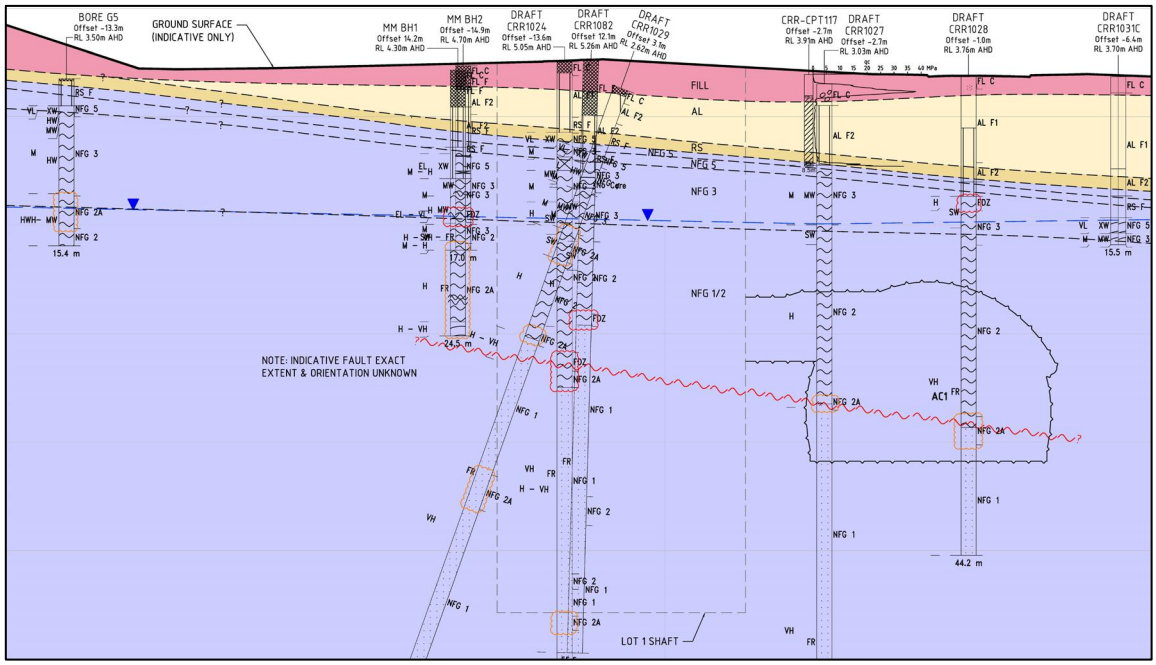


Figure 11: Albert Street Station geotechnical section – showing interpreted low-angle fault.

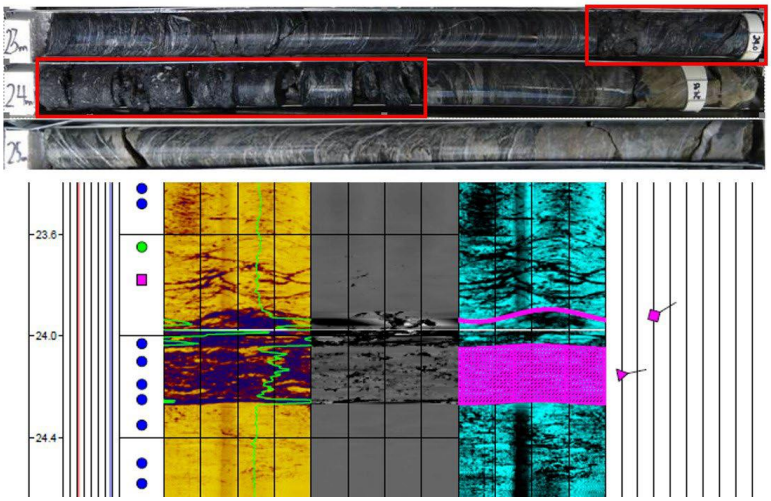


Figure 12: Borehole CRR1082 core photo and televiewer image showing low-angle fault at the Albert Street Station Lot 1 shaft.

4.2 DESIGN CONSIDERATIONS

There was better site investigation coverage and a higher level of confidence in the fault location and character for the Albert Street Station geotechnical model compared to Roma Street Station, therefore the ground support and reinforcement designs could be developed with more certainty at the design phase. Extensive 2D and 3D numerical modelling was undertaken to assess the behaviour and deformation of the Albert Street Station shaft, cavern and surrounding area to inform the design, construction sequence and the predicted effects on existing infrastructure. The design solutions developed to address the low-angle fault included:

- A passive shotcrete lining for the primary cavern crown support, combined with a three-heading excavation sequence in the area of influence of the fault, shaft and adits.
- Stitch bolts and concrete replacement for the rock pillar between the Albert Street Station cavern and the Lot 1 shaft, Figure 13.
- Heavier primary ground support for the walls of the cavern and shaft where the fault daylights, Figure 14, including tensioned anchors in the shaft.
- Underpinning of shaft piles where they are founded within or close to the fault.

- Three rows of temporary props within the shaft, with continuous load and displacement monitoring and adjustable jacks to maintain the support within defined upper and lower limits during the shaft and cavern excavation. These props were required for other geological conditions as well as the fault (potential large rock wedges along foliation parallel defects in the NFG) and very tight displacement criteria related to the adjacent high-rise buildings.
- Carefully managed excavation and support sequence and extensive deformation monitoring for the cavern, shaft and adjacent existing infrastructure.
- Removal and concrete replacement of fault materials in the cavern invert.
- A thick permanent concrete lining with reinforcement for the cavern to cater for ground loading associated with the fault.
- A robust permanent station building design to consider contrasting stiffness and ground loads.

These were assigned and managed via the PTT, Permit to Excavate (PTE) and Hold Point processes during construction.

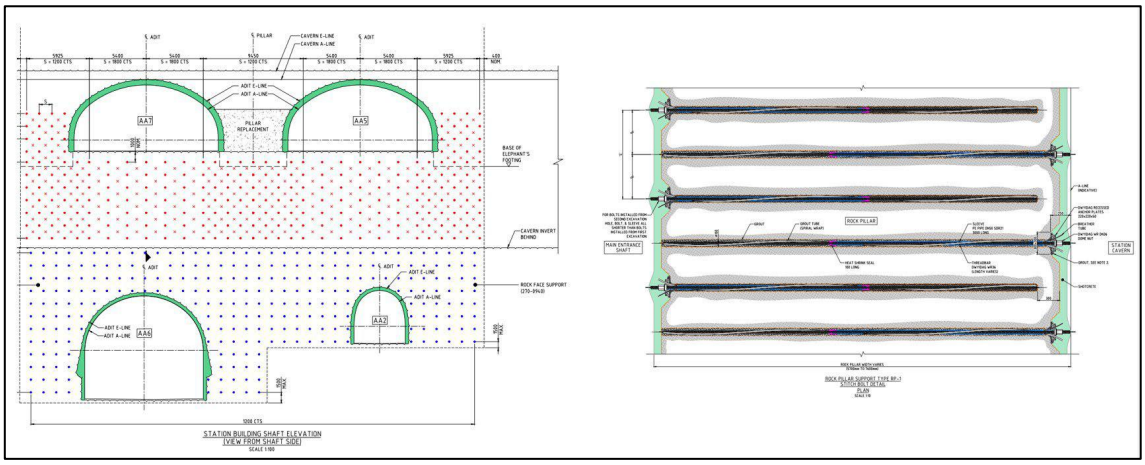


Figure 13: Stitch bolt ground support and concrete replacement of the pillar between the Albert Street Station cavern and the Lot 1 shaft.

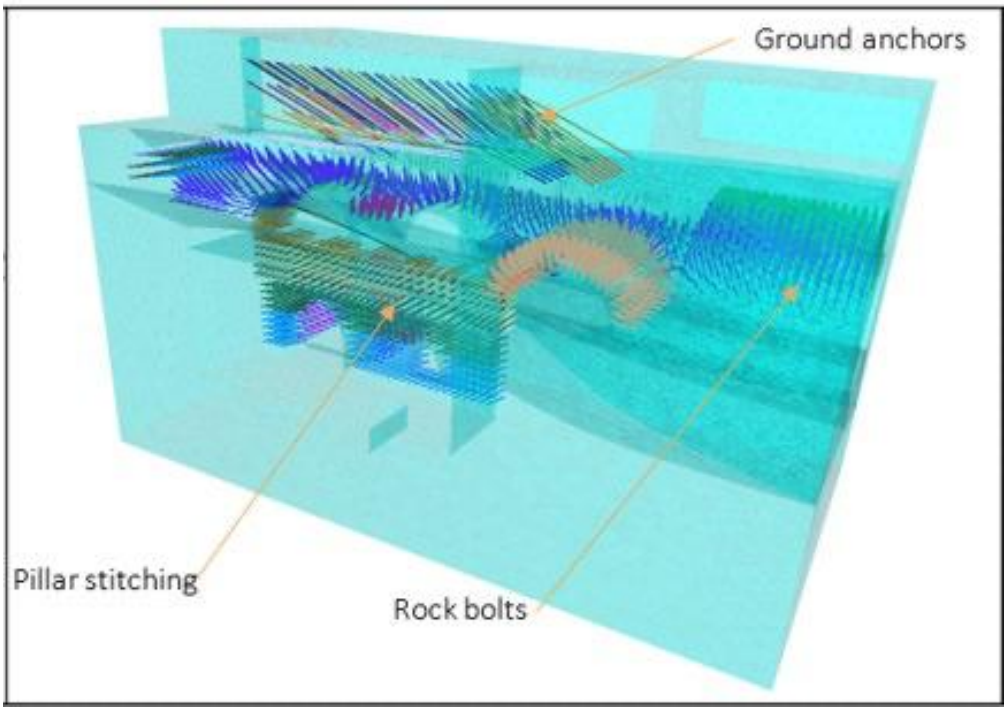


Figure 14: 3D model showing the ground support and pillar stitching elements for the Albert Street Station cavern and the Lot 1 shaft.

4.3 CONSTRUCTION OUTCOMES

Verification of the low-angle fault was undertaken during construction via geotechnical mapping, endoscopes, and monitoring. The fault was persistent as expected and was variable in character along its strike. Figure 15 shows the approximate location of the fault intersecting the Albert Street Station Lot 1 shaft. It varied from a 2m thick zone of FCZ and FDZ, with anastomosing fault splays, Figure 16, to a discrete single fault with around 100mm of brecciated rock infill, Figure 17. The fault was wider than expected in the cavern invert, with a broad crushed zone requiring treatment in the floor, Figure 18. However, in the critical zones (i.e. the shaft walls and pillar) the fault conditions and location were within the design expectations therefore construction was able to continue with no significant delay or design change. This fault is expected to extend into the surrounding properties around the Albert Street Station project site and may need to be considered for future basement excavations or underground works in this area.



Figure 15: Albert Street Station Lot 1 shaft showing cavern adits, temporary props, stitching bolts, concrete pillar replacement and approximate location of the low-angle fault.

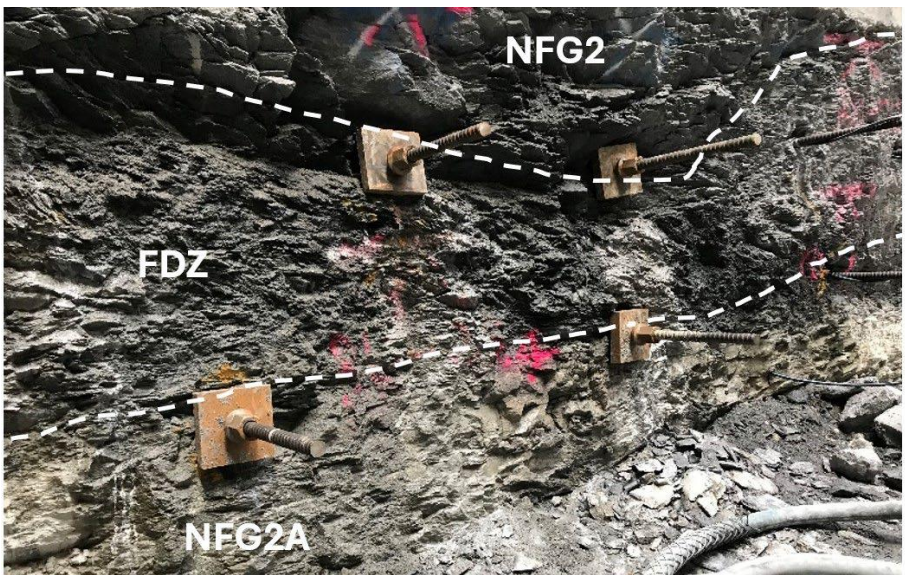


Figure 16: Pillar stitch bolts in low-angle fault at Albert Street Station.

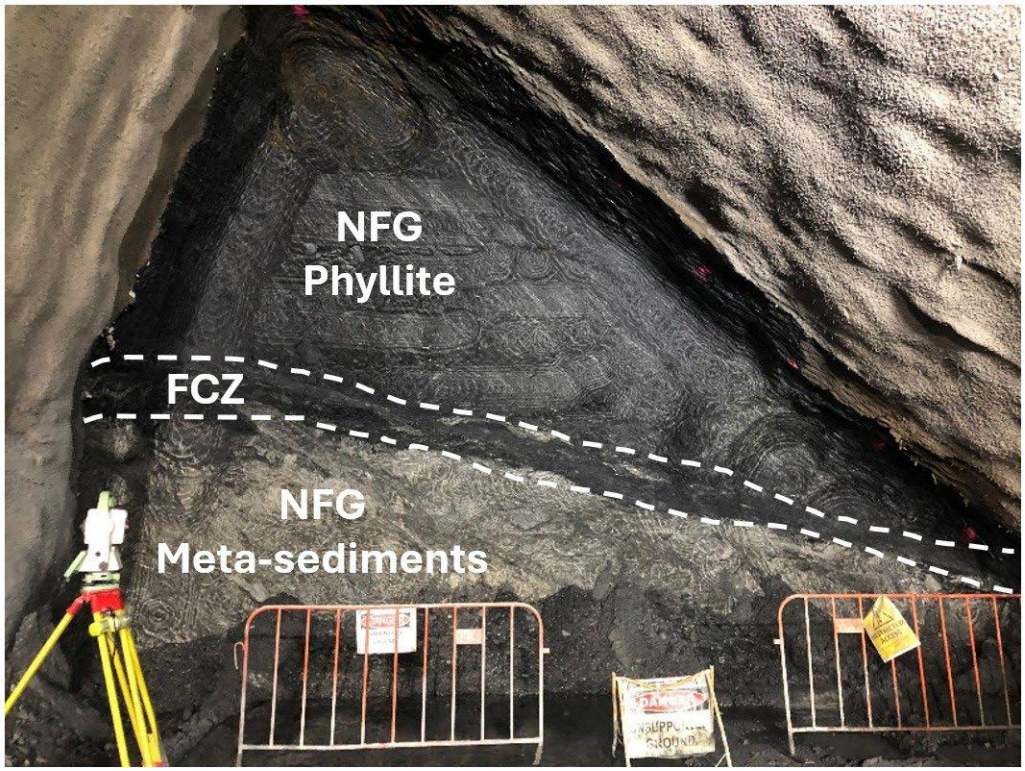


Figure 17: Low-angle fault encountered in the Albert Street Station cavern heading during construction.



Figure 18: Excavation of fault materials for the Albert Street Station cavern invert floor treatment.

5 CASE STUDY 3 – UNCONFORMITY ZONE AT BOGGO ROAD STATION

5.1 GEOTECHNICAL MODEL

Bogga Road Station is located within the Aspley Formation and Brisbane Tuff geological units to the south of the Brisbane CBD. The initial investigation boreholes encountered an Unconformity Zone (UZ) between the overlying Tuff and underlying Aspley units, located close to the invert level of the shaft for the proposed station box building, Figures 19 and 20. The UZ was assessed to be highly variable, ranging from a good quality rock-to-rock contact, to low shear strength and low stiffness brecciated and sheared rock and soil materials up to 1m thick. The UZ was considered to have potential implications for shaft stability, ground loading, founding conditions, and as a potential source of displacement which could impact exiting infrastructure. Additional geotechnical boreholes were drilled from within the shaft excavation during the construction phase to improve understanding of this feature at critical locations where large structural loads or spans were identified in the station box design.

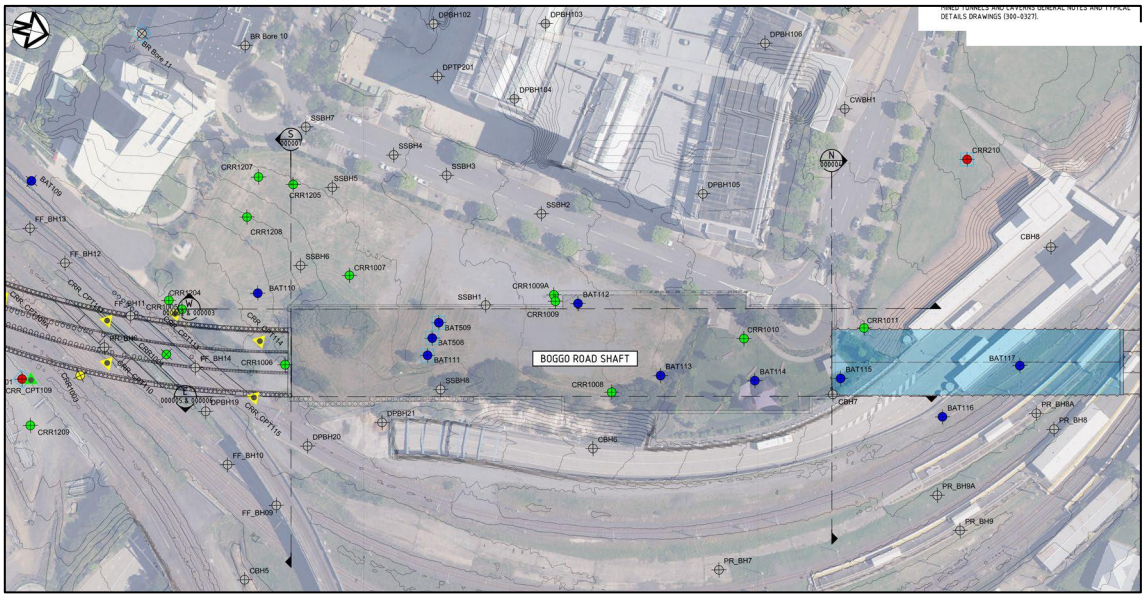


Figure 19: Boggo Road Station borehole plan (refer to Figure 2 for legend).

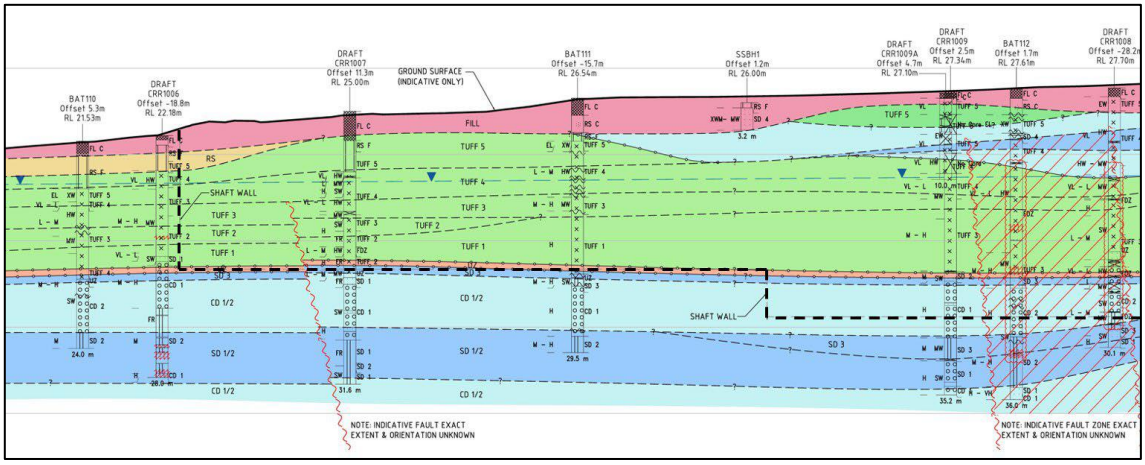


Figure 20: Boggo Road Station geotechnical section – showing inferred Unconformity Zone (orange unit) at shaft invert level between Brisbane Tuff (green units) and Aspley Formation (blue units).

5.2 DESIGN CONSIDERATIONS

The design solutions developed to cater for the UZ at the Boggo Road Station shaft included:

- Heavier primary ground support for the shaft walls where the UZ daylights.
- Underpinning or deepening of shaft piles where they are founded within or close to the UZ.
- A review of additional construction phase investigations, Figure 21, ground-structure interaction assessments and geotechnical loading and settlement inputs into the permanent station box structural design to cater for the UZ materials. The design solutions introduced for the station box included:
  - Removal and concrete replacement of adverse UZ materials where close to the shaft invert, or
  - Inclusion of additional reinforcement in the station box slab and walls to span across or enable transfer load around zones of lower stiffness in the foundation associated with the UZ.
- Carefully managed excavation and support sequence and deformation monitoring of the shaft and adjacent existing infrastructure.
- Staged construction of the station-box structure to manage deformations.

These were assigned and managed via the PTE, Hold Point and Request for Information (RFI) processes during construction.

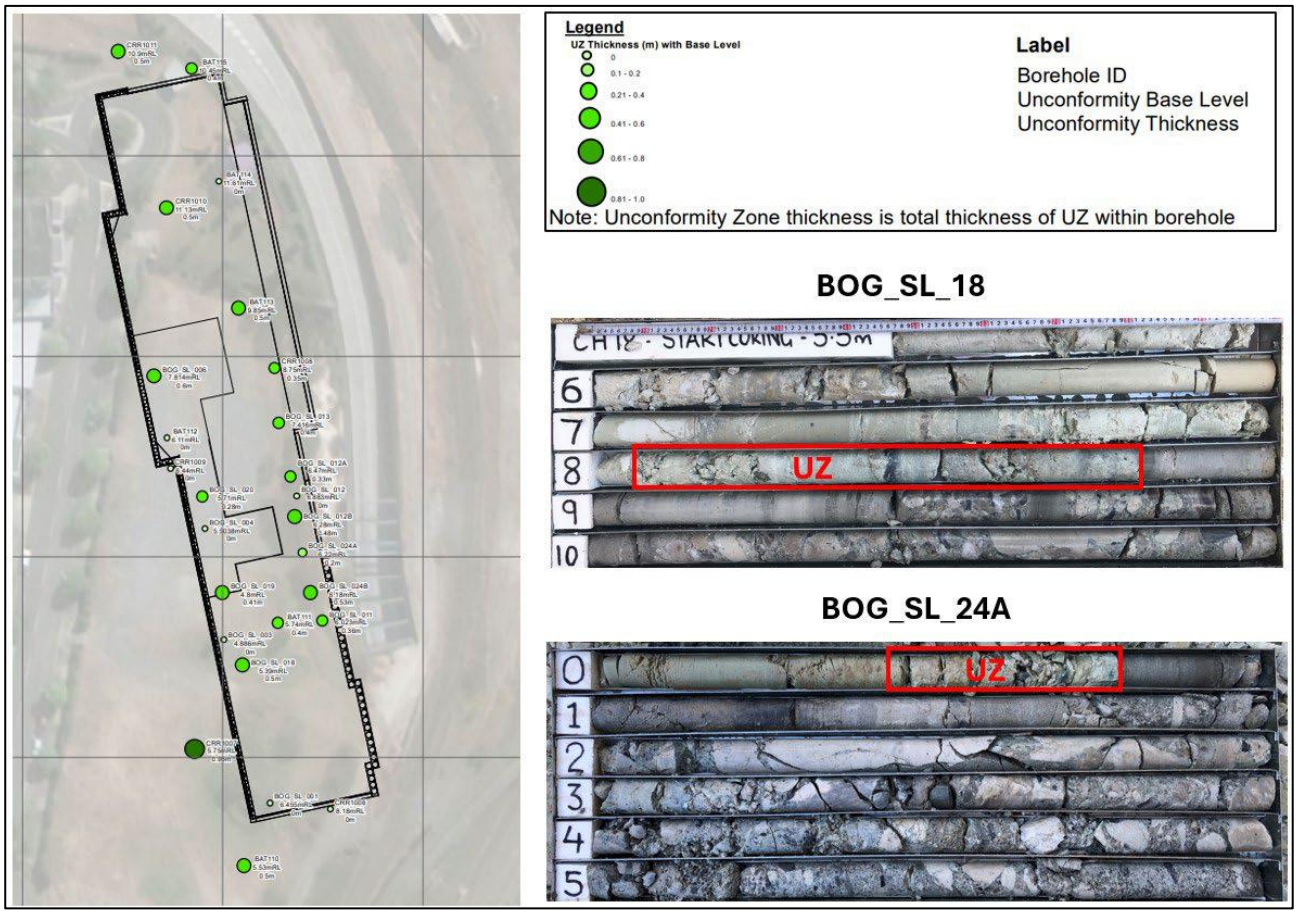


Figure 21: Construction phase geotechnical boreholes to investigate the relative level, thickness and character of the Unconformity Zone below the Boggo Road Station shaft invert. Typical core photographs are shown.

5.3 CONSTRUCTION OUTCOMES

Verification of the UZ was undertaken during construction via additional boreholes with televiewer imaging, geotechnical mapping, endoscopes, piling inspections and monitoring. The UZ was persistent and observed to be undulating in shape over short distances, inferred to be associated with the paleo-erosion surface prior to deposition of the overlying volcanic tuff materials. It was variable in character along its strike, ranging from a clean rock-to-rock contact to a 1m thick zone of clast or matrix supported brecciated rock with zones of soil, including high plasticity clay, up to 0.5m thick, Figure 22. Slickensides and other signs of shearing were observed in places. Significant groundwater seepage occurred at some locations. Removal and replacement of the UZ materials was undertaken in the Boggo Road Station shaft invert, Figure 23.

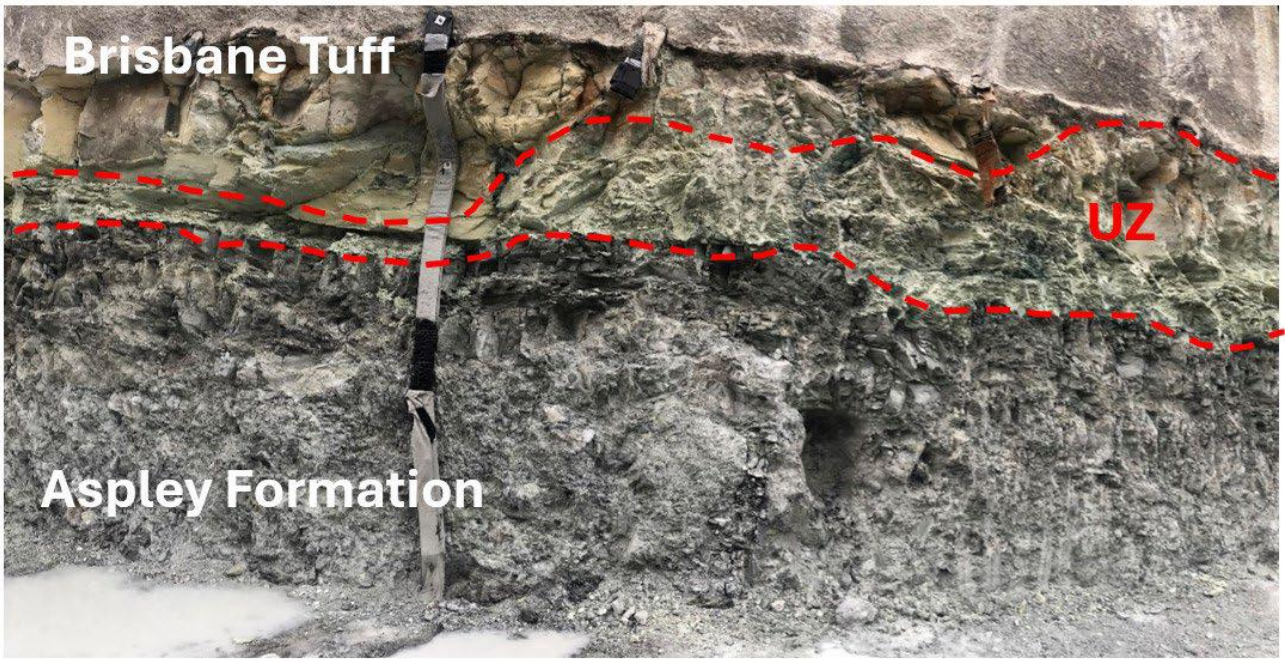


Figure 22: Unconformity Zone between the overlying Brisbane Tuff and underlying Aspley Formation geological units encountered in the Boggo Road Station shaft excavation during construction.



Figure 23: Excavation of Unconformity Zone materials for the Boggo Road Station invert floor treatment.

6 CONCLUSIONS

A range of challenging geological conditions were considered and managed during the design and construction of CRR. Adverse conditions associated with the Normanby Fault Zone were contended with in several locations, including major fault zones up to 15m in width, and persistent discrete faults up to 2m in width. A similar range of conditions, including potentially wider fault zones, are expected elsewhere in the Normanby Fault Zone within the Brisbane CBD. Highly variable conditions were observed at geological unconformities between the Brisbane Tuff, Aspley Formation and NFG units. These were encountered at several locations at CRR to the south of the Brisbane CBD including the southern dive structure, mined tunnels and Boggo Road and Woolloongabba Stations.

Case studies for three selected examples are presented in this paper, which demonstrate the importance of appropriate site investigations, understanding the level of confidence in geotechnical models, allowing for geotechnical variability in design, and the verification and monitoring of ground conditions and performance during construction. These examples comprised zones of significantly lower strength and stiffness materials bounded by high strength rock. This contrast in geotechnical properties can present issues related to ground loads on tunnel and shaft linings and ground support, kinematic stability mechanisms, ground deformation, founding conditions and load transfer, arching & bridging actions for reinforced concrete structures.

The project has provided information to better understand a variety of adverse ground conditions in Brisbane and it is hoped this may be useful for future ground-engineering projects.

7 ACKNOWLEDGMENTS

The author would like to acknowledge the Pulse consortium and the CBGU JV for granting permission to publish this paper. The author also wishes to express their appreciation of their colleagues at PSM and other designers at CRR, as well as the CBGU JV construction team to successfully navigate these, and other, geological challenges encountered on this project.

8 REFERENCES

Bennett, C. and Norbert, M. (2014). Tunnelling within the Bunya Phyllite of Legacy Way, Brisbane, Queensland. *15th Australasian Tunnelling Conference*.

Bryan, W., & Jones, O. (1951). Geological Map of The City of Brisbane and Explanatory Notes. *University of Queensland Press.*

Bryan, W., & Jones, O. (1954). Contributions to the geology of Brisbane No. 2. The structural history of the Brisbane Metamorphics. *Proceedings of the Royal Society of Queensland Vol. 65,* 25-50.

Cammack, R., Bertuzzi, R., Smith, A., Brehaut, R. (2022). Rock Mass parameters for the Brisbane CBD. *Australian Geomechanics Journal Volume 57, Number 4 - December 2022,* 47-72.

Cammack, R., Shen, B., Kobler, M. (2023). Geotechnical Characterisation of the Normanby Fault Zone for Roma Street Station Cavern Design, Cross River Rail, Brisbane. *Australasian Tunnelling Conference 2023: Conference Proceedings: Trends and Transitions in Tunnelling.* 141-151.

Grubb, K. (1989). Engineering Geology of the Central Business District of Brisbane. (Masters by Research Thesis). *Queensland University of Technology.*

Holcombe, R. (1977). Structure and Tectonic History of the Brisbane Metamorphics in the Brisbane Area. *Journal of the Geological Society of Australia, Vol. 24,* Pt 8, 475-490.

Shen, B., Clarke, S., Rogan, A. McCormack, P. (2022). Design And Construction of Roma Street Station Cavern, Cross River Rail, Brisbane. *Australian Geomechanics Journal. Volume 57, Number 4 - December 2022,* 115-128.

Willmott, E. (2012). Rocks and landscapes of Brisbane and Ipswich. *Geological Society of Australia – Queensland Division, 2nd Ed.,* 86.

https://doi.org/10.56295/1ACEG37

SITE INVESTIGATION AND GEOLOGICAL CHALLENGES FOR A RAIL LEVEL CROSSING PROJECT IN SEQ

Pramod Thakur[1] and Craig Brock[2]

1. Technical Executive, WSP Australia

2. Senior Associate Engineering Geologist, WSP Australia

ABSTRACT

An understanding of geology is very important to minimise design and construction uncertainties and challenges for any site. WSP was engaged to deliver a detailed design of an overpass bridge and associated structures to replace a very busy rail level crossing for a rail track in a metro area of Southeast Queensland (SEQ). The design services included design of an overpass bridge, earthworks, approach embankments, retaining walls, etc. Considering the design life of 100 years for these structures, a detailed geotechnical investigation (GI) and interpretation of the GI data were required to be fed into the design. As the site was located in an urban area, carrying out geotechnical investigation was not an easy task. It required dealing with various stakeholders, local community, and working night shifts to manage technical requirements and public expectations.

The project conceptual ground model benefited from some previous intrusive site investigations. However, WSP noted that the previous boreholes had limited rock coring and had relatively un-explained SPT refusals in soil material at depths of less than 10 metres below ground level. WSP scoped additional geotechnical investigation as per the Department of Transport and Main Roads (DTMR) geotechnical design standards and project specifications. When the geotechnical investigation was complete, the encountered materials were weakly and moderately cemented units, interlayered with poorly consolidated materials that are typically dominated by Residual (Sandy CLAY) to about 25 m below ground level overlying very low strength (UCS < 1.5 MPa) Sedimentary rock (Sandstone/Siltstone/Claystone) to the borehole termination depth of approximately 40 m bgl. This created additional challenges for pile foundation design and constructability issues.

This paper discusses how the challenges during geotechnical investigation were overcome and interpretation of the encountered strata for feeding into the design to manage geotechnical uncertainties considering constructability within a constrained environment.

1 PROJECT DESCRIPTION

WSP Australia was engaged to deliver a detailed design of a railway overpass bridge and associated structures to replace a busy rail level crossing for a rail track in a metro area of Southeast Queensland. The proposed development primarily comprises a new 92 m long, three span bridge, over the existing rail track including over 200 m of approach embankments either side of the bridge supported by Reinforced Soil Structure (RSS) walls, a pedestrian underpass, and an upgrade of an intersection and pavement. Both the geotechnical site investigation and the subsequent detailed design were completed in accordance with the relevant Department of Transport and Main Roads (DTMR) standards.

Figure 1 is an overlay of the project site showing the alignment of the proposed bridge and the upgrades to the surrounding approach roads.

This paper describes the site and some of the constraints in relation to completing the geotechnical investigation and the detailed design of the proposed structures. The geological setting and the initial project conceptual ground model are discussed followed by interpretation of the additional site investigation works which led to a modified 3D geotechnical design model. The apparent lack of correlation between in-situ dynamic cone penetration (DCP) tests and standard penetration tests (SPT) during the additional site investigation is discussed. Finally, the paper presents recommended geotechnical design parameters based on the 3D ground model and the relevant DTMR standards for geotechnical design.

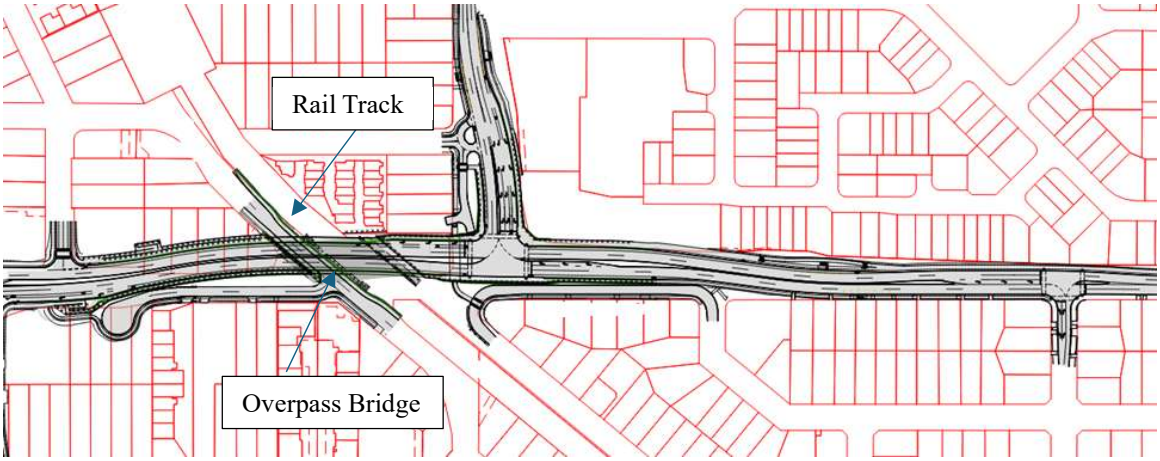


Figure 1: Proposed development layout.

2 SITE CONSTRAINTS

The project involves the construction of a bridge and approach works, removal of the existing level crossing, construction of a new intersection and road pavement upgrades. Existing infrastructure within the project site that had to be considered included an active petrol station, rail line with overhead electrical lines, active commercial/retail buildings, private properties and buried services. Figure 2 shows an aerial view of the project site centred on the existing rail crossing.



Figure 2: Existing conditions at project site (Google Earth, 2024).

3 GEOLOGICAL SETTING

The project is located in the Oxley Basin, the Oxley Group of rocks comprises three sedimentary formations that are said to be lateritised towards the basin's southern extent (Geological Survey of Queensland, 2023). The geological map of the project site indicates that the majority of the road alignment is underlain by the Sunnybank Formation (of the Oxley Group) unconformably overlying the Triassic/Jurassic age Woogaroo Subgroup. Figure 3 shows the project site with the local geology overlay, and Table 1 provides a description of the geological units expected to be encountered on the project site.

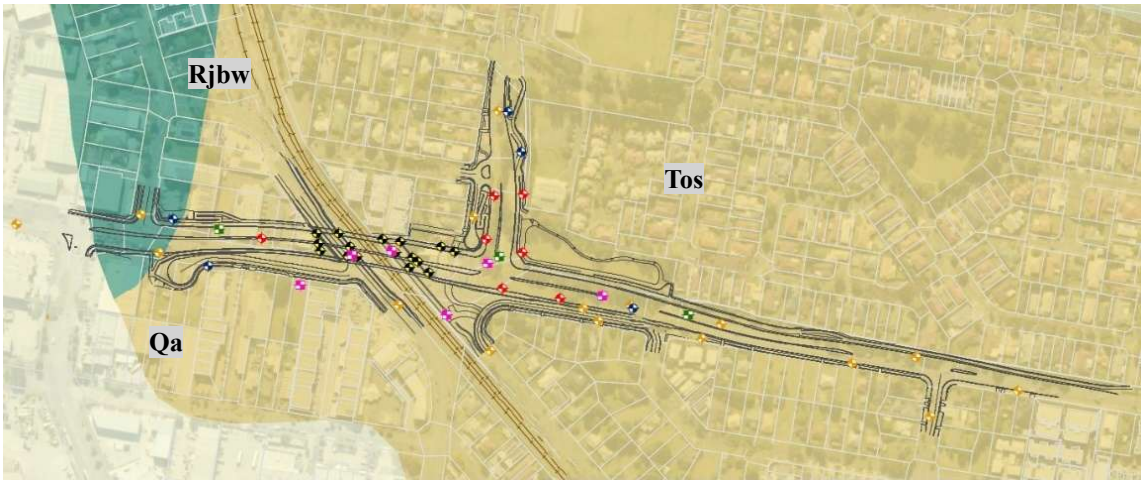


Figure 3: Project layout, local geology, and proposed and existing borehole locations.

Table 1: Geological unit description

Geological Unit	Description
Rjbw	Woogaroo Subgroup (Stratified unit including Volcanic and Metamorphic) – Sublabile to quartzose sandstone, siltstone, quartz – rich granule to cobble conglomerate and coal.
Tos	Sunnybank formation (Stratified unit including Volcanic and Metamorphic) – Lacustrine and fluviatile quartzose to sublabile sandstone, conglomerate, silty clay, siltstone, clayey mudstone: mildly lateritised.
Qa	Alluvium – Clay, silt, sand, and gravel: flood-plain alluvium.

The Sunnybank Formation is said to consist of up to 164 m of claystone, sandstone, conglomerate and limestone deposited in a fluvial to lacustrine environment (Geological Survey of Queensland, 2023). The sedimentary rocks of the Oxley group have been undisturbed by folding and are considered to be relatively unconsolidated and soft (Willmott, 2012).

The Sunnybank Formation includes weakly and moderately cemented units, interlayered with poorly consolidated materials that are typically dominated by sandy clay. The Formation was subject to deep (lateritic) weathering processes when it was subaerially exposed. Superficial soils are typically red earth (lateritic red soils and laterite podzol) that may be described as clay, with irregularly shaped nodules of limonite and haematite.

The Sunnybank Formation includes vertically and laterally non-persistent beds of quartzose (grading up from pebbly conglomerate) sandstone, clayey/weathered feldspathic sandstone and sandy mudstone, any of which may be moderately cemented, typically low and partly medium strength.

Towards the western end of the project site the geology was anticipated to transition to the Woogaroo Subgroup and surficial deposits of quaternary aged alluvium. The Woogaroo Subgroup is dominated by grey interbedded sandstone and siltstone, with some interbedded conglomerate and some carbonaceous shaly mudstone.

4 GEOTECHNICAL INVESTIGATION

4.1 INVESTIGATION REQUIREMENTS

Knowledge of the properties of the subsoil layers and their lateral variation are important for an accurate site characterisation. According to the Department of Transport and Main Roads (DTMR) Geotechnical Design Standard Minimum Requirements (DTMR, 2020a), geotechnical investigations are required to inform the design of the foundations of all bridges and other structural elements. The scope of work for any site investigation needs to ensure that the site geological model can reasonably be established and adequately inform the design. Additional site investigation requirements are also specified based on the proposed structure types. DTMR (2020a) requires a minimum of two boreholes to be drilled at every abutment and pier location. Also, the boreholes to be drilled

should be at intervals not exceeding 10 m along the width of every abutment and pier of all bridges. For bored piles, the boreholes are to be extended to a minimum of 5 m into competent bedrock (moderately weathered and medium strength or better rock).

In addition, the Main Roads Technical Specification MRTS63 (DTMR, 2020b) requires the depth of at least three boreholes or 50% of all the boreholes at a proposed bridge location to be a minimum of 2 x pile diameter deeper than the proposed pile base with no weak layers identified. MRTS63 further states that the maximum distance between the boreholes and proposed pile location to be as per the following pile ultimate loading:

- ≤2,000 kN: borehole can be 10 m away from the pile location.
- ≤10,000 kN: borehole to be within 10 m from the pile.
- >10,000 kN: borehole to be at the pile location.

4.2 CONCEPTUAL GROUND MODEL

There were some existing boreholes available from the Business Case design of the project (Figure 4). The conceptual ground model was developed based on this data. As there were only two boreholes (BH6 and BH7) at the bridge location, additional investigation was required. Moreover, these boreholes had limited rock coring and had relatively un-explained Standard Penetration Test (SPT) refusals in soil material at depths of less than 10 metres below ground level. These previous intrusive works were not sufficient to meet the DTMR and project requirements. Therefore, an additional geotechnical investigation scope was developed with consideration of the project objectives and the locations of the previous investigation completed at the site.



Figure 4: Existing geotechnical investigation locations.

4.3 ADDITIONAL INVESTIGATION AND METHODOLOGY

An additional geotechnical investigation was proposed to inform the detailed design of the bridge and associated structures in accordance with the project specification. The investigation included the following number of additional boreholes, and the locations of these boreholes are shown in Figure 3.

- 14 boreholes for the proposed bridge.
- 14 boreholes for the proposed retaining walls and pedestrian underpass.
- 19 boreholes to investigate the pavement subgrade of the road alignments.

In addition, a number of laboratory tests (e.g. Atterberg Limits, Aggressivity, Point Load Index, Uniaxial Compressive Strength, 4 Days-soaked California Bearing tests for pavement, etc.) were conducted on the materials retrieved during the investigation.

Given the urban environment there were many site constraints to consider. Constraints to the site investigation included:

- Dense urban environment comprising residential and light industrial / commercial properties adjoining the road corridor.
- Potentially contaminated soils (including a petrol station).

- A number of buried services.
- A busy road where the site investigation had to be completed with no disruption to the daytime traffic.

Careful planning and coordination were required to carry out the proposed investigation. In addition, the following methodologies were implemented to minimise the disruption to the public and manage the site constraints:

- Public consultation was conducted before any works commenced on site.
- Boreholes along the existing road alignment were completed at night under lights and with all relevant traffic management and permits in place.
- For the boreholes located within 3 m of underground services, hand auger and/or non-destructive drilling (NDD) techniques were used from the surface through the fill material until natural soil was confirmed.
- When drilling at the petrol station, gas monitoring was carried out and the drilling rig was shut down during re-fuelling activities.

Following the NDD of the boreholes, drilling was advanced through the soil using auger and rotary wash boring techniques until rock was encountered. At the bridge borehole locations, the boreholes were advanced through rock using diamond rotary coring techniques. The encountered materials in the boreholes were logged in accordance with AS1726-2017.

Standard Penetration Tests (SPT) were completed in the bridge and retaining wall boreholes at approximately 1.5 m intervals until refusal (SPT, N > 50). Dynamic Cone Penetration (DCP) tests were completed adjacent to each borehole to assess strength of soils within top 3 m.

5 SUBSURFACE PROFILE AND GROUND WATER

Based on the materials encountered in the boreholes, the typical subsurface profile at the project site consists of the following:

- Fill – Generally comprising firm Gravelly CLAY, medium dense to dense Clayey and Gravelly SAND up to 1 m below ground level (bgl). In absence of compaction tests results, the fill encountered was generally considered to be un-controlled as per AS3798-2007.
- Alluvium – Encountered as a thin layer in a small number of borehole locations. Where encountered it was described as grey Sandy CLAY or Clayey SAND.
- Residual Soil / Extremely Weathered Material – generally stiff to hard CLAY and dense to very dense Clayey SAND, encountered up to 31.5 m bgl. Inferred lateritised zones at shallow depths is shown in Figure 5.
- Rock – highly weathered to fresh Siltstone, Sandstone, and Claystone, generally very low to low strength.



Figure 5: Inferred lateritised zone in cored soil (WSP, 2024).

The ground conditions were generally consistent with the published geology. The SPT refusals (> 50 blows/150 mm penetration) at shallow depths (< 10 m bgl) from the conceptual ground model were encountered during the additional ground investigation. These refusals have been interpreted to represent weakly cemented or lateritised horizons. In places, these layers have been described as rock (unable to disaggregate by hand) in accordance with AS1726-2017.

Groundwater was encountered during the investigation and data from groundwater monitoring wells installed as part of the project indicated that groundwater was generally < 2 m below the existing ground surface.

6 GEOTECHNICAL GROUND MODEL

6.1 GEOTECHNICAL UNITS

When the geotechnical investigation was complete, the encountered materials were summarised as weakly and moderately cemented units interlayered with poorly consolidated materials that are typically dominated by Residual (Sandy CLAY) to about 25 m bgl overlying very low strength (UCS < 1.5 MPa) sedimentary rock (Sandstone/Siltstone/Claystone) to the borehole termination depths of approximately 40 m bgl.

In general, the geotechnical units interpreted for the geotechnical model and design were:

- Fill overlying
- Residual Soil overlying
- Extremely Weathered Material overlying
- Weathered Sunnybank Formation (Sandstone/Siltstone/Claystone).

6.2 3D MODEL AND GEOLOGICAL SECTIONS

The borehole data from the site investigations was imported into Leapfrog, a leading 3D geological modelling software, to assist with the development of the 3D ground model. The geotechnical units were imported based on the geological sequence interpreted from the borehole logs. The 3D geological model for the site is shown in Figure 6.

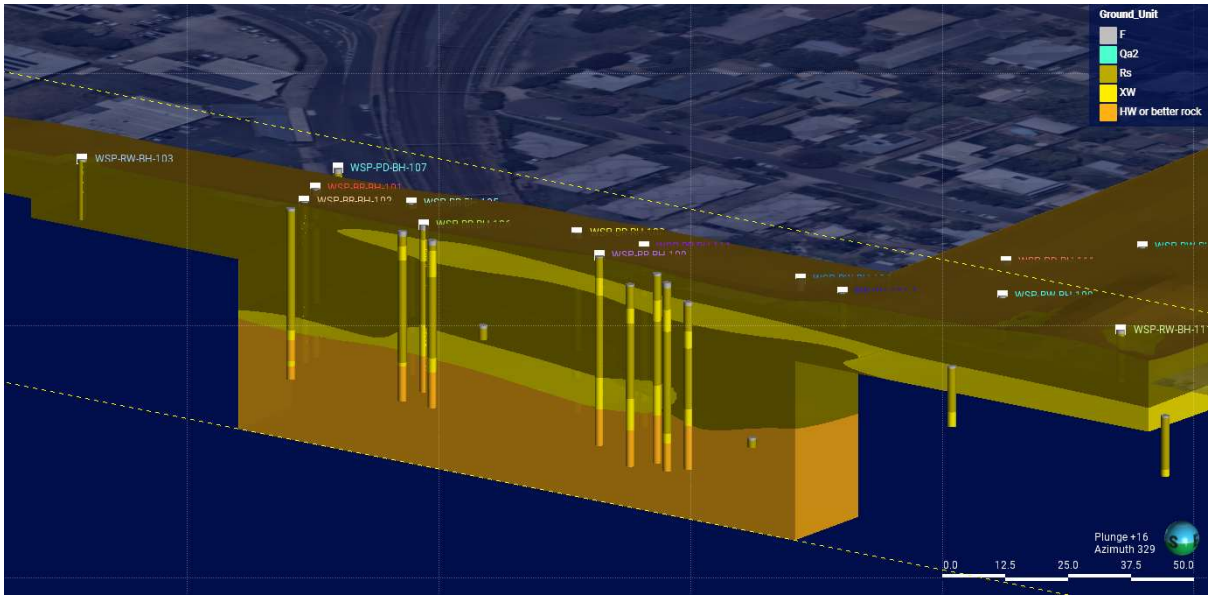


Figure 6: 3D Geological model of the site.

The geological sections along the bridge abutments and piers, and RSS walls were extracted from Leapfrog Works in 2D. These inferred geological sections formed the basis of the geotechnical model for design. Figure 7 shows an example of a geological sections at one of the bridge abutments.

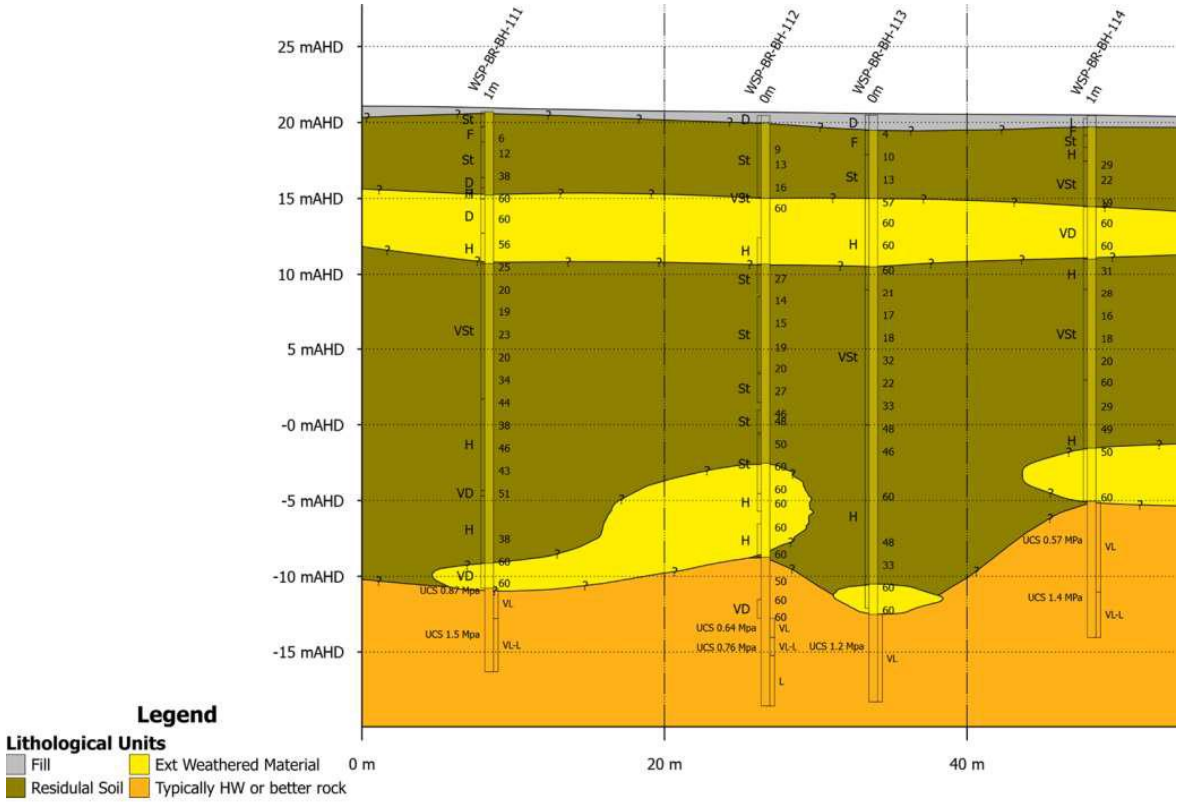


Figure 7: Inferred geological section through a bridge abutment from Leapfrog.

7 INTERPRETATION OF THE GI DATA

Accurate geotechnical interpretation of the encountered materials at the site is very important for a robust and economical design. Therefore, a hand-drawn geological section was developed to commence the design prior to the completion of laboratory testing and 3D modelling. These sketches in combination with SPT and core photography helped to confirm the lateral extent of both the cemented horizons near the surface and the very low to low strength rock at depth.

As part of the review of the field testing, it was observed that the SPT, N values indicated the materials in the upper layer (within top 3 m) to be of firm to stiff consistency. Considering the height of the approach embankments (up to 10 m), foundation improvement was required to minimise the differential settlements and satisfy the bearing capacity. Remove and replace was considered the economical option. However, considering the close proximity of rail track, buildings, and underground services; excavating up to 3 m to carry out remove and replace was not viable. Therefore, Dynamic Cone Penetration (DCP) test data available for the top 3 m was reviewed. A summary of the SPT, N and DCP values at each borehole location is presented in Table 2. The material consistency was interpreted from the SPT, N and DCP values as per HB 160 (AS 2006).

Table 2: Summary of SPT, N and DCP values with corresponding material consistency

BH ID	Depth (m bgl)	Material Type	SPT N value	SPT corelated Consistency	DCP blow count/100 mm penetration	DCP corelated Consistency
103	1	CLAY, high plasticity	11	Stiff	5	Very stiff
108	1	CLAY, high plasticity	8	Firm-Stiff	5	Very stiff
108	2.5	CLAY, high plasticity	12	Stiff	14	Hard
110	1.5	Sandy CLAY, high plasticity	2	Soft	7	Very stiff
111	1.5	Clay, low plasticity	6	Firm	8	Very stiff
112	2	CLAY, medium to high plasticity	9	Stiff	19	Hard
101	1.5	Silty CLAY, medium plasticity	8	Firm-Stiff	17	Hard

BH ID	Depth (m bgl)	Material Type	SPT N value	SPT corelated Consistency	DCP blow count/100 mm penetration	DCP corelated Consistency
102	1.5	Clay, medium plasticity	6	Firm	3	Stiff
103	1.5	Clay, high plasticity	5	Firm	9	Very stiff
105	1.5	Clay, high plasticity	9	Stiff	8	Very stiff
106	1.5	Clay, med plasticity	6	Firm	20+	Hard
108	1.5	Clay, low Plasticity	Refusal	Hard	6	Very stiff
109	1.5	Sandy CLAY low plasticity	Refusal	Hard	17	Hard
110	1.5	Clay medium to high plasticity	6	Firm	6	Very stiff
111	1.5	Sandy Clay low to medium Plasticity	8	Firm to stiff	7	Very stiff
112	1.5	Sandy Clay (low to medium plasticity	5	Firm	4	Stiff
113	1.5	Clay, high plasticity	15	Stiff to Very stiff	8	Very stiff

SPT, N values indicated the encountered ground to be firm to stiff consistency while the DCP values indicated the soils to be primarily very stiff to hard consistency with some localised stiff materials. It is envisaged that the materials may have lost strength due to ground disturbance during borehole drilling resulting in lower SPT, N values. As a result, the materials' consistency based on the DCP values was adopted in the design which helped to minimise the ground improvement requirement and saved construction time and cost.

8 GEOTECHNICAL DESIGN PARAMETERS

Once the field and laboratory tests were completed, the geotechnical design parameters were determined to complete the geotechnical design of the approach embankments, pile foundation, and retaining walls.

8.1 GEOTECHNICAL PARAMETERS FOR SOIL

8.1.1 Unit weight

Soil unit weight can typically be related to the consistency / density of the material. AS4678-2002 recommends a typical unit weight of the materials. A summary of the design values for bulk unit weight for various materials encountered at the site is presented in Table 3.

Table 3: Adopted unit weight of the soil/rock encountered

Materials	Consistency/Density/Strength	Unit Weight (kN/m^3)
Cohesive materials	Firm	18
	Stiff to very stiff	19
	Hard	20
Granular materials	Medium dense	19
	Dense	20
	Very dense	21
Extremely weathered materials	Hard/Very dense	21
Siltstone/Claystone/sandstone	Moderately to highly weathered, very low strength	21
	Slightly weathered to fresh, low strength	22

8.1.2 Undrained shear strength

The undrained shear strength (s_u) of cohesive materials was determined using the SPT, N values based on the relationship given by Terzaghi and Peck (1967).

$$s_u = 6 \times N \quad (kPa) \qquad (1)$$

8.1.3 Effective strength parameters

The effective strength parameters (cohesion, *c'*, and friction angle, ϕ') for cohesive soils were determined based on engineering judgement and correlations between plasticity index (I_p) and friction angle (ϕ') shown in Figure 8 obtained from AS4678-2002.

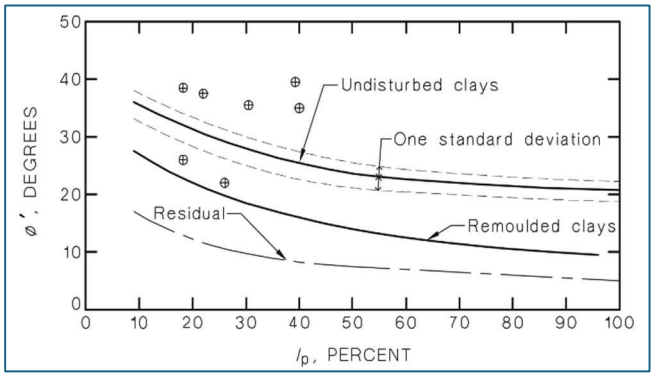


Figure 8: Correlation between ϕ' and plasticity index I_p (AS4678-2002).

The Atterberg Limit tests on the encountered cohesive materials indicated the Plasticity Index (I_p) in a range of 30 to 50 %.

The friction angle of cohesionless soils were determined using empirical correlations between SPT, N values and ϕ′, as indicated in published literature (Bowles 1997) and engineering judgment. In general, Equation 2 was used for determining the friction angle of cohesionless soils.

$$\emptyset' = (0.36 \times N) + 27 \qquad (2)$$

Equation 2 may result in high ϕ' values for SPT completed within very dense granular materials. Therefore, a maximum friction angle (ϕ') of 39° has been used for very dense materials at this site.

Based on this, the recommended effective strength parameters for the encountered materials are summarised in Table 4.

Table 4: Recommended value of effective strength parameters

Materials	Consistency/Density	Effective Cohesion, c' (kPa)	Effective Friction, ϕ' (°)
Cohesive materials	Stiff	3	26
	Stiff to very stiff	4	28
	Hard	5	30
Granular materials	Medium dense	-	33
	Dense	-	36
	Very dense	-	39

8.1.4 Elastic modulus and Poisson's ratio

For cohesive soils, Duncan and Buchignani (1976) recommended that undrained Young's modulus (E_u) was linearly proportional to s_u and proposed the Equation 3.

$$E_u = Ks_u \quad (kPa) \tag{3}$$

Where K is the constant of proportionality and is a function of Plasticity Index (PI), and Overconsolidation Ratio (OCR) as shown in Figure 9. As the encountered soil has PI in a range of 30 to 50, K = 350 was adopted.

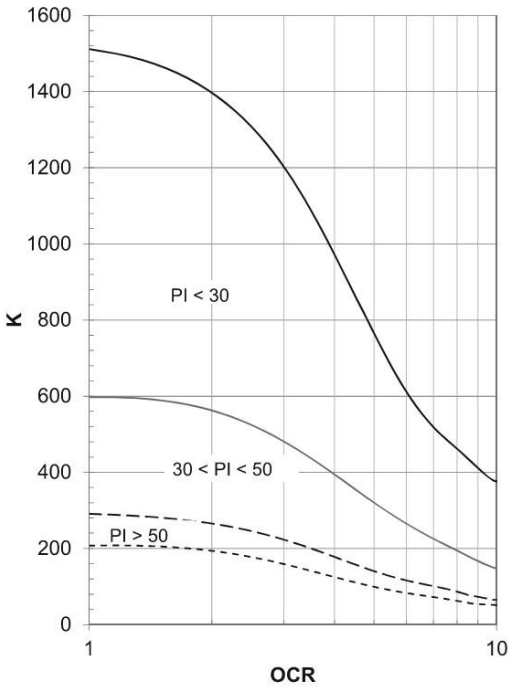


Figure 9: K-factor variation based on OCR (Duncan and Buchignani, 1976).

Drained elastic modulus (E') for the cohesive soils were estimated from the E_u through an elastic relationship with the drained Poisson's Ratio (ν'):

$$E' = \frac{2(1+\nu')}{3} E_u \tag{4}$$

For the cohesionless soils, a correlation between elastic modulus and SPT, N value was selected as follows, which is recommended for clayey sands (Clayton 1995):

$$E' = 2000 \times N \quad (kPa) \tag{5}$$

A Poisson's ratio (ν) of 0.3 has been adopted for all soil and rock layers.

8.2 GEOTECHNICAL PARAMETERS FOR ROCK

8.2.1 Strength and weathering characteristics

The Sunnybank Formation includes weakly and moderating cemented units, interlayered with poorly consolidated materials. The formation was subject to deep (lateritic) weathering processes, with the weathering being both contemporaneous with and subsequent to its period of deposition. Rock recovered in the boreholes as slightly weathered and fresh, was still very low to low strength.

Generally, the extremely weathered material encountered in the boreholes was recovered as hard clay / sandy clay (inferred as residual soil and extremely weathered material) generally up to a depth of 24 m at Abutment A and to 30.5 m bgl at Abutment B. Below this depth, the rock (Siltstone, Sandstone, Claystone) was recovered as very low to low strength through to the termination depths of the boreholes.

8.2.2 Rock Strength

The bridge boreholes encountered extremely weathered materials with SPT refusal (N > 50) at shallow depth of around 5 m bgl and before rock coring at a depth between 24 m and 30.5 m bgl. Ignoring the contribution of this materials for pile skin resistance would have made the pile very deep and uneconomical. Therefore, equivalent uniaxial compressive strength (UCS) for this material was estimated as per the recommendations made in CIRIA

(1999). Figure 10 presents relationship between SPT and equivalent compressive strength for extremely weathered material with rock structure (Weak Rock).

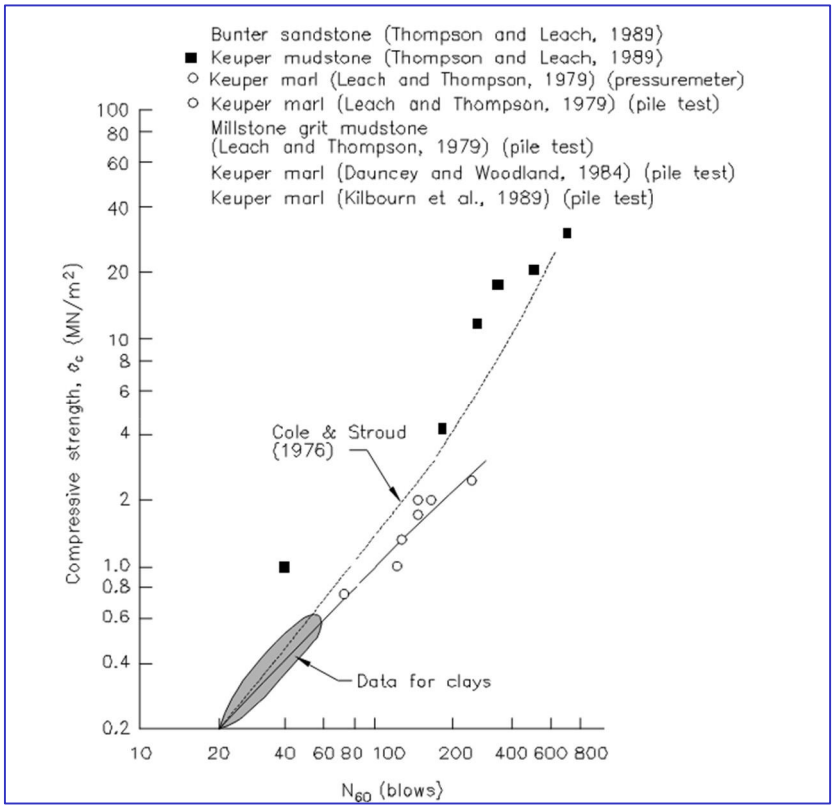


Figure 10: Correlations between SPT N_{60} and Compressive Strength of Weak Rock (CIRIA, 1999).

For the extremely weathered materials encountered at the site with lower bound SPT N of 60, a design UCS of 0.6 MPa was adopted.

The point load strength (Is_{50}) and UCS at respective depth from bridge boreholes were plotted and are presented in Figure 11. The line of best fit indicates a factor of 10 between Is_{50} and UCS (i.e. UCS = 10 x Is_{50}). The relationship is lower than the ratio suggested in AS1726-2017; however, it is in line with the relationship reported by Look (2007) for low strength rock.

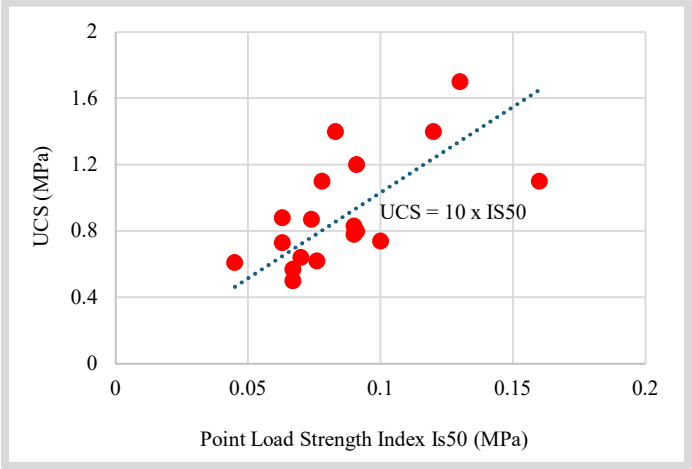


Figure 11: UCS vs Point Load Index strength correlation

This suggests that the inferred UCS of the rock encountered at the bridge site ranges between 0.6 to 1 MPa.

In addition, the UCS tests were plotted against depth at the bridge location and is shown in Figure 12. Based on the results of the UCS tests, it was found that the Rock UCS ranges between 0.6 MPa to 2.3 MPa. Moreover, the

data are concentrated between 0.6 MPa and 0.9 MPa. Therefore, a design UCS of 0.75 was adopted for determining pile design parameters. This was consistent with the inferred values of UCS from Is_{50}.

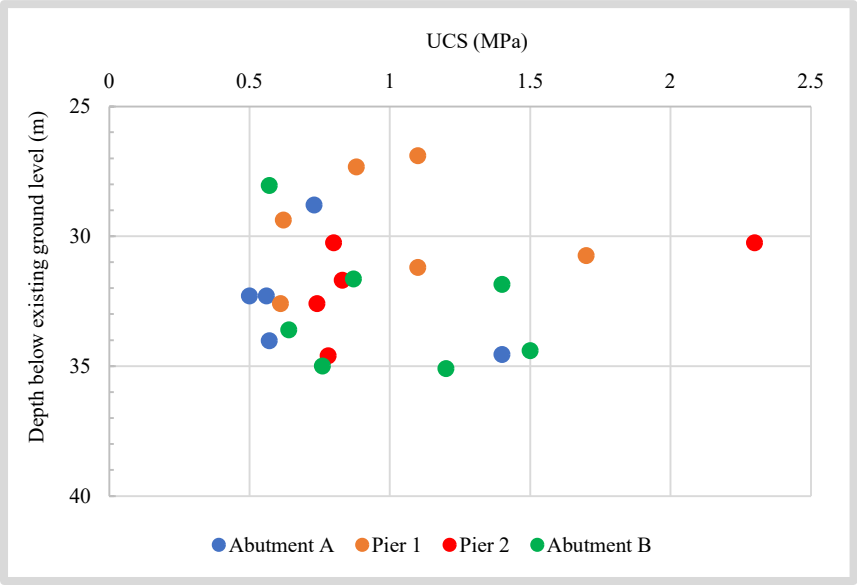


Figure 12: Variation of Rock UCS with Depth at Bridge Location

8.2.3 Pile design parameters

Based on the materials encountered at the bridge site, majority of the pile embedment is expected to be within the Residual Soil/Extremely weathered materials of very stiff to hard consistency and very low to low strength rock. The piles are expected to be terminated in very low to low strength rock.

For soil materials (i.e. residual soil and extremely weathered material), the ultimate skin friction (f_{su}) was determined using the following relationship:

$$f_{su} = \alpha \times s_u \quad (kPa) \tag{6}$$

Where α was obtained as recommended in MBIE (2014). From Figure 13 below, a value of 0.4 was adopted for the bored piles within the very stiff to hard residual soils.

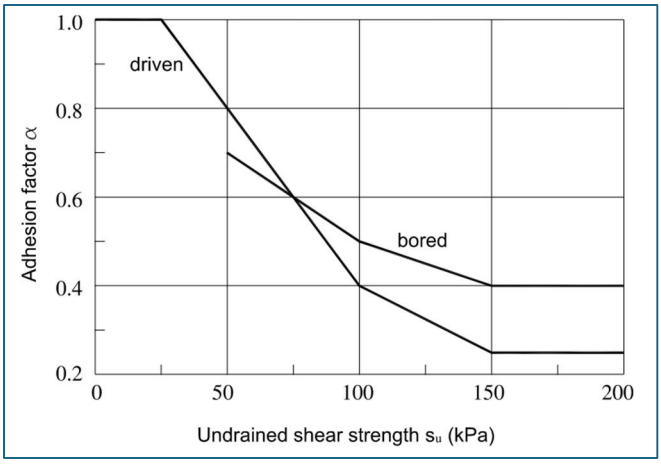


Figure 13: Adhesion factor for piles in cohesive soils (MBIE, 2014).

For very low to low strength rock, the f_{su} and ultimate base bearing (f_{bu}) were determined as per Zhang and Einstein (1998).

$$f_{su} = \beta \times \sqrt{UCS} \quad (MPa) \tag{7}$$

$$f_{bu} = \gamma \times \sqrt{UCS} \quad (MPa) \tag{8}$$

Where β varies between 0.3 and 0.8 depending on the rock socket roughness whereas γ ranges between 3 and 6.6. For robustness, $\beta = 0.4$ and $\gamma = 4$ was adopted for this site.

Based on the above, the recommended pile design parameters for the site are summarised in Table 5.

Table 5: Recommended pile design parameters

Materials Unit	Design s_u (kPa) or *UCS* (MPa)	Ultimate Skin Friction, f_{su} (kPa)	Ultimate Base Bearing, f_{bu} (kPa)
Residual (very stiff)	s_u = 190	75	-
Residual (hard)	s_u = 250	100	-
Extremely weathered materials	UCS = 0.6	300	-
Sandstone/Siltstone/Claystone (very low strength)	UCS = 0.75	350	3500

Rock mass modulus (E_r) is another important parameter for estimating pile settlement. For very low strength rock, the rock mass modulus was determined as per Rowe and Armitage (1987) using Equation 9.

$$E_r = 215 \times \sqrt{UCS} \quad (MPa) \tag{9}$$

The recommended value of E_r was 185 MPa.

9 CONSTRUCTABILITY CONSIDERATIONS

As the project is nearby a rail track and other structures, a steel liner to 10 m bgl has been recommended to provide pile hole stability. In addition, a recent project in similar materials encountered borehole instability due to groundwater and very low strength Sunnybank Formation rock, so a polymer supported pile hole has been proposed. The project is yet to be constructed, no construction issues have been discussed.

10 CONCLUSION

The paper presented the importance of good understanding of the site geology and having sufficient geotechnical investigation data to inform the detailed design of a railway overpass bridge and associated structures. Review of the existing data indicated the existing boreholes were limited and does not satisfy the project specification. Therefore, additional geotechnical investigation comprising of 14 bridge boreholes, 14 retaining wall boreholes, and 19 pavement boreholes was proposed and conducted to inform the design and minimise the construction risks. The bridge boreholes were drilled up to 40 m bgl, retaining wall boreholes were drilled up to 15 m bgl, and pavement boreholes were drilled to 2 m bgl. SPT tests were conducted at 1.5 m intervals to the top of rock. In addition, DCP tests were conducted at each borehole in upper 3 m or earlier refusal. Soil/rock samples retrieved were sent for laboratory testing.

The geotechnical investigation campaign required meticulous planning and managing stakeholders' expectations. The project being in urban setting the road was required to be opened during the day so most of the investigations were conducted during the night under traffic control to keep the road partially open.

Comparison of inferred soil strength from SPT, N and DCP values indicated reasonable discrepancy. The undrained shear strength of the soil in upper strata determined from the SPT, N values showed to be firm to stiff consistency requiring foundation improvement using remove and replace. However, the soil consistency based on the DCP tests indicated very stiff to hard consistency. As the DCP measures soil strength nearly in undisturbed state, it was decided to adopt in the design.

A 3D geological model was developed using Leapfrog to estimate the extent of soil/rock strata. Then 2D geological sections were produced to prepare a geotechnical model at each abutment, pier, and wall location. Field and laboratory test data were used to determine geotechnical design parameters using empirical correlations published in literatures and was recommended for detailed design.

The train track needed to be in operation and due to presence of buildings and services nearby the bridge site, steel liner was recommended to be screwed or inserted in pre-augured borehole to 10 m bgl. Moreover, polymer supported pile hole was advised considering the Sunnybank Formation may soften under water.

11 ACKNOWLEDGEMENTS

The authors are thankful to the client and WSP Australia Pty Ltd (WSP) for providing the opportunity to present the paper.

12 REFERENCES

AS 1726-2017. Geotechnical Site Investigations, *Standards Australia*, 1-75.

AS 4678-2002. Earth Retaining Structures, *Standard Australia*, 60-68.

Bowles, J. E. (1997). Foundation Analysis and Design, *5th Edn*, *McGraw Hill*, 135-210.

CIRIA (1999). Pile Foundations in Weak Rock, Report 181, *ciria London*, 17-37.

Clayton C.R.I. (1995). The Standard Penetration Test (SPT): Methods and Use*, CIRIA Report 143*, 77-94.

DTMR (2020a). Geotechnical Design Standards – Minimum Requirements Standards, *Department of Transport and Main Roads, Queensland Government*, 1-36.

DTMR (2020b). Transport and Main Roads Technical Specification MRTS63 Cast-In-Place Piles, *Department of Transport and Main Roads, Queensland Government*, 1-22.

Duncan, J.M. and Buchignani, A. L., (1976). An Engineering Manual for Settlement Studies, *University of California, Berkeley*, 22-71.

Geological Survey of Queensland, (2023). *Geology of Queensland*, Brisbane: Geological Survey of Queensland,594-595

HB 160-2006. Handbook-Soils Testing, *Standards Australia*, 1-113.

Look, B. G. (2007). Handbook of Geotechnical Investigation and Design Tables, *Taylor & Francis*, 65-76.

MBIE (2014). Acceptable Solutions and Verifications Methods, B1 Structures, *Ministry of Business, Innovation & Employment New Zealand*, 51-67.

Rowe, R.K. and Armitage, H.H. (1987). A design method for drilled piers in soft rock, *Canadian Geotechnical Journal,* 24(1), pp. 126-142.

Terzaghi, K. and Peck, R.B. (1967). Soil Mechanics in Engineering Practice. 2nd Edition, *John Wiley & Sons Inc., New York*, 729.

Willmott, W.F. (2012). Rocks and Landscapes of Brisbane and Ipswich, *2nd Edn., Geological Society of Australia, Queensland Division, Brisbane, Qld, 10-11*.

Zhang, L. and Einstein, H. H. (1998). End Bearing Capacity of Drilled Shafts in Rock, *J. of Geotech and Geoenv Eng ASCE*, 124 (7), 574-584.

https://doi.org/10.56295/1ACEG38

RESERVOIRS AND LANDSLIDES – THE CLYDE DAM EXPERIENCE

Don Macfarlane

Engineering Geology Consultant

ABSTRACT

Most dams and reservoirs are located in natural valleys resulting from fluvial or glacial erosion. In valleys with geologic structure that involves layering parallel or sub-parallel to the topographic slope there is greater potential for landslides into reservoirs.

The risk of landslide occurrence into reservoirs is enhanced by the submergence of the slope toe and by rapid drawdown conditions. Rapid failures may cause waves that endanger the dam.

Clyde dam (and its power station) was always controversial and was eventually completed 15 years after site works began. But then lake filling was delayed by the need to stabilise large landslides in the very mica-rich schist around the perimeter.

Between 1988 and 1992 New Zealand's Clyde Power Project was responsible for the investigation, analysis and design, and then construction of stabilisation works on 10 large landslides in the Otago Schist, mostly in the Cromwell Gorge, a 20 km section of the reservoir waiting to be formed upstream from the Clyde Dam. The engineering geology team was responsible for planning, supervising and assessing the site investigations which were undertaken concurrently with design and construction. Key issues confronted by the team were complex geological conditions, highly variable groundwater conditions and tight deadlines. No two landslides were the same. Lake filling and power generation was delayed by three years.

Regional studies of landslides, seismic hazard assessment and interactive groundwater modelling were key inputs but ultimately the success of the project was due to teamwork and commitment. The geologists eventually logged 42 km of cored holes, 100 km of drain holes and 16 km of tunnels. Plus mapping the foundations for buttresses at 4 landslides and for a raincoat over another.

This is the summary story of what we did and how we did it. With a bit about why…. The focus is on the role of the engineering geologists – because without us the project would not have been completed in the timeframe achieved.

Background References

Brown, R.; Gillon, M; Deere, D. (1993). Landslide stabilisation at the Clyde Power Project, New Zealand. Geotechnical Practice in Dam Rehabilitation. Sponsored by Geotechnical Engineering Division, *ASCE*. April 25-28, 1993, Raleigh, North Carolina

Gillon, M.D.; Hancox, G.T. (1992). Cromwell Gorge landslides: a general overview. *Proceedings 6th International Symposium on Landslides*, Christchurch. Volume 1, p83-103

Macfarlane, D.F. (2009). Observations and predictions of behaviour of large, slow-moving landslides in schist, Clyde Dam reservoir, New Zealand. *Engineering Geology 109*, p5-15

Macfarlane, D.; Silvester, P. (2019). Performance and management of the Cromwell Gorge landslides, Clyde Dam reservoir. *NZSOLD/ANCOLD Conference*, Auckland, October 2019.

https://doi.org/10.56295/1ACEG39

UNCOVERING GEOHAZARDS AFFECTING INFRASTRUCTURE IN THE HIMALAYAS

Ranjan Kumar Dahal
Central Department of Geology, Tribhuvan University, Kirtipur, Kathmandu, Nepal

ABSTRACT

The Himalayan region, formed by the ongoing collision of the Indian and Eurasian plates, is among the most geologically active zones in the world. Infrastructure development across this mountainous terrain faces severe threats from geohazards such as landslides, earthquakes, glacial lake outburst floods (GLOFs), and Deep-Seated Gravitational Slope Deformations (DGSDs). These hazards, intensified by climate change and poorly planned construction, have resulted in repeated damage to roads, bridges, hydropower plants, and settlements. Events like the 2021 Melamchi flood and persistent ground deformation at Pakyong Airport in India exemplify the vulnerability of infrastructure to complex geomorphological and hydrometeorological processes. Many urban and rural areas across Nepal, India, and Bhutan are situated on DGSDs terrain without proper hazard assessment. This paper highlights the nature and impact of these geohazards, supported by recent case studies, and stresses the need for precise engineering geological investigations, hazard mapping, and risk-informed planning. Without incorporating geohazard science into infrastructure development, the Himalayan region remains exposed to growing disaster risks, leading to increased economic losses and compromised resilience. Strengthening geotechnical solutions, monitoring systems, and regional cooperation are essential steps toward safer infrastructure in this geologically young mountain environment.

1 INTRODUCTION

The Himalayas, a 2,400 km long mountain chain stretching across eight countries from Afghanistan to Myanmar, are the youngest and most tectonically active mountain range in the world. They were formed by the ongoing collision between the Indian and Eurasian tectonic plates. This active tectonic setting has led to complex geological conditions, marked by frequent earthquakes, floods, landslides, and rapidly eroding landscapes in high-altitude regions. Beyond their geological significance, the Himalayas have a major influence on the socio-economic conditions of South Asia, particularly in Pakistan, northern India, Nepal, and Bhutan (Figure 1). The region is home to millions of people and is the source of major rivers that support agriculture, energy generation, and water supply for nearly half of the global population. The presence of key road networks, hydropower projects, and expanding infrastructure reflects the economic importance of the Himalayas, but also reveals high exposure to geohazards of the region.

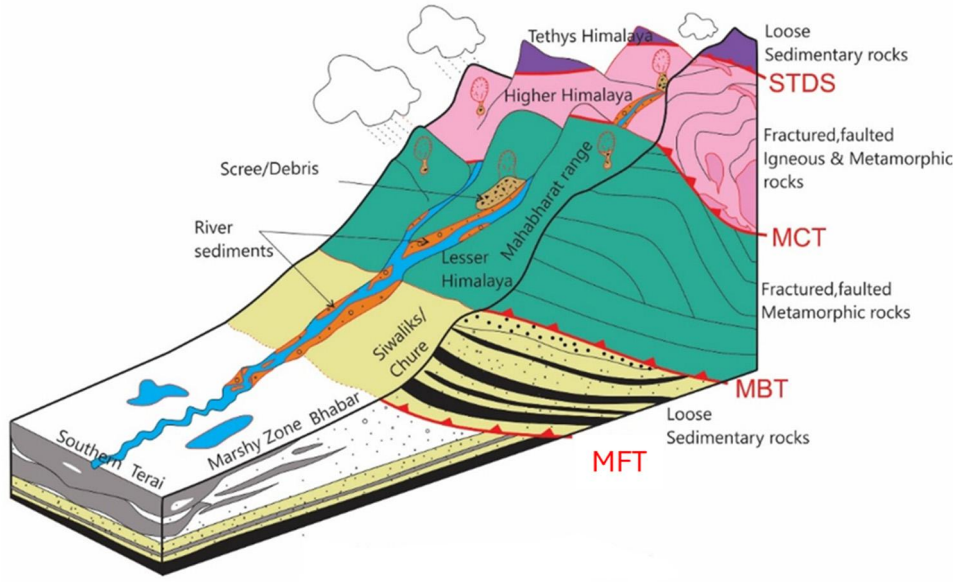


Figure 1: Geological and geomorphological settings of the Himalaya (source: DMG, 2025)

Geohazards in the Himalayas are natural geological and climatic processes that pose serious threats to human lives, livelihoods, and infrastructure. Major hazards include landslides and Deep-Seated Gravitational Slope Deformations (DGSDs), which occur frequently due to steep slopes, earthquakes, intense monsoon rainfall, and ongoing tectonic

activity. Earthquakes, generated by active faults such as the Main Frontal Thrust (MFT) and Main Boundary Thrust (MBT), often cause widespread damage and trigger secondary hazards like landslides. Glacial lake outburst floods (GLOFs) are becoming increasingly common due to the rapid retreat of glaciers and the melting of permafrost, forming unstable glacial lakes dammed by loose moraine. These risks are further intensified by poorly planned development, expanding road construction in both national and rural areas, and the growing impacts of climate change across the Himalayan region.

The objective of this paper is to examine the nature and extent of geohazards in the Himalayan region and to assess their direct and indirect impacts on critical infrastructure such as roads, bridges, hydropower plants, settlements, and related systems. Given the region's complex tectonic setting and growing human activity, infrastructure is often built in areas highly prone to natural hazards. This study focuses on how geohazards, particularly landslides (including DGSDs), earthquakes, and GLOFs, disrupt essential services, result in economic losses, and pose risks to long-term development. The paper also explores practical strategies to reduce these risks, including geotechnical engineering solutions, hazard mapping, early warning systems, and risk-informed planning. By examining both the challenges and the available mitigation options, the paper supports a more informed and cautious approach to infrastructure development in the Himalayan region.

2 Geohazard Context in the Himalayas

The Himalayas present a hazardous environment for infrastructure due to the interplay of tectonic activity, climate extremes, fragile geology, and human interventions. Historical earthquakes such as the 1934 Bihar–Nepal and the 2015 Gorkha Earthquake events have caused widespread damage to roads, bridges, hydropower facilities, and settlements. Intense monsoonal rainfall, snowmelt, and the rapid retreat of glaciers and permafrost melting (Figure 2a) and rainfall in the higher altitue contribute to frequent landslides, debris flow, flash floods, and glacial lake outburst floods (GLOFs), threatening downstream infrastructure.

The 2021 Melamchi flood, which struck north of Kathmandu on June 15, was one of the most devastating disasters in central Nepal in recent years. Triggered by intense monsoon rainfall, the flood and debris flow swept through the Melamchi and Indrawati river corridors, causing widespread destruction. The disaster severely damaged the Melamchi Water Supply Project (MWSP), a flagship national project designed to supply 170 million liters of drinking water per day to Kathmandu Valley. Key infrastructure, including the headworks, access roads, tunnels, and intake structures, were either submerged or washed away. The flood also destroyed over a dozen motorable and pedestrian bridges, and inundated several settlements, including parts of Melamchi Bazaar (Figure 2b). More than 260 households were directly affected, and over 500 families had to be evacuated. Agricultural lands, worth millions of rupees, were buried under debris, and numerous fisheries along the riverbanks were completely destroyed. Estimates suggest that the total economic loss exceeded NPR 30 billion (approximately USD 250 million). Recovery and reconstruction efforts have been slow, hindered by the complexity of terrain and recurring monsoon threats. The Melamchi disaster highlighted critical gaps in engineering geological investigation in before the project construction, river basin management, and the resilience of large infrastructure projects to climate-induced disasters.

Likewise, Deep-Seated Gravitational Slope Deformations (DGSDs) are widespread across the Himalayan region but often remain undetected until triggered by external factors such as intense rainfall or seismic events, resulting in large-scale slope failures. A best example is the Pakyong Airport in Sikkim, India (Figure 2c), where progressive ground deformation attributed to DGSDs has caused persistent instability over the past three years. Despite ongoing monitoring efforts, a comprehensive long-term mitigation strategy with specific engineering geological understanding has not yet been implemented. The airport continues to experience creeping slope movements, widespread cracking, and significant structural damage, particularly in the mechanically stabilized earth (MSE) walls and retaining structures. This case exemplifies the critical oversight of engineering geomorphology and engineering geological site characterization in infrastructure development across the Himalayan terrain.

Similarly, several towns in Nepal, including Tansen, Tamghas, Mangalsen, Baitadi, Ilam, Okhaldhunga, and Gorkha, and in India, such as Darjeeling, Kurseong, Nainital, Joshimath and Pithoragarh, are located on DGSD-prone slopes. The Bhawanijhora Landslide in Bhutan is a prominent example of a transboundary landslide disaster, closely associated with DGSD. The debris flow originates in Bhutan and deposits downstream in India, highlighting the cross-border implications of geomorphological hazards in the Himalayan region (Figure 2d). These areas frequently exhibit symptoms of ground instability, including cracks in buildings, tilting of structures, and progressive ground displacement, especially during the monsoon season and following seismic activity. However, systematic engineering geological investigations and site-specific stabilization measures remain largely inadequate. The lack of understanding and mitigation of DGSD processes continues to pose a serious threat to the sustainability of urban infrastructure and settlements in these vulnerable Himalayan mountainous regions.

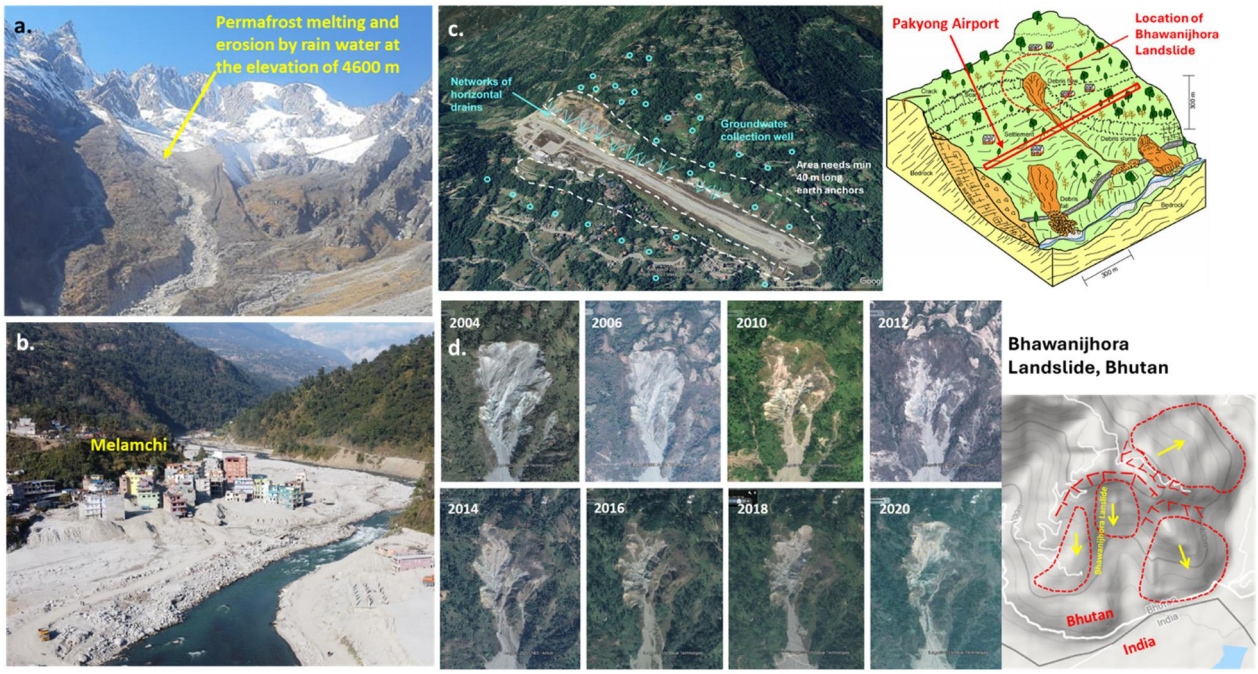


Figure 2: Illustrations of geohazard issues in the Himalaya: a) Permafrost melting and headward erosion – Observed in the Melamchi River basin at an elevation of approximately 4,600 meters, where permafrost degradation is accelerating headward erosion processes. b) Burial of Melamchi Town – Resulting from the catastrophic July 15, 2021 flash flood, triggered by a combination of glacial lake outburst flood (GLOF) and landslide dam outburst flood (LDOF), which buried large sections of the town. c) Pakyong Airport instability – Constructed on a DGSD-affected slope, the site has experienced ongoing ground deformation and structural failures due to creeping slope movements. Suitable mitigation measures needed for the site is also illustrated in the image. d) Bhawanijhora Landslide – A typical transboundary landslide occurring within DGSD terrain, demonstrating complex interactions of gravitational deformation. The geomorphological settings of both the Pakyong Airport and Bhawanijhora landslide sites are consistent with the DGSD model characteristic of the Himalayan region.

Human activities such as slope-cutting for road construction, and poor drainage design further aggravate geohazards in the rural areas. Many major infrastructure projects are implemented without adequate engineering geological studies or long-term hazard planning. The under construction Kathmandu–Terai Madhesh Fast Track has encountered repeated slope failures, tunnel deformation, and drainage issues, partly due to DGSDs. Key road networks like the Prithvi Highway, B.P. Highway, and Mid-Hill Highway, along with several hydropower projects, suffer frequent disruptions from monsoon-triggered landslides and erosion. In many cases, reactive maintenance replaces preventive measures without proper understanding of engineering geological settings of the site, resulting in escalating costs and further vulnerability.

3 Major Geohazards Affecting Infrastructure

3.1. LANDSLIDES

In Nepal, landslides are among the most frequent and destructive natural disasters, occurring annually and causing substantial social and economic losses, particularly in mountainous regions (Dahal and Hasegawa, 2008). Fatalities due to landslides remain consistently high. Figure 4 illustrates the multi-hazard landscape of Nepal, where landslides are identified as a recurring threat. An analysis of data from the past 50 years reveals that landslides have caused an average of 110 deaths per year, with annual fatalities reaching as high as 1,350 in extreme cases.

For instance, during the early monsoon period in 2021 (June 10 to June 16), landslides and floods claimed at least 20 lives. Numerous villages and settlements along river basins were severely affected by landslide dam outburst floods (LDOFs), highlighting the urgent need for proactive measures.

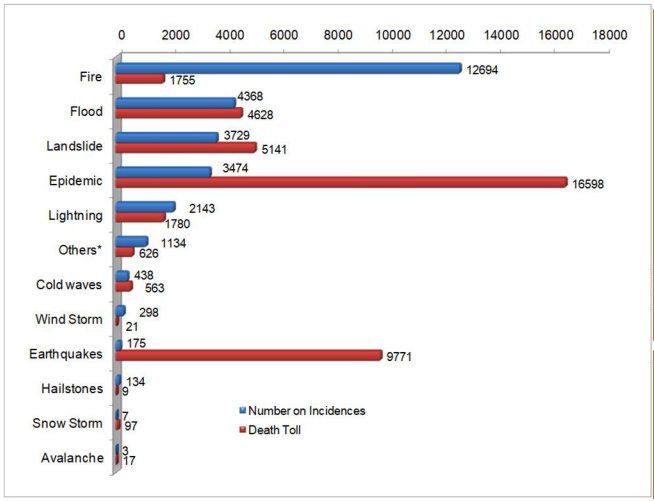
In late September 2024, central Nepal experienced one of its most devastating natural disasters in recent history, as unprecedented monsoon rainfall triggered widespread flooding and landslides across the region.

Between September 26 and 30, the Kathmandu Valley received over 700 mm of rain, nearly half its annual average—over just three days. This deluge caused the Bagmati River to overflow, inundating large parts of Kathmandu and Patan. The resulting floods and landslides led to at least 246 confirmed deaths nationwide, with over 4,000 people rescued and more than 1,200 homes destroyed or severely damaged. Infrastructure damage was extensive: 25 bridges, 37 highways, and 11 hydropower stations were impacted, while seven major highways leading out of Kathmandu were blocked by debris. The disaster also disrupted power, water, and telecommunications services across multiple districts. In the Kathmandu Valley alone, at least 73 fatalities were reported. Rescue operations were hampered by blocked roads and ongoing landslides, with entire vehicles, including buses, buried under debris.



Figure 3: Damage and loss scenario during extreme rainfall of September 26 and 30, 2024. Red box is official data of National Disaster Risk Reduction and Management (NDRRMA), Government of Nepal.

To reduce the impacts of future disasters, it is crucial to identify and monitor areas that are highly susceptible to landslides in advance. Landslide hazard assessment is fundamental for understanding the geomorphological and geotechnical characteristics of vulnerable terrain, especially under the stress of extreme climatic events. These assessments support systematic data collection, risk evaluation, and the development of site-specific mitigation strategies. In particular, landslide hazard maps provide essential insights into the spatial distribution of susceptibility across different regions. They serve as critical tools for local communities and government agencies, enabling evidence-based planning and the implementation of targeted, action-oriented disaster risk reduction interventions.



Landslide Index No: ..... District ID +Municipal ID + Landslide ID (All are 2 digit code)

Major Description

Location (District/Municipality/Ward): .....

Coordinate of landslide: .....

Top, ... Bottom, ... Right, ... Left

Approximate Area (sq. m.): .....

Aspect: .....

Elevation: Max. .....m. Min. .....in m.

Date of incident:

History of previous failures:

Type of Landslides classification by Varnes (1978)

Type of movement			Type of material: Engineering soils – Predominantly fine	Engineering soils – Predominantly coarse	Bedrock
Falls			Earth fall	Debris fall	Rock fall
Topples			Earth topple	Debris topple	Rock topple
Slides	Rotational	Few Units	Earth slump	Debris slump	Rock slump
	Translational	Few units	Earth block slide	Debris block slide	Rock block slide
		Many units	Earth slide	Debris slide	Rock slide
Lateral spreads			Earth spread	Debris spread	Rock spread
Flows			Earth flow	Debris flow	Rock flow
			(Soil creep)		(Deep creep)
Complex			Combination of two or more principal types of movement		

Causes of Sliding:

a) Toe cutting, Heavy rain, Steep slope

b) Lack of water management, Heavy rain, Steep slope

c) Cracked rocks, Heavy rain, Steep slope, Earthquake

d) Others .....

Geology:	Probability of Occurrence/Reoccurrence			Quantification of damage to the element		
	High	Medium	Low	High	Medium	Low

Type of Landslide in term of Treatability (Tick in Appropriate type):

Easily Treatable | Moderately Treatable | Difficultly Treatable

Element at Risk

Settlement / National Heritage / Lives/Roads or Other ifrastructure

Village Name: ..... National Heritage Name: ..... Road or Infrastructe at risk .....

No of ..... No of people displaced ..... No. of people Killed .....

Road Type (Tick in Appropriate type)

Dirt | Grave | Asphalt road

Length of Road affected in meters .....

Irrigation Type (Tick in Appropriate type) — Command area in ha.

Community | Multi community | Multi VDC — Affected Length in meters

Drinking water supply Type (Tick in Appropriate type) — No. of User Households

Community | Multi community | Multi VDC — Length in meters

Hydropower (Tick in Appropriate type)

Intake: | Dam: | Tunnel | Statio | Stilling basin

Land use

Agriculture | National Forests | Community Forests | Pasture lands | / Shrub /

Landslides Blocking Stream / River (Tick Appropriate type)

None (no signs of blockage of rivers)	Partially (partially blocked the river)	Complete (completely blocked the river, and still blocking)	Complete and broken through (blocked the river but later broken through)

Figure 4: Multi-hazard scenario of Nepal by its number of incidences and death toll, 1971-2018 (Source: MoHA, 2018) and table on right is a recommended sheet for landslide data collection in after the disaster.

To reduce the impacts of future disasters, it is crucial to identify and monitor areas that are highly susceptible to landslides in advance. Landslide hazard assessment is fundamental for understanding the geomorphological and engineering geological characteristics of vulnerable terrain, especially under the stress of extreme climatic events. These assessments support systematic data collection (see Figure 4), risk evaluation, and the development of site-specific mitigation strategies. In particular, the field data always helps to produce accurate landslide hazard maps, which provide essential insights into the spatial distribution of susceptibility across the affected regions. Government should understand that hazard maps serve as critical tools for local communities and government agencies, enabling evidence-based planning and the implementation of targeted, action-oriented disaster risk reduction interventions.

3.2. EARTHQUAKES

Nepal lies in one of the most seismically active regions in the world due to the ongoing subduction of the Indian Plate beneath the Eurasian Plate along the Himalayan arc. The convergence rate of approximately 45 mm/year has led to the formation of a series of major thrust faults—namely, the Main Central Thrust (MCT), Main Boundary Thrust (MBT), and the highly seismogenic Main Frontal Thrust (MFT). These active tectonic structures continuously accumulate strain, which is periodically released through large-magnitude earthquakes (Lavé and Avouac, 2000; Bilham, 2004).

Nepal has experienced several significant seismic events over the past century, including the devastating 1934 Mw 8.0 Bihar-Nepal Earthquake and the 2015 Gorkha Earthquake of Mw 7.8. These events demonstrate the country's high vulnerability to seismic hazards, particularly due to the concentration of population and infrastructure along the thrust zones.

In addition to ground shaking and surface rupture, earthquake-induced landslides represent a major secondary hazard. Though not comprehensively documented, historical earthquakes such as the 1934 Bihar-Nepal, 1950 Assam, and 2005 Kashmir earthquakes triggered numerous landslides across the Himalaya. The 2015 Gorkha Earthquake alone resulted in thousands of co-seismic landslides that caused extensive damage to settlements, transportation networks, and natural river systems (Roback et al., 2018; Dahal, 2015).

Despite the well-established relationship between seismicity and Himalayan tectonics, the systematic study and documentation of earthquake-induced landslides in Nepal remain limited. These landslides often cause more widespread and prolonged damage than the seismic shaking itself, underscoring the need for integrated seismic and landslide risk assessment and preparedness.

3.3. GLACIAL LAKE OUTBURST FLOODS AND FLASH FLOODS

Glacial Lake Outburst Floods (GLOFs) represent one of the most serious climate-induced hazards in Nepal. As glaciers are retreating rapidly, leading to the formation and expansion of glacial lakes, many of which are dammed by unstable terminal moraines. Dams of glacial lake usually fail due to icefalls, rockfall into the lake, landslides into the lake, heavy rainfall in high altitude, or internal pressure build up they release massive volumes of water and debris downstream in a sudden and highly destructive manner. Nepal currently has over a thousand identified glacial lakes, with more than two dozen considered potentially dangerous. Historic events like the 1985 Dig Tsho GLOF or Thame GLOF of 2024 in eastern Nepal highlight the scale of destruction such events can cause, including loss of infrastructure, disruption of livelihoods, and degradation of river ecosystems. GLOFs pose a direct threat to mountain communities, hydroelectric plants, roads, bridges, and agricultural lands situated along river valleys. Despite their high risk, monitoring and mitigation systems for GLOFs in Nepal remain limited.

Riverbank failures due to flash floods are a widespread and recurring hazard in Nepal, especially during the monsoon season when rivers experience high discharge and increased erosive power. These failures are driven by river undercutting, saturation of banks, and the collapse of loosely consolidated alluvial materials. In mountainous regions, steep gradients and unregulated river systems exacerbate the risk of lateral erosion, leading to the loss of settlements, roads, and agricultural land. In the Terai and Middle hills, human activities such as gravel mining and construction too close to riverbanks further destabilize these fragile areas. Addressing riverbank failures in Nepal requires a combination of engineering measures (such as revetments and check dams), ecological approaches (such as riparian vegetation and bioengineering), and regulatory planning tools like river corridor zoning and setback enforcement. Public awareness and integrated watershed management are also essential to ensure long-term stability and safety of river-adjacent communities.

On 15 June 2021, Melamchi Municipality in Sindhupalchok District experienced a devastating flood, followed by a second major event on 31 July 2021. These floods caused extensive damage to 255 households, destroyed two concrete and two suspension bridges, and inundated thousands of hectares of agricultural land, isolating the municipality and its surrounding areas for several weeks. Although the scale of destruction was immense, early warning from upstream communities played a critical role in preventing human casualties. Scientific investigations suggest that the main trigger

of the flood was the outburst of Pemdan Glacial Lake (Figure 5), which led to the breaching of an old natural dam near Bhemathan. This initiated rapid riverbed erosion, sediment mobilization, and a cascading series of landslides along the Melamchi River (Figure 5). The downstream impacts extended up to the Sipaghat area of the Indrawati River, with severe debris deposition particularly around low-clearance bridges. Based on flood hazard modelling, settlements from Talamarang to Sipaghat are vulnerable to high-magnitude floods with 100-year return periods and should be avoided for permanent habitation. The 2021 event revealed the inadequacy of the earlier 20-meter river setback, prompting the development of new setback standards, risk-sensitive land use plans, and structural as well as bioengineering mitigation measures. The total estimated cost for implementing a comprehensive rehabilitation and disaster mitigation plan in the Melamchi area is over NPR 3.38 billion.



Figure 5, Pemdan Glacial Lake in 4750 m and status of erosion in Pemdan creek and burst of the lake.

4 Monitoring and Early Warning Systems

Suitable monitoring and early warning systems (EWS) are major components of disaster risk reduction in the geohazard-prone regions of the Himalayas. Given the frequent occurrence of landslides, floods, earthquakes, and glacial lake outburst floods (GLOFs), timely detection and communication of potential threats can save lives, minimize economic losses, and protect ongoing development efforts. Monitoring involves the continuous observation of environmental and geological conditions using tools such as automated rainfall gauges, ground motion sensors, GPS, satellite imagery, and remote sensing technologies. These tools help detect changes in slope stability, precipitation, snow cover, seismic activity, and glacial lake dynamics, critical indicators of impending geo-disasters. Early warning systems translate this data into actionable information, which must be effectively communicated to at-risk communities before a disaster hits.

In Nepal, early warning systems have been developed at both local and regional scales. Local systems focus on specific slopes or communities and rely on real-time monitoring and alerts when conditions change. Regional systems, which cover broader geographic areas, utilize rainfall forecasts and other environmental data to provide advance warnings to a larger population. Both systems face specific challenges: local systems require accurate, low-cost, and sustainable monitoring technologies, while regional systems demand improved forecasting capabilities, access to free and high-resolution data, and the development of geographically specific and impact-based forecasts that consider vulnerability and exposure. Community-based early warning systems (CBEWS), piloted in river basins like the Koshi and Karnali, offer valuable models for localized preparedness but face limitations in scale, infrastructure, and public response.

To build a more robust EWS network in Nepal, several key actions can be recommended: improving the use of existing knowledge and data products, localizing hazard and susceptibility assessments, developing impact-based forecasting, enhancing forecast accuracy, strengthening governance and coordination, increasing data collection, and promoting slope-scale, community-managed warning systems. Various projects have already produced national and local hazard, vulnerability, and susceptibility maps, but their uptake by national, municipal, and local stakeholders remains inconsistent. Assessing awareness and use of these products, identifying gaps, and addressing barriers to access and implementation will be crucial.

5 Risk Reduction Strategies

Action oriented disaster risk reduction requires a comprehensive approach that integrates engineering solutions, strong policy frameworks, community involvement, and international collaboration. Engineering interventions such as bioengineering, slope stabilization, and seismic-resistant design help for mitigating physical risks, particularly in hazard-prone regions of the Himalaya. These measures enhance the resilience of infrastructure and reduce the likelihood of catastrophic failure during extreme events like landslides, earthquakes, and floods. Equally important are refined and evidence-based policy frameworks and the enforcement of building codes, which ensure that development is aligned with safety standards and hazard assessments. Institutionalizing risk-sensitive land use planning and regulating construction in vulnerable areas are essential components of long-term risk management. This was well practiced in Melamchi and local government is now implementing such land use planning. Similarly, international cooperation and funding support are vital for capacity building, technology transfer, and the implementation of large-scale resilience programs, especially in the Himalaya. These collaborative efforts help bridge resource gaps and promote shared learning, ultimately contributing to more sustainable and inclusive disaster risk reduction outcomes.

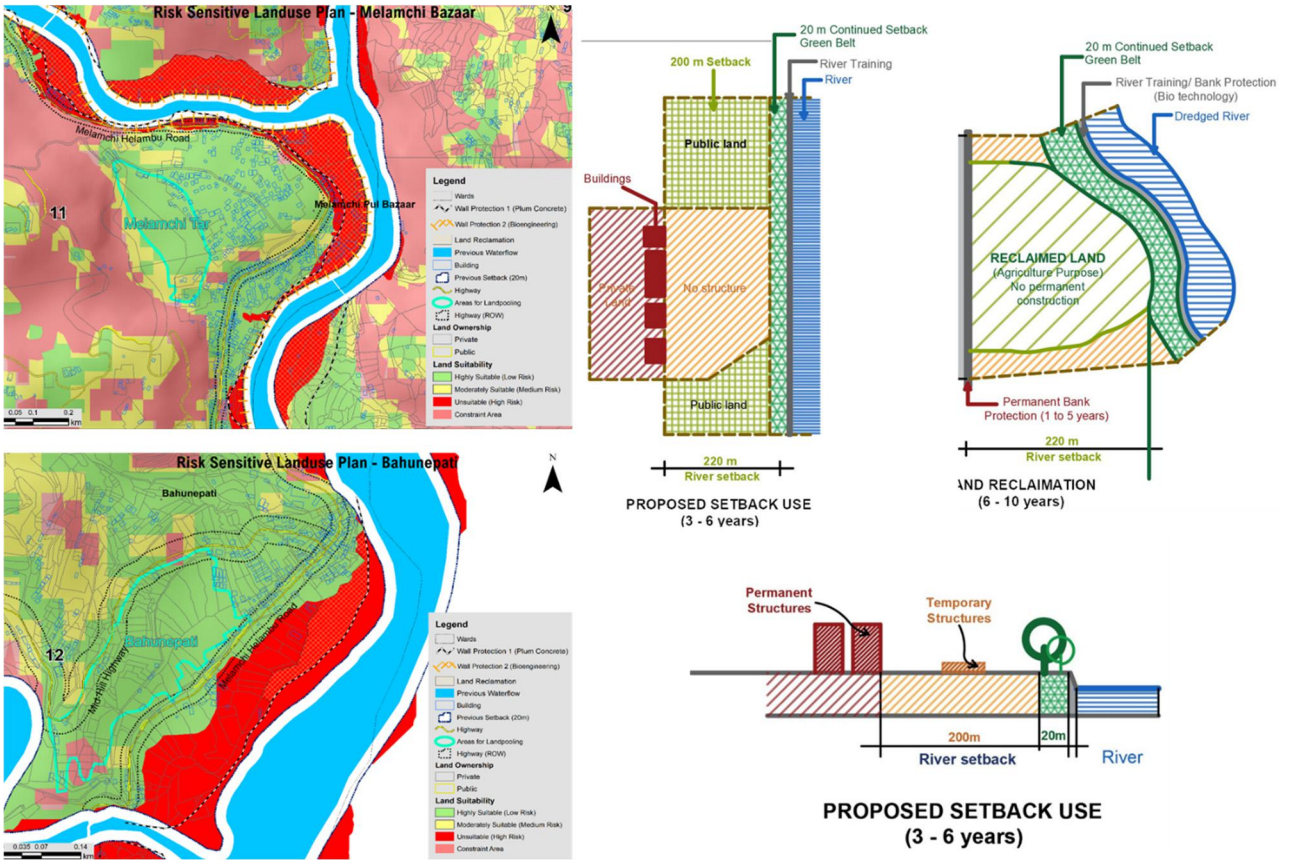


Figure 6, Risk-Sensitive Land Use Planning and Setback Implementation following the Melamchi Flood Event in the Melamchi River Valley, Nepal

6 Conclusion

The Himalayas represent not only a remarkable geological formation but also one of the most hazardous regions on Earth. As this study has shown, the combination of active tectonics, intense monsoon systems, steep topography, and increasing human intervention for development activities has created a complex risk environment, one where infrastructure and communities are persistently vulnerable to geohazards. From recurrent landslides and catastrophic floods to seismic

events and glacial lake outburst floods, the impacts on roads, hydropower, settlements, and lifeline systems are widespread and intensifying.

The Melamchi disaster and the instability at Pakyong Airport of Sikkim, India exemplify the exclusive consequences of overlooking engineering geological assessments and the pervasive threat of Deep-Seated Gravitational Slope Deformations. Meanwhile, repeated earthquake and landslide events underscore the urgent need for science-based approaches to development planning and disaster mitigation.

In fact, a paradigm shift is needed, from reactive disaster response to proactive, risk-informed infrastructure development. This includes thorough engineering geological site investigations, detailed hazard mapping, monitoring systems, resilient design practices, and the integration of engineering geology into every phase of infrastructure planning and policy. With climate change adding further uncertainty, there is little room for complacency. The safety, sustainability, and resilience of Himalayan infrastructure and the wellbeing of millions who depend on it hinge on scientific ability to understand, anticipate, and adapt to the evolving geohazard landscape of the Himalaya.

7 References

DMG, 2025, General Geology, available in https://dmgnepal.gov.np/en/pages/general-geology-4128, accessed on 2025-05-11.

Dahal R.K. (2015) Engineering Geological Issues after Gorkha Earthquake 2015 in Nepal - a preliminary understanding, Proceedings of 10th Asian Regional Conference of IAEG, Kyoto, Japan, September 26-27, 2015. 7p.

Roback K, , Clark M. K., West A. J., Zekkos D., Li G, Gallen S. F., Chamlagain D., Godt J. W. (2018) The size, distribution, and mobility of landslides caused by the 2015 Mw7.8 Gorkha earthquake, Nepal, Geomorphology, 301,121-138.

Avouac J.P., Meng L., Wei S., Wang, T. & Ampuero J.P., 2015. Lower edge of main Himalayan Thrust unzipped by the 2015 Gorkha earthquake. Nature Geoscience. vol. 8. pp. 708–711.

Bilham R., 2004. Earthquakes in India and the Himalaya: tectonics, geodesy, and history. Ann. Geophys. vol. 47. 839–858.

https://doi.org/10.56295/1ACEG40

ENGINEERING GEOLOGY IN AUSTRALIA: A PROFESSION AT THE FAULT LINE OF POLICY, PRACTICE, AND PERFORMANCE

Christian Dodge
Engineering Geologist & Geotechnical Engineer

ABSTRACT

Australia's built and natural environment sectors are facing escalating costs, delays, and safety risks due to systemic shortcomings in ground risk management. This paper explores the under-recognition of engineering geology as a profession and its consequences on project performance, immigration policy, and national standards. Through comparative analysis with other high-income English-speaking nations, the study highlights inconsistencies in role definitions, education pathways, and professional accreditation. It proposes a framework for reform, including the establishment of a dedicated registration pathway for engineering geologists, improved integration of geoscience in engineering education, and the adoption of a hazard-first approach to ground risk management. The findings underscore the urgent need for structural change to mitigate socio-economic impacts and enhance national resilience.

1 INTRODUCTION

Despite a record-breaking infrastructure cycle funded by mineral exports, Australia's approach to ground risk management remains questionable. Its failure to formally recognise key ground engineering vocations—particularly Engineering Geology—is evident in both economic indicators and professional frameworks.

Ground risk management relies on a multidisciplinary sector, where competence stems from education and ongoing professional development. Yet inconsistent recognition, especially in registration requirements, undermines this workforce. As Packer et al. (2024) note, the absence of legislative accreditation for Engineering Geologists in Australia triggers a cascade of impacts—limiting practice, distorting migration pathways, and weakening sector resilience. This sequence is shown in **Figure 1**.



Figure 1: Detrimental sequence caused by the lack of legislative professional accreditation

To investigate this the Australian ground engineering sector must be examined by comparison to other English-speaking high-income economies with respect to:

- The roles and titles within the sector
- Education and skills in ground engineering
- Occupation recognition, registration and immigration
- Engineering geological hazards and the socio-economic effects on Australian
- Standards in ground risk management

Where appropriate recommendations will be made for how Australia can make progress in its ground engineering sector by taking best practice and pragmatism from other similar nations.

2 ENGINEERING GEOLOGY AND THE GROUND ENGINEER SECTOR

The term ground engineering is a recognition of the geoscience connection to civil engineering. How those enter into and practice within the sector vary internationally but the drivers from education, job title (given by employers), occupational skills and competence (directed governing institution and/or skill assessment bodies) should be to be consistent, but it seems this is not the case throughout the industry.

2.1 ROLES AND TITLES

Fookes (1997) defined three ground engineering roles (**Figure 2**) noting that while Geological Engineer is uncommon in British practice, it is recognized in North America. Later Sections 2.2 and 2.3 address how evolving sector demands and education governance blur these distinctions.

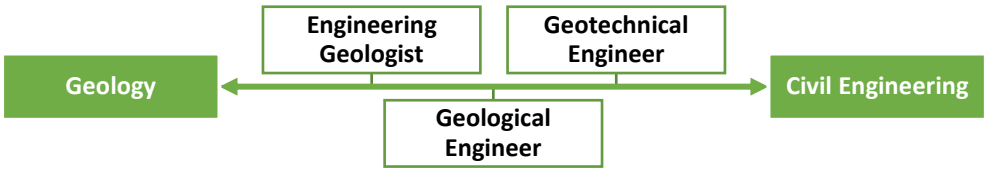


Figure 2: Roles in Ground Engineering based on technical training according to Fookes (1997)

There are three core principles to the ground engineering sector in which all three occupations are involved in. These are

- Site and earth materials characterisation
- Hazard identification and risk management, and
- Engineering design

Based on the definition of each occupation in nine comparable English-speaking economies (UK, Ireland, United States, Canada, Australia, New Zealand, South Africa, Hong Kong and Singapore) each has been plotted on the Ternary diagram in **Figure 3** to try to appreciate the amount of involvement the three occupation types have in each of these principles and how these might vary Across the 9 nations. Countries where the various role titles are recognised and used as job titles are detailed in **Table 1** which is appended to this paper. It should be noted that Geological Engineer is only recognised in Canada and the US, there were no definitions for any of the three occupations in any Singapore based reference.

Nevertheless, the **Figure 3**shows a broad spectrum of variance amongst the discipline for these occupations. Traditionally it might have been expected that engineering design would feature only in the engineering occupation definitions, but this was not case with design activity in relation to engineering featuring in the Engineering Geologist definitions for Australia, New Zealand, US, Canada and South Africa.

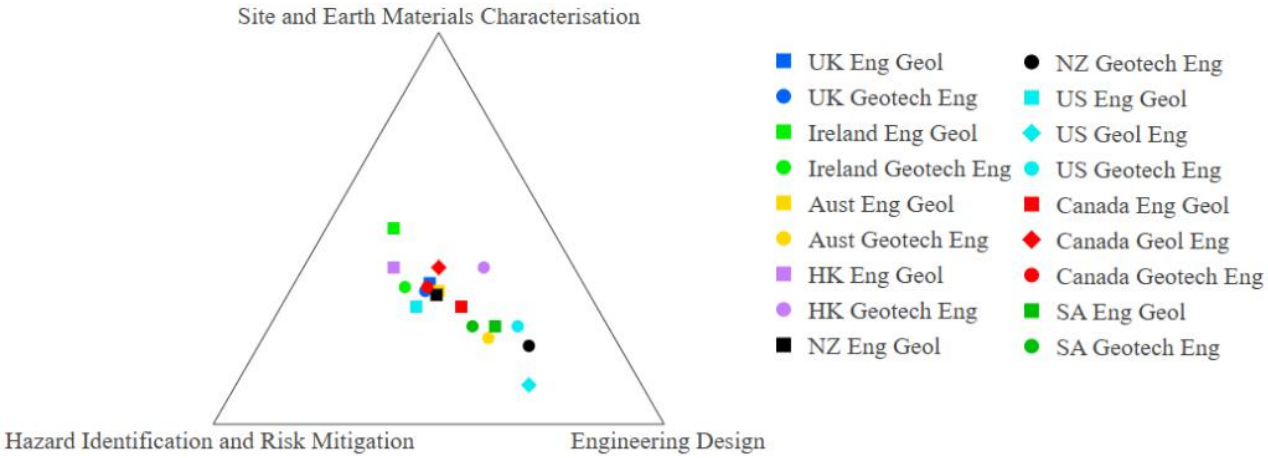


Figure 3: Nations where the various roles and titles are recognised and defined

It is noted that while the International Association of Engineering Geology and the Environment (IAEG) is recognised by these countries but the context here is regarding application of role titles and descriptions either by their governments, industry bodies or the local employment sector. Another interesting aspect is how design is mentioned in the engineering geologist definitions for Australia, New Zealand, US, Canada and South Africa. Furthermore, the UK government definition for Geotechnical Engineer covers engineering geology.

Fookes notes in his paper that the term Geotechnical Engineer could reflect any aspect within ground engineering, and this is seen in job title data not only in the UK but also in North America i.e. the job title is Geotechnical Engineer, yet the description is either one of engineering geology or site investigation.

Professionals with geological training often work in ground engineering under varied titles, including ‘engineer’, depending on the country. Many enter with geology degrees and gain engineering competence through formal study or practical experience, recognised by local employment markets.

While job titles may appear similar, their definitions, and who defines them, vary significantly. Ideally, employers would shape role expectations via industry bodies (e.g. AIG, SEG), which would inform government policy on education and immigration. This could support consistent national frameworks for assessing qualifications and experience.

However, across English-speaking high-income nations, title definitions remain fragmented. Australia reflects a broader inconsistency, not an exception.

2.2 INTERNATIONAL EDUCATION

Presumably based on this experience until the late 1990s, Fookes also detailed the areas of training included between the civil engineering and geological sciences disciplines.

- Geology areas of expertise based on technical training – Physical Geology, Petrology, Structural Geology, Palaeontology, Stratigraphy, Geomorphology, Field Mapping Techniques
- Civil Engineering areas of expertise based on technical training – Physics, Statics, Dynamics, Material Strength, Highways, Hydraulics, Mechanics, Thermodynamics, Structures, Public Health

A key divergence is governance: engineering programs follow international accords (Washington/Sydney/Dublin), supposedly creating consistent outcomes with varying yet minimal earth science content (<3 modules in most civil degrees; **Figure 4**)

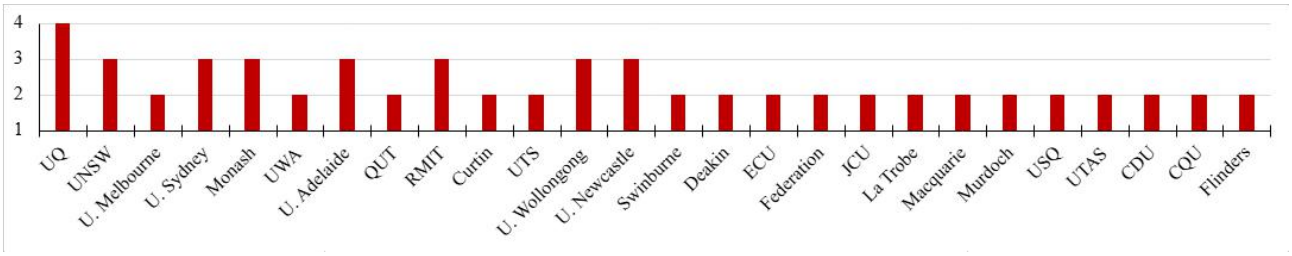
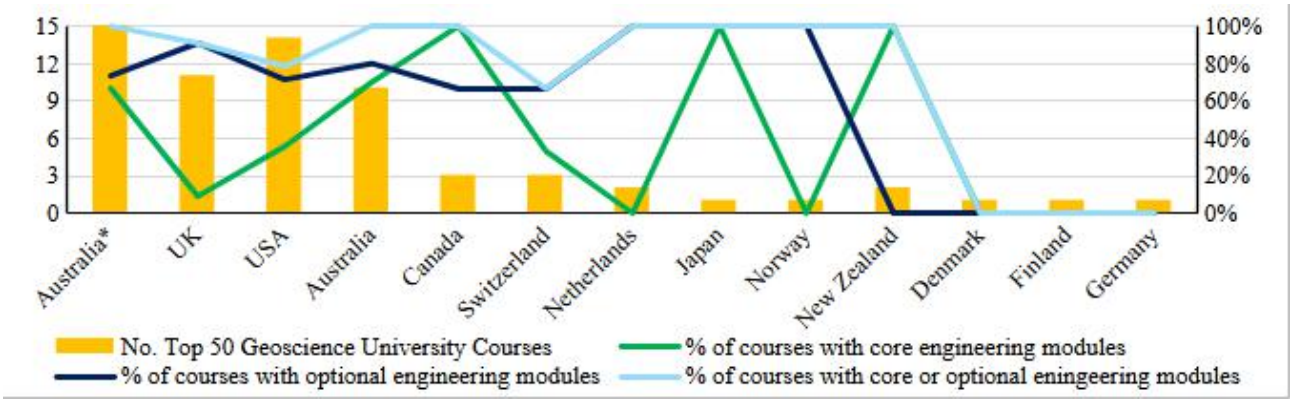


Figure 4: Number of applied earth science modules on 4-year Civil Engineering Degree programs



*denotes all Australian courses (even those outside the global top 50)

Figure 5: Comparison of quantity of engineering content on the global top 50 Geoscience courses and those of Australia

By contrast the education of Geology varies even more significantly and examples can be seen in the variation in the global top 50 Geoscience courses (TopUniversities.com, 2025). **Figure 5** shows the number of Geology or Earth Science Bachelor courses in the top 50 global rankings by country compared with all the Australian courses. Also shown in the figure is the percentage of those courses which have engineering content (such as Engineering Geology, Geological Engineering, Geotechnics, Geotechnical Engineering, Rock/Soil Mechanics) by country either optionally or as requisite. Limitations should be noted with this data for example what is considered core and optional will vary with major/minor degrees. However, what should be observed from this is what potential learning outcomes can be taken from someone with a geoscience degree in terms of engineering content by contrast with those on Washington accord programmes.

Australian geoscience programs rank well globally for applied and engineering content, though Canada and New Zealand appear stronger in depth. A broader trend shows a tiered university system: elite institutions (e.g. Russell Group, Ivy League) emphasise academic geology, while others tailor curricula to local industry needs, often with applied modules concentrated in final-year study.

With no single unified agreement in Geoscience like the Washington Accord for Engineering, the International Union of Geological Sciences has established 'The Commission on Geoscience Education since 2004'. The commission's objectives include:

- Establishing a global geoscience education network
- Developing guidelines for good practice in geoscience education
- Coordinating geoscience education activities at the international level

Despite positive developments, current geoscience programs remain distant from Washington Accord alignment or show limited intent to develop an equivalent accord for applied geoscience. Many courses globally include engineering content, but flexible module structures and mixed major/minor pathways complicate comparisons with the International Engineering Alliance's three-tier system.

In Australia, recognition in engineering hinges on educational background and IEA alignment. Yet meaningful assessment requires a detailed review of transcripts and course specifications by a suitably qualified evaluator, an uncommon resource, with no transparent evaluation framework currently in place.

Compounding this, some geoscience degrees offer more ground engineering content than Washington Accord programs. This exposes serious flaws in how competence for registration is assessed, especially when typical geoscience curricula and learning outcomes are examined closely.

2.2.1 Detailed Learned Outcomes

Paul (2024) discusses the state of geological education in Australia. Within the paper is the indicative pathway to Geomechanics. However, this is misleading on at least three specific issues as case examples

Dip, strike, and dip direction are core mapping techniques taught universally in geology degrees, typically followed by stereographic projection methods. These skills are introduced in mid-degree years and underpin rock mechanics modules in applied final-year curricula. Mathematical approaches to planar and wedge failure are generally covered in engineering geology units, forming a bridge between geoscience and engineering practice, an intersection explored later in this paper.

Though civil engineering physics isn't the focus here, it's incorrect to assume physics is peripheral in geoscience education. Biology is limited to palaeontology electives, while chemistry features in mineralogy and petrology. Physics, however, is central to informing topics like the Hjulström curve, seismology, geophysics, and rock/soil mechanics.

This distinction is critical when evaluating the scientific competence of geoscience-trained professionals. Assumptions of deficiency in core science knowledge during skills assessments or registration processes are not only unfounded but risk undervaluing a curriculum deeply rooted in applied physical science.

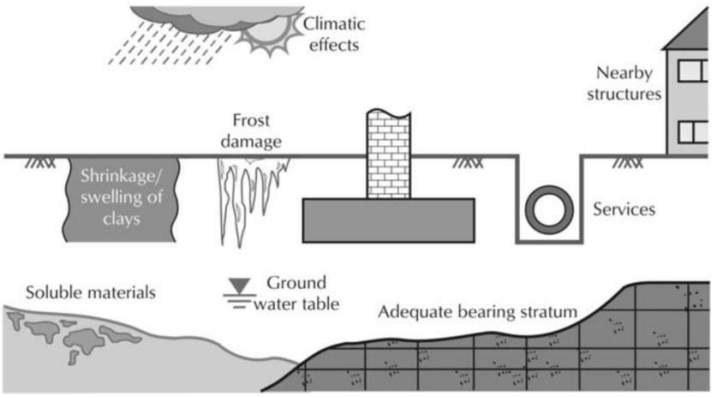


Figure 6: Geohazards defining limit states

Engineering geology extends beyond model development; it centres on hazard identification and risk assessment and mitigation. Limit states in geotechnical design are derived from geohazards, as illustrated in **Figure 6** taken from Bond & Harris (2006) and discussed further in Section 4.

2.3 GROUND ENGINEERING SPECTRUM AND SKILLS

Fookes originally drew clear lines between Engineering Geology (defining ground conditions) and Civil Engineering (calculating ground stability). However, these boundaries have since blurred and relying solely on educational background to assess competence risks overlooking skilled professionals. Traditionally, geologists led hazard identification and

ground investigation design, producing geological models, while civil engineers handled parametrisation and geotechnical modelling, but this division is no longer universal.

Paul's pathways diagram provides a critical spectrum based on the tree of education provision as shown in **Figure 7** and it is important that this is compared with the industry skills spectrum for ground engineering shown in **Figure 8**.

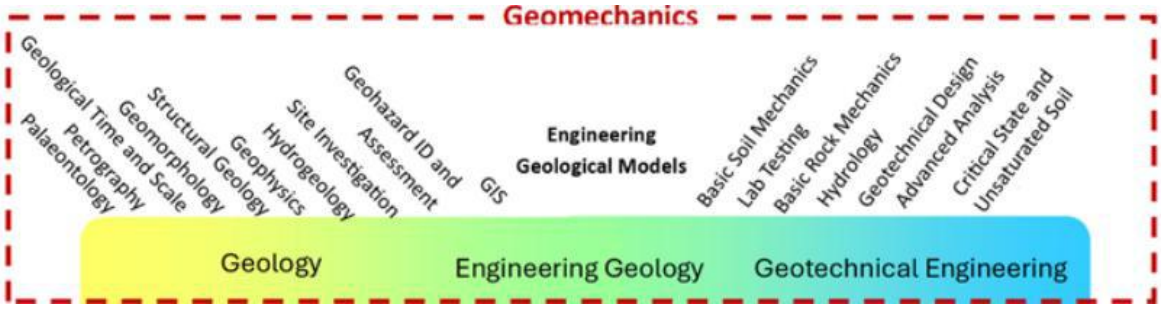


Figure 7: Geomechanics spectrum of education content

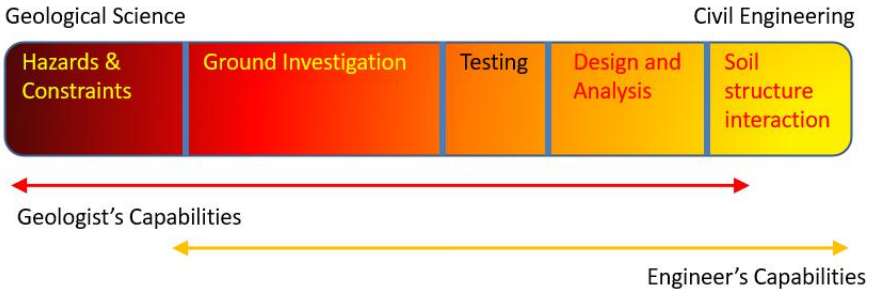


Figure 8: Ground Engineering Skills Spectrum

These two diagrams highlight a key discrepancy between the learning outcomes from the ground engineering education sector in Australia and the capabilities of ground engineering staff across the sector internationally.

Figure 8 is based on the skills capabilities observed in the UK by Geology graduates with applied final-year modules and accredited ground engineering training, Geology graduates without applied modules but a ground engineering MSc and accredited training, Civil Engineering graduates with a ground engineering related MSc.

UK geology graduates are well-equipped to identify hazards and conduct risk assessments, applying field and lab skills to produce engineering geological models from concept to construction. With project experience and structured training, they progress into limit state definition and stability analysis, occasionally extending into advanced numerical methods like FEA, though typically not into constitutive modelling.

Conversely, civil engineering graduates with ground engineering Masters may be proficient in constitutive models but often lack the earth science foundation for hazard identification. This highlights a flaw in registration frameworks that assess competence solely through engineering education, overlooking geoscience-trained professionals with relevant expertise.

2.4 REGISTRATION, OCCUPATIONS AND IMMIGRATION

Packer et al. (2024) highlighted the absence of formal accreditation for engineering geologists in Australia and the registration challenges they face. Due to international variability in titles (Section 2.1), overseas professionals applying under ANZSCO 233212 (Geotechnical Engineer) must obtain state registration for permanent residency, mandatory in all states by 2027.

For those without Washington, Sydney, or Dublin Accord qualifications, the immigration skills assessment via Engineers Australia mirrors the Stage 1 registration process, making it unlikely that geoscience-trained applicants will succeed.

As discussed earlier, many overseas ground engineering professionals with geological degrees hold titles like Geotechnical or Geological Engineer. However, without registration, they cannot legally practise in some states—risking prosecution and jeopardizing visa eligibility. This issue is compounded by the lack of ANZSCO codes for Engineering Geologists or Geological Engineers.

Practitioners with geoscience backgrounds may apply under ANZSCO 234411 (Geologist), but success hinges on alignment with VETASSESS's narrow task list, focused on resource exploration, specimen analysis, environmental impact, and lab supervision, rather than engineering-related ground investigation or design. Those focused on ground characterisation, parameterisation, and design, toward the right of **Figure 8**, will struggle to meet these criteria.

This misalignment creates a significant barrier for qualified international professionals seeking entry into Australia's ground engineering and engineering geology workforce.

However, Australia is not unique in coupling its immigration requirements with registration. Out of the 9 high-income English-speaking nations mentioned previously, 7 require compulsory registration for Civil/Geotechnical Engineers but only 2 require it for Geologists/Engineering Geologists.

However, as registration is State led for Australia, it is important to put this comparison into context with similar nations and state unions.

Figure 9 shows that Australia is the only state where 100% of states do not require registration of Engineering Geologists. As Packer et al highlight in their paper, there isn't a compulsory registration for Engineering Geologists in Australia.

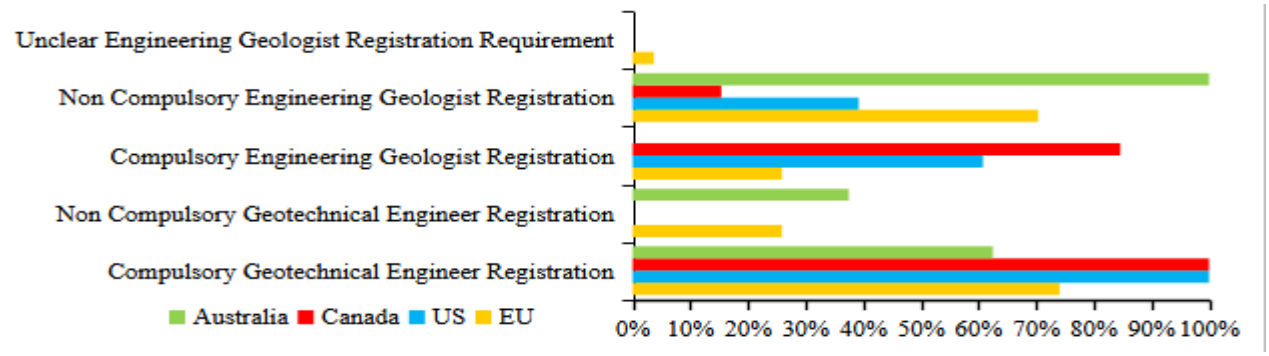


Figure 9: Percentages of states requiring registration for Geotechnical Engineers and Engineering Geologists.

Given the issues described so far regarding registration, occupation, education and skills recognition and the contribution this is creating to immigration coupled with the acute skills shortage Australia appears relentless in trying to backfill. The impacts must be being felt and observed by some measure.

3 SOCIO ECONOMIC IMPACT

Economic impacts often reveal skill shortages, yet data linking ground risk management to performance remains limited. One proxy is how well projects handle ground conditions. With adequate engineering geology expertise in transport, water, mining, and energy sectors, geological hazards could be more reliably identified and mitigated.

A review of news and articles on projects commissioned since 2000 reveals that ground-related challenges have significantly impacted infrastructure projects across Australia, particularly in tunnelling, often resulting in billion-dollar cost overruns, construction halts, or deferrals. **Figure 10** provides a summary of those findings. Notably, most ground conditions were unremarkable, except for one mining project facing extreme subsurface temperatures.

Rather than faulting individual projects, the evidence points to a broader misalignment in ground risk recognition by the Australian Government, as highlighted in the National Study of Infrastructure Risk.

A summary of the top five risks of projects from the government vs national construction contractors shows the stark difference the government agencies have when it comes to ground risks when compared to the contracting companies. The study showed the top 5 risks of each in order of importance:

- National Construction Contractors - utilities and ground conditions, land contamination, shortage of professional talent, shortage of general labour, complex policy and regulation
- Government - contractor capacity, shortage of professional talent, project management skills, shortage of general labour, planning approvals

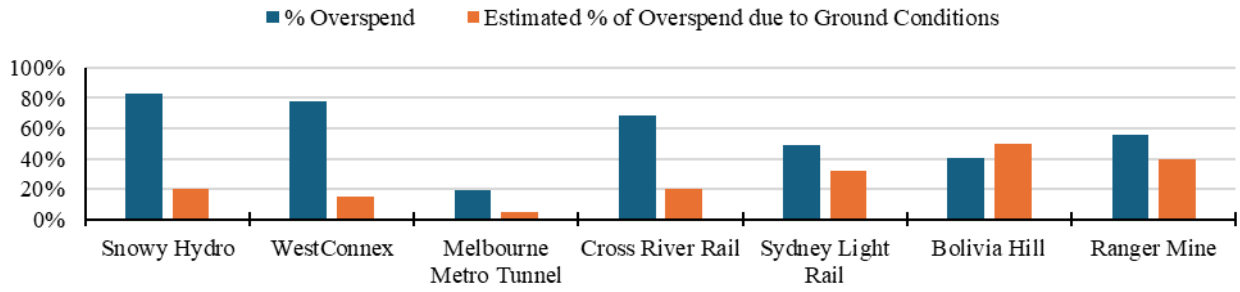


Figure 10: Selection of projects impacted by ground conditions

The study also highlights skills shortages in professional areas, geotechnical engineering and tunnelling, land contamination and challenging ground conditions as common delivery risks which are amplified by project and systemic risks such as insurance liabilities, climate change, geological hazards, cost and delivery risks. It should be noted however, that these are mostly hardest felt by the transport infrastructure sector.

The study also stated the same reoccurring theme that ground conditions are often poorly understood during the early stages of project planning, despite that being the most effective time to mitigate associated risks. Both industry experts and contractors agree that proactive hazard identification and mitigation should occur before construction begins, particularly for unpredictable or poorly characterised subsurface elements. The implication is clear; delayed recognition of ground risks leads to avoidable complications, and early-phase 'geotechnical' input is essential for project resilience.

It is ironic that the failure to understand ground conditions early in the planning and development of projects is still said today despite **Figure 11** which Fookes purported in 1997.

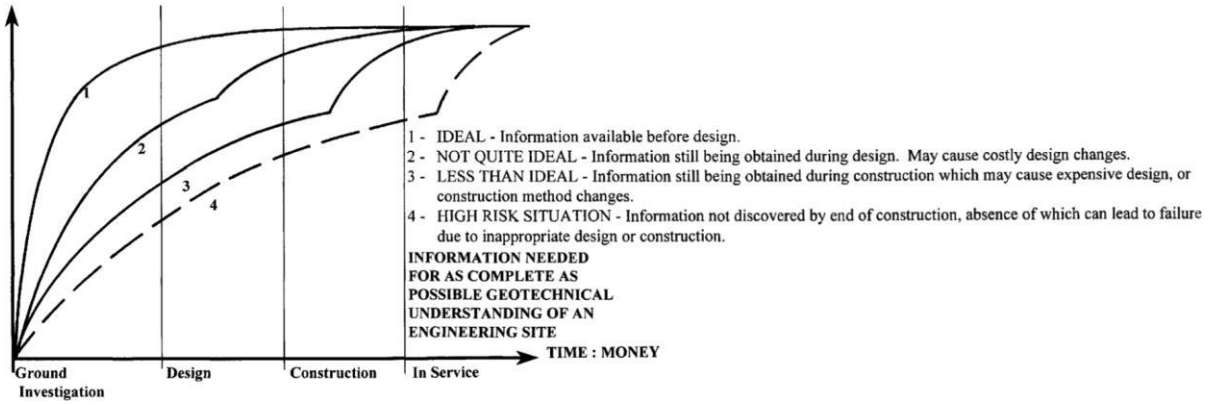


Figure 11: The optimisation of ground condition information gathering during the stages of a project.

The study found that inadequate planning significantly contributes to uncertainty in ground conditions, with cost uplifts in transport projects—particularly those involving tunnelling—ranging from 60–80%. Unpredictable subsurface conditions were a consistent challenge across major infrastructure projects, and industry participants indicated a declining willingness to absorb such risks. This underscores the need for stronger collaboration between government and contractors to manage geotechnical uncertainty. The $2 billion cost overrun on Melbourne Metro was partly attributed to unexpected soil density, which delayed excavation. Stakeholders broadly support shared risk models, but concerns remain over the use of 'no-reliance' geotechnical data during tendering. Contractors argue that if provided information proves inaccurate, they should be entitled to time and cost relief. Melbourne's inconsistent geology heightens the risk of undetected subsurface features, and even comprehensive pre-construction sampling may miss critical anomalies. Ultimately, the severity of unknown ground conditions depends heavily on regional geology, and full understanding prior to construction is rarely achievable.

Poorly informed views such as these are undermining the industry. Melbourne's geology is not inherently unpredictable; it's poorly understood due to limited investigation. Ground certainty depends on informed analysis, not geology alone. A shortage of expertise is hindering the detection of unforeseen conditions, reinforcing the need for comprehensive, phased investigations including geophysics.

A further measure of geohazard impact is Australia's landslide fatality rate, which ranks high among peer nations. Countries with effective ground risk management typically adopt preventative strategies. Despite differences in climate and terrain, the 12-year comparative data (2004–2016) offers a compelling socioeconomic lens.

Figure 12 shows Australia ranks fourth in average annual landslide fatalities among high-income English-speaking nations, second when adjusted for population, and third by population density, behind only New Zealand, the US, and Canada.

These rankings suggest a shortfall in geohazard risk management capability. While population density may also reflect regulatory effectiveness, the elevated fatality rates warrant closer scrutiny of how ground risks are currently managed.

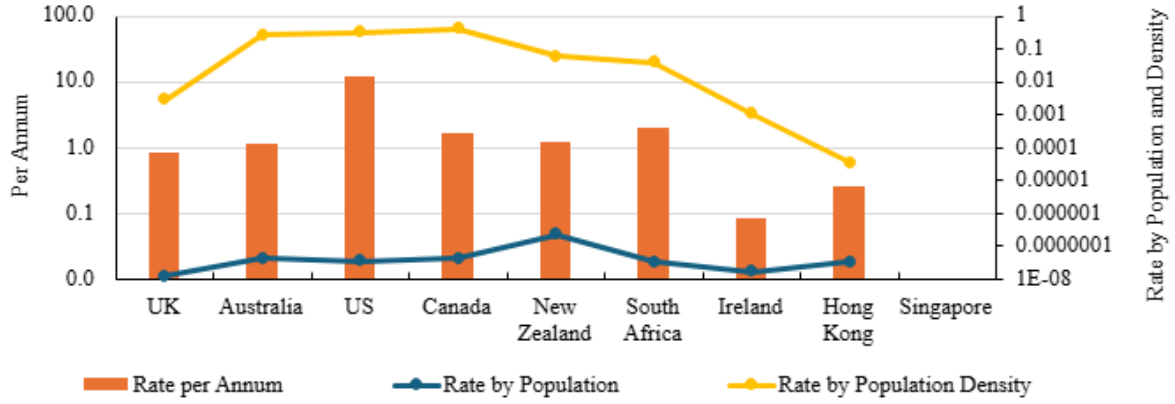


Figure 12: Comparison of average annual rate of landslide fatalities by population size and density

4 GROUND RISK MANAGEMENT STANDARDS

Ground risk management begins with identifying hazards through prior knowledge and desktop research i.e. a Desk Study or Literature Review. This stage aims to recognise and preliminarily quantify risks, forming initial conceptual and geological models. These models remain dynamic and are refined throughout the ground investigation process. Following a phased approach of investigation survey techniques which will target; hazards so that they can be risk assessed, geological complexity and uncertainty, qualitative data acquisition of ground information to enable ground characterisation and parameterisation for design.

Following this the objective should be for geological hazards to be risk assessed, mitigated and transferred. The conceptual, geological and engineering models fully developed to define receptors, RAG (red - amber - green) rate site hazards, and convey uncertainty. The design limit states fully developed with geological hazards considered and designed for.

The next section of will go into the aspects of this process which are directly relevant to engineering geology and affected by the topics covered so far but also how other nations approach these methods.

4.1 HAZARDS

Identifying and understanding ground hazards comes from a knowledge of, tectonic stress history, erosion and depositional history, historical and current climate, previous development, recent military conflict.

While geoscientists are naturally equipped for this work, engineers with strong geological competence also contribute. The key lies in linking hazards to the design limit state and anticipating the next phase, typically ground investigation, where health and safety issues emerge. This is where engineering geologists begin developing design skills, while engineers often overlook their need to deepen geological understanding in ground engineering.

Rumsfeld (2011) is often attributed to the categorisation of hazards into four classifications.

- Known knowns – expected and identified hazards e.g. dams prone to slope instability
- Known unknowns – hazards that are identifiable but have not been researched for the project at hand
- Uknown knowns – identifiable hazards that are not recognised as identifiable
- Uknown unknowns – unexpected and unprecedented hazards that cannot be researched

How this classification allows for the illustration of hazards and the links to health and safety and design limit states as shown in **Figure 13**

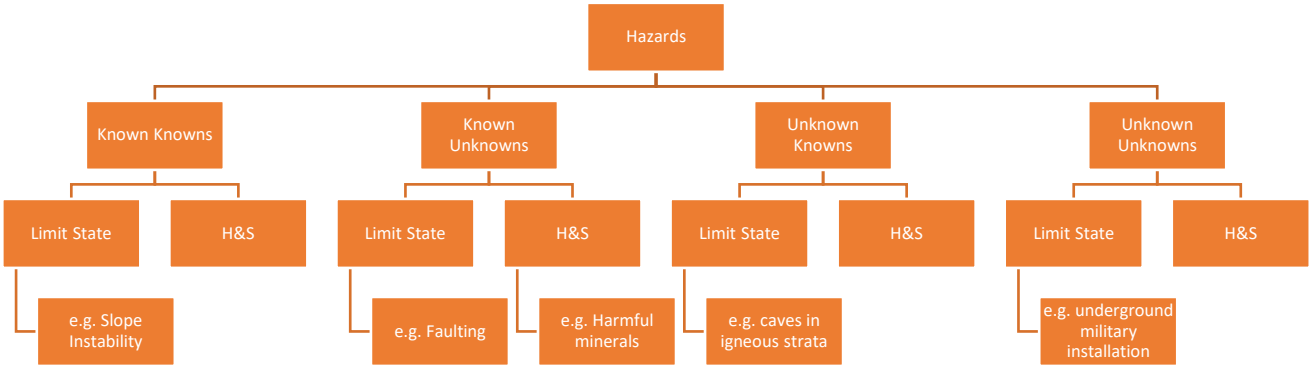


Figure 13: Hazard categories and the connectivity with design and Health and Safety

4.2 DESK STUDY

The desk study is the key initial step for identifying ground hazards and typically precedes site investigations. Its requirement, along with the scope of risk assessments and sources consulted, varies across countries. **Figure 14** shows the varying national ground engineering standards and their requirements for a desk studies and risk assessments in the early phases based on the author's review.

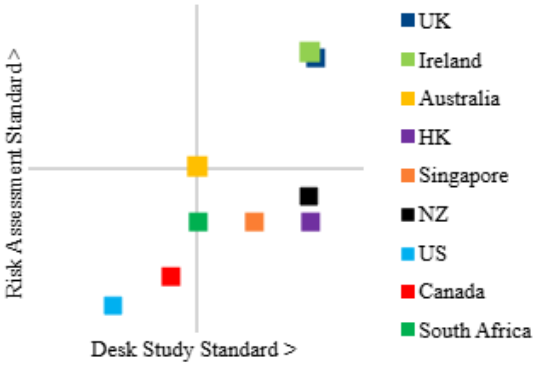


Figure 14: National ground engineering standards and the mandating of desk studies

While some national standards don't explicitly define the desk study as a formal investigation stage, they do emphasise preliminary assessments. At minimum, guidance should be provided on typical information sources, especially in standards framed as best practice versus minimum compliance.

The level of detail varies widely. The UK's BS5930 outlines desk study requirements extensively, including content, interpretation, sources, structure, and links to health and safety legislation, reinforcing a hazard-led approach.

In contrast, Australia's decentralised data landscape complicates desk study compilation. While national and state portals offer impressive spatial coverage, usability and geological data quality vary. Inconsistencies across state geological maps, such as missing sections, dip markers, or linear features, can hinder interpretation. Key geohazard maps like subsidence (QLD & NSW only) and naturally occurring asbestos (NOA, NSW only) are not universally available.

Understanding map limitations is critical. NOA maps, for instance, only reflect surface geology, requiring users to infer subsurface potential from regional structure. Similarly, detailed units may appear in one area due to supporting data but be absent elsewhere, despite likely presence. These nuances demand education for non-geoscientists and should be addressed in AS1726. Moreover, some listed sources aren't available nationwide, and valuable datasets like geophysical maps are omitted.

Sector-specific guidelines (e.g. CD622, QLD Geotechnical Guideline) often provide more detailed requirements than AS1726, especially for infrastructure projects. Overall, there are clear disparities in desk study expectations across national, state, and sector standards.

4.3 MODELS

Model development is integral to identifying, assessing, and mitigating ground engineering risk. Broadly, there are three types of models in ground engineering.

- Conceptual model (CSM) – Originating from contamination studies, CSMs highlight hazards and receptors to guide targeted investigations. Common in infrastructure and dam projects, they are schematic rather than factual.
- Geological Model – A dynamic, evolving subsurface representation refined through investigation. Initially basic, it gains precision with data and typically uses modelling software. QA processes are essential for complex projects.
- Geotechnical or Engineering Ground Model – A simplified, parametrised version used for design. Though often associated with later stages, early versions can emerge from desk studies—provided derivation is justified.

ANCOLD references all three, but most Australian state guidelines do not, except the Northern Territory's CSM guidance. Internationally, Canada and the UK mandate CSMs under environmental standards; ISO 21365:2020 offers broader applicability. IAEG's Commission 25 is the only document integrating all three models.

Countries with clearer engineering geology recognition such as Hong Kong, New Zealand, Canada, the UK, and Ireland better incorporate these models into design frameworks. In contrast, AS1726 focuses on investigation scope rather than hazard-led model development, limiting its alignment with risk-based approaches.

4.4 RISK ASSESSMENT, MANAGEMENT AND REGISTER

Risk assessment is closely tied to model development, yet its implementation varies more widely across countries and sectors than desk studies or modelling. Ireland, Hong Kong, and the UK embed live risk registers from project inception in national standards and infrastructure guidelines. Other countries may use geotechnical risk registers as management tools, but adoption depends on project scale and sector.

AS1726 references geotechnical risk assessment only late in the process—within the interpretive report—limiting alignment with hazard-led engineering geology approaches. In Australia, risk registers appear in state-level requirements for mine closure, rehabilitation, and environmental hazard management. Canadian-developed guidelines also promote their use in stockpile, waste dump, and open pit slope design.

5 CONCLUSIONS AND A WAY FORWARD FOR AUSTRALIA

The fatality statistics alone should compel urgent action. The regulatory threats facing geoscience-trained ground engineering professionals in Australia are not only financially damaging—they are costing lives.

The following sections summarise key findings and offer targeted recommendations to address the interconnected issues outlined in this paper.

5.1 RECOGNITION

Government ignorance of the discipline as an occupation is not accepted. While OSCA recognises Engineering Geologist as a Geologist specialisation (ABS, 2024), this must be reflected in the ANZSCO 234411 classification to ensure consistency in migration pathways. Otherwise, fluctuating demand across subfields (e.g. Engineering Geologists vs Palaeontologists) risks undermining visa allocations or removing the broader occupation from state lists.

To address this, two options exist. Petition Engineers Australia to recognise applied geoscience graduates as qualified for engineering tasks as supported in Section 2.3. Otherwise, Advocate for Engineering Geoscientists, including Engineering Geophysicists, to be recognised as a standalone occupation with a dedicated skills assessment body.

5.2 ALIGNMENT OR DEVOLUTION

Engineers Australia's reliance on the International Engineering Alliance (IEA) accords creates an exclusionary framework that undermines the role of geoscience-trained professionals in ground engineering. The IEA's vague educational criteria contrast with ABET's clearer definition of engineering as the applied use of mathematical and natural sciences, criteria geology inherently meets, especially in hazard-related applications.

Despite the mathematical rigor in applied geological education, EA is unlikely to diverge from IEA standards. This reinforces the need for an independent body to assess engineering geology qualifications for registration and immigration, based on actual competencies rather than rigid accords.

Geologists working in civil engineering, particularly in ground design, clearly meet engineering thresholds. Arguments that exclude them based on "design" misunderstand the nature of geotechnical calculations, which relate to ground limit states, not structural elements. The design of natural rock slopes, for instance, demands structural geology expertise, not just civil engineering credentials.

If EA does not reform its recognition policies, alternative governance must be pursued to ensure fair registration and protect public safety.

5.3 GOVERNANCE, IMMIGRATION AND REGISTRATION

There are currently three industry bodies which offer governance in terms of professional qualification or registration to the Engineering Geology occupation for Australia; Australian Institute of Geoscientists (AIG), Geological Society of Australia (GSA), Australasian Institute of Mining and Metallurgy (AusIMM)

The absence of a unified professional body has caused issues elsewhere, such as in the UK, where merging the Institute of Geologists into the Geological Society led to the Royal Charter, Chartered Geologist (CGeol) status, and the foundation for Ground Engineering Registration. Ireland followed suit, with Engineers Ireland and the Institute of Geologists of Ireland formally supporting RoGEP alongside UK institutions like ICE, GSL, and IOM3.

Australia could adopt a similar model to New Zealand's PEngGeol qualification. This is feasible, as most state legislation does not specify which body must assess engineering registration or define qualification criteria in detail. Thus, states could theoretically endorse a dedicated assessment body for Engineering Geologists.

An internationally affiliated body, such as IAEG, linked with ISSMGE, ISRM, and governed under FedIGS, would be ideal. Their collaborative stance reinforces the reality that engineering geology and geotechnical engineering are interwoven disciplines. Whether trained in civil engineering or geoscience, practitioners are equipped to contribute across the ground engineering spectrum.

It should then fall on this internationally accredited Australian Engineering Geology governance body to lobby Australian Home Affairs and Immigration departments to recognise Engineering Geologists as its own occupation. Then advise VETASSESS on how the tasks specified on the skills assessment information should reflect that of Engineering Geologists. Alternatively, become its own skills assessment body for immigration, registration and professional qualification.

Lastly the same industry body will likely be the conduit to improving the standards relating to ground engineering through the technical knowledge of members and self-appointed technical committees in line with the international governance inputs.

5.4 GROUND RISK MANAGEMENT & STANDARDS

As already mentioned in Section 4, desk study compilation in Australia is often inefficient due to fragmented data sources and inconsistent presentation. This may discourage clients and practitioners from engaging in this critical phase. To improve uptake, state and federal datasets should be centralised via user-friendly portals, with clear guidance on data limitations and training for non-geoscientists. AS1726 should explicitly address this need.

Comparative analysis shows AS1726 lacks emphasis on hazard identification through desk studies. Greater alignment with state and sector guidelines, and international best practice, is needed. Rather than setting a minimum baseline, AS1726 should reflect optimal standards and promote a hazard-first approach.

Consistency across national, state, and sector frameworks should centre on three pillars: hazard identification, ground models, and risk registers. These elements, illustrated in **Figure 15** form the basis of the Ground Engineering Risk Management Process (GERMP).

What is covered by these three components are:

- Early hazard identification – this includes reinforcement of a well put together and detailed desk study which assigns what hazards fall into the 4 'Rumsfeld' categories.
- Engineering Geological Models – as per IAEG's Commission 25 (C25) and like ANCOLD, covering conceptual, geological and engineering models
- A live risk register – linking with the EGM and the hazards identified a live risk register works as the key conduit for ensuring adequate geotechnical design and limit state development. The risk register remains live from inception to commissioning and should conform into the overall project risk register following the completion of geotechnical construction.

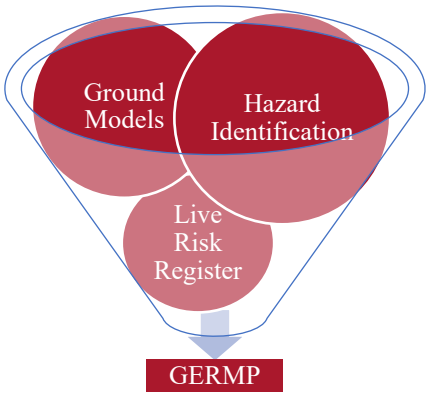


Figure 15: Core components of a Ground Engineering risk management process

An example full flow process for this is illustrated in **Figure 16**

The proposed flow diagram aims to supplement or replace Figure 1 in AS 1726:2017 by shifting the focus of ground investigations toward hazard identification from project inception. Instead of defining scope and objectives upfront, the process begins by identifying hazards, which in turn define the design limit states.

Where hazard data exists, the desk study or literature review begins by default; where it doesn't, the hazard is logged and the risk register initiated, activating two of the three core GERMP elements. The desk study should yield early geological and conceptual models that combine factual geology with interpretive uncertainty, allowing practitioners to assess potential impacts on receptors and assign risk ratings. This links hazard identification, model limitations, and live risk assessment directly to design development.

Even if the desk study concludes with all available data consulted, the geological model and risk register must remain live, acknowledging that new hazards may emerge during subsequent investigation stages. Maintaining flexibility and strategic focus is essential, which is why remote and non-intrusive methods should be considered next.

A resurgence in remote techniques—such as photogrammetry, LiDAR, airborne geophysics, satellite sensing, muography, and InSAR, offers a chance to reassess hazards while prioritising safety, sustainability, and innovation before intrusive works begin. These methods help refine live models and the risk register before putting boots on the ground.

The intrusive investigation phase should follow a hazard- and risk-led approach, targeting engineering and ground characterisation. Given the remote nature of many Australian sites, this stage should maximise onsite efficiency through advanced methods like downhole and cross-hole geophysics, televiewers, instrumented drilling, and dual rigs combining sonic, rotary percussive, and CPT capabilities. Results from this phase feed back into the live models and risk register, which continue to evolve through design and construction.

Throughout, the risk register should be updated to reflect mitigated hazards and transferred residual risks across stakeholders. The ground model must be validated during construction to support commercial decision-making and manage project complexity.

6 CLOSING REMARKS

This strategic shift will require most importantly collaboration from across the ground engineering spectrum but also an education from those in engineering geology to take best practice from Australia and other nations beyond those mentioned in this paper.

Terzaghi once said that engineering geology preceded soil mechanics by over a century, the first geological map of a country was prepared and published by a civil engineer, William Smith, in 1815, and not by geologists, and the first textbook on engineering geology was published as early as 1875. He also noted the crucial efficiency of geological reports for engineering projects, after several engineering failures he gave focus to engineering geological site investigation and gave the engineering geology courses himself at Harvard University.

This demonstrates that geotechnical engineering does not stop where engineering geology starts, it is one discipline, the ground engineering discipline and competent practitioners come from various relevant educational backgrounds with varying engineering and geological content. To progress where the industry has failed in Australia, better education, recognition, representation and standardisation is needed.

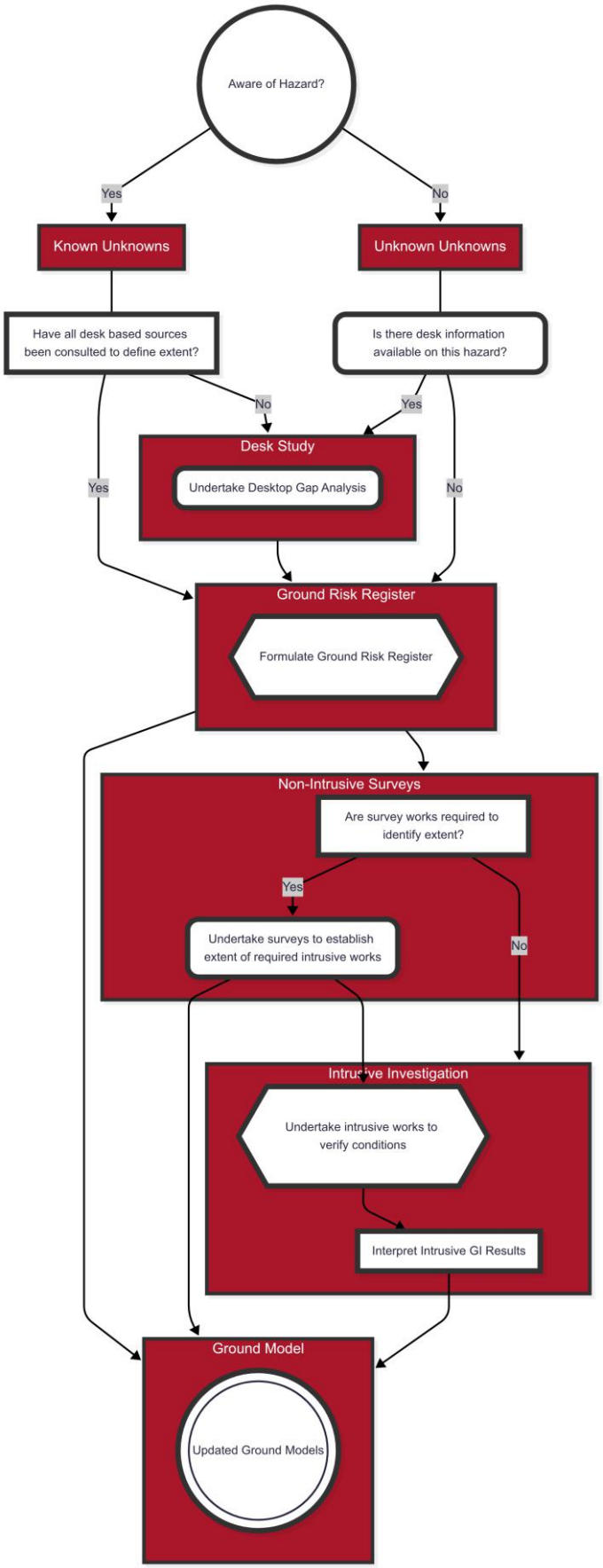


Figure 16: A Prototype of a Ground Engineering Risk Management Process

REFERENCES

ABC News, 2022a. *Ranger uranium mine cleanup cost blowout to $2.2 billion.* [online] Available at: https://www.abc.net.au/news/rural/2022-02-02/ranger-uranium-mine-cleanup-cost-blowout-to-2-2-billion/100798666 [Accessed 27 June 2025].

ABC News, 2022b. *Kakadu's Ranger uranium mine rehabilitation faces major challenges.* [online] Available at: https://www.abc.net.au/news/2022-06-19/kakadu-ranger-uranium-mine-rehabilitation/101147762 [Accessed 27 June 2025].

Accreditation Board for Engineering and Technology (ABET), (2021) *Criteria for Accrediting Engineering Programs*. [online] Available at: https://www.abet.org/accreditation/

American Profession Guide (n.d.) *Professional Organizations for Geotechnical Engineers*. Available at: https://americanprofessionguide.com/professional-organizations-for-geotechnical-engineers/ (Accessed: 16 June 2025).

ASTM International, 2018. ASTM D420-18: *Standard guide for site characterization for engineering design and construction purposes*. West Conshohocken, PA: ASTM International.

Australian Institute of Geoscientists (AIG) (n.d.) *Careers in Geoscience: Engineering Geology*. Available at: https://www.aig.org.au/education/careers-in-geoscience/careers-in-geoscience-engineering-geology/ (Accessed: 16 June 2025).

Australian National University (ANU) (n.d.) Earth Science Major – Course Structure. Available at: https://programsandcourses.anu.edu.au/major/EART-MAJ (Accessed: 16 June 2025).

Australian Bureau of Statistics (2024) *OSCA - Occupation Standard Classification for Australia, 2024, Version 1.0: 244531 Engineering Geologist*. Available at: https://www.abs.gov.au/statistics/classifications/osca-occupation-standard-classification-australia/2024-version-1-0/browse-classification/2/24/244/2445/244531 (Accessed: 20 June 2025).

Big Rigs, 2021. *$43 million to finish Bolivia Hill upgrade.* [online] Available at: https://bigrigs.com.au/2021/02/25/43-million-to-finish-bolivia-hill-upgrade/ [Accessed 27 June 2025].

Blais-Stevens, A., Behnia, P. and Castagner, A., 2019. *Historical landslides that have resulted in fatalities in Canada (1771–2018)*. Ottawa: Geological Survey of Canada.

Bond, A. and Harris, A., 2006. *Decoding Eurocode 7*. 1st ed. London: CRC Press.

BS EN ISO 21365:2020. *Conceptual site models for contaminated sites – Specification*. London: British Standards Institution.

BSI (British Standards Institution), 2015. *BS 5930:2015 Code of practice for ground investigations*. London: BSI.

California Institute of Technology (Caltech) (n.d.) *Undergraduate Program – Geological and Planetary Sciences*. Available at: https://www.gps.caltech.edu/academics/undergraduate-program (Accessed: 16 June 2025).

Canadian Geotechnical Society (CGS) (n.d.) *Engineering Geology & Geological Engineering Division*. Available at: https://www.cgs.ca/division_engineering_geology.php (Accessed: 16 June 2025).

Canadian Geotechnical Society (CGS), 2023. *Canadian Foundation Engineering Manual*. 5th ed. Ottawa: CGS.

CD 622, 2020. *Managing geotechnical risk*. Highways England.

Central Queensland University 2025*, Bachelor of Engineering (Honours) (Civil)*, CQU, Rockhampton.

Charles Darwin University 2025, *Bachelor of Engineering (Honours) (Civil)*, CDU, Darwin.

Civil Engineering and Development Department (CEDD) (2007) *Engineering Geological Practice in Hong Kong.* GEO Publication No. 1/2007. Available at: https://www.cedd.gov.hk/filemanager/eng/content_149/ep1_2007.pdf (Accessed: 16 June 2025).

Columbia University (n.d.) *Geology – Department of Earth and Environmental Sciences*. Available at: https://eesc.columbia.edu/content/geology (Accessed: 16 June 2025).

Construction Jobs Ireland (n.d.) *Your career as a Geotechnical Engineer*. Available at: https://www.constructionjobsireland.ie/career-advice/your-career-as-a-geotechnical-engineer/ (Accessed: 16 June 2025).

CSA Z1000-14, 2014. *Occupational Health and Safety Management*. Toronto: Canadian Standards Association.

Curtin University 2025, *Bachelor of Engineering (Honours) (Civil)*, Curtin University, Perth.

Curtin University (n.d.) *BSc Geology – Course Information*. Available at: https://www.curtin.edu.au/study/offering/course-ug-bachelor-of-science-bsc-glb--g-bsc/ (Accessed: 16 June 2025).

Deakin University 2025, *Bachelor of Engineering (Honours) (Civil)*, Deakin University, Geelong.

ECO Canada (n.d.) *Geotechnical Engineer Career Profile*. Available at: https://eco.ca/career-profiles/geotechnical-engineer/ (Accessed: 16 June 2025)

Edith Cowan University 2025, *Bachelor of Engineering (Honours) (Civil)*, ECU, Perth.

Engineering New Zealand (2025) *Professional Engineering Geologist Assessment Guidance*

Engineers Australia (2022) *Geotechnical Engineering: Area of Practice / Area of Engineering*. Available at: https://www.engineersaustralia.org.au/sites/default/files/2022-07/geotechnical_engineering_aop_aoe_-_final.pdf (Accessed: 16 June 2025).

ETH Zurich (n.d.) *Bachelor in Earth and Climate Sciences*. Available at: https://eaps.ethz.ch/en/studies/bachelor/earth-climate-sciences.html (Accessed: 16 June 2025).

Eurocode 7, 2004. *Geotechnical design - Part 1: General rules*. Brussels: European Committee for Standardization (CEN)
Federation University Australia 2025, *Bachelor of Engineering (Honours) (Civil)*, Federation University, Ballarat.
Flinders University 2025, *Bachelor of Engineering (Honours) (Civil)*, Flinders University, Adelaide.
Flinders University (n.d.) *BSc Geology – Course Information*. Available at: https://www.flinders.edu.au/study/courses/undergraduate/geology (Accessed: 16 June 2025).
Fookes, P. G., (1997). *Geology for Engineers: the Geological Model, Prediction and Performance*. *Quarterly Journal of Engineering Geology*, 30, 293-424. The First Glossop Lecture. The Geological Society
Froude, M.J. and Petley, D.N., 2018. *Global fatal landslide occurrence from 2004 to 2016*. *Natural Hazards and Earth System Sciences*, 18(8), pp.2161–2181. https://doi.org/10.5194/nhess-18-2161-2018
Geoscience Australia (2012): *Landslide Search*. [software]. https://pid.geoscience.gov.au/dataset/ga/74273
Geotechnical Engineering Office (GEO), 1987. Geoguide 2: Guide to site investigation. Hong Kong: Civil Engineering and Development Department.
Government of Canada (2021*) National Occupational Classification (NOC) Profile: 21331 – Geological Engineers*. Available at: https://noc.esdc.gc.ca/Structure/NOCProfile?GocTemplateCulture=en-CA&code=21331&version=2021.0 (Accessed: 16 June 2025).
GradIreland (2023) *Geologist, engineering job description*. Available at: https://gradireland.com/careers-advice/job-descriptions/geologist-engineering (Accessed: 16 June 2025)
Harvard University (n.d.) *Undergraduate Program – Earth and Planetary Sciences*. Available at: https://eps.harvard.edu/undergraduate-program (Accessed: 16 June 2025).
IAEG (International Association for Engineering Geology and the Environment), 2024. *Guidelines for the Development and Application of Engineering Geological Models on Projects*.
Imperial College London (n.d.) *BSc Geology*. Available at: https://www.imperial.ac.uk/study/courses/undergraduate/geology-bsc/ (Accessed: 16 June 2025).
Infrastructure Australia 2021, *A national study of infrastructure risk, Infrastructure Australia*, Canberra.
James Cook University 2025, *Bachelor of Engineering (Honours) (Civil)*, JCU, Townsville.
James Cook University (n.d.) *BSc Geology – Course Information*. Available at: https://www.jcu.edu.au/courses/bachelor-of-science (Accessed: 16 June 2025).
La Trobe University 2025, *Bachelor of Engineering (Honours) (Civil)*, La Trobe University, Melbourne.
Ludwig Maximilian University of Munich (n.d.) *BSc Earth Sciences – Course Structure*. Available at: https://www.en.geophysik.uni-muenchen.de (Accessed: 16 June 2025).
Macquarie University 2025, *Bachelor of Engineering (Honours) (Civil)*, Macquarie University, Sydney.
Macquarie University (n.d.) *BSc Geology – Course Information*. Available at: https://courses.mq.edu.au/2024/international/bachelor-of-science/geology (Accessed: 16 June 2025).
Massachusetts Institute of Technology (MIT) (n.d.) *Earth, Atmospheric, and Planetary Sciences* (Course 12). Available at: https://catalog.mit.edu/degree-charts/earth-atmospheric-planetary-sciences-course-12/ (Accessed: 16 June 2025).
Monash University 2025, *Bachelor of Engineering (Civil)*, Monash University, Melbourne.
Monash University (n.d.) *BSc Earth Science – Course Information*. Available at: https://www.monash.edu/science/schools/earth-atmosphere-environment/study/undergraduate-courses (Accessed: 16 June 2025).
Murdoch University 2025, *Bachelor of Engineering (Honours) (Civil)*, Murdoch University, Perth.
New Zealand Geotechnical Society (NZGS) (n.d.) *Working in Geotechnics*. Available at: https://www.nzgs.org/careers/working-in-geotechnics/ (Accessed: 16 June 2025).
New Zealand Geotechnical Society (NZGS), 2005. NZGS 200: *Guidelines for the field classification and description of soil and rock for engineering purposes*. Wellington: NZGS.
NSAI (National Standards Authority of Ireland), 2007. *I.S. EN 1997-2:2007 Eurocode 7 – Geotechnical design – Part 2: Ground investigation and testing*. Dublin: NSAI.
Packer, M., Nash, T., Bennett, C. & Doe, A. 2024, *'Establishing professional accreditation pathways for Australian engineering geologists in the civil design and construction industry'*, Australian Geomechanics, vol. 59, no. 3, pp. 23-29.
Paul, D. 2024, *'The state of engineering geology education in Australia'*, Australian Geomechanics, vol. 59, no. 3, pp. 17-22.
Pennsylvania State University (Penn State) (n.d.) *Earth Sciences, B.S. – Program Requirements*. Available at: https://bulletins.psu.edu/undergraduate/colleges/earth-mineral-sciences/earth-sciences-bs/ (Accessed: 16 June 2025).
Prospects.ac.uk (n.d.) *Geotechnical engineer job profile*. Available at: https://www.prospects.ac.uk/job-profiles/geotechnical-engineer (Accessed: 16 June 2025).
Public Accountant, 2022. *3 lessons from major project failures.* [online] Available at: https://publicaccountant.com.au/features/3-lessons-from-major-project-failures/ [Accessed 27 June 2025]
Queensland University of Technology 2025, *Bachelor of Engineering (Honours) (Civil)*, QUT, Brisbane.
RMIT University 2025, *Bachelor of Engineering (Civil)*, RMIT, Melbourne.

Rumsfeld, D. 2011, *Known and Unknown: A Memoir*, Sentinel, New York.
Society of Exploration Geophysicists (SEG) (2023) *Engineering Geologist Job Description*. Available at: https://careers.seg.org/career/engineering-geologist/job-descriptions (Accessed: 16 June 2025).
South African Institute for Engineering and Environmental Geologists (SAIEG) (n.d.) *About SAIEG*. Available at: https://www.saieg.co.za/ (Accessed: 16 June 2025).
South African Geotechnical Division (n.d.) *What is Geotechnical Engineering*. Available at: https://www.geotechnicaldivision.co.za/about-us/what-is-geotechnical-engineering/ (Accessed: 16 June 2025).
South African Bureau of Standards (SABS), 2012. *SANS 634:2012 Geotechnical investigations for township development*. Pretoria: SABS.
SPRING Singapore, 2010. *SS EN 1997-2:2010 Eurocode 7 – Geotechnical design – Part 2: Ground investigation and testing*. Singapore: SPRING Singapore.
Standards Australia, 2017. *AS 1726:2017 Geotechnical site investigations*. Sydney: Standards Australia.
Stanford University (n.d.) *Earth and Planetary Sciences Major*. Available at: https://majors.stanford.edu/majors (Accessed: 16 June 2025).
Swinburne University of Technology 2025, *Bachelor of Engineering (Honours) (Civil)*, Swinburne University, Melbourne. Available at: https://www.swinburne.edu.au/course/unit/c/cve40001/
The Geological Society (n.d.) *Engineering Geology Sector*. Available at: https://www.geolsoc.org.uk/Geology-Career-Pathways/Careers/Job-Sectors/Engineering-Geology-Sector.html (Accessed: 16 June 2025)
TII (Transport Infrastructure Ireland), 2020. *Geotechnical risk management guidelines*.
TopUniversities.com (2025) *QS World University Rankings by Subject 2025: Geology*. Available at: https://www.topuniversities.com/university-subject-rankings/geology (Accessed: 16 June 2025).
U.S. Bureau of Labor Statistics (2025) *Mining and Geological Engineers*. Available at: https://www.bls.gov/ooh/architecture-and-engineering/mining-and-geological-engineers.htm (Accessed: 16 June 2025).
UK Government (n.d.) Work Permits (UK) *Internal Caseworker Guidance: Geotechnical Engineer*. Available at: https://assets.publishing.service.gov.uk/media/5a80b77740f0b62305b8cc00/geotechnicalengineer.pdf (Accessed: 16 June 2025).
University of Oxford. (n.d.). *Department of Earth Sciences – Undergraduate Courses*. University of Oxford.
University of Portsmouth. (2017). *BSc (Hons) Geology Course Specification*. University of Portsmouth
University of Queensland 2025, *Bachelor of Engineering (Honours) (Civil)*, UQ, Brisbane. Available at: https://study.uq.edu.au/study-options/programs/bachelor-engineering-honours-2455/geotechnical-engineering-geotec2455
University of New South Wales 2025, *Bachelor of Engineering (Honours) (Civil)*, UNSW, Sydney.
University of Melbourne 2025, *Bachelor of Engineering (Civil)*, University of Melbourne, Melbourne.
University of Sydney 2025, *Bachelor of Engineering (Civil)*, University of Sydney, Sydney. Available at: https://www.sydney.edu.au/courses/subject-areas/spec/geotechnical-engineering.html
University of Western Australia 2025, *Bachelor of Engineering (Honours) (Civil)*, UWA, Perth.
University of Adelaide 2025, *Bachelor of Engineering (Honours) (Civil)*, University of Adelaide, Adelaide.
University of Technology Sydney 2025, *Bachelor of Engineering (Honours) (Civil)*, UTS, Sydney.
University of Wollongong 2025, *Bachelor of Engineering (Honours) (Civil)*, University of Wollongong, Wollongong.
University of Newcastle 2025, *Bachelor of Engineering (Honours) (Civil)*, University of Newcastle, Newcastle.
University of Southern Queensland 2025, *Bachelor of Engineering (Honours) (Civil)*, USQ, Toowoomba.
University of Tasmania 2025, *Bachelor of Engineering (Honours) (Civil)*, UTAS, Hobart.
University of Oxford (n.d.) *Earth Sciences (Geology)*. Available at: https://www.ox.ac.uk/admissions/undergraduate/courses/course-listing/earth-sciences-geology (Accessed: 16 June 2025).
University of Cambridge (n.d.) *Course Structure – Department of Earth Sciences*. Available at: https://www.esc.cam.ac.uk/join-us/prospective-undergraduates/course-structure (Accessed: 16 June 2025).
University of California, Berkeley (n.d.) *Geology – Undergraduate Program*. Available at: https://guide.berkeley.edu/undergraduate/degree-programs/geology/ (Accessed: 16 June 2025).
University of Tokyo (n.d.) *Undergraduate Program – Earth and Planetary Science*. Available at: https://www.s.u-tokyo.ac.jp/en/education/undergraduate/ (Accessed: 16 June 2025).
University of British Columbia (UBC) (n.d.) *Courses & Registration – Earth, Ocean and Atmospheric Sciences*. Available at: https://www.eoas.ubc.ca/undergrads/courses-registration (Accessed: 16 June 2025).
University of Washington (n.d.) *Undergraduate Program – Earth and Space Sciences*. Available at: https://ess.uw.edu/education/undergraduate-program/ (Accessed: 16 June 2025).
University of California, Los Angeles (UCLA) (n.d.) *Geology BS – Course Requirements*. Available at: https://catalog.registrar.ucla.edu/major/2021/GeologyBS (Accessed: 16 June 2025).
University of Edinburgh (n.d.) *BSc Geology – Course Structure*. Available at: https://www.ed.ac.uk/studying/undergraduate/degrees/index.php?action=programme&code=F600 (Accessed: 16 June 2025).

University of Toronto (n.d.) *BSc Geological Sciences – Course Information*. Available at: https://artsci.calendar.utoronto.ca/section/Geological-Sciences (Accessed: 16 June 2025).
University of Sydney (n.d.) *BSc Geology – Course Information*. Available at: https://www.sydney.edu.au/handbooks/science/subject_areas_ug/geosciences.shtml (Accessed: 16 June 2025).
University of Manchester (n.d.) *BSc Earth and Planetary Sciences*. Available at: https://www.manchester.ac.uk/study/undergraduate/courses/2025/12106/bsc-earth-and-planetary-sciences/ (Accessed: 16 June 2025).
University of Adelaide (n.d.) *BSc Geology – Course Structure*. Available at: https://www.adelaide.edu.au/degree-finder/bge_geolsc_b.html (Accessed: 16 June 2025).
University of Western Australia (UWA) (n.d.) *BSc Geology – Course Information*. Available at: https://www.uwa.edu.au/study/courses/geology (Accessed: 16 June 2025).
University of Queensland (n.d.) *Bachelor of Science – Earth Science Major*. Available at: https://study.uq.edu.au/study-options/programs/bachelor-science-2461/earth-science-earthc2461 (Accessed: 16 June 2025).
University of Bristol (n.d.) *Geology – Course Structure*. Available at: https://www.bristol.ac.uk/earthsciences/ugrad/course-list/geology/ (Accessed: 16 June 2025).
University of Texas at Austin (n.d.) *BS Geological Sciences – Course Information*. Available at: https://catalog.utexas.edu/undergraduate/natural-sciences/degree-programs/geological-sciences/ (Accessed: 16 June 2025).
University of Oslo (n.d.) *BSc Geology – Course Structure*. Available at: https://www.uio.no/english/studies/programmes/geology/ (Accessed: 16 June 2025).
University of Zurich (n.d.) *BSc Earth Sciences – Course Information*. Available at: https://www.ieu.uzh.ch/en/studies/bachelor/earth_sciences.html (Accessed: 16 June 2025).
University of California, San Diego (UCSD) (n.d.) *BS Earth Sciences – Course Information*. Available at: https://catalog.ucsd.edu/curric/ESYS-ug.html (Accessed: 16 June 2025).
University of Amsterdam (n.d.) *BSc Earth Sciences – Course Structure*. Available at: https://www.uva.nl/en/programmes/bachelors/earth-sciences/earth-sciences.html (Accessed: 16 June 2025).
University of Melbourne (n.d.) *BSc Geology – Course Information*. Available at: https://study.unimelb.edu.au/find/courses/undergraduate/bachelor-of-science/major/geology/ (Accessed: 16 June 2025).
University of Leeds (n.d.) *Geology BSc – Course Details*. Available at: https://courses.leeds.ac.uk/i683/geology-bsc (Accessed: 16 June 2025).
University of Geneva (n.d.) *BSc Earth Sciences – Course Information*. Available at: https://www.unige.ch/sciences/terre/en/enseignement/bachelor/ (Accessed: 16 June 2025).
University of Helsinki (n.d.) *BSc Geology – Course Information*. Available at: https://www.helsinki.fi/en/degree-programmes/bachelors-programme-science/geology (Accessed: 16 June 2025).
University of Arizona (n.d.) *BS Geosciences – Course Information*. Available at: https://www.geo.arizona.edu/undergraduate-program (Accessed: 16 June 2025).
University of Utah (n.d.) *BS Geology – Course Information*. Available at: https://earth.utah.edu/undergraduate/geology.php (Accessed: 16 June 2025).
University of Alberta (n.d.) *BSc Geology – Course Information*. Available at: https://apps.ualberta.ca/catalogue/program/science/1720 (Accessed: 16 June 2025).
University of St Andrews (n.d.) *Modules – Earth and Environmental Sciences*. Available at: https://www.st-andrews.ac.uk/subjects/modules/ (Accessed: 16 June 2025).
University of Copenhagen (n.d.) *BSc Geology-Geoscience – Course Information*. Available at: https://studies.ku.dk/bachelors/geology-geoscience/ (Accessed: 16 June 2025).
University of Bristol (n.d.) *BSc Environmental Geoscience – Course Information*. Available at: https://www.bristol.ac.uk/study/undergraduate/2024/environmental-geoscience/ (Accessed: 16 June 2025).
University of Glasgow (n.d.) *BSc Geology – Programme Structure*. Available at: https://www.gla.ac.uk/undergraduate/degrees/geology/ (Accessed: 16 June 2025).
University of Otago (n.d.) *BSc Geology – Course Information*. Available at: https://www.otago.ac.nz/geology/study/index.html (Accessed: 16 June 2025).
University of Tasmania (n.d.) *BSc Geology – Course Information*. Available at: https://www.utas.edu.au/courses/cale/courses/s3a-bachelor-of-science-geology (Accessed: 16 June 2025).
University of Durham (n.d.) *GEOL1101: Understanding Earth Sciences*. Available at: https://www.durham.ac.uk/study/modules/undergraduate/geol1101.php (Accessed: 16 June 2025).
University of Wollongong (n.d.) *BSc Geology – Course Information*. Available at: https://www.uow.edu.au/study/undergraduate/geology-degree/ (Accessed: 16 June 2025).
University of Auckland (n.d.) *BSc Geology – Course Information*. Available at: https://www.auckland.ac.nz/en/study/study-options/find-a-study-option/geology.html (Accessed: 16 June 2025).
University of New South Wales (UNSW) (n.d.) *BSc Geology – Course Information*. Available at: https://www.unsw.edu.au/science/study/undergraduate/bachelor-of-science/geology (Accessed: 16 June 2025).

University of Newcastle (n.d.) *BSc Geology – Course Information*. Available at: https://www.newcastle.edu.au/degrees/bachelor-of-science-geology (Accessed: 16 June 2025).
Utrecht University (n.d.) *BSc Earth Sciences – Course Information*. Available at: https://www.uu.nl/bachelors/en/earth-sciences (Accessed: 16 June 2025).
Vocational Training Council (VTC) (n.d.) *Geotechnical Engineers*. Available at: https://occupation-dictionary.vtc.edu.hk/occupation/geotechnical-engineers (Accessed: 16 June 2025).
WPC Consulting, 2023. *Infrastructure budget blowouts: A critical look at Australian mega projects.* [online] WPC Consulting. Available at: https://www.wpcconsulting.com.au/post/infrastructure-budget-blowouts-a-critical-look-at-australian-mega-projects [Accessed 27 June. 2025]
Yale University (n.d.) *Undergraduate Program – Earth and Planetary Sciences*. Available at: https://earth.yale.edu/undergraduate-program (Accessed: 16 June 2025).
Yang, J., 2022. *Geotechnical challenges and solutions for the Bolivia Hill upgrade. Australian Geomechanics,* 57(2), pp. 65–78.

Table 1: Nations where the various roles and titles are recognised and defined

COUNTRY	ENGINEERING GEOLOGIST	GEOLOGICAL ENGINEER	GEOTECHNICAL ENGINEER
UK	Engineering geologists are involved in processes that modify surface and sub-surface geology for the built environment (Geological Society, 2025)	*Not Recognised*	Geotechnical engineers assess the properties and behaviour of soil and rock formations. Geotechnical engineering is a collective term for the more individual disciplines of: • Soil mechanics • Foundation engineering • Engineering geology and hydrology • Environmental science • Rock mechanics • Rock engineering (UK Government, 2006) Geotechnical engineers use their expertise in soil and rock to assess risks and address challenges on a variety of infrastructure projects. (Prospects, 2025)
Ireland	Engineering geologists apply their knowledge of rocks and soils to civil engineering projects such as bridges, factories and dams (GradIreland, 2023)	*Not Recognised*	As a geotechnical (geotech) engineer you will support construction and design professionals by carrying out tests and analysis to ensure risks to both people and the environment are mitigated against when planning a construction project. (Construction Jobs Ireland, 2025)
Australia	Engineering geoscientist's role focusses primarily on the understanding of geological and geotechnical conditions and how they may change in time and space in regard to particular engineering projects such as major construction, infrastructure, mining and resource developments and include ground and slope stabilisation, foundations characterisation and design, interpretive modelling, sourcing of suitable materials, recognition of hazards and risk factors and the forensic investigations after failures. They are specialist geologists dealing in the measurement, assessment and review of soils, water and rocks and the engineering impacts of natural processes or human activities such as construction projects, urban or industrial development, mining and resource developments and	*Not Recognised*	Geotechnical engineers identify, design and implement practical solutions to engineering problems concerning soil, rock and groundwater. They apply scientific and engineering techniques to predict and manage the behaviour of the ground where it interacts with or responds to human activity (Engineers Australia, 2022)

COUNTRY	ENGINEERING GEOLOGIST	GEOLOGICAL ENGINEER	GEOTECHNICAL ENGINEER
	the maintenance and monitoring of the outcomes of these projects. (AIG, 2025)		
Hong Kong	*Engineering Geologists are…* primarily concerned with the determination of geological and hydrogeological conditions to facilitate ground engineering with respect to the recognition and management of geotechnical risk. This requires the application of geological knowledge and skills to define and communicate the potential and actual variations in ground conditions that are relevant to the engineering project at hand. (CEDD, 2007)		Geotechnical Engineers plan, organise, perform site investigation (on geotechnical aspects) to determine and design the type of foundations, earthworks, and/or pavement subgrades required for the intended man-made structures to be built. (VTC, 2025)
Singapore	*No definition given by a Singapore source or body*	*Not Recognised*	*No definition given by a Singapore source or body*
New Zealand	A Professional Engineering Geologist (PEngGeol) applies specialised knowledge of geology to evaluate and manage the interaction between geological conditions and engineering activities. They play a key role in identifying and mitigating ground-related risks, ensuring the safety, efficiency and sustainability of infrastructure and resource development projects. Professional engineering geologists demonstrate their competence by integrating geoscience expertise with engineering practices. (Engineering New Zealand, 2025) Engineering geologists are specialist earth scientists who apply the geological sciences to engineering study to account for geological factors regarding the location, design, construction, operation and maintenance of engineering works in the design. Engineering geologists provide geological and geotechnical recommendations, analysis, and design associated with human development and various types of structures. The principal objective of the engineering geologist is, by careful investigation and	*Not Recognised*	Geotechnical engineers are specialist civil engineers who analyse, plan and construct foundations and support structures. These professionals use engineering principles and applications to ensure a structure's stability and longevity. Geotechnical engineers often work in offices; they also conduct site visits and field work. The principal objective of the geotechnical engineer is the protection of life and property against damage caused by various geological conditions by careful design of underground or ground supporting structures. (NZGS, 2025)

COUNTRY	ENGINEERING GEOLOGIST	GEOLOGICAL ENGINEER	GEOTECHNICAL ENGINEER
	characterisation of the ground, the protection of life and property against damage caused by various geological conditions. There is a large overlap between engineering geology and geotechnical engineering. In simple terms, engineering geologists identify and define a problem, then geotechnical engineers design the solution (NZGS, 2025)		
United States	Engineering Geologists are indispensable professionals who analyse geological data to inform the design, construction, and maintenance of infrastructure projects, thereby ensuring stability and safety (SEG, 2023)	Geological engineers design mines to safely and efficiently remove minerals for use in manufacturing and utilities (U.S. Bureau of Labor Statistics 2025).	Geotechnical engineers assess ground conditions and design foundations, slopes, and earth retaining structures. (American Profession Guide, 2025)
Canada	Engineering Geologists have specialized knowledge in geological sciences and the principles and methods of engineering analysis acquired through professional education and practical experience. Engineering geologists are qualified to apply such knowledge, skill, and judgment to a wide variety of civil and mining works, and the prevention and remediation of geological hazards. They complete geological and geotechnical studies, inspections and analyses of, and provide recommendations and geological design associated with natural and built environments. They also develop measures to prevent, mitigate, and remediate geological hazards. Engineering geologists are critical to and should be considered as the principal developers of the conceptual ground model for a given site. (CGS, 2025)	Geological engineers conduct geological and geotechnical studies to assess suitability of locations for civil engineering, mining and oil and gas projects; and plan, design, develop and supervise programs of geological data acquisition and analysis and the preparation of geological engineering reports and recommendations. (Government of Canada, 2021)	Geotechnical Engineers analyse soil, rock, groundwater, and other earth materials to inform and guide construction projects and environmental conservation. Their work supports infrastructure development like buildings, bridges, and dams, balancing technical requirements with environmental stewardship. This profession requires a blend of fieldwork, analysis, and collaboration with multidisciplinary teams to solve complex engineering problems. (ECO Canada, 2025)
South Africa	Engineering geologists investigate and provide geologic and geotechnical recommendations, analysis, and design associated with human development. (SAIEG, 2025)	*Not Recognised*	Geotechnical engineers are responsible for structures' foundations. Work includes assessing data from the field, finding ways to ensure foundations or slopes are stable, designing foundations, and overseeing work on a construction site

COUNTRY	ENGINEERING GEOLOGIST	GEOLOGICAL ENGINEER	GEOTECHNICAL ENGINEER
			(South African Geotechnical Division, 2025).

https://doi.org/10.56295/1ACEG41

A SCALABLE MACHINE LEARNING MODELLING TOOL FOR MAPPING LANDSLIDE RUNOUT USING A CASE STUDY IN HAWKES BAY, NEW ZEALAND

Alex Stokes
Independent Engineering Geologist

ABSTRACT

Understanding landslide runout is crucial for land use planning, utility networks, and assessing infrastructure resilience on slopes. Recent guidance recommends incorporating landslide runout models along with climate change implications when assessing land for development. The advancement of machine learning (ML) techniques can offer new insights and a tool to be used alongside current methods. A range of data inputs from land-use, remote observations, and field measurements can all be used for training models and as inputs to landslide runout predictions.

Modelling potential landslide runout scenarios requires extensive volumes of data. A ML trained model has been developed to map landslide runout direction and distance for a case study in Hawkes Bay, New Zealand following rainstorm events in January 2023 and then cyclone Gabrielle February 2023. A steepest path hydrological flow path model was developed alongside the ML approach for landslide runout direction. Ten thousand landslide runouts were used in the training along with features engineered from a 1 m resolution Digital Elevation Model (DEM).

The results show the model is capable of predicting expected runout distances with a reasonable degree of accuracy. To improve the results and create a probabilistic output for hazard mapping, a stochastic parameter should be incorporated into the model, along with additional disposing factors such as vegetation density, source size and topographic wetness. The hydrological flow path model performed better than the ML runout direction model in certain scenarios, most likely due to the large precipitation volumes triggering high water content debris flows and debris floods. This highlights the inherent complexity of modelling landslide debris trails and why a probabilistic Monte Carlo modelling approach will be best placed for quantifying the uncertainty into a hazard map.

1 INTRODUCTION

Landslides have killed more people in Aotearoa New Zealand than other geological hazards combined (de Vilder et al., 2024) and New Zealand has been identified as one of the most vulnerable economies in the world to the impact of natural disaster as a percentage of GDP (NZGS, 2024). In the case of New Zealand, it is therefore important to understand landslide risk in the most cost-efficient way.

The analysis of landslides can broadly be broken down into two categories –

1. identification of terrain which is susceptible to landsliding,
2. *the source* and the direction and distance of the landslide path, *the runout*.

However, landslides are complex processes with many degrees of freedom influencing their triggering mechanism, source and runout. Traditionally landslides have been categorised into different types (Varnes, 1978) depending on host material which then has been linked, based on empirical data, to their typical runouts (Brideau et al., 2021). Debris flows type are particularly hazardous when considering runout given the potential for large travel distances, particularly when confined into channelised debris flows (Cascini et al., 2014).

There are many methods which are often combined to assess landslide runout out including geomorphological mapping (Parry, 2011), numerical modelling (Hungr and McDougall, 2009; Ceccato et al., 2024), topographic zoning (WSP, 2023), and back analysis (Sun et al., 2021). The appropriate method for assessing landslide runout is often case dependent – client requirements, potential risk, project budget, type of landslide, available expertise, data available, access and time constraints. A big data probabilistic model is most appropriate for insurance risk models, initial input into landslide risk analysis for land planning, utility networks and infrastructure resilience. For site specific landslide runout analysis, a more involved approach such as a Natural Terrain Hazard Survey (Ho and Roberts, 2016) would be more appropriate. This paper is a preliminary approach for probabilistic modelling of landslide *runout*. Our research has previously developed a probabilistic model of landslide susceptibility *source* for New Zealand (Stokes, in press) which this study uses.

All the above methods rely, to different degrees, on empirical historical data and the future being linked to the environments of the past (Lee, 2024). Current and future developing uncertainties such as climate and land use change

inhibit our ability to predict both landslide source and runout to the absolute. We have shown that the general source model can be calibrated to different rainfall events and land-use allowing for the landslide susceptibility to be predicted for a rainfall event of a given magnitude or land use change (Stokes, in press). There is of course uncertainty over what magnitude rainfall triggering event is appropriate for predicting future events. Current guidance for climate-change scenarios that need to be considered in analysis is generally not provided definitively, which is not surprising given the dynamic uncertainty (de Vilder et al., 2024). Therefore, a big data probabilistic approach can aid in decision making in such scenarios but cannot provide absolutes.

Probabilistic models rely on large datasets and appropriate statistical methods to develop return periods and correlations. Recent advances in statistics coupled with machine learning (ML) and availability of computing power allows for many more variables to be included in models enabling the prediction of much more complex non-linear processes to be developed. Obviously, this approach has limits, such as uncertain prediction outside of the limits of the training data, and to some extent model opaqueness, but the application of this method has already been successful in many fields. Within the field of ML, a Generative Adversarial Network (GAN) is a method which uses fake data to train a predictive model alongside real data. The use of GANs has been explored for landslide susceptibility assessments by (Al-Najjar and Pradhan, 2021) and (Stokes, in press) and debris avalanche footprints (Mead and Kereszturi, 2023). This paper presents a novel approach to modelling landslides which uses a GAN to predict landslide direction and runout distance from any start point. The model uses the output from a landslide susceptibility analysis (Stokes, in press) to model the runout from areas of high landslide susceptibility.

2 STUDY AREA

The sample dataset utilised the 10,000[1] debris trails from the New Zealand Landslide Database located in Hawkes Bay, New Zealand (Figure 1). The landslide type was predominantly rainfall induced shallow soil debris flows[2]. The dataset has been chosen given the large amount of landslide in a very local area, similar mechanism of occurrence, triggered by a single event and with the underlying geology being consistent over the study area comprising Paleogene to Neogene sandstone, mudstone and limestone (Figure 7 in the Appendix).

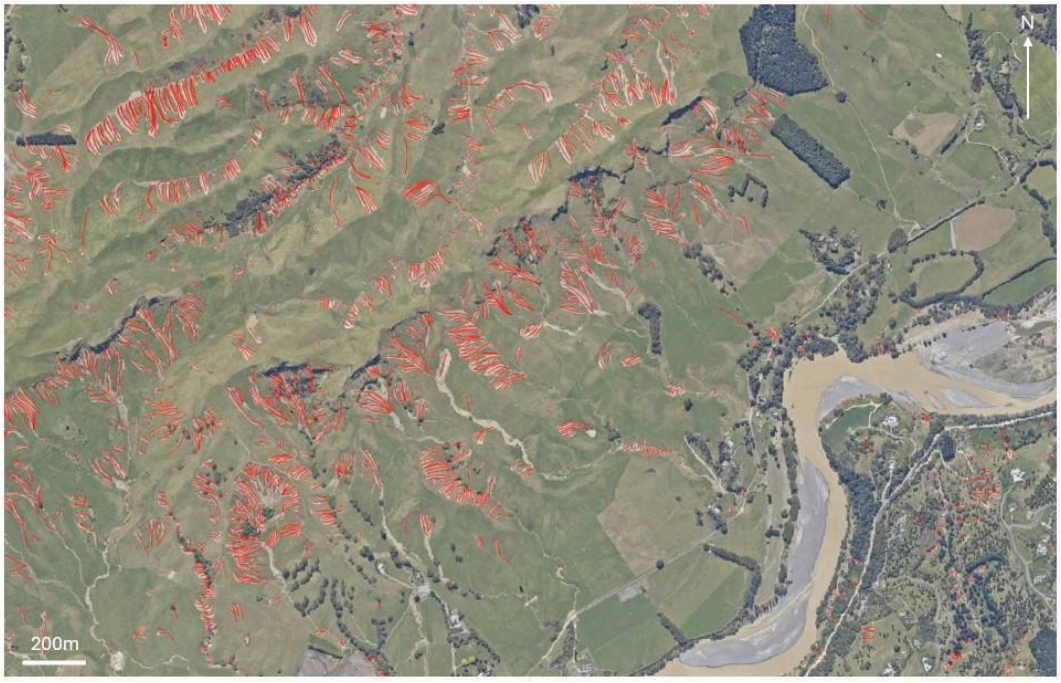


Figure 1: Extract of Landslide Runouts (red) in Study Area. Tukituki River, Hawkes Bay. Aerial Photograph downloaded from LINZ and captured between 19-21 February 2023.

[1] The dataset does not include exact information on the date of occurrence but based on an assessment using recent aerial imagery most if not all the landslides would have occurred following the Cyclone Gabrielle rainfall event in February 2023.
[2] although this isn't confirmed for all landslides

3 METHODOLOGY

There are many approaches of numerical modelling landslide runout. These range from a

- (Brideau et al., 2021) - purely empirical travel angle calculation,
- (Hungr and McDougall, 2009) - dynamic 'method of slices', and
- (Mikos and Bezak, 2021) - numerical physical finite volume models

These methods are limited as they can only be used modelling a single event at a time.

ML is the approach that has been employed in this paper and is considerable relevant through its successes across multiple disciplines (Scalia, 2022) and is being used more commonly in earth science (Dramsch, 2020) with many examples in the field of landslide susceptibility and runout by (Chen et al., 2024). ML differs from many of the traditional methods as it doesn't not rely on physical geometric process modelling but instead is rooted in the statistical and probabilistic branch of mathematics. There are many advantages to using this method:

1. It can utilise the large amounts of data which is now available.
2. The processing power requirements are lower than physical models which is particularly useful for large areas.
3. The flexible nature of the modelling method – physical models tend to be very set in stone with the data requirements for the model. An ML approach can be adapted to the available data and the model will quantify the predictive power of the output based on the data provided. For example, if the data does not include source volumes the model will still be able to produce a prediction, but the certainty of the model will be reduced.

3.1 Model Framework

The model utilises a variation of the GAN framework developed in the field of machine learning (Goodfellow et al., 2014) which has had considerable success in tasks such as realistic image generation and downscaling climate models (Rampal et al., 2025). The basic framework of a GAN is shown in Figure 2.

A GAN consists of two ML models a Generator and a Discriminator. In the context of realistic image generation, the generator creates fake images which could just be noise. The Discriminator is then trained to identify the difference between the fake images and real images. Repeated training of the models can lead to generated fake images which are authentic to human observers. This framework has been selected based on the information that is available – a database of real landslide debris trails. The general GAN inspired framework is shown in Figure 3. Instead of fake images the Generator creates fake (synthetic) landslide debris trails using an adapted random walk algorithm. Using a number of features extracted from the real and synthetic debris trails and a high-resolution DEM the Discriminator model is trained on a balanced dataset. The final step of the model is the 'Expert Discriminator' a landslide expert who assesses whether the landslide debris trails that have been generated are satisfactory.

The GAN model uses the combination of two gradient boosted decision tree machine learning architectures, an XGboost Classifier and an XGboost Regressor (Chen, 2016). Both architectures are highly reputable and have been successfully implemented across multiple disciplines and including recently to model landslide runout (Qui and Ghen, 2024). The classifier is used to predict the direction of landslide runout and the regressor is used to predict the termination point of the landslide.

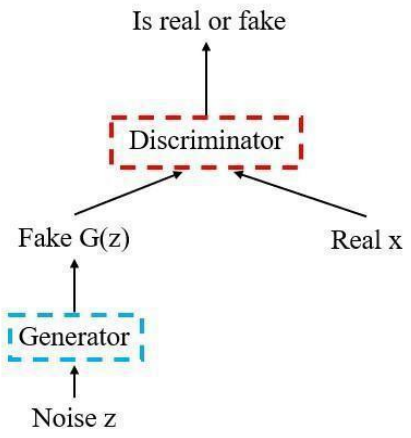


Figure 2: Generalised GAN Architecture after (Goodfellow et al., 2014)

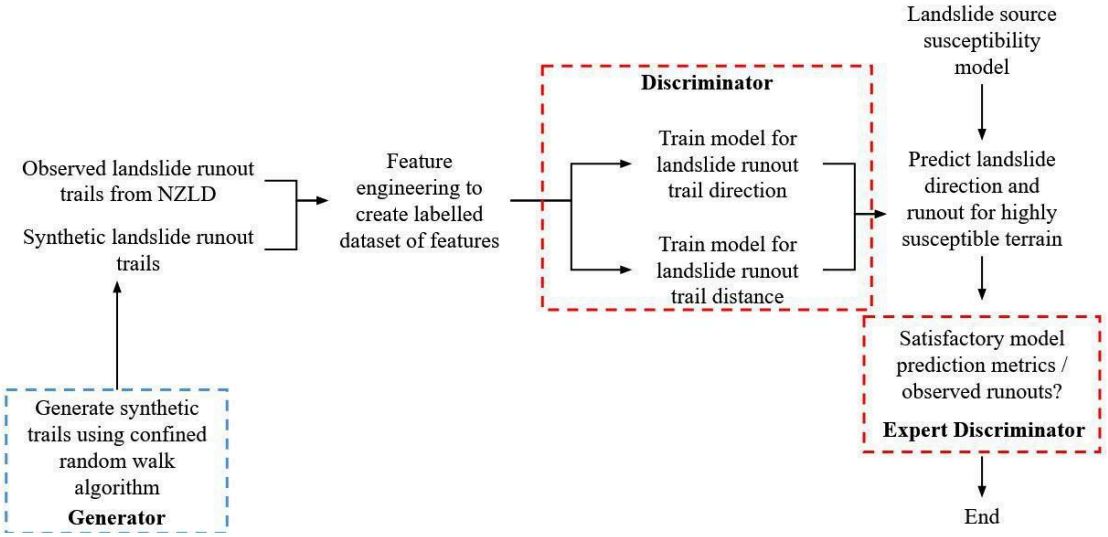


Figure 3: GAN inspired model architecture for landslide debris trail prediction

3.1 Selection of disposing factors

Factor or feature selection is critical for a good quality machine learning model (Qiu and Geng, 2024). Features must be engineered that provide the model with the most appropriate information for explaining how the system under study behaves. This is often and favourably derived from expert knowledge, but in its absence (or alongside) a brute force approach using statistical measures is possible. Features important for predicting landslide runout are well documented in the literature (McDougall, 2014; Reid et al., 2025) and include (but not limited to) height-to-length ratio (H/L), angle of reach, drop height between source area and endpoint, mean gradient of travelling path, mean curvature of travelling path, volume of failure mass, and normalised difference vegetation index, degree of channelisation. All these features can be calculated from a high-resolution DEM for any given runout footprint except for normalised difference vegetation index and volume of failure mass. As the model has been designed to predict runout length and direction different relevant disposing factors were included in each model.

3.2 Direction of landslide runout

The direction of landside runout is often modelled using hydrological flowlines which estimate the flow direction of water over a terrain using a simple algorithm which follows downward topographic movement. However, landslide processes differ from hydrologic processes so an ML model trained on actual landslide runout paths may provide more accurate predictions than one simply following the likely hydrologic flow path.

Two separate models have been used for the direction of landslide runout:

1. Hydrologic flow path model – This simply follows the direction of maximum H/L which is the steepest path.
2. XGboost classifier model – A ML boosted decision tree model which is trained on synthetic and real data using the following disposing factors: height-to-length ratio (H/L), angle of reach, drop height between source area and endpoint, mean gradient of travelling path, mean curvature of travelling path and degree of channelisation. The model predicts whether a trail is real or synthetic based on these factors.

3.3 Termination of landslide runout

To model the termination of a landslide the XGBoost regression architecture was employed. The model was trained using height-to-length ratio (H/L), angle of reach, drop height between source area and endpoint, mean gradient of travelling path, mean curvature of travelling path and degree of channelisation. The 'label' which is being predicted is the point along the debris trail, a value between 0 and 1. As it is a regression model, it can just be trained on the actual landslides trails and doesn't require any synthetic 'fake' runout out data.

3.2 Collinearity assessment of factors

Assessing the collinearity of factors or features is an important step when developing a machine learning model. Collinearity refers to the non-independence of predictor variables (Dormann et al., 2013). A 'folk lore' exists that a

feature should not be included if its correlation coefficient is >0.7 with another feature as this can severely distort model estimation and prediction (Dormann et al., 2013).

3.3 Model Development

Prior to model development an appropriate study area was selected manually in the GIS environment QGIS. The relevant data was then cropped to reduce the memory requirements. The model was then developed in Python using the Integrated Development Environment (IDE) Visual Studio Code. The python modules used were geopandas, pandas, numpy, shapely, xgboost, sklearn, multiprocessing and rasterio. Each of the steps shown in the GAN inspired model architecture (Figure 3) required extensive functions to be written, a general step-by-step pseudo code of the method is provided in the Appendix at the end of the paper.

4 RESULTS

4.1 Determination of input variables

The collinearity of features input in the model has been calculated. The features associated with measuring the channel width and height have high collinearity and the features for related to measuring the angle of reach also have high collinearity. Given the current model architecture used will reduce the weight of features that are highly colinear, it is not necessary to remove them from the model.

4.2 Trained Model Validation Metrics

Both models were trained and tested using a 2/3 to 1/3 split ratio. The model metrics show the trained directional model can distinguish the difference between real and synthetic debris trails with a high level of accuracy, 91%. This is not surprising given the initial trails are generated from a random walk algorithm. The regression based trained runout trail distance model has a moderate performance with a relative Mean Absolute Error (MAE) of 31%.

4.3 Estimate of travel distance and direction

Over 6,000 debris trails were predicted using the model from the same start points as the original 11,000 real debris trails. Figure 4 shows a visual comparison between:

a) real debris trails from the event,
b) the initial random walk trails,
c) the predicted debris trails using the ML direction/runout model, and
d) the predicted debris trails using direction of max H/L with the ML runout model.

A preliminary set of results compares the real and predicted synthetic debris trails using the common metrics in Figure 5:

a) runout length,
b) total drop height, and
c) angle of reach.

A visual comparison between the three figures, Figure 4, Figure 5 and Figure 6, shows general correlation. The real trails frequency exhibits a behaviour more like a natural complex system with a power law relationship, a property of a system at self-organised criticality in Figure 5 (top) and (middle) (Bak et al., 1987) and a characteristic smooth gaussian distribution in Figure 5 (bottom) (Sornette, 2007). This is less pronounced in the synthetic debris flows frequency plots.

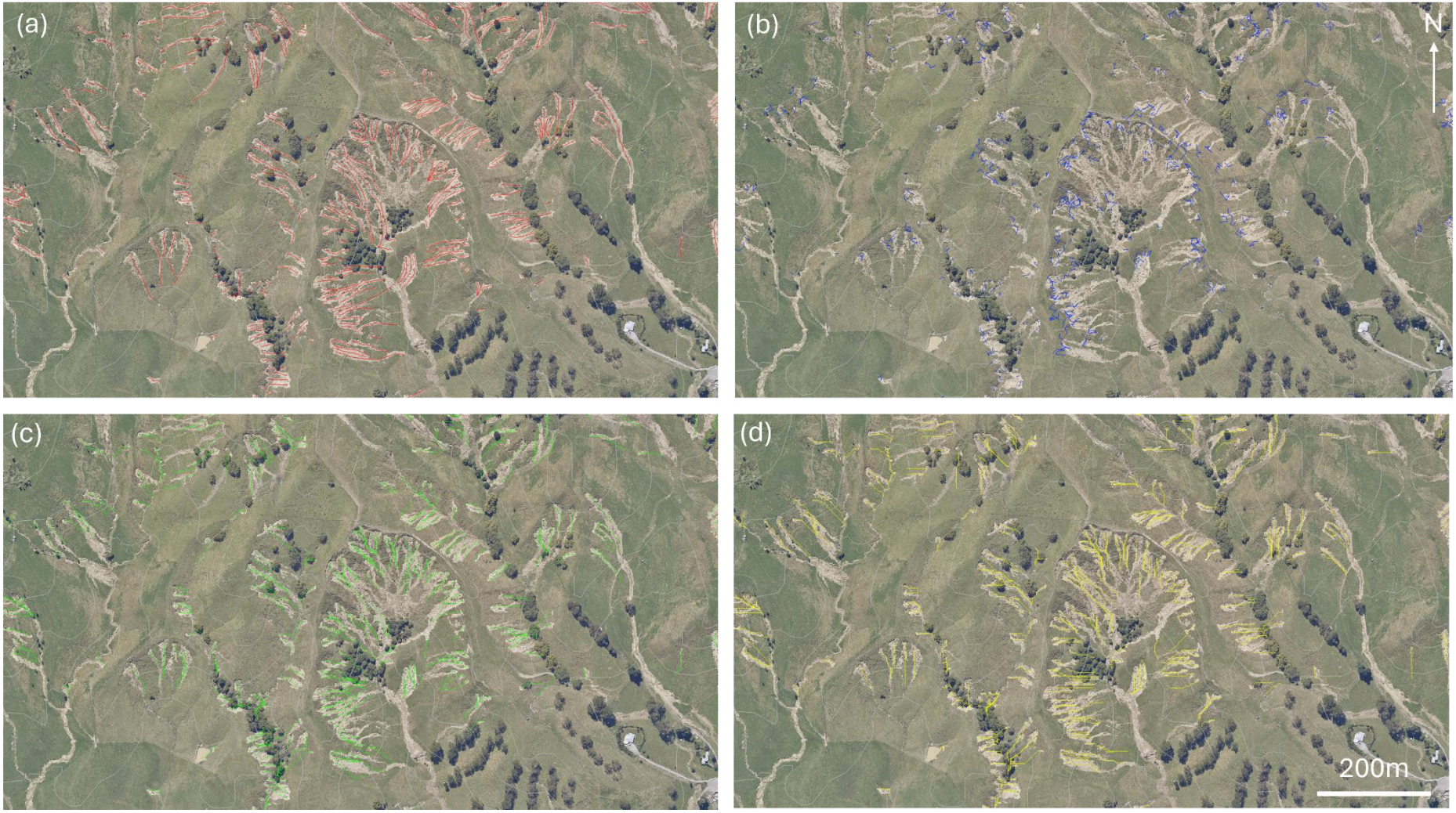


Figure 4: Example model output for a specific location in the study area. (a) The real debris trails. (b) The initial generated random walk debris trails. (c) The predicted debris trails from the ML Direction and ML runout models. (d) The predicted debris trails from the hydrologic flow path direction and ML runout model.

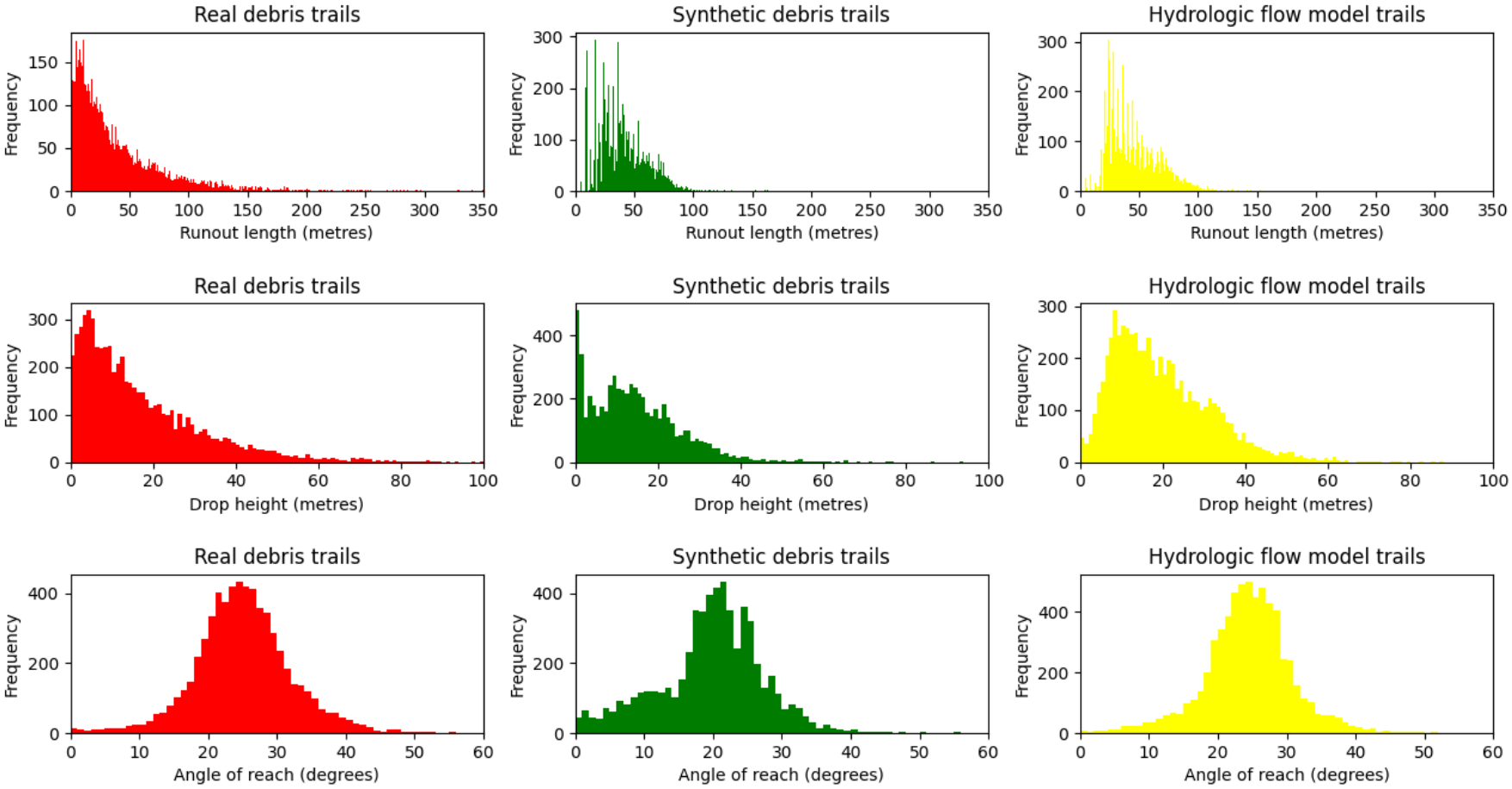


Figure 5: Comparison between real and predicted synthetic debris trails using the ML Direction model and hydrologic flow model. Common metrics (top) runout length, (middle) total drop height and (bottom) angle of reach.

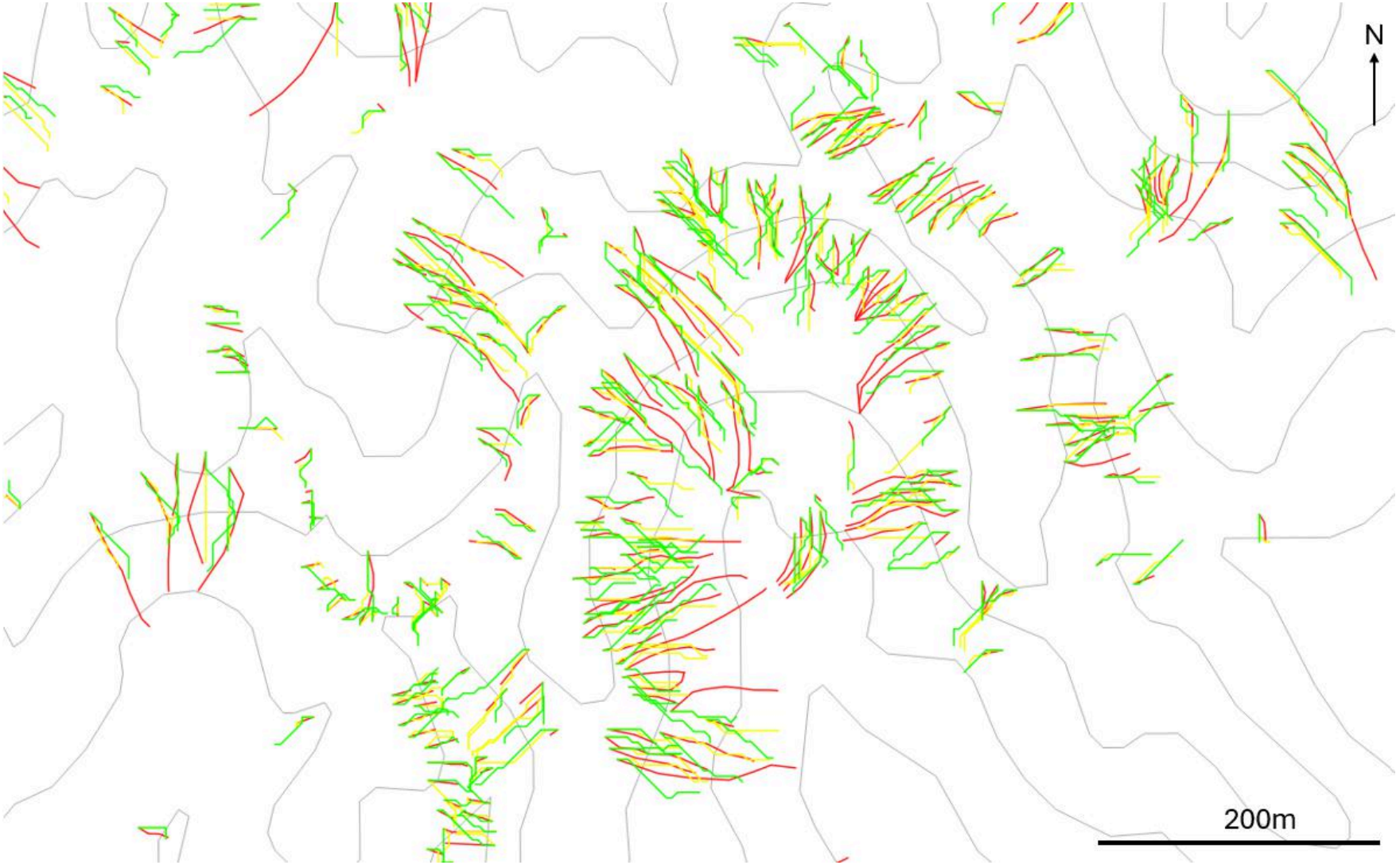


Figure 6: Landslide debris runout overlay of trails in Figure 4. Red – The real debris trails (Figure 4a). Green – The predicted debris trails from ML direction and ML runout models (Figure 4c). Yellow – The predicted debris trails from the hydrologic flow path direction and ML runout model (Figure 4d).

5 DISCUSSION AND LIMITATIONS

5.1 Discussions

The results show a model can be trained to predict landslide runout and direction from real and random data. However, the direction and distance of the predicted runout are not always consistent with the real data. The ML approach for both direction and distance of the debris trail (Figure 4c) has an accuracy of greater than 90% when considering the spatial overlap between the real and synthetic debris trails (Figure 6). The hydrological flow path direction model (Figure 4d) and ML distance model has an accuracy of 97% (Figure 6). There are some notable exceptions in the output where the ML direction debris trails appear to not follow exactly the same path as the real debris trails. The lowest correlation is where the landslide occurs close or on a spurline. In these situations, it is likely there are a few alternative paths the debris trail could take at the beginning of the trail leading to much larger differences further along. The hydrological flow path model performed better in such situations (Figure 4d). Given the trigger event was an unprecedented very high-volume short duration rainfall event, some of the trails might include secondary sedimentation of the landslide deposit which could be classified as a colluvial deposit or debris flood deposit (Jakob and Hungr, 2005; Church and Jakob, 2020). These deposits are more water dominated so are more likely to follow a hydrologic flow path and also typically have a longer runout than the landslide debris alone.

The differences observed between the three datasets – real debris trails (Figure 4a), ML-direction/ML-distance debris trails (Figure 4c) and H/L max direction/ML-distance debris trails (Figure 4d) can be accounted for by the complexity of landslide runouts. Landslide debris trails are influenced by many factors which are difficult or impossible to account for in a model. There is potential for improving the model by adding factors including calibration to rainfall (von Ruette et al., 2016), storm direction / slope aspect, topographic wetness index, vegetation density and subsurface information. But this reductionist approach has limits and may not be able to account for the inherent chaos and complexity in the system (Lee, 2024). In the context of landslide debris trails, no two events or locations are the same. Nevertheless, the likeness of the synthetic trails to the natural system (the real trails) (Figure 5) could be increased through model refinement.

The end goal of this approach was not to directly replicate the real debris trails but to produce landslide hazard zonation maps which consider multiple possibility trail routes and runouts. This goal on the whole was achieved by this method.

5.2 Refinement of the model

A way of countering the unpredictable nature of debris trails is to use a stochastic approach, such as a Monte Carlo simulation, notably used in climate change models (Randall et al., 2004). This can be added easily into the ML modelling approach and after multiple landslide debris runouts, it is then possible to synthesise the output into a coherent probabilistic map. A probabilistic runout map based on many landslide runouts will have a much more explaining power and provide the end user with a practical output which depicts the hazard opposed to a map based on single debris trails.

5.3 Limitations

It is important to acknowledge the limitations of this ML modelling approach (Baynes and Parry, 2024). In its current form, it cannot replace physical models of debris trails, which provide velocity, energy, and inundation estimates for detailed hazard assessments at specific locations. However, the relatively low computational demands of this method enable the analysis of larger datasets and the prediction of many more debris trails across a broader scale—something not feasible with conventional physical models. For detailed design in a specific use case, a physical model combined with expert judgement remains essential.

The methodology introduces an *expert discriminator* – a human landslide expert to determine whether the final landslide debris trails generated by the model are plausible. It would defeat the whole object of this method, and likely not possible, for every single trail to be inspected. It is likely that a sample would be inspected; the size of which has not been determined at this stage.

There are also limitations to the real debris trails used for training the ML models. These have been collected by aerial photograph interpretation following the event without ground truthing. Some of the debris trails may have been obscured by vegetation and there could be human error involved in interpretation.

Finally, the study area selected consisted of 10,000 debris trails from a single event in a single geology material type which can be considered a large sample. The predictive power of the model in other geology types in other events will likely be limited given the confinements of the modelling process.

6 CONCLUSION

The modelling approach and framework have been selected based on the high level of success achieved in other fields of study and the availability of large datasets. The results have yielded promising predictions based on visual comparison and metrics (Figure 6). However, the results are not yet satisfactory for use in hazard prediction. Introducing a Monte Carlo simulation approach into the modelling framework will increase the predictability and confidence in the output which can be synthesised into a probabilistic landslide runout map. Adding additional disposing factors such as vegetation and topographic wetness may also increase the predictability. The scaling up of the method should be possible through code parallelism and optimisation without the need of costly high-performance computing.

7 APPENDIX

A summary of the pseudocode followed for the methodology is provided below:

Generate synthetic trails using confined random walk algorithm:

1. *Start points of sampled debris trails selected.*
2. *Random points added sequentially within a maximum specified distance of previous point.*
3. *Next point selected within a certain distance of the previous point*
4. *Algorithm is stopped with the same number of points as the original sampled debris trail.*

There are many ways to develop this algorithm. GAN models tend to start with random noise implying a large amount of flexibility (Goodfellow et al., 2014).

Feature engineering to create labelled dataset of feature:

1. *Create data dictionary for each debris trail*
2. *Iterate through each point of the debris trail and:*
    a. *Extract height from DEM*
    b. *Calculate angle of debris trail (iterative and total), drop height (iterative and total), plan length, full length andsinuosity of trail*
    c. *Calculate DEM height at 5m, 10m, and 15m perpendicular to trail direction to measure confinement*
    d. *Calculate how far along the debris trail the point is*
3. *Concatenate all data dictionaries into a pandas dataframe.*

Train model for landslide runout trail direction:

1. *Select relevant features for landslide runout trail direction*
2. *Create balanced dataset of real and synthetic data*
3. *Train XGBoost model on real and synthetic data to identify the correct landslide direction*

Train model for landslide runout trail distance:

1. *Select relevant features for landslide runout trail distance and create balanced dataset of real and synthetic data*
2. *Train XGBoost regression model on real and synthetic data to identify the correct landslide runout distance*

Landslide source susceptibility model:

1. *Extract data from landslide susceptibility model within study area.*
2. *Select 10,000 locations which are highly susceptible to landslides (Relative Probability >0.7).*
3. *Use these points as start points for landslide prediction.*

Predict landslide direction and runout for highly susceptible terrain:

1. *Select each start point*
2. *Create features for all possible directions in the Von Neumann neighbourhood for the point.*
3. *Use trained direction model to predict most likely landslide direction.*
4. *Use trained distance model to predict if the current point is the end of the landslide runout trail.*
5. *Iterate back through steps 2 to 5 until the model predicts it has reached the end of the landslide trail.*
6. *Then select a new start point – step 1.*
7. *If the generated landslide trails are as expected by an expert discriminator, then end the model otherwise use generated landslide trails to retrain the direction model to improve model parameters.*

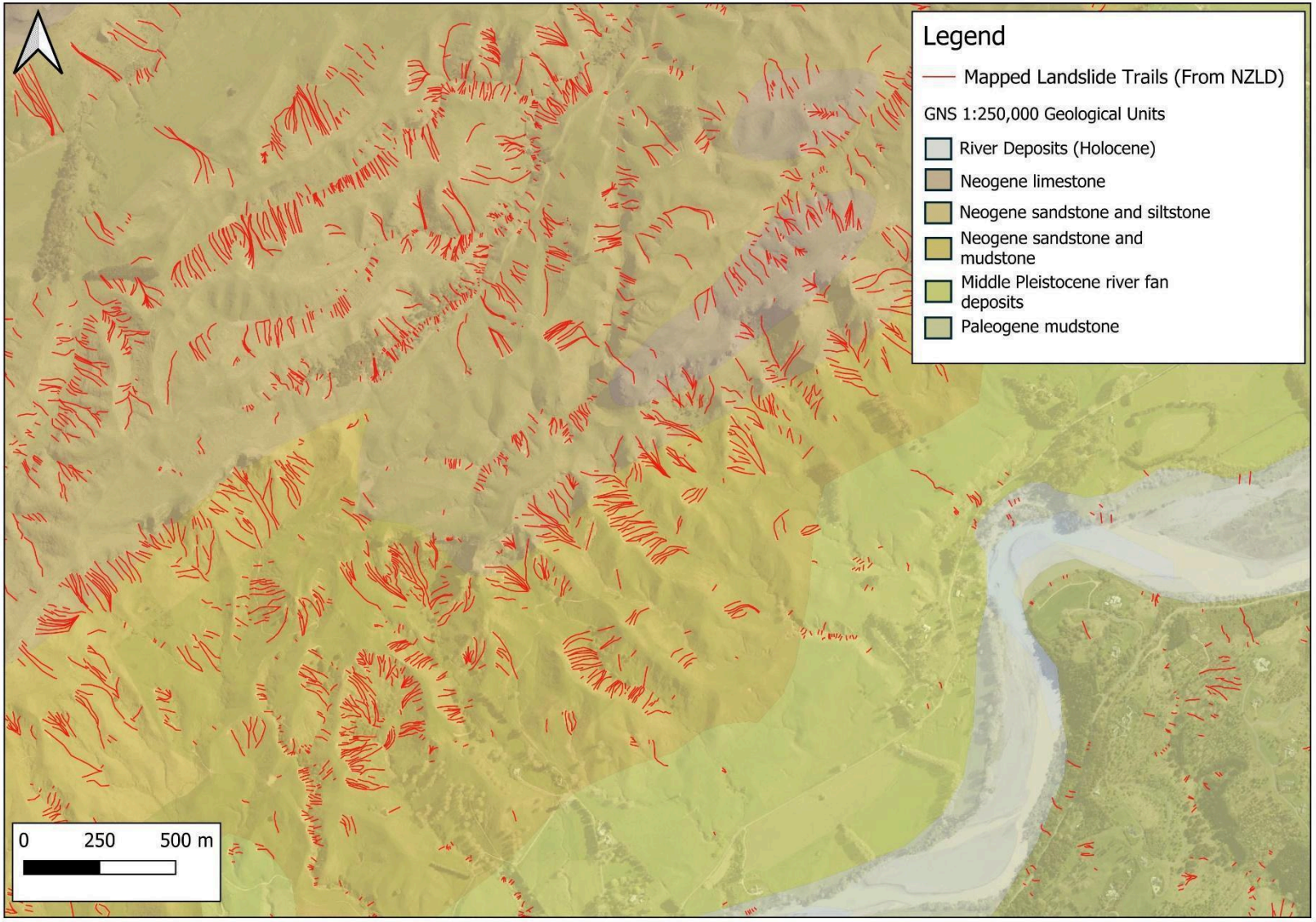


Figure 7: Typical geological units in the study area comprising Paleogene to Neogene Mudstone, Sandstone and Limestone.

8 REFERENCES

Al-Najjar H. A. H., Pradhan, B. (2021). Spatial landslide susceptibility assessment using machine learning techniques assisted by additional data created with generative adversarial networks. *Geoscience Frontiers* 12: 625-637.

Bak, P., Tang, C., & Wiesenfeld, K. (1987). Self-organized criticality: An explanation of 1/f noise. *Physical Review Letters, 59*(4), 381–384.

Baynes, F. J. and Parry, S. (2024). Guidelines for the development and application of engineering geological models on projects. Version 2.0. *International Association for Engineering Geology and the Environment (IAEG)* Commission 25 Publication No. 1, 81 pp.

Brideau, M. A., de Vilder, S., Massey, C., Mitchell, A., McDougall, S., Aaron, J. (2021). V1.0 Empirical Landslide Runout Relationships, compiled from international examples, for various landslide types. Understanding and Reducing Landslide Disaster Risk, *ICL Contribution to Landslide Disaster Risk Reduction*.

Cascini, L., Cuomo, S., Pastor, M., Sorbino, G., & Piciullo, L. (2014). SPH run out modelling of channelised landslides of the flow type. *Geomorphology, 214*, 502–513.

Ceccato, F., Yerro, A., & Di Carluccio, G. (2024). Simulating landslides with the material point method: Best practices, potentialities, and challenges. *Engineering Geology, 338*, 107614.

Chen, L., Ma, P., Fan, X., Wang, X., & Ng, C. W. W. (2024). A knowledge-aware deep learning model for landslide susceptibility assessment in Hong Kong. *Science of The Total Environment*, 941, 173557.

Chen, T., & Guestrin, C. (2016). XGBoost: A scalable tree boosting system. *arXiv*. arXiv.1603.02754.

Church, M., & Jakob, M. (2020). What is a debris flood? *Water Resources Research, 56*, e2020WR027144.

De Vilder S. J., Kelly S. D., Buxton R. B., Allan S, and Glassey P. J. (2024). Landslide planning guidance: reducing landslide risk through land-use planning. Lower Hutt (NZ): GNS Science. 77 p. *(GNS Science miscellaneous series; 144).*

Dormann, C. F., Elith, J., Bacher, S., Buchmann, C., Carl, G., Carré, G., García Marquéz, J. R., Gruber, B., Lafourcade, B., Leitão, P. J., Münkemüller, T., McClean, C., Osborne, P. E., Reineking, B., Schröder, B., Skidmore, A. K., Zurell, D., & Lautenbach, S. (2013). Collinearity: A review of methods to deal with it and a simulation study evaluating their performance. *Ecogeography, 36*, 27-46.

Dramsch, J. S. (2020). Chapter One - 70 years of machine learning in geoscience in review. In *Advances in Geophysics* (Vol. 61, pp. 1–55). Elsevier.

Goodfellow, IJ., Pouget-Abadie, J., Mirza, M., Xu, B., Warde-Farley, D., Ozair, S., Courville, A., & Bengio, Y. (2014). Generative adversarial networks. arXiv. (*arXiv*:1406.2661).

Ho H.Y. and Roberts KJ. (2016). Guidelines for Natural Terrain Hazard Studies. GEO Report No. 138 (Second Edition). Geotechnical Engineering Office. HKSAR.

Hungr, O., & McDougall, S. (2009). Two numerical models for landslide dynamic analysis. *Computers & Geosciences, 35*(5), 978–992.

Jakob, M., & Hungr, O. (2005). Debris-flow hazards and related phenomena. *Springer Science & Business Media.*

Randall, D. A., Wood, R. A., Bony, S., Colman, R., Fichefet, T., Fyfe, J., Kattsov, V., Pitman, A., Shukla, J., Srinivasan, J., Stouffer, R. J., Sumi, A., & Taylor, K. E. (2007). Climate models and their evaluation. In S. Solomon, D. Qin, M. Manning, Z. Chen, M. Marquis, K. B. Averyt, M. Tignor, & H. L. Miller (Eds.), *Climate Change 2007: The Physical Science Basis*. Contribution of Working Group I to the Fourth Assessment Report of the Intergovernmental Panel on Climate Change. Cambridge University Press

Lee, J.M.; Bland, K.J.; Townsend, D.B.; Kamp, P.J.J. (compilers) (2011). Geology of the Hawke's Bay area. Institute of Geological & Nuclear Sciences 1:250,000 geological map 8. 1 sheet + 93 p. Lower Hutt, New Zealand. GNS Science.

Lee, M. (2024). 24th Glossop Lecture: Landslide Risk Assessment: Radical Uncertainty and Engineering Geomorphology. Geological Society of London.

McDougall S. 2017. (2014). Canadian geotechnical colloquium: landslide runout analysis—current practice and challenges. *Can Geotech J* 54:605–620.

Mead, S., and Kereszturi G. (2023). Generative Adversarial Networks to Forecast Debris Avalanche Hazard. *IAVCEI* 2023.

Mondini, A. C., Guzzetti, F., & Melillo, M. (2023). Deep learning forecast of rainfall-induced shallow landslides. *Nature Communications*, *14*, Article 2466.

NZGS (New Zealand Geotechnical Society). (2024). Slope stability geotechnical guidance series: unit 1 – general guidance. Version 1.

Parry, S. (2011). Chapter Fifteen - The Application of Geomorphological Mapping in the Assessment of Landslide Hazard in Hong Kong. *Developments in Earth Surface Processes.* 15. 413-441.

Qiu, C., & Geng, X. (2024). Travel distance estimation of landslide-induced debris flows by machine learning method in Nepal Himalaya after the Gorkha earthquake. *Bulletin of Engineering Geology and the Environment*, 83(395).

Rampal, N., Gibson, P. B., Sherwood, S., Abramowitz, G., & Hobeichi, S. (2025). A reliable generative adversarial network approach for climate downscaling and weather generation. *Journal of Advances in Modeling Earth Systems, 17*.

Reid, M.E., Brien, D.L., Cronkite-Ratcliff, C., and Perkins, J.P. (2025). Grfin Tools—User guide and methods for modelling landslide runout and debris-flow growth and inundation: *U.S. Geological Survey Techniques and Methods*, book 14, chap. A3, 105 p.

Scalia, G. (2022). Machine learning for scientific data analysis (pp. 115–126). In *Special Topics in Information Technology* (SpringerBriefs in Applied Sciences and Technology).

Sornette, D. (2007). Probability distributions in complex systems. *arXiv. preprint arXiv:0707.2194*.

Stokes, A. J. H, (in press). The use of machine learning in mapping rainfall induced landslide source susceptibility using a case study in Gisborne, New Zealand. *NZGS Symposium 2025*.

Sun, X., Zeng, P., Li, T., Wang, S., Jimenez, R., Feng, X., & Xu, Q. (2021). From probabilistic back analyses to probabilistic run-out predictions of landslides: A case study of Heifangtai terrace, Gansu Province, China. *Engineering Geology, 280*, 105950.

Varnes, D. J. (1978). Slope movement types and processes. In R. L. Schuster & R. J. Krizek (Eds.), Landslides: Analysis and control (pp. 11–33). Washington, D.C.: *National Academy of Sciences.*

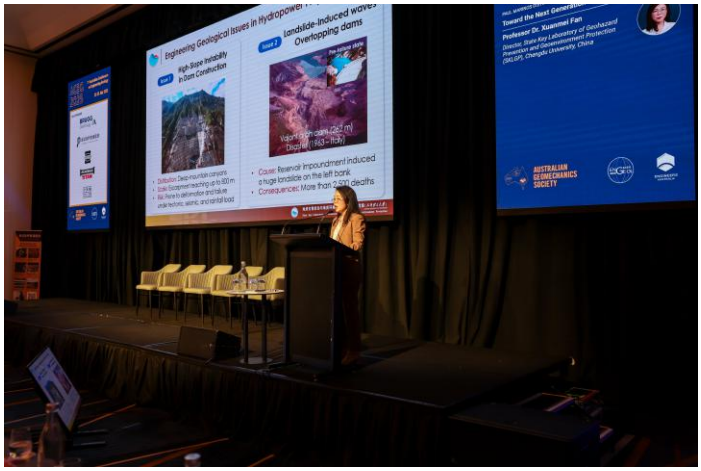
von Ruette, J., Lehmann, P., & Or, D. (2016). Linking rainfall-induced landslides with predictions of debris flow runout distances. *Landslides, 13*, 1097–1107.

WSP. (2023). Tauranga Landslide Slope Hazard (IDC Zones) Study. Technical Report.


ACEG
2025
AUSTRALIAN
GEOMECHANICS
SOCIETY


ACEG
2025
AUSTRALIAN
GEOMECHANICS
SOCIETY



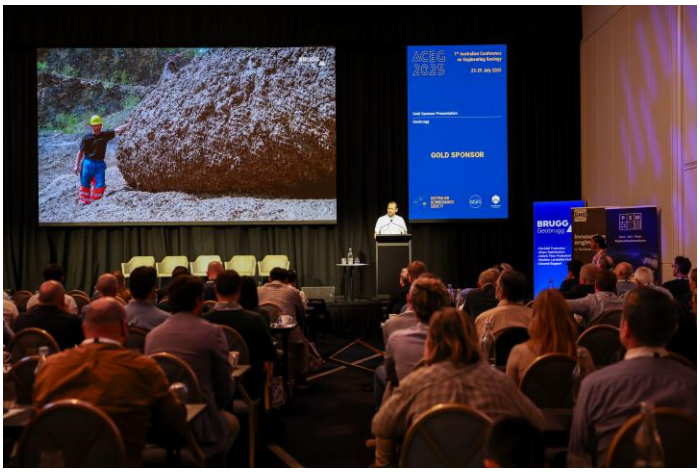

Landslide-Induced waves
Overtopping dams
AUSTRALIAN
GEOMECHANICS
SOCIETY


SCOPEGEO
ETROGRAPHIC AND
OLOGICAL SERVICES
ACEG
2025
AUSTRALIAN
GEOMECHANICS
SOCIETY


ACEG
2025
AUSTRALIAN
GEOMECHANICS
SOCIETY


AUSTRALIAN
GEOMECHANICS
SOCIETY
ACEG
2025
AUSTRALIAN
GEOMECHANICS
SOCIETY


SCOPEGEO
ACEG
2025
AUSTRALIAN
GEOMECHANICS
SOCIETY


ACEG 2025
GOLD SPONSOR
BRUGG


Water is the enemy
ACEG 2025
BRUGG




MACQUARIE


ACEG 2025
AUSTRALIAN GEOMECHANICS SOCIETY

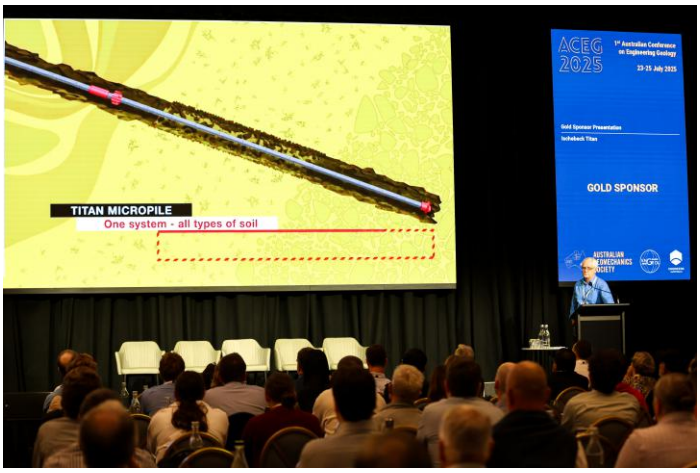

ACEG 2025
AUSTRALIAN GEOMECHANICS SOCIETY


ACEG – July '25
ACEG 2025
AUSTRALIAN GEOMECHANICS SOCIETY


SCOPEGEO
PETROGRAPHIC AND GEOLOGICAL SERVICES
www.scopegeo.com
0417 355 766
ACEG 2025
GOLD SPONSOR
ACEG 2025
AUSTRALIAN GEOMECHANICS SOCIETY



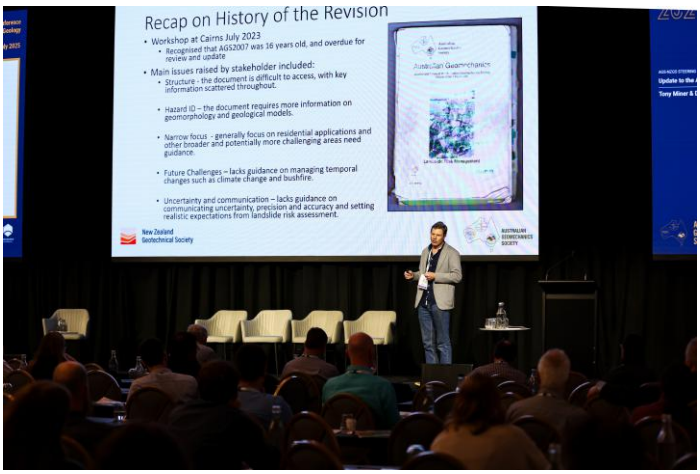

AUSTRALIAN GEOMECHANICS SOCIETY
BRUGG
Geobrugg


TITAN MICROPILE
One system - all types of soil
ACEG 2025
GOLD SPONSOR


Engineering Geology for Reservoir Landslides
Clyde Dam
New Zealand
ACEG 2025


AUSTRALIAN GEOMECHANICS SOCIETY


Civil Tunnelling
ACEG 2025
GOLD SPONSOR


Recap on History of the Revision
Workshop at Cairns July 2023
Recognised that AGS2007 was 16 years old, and overdue for review and update
Main issues raised by stakeholder included:
Structure - the document is difficult to access, with key information scattered throughout.
Hazard ID – the document requires more information on geomorphology and geological models.
Narrow focus - generally focus on residential applications and other broader and potentially more challenging areas need guidance.
Future Challenges – lacks guidance on managing temporal changes such as climate change and bushfire.
Uncertainty and communication – lacks guidance on communicating uncertainty, precision and accuracy and setting realistic expectations from landslide risk assessment.
New Zealand Geotechnical Society


ACEG 2025
AUSTRALIAN GEOMECHANICS SOCIETY


engage and contribute
in these areas
Australian Conference on Engineering Geology 2025
ACEG
2025
AUSTRALIAN
GEOMECHANICS
SOCIETY


ACEG
2025
AUSTRALIAN
GEOMECHANICS
SOCIETY


ACEG
2025
AUSTRALIAN
GEOMECHANICS
SOCIETY


ACEG
2025
AUSTRALIAN
GEOMECHANICS
SOCIETY


ENGINEERS
AUSTRALIA
ACEG
2025
AUSTRALIAN
GEOMECHANICS
SOCIETY


ENGINEERS
AUSTRALIA
ACEG
2025
AUSTRALIAN
GEOMECHANICS
SOCIETY


ACEG
2025
AUSTRALIAN
GEOMECHANICS
SOCIETY


ACEG
2025
AUSTRALIAN
GEOMECHANICS
SOCIETY


BRUGG
Geobrugg
SCOPEGEO
TITAN
LaRGE
2026
ACEG
2025
AUSTRALIAN
GEOMECHANICS
SOCIETY


BRUGG
SCOPESCO
RICHMIX
TITAN
Risk Ass
Melbourne, V


Khumbu glacier – erosion on end moraine
Everest
'Kalapathhar'
base camp of ML
Khumbu Glacier
ACEG
2025
1st Australian Conference on Engineering Geology
23-25 July 2025
AUSTRALIAN GEOMECHANICS SOCIETY


ogy (NAST)
ersity, Matsue, JAPAN
AUSTRALIAN GEOMECHANICS SOCIETY


our
onsor
eca
AUSTRALIAN GEOMECHANICS SOCIETY


AUSTRALIAN GEOMECHANICS SOCIETY
AUSTRALIAN GEOMECHANICS SOCIETY


GS
MEN IN AGS]
ACEG
2025
AUSTRALIAN GEOMECHANICS SOCIETY

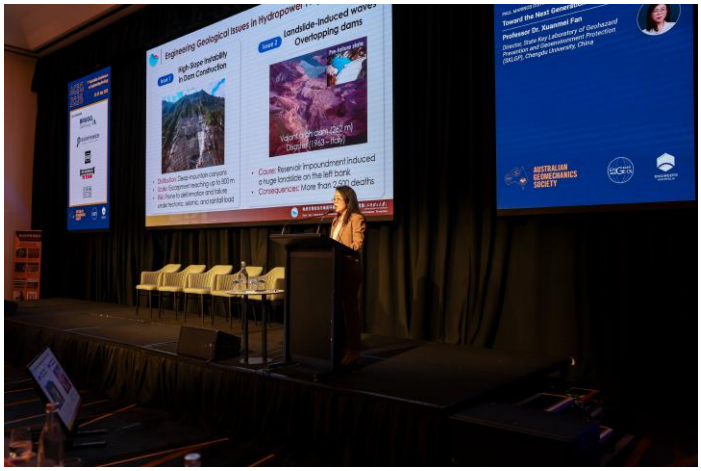

st ACEG – July '25
AUSTRALIAN GEOMECHANICS SOCIETY
ACEG
2025
AUSTRALIAN GEOMECHANICS SOCIETY


ACEG
202
AUSTRALIAN GEOMECHANICS SOCIETY


ACEG
2025
AUSTRALIAN
GEOMECHANICS
SOCIETY


ACEG
2025
AUSTRALIAN
GEOMECHANICS
SOCIETY



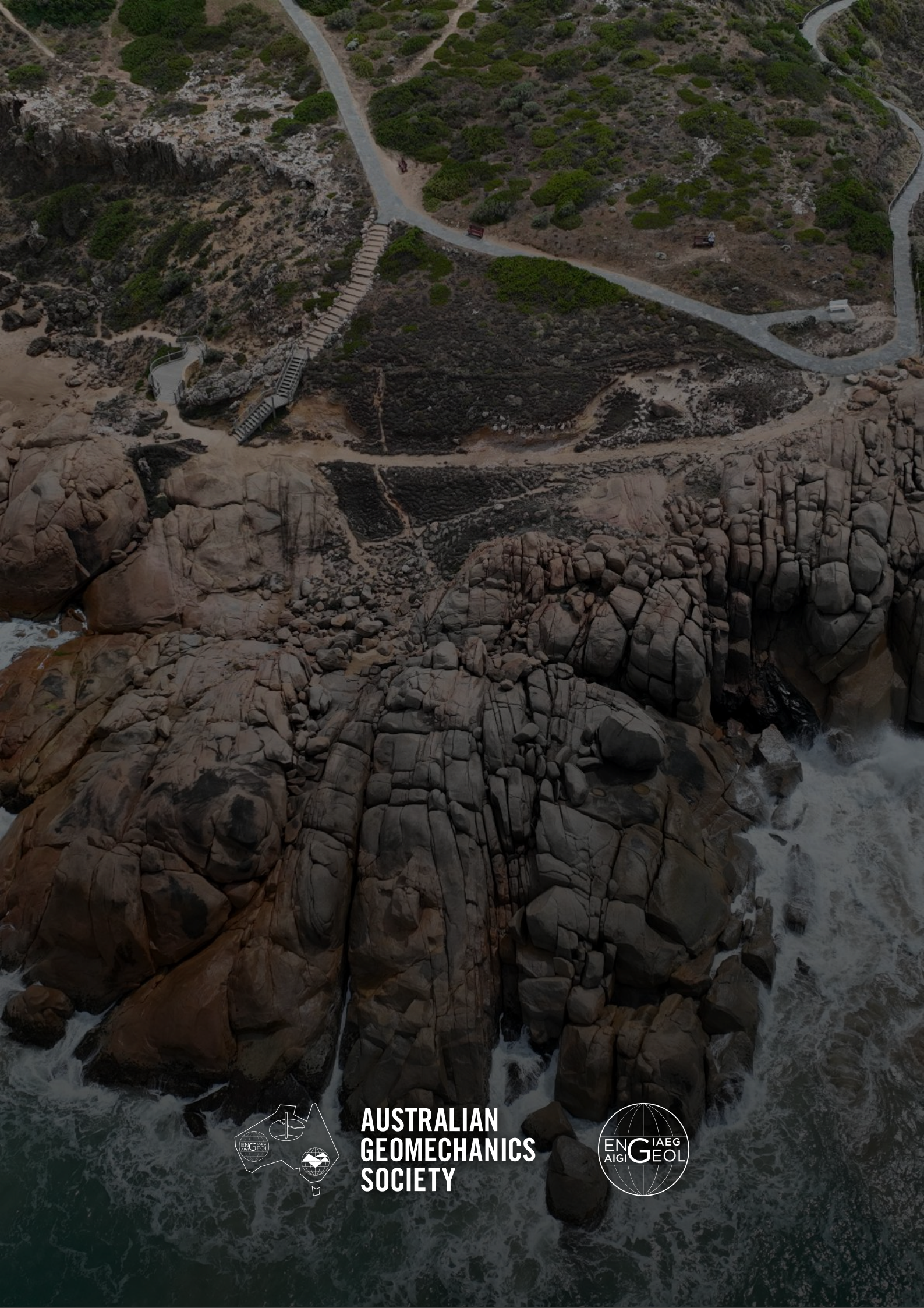

Landslide-Induced waves
Overtopping dams
AUSTRALIAN
GEOMECHANICS
SOCIETY


SCOPEGEO
ETROGRAPHIC AND
OLOGICAL SERVICES
ACEG
2025
AUSTRALIAN
GEOMECHANICS
SOCIETY


ACEG
2025
AUSTRALIAN
GEOMECHANICS
SOCIETY


AUSTRALIAN
GEOMECHANICS
SOCIETY
ACEG
2025
AUSTRALIAN
GEOMECHANICS
SOCIETY


SCOPEGEO
ACEG
2025
AUSTRALIAN
GEOMECHANICS
SOCIETY



AUSTRALIAN
GEOMECHANICS
SOCIETY